VOYAGER SPACECRAFT SYSTEM

FINAL TECHNICAL REPORT

VOLUME A

PREFERRED DESIGN FOR FLIGHT SPACECRAFT AND HARDWARE SUBSYSTEMS

PART II

prepared for

JET PROPULSION LABORATORY
CALIFORNIA INSTITUTE OF TECHNOLOGY
PASADENA, CALIFORNIA

UNDER
CONTRACT NO. 951111
JULY 1965

THE BOEING COMPANY • AERO-SPACE DIVISION • SEATTLE, WASHINGTON

THE BOEING COMPANY

SEATTLE, WASHINGTON 98124

LYSLE A. WOOD
VICE PRESIDENT-GENERAL MANAGER
AERO-SPACE DIVISION

July 29, 1965

Jet Propulsion Laboratory
California Institute of Technology
4800 Oak Grove Drive
Pasadena, California

Gentlemen:

This technical report culminates nearly three years of Mariner/Voyager studies at Boeing. During this time, we have gained an appreciation of the magnitude of the task, and feel confident that the experience, resources and dedication of The Boeing Voyager Team can adequately meet the challenge.

The Voyager management task is accentuated by three prime requirements: An inflexible schedule of launch opportunities; the need for an information-retrieval system capable of reliable high-traffic transmission over interplanetary distances; and a spacecraft design flexible enough to accommodate a number of different mission requirements. We believe the technical approach presented here satisfies these design requirements, and that management techniques developed by Boeing for space programs will assure delivery of operable systems at each critical launch date.

Mr. E. G. Czarnecki has been assigned program management responsibility. His group will be ably assisted by Electro-Optical Systems in the area of spacecraft power, Philco Western Development Laboratories will be responsible for telecommunications, and the Autonetics Division, North American Aviation will provide the auto-pilot and attitude reference system. This team has already demonstrated an excellent working relationship during the execution of the Phase IA contract, and will have my full confidence and support during subsequent phases.

This program will report directly to George H. Stoner, Vice President and Assistant Division Manager for Launch and Space Systems. Mr. Stoner has the authority to assign the resources necessary to meet the objectives as specified by JPL.

The Voyager Spacecraft System represents to us more than a business opportunity or a new product objective. We view it as a chance to extend scientific knowledge of the universe while simultaneously contributing to national prestige and we naturally look forward to the opportunity of sharing in this adventure.

Lysle A. Wood

Lysle A. Wood

CONTENTS

CONTENTS
(Cont.)

CONTENTS
(Cont.)

CONTENTS
(Cont.)

CONTENTS
(Cont.)

CONTENTS
(Cont.)

CONTENTS
(Cont.)

INTRODUCTION

INTRODUCTION

In fulfillment of the Jet Propulsion Laboratory (JPL) Contract 951111, the Aero-Space Division of The Boeing Company submits the Voyager Spacecraft Final Technical Report. The complete report, responsive to the documentation requirements specified in the Statement of Work, consists of the five following documents:

VOLUME	TITLE	BOEING DOCUMENT NUMBER
A	Preferred Design Flight Spacecraft and Hardware Subsystems	D2-82709-1
	Part I	
	Section 1.0 Voyager 1971 Mission Objectives and Design Criteria	
	Section 2.0 Design Characteristics and Restraints	
	Section 3.0 System Level Functional Descriptions of Flight Spacecraft	
	Part II	
	Section 4.0 Functional Description for Spacecraft Hardware Subsystems	
	Part III	
	Section 5.0 Schedule and Implementation Plan	
	Section 6.0 System Reliability Summary	
	Section 7.0 Integrated Test Plan Development	
B	Alternate Designs Considered--Flight Spacecraft and Hardware Subsystems	D2-82709-2
C	Design for Operational Support Equipment	D2-82709-3
D	Design for 1969 Test Spacecraft	D2-82709-4
E	Design for Operational Support Equipment for 1969 Test Flight Spacecraft	D2-82709-5

For convenience the highlights of the above documentation have been summarized to give an overview of the scope and depth of the technical effort and management implementation plans produced during Phase IA. This summary is contained in Volume 0, Program Highlights and Management Philosophy, D2-82709-0. A number of supporting documents are provided to furnish detailed information developed through the course of the contract and to provide substantiating reference material which would not otherwise be readily available to JPL personnel. Additionally, a full scale mockup of the preferred design spacecraft has been assembled. This mockup, shown in Figure 1, has been delivered to JPL. The mockup has been provided with the view that it would be of value to JPL in subsequent Voyager Spacecraft System planning. Mr. William M. Allen, President of The Boeing Company, Mr. Lysle A. Wood, Vice-President and Aero-Space Division General Manager, Mr. George H. Stoner, Vice-President and Assistant Division Manager responsible for Launch and Space Systems activities, and Mr. Edwin G. Czarnecki, Voyager Program Manager, are shown with the mockup.

During the 3-month period covered by Contract 951111, Boeing has:

1) Performed system analysis and trade studies necessary to achieve an optimum or preferred design of the Flight Spacecraft.
2) Determined the requirements and constraints which are imposed upon the Flight Spacecraft by the 1971 mission and by the other systems and elements of the project, including the science payload.
3) Developed functional descriptions for the Flight Spacecraft and for each of its hardware subsystems, excluding the science payload.

Figure 1: Preferred Design Mockup

Left to Right:

William M. Allen
Edwin G. Czarnecki
Lysle A. Wood
George H. Stoner

4) Determined the requirements for the Flight Spacecraft associated Operational Support Equipment (OSE) necessary to accomplish the Voyager 1971 mission.

5) Developed a preliminary design of the OSE.

6) Developed functional descriptions for the OSE.

7) Determined the objectives of a 1969 test flight and the design of the 1969 Test Flight Spacecraft using the Atlas/Centaur Launch Vehicle. An alternate test flight program is presented which utilizes the Saturn 1B/Centaur Launch Vehicle.

8) Deveoped functional descriptions for the Flight Spacecraft Bus, and its hardware subsystems, and OSE for the 1969 test spacecraft.

9) Updated and supplemented the Voyager Implementation Plan originally contained in the response to JPL Request for Proposal 3601.

The Voyager program management Team, shown in Figure 2 is under the direction of Mr. Edwin G. Czarnecki. Mr. Czarnecki is the single executive responsible to JPL and Boeing management for the accomplishment of the Voyager Spacecraft Phase IA, and will direct subsequent phases of the program. He reports directly to Mr. George H. Stoner who has the authority to commit those corporate resources necessary to fulfill JPL's Voyager Spacecraft System objectives.

Although Boeing has a technical management capability in all aspects of the Voyager Program, it is planned to extend this capability in depth through association with companies recognized as specialists in certain fields. Use of team members to strengthen Boeing's capability was considered early during pre-proposal activities. The basic concept

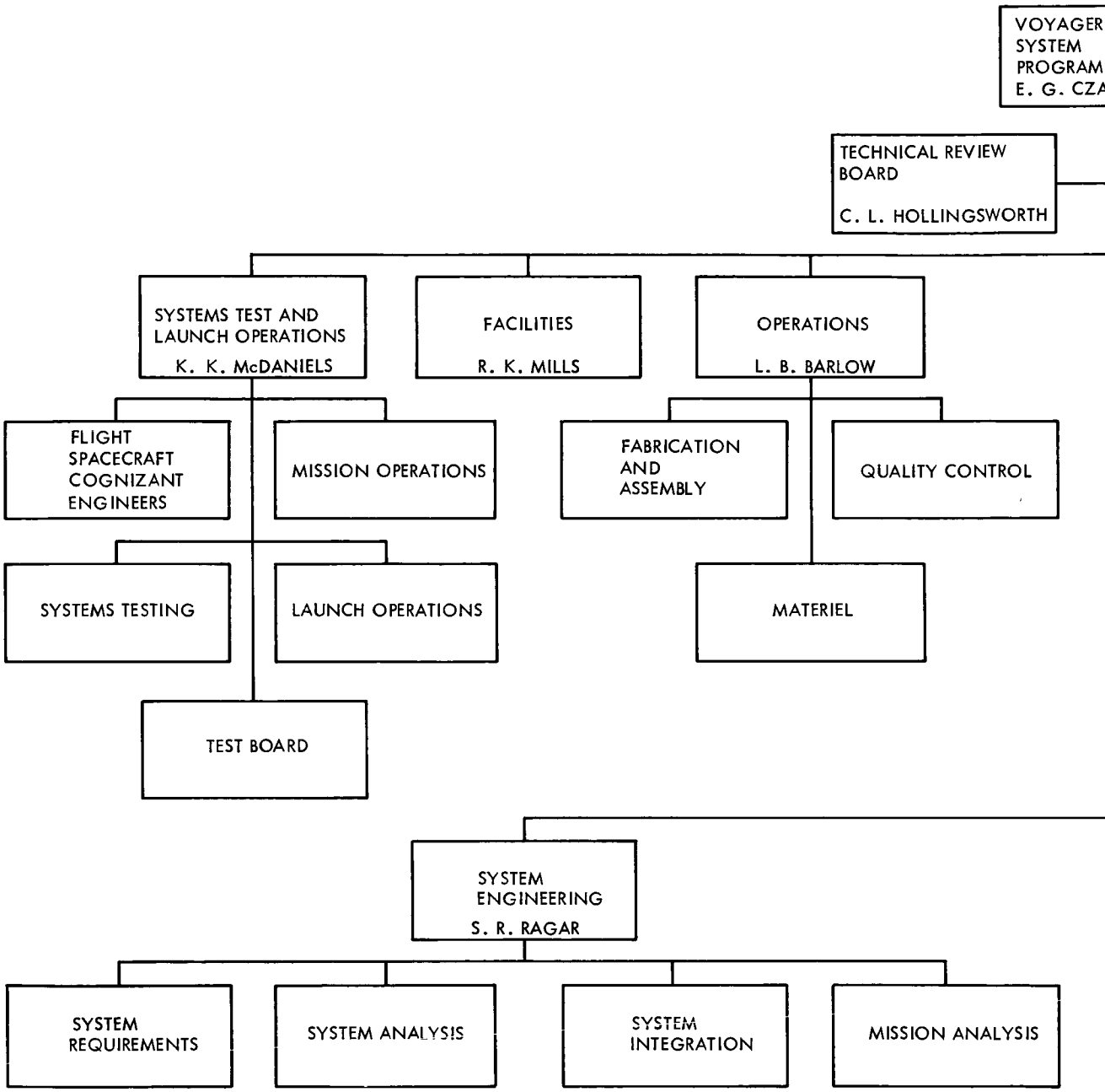
VOYAGER
SYSTEM
PROGRAM
E. G. CZA
TECHNICAL REVIEW
BOARD
C. L. HOLLINGSWORTH
SYSTEMS TEST AND
LAUNCH OPERATIONS
K. K. McDANIELS
FACILITIES
R. K. MILLS
OPERATIONS
L. B. BARLOW
FLIGHT
SPACECRAFT
COGNIZANT
ENGINEERS
MISSION OPERATIONS
FABRICATION
AND
ASSEMBLY
QUALITY CONTROL
SYSTEMS TESTING
LAUNCH OPERATIONS
MATERIEL
TEST BOARD
SYSTEM
ENGINEERING
S. R. RAGAR
SYSTEM
REQUIREMENTS
SYSTEM ANALYSIS
SYSTEM
INTEGRATION
MISSION ANALYSIS

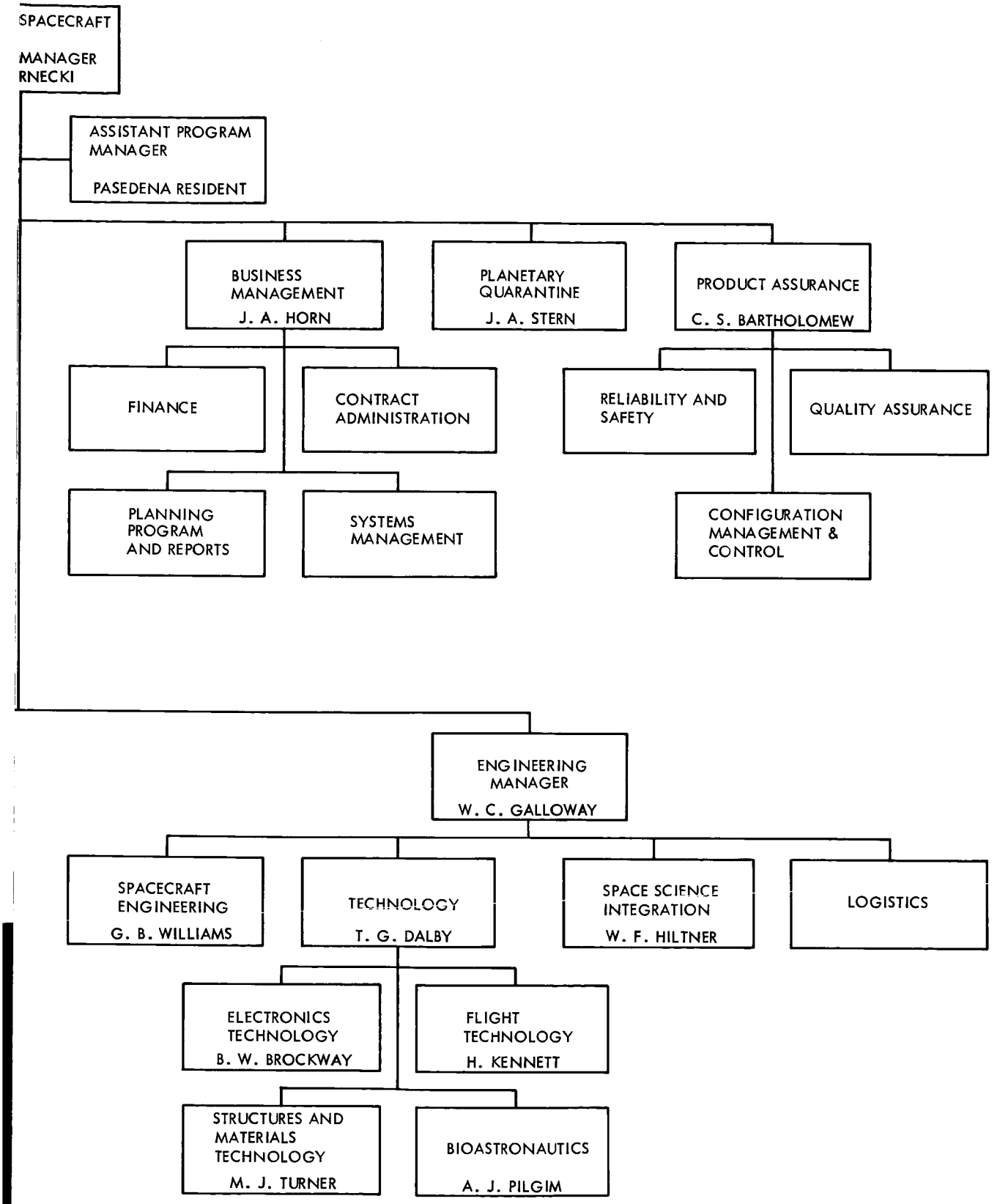

Figure 2 Boeing Voyager
Spacecraft Systems Management Structure

was to add team members who would complement Boeing experience and capability, and significantly improve the amount and quality of technical and management activities. Based upon competitive considerations including experience and past performance and giving strongest emphasis to technical qualifications and management willingness to support the Voyager effort, Autonetics, Philco Western Deveopment Laboratories, and Electro-Optics Systems were chosen as team members. This team arrangement, subject to JPL approval, is shown in Figure 3. The flight spacecraft design and integration task to be accomplished by this team is illustrated in Figure 4. Discussions leading to the formation of this team were initiated late in 1964, formal work statement agreements have been arrived at, and there has been a continuous and complete free exchange of information and documentation; permitting the Boeing team to satisfy JPL's requirements in depth and with confidence.

BOEING VOYAGER TEAM VOYAGER SPACECRAFT AND SPACE SCIENCES PAYLOAD INTEGRATION CONTRACTOR The Boeing Company Seattle, Washington Mr. E. G. Czarnecki - Program Manager		
SUBCONTRACTOR Autonetics, North American Aviation Anaheim, California Autopilot and Attitude Reference Subsystem Mr. R. R. Mueller Program Manager	SUBCONTRACTOR Philco, Western Development Laboratories Palo Alto, California Telecommunications Subsystem Mr. G. C. Moore Program Manager	SUBCONTRACTOR Electro-Optical Systems Incorporated Pasadena, California Electrical Power Subsystem Mr. C. I. Cummings Program Manager

Figure 3

SUMMARY--VOLUME A

The Boeing team's flight spacecraft represents a conservative design based upon selection of space-proven components. The design meets the objectives of the Voyager program for 1969 through 1977 opportunities. The 250-pound science payload, as well as the 2300 or 4500 pound flight capsule can be accommodated and all program and mission objectives achieved.

The Voyager Spacecraft is shown in Figure 4 with equipment deployed in the operational configuration. It is 30 feet wide from solar panel tip to solar panel tip, and the body is 59-inches high. The 31-foot magnetometer boom and 17- and 18-foot antenna booms are shown in position. Estimated weight at this state of the preliminary design is 1565 pounds for the spacecraft, and 3400 pounds for the propulsion module. A contingency of 285 pounds of the specification weight of 5250 pounds is available for selective use during the detail design phase. The 20 equipment modules are fastened to the central magnesium shell with cooling provided by thermal radiation from the external faces of the package. Thermal control is by space-facing louvers.

Outstanding design features of the Boeing team's Voyager Spacecraft are its ability to perform reliably, transmit data to Earth at encounter at the 50,000 bit-per-second rate generated in the science package, and meet all mission energy requirements through 1977 with a single propulsion module design. Use of redundancy in critical components and selection of proven designs requiring a minimum of additional development

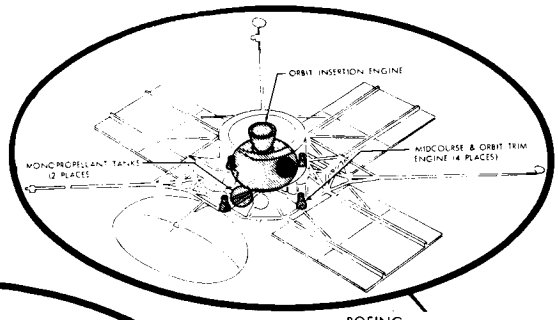

BOEING
PROPULSION SUBSYSTEM

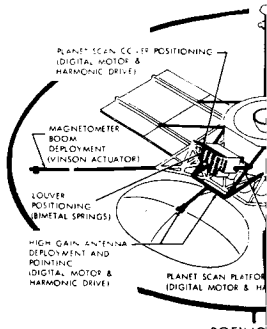

BOEING
MECHAN

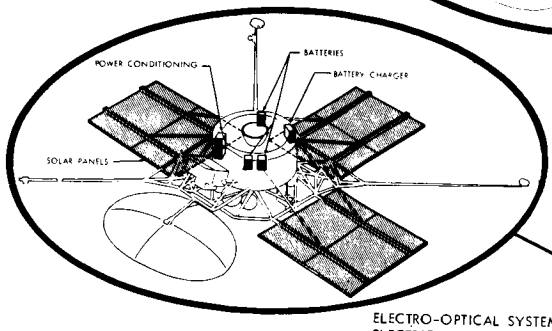

ELECTRO-OPTICAL SYSTEMS
ELECTRICAL POWER SUBSYSTEM

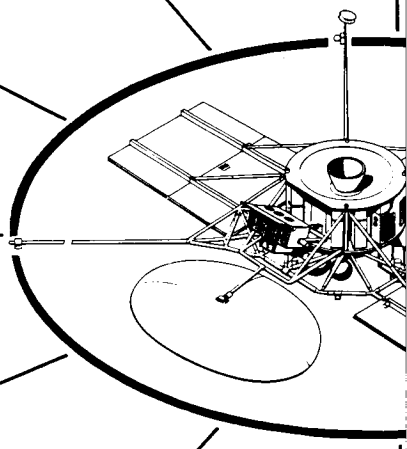

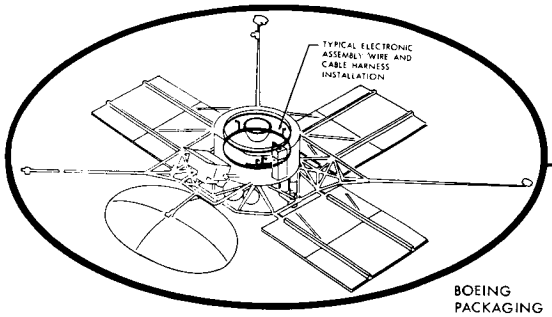

BOEING
PACKAGING & CABLING

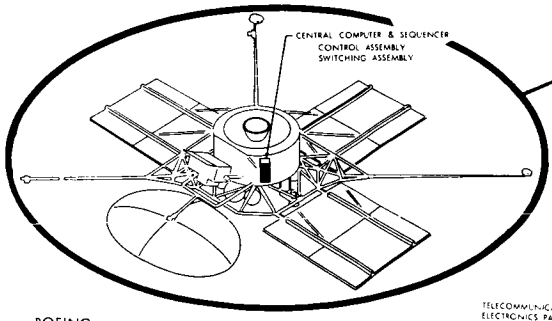

BOEING
CENTRAL COMPUTER & SEQUENCER SUBSYSTEM

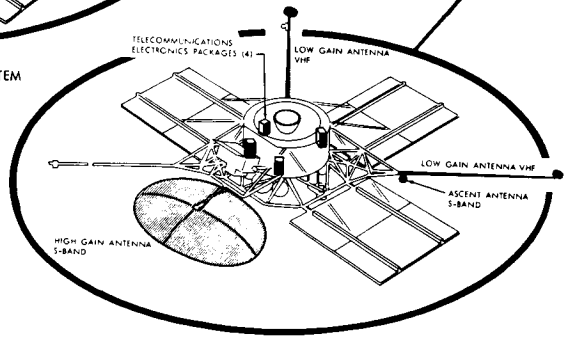

PHILCO
TELECOMMUNICATIONS SUBSYSTEM

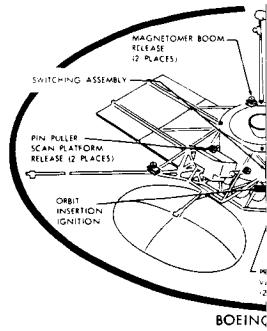

BOEING
PYROTE

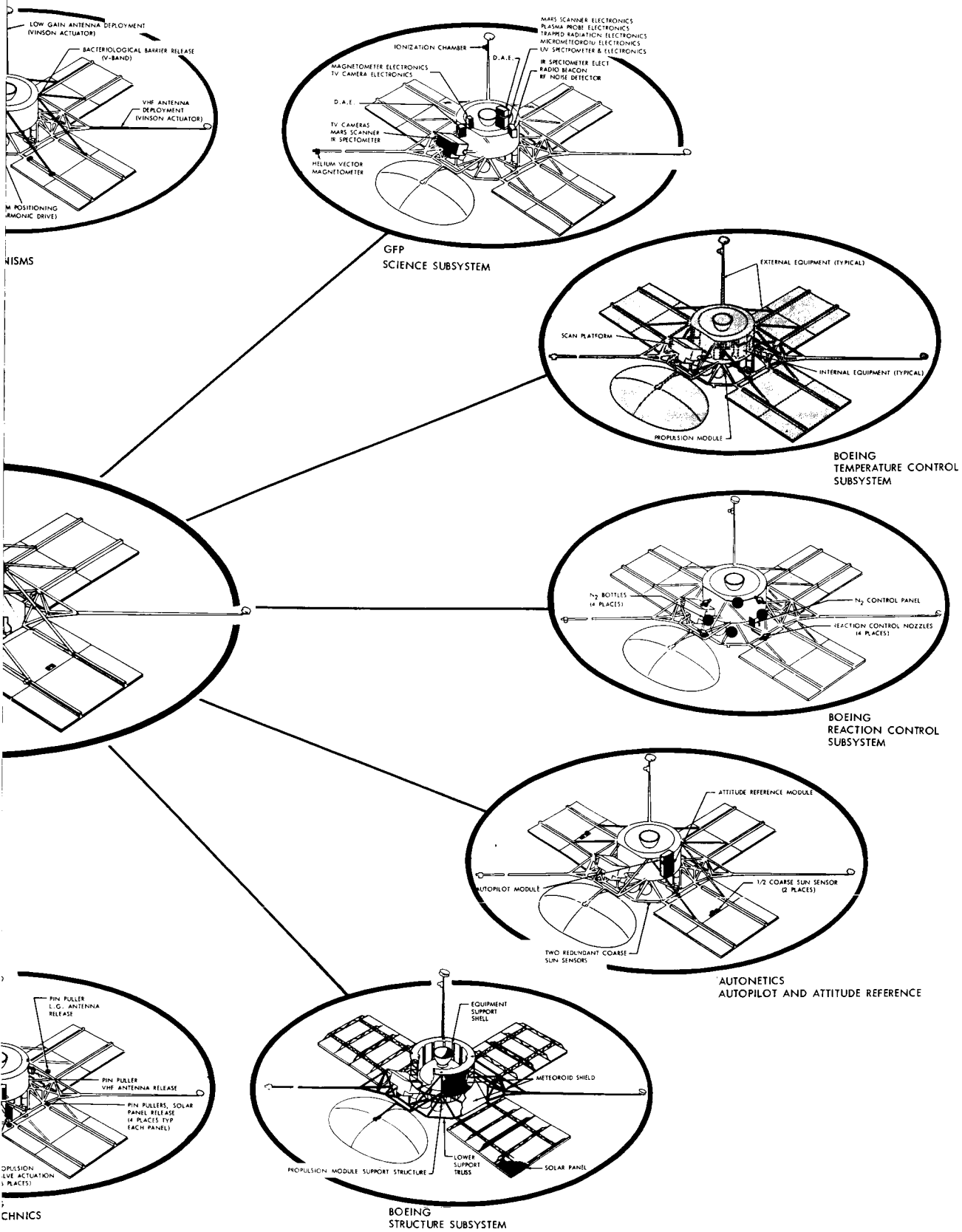

Figure 4. Voyager Flight Spacecraft Subsystem Integration

resulted in an overall mission success probability of 47 percent, exceeding the specified 45 percent, including an allocation of 0.674 for the science payload.

The spacecraft can enter biologically safe orbits with periods as low as 18 hours from Mars approach velocities as high as 3.5 km/sec., or with periods less than 9 hours from approach velocities as high as 3.0 km/sec. The 18-hour orbit provides coverage of four different swaths of Mars surface in the first three days after encounter.

In 1971, orbits are available which have no occultation of Canopus or the Sun for the first 60 days in orbit. The periapsis positions are at southern latitudes and at illumination angles which favor the black and white TV experiment. Some adjustment of periapsis position is available with "off-periapsis" orbit insertion techniques. The "off-periapsis" insertion technique allows the utilization of the fixed-total-impulse solid motor for all approach velocities considered.

The telecommunications design includes completely redundant radio subsystems. It features an 8' x 12' paraboloidal high-gain antenna, two 50-watt traveling wave tubes and bi-orthogonal block coding to obtain the high data rate. The 50-watt tube selection is supported by three separate tube designs including test data. Detailed link calculations substantiate a positive communication link margin under worst-case conditions at Mars encounter, with a calculated 48,000 bits per second data rate. (Upon definition of the precise science payload data rate, the telecommunications link can be optimized to that value.) For

longer communication ranges, alternate lower data modes and two tape recorders with storage capability for 2×10^8 bits of scientific data are provided. Two 72,000 bit buffers provide temporary storage of spacecraft engineering and capsule data.

The spacecraft propulsion subsystem consists of a solid motor with an oblate spheroidal case for Mars orbit insertion and four 50-pound thrust, jet vane controlled, hydrazine engines operating in pairs for midcourse and orbit trim. The solid propellant motor with a specific impulse of about 300 pounds force seconds per pound mass delivers 10,500 pounds maximum thrust and burns regressively to provide not more than 2.2 g's acceleration. Solid motor TVC is by a Freon secondary injection system. With the available 2306 pounds of solid propellant, an orbit insertion velocity increment of 5700 feet per second is attained. The 50-pound thrust monopropellant engines with a specific impulse of 235 pound force seconds per pound mass have multiple restarting capability. These engines utilize the spontaneous decomposition catalyst. Hydrazine fuel capacity is adequate for 929 total seconds of operation.

Reaction control is produced by expulsion of sterile nitrogen through two redundant sets of eight .25 pound thrusters each, which are body-mounted on the spacecraft. Four titanium tanks contain 60 pounds of cold nitrogen for reaction control and propulsion requirement. The 45 pounds allocated to reaction control is adequate for the 6-month orbital mission with a safety factor of 2. Under nominal conditions, the nitrogen supply is adequate for four years. Both propulsion systems, plus the reaction control subsystem, are assembled in a single sub-module mounted

in the spacecraft. This modular arrangement permits complete assembly and checkout, including sterilization, prior to installation on the spacecraft. The propulsion and reaction control systems including all fuel and gas supplies are sterilized to avoid planetary contamination by propulsion ejecta.

The selected attitude reference and autopilot subsystems are comprised of an attitude reference module, autopilot module, and coarse and fine Sun sensors. The attitude reference module includes three redundant Autonetics G-10 gas-bearing gyros, two redundant accelerometers, two redundant Canopus sensors and two fine Sun sensors. The coars Sun sensors are located on two solar panels. The autopilot is an analog type and maintains spacecraft orientation to within $\pm$0.4 degree in cruise, $\pm$0.2 degree in Mars orbit, and the limit cycle period is several hours. All selected components are existing designs with operation and qualification experience.

The electrical power system is similar to Mariner IV, with three solar panels, 8-1/2' x 13', consisting of two sections each. The total area of 236 square feet provides 627 watts of power at the distance of Mars from the Sun. A flat solar cell arrangement is used; three silver cadmium batteries are provided for use during off-Sun periods. The power subsystem regulates and distributes the electrical power to subsystems where additional power conditioning is performed. A 50-percent increase in power is possible by addition of one section to each solar panel.

The Voyager central computer and sequencer (CC&S) provides timing functions and command signals to all other spacecraft subsystems. A magnetic core memory provides storage for 256 21-bit words and a capability to execute 333 different commands. The CC&S minimizes the need for detail ground commands by incorporating preplanned operational sequences. All commands and stored instructions can be monitored and controlled from the ground for complete analysis and control during the entire mission. A modified NASA Lunar Orbiter programmer has been selected as the basic element. This memory-oriented digital computer has been space-qualified and addition of redundant data processing and switching circuits provide a highly reliable unit.

The spacecraft structure includes a simple truss base, 10 feet wide at the bottom and 5 feet wide at the top, fabricated of 6AL4V titanium tubing. This base attaches to the Centaur adapter and supports the antenna and solar panel appendages. The electronic packages are connected to a five-foot diameter, cylindrical, magnesium shell installed above the truss. The flight capsule is supported by an adapter ring with loads carried by four columns through the cylindrical shell.

A number of major technical problems were encountered and studied in developing the preliminary design. The most significant of these were as follows:

1) The assessment of the most reliable and highest power transmitter tube meeting the Voyager requirements;

2) The overall spacecraft magnetics problem with particular attention to the magnetic focusing field for the traveling wave tube.

3) Availability and reliability of spacecraft recorders.

4) Selection of a reliable secondary battery with adequate recycle life.

5) Estimation of solar panel degradation from electromagnetic radiation and meteoroids during the mission.

6) The trade-off between proven instruments versus new and inherently simpler instruments.

7) Determination of the degree and type of redundancy, for example, using two identical instruments of two difference designs.

8) The effect of the solid engine exhaust on the structure and solar panel temperature.

9) Accommodating the length of the orbit insertion engine.

10) Selection of installation technique for the equipment packages.

11) Selection of the thrust vector control technique.

12) Effect of heat soak sterilization on equipment.

These problems are the key technical considerations in developing the preferred design.

The subsystems of the Boeing team's spacecraft provide a conservative and highly reliable design. No state-of-the-art advances are required to meet the design criteria for any subsystem.

CONTENTS

4.0 SUBSYSTEM LEVEL FUNCTIONAL DESCRIPTIONS

The subsystems incorporated in the preferred design of the Voyager Spacecraft are described in this section. The description of telecommunications covers details of the chosen system and the link analysis as requested by JPL. Description of the electrical power subsystem includes consideration of solar panel structure as well as electrical characteristics of the panels, of batteries, and of power conditioning equipment. The discussion of the spacecraft propulsion subsystem covers engines for midcourse correction, orbit insertion (including thrust vector control), and orbit trim. Treatment of engineering mechanics includes a description of thermal control methods and equipment, of equipment packaging, mounting and cabling, of the spacecraft structure, of actuating mechanisms, and of the pyrotechnic subsystem. (Since firing of pyrotechnics is controlled by the CC&S, part of the discussion appears in that section.) Weight, center of gravity location, and moments and products of inertia are also covered in this discussion. A brief treatment of general characteristics of a typical spacecraft science subsystem is included in order to examine the impact of this subsystem on the rest of the spacecraft. The attitude reference and autopilot subsystem is described in terms of its modes of operation and the hardware selected; the associated reaction control subsystem is similarly described. Finally, the central computer and sequencer, which includes both data processing and power switching circuitry, is described.

4.1 TELECOMMUNICATIONS

4.1.1 Summary

The primary purpose of the Voyager telecommunications system is to return to Earth the maximum possible amount of scientific data within the constraints of vehicle size and weight, and subsystem performance and reliability. The communication system selected for Voyager is a fully redundant conventional S-band system using a 50-watt traveling wave tube (TWT) and an 8' x 12' paraboloidal high-gain antenna. This, coupled with the 210 foot ground antenna, allows real time transmission of high-rate scientific data (48,000 bits/sec) for approximately 2 months after encounter in the nominal case.

Two tape recorders allow storage of 2×10^8 bits for those periods when Earth transmission is prevented by occultation, or when link margins will not support high-rate transmission.

Exceptional system versatility is supplied by the wide variety of operational modes available. A low-noise tunnel diode preamplifier in the radio subsystem allows reception of ground commands through the omnidirectional low-gain antenna for up to 2 months after encounter, thus allowing for corrective action when the link through the high-gain antenna is not operational for any reason.

Major elements of the system and their functional interrelations are illustrated in Figure 4.1-1. The design features that provide a significant improvement in performance over current deep space systems are:

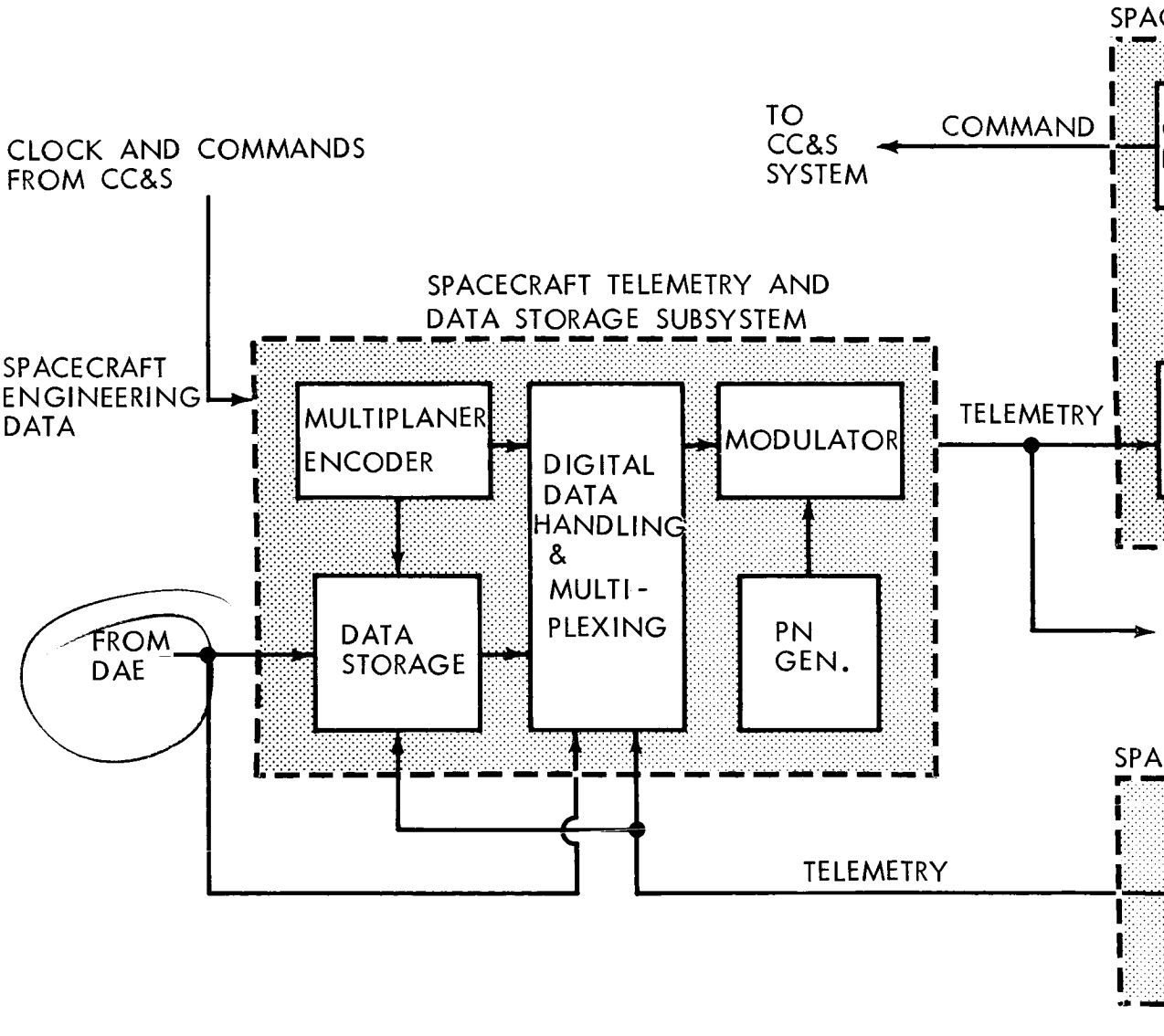
SPA
TO
CC&S
SYSTEM
COMMAND
CLOCK AND COMMANDS
FROM CC&S
SPACECRAFT TELEMETRY AND
DATA STORAGE SUBSYSTEM
SPACECRAFT
ENGINEERING
DATA
MULTIPLANER
ENCODER
DIGITAL
DATA
HANDLING
&
MULTI-
PLEXING
MODULATOR
TELEMETRY
FROM
DAE
DATA
STORAGE
PN
GEN.
SPA
TELEMETRY

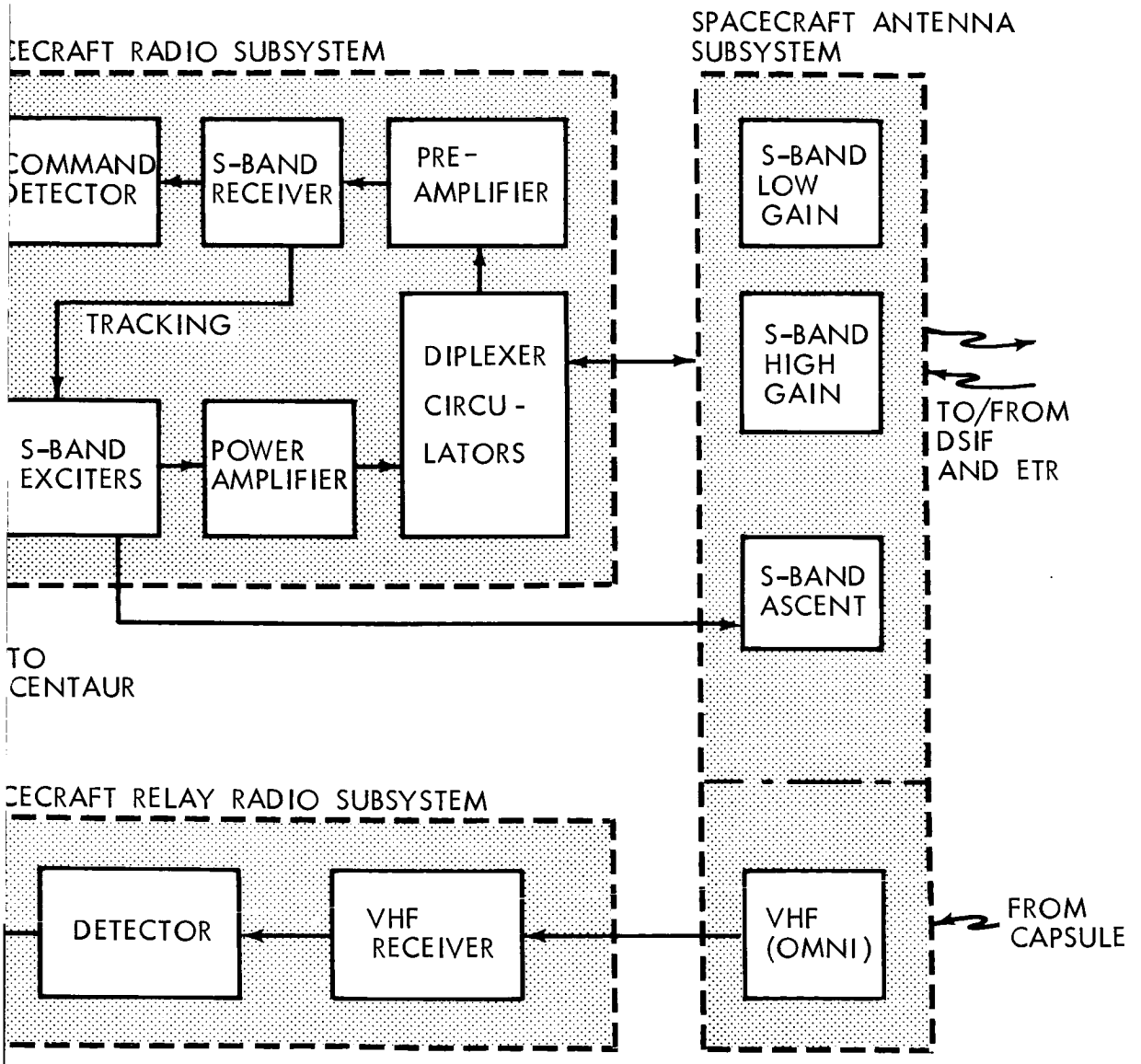

Figure 4.1-1: Spacecraft Telecommunication Functional Grouping

1) A 50-Watt Power Amplifier -- Traveling wave tube amplifiers operating at this power level can be through the engineering prototype stage by July 1966. The TWT has been selected for Voyager because of its advanced development and history of reliable performance.

2) An 8 by 12 foot Paraboloidal High-Gain Antenna Providing 34.3 Decibel Gain -- This antenna is the maximum size, rigid, nonsegmented antenna that will fit within the vehicle shroud and be compatible with the Boeing-designed spacecraft. This antenna is gimbaled about two axes and pointed to an accuracy of ± 0.6 degree total error in each axis to minimize pointing losses. Careful study of servo design, installation, and vehicle attitude stabilization indicates that this accuracy can be achieved.

3) Biorthogonal Block Coding of the Digital Data Stream -- A 16, 5 code provides the equivalent of 2 decibel in link gain without degradation of the specified bit error rate ($P_e^b = 5 \times 10^{-3}$).

The combination of the above features, together with utilization of the 210-foot receiving antennas being developed for the deep space stations, results in a system that can provide a 48,000-bit-per-second data rate at Mars encounter. Assuming an encounter date of December 23, 1971, a positive margin will exist at this data rate for encounter plus 73 days under nominal performance and for encounter plus 10 days at worst-case conditions.

Two high-capacity tape recorders (10^8 bits each) are provided for back-up of the real time mode and for storage and delayed playback of planetary science data. Two 72,000-bit-core buffers are provided for temporary storage of spacecraft engineering and capsule data as required during maneuvers and periods of occultation.

Two subcarriers are used for simultaneous transmission of low- and high-rate data. Engineering , capsule, and cruise science are all multiplexed (without biorthogonal coding) on to a lower subcarrier. Planetary science is coded and modulates a higher subcarrier.

Other features of interest are:

1) Incorporation of a low-noise preamplifier into one receiver channel. This provides a command reception capability on the low-gain antenna for as long as 2 months beyond encounter under nominal conditions and 6 months beyond encounter if the 100-kw, ground transmitter is used.

2) Incorporation of a 5-bit-per-second emergency telemetry mode provides engineering data for as long as 3 months beyond encounter, if communication via the high-gain antenna is lost for any reason.

3) Use of a 1-watt solid-state exciter, operating through a low-gain ascent antenna for the first 24 hours after launch, permits delaying activation of the high-level power amplifier until outgassing is completed.

The following items require development work that can be completed by July, 1966.

1) 50-Watt TWT -- At least one manufacturer has operated existing tubes at 50-watt power levels. (Watkins-Johnson Proposal for 50 Watt TWTA, File No. 65P-3106.) An industry survey indicates that an engineering model of a tube optimized for long-life space operation can be delivered within 6 months after the Phase IB go-ahead with production prototypes available 6 months later.

2) Preamplifiers -- A tunnel diode preamplifier for space application has been developed (Microstate Electronics Corporation, Proposal on Low Noise Preamplifier P1-85-A), but initial models exhibited a high degree of temperature sensitivity. Development is continuing and this device should be available in final form in early 1966.

3) Tape Recorders -- Space qualified tape recorders are currently available but do not have the desired 10^8 bit capacity. Preliminary development work has been carried out or is underway by at least three companies -- Kinelogic, Raymond Engineering, and Ampex. The use of electronic switching of the record/playback heads requires close alignment and control of magnetic tape tolerances. Further development will be required before space qualification can be assured. For this reason, completion of development of a prototype moded will require approximately 6 months after Phase IB go-ahead.

The preferred design configuration has an 84.16-percent probability of full functional capability for a 5880-hour mission duration. The preferred configuration incorporates redundant command receivers, command detectors, ranging units, exciters, power amplifiers, and planetary science tape recorders. Subcomponent redundancy is provided in the analog multiplexer to ensure highest reliability in the engineering data channel. The reliability estimate is based on standard ground rules defined in the "Voyager '71 Program Reliability Analysis and Prediction Standards" Boeing Document D2-23834-1, Revision A. A detailed block diagram of the preferred telecommunication system is shown in Figure 4.1-3. A summary of system performance parameters is presented in Figure 4.1-2.

Section 4.1.2 provides a functional description of the Voyager telecommunication system spacecraft and ground elements. Section 4.1.3 contains a detailed description of each of the four subsystems comprising the Voyager spacecraft telecommunication system. Section 4.1.4 is the detailed link analysis developed in accordance with the JPL Telecommunications Design Control Tables. Section 4.1.5 contains a summary of the telecommunication system reliability analysis.

SPACECRAFT TELEMETRY AND DATA STORAGE SUBSYSTEM

Mode	Mission Phase	Type of Data and Rate	Data Rates	Modulation	Nominal Mod. Index	Subcarrier Frequencies	Bit Error Rate
1	Launch Acquisition Cruise Maneuvers	Engr. at 11 1/9 Capsule at 11 1/9	22 2/9 bps	Dual Ch. Coherent PSK/PM	Sync: +0.35 rad Data: ±1.28 rad	200 cps 400 cps	$5x10^{-3}$
2	Cruise	Engr. at 11 1/9 Capsule at 11 1/9 Science at 111 1/9	133 1/3 bps	Single Channel Coherent PSK/PM	±1.40 rad	533 1/3 cps	$5x10^{-3}$
3	Post - Maneuver Option	Engr. at 11 1/9 Capsule at 11 1/9 Stored Engr. at 111 1/9	133 1/3 bps	Single Channel Coherent PSK/PM	±1.40 rad	533 1/3 cps	$5x10^{-3}$
4	Emergency Cruise or Encounter	Engr. at 5 5/9	5 5/9 bps	Dual Channel Coherent PSK/PM	Sync: ±0.70 rad Data: ±1.30 rad	50 cps 100 cps	$1x10^{-2}$
5A	Primary Encounter & Orbital	Engr. at 66 2/3 Science at 166 2/3 Capsule at 166 2/3	Telemetry Ch. 400 bps Planetary Ch. 8000 bps	PSK/PM Coded PSK/PM	±0.56 rad ±1.44 rad	1.6 kc 102.4 kc	$5x10^{-3}$
5B	Optional Late Orbital	Engr. at 66 2/3 Science at 166 2/3 Capsule at 166 2/3	Telemetry Ch. 400 bps Planetary Ch. 4000 bps	PSK/PM Coded PSK/PM	±0.73 rad ±1.40 rad	1.6 kc 102.4 kc	$5x10^{-3}$
5C	Optional Late Orbital	Engr. at 66 2/3 Science at 166 2/3 Capsule at 166 2/3	Telemetry Ch. 400 bps Planetary Ch. 2000 bps	PSK/PM Coded PSK/PM	±0.85 rad ±1.28 rad	1.6 kc 102.4 kc	$5x10^{-3}$
6	Optional Encounter & Orbital	Engr. at 66 2/3 Science at 166 2/3 Capsule at 166 2/3	Telemetry Ch. 400 bps Planetray Ch. 48,000 bps	PSK/PM Coded PSK/PM	±0.50 rad ±1.50 rad	9.6 kc 614.4 kc	$5x10^{-3}$

DATA	TYPE OF STOAGE	INPUT RATE	CAPACITY	STORAGE PERIOD	OUTPUT RATE
Planetary	Tape Recorder	50,000 bps	10^8 bits	36 minutes	8000/4000/2000 bps
Engineering	Core	11 1/9 bps	$7.2x10^4$ bits	1.8 hours	111 1/9 bps
Capsule	Core	10/100 bps	$7.2x10^4$ bits	2 hours/12 minutes	11 1/9/166 2/3 bps

SPACECRAFT RADIO SUBSYSTEM

UNIFIED S-BAND (221/240); TRACKING, COMMAND, AND TELEMETRY

- Receive - 2115 ± 5 Mc
- Noise Temperature - 704°K
- Command Channel:
  - Modulation - Single Channel Coherent PSK/PM
  - Bit Rate - 1 bit/second
- Transmit - 2295 ± 5 Mc
- Low-Power Mode -- 1 watt
- High-Power Mode -- 50 watts

SPACECRAFT ANTENNA SUBSYSTEM

Antenna	Frequency	Type	Polarization	Gain
Ascent	2295 Mc	Bi-Conical Horn Pyramidal Horn	Circular Linear	0 db
Relay	100 Mc	Dipole Array	Linear	+5 db
Low Gain	2115/2295 Mc	Bi-Conical Horn	Circular	+1 db
High Gain	2115/2295 Mc	8' x 12' Parabolic Dish	Circular	+34.3 db

SPACECRAFT RELAY RADIO SUBSYSTEM

Frequency:	100 Mc Nominal
Modulation:	PCM/PSK/FM
Noise Figure:	4 db
Data Rates:	10/100 bps

WEIGHT/POWER

Radio Subsystem:	87.0 lbs	169.4 watts
Telemetry and Data Storage Subsystem	58.0 lbs	31.0 watts
Relay Radio Subsystem	7.5 lbs	5.2 watts
Antenna Subsystem	54.3 lbs	6.0 watts
TOTAL	206.8 lbs	211.6 watts

Figure 4.1-2: Typical Voyager Deep Space Station

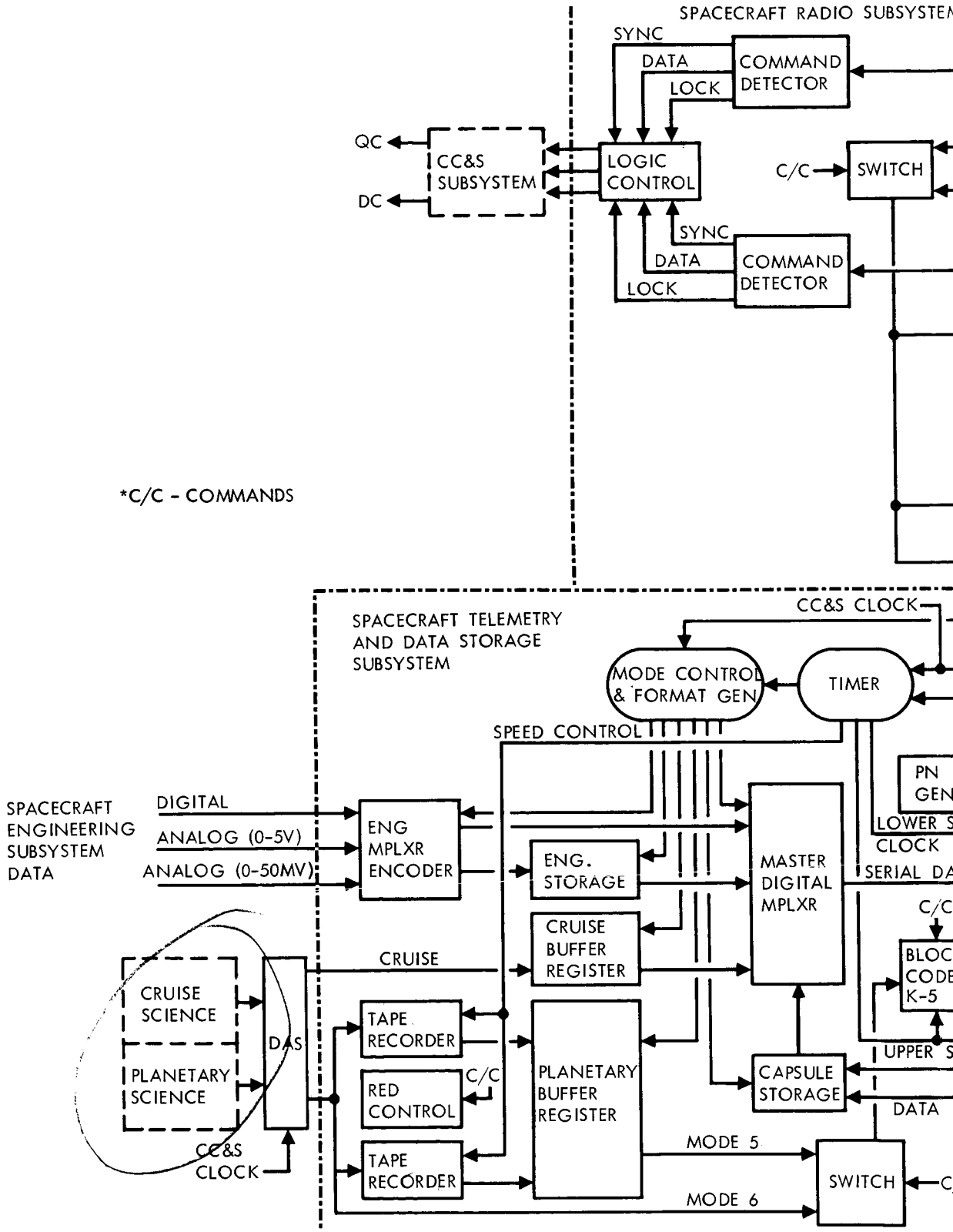
SPACECRAFT RADIO SUBSYSTEM
SYNC
DATA
LOCK
COMMAND DETECTOR
QC
DC
CC&S SUBSYSTEM
LOGIC CONTROL
C/C
SWITCH
SYNC
DATA
LOCK
COMMAND DETECTOR
*C/C - COMMANDS
SPACECRAFT TELEMETRY AND DATA STORAGE SUBSYSTEM
CC&S CLOCK
MODE CONTROL & FORMAT GEN
TIMER
SPEED CONTROL
PN GEN
LOWER S
CLOCK
SERIAL DA
SPACECRAFT ENGINEERING SUBSYSTEM DATA
DIGITAL
ANALOG (0-5V)
ANALOG (0-50MV)
ENG MPLXR ENCODER
ENG. STORAGE
MASTER DIGITAL MPLXR
C/C
BLOC CODE K-5
CRUISE BUFFER REGISTER
CRUISE
CRUISE SCIENCE
PLANETARY SCIENCE
DAS
TAPE RECORDER
RED CONTROL
C/C
PLANETARY BUFFER REGISTER
CAPSULE STORAGE
UPPER S
DATA
CC&S CLOCK
TAPE RECORDER
MODE 5
MODE 6
SWITCH
C

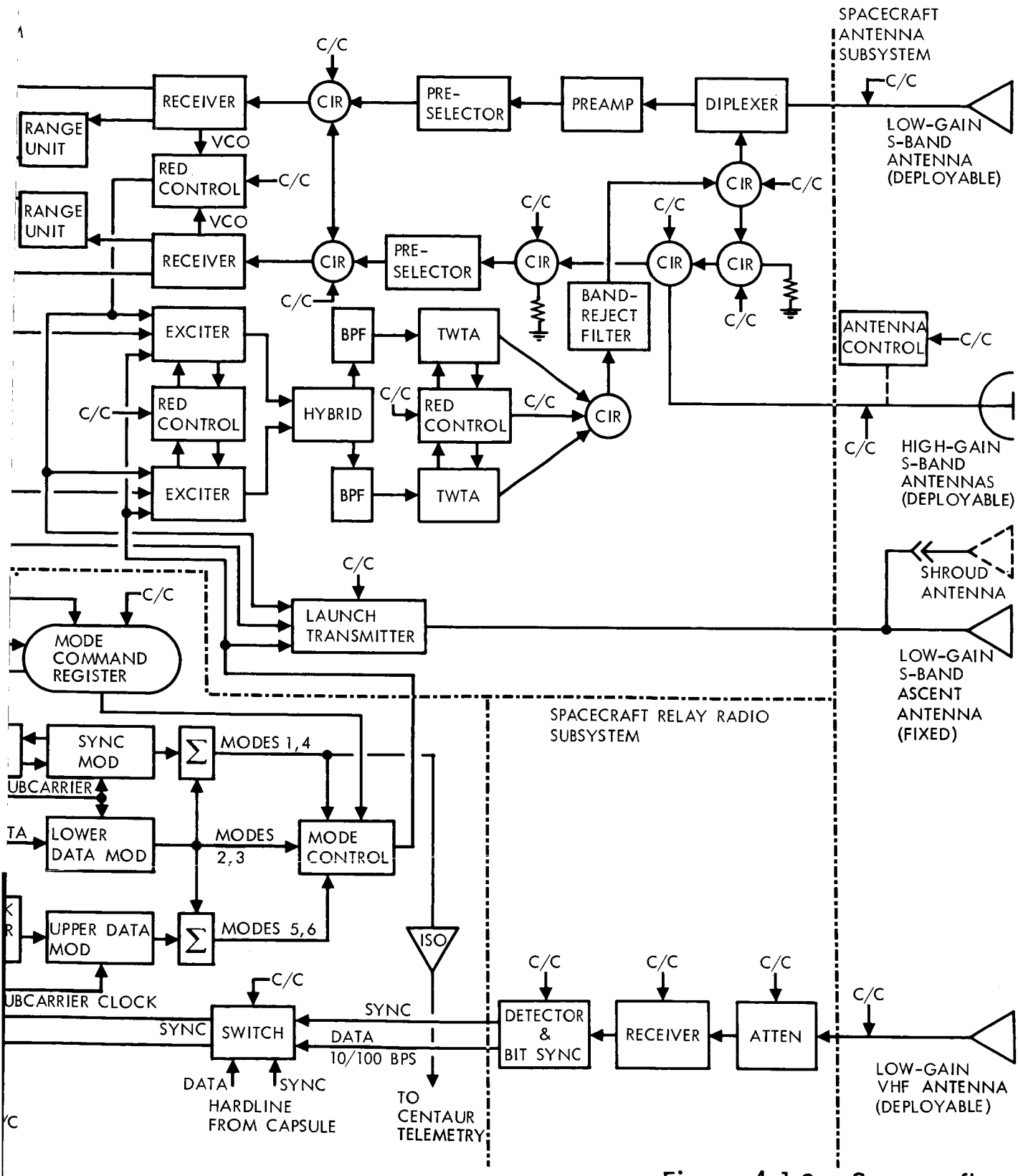

Figure 4.1-3: Spacecraft Telecommunication Subsystem

4.1.2 Telecommunications System--Spacecraft and Ground Elements

4.1.2.1 Scope

This functional description covers the overall functional requirements for the 1971 Voyager telecommunication system including the ground and spacecraft functions required for relaying capsule data and for tracking, telemetering, and commanding of the spacecraft. The telecommunications subsystem is designed to perform the functions highlighted on the accompanying mission sequences matrix.

4.1.2.2 Applicable Documentation

The following documents were the basis for determining the functional descriptions of the telecommunication system and its subsystems.

The Deep Space Network, JPL Engineering Planning Document 283

Telecommunication Development GSDS Ground Command System, JPL Specification GMG-50109-DSN-A

Voyager 1971 Program Reliability Analysis and Prediction Standards, Boeing Document D2-23834-1 Rev. A, dated 26 April 1965

Mars Mission Communication Analysis, Philco Report WDL-TR-2531

Environmental Test Specification, R.F. Interference Control for Spacecraft and Ground Control Equipment, JPL specification Number 30236A

Spacecraft Telecommunication System MC-4-310-A, Mariner C Functional Specification

Mars Mission Antenna Studies, Boeing Document D2-82731-1

Lunar Orbiter Low-Gain Antenna Development, Boeing Document D2-36355-1

R. W. Hartop, Power Loss Between Arbitrarily Polarized Antennas, JPL Technical Report No. 32-457, September 1, 1964

Voyager Design Study, Part II, Volume III, Subsystem Design, GE, MSVD Document No. 635D801, 15 October 1963; pp 1-189, 1-203

	1.0 PRELAUNCH AT ETR	2.0 LAUNCH & INJECTION (INCLUDES COUNTDOWN)
GROUND COMPLEX (MOS, LOS, & DSN)	OPERATIONAL READINESS TEST, S/C-DSN COMPATIBILITY TEST SCHED & COORD ETR ACTIVITIES C/O & SUPPORT MOS (DSN ONLY) LOAD CC&S WITH FLIGHT PROGRAM	MOS/LOS A) COMMAND LIFTOFF B) TRACK VEHICLE DURING BOOST C) SUPPLY FLIGHT COMMANDS (AS REQ) D) RECEIVE & ANALYZE DATA FROM S/C & BOOSTER E) STANDBY ON ALERT F) COMMUNICATE WITH ETR CHANGE FROM MOS/LOS ON INJECTION INTO TRA A) PROVIDE SFOF/DS IF DSN SEARCH DATA B) RECEIVE ANTENNA SI C) SEARCH FOR & ACQU D) ESTABLISH & VERIFY E) TRACK S/C (1-WAY) F) RECEIVE & ANALYZE
SPACECRAFT TELECOMMUNICATIONS	SUBSYSTEM C/O & STATUS MONITORING	A) TRANSMIT ENGINEERING DATA VIA CENTAUR TELEMETRY B) TRANSMIT ENGINEERING DATA VIA LOW POWER LAUNCH EXCITER C) RECEIVE POWER FROM F/P
CENTRAL COMPUTER & SEQUENCER (CC&S)	A) SUBSYSTEM C/O & STATUS B) COMMAND OTHER SUBSYSTEMS FOR C/O & STATUS MONITORING C) READY ALL SUBSYSTEMS FOR LAUNCH D) LOAD CC&S WITH FLIGHT PROGRAM	PROVIDE BACKUP COMMANDS AS REQUIRED
ATTITUDE REFERENCE SUBSYSTEM AUTOPILOT SUBSYSTEM REACTION CONTROL SUBSYSTEM (RCS)	SUBSYSTEM C/O & STATUS MONITORING	A) ATTITUDE REFERENCE — GYROS OFF DURING LAUNCH B) AUTOPILOT — OFF C) RCS — OFF
MIDCOURSE CORRECTION PROPULSION SYSTEM ORBIT INJECTION PROPULSION SYSTEM	SUBSYSTEM C/O & STATUS MONITORING	
ELECTRICAL POWER SUBSYSTEM	SUBSYSTEM C/O & STATUS MONITORING	A) PROVIDE ENGRG DATA FOR TELECOMUNICATIONS SUBSYSTEM B) PROVIDE BATTERY POWER TO: • TELECOMMUNICATIONS SUBSYSTEM • CC&S • ATTITUDE REFERENCE SUBSYSTEM • AUTOPILOT SUBSYSTEM
S/C STRUCTURE SUBSYSTEM S/C MECHANISMS SUBSYSTEM INSTALLATION CABLES & TUBING	SUBSYSTEM C/O & STATUS MONITORING	A) PROVIDE PHYSICAL SUPPORT FOR ALL EQUIPMENT B) PROVIDE ATTACHMENT FOR CAPSULE C) SUPPORT FLT CAPSULE
TEMPERATURE CONTROL SUBSYSTEM	SUBSYSTEM C/O & STATUS MONITORING SPACECRAFT COOLING SUPPLIED BY CENTAUR	A) PROVIDE HEAT SINK COOLING CAPABILITY UP TO SHROUD JETTISON B) TEMPERATURE CONTROL AFTER SHROUD JETTISON
PYROTECHNIC SUBSYSTEM	SUBSYSTEM C/O & STATUS MONITORING	
SCIENCE EXPERIMENTS (GFE)	SUBSYSTEM C/O & STATUS MONITORING S/C MAGNETIC MAPPING (FAT)	
DATA AUTOMATION EQUIPMENT (GFE)		

REPEAT UP TO FO

3.0 ACQUISITION

4.0 INTERPLANETARY CRUISE

TO DSN CONTROL ISMARS ORBIT WITH ANTENNA ARCH DATA IRE S/C CONTROL OF S/C :NGRG DATA	DSN A) MONITOR BOOSTER SEPARATION B) MONITOR SOLAR PANEL DEPLOYMENT C) MONITOR ANTENNA DEPLOYMENT D) PROVIDE COMMANDS TO BACK UP CC&S AS REQUIRED E) TRACK S/C F) REC DATA G) MONITOR SCIENCE DEPLOYMENT DSN H) MONITOR & VERIFY ACQUISITION OF SUN I) MONITOR & VERIFY ACQUISITION OF CANOPUS J) COMMAND REACQUISITION OF CANOPUS (AS REQD) K) MONITOR S/C TRAJECTORY L) UPDATE CC&S TRAJECTORY PARAMETERS FOR PITCH, YAW, & ROLL M) COMPUTE CC&S PITCH,YAW,&ROLL POLARITY	DSN A) TRACK S/C B) RECEIVE & DISPLAY SCIENCE & ENGINEERING DATA C) MONITOR S/C & CAPSULE STATUS D) PROCESS DATA ON EARTH TO OBTAIN GUIDANCE COMMANDS (STORED COMMANDS & START TIMES)	A) PR B) PR C) PR D) PR E) RE • [illegible] • [illegible] • [illegible] F) TR/
	A) TRANSMIT ENGINEERING DATA B) RECEIVE POWER FROM E/P C) RECEIVE VIA LOW-POWER LAUNCH EXCITER DETECT & SEND TO CC&S COMMAND SIGNALS FROM EARTH D) TRANSMIT CELESTIAL REFERENCE ACQUISITION TO DSN E) TRANSMIT VERIFICATION OF DEPLOYMENT OF SOLAR PANELS, ANTENNAS, ETC TO EARTH F) TWO-WAY TRACKING		A) RE B) RE C) RE D) RE E) SW F) RE G) ST TR TO
	A) COMMAND SIGNALS TO PYROTECHNICS & MECH TO DEPLOY • SOLAR PANELS • HIGH-GAIN ANTENNA • VHF ANTENNA • LOW-GAIN ANTENNA • SCIENCE BOOM B) SWITCH ON GYROS & SELECT MODES C) ENABLE SUN-SENSOR ROLL AND PITCH CONTROL D) RECEIVE SUN PRESENCE SIGNAL E) TURN ON CANOPUS TRACKER F) SWITCH ROLL CONTROL TO CANOPUS SENSOR G) ACTIVATE MAGNETOMETER (CALIBRATION ROLL) H) RECEIVE CANOPUS PRESENCE OUTPUT SIGNAL I) TRANSMIT VERIFICATION TO TELECOMMUNICATION SUBSYSTEM (CANOPUS & SUN PRESENCE) J) PERFORM COMMAND FUNCTIONS FOR CANOPUS OVERRIDE AS REQUIRED K) BACKUP COMMANDS AS REQUIRED	A) COMMAND TELECOMMUNICATION TO DATA MODE NO. 2 B) COMMAND CRUISE SCIENCE ON (WARMUP) — SCIENCE INSTRUMENTS C) COMMAND DATA RECORDERS ON D) COMMAND TWTA ON E) SWITCH CANOPUS ANGLE AS REQUIRED F) INITIATE CRUISE SCIENCE DATA ACQUISITION G) COMMAND TELECOMMUNICATION CHANGE FROM OMNI TO HIGH-GAIN ANTENNA H) UPDATE HIGH-GAIN ANTENNA POSITION (AS REQUIRED) I) COMMAND TELECOMMUNICATIONS — CHANGE DATA TRANSMISSION RATES J) COMMAND RECALIBRATION OF SCIENCE ELEMENTS AS REQUIRED K) BACKUP COMMANDS AS REQUIRED	A) CO B) RE C) SW D) CO E) RE F) SW G) AR H) PR I) RE J) DI K) CO L) CO M) CO N) BA
	A) RECEIVE CC&S COMMAND SWITCH ON GYROS, RCS, & AUTOPILOT B) DAMP ROTATION C) YAW & PITCH SPACECRAFT TO ACQUIRE SUN D) RELAY SUN ACQUISITION SIGNAL TO CC&S E) TURN ON CANOPUS SENSOR, ROLL 360 TO CALIBRATE MAGNETOMETER F) ROLL TO ACQUIRE CANOPUS & PROVIDE STAR MAP G) RELAY ACQUISITION SIGNAL (CANOPUS) TO CC&S H) PERFORM CANOPUS OVERRIDE ROLL MANEUVER AS REQUIRED	A) UPDATE CANOPUS CONE ANGLE ON COMMAND B) SWITCH AUTOPILOT TO CRUISE MODE C) MAINTAIN S/C ATTITUDE TO CELESTIAL REFERENCES DURING CRUISE	A) SW B) RO C) YA D) AU TO E) TU F) PR TO G) TU
			MIDCO A) AR B) AR C) FI D) SH E) IS F) IS
	A) PROVIDE POWER TO PYROTECHNIC SUBSYSTEMS FOR SQUIB FIRINGS B) PROVIDE POWER TO MECHANISMS C) ACTIVATE SOLAR POWER SYSTEM AFTER SUN ACQUISITION (AUTOMATIC) D) TRANSMIT "VOLTAGE SATISFACTORY" SIGNAL TO CC&S E) PROVIDE POWER TO: • TELEMETRY • CC&S • TEMPERATURE CONTROL • AUTOPILOT	A) PROVIDE CONDITIONED SOLAR ELECTRICAL POWER TO: • TELEMETRY • CAPSULE • CC&S • ATTITUDE REF • AUTOPILOT • TEMPERATURE CONTROL • SCIENCE B) CHARGE BATTERIES	A) PF • [illegible] • [illegible] • [illegible] • [illegible] • [illegible] • [illegible] • [illegible] • [illegible]
	A) PROVIDE PHYSICAL SUPPORT FOR ALL EQUIPMENT B) DRIVE SOLAR PANELS TO LIMIT STOPS C) PROVIDE DOT & LOCK SIGNALS TO TELEMETRY D) DRIVE HIGH-GAIN ANTENNA TO OPERATING POSITION & LOCK E) DRIVE VHF & OMNI ANTENNAS TO OPERATING POSITION & LOCK F) DRIVE MAGNETOMETER BOOM TO OPERATING POSITION & LOCK G) SUPPORT FLT CAPSULE	A) SUPPORT S/C ASSEMBLIES B) SUPPORT S/C COMPONENTS C) MAINTAIN ADEQUATE ALIGNMENT BETWEEN COMPONENTS D) PROVIDE ACCEPTABLE STATIC & DYNAMIC LOAD ENVIRONMENTS E) SUPPORT FLIGHT CAPSULE	A) SI B) SI C) M D) PI E) SI
	PROVIDE TEMPERATURE CONTROL	PROVIDE TEMPERATURE CONTROL	PROV
	RECEIVE SQUIB FIRING SIGNALS FOR DEPLOYMENT OF: • SOLAR PANEL • MAGNETOMETER BOOM • LOW-GAIN ANTENNA • HIGH-GAIN ANTENNA • VHF ANTENNA		A) RE B) PI C) IN
	A) CALIBRATE MAGNETOMETER DURING S/C ROLL B) CALIBRATE OTHER SCIENCE INSTR AS REQUIRED	A) RECEIVE CRUISE SCIENCE "ON" COMMAND B) ACQUIRE CRUISE SCIENCE DATA C) TRANSFER CONDITIONED DATA TO DAE D) RECEIVE POWER FROM E/P E) RECALIBRATE SCIENCE EXPERIMENTS AS REQUIRED	A) RI B) TU
		A) RECEIVE DAE "ON" COMMAND B) PROCESS & TRANSFER DATA TO TM	

UR TIMES

5.0 INTERPLANETARY TRAJECTORY CORRECTION

VIDE ROLL TURN MAGNITUDE & DIRECTION
VIDE YAW TURN MAGNITUDE & DIRECTION
VIDE MIDCOURSE MOTOR BURN DURATION AND ΔV
VIDE INITIATE MANEUVER SEQUENCE COMMAND
EIVE VERIFICATION OF CORRECTION MANEUVER
EGREES OF YAW & ROLL
HRUST DURATION
EACQUISITION OF CELESTIAL REFERENCES
CK SPACECRAFT

EIVE ROLL & YAW TURN COMMAND & RELAY TO CC&S
EIVE ANTENNA POSITIONING DATA & RELAY TO CC&S
EIVE MOTOR BURN DURATION AND & ΔV RELAY TO CC&S
EIVE INITIATE MANEUVER COMMAND & RELAY TO CC&S
ITCH TO DATA MODE NO. 1 (FOR LATE MIDCOURSE MANEUVERS)
AV VERIFICATION OF CORRECTION MANEUVER TO DSN
RE AND/OR TRANSMIT ENGINEERING DATA TO DSN (MODE 3)
NSMIT ENGINEERING (SPACECRAFT & CAPSULE) + CRUISE SCIENCE
ISN (MODE 2)

MMAND TELECOMMUNICATION TO DATA MODE NO. 1
EIVE TRAJECTORY CORRECTION PARAMETERS
ITCH GYROS TO RATE CONTROL
MMAND ANGULAR MANEUVER
EIVE GYRO SIGNALS & SUM FOR ANGULAR MANEUVERS
ITCH ATTITUDE REFERENCE TO AUTOPILOT SUBSYSTEM
M PROPULSION SYSTEM
VIDE COMMAND TO INITIATE ATTITUDE MANEUVER & ΔV MANEUVER
EIVE ACCELEROMETER SIGNALS & INTEGRATE FOR ΔV MANEUVER
ARM PROPULSION SYSTEM
MMAND REVERSE ANGULAR MANEUVER
MMAND REACQUIRE CELESTIAL REFERENCES
MMAND AUTOPILOT SELECTION CONTROL
KUP COMMANDS AS REQUIRED

ITCH TO GYRO CONTROL
L S/C AND VERIFY
/ S/C AND VERIFY
OPILOT — PROVIDE COMMAND
VC DURING MOTOR BURN
N ON ACCELEROMETERS
VIDE ACCELERATION DATA
C&S
N OFF ACCELEROMETER

RSE PROPULSION SYSTEM

M PRESSURIZATION SYSTEM (FIRE SQUIB VALVE)
M PROPELLANT FEED SUBSYSTEM (FIRE SQUIB VALVE)
PROGRAMMED ENGINES (OPERATE SOLENOID VALVE)
T DOWN ENGINE
LATE PROPELLANT FEED SUBSYSTEM
LATE PRESSURIZATION SUBSYSTEM

VIDE CONDITIONED SOLAR OR BATTERY POWER TO:
ELEMETRY
C&S
UTOPILOT
TTITUDE REFERENCE
EACTION CONTROL
ROPULSION
EMPERATURE CONTROL
YROTECHNIC
APSULE

PPORT S/C ASSEMBLIES
PPORT S/C COMPONENTS
NTAIN ADEQUATE ALIGNMENT BETWEEN COMPONENTS
VIDE ACCEPTABLE STATIC & DYNAMIC LOAD ENVIRONMENTS
PORT FLIGHT CAPSULE

E TEMPERATURE CONTROL

OVE PROPULSION SYSTEM INHIBIT
VIDE IGNITION
IBIT PROPULSION SYSTEM

EIVE CC&S COMMAND "CRUISE SCIENCE OFF"
N OFF CRUISE SCIENCE

6.0 S/C CAPSULE SEPARATION

A) INITIATE PRESEPARATION SEQUENCE
B) RECEIVE CAPSULE STATUS DATA
C) COMMAND SEPARATION
D) VERIFY CAPSULE PROGRAM
E) VERIFY SEPARATION
F) TRACK CAPSULE & SPACECRAFT

A) RECEIVE PRESEPARATION SEQUENCE COMMANDS & RELAY TO CC&S
B) SWITCH TO DATA MODE NO. 2
C) TRANSMIT CAPSULE ENGRG DATA TO DSN
D) RECEIVE SEPARATION COMMAND FROM DSN & ROUTE TO CC&S
E) STORE AND/OR TRANSMIT ENGINEERING DATA TO DSN (MODE 3)
TRANSMIT ENGINEERING (SPACECRAFT & CAPSULE) + CRUISE SCIENCE TO DSN (MODE 2)

A) LOAD CAPSULE WITH 5 OR MORE COMMANDS
B) COMMAND CAPSULE SEQUENCING
C) COMMAND TELECOMM SWITCH TO DATA MODE NO. 1
D) COMMAND GYROS ACTIVATE (CAPSULE)
E) COMMAND GYROS ESTABLISH POLARITY (CAPSULE)
F) COMMAND GYROS TO ATTITUDE CONTROL MODE (CAPSULE)
G) COMMAND DATA TAPE RECORDER OFF
H) COMMAND CAPSULE ACTIVATE ENTRY SCIENCE
I) COMMAND CAPSULE ACTIVATE TELE-COMM & VERIFY RADIO LINK (VHF)
J) SELECT T/M MODE FOR TRANSMISSION OF CAPSULE DATA
K) COMMAND:
BIOBARRIER SEPARATION
S/C ORIENT TO SEPARATION ATTITUDE
ELECTRICAL CONNECTION SEPARATION
VERIFY SEPARATION
L) COMMAND REORIENT S/C & REACQUIRE CELESTIAL REFERENCES
M) BACKUP COMMANDS AS REQUIRED
N) RECEIVE S/C ORIENTATION PARAMETERS

A) SWITCH TO GYRO CONTROL
B) PERFORM ROLL TURN & VERIFY
C) PERFORM YAW TURN & VERIFY
D) MAINTAIN ATTITUDE DURING SEPARATION
E) PERFORM YAW TURN (INVERSE TO C) & VERIFY
F) PERFORM ROLL TURN (INVERSE TO B) & VERIFY
G) REACQUIRE CELESTIAL REFERENCES
H) RETURN TO CELESTIAL REFERENCE ATTITUDE CONTROL MODE

A) PROVIDE CONDITIONED SOLAR OR BATTERY POWER TO:
- T/M
- CC&S
- AUTOPILOT
- ATTITUDE REF
- REACTION CONTROL
- TEMPERATURE CONTROL
- PYROTECHNICS
- CAPSULE

A) SUPPORT S/C ASSEMBLIES
B) SUPPORT S/C COMPONENTS
C) MAINTAIN ADEQUATE ALIGNMENT BETWEEN COMPONENTS
D) PROVIDE ACCEPTABLE STATIC & DYNAMIC LOAD ENVIRONMENTS
E) SUPPORT FLIGHT CAPSULE

PROVIDE TEMPERATURE CONTROL

A) RECEIVE SIGNAL TO REMOVE CAPSULE SEPARATION INHIBIT
B) RECEIVE SIGNAL TO FIRE CAPSULE UMBILICAL SEPARATION
C) RECEIVE SIGNAL TO FIRE BIOBARRIER REMOVAL
D) RECEIVE SIGNAL TO FIRE CAPSULE SEPARATION
E) RECEIVE SIGNAL FOR SEPARATION INHIBIT

A) RECEIVE CC&S COMMAND "CRUISE SCIENCE OFF"
B) TURN OFF CRUISE SCIENCE

7.0 FLIGHT CAPSULE TRAJECTORY DEFLECTION → 9.0 FLIGHT CAPSULE CRUISE → 10.0 FLIGHT CAPSULE ENTRY →

→ 8.0 FLIGHT S/C CRUISE →

A) TRANSMIT ORBIT INJECTION PARAMETERS • ROLL MAGNITUDE & DIRECTION • YAW MAGNITUDE & DIRECTION • MOTOR BURN START TIME B) TRACK FLIGHT SPACECRAFT C) RECEIVE, REDUCE & DISPLAY SCIENCE & ENGINEERING DATA D) PROVIDE COMMANDS TO BACK UP CC&S AS REQUIRED	A) RECEIVE, DECODE, & DISPLA B) RELAY UPDATED ORBIT INJE C) PROVIDE COMMAND TO INIT D) PROVIDE BACKUP COMMAN E) TRACK S/C F) VERIFY ORBIT INSERTION
A) RECEIVE ROLL & YAW TURN MAGNITUDE & DIRECTION COMMAND & RELAY TO CC&S B) RECEIVE ANTENNA POSITIONING DATA & RELAY TO CC&S C) RECEIVE MOTOR-BURN START TIME, RELAY TO CC&S D) RECEIVE CAPSULE DATA, CONDITION & RELAY TO GROUND E) TRANSMIT FLIGHT SPACECRAFT ENGINEERING, CAPSULE ENGRG, & SCIENCE DATA TO GROUND VIA MODE 2	A) UPDATE ROLL-TURN MAGNITI B) UPDATE YAW-TURN MAGNITU C) UPDATE MOTOR-BURN STAR D) UPDATE INITIATE MANEUVER E) SWITCH TO DATA MODE NO. F) REACQUIRE EARTH AFTER RO G) RELAY VERIFICATION OF MA
A) COMMAND SWITCH TO DATA MODE NO. 2 B) COMMAND CANOPUS CONE ANGLE SETTING C) COMMAND ANTENNA STEP (AS REQUIRED) D) RECEIVE ORBIT INJECTION PARAMETERS E) PROVIDE SIGNAL TO PYRO & MECHANISMS TO DEPLOY SCAN PLATFORM (CRUISE SCIENCE T/M OFF) & SWITCH TO DATA MODE NO. 1 F) SWITCH ON DATA RECORDER-COMMAND TELECOMMUNICATIONS RECEIVE CAPSULE DATA G) BACKUP COMMANDS AS REQUIRED	A) UPDATE STORED ROLL, PITC B) UPDATE STORED VELOCITY M C) INITIATE MANEUVER SEQUEN D) COMMAND ORIENTATION OF E) COMMAND THRUST FOR ORB F) COMMAND RETURN TO CRUI G) BACKUP COMMANDS AS REQ
	A) SWITCH TO GYRO CONTROL
A) UPDATE CANOPUS CONE ANGLE ON COMMAND B) SWITCH AUTOPILOT TO CRUISE MODE C) MAINTAIN S/C ATTITUDE TO CELESTIAL REFERENCES DURING CRUISE	B) PROVIDE ROLL TO PROPER A C) YAW TO PROPER ATTITUDE & D) AUTOPILOT – PROVIDE COM E) TURN ON ACCELEROMETER F) PROVIDE ACCELEROMETER D G) TURN OFF ACCELEROMETER H) YAW BACK AFTER MOTOR BU I) ACQUIRE SUN & VERIFY J) ROLL BACK TO PROGRAMME K) ACQUIRE CANOPUS & VERIF L) SWITCH AUTOPILOT FROM G
	ORBIT INSERTION ENGINE A) ARM TVC B) ARM IGNITER C) FIRE MOTOR & PROVIDE T D) TERMINATE THRUST (MOTO
A) PROVIDE CONDITIONED SOLAR ELECTRICAL POWER TO: • T/M • CC&S • AUTOPILOT • ATTITUDE REF • REACTION CONTROL • TEMPERATURE CONTROL D) CHARGE BATTERIES	A) PROVIDE CONDITIONED SOLA • TELEMETRY • CC&S • ATTITUDE REFERENCE SU • AUTOPILOT • TEMPERATURE CONTROL • PULSE TO PYROTECHNIC • PULSE TO PROPULSION
A) SUPPORT S/C ASSEMBLIES B) SUPPORT S/C COMPONENTS C) MAINTAIN ADEQUATE ALIGNMENT BETWEEN COMPONENTS D) PROVIDE ACCEPTABLE STATIC & DYNAMIC LOAD ENVIRONMENTS E) DRIVE SCAN PLATFORM TO DEPLOYED POSITION & LOCK	A) SUPPORT S/C ASSEMBLIES B) SUPPORT S/C COMPONENTS C) MAINTAIN ADEQUATE ALIG D) PROVIDE ACCEPTABLE STA
PROVIDE TEMPERATURE CONTROL	PROVIDE TEMPERATURE CONTRO
RECEIVE SQUIB FIRING SIGNAL FOR UNLATCHING OF SCAN PLATFORM	A) RECEIVE & EXECUTE COMMA PROPULSION ENGINE B) RECEIVE & EXECUTE SIGNAL C) RECEIVE & EXECUTE COMMA STOP D) RECEIVE & EXECUTE SIGNAL
A) RECEIVE CRUISE SCIENCE "ON" COMMAND B) ACQUIRE CRUISE SCIENCE DATA C) TRANSFER CONDITIONED DATA TO DAE D) RECEIVE POWER FROM EIP E) RECALIBRATE SCIENCE EXPERIMENTS AS REQUIRED	SCIENCE OFF DURING ORBIT IN
A) RECEIVE DAE "ON" COMMAND B) PROCESS & TRANSFER DATA TO TM	

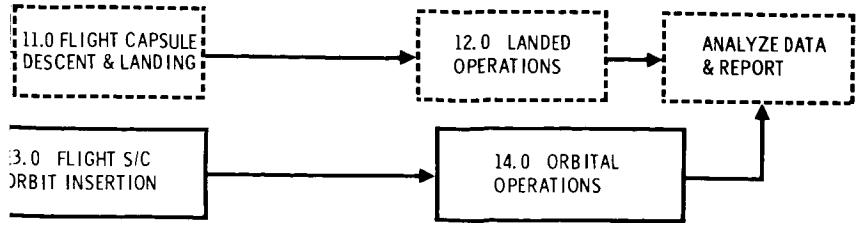

Y ENGINEERING DATA STION PARAMETERS IATE INSERTION MANEUVER S TO CC&S AS REQUIRED	A) RECEIVE, DECODE, & DISPLAY SCIENCE DATA B) RECEIVE AND ANALYZE ENGINEERING DATA C) TRACK S/C D) RECEIVE & DISPLAY CAPSULE DATA E) PROVIDE DATA FOR ORBITAL TRIM (IF REQUIRED) F) RECEIVE VERIFICATION OF ORBITAL TRIM MANEUVER G) TERMINATE MISSION
IDE & DIRECTION COMMAND & RELAY TO CC&S IDE & DIRECTION COMMAND & RELAY TO CC&S TIME & RELAY TO CC&S & RELAY TO CC&S 2 OR 5A AS REQUIRED LL TURNS & MOTOR BURN NEUVERS	A) TRANSMIT SCIENCE & ENGINEERING DATA VIA DATA MODES 5 AND 6 B) RECORD ENGINEERING & SCIENCE DATA AS COMMANDED C) RECEIVE, STORE & RELAY CAPSULE DATA ON COMMAND (MODES 5 AND 6) D) RECEIVE & RELAY DATA FOR ORBIT TRIM IF REQUIRED
H, & YAW MAGNITUDE & SIGN AGNITUDE CE S/C TO INJECTION ATTITUDE T INSERTION SE ATTITUDE UIRED	A) COMMAND ORBITAL TRIM MANEUVER (IF REQUIRED) B) SWITCH DATA MODES AS NECESSARY C) RECEIVE ANY ORBITAL OPERATION CHANGES & SEQUENCES D) COMMAND POSITIONING OF SCIENCE SCAN PLATFORM E) SWITCH ON ORBITAL SCIENCE F) SELECT RECORDED SCIENCE READOUT TO TELECOMMUNICATIONS G) BACKUP COMMANDS AS REQUIRED H) STORE DATA FOR ORBIT TRIM (IF REQUIRED) I) TERMINATE MISSION ON COMMAND (IF REQUIRED)
TTITUDE & VERIFY ROLL VERIFY MAND TO TVC DURING MOTOR BURN ATA TO CC&S RN) ATTITUDE Y YRO – CONTROL TO CELESTIAL REFERENCE CONTROL	A) MAINTAIN S/C ATTITUDE TO CELESTIAL REFERENCES B) SWITCH AUTOPILOT TO GYRO CONTROL DURING OCCULTATION C) REACQUIRE CELESTIAL REFERENCES FOLLOWING OCCULTATION D) REORIENT S/C FOR ORBITAL TRIM MANEUVER USING GYRO CONTROL E) PROVIDE TVC DURING ENGINE FIRING F) REACQUIRE CELESTIAL REFERENCES FOLLOWING MANEUVERS G) UPDATE CANOPUS CONE ANGLES ON COMMAND
HRUST & TVC R BURNS TO DEPLETION)	MIDCOURSE A) ARM PRESSURIZATION & PROPELLANT FEED SUBSYSTEMS B) PROVIDE THRUST (FIRE PROGRAMMED ENGINES) FOR ORBIT TRIM IF REQUIRED C) TERMINATE THRUST ON COMMAND D) ISOLATE PROPELLANT FEED SUBSYSTEM E) ISOLATE PRESSURIZATION SUBSYSTEM
R OR BATTERY POWER TO: BSYSTEM S	A) PROVIDE CONDITIONED SOLAR OR BATTERY POWER TO: • TELEMETRY • CC&S • ATTITUDE REFERENCE SUBSYSTEM • AUTOPILOT • TEMPERATURE CONTROL • STRUCTURES & MECHANISMS • SCIENCE
MENT BETWEEN COMPONENTS IC & DYNAMIC LOAD ENVIRONMENTS	A) SUPPORT S/C ASSEMBLIES B) SUPPORT S/C COMPONENTS C) MAINTAIN ADEQUATE ALIGNMENTS BETWEEN COMPONENTS D) PROVIDE ACCEPTABLE STATIC AND DYNAMIC LOAD ENVIRONMENTS E) POSITION SCAN PLATFORM
L	PROVIDE TEMPERATURE CONTROL
ND SIGNAL TO REMOVE INHIBIT FOR FOR PROPULSION ENGINE START ND SIGNAL FOR PROPULSION ENGINE FOR PROPULSION INHIBIT	
SERTION	A) TURN ON ORBITAL SCIENCE INSTRUMENTS B) ACQUIRE ORBITAL SCIENCE DATA C) TRANSFER CONDITIONED DATA TO DAE D) RECALIBRATE SCIENCE EXPERIMENTS AS REQUIRED
	A) RECEIVE DAE "ON" COMMAND B) PROCESS & TRANSFER DATA TO TM

Mission Sequences Matrix

RCI-30-29, Range Frequency Scheduling

Brochure, Reflector Structure Development and Fabrication Programs, Electro-Optical Systems, Inc. No. 64-1062 (Supplement).

4.1.2.3 Telecommunications System--Functional Description

The 1971 Voyager telecommunications system (spacecraft and ground elements) is designed to perform the following functions.

1) Spacecraft:

   a) Receive and detect commands sent from the DSIF and direct them to the spacecraft central computer and sequencer (CC&S) subsystem;

   b) Telemeter certain engineering parameters and scientific phenomena from the spacecraft to the DSIF stations;

   c) Coherently receive and retransmit the command carrier signal in order to provide two-way doppler tracking;

   d) Provide turnaround ranging capability;

   e) Receive certain engineering information from the capsule when attached to the spacecraft bus and also during capsule cruise phase and then telemeter the data to the DSIF stations;

   f) Receive data from up to two capsules, after landing on Mars and retransmit to the DSIF stations.

2) Ground System:

   a) Track the relative angular position and radial velocity and range of the spacecraft with respect to designated coordinate systems to enable the Space Flight Operations Facility to compute the parameters of the spacecraft trajectory.

b) Provide for processing all spacecraft data as required for ground handling and distribution.

Spacecraft Subsystems--The spacecraft portion of the telecommunications system has been divided into four functional equipment groups outlined in Figure 4.1-3. A summary description of the subsystem elements follows.

Spacecraft Antenna Subsystem--Consists of low-gain, low-gain ascent/and steerable high-gain antennas to be used for transmission and reception of rf energy at S-band frequencies plus a VHF antenna for communication with the capsule when it becomes separated from the spacecraft. The spacecraft antenna subsystem will:

1) Transmit rf signals from the spacecraft radio subsystem to the DSIF;
2) Receive rf signals from the DSIF and couple these into the spacecraft radio subsystem.

The spacecraft antennas are capable of being switched to permit transmission over either the ascent, low-gain, or high-gain antennas. The modes for this switching will permit the following combinations:

1) Transmission and reception via the low-gain antenna;
2) Transmission and reception via the high-gain antenna;
3) Transmission via high-gain antenna and reception via low-gain antenna;
4) Transmission via the ascent antenna and reception via the low-gain antenna.

The high-gain antenna is capable of being pointed toward the Earth by stored program and real time commands from the CC&S. The VHF antenna is used for receiving transmissions from the capsule during the descent phase and after the Mars landing period. A more detailed description is contained in Section 4.1.3.4.

Spacecraft Radio Subsystem--Consists of rf components, preamplifier, and S-band receivers; a command detector (for use in command link); a launch transmitter; an S-band exciter and power amplifier (used by tracking and telemetry links); and a ranging unit. The spacecraft radio subsystem will:

1) Receive and demodulate the rf phase modulated command signal of the DSN;
2) Detect the synchronization signal and the command word bits and direct to the command decoder of the central computer and sequencer (CC&S);
3) Receive phase lock-on and track the DSN command carrier frequency;
4) Convert coherently the received carrier frequency by a 240/221 ratio and retransmit this frequency as the telemetry carrier (When a DSN command carrier is not present, an internally generated carrier frequency is substituted);
5) Demodulate the range code video information transmitted from the DSN on the command frequency carrier and modulate the telemetry carrier with this information for retransmission to the DSN;
6) Phase modulate the telemetry carrier with a baseband consisting of PN sync and/or data subcarrier from the telemetry and data storage subsystem;
7) Amplify the modulated telemetry carrier for transmission to the DSN.

The detected command bit rate is fixed at a rate of 1 bit per second.

The two levels of rf power for spacecraft data transmission are:

1) Low power level for transmission of data from launch to completion of outgassing;
2) High power level for transmission of data in all modes after outgassing is completed.

The transmitted rf carrier has two modes--noncoherent and coherent. When the transponder receiver is not receiving a signal, the phase and frequency of the unmodulated transmitted carrier is controlled by a crystal oscillator. When the transponder is locked to a ground signal, the phase and frequency of the unmodulated transmitted carrier will be 240/221 times the phase and frequency of the unmodulated received carrier. A more detailed description is contained in Section 4.1.3.1.

Spacecraft Telemetry and Data Storage Subsystem--Consists of engineering data acquisition elements required to:

1) Time-division multiplex, encode, and format all spacecraft engineering telemetry, capsule, cruise science, and planetary science data;
2) Provide subcarriers modulated with the above data;
3) Store spacecraft engineering, capsule, and planetary science data.

The telemetry and data storage subsystem will:

1) Accept scientific data from the data automation system (DAS);

2) Accept planetary science data and process for real-time transmission;

3) Store planetary science data and readout at rates compatible with telecommunications link capability;

4) Accept capsule data via hardwire connection prior to separation;

5) Accept capsule data, transmitted during capsule descent and entry phases, from the spacecraft relay radio subsystem;

6) Accept capsule data, transmitted from the Mars surface, from the spacecraft relay radio subsystem;

7) Store capsule data during the maneuver phases and during Mars insertion burn period and play back this data upon command;

8) Accept analog engineering measurements within a predetermined set of levels, time division sample this data, and convert data to digital form;

9) Accept digital engineering data;

10) Store engineering data during maneuver and insertion burn phases and play back this data upon command;

11) Time-multiplex engineering data with capsule and scientific data;

12) Generate a PN synchronization code for use with Mode 1 and Mode 4 telemetry;

13) Generate and add biorthogonal coding to planetary science data;

14) PSK modulate the data and synchronizing signals on appropriate subcarriers;

15) Multiplex data and synchronizing signals.

There are six telemetry data modes:

1) TLM-1: Real-time engineering + capsule data at 22 2/9 bits per second (total);

2) TLM-2: Real-time engineering + capsule + cruise science data at 133 1/3 bits per second;

3) TLM-3: Real-time engineering + capsule + playback of engineering data at 133 1/3 bits per second;

4) TLM-4: Real-time engineering at 5 5/9 bits per second;

5) TLM-5a: Real-time engineering, capsule, and cruise science at 400 bits per second and playback of planetary science at 8000 bits per second;

TLM-5b: Real-time engineering, capsule, and cruise science at 400 bits per second and playback of planetary science at 4000 bits per second;

TLM-5c: Real-time engineering, capsule and cruise science at 400 bits per second and playback of planetary science at 2000 bits per second;

6) TLM-6: Real-time engineering capsule, and cruise science at 400 bits per second and real time readout of planetary science at 48,000 bits per second.

The spacecraft data handling and storage subsystem is capable of formating data for output rates of 5-5/9, 22-2/9, 133-1/3, 400, 2000, 4000, 8000, and 48,000 bits per second. The 48,000- and 8000- to 2000-bits-per-second planetary-science data will be formatted into a biorthogonal code before separate subcarrier modulation. Further definition of the spacecraft telemetry and data storage subsystem is contained in Section 4.1.3.2.

Spacecraft Relay-Radio Subsystem--Consists of a VHF receiver and detector. This subsystem provides a telemetry link from separated capsule to the spacecraft bus for subsequent relay to Earth. Two capsules may be accommodated sequentially, but not simultaneously. The relay-radio subsystem will:

1) Receive and detect VHF telemetry signals sent from the separated capsule prior to landing. The detected data will be at the nominal rate of 10 bits per second and will be directed to the spacecraft telemetry and data storage subsystem for real time transmission to the DSIF as a primary mode. The data will also be stored during maneuver or spacecraft engine burn phases for subsequent playback.
2) Receive and detect VHF telemetry signals sent from either of two capsules after they have landed on the Mars surface. The detected data will be at the assumed nominal rate of 100 bits per second and will be directed to the spacecraft telemetry and data storage system for formating into the modulation baseband and subsequent real time transmission to the DSIF. Section 4.1.3.3 contains additional description at the relay-radio subsystem.

Ground Subsystems--The following DSIF subsystems will be required to support the Voyager mission--ground telemetry subsystem, ground command subsystem, ground instrumentation subsystem, and ground ranging subsystem. A description of the mission dependent equipment to supplement the existing DSIF subsystems is contained in Boeing Document D2-82709-3. The typical DSIF station configuration is illustrated in Figure 4.1-4.

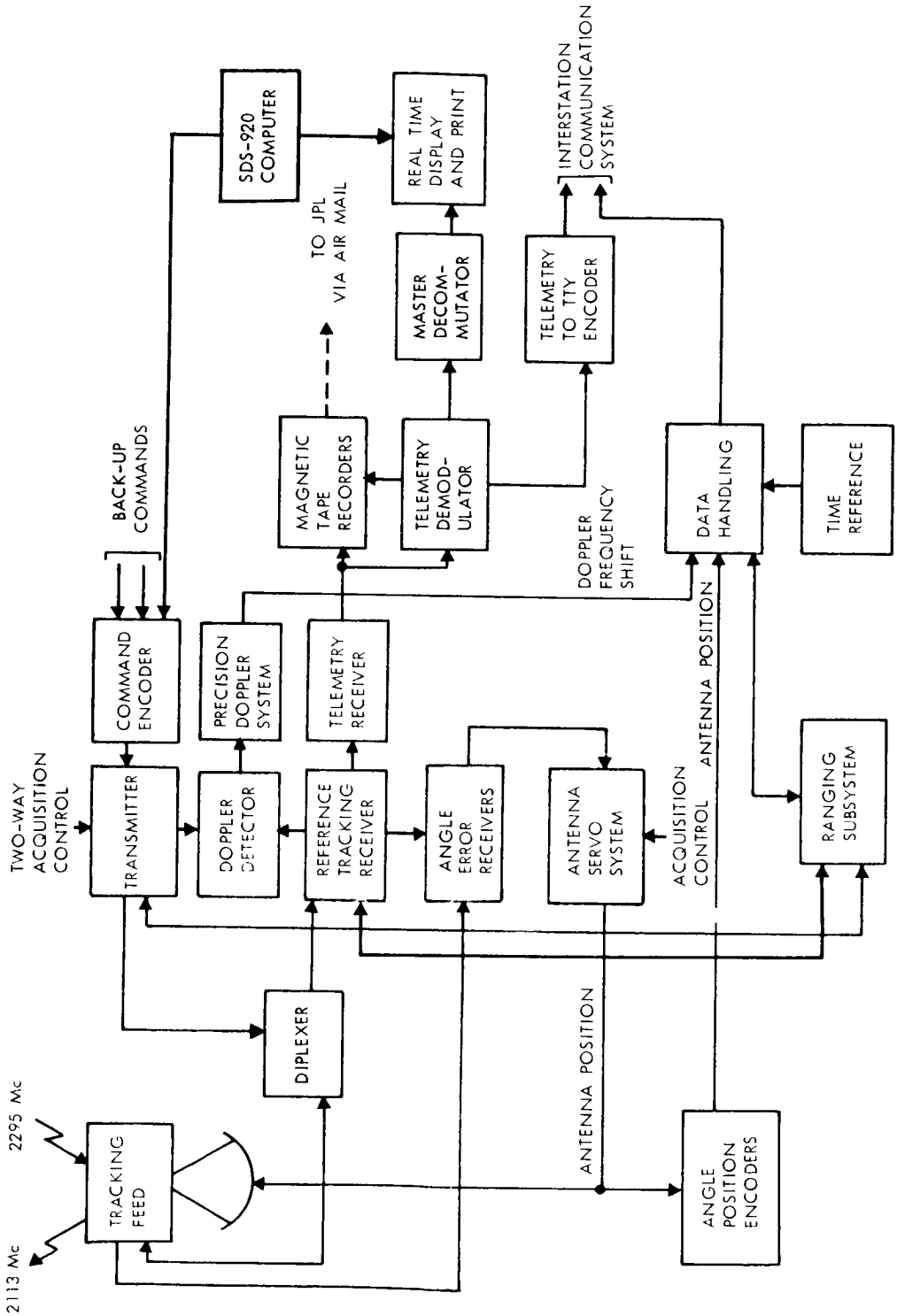

Figure 4.1-4: Typical Voyager Deep Space Station

Phases of Operation

The configuration of the spacecraft and ground telecommunications system is detailed in Table 4.1-1 for the five major phases of the mission. Each configuration is defined in terms of spacecraft and ground elements.

Data Handling Capability

A summary of the overall telecommunications data handling capability is presented below.

Engineering Data--

Real Time--Accommodate 11-1/9 bits per second (including frame synchronchronization) for all operating modes up to Mars orbit insertion. Accommodate up to 66-2/3 bits per second during Mars-orbit modes. In emergency mode, accommodate 5-5/9 bits per second.

Stored--As a backup, store data at 11-1/9 bits per second for up to 2 hours during second and optional third midcourse maneuver, capsule separation, and Mars-orbit injection maneuvers. Playback at rate of 111-1/9 bits per second using Telemetry Mode 3.

Capsule Data--

Real-Time (Preseparation)--Accepts data at 10 bits per second and transmits at rate of 11-1/9 bits per second (including synchronization) for all modes until capsule separation.

Table 4.4-1: TELECOMMUNICATION OPERATIONAL CONFIGURATION

Mission Phase	Description	Time Period	Maximum Range to Earth (KM)	Spacecraft Configuration: Ground Antenna	S/C Antenna	S-Band Radio	Relay Radio	TLM Data Mode
	LAUNCH PHASE							
A-1	Launch to Shroud Separation	200 sec		Sta71+ETR	Shroud	1 watt		1(22 bps)
2	Shroud Separation to Centaur Separation	30 min			Ascent	↓		1
3	Johnnesberg Acquisition	30-60 min		2'DSIF	Ascent			1
4	Johnnesberg Acqui. to completion of outgassing	8-24 hrs	0.3×10^6	85'DSIF	Ascent			1
	CRUISE PHASE							
B-1	Completion of outgassing to 1st Maneuver	1-5 days	1.5×10^6	85'DSIF	Lo-gain	50 watts		2(133 bps)
2	1st Maneuver to activation of Hi-gain antenna	5-80 dys	20×10^6	↓	Lo-gain	↓		2
3	Activation of Hi-gain antenna to Mars encounter	100-215 days	157×10^6		Hi-gain			2
4	Turn-around Ranging	0-20 dys	5.3×10^6		Lo-gain			1
	MANEUVER PHASES							
C-1	1st Midcourse Maneuver	5th day	1.5×10^6		Lo-gain			2
2	2nd Midcourse Maneuver	25 to 100th day	29×10^6		Lo-gain			1
3	Optional 3rd Midcourse				Hi-gain			2
4	Capsule Separation	210th day	150×10^6	210'DSIF	Hi-gain + VHF		10 b/s	1
5	Mars Orbit Injection	215th day	157×10^6	↓	Hi-gain + VHF	↓	↓	1
	PLANETARY APPROACH PHASE							
D-1	Capsule Separation to Landing (Normal)	210-215 days	150×10^6		Hi-gain + VHF			2
2	Playback of Stored Engineering Data From Capsule Separation							3(133 1/3 bps)
3	Playback of Stored Capsule Data From Capsule Separation							5a(400b/s)
4	Engine Burn	215th day	157×10^6					1
5	Play back of Stored Engr. Data From Mars Orbit Injection and Engine Burn							3(133 1/3 bps)
6	Playback of Stored Capsule Data From Mars Orbit Injection and Engine Burn							5a(400b/s)
	MARS ORBIT PHASE							
E-1	Real Time Planetary Science and Capsule Data	215-225 days	170×10^6	210'DSIF			100 b/s	6(48kb/s)
2	Stored Planetary Science	225-300	268×10^6		Hi-gain			5a(8kb/s)
3	Stored Planetary Science	300-395	370×10^6		Hi-gain			5b(4kb/s)

Real-Time (Postseparation)--Receive data at 10 bits per second via VHF relay and retransmit at 11-1/9 bits per second during capsule descent mode. Receive at 100 bits per second via VHF relay, temporarily store, and retransmit at 166-2/3 bits per second during nominal 2-day period of capsule landing on Mars.

Stored--As a backup, record at 10 bits per second for 2 hours during capsule separation and Mars-orbit injection maneuvers. Playback at rate of 166-2/3 bits per second using Telemetry Mode 5a.

Cruise Science Data--

Real Time--Accept data at a rate of 100 bits per second and transmit at rate of 111-1/9 bits per second (including synchronization) during cruise. Transmit at up to 166-2/3 bits per second during Mars-orbit phases.

Stored--Not required.

Planetary Science Data--

Real Time--Transmit at a rate of 48,000 bits per second for 10 to 73 days depending on link margins.

Stored--Record at nominal rate of data automation system (assume 48,000 bits per second) until 10^8-bit recorder capacity is filled. Playback at 8000 bits per second during the first 85 to 140 days of Mars orbit and at 4000 bits per second for the remainder of the 6-month mission. If desired, the redundant recorder could be used to store an additional 10^8 bits of

information at some sacrifice of mission reliability. Figure 4.1-5 shows the total number of information bits accumulated during the 6-month orbital period as a function of data modes reflected in this design.. The data model assumed in this evaluation was:

Orbital period 18 hours;

Only high-quality data would be transmitted in real time (Mode 6);

Therefore, data collected only within ±1 hour relative to periapsis.

Record and playback of data (Modes 5) are limited to the storage capacity of 1.1×10^8 bits.

One television picture consists of 1×10^6 bits.

An evaluation of the data at the end of the first 30 days reveals:

Under nominal Mode 6 conditions, data equivalent to 14,000 pictures can be returned to Earth.

Under worst case conditions on Mode 6 only, data equivalent to 7500 pictures can be returned to Earth.

Using only Mode 5, only 4400 pictures can be transmitted back to Earth.

At the end of the 6-month readout period, the number of pictures returned for each of the above three conditions is (1) 49,000, (2) 29,500, and (3) 26,000.

4.1.2.4 Interface Definition, Boundary Definitions and Characteristics

The detail boundary definitions and interface characteristics between the spacecraft telecommunication subsystems and the other spacecraft systems are specified in the subsystem descriptions contained in Section 4.1.3. Tables 4.1-2 and 4.1-3 provide a preliminary list of the

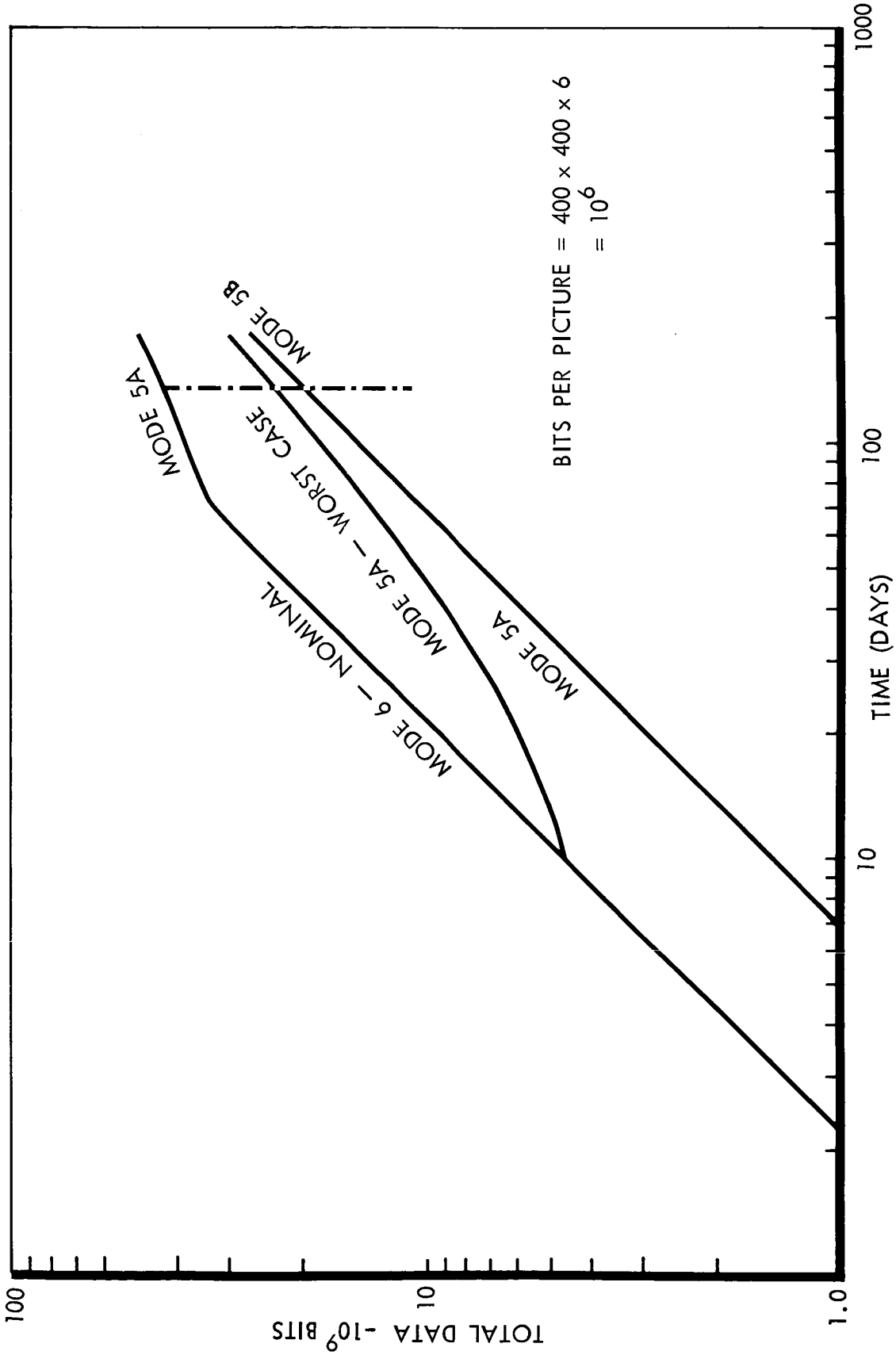

Figure 4.1-5: Total Information Bits Versus Mission Time

Table 4.1-2: TELECOMMUNICATIONS SYSTEM COMMAND REQUIREMENTS

NO.	SUBSYSTEM	FUNCTION	STORED	RTC	TYPE
1	Radio	T_X Power	X	X	Pulsed
2		Sw Exciters		X	Pulsed
3		Sw TWTA		X	Pulsed
4		Sw REC/C.D./Range		X	Pulsed
5		Ranging On/Off		X	Pulsed
6	Relay	Relay Radio	X	X	Pulsed
7		Sw. Sensitivity	X	X	Pulsed
8		Sw. Frequency		X	Pulsed
9		Sw. Data Rate	X	X	Pulsed
10	T/M	Sw. Tape Rec. (T/R)		X	Pulsed
11		T/R Mode	X	X	Pulsed
12		T/R On/Off	X	X	Pulsed*
13		Select T/M Mode	X	X	Quant.
14		Store Eng Data	X	X	Pulsed
15		Store Capsule Data	X	X	Pulsed
16		Sw Capsule Data Source	X	X	Pulsed
17		Select Clock Ref.		X	Pulsed
18		Select Block Coding		X	Pulsed
19	Antenna	Position	X	X	Pulsed
20		Position	X	X	Pulsed
21		Position	X	X	Pulsed
22		Position	X	X	Pulsed
23		Rec Low Gain-Tx Low Gain	X	X	Pulsed
24		Rec Low Gain-Tx High Gain	X	X	Pulsed
25		Rec High Gain-Tx High Gain	X	X	Pulsed

* 3 Bits

Table 4.1-3 TELECOMMUNICATIONS SYSTEM TELEMETRY REQUIREMENTS

NO.	SUBSYSTEM	PARAMETER	SCALE	RATE	NO.	SUBSYSTEM	PARAMETER	SCALE	RATE
1	Radio	Receiver S.P.E.	0-5V	1/60	16	T/M	T/R T^{o}	0-5V	1/600
2		Rec. AGC Course	0-5v	1/60	17		T/R Status	Digital	1/600
3		Rec. AGC Fine	0-50MV	1/600	18		T/R Pressure #1	0-5V	1/600
4		L.O. Drive	0-5-MV	1/600	19		T/R Pressure #2	0-5V	1/600
5		VCO Temp	0-5V	1/600	20		Full Scale Ref.	0-5V	1/600
6		Aux. Osc. Temp	0-5V	1/600	21		Low Scale Ref.	0-5V	1/600
7		Exciter Drive	0-5V	1/600	22		Eng. Memory	Digital	1/600
8		TWTA Drive	0-5V	1/600	23		Capsule Memory	Digital	1/600
9		Trans. Pwr. Out	0-5V	1/600	24		Mode State	0-5V	1/60
10		Command Det.	Digital	1/60	25		Slow Deck Pos.	0-5V	1/60
11	Relay	Receiver f	0-5V	1/60	26	Antenna			
	Radio				27		High-Gain Hinge Angle	10 Bit	1/60
12		T/M Det. VCO #1	0-5V	1/600	28		High-Gain Swivel Angle	10 Bit	1/60
13		T/M Det. VCO #2	0-5V	1/600	29		High-Gain Deploy	1 Bit	1/200
14		Low Rate Corr.	0-5V	1/600	30		High-Gain Deploy	1 Bit	1/1200
15		High Rate Corr.	0-5V	1/600	31		Low-Gain Deploy	1 Bit	1/1200
					32		High-Gain Hinge Temp	5 V	1/1200
					33		High-Gain Swivel Temp	5 V	1/1200
					34		VHF Deploy	1 Bit	1/200

specific command functions and telemetry points required for the telecommunication subsystem. Table 4.1-4 provides a summary of the physical interfaces between the telecommunication subsystems. The rf interfaces are defined by Table 4.1-5 in Section 4.1.3.1 and Table 4.1-9 in Section 4.1.3.3.

Reliability Parameters--The spacecraft telecommunication system reliability probability of success for the preferred design configuration is estimated to be 0.8416 for all functions for a 5880-hour mission duration. This estimate is based upon incorporated redundancy, a parts-count analysis, part-failure rates, and ground rules defined in the "Voyager '71 Program Reliability Analysis and Prediction Standards," Boeing Document D2-23834-1. The reliability model, equipment redundancy description, and detailed analysis is delineated in Section 4.1.5.

Telecommunication Link Performance Parameters--The performance of the telecommunication links is summarized in Figures 4.1-6, 4.1-7, 4.1-8 and 4.1-9. These graphs define the data channel margins versus time and mission phases for the telemetry, command and ranging functions. More detailed information is contained in Section 4.1.4, Link Analysis.

Telemetry Margins--Figures 4.1-6 and 4.1-7 show that the data margins under conditions of maximum worst case tolerances are positive for all mission phases. Communication will therefore be continuous except for periods of roll maneuver when the spacecraft high-gain antenna will not be tracking Earth.

ASSEMBLY AND SUBASSEMBLY	NO. OF UNITS	VOLUME	WEIGHT (Pounds)	ELECTRICAL Power Dissipated		DUTY CYCLE L = Launch C = Cruise E = Encounter O = Orbit	T/A THERMAL LIMIT OPERATING CONDITION	
				Input Watts	Internal Watts		Min T/A Temp °F	Max T/A Temp °F
Receiver and Exciter Assembly								
Receivers	2		8.5	5.6	5.6	All Modes	-13	+167
Command Detectors	2		6.0	1.5	1.5	All Modes	-13	+167
Ranging	2		1.0	1.0	1.0	To L + 20 Days	-13	+167
Exciter	2		2.8	5.4	5.2	C+E+O	-13	+167
Launch Transmitter	1		2.2	20.0	19.0		-13	+167
Redundancy Control and Logic	1		4.5	0.6	0.6	All Modes	-13	+167
Preamplifier	1		1.0	0.25	0.25	All Modes	-13	+158
Converter-Exciter 1	1		1.3	1.1	1.1	C+E+O	-13	+167
Converter-Launch Transmitter, and Exciter 2	1		1.3	1.1/ 4.3	1.1/ 4.3	C+E+O Launch	-13	+167
Converter, Receiver, Command Detector and Ranging	2		2.7	1.9	1.9	C+E+O	-13	+167
Converter, Red. Cont. Logic	1		1.3	1.7	1.7	C+E+O	-13	+167
Cabling			4.2				-13	+167
Subtotal		16x8x8	36.8	33.3 19.2	32.3 19.0	Launch C+E+O-1 watt when ranging OFF		
RF - P.A. Assembly								
Structure	1		3.0				-13	+185
Diplexer	1		1.5				-13	+185
4-Port Circulator Switch	3		8.2	0.18	0.18	All Modes	-13	+185
Preselector	2		1.5					
P.A. Structure	1		4.0					
TWTA	2		18.0	150.0	100.0	C+E+O	-13	+185
Isolator	3		4.6				-13	+185
Band Pass Filter	3		3.0				-13	+185
Band-Reject Filter	1		0.8				-13	+185
Hybrid	1		1.0				-13	+185
Circulator Switch (3-Port)	1		0.8	0.03	0.03	All Modes	-13	+185
Cabling			4.0				-13	+167

Subtotal		16x8x26	50.4	150.2	100.2	Launch C+E+O			
Planetary Science Recorder Assembly				25.0	25.0				
Tape Recorder	2		30.0	Record 2.4	2.4	Encounter & Orbital	-13	+122	
				Playback 1.2		Liftoff (1.2)	-13	+167	
Cabling			2.0	Liftoff					
Subtotal		16x8x28	32.0	25.0	25.0				
Telemetry Processor Assembly									
Engineering Core Memory	1		5.0	0.5	0.5	All Modes	-13	+167	
Capsule Core Memory	1		5.0	0.5	0.5	All Modes	-13	+167	
Eng. Multiplexer/ Encoder/Modulator	1		11.5	3.3	3.3	All Modes	-13	+167	
Converter	1		1.5	1.7	1.7	All Modes	-13	+167	
Cabling			3.0				-13	+167	
Subtotal		16x8x7	26.0	6.0	6.0	All Modes			
Relay Radio Assembly									
Receiver	1		3.0	2.10	2.10	E & O	-13	+167	
Telemetry Detector	1		2.5	1.53	1.53	E & O	-13	+167	
Converter	1		1.0	1.57	1.57	E & O	-13	+167	
Cabling			1.0			E & O	-13	+167	
Subtotal		8x8x4	7.5	5.2	5.2	E & O			
Antenna (Including Ancillary Hardware)									
Ascent Antenna Assembly			3.5			Standby			
Low-Gain Antenna Assembly			6.4	1.0		Maneuver Average			
High-Gain Antenna Assembly			38.0	6.0		Maneuver Peak			
Relay Antenna Assembly			6.4	120.0					
Subtotal			54.3	1.0		Standby			
				6.0		Maneuver Average			
Subsystem Totals			206.8	39.5	38.5	Launch			
				182.4	132.2	Cruise (Ranging On)			
				181.4	131.2	Cruise (Ranging Off)			
NOTE: All Input Electrical Power = 35.0 + 1.75 v.d.c. –						Encounter and Orbital (Assume Relay Radio On and Tape Recorders On)			Additional 5 watts (average) required during maneuvers. (120 peak)
				211.6	161.4				

Table 4.1-4: Telecommunications System Assembly Physical Characteristics

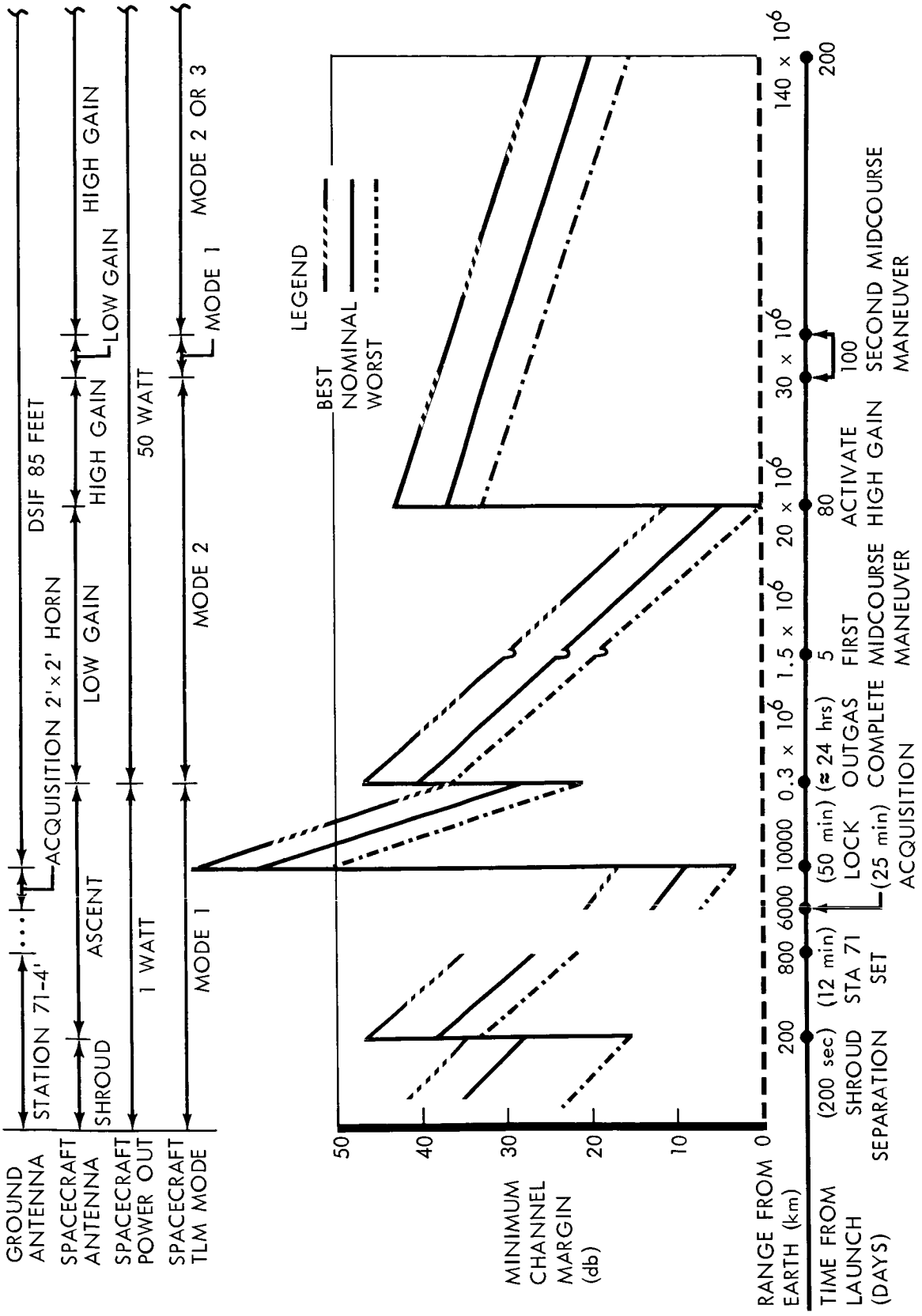

Figure 4.1-6: Telemetry Link Performance

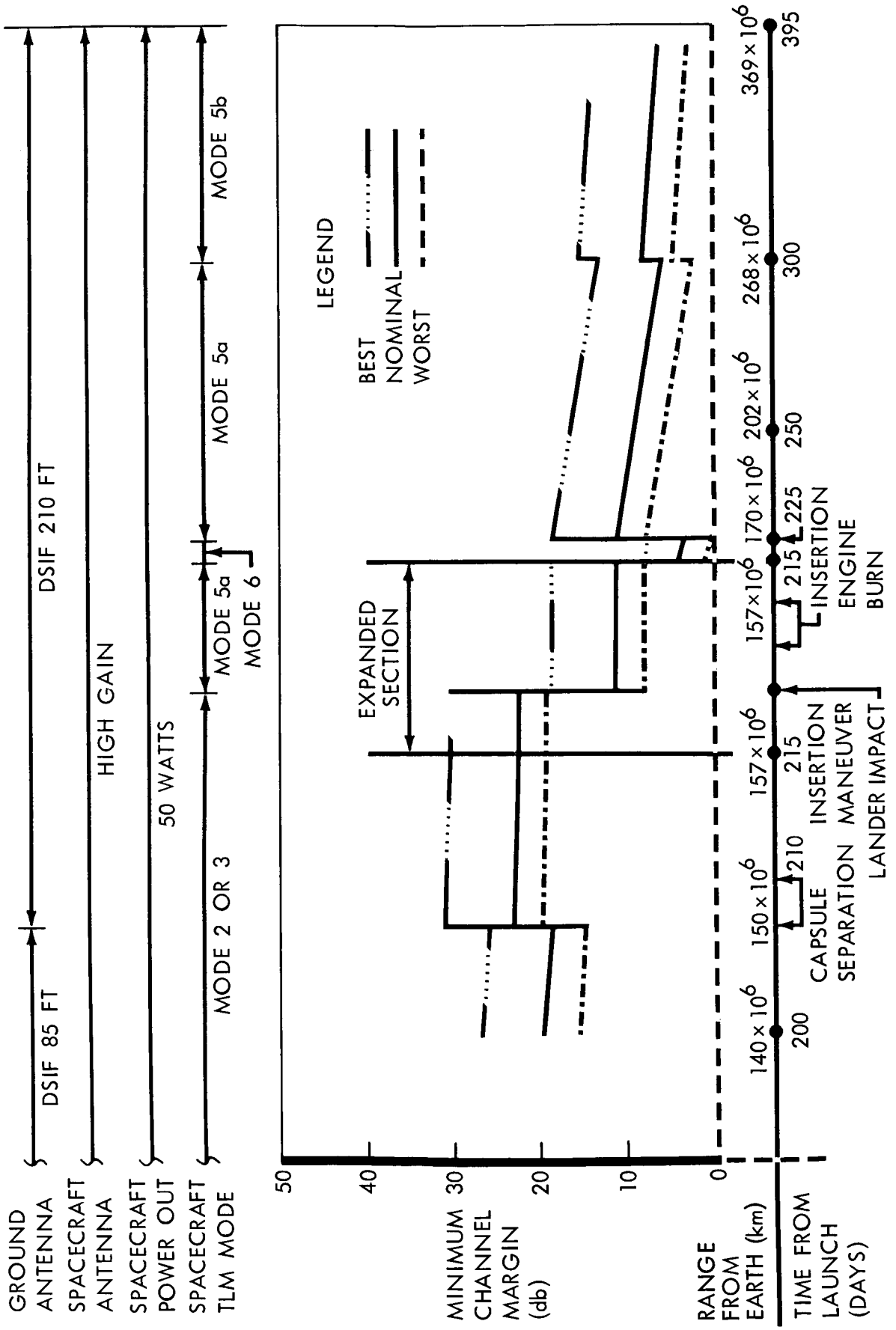

Figure 4.1-7: Telemetry Link Performance

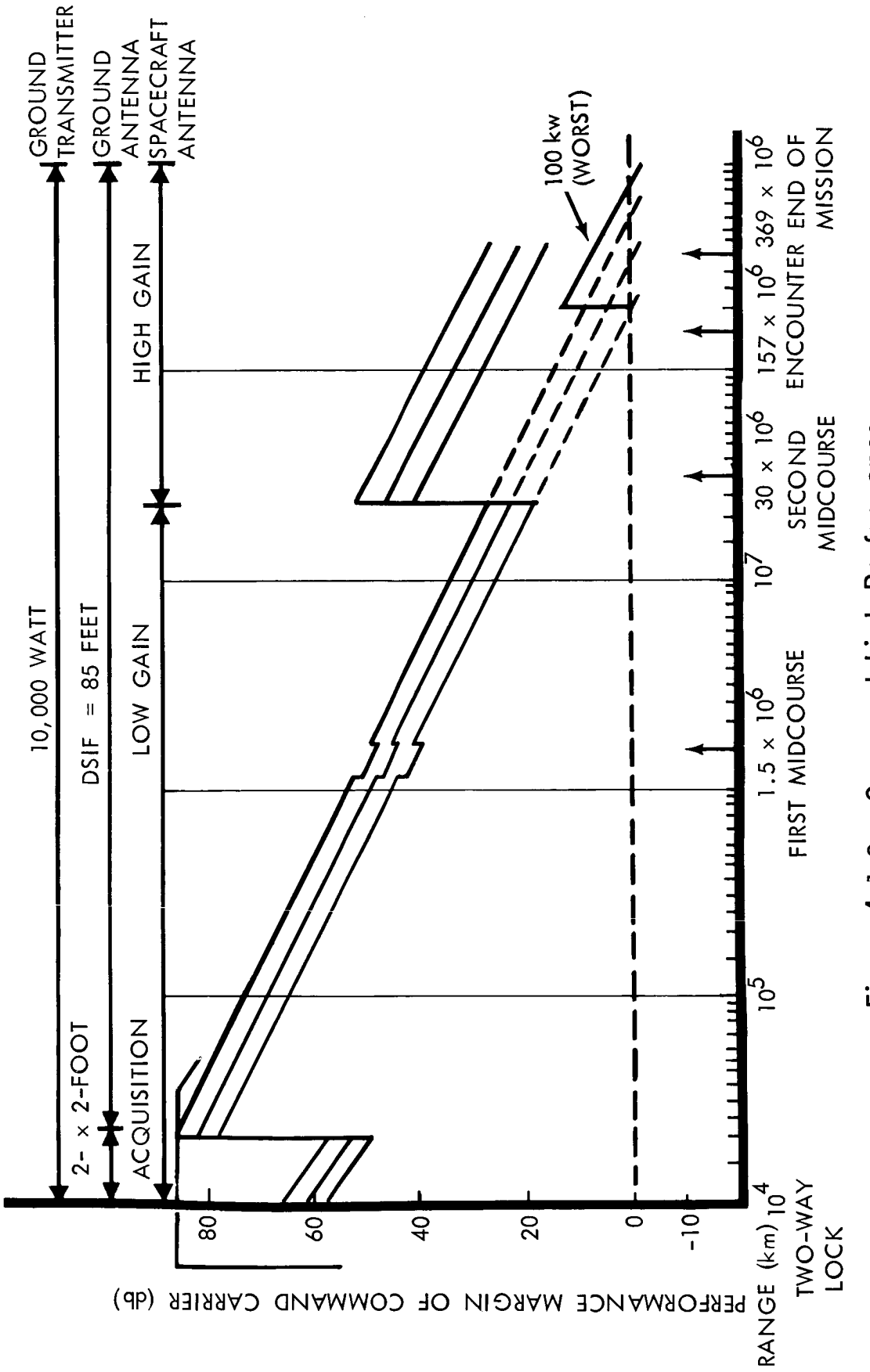

Figure 4.1-8: Command Link Performance

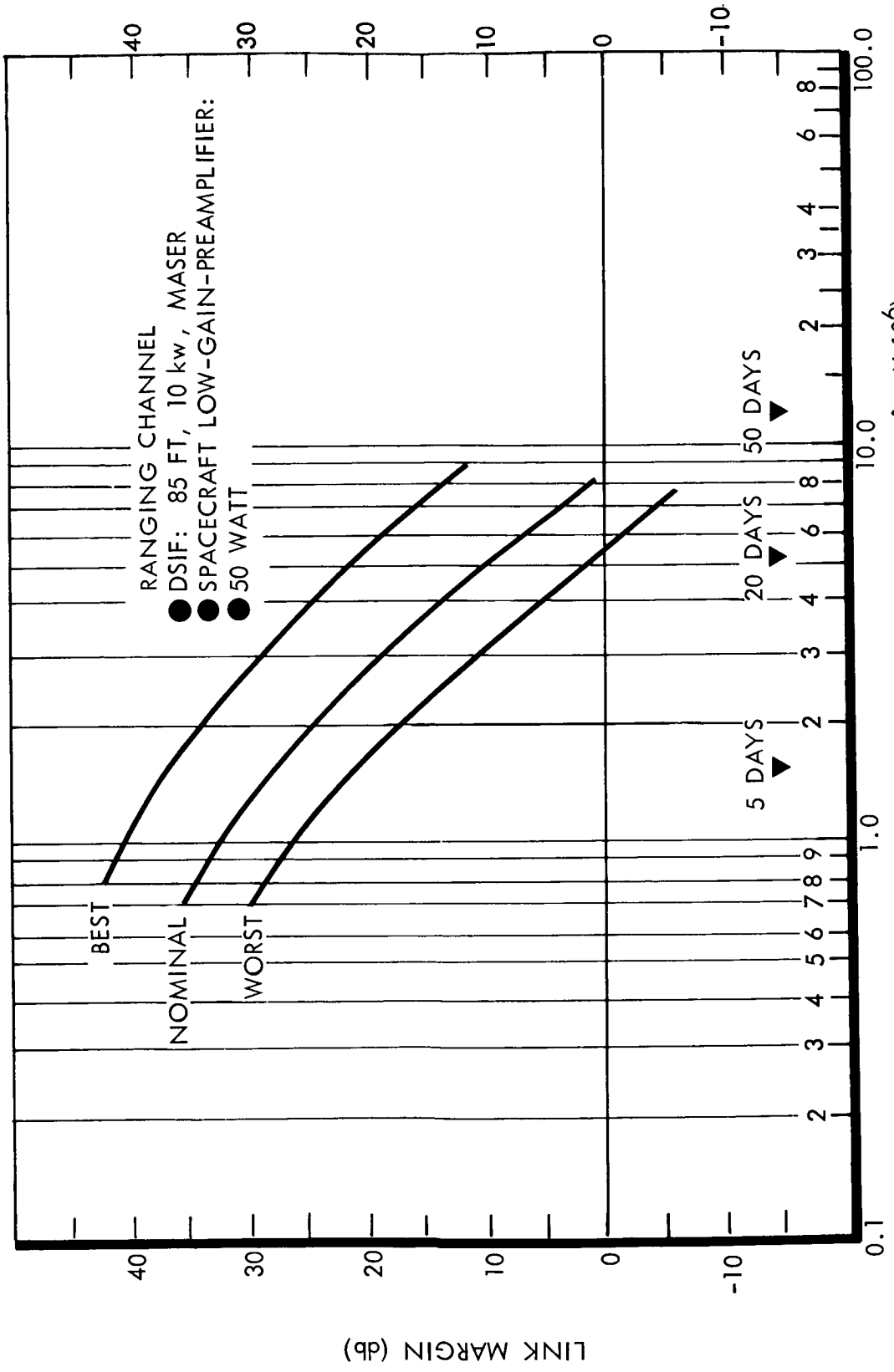

Figure 4.1-9: Voyager Ranging Link

As discussed in Section 4.1.2.3, Mode 5 will provide high margins for the transmission of planetary science data throughout the 6-month orbital mission. Mode 6 provides the capability to transmit planetary science data in real time for a minimum of 10 days after orbit insertion under conditions of worst case commication link tolerances. Under the most favorable conditions this capability could extend throughout the 6-month orbital mission; however, if nominal conditions prevail, communications using this mode will be limited to about 73 days of orbital operation. The decision to use this mode after 10 days must therefore be based on assessment of the link operating conditions.

Command Margins--Figure 4.1-8 shows that the planned use of the spacecraft high-gain antenna after 80 days results in more than sufficient margin to permit 10-kw transmitter operation for the whole mission. If the high-gain antenna should fail, positive link margins are provided by the spacecraft low-gain antenna and 10-kw transmitter until encounter and for the entire mission when used in conjunction with the 100-kw transmitter.

Ranging Margins--Figure 4.1-9 shows that simultaneous ranging and transmission of data in Mode 1 is provided up to a range of 5.3×10^6 kilometers.

4.1.2.5 Physical Characteristics and Constraints

Size, Weight, Power, and Thermal Characteristics--The size, weight, power and thermal characteristics of the telecommunication subsystem spacecraft assemblies and constituent components are listed in Table 4.1-4. Figure 4.1-10 defines the mission power profile for the telecommunications subsystem.

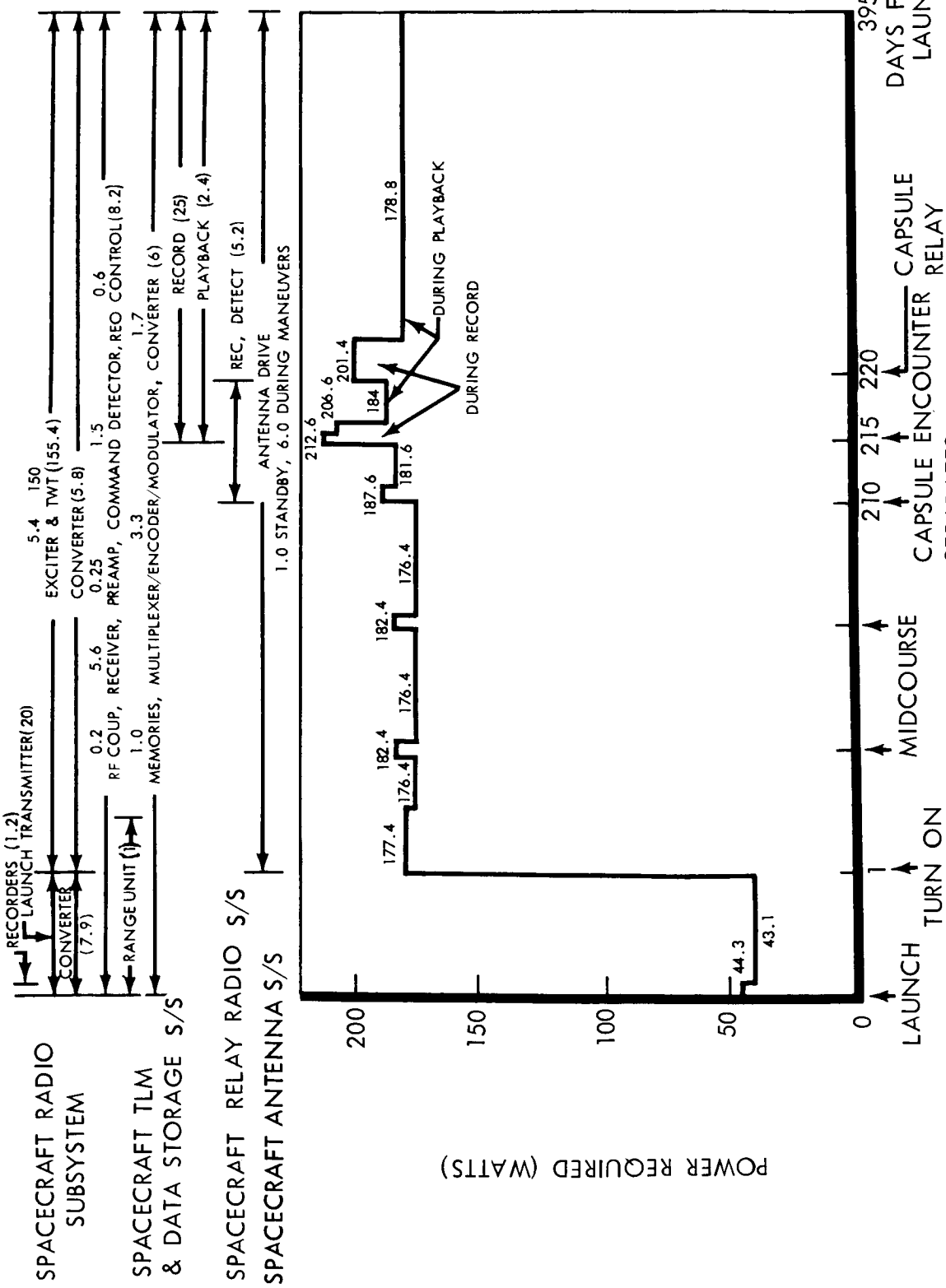

Figure 4.1-10: Spacecraft Telecommunication Subsystem Power Requirements

Magnetic Characteristics--The traveling wave tube of the telecommunications system presents the major source of magnetic interference in the spacecraft, however the ferrite switches and circulators used in the rf circuits also contribute. The magnitude of the fields introduced by these components at the magnetometer will be minimized by orienting and/or compensating the various components to produce, effectively, high order multipole fields and to minimize the residual dipole field. For example, data supplies by Hughes (Technical and Cost Proposal, R-5431, Hughes Aircraft Company, Microwave Tube Division), indicates that fields of less than one gamma are possible, in specific directions, at distances of 40 inches when their travelling wave tube is magnetically compensated. Magnetic components in each subsystem are evaluated and discussed in Section 4.1, D2-82709-2.

Operating Constraints--The following shall apply.

Maximum Communication Range--The maximum required communication range shall not exceed 3.70×10^8 kilometers.

High-Gain Antenna Pointing--The peak radiation vector of the high-gain antenna shall be aligned with the Earth probe line to within approximately 1.0 degree at encounter plus 6 months (1.0-decibel pointing loss).

Spacecraft Occultation--During the period when communication is required, neither the target planet nor an appreciable part of its atmosphere shall pass between the spacecraft and Earth.

Midcourse Capsule Separation and Orbit Insertion Maneuvers--The event sequence for maneuvers is presented in detail in Section 3.9. When

communication to Earth is via the low-gain antenna, the initial roll maneuver may cause momentary loss of communication if the pattern null passes through the line of sight to Earth. Maneuvers must be planned to limit low-gain antenna pointing losses to not more than 1 decibel at the terminal position of any individual axis attitude change. Section 4.1.3.4 describes the antenna pattern.

The high-gain antenna will not track the Earth during roll maneuvers of any sequence. Time is allowed for reacquisition at the end of each roll maneuver when the high-gain antenna is in use. The high-gain antenna can be slewed to maintain continuous orientation to Earth during yaw maneuvers. The high-gain antenna pointing problem during maneuvers is described more fully in Section 4.1.3.4, Spacecraft Antenna Subsystem.

Radio Frequency Interference--All spacecraft components are to comply with JPL 30236A. Furthermore, spurious signals coupled to the S-band receiver inputs must be less than -162 dbm for coherent signals and -184 dbm/cps for non-coherent signals in the 2115-$\pm$ 5-megacycle band. Spurious signals coupled into the VHF receiver must be less than -140 dbm for coherent signals and -170 dbm/cps for noncoherent signals in the 100 $\pm$ 1 megacycle band.

Packaging Characteristics--The following component packaging approaches will be used for the spacecraft elements of the Telecommunication System.

Digital and video circuits will be packaged in encapsulated modules of standard sizes as defined by Standard 2-10849. These modules are assembled

to form the subsystem components by attaching them to the component chassis and interconnecting them by means of multiple lead wiring panels. Connections to the wiring panel as well as all module internal connections will be welded.

A flat-pack-module configuration, as illustrated in Figure 4.1-11, will be used for microelectronic circuits. This module consists of a group of printed circuit assemblies stacked upon a standardized header assembly. Flat-pack integrated circuits are welded directly to the module etched-circuit boards which are in turn welded to risers leading to the external terminals.

Analog circuits will be packaged cordwood fashion, using mylar substrates for routing and support, with interconnections resistance welded to either the part leads or gold-plated Dumet risers. Nickel ribbon is known to be acceptable for the interconnections from an assembly and process standpoint; however, it is undesirable from a magnetic interference standpoint. Alternate materials will be considered.

Modular construction is also used for radio frequency circuits. The size of a module is dependent upon the many requirements that constitute the total design; however, a given modular subassembly will never be less than an individual functional portion of the circuit.

Figure 4.1-12 shows the packaging approach for a typical IF amplifier. The module consists of a gold plated aluminum frame onto which are cemented

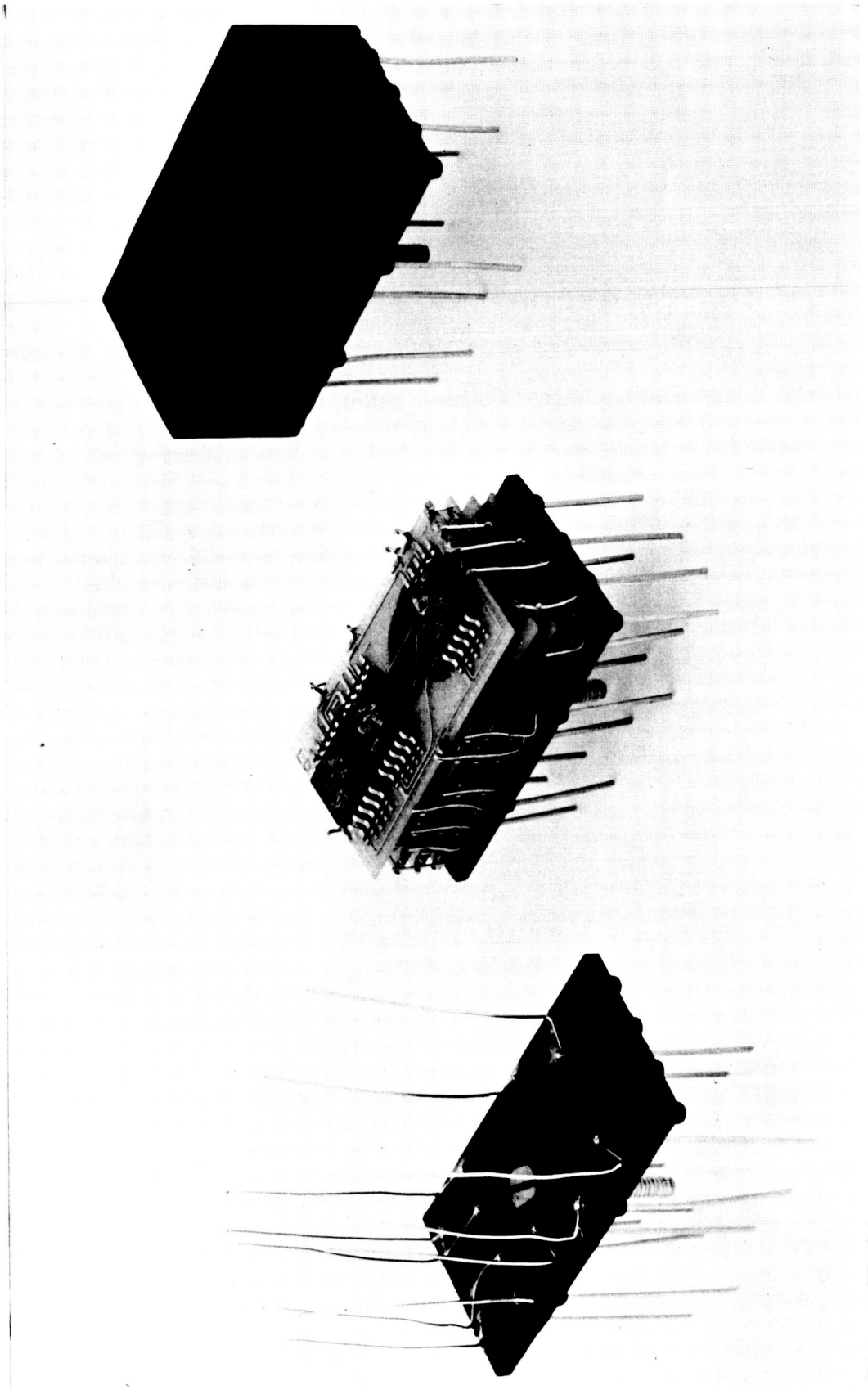

Figure 4.1-11: Typical Flat-Pack Module Configuration

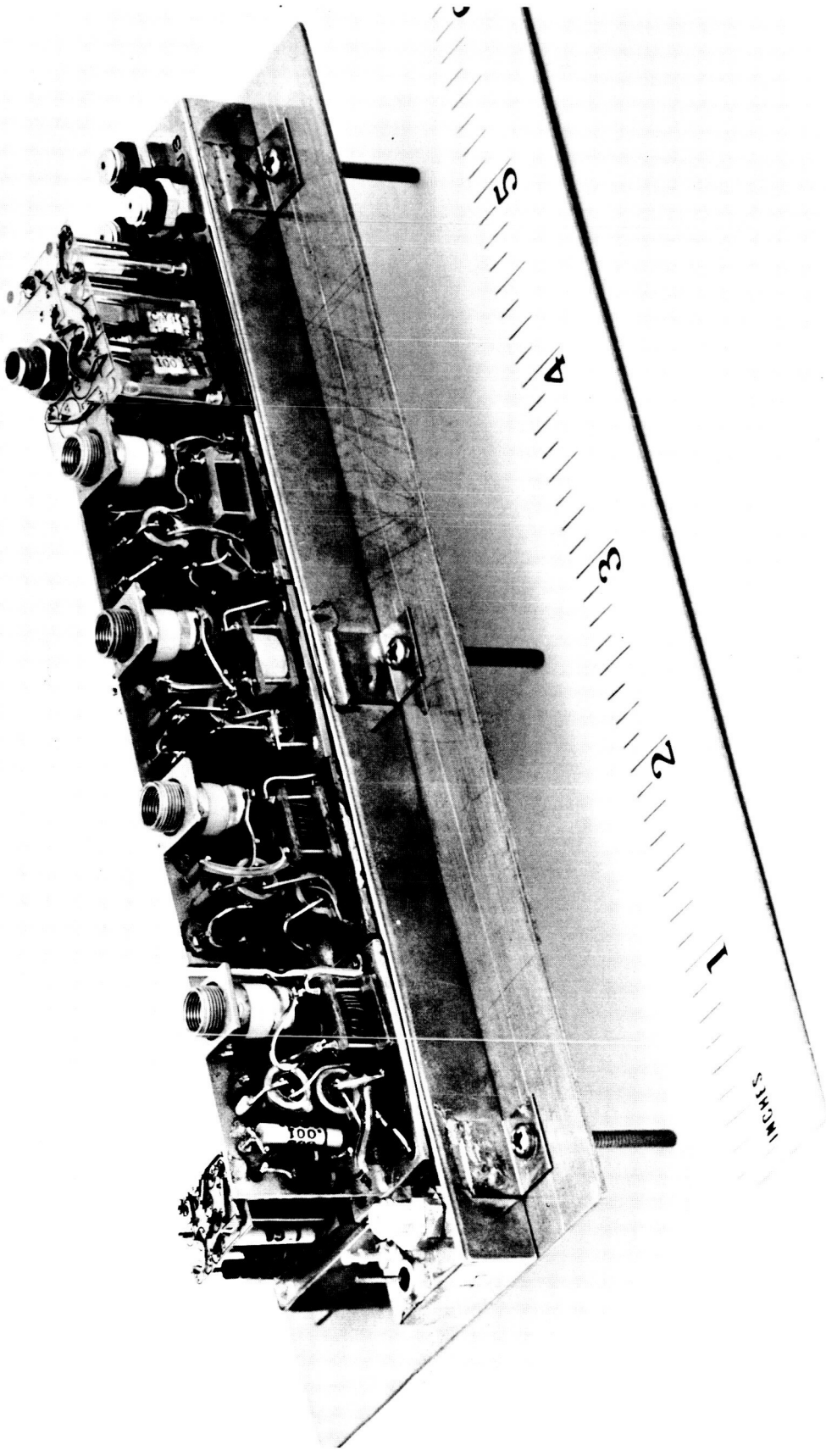

Figure 4.1-12: Typical if Amplifier Configuration

the electronic components. The metal frame also contains the mechanical components required for mounting the module and acquiring electrical continuity through the partitioning web and through the mounting flange. The electronic parts are interconnected by the use of a miniature resistance welding techniques. The inter-connection ribbons are wired from point to point. This three-dimensional wiring technique, a departure from the usual welded module matrix or plannar technique, is used to obtain the shortest lead lengths possible.

An electroformed copper shielding cover is placed over the assembly and soldered to the mounting flange. The module is encapsulated with a lightweight, low-dielectric-constant, polyurethane foam.

Interconnections between radio-frequency modules are made by welding short jumper wires from one module to the next.

Components are assembled into assemblies depending upon functional requirements. The assemblies will be either 8 by 8 by X inches or 8 by 16 by X inches and will use standard mounting flanges for attachment to the spacecraft structure.

State of Development--These packaging approaches are based on proven techniques used by Philco, on the JPL Sequence Generator, the Space Radiation Monitoring System for the Air Force Special Weapons Center, and a lightweight S-Band Deep Space Transponder.

4.1.2.6 Safety Considerations

High Voltages--Precaution must be exercised in handling the rf power amplifiers while operating due to the presence of high voltages.

Electromagnetic Radiation--Personnel must be prohibited from areas where the electromagnetic fields radiated by the telecommunication subsystem antennas exceeds 0.01 watt per square centimeter.

Prelaunch Testing--Precautions must be taken to ensure that the high-power rf power amplifier is not operated when the presence of rf energy might create a hazard to pyrotechnic devices. In addition, all requirements of ETR Range Communication Instructions, particularly frequency scheduling, RCI, 30-29 must be complied with.

4.1.3 Spacecraft Telecommunication Subsystems

This section describes characteristics of the subsystems that comprise the spacecraft element of the telecommunication system. These characteristics are defined in terms of functions performed by these subsystems and the features of a design to perform these functions.

4.1.3.1 Spacecraft Radio Subsystem

Functional Description--The spacecraft radio subsystem described in this section performs the following functions:

1) Receive and demodulate the rf phase modulated command signal of the DSN
2) Detect the synchronization signal and the command word bits and direct to the command decoder of the central computer and sequencer (CC&S)
3) Receive, phase lock-on, and track the DSN command carrier frequency
4) Coherently convert the received carrier frequency by a 240/221 ratio and retransmit this frequency as the telemetry carrier
5) Demodulate the range code video information transmitted from the DSN on the command frequency carrier and modulate the telemetry carrier with this information for retransmission to the DSN
6) Receive a modulation baseband consisting of PN sync and/or data subcarrier(s) from the telemetry and data storage subsystem for application to the telemetry carrier

The following paragraphs discuss the operating modes, subsystem configuration, switching logic, and component implementations that have been selected to meet these functional requirements.

Modes of Operation--To accomplish the above functions the following modes of operation will be provided:

RF Transmission Modes--There will be two levels of rf power for spacecraft data transmission:

1) Low-power level (1 watt) for transmission of data from launch to completion of outgassing
2) High-power level (50 watt) for transmission of data in all modes after outgassing is completed

Phase Control Modes--The control of the unmodulated phase and frequency of the transmitted rf carrier will have two modes, noncoherent and coherent. When the transponder receiver is not receiving a signal, the phase and frequency of the unmodulated transmitted carrier will be controlled by a crystal oscillator. When the transponder is locked to a ground signal, the phase and frequency of the unmodulated transmitted carrier will be 240/221 times the phase and frequency of the unmodulated received carrier.

Ranging Modes--The video channel for the operation of "turn-around" ranging will be enabled and disabled by command.

Antenna Operating Modes--The following antenna operating modes will be provided:

1) Receive on low-gain, transmit on ascent antenna;
2) Receive and transmit on low-gain antenna;

3) Receive on low-gain, transmit on high-gain antenna;

4) Receive and transmit on high-gain antenna.

Subsystem Configuration--The preferred design for the radio subsystem is indicated in Figure 4.1-13. The design uses components presently designed (Mariner C equipment preferable) to the maximum extent possible.

The 50-watt travelling wave tube requires significant development effort. Three qualified suppliers (1,2,3) have presented data to show that reasonable extrapolation of existing 20-watt S-band designs will result in a design capable of development freeze by July 1, 1966. Copies of these proposals are included with this report as backup data. Detailed schedules showing the necessary milestones for the development of a TWT during Phase IB are provided in Section 5.0 of this report. The program approach will be to subcontract further development to one or two of the vendors who already have 20-watt S-band tubes under development. The cathode structure will be scaled to provide the necessary current density and three engineering prototypes will be constructed and tested. Laboratory results will be compared with results of analytical studies

[1]Watkins Johnson--Technical discussion to modify the W-J-269 or WJ-295 File No. W-J 65P-3106

[2]Eitel-McCullough "Technical Proposal for a 50 Watt Power Amplifier TWTA."

[3]Hughes Microwave Tube Division R-5341

[4]International Microwave Corp - Proposal on Tunnel Diode Amplifiers-70311.

[5]Microstate Electronics - Low Noise Preamplifier P 1 - 85A

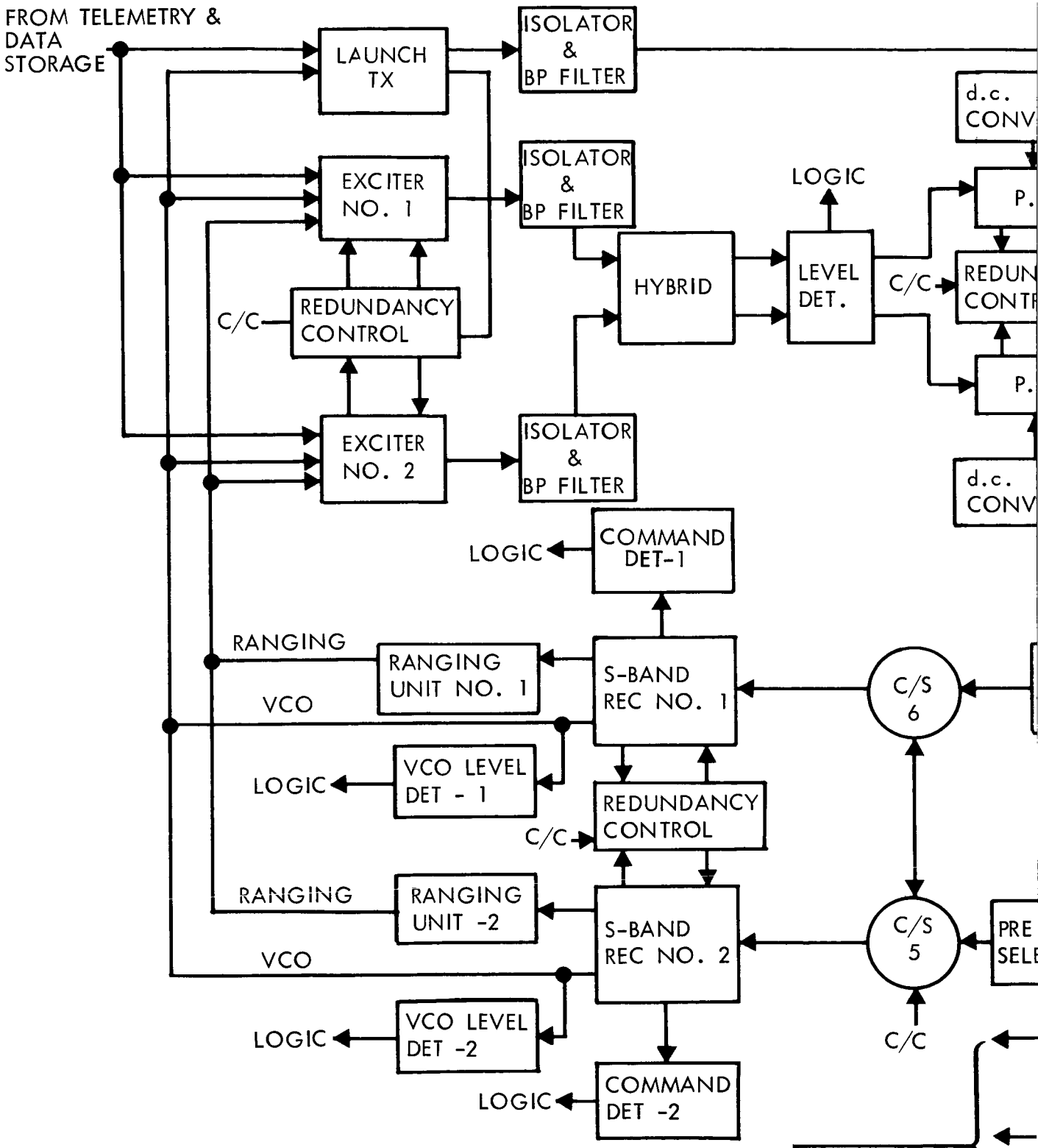
FROM TELEMETRY & DATA STORAGE
LAUNCH TX
ISOLATOR & BP FILTER
EXCITER NO. 1
ISOLATOR & BP FILTER
LOGIC
HYBRID
LEVEL DET.
C/C
REDUNDANCY CONTROL
C/C
EXCITER NO. 2
ISOLATOR & BP FILTER
d.c. CONV
P.
REDUN CONTR
P.
d.c. CONV
LOGIC
COMMAND DET-1
RANGING
RANGING UNIT NO. 1
S-BAND REC NO. 1
C/S 6
VCO
LOGIC
VCO LEVEL DET - 1
REDUNDANCY CONTROL
C/C
RANGING
RANGING UNIT -2
S-BAND REC NO. 2
C/S 5
PRE SELE
VCO
LOGIC
VCO LEVEL DET -2
C/C
LOGIC
COMMAND DET -2
1-REC-1; COMM DET.-1; RU-1
2-REC-2; COMM DET.-2; RU-1
3-LAUNCH TX; EX-1
d.c. CONVERTERS

(1)

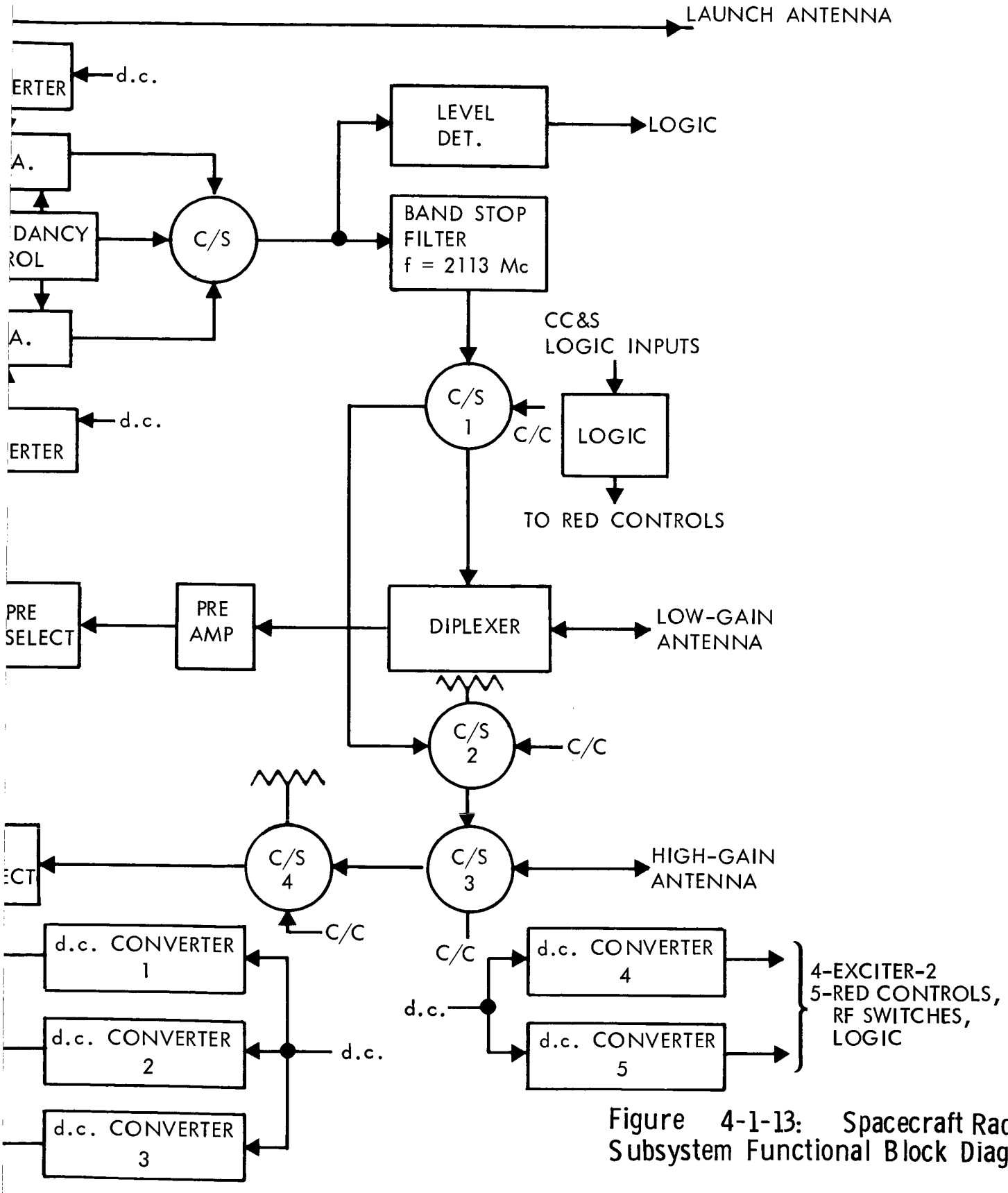

Figure 4-1-13: Spacecraft Radio Subsystem Functional Block Diagram

to estimate the mean time to fail. A review of manufacturing procedures, selection of materials, and structural integrity will extablish confidence in the chosen parameters. A design review will be held before the end of Phase IB to freeze the design concept.

The tunnel diode preamplifier requires some development effort during Phase IB. Two suppliers (4 & 5) are developing devices that show promise of meeting the Voyager requirements. This continuing work will be closely monitored.

The design provides maximum reliability consistent with available weight and power through redundant components. Specific features include:

1) S-band switching accomplished entirely by ferrite circulator switches. This approach provides the most reliable switch function even though additional sections must be added to obtain the required isolation.
2) Complete redundancy for such critical components as the receiver/command detector/ranging unit, exciters, and power amplifiers.
3) Redundancy controlled successively by internal sensing, by ground command, or by CC&S pulse (when not inhibited by receiver acquisition or internal sensing.)

Circulator switches number 2 and 4 are used to minimize interference effects from reception through the high-gain antenna when receiving on the low-gain antenna and transmitting on the low- or high-gain antenna.

Redundant exciters and 50-watt TWT rf power amplifiers provide the transmitting function after launch. A separate 1-watt solid-state transmitter is used to supply the rf power to eliminate the risk of high voltage arcing in the TWT rf power amplifier at critical atmospheric pressures.

Although it is desirable to minimize redundancy switching, the use of active component redundancy with rf equipment is generally not feasible and studies reveal that it was not possible to incorporate sufficient active redundancy within each component to meet the Voyager communication reliability needs. Section 4.1.5 contains a reliability analysis of the subsystem, and a study of the reliability of alternate configurations is contained in Section 4.1.5 of Volume B.

Switching Logic--As a design objective, first priority has been given to automatic detection and correction of component failu es. This approach reduces the need to telemeter large quantities of data to Earth for analysis and removes the command link as a series function required to accomplish the redundancy switching.

1) Antenna Switching - The objective of antenna switching logic shown in Figure 4.1-14 is to return the receiver input to the low-gain antenna in the event of antenna steering or attitude control failures.

2) Exciter and Power Amplifier Switching - Figure 4.1-14 shows the logic for activating the redundant exciters and power amplifiers. Automatic failure sensing for these components is accomplished by monitoring their rf power outputs.

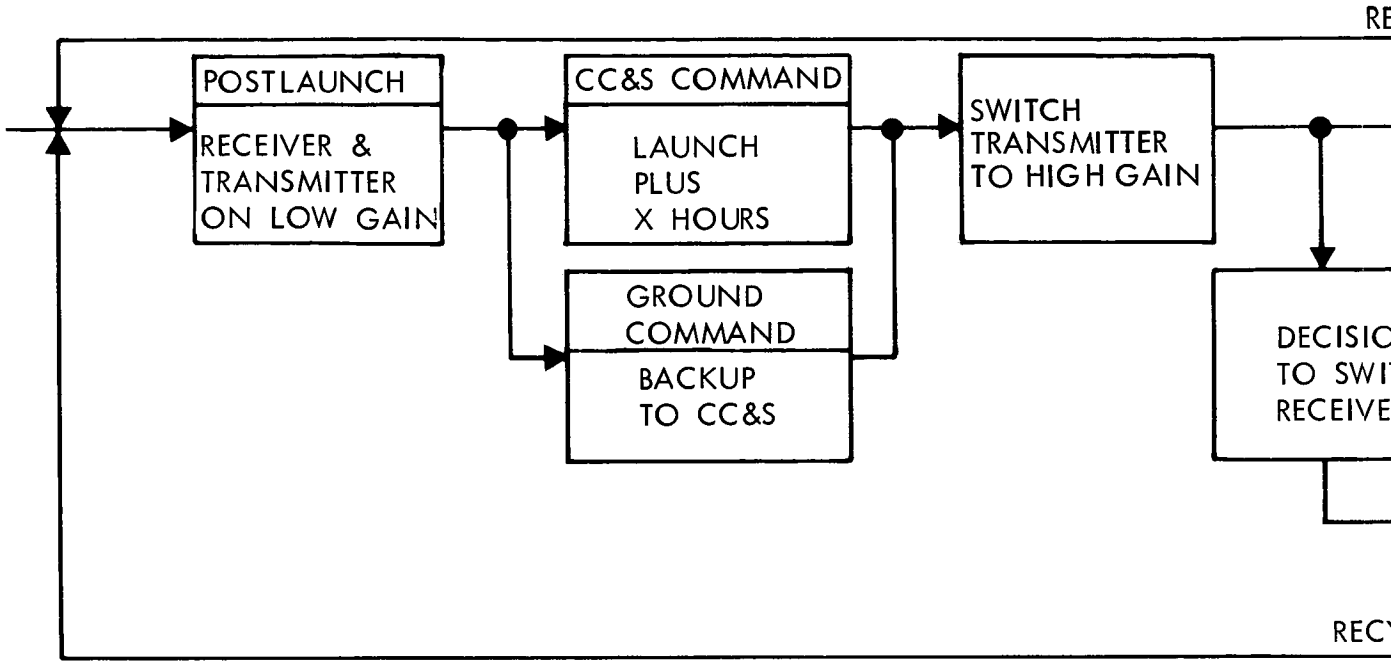

(a) ANTENNA SWITCHING LOGIC

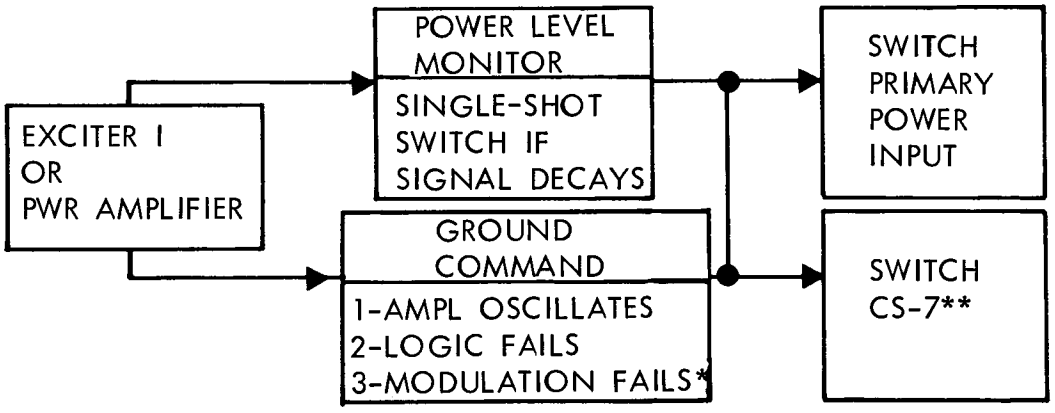

(b) EXCITER & POWER AMPLIFIER SWITCHING LOGIC

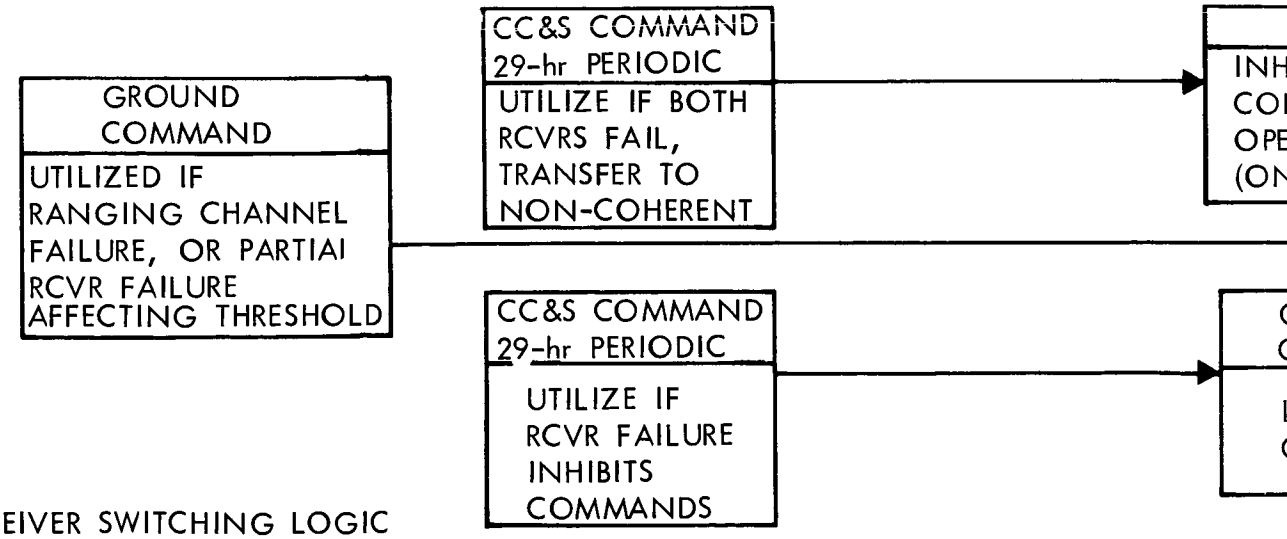

(c) RECEIVER SWITCHING LOGIC

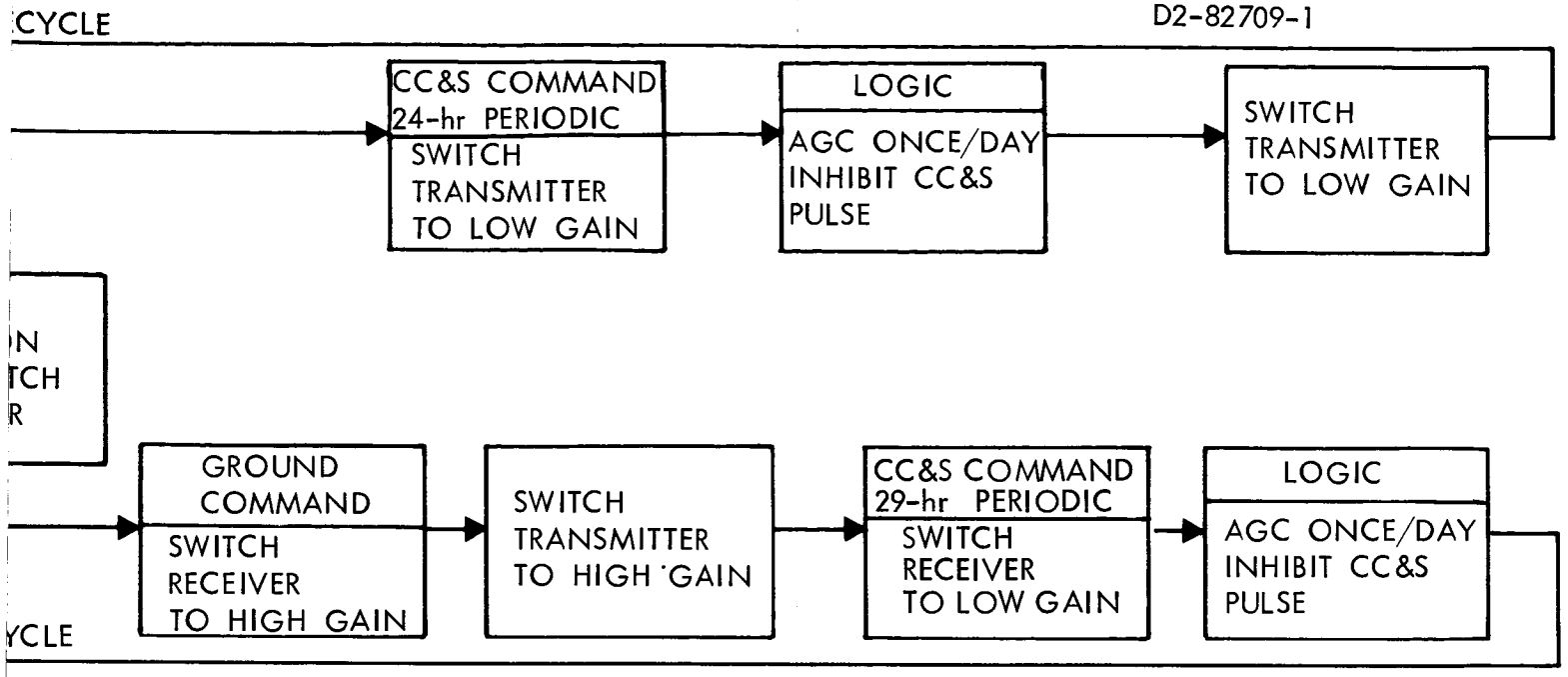

* EXCITER ONLY
** PWR AMPLIFIER ONLY

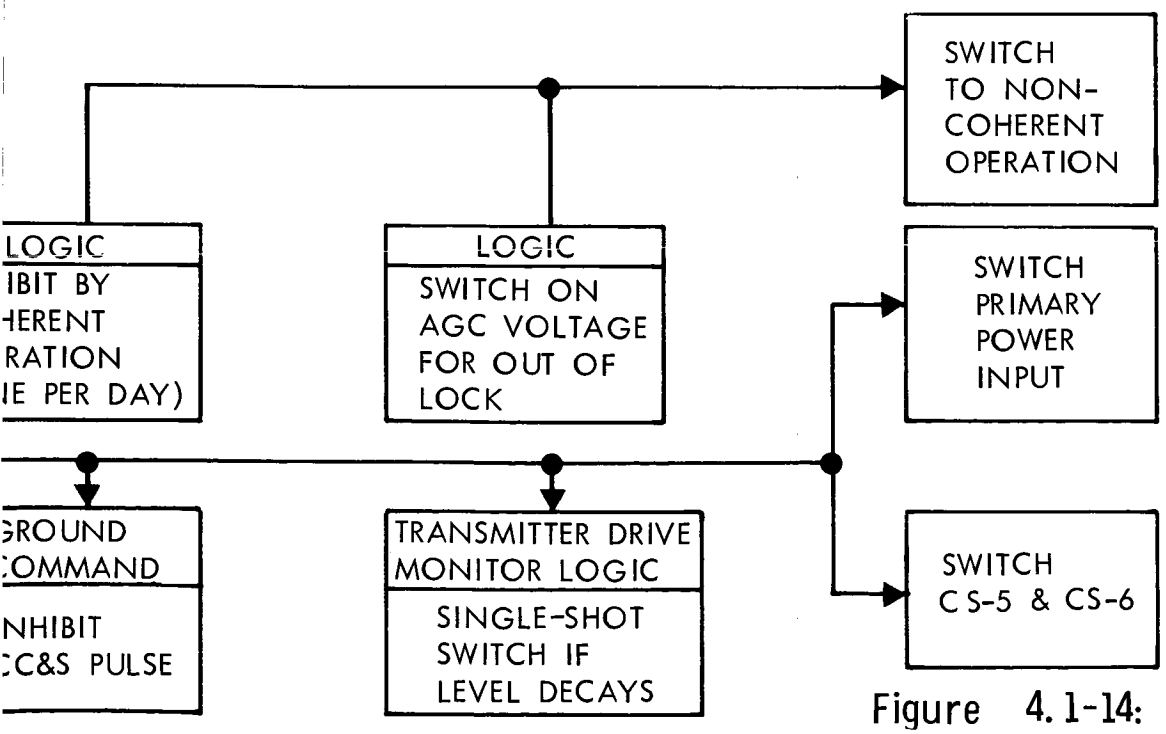

Figure 4.1-14: Spacecraft Radio Subsystem Switching Logic

3) Receiver and Command Detector - The logic shown in Figure 4.1-14 provides for switching receivers if either:

a) The receiver VCO output drops below an acceptable level

b) The capability to receive commands is lost

If the receiver is not coherently locked to the ground station during the prescribed interval, a timed pulse from the CC&S is accepted as the switching signal.

Component Descriptions

Preamplifier--The preamplifier will use a germanium tunnel diode in a four-port circulator to provide a gain of 15 db with a noise figure of 4.5 db. Further information of the selection of this device is contained in D2-82709-2.

Receiver--The receiver configuration is identical to that of the Mariner C unit, and consists of a narrowband, double superhetrodyne automatic phase-tracking device capable of receiving both ranging and command signals. The functional block diagram of the receiver is shown in Figure 4.1-15. The receiver has an input frequency of 2113 Mc, which is converted to 48 Mc in a mixer preamplifier that consists of a low noise balanced mixer followed by a solid-state amplifier. The following IF amplifier provides AGC over a 100 db dynamic range. This module also converts the IF to 9.5 Mc by mixing with a 57-Mc local oscillator signal from the voltage-controlled crystal oscillator. The signal is further band limited, amplified, and limited by the 9.5-Mc IF amplifier.

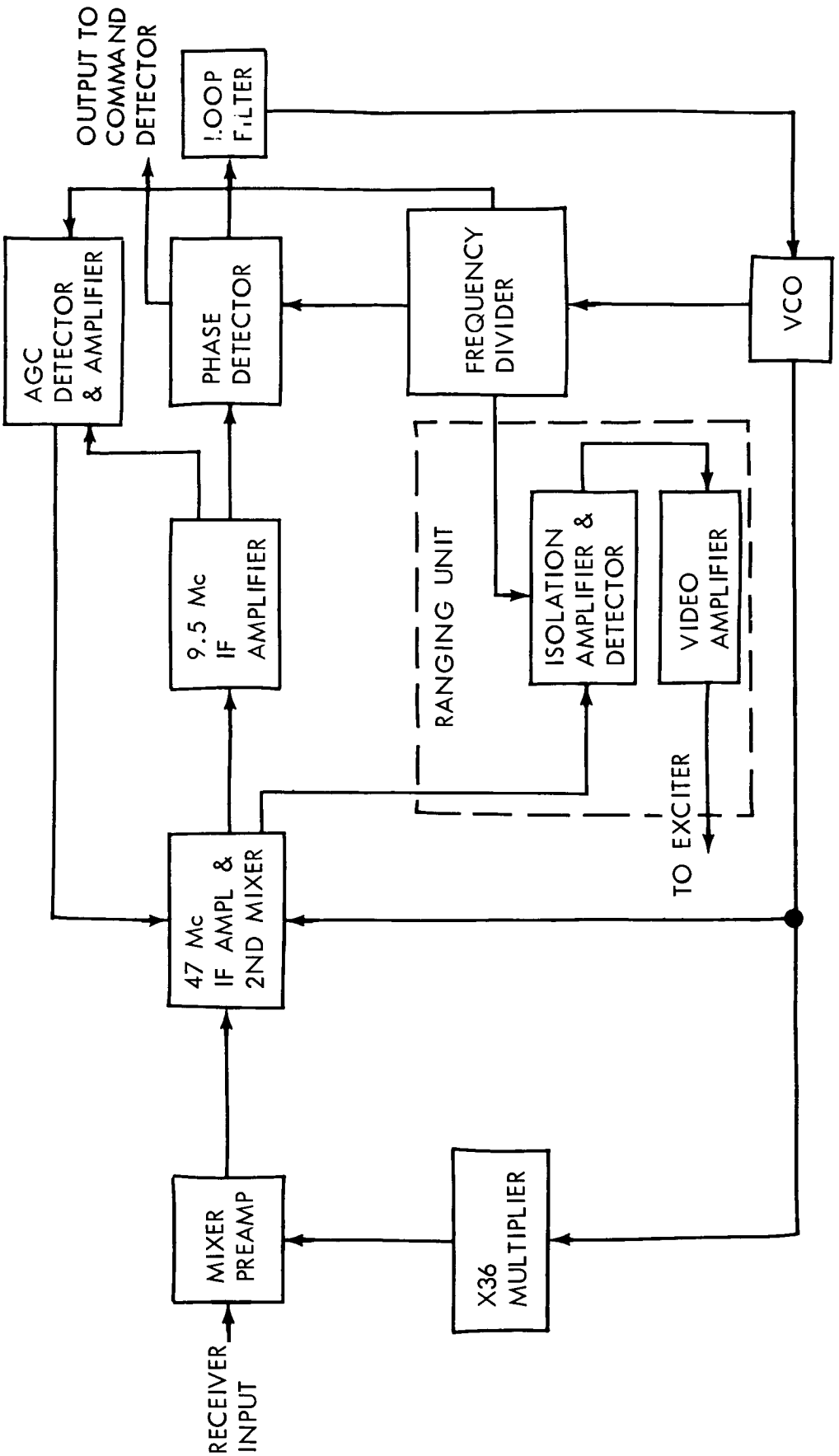

Figure 4.1-15: S-Band Receiver Block Diagram

A voltage controlled oscillator (VCO) generates all the references and local oscillator (L. O.) signals present in the receiver; therefore making the receiver fully coherent when in lock.

Both a coherent phase and AGC detector are provided for signal detection and gain control. A frequency divider is included to minimize coherent leakage from the phase and AGC detector reference channels.

Ranging Unit--The ranging unit consists of a 9.56 Mc isolation amplifier and balanced detector followed by a video amplifier. The purpose of the ranging unit is to amplify and demodulate the ranging signal received from the ground station; and amplify further, and modulate the exciter output with the baseband ranging signal. The isolation amplifier prevents coherent leakage from the detector from entering the 9.56 Mc IF.

Exciter--The exciter provides a signal source to the power amplifiers to generate the transmitter carrier and provide for modulating the carrier and switching the transmitter modes. It consists of a crystal controlled oscillator, switching amplifier (for VCO selection) and phase modulator. A transfer signal from the receiver AGC will transfer the driver from the auxiliary oscillator to the receiver VCO.

Launch Transmitter--The launch transmitter is very similar to the exciter (Figure 4.1-16), except the power output is greater. The exciter is modified by adding a push-pull amplifier stage after the power

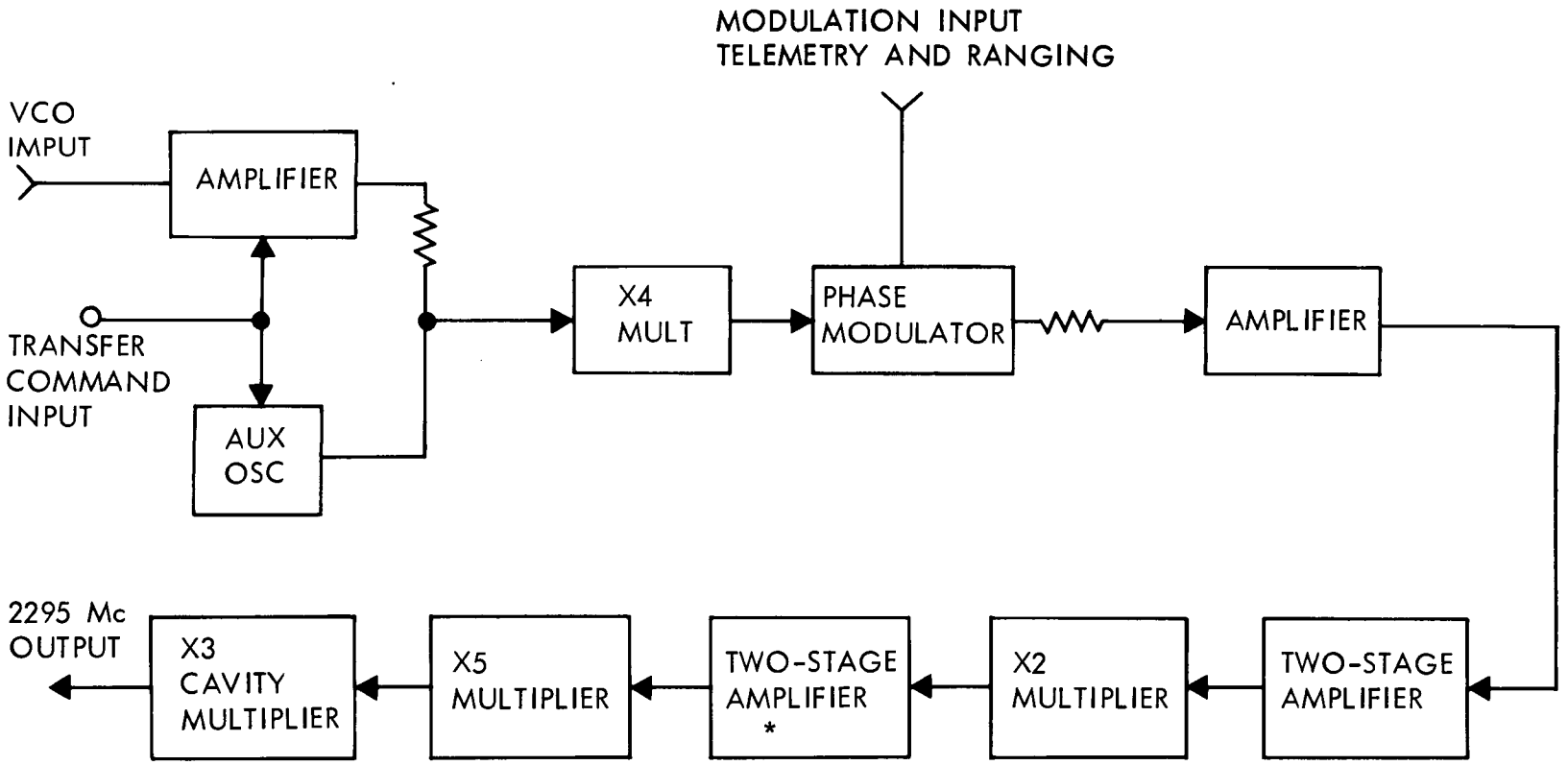

Figure 4.1-16: Launch Transmitter Block Diagram

amplifier. Only 7 or 8 db additional gain is required to reach the required output level of 1 watt. The final multiplier stages will be modified to handle the power increase.

RF Power Amplifier and Power Supply--A traveling wave tube amplifier has been established as the preferred power amplifier device. A 50-watt S-band unit with a saturated gain of 30 db operating at an overall efficiency of approximately 35 percent with depressed collector will be used.

Bandpass Filters--Bandpass filters are used at the output of the exciters and launch transmitter to minimize all spurious signals.

Isolators--A ferrite isolator is used between the exciter and the bandpass filter to provide exciter stability.

Command Detector--The single channel command detector (SCCD) detects PCM data and bit synchronization signals from a received subcarrier that is modulated by a pseudo-random synchronization code and command data. The block diagram in Figure 4.1-17 shows the SCCD as a combination of three detectors: a synchronization detector, which contains a phase lock-loop and a PN code generator as part of a correlator; a data detector; and a quadrature detector. A frequency counter controlled by the CC&S clock is included for the purpose of determining VCO frequency for telemetry transmission. This configuration is similar to the command detector supplied by Philco to JPL under Contract 950416.

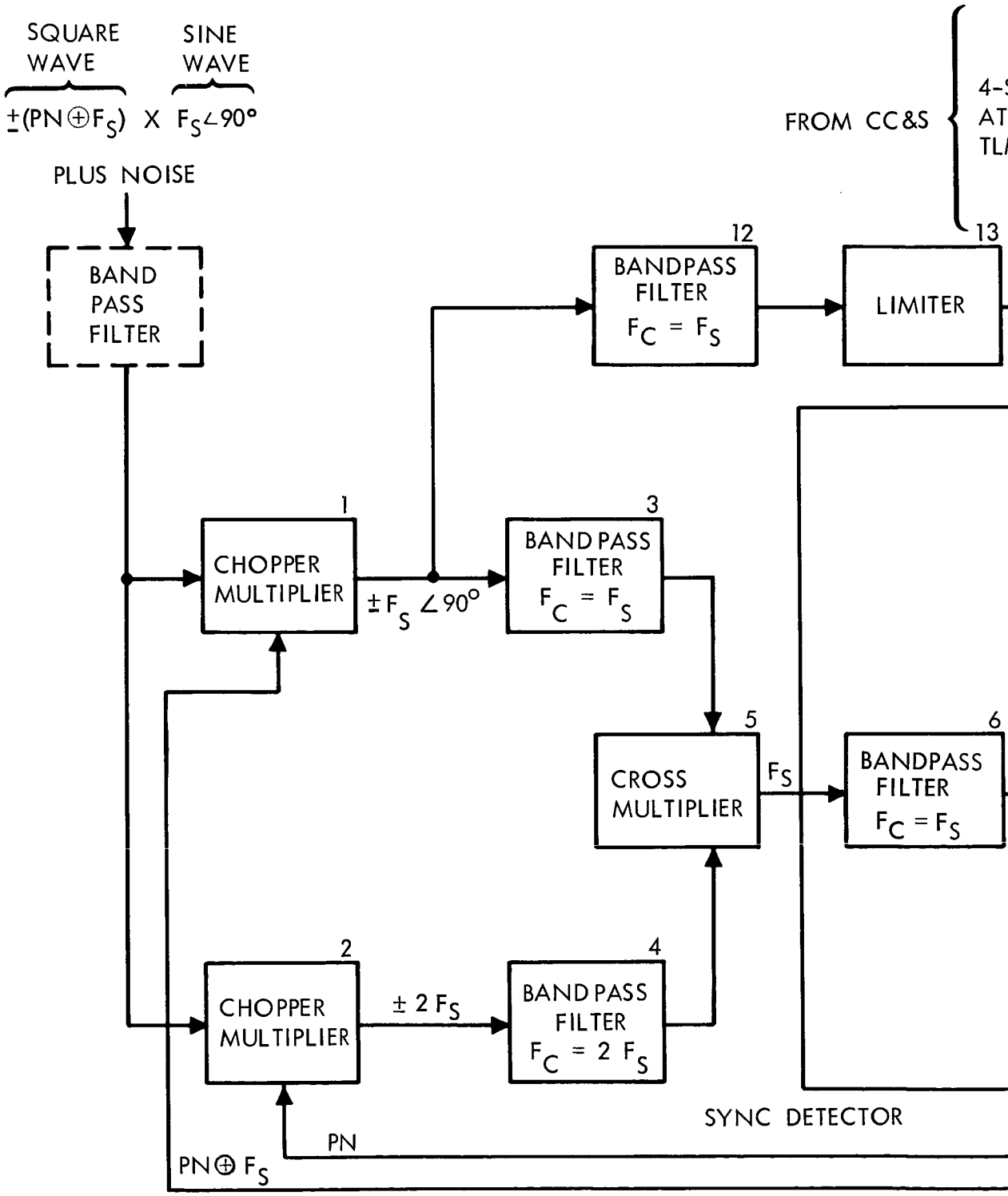
SQUARE WAVE
SINE WAVE
±(PN⊕F_S) X F_S∠90°
PLUS NOISE
BAND PASS FILTER
FROM CC&S
4-
AT
TL
12
BANDPASS FILTER
F_C = F_S
LIMITER
13
1
CHOPPER MULTIPLIER
±F_S ∠90°
3
BAND PASS FILTER
F_C = F_S
5
CROSS MULTIPLIER
F_S
6
BANDPASS FILTER
F_C = F_S
2
CHOPPER MULTIPLIER
± 2 F_S
4
BAND PASS FILTER
F_C = 2 F_S
SYNC DETECTOR
PN
PN⊕ F_S

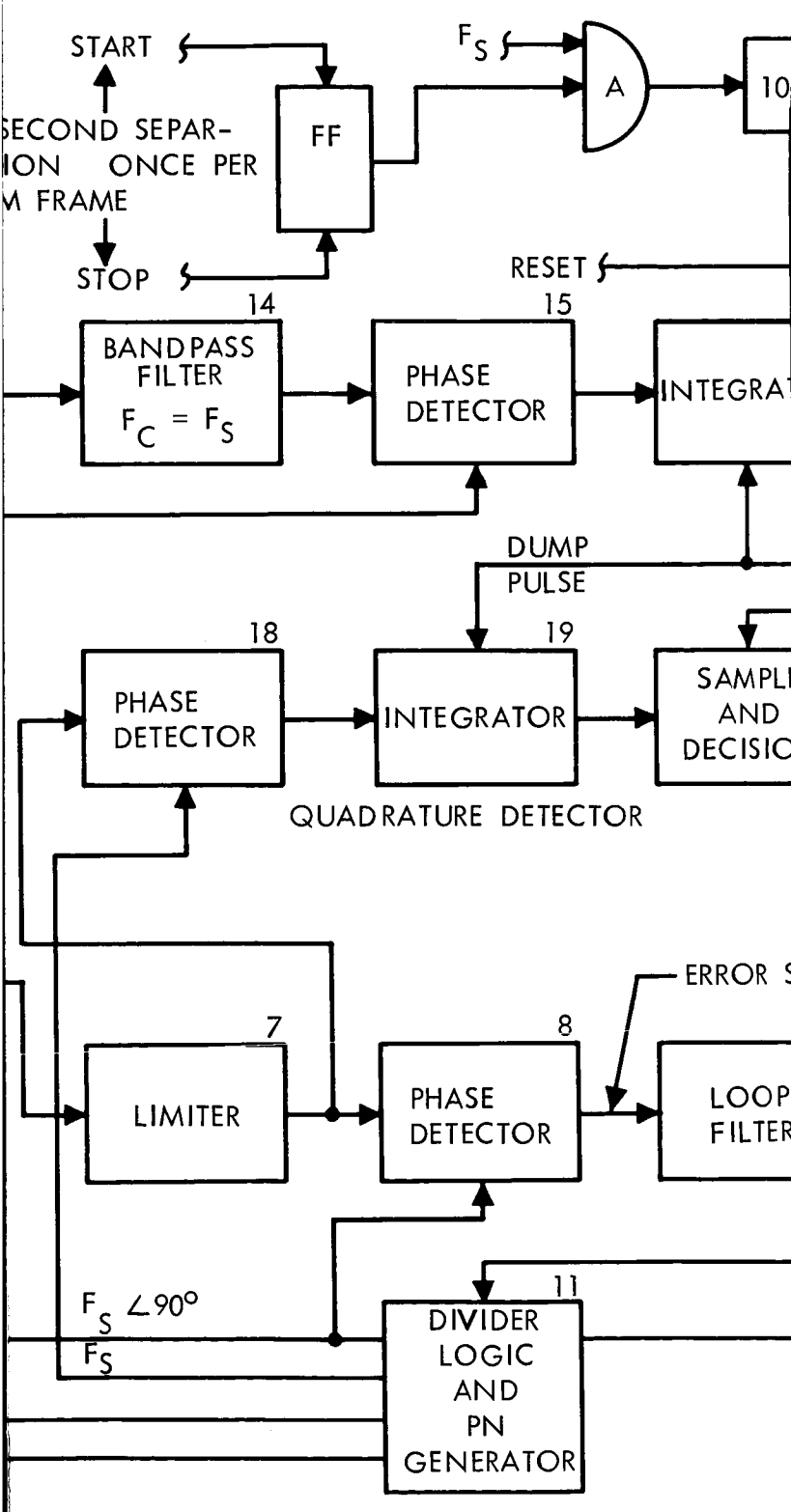
START
SECOND SEPAR-
ION ONCE PER
M FRAME
STOP
FF
F_S
A
10
RESET
14
BANDPASS
FILTER
$F_C = F_S$
15
PHASE
DETECTOR
INTEGRA
DUMP
PULSE
18
PHASE
DETECTOR
19
INTEGRATOR
SAMPLI
AND
DECISIO
QUADRATURE DETECTOR
ERROR S
7
LIMITER
8
PHASE
DETECTOR
LOOP
FILTER
$F_S \angle 90°$
F_S
11
DIVIDER
LOGIC
AND
PN
GENERATOR

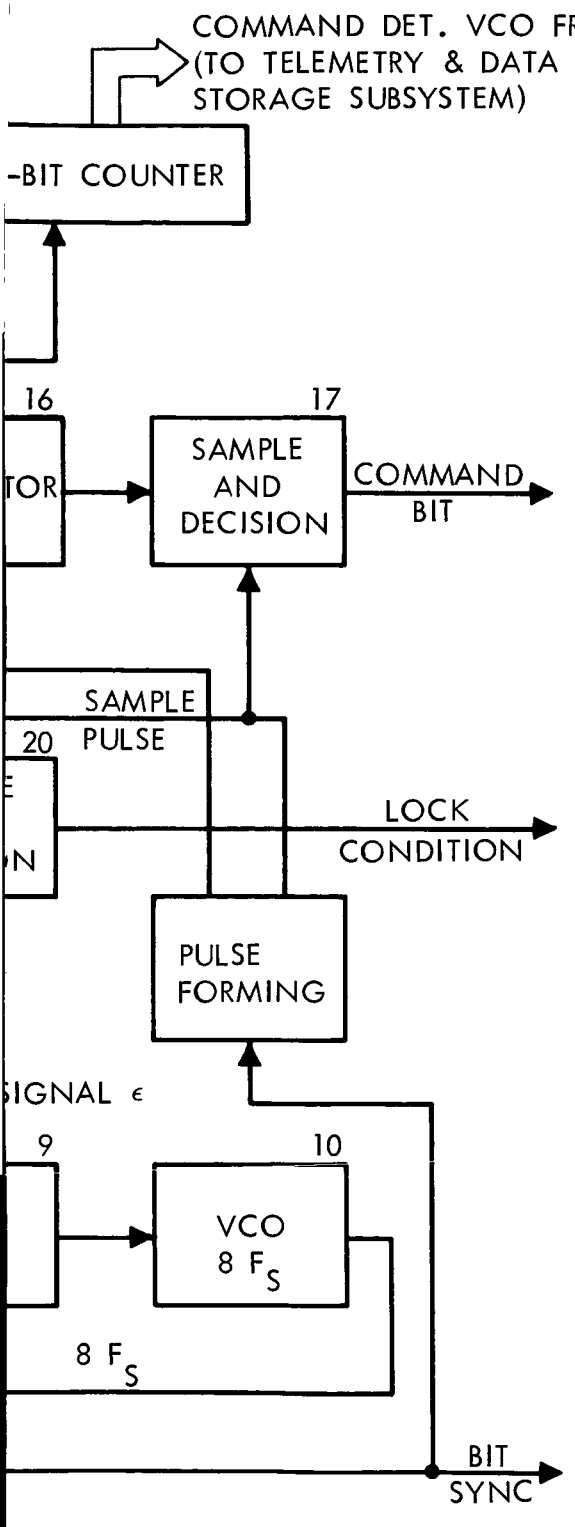

Figure 4.1-17: Command Detector

DC-to-DC Power Converters--The dc-to-dc power converters supply regulated dc voltages to the radio subsystem from the Spacecraft Bus power supply. The power converter functional design for all components (Figure 4.1-18) can be divided into the three basic functions of regulation, conversion, and filtering.

The master oscillator is normally synchronized from the CC&S clock, but operates as a free running oscillator if the synchronization signal fails. Regulation is accomplished by a pulse-width modulation technique that maintains constant volt-second pulses. These pulses drive a power amplifier that accomplishes the power switching and transformation to the appropriate voltage.

Interface Definition

Electrical Interfaces--A summary of the electrical interface characteristics between other spacecraft, subsystems, and the radio subsystem is listed in Table 4.1-5. Detailed telemetry and command interfaces are contained in Section 4.1.2.4.

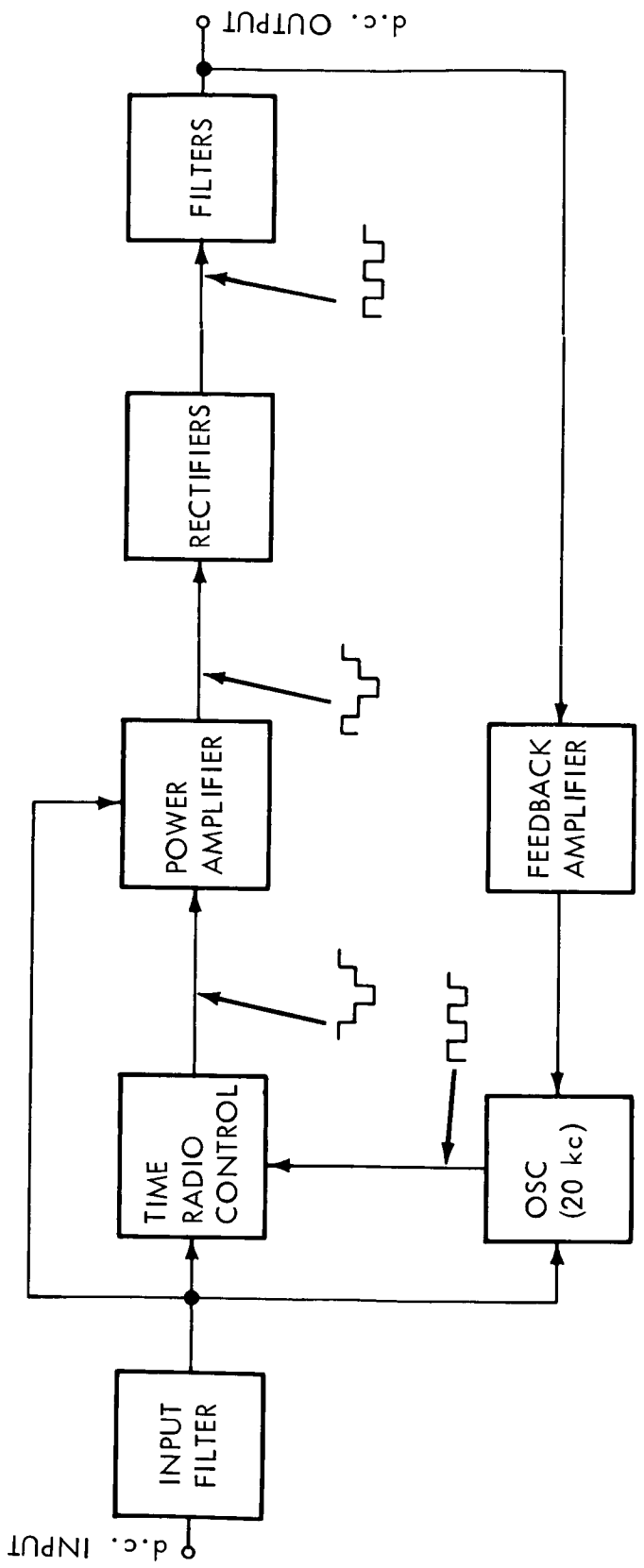

Figure 4.1-18: d.c. To d.c. Converter-Spacecraft Radio Subsystem

Table: 4.1-5 SPACECRAFT RADIO SUBSYSTEM - ELECTRICAL INTERFACES

INTERFACE	INPUT IMPEDANCE	OUTPUT IMPEDANCE	SIGNAL LEVEL	FREQUENCY
I Antenna Subsystem				
Low Gain				
Receive	50 ohms 1.3/1 VSWR	N/A	-50 to -156 dbm	2115 ± 5 Mc
Transmit	N/A	50 ohms 1.3/1 VSWR	+47 dbm	2295 ± 5 Mc
High Gain				
Receive	50 ohms 1.3/1 VSWR	N/A	-50 to -151 dbm	2115 ± 5 Mc
Transmit	N/A	50 ohms 1.3/1 VSWR	+47 dbm	2295 ± 5 Mc
Omni Launch	N/A	50 ohms 1.3/1 VSWR	+30 dbm	2295 ± 3 Mc
II CC&S Subsystem				
Detected Commands VCO Counter Start Stop Reset	N/A	1,000 ohms	3.7V for a one 40.4V for a zero	1 BPS
Control Commands (see Section 4.1.2.4)	1,000 ohms	N/A	1 volt peak	100 ms Pulse
III Telemetry & Data Storage				
Subsystem Modulation	1,000	N/A	N/A	Subcarrier Frequencies 50 cps to 614.4 kc
Measurements (see Section 4.1.2.4)	N/A	1,000 ohms	0 - 5 VDC	dc

Table 4.1-5 (continued)

INTERFACE	INPUT IMPEDANCE	OUTPUT IMPEDANCE	SIGNAL LEVEL	FREQUENCY
IV Power Converters				
Receiver/Detector	N/A	N/A	35 ± 1.75 Volts	DC
Exciter	N/A	N/A	35 ± 1.75 Volts	DC
Power AMP	N/A	N/A	35 ± 1.75 Volts	DC
Logic/Switching	N/A	N/A	35 ± 1.75 Volts	DC

Mechanical Interface--See Section 4.1.2.6 for sizes of spacecraft assemblies. Equipment installation arrangement is shown in Section 3.1.

Thermal Interfaces--Thermal interface criteria are listed in Section 4.1.2.6. A major thermal problem arises from the 100 watts of heat dissipated by the power amplifier. Special mounting provisions and thermal control design measures have been taken which assure operation within required temperature limits (see Section 4.4). During the short period (in the boost phase) when the amplifier is not operating due to the out-gassing-arcing problem, standby heat is needed to prevent the unit from cooling below its lower limit.

Performance Parameters--Performance parameters for each key component are listed in Table 4.1-6.

PREAMPLIFIER

Center Frequency: 2115 + 5 Mc
Bandwidth (3 db) : 50 Mc
Gain : 15 ±1 db
Gain Compression : 2 db @ -65 dbm
Failure Rate: 0.095%/1000 hrs

RECEIVER

RF Frequency: 2115 Mc Nominal
Frequency Tracking Range : ±60 kc
Noise Figure : 10, +0, -2 db
Threshold: -151, +2, -1 db
Dynamic Range: -70 dbm to threshold
APC Loop Bandwidth: 20 cps threshold
267 cps Strong signal
AGC Noise Bandwidth: 1.0 cps threshold
2.0 cps at -70 dbm
Modulation Frequency Response : -1.5 db from
100 cps to 2.0 kc
Residual Phase Modulation: 3^{o} peak at -70 dbm
Failure Rate: 1.285%/1000 hrs

EXCITER

RF Frequency: 2295 Nominal
Power Output : 250 mw
Power Variation: ±1.5 db
Phase Control: Auxiliary OSC or
Receiver VCO
Aux. OSC Frequency Stability: $\pm 10^{-7}$ short term
$\pm 10^{-6}$ long term
Phase Deviation Capability: ±4 radians
Modulation Frequency Response: ±3 db at 1.8 Mc
Spurious RF Outputs: 40 db below unmodulated
carrier
Failure Rate: 0.278%/1000 hrs

LAUNCH TRANSMITTER

Same as exciter except:
Power Output: 1.0 watt
Failure Rate: 0.292%/1000 hrs

POWER AMPLIFIER

Power Output: 50 watts
Saturated Gain: 30 db
Failure Rate: 2.092%/1000 hrs

DIPLEXER

Insertio
Isolatio
Failure

PRESELECTOR

Bandwi
Rejecti
Failure

BAND REJECT F

Center
Rejecti
Insertio
Failure

BANDPASS FIL

Insertio
Bandwi
Isolatio
Failure

RANGING UN

Input
Video
Output
Failure

COMMAND DE

Bit Rat
Noise
Loop
Input
Failure

CIRCULATOR SW

Insertio
Isolatio
Switch
Failure

n Loss: 0.5 ± 0.1 Receiver
0.3 ± 0.1 Transmit
n: 100 db xmtr to Receiver
40 db Receiver to xmtr
Rate: 0.010%/1000 hrs

dth (3 db): 40 Mc
on: 40 db at ±94 Mc
100 db at ±182 Mc
Rate: 0.010%/1000 hrs

ILTER
Frequency: 2115 Mc Nominal
on: 100 db over -10 Mc
n Loss: 0.3 db at 2295 Mc
Rate: 0.010%/1000 hrs.

ER
on Loss: 1.0 db
dth 30 Mc
on: 100 db at ± 182 Mc
Rate: 0.010%/1000 hrs

T
requency: 9.56 Mc
Bandwidth (3 db), 50 cps to 2 Mc
: Amplitude-limited square wave
Rise-and-fall times ∠ 140 ns
Rate: 0.0657%/1000 hrs

TECTOR
e: 1 bit/sec
Bandwidth: 2 cps threshold
Gain (strong sig.): 500
S/N (Icps): 18 db
Rate: 0.243%/1000 hrs

VITCH (3 port)
n Loss: 0.2, +0.2, -0.0 db
on: 20 db minimum
ng Power: 30 mw
Rate: 0.020%/1000 hrs

Table 4.1-6: Component Performance Parameters

CIRCULATOR SWITCH (4 port)

Insertion Loss: 0.3, $\pm$ 0.2, - 0 db
Isolation: 20 db minimum
Switching Power: 60 mw
Failure Rate: 0.040%/1000 hrs

ANTENNA INTERFERENCE

20 db minimum high gain/omni
Isolation for reception or transmission

POWER SUPPLIES

Input Voltage: 35 $\pm$1.75
Regulation: 0.5% except TWT
0.1% TWT

GENERAL

All RF components between the power amplifier output and the antenna terminals will be designed to prevent multipactor breakdown

4.1.3.2 Spacecraft Telemetry and Data Storage Subsystem

Functional Description--This section describes the functional requirements and the implementation of the Voyager spacecraft telemetry and data storage subsystem (TDSS). The design involves digitally multiplexing the outputs of several synchronous and asynchronous PCM formats into a single bit stream. All capsule and bus engineering and science data must be processed into selected transmission formats. These formats must change as a function of mission phase and communication link parameters to accommodate the changing data requirements and system constraints. The system must operate reliably for many months at interplanetary distances under a variety of environmental conditions.

All of the components selected for use in the Voyager telemetry and data storage subsystem are based on established and proven technology, however, the state of development of magnetic tape recorders with the required storage capacity necessitates a development program to integrate existing technology into flight hardware. The capability to store more than 10^8 bits on magnetic tape, and design of long-life bearings and drive mechanisms, and the development of suitable electronic circuits have been separately accomplished. During Phase IB, one or more of the suppliers who have previously developed data recorders will be contracted to assemble and test a complete unit meeting Voyager requirements. A failure analysis will be conducted to establish confidence in the optimum choice of materials, processes, and design concepts. A design review will be held resulting in a freeze of the design concept before July 1, 1966.

This subsystem performs the following functions:

1) Process spacecraft engineering telemetry data

2) Accept spacecraft scientific and capsule data

3) Store the above data as required for nonreal-time transmission

4) Multiplex and format data listed above

5) Generate subcarrier frequencies and implement the modulation requirements for transmission to DSN stations

Modes of Operation--To accomplish the above functions during changing mission phases, the telemetry and storage functions will be performed in predetermined modes. Mode configurations have been selected considering the following factors:

1) Data storage requirements when the spacecraft-to-Earth radio link is not available;

2) Bit rate requirements for the various data sources;

3) Transmission channel capacity during the mission;

4) Simplicity and reliability.

The telemetry encoding modes are listed in Figure 4.1-2.

Subsystem Definition--The preferred design of the spacecraft telemetry and data storage subsystem will provide the following minimum capabilities:

Engineering and Capsule Data Storage--For backup during maneuvers, when the telemetry link via the spacecraft high-gain antenna is not available, both the capsule data and engineering data will be recorded for transmission

at a later time. The maximum recording period will be 2 hours and at 10 bits per second, the minimum required capacity of each buffer is 72 kilobits.

Planetary Science Data Storage--If the major portion of the planetary science data is generated at or near periapsis, it is desirable that the storage capacity equal the amount of data that can be transmitted between the experiment operations. For an assumed 17-hour period of transmission at a data rate of 8,000 bits per second, 4.9×10^8 bits could be transmitted. Data storage capacities of this magnitude are not currently practical however, and tape recorders providing less capacity represent a much lower program risk and can be used with but little deterioration in mission value. Surveys of qualified vendors indicate that an increase in storage capacity from approximately 10^8 to over 10^9 may result in an order-of-magnitude increase in development complexity. For this reason two (to provide redundancy) tape recorders providing 1.1×10^8 bits of storage per recorder were selected as the preferred design. These recorders accept data from the data automation equipment at 50 kilobits per second.

Data Formats and Subcarrier Modulation--Data bit rates and modulation formats as a function of telemetry modes and mission phases are given in Figure 4.1-2. During Mode 1, engineering and capsule data are time multiplexed and transmitted at a rate of 22-2/9 bits per second on a 400 cps biphase modulated subcarrier. Synchronization is provided by means of a pseudo-noise code modulating a 200-cps square wave subcarrier. During Mode 2, engineering, capsule, and cruise science data are time multiplexed

and transmitted at a bit rate of 133 1/3 bits per second on a biphase modulated subcarrier. Mode 3 is identical with Mode 2 with the exception that stored engineering data are substituted for cruise science data. During Mode 4, only engineering data at 5 5/9 bits per second are transmitted. Modulation during this mode is the same as Mode 1 with the exception that the subcarrier frequencies for data and sync are 100 cps and 50 cps. Modes 5A, 5B, 5C and 6 are identical with the exception of the planetary science data rate. During these modes, the planetary science data are transmitted on bi-phase-modulated subcarriers at the bit rates as shown in Figure 4.1-2. During Mode 6, the planetary science recorder is bypassed and data are transmitted at the DAS output rate of 48,000 bits per second. Block encoding for the planetary science data is performed prior to subcarrier modulation. This process encodes 5-bit data into 16-bit biorthogonal code words. During Modes 5 and 6, the various data shown in Figure 4.1-2 are time multiplexed and transmitted at a rate of 400 bits per second on a bi-phase-modulated subcarrier.

The data multiplexing format for the low-frequency subcarrier channel is shown in Figure 3.6-1. The basic concept is one in which 7 bits at a time are transmitted from each data source associated with any particular mode. The transmission of 12 such words constitutes a multiplexed frame. The beginning of each frame is identified by a 7-bit Barker code for frame recognition at the receiving stations. The number of times each data source is sampled in a frame (number of 7-bit words) is proportional to the data source rate referred to the transmitted bit rate. The transmitted bit is equal to the sum of the individual bit rates.

This time-multiplexed technique does not require any consideration of individual data synchronization signals (frame sync, work sync, etc.). This is possible because the MDE equipment can reassemble data from each source by merely recognizing the Barker code frame sync and direct incoming data into memory devices allocated for each data type. The data in each memory is thus continuous as if no sampling had ever occurred. In this configuration data synchronizing signals can be detected by normal techniques. With this basic data formating technique, no more than two subcarriers are transmitted at once. During Modes 5 and 6 the planetary science word rate is synchronized to the lower subcarrier channel frequency in order to facilitate the detection of planetary science data.

Component Descriptions--The block diagram of the telemetry and data storage subsystem is shown in Figure 4.1-19.

The planetary science data is either recorded at a nominal 50-kilobit [illegible] then played back at one of three playback rates selected by the CC&S or transmitted in real time. Planetary science data is divided into 5-bit blocks. Each block is applied to the input of a 16-bit feedback shift register that transforms it into a 16-bit biorthogonally coded word. The feedback shift register output, in turn, modulates the upper subcarrier during operation in Mode 5. Use of this coding technique provides up to 2-db improvement in link margins. See D2-82709-2 Section 4.1.2 for detailed discussion.

The five lower frequency data subcarriers are obtained by bandpass filtering the appropriately divided digital signals obtained from the upper subcarrier

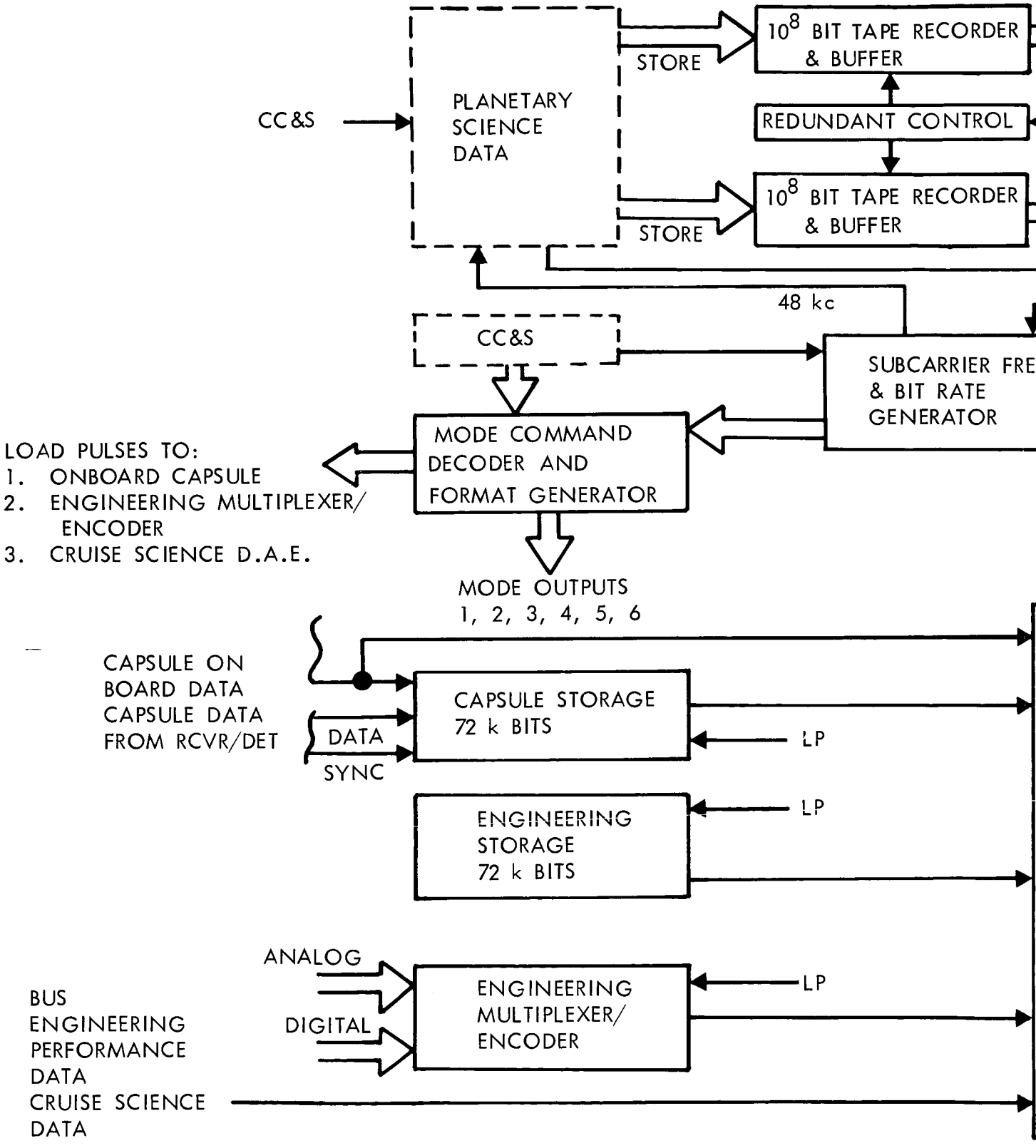
CC&S
PLANETARY SCIENCE DATA
STORE
STORE
10^8 BIT TAPE RECORDER & BUFFER
REDUNDANT CONTROL
10^8 BIT TAPE RECORDER & BUFFER
48 kc
CC&S
SUBCARRIER FRE & BIT RATE GENERATOR
MODE COMMAND DECODER AND FORMAT GENERATOR
LOAD PULSES TO:
1. ONBOARD CAPSULE
2. ENGINEERING MULTIPLEXER/ ENCODER
3. CRUISE SCIENCE D.A.E.
MODE OUTPUTS 1, 2, 3, 4, 5, 6
CAPSULE ON BOARD DATA
CAPSULE DATA FROM RCVR/DET
DATA
SYNC
CAPSULE STORAGE 72 k BITS
LP
ENGINEERING STORAGE 72 k BITS
LP
ANALOG
DIGITAL
ENGINEERING MULTIPLEXER/ ENCODER
LP
BUS ENGINEERING PERFORMANCE DATA
CRUISE SCIENCE DATA

1

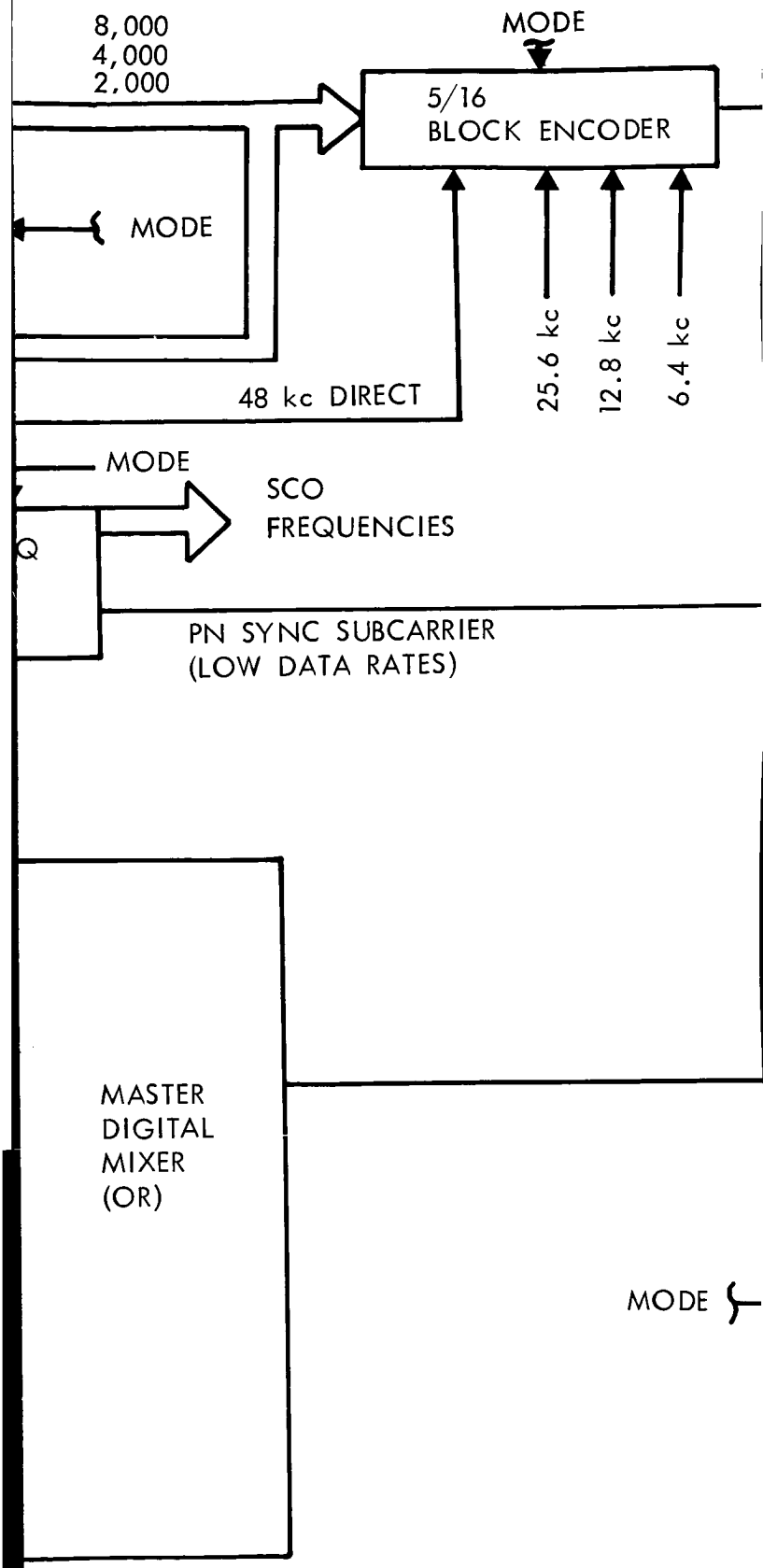

Figure 4.1-19: Telemetry A

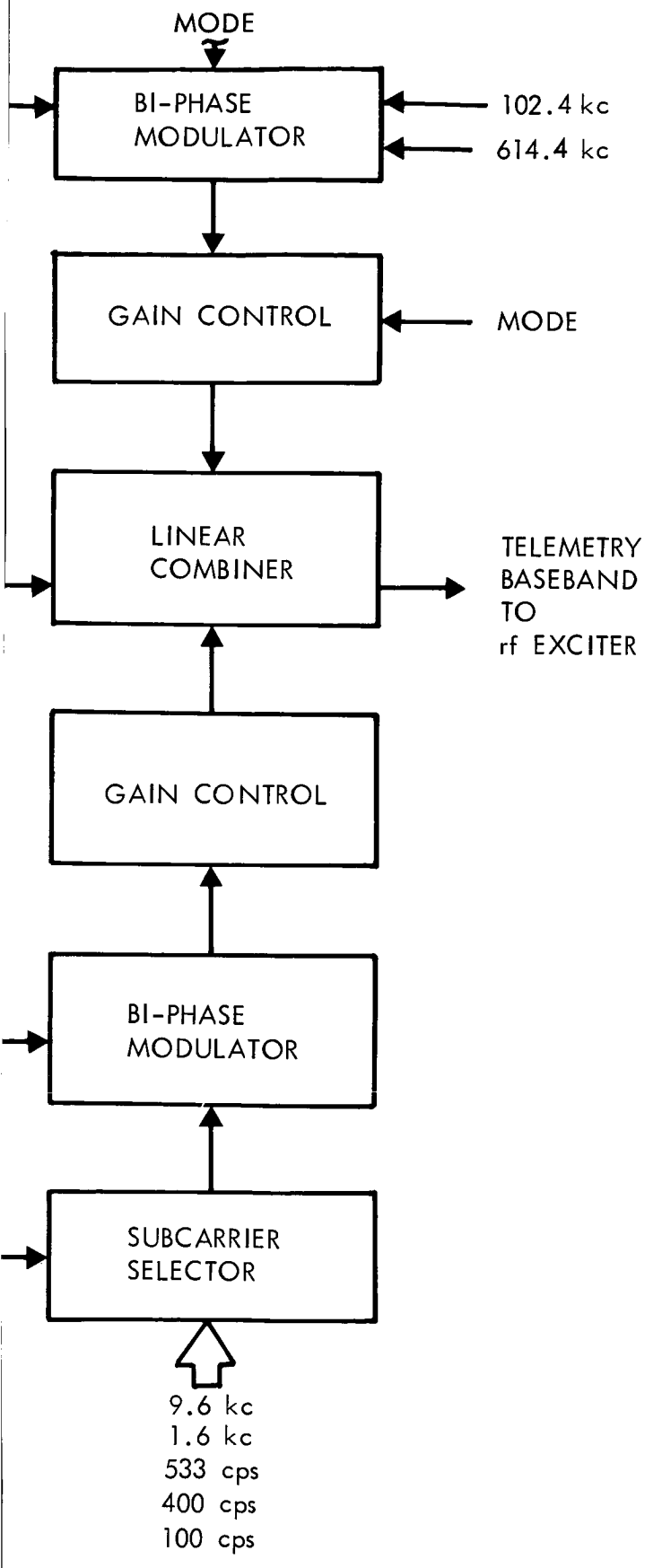

nd Data Storage Subsystem Block Diagram

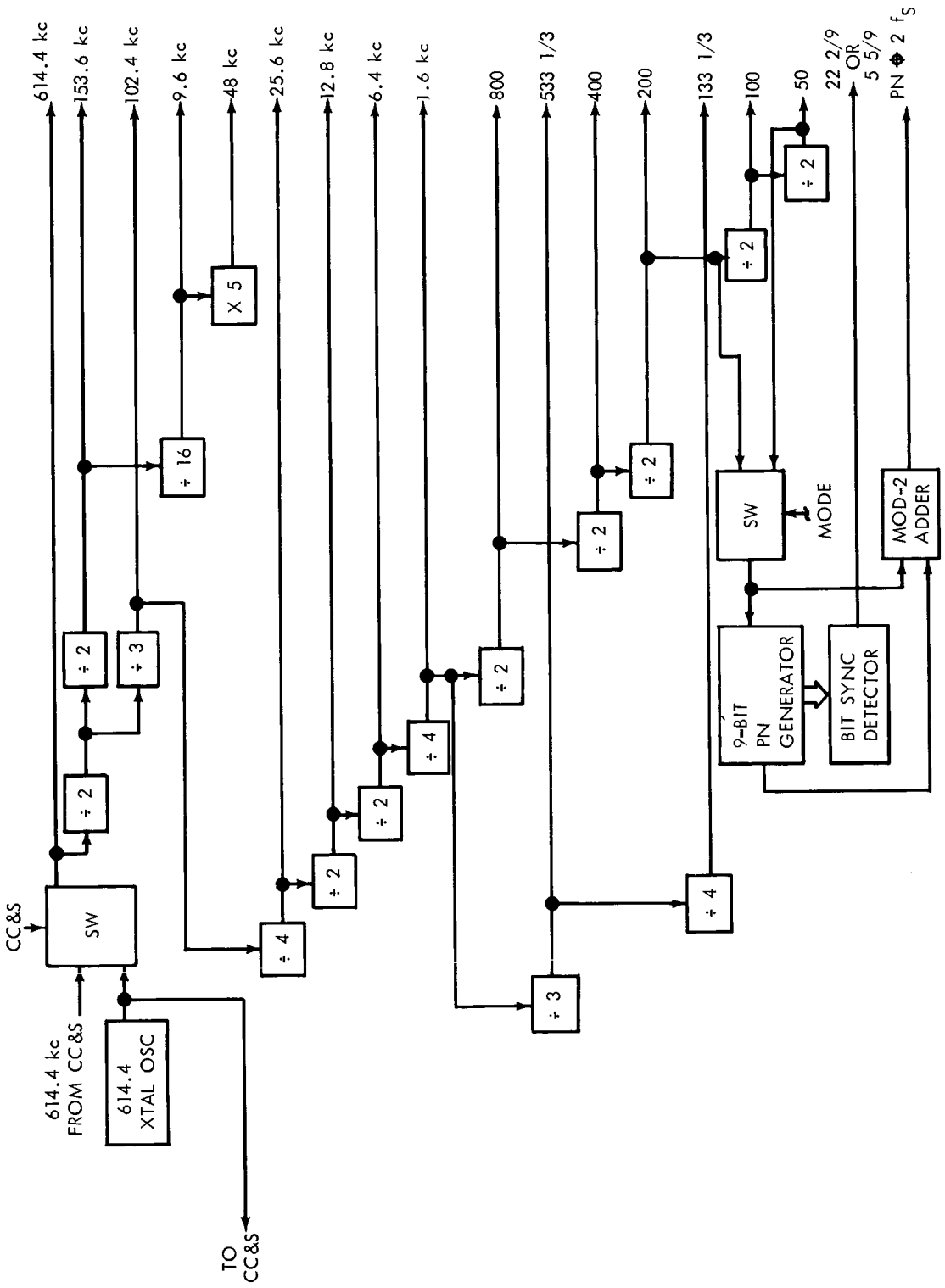

Figure 4.1-20: Subcarrier Frequency And Bit Rate Generator

frequency. This synchronization of upper and lower frequency subcarriers facilitates the acquisition of word sync during the recovery of planetary science data at the receiving site.

Time multiplexing of all lower frequency subcarrier data is obtained by furnishing load pulses to the three on-board data processors. No data are lost since the activation signal to each data processor is synchronized.

Subcarrier Frequency and Bit Rate Generator--The block diagram is shown in Figure 4.1-20. All subcarrier frequencies and bit synchronization signals are obtained by dividing down the 614.4-kc reference frequency. The reference frequency can be selected from either a local or external source via CC&S. The low data rate PN-modulated synchronization subcarrier is obtained by feeding 200 cps or 50 cps (2fs) to a 63-bit pseudo-noise (PN) generator and Modulo 2 adding the output with 2 fs.

Engineering Multiplexer and Encoder--The engineering multiplexer and encoder is similar in design to that used on the NASA Lunar Orbiter. Data output rate and timing will be controlled by the FORMAT generator. Word and bit sequencing will be controlled internally. The data format is shown in Section 3.0 of this volume.

The desired accuracy of all analog channels is exceeded by the use of a seven-bit binary analog to digital converter. Ten-to-one subcommutators are used to reduce the length of the frame cycle time.

For the purpose of time multiplexing, all spacecraft engineering data are divided into seven-bit words. A 32-bit frame sync code word is added to the engineering data frame and sufficient excess bits added to fill all words and subframes. The frame length is determined by the number of words used in this way.

Word Counter--Absolute control of the engineering multiplexer and encoder equipment is maintained by the FORMAT generator. Internal control of word count and word subcommutation is maintained by the word counter. Thus, the bit stream may be stopped at any time and started at any time later by merely stopping and starting the load pulses.

Analog Multiplexer--Signal conditioning is done ahead of the low duty cycle multiplexer. The data switches will be field-effect transistors arranged in parallel-series quad configuration to provide necessary reliability.

Analog-to-Digital Converter--The Analog-to-Digital Converter is a successive approximation 7-bit binary encoder.

Digital Multiplexer--This multiplexer is predominantly a switch array as the timing is accomplished externally.

Mixer--The mixer is an "OR" gate to mix the analog and digital data streams.

Engineering Data Core Memory--The bit organized type of memory is ideally suited for slow data rate; the number of logic and driver circuits are reduced to the theoretical minimum. The overall block diagram of the proposed memory is shown in Figure 4.1-21.

Write-in and readout are performed one bit at a time. One vertical line is selected by action of the 15 and 19 stage driver rings. Likewise, a horizontal line is selected by the action of the 16- and 17-stage driver rings. The total bit storage is the product 16 x 17 x 15 x 19 or 77,520 bits.

Prior to storing data, all storage cores are reset to "1" state by a single "set wire" through the storage array. The read command enables the read AND gate and allows the clock pulses to start the read drivers. The output pulse from the core is sampled by a narrow strobing pulse.

Current Steering Switch--Current steering switches have been used extensively in serial access core memory systems with high performance and reliability.

Operation of the current steering switch is dependent upon the flux change of one of N parallel cores, steering current through an associated diode. The flux change will back bias all other diodes associated with that phase.

Ring Drivers--The multi-phase driver is essentially a set of blocking oscillators containing square loop transformer cores. This circuit has

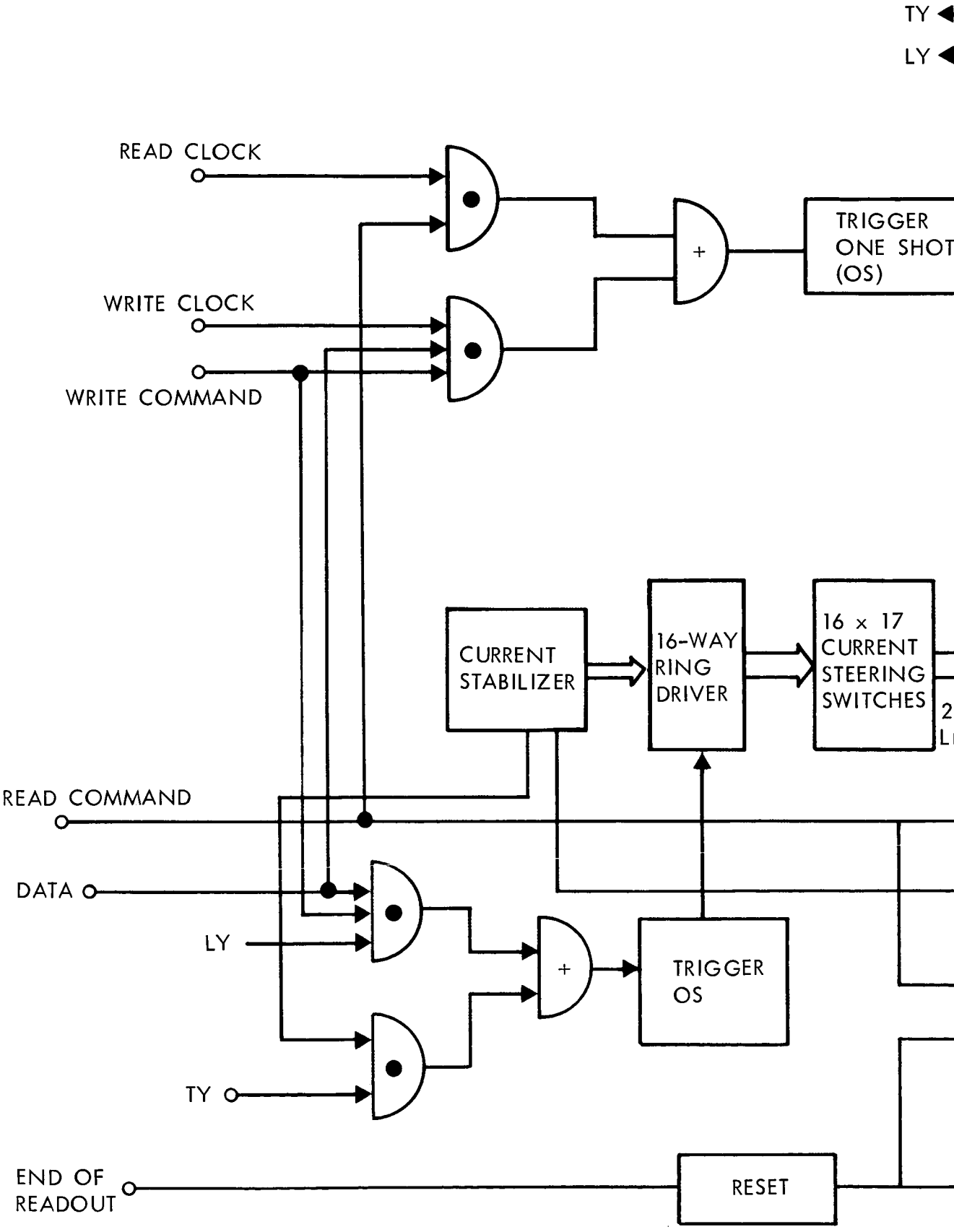
TY
LY
READ CLOCK
WRITE CLOCK
WRITE COMMAND
+
TRIGGER
ONE SHOT
(OS)
CURRENT
STABILIZER
16-WAY
RING
DRIVER
16 x 17
CURRENT
STEERING
SWITCHES
READ COMMAND
DATA
LY
+
TRIGGER
OS
TY
END OF
READOUT
RESET

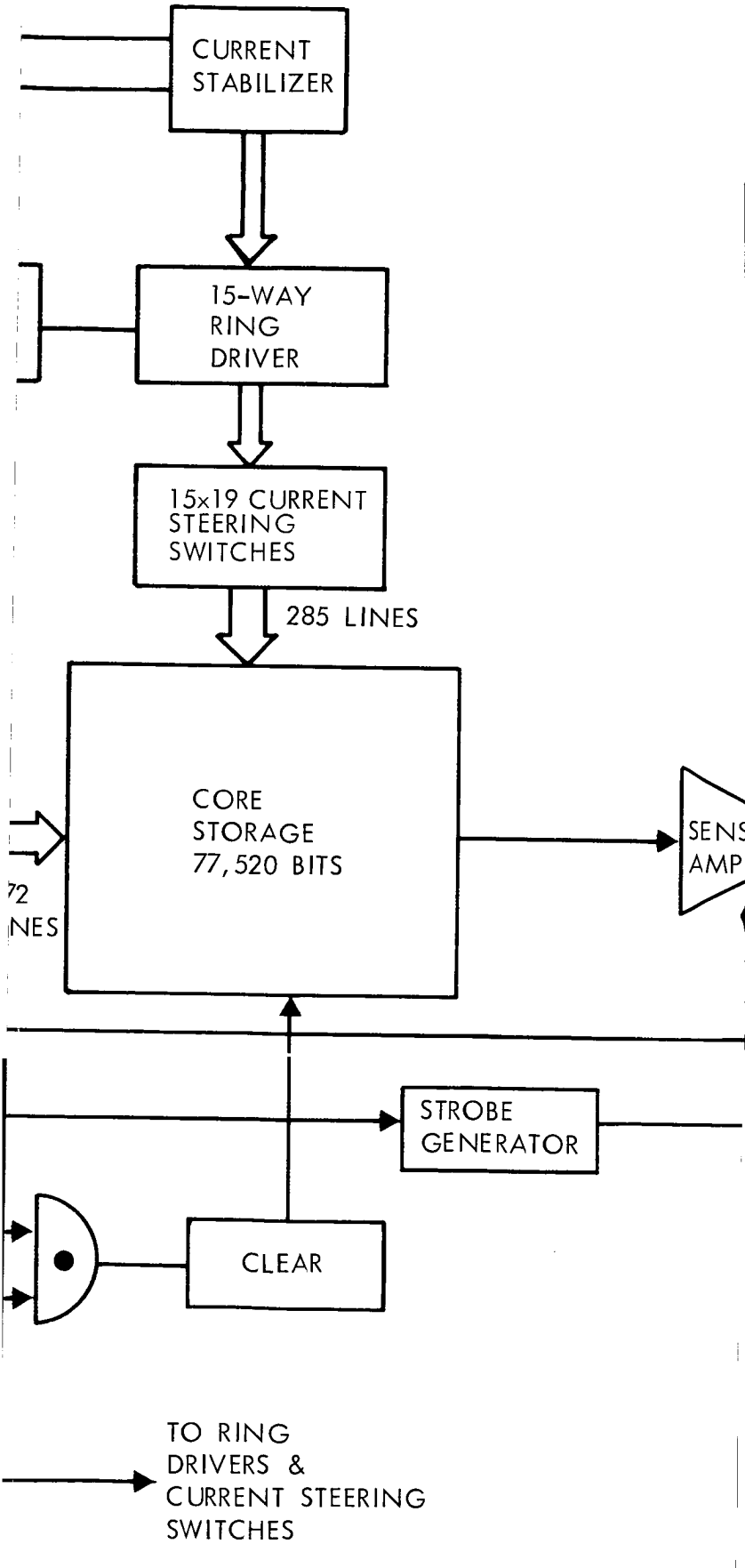
CURRENT STABILIZER
15-WAY RING DRIVER
15x19 CURRENT STEERING SWITCHES
285 LINES
CORE STORAGE 77,520 BITS
72
INES
SENS
AMP
STROBE GENERATOR
CLEAR
TO RING DRIVERS & CURRENT STEERING SWITCHES

Figure 4

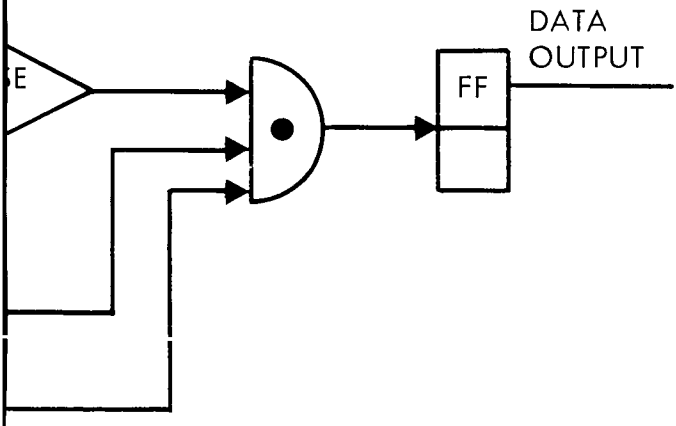

. 1-21: Block Diagram Data Storage Memory

proven to be an extremely reliable method of providing sequential access to ferrite core memories with zero power drain between memory cycles, retaining the next bit address even if power supply voltages are switched off between operations.

Capsule Data Core Memory--The core memory used to store capsule data is identical to that described for the Engineering Data. This memory also serves the additional purpose of buffering the 100 bit per second real-time capsule data.

Planetary Science Tape Recorder--A continuous motion magnetic tape recorder is used to store Planetary Science data on the spacecraft for subsequent playback at a lower rate required by the communication link.

Block Diagram--Components of the tape recorder data storage system are shown by Figure 4.1-22. This block diagram indicates the signal flow and the power distribution throughout the system.

Tape Transport--The selected design provides constant tension winding as the tape pack diameters change. The unit consists of a peripheral drive reel-to-reel transport driven by one synchronous motor for record and another for the three playback speeds.

End-of-Tape Sensors--A strip of oxide removed from each end of the tape leaving only the transparent mylar backing for activating photoelectric switches from a lamp provides end of tape sensing. Planetary science data are received at a serial bit rate of 50,000 bps. The 50,000 bps

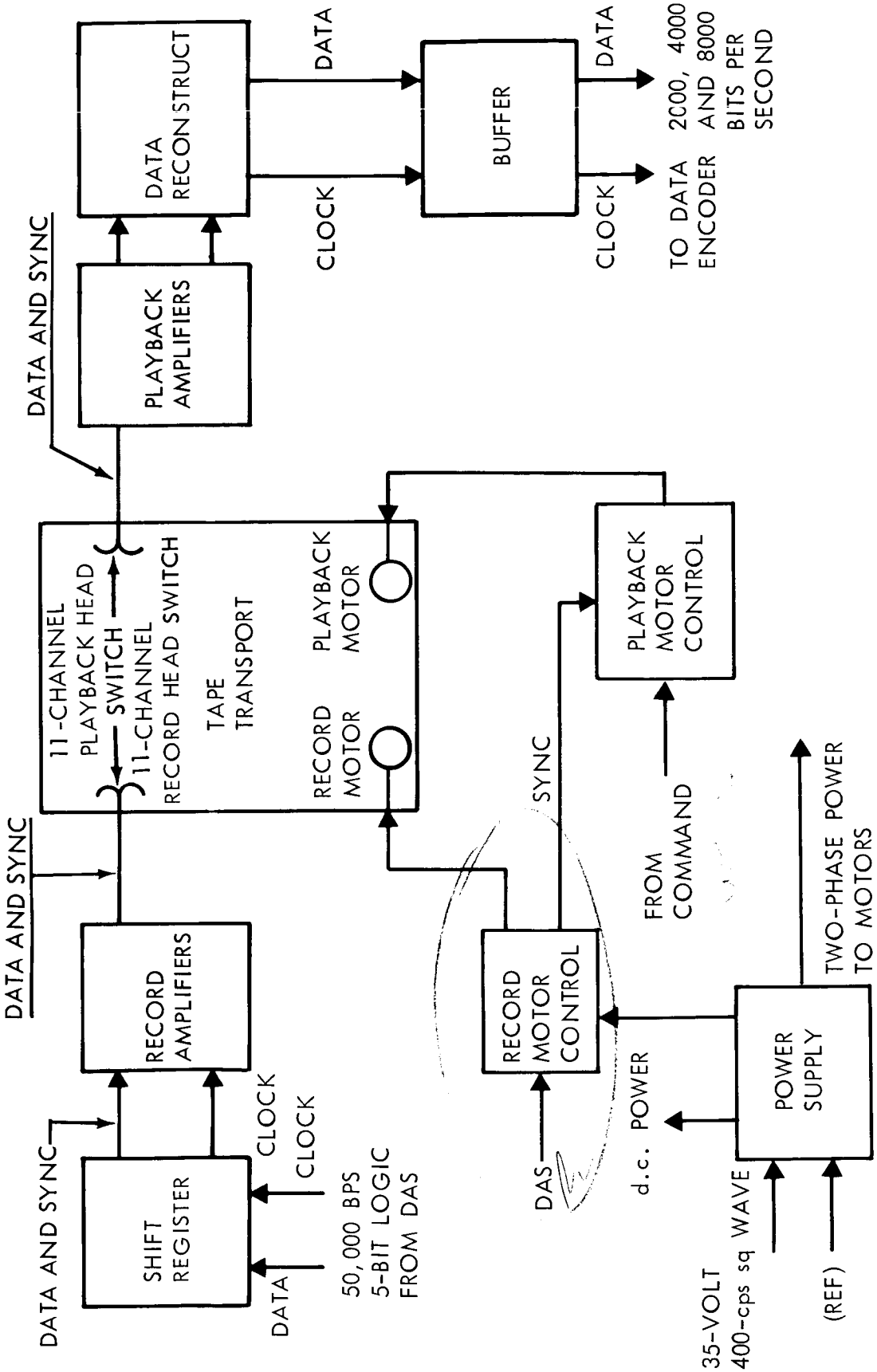

Figure 4.2-22: Planetary Science 10^8 Bit Data Recorder And Buffer

NRZ digital data will be recorded serially at a 40 ips tape speed. The linear packing density will be 1250 bits/track inch. Eleven parallel tracks and 650 feet of mylar backed tape will allow 10^8 total bits of data recording. A time period of 3.25 minutes will be required to record one track of data before the tape transport is reversed and the record electronics are switched for recording back on the next track until all eleven data tracks are filled, thus 36 minutes of continuous data can be recorded before tape capacity is exceeded. This approach minimizes the problems associated with tape skew when very wide tape is utilized.

Interface Definition--The electrical interface between the telemetry and data storage subsystem and other spacecraft subsystems is presented in Table 4.1-7. Physical characteristics and thermal limits are listed in Table 4.1-4.

Reliability--The telemetry and data storage subsystem reliability probability of success for the preferred design configuration is estimated to be 88.49% for all associated functions for 5880 hours mission operational duration. This estimate is based upon incorporated redundancy, a parts count analysis, part failure rates and the ground rules defined in the Voyager '71 Program Reliability Analysis and Prediction Standards, D2-23834-1, Revision A, dated April 26, 1965.

The reliability model, equipment redundancy description, and detailed analyses of the preferred design are delineated in Section 4.1.5. See Volume B, Section 4.1.6 for analyses of redundancy applications which

Table 4.1-7: Telemetry and Data Storage Subsystem Electrical Interfaces

INTERFACE WITH	FUNCTION	Z IN	Z OUT	SIGNAL LEVEL
1. Science Payload	Planetary Science Output	1000 Ohms	NA	0 -4V (Digital)
	Cruise Science Output	1000 Ohms	NA	0 -4V (Digital)
	Cruise Science Load Pulses	NA	1000 Ohms	0 -4V (Digital)
	Planetary Science Control to Recorder	1000 Ohms	NA	0 -4V (Digital)
2. Radio Relay Subsystem	Capsule Data	1000 Ohms	NA	0 -4V (Digital)
	Capsule Sync	1000 Ohms	NA	0 -4V (Digital)
3. Spacecraft Analog Data (See Measurement List for Quantity)	Analog Data Channels From Subsystems or Signal Conditioner	500 K Ohms	NA	0 -5V (Analog)
4. Spacecraft Digital Data (See Measurement List for Interface)	Digital Data Channels From Subsystems	>20K	NA	0 -4V (Digital)
5. Capsule (Before Separation)	Capsule Data Output	1000 Ohms	NA	0 -4V (Digital)
	Capsule Bit Sync	1000 Ohms	NA	0 -4V (Digital)
6. Centaur Telemetry Subsystem	Spacecraft Data Modulating Low-Frequency Subcarrier	50 Ohms, Ground Isolated from Spacecraft	NA	5V RMS (Analog)
7. Deep-Space Radio System	Composite Subcarrier Baseband Signals to Modulate RF Carrier	NA	50 Ohms or 1000 Ohms	5V RMS (Analog)
8. CC&S	Select TM Mode Bit 1	1000 Ohms	NA	0-4V (Digital)
	Select TM Mode Bit 2	1000 Ohms	NA	0-4V (Digital)
	Select TM Mode Bit 3	1000 Ohms	NA	0-4V (Digital)
	Tape Recorder On/Off	1000 Ohms	NA	0-4V (Digital)
	Select Tape Recorder Mode Bit 1	1000 Ohms	NA	0-4V (Digital)
	Select Tape Recorder Mode Bit 2	1000 Ohms	NA	0-4V (Digital)
	Select Tape Recorder	1000 Ohms	NA	0-4V (Digital)
	Store Engr Data	1000 Ohms	NA	0-4V (Digital)
	Store Capsule Data	1000 Ohms	NA	0-4V (Digital)
	614.4 KC Squarewave	1000 Ohms	NA	0-4V (Digital)
	Select Block Coding	1000 Ohms	NA	0-4V (Digital)
	Select CC&S Clock Reference	1000 Ohms	NA	0-4V (Digital)
	Select Capsule Data Source	1000 Ohms	NA	0-4V (Digital)

should be considered during future studies. The associated functional and component reliabilities are summarized in Table 4.1-8.

Table 4.1-8: TELEMETRY & DATA STORAGE SUBSYSTEM PROBABILITY OF SUCCESS

	Failure Rate %/1000 Hr.	t Mission Time Hours	t Product	P_s (t) Probability Success
1. Planetary Science Tape Recorder*	0.0806	720	0.00058	0.99942
2. Engineering Core Memory	1.537	6	0.0000921	0.999908
3. Capsule Core Memory				
Buffer Mode	0.217	5160	0.0112	0.9888
Storage Mode	1.537	6	0.0000921	0.999908
4. Engineering Multiplexer Encoder**	1.2396**	5880	0.0729	0.9296
5. Gate Generator	0.250	5880	0.0147	0.9853
6. Subcarrier/Timing Generator	0.386	5880	0.0226	0.9621
7. Modulator	0.0328	3880	0.00193	0.99807

* Standby Recorder Redundancy
** Quad Redundant Analog

TOTAL SUBSYSTEM	0.122	0.8849

FUNCTION PROBABILITIES:	P_s(t)	t (Hrs)
Planetary Science Data	0.9648	720
Engineering/Cruise Science Data Real Time	0.8994	5880
Engineering/Cruise Science Data with Storage	0.8993	5880/6
Capsule Data Real Time	0.9637	5160
Capsule Data with Storage	0.9636	5160/6

4.1.3.3 Spacecraft Relay Radio Subsystem

Functional Description--The relay radio subsystem provides equipment for the reception of the capsule VHF rf signal and subsequent telemetry detection. The relay link is utilized in the Voyager mission during the capsule landing phases as a telemetry data relay between the capsule and Earth and is required to function after Spacecraft/Capsule separation during descent and landing. After Capsule landing, the capsule/orbiting-spacecraft/Earth link is used as a backup alternate to the direct Capsule-Earth communications link.

The functional diagram of the relay radio subsystem equipment is shown in Figure 4.1-23a. Included are the VHF receiver, telemetry detector, and associated d.c. to d.c. convertor. Two data detection rates are provided by the telemetry detector for the two capsule telemetry modes, (descent mode and landed mode). Also, receiver capability is provided to operate at two selectable capsule transmission frequencies to support alternate telemetry reception from up to two capsules. All the components of the relay radio subsystem utilize previously flight proven technology and no completely new development is required. The relay radio modes of operation are:

1) Capsule Descent Mode--The relay radio subsystem receives and detects VHF telemetry signals transmitted from the separated capsule. The detected data bit rate, 10 bits per second nominal, is directed to the spacecraft telemetry and data storage subsystem for relay in real time over the spacecraft-Earth RF link as the primary operational mode.

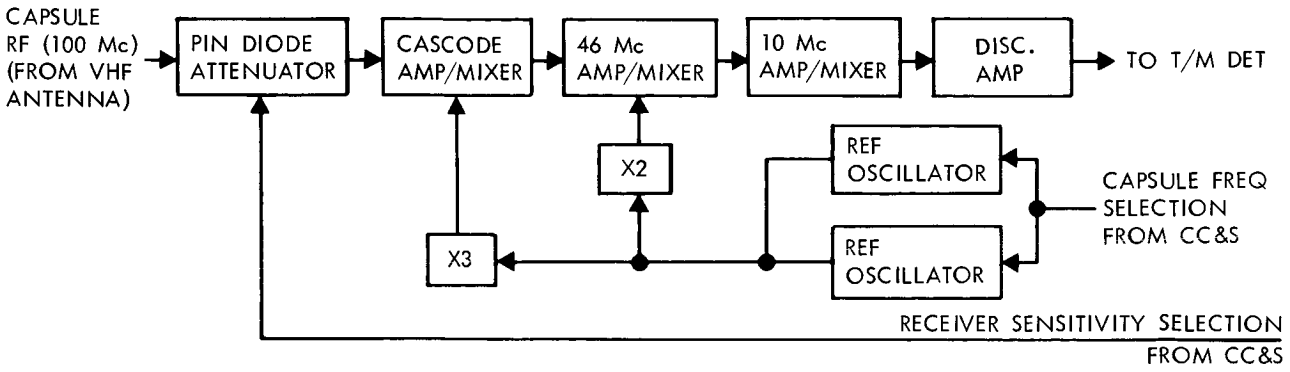

B. RELAY RADIO RECEIVER

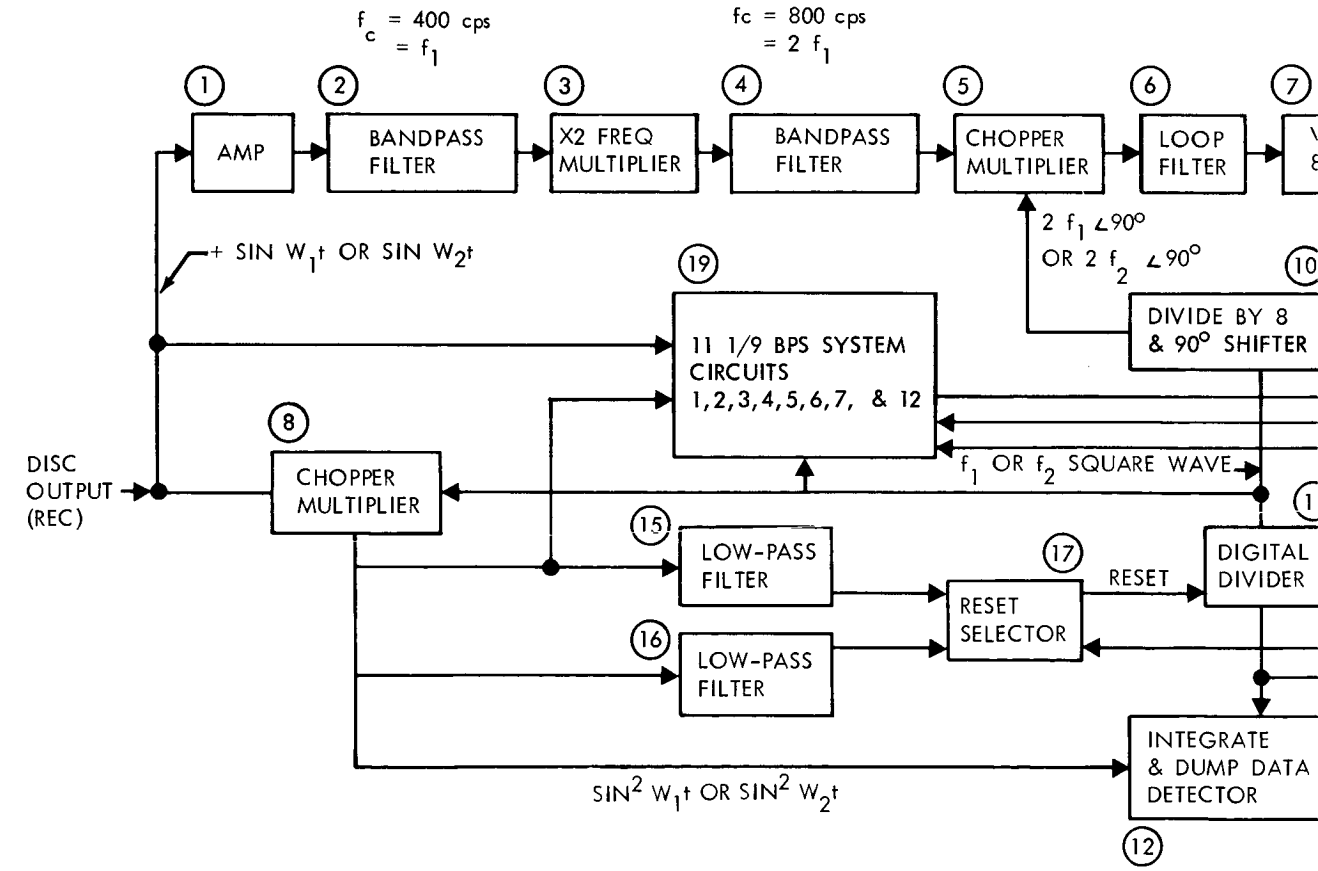

C. RELAY RADIO TELEMETRY DETECTOR

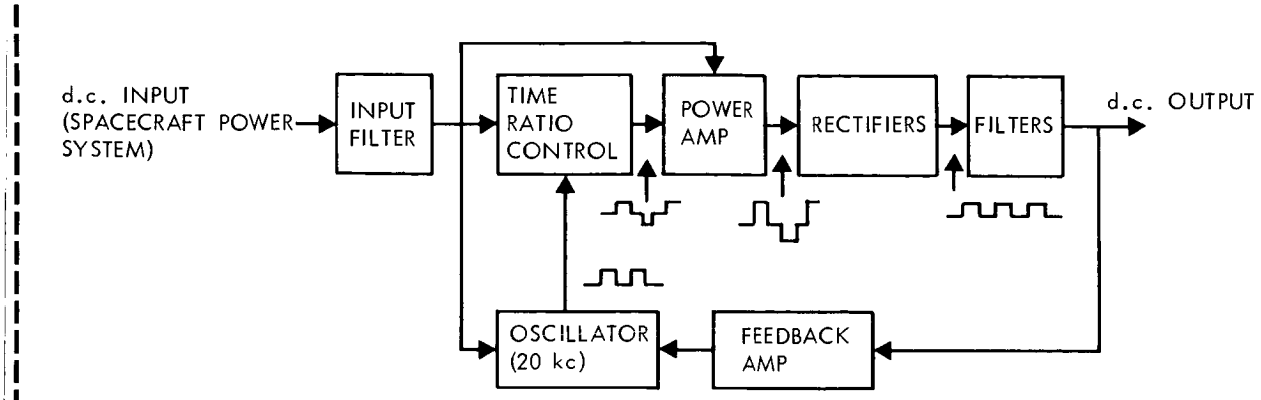

D. RELAY RADIO d.c./d.c. CONVERTER

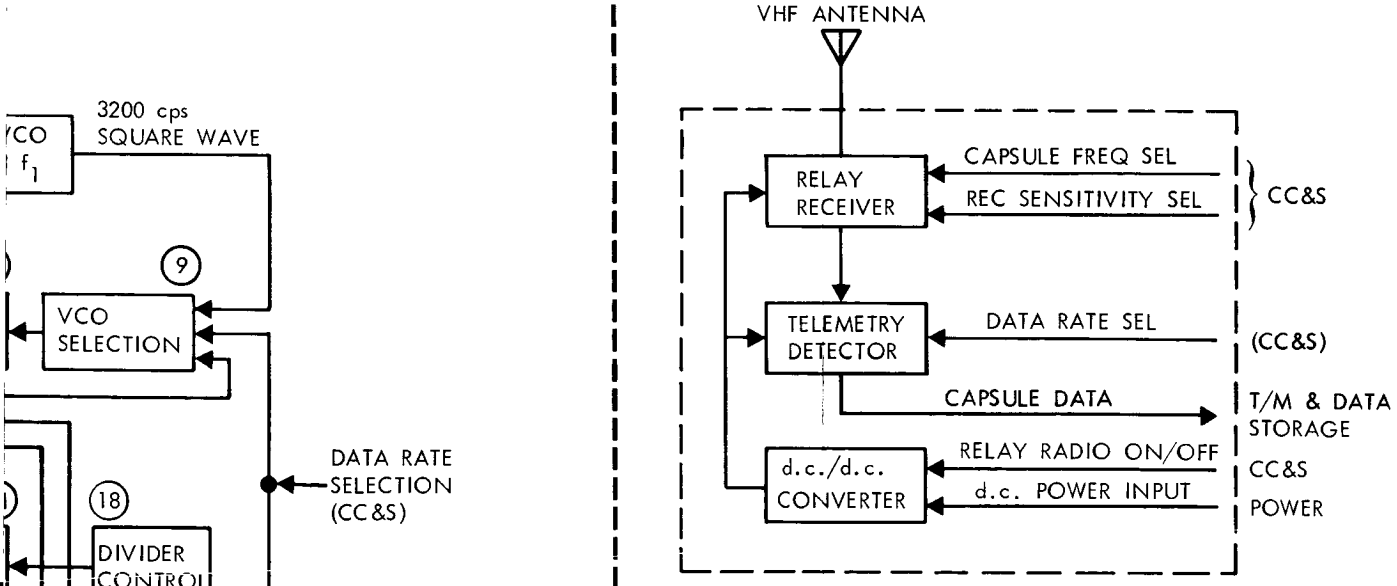

A. RELAY RADIO FUNCTIONAL DIAGRAM

Figure 4.1-23: Relay Radio

2) Capsule Landed Mode--The relay radio system is employed as an alternate backup to the prime capsule-Earth rf link to receive and detect VHF signals from up to two capsules after they have landed on the Mars surface. The detected data bit rate, which is assumed to be 100 bits per second, is directed to the spacecraft telemetry and data storage subsystem for formatting into the modulation baseband and subsequent relay in real time over the spacecraft-Earth rf link.

Alternate modes are incorporated for storage of capsule data during the critical phases of the spacecraft orbital insertion maneuver and subsequent playback of data upon command.

The relay receiver design is based on capsule data rates and rf power levels derived in the relay link analysis (D2-82709-2, Section 4.1.8). A lower data bit rate reduces the required capsule rf power, thereby increasing the confidence in development of the relay link.

Component Descriptions--The receiver and telemetry detector are described below:

Receiver--The receiver block diagram is shown in Figure 4.1-23b. The unit is a double conversion FM receiver with intermediate frequencies at 46 and 10 Mc. This IF selection allows maximum use of the existing S-band designs. The 100-Mc input signal is received by a voltage controlled PIN diode attenuator at the receiver input. This unit provides a

switchable attenuation of 0.5 or 30 decibel. Its purpose is to eliminate receiver overload when the capsule is in close proximity to the spacecraft. Depending on capsule transmitter power and mutual antenna coupling, the receiver input power could be as high as 0.5 watt under this condition. The attenuator activation is derived from a CC and S timing signal.

A narrow-band cascode amplifier and balanced mixer module follows the diode attenuator. It provides an input noise figure no greater than 3 decibel and about 20-decibel gain. The response of the unit is such as to provide a minimum of 80-decibel rejection to the image frequencies of the desired 46-Mc and 10-Mc signals. The resulting 46-Mc signal is then amplified (40-decibel total gain) and converted down to 10 Mc. A crystal filter at the input of the 10-Mc IF amplifier reduces the bandwidth to 3.5 kc. This bandwidth is the minimum possible consistent with required doppler, oscillator drift and modulation requirements. The 10-Mc IF also provides limiting and further amplification (as required) of up to 80 decibel. The 10-Mc amplifier is followed by a balanced diode discriminator and isolation amplifier. A total gain margin of 20 decibel at threshold is provided in the receiver signal path for protection against environmental and component degradation. The crystal controlled reference oscillators are provided to drive the first and second mixers. Either oscillator is switchable through application of DC power as controlled by command from the CC and S. This mechanization allows for selection of reception from either of two capsules.

Telemetry Detector--The relay radio telemeter detector converts the input subcarrier baseband to a PCM signal and its related bit sync train. The input signal has one of two forms for the two data rates to be received.

a) $\pm$ Sin $2\pi f_1 t$ (Capsule Bit Rate of 100 BPS, f_1=400 cps)

b) $\pm$ Sin $2\pi f_2 t$ (Capsule Bit Rate of 10 BPS, f_2 = 200 cps)

The plus/minus notation implies PCM/PSK modulation of the subcarriers f_1 and f_2. These subcarrier frequencies result in four (4) and twenty (20) subcarrier cycles per data bit for the two subcarriers. A CC and S pulse is provided to switch demodulation data rates.

The modulation on both subcarriers is assumed to be differentially coherent PCM/PSK with the following Data/Subcarrier characteristics:

a) The PCM data stream is one in which a logic "1" is denoted as a transition from one logic state to the other logic state (no transition for a logic "0").

b) The PCM data are synchronous with the subcarrier.

c) The modulation results in biorthogonal signals. Plus Sin $2\pi f_1 t$ is transmitted for one binary state and minus Sin $2\pi f_1 t$ for the other binary state.

The operation of the Telemetry Detector (Figure 4.1-23c) is similar to a Differential PSK Detector. The following explanation is applicable to a system with one data rate; dual circuits are needed to handle two data rates. The input signal is passed through the bandpass filter centered at f_1 (the subcarrier frequency). The signal is essentially squared by a full wave rectifier to remove the modulation. The signal is then passed through the second bandpass filter centered

at $2f_1$. Multiplier (5), loop filter (6), VCO (7), and the 90^o phase shifting circuit constitute a phase lock loop operating at $8f_1$. After lock has been achieved the output of the $\div$ 8 circuit (10) is a reconstructed version of the modulator subcarrier signal, sin w_1t. Phasing between the reconstructed signal and the modulator reference is within a 180 degree ambiguity and the static error is maintained arbitrarily low by employing a large open loop gain.

After the loop has acquired lock and the local reference has been derived proper data detection occurs. The reconstructed reference and the input signal are multiplied together by circuit (8) to produce a $\pm$ Sin^2w_2t signal. The divider circuit (11) divides the reconstructed reference by N (there are N subcarrier cycles per data bit) to produce bit sync. Both signals are inputs to the integrate and dump data detector, which reconstructs the PCM data stream. The detected data at this point is NRZM (differentially coded). A converter circuit (14) converts the NRZM signal into a full-bauded non-return to zero PCM signal.

Bit sync is obtained by the overflow of the divider circuit (11). It remains for the start of the division action of this circuit to be referenced to the start of a bit period. This is accomplished by the low pass circuit (15) which recognizes data crossovers and provides a reset to the counters in circuit (11). Dual circuits are included to handle both data rates. The control circuits are (9), (13), (17) and (18). The block diagram illustrates all of the circuits required for the 100 bits/second data signal detection. Block (19) contains the

circuits required for the ten bits/second data signal detection. Circuits (10), (8), (11) and (14) are common to the detection of both data rate signals.

Interface Definition--A summary of the electrical interface characteristics existing between the Relay Radio Subsystem and other spacecraft subsystems is listed in Table 4.1-9. The assumed capsule interface is detailed in Table 4.1-10.

Performance Parameters--The relay radio performance parameters for the Receiver, Telemetry Detector, and Power Convertor are given in Tables 4.1-11 through 4.1-13, respectively. The Relay Radio Subsystem reliability (probability of success) for the preferred design configuration is calculated to be 99.88% for all associated functions for 217 hours mission operational duration. The reliability model, equipment redundancy description and detailed analysis are delineated in Section 4.1.5.

TABLE 4.1-9: RELAY RADIO OPERATIONAL ELECTRICAL INTERF				
INTERFACE WITH	FUNCTION	Z_{IN}	Z_{OUT}	
VHF ANTENNA	RECEIVE CAPSULE	50 OHMS	N/A	-1
	r.f. SIGNAL	1.5/1 VSWR (NORMAL) 50/1 VSWR (ATTEN.)		
POWER	d.c. INPUT POWER	250 OHMS	N/A	+3
CC&S COMMAND	SYSTEM ON/OFF	1000 OHMS	N/A	1 V
	RECEIVER SENSITIVITY	1000 OHMS	N/A	1 V
	FREQUENCY SELECTION	1000 OHMS	N/A	1 V
	DATA DEMOD. BIT RATE	1000 OHMS	N/A	1 V
TELEMETRY & DATA STORAGE DATA OUTPUT	DEMOD. CAPSULE DATA	N/A	1000 OHMS	3. 0.
T/M MEASUREMENTS	RECEIVER FREQUENCY	N/A	1000 OHMS	0-
	T/M DETECTOR VCO #1	N/A	1000 OHMS	0-
	T/M DETECTOR VCO #2	N/A	1000 OHMS	0-
	LOW BIT RATE CORR.	N/A	1000 OHMS	0-
	HIGH BIT RATE CORR.	N/A	1000 OHMS	0-

TABLE 4.1-11: RELAY RADIO RECEIVER PERFORMANCE PARAMETERS	
Z_{IN}	50Ω; VSWR 1.5/1.0 MAX (ATTN. OUT) 50Ω; VSWR 50/1.0 (ATTN. IN)
f_{INPUT}	100Mc
$f_{STABILITY}$	±1 PART IN 10^6 LONG TERM ±1 PART IN 10^7 SHORT TERM
$f_{STABILITY}$ VS. T^0	±3 PARTS IN 10^6 FOR RANGE -25°C TO +75° C
NOISE FIGURE	4 DB MAX (OVERALL ENVIRONMENTAL COND.)
PREDETECTION B.W.	3.5 KC ± 150 CPS
GAIN MARGIN	20 DB MIN. AT THRESHOLD
THRESHOLD SENSITIVITY	-122 DBM ±1 DB FOR PREDETECTION $\frac{S}{N}$ RATIO OF 12 DB
DYNAMIC RANGE	+37 DBM TO THRESHOLD
MODULATION SENSITIVITY	1 V P-P FOR 500 CPS INPUT FREQ. DEVIATION
Z_{OUT}	1000 ±50 OHMS
IMAGE REJECTION	8 DB MIN TO INPUT f'S OF 8 & 46 Mc
INPUT RF LOSSES	@100 Mc=1.25 DB MAX BETWEEN ANTENNA & RECEIVER
RELIABILITY	MAX. FAILURE RATE OF 0.318%/1000 OHMS

TABLE 4.1 PERFO
Z_{IN}
INPUT S/N
ERROR PRO
OUTPUT LE
OUTPUT FO
RELIABILITY

ACES	SIGNAL LEVEL
	22 to + 27 DBM
	35 ± 1.75 v.d.c. (5.2 WATT)
	VOLT PEAKS 100 MS PULSE
	VOLT PEAKS 100 MS PULSE
	VOLT PEAKS 100 MS PULSE
	VOLT PEAKS 100 MS PULSE
	7 v FOR A "ONE", 4 v FOR A ZERO
	5 v
	5 v
	5 v
	5 v
	5 v

-12: TELEMETRY DETECTOR ORMANCE PARAMETERS	
	100,000 ±10%
RATIO	12 DB NOMINAL
.	$<1 \times 10^{-7}$ FOR DETECTOR OUTPUT
VEL	<0.4 FOR "ZERO" ; >3.7 FOR "ONE"
RMAT	NRZ
	MAX. FAILURE RATE OF 0.163%/1000 HRS.

TABLE 4.1-10: CAPSULE INTERFACE

FREQUENCY	100 Mc (NOMINAL) ± 4 PARTS IN 10⁸
MOD.	PCM/PSK/FM
ENTRY BIT RATE	10 BPS/200 CPS S.C.
ORBITAL BIT RATE	100 BPS/400 CPS S.C.
MOD INDEX	0.7 RADIAN
DOPPLER (RECEIVED)	± 500 CPS MAX.
$T_X P_O$ - ENTRY	2 WATTS
$T_X P_O$ - ORBITAL	14 WATTS
RF LOSS-T_X TO ANTENNA	1.25 DB
ANTENNA GAIN	0 DB RELATIVE TO S/C DIRECTION

TABLE 4.1-13: POWER SUPPLY PERFORMANCE PARAMETERS

TYPE	d.c. TO d.c. CONVERTER
V_{IN}	+35 ±1.75 v.d.c.
OUTPUT	REC. 100 MA @ + 15.0V = 1.5 WATTS 40 MA @ - 15.0V = 0.6 WATTS T/M DET. 86 MA @ +6.0 v = 0.52 WATTS 86 MA @ -6.0 v = 0.52 WATTS 41 MA @ + 12 v = 0.49 WATTS
V_{OUT} TOLERANCE	+ 0.5%
V_{OUT} RIPPLE	MAX. ≥ ±0.15% OF RESP. VOLT
SWITCHING FREQUENCY	20 KC NOM.
EFF. (η)	70%
RELIABILITY	MAX. FAILURE RATE = 0.0854%/1000 HRS.

4.1.3.4 Spacecraft Antenna Subsystem

The spacecraft antenna subsystem consists of four S-band antennas and one VHF antenna, including their associated transmission lines, and the connectors required to connect to the appropriate terminals of the Radio Subsystem.

High-Gain Antenna--For long range data transmission a High-Gain Antenna is provided with its associated controls and transmission lines, connecting to the radio subsystem. The high-gain antenna is capable of steering about two orthogonal axes in order to maintain pointing along the Earth-vector locus. It also is necessary for this antenna to be steered toward the Earth direction during the injection maneuver, and possibly during a late midcourse maneuver.

Performance Parameters--The principal performance parameters are the gain (referred to isotropic level), and the polarization. Secondary performance parameters are sidelobe levels and cross-polarization characteristics.

The choice of an 8-by 12-foot paraboloidal dish as the preferred high-gain antenna results from the parametric curves of Figure 4.1-24. The system trade-offs leading to this selection are discussed in D2-82709-2, Section 4.1.8. The operating point for the preferred system is shown at 50 watts and an 8 by 12 foot aperture, for 135 kw ERP and 48,000 bits per second.

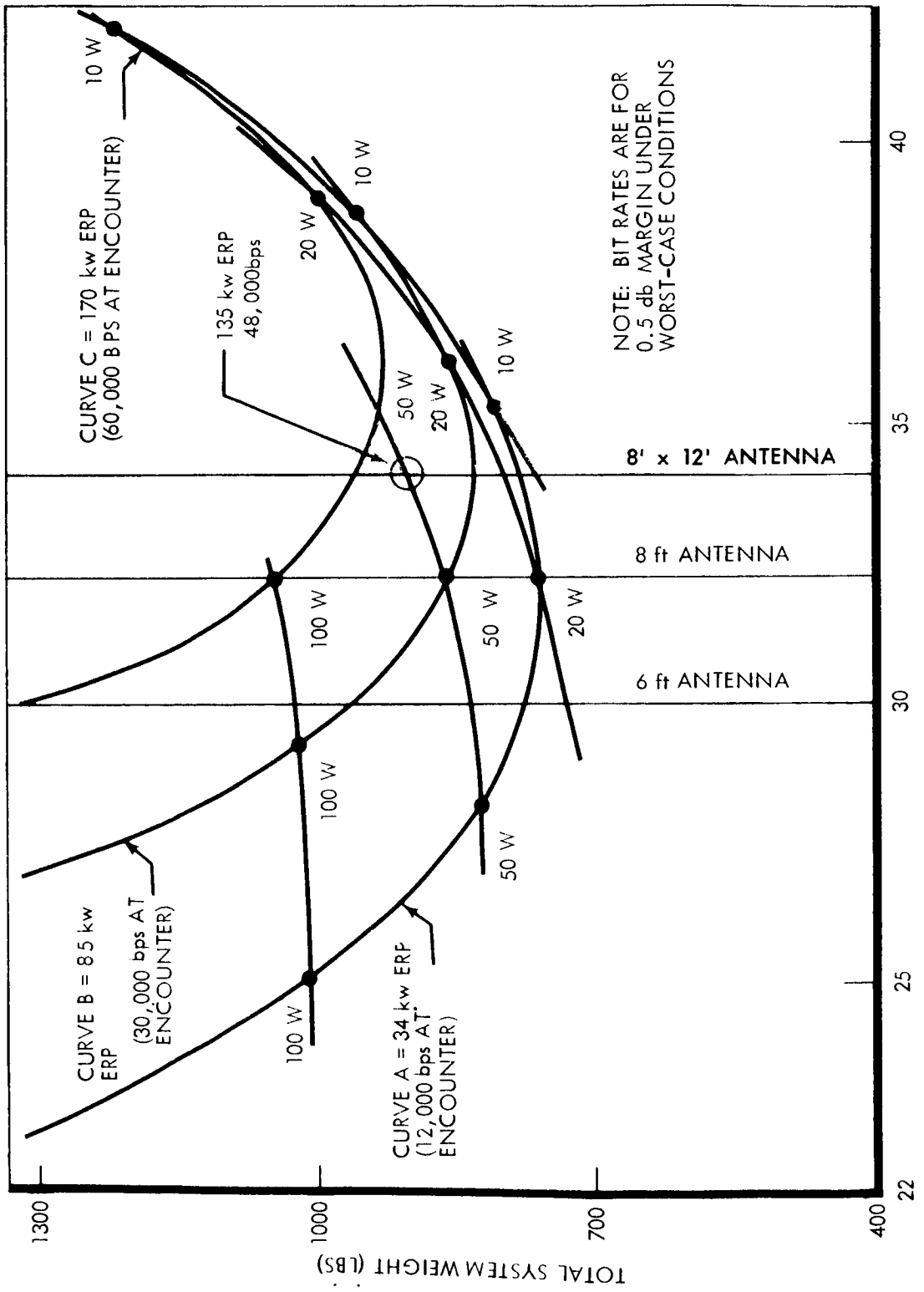

Figure 4.1-24: Total System Weight (Includes Tel./Com., A/C System, Elect. Pwr. Ther. Con., And Antenna) Versus Antenna Gain

Gain estimates for the 8 by 12 foot antenna have been made on the basis of Mariner C performance parameters. The performance of the selected antenna is:

Frequency	Aperture Efficiency	Gain (for min. aperture efficiency)
2,295 mc	0.50 - 0.65	34.3 db
2,115 mc	0.36 - 0.57	32.1 db

Main-Beam Performance Parameters--The parameter used to describe the main beam width is the angular width between half-power points (3-db beam width). A suitable estimate for antennas of this type is $70/(D/\lambda)$ degrees; this yields the values tabulated below for the beam widths in the major axes of the reflector.

Frequency	8 feet (Y axis)	12 feet (X axis)
2295 mc	3.8^{o}	2.5^{o}
2115 mc	4.1^{o}	2.7^{o}

Pointing Losses, Cruise and Orbit--The pointing losses are derived from the equisignal contours of Figure 4.1-25. As discussed in Section 4.1.8 of Boeing Document D2-82709-2, $\pm$ 0.6 degrees has been selected as the antenna pointing requirement.

The resulting maximum pointing loss is 1 db. Figure 4.1-26 shows the pointing loss as a function of errors about each antenna axis.

Pointing Losses, Maneuvers--When the Spacecraft attitude is controlled by inertial references during maneuver sequences, increased attitude errors

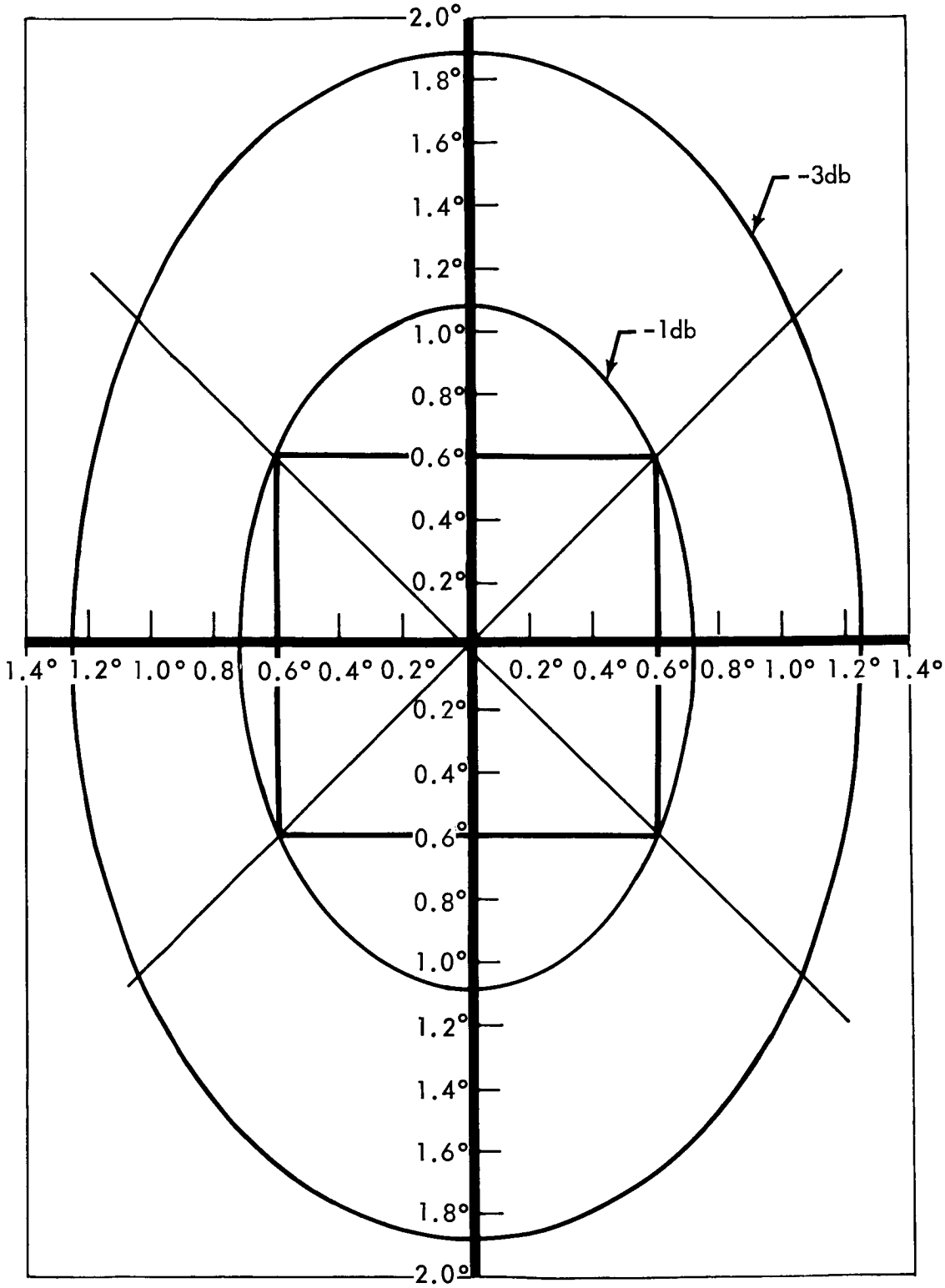

Figure 4.1-25: Equisignal Contours, 8' x 12' Reflector (2,295 mc)

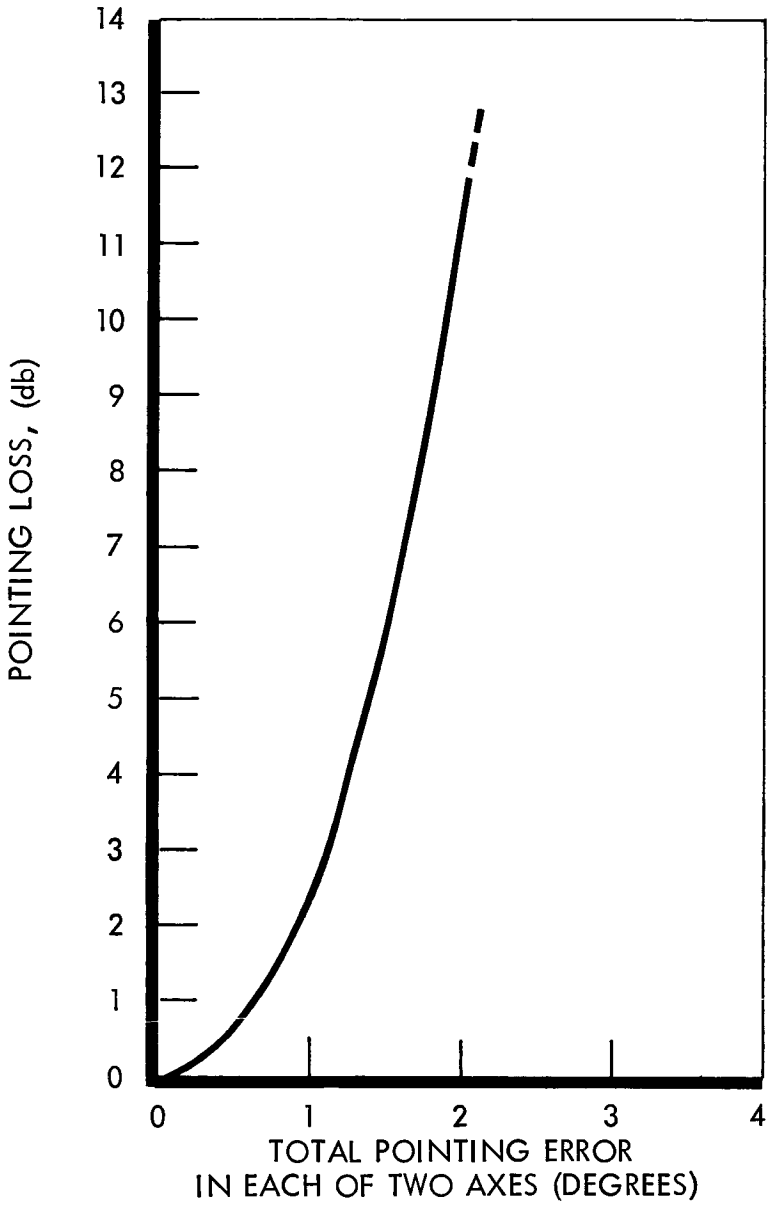

Figure 4.1-26: Pointing Loss, 8' x 12' Elliptical Paraboloid (f = 2,295 mc)

occur. During the orbit injection, motor-burn period deflections of the high-gain antenna supporting structure also add to the pointing error. Table 4.1-14 presents a summary of the pointing losses under all conditions.

Polarization Losses--Polarization losses are calculated from equations tabulated by Hartop (JPL Technical Report No. 32-457, 1 September 1964):

$$10 \log_{10} \frac{(R_1^2 + 1)\ (R_2^2 + 1)}{(R_1 R_2 + 1)^2} \leq P \leq 10 \log_{10} \frac{(R_1^2 + 1)\ (R_2^2 + 1)}{(R_1 + R_2)^2},$$

corresponding to 0 and 90 degree orientations of the polarization ellipses. Using the on-axis axial ratios tabulated earlier,

at 2295 Mc: $R_1 = 1.084$ (0.7 db DSIF ellipticity)

$R_2 = 1.1 - 1.2$

at 2115 Mc: $R_1 = 1.3 - 1.9$

$R_2 = 1.19$ (1.5 db ellipticity)

The on-axis polarization losses are then:

$0.02 \text{ db} \leq P\ (2295) \leq 0.07 \text{ db}$

$0.02 \text{ db} \leq P\ (2115) \leq 0.65 \text{ db}$

Maximum rf Power Level--Limitations on rf power levels in antennas and transmission lines arise from air breakdown, rf vacuum breakdown ("multipacting"), and heating caused by transmission line losses.

1) Air Breakdown - Since high-power transmitter operation will be deferred until after outgassing of components, the possibility of rf breakdown in air should not arise, provided that high-power transmission lines are vented to ensure that air pressure within transmission lines and transmission-line components is less than

Table: 4.1-14 : HIGH-GAIN ANTENNA--POINTING LOSSES

Mission Phase	Error Source	Per Axis Error	Cone Angle Error	Pointing Loss (db)
Cruise and Orbit[1]	Attitude-Control Limit Cycle	$\pm 0.20^{o}$		
	A/C Reference Senser	$\pm 0.10^{o}$		
	Structure	$\pm 0.20^{o}$		
	Antenna Control (Step = 0.20^{o})	$\pm 0.10^{o}$		
		$\pm 0.60^{o}$	0.85^{o}	1.0 db
Midcourse Maneuver	Attitude Error[2] (3-Sigma)		1.05^{o}	
			0.85^{o}	
			1.35^{o} (RSS)	2-1/2 db
			1.90^{o} (Absolute Sum)	4-1/2 - 5 db

(1) Applicable when $\pm$ 0.2° attitude-control limit-cycle used, including encounter and orbit.

(2) Section 3.8, Guidance and Navigation--Maneuver Error Allocation.

Table 4.1-14: HIGH-GAIN ANTENNA--POINTING LOSSES (Continued)

Mission Phase	Error Source	Per Axis Error	Cone Angle Error	Pointing Loss (db)
Insertion Maneuver (Excluding motor burn internal)	Attitude Error(2) (3-Sigma)		1.08° 0.85°	
			1.37° (RSS)	2-3/4 db
			1.93° (Absolute Sum)	5--5-1/2 db
Insertion Motor Burn	Attitude Error(2) (3-Sigma)		1.08° 0.85°	
	Deflection(3)		0.75°	
			1.56° (RSS)	3 d db
			2.68° (Absolute Sum)	9-1/2 - 10 db

(2) Section 3.8, Guidance and Navigation--Maneuver Error Allocation.

(3) Deflection 3/4° (± 3/4° damped oscillation), in pitch plane.

0.10 mm Hg (reduced to 290°K) at initiation of TWTA operation.

2) RF Vacuum Breakdown (Multipacting) - The rf voltage between electrodes in a vacuum can be limited by a secondary electron-emission resonance phenomenon. The threshold voltage for this effect is a function of frequency, electrode spacing, and configuration, and of the electrode material, including its surface condition. The threshold voltage for initiation of multipacting is estimated at 250 to 425 volts rms for parallel-plane electrodes 0.070 inch apart (the slot width) at 2295 Mc. Power-handling capacity is estimated at 63 to 180 watts per slot, for a resonant slot impedance estimated at 1000 ohms. Since the applied power level is 12-1/2 watts per slot, the margin below the multipacting threshold appears adequate.

Safety Considerations--Personnel exposed to radiation from the high-gain antenna, when tested at the 50-watt level, should be at a sufficient distance to ensure that power density incident on body surfaces will not exceed 0.01 watt per square centimeter.

Position Control--The high-gain antenna (HGA) is deployed on a boom extending in the direction of the negative Y (yaw) axis of the spacecraft. A two-axis drive is provided, with the swivel axis oriented parallel to the Y-axis and the hinge axis lying in the X-Z plane. From the swivel gimbal position, which aligns the hinge axis with the X axis, the swivel axis can scan $\pm$ 180 degrees. When the hinge axis is parallel to the X axis, the hinge gimbal can scan from 40 degrees above the negative Z axis down through the negative Y axis and to within 10 degrees of the positive

Z axis. Therefore, the two gimbals can sweep the HGA over slightly more than a hemisphere, which is nearly centered on the negative Y axis.

With the addition of vehicle roll motion, the antenna can sweep 4 π steradians, less the 10-degree cone about the positive Z-axis. With this configuration, the HGA can track Earth continuously during cruise (Figure 4.1-27), and during maneuvers, subject to the acceptance by other subsystems of the following constraints:

1) Vehicle maneuver away from cruise attitude is executed by a roll rotation first, followed by a yaw rotation, and the return is in reverse sequence.
2) If the normal roll angle command (ϕ) would carry Earth out of the HGA hemisphere of coverage, the roll command must be changed to (ϕ - 180 degrees).
3) The positive Z axis must not approach the Earth line of sight closer than the 10-degree limit on HGA field of view.
4) The programmer must generate the appropriate pointing angles in the form of incremental position commands to the gimbal drive mechanisms. During vehicle roll rotation, the required hinge and swivel angle commands are arc sin and arc tangent functions, respectively, of vehicle roll attitude (modified by the Earth cone angle).

Continuous tracking during roll maneuver carries a high penalty in terms of programmer complexity. Instead, the programmer will command the final positions of the hinge and swivel axes, which will place Earth back within the HGA field of view at the completion of the vehicle roll rotation. The HGA link can be re-established while the vehicle is still on the Sun

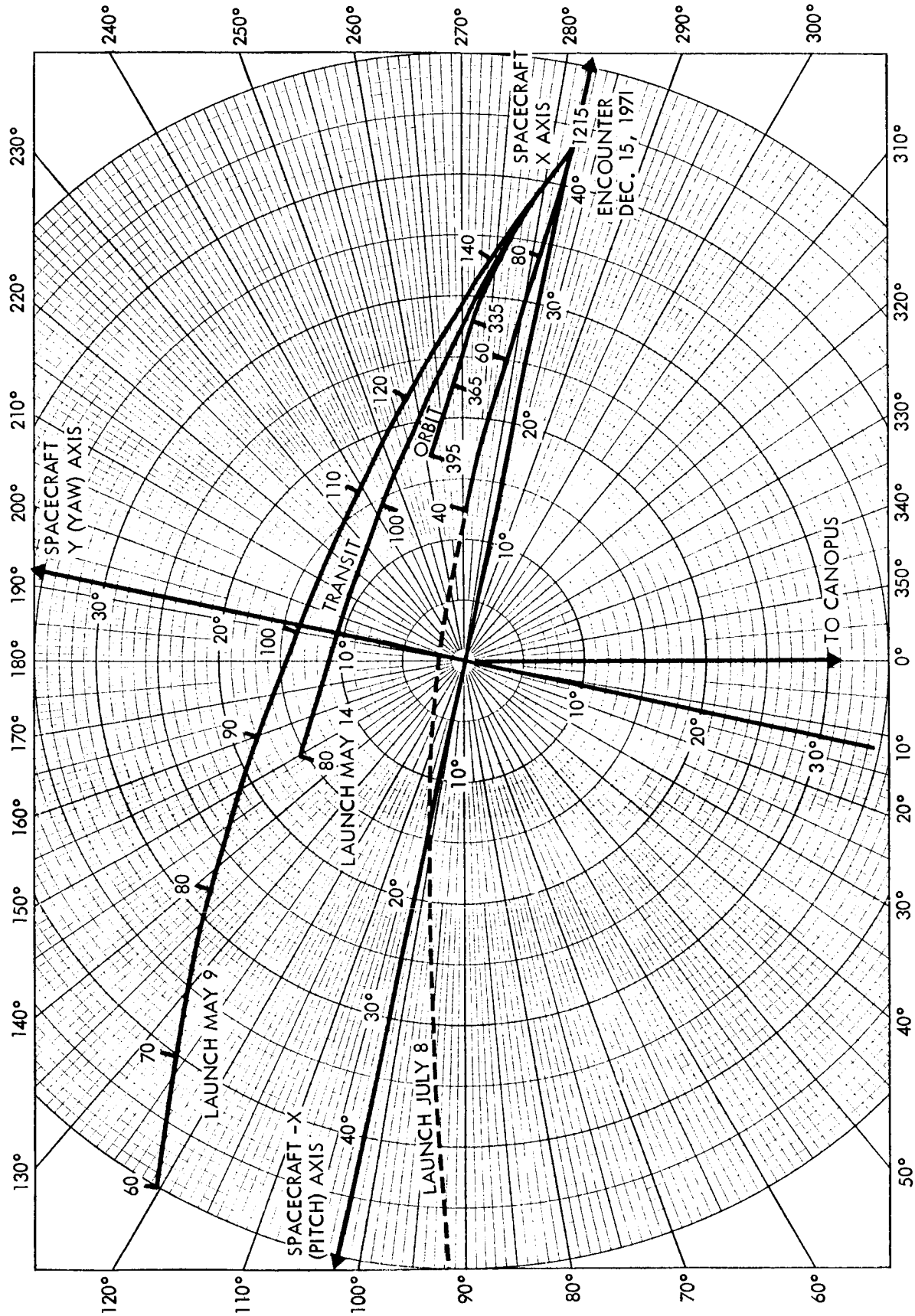

Figure 4.1-27: Earth Cone & Clock Angles

line. The subsequent yaw rotation can be compensated directly by a fixed rate counterrotation of the swivel gimbal, and HGA communication will not be interrupted during the portion of the maneuver that is off the Sun line.

The antenna is rotated in each axis in increments of 0.176 degree. The position error caused by gimbal angle quantization is only ±0.088 degree. An error of ±0.2 degree results from mechanical tolerances. Other errors caused by structural misalignments are calibrated out early in the mission. Total pointing losses for each mission phase have been previously tabulated in Table 4.1-14.

The antenna gimbal drives can produce gimbal rates up to 2 degrees per second, which is greater than the maximum required rate during spacecraft maneuvers by a factor of 6. The gimbal actuators mechanically detent their shafts in between stepping commands without application of electrical power. Thus the antenna is locked in attitude during cruise except during stepping pulses, which are required no oftener than once a day. This positive locking is essential during orbit insertion where acceleration up to 2.2g will occur.

Gimbal Drive Mechanization--A functional block diagram of the gimbal drives is shown in Figure 4.1-28. Gimbal actuation is by stepper motor (Abrams Instrument Corp, Model DMA) driving through a gear reduction (United Shoe Machinery, harmonic drive) of 205 to 1. This gear ratio, combined with the motor-stepping characteristic (36 degrees per step), produces a requirement for 11-bit encoding of antenna gimbal angle.

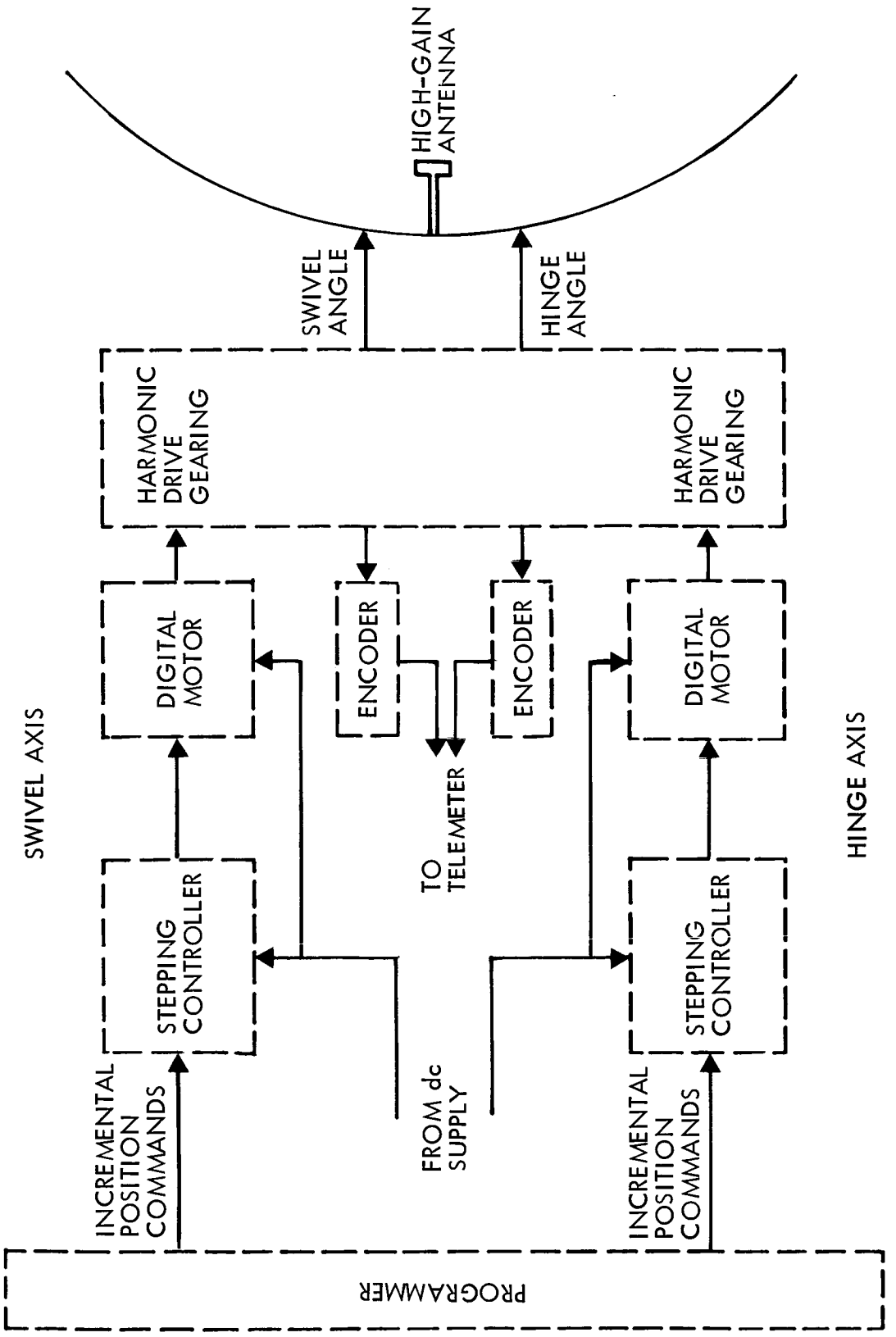

Figure 4.1-28: High-Gain Antenna Position Control

Redundant readout of gimbal angle is provided by a 10-bit absolute encoder (Northern Precision Laboratories). Both the motor and encoder are being used in the high-gain antenna controller for the NASA Lunar Orbiter and have been subjected to extensive testing in environmental conditions more severe than those anticipated in this application. Selection of a harmonic drive gear provides a hermetically sealed enclosure for the motor and encoder at no addition penalty in weight and volume. Position-indexing of the motor, load, and encoder is maintained within the limits of the drive backlash, which is held within $\pm$ 2 minutes of arc.

The motor-stepping controller utilizes solid-state logic and power-switching circuits, which were developed for similar applications on the NASA Lunar Orbiter. Power consumed during stepping is essentially motor power (50 watts during 50-millisecond pulse time); power consumption is negligible at all other times.

S-Band Low-Gain Antenna--The low-gain antenna is required to provide nearly spherical coverage to allow communication early in the transit trajectory, and provide for command reception in the later phases in the event of attitude control malfunction. The biconical circularly-polarized horn antenna has been selected. It provides coverage over 95 percent of a sphere at moderate gain levels (+2 db to -6 db). The biconical horn antenna consists of a slot radiator section and two conical caps and is sketched in Figure 4.1-29. Shunt susceptance elements mounted in the transmission line match the antenna impedance to that of the transmission line.

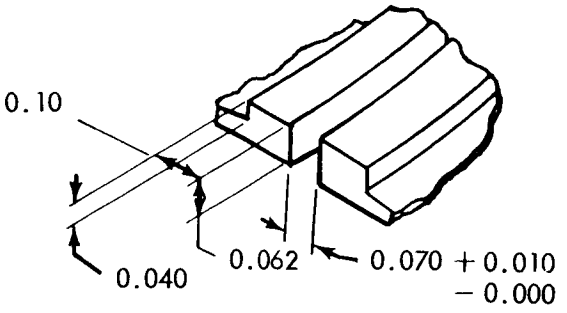

SLOT DETAIL

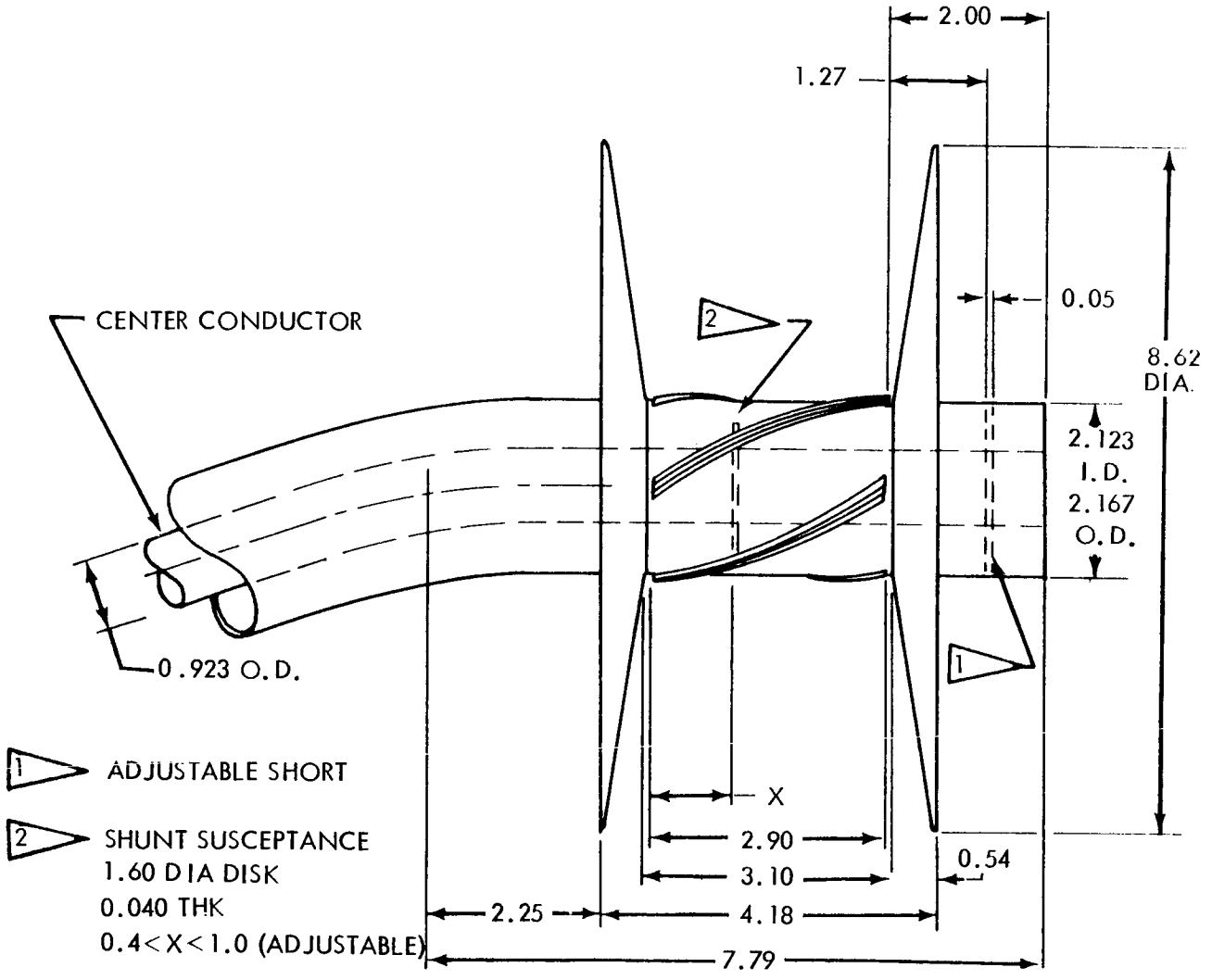

NOTE: DIMENSIONS IN INCHES

Figure 4.1-29: Low-Gain Antenna

The antenna pattern is toroidal. The antenna axis is the axis of the toroid. Antenna axis orientation is given by two angles: a rotation in the X-Y plane measured from the X axis, CCW positive, and a tilt of the axis out of the X-Y plane with positive angles above the plane. The two orientation angles are 87^{o} and 5^{o} for the rotation and tilt respectively of the antenna axis. With these angles the coverage provided is shown in Figure 4.1-30. Typical Earth look angles from the vehicle are shown. All anticipated look angles for the predicted Earth trajectories are well within the pattern coverage provided by this antenna. Maintenance of gain during an arbitrary maneuver requires constraints on the sequence of maneuvers employed in reaching the designated attitude.

Polarization Losses, Cruise and Orbit--The following values are also applicable during pre-maneuver rotations when a sequence of rotations suitable for maintaining near-maximum gain is followed.

Polarization losses are calculated, as for the high-gain antenna, from these axial ratios:

At 2295 Mc: $R_1 = 1.084$

$R_2 = 1.59$

At 2115 Mc: $R_3 = 1.59$

$R_4 = 1.19$

Then:

$$0.16 \text{ db} \leqslant P\ (2295) \leqslant 0.31 \text{ db}$$

$$0.08 \text{ db} \leqslant P\ (2115) \leqslant 0.41 \text{ db}$$

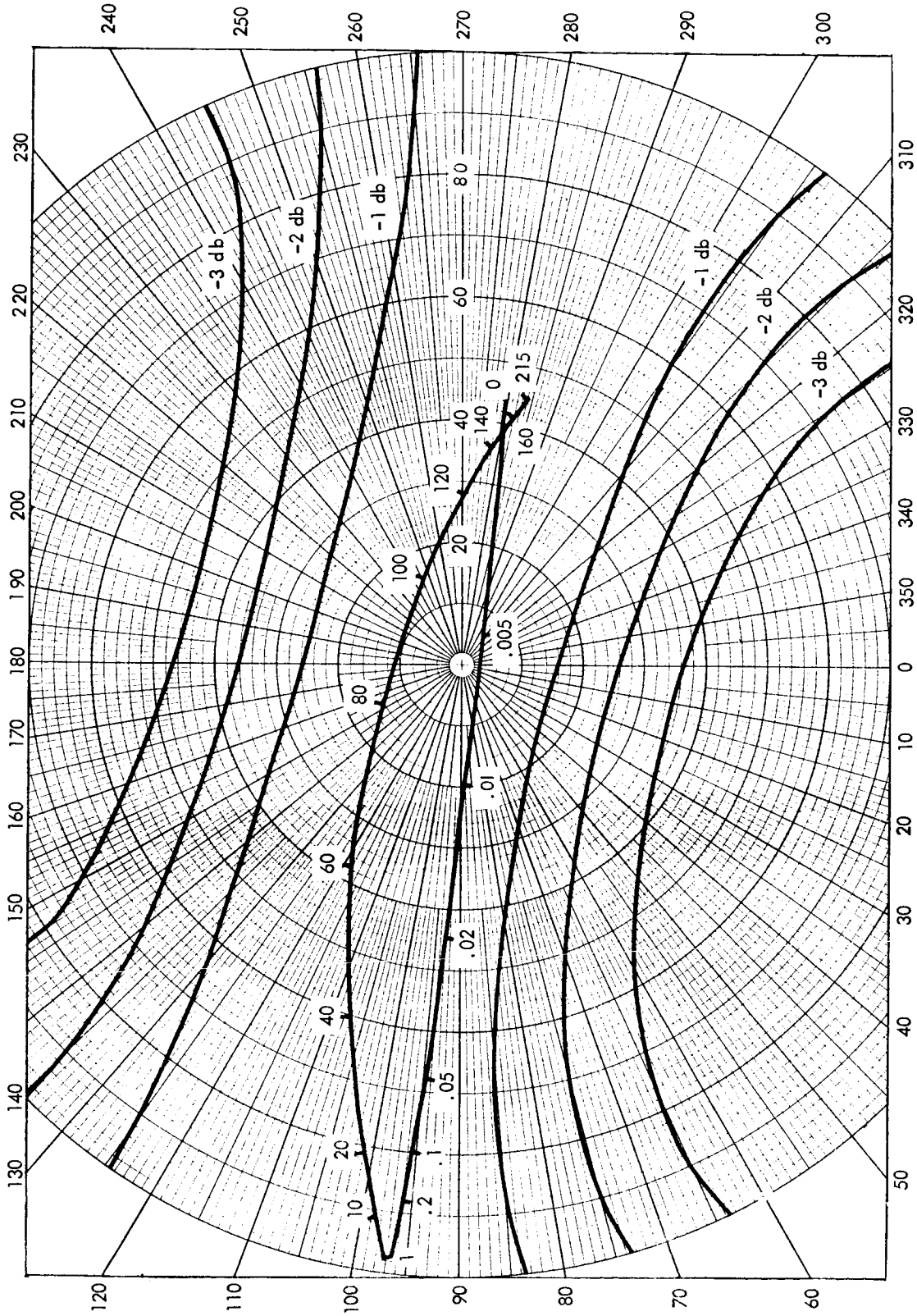

Figure 4.1-30: Low-Gain Antenna Coverage For Dipole Pattern

Ascent Antennas--Four elements are used to provide communication before and during the boost phase of the mission.

Shroud Antenna--A circularly-polarized S-band horn antenna installed in a radome, provides coverage during launch. The cylindrical portion of the shroud is recommended for this location, in order to provide maximum coverage to Station 71 during the boost phase and up to shroud separation. The antenna receives rf energy from the launch exciter through an rf coupler connected to the transmission line which leads to the acquisition antennas. At shroud separation, the antenna is disconnected and rf power is transferred to the acquisition antennas.

RF Coupler--The direct coupling through a separable connector to the launch-exciter-acquisition antenna transmission line provides a simple means of obtaining almost complete energy transfer to the shroud antenna. The connector is preferable to a loosely-coupled probe or a closely fitting antenna cover-type coupler. The loosely-coupled probe would have coupling losses of about 20 db, while an antenna cover would be difficult to separate. A sketch of the coupler is shown in Figure 4-1-31.

Acquisition Antennas--Two antennas are used to provide approximately spherical coverage after shroud separation; a circularly polarized omnidirectional antenna similar to the low-gain antenna shown in Figure 4.1-29, and a pyramidal horn. The onmidirectional antenna is mounted on the nose of the capsule so that it has a dipole type pattern about the vehicle's roll axis. Pattern coverage is over the major

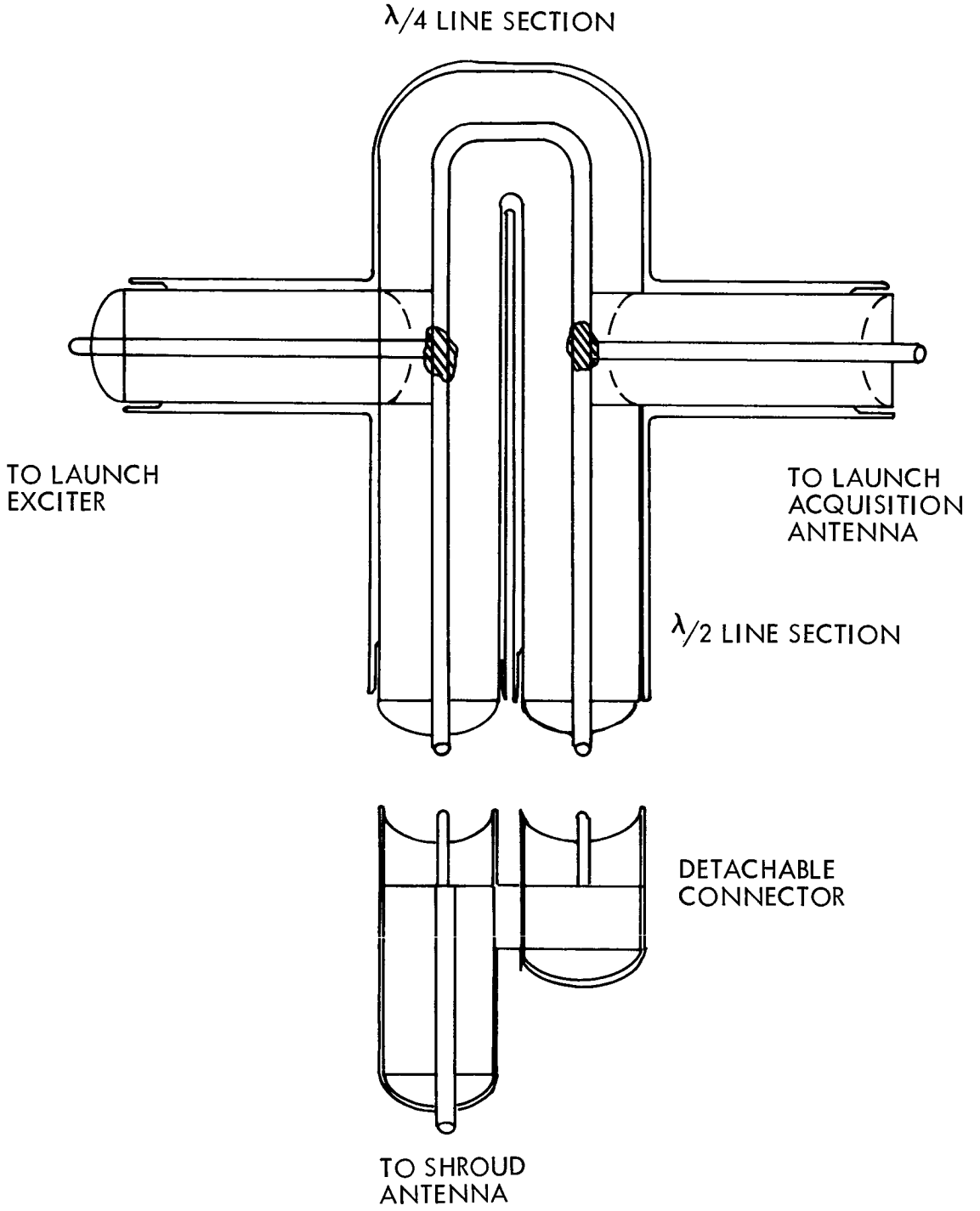

Figure 4.1-31: RF Coupler

portion of the sphere except for the region behind the vehicle (along the negative Z-axis) which is shadowed by the capsule and vehicle. A horn antenna pointed along the negative Z-axis is used to fill in the region shadowed by the vehicle. Since some interference lobes in the overlap region are unavoidable, experimental optimization of horn parameters will be required. The higher gain of the horn antenna requires a power divider between the two antennas to provide a uniform signal level around the vehicle. Approximately 75 percent of the power is radiated by the onmidirectional antenna.

Relay Antenna--The Relay (VHF) Antenna is a single low-gain VHF antenna, connected to the relay radio subsystem by its transmission line. The need for increased gain at apoapsis indicated the need for an antenna with increased gain in one hemisphere in order to reduce the variation in received signal level during an orbit. The two-element dipole array provides this capability while having only a small effect on communications immediately following separation.

The two-element array configuration is shown in Figure 4.1-32 and consists of a radiating element together with a parasitic reflector. The spacing and length of the parasitic element determines the radiation characteristics of the antenna. Proper spacing and length gives an antenna with 7 db gain and front to back ratio of 5 db. A simple impedance-matching network at the base of the antennas radiating element matches the antenna impedance to that of the transmission line.

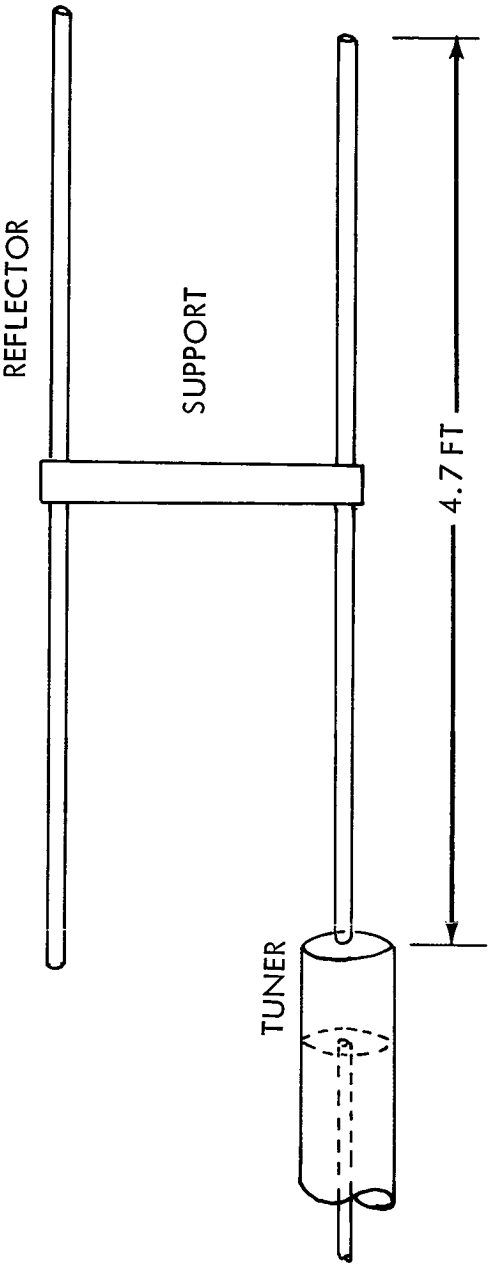

Figure 4.1-32: Linearly-Polarized Antennas For 100 mc

The orientation angles for the antenna axis are 82° and -15° for the rotation and tilt angles respectively. The Mars look angles and the gain contours for a dipole antenna pattern are shown in Figures 4.1-33 and 4.1-34 for the 1st and 240th orbit, respectively.

Transmission Lines--A number of different types of transmission lines exist that can be used for the antenna systems. The types considered are flexible, ridged and standard waveguide, Styroflex and Foamflex coaxial cable. Of the coaxial cables, Styroflex is preferred because of the more rapid outgassing possible. A list of estimated cable losses for various transmission lines for the antenna systems is given in Table 4.1-15. A VSWR loss of 0.1 db is charged to all systems along with a rotary-joint loss of 0.2 db per rotary joint where applicable. The rotary joints in the cable runs account for a large part of the losses; a reduction of the losses in these items gives the greatest improvement in performance. Reducing cable losses by using wave-guide instead of coaxial cable gives a relatively small increase in performance.

Performance Parameters--Table 4.1-16 contains a summary of antenna subsystem performance parameters.

Weights and Power Consumption--The weight and input power requirements are summarized in Table 4.1-17. Interface Definition Table 4.1-18 contains a summary of all Antenna Subsystem Interfaces.

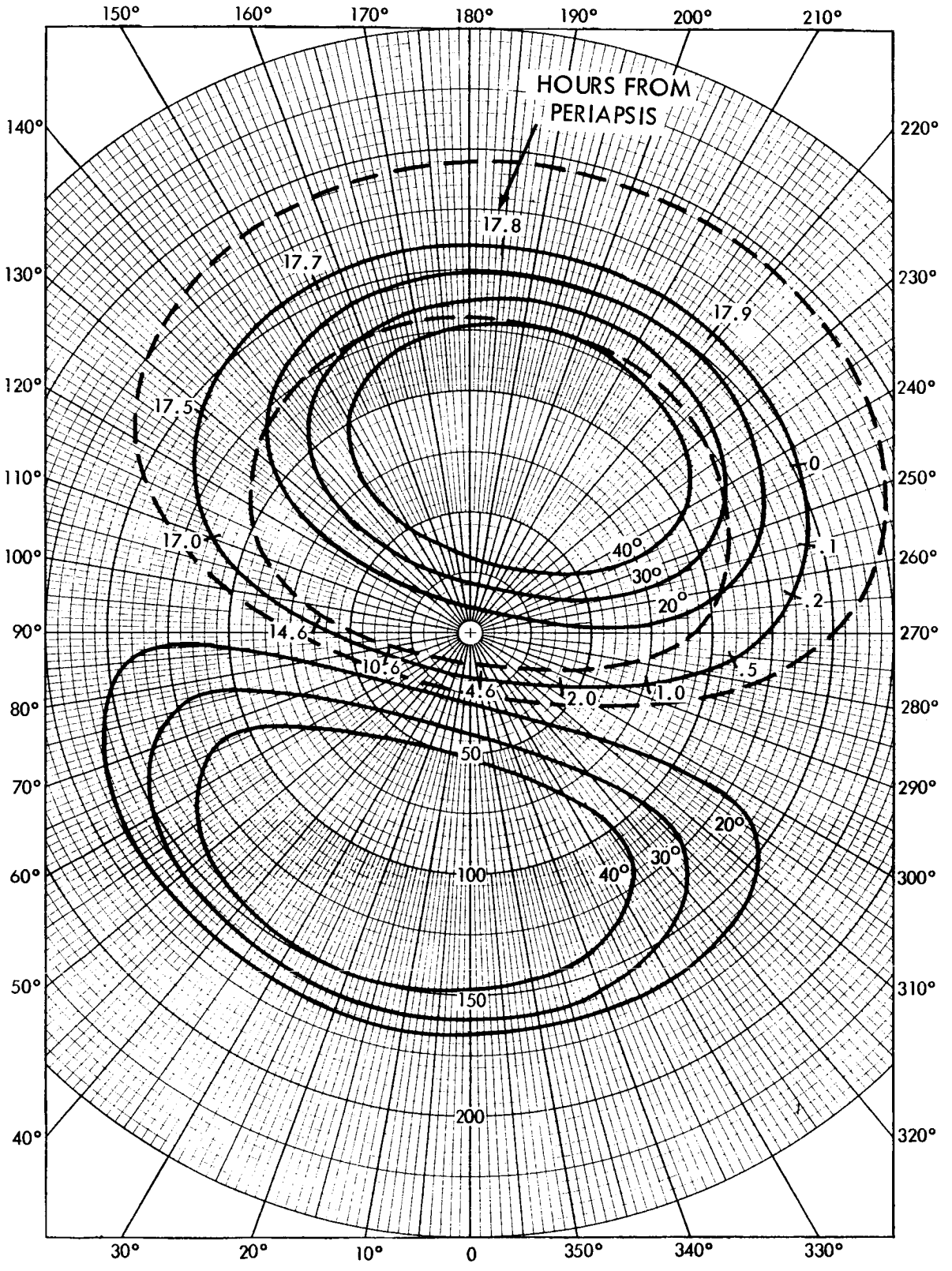

Figure 4.1-33: VHF Antenna Coverage 1st Orbit

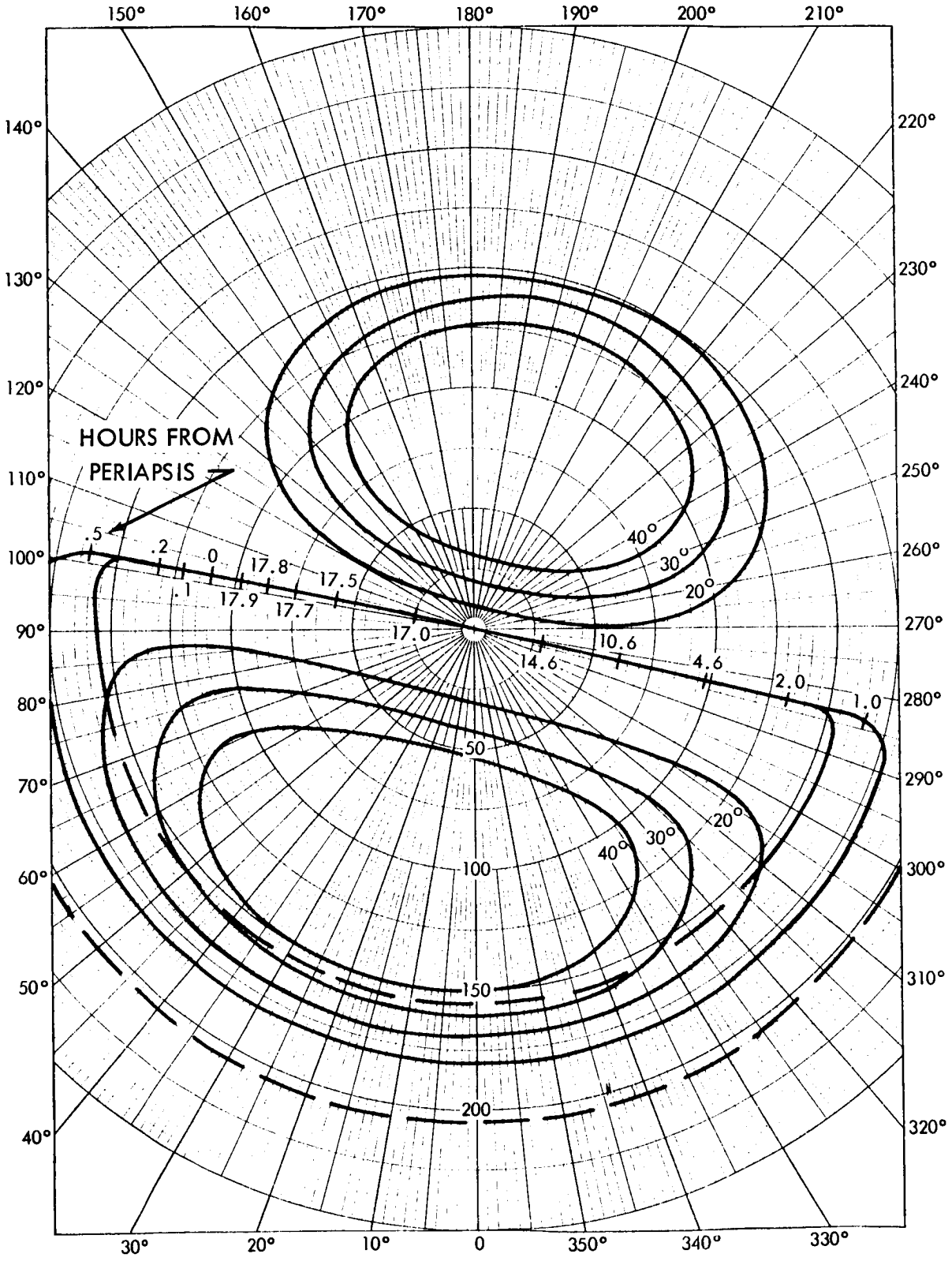

Figure 4.1-34 VHF Antenna Coverage 240th Orbit

Table 4.1-15: TRANSMISSION LINE LOSSES

Antenna	Frequency	Maximum Cable Length	Cable Size	Total Cable Loss (db)	Number of Rotary Joints	Total Loss	Weight (lb/ft)
Relay	VHF	28'	RG 142 3/8" 1/2" 7/8" RG 143	1.06 0.32 0.22 0.12 0.7	0 2 2 2 0	1.16 0.82 0.72 0.62 0.8	0.045 0.097 0.165 0.5 0.108
Low Gain	S-Band	11' boom 16' cable	 1/2" 7/8" 1-5/8"	0.086 0.72 0.42 0.26	1	 1.1 0.81 0.65	 0.93
High Gain	S-Band	4' feed 7' cable	boom boom 7/8" 1-5/8"	0.04 0.056 0.18 0.11	4	 1.0 1.12 1.05	0.27
Ascent	S-Band	21' boom 14' cable 35' cable	boom 7/8" 1-5/8" 7/8" 1-5/8"	0.17 0.36 0.22 0.94 0.56		 0.63 0.49 1.04 0.66	

Table 4.1-16: SPACECRAFT ANTENNAS--PERFORMANCE PARAMETERS

	Radio Frequency	Gain (Referred to Isotropic Level)	Axial Ratio	Impedance/ VSWR
High-Gain Antenna	2,115 ±5 mc	+32.1 -- +34.1 db	1.3 - 1.9	50 ohms 1.6:1
	2,294 ±5 mc	+34.3 -- +35.4 db	1.1 - 1.2	50 ohms 1.3:1
Low-Gain Antenna	2,115 ±5 mc	+1 -- +2 db (See Fig. 4.1.3.4-7)	1.6	50 ohms 1.7:1 (1)
	2,295 ±5 mc	+1 -- +2 db	1.6	50 ohms 1.3:1
Ascent Antennas				
Shroud Antenna	2,295 ±3 mc	-10 -- -19 db		50 ohms 1.3:1
Acquisition Antennas	2,295 ±3 mc	-2 db over 90% of sphere (design goal)		50 ohms 1.3:1
+Z Ascent	2,295 ±3 mc	(+Z and -Z connected through power divider for above performance)	Variable	--
-Z Ascent	2,295 ±3 mc			--
Relay (VHF) Antenna	100 mc (nominal)	+5 -- +7 db	linearly polarized	50 ohms 1.5:1

(1) Actual performance for antenna illustrated in Figure 4.1.3.4-8: 1.2:1 at 2,295 mc
1.7:1 at 2,115 mc;

Parameter is adjustable.

Table 4.1-17: WEIGHTS AND POWER CONSUMPTION

	Weight	Power
Low-Gain Antenna		
Antenna Assembly	1.5 lb	--
Boom Assembly	4.9 lb	--
High-Gain Antenna		
Antenna Dish Assembly	38.0 lb	--
*Boom Assembly - 22.0 lb		--
*Drive Units - 9.5 lb		Maneuver: 120 watt peak, 1-50 ms pulse/sec; 6 watts average.
*Weight for these items is included under Spacecraft Mechanisms Subsystem.		Cruise & Orbit Less than one pulse/day; Less than one watt average.
Ascent Antennas		
Shroud Antenna	1.5 lb	
RF Coupler	0.5 lb	
Acquisition Antenna	1.5 lb	
Relay Antenna (VHF)		
VHF Antenna Assembly	1.5 lb	
VHF Boom	4.9 lb	
Total	54.3 lb.	

Table 4.1-18: INTERFACE DEFINITION--SPACECRAFT ANTENNA SUBSYSTEM

A. High-Gain Antenna--Electrical Interfaces

Interface	Impedance	Signal Level	Frequency
Spacecraft Radio Subsystem	50 ohms 1.3:1 VSWR	Receive: -50 to -151 dbm Transmit: +47 dbm	2,115 ±5 mc 2,295 ±5 mc

-- Thermal Interfaces

Thermal

Reflector surface temperatures/thermal gradients require thermal control to assure reflector edge deflection of less than ±0.06 inches from mean. Corresponding reflector RMS surface deviations from true paraboloidal contour are to be determined, but will be of the order of 0.3 inches. (This estimate is somewhat dependent on the periodicity of surface deviations.)

Antenna Feed will require thermal control to assure dimensional/physical stability of conductors and dielectrics, within temperature limits to be determined.

Antenna Feed Support structure will require thermal control to assure angular alignment (corresponding to transverse displacements at focus) of 0.05° or less.

-- Mechanical Interfaces

Mechanisms Subsystems

The high-gain antenna will be supported on a deployment/two-axis drive mechanism (Ref. Section 4.4.4, Mechanisms Subsystems) R-F transmission lines will be carried on or through the deployment/drive mechanisms (including deployment and drive articulation), from a connector joining to a transmission line to the spacecraft radio subsystem, to a connector at the antenna joining a transmission line to the antenna feed.

Table 4.1-18: INTERFACE DEFINITION--SPACECRAFT ANTENNA SUBSYSTEM (Continued)

Interface	Impedance	Signal Level	Frequency
B. High-Gain Antenna Position Control -- Electrical Interfaces			
CC&S			
Swivel Axis	6,000 ohms	0, +6V.	DC pulse
Hinge Axis	6,000 ohms (CC&S output)	0, +6V.	
Spacecraft Telemetry and Data Storage	6,000 ohms (encoder internal)	0, +6V.	DC pulse 11 conductors (10-bit code)
Spacecraft Power Subsystem	NA	Maneuver: 60 watts per axis, 50-ms pulse; total 120 watts peak, 6 watts.	DC pulse (26V. nominal)
		Cruise and Orbit: Less than one 60-watt pulse per axis per day.	DC pulse
-- Magnetic Interface			
Magnetic	Stepping motors (2) are solenoid-type, without permanent magnets, and energized only by 50-millisecond pulses as noted under Power Subsystem above.		

Table 4.1-18: INTERFACE DEFINITION--SPACECRAFT ANTENNA SUBSYSTEMS(Continued)

Interface	Impedance	Signal Level	Frequency
C. Low-Gain Antenna	-- Electrical Interfaces		
Spacecraft Radio Subsystem	50 ohms		
	Receive: 1.7:1 VSWR	-50 to -156 dbm	2,115 ±5 mc
	Transmit: 1.3:1 VSWR	+47 dbm	2,295 ±5 mc
Mechanisms Subsystems	-- Mechanical Interface The Low-Gain Antenna is supported on a deployable boom (Ref. Section 4.4.4, Mechanisms Subsystems). An R-F transmission line on an interval with the boom and mechanism will be carried from the antenna to a connector joining a transmission line to the Radio Subsystem.		
D. Ascent Antennas	-- Electrical Interfaces		
Spacecraft Radio Sub-System:			
Shroud Antenna	50 ohms 1.3:1 VSWR	+30 dbm	2,295 ±3 mc
RF Coupler	50 ohms	+30 dbm	2,295 ±3 mc
Acquisition Antennas (2) at Common Input:	50 ohms	+30 dbm	2,295 ±3 mc

Table 4.1-18: INTERFACE DEFINITION--SPACECRAFT ANTENNA SUBSYSTEMS (Continued)

Interface	Impedance	Signal Level	Frequency
	-- Shroud Interface		
Shroud	The Shroud Antenna will be installed in the cylindrical portion of the shroud, behind Saturn Station 2048. A transmission line will join the Shroud Antenna to the Radio Subsystem at a separable connector (RF Coupler)		
	-- Capsule Interface		
Capsule	The "+Z Ascent Antenna" will be mounted on the canister enclosing the Flight Capsule (Ref. Model 945-6026A, Dwg, 25-50034A). A transmission line will join the "+Z Ascent Antenna" to a power divider located at or near the "-Z Ascent Antenna," which is mounted on spacecraft structure.		
E. Relay (VHF) Antenna --Electrical Interfaces			
Spacecraft Relay Radio Subsystem	50 ohms 1.5:1 VSWR	-222 to +27 dbm	100 mc (nominal)
Mechanisms Subsystems	The Relay Antenna is supported on a deployable boom (Ref. Section 4.4.4, Mechanisms Subsystems). An R-F transmission line within the boom and mechanism will be carried from the antenna to a connector joining a transmission line to the Relay Radio Subsystem.		
F. Transmission Lines -- Thermal Interfaces			
Thermal	Transmission lines (including coaxial cables and waveguides which are separate from or integral with structural elements, as well as transmission line components such as connectors and rotary joints) will require thermal control to assure dimensional/physical stability of conductors and dielectrics, within temperature limits to be determined (by allowable center-conductor temperature--nominally 482°F for Teflon, 175°F for polyethylene).		

4.1.4 Telecommunications Link Analysis

4.1.4.1 Introduction

Performance of each telecommunication link in the recommended design is discussed in this section. The command and ranging channels were analyzed for the DSIF-to-spacecraft links, and the telemetry and ranging channels were analyzed for the spacecraft-to-DSIF links. Power levels and performance margins were determined for the data transmission modes used in each phase of the mission.

The telecommunication performance analysis was established by use of design control tables in accordance with JPL Specification No. 3393-19-65, entitled, "Explanation of the Telecommunications Design Control Tables," dated April 28, 1965.

The criteria and analysis used to derive the various system parameters including carrier and data threshold values, acquisition times, probability of loss of synchronism, and modulation indices and losses are presented in a specific format to meet the requirements of JPL document, "Contractor Performance Measures of the Telecommunications System," transmitted by JPL cover letter from Mr. A. Gluckson to The Boeing Company on May 17, 1965.

The design control tables permit a realistic evaluation of the received power, performance margins, and tolerances for the carrier and all subcarriers for each data mode and set of subsystem parameters. Determination of performance parameters at selected points allows scaling to all communication distances where the data mode and subsystem parameters apply.

These tables indicate the sources of the values and tolerances established for each parameter. This feature permits verification of the parameters and results in the program study phase. During the design and implementation phases, the design control tables show the required and expected performance for each parameter and its reference or source of derivation within the text.

Flight Sequence and Data Mode Requirements--Variations in communication distance and data transmission requirements in the various mission phases necessitate several combinations of data modes, antennas, transmitters, and receivers. Table 4.1.4-1 shows the communication range, antennas, transmitters, and data modes used in the mission phases from launch through orbital operations. The mission phases and data modes are reviewed to provide background information for subsequent descriptions of link performance.

The launch phase extends from liftoff through initial two-way acquisition of the spacecraft by Johannesburg after spacecraft injection into trans-Mars trajectory. The spacecraft transmits at low power through the shroud antenna until shroud separation. After the shroud is removed, the spacecraft transmits through the ascent antenna to DSIF station 71 until the spacecraft disappears below the radio horizon. The next contact with the spacecraft occurs when the Johannesburg acquisition antenna acquires the spacecraft after cruise injection.

The cruise phase begins within 1 hour after launch when the DSIF operation is switched from the acquisition antenna to the 85-foot antenna. The

MISSION PHASE	DESCRIPTION	COMMUNICATION RANGE (km)	DSIF	
			ANTENNA	POWER(kw)
LAUNCH	SPACECRAFT SHROUD	0-200	DSIF 71 4 ft	--
"	SPACECRAFT ASCENT	200-2000	DSIF 71 4 ft	--
"	ACQUISITION JOHANNESBURG	6000-12,000	JOHAN-NESBURG 2x2 ft HORN	10
CRUISE	SPACECRAFT ASCENT	1.2×10^{4}-3×10^{5}	85 ft	"
"	SPACECRAFT LOW-GAIN	3.10^{5}-1.9×10^{7}	85 ft	"
"	S/C LOW-GAIN MANEUVERS	1.5×10^{6}-3×10^{7}	85 ft	"
"	S/C HIGH-GAIN	1.9×10^{7}-1.44×10^{8}	85 ft	"
"	OPTIONAL LATE M/C MANEUVERS	1.2×10^{8}-1.4×10^{8}	85 ft	"
"	DATA PLAYBACK **	1.2×10^{8}-1.4×10^{8}	85 ft	"
CAPSULE SEP. & DESCENT	SEPARATION MANEUVER	1.44×10^{8}	210*/85 ft	"
"	DATA PLAYBACK**	1.44×10^{8}	"	"
"	PRE-ENCOUNTER CRUISE	1.44×10^{8}-1.57×10^{8}	"	"
"	INSERTION MANEUVER	1.57×10^{8}	"	"
"	DATA PLAYBACK**	1.58×10^{8}	"	"
"	CAPSULE IMPACT	1.57×10^{8}	"	"
MARS ORBIT INSERTION	INSERTION BURN	1.57×10^{8}	"	"
"	POSTBURN PLAYBACK	1.57×10^{8}	"	"
"	POSTINSERTION MANEUVER	1.57×10^{8}	"	"
"	DATA PLAYBACK**	1.57×10^{8}	"	"
ORBITAL OPERATIONS	EARLY ORBIT	1.57×10^{8}-3.34×10^{8}	"	"
"	REAL-TIME PLANETARY DATA READOUT	1.57×10^{8}-1.70×10^{8}	"	"
"	ORBIT	3.34×10^{8}-3.69×10^{8}	"	"
"	LATE ORBIT	$3.34\text{-}10^{8}$-3.69×10^{8}	"	"
ALL MODES	EMERGENCY	3×10^{7}-3.69×10^{8}	210/85 ft	100

NOTE: *) TELEMETRY RECEPTION USED 210 FOOT NET WHILE COMMAND TRANSMISSION REMAINS O.
**) OPTIONAL
***) TELEMETRY ON ASCENT ANTENNA, COMMAND, ON LOW GAIN ANTENNA

SPACECRAFT		COMMAND LINK	RANGING CAPABILITY	TELEMETRY MODE	APPLIC
ANTENNA	POWER (w)				TELEMETR
SHROUD	1	NO	NO	1	TABLE 4.1.4-
ASCENT	1	NO	NO	1	TABLE 4.1.4-
ASCENT/ LOW-GAIN ***	1	CARRIER ONLY	NO	1	TABLE 4.1.4
ASCENT/ LOW-GAIN ***	1	YES	NO	2	TABLE 4.1.4 -
LOW-GAIN	50	YES	YES	2	TABLE 4.1.4-
LOW-GAIN	50	YES	NO	1	TABLE 4.1.4
HIGH-GAIN	50	YES	NO	2	TABLE 4.1.4-
"	50	YES	NO	2	SCALED FRO 4.1.4-18
"	50	YES	NO	3	SCALED FRO 4.1.4-18
"	50	YES	NO	2	SCALED FRO 4.1.4-18
"	50	YES	NO	3	SCALED FRO 4.1.4-18
"	50	YES	NO	2	TABLE 4.1.4
"	50	YES	NO	2	SCALED FRO 4.1.4-18
"	50	YES	NO	3	SCALED FRO 4.1.4-18
"	50	YES	NO	5a	TABLE 4.1.4
"	50	YES	NO	5a	SCALED FRO 4.1.4-20
"	50	YES	NO	5a	SCALED FRO 4.1.4-20
"	50	YES	NO	5a	SCALED FRO 4.1.4-20
"	50	YES	NO	3	SCALED FRO 4.1.4-18
"	50	YES	NO	5a	TABLE 4.1.4
"	50	YES	NO	6	TABLE 4.1.4
"	50	YES	NO	5b	TABLE 4.1.4
"	50	YES	NO	5c	TABLE 4.1.4
LOW-GAIN	50	YES	NO	4	TABLE 4.1.

N 85 FOOT NET

Table 4.1.4-1: Flight Sequences & Data Mode Requirements

ABLE DESIGN CONTROL TABLES		RANGING
Y	COMMAND	
11	---	
3	---	
14	TABLE 4.1.4-25	
15	TABLE 4.1.4-26	
17	TABLE 4.1.4-26	TABLE 4.1.4-28 & 29
-16	SCALED FROM TABLE 4.1.4-26	
18	TABLE 4.1.4-27	
A TABLE	TABLE 4.1.4-27	
A TABLE	TABLE 4.1.4-27	
M TABLE	TABLE 4.1.4-27	
M TABLE	TABLE 4.1.4-27	
-20	TABLE 4.1.4-27	
M TABLE	TABLE 4.1.4-27	
M TABLE	TABLE 4.1.4-27	
-18	TABLE 4.1.4-27	
M TABLE	SCALED FROM TABLE 4.1.4-27	
M TABLE	SCALED FROM TABLE 4.1.4-27	
M TABLE	SCALED FROM TABLE 4.1.4-27	
M TABLE	SCALED FROM TABLE 4.1.4-27	
-20	TABLE 4.1.4-27	
-21	TABLE 4.1.4-27	
-22	TABLE 4.1.4-27	
-23	TABLE 4.1.4-27	
-19	TABLE 4.1.4-26	

cruise phase lasts until the spacecraft is oriented for capsule separation at about 10 days before arrival at Mars.

The capsule separation phase begins when the spacecraft is oriented for capsule release. The phase is considered to last until the capsule impacts on Mars. After separation, the spacecraft returns to normal cruise phase with capsule data obtained via the VHF relay link.

The Mars orbit insertion phase begins after capsule impact when the spacecraft has been oriented for insertion firing. It ends when the spacecraft has been inserted into the desired orbit and has reacquired the Sun and Canopus. Total duration of the phase is less than 1 day including any time needed for postburn playback of stored engineering and capsule data.

The remainder of the spacecraft lifetime constitutes the orbital operations phase, which is characterized by extremely high-data-rates needed for the transmission of planetary science data. Telemetry link performance permits real-time planetary data transmission for at least 10 days after encounter. Three lower data rates are provided for planetary science data transmissions in the later orbital periods.

Data Mode Descriptions--Telemetry data modes are reviewed in the following paragraphs and are discussed fully in Section 4.1.4.2. Mode 1 provides engineering and capsule data at a combined rate of 22-2/9 bits per second on a sinusoidal subcarrier with a pseudo-random bit synchronization code on a square-wave subcarrier. Mode 2 combines cruise science data with

engineering and capsule data at a rate of 133-1/3 pits per second on a single subcarrier. Mode 3 substitutes stored engineering for cruise science data to provide delayed readout after maneuvers at 133-1/3 bits per second. Mode 4 is used in emergencies to provide telemetry readout at 5-5/9 bits per second where system degradation such as high-gain antenna failure or extreme range precludes using Mode 1. Mode 5a has a lower subcarrier channel capable of 400 bits per second of engineering, cruise science, and capsule data, and an upper subcarrier channel for playback of planetary science data at a rate of 8000 bits per second. Modes 5b and 5c differ from 5a by having planetary science readout rates of 4000 and 2000 bits per second, respectively, and a 400-bits-per-second lower channel. Mode 6 has a 48,000-bit-per-second capability on the upper subcarrier for real-time transmission of planetary science data and a 400-bit-per-second subcarrier for cruise science, capsule, and engineering data.

The command link transmits command data at a rate of 1 bit per second on a single subcarrier along with a PN code sequence for synchronization, which is modulo 2 added to the command data and transmitted on the same subcarrier. The command carrier without modulation is transmitted to the spacecraft for initial acquisition at Johannesburg.

The turnaround ranging link modulates the command carrier with a PN range code word for transmission to the spacecraft. The spacecraft operates in telemetry Mode 1 for ranging with the range code transmitted back to the DSIF as additional modulation.

Choice of Critical Design Control Tables--Table 4.1.4-1 lists command, ranging, and telemetry modes that have sufficiently distinct characteristics to require individual design control tables. The performance during all periods can be found by scaling from the indicated tables. Maneuver modes differ from normal cruise modes only in the amount and tolerances for spacecraft antenna pointing error that can occur. Thus, the design control tables for cruise modes can be made applicable to maneuver cases by modifying the tables for the differences in the nominal value and the positive and negative tolerances. It is also possible to scale the tables to reflect the use of the 210-foot antenna instead of the 85-foot antenna for telemetry, or to show the effect of using the 100-kilowatt transmitter instead of 10-kilowatt transmitter for command. The performance of telemetry mode 5a during the insertion maneuvers can also be determined by scaling.

DSIF Parameters--The Deep Space Instrumentation Facility (DSIF) provides the ground terminals for telemetry, command, and ranging contact with the spacecraft. Pertinent characteristics of the DSIF stations usable with the spacecraft are shown in Table 4.1.4-2. DSIF station 71 at Cape Kennedy receives telemetry from liftoff until the spacecraft disappears below the radio horizon. The first station to contact the spacecraft after injection is normally Johannesburg. There, a 2 by 2 foot horn monopulse acquisition antenna transmits the command carrier for frequency acquisition and acquires and tracks the spacecraft telemetry transmission in frequency and direction. After sufficient tracking information is obtained with the acquisition antenna, tracking is transferred to the

Table 4.1.4-2: VOYAGER DSIF PARAMETERS

	Receive	Transmit	References
Ground Transmitter Power			
Present Capability		10 kw+.5 db -0	EPD 283 EPD 258
Planned Capability (Goldstone Venus Station now)		100 kw+.5 db -0	EPD 283 EPD 258
Ground Circuit Loss			
210-foot diplexed, non-tracking feed		-0.2 ±0.1 db	TM 33-83 R1
210-foot diplexed and tracking		-0.4 ±0.1 db	EPD 283
210-foot maser	-0.2 +0.1 db -0.0		EPD 283
210-foot paramp	-0.3 ±0.1 db		EPD 283
85-foot diplexed and tracking		-0.4 ±0.1 db	EPD 283
85-foot maser	-0.2 +0.1 db -0.0		EPD 283
85-foot paramp	-0.3 ±0.1 db		EPD 283
Acquisition Antenna	-0.5 ±0.2 db	-0.5 ±0.2 db	MC-4-310A
Station 71 (1)	-0.5 ±0.2 db		
Ground Antenna Gain			
210-foot	61 db +1.0 db -0.5	60.3 db +1.0 db -0.5 db	EPD 283
85-foot	53 +1.0 db -0.5 db	51.0 db +1.0 db -0.5 db	EPD 283
Acquisition Antenna	21 db +1.0 db	20 db +2.0 db	EPD 258
Station 71 (4-foot)	26.5 db +1.0 db -0.0 db		Section 4.1.4.2
Antenna Pointing Loss			
210-foot	-0.1 db ±0.1 db	-0.1 db ±0.1 db	EPD 283(2)
85-foot	-0.0 db +0.0 db -0.1 db	-0.0 db +0.0 db -0.1 db	EPD 283(2)
Station 71	-0.5 db ±0.5 db		Section 4.1.4.2
System Noise Temperature			
210-foot listen feed only, maser	25°K		EPD 283
210-foot diplex or tracking	35°K		EPD 283
210-foot diplexed and tracking	45°K		EPD 283
85-foot diplexed, track, maser	45°K +10°K - 5°K		EPD 283
85-foot diplexed, track, paramp	270°K ±50°K		EPD 283
Acquisition Site, paramp	270°K ±50°K		EPD 283
Station 71 10-db NF receiver	2640°K -610°K 760°K		Table 4.1.4-12

(1) Assumed same as for acquisition antenna (2) Computed from 0.02-degree angle error

85-foot antenna. The 85-foot antennas are used throughout the cruise phase until immediately before encounter. Telemetry reception is switched to the 210-foot network at encounter while command transmission remains on the 85-foot network.

Most of the details concerning DSIF Station 71 have not been released; circuit losses have been assumed to be the same as for the Johannesburg acquisition antenna. Antenna pointing losses from the 210-foot and 85-foot antennas were computed from the angular pointing accuracies stated in EPD 283 and theoretical antenna patterns. Of the three combinations of noise-temperature and feed listed for the 210-foot antenna, the nominal system temperature used in the performance analysis is 35°K for a tracking, listen-only feed.

Spacecraft Parameters--Following paragraphs discuss spacecraft parameters.
Transmitter Power--The TWT power amplifier output is specified as a minimum of 50 watts into a load VSWR of 2:1. This high-power transmitter will not be used until 1 to 5 days after launch for two basic reasons: primary power is limited until the Sun has been acquired, and the power-supply high voltages would cause breakdown during the launch and early flight pressure environment.

The low-power solid-state transmitter used during the launch and early flight phase is conservatively specified at 1 watt into a load VSWR of 2:1.

Antenna Gain--The four different S-Band antennas on the Voyager spacecraft are the high-gain, low-gain, ascent, and shroud antennas. The gain characteristics given below are with respect to an isotropic radiator of matching polarization.

The high-gain spacecraft antenna, a paraboloidal reflector with an 8- by 12-foot aperture, is specified for telemetry transmission (2295 megacycles) to provide a gain of 34.3 to 35.4 decibels corresponding to antenna efficiencies of 50 to 65 percent. On command reception, the gains are 32.1 to 34.1 decibels corresponding to antenna efficiencies of 36 to 57 percent.

The low-gain biconical spacecraft antenna is similar to the antenna planned for the Lunar Orbiter. The selected location and orientation of this antenna provides an antenna gain of +1 to +2 decibels over the mission period as shown in the combined trajectory and antenna gain plot of Figure 4.1-33 of Section 4.1.3.4, "Antenna Subsystem." The ascent antenna system is used for telemetry transmission during launch, Johannesburg acquisition, and early cruise. The variation in launch time and spacecraft tumbling before Sun and Canopus acquisition causes a large excursion in spacecraft look angles to Station 71 and Johannesburg. Thus, the ascent antenna system is specified as needing nearly spherical gain requirements. The initial antenna design to satisfy this requirement consists of a two-antenna system fed from a tee power divider. One antenna is mounted on the spacecraft rear surface giving coverage aft and downward. The second antenna is mounted on the tip of the capsule providing some aft coverage and coverage of the forward hemisphere. The overall gain for this antenna

system is -2 decibels over 90 percent of the sphere as a design goal pending experimental verification and optimization on the pattern range.

The shroud antenna system is used during prelaunch checkout and the initial launch phase for telemetry transmission. The antenna is a slot type, fed from a special tee junction in the ascent antenna feed line. The net worst-case gain of the shroud antenna will be -10 to -19 db along the booster axis.

Antenna Pointing Loss--The maximum antenna pointing loss for the 8 by 12 foot high-gain spacecraft antenna has been established by the detailed pointing-error analysis of Section 4.1.3.4 for all mission phases. The significant pointing losses are:

Cruise and orbit:	-1 db
Midcourse maneuvers:	-2.5 to -5 db
Insertion burn:	-3 to -4 db
End of insertion burn:	-3 to -6 db

The low-gain biconical antenna provides a nearly spherical pattern and will have no pointing loss during the normal cruise and orbit periods. During maneuvers, a maximum pointing loss of 1 db has been allowed up to ranges corresponding to 100 days from launch. This loss is relative to the antenna gain-pattern orientation during cruise and orbital mission phases.

RF Circuit Losses--The spacecraft rf circuit losses have been determined for each combination of transmitter, receiver, and antenna.

The results are detailed in the simplified switching diagram of Figure 4.1.4-1. The nominal value and tolerances account for variations in temperature, line length, and production tolerances. These numbers would become specification values when component orders are placed. The total losses indicated for each transmit-receive combination have been used in the design control table evaluations.

Spacecraft Receiving System Effective Noise-Temperature--Receiving system noise-temperature data is required to determine the receiver noise spectral density. System noise-temperature must be calculated for two distinct spacecraft receiving modes: one is the low-gain antenna/diplexer/preamp/receiver system; the other is the high-gain antenna/rf-components/receiver system.

Figure 4.1.4-2 shows the model used to determine the system noise temperature for reception through the low-gain antenna.

Figure 4.1.4-2: SYSTEM NOISE-TEMPERATURE MODEL

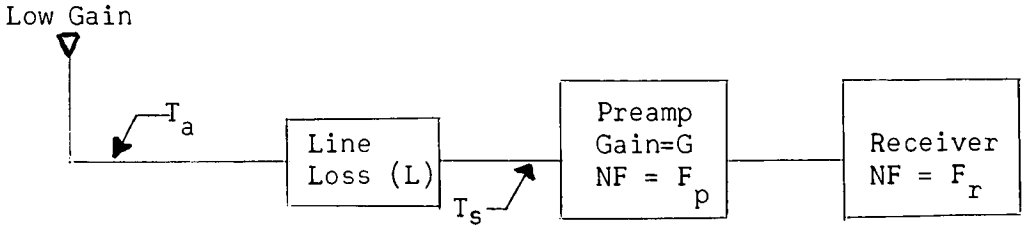

The system noise-temperature (T_s) referred to the preamplifier input is given by:

$$T_s = \underbrace{\frac{T_a}{L}}_{\text{Antenna}} + \underbrace{\left(\frac{L-1}{L}\right)T_L}_{\text{Lossy Network}} + \underbrace{(F_p - 1)T_o}_{\text{Preamp}} + \underbrace{\left(\frac{F_r-1}{G}\right)T_o}_{\text{Receiver}}$$

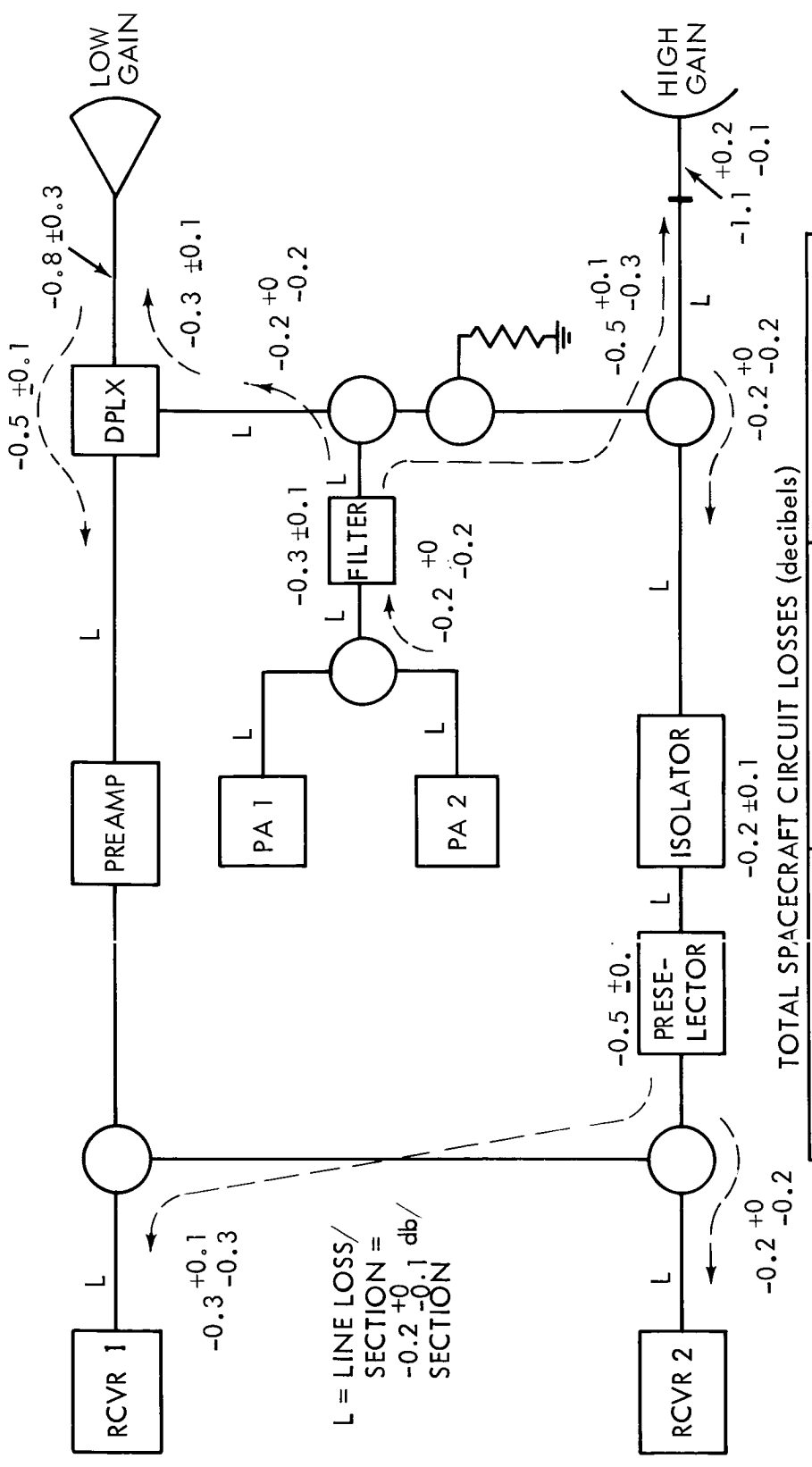

TOTAL SPACECRAFT CIRCUIT LOSSES (decibels)

RECEIVER, LOW-GAIN ANTENNA -1.5 +0.4 -0.5	TRANSMITTER, LOW-GAIN ANTENNA -2.6 +0.5 -1.3	TRANSMITTER, HIGH-GAIN ANTENNA -2.7 +0.4 -1.0	
RECEIVER 1, HIGH-GAIN ANTENNA -3.1 +0.5 -1.2	RECEIVER 2, HIGH-GAIN ANTENNA -3.0 +0.4 -1.1	EXCITER TRANSMITTER VIA ASCENT ANTENNA -0.6 +0.4 -0.6	

Figure 4.1.4-1: RF Circuit Losses

where:

T_o = 290°K

T_a = 30°K contribution due to Earth through the first midcourse maneuver

T_a = 0°K for planetary

T_L = 308°K median compartment temperature

Table 4.1.4-3 presents the results of the system noise-temperature calculations based on the best-, nominal-, and worst-case circuit loss and receiver noise figure values.

Table 4.1.4-3: SYSTEM NOISE-TEMPERATURE--LOW-GAIN ANTENNA

	L	EFF. TEMP., °K		F_p	PREAMP EFF., °K TEMP.	F_R	G	RCUR TEMP.	T_s, °K	T_s, °K
		NTWK	ANT.							
	db	$\frac{L-1}{L} T_L$	$\frac{T_a}{L}$	db	$(F_p-1)290$	db	db	°K	Near Earth	Planetary
Worst	-2.0	114	19	5.0	625	11	13	168	926	907
Nominal	-1.5	91	21.2	4.5	530	10	15	82.5	724.7	703.5
Best	-1.1	65	23.3	4.5	530	9	17	40.3	662.6	639.3

The model used to compute the system noise temperature for reception through the high-gain antenna is the same as shown in Figure 4.1.4-2 except that the preamplifier is removed. The system noise temperature referred to the receiver input is then given by:

$$T_s = \frac{T_a}{L} + \left(\frac{L-1}{L}\right)T_L + \left(F_r-1\right)T_o$$

Calculations have been made to determine the magnitude of solar flux entering through the high-gain antenna side lobes during the closest

approach to the Sun line (at 90 days). These calculations show that T_a is less than 25°K and may be neglected compared to the receiver temperature.

Table 4.1.4-4 shows the system noise-temperature values for the appropriate spacecraft circuit loss values developed previously in Figure 4.1.4-1.

TABLE 4.1.4-4: SYSTEM NOISE-TEMPERATURE--HIGH-GAIN ANTENNA

	L db	Network Temp. $\left(\frac{L-1}{L}\right)T_L$ °K	F_r db	Rcvr. Temp. (F_r-1) 290, °K	T_s, °K
Worst	-4.3	193	11	3360	3553
Nominal	-3.1	157	10	2610	2767
Best	-2.6	139	9	2010	2149

Antenna Polarization Losses--The design control tables used values of polarization losses between the spacecraft high- and low-gain antennas and the DSIF antennas based on preliminary calculations of antenna axial ratios. Best-, nominal-, and worst-case losses were determined corresponding to major-axis misalignment of 0, 45, and 90 degrees, respectively. These losses are listed below in Table 4.1.4-5. Subsequent calculations as detailed in Section 4.1.3.4 have shown a slight increase in values for the command and low-gain telemetry case. The primary high-gain telemetry link value is still as shown in Table 4.1.4-5.

Table 4.1.4-5: ANTENNA POLARIZATION LOSS		
	Telemetry	Command
Spacecraft high-gain--DSIF	0.0 db $^{+0.0\ db}_{-0.1\ db}$	0.0 db $^{+0.0\ db}_{-0.1\ db}$
Spacecraft low-gain--DSIF	0.0 db $^{+0.1\ db}_{-0.1\ db}$	0.0 db $^{+0.2\ db}_{-0.2\ db}$

4.1.4.2 Spacecraft-to-Earth Telemetry Links

Six different spacecraft-to-earth telemetry link modes have been established to support all phases of the Voyager mission and to ensure adequate margins and backup modes for particularly critical events throughout the mission. The basic goal on the selection of specific modes and operating parameters for each mode has been to maximize the quantity of data that can be acquired successfully by the Deep Space Network (DSN).

To select spacecraft modulation parameters for each mode, it has been necessary to define specific performance criteria for each mode, to define channel thresholds to meet these criteria, and to calculate the modulation parameters that yield optimum channel performance at the defined thresholds. Particular emphasis has been placed on:

1) The selection of carrier threshold bandwidths and signal-to-noise ratios for each mode that maximizes the power available in the data channels
2) The selection of realistic data channel threshold $\frac{ST}{(N/B)}$'s that include all identifiable channel losses
3) The selection of carrier modulation indices for each subcarrier to minimize total rf power required at the specified mode threshold

4) The selection of specific bit rates, subcarrier frequencies, and modulation indices to achieve a minimum level of inter-modulation distortion in all channels

5) The analysis of the performance margins that will exist throughout the mission for each mode for the specific spacecraft and ground system parameters that have been selected

The selected modes, channel thresholds, threshold bandwidths, bit rates, subcarrier frequencies, modulation indices, and modulation losses are summarized in Figure 4.1.4-3. This section presents the rationale for selecting the numbers in Figure 4.1.4-3 and documents the resulting spacecraft-to-Earth telemetry data link performance.

Selection of Tracking Receiver Parameters--The tracking receiver parameters that must be specified for each telemetry mode are the threshold loop noise bandwidth, $2B_{LO}$, and the required threshold carrier signal-to-noise ratio referred to $2B_{LO}$, $(S/N)2B_{LO}$. The criterion used in selecting these parameters is the minimization of total system losses in the data channels. This criterion is somewhat more inclusive than the more common rms error, peak phase error, or out-of-lock probability tracking loop criterion in that it includes the effects on the demodulated baseband of noise and doppler errors in the loop as well as the modulation losses, due to the division of available power between the carrier loop and the data channels.

In the ground receiver threshold loop noise bandwidths, $2B_{LO}$, three receiver threshold loop noise bandwidths are available at the DSN sites; 12 cps, 48 cps, and 152 cps. A 5 cps bandwidth is planned per EPD-283.

MODE	TELEMETRY CHANNEL DATA TYPE & RATES	CHANNEL	SUBCARRIER FREQUENCY	PHASE DEVIATION PEAK RADIANS		
				MIN	NOM	MAX
I	S/C ENGRG @ 11 1/9 bps CAPSULE ENGRG @ 11 1/9 bps	CARRIER				
		SYNC	200 c/s	0.32	0.35	0.38
		DATA	400 c/s	1.15	1.27	1.41
II OR III	S/C ENGRG @ 11-1/9 bps CAPSULE ENGRG @ 11-1/9 bps CRUISE SCI @ 111-1/9 bps OR STORED S/C ENGRG	CARRIER				
		DATA	533-1/3 c/s	1.26	1.40	1.54
IV	S/C ENGRG @ 5 - 5/9 bps	CARRIER				
		SYNC	50 c/s	0.63	0.70	0.77
		DATA	100 c/s	1.17	1.30	1.43
VA	S/C ENGRG @ 66-2/3 bps CRUISE SCI @ 166-2/3 bps CAPSULE ENGRG & SCI @ 166-2/3 bps	CARRIER				
		LOWER	1.6 kc	0.50	0.56	0.62
		UPPER	102.4 kc	1.30	1.44	1.58
VB	SAME AS VA	CARRIER				
		LOWER	1.6 kc	0.66	0.73	0.80
		UPPER	102.4 kc	1.26	1.40	1.54
VC	SAME AS VA	CARRIER				
		LOWER	1.6 kc	0.77	0.85	0.93
		UPPER	102.4 kc	1.15	1.28	1.41
VI	SAME AS VA	CARRIER				
		LOWER	9.6 kc	0.45	0.5	0.55
		UPPER	614.4 kc	1.35	1.50	1.65
COMMAND	SINGLE CHANNEL SYSTEM	CARRIER				
		SYNC	(SEE NOTE 1)			
		DATA		0.80	0.89	0.98

NOTE 1: CHARACTERISTICS ASSUMED FOR SINGLE-CHANNEL COMMAND DETECTOR AS SU
JPL UNDER CONTRACT NO. 950416 (PHILCO)

NOTE 2: GOVERNS LINK THRESHOLD

CARRIER MOD LOSS P_c/P_t db	SYNC OR SUBCARRIER MOD LOSS P_{sc1}/P_t db	UPPER SUBCARRIER MOD LOSS P_{sc2}/P_t db	MISSION PHASE	$2B_{Lo}$ cps	$\frac{S}{N}_{2B_{LO}}$ db	INF BIT RAT (bps
-4.7 $^{+1.0}_{-1.1}$	-13.6 $^{+1.7}_{-1.6}$	-3.3 $^{+0.5}_{-0.6}$	LAUNCH ACQUISITION MANEUVERS	152 48.0 12.0 0.5	9.0 14.0 ± 0.5	22-2
-4.9 $^{+1.0}_{-1.3}$	-2.4 $^{+0.4}_{-0.4}$		CRUISE & POST MANEUVER OPTION	12.0	15.0	133-1
-6.5 $^{+1.4}_{-1.5}$	-8.0 $^{+1.6}_{-1.8}$	-5.0 $^{+0.9}_{-1.0}$	EMERGENCY CRUISE OR ENCOUNTER	5.0 0.5	6.0 14.0 ± 0.5	5-5
-6.0 $^{+1.2}_{-1.5}$	-13.7 $^{+1.9}_{-2.3}$	-2.9 $^{+0.5}_{-0.6}$	PRIMARY ENCOUNTER AND ORBITAL	48.0 12.0	15.0	40 800
-6.2 $^{+1.3}_{-1.5}$	-11.3 $^{+1.8}_{-1.9}$	-3.6 $^{+0.6}_{-0.7}$	OPTIONAL LATE ORBITAL	12.0	15.0	40 400
-5.8 $^{+1.2}_{-1.2}$	-9.3 $^{+1.6}_{-1.6}$	-4.4 $^{+0.7}_{-0.8}$	OPTIONAL LATE ORBITAL	12.0	15.0	4 20
-6.4 $^{+1.4}_{-1.9}$	-15.2 $^{+2.1}_{-2.6}$	-2.7 $^{+0.5}_{-0.6}$	OPTIONAL ENCOUNTER AND ORBITAL	12.0	15.0	48,
-1.8 $^{+0.3}_{-0.5}$	-4.8 $^{+0.6}_{-0.8}$		ALL PHASES	20.0 2.0	9.0 db 15.0 db (NOTE 2)	1

UPPLIED TO

Figure 4.1.4-3: Telemetry an

O E)	TRANS-MITTED BIT RATE (bps)	EFFECTIVE ST $\overline{N}/B$ (db)	P_e^b EFFECTIVE BIT ERROR RATE	CHANNEL THRESHOLD P_{sc}/N_o	RF THRESHOLD P_t/N_o db
/9	22-2/9	7.6 ± 0.5	5×10^{-3}	+30.8 +25.8 +19.8 +11.0 +21.1	+35.5 +30.5 +24.5 +24.6 +24.4
/3	133-1/3	7.2 ± 0.5	5×10^{-3}	+25.8 +28.5	+30.7 +30.9
/9	5-5/9	7.7 ± 0.5	1×10^{-2}	+13.0 +11.0 +15.1	+19.5 +19.0 +20.1
0 0	400 25,600	7.2 ± 0.5 5.0 ± 0.5	5×10^{-3} 5×10^{-3}	+31.8 +25.8 +33.2 +44.0	+37.8 +31.8 +46.9 +46.9
)0)0	400 12,800	7.2 ± 0.5 5.0 ± 0.5	5×10^{-3} 5×10^{-3}	+25.8 +33.2 +41.0	+32.0 +44.5 +44.6
)0)0	400 6400	7.2 ± 0.5 5.0 ± 0.5	5×10^{-3} 5×10^{-3}	+25.8 +33.2 +38.0	+31.6 +42.5 +42.4
400 000	400 153,600	7.2 ± 0.5 5.0 ± 0.5	5×10^{-3} 5×10^{-3}	+25.8 +33.2 +51.8	+32.2 +48.4 +54.5
	1	$10.5\ ^{+0.5}_{-0.0}$	1×10^{-5}	+22.0 +18.0 —	+23.8 +22.8 —

d Command Modulation-Mode Parameters

3

Threshold loop noise bandwidths, $2B_{LO}$'s have been chosen for each mode so as to minimize the sum of the peak steady-state plus rms random errors in the loop. Steady-state errors primarily caused by doppler offset, oscillator instabilities, and doppler rate, increase with decreasing loop noise bandwidth. Random errors, primarily caused by the thermal noise, decrease with decreasing loop noise bandwidth while random errors, due to oscillator phase noise, increase with decreasing bandwidth. The calculations of loop errors and resulting data channel losses due to noise, doppler, and other disturbances are complicated by the nonlinear variation in loop bandwidths with input signal power caused by the predetection limiter. The expressions used in these calculations are defined as:

1) Thermal noise - The rms phase error, σ_n, and the data channel signal degradation L_{σ_n} due to σ_n are given as a function of $(S/N)_{2B_{LO}}$ below and are plotted in Figure 4.1.4-4.

$$L_{\sigma_n} = -4.3\ 43\ \sigma_n^2, \text{ db, Gilcrest}^1 \qquad (1)$$

$$\sigma_n^2 = \frac{\pi}{3} + 4 \sum_{n=1}^{\infty} \frac{(-1)^n I_n(R)}{n^2 I_o(R)}, \text{ Viterbi}^2 \qquad (2)$$

$$\frac{B_L}{B_{LO}} = \frac{1}{3} (1 + 2 \alpha/\alpha_o), \text{ Martin}^3 \qquad (3)$$

$$\alpha^2 = \frac{1}{1 + \frac{4}{\pi} (\frac{N}{S})_{B_{if}}}, \text{ Martin}^3 \qquad (4)$$

where

σ_n = rms phase error due to thermal noise, radians

$2B_{LO}$ = Two sided loop noise bandwidth at threshold = 12 cps

$2B_L$ = Two-sided loop noise bandwidth above threshold, cps

$$L\,\sigma_n\ (db) = -4.343\ \sigma_n^2$$

$$\sigma_n^2 = \frac{\pi}{3} + 4 \sum_{n=1}^{\infty} \frac{(-1)^n\ I_n(R)}{n^2\ I_o(R)}$$

$$R = 2(S/N)_{2B_L}$$

$$\frac{B_L}{B_{LO}} = \frac{1}{3}\left(1 + 2\frac{\alpha}{\alpha_o}\right)$$

$$\alpha^2 = \frac{1}{1 + \frac{4}{\pi}\left(\frac{N}{S}\right)_{Bif}}$$

$\alpha_o = 0.0685$

$2B_{LO} = 12$ cps

$B_{if} = 2$kc

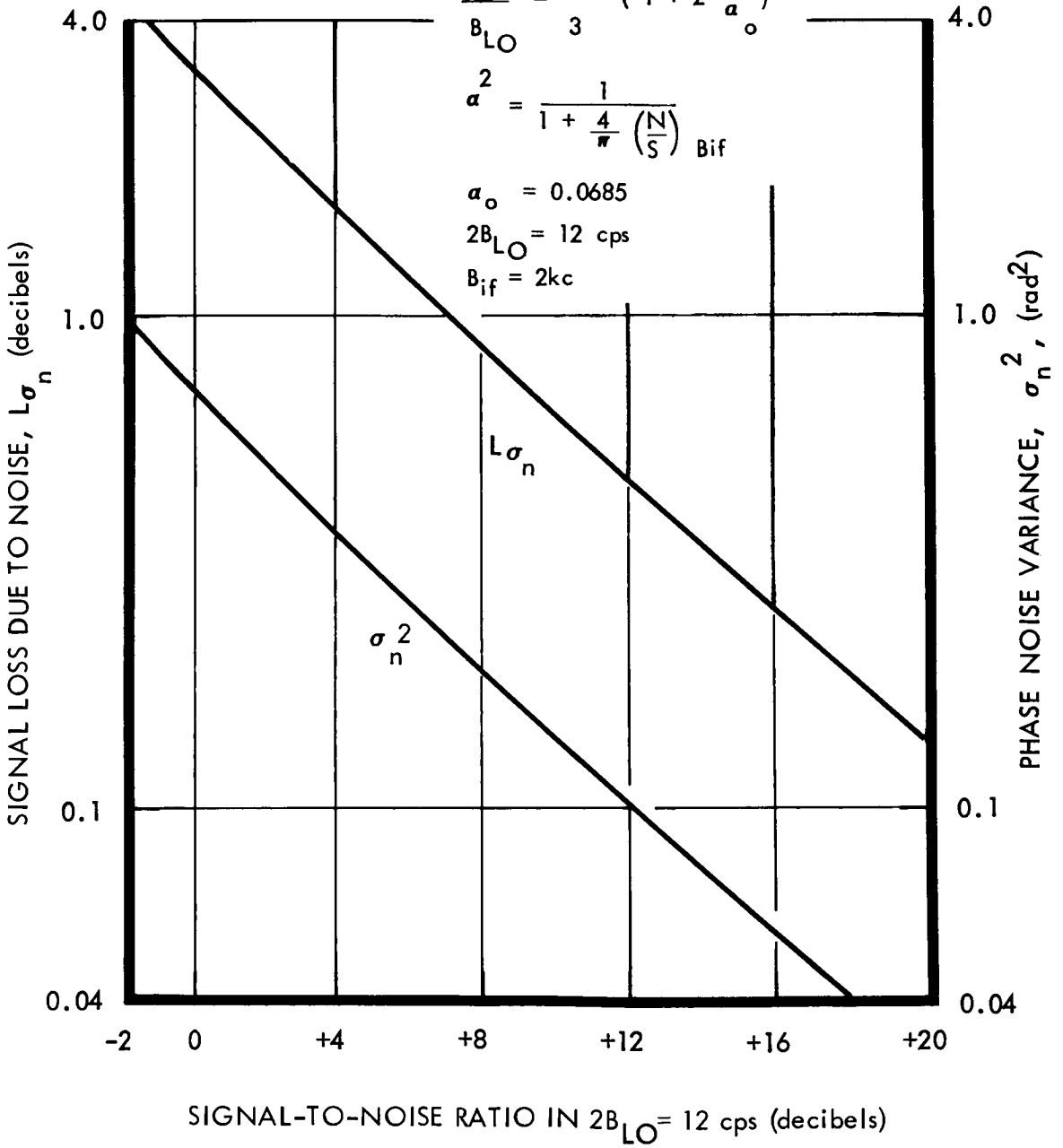

Figure 4.1.4-4: Signal Losses versus Signal-To-Noise Ratio in the Carrier APC Loop

I_n = Modified Bessel functions of order n

$R = 2\,(S/N)_{2B_{LO}}$

α_o = Limiter suppression factor at $(S/N)_{2B_{LO}} = 0$ db

α = Limiter suppression factor at $(S/N)_{2B_{LO}} > 0$ db

B_{if} = Prelimiter noise bandwidth = 2 kc

2) Frequency Uncertainties - The power loss due to a frequency offset into the loop is given by

$$L_f = \cos^2 e_f = \cos^2 \left[\frac{360\,\Delta f}{T_1\ 8/9(2B_{LO})\ 2\ (\frac{\alpha}{\alpha_o})} \right], \text{ Martin}^3 \quad (5)$$

where L_f = Power loss in the data channel due to Δf, db.

e_f = Peak phase error due to Δf, degrees.

Δf = Peak frequency offset, cps.

T_1 = Time constant of the low pass filter, seconds.

3) Frequency Ramp - The power loss due to a frequency ramp into the loop is given by

$$L_f^{\bullet} = \cos^2 e_f^{\bullet} = \cos^2 \left[\frac{360\ \dot{f}}{\frac{8}{9}\,(2B_{LO})^2\ \ \frac{\alpha}{\alpha_o}} \right], \text{ Martin}^3 \quad (6)$$

---

1) C. E. Gilcrest, "Space Programs Summary", No. 37-16, Volume IV, Jet Propulsion Laboratory, Pasadena, California, August 31, 1962, pp. 87.

2) A. J. Viterbi, "Phased Locked Loop Dynamics in the Pressure of Noise by Fokker-Planck Techniques", PROC IRE, Vol. 51, pp. 1743, December 1963.

3) B. D. Martin, "The Pioneer IV Lunar Probe: A Minimum Power FM/PM System Design", TR 32-215, Jet Propulsion Laboratory, Mar. 15, 1962.

where $L_{\dot{f}}$ = Power loss in the data channel due to f, db.

$e_{\dot{f}}$ = Peak phase error due to $\dot{f}$ degrees.

$\dot{f}$ = Maximum doppler rate, cycles/second^2

Peak phase errors, e_f and $e_{\dot{f}}$, of equations (5) and (6) are plotted in Figure 4.1.4-5 over the parameter range of interest. Note that the factor α/α_0 is a function of $(S/N)_{2B_{LO}}$ and of the specified $2B_{LO}$.

4) Oscillator Noise - Measurements at Philco on S-band transponder exciters indicate that the spacecraft VCO will cause a 4 degree rms phase error in $2B_{LO}$ = 20 cps, 7 degrees in $2B_{LO}$ = 12 cps, and 20 degrees in $2B_{LO}$ = 5 cps. Crystal oscillator phase error due to vibration must also be considered in specifying tracking loop bandwidths during powered flight. Typical crystals will exhibit an additional 4 degrees of phase error in a $2B_{LO}$ = 100 cps for each G of acceleration. This data will be used with equation (1) to calculate signal losses due to oscillator noise.

The expected peak doppler and doppler rates for the various mission phases are shown in Table 4.1.4-6 along with the $2B_{LO}$'s, which have been selected for use in the link calculations. It can be seen from Figure 4.1.4-5 that doppler errors during cruise and orbit phases will be dominated by the effects of Earth rotation and that the minimum $2B_{LO}$ = 12 cps can be used to minimize the effects of thermal noise.

Because of the large doppler and doppler rates indicated during initial acquisition over Johannesburg, a $2B_{LO}$ of 152 cps has been

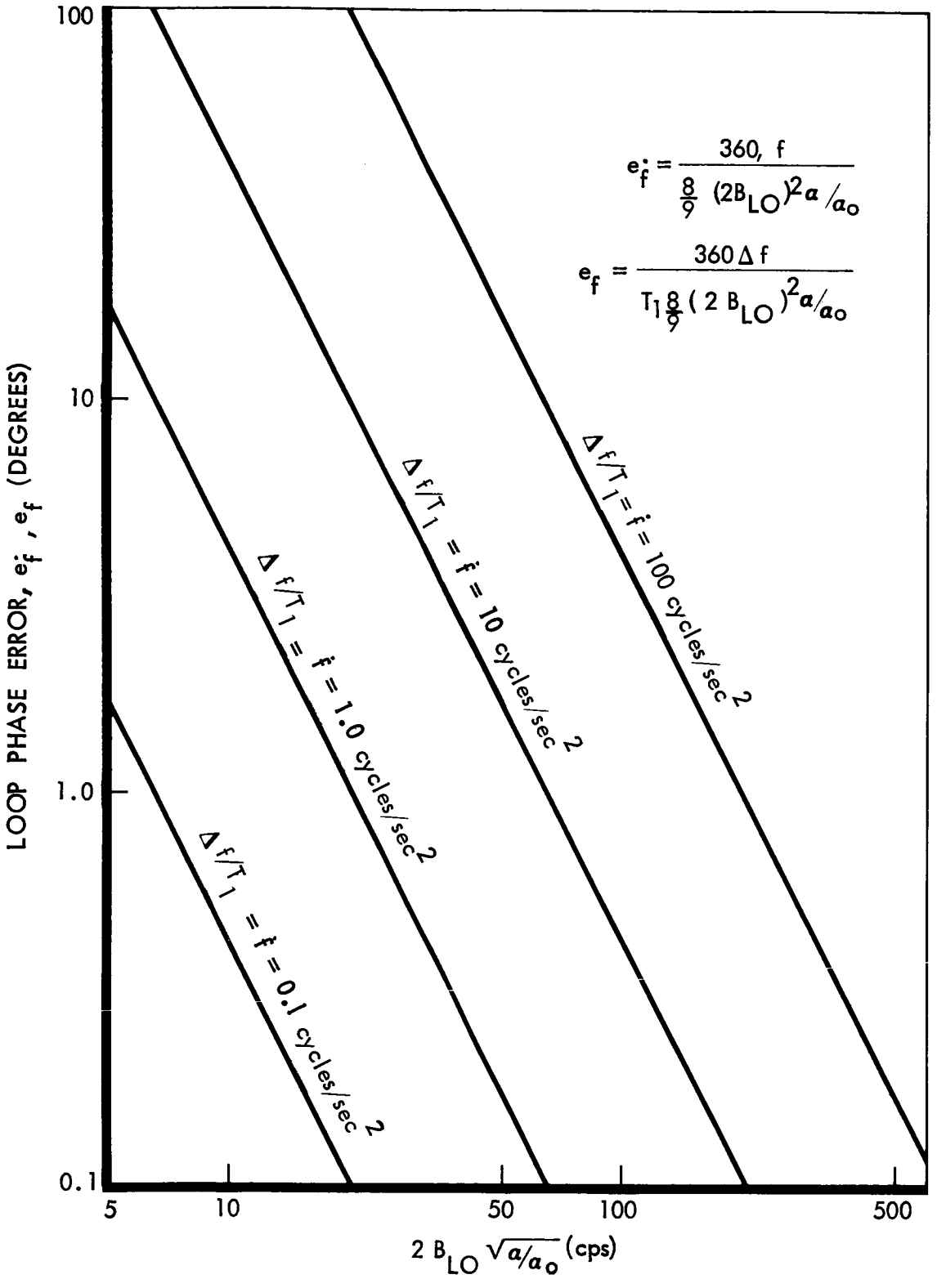

Figure 4.1.4-5: Tracking-Loop Phase Errors Due to Doppler and Doppler Rate

Table 4.1.4-6: DOPPLER AND DOPPLER RATES AND SELECTED GROUND BANDWIDTHS ($2B_{LO}$'s)

Flight Period	Ground Site	Time From Launch	Telemetry Data Mode	f_d(max) KC/Sec	f_d(max)** Cycles/Sec^2	Selected $2B_{LO}$(cps)
Launch	Station 71		M1	49	276	152
Injection	(Out of View)	15-22 Min.	M1	90	158	---
Acquisition Johannesburg	Johannesburg	25-50 Min.	M1	84	163	152/48
Tracking Johannesburg	Johannesburg	50-525 Min.	M2	83.7	7.3	12
Cruise*	DSN Net	525 Min-215 Days	M2 or 3	54.5	0.449	12
Orbit Insertion	DSN Net	215 Days	M5a	273	136	48
Orbit	DSN Net	215-395 Days	M5abc, M6	261	.017	12
Emergency	DSN Net	Any	M4	-	-	5

*During midcourse maneuver M1 is employed.

**Does not include Earth rotation.

used in the link chart (Table 4.1.4-14) for this contact. Because of the need to use the low gain acquisition horn, the 1-watt transmitter and the wide $2B_{LO}$, the carrier channel reaches greyout threshold at 15,000 km approximately 55 minutes after launch and 29 minutes after initial contact. The use of the $2B_{LO}$ = 152 cps has an additional disadvantage in that the telemetry Mode 1 subcarriers at 200 cps and 400 cps are low enough to cause modulation error in the carrier loop, which will cause loss of data channel powers. To determine the actual loop performance at the lower $2B_{LO}$'s, the loop errors were calculated for the actual signal levels, doppler, and doppler rates that can be expected at Johannesburg for both $2B_{LO}$ = 12 cps and 48 cps. The results, shown in Figures 4.1.4-6 and -7, indicate that the sum of the steady-state errors due to doppler and doppler rate will always be less than rms noise errors for $2B_{LO}$ = 48 cps. For $2B_{LO}$ = 12 cps, the total error remains below 55 degrees, but above 40 degrees. However, after the first 10 minutes of tracking, the principal error contribution is due to Δ f. Thus, there are several alternatives to the use of $2B_{LO}$ = 152 cps at Johannesburg, which could improve the data link margin of this site during the critical first contact. These are:

1) Use of $2B_{LO}$ = 48 cps

2) Selection of $2B_{LO}$ = 12 cps after the first 10 minutes of contact.

3) Switchover to the 85-foot antenna after one-way acquisition.

During the launch phase, the use of $2B_{LO}$ = 152 cps is dictated by adequate signal margins and high doppler rates. However, if telemetry Mode 1 is used during launch, the tracking loop will interfere with the Mode 1 sync and data subcarriers during strong signal conditions. Thus, the alternate to consider during the launch phase is the use of telemetry Mode 2.

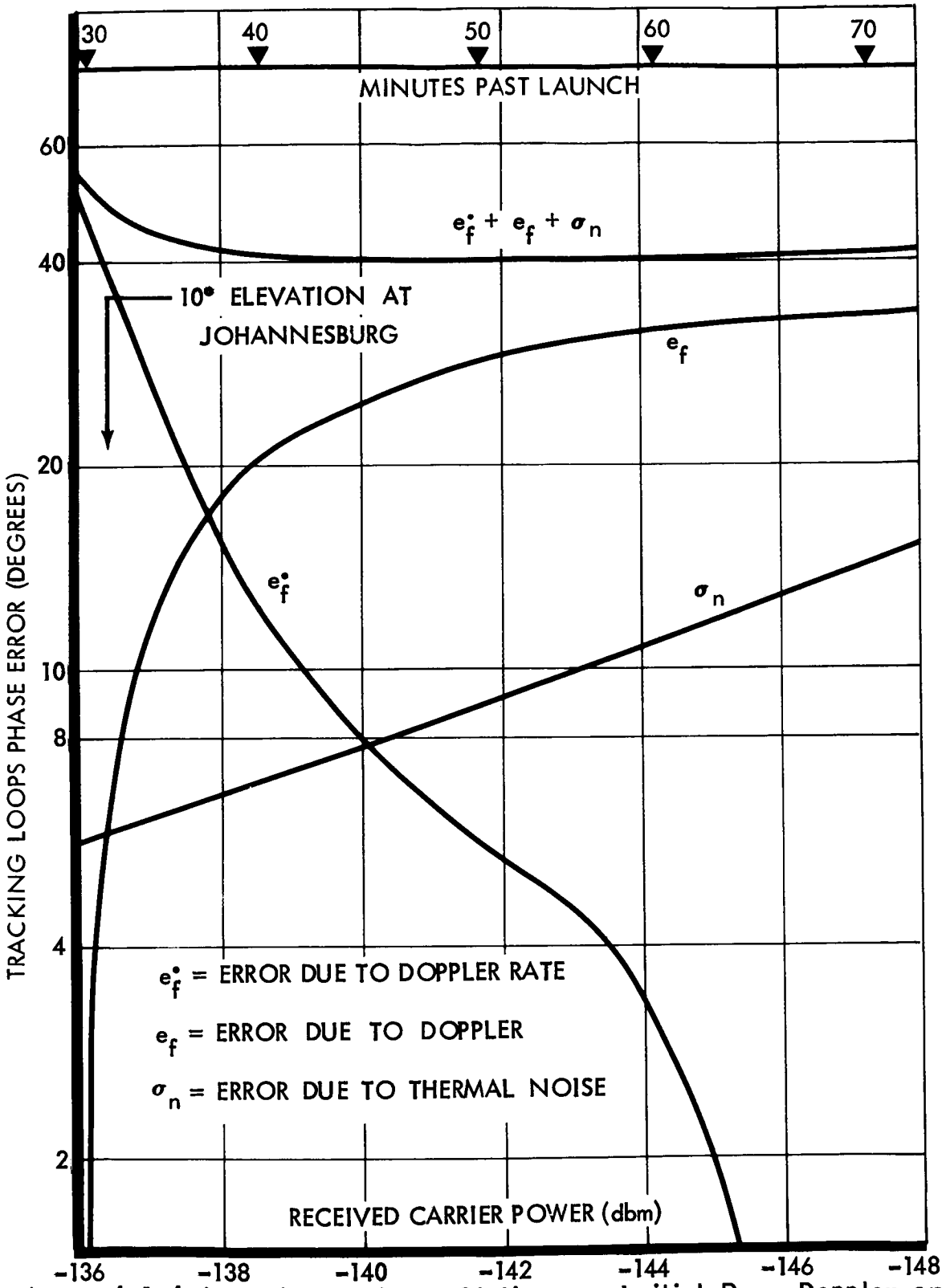

Figure 4.1.4-6: Johannesburg Station — Initial-Pass Doppler and Noise Errors in Tracking Loop $2B_{LO}$ = 12 cps

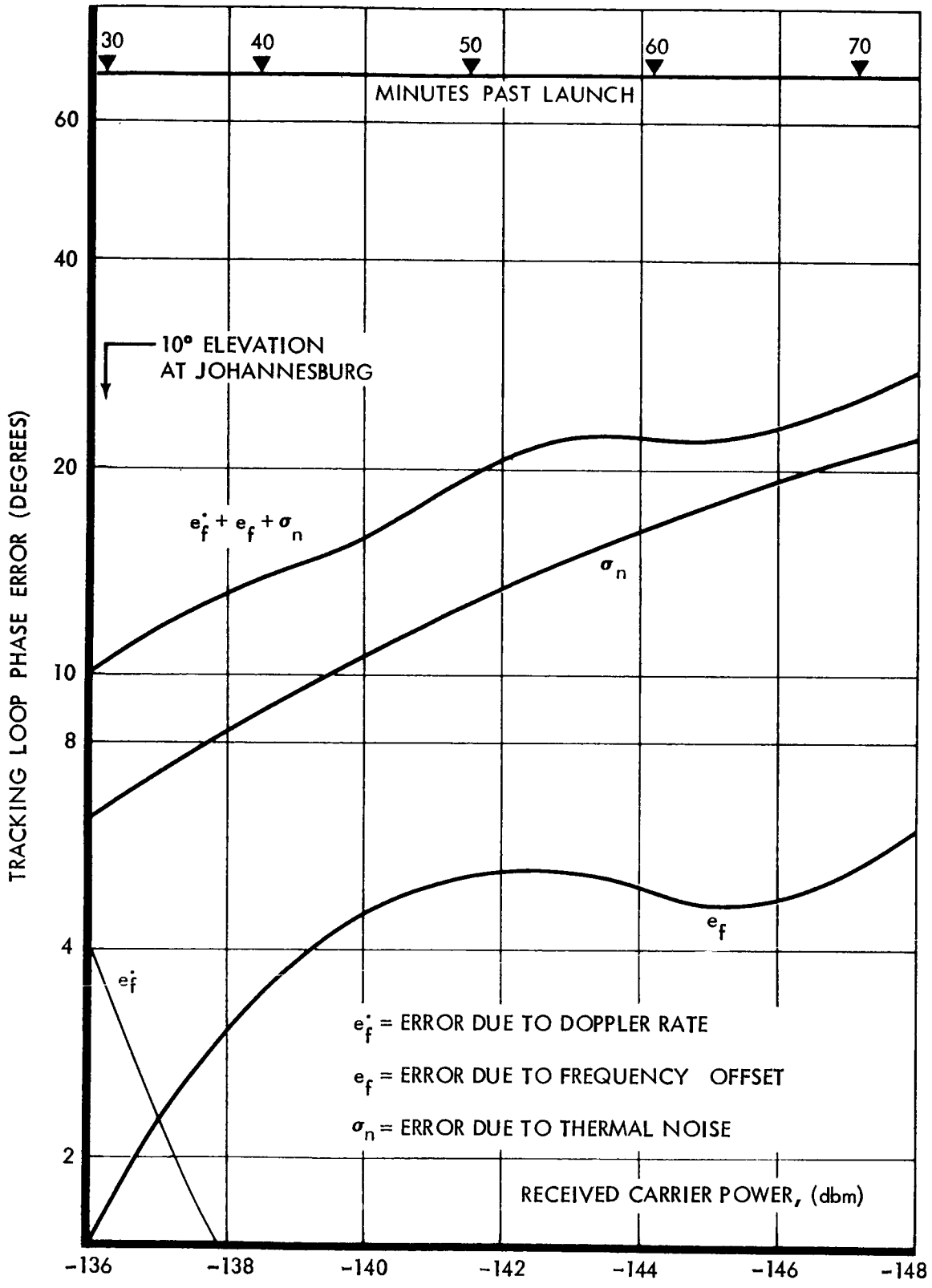

Figure 4.1.4-7: Johannesburg Station — Initial Pass Doppler and Noise Errors in Tracking Loop $2B_{LO}$ = 48 cps

During orbit insertion, the expected doppler errors from Figure 4.1.4-5 and Table 4.1.4-6 will require a $2B_{LO}$ = 48 cps or greater. Using the high-gain antenna, the link will support Mode 5a telemetry with a $2B_{LO}$ = 152 cps.

In the case of receiver threshold signal-to-noise ratios for those modes that are carrier power limited, the carrier loop SNR in $2B_{LO}$ must be defined to minimize the total losses in the data channel. Let

$$L_d = L_m + L_c$$

$$L_c = L_{\sigma_n} + L_{\dot{f}} + L_o + L_f$$

where

L_d = Total data channel signal losses (db)

L_c = Data channel losses due to an imperfect carrier reference

L_m = Data channel modulation loss = $\frac{\text{data channel power}}{\text{Total Power}}$, db

L_{σ_n} = Loss due to jitter on the carrier reference due to thermal noise in the loop, db.

L_f = Loss due to phase error in the loop due to doppler and oscillator frequency uncertainties, db.

$L_{\dot{f}}$ = Loss due to phase error in the loop due to doppler rate, db.

L_o = Loss due to phase jitter in the loop due to oscillator noise.

Modulation losses (L_m) for each data channel result from the division of power between carrier and data channels, and depend on the peak phase deviations assigned to each subcarrier. For carrier-power-limited modes, the allocation of a large amount of power to the carrier will increase data channel modulation losses, but will decrease losses due to thermal noise, doppler, and oscillator phase instabilities in the reconstructed carrier

reference. Thus, there is an optimum threshold definition for the carrier loop SNR and $2B_{LO}$ which minimizes the total power required at the defined threshold.

Mode 1 is a carrier-power-limited mode. Therefore, in order to define the Mode 1 carrier threshold to minimize the total data losses (L_d) the modulation losses (L_m) and the losses due to the carrier reference (L_c) were calculated for a range of $(\frac{S}{N})_{2B_{LO}}$ for $2B_{LO}$ = 12 cps. The results shown in Figure 4.1.4-8 indicate that a carrier threshold definition of

$$(S/N)\ 2B_{LO} = +9 \text{ db}, \quad 2B_{LO} = 12 \text{ cps}$$

yields a minimum L_d = -4.24 db. The modulation losses L_m have been calculated from equations (11) through (15) given in the next section and indicate how subcarrier power falls off as the modulation indices are lowered and more power is allocated to the carrier. Note, however, that L_m approaches a minimum which corresponds to the knee of the P_{sc}/P_t curve illustrated in Figure 4.1.4-9. Losses due to thermal noise, doppler, doppler rate, and oscillators jitter have been calculated from equations (1) through (6) above. Signal-to-noise thresholds for Modes 2 through 6 have been determined in a similar manner and are indicated in Table 4.1.4-7 together with the associated data losses. Note that the data channel losses due to the carrier phase error (L_c) are included in the data channel threshold $\frac{ST}{(N/B)}$'s as shown in Table 4.1.4-8.

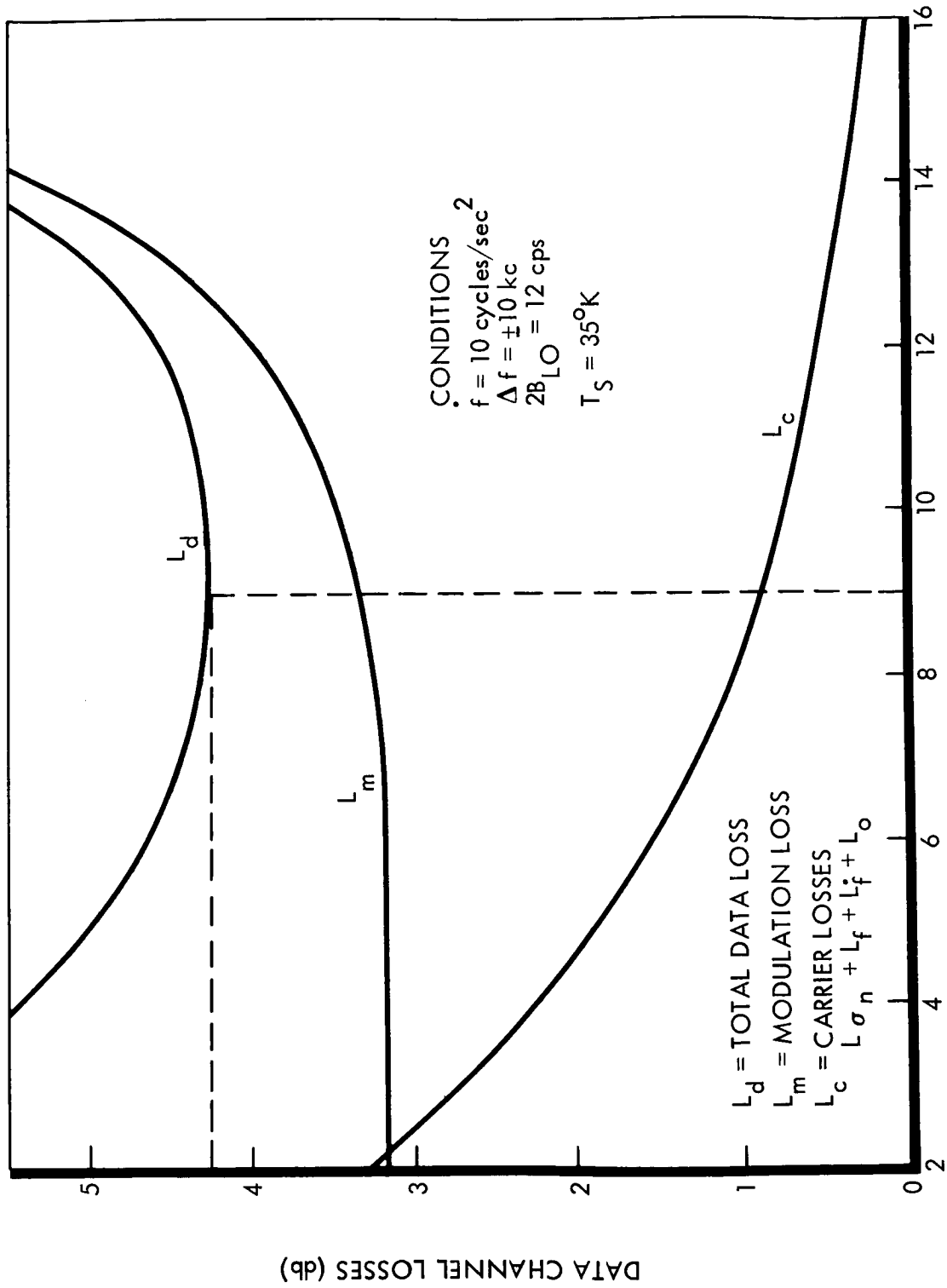

Figure 4.1.4-8: Optimum Carrier Channel Threshold Definition for Mode 1

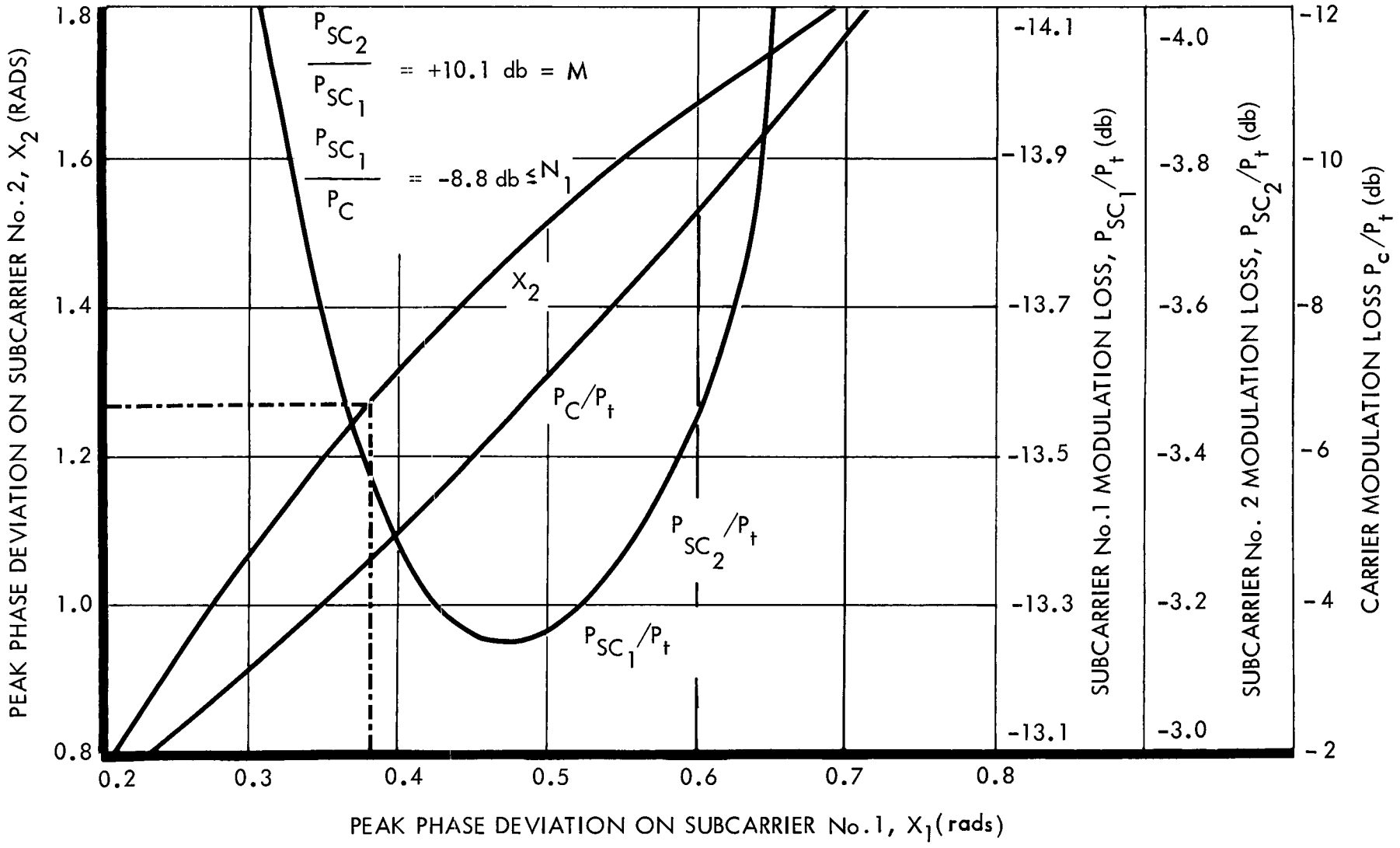

Figure 4.1.4-9: Optimum Modulation Parameters — Mode 1 Telemetry

Table 4.1.4-7: CARRIER THRESHOLDS AND DATA CHANNEL LOSSES

Telemetry Mode / Source of Loss	1		2	3	4	5	6	
Carrier Loop $2B_{LO}$, cps	12	152	12	12	5	12	152	12
Required $(S/N)2B_{LO}$, db	+9	+9	+15	+15	+6	+15	+15	+15
Maximum Frequency Offset, Δf, kc (VCO aiding assumed)	10	10	10	10	10	10	10	10
Maximum Doppler Rate, f, cpsps	10	276	7.3	.45	1.0	1.0	136	1.0
Thermal Noise Loss, L_{σ_n}, db	-0.7	-.2	-.3	-.3	-1.1	-.3	-.2	-.3
Frequency Uncertainty Loss, L_f, db	-.06	-.06	-.06	-.06	-.06	-.06	---	-.06
Doppler Rate Loss, $L_{\dot{f}}$, db	-.13	-.02	-.01	---	---	---	---	---
Oscillator Noise Loss, L_o, db	-.01	---	-.01	---	-0.6	---	---	-.01
Total Data Channel Losses Due to Carrier Phase Error, L_c, db	-0.9	-0.3	-0.4	-0.4	-1.7	-0.4	-0.2	-0.4

Optimization of Data Link Modulation Parameters--The rationale by which the modulation parameters have been assigned for each telemetry mode may be summarized as follows:

1) Define carrier channel criteria and thresholds
2) Define data channel threshold criteria
3) Define data channel design thresholds that achieve these criteria.
4) Derive modulation parameters that achieve maximum performance at the design thresholds specified above.
5) Calculate for each channel the actual performance that results from the modulation indices derived above.

Carrier channel thresholds have been derived in the previous section and are listed in Table 4.1.4-7.

Telemetry Data Channel Threshold Criteria--The telemetry data channel threshold SNR in 1.0 cps will be established at a value such that a bit error probability of 5 parts in 10^3 or less can be obtained at the output of the data detector. For the emergency low data rate mode the bit error probability will be 1 part in 10^2. For the coded data, the equivalent word error rate is 1.1×10^{-2} for a 5-bit data word.

Sync Channel Threshold Criteria--A separate sync channel will be used when the low data rates of Modes 1 and 4 are transmitted. The threshold SNR in $2B_{LO}$ of the sync tracking loop will be established at a value such that the data channel degradation due to sync and carrier tracking loop phase errors is minimized.

Data and Sync Channel Thresholds--Data and sync channel thresholds are defined as the signal power to noise spectral density, S/N_o required in the first order sideband of the appropriate channel at the input to the carrier demodulator. Threshold requirements are referenced to the unmodulated RF carrier power so that the effect of imperfect carrier demodulation can be included in the data and sync channel power requirements. Table 4.1.4-8 summarizes losses due to carrier, subcarrier, demodulators, bit detectors, filter, etc., for each mode and lists the resulting S/N_o requirements for each mode. The required S/N_o numbers for each channel are used later to compute the optimum carrier phase deviations for each subcarrier.

Carrier and Data Channel Power Allocation--Once the required signal power to noise density ratios (S/N_o) have been specified for carrier, data, and sync channels for all modes, the carrier phase deviations for each subcarrier can be determined so as to minimize the total power required to meet the threshold requirements. This section describes the techniques used to compute the optimum phase deviations and defines the exact mathematical expressions used in the calculations. The details of the computation for Mode 5a are given, and the deviations, modulation losses, and resulting total power thresholds are summarized for each channel and each mode in Figure 4.1.4-3.

In the design of a multiple subcarrier PSK/PM telemetry system, it is necessary to divide the available power between the carrier and each data channel so as to maximize the distance over which the link will operate.

TELEMETRY MODE	1		2
CHANNEL / LOSS ALLOCATION	SYNC	DATA	DATA
BIT ERROR RATE, P_b^e	---	5×10^{-3}	5×10^{-3}
THEORETICAL ST/(N/B), db	---	+5.4	+5.4
THEORETICAL (S/N) IN $2B_{LO}$, db	+9.0	---	---
BANDPASS FILTER, db	0.9	0.1	0.2
LIMITER SUPPRESSION, db	1.0	0.3	0.1
PN⊕fs DETECTOR, db	0.9	---	---
SUBCARRIER DETECTOR, db	0.2	0.8	0.6
BIT DETECTOR, db	---	0.1	0.5
INTERMODULATION DISTORTION, db	1.1	---	---
CARRIER DEMOD. LOSSES, L_c	0.9	0.9	0.4
REQUIRED ST/(N/B), TOTAL, db	---	7.6	7.2
REQUIRED (S/N) IN $2B_{LO}$ TOTAL, db	14.0	---	---
BIT RATE, 1/T, bps-db	---	+13.5	+21.3
$2B_{LO}$, cps-db	-3.0	---	---
REQUIRED S/N PER CHANNEL, db°	+11.0	+21.1	+28.5

*) TRANSMITTED BIT RATE EQUALS $1/T_S$

Table 4.1.4-8: Data and Sync Channel Thresholds and Error Budgets

3	4		5		6		COMMENTS
DATA	SYNC	DATA	DATA NO.1	DATA NO.2	DATA NO.1	DATA NO.2	
$\times 10^{-3}$	---	10^{-2}	5×10^{-3}	5×10^{-3}	5×10^{-3}	5×10^{-3}	
+5.4	---	+4.6	+5.4	+3.3	+5.4	+3.3	
---	+9.0	---	---	---	---	---	
0.2	0.5	0.1	0.2	0.2	0.2	0.2	BW = $4/T_s$ *
0.1	0.7	0.3	0.1	0.1	0.1	0.1	
---	0.8	---	---	---	---	---	
0.6	0.2	0.8	0.6	0.6	0.6	0.6	
0.5	---	0.2	0.5	0.3	0.5	0.3	
---	1.1	---	---	0.1	---	0.1	
0.4	1.7	1.7	0.4	0.4	0.4	0.4	
7.2	---	7.7	7.2	5.0	7.2	5.0	
---	14.0	---	---	---	---	---	
21.3	---	+7.2	+26.0	+39.0 +36.0 +33.0	+26.0	+46.8	MODE 5a MODE 5b MODE 5c
---	-3.0	---	---	---	---	---	
28.5	+11.0	+14.9	+33.2	+44.0 +41.0 +38.0	+33.2	+51.8	MODE 5a MODE 5b MODE 5c

When a subcarrier phase modulates a carrier, the useable sideband power resides in the first order sideband and the remaining components appear as distortion products. When two or more subcarriers are present, each generates a useable first order sideband. In this case, odd order sum and difference sidebands are also generated, which result in wasted power and intermodulation distortion. The magnitude of sidebands and distortion products are complex functions of the phase deviations assigned to each subcarrier. Thus, the proper approach to follow in the design of an efficient multiple subcarrier PM link is one which assigns to each subcarrier a carrier phase deviation such that:

1) The carrier channel threshold is equal to or better than any of the subcarrier channel thresholds.
2) All subcarrier channels threshold simultaneously as total received power is decreased.
3) The useful power in the first order sidebands is as large as possible consistent with constraints 1) and 2) above.

In addition to choosing the proper phase deviations, the design must specify subcarrier frequencies to minimize the cross product distortion generated in the demodulator that falls into the useful first order sidebands.

When the data channel power requirements are large compared to the carrier channel power requirements, constraint 1) above has no practical effect on the selection of indices because there will exist a unique set of subcarrier modulation indices, which maximizes the power in the subcarrier channels. For narrowband data when the carrier channel threshold is poorer than the minimum data channel threshold, constraint 1) applies

and the modulation indices must be chosen so as to equalize carrier and data channel thresholds.

It is important to note the the deviations resulting from thes derivations are only optimum with respect to thermal noise. To determine whether or not these indices can be used, the intermodulation distortion produced by various nonlinearities in the channel must be determined. In a properly designed system, the major source of this distortion will be the sinusoidal characteristic of the phase detector in the carrier phase demodulator.

The design approach followed here is similar to that described by Martin. For a multiple subcarrier PSK/PM system the RF signal at the input to the receiver on the ground can be represented by

$$E(t) = \sqrt{2}\ A \sin\left[\omega_c t + \phi_1(t)\right] + n(t) \tag{7}$$

$$\phi_1(t) = \sum_{i=1}^{N} x_i \cos\left[\omega_i t + \frac{\pi}{2} U_i(t)\right] + \sum_{j=1}^{M} Y_j V_j(t) \tag{8}$$

where

$n(t)$ = Band-limited white gaussian noise centered about the carrier frequency with one-sided spectral density N_o and bandwidth B_{if}.

$\sqrt{2}\ A$ = Amplitude of a sinusoidal carrier of power A^2.

ω_c = Carrier Frequency, rad/sec.

N = Number of sine wave subcarriers

ω_i = Frequency of i^{th} sine subcarrier, rad/sec.

x_i = Peak phase deviation of i^{th} sine subcarrier, radians

$U_i(t)$ = PCM Signal modulated on the i^{th} subcarrier with binary values ± 1.

M = Number of square wave subcarriers

Y_j = Peak phase deviation of the j^{th} square wave, radians

$V_j(t)$ = PCM signal modulated on the j^{th} square wave subcarrier with binary values $\pm$ 1.

The received signal is demodulated in a product demodulator by a reference signal of the form

$$E_r(t) = \sqrt{2} \text{ Cos } \left[\omega_c t + \phi_2(t)\right]$$

where

$\phi_2(t)$ = random phase error on the reference carrier. The noise process, n(t) can be represented by

$$n(t) = \sqrt{2}\, n_1(t) \text{ Sin } \omega_c t + \sqrt{2}\, n_2(t) \text{ Cos } \omega_c t$$

where n(t) and $n_2(t)$ are independent stationary wideband gaussian processes with one-sided spectral densities of N_o extending from dc to $B_{if/2}$. The output of the product demodulator is then given by:

$$E_o(t) = E(t)E_r(t) = A \text{ Sin } \left[\phi_1(t) - \phi_2(t)\right] - n_1(t) \text{ Sin } \phi_2(t) + n_2 \text{ Cos } \phi_2(t) \qquad (9)$$

plus the high frequency terms centered about $2\omega_c$ which are not of interest.

The power that remains in the carrier and in each of the subcarrier channels may be determined by expanding equations (7) and (8) in terms of sums of products of sines and cosines of the individual subcarrier components and applying the expressions:

$$\text{Cos } (x\text{Cos } y) = J_o(x) + 2 \sum_{k=1}^{\infty} (-1)^k J_{2k}(x) \text{ Cos } 2ky$$

$$\text{Sin } (x \text{ Cos } y) = 2 \sum_{k=1}^{\infty} (-1)^{k-1} J_{2k-1}(x) \text{ Cos } (2k-1)y \qquad (10)$$

$$\text{Cos } \left[xU(t)\right] = \text{Cos } x, \quad \text{Sin } \left[xU(t)\right] = U(t) \text{ Sin } X$$

$$U(t) = \pm 1$$

From these substitutions the power which remains in the carrier is

$$P_c = \prod_{i=1}^{N} J_o^2 (x_i) \prod_{j=1}^{M} \cos^2 (Y_j) \, P_t \qquad (11)$$

where

P_c = Carrier power

P_t = Total power

J_o = Zero-order Bessel function

x_i = Phase deviation of the i^{th} sine wave subcarrier

Y_j = Phase deviation of the j^{th} square wave subcarrier

The recoverable power in the first order sideband of the n^{th} sine wave subcarrier is

$$P_{sc_n} = 2J_1^2 (x_n) \sum_{\substack{i=1 \\ \neq n}}^{N} J_o^2 (x) \sum_{j=1}^{M} \cos^2 (Y_j) \, P_t \qquad (12)$$

where

P_{sc_n} = Power in the n^{th} sine wave subcarrier

J_1 = First-order Bessel function

The recoverable power in the first order sideband of the n^{th} square wave subcarrier is

$$P_{ss_n} = \frac{8}{\pi^2} \sin^2 (y_m) \prod_{i=1}^{N} J_o^2 (x_i) \prod_{\substack{j=1 \\ \neq m}}^{M} \cos^2 (Y_j) \, P_t \qquad (13)$$

where the $8/\pi^2$ factor is due to the fact that only the first harmonic of the square wave will be recovered in the subcarrier demodulator.

Equations (11), (12), and (13) express the power that will fall in the individual carrier and data channels in terms of the individual subcarrier modulation indices. Carrier and data channel thresholds have been specified in the previous section in terms of the signal-to-noise ratios required in each channel to meet the minimum performance criteria. From these channel thresholds, the individual indices, x_1, and x_2 can be

determined so as to minimize the total power required to provide exactly the right amount of power in the carrier and in each subcarrier channel.

If the resulting intermodulation levels are acceptable, then this set of indices may be considered to be the optimum set. To illustrate the application of this optimization technique, consider the case in which two sine wave subcarriers modulate the carrier. To satisfy constraint (2) as stated earlier, the phase deviations must be chosen so that:

$$\frac{P_{sc_2}}{P_{sc_1}} = \frac{J_1^2(x_2)}{J_o^2(x_2)} \cdot \frac{J_o^2(x_1)}{J_1^2(x_1)} = M \qquad (14)$$

where M is a specified constant equal to the ratio of the powers required in each channel.

To satisfy constraint (1) stated earlier, x_1, and x_2 must be constrained such that

$$\frac{P_{sc_i}}{P_c} = \frac{2\,J_1^2(x_i)}{J_o^2(x_i)} \leq N_i, \quad i = 1, 2 \qquad (15)$$

where the N_i are specified constants equal to the ratio of the power required in the i^{th} subcarrier to the power required in the carrier channel. In practice only one N need be specified since $N_2 = N_1 + M$ if x_1 and x_2 are chosen to satisfy equation (14).

The x_1 for the recommended telemetry communication modes have been calculated and are tabulated in Figure 4.1.4-3 together with the resulting performance of each channel. The procedure used in these calculations may be summarized as:

1) Specify the bit rate, 1/T, and the signal energy to noise density ratio, ST/N/B required in each data channel to meet the specified bit error probability.
2) Specify the SNR required in the carrier tracking loop design threshold noise bandwidth $2B_{LO}$ to minimize carrier and subcarrier demodulation losses due to reference phase jitter at the data channel threshold design point specified in (1) above.
3) Calculate M and N from (1) and (2) above.
4) Solve equation (14) and plot x_1 as a function of x_2.
5) Solve equation (11) and plot P_c/P_t as a function of x_1 with constraint $x_1 = f(x_2)$ given by (4) above.
6) Solve equation (12) and plot P_{sc_1}/P_t as a function of x_1 with the constraint $x_1 = f(x_2)$ given by (4) above.
7) Solve equation (15) for the equality condition and bound the values of x_1 and x_2 expressed by $x_1 = f(x_2)$.
8) Select x_1 and x_2 to maximize P_{sc_1}/P_t and P_{sc_2}/P_t on the plot given by (5) above and constrained by (7) above.

Graphical solutions for telemetry Modes 1, 4, 5a, 5b, and 5c are shown in the figures which follow for the values of M and N indicated. Modes 2 and 3 require only one subcarrier so that a direct solution for x_1 is possible by solving equation (15).

1) Mode 1-Figure 4.1.4-9--For Mode 1, subcarrier No. 1 is a square wave and subcarrier No. 2 is a sine wave. x_2, P_{sc_1}/P_t, P_{sc_2}/P_t are plotted against x_1. It can be seen that maximum subcarrier power is available for $x_1 = 0.46$, and $x_2 = 1.44$. However, equation (15) indicates that in this case $x_1 \leq 0.38$ in order to satisfy the carrier threshold requirements. Thus, the recommended parameters are $x_1 = 0.38$, $x_2 = 1.27$; the resulting modulation losses may be read from the appropriate curves. Note that the $8/\pi^2$ power loss factor inherent in square wave demodulation is included in equation (13) rather than in the required $(\frac{ST}{N/B})$.

2) Modes 2 and 3--A single sine wave subcarrier is used in this mode. From Figure 4.1.4-3 N = +2.7 db, so that from equation (15), $x_1 = 1.40$ radians.

3) Mode 4--The Mode 4 modulation indices should be determined under the same carrier threshold restriction as the choice of Mode 1. The indices used are $x_1 = 0.7$ and $x_2 = 1.3$ as shown in Figure 4.1.4-10. The figure indicates optimum indices are near $x_1 = 0.61$ and $x_2 = 1.15$.

4) Mode 5a, Figure 4.1.4-11--Two sine wave subcarriers are used in this mode. Subcarrier power is optimized for $x_1 = 0.60$, $x_2 = 1.50$, a point corresponding to the bottom of the P_{sc_1}/P_t curve. From equation (15) the constraint on x_1 is $x_1 \leq 1.13$,

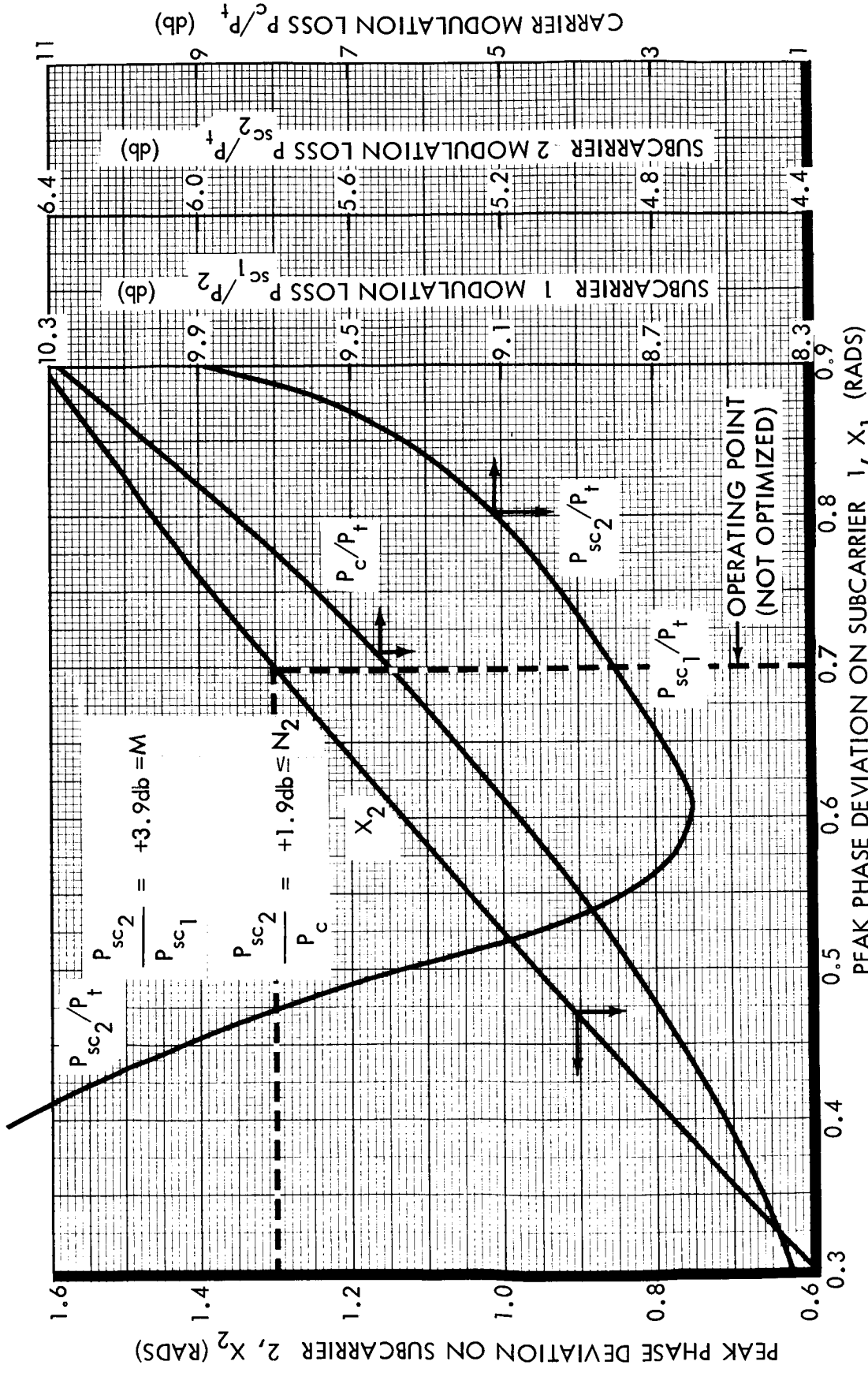

Figure 4.1.4-10: Optimum Modulation Parameters — Mode 4 Telemetry

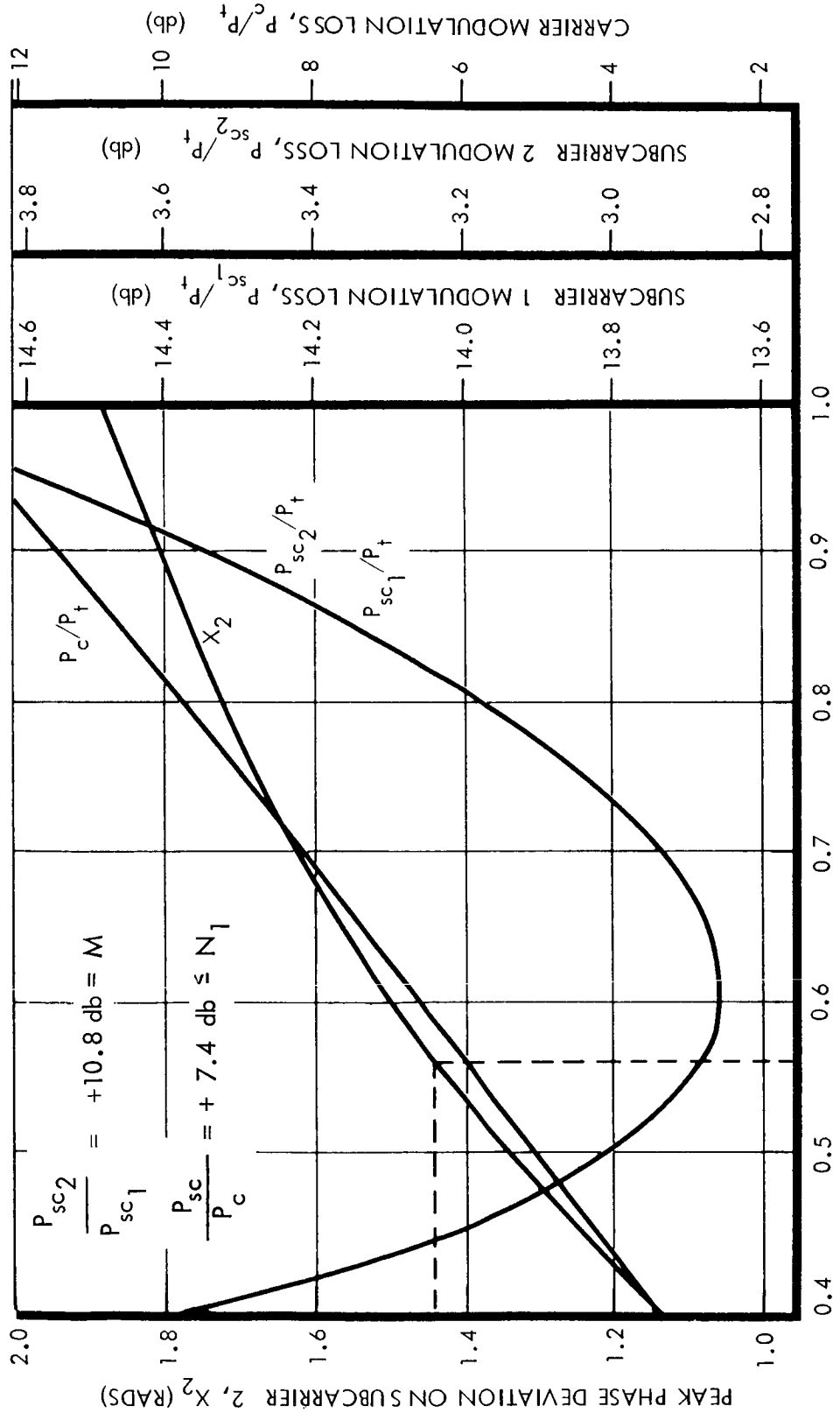

Figure 4.1.4-11: Optimum Modulation Parameters — Mode 5a Telemetry

so that the x_1 may be selected from the bottom of the power curve. The recommended parameters, $x_1 = 0.56$, $x_2 = 1.44$ which lie just to the right of the optimum point were selected to hold the peak deviation on channel two to less than 1.45 to limit demodulation phase non-linearities in that channel. The resulting power degradation from optimum is less than 0.03 db.

5) Mode 5b, 5c, Figure 4.1.4-12 and 4.1.4-13--The solution for these modes is similar to that for 5a, the major change being a slight shift to the right in the location of maximum point on the subcarrier power curve.

6) Mode 6--The modulation indices for Mode 6, the real time transmission mode can be optimized by following the same procedure as for Modes 5a, b, and c. The modulation indices used in the link analysis are $x_1 = 0.5$ and $x_2 = 1.5$. Further iterations are required to fully optimize these parameters.

To maintain a near optimum power allocation throughout the duration of the mission, the allowable tolerances on the modulation indices for each subscrrier must be carefully controlled.

Intermodulation Products--The previous section has derived expressions for the power in the carrier and the first order sidebands of the telemetry signals for the various data modes. It is necessary to evaluate the higher order sidebands to determine the level of intermodulation distortion that will exist in each of the first order sidebands. For the

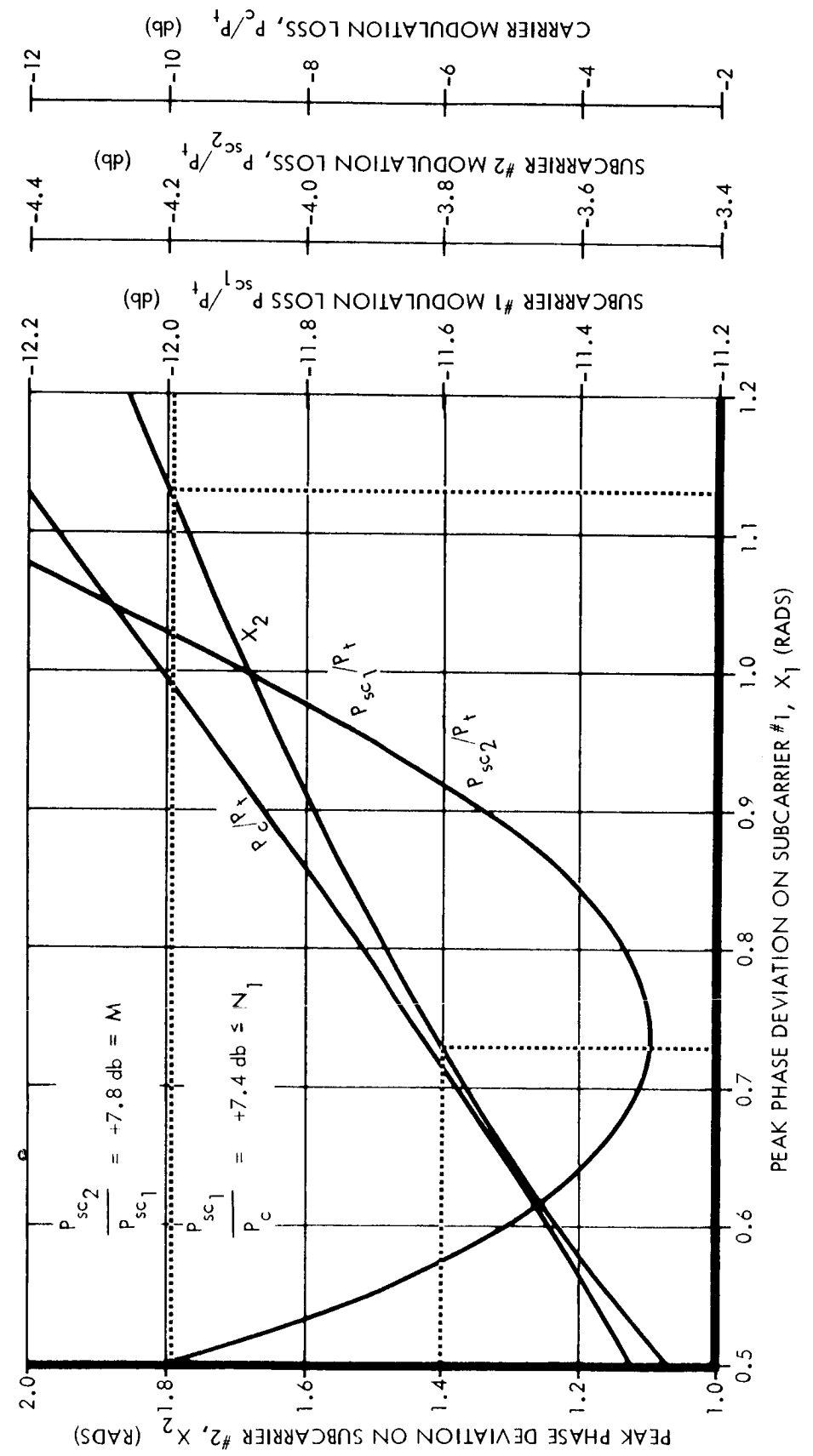

Figure 4.1.4-12: Optimum Modulation Parameters — Mode 5b Telemetry

Figure 4.1.4-13: Optimum Modulation Parameters – Mode 5c Telemetry

case of two sinewave subcarriers, and an ideal product demodulator, the signal at the output of the carrier demodulator can be written from equations (8) and (9) of the previous section as:

$$E_o(t) = A \sin \left[X_1 \sin (\omega_1 t \pm \pi/2) + X_2 \sin (\omega_2 t \pm \pi/2) \right] \quad (16)$$

where

X_1, X_2 = peak phase deviations of the respective subcarriers, radians

ω_1, ω_2 = radian frequency of the respective subcarriers, radians/sec.

Application of the identities of equation (10) to equation (16) will yield a Bessel function expansion for the output of the carrier demodulator as follows:

$$E_o(t) = \frac{1}{2} \left[\sum_{n_1 = -\infty}^{+\infty} \sum_{n_2 = -\infty}^{+\infty} J_{n_1}(X_1) J_{n_2}(X_2) \sin (n_1\omega_1 + n_2\omega_2)t \right] \quad (17)$$

For an ideal demodulator E_o (t) will only contain modulation products for which the sum of n_1 and n_2 is an odd number.

The terms of equation (17) for $n_1 = \pm 1$, $n_2 = 0$ represent the useful power in the first-order sideband of data channel No. 1. The terms for $n_1 = 0$, $n_2 = \pm 1$ represent the useful power in the first order sideband of data channel No. 2. Terms resulting for all other combinations of n_1 and n_2 will result in higher-order terms, some of which fall within the data channels and cause intermodulation distortion, and some of which re-

sult in wasted power that cannot be recovered. The signal power lost due to these terms has already been accounted for in the modulation losses indicated in Figure 4.1.4-3 since the subcarrier power represented by equations (12) and (13) includes only the first-order terms for each channel. The total power lost in higher-order terms varies from 10 to 20 percent for the prime telemetry modes. The use of a subcarrier PM communication system and the resulting loss of usable power as indicated by the truncation of the higher order terms in equation (17) is best justified by the increased communication and tracking capability that results from the use of narrowband phase lock tracking techniques.

These intermodulation products that produce distortion in the data channels must be evaluated to ensure that the selected modulation indices and subcarrier frequencies do not degrade the data at threshold. All those products that fall within a bandwidth equal to four times the transmitted bit rate have been calculated and are listed in Table 4.1.4-9 for each telemetry mode. Sinewave subcarriers have been assumed in these calculations for all modes so that the results indicated for Modes 1 and 4 are worse than may be expected for the square wave sync subcarriers.

Table 4.1.4-9: TELEMETRY CHANNEL INTERMODULATION PRODUCTS

MODES	CHANNELS	P_{sc}/P_t [1] db	P_{im}/P_t [2] db	P_{im}/P_{sc} [3] db
1	Sync	-13.6	-35.5	-21.9
	Data	- 3.3	-27.1	-23.8
2,3	Data	- 2.4	-	-
4	Sync	- 8.0	-20.1	-22.1
	Data	- 5.0	-22.2	-17.2
5a	Data #1	-13.7	-	-
	Data #2	- 2.9	-27.5	-24.6
5b	Data #1	-11.3	-	-
	Data #2	- 3.6	-23.4	-19.8
5c	Data #1	- 9.3	-	-
	Data #2	- 4.4	-21.1	-16.7
6	Data #1	-15.2	-	-
	Data #2	- 2.7	-29.1	-26.4

NOTES:

1) P_{sc}/P_t = Ratio of subcarrier power to total power.

2) P_{im}/P_t = Ratio of intermodulation power in 4/T bandwidth to total power.

3) $P_{im}/P_{sc} = (P_{im}/P_t) / (P_{sc}/P_t)$.

Sync Acquisition Times for Telemetry System--The detectors to be used for telemetry subcarrier and bit synchronization are the JPL-developed, two-channel PN detector for Modes 1 and 4 and a Costas-type detector for Modes 2, 3, 5 and 6. The advantages of these devices have been discussed in Section 4.1.2, Volume B.

1) Costas Loop Acquisition Time--The characteristics of the Costas loop bit acquisition times are shown graphically in Figure 4.1.4-14. The results are per actual test data obtained on a Costas loop bi-phase demodulator and bit synchronizer (Telemetrics Inc. Model #6233). The general acquisition characteristics are as follows:

   a) The ST/N/B threshold level for bit sync acquisition is dependent upon the ratio of the subcarrier-to-bit rate.

      Lower subcarrier-to-bit rate ratios improve the threshold levels and lower the sync acquisition time.

      Increased subcarrier-to-bit rate ratios degrade threshold values and increase sync acquisition times.

   b) Larger offsets (up to 10% maximum allowed) between the incoming bit rate and the Costas bit rate generator require longer acquisition times.

   c) Increased bit transition density decreases acquisition times.

2) PN Synchronization Double Channel System--The acquisition of the basic PN code sync system has been described by Springett[4] of JPL. Above sync acquisition threshold the PN sync system mean acquisition time can be expressed as:

---

[4] JPL Technical Report No. 32-495 January 15, 1965.

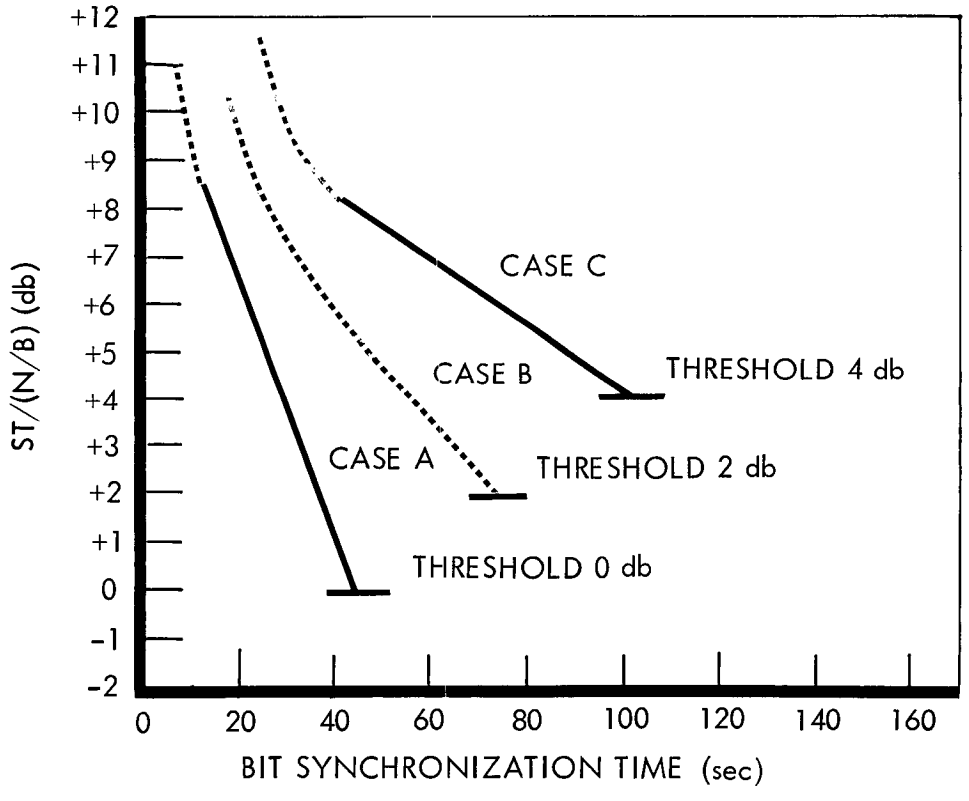

CASE A
- SUBCARRIER/BIT RATE:32/1
- OFFSET OF COSTA'S LOOP BIT RATE GENERATOR:10%
- BIT RATE : 489 bps

CASE B
- SUBCARRIER/BIT RATE:128/1
- OFFSET OF COSTA'S LOOP BIT RATE GENERATOR : 10%
- BIT RATE : 122 bps

CASE C
- SUBCARRIER/BIT RATE:256/1
- OFFSET OF COSTA'S LOOP BIT RATE GENERATOR : 10%
- BIT RATE : 61 bps

Figure 4.1.4-14: Costa's Loop Acquisition Time

$$Ta = \frac{L}{\frac{K}{3} B_{LO} \left(1 + 2 \frac{\sigma}{a_o}\right) - \Delta_f} \quad \text{seconds} \quad (18)$$

where, T_a = mean acquisition time

L = the PN code length in bits

$\frac{\sigma}{a_o}$ = 8.7 at operating threshold

$2B_{LO}$ = 0.5 cps at design threshold

Δ_f = Oscillator instability or frequency offset

The value of K varies from 2 at signal-to-noise ratios near threshold to 1.89 at signal-to-noise ratios much above threshold. At system threshold, $(\frac{S}{N})_{2B_{LO}}$ is 14 db at the detector input, which is equivalent to a $(\frac{S}{N})_{2B_{LO}}$ of 9 db within the loop.

Acquisition times of a typical PN sync code loop is depicted in Figure 4.1.4-15 where equation (18) has been graphed for K = 2, $\Delta f_o = 0$; and also for K = 2, Δf_o = 0.1 cps.

Table 4.1.4-10 summarizes the mean threshold acquisition times for the proposed telemetry Modes 1 through 6. The mean bit synchronization time for each mode is shown assuming characteristics of the Costas loop phase-lock bit synchronizer and demodulator and the double channel JPL PN sync code detector.

Modes 1 and 4 should have a mean acquisition time of 21 seconds at threshold ST/N/B, equal to 14.0 db. Modes 2, 3, 5 and 6 should have

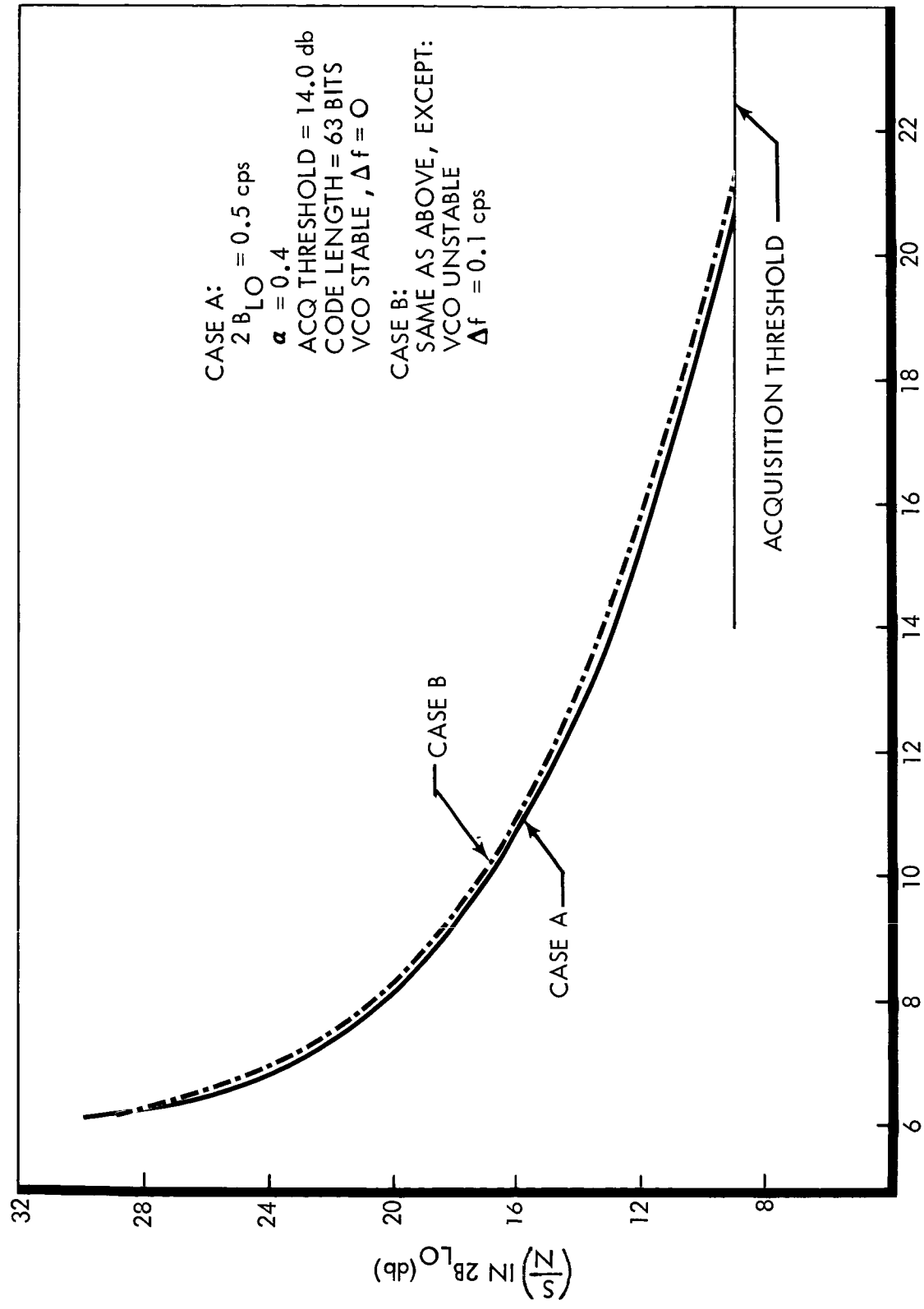

Figure 4.1.4-15: Two Channel Sync Acquisition Time

Table 4.1.4-10: MEAN ACQUISITION TIME FOR VOYAGER TLM MODES

MODE	CHANNEL	RATIO SUBCARRIER TO BIT RATE fsc/fo	TYPE SYNC BIT DETECTION	SYNC THRESHOLD	MEAN ACQUISITION SYNC TIME SECONDS
1,4	PN SYNC ENGINEERING	1/1 18/1	DOUBLE CHANNEL PN SYNC CODE PLL	$+14 = (S/N)_{2B_{LO}}$ Detector Input	21
2,3	CRUISE SCIENCE	4/1	COSTAS	$0.0db = \frac{ST}{N/B}$	45
5a	CRUISE SCIENCE	4/1	COSTAS	$0.0db = \frac{ST}{N/B}$	45
	PLANETARY SCIENCE	12.8/1		$0.0db = \frac{ST}{N/B}$	45
5b	CRUISE SCIENCE	4/1	COSTAS	$0.0db = \frac{ST}{N/B}$	45
	PLANETARY SCIENCE	25.6/1		$0.0db = \frac{ST}{N/B}$	45
5c	CRUISE SCIENCE	4/1	COSTAS	$0.0db = \frac{ST}{N/B}$	45
	PLANETARY SCIENCE	51.2/1		$0.0db = \frac{ST}{N/B}$	45
6	CRUISE SCIENCE	24/1	COSTAS	$0.0db = \frac{ST}{N/B}$	45
	PLANETARY SCIENCE	12.8/1		$0.0db = \frac{ST}{N/B}$	45

mean acquisition times of 45 seconds at 0 db $\frac{S\ T}{(N/B)}$ threshold for all cases.

Probability of Loss of Bit Sync at Threshold--

1) Modes 1 and 4

The telemetry demodulators for Modes 1 and 4 are two-channel PN synchronized detectors as developed by JPL. In this system bit sync and subcarrier sync are accomplished simultaneously by the same circuit. The sync channel threshold $(\frac{S}{N})_{2B_{LO}}$ = +9 db within the loop has been specified in the preceding discussion of data and sync channel threshold (see Table 4.1.4-8). The design parameters are $2B_{LO}$ = 0.5 cps and α_o = 0.031.

The operating $(\frac{S}{N})_{2B_L} = (\frac{S}{N})_{2B_{LO}} - \frac{2B_L}{2B_{LO}}$, db

or, $(\frac{S}{N})_{2B_L} = (\frac{S}{N})_{2B_{LO}} - 1/3\ (1 + 2\ \frac{\alpha}{\alpha_o})$, db

For the above threshold conditions $(\frac{S}{N})_{2B_L}$ = +7.14 db.

The phase error in the loop is 0.324 radians as calculated from equation (2).

The loop will go out of lock whenever the rms value of noise voltage (σ_n) exceeds $\frac{\pi}{2}$ radians. Since $\frac{\pi}{2} \Big/ \sigma_n$ = 4.85 the noise must exceed 4.85 σ_n in magnitude. The normal probability distribution function describes the characteristics of the noise so that the probability of losing bit sync is found to be less than 1 x 10^{-6}.

2) Modes 2, 3, 5 and 6

In Modes 2, 3, 5 and 6 subcarrier lock is achieved in a Costas-type phase-lock demodulator in which the PCM data is forced to appear at the in-phase channel detector output. This PCM signal is then processed by a second loop slaved to the subcarrier loop which generates bit sync from the data train. If the bit sync loop slips a cycle, a bit error will occur; however, loss of bit sync will not necessarily take place when a bit error is made.

In the case of the uncoded data links of Modes 2, 3, 5 and 6, the output of the Costas demodulator will be the PCM data stream with a threshold bit error rate of 5×10^{-3}. For the case of the coded data links, the transmitted bit stream is detected and is then further processed by the decoder to provide the uncoded PCM data at the desired error rate. In either case, the $\frac{ST}{(N/B)}$ to the detector is above that required to assure operation of the sync loop above threshold. Therefore, the probability of loss of bit sync will be equal to or less than 5×10^{-3}.

Probability of Loss of Word and Frame Sync at Threshold--Recovery of the PCM data requires detection of the 7 bit sync word in the 91 bit master frame and the individual PCM subchannel frame sync words. In the case of the Bus Multiplexer/Encoder, the subchannel frame is 784 bits long. Detection of both the master frame sync word and the subchannel frame sync word is required for data word identification.

A 7 bit Barker code word is being used to synchronize the 91 bit master frame because of its excellent autocorrelation properties. The total probability (P_f) of false sync while the recognizer is searching the non-sync word positions is approximately:

$$P_f = 1 - (G_m)^{d-1}$$

where d = number of bits in the frame

$$G_m = 1 - (1/2)^m \sum_{r=o}^{e} \binom{m}{r} = 1 - P_i$$

P_i = probability of a false sync pattern in one sample of random data.

m = number of bits in the sync word

e = number of errors accepted by the recognizer

For m = 7, e = o, d = 91, $G_m = 0.9922$ and $P_f = 0.4944$.

This means a 49.4 percent probability of false sync during each frame.

Probability (P_c) of receiving the true sync is:

$$P_c = \sum_{r=o}^{e} \binom{m}{r} (P_e^b)^r \quad (1 - P_e^b)^{m-r}$$

where P_e^b is the bit error probability.

In our case e = o, m = 7, and $P_e^b = 5 \times 10^{-3}$.

$P_c = (0.995)^7 = 0.9655$.

Probability (P_t) of true sync in one frame is:

$$P_t = (1-P_f)\, P_c = (0.5056) \cdot (0.9655) = 0.4881$$

Probability (P_o) that no sync will occur:

$$P_o = (1-P_f) \cdot (1-P_c) = (0.5056) \quad (0.0345) = 0.0176$$

These probabilities indicate a relatively sluggish acquisition in one frame during search as is typical with word sync. However, the master frame is only 91 bits long and the probability of acquiring sync rises

rapidly in a few frames by using the proper techniques. To acquire and maintain sync the standard search, check and lock mode techniques will be used. It is clear from the above probabilities and by considering the use of a memory circuit to discriminate against random false sync indications, true sync can be readily acquired and maintained in 6 to 10 frames.

A 32 bit sync word is planned for the engineering subchannel frame of 784 bits. This sync word is excessive as long as the frame is synchronously blocked at the word intervals. However, emergency mode considerations make it advisable to employ a sync word of this length. Assuming a worst case failure mode with no master frame sync and a 3 percent bit error rate which is below the required bit error rate of 0.5 percent:

$P_i = 1 \times 10^{-6}$ for e = 3, m = 32, and d = 784

$P_c = 0.985$

$P_f \simeq P_i \ (d-1) = 7.83 \times 10^{-4}$

Since P_f is so small, $P_t = P_c = 0.985$, indicating that the sync acquisition is adequate.

Probability of the loss of master frame sync is determined by requiring 3 false indications to change from the lock to the check mode and 1 false indication to change from the check to the search mode. At the threshold level of 5×10^{-3} bit error rate, the probability of not receiving the true pattern in lock mode is $(1 - P_e^b)^7$ which is 0.0348. The probability of loss of master frame and word sync due to this bit error rate is $(0.0348)^4$ or 1.5×10^{-6}.

Effective Bit Error Rate for Bi-orthogonal Coded Data--An (n,k) M'ary bi-orthogonal code is one that consists of $M = 2^k$ words, each word of which contains k binary information bits and n binary coded bits. For any bi-orthogonal alphabet

$$M = 2^k, \quad n = 2^{k-1}, \quad M/2 = n$$

M/2 of the code words are chosen to be mutually orthogonal to each other while the remaining M/2 are the binary complements of the first M/2 words. Viterbi[5] has shown that the word error probability for a bi-orthogonal coded system may be expressed as a function of the received energy per word-to noise spectral density-ratio as:

$$P_w(k) = \int_{-\sqrt{2a}}^{\infty} \phi(x) \left[1 - 2\,\mathrm{erfc}\left(x + \sqrt{2a}\right)\right]^{M/2 - 1} dx$$

where

$P_w(k)$ = Word error probability for an $M = 2^k$ word code

$a = ST/N_o$

S = Received signal power, watts

T = Word period, sec

N_o = Receiver noise spectral density, watts/cps

$$\phi(X) = \frac{1}{\sqrt{2\pi}} \exp\left(-x^2/2\right)$$

$$\mathrm{erfc}(x) = \int_x^{\infty} \phi(y)\, dy$$

$M = 2^k$ = number of words in the alphabet

k = number of information bits per word.

[5] A. J. Viterbi, "On Coded Phase Coherent Communication", IRE TRANS., Vol. Set-7, March 1961, pp. 3-14.

The effective bit error rate of a (n, k) bi-orthogonal code may be computed by considering the decision process required in the detector. If M/2 correlators are used in the detector, the correct word will be selected if--and only if--the absolute values of the outputs of all other correlators are less than that of the correct one, and if the sign of the output has the correct polarity. The probability of selecting the code word complementary to the transmitted word is much lower than that of selecting the word orthogonal to it. Following Viterbi this probability, which shall be termed an error of the first kind, is given by

$$P_1(k) = \int_{-\infty}^{-\sqrt{2a}} \phi(x) \left[1 - 2\,\mathrm{erfc}\left(x + \sqrt{2a}\right)\right]^{\frac{M}{2} - 1} dx$$

where P_1 = Probability of an error of the first kind. The probability of selecting one of $(2^k - 2)$ code words orthogonal to the transmitted word, which shall be termed an error of the second kind, is

$$P_2(k) = P_w(k) - P_1(k) = \int_{-\sqrt{2a}}^{\infty} \phi(x) \left[1 - 2\,\mathrm{erfc}\left(x + \sqrt{2a}\right)\right]^{M/2 - 1} dx - P_1(k)$$

If it is assumed that complementary data words are encoded into complementary transmitted words, then an error of the first kind will cause k error bits, while an error of the second kind will cause

$$\frac{(k - 1)\, 2^k - 2}{k\,(2^{k-1} - 1)} \quad \text{error bits.}$$

Thus the total bit error probability for bi-orthogonal codes is

$$P_b(k) = P_1(k) + \frac{(k-1)2^{k-2}}{k(2^{k-1}-1)}\, P_2(k)$$

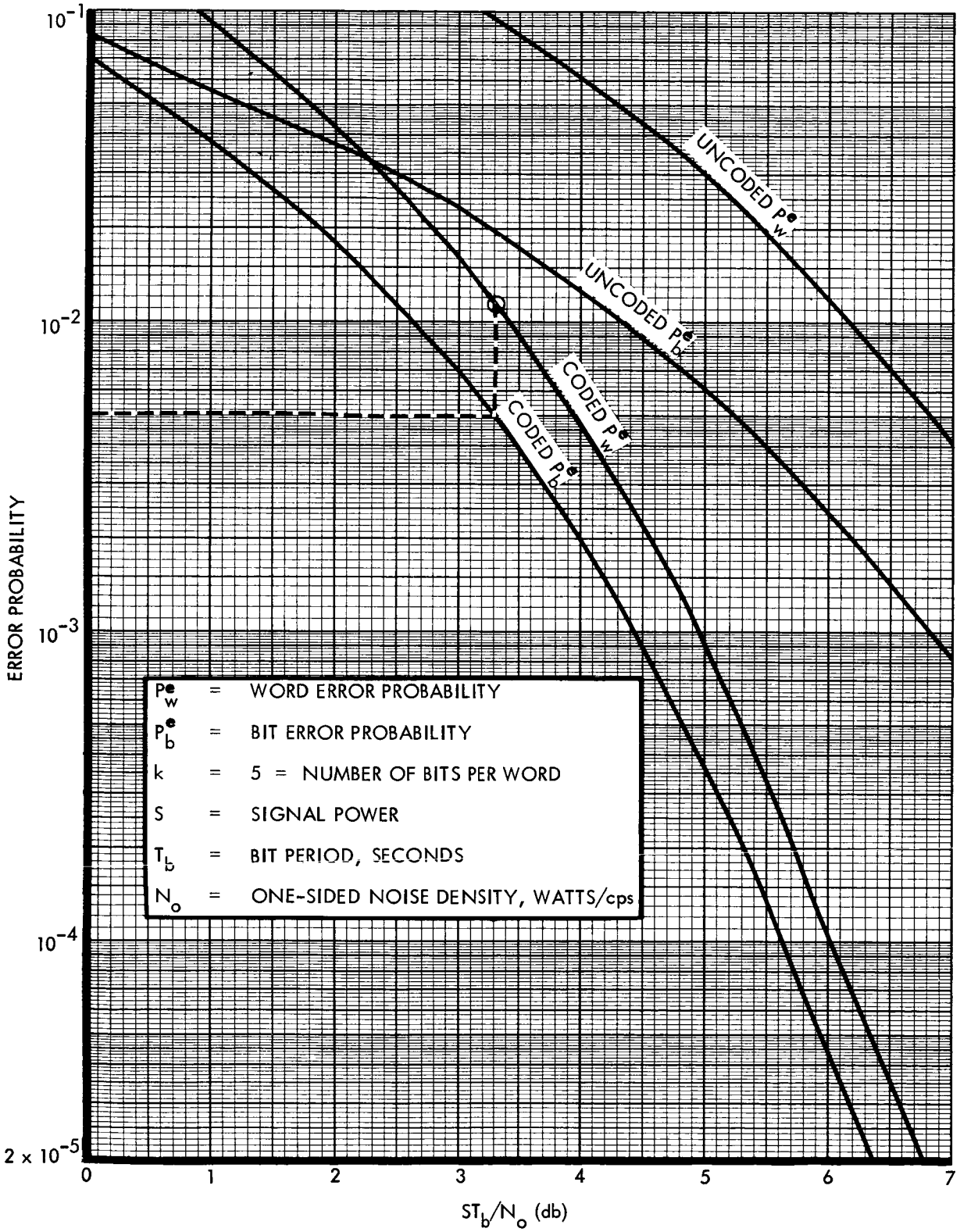

Figure 4.1.4-16: Bit & Word Error Probability for a (16, 5) Biorthogonal Code

In comparing the bit error rate performance of block coded binary systems, one must remember that the word period, T, is related to the bit period, T_b, by

$$T_b = \frac{T}{k} = \frac{T}{\log_2 M}$$

A bi-orthogonal code has been recommended for Modes 5 and 6 for which M = 32, n = 16, and k = 5. The resulting bit and word error rates are plotted in Figure 4.1.4-16 as a function of ST_b/N_o, the bit energy-to-noise density ratio. Bit and word error rate curves for uncoded coherent PSK are included for comparison. The uncoded word error rate was calculated from

$$P_w^e = 1 - (1 - P_b^e)^k \quad \text{where } k = 5$$

For the (16, 5) code selected, an (ST_b/N_o) = 3.3 db is required to meet the required bit error rate of 5×10^{-3}. The equivalent word error rate for this (ST_b/N_o) is $P_w(5) = 1.1 \times 10^{-2}$.

Telemetry-Link Performance Analysis--The specific design control tables developed for the telemetry-link modes are discussed in this section. These tables have been detailed in accordance with Jet Propulsion Laboratory Memo 3393-19-65, "Explanation of the Telecommunication Design Control Table," April 28, 1965. The tables presented were chosen to show the maximum capability of each telemetry data mode operating with the various anticipated spacecraft-DSIF component combinations.

Most of the entries in the design control table concerned with spacecraft hardware parameters have been developed in Section 4.1.4.1. The

corresponding ground parameters are tabulated in the same section under "DSIF Parameters." The items associated with modulation, such as derivation of modulation indices, losses, and threshold values, are also presented earlier in this section.

The discussion of the input data to a particular design control table will be limited to those items peculiar to that mode and system configuration.

The performance graphs presented for each design control table will show, as a minimum, the limiting-channel performance. A limiting channel is the one that reaches greyout first, where greyout is defined as nominal margin equal to worst-case tolerances.

Mode 1 Launch--Spacecraft: Shroud, 1-watt; DSIF: 4-foot, 10-db NF Receiver

Design Control Table 4.1.4-11 has been developed to establish the telemetry link performance during the early launch phase from liftoff to shroud ejection. As shown in the table, telemetry data Mode 1 has been used during this phase for transmission of spacecraft and capsule engineering data at 22-2/9 bps to Station 71. However, telemetry Mode 2 might be a desirable alternate because of possible interference of the subcarriers with the carrier tracking loop. Telemetry data will also be transmitted via the prime Centaur telemetry link to ETR stations.

The items significantly different from those of the normal flight configuration are the 1-watt launch transmitter and shroud antenna on the spacecraft, the 4-foot antenna, 10-db noise figure receiver, and the $2 B_{LO}$ tracking bandwidth of 152 cps on the ground. The gain of the 4-foot antenna is calculated to be 26.5 to 27.5 db, corresponding to 53- and 65-percent efficiency. The pointing loss of the antenna has been established by assuming that it could track with an angle accuracy of better than 2.2 degrees, which corresponds to a maximum pointing loss of -1 db.

The ground-system noise temperature (T_s) is calculated from the relation:

$$T_s = \left(\frac{L-1}{L} + F_r - 1\right) 290^{\circ}K$$

where: L is the ground circuit loss assumed to be 0.5 $\pm$0.2 db;

F_r is the ground receiver noise figure of 10 $\pm$1 db.

TELECOMMUNICATION DESIGN CONTROL Table 4.1.4-11

PROJECT: VOYAGER DATE

CHANNEL: SPACECRAFT - EARTH TELEMETRY LINK MODE L PAGE 1

MODE: LAUNCH: S/C SHROUD - 1 WATT, DSIF 4 FT. - 10 db NF RECEIVER

NO.	PARAMETER	VALUE	TOLERANCE	SOURCE
1	Total Transmitter Power	+ 30.0 dbm	+2.0 db - 0.0 db	SECTION 4.1.4.1
2	Transmitting Circuit Loss	- 0.6 db	+0.4 db - 0.6 db	FIGURE 4.1.4-1
3	Transmitting Antenna Gain	- 10.0 db	+0.0 db - 9.0 db	SECTION 4.1.4.1
4	Transmitting Antenna Pointing Loss	Included in 3		SECTION 4.1.4.1
5	Space Loss @ 2295 Mc, R = 200 km	- 145.7 db	-	—
6	Polarization Loss	Included in 3		—
7	Receiving Antenna Gain	+ 26.5 db	1.0 db - 0.0 db	TABLE 4.1.4-2
8	Receiving Antenna Pointing Loss	- 0.5 db	+0.5 db - 0.5 db	TABLE 4.1.4-2
9	Receiving Circuit Loss	- 0.5 db	+0.2 db - 0.2 db	TABLE 4.1.4-2
10	Net Circuit Loss	- 130.8 db	+2.1 db -10.3 db	—
11	Total Received Power	- 100.8 dbm	+4.1 db -10.3 db	—
12	Receiver Noise Spectral Density (N/B) T System = $2642^{+763}_{-609}{}^{\circ}K$	- 164.4 dbm	1.1 db - 1.1 db	TABLE 4.1.4-12
13	Carrier Modulation Loss	- 4.7 db	+1.0 db - 1.1 db	FIGURE 4.1.4-3
14	Received Carrier Power	- 105.5 dbm	+5.1 db -11.4 db	—
15	Carrier APC Noise BW ($2B_{LO}$ = 152 cps)	+ 21.8 db	+0.0 db - 0.5 db	FIGURE 4.1.4-3
	CARRIER PERFORMANCE -- TRACKING (One-Way)			
16	Threshold SNR in $2B_{LO}$	+ 9.0 db	-	FIGURE 4.1.4-3
17	Threshold Carrier Power	- 133.6 dbm	+1.1 db - 1.6 db	—
18	Performance Margin	+ 28.1 db	+6.7 db - 12.5 db	—
	CARRIER PERFORMANCE -- TRACKING (Two-Way)			
19	Threshold SNR in $2B_{LO}$	NOT APPLICABLE		
20	Threshold Carrier Power			
21	Performance Margin			

TELECOMMUNICATION DESIGN CONTROL TABLE 4.1.4-11

PROJECT: VOYAGER DATE
CHANNEL: SPACECRAFT--EARTH TELEMETRY LINK MODE 1 PAGE 2 of
MODE: LAUNCH; S/C SHROUD - 1 WATT, DSIF 4 FT. - 10 db NF RECEIVER

NO.	PARAMETER	VALUE	TOLERANCE	SOURCE
	CARRIER PERFORMANCE - DATA			
22	Threshold SNR in $2B_{LO}$	+9.0 db		Figure 4.1.4-3
23	Threshold Carrier Power	-133.6 dbm	+1.1 db -1.6 db	--
24	Performance Margin	+28.1 db	+6.7 db -12.5 db	--
	DATA CHANNEL			
25	Modulation Loss	-3.3 db	+0.5 db -0.6 db	Figure 4.1.4-3
26	Received Data Subcarrier Power	-104.1 dbm	+4.6 db -10.9 db	--
27	Bit Rate (1/T) 22-2/9 bps	+ 13.5 db	--	--
28	Required ST/N/B	+7.6 db	+0.5 db -0.5 db	Figure 4.1.4-3
29	Threshold Subcarrier Power	-143.3 dbm	+1.6 db -1.6 db	--
30	Performance Margin	+39.2 db	+6.2 db -12.5 db	--
	SYNC CHANNEL			
31	Modulation Loss	-13.6 db	+1.7 db -1.6 db	Figure 4.1.4-3
32	Receiver Sync Subcarrier Power	-114.4 dbm	+5.8 db -11.9 db	--
33	Sync APC Noise BW($2B_{LO}$ = 0.5 cps)	-3.0 db	+0.4 db -0.4 db	Figure 4.1.4-3
34	Threshold SNR in $2B_{LO}$	+14.0 db	+0.5 db -0.5 db	Figure 4.1.4-3
35	Threshold Subcarrier Power	-153.4 dbm	+2.0 db -2.0 db	- --
36	Performance Margin	+39.0 db	+7.8 db -13.9 db	--

COMMENTS:

The calculations and resultant system noise temperatures are given in Table 4.1.4-12.

TABLE: 4.1.4-12: SYSTEM NOISE TEMPERATURE--STATION 71

Condition	L		L-1	F		T_s	
	db	Num	L	(db)	F-1	^oK	N/B (dbm/cps)
Best	0.3	1.072	0.067	9	6.94	2033	-165.5
Nominal	0.5	1.122	0.109	10	9.0	2642	-164.4
Worst	0.7	1.175	0.149	11	11.59	3405	-163.3

The results of the design control table evaluation are presented in Figure 4.1.4-17 for the limiting case (i.e., the carrier channel). The link, under worst-case system performance, will give a margin of +15.5 db at the nominal shroud ejection slant range of 200 km (altitude greater than 500,000 feet). The performance graph shows that, even with the shroud antenna and the wide 2 B_{LO} tracking bandwidth of 152 cps on the ground, the link is capable of operating at a slant range in excess of 1000 km, which should exceed the line-of-sight limit (elevation angles $\leq$ 10 degrees) of Station 71. The one parameter not included in the design control table evaluation is plume attenuation during boost. However, the performance margins during this phase should adequately allow for this effect. In addition, the amount of this degradation depends strongly on the geometric relations between launch pad, ground station, trajectory parameters, and booster plume characteristics.

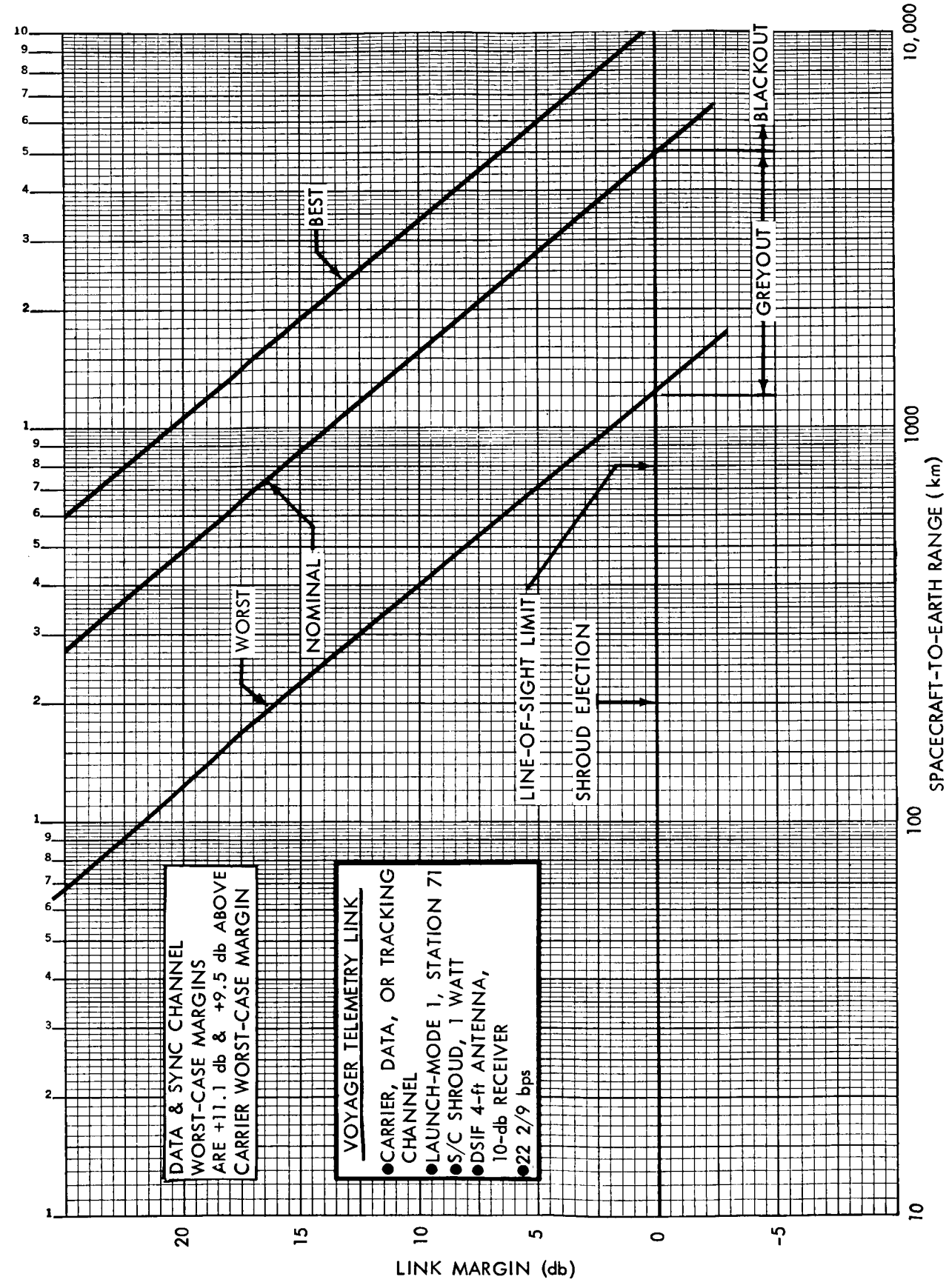

Figure 4.1.4-17:

Mode 1 Launch--Spacecraft: Ascent, 1-watt; DSIF: 4-foot, 10-db NF Receiver

During this flight phase, the shroud has been ejected and the spacecraft is sending telemetry data to Station 71 via the spacecraft ascent antenna. Design Control Table 4.1.4-13 evaluates the link for the same parameters as Table 4.1.4-11, except that the ascent antenna parameters are used instead of those for the shroud antenna. The ascent antenna system worst-case gain characteristics are 17 db better than those of the shroud antenna--this improvement is evident on the system performance graph Figure 4.1.4-18. The link performance under worst-case conditions will give a +20 db margin at the Station 71 line-of-sight limit.

TELECOMMUNICATION DESIGN CONTROL Table 4.1.4-13

PROJECT: VOYAGER DATE

CHANNEL: SPACECRAFT - EARTH TELEMETRY MODE 1 PAGE 1

MODE: LAUNCH: S/C ASCENT - 1 WATT, DSIF 4 FT. - 10 db NF RECEIVER

NO.	PARAMETER	VALUE	TOLERANCE	SOURCE
1	Total Transmitter Power	+ 30.0 dbm	+2.0 db - 0.0 db	SECTION 4.1.4.1
2	Transmitting Circuit Loss	- 0.6 db	+0.4 db - 0.6 db	FIGURE 4.1.4-1
3	Transmitting Antenna Gain	0.0 db	+2.0 db - 2.0 db	SECTION 4.1.4.1
4	Transmitting Antenna Pointing Loss	INCLUDED IN 3		—
5	Space Loss @ 2295 Mc, R = 2,000 km	- 165.7 db	-	—
6	Polarization Loss	INCLUDED IN 3		—
7	Receiving Antenna Gain	+ 26.5 db	+1.0 db - 0.0 db	SECTION 4.1.4.1
8	Receiving Antenna Pointing Loss	0.0 db	+0.0 db - 0.0 db	TABLE 4.1.4-2
9	Receiving Circuit Loss	- 0.5 db	+0.2 db - 0.2 db	TABLE 4.1.4-2
10	Net Circuit Loss	- 140.3 db	+3.6 db - 2.8 db	—
11	Total Received Power	- 110.3 dbm	+5.6 db - 2.8 db	—
12	Receiver Noise Spectral Density (N/B) T System = 2642°K $^{+763^{\circ}K}_{-609^{\circ}K}$	- 164.4 dbm	+1.1 db - 1.1 db	TABLE 4.1.4-12
13	Carrier Modulation Loss	- 4.7 db	+1.0 db - 1.1 db	FIGURE 4.1.4-3
14	Received Carrier Power	- 115.0 dbm	+6.6 db - 3.9 db	—
15	Carrier APC Noise BW ($2B_{LO}$ = 152cps)	+ 21.8 db	+0.0 db - 0.5 db	FIGURE 4.1.4-3
	CARRIER PERFORMANCE -- TRACKING (One-Way)			
16	Threshold SNR in $2B_{LO}$	+ 9.0 db	-	FIGURE 4.1.4-3
17	Threshold Carrier Power	- 133.6 dbm	+1.1 db - 1.6 db	—
18	Performance Margin	+ 18.6 db	+8.2 db - 5.0 db	—
	CARRIER PERFORMANCE -- TRACKING (Two-Way)			
19	Threshold SNR in $2B_{LO}$	+ 9.0 db	-	FIGURE 4.1.4-3
20	Threshold Carrier Power	- 133.6 dbm	+1.1 db - 1.6 db	—
21	Performance Margin	+ 18.6 db	+8.2 db - 5.0 db	—

TELECOMMUNICATION DESIGN CONTROL TABLE 4.1.4-13

PROJECT: VOYAGER DATE
CHANNEL: SPACECRAFT - EARTH TELEMETRY MODE 1 PAGE 2 of
MODE: LAUNCH: S/C ASCENT - 1 WATT, DSIF 4 FT. - 10 db NF RECEIVER

NO.	PARAMETER	VALUE	TOLERANCE	SOURCE
	CARRIER PERFORMANCE - DATA			
22	Threshold SNR in $2B_{LO}$	+9.0 db	--	Figure 4.1.4-3
23	Threshold Carrier Power	-133.6 dbm	+1.1 db -1.6 db	--
24	Performance Margin	+18.6 db	+8.2 db -5.0 db	--
	DATA CHANNEL			
25	Modulation Loss	-3.3 db	+0.5 db -0.6 db	Figure 4.1.4-3
26	Received Data Subcarrier Power	-133.6 dbm	+6.1 db -3.4 db	--
27	Bit Rate (1/T) 22 2/9 bps	+13.5 db	--	--
28	Required ST/N/B	+7.6 db	+0.5 db -0.5 db	Figure 4.1.4-3
29	Threshold Subcarrier Power	-143.3 dbm	+1.6 db -1.6 db	--
30	Performance Margin	+29.7 db	+7.7 db -5.0 db	--
	SYNC CHANNEL			
31	Modulation Loss	-13.6 db	+1.7 db -1.6 db	Figure 4.1.4-3
32	Receiver Sync Subcarrier Power	-123.9 dbm	+7.3 db -4.4 db	--
33	Sync APC Noise BW($2B_{LO}$ = 0.5 cps)	-3.0 db	+0.4 db -0.4 db	Figure 4.1.4-3
34	Threshold SNR in $2B_{LO}$	+14.0 db	+0.5 db -0.5 db	Figure 4.1.4-3
35	Threshold Subcarrier Power	-153.4 dbm	+2.0 db -2.0 db	--
36	Performance Margin	+29.5 db	+9.3 db -6.4 db	--

COMMENTS:

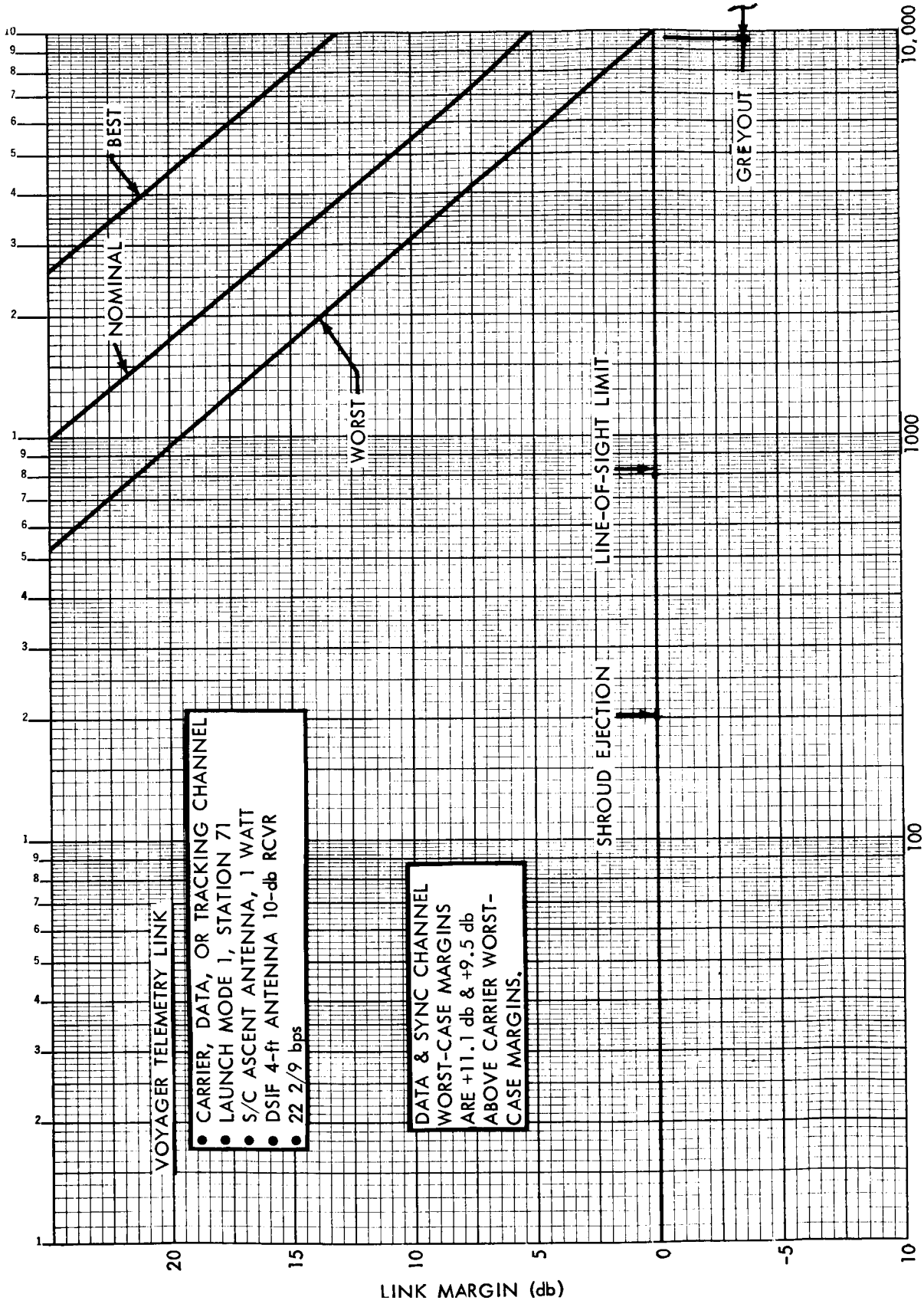

Figure 4.1.4-18:

Mode 1 Acquisition (Johannesburg)--Spacecraft: Ascent, 1-watt; DSIF: 2 by 2-foot horn, Paramp

In this phase of the flight, the initial two-way acquisition and tracking of the spacecraft is accomplished by Johannesburg before operational control and cruise tracking by the DSN antenna. The spacecraft configuration will contain the ascent antenna and 1-watt transmitter to conserve prime power prior to Sun acquisition and to prevent the use of high voltages until completion of outgassing. The Johannesburg ground station will be in its acquisition mode using the 2 by 2-foot horn antenna with 10-kw transmitter diplexed with a paramp receiver front end. Initial acquisition will be accomplished by illuminating the horizon at the predicted azimuth until the spacecraft signal is detected. One-way tracking is then initiated, and the uplink frequency is varied to achieve two-way lock and tracking. Based on Lunar Orbiter studies, it is expected that the acquisition sequence and transfer to the 85-foot antenna will require 20 minutes. The trajectory analyzed for the Voyager mission indicates that injection into the trans-Mars trajectory will be complete before contact and the slant range variation during the first 20 minutes of Johannesburg contact will be 6000 to 10,000 km. The initial doppler rates might be sufficiently high to require the 152-cps 2 B_{LO} bandwidth at the ground.

The telemetry link performance has been evaluated for this equipment configuration in Design Control Table 4.1.4-14. There are no table entries that have not been discussed or tabulated in previous sections. The system performance graph (Figure 4.1.4-19) shows that the link will have a

TELECOMMUNICATION DESIGN CONTROL Table 4.1.4-14

PROJECT: VOYAGER DATE

CHANNEL: SPACECRAFT - EARTH TELEMETRY LINK MODE 1 PAGE 1

MODE: ACQUISITION JOHANNESBURG: S/C ASCENT - 1 WATT, DSIF 2 x 2 FT. HORN-PARAMP

NO.	PARAMETER	VALUE	TOLERANCE	SOURCE
1	Total Transmitter Power	+ 30.0 dbm	+2.0 db - 0.0 db	SECTION 4.1.4.1
2	Transmitting Circuit Loss	- 0.6 db	+0.4 db - 0.6 db	FIGURE 4.1.4-1
3	Transmitting Antenna Gain	0.0 db	+2.0 db - 2.0 db	SECTION 4.1.4.1
4	Transmitting Antenna Pointing Loss	INCLUDED	IN 3	
5	Space Loss @ 2295 Mc, R = 10,000 km	- 179.7 db	-	
6	Polarization Loss	INCLUDED	IN 3	
7	Receiving Antenna Gain	+ 21.0 db	+1.0 db - 1.0 db	TABLE 4.1.4-2
8	Receiving Antenna Pointing Loss	0.0 db	+0.0 db - 0.0 db	TABLE 4.1.4-2
9	Receiving Circuit Loss	- 0.5 db	+0.2 db - 0.2 db	TABLE 4.1.4-2
10	Net Circuit Loss	- 159.8 db	+3.6 db - 3.8 db	
11	Total Received Power	- 129.8 dbm	+5.6 db - 3.8 db	
12	Receiver Noise Spectral Density (N/B) T System = 270°K $^{+50°K}_{-50°K}$	- 174.3 dbm	+0.7 db - 0.9 db	TABLE 4.1.4-2
13	Carrier Modulation Loss	- 4.7 db	+1.0 db - 1.1 db	FIGURE 4.1.4-3
14	Received Carrier Power	- 134.5 dbm	+6.6 db - 4.9 db	
15	Carrier APC Noise BW ($2B_{LO}$ = 152 cps)	+ 21.8 db	+0.0 db - 0.5 db	FIGURE 4.1.4-3
	CARRIER PERFORMANCE -- TRACKING (One-Way)			
16	Threshold SNR in $2B_{LO}$	+ 9.0 db	-	FIGURE 4.1.4-3
17	Threshold Carrier Power	- 143.5 dbm	+0.7 db - 1.4 db	
18	Performance Margin	+ 9.0 db	+8.0 db - 5.6 db	
	CARRIER PERFORMANCE -- TRACKING (Two-Way)			
19	Threshold SNR in $2B_{LO}$	+ 9.0 db	-	FIGURE 4.1.4-3
20	Threshold Carrier Power	- 143.5 dbm	+0.7 db - 1.4 db	
21	Performance Margin	+ 9.0 db	+8.0 db - 5.6 db	

TELECOMMUNICATION DESIGN CONTROL TABLE 4.1.4-14

PROJECT: VOYAGER DATE

CHANNEL: SPACECRAFT--EARTH TELEMETRY LINK MODE 1 PAGE 2 of

MODE: ACQUISITION JOHANNESBURG; S/C ASCENT - 1 WATT, DSIF 2x2 FT. HORN-PARAMP

NO.	PARAMETER	VALUE	TOLERANCE	SOURCE
	CARRIER PERFORMANCE - DATA			
22	Threshold SNR in $2B_{LO}$	+9.0 db	--	Figure 4.1.4-3
23	Threshold Carrier Power	-143.5 dbm	+0.7 db -1.4 db	--
24	Performance Margin	+9.0 db	+8.0 db -5.6 db	--
	DATA CHANNEL			
25	Modulation Loss	-3.3 db	+0.5 db -0.6 db	Figure 4.1.4-3
26	Received Data Subcarrier Power	-133.1 dbm	+6.1 db -4.4 db	--
27	Bit Rate (1/T) 22-2/9 bps	+13.5 db	--	--
28	Required ST/N/B	+7.6 db	+0.5 db -0.5 db	Figure 4.1.4-3
29	Threshold Subcarrier Power	-153.2 dbm	+1.2 db -1.4 db	--
30	Performance Margin	+20.1 db	+7.5 db -5.6 db	--
	SYNC CHANNEL			
31	Modulation Loss	-13.6 db	+1.7 db -1.6 db	Figure 4.1.4-3
32	Receiver Sync Subcarrier Power	-143.4 dbm	+7.3 db -5.4 db	--
33	Sync APC Noise BW($2B_{LO}$ = 0.5 cps)	-3.0 db	+0.4 db -0.4 db	Figure 4.1.4-3
34	Threshold SNR in $2B_{LO}$	+14.0 db	+0.5 db -0.5 db	Figure 4.1.4-3
35	Threshold Subcarrier Power	-163.3 dbm	+1.6 db -1.8 db	--
36	Performance Margin	+19.9 db	+9.1 db -7.0 db	--

COMMENTS:

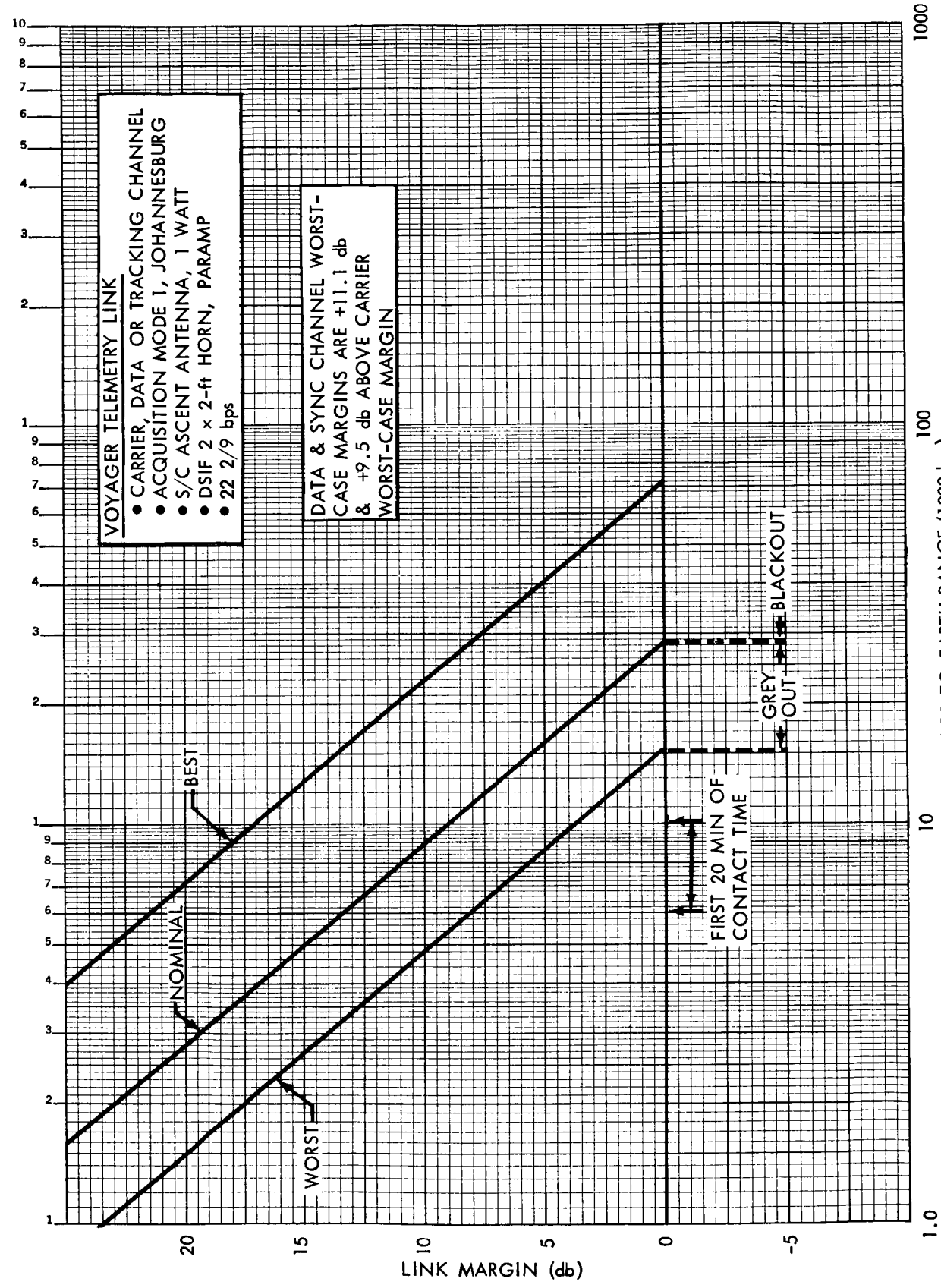

Figure 4.1.4-19:

performance margin of +3.5 db worst case at the end of the first 20 minutes of station contact. The corresponding slant range at this point is 10,000 km. The link does not enter greyout until the range is 15,000 km, which occurs about 35 minutes after initial station contact. It is possible to switch to the 48-cps loop bandwidth to extend the greyout range as the doppler rate becomes negligible within 25 minutes after initial contact.

Mode 2 Cruise--Spacecraft: Ascent, 1-watt; DSIF: 85-foot, Maser

After completion of the acquisition sequence at Johannesburg, tracking of the spacecraft is transferred to the 85-foot DSN stations. This period is the start of the cruise flight phase, and the telemetry data Mode 2 is selected to allow transmission of cruise science along with spacecraft and capsule engineering data. Design Control Table 4.1.4-15 has been evaluated for the 1-watt power level and ascent antenna to establish the maximum range of operation for the low power mode. Doppler parameters are low in this phase, and the 12-cps $2B_{LO}$ has been selected for use. System Performance Figure 4.1.4-20 shows that this link can operate above greyout conditions to a range of 2.7×10^6 km (10 days). A performance margin of +5 db above worst case is provided at the first midcourse maneuver occurring nominally at 5 days. Normally, operation is switched to the low-gain antenna and 50-watt transmitter as soon as high voltages can be used, usually about 24 hours after launch.

TELECOMMUNICATION DESIGN CONTROL Table 4.1.4-15

PROJECT: VOYAGER DATE

CHANNEL: SPACECRAFT-EARTH TELEMETRY LINK MODES 2 OR 3 PAGE 1

MODE: CRUISE: S/C ASCENT - 1 WATT, DSIF 85 FT. - MASER

NO.	PARAMETER	VALUE	TOLERANCE	SOURCE
1	Total Transmitter Power	+ 30.0 dbm	+2.0, -0.0 db	SECTION 4.1.4.1
2	Transmitting Circuit Loss	- 0.6 db	+0.4, -0.6 db	FIGURE 4.1.4-1
3	Transmitting Antenna Gain	0.0	+2.0, -2.0 db	SECTION 4.1.4.1
4	Transmitting Antenna Pointing Loss	Included in (3)		
5	Space Loss @ 2295 Mc, R = 2×10^6 km	-225.7 db		-
6	Polarization Loss	Included in (3)		
7	Receiving Antenna Gain	+ 53.0 db	+1.0, -0.5 db	TABLE 4.1.4-2
8	Receiving Antenna Pointing Loss	0.0 db	+0.0, -0.1 db	TABLE 4.1.4-2
9	Receiving Circuit Loss	- 0.2 db	+0.1, -0.0 db	TABLE 4.1.4-2
10	Net Circuit Loss	-173.5 db	+3.5, -3.2 db	-
11	Total Received Power	-143.5 dbm	+5.5, -3.2 db	-
12	Receiver Noise Spectral Density (N/B) $T_{System} = 45^{+10}_{-5}\ ^{\circ}K$	-182.1 dbm	+0.9, -0.5 db	TABLE 4.1.4-2
13	Carrier Modulation Loss	- 4.9 db	+1.0, -1.3 db	FIGURE 4.1.4-3
14	Received Carrier Power	-148.4 dbm	+6.5, -4.5 db	-
15	Carrier APC Noise BW ($2B_{LO}$=12.0 cps)	+ 10.8 db	+0.0, -0.5 db	FIGURE 4.1.4-3
	CARRIER PERFORMANCE -- TRACKING (One-Way)			
16	Threshold SNR in $2B_{LO}$	+ 9.0 db	-	FIGURE 4.1.4-3
17	Threshold Carrier Power	-162.3 dbm	+0.9, -1.0 db	-
18	Performance Margin	+ 13.9 db	+7.5, -5.4 db	-
	CARRIER PERFORMANCE -- TRACKING (Two-Way)			
19	Threshold SNR in $2B_{LO}$	+ 9.0 db	-	FIGURE 4.1.4-3
20	Threshold Carrier Power	-162.3 dbm	+0.9 - 1.0 db	-
21	Performance Margin	+ 13.9 db	+7.5, -5.4 db	-

TELECOMMUNACTION DESIGN CONTROL TABLE 4.1.4-15

PROJECT: VOYAGER DATE
CHANNEL: SPACECRAFT--EARTH TELEMETRY LINK MODES 2 or 3 PAGE 2 of
MODE: CRUISE: S/C ASCENT - 1 WATT, DSIF 85 ft. - MASER

NO.	PARAMETER	VALUE	TOLERANCE	SOURCE
	CARRIER PERFORMANCE - DATA			
22	Threshold SNR in $2B_{LO}$	+15.0 db	--	Figure 4.1.4-3
23	Threshold Carrier Power	-156.3 dbm	+0.9 db -1.0 db	--
24	Performance Margin	+7.9 db	+7.5 db -5.4 db	--
	DATA CHANNEL			
25	Modulation Loss	-2.4 db	+0.4 db -0.4 db	Figure 4.1.4-3
26	Received Data Subcarrier Power	-145.9 dbm	+5.9 db -3.6 db	--
27	Bit Rate (1/T) 133-1/3 bits/sec	+21.3 db	--	--
28	Required ST/N/B	+7.2 db	+0.5 db -0.5 db	Figure 4.1.4-3
29	Threshold Subcarrier Power	-153.6 dbm	+1.4 db -1.0 db	Figure 4.1.4-3
30	Performance Margin	+7.7 db	+6.9 db -5.0 db	--
	DATA CHANNEL			
31	Modulation Loss			
32	Received Data Subcarrier Power			
33	Bit Rate (1/T)			
34	Required ST/N/B			
35	Threshold Subcarrier Power			
36	Performance Margin			

COMMENTS:

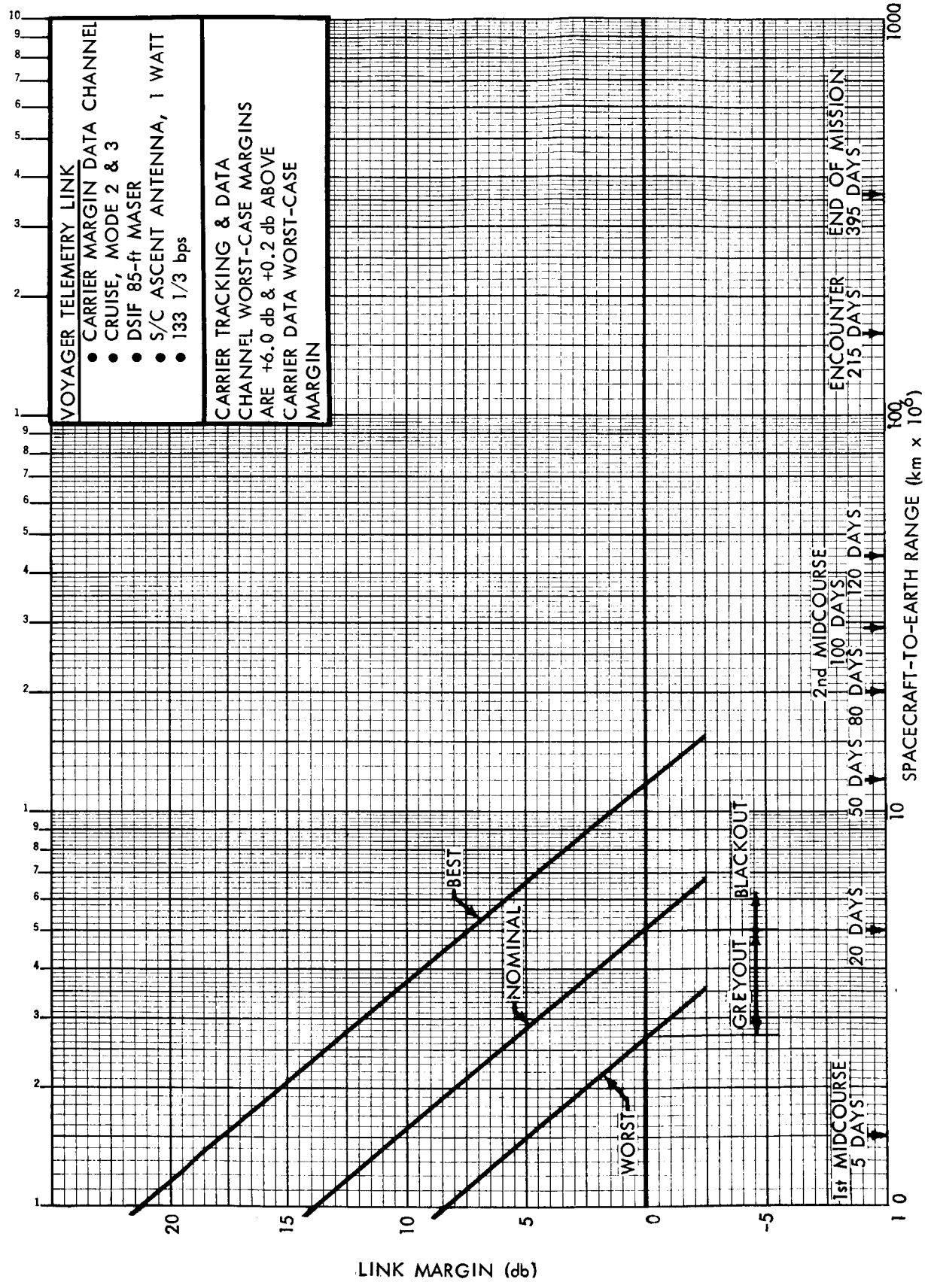

Figure 4.1.4-20.

Mode 1 Cruise--Spacecraft: Low-Gain, 50-watt; DSIF: 85-foot, Maser

Design Control Table 4.1.4-16 is evaluated to present the maximum capability of telemetry data for Mode 1 operating with the low-gain spacecraft antenna and 50-watt transmitter power. The table itself is for the non-maneuvering case and 85-foot ground antenna. Scaling techniques are used to establish the performance for the maneuvering conditions (1 db of additional pointing loss on the low-gain pattern) and for operation with the 210-foot ground antenna. Scaling to attain the performance with the 210-foot antenna must consider the antenna gain and system noise temperature improvement to arrive at the correct nominal, best, and worst-case tolerance values.

System Performance Figure 4.1.4-21 shows Mode 1 capability with the 85-foot antenna under maneuvering and non-maneuvering conditions. The second midcourse maneuver will occur between 25 and 100 days after launch. Under worst-case conditions, and assuming that the midcourse correction is delayed until the 100th day, the link performance margin would be +0.5 db using the low-gain antenna. There is a very high probability that this maneuver will be performed prior to the fiftieth day, in which case the margin under worst-case conditions will be at least +8.0 db.

System Performance Figure 4.1.4-22 presents the maximum Mode 1 range capability using the spacecraft low-gain antenna with the 210-foot ground antenna. This graph shows that during the second midcourse maneuver, use of this antenna would provide a worst-case performance margin of +10 db

TELECOMMUNICATION DESIGN CONTROL Table 4.1.4-16

PROJECT: VOYAGER DATE

CHANNEL: SPACECRAFT - EARTH TELEMETRY LINK MODE 1 PAGE 1

MODE: CRUISE: S/C LOW GAIN - 50 WATTS, DSIF 85 FT - MASER

NO.	PARAMETER	VALUE	TOLERANCE	SOURCE
1	Total Transmitter Power	+ 47.0 dbm	+2.0, - 0.0 db	SECTION 4.1.4.1
2	Transmitting Circuit Loss	- 2.6 db	+0.5, -1.3 db	FIGURE 4.1.4-1
3	Transmitting Antenna Gain	+ 1.0 db	+1.0, -0.0 db	SECTION 4.1.4.1
4	Transmitting Antenna Pointing Loss	0.0 db	+0.0, -0.0 db	SECTION 4.1.4.1
5	Space Loss @ 2295 Mc, $R = 30 \times 10^6$ km	- 249.2 db		-
6	Polarization Loss	0.0 db	+0.1, -0.1 db	TABLE 4.1.4-5
7	Receiving Antenna Gain	+ 53.0 db	+1.0, -0.5 db	TABLE 4.1.4-2
8	Receiving Antenna Pointing Loss	0.0 db	+0.0, -0.1 db	TABLE 4.1.4-2
9	Receiving Circuit Loss	- 0.2 db	+0.1, -0.0 db	TABLE 4.1.4-2
10	Net Circuit Loss	- 198.0 db	+2.7, -2.0 db	-
11	Total Received Power	- 151.0 dbm	+4.7, -2.0 db	-
12	Receiver Noise Spectral Density (N/B)	- 182.1 dbm	+0.9, -0.5 db	TABLE 4.1.4-2
13	T System=45^{+10}_{-5} °K Carrier Modulation Loss	- 4.7 db	+1.0, -1.1 db	FIGURE 4.1.4-3
14	Received Carrier Power	- 155.7 dbm	+5.7, -3.1 db	
15	Carrier APC Noise BW ($2B_{LO}$ = 12 cps)	10.8 db	+0.0, -0.5 db	FIGURE 4.1.4-3
	CARRIER PERFORMANCE -- TRACKING (One-Way)			
16	Threshold SNR in $2B_{LO}$	+ 9.0 db	- -	FIGURE 4.1.4-3
17	Threshold Carrier Power	- 162.3 dbm	+0.9, - 1.0 db	-
18	Performance Margin	+ 6.6 db	+6.7, -4.0 db	-
	CARRIER PERFORMANCE -- TRACKING (Two-Way)			
19	Threshold SNR in $2B_{LO}$	+ 9.0 db	- -	FIGURE 4.1.4-3
20	Threshold Carrier Power	- 162.3 dbm	+0.9, -1.0 db	-
21	Performance Margin	+ 6.6 db	+6.7, -4.0 db	-

TELECOMMUNICATION DESIGN CONTROL TABLE 4.1.4-16

PROJECT: VOYAGER
CHANNEL: SPACECRAFT--EARTH TELEMETRY LINK MODE 1
MODE: CRUISE: S/C LOW GAIN - 50 WATTS, DSIF 85 FT. - MASER

DATE
PAGE 2 of

NO.	PARAMETER	VALUE	TOLERANCE	SOURCE
	CARRIER PERFORMANCE - DATA			
22	Threshold SNR in $2B_{LO}$	+9.0 db	--	Figure 4.1.4-3
23	Threshold Carrier Power	-162.3 dbm	+0.9 db -1.0 db	--
24	Performance Margin	+6.6 db	+6.7 db -4.0 db	--
	DATA CHANNEL			
25	Modulation Loss	-3.3 db	+0.5 db -0.6 db	Figure 4.1.4-3
26	Received Data Subcarrier Power	-154.3 dbm	+5.2 db -2.6 db	--
27	Bit Rate (1/T) 22-2/9 bps	+13.5 db	--	--
28	Required ST/N/B	7.6 db	+0.5 db -0.5 db	Figure 4.1.4-3
29	Threshold Subcarrier Power	-161.0 dbm	+1.4 db -1.0 db	--
30	Performance Margin	+6.7 db	+6.2 db -4.0 db	--
	SYNC CHANNEL			
31	Modulation Loss	-13.6 db	+1.7 db -1.6 db	Figure 4.1.4-3
32	Receiver Sync Subcarrier Power	-164.6 dbm	+6.4 db -3.6 db	--
33	Sync APC Noise BW($2B_{LO}$ = 0.5 cps)	-3.0 db	+0.4 db -0.4 db	Figure 4.1.4-3
34	Threshold SNR in $2B_{LO}$	14.0 db	+0.5 db -0.5 db	Figure 4.1.4-3
35	Threshold Subcarrier Power	-171.1 dbm	+1.8 db -1.4 db	--
36	Performance Margin	+6.5 db	+7.8 db -5.4 db	--

COMMENTS:

NOTE 1. The midcourse maneuver performance is obtained from this chart by scaling to include low gain pointing loss of -1.0 db $^{+1.0}_{-0.0}$ db; that is, reduce nominal margin by 1.0 db, raise best tolerance by 1.0 db, worst tolerance is same.

NOTE 2. The maneuver performance using DSIF 210FT is obtained from scaling this chart by adding +8.0 db to nominal margin, +2.0 db to best tolerance, and +0.9 to worst tolerance.

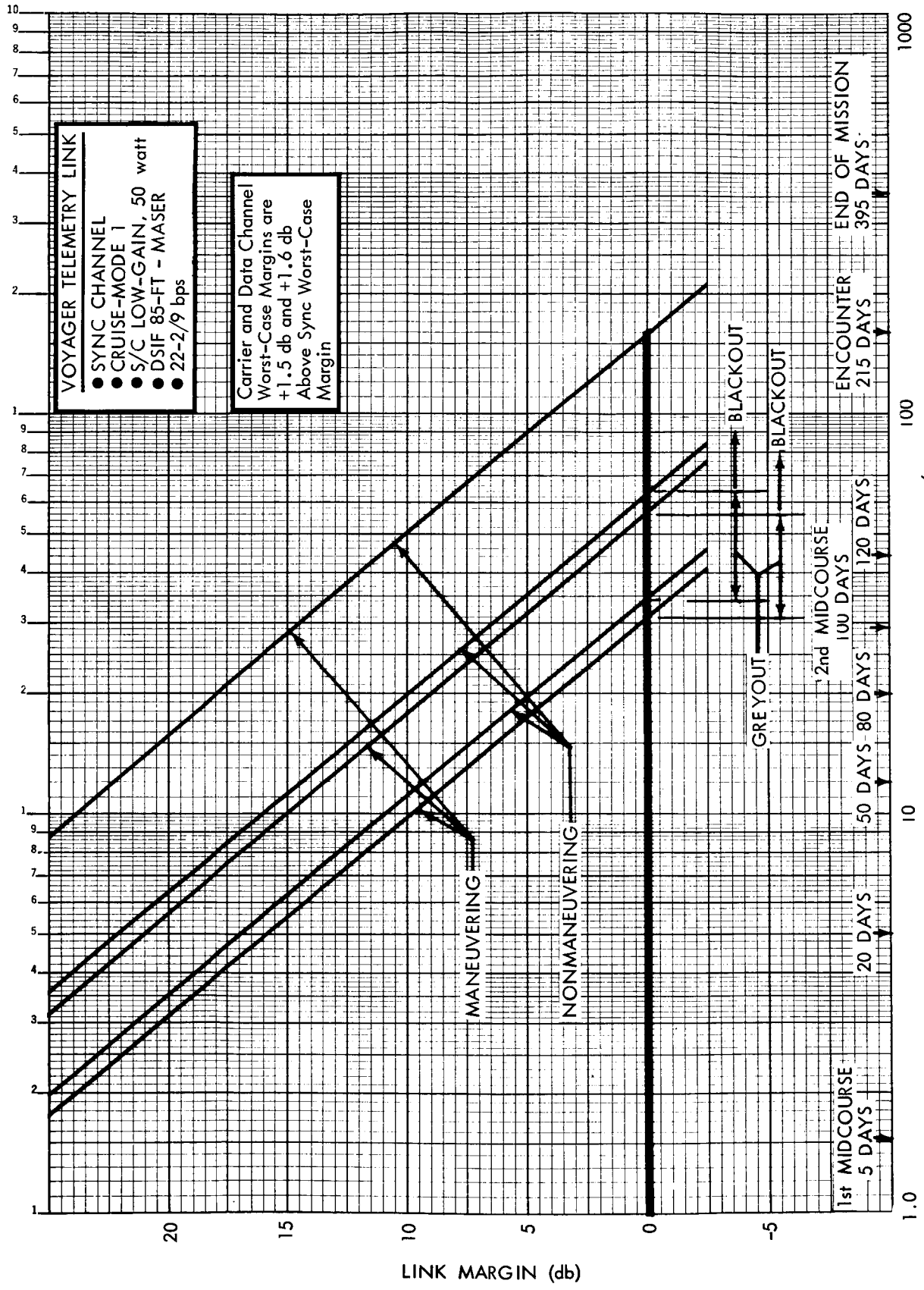

Figure 4.1.4-21:

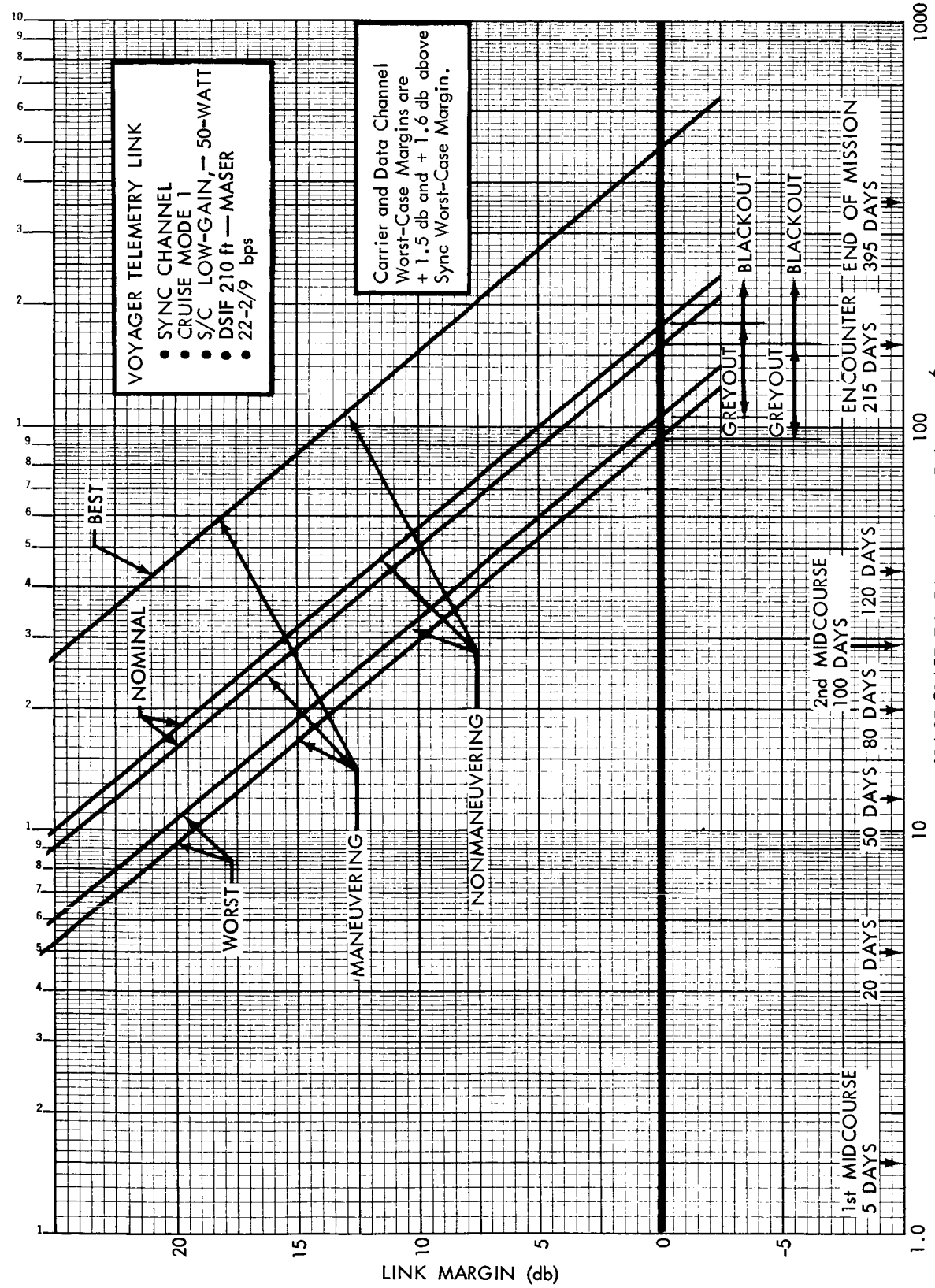

Figure 4.1.4-22:

compared to +0.5 db using the 85-foot antenna. The graph also shows that the 210-foot antenna and low-gain antenna combination would allow a late midcourse maneuver without greyout conditions to a range of 94×10^6 km (170 days). It is also seen that the use of Mode 1 via the low-gain during the encounter phase would involve system operation in greyout. For this reason the high-gain antenna system is designed to operate during encounter maneuvers and provide adequate Mode 1 capability.

Mode 2 or 3 Cruise--Spacecraft: Low-Gain, 50-watt; DSIF: 85-foot, Maser

During cruise flight, Mode 2 telemetry data is used for transmission of engineering and cruise science. Mode 3, which is identical from a data-rate standpoint, also may be selected. Mode 3 is a post-maneuver option where engineering data stored during maneuvers (engineering data is also transmitted during maneuvers) may be played back in place of the cruise science data.

Design Control Table 4.1.4-17 evaluates the Mode 2 or Mode 3 performance for the low-gain antenna and 50-watt transmitter with the 85-foot ground antenna. The basic input parameters to the chart have been treated previously and may be found by reference to the source column entries. System Performance Figure 4.1.4-23 shows the link may be used without greyout to ranges of 19×10^6 km ($\sim$ 80 days). At this point, it is planned to switch to the high-gain spacecraft antenna as the tracking rates requirements are quite low ($\sim 1^\circ$/day). An alternate choice at the 80 day point would be to switch over at the ground to the 210-foot network. Since use of the high-gain antenna is feasible and the mission guidelines suggest continued use of the 85-foot net until the encounter period, the switchover to high-gain antenna at 80 days has been selected.

TELECOMMUNICATION DESIGN CONTROL Table 4.1.4-17

PROJECT: VOYAGER DATE

CHANNEL: SPACECRAFT-EARTH TELEMETRY LINK MODES 2 OR 3 PAGE 1

MODE: CRUISE: S/C LOW-GAIN -- 50 WATTS, DSIF 85 FT. - MASER

NO.	PARAMETER	VALUE	TOLERANCE	SOURCE
1	Total Transmitter Power	+ 47.0 dbm	+2.0, - 0.0 db	SECTION 4.1.4.1
2	Transmitting Circuit Loss	- 2.6 db	+0.5, - 1.3 db	FIGURE 4.1.4-1
3	Transmitting Antenna Gain	+ 1.0 db	+1.0, - 0.0 db	SECTION 4.1.4.1
4	Transmitting Antenna Pointing Loss	0.0 db	+0.0, - 0.0 db	SECTION 4.1.4.1
5	Space Loss @ 2295 Mc, $R = 1.86 \times 10^{9}$ km	-245.0 db	- -	
6	Polarization Loss	0.0 db	+0.2, -0.2 db	TABLE 4.1.4-5
7	Receiving Antenna Gain	+ 53.0 db	+1.0, -0.5 db	TABLE 4.1.4-2
8	Receiving Antenna Pointing Loss	0.0 db	+0.0, -0.1 db	TABLE 4.1.4-2
9	Receiving Circuit Loss	- 0.2 db	+0.1, -0.0 db	TABLE 4.1.4-2
10	Net Circuit Loss	-193.8 db	+2.8, -0.0 db	
11	Total Received Power	-146.8 dbm	+4.8, -2.1 db	
12	Receiver Noise Spectral Density (N/B) T System = 45 $^{+10}_{-5}$ ^{o}K	-182.1 dbm	+0.9, -0.5 db	TABLE 4.1.4-2
13	Carrier Modulation Loss	- 4.9 db	+1.0,-1.3 db	FIGURE 4.1.4-3
14	Received Carrier Power	-151.7 dbm	+5.8, -3.4 db	
15	Carrier APC Noise BW ($2B_{LO}$ =12.0cps)	+ 10.8 db	+0.0, -0.5 db	FIGURE 4.1.4-3
	CARRIER PERFORMANCE -- TRACKING (One-Way)			
16	Threshold SNR in $2B_{LO}$	+ 9.0 db	- - -	FIGURE 4.1.4-3
17	Threshold Carrier Power	-162.3 dbm	+0.9, -1.0 db	
18	Performance Margin	+ 10.6 db	+6.8, -4.3 db	
	CARRIER PERFORMANCE -- TRACKING (Two-Way)			
19	Threshold SNR in $2B_{LO}$	+ 9.0 db	- -	FIGURE 4.1.4-3
20	Threshold Carrier Power	-162.3 dbm	+0.9, -1.0 db	
21	Performance Margin	+ 10.6 db	+6.8, -4.3 db	

TELECOMMUNICATION DESIGN CONTROL TABLE 4.1.4-17

PROJECT: VOYAGER DATE
CHANNEL: SPACECRAFT--EARTH TELEMETRY LINK MODES 2 or 3 PAGE 2 of 2
MODE: CRUISE: S/C LOW-GAIN - 50 WATTS, DSIF 85 FT. - MASER

NO.	PARAMETER	VALUE	TOLERANCE	SOURCE
	CARRIER PERFORMANCE - DATA			
22	Threshold SNR in $2B_{LO}$	+15.0 db	--	Figure 4.1.4-3
23	Threshold Carrier Power	-156.3 dbm	+0.9 db -1.0 db	--
24	Performance Margin	+4.6 db	+6.8 db -4.3 db	--
	DATA CHANNEL			
25	Modulation Loss	-2.4 db	+0.4 db -0.4 db	Figure 4.1.4-3
26	Received Data Subcarrier Power	-149.2 dbm	+5.2 db -2.5 db	--
27	Bit Rate (1/T) (133-1/3 bits/sec)	+21.3 db	--	--
28	Required ST/N/B	+7.2 db	+0.5 db -0.5 db	Figure 4.1.4-3
29	Threshold Subcarrier Power	-153.6 dbm	+1.4 db -1.0 db	--
30	Performance Margin	+4.4 db	+6.2 db -3.9 db	--
	SYNC CHANNEL			
31	Modulation Loss			
32	Receiver Sync Subcarrier Power			
33	Sync APC Noise BW($2B_{LO}$ =			
34	Threshold SNR in $2B_{LO}$			
35	Threshold Subcarrier Power			
36	Performance Margin			

COMMENTS:

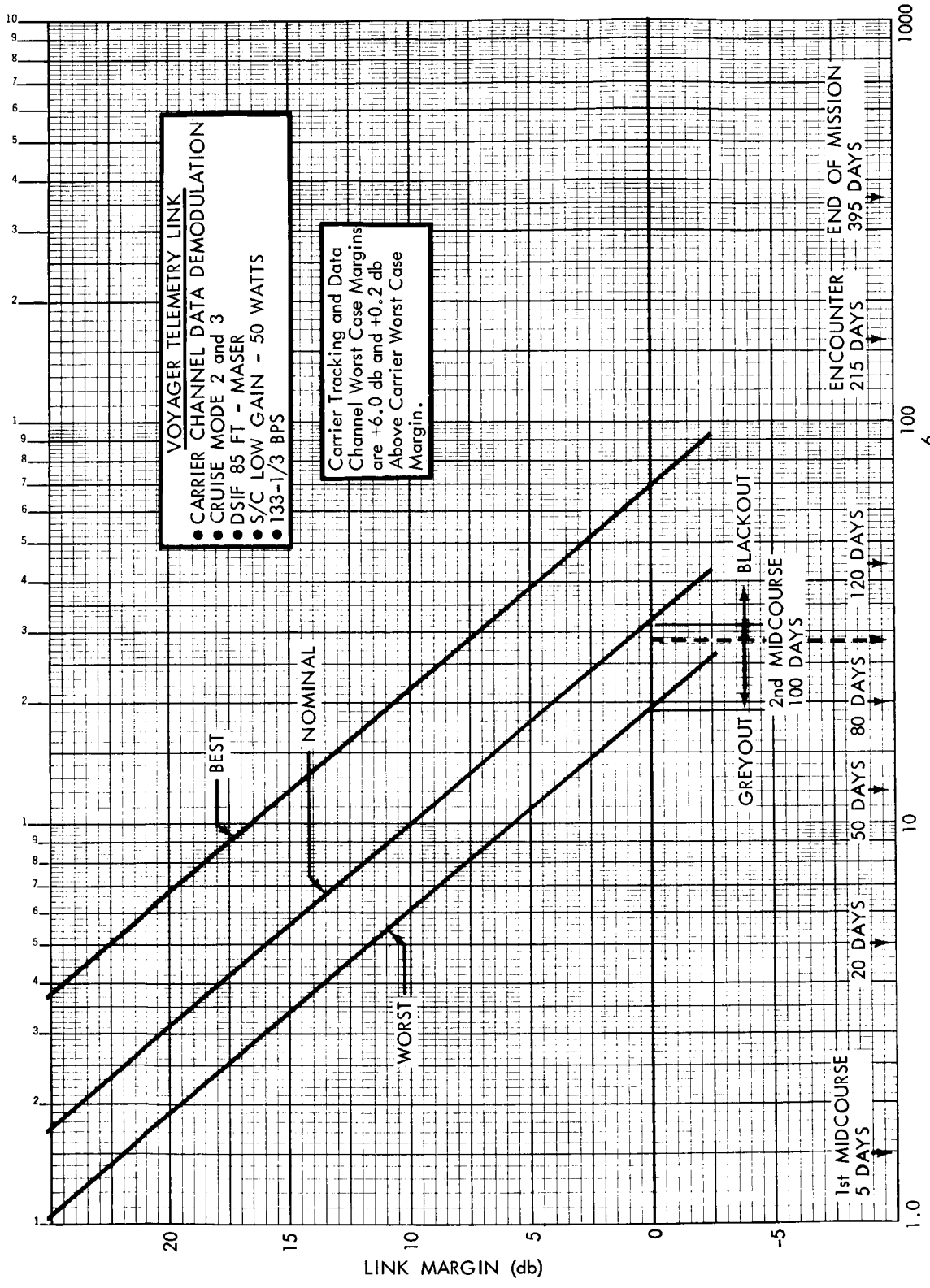

Figure 4.1.4-23:

Mode 2 or 3 Cruise--Spacecraft: High-Gain, 50-watt; DSIF: 85-foot, Maser

After 80 days, the telemetry data Mode 2 is switched to the high-gain antenna working with the 85-foot ground antenna. Design Control Table 4.1.4-18 evaluates the performance of this link configuration. The table input parameters are the same as the previous chart, except that the high-gain antenna parameters are substituted for the low-gain antenna parameters. Scaling was performed from the table parameters to two other cases. One scaling was made to show the performance at encounter after switchover to the 210-foot net. The second scaling was made to establish the Mode 2 performance during encounter maneuvers using the high-gain spacecraft antenna (-6 db maneuver pointing loss) and the 210-foot ground antenna.

System Performance Figure 4.1.4-24 shows Mode 2 operation with 85-foot antennas to provide a worst case margin of +14 db and +7 db at encounter and end of mission, respectively. Switchover to the 210-foot antennas would provide corresponding margins under maneuvering conditions of +19 db and +12 db.

TELECOMMUNICATION DESIGN CONTROL TABLE 4.1.4-18

PROJECT: VOYAGER DATE

CHANNEL: SPACECRAFT-EARTH TELEMETRY LINK MODES 2 or 3 PAGE 1

MODE: CRUISE: S/C HIGH GAIN - 50 WATTS, DSIF 85 FT. - MASER

NO.	PARAMETER	VALUE	TOLERANCE	SOURCE
1	Total Transmitter Power	+ 47.0 dbm	+2.0, -0.0 db	SECTION 4.1.4.1
2	Transmitting Circuit Loss	- 2.7 db	+0.4, -1.0 db	FIGURE 4.1.4-1
3	Transmitting Antenna Gain	+ 34.3 db	+1.1, -0.0 db	SECTION 4.1.4.1
4	Transmitting Antenna Pointing Loss	- 0.5 db	+0.5, -0.5 db	SECTION 4.1.4.1
5	Space Loss @ 2295 Mc, $R = 1.60 \times 10^8$ km	-263.7 db	- - -	- - -
6	Polarization Loss	0.0 db	+0.0, -0.1 db	TABLE 4.1.4-5
7	Receiving Antenna Gain	+ 53.0 db	+1.0, -0.5 db	TABLE 4.1.4-2
8	Receiving Antenna Pointing Loss	0.0 db	+0.0, -0.1 db	TABLE 4.1.4-2
9	Receiving Circuit Loss	- 0.2 db	+0.1, -0.0 db	TABLE 4.1.4-2
10	Net Circuit Loss	-179.8 db	+3.1, -2.2 db	- - -
11	Total Received Power	-132.8 dbm	+5.1, -2.2 db	- - -
12	Receiver Noise Spectral Density (N/B) $T_{System} = 45^{+10}_{-5}\ ^{o}K$	-182.1 dbm	+0.9, -0.5 db	TABLE 4.1.4-2
13	Carrier Modulation Loss	- 4.9 db	+1.0, -1.3 db	FIGURE 4.1.4-3
14	Received Carrier Power	-137.7 dbm	+6.1, -3.5 db	- - -
15	Carrier APC Noise BW ($2B_{LO} = 12.0$ cps)	+ 10.8 db	+0.0, -0.5 db	FIGURE 4.1.4-3
	CARRIER PERFORMANCE -- TRACKING (One-Way)			
16	Threshold SNR in $2B_{LO}$	+ 9.0 db	- -	FIGURE 4.1.4-3
17	Threshold Carrier Power	-162.3 dbm	+0.9, -1.0 db	- - -
18	Performance Margin	+ 24.6 db	+7.1, -4.4 db	- - -
	CARRIER PERFORMANCE -- TRACKING (Two-Way)			
19	Threshold SNR in $2B_{LO}$	+ 9.0 db	- - -	FIGURE 4.1.4-3
20	Threshold Carrier Power	-162.3 dbm	+0.9, -1.0 db	- - -
21	Performance Margin	+ 24.6 db	+7.1, -4.4 db	- - -

TELECOMMUNICATION DESIGN CONTROL TABLE 4.1.4-18

PROJECT: VOYAGER DATE
CHANNEL: SPACECRAFT--EARTH TELEMETRY LINK MODES 2 or 3 PAGE 2 of 2
MODE: CRUISE; S/C HIGH GAIN - 50 WATTS, DSIF 85 ft. - MASER

NO.	PARAMETER	VALUE	TOLERANCE	SOURCE
	CARRIER PERFORMANCE - DATA			
22	Threshold SNR in $2B_{LO}$	+15.0 db	--	Figure 4.1.4-3
23	Threshold Carrier Power	-156.3 dbm	+0.9 db -1.0 db	--
24	Performance Margin	+18.6 db	+7.1 db -4.4 db	--
	DATA CHANNEL			
25	Modulation Loss	-2.4 db	+0.4 db -0.4 db	Figure 4.1.4-3
26	Received Data Subcarrier Power	-135.2 dbm	+5.5 db -2.6 db	--
27	Bit Rate (1/T) 133-1/3 bits/sec.	+21.3 db	--	--
28	Required ST/N/B	+7.2 db	+0.5 db -0.5 db	Figure 4.1.4-3
29	Threshold Subcarrier Power	-153.6 dbm	+1.4 db -1.0 db	--
30	Performance Margin	+18.4 db	+6.5 db -4.0 db	--
	SYNC CHANNEL			
31	Modulation Loss			
32	Receiver Sync Subcarrier Power			
33	Sync APC Noise BW($2B_{LO}$ =			
34	Threshold SNR in $2B_{LO}$			
35	Threshold Subcarrier Power			
36	Performance Margin			

COMMENTS:

1) For DSIF 210 ft. antenna, all performance margins are increased by adding +9.0 db for nominal values, +1.0 db for maximum tolerance and +0.9 db for minimum tolerance.

2) For maneuvers at or near encounter using the DSIF 210 ft. antenna, all performance margins are increased by adding +4.0 db for nominal values, +1.0 db for maximum tolerances and +0.9 db for minimum tolerance assuming a high gain pointing loss of -6 db (worst case).

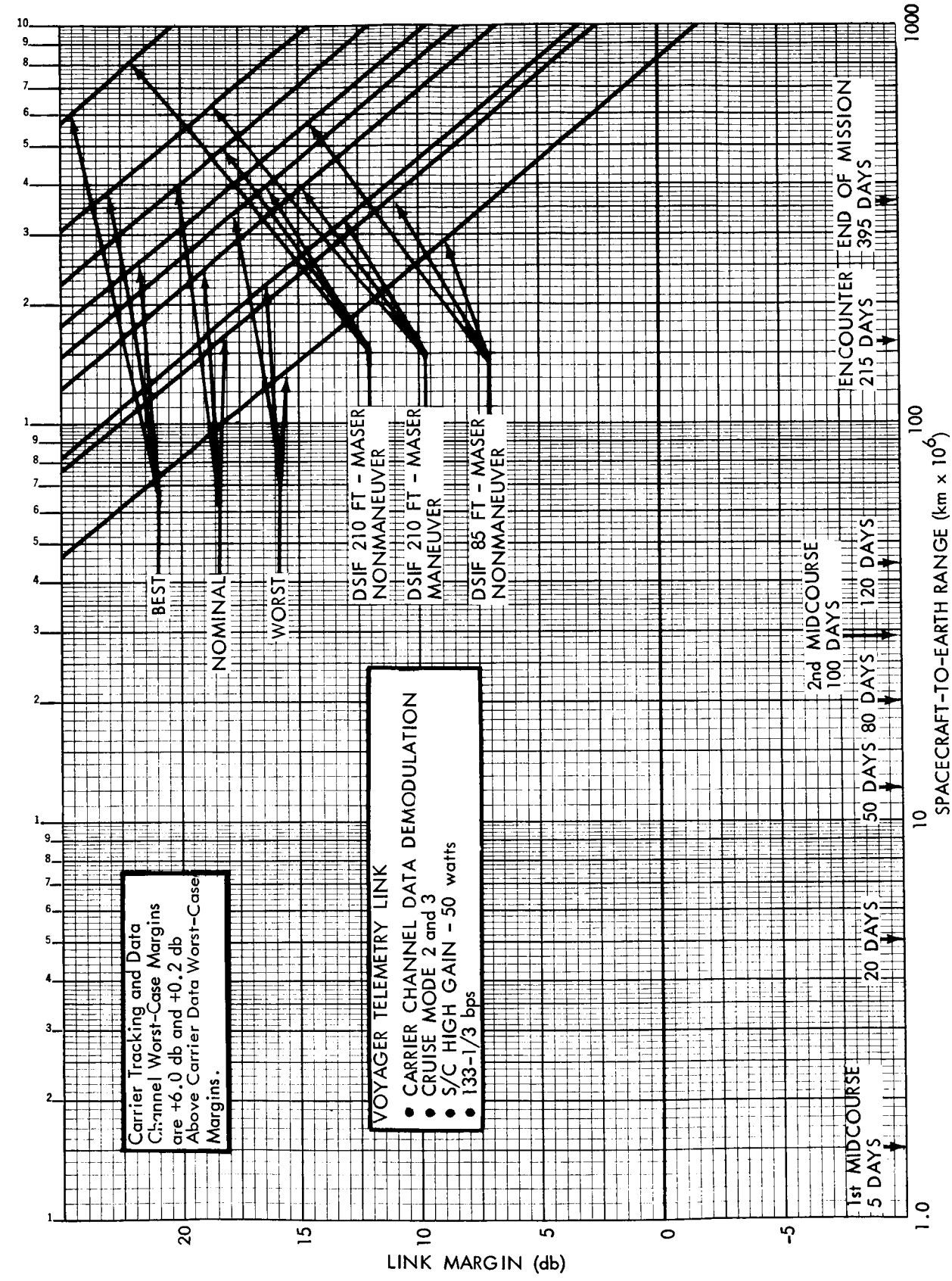

Figure 4.1.4-24:

Mode 4 All Phases--Spacecraft: Low-Gain, 50-watt; DSIF: 210-foot, Maser

Mode 4 has been incorporated as an emergency mode to provide capability to transmit spacecraft engineering data via the low-gain antenna at ranges beyond Mode 1 - low-gain greyout. An example of the use of Mode 4 would be a case of high-gain antenna mispointing. The antenna position would be reported as engineering data in Mode 4 over the low-gain antenna. Ground computations would determine the correct high-gain position and send the appropriate commands to step the antenna into position. Design Control Table 4.1.4-19 evaluates the Mode 4 link performance. To establish maximum capability the ground tracking bandwidth, 2 B_{LO}, has been chosen as 5 cps consistent with EPD 283. The carrier channel is the limiting-range case, and to extend its performance the required threshold signal-to-noise ratio for data demodulation has been reduced from 9 db to 6 db. The increased carrier noise degradation resulting in the data channel has been evaluated along with the reduced data rate (5-5/9 bps) and bit error rate achieved in establishing the required $\frac{ST}{N/B}$ as detailed earlier in this section.

System Performance Figure 4.1.4-25 for Mode 4 indicates that the link enters gr yout one month beyond encounter and enters blackout three and one-half months beyond encounter.

TELECOMMUNICATION DESIGN CONTROL TABLE 4.1.4-19

PROJECT: VOYAGER DATE

CHANNEL: SPACECRAFT - EARTH TELEMETRY LINK MODE 4 PAGE 1

MODE: EMERGENCY (ALL MISSION PHASES): S/C LOW GAIN - 50 WATTS, DSIF 210 FT - MASER

NO.	PARAMETER	VALUE	TOLERANCE	SOURCE
1	Total Transmitter Power	+ 47.0 dbm	+2.0, -0.0 db	SECTION 4.1.4.1
2	Transmitting Circuit Loss	- 2.6 db	+0.5, -1.3 db	FIGURE 4.1.4-1
3	Transmitting Antenna Gain	+ 1.0 db	+1.0, -0.0 db	SECTION 4.1.4.1
4	Transmitting Antenna Pointing Loss	+ 0.0 db	+0.0, -0.0 db	SECTION 4.1.4.1
5	Space Loss @ 2295 ± 5 Mc , R = 1.19×10^8 km	-261.2 db	- -	
6	Polarization Loss	0.0 db	+0.1, -0.1 db	TABLE 4.1.4-5
7	Receiving Antenna Gain	+ 61.0 db	+1.0, -0.5 db	TABLE 4.1.4-2
8	Receiving Antenna Pointing Loss	- 0.1 db	+0.1, -0.1 db	TABLE 4.1.4-2
9	Receiving Circuit Loss	- 0.2 db	+0.1, -0.0 db	TABLE 4.1.4-2
10	Net Circuit Loss	-202.1 db	+2.8, -2.0 db	
11	Total Received Power	-155.1 dbm	+4.8, -2.0 db	
12	Receiver Noise Spectral Density (N/B) T System $35^{+0.0}_{-10.0}{}^{\circ}K$	-183.1 dbm	+0.0, -1.5 db	TABLE 4.1.4-2
13	Carrier Modulation Loss	- 6.5 db	+1.4, -1.5 db	FIGURE 4.1.4-3
14	Received Carrier Power	-161.6 dbm	+6.2, - 3.5 db	
15	Carrier APC Noise BW ($2B_{LO}$= 5 cps)	+ 7.0 db	+0.0, -0.5 db	FIGURE 4.1.4-3
	CARRIER PERFORMANCE — TRACKING (One-Way)			
16	Threshold SNR in $2B_{LO}$	+ 9.0 db	- - -	FIGURE 4.1.4-3
17	Threshold Carrier Power	-167.1 dbm	+0.0, -2.0 db	
18	Performance Margin	+ 5.5 db	+8.2, -3.5 db	
	CARRIER PERFORMANCE — TRACKING (Two-Way)			
19	Threshold SNR in $2B_{LO}$	+ 9.0 db	- - -	FIGURE 4.1.4-3
20	Threshold Carrier Power	-167.1 dbm	+0.0, -2.0 db	
21	Performance Margin	+ 5.5 db	+8.2, -3.5 db	

Mode 5a Orbital--Spacecraft: High-Gain, 50-watt; DSIF: 210-foot, Maser

Mode 5a is the initial orbital planetary data playback mode. Mode 5a operation will be initiated at capsule impact because Mode 2 does not offer a high data rate channel for expected increase in capsule data rate after impact. Design Control Table 4.1.4-20 evaluates Mode 5a performance. In this mode the telemetry (lower) channel data rate is 400 hps and the planetary (upper) channel data rate is 8000 bps.

Two System Performance graphs (Figures 4.1.4-26 and 4.1.4-27) show the performance of the telemetry data and planetary data channels, respectively. At encounter, the planetary channel has a worst-case margin of +8 db and does not enter greyout until after the end of mission. The telemetry data channel has an encounter worst-case margin of +6.5 db and enters greyout 4.5 months into the orbital phase. Further optimization of the power allocations between the channels will allow simultaneous thresholding of the channels at about 6 months into the orbital phase.

While the insertion burn occurs, the telemetry link will continue to operate in Mode 5a through the high-gain antenna with an additional 5 db loss caused by antenna pointing errors.

The previous analysis under "Receiver Threshold Loop Noise Bandwidths" showed it will be necessary for the DSIF ground station to utilize either a $2B_{LO}$ of 48 cps or 152 cps to accommodate the anticipated Doppler effects during burn.

TELECOMMUNICATION DESIGN CONTROL TABLE 4.1.4-20

PROJECT: VOYAGER DATE

CHANNEL: SPACECRAFT - EARTH TELEMETRY LINK MODE 5A PAGE 1

MODE: ORBITAL: S/C HIGH GAIN - 50 WATTS, DSIF 210 FT. - MASER

NO.	PARAMETER	VALUE	TOLERANCE	SOURCE
1	Total Transmitter Power	+ 47.0 dbm	+2.0, -0.0 db	SECTION 4.1.4.1
2	Transmitting Circuit Loss	- 2.7 db	+0.4, -1.0 db	FIGURE 4.1.4-1
3	Transmitting Antenna Gain	+ 34.3 db	+1.1, - 0.0 db	SECTION 4.1.4.1
4	Transmitting Antenna Pointing Loss	- 0.5 db	+0.5, -0.5 db	SECTION 4.1.4.1
5	Space Loss @ 2295 Mc, R = 1.60×10^8 km	-263.7 db		--
6	Polarization Loss	0.0 db	+0.0, -0.1 db	TABLE 4.1.4-5
7	Receiving Antenna Gain	+ 61.0 db	+1.0, -0.5 db	TABLE 4.1.4-2
8	Receiving Antenna Pointing Loss	- 0.1 db	+0.1, -0.1 db	TABLE 4.1.4-2
9	Receiving Circuit Loss	- 0.2 db	+0.1, -0.0 db	TABLE 4.1.4-2
10	Net Circuit Loss	-171.9 db	+3.2, -2.2 db	--
11	Total Received Power	-124.9 dbm	+5.2, -2.2 db	--
12	Receiver Noise Spectral Density (N/B)	-183.2 dbm	+0.0, - 1.4 db	TABLE 4.1.4-2
	T System = 35^{+0}_{-10} °K			
13	Carrier Modulation Loss	- 6.0 db	+1.2, - 1.5 db	FIGURE 4.1.4-3
14	Received Carrier Power	-130.9 dbm	+6.4, -3.7 db	--
15	Carrier APC Noise BW ($2B_{LO}$=12.0cps)	+ 10.8 db	+0.0, -0.5 db	FIGURE 4.1.4-3
	CARRIER PERFORMANCE — TRACKING (One-Way)			
16	Threshold SNR in $2B_{LO}$	+ 9.0 db		FIGURE 4.1.4-3
17	Threshold Carrier Power	-163.4 dbm	+0.0, -1.9 db	--
18	Performance Margin	+ 32.5 db	+8.3, -3.7 db	--
	CARRIER PERFORMANCE — TRACKING (Two-Way)			
19	Threshold SNR in $2B_{LO}$	+ 9.0 db	- -	FIGURE 4.1.4-3
20	Threshold Carrier Power	-163.4 dbm	+0.0, - 1.9 db	--
21	Performance Margin	+ 32.5 db	+8.3, -3.7 db	--

TELECOMMUNICATION DESIGN CONTROL TABLE 4.1.4-20

PROJECT: VOYAGER DATE

CHANNEL: SPACECRAFT--EARTH TELEMETRY LINK MODE 5A PAGE 2 of

MODE: ORBITAL: S/C HIGH GAIN - 50 WATTS, DSIF 210 FT. - MASER

NO.	PARAMETER	VALUE	TOLERANCE	SOURCE
	CARRIER PERFORMANCE DATA			
22	Threshold SNR in $2B_{LO}$	+15.0 db	--	Figure 4.1.4-3
23	Threshold Carrier Power	-157.4 dbm	+0.0 db -1.9 db	--
24	Performance Margin	+26.5 db	+8.3 db -3.7 db	--
	DATA CHANNEL -- PLANETARY DATA			
25	Modulation Loss	-2.9 db	+0.5 db -0.6 db	Figure 4.1.4-3
26	Received Data Subcarrier Power	-127.8 dbm	+5.7 db -2.8 db	--
27	Bit Rate (1/T) 8000 bits/sec	+39.0 db	--	--
28	Required ST/N/B	+5.0 db	+0.5 db -0.5 db	Figure 4.1.4-3
29	Threshold Subcarrier Power	-139.2 dbm	+0.5 db -1.9 db	--
30	Performance Margin	+11.4 db	+7.6 db -3.3 db	--
	DATA CHANNEL -- TELEMETRY DATA			
31	Modulation Loss	-13.7 db	+1.9 db -2.3 db	Figure 4.1.4-3
32	Received Data Subcarrier Power	-138.6 dbm	+7.1 db -4.5 db	--
33	Bit Rate (1/T) 400 bits/sec	+26.0 db	--	--
34	Required ST/N/B	+7.2 db	+0.5 db -0.5 db	Figure 4.1.4-3
35	Threshold Subcarrier Power	-150.0 dbm	+0.5 db -1.9 db	--
36	Performance Margin	+11.4 db	+9.0 db -5.0 db	--

COMMENTS:

1) During insertion burn, antenna pointing losses and wider carrier tracking loop bandwidth reduce all performance margins by 5 db in data channels and 16 db in carrier channel.

2) For post-insertion playback, all nominal performance margins are reduced by 5 db due to higher pointing loss for spacecraft high-gain antenna. This degradation still gives performance above "grey-out" level.

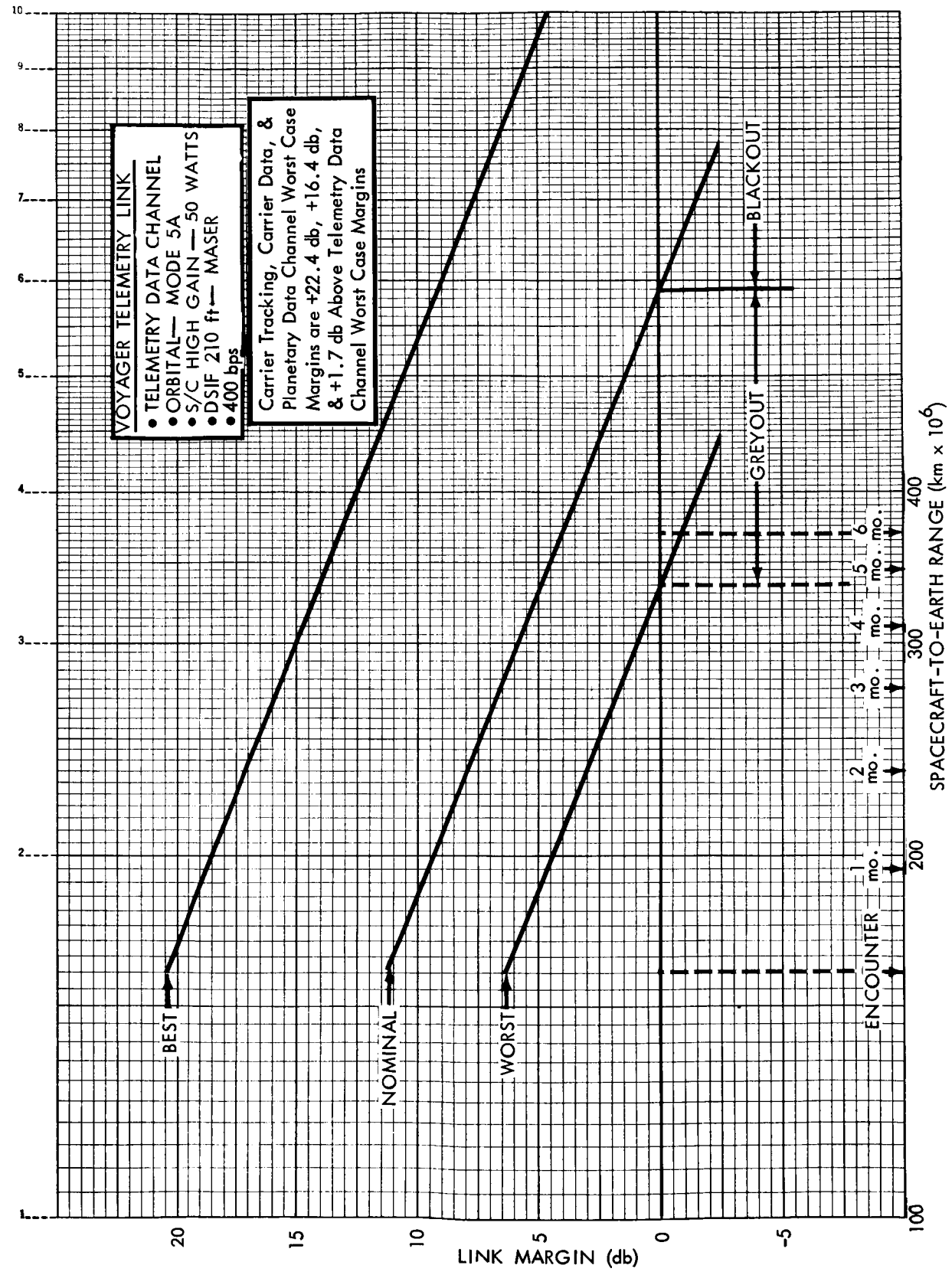

Figure 4.1.4-26:

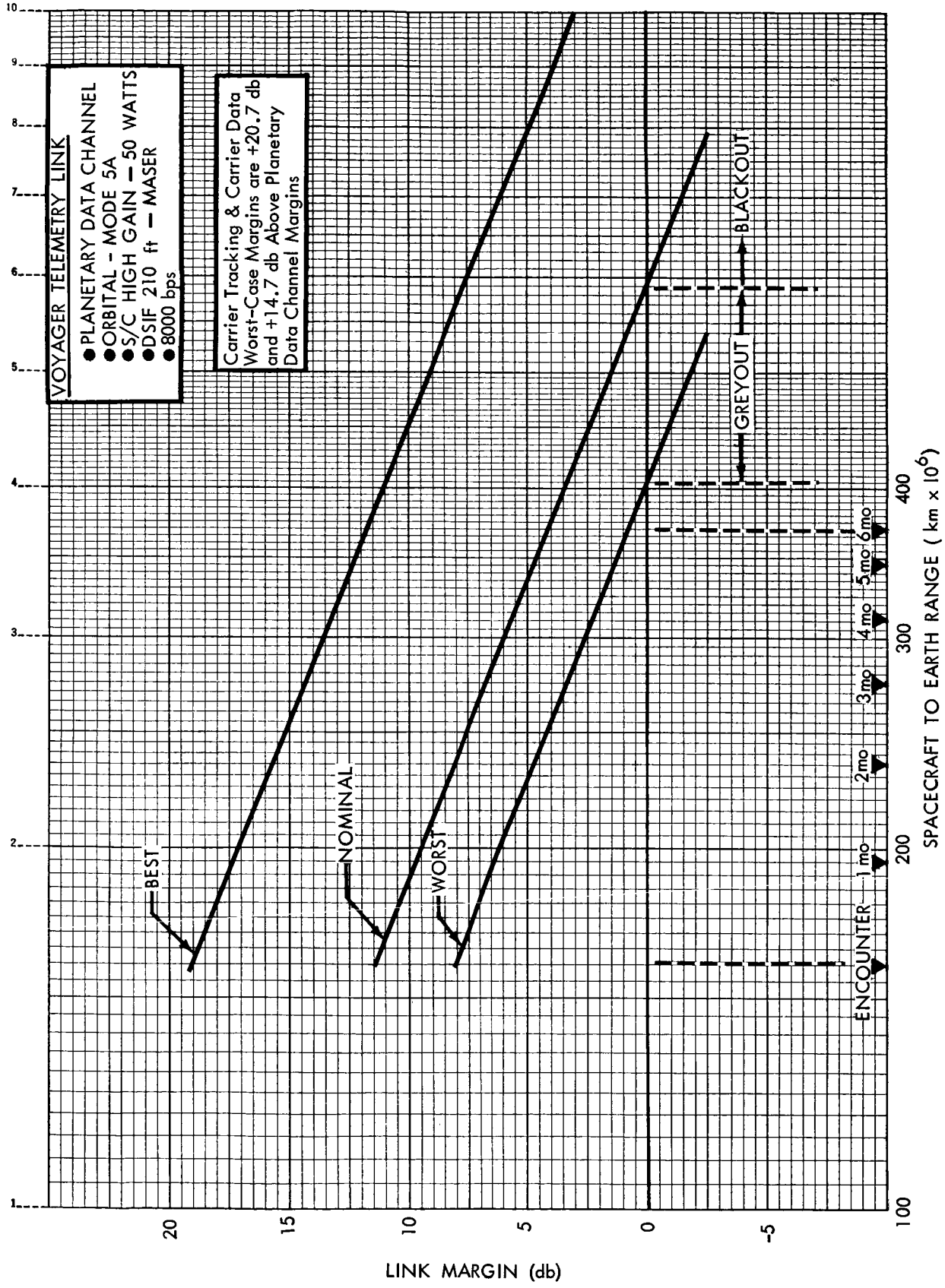

Figure 4.1.4-27:

Design Control Table 4.1.4-20 can be scaled to determine the link performance during the burn period by reducing each data channel nominal margin by 5 db due to pointing loss, and the carrier channel nominal margin by 16 db (5 for pointing loss and 11 for the 152 cps $2B_{LO}$). This scaling applied to system performance (Figures 4.1.4-26 and -27) shows that during burn the telemetry data channel has a worst-case margin of +1.5 db, while the planetary data channel margin is +3.1 db. The corresponding margin in the carrier tracking channel scaled from Table 4.1.4-20 is +12.8 db.

Mode 6 Orbital (Real Time)--Spacecraft: High-Gain, 50-watt; DSIF: 210-foot, Maser

Mode 6 is implemented to allow real-time transmission of planetary science data during the early orbital period. The telemetry (lower) subcarrier has 400 bps of engineering, cruise science, and relayed capsule data. The planetary (upper) subcarrier has 48,000 bps of real-time planetary science data.

Design Control Table 4.1.4-21 evaluates the link performance based on the input parameters derived as indicated in the source column. Figure 4.1.4-28 shows that the planetary channel has a worst-case margin at encounter of +0.5 db. Thus, real time planetary data transmission is possible for the first 10 days after encounter before entering greyout. It is also possible under nominal conditions to maintain the real-time link for 73 days before blackout. The telemetry channel performance is much better, and as shown in the system performance graph, Figure 4.1.4-29, will have a worst-case margin of +4.5 db at encounter and will not enter greyout until 2.5 months after encounter.

An additional system performance chart (Figure 4.1.4-30) is presented to show the combined performance and sequential switchover of Mode 6 and Mode 5a. This figure shows both switchover from Mode 6 and to Mode 5a on worst-case conditions (10 days) and the switchover on nominal conditions (73 days).

TELECOMMUNICATION DESIGN CONTROL TABLE 4.1.4-21

PROJECT: VOYAGER DATE

CHANNEL: SPACECRAFT - EARTH TELEMETRY LINK MODE 6 PAGE 1

MODE: EARLY ORBIT: S/C HIGH GAIN - 50 WATTS, DSIF 210 FT. - MASER

NO.	PARAMETER	VALUE	TOLERANCE	SOURCE
1	Total Transmitter Power	+ 47.0 dbm	+2.0, -0.0 db	SECTION 4.1.4.1
2	Transmitting Circuit Loss	- 2.7 db	+0.4, -1.0 db	FIGURE 4.1.4-1
3	Transmitting Antenna Gain	+ 34.3 db	+1.1, -0.0 db	SECTION 4.1.4.1
4	Transmitting Antenna Pointing Loss	- 0.5 db	+0.5, -0.5 db	SECTION 4.1.4.1
5	Space Loss	-263.7 db		--
6	@2295 Mc, R =1.60x10^8km Polarization Loss	0.0 db	+0.0, -0.1 db	TABLE 4.1.4-5
7	Receiving Antenna Gain	+ 61.0 db	+1.0, -0.5 db	TABLE 4.1.4-2
8	Receiving Antenna Pointing Loss	- 0.1 db	+0.1, -0.1 db	TABLE 4.1.4-2
9	Receiving Circuit Loss	- 0.2 db	+0.1, -0.0db	TABLE 4.1.4-2
10	Net Circuit Loss	-171.9 db	+3.2, -2.2 db	--
11	Total Received Power	-124.9 dbm	+5.2, -2.2 db	--
12	Receiver Noise Spectral Density (N/B) T System = 35 $^{+U}_{-10}$ ^{o}K	-183.2 dbm	+0.0, - 1.4 db	TABLE 4.1.4-2
13	Carrier Modulation Loss	- 6.4 db	+1.4, -1.9 db	FIGURE 4.1.4-3
14	Received Carrier Power	-131.3 dbm	+6.6, -4.1 db	--
15	Carrier APC Noise BW ($2B_{LO}$=12.0 cps)	+ 10.8 db	+0.0, -0.5 db	FIGURE 4.1.4-3
	CARRIER PERFORMANCE — TRACKING (One-Way)			
16	Threshold SNR in $2B_{LO}$	+ 9.0 db	- - -	FIGURE 4.1.4-3
17	Threshold Carrier Power	-163.4 dbm	+0.0, -1.9 db	--
18	Performance Margin	+ 32.1 db	+8.5, -4.1 db	--
	CARRIER PERFORMANCE — TRACKING (One-Way)			
19	Threshold SNR in $2B_{LO}$	+ 9.0 db	- -	FIGURE 4.1.4-3
20	Threshold Carrier Power	-163.4 dbm	+0.0, - 1.9 db	--
21	Performance Margin	+ 32.1 db	+8.5, -4.1 db	--

TELECOMMUNICATION DESIGN CONTROL TABLE 4.1.4-21

PROJECT: VOYAGER DATE
CHANNEL: SPACECRAFT--EARTH TELEMETRY LINK MODE 6 PAGE 2 of 2
MODE: EARLY ORBIT: S/C HIGH GAIN - 50 WATTS, DSIF 210 FT. - MASER

NO.	PARAMETER	VALUE	TOLERANCE	SOURCE
	CARRIER PERFORMANCE--DATA			
22	Threshold SNR in $2B_{LO}$	+15.0 db	--	Figure 4.1.4-3
23	Threshold Carrier Power	-157.4 dbm	+0.0 db -1.9 db	--
24	Performance Margin	+26.1 db	+8.5 db -4.1 db	--
	DATA CHANNEL—PLANETARY DATA			
25	Modulation Loss	-2.7 db	+0.5 db -0.6 db	Figure 4.1.4-3
26	Received Data Subcarrier Power	-127.6 dbm	+5.7 db -2.8 db	--
27	Bit Rate (1/T) 48,000 bits/sec	+46.8 db	--	--
28	Required ST/N/B	+5.0 db	+0.5 db -0.5 db	Figure 4.1.4-3
29	Threshold Subcarrier Power	-131.4 dbm	+0.5 db -1.9 db	--
30	Performance Margin	+3.8 db	+7.6 db -3.3 db	--
	DATA CHANNEL -- TELEMETRY DATA			
25	Modulation Loss	-15.2 db	+2.1 db -2.6 db	Figure 4.1.4-3
26	Received Data Subcarrier Power	-140.1 dbm	+7.3 db -4.8 db	--
27	Bit Rate (1/T) 400 bits/sec	+26.0 db	--	--
28	Required ST/N/B	+7.2 db	+0.5 db -0.5 db	Figure 4.1.4-3
29	Threshold Subcarrier Power	-150.0 dbm	+0.5 db -1.9 db	--
30	Performance Margin	+9.9 db	+9.2 db -5.3 db	--

COMMENTS:

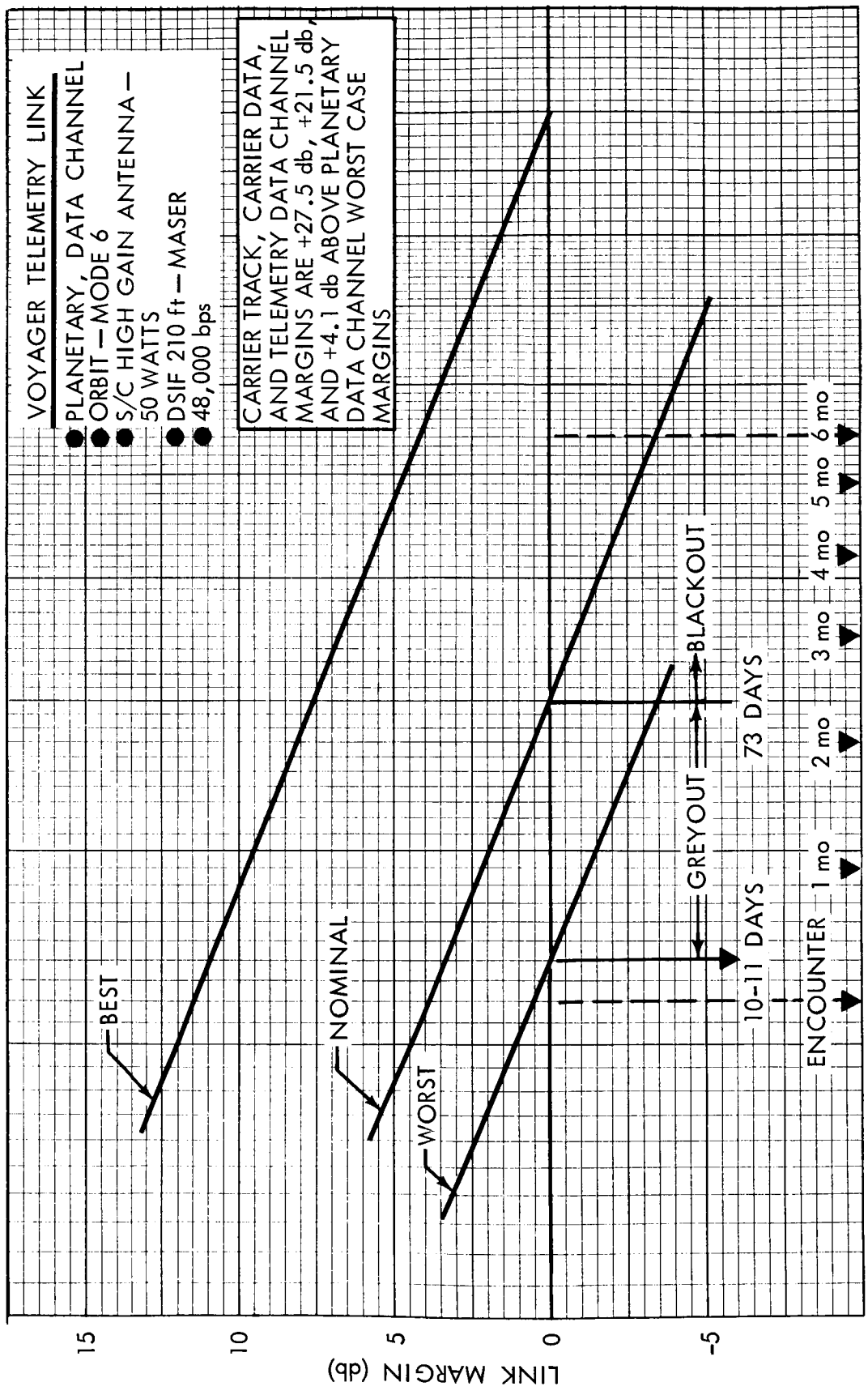

Figure 4.1.4-28:

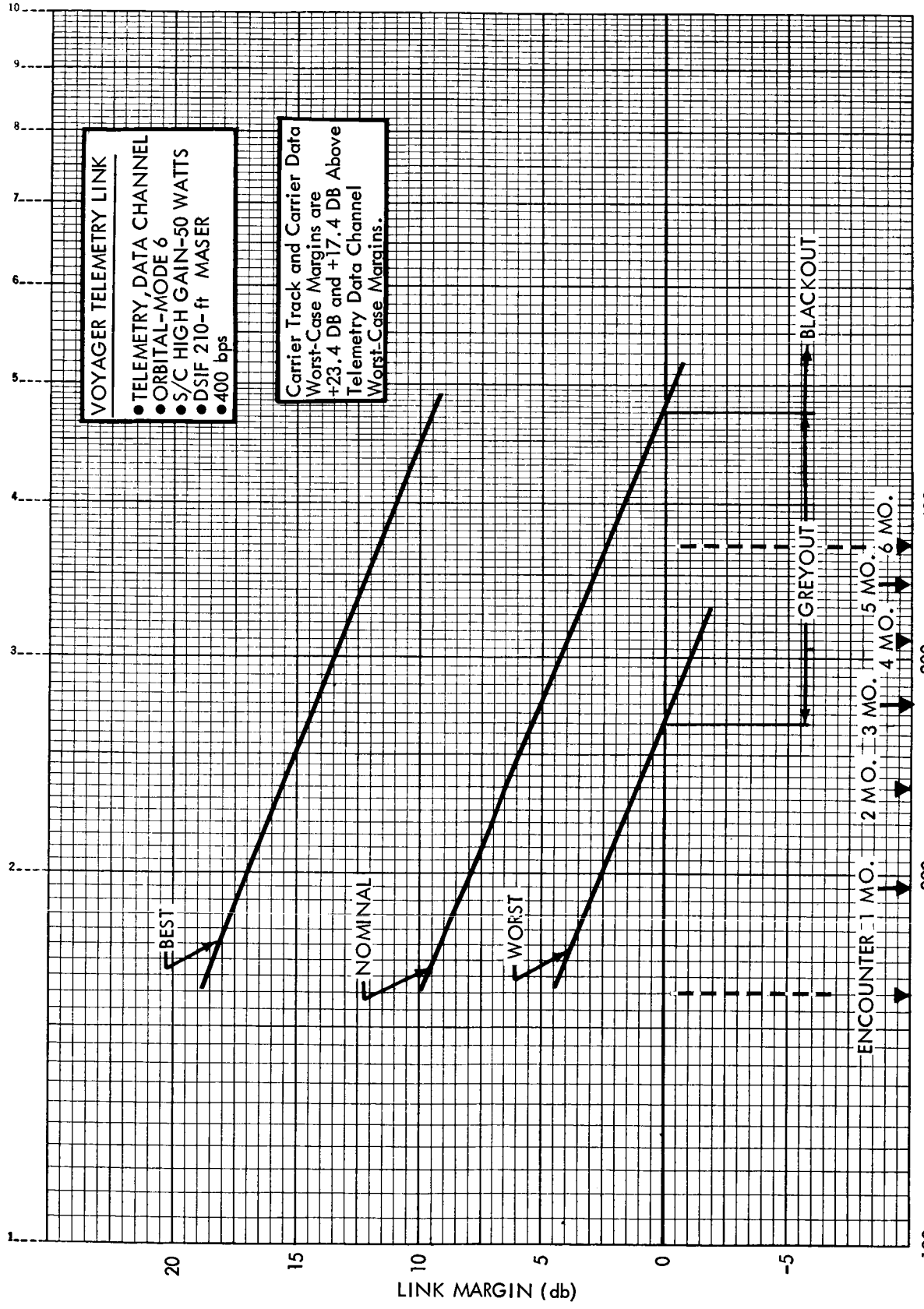

Figure 4.1.4 - 29:

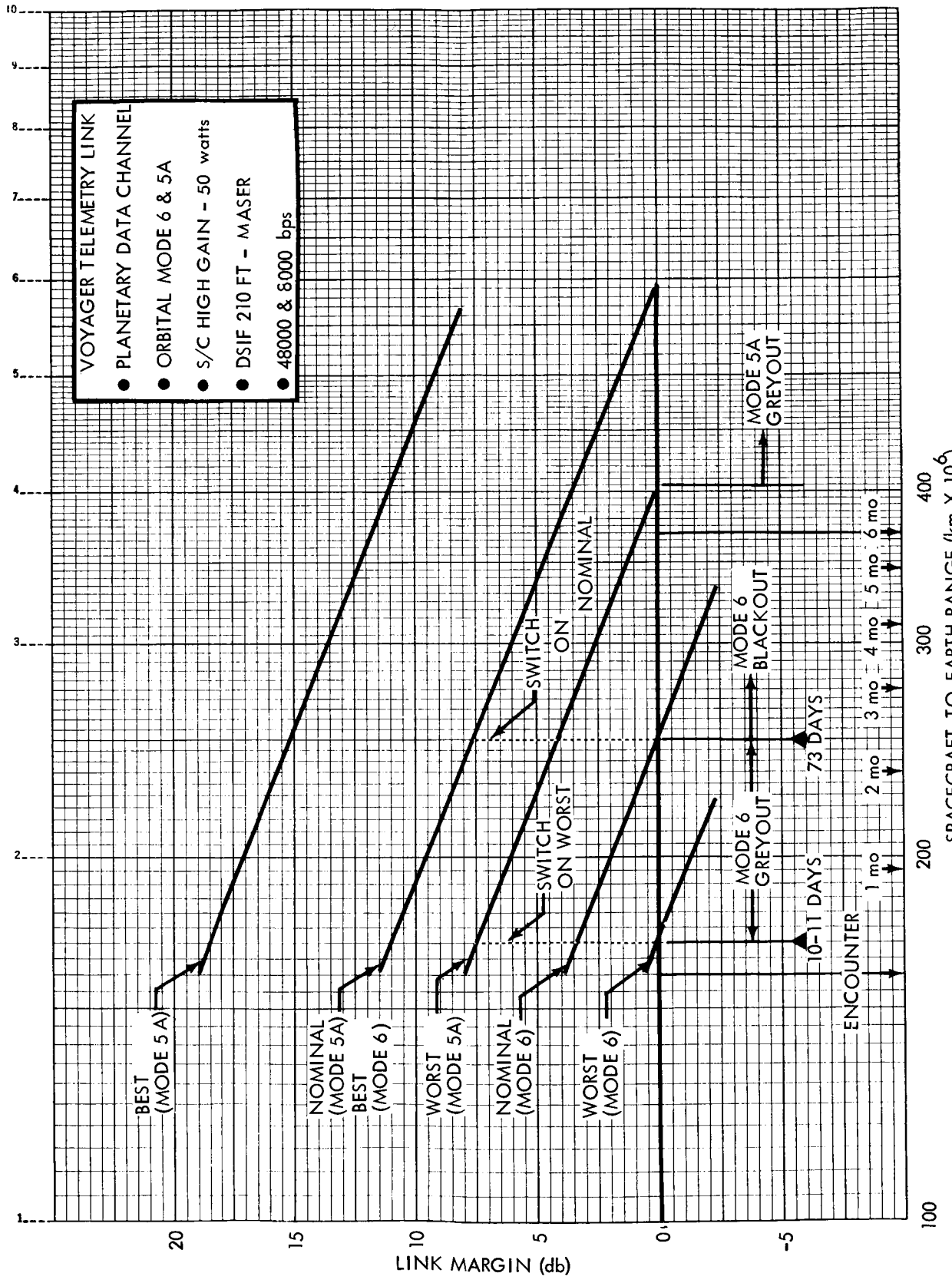

Figure 4.1.4-30:

Mode 5b Orbital--Spacecraft: High-Gain, 50-watt; DSIF: 210-foot, Maser

As the spacecraft reaches greyout range for Mode 5a, the telemetry mode is switched by command to Mode 5b. Table 4.1.4-22 is the design control table for Mode 5b. It was evaluated at a communication range of 2.5 x 10^8 km. The performance margin of the lower or telemetry channel as a function of distance is shown in Figure 4.1.4-31. Figure 4.1.4-32 shows the performance margin for the planetary data channel. This mode allows transmission of 4000 bps of planetary data to a greyout range of 4.6 x 10^8 km. This range is in excess of a 6-month orbit. The lower telemetry subcarrier remains the same as in Mode 5a.

TELECOMMUNICATION DESIGN CONTROL TABLE 4.1.4-22

PROJECT: VOYAGER DATE

CHANNEL: SPACECRAFT - EARTH TELEMETRY LINK MODE 5B PAGE 1

MODE: ORBITAL: S/C HIGH GAIN - 50 WATTS, DSIF 210 FT. - MASER

NO.	PARAMETER	VALUE	TOLERANCE	SOURCE
1	Total Transmitter Power	+ 47.0 dbm	+2.0, - 0.0 db	SECTION 4.1.4.1
2	Transmitting Circuit Loss	- 2.7 db	+0.4, - 1.0 db	FIGURE 4.1.4-1
3	Transmitting Antenna Gain	+ 34.3 db	+1.1, - 0.0 db	SECTION 4.1.4.1
4	Transmitting Antenna Pointing Loss	- 0.5 db	+0.5, - 0.5 db	SECTION 4.1.4.1
5	Space Loss @ 2295 Mc, $R = 2.5 \times 10^8$ km	-267.7 db	-	-
6	Polarization Loss	0.0 db	+0.0, - 0.1 db	TABLE 4.1.4-5
7	Receiving Antenna Gain	+ 61.0 db	+1.0, - 0.5 db	TABLE 4.1.4-2
8	Receiving Antenna Pointing Loss	- 0.1 db	+0.1, - 0.1 db	TABLE 4.1.4-2
9	Receiving Circuit Loss	- 0.2 db	+0.1, - 0.0 db	TABLE 4.1.4-2
10	Net Circuit Loss	-175.9 db	+3.2, - 2.2 db	-
11	Total Received Power	-128.9 dbm	+5.2, - 2.2 db	-
12	Receiver Noise Spectral Density (N/B) $T_{System} = 35^{+0}_{-10}{}^{\circ}K$	-183.2 dbm	+0.0, - 1.4 db	TABLE 4.1.4-2
13	Carrier Modulation Loss	- 6.2 db	+1.3, - 1.5 db	FIGURE 4.1.4-3
14	Received Carrier Power	-135.1 dbm	+6.5, - 3.7 db	-
15	Carrier APC Noise BW ($2B_{LO}$ =12.0cps	+ 10.8 db	+0.0, - 0.5 db	FIGURE 4.1.4-3
	CARRIER PERFORMANCE — TRACKING (One-Way)			
16	Threshold SNR in $2B_{LO}$	+ 9.0 db	-	FIGURE 4.1.4-3
17	Threshold Carrier Power	-163.4 dbm	+0.0, - 1.9 db	-
18	Performance Margin	+ 28.3 db	+8.4, - 3.7 db	-
	CARRIER PERFORMANCE — TRACKING (Two-Way)			
19	Threshold SNR in $2B_{LO}$	+ 9.0 db	-	FIGURE 4.1.4-3
20	Threshold Carrier Power	-163.4 dbm	+0.0, - 1.9 db	-
21	Performance Margin	+ 28.3 db	+8.4, - 3.7 db	-

TELECOMMUNICATION DESIGN CONTROL TABLE 4.1.4-22

PROJECT: VOYAGER DATE
CHANNEL: SPACECRAFT--EARTH TELEMETRY LINK MODE 5B PAGE 2 of
MODE: ORBITAL: S/C HIGH GAIN - 50 WATTS, DSIF 210 FT. - MASER

NO.	PARAMETER	VALUE	TOLERANCE	SOURCE
	CARRIER PERFORMANCE -- DATA			
22	Threshold SNR in $2B_{LO}$	+15.0 db	--	Figure 4.1.4-3
23	Threshold Carrier Power	-157.4 dbm	+0.0 db -1.9 db	--
24	Performance Margin	+22.3 db	+8.4 db -3.7 db	--
	DATA CHANNEL-- PLANETARY DATA			
25	Modulation Loss	-3.6 db	+0.6 db -0.7 db	Figure 4.1.4-3
26	Received Data Subcarrier Power	-132.5 dbm	+5.8 db -2.9 db	--
27	Bit Rate (1/T) 4000 bits/sec	+36.0 db	--	--
28	Required ST/N/B	+5.0 db	+0.5 db -0.5 db	Figure 4.1.4-3
29	Threshold Subcarrier Power	-142.2 dbm	+0.5 db -1.9 db	--
30	Performance Margin	+9.7 db	+7.7 db -3.4 db	--
	DATA CHANNEL--TELEMETRY DATA			
31	Modulation Loss	-11.3 db	+1.8 db -1.9 db	Figure 4.1.4-3
32	Received Data Subcarrier Power	-140.2 dbm	+7.0 db -4.1 db	--
33	Bit Rate (1/T) 400 bits/sec	+26.0 db	--	--
34	Required ST/N/B	+7.2 db	+0.5 db -0.5 db	Figure 4.1.4-3
35	Threshold Subcarrier Power	-150.0 dbm	+0.5 db -1.9 db	--
36	Performance Margin	+9.8 db	+8.9 db -4.6 db	--

COMMENTS:

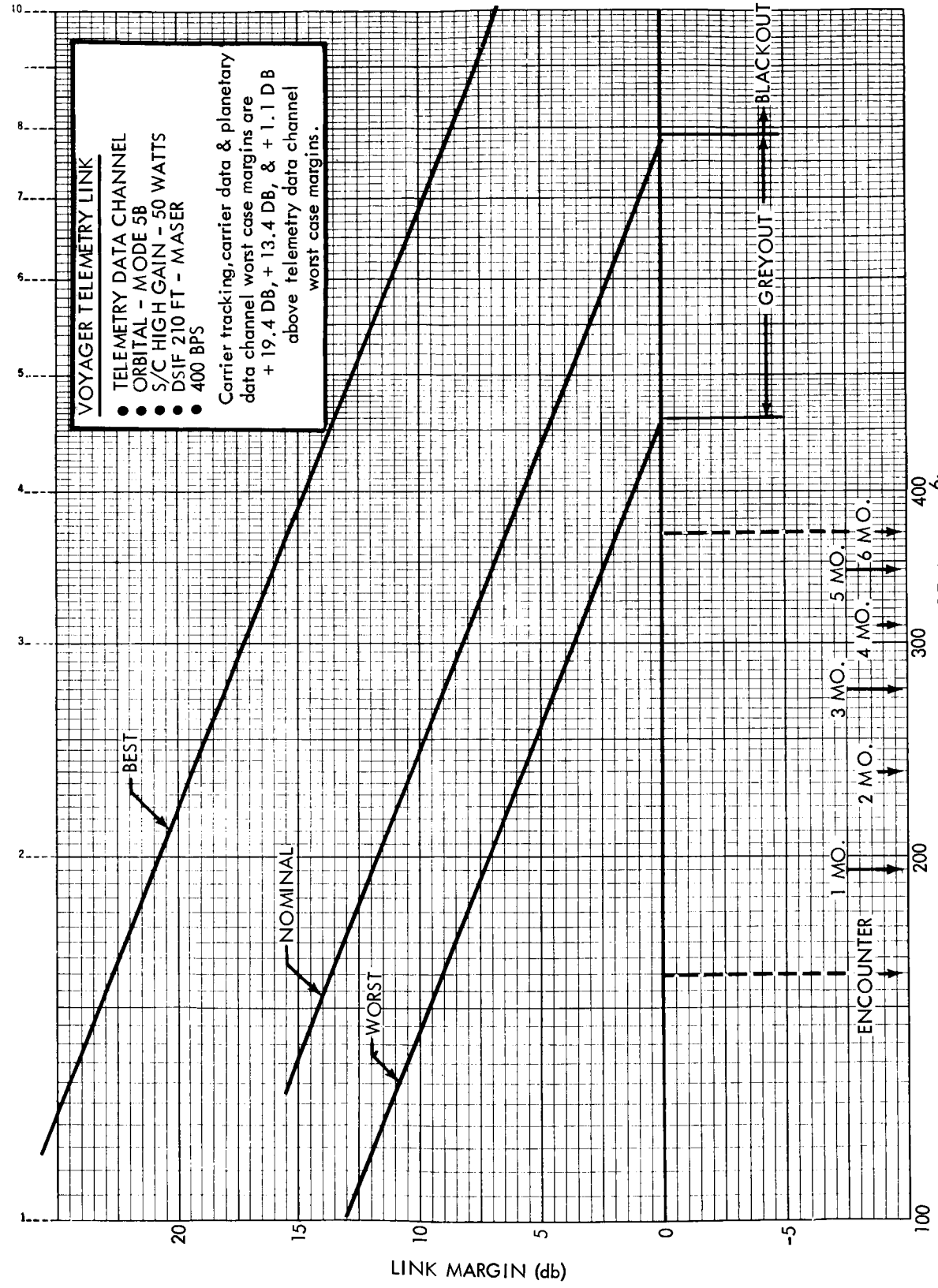

Figure 4.1.4-31:

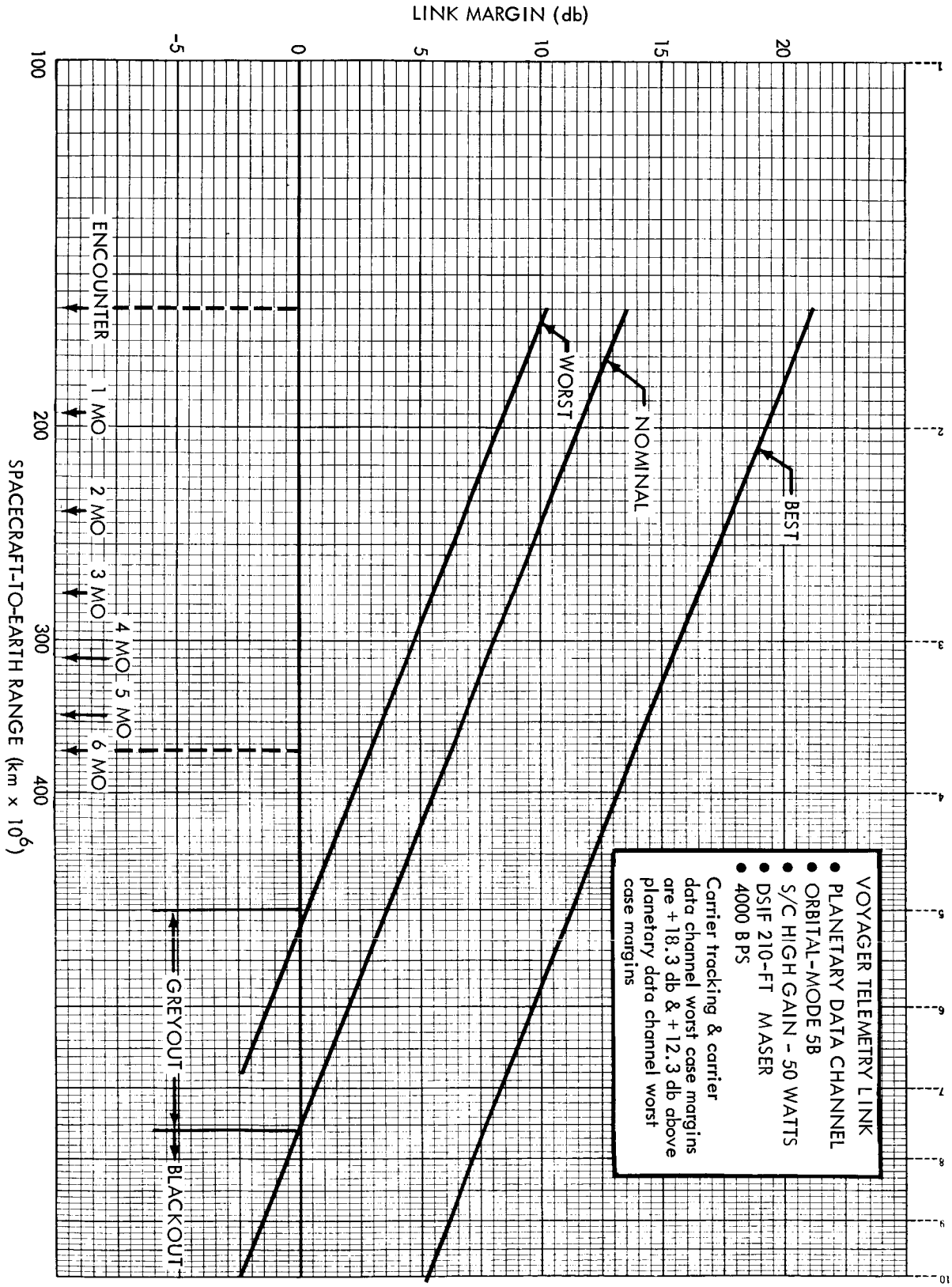

Figure 4.1.4-32:

Mode 5c Orbital--Spacecraft: High-Gain, 50-watt; DSIF: 210-foot, Maser

This data mode provides a capability for transmitting planetary data at 2000 bits per second. The planetary data is placed on one subcarrier, and the telemetry subcarrier carries the same data as before. Modulation indices and modulation losses for this mode have been described earlier.

The design control table for this link, Table 4.1.4-23, shows the performance margin at the end of the mission, 3.69×10^8 km, to be +8.5 db (with a positive tolerance of +8.7 db and a negative tolerance of -4.3 db) on the telemetry data channel and +8.6 db with tolerances of +7.8 db and -3.5 db on the planetary data channel. Performance-margin graphs for these channels are provided in Figures 4.1.4-33 and 4.1.4-34.

This mode can also provide planetary data readout capability with the 85-foot DSIF antenna for 28 days after encounter if the 210-foot antenna is unavailable for any reason. The performance with the 85-foot antenna is found by subtracting 9.0 db from the nominal value, 1.0 db from the positive tolerance, and 0.9 db from the negative tolerance computed in the design control table for this mode. At encounter the performance margin of the telemetry channel is +6.9 db with tolerances of +7.7 db and -5.2 db with the 85-foot receiving antenna.

TELECOMMUNICATION DESIGN CONTROL TABLE 4.1.4-23

PROJECT: VOYAGER DATE

CHANNEL: SPACECRAFT - EARTH TELEMETRY LINK MODE 5C PAGE 1

MODE: ORBITAL: S/C HIGH GAIN - 50 WATTS, DSIF 210 FT - MASER

NO.	PARAMETER	VALUE	TOLERANCE	SOURCE
1	Total Transmitter Power	+ 47.0 dbm	+2.0, -0.0 db	SECTION 4.1.4.1
2	Transmitting Circuit Loss	- 2.7 db	+0.4, -1.0 db	FIGURE 4.1.4-1
3	Transmitting Antenna Gain	+ 34.3 db	+1.1, -0.0 db	SECTION 4.1.4.1
4	Transmitting Antenna Pointing Loss	- 0.5 db	+0.5, -0.5 db	SECTION 4.1.4.1
5	Space Loss @ 2295 Mc, R =3.69×10^8km	-271.0 db	- -	--
6	Polarization Loss	0.0 db	+0.0, -0.1 db	TABLE 4.1.4-5
7	Receiving Antenna Gain	+ 61.0 db	+1.0 -0.5 db	TABLE 4.1.4-2
8	Receiving Antenna Pointing Loss	- 0.1 db	+0.1, -0.1 db	TABLE 4.1.4-2
9	Receiving Circuit Loss	- 0.2 db	+0.1, -0.0 db=	TABLE 4.1.4-2
10	Net Circuit Loss	-179.2 db	+3.2, -2.2 db	--
11	Total Received Power	-132.2 dbm	+5.2, -2.2 db	--
12	Receiver Noise Spectral Density (N/B) T System = 35^{+0}_{-10}°K	-183.2 dbm	+0.0, -1.4 db	TABLE 4.1.4-2
13	Carrier Modulation Loss	- 5.8 db	+1.2, -1.2 db	FIGURE 4.1.4-3
14	Received Carrier Power	-138.0 dbm	+6.4, -3.4 db	
15	Carrier APC Noise BW ($2B_{LO}$ =12cps	+ 10.8 db	+0.0, -0.5 db	FIGURE 4.1.4-3
	CARRIER PERFORMANCE — TRACKING	(One-Way)		
16	Threshold SNR in $2B_{LO}$	+ 9.0 db		FIGURE 4.1.4-3
17	Threshold Carrier Power	-163.4 dbm	+0.0, -1.9 db	--
18	Performance Margin	+ 25.4 db	+8.3, -3.4 db	--
	CARRIER PERFORMANCE — TRACKING	(Two-Way)		
19	Threshold SNR in $2B_{LO}$	+ 9.0 db		FIGURE 4.1.4-3
20	Threshold Carrier Power	-163.4 dbm	+0.0, -1.9 db	--
21	Performance Margin	+ 25.4 db	+8.3, -3.4 db	--

TELECOMMUNICATION DESIGN CONTROL TABLE 4.1.4-23

PROJECT: VOYAGER DATE
CHANNEL: SPACECRAFT--EARTH TELEMETRY LINK MODE 5C PAGE 2 of
MODE: ORBITAL: S/C HIGH GAIN - 50 WATTS, DSIF 210 FT. - MASER

NO.	PARAMETER	VALUE	TOLERANCE	SOURCE
	CARRIER PERFORMANCE -- DATA			
22	Threshold SNR in $2B_{LO}$	+15.0 db	--	Figure 4.1.4-3
23	Threshold Carrier Power	-157.4 dbm	+0.0 db -1.9 db	--
24	Performance Margin	+19.4 db	+8.3 db -3.4 db	--
	DATA CHANNEL--PLANETARY DATA			
25	Modulation Loss	-4.4 db	+0.7 db -0.8 db	Figure 4.1.4-3
26	Received Data Subcarrier Power	-136.6 dbm	+5.9 db -3.0 db	--
27	Bit Rate (1/T) 2000 bits/sec	+33.0 db	--	---
28	Required ST/N/B	+5.0 db	+0.5 db -0.5 db	Figure 4.1.4-3
29	Threshold Subcarrier Power	-145.2 dbm	+0.5 db -1.9 db	--
30	Performance Margin	+8.6 db	+7.8 db -3.5 db	--
	DATA CHANNEL-- TELEMETRY DATA			
31	Modulation Loss	-9.3 db	+1.6 db -1.6 db	Figure 4.1.4-3
32	Received Data Subcarrier Power	-141.5 dbm	+6.8 db -3.8 db	--
33	Bit Rate (1/T) 400 bits/sec	+26.0 db	--	--
34	Required ST/N/B	+7.2 db	+0.5 db -0.5 db	Figure 4.1.4-3
35	Threshold Subcarrier Power	+150.0 dbm	+0.5 db -1.9 db	--
36	Performance Margin	+8.5 db	+8.7 db -4.3 db	--

COMMENTS:

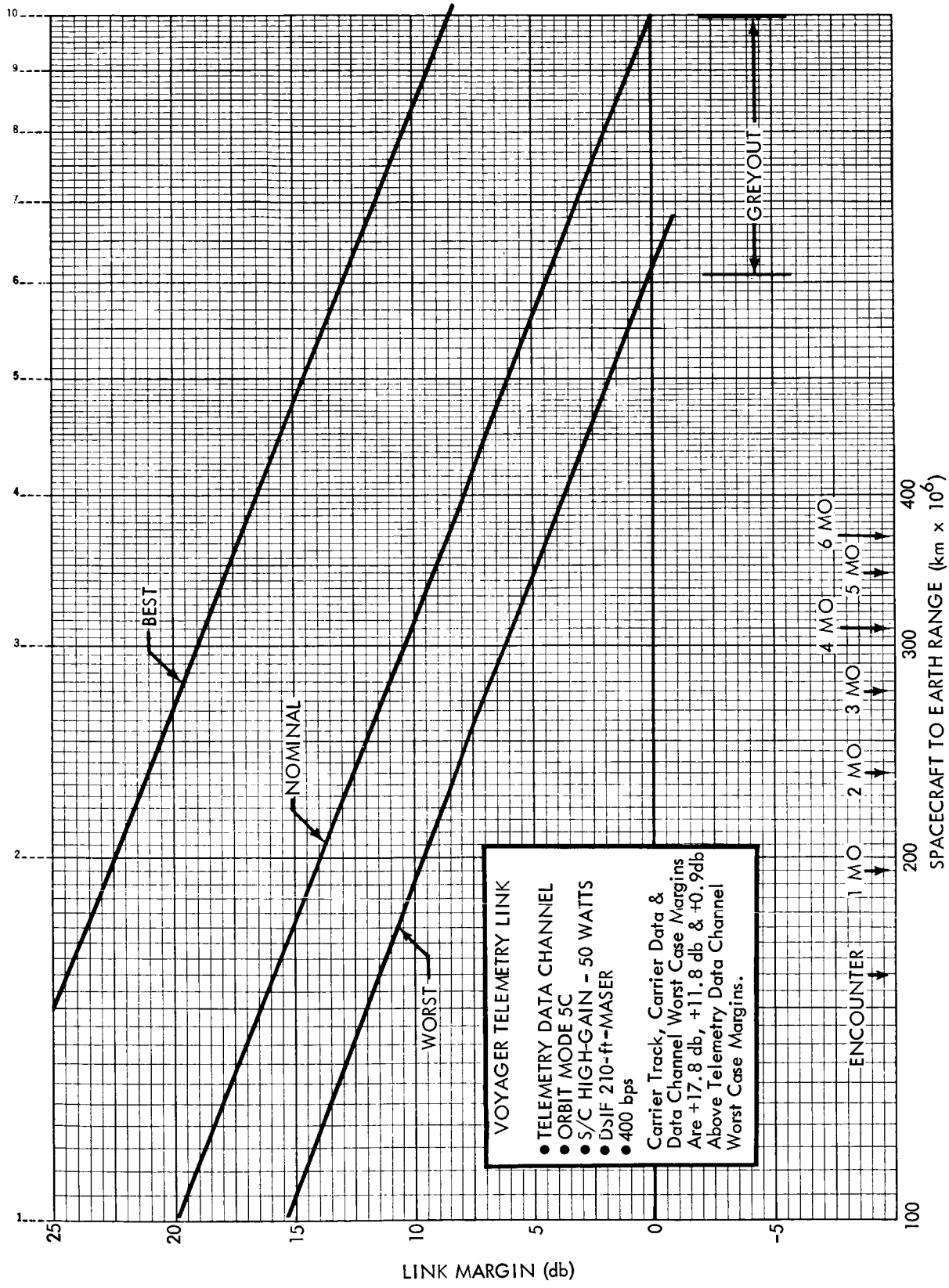

Figure 4.1.4-33:

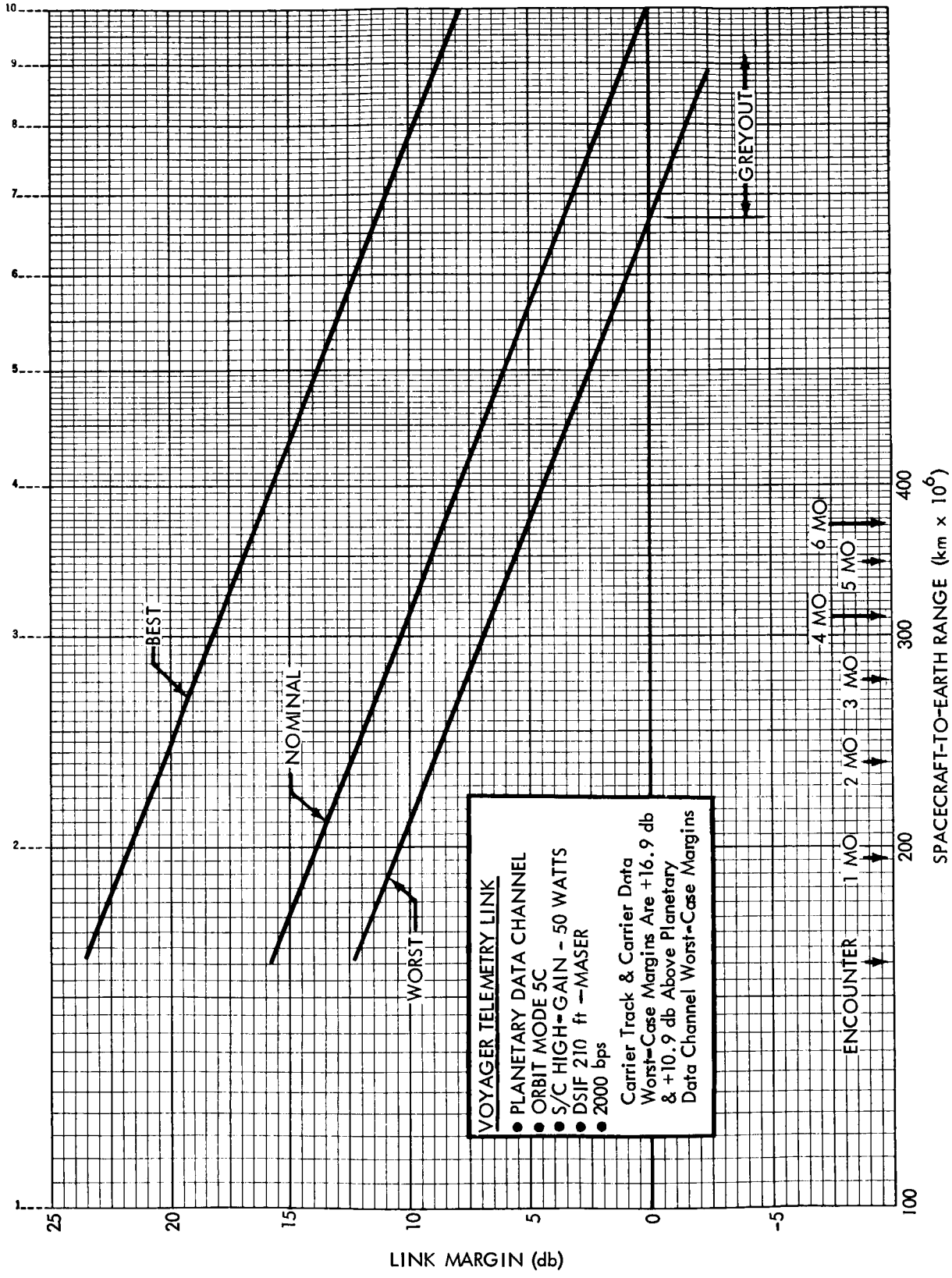

Figure 4.1.4-34:

4.1.4.3 Earth to Spacecraft Command Data Link

The performance of the command data link will be established in the following sections with the use of design control tables and performance graphs. Prior to constructing the design control tables, it is necessary to present a derivation of certain link parameters and to present supporting analysis and criteria for the selection of various threshold parameters used in establishing the command data link performance. The identical procedure of the previous section will be used to derive the command link modulation parameters.

Threshold Criteria

The carrier channel performance criteria

1) Carrier Channel Tracking Performance Criterion--The one-way tracking threshold of the carrier loop will be established such that the probability of losing lock due to phase jitter is less than 1×10^{-4}. (The uplink will operate only in the one-way tracking mode. When so operated, the downlink is in the two-way mode);

2) Carrier Channel Data Demodulation Performance Criterion--The threshold of the carrier loop will be established at a value such that the data channel degradation due to carrier tracking loop and subcarrier tracking loop phase errors and modulation losses is minimized.

Command data channel threshold criterion--The signal-to-noise ratio in 1 cps will be established at a value such that a bit-error probability of 1 part in 10^5 or less can be obtained at the output of the data detector.

Threshold Definition

Carrier Threshold for Tracking--The probability of losing lock of 1×10^{-4} implies that the root-mean-square phase error of the transponder carrier tracking loop be

$$\sigma_n = 90^\circ/4 = 22.5 \text{ degrees}$$

for a Gaussian phase distribution.

This value, with the transponder constants of $2B_{LO} = 20$ cps, and $\alpha_o = 0.0512$ and Equation (2) of Section 4.1.4.2 sets the threshold requirement as $\left(\frac{S}{N}\right)_{2B_{LO}} = 9$ decibel

Carrier Threshold for Data Demodulation--To define the point at which the tracking loop threshold satisfies the carrier channel data performance criterion, the design procedure outlined in Section 4.1.4.2 is used. The results of this optimization are shown in Figure 4.1.4-35. The best operating point shows a carrier threshold value of 5.6 decibel in $2B_{LO}$.

This point also defines the modulation index, which, for a 10-percent variation of index due to hardware tolerances is 1.31 ± 0.13 radians, (peak). It was not possible to incorporate these numbers into the link analysis where an index of $0.89 \begin{smallmatrix}+.09\\-.09\end{smallmatrix}$ radian (peak) and a threshold of 9 decibel was used.

Data and Sync Threshold--It has been shown by measurement (This data was accululated during the performance of JPL Contract No. 950416 by Philco

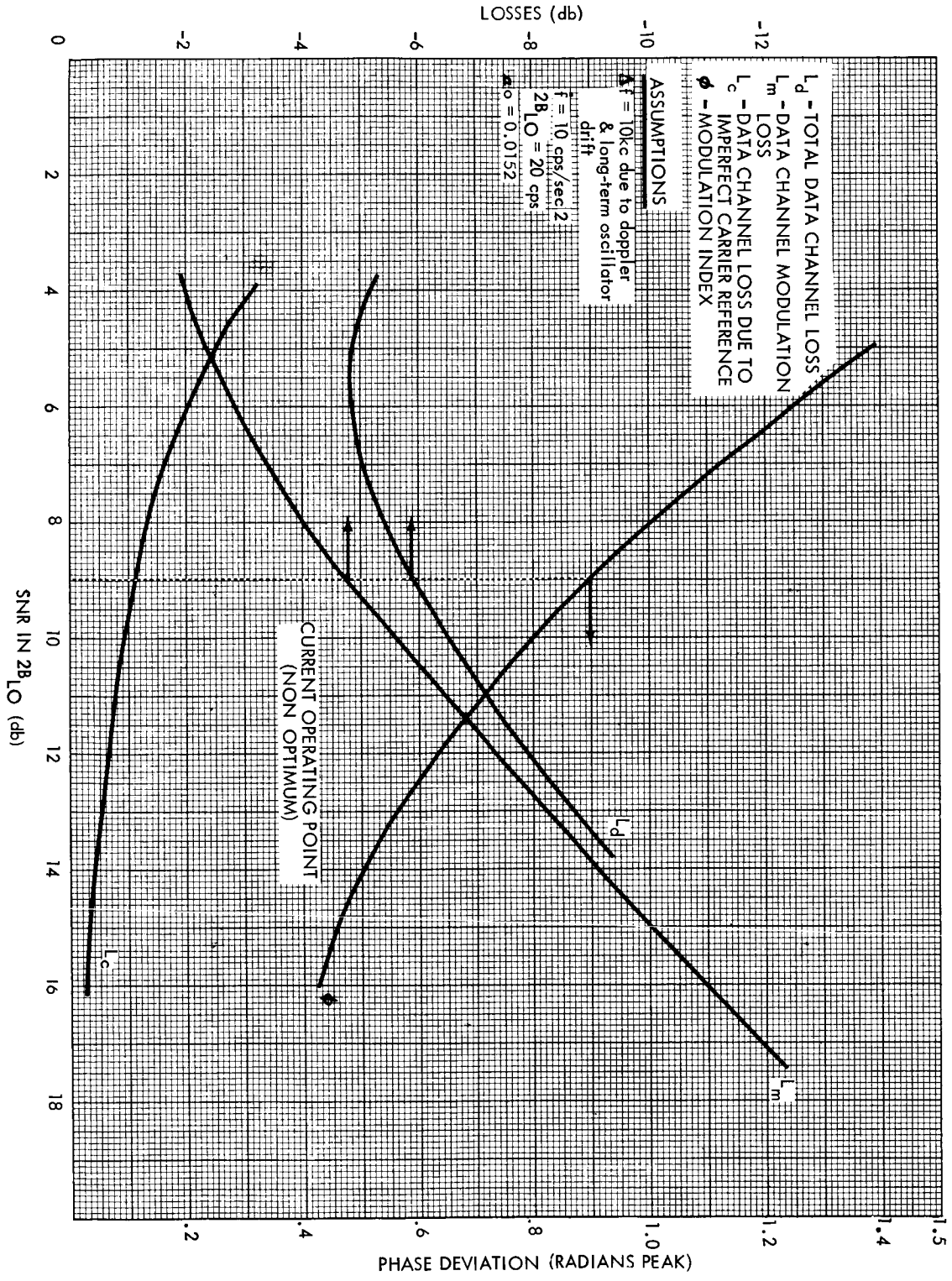

Figure 4.1.4-35: Optimum Carrier Threshold Definition

which called for design and fabrication of a single channel system.) that if the signal-to-noise ratio in 1 cps is 18 decibel at the detector input, the sync loop is able to acquire the signal and remain in lock with a small amount of phase jitter, and the bit error rate is less than 1×10^{-5}. Tests indicate that if the signal-to-noise ratio is reduced from 18 db, the bit error rate increases almost immediately to values above 1×10^{-5}. Therefore, the sync threshold SNR in 1 cps has been set at $18 \begin{smallmatrix}+1.2\\-0.0\end{smallmatrix}$,db.

Tests also show that the data demodulator section of the single channel system performs within 0.9 to 1.4 db of theoretical value with a perfect sync channel reference (hard-wire). For a bit error rate of 1×10^{-5}, the theoretical $\frac{ST}{N/B}$ is 9.6 decibel. Therefore, under the above conditions, the data channel input $\frac{ST}{N/B}$ is $10.5 \begin{smallmatrix}+0.5\\-0.0\end{smallmatrix}$.

Command Signal Spectra--The single channel system transmits both the data and the PN* sequence mod-2 combined on a single sinusoidal subcarrier at a frequency of f_s.

The transmitted spectrum is,

$$f_c(t) = K \sin \left[W_c t + \Delta\phi a(t) \cos (2\pi f_s t)\right]$$

where

$a(t) = D \oplus PN^* =$ (Data) mod-2 (PN* Sequence) = composite bit stream

$\Delta\phi$ = Phase deviation for composite signal

$\cos 2\pi f_s t$ = sinusoidal subcarrier, $f_s \angle 90^\circ$

At the carrier demodulator output, the recovered data spectrum, f_r,

can be represented as

$$f_r(t) = \sum_{n=-\infty}^{\infty} J_n(\Delta\phi)\, a(t) \sin (n\, 2\pi f_s)t.$$

The desired power components are given by

P_c = carrier power = $J_o^2(\Delta\phi)\ P_t$

$P_{s/c}$ = composite data signal = $2\, J_1^2(\Delta\phi)\ P_t$

where

P_t = total power

The power remaining in the higher order terms, P_W, can be expressed as

$$P_W = P_t - P_c - P_{s/c} = P_t \left[1 - J_o^2(\Delta\phi) - 2\, J_1^2(\Delta\phi)\right]$$

For modulation indices up to 1.2 radians, P_W is below 5 percent of total power. Any attempt to recover this value will only result in performance degradations because of the additional noise power that is admitted. Therefore, the higher order terms are of no interest.

Modulation Losses--For the selected modulation index of 0.89 $\pm$0.09 radian peak the carrier modulation loss is

$$L_c = \frac{P_c}{P_t} = -1.8\ {}^{+0.3}_{-0.5}\ \text{decibel}$$

and the data channel modulation losses are

$$L_{s/c} = \frac{P_{s/c}}{P_t} = -4.8\ {}^{+0.6}_{-0.8}\ \text{decibel}$$

Doppler Offset and Doppler Rate Considerations--It can be shown that doppler offset and doppler rate have the same effect on the carrier tracking loop. The phase error produced in the loop is shown in

Figure 4.1.4-5 as a function of the loop parameter $2B_{LO}\sqrt{\alpha/d_o}$ and doppler rate, $\dot{f}$, or normalized dopper offset $\frac{\Delta f}{T_1}$, where the normalization factor T_1 is the time-constant of the tracking loop low pass filter. For the transponder loop under consideration, T_1 = 240 sec.

The table shows that for a frequency offset of 10 kc the transponder carrier loop will have a peak phase error of less than 15 degrees so that the resultant data power loss, from Equation 5, Section 4.1.4.2, is 0.3 decibel.

Losses produced by the doppler rate frequency ramp must also be considered. However, the mission trajectory indicates that the accelerations during phases where ground commands must be received are in the order of 0.4 m/sec^2, so that the doppler rate remains below 3.5 cycles/sec^2. The error in the carrier loop therefore is less than 1.2 degrees and is negligible. (Equation 6, Section 4.1.4.2).

During engine burns and first acquisition, the doppler rates will be high. Although no commands will be sent during that time, it is desirable to maintain the spacecraft transponder locked to the ground signal.

One performance measure during this condition is the probability of loss of lock, considering both the effects of doppler rate and phase jitter.

The probability of loss of lock can be assumed to be the probability that the absolute phase error exceeds 90 degrees. Loop error due to noise, e_n, as derived by Viterbi (Viterbi, A.J., "Phase-Locked Loop Dynamics in the Presence of Noise by Fokker-Planck Techniques", PROC. IEEE, Dec '63, pp 1737.) is treated as a Gaussian variable with a zero mean while error due to doppler rate, $e_f^{\cdot}$, is treated as a bias. This bias tends to shift the Gaussian distribution curve so that the composite error has a Gaussian distribution with a mean of $e_f^{\cdot}$ and a variance of e_n^2. The probability of losing lock (Prob$\left[\,|e| > 90^o\,\right]$) can now be calculated. Figure 4.1.4-36 shows these probabilities as a function of signal-to-noise ratios in the 20 cps-$2B_{LO}$ bandwidth of the receiver with various doppler rates as a parameter. Table 4.1.4-24 displays the worst case values of interest during the critical maneuvers.

Table 4.1.4-24

SPACECRAFT RECEIVER PERFORMANCE DURING HIGH DOPPLER RATES

DSN Configuration: 85-foot Antenna with 10 kw of Power

	Spacecraft Antenna	Worst Case S/N in $2B_{LO}$ (decibels)	One-Way Doppler Rate (cps^2)	Doppler Rate Phase Error (degrees)	Prob. of Loss of Lock
Johannesburg Acquisition	Low-Gain	62.5*	82	< 10	$<<10^{-5}$
Orbit Insertion	Low-Gain	7.8**	68	27	$1x10^{-2}$
Orbit Insertion	High-Gain	26.5	68	4.8	$<<10^{-5}$

* Shows maximum worst case tolerance. In practice transmitter power would be reduced.

** Link is in "grey-out" by 1.2 db.

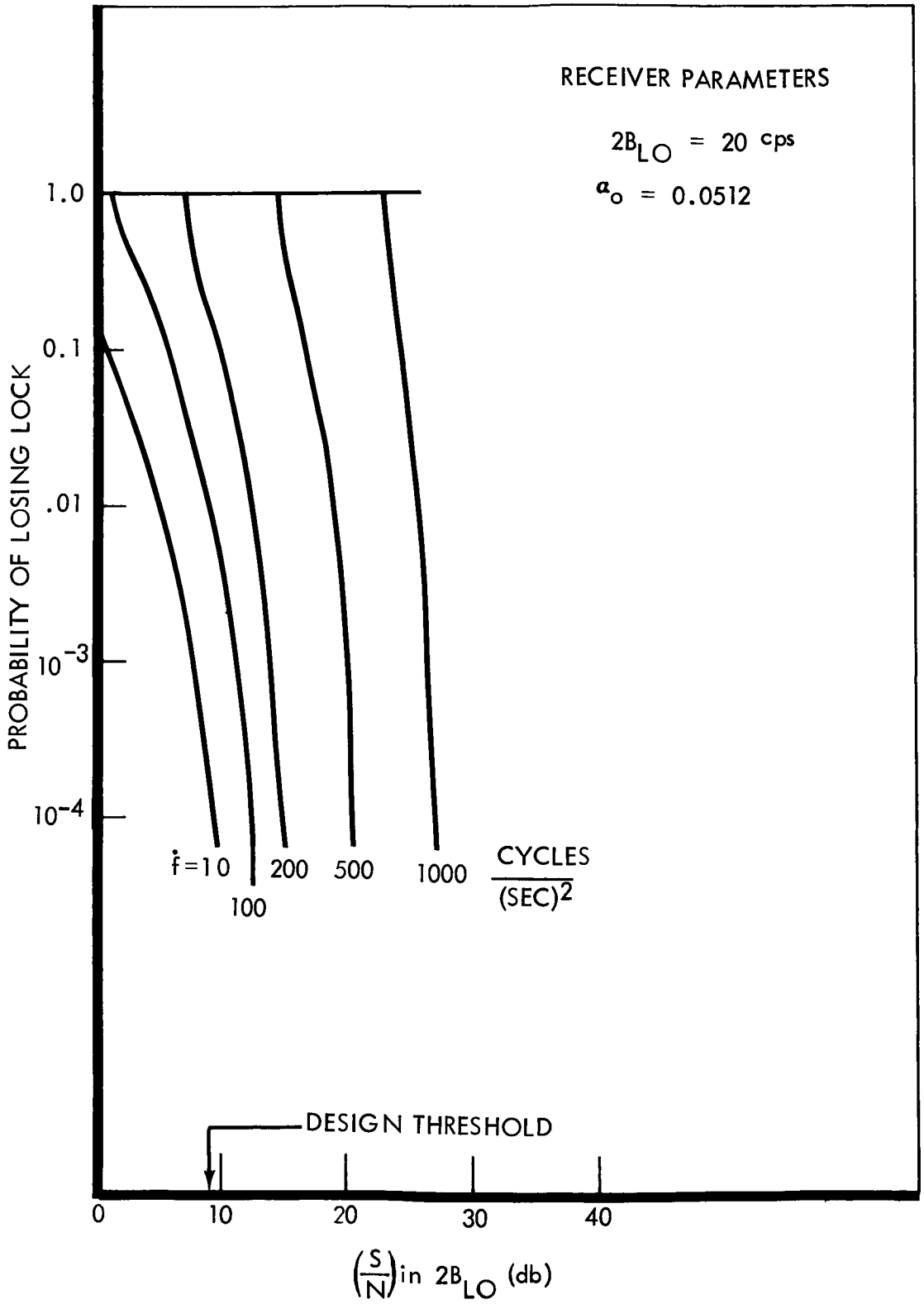

Figure 4.1.4-36: Probability of Receiver Loss of Lock

Probability of Bit Error and Out-of-Lock Indication--Both the two-channel and single channel PN-synchronized systems provide an in-lock and out-of-lock indication. The received data is accepted only if an in-lock indication persists during the reception of the entire command word. If at any time an out-of-lock indication occurs, the part of the word received up to that time is discarded and the command reception must start over again.

Considering that the sync detector sets the bound on the required signal input and that the sync detector tends to have a sharper threshold effect than the data channel (mainly due to self-noise in the phase locked loop) it is logical to sense the quality of the sync channel for a measure of data goodness.

The operation of the two channel system out-of-lock indicator has been analyzed (JPL Space Programs Summary No. 37-30 Vol. II, November 1964, pp 26-31(Conf)). Although the single channel signal to the phase detectors is not identical to that for the two-channel system, the relationship between the sync loop in-lock quality and out-of-lock indicator will be the same. Therefore, the approach of that analysis can be extended to include the operating characteristics of the single channel system.

First, the probability of an out-of-lock indication P_{ol}, as a function of input signal to noise ratio, with bias voltage as a parameter has to be determined. The slope of P_{ol} with respect to signal-to-noise ratio is expected to be much steeper for the single channel system than that of the

two-channel detector. This is attributed to the effects of the additional limiter and the cross-multiplier in the single channel demodulator. The steep slope is a desirable feature, because a small degradation in input signal-to-noise ratio can now be sensed. That is, at an input signal-to-noise ratio slightly below the selected threshold signal-to-noise ratio, P_{ol} is near 1, ensuring that bits detected under conditions where the bit-error probability is larger than the design value, will not be admitted. Furthermore, when the input signal-to-noise ratio is slightly above the design value, P_{ol} is many orders of magnitude below 1, so that the probability of losing good data is very low.

Once the shape of the P_{ol} curves have been derived, the effects of hardware tolerance have to be considered. It is desirable to get the same P_{ol} for a given input signal-to-noise ratio under all encountered environments.

The question where the lock bias should be set must be answered. This answer will involve a trade-off between the probability of admitting data when a bit error is likely and the probability of not admitting data when when bit errors are not likely. A very steep-sloped P_{ol} versus signal-to-noise ratio characteristic that has negligible tolerances with respect to signal-to-noise ratio is obviously set such that design probability of bit error equals P_{ol}. This setting will ensure that the bit error rate will never drop appreciably below design point and that good data is not inhibited. For lower slopes of P_{ol}, one must also consider the data word length and the error detection capability of the data. For instance,

if an n-bit word is inhibited due to an out-of-lock indication during any single bit, the P_{ol} need only be set to 1/n of the design threshold value.

Further analysis must be performed in this area to arrive at the exact P_{ol} versus signal-to-noise ratio characteristic. This characteristic must be known before one can evaluate the probability of an out-of-lock indication and the bit error rate, given an out-of-lock indication.

Command Sync Acquisition--The acquisition characteristics of the single channel system above threshold can be calculated using the same techniques described in Section 4.1.4.2 under "Sync Acquisition Time for Telemetry System."

Acquisition time is related to the sync loop parameters by the expressions

$$T_a = \frac{1}{KB_L} = \text{acquisition time, seconds}$$

where

$$\frac{B_L}{B_{LO}} = \frac{1}{3}\left(1 + 2\frac{\alpha}{\alpha_o}\right)$$

$$\alpha^2 = \frac{\pi}{\pi + 4\left(\frac{N}{S}\right)_{BW}}$$

L = PN sequence length, bits

These equations assume a stable VCO Kis 2 near threshold and K = 1.89 at input signal-to-noise ratios much higher than the threshold value. For an unstable VCO, the acquisition equation changes to:

$$T_a = \frac{L}{KB_L - \Delta f}$$

where Δf is the frequency uncertainty of the VCO. For frequencies of interest, this value is about 0.25 cps. Figure 4.1.4-37 presents the acquisition characteristics for the command link above threshold for conditions of both a stable and unstable VCO.

Command Link Performance Analysis--Performance evaluation of the command link is divided into three major phases on the basis of transmitting and receiving antenna combinations. Design control tables have been prepared to establish command link performance for initial acquisition using the spacecraft low-gain antenna and for cruise flight using the 85-foot DSIF antenna and the spacecraft high-and low-gain antenna. System performance figures are presented for showing the most critical channel for each phase. The most critical channel for the command link is the channel that reaches grey-out conditions at the lowest communications distance. Scaling procedures to obtain performance margins for other phases are also described.

Earth-Spacecraft Tracking, Acquisition Johannesburg; Spacecraft:Low-Gain, Preamp ; DSIF Acquisition Antenna, 10-kilowatt.--This operating phase occurs within the first hour after launch when DSIF Station 51 at Johannesburg is attempting initial contact with the spacecraft. This phase differs from other phases in that the carrier is transmitted without modulation through the 2 by 2 foot horn acquisition antenna. The signal is received by the low-gain antenna aboard the spacecraft.

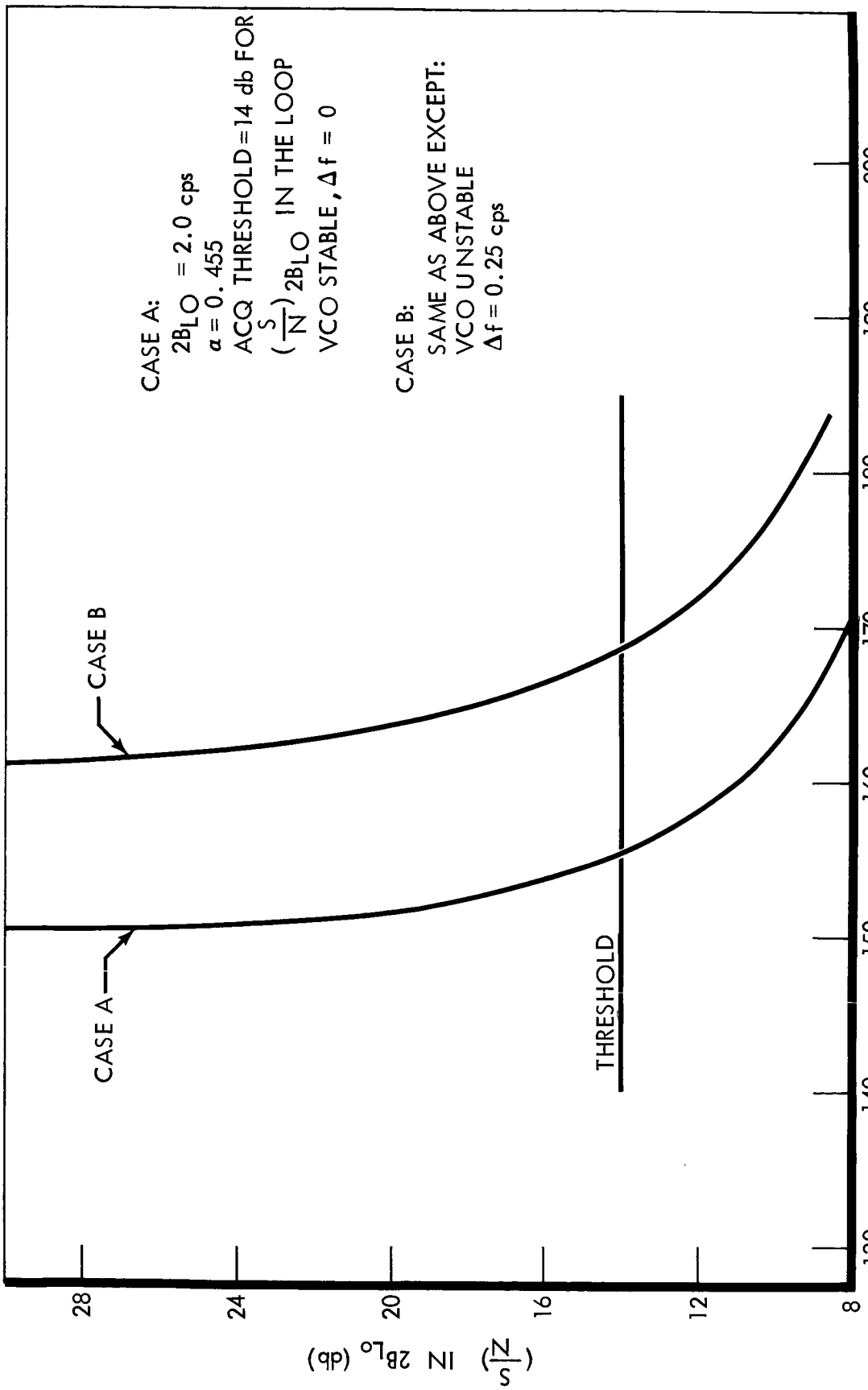

Figure 4.1.4.-37: Command Dectector Mean Acquistion Time

Table 4.1.4-25 is the design control table for this phase. The carrier performance margin is graphed in Figure 4.1.4-38 as a function of communication range.

At the 10,000 kilometer range, the received power is -90 dbm, and the carrier performance margin is nominally +58.0 decibels with tolerances of +5.2 decibels and -4.5 decibels. The high margin is the result of using the full transmitter capability of 10 kilowatts. At this signal-to-noise ratio, the spacecraft receiver can acquire the command carrier in less than 1 second after the spacecraft enters the acquisition antenna pattern as shown in the acquisition analysis.

Earth-Spacecraft Command Link, Cruise; Spacecraft: Low-Gain Antenna, Preamp; DSIF: 85-foot, 10-kilowatt--The second command phase uses the spacecraft low-gain antenna to receive commands transmitted from the DSIF 10 kilowatt transmitters and 85-foot antennas. This phase is used from completion of initial acquisition until activation of the high-gain antenna 80 days later. The system noise temperature in this phase is lower by 21°K than in the acquisition phase, because the Earth subtends a smaller solid angle as the communication range increases.

Table 4.1.4-26 is the design control table for this phase. It shows that the command link reaches grey-out at 1.56×10^8 kilometers with the 10 kilowatt transmitter, although it normally is not used past 2×10^7 kilometers. In emergencies, it is possible to use the 100 kilowatt transmitter during this phase to transmit commands over any range to the end

TELECOMMUNICATION DESIGN CONTROL TABLE 4.1.4-25

PROJECT: VOYAGER DATE

CHANNEL: Earth-Spacecraft, Tracking PAGE 1 of 1

MODE: Acquisition Johannesburg: S/C:Low Gain, Preamp:DSIF:Acq, Antenna, 10 KW

NO.	PARAMETER	VALUE	TOLERANCE	SOURCE
1	Total Transmitter Power	+70.0 dbm	+0.5 db -0.0 db	Table 4.1.4-2
2	Transmitting Circuit Loss	-0.5 db	+0.2 db -0.2 db	Table 4.1.4-2
3	Transmitting Antenna Gain	+20.0 db	+2.0 db -2.0 db	Table 4.1.4-2
4	Transmitting Antenna Pointing Loss	-0.0 db	+0.0 db -0.0 db	Table 4.1.4-2
5	Space Loss @ 2215 Mc R = 10,000 km	-179.0 db		--
6	Polarization Loss	-0.0 db	+0.2 db -0.2 db	Table 4.1.4-5
7	Receiving Antenna Gain	+1.0 db	+1.0 db -0.0 db	Section 4.1.4.1
8	Receiving Antenna Pointing Loss	Included in	(7)	--
9	Receiving Circuit Loss	-1.5 db	+0.4 db -0.5 db	Figure 4.1.4-1
10	Net Circuit Loss	-160.0 db	+3.8 db -2.9 db	--
11	Total Received Power	-90.0 dbm	+4.3 db -2.9 db	--
12	Receiver Noise Spectral Density (N/B) T System = $725\ ^{+201}_{-62}\ ^{o}K$	-170.0 dbm	+1.1 db -0.4 db	Table 4.1.4-3
13	Carrier Modulation Loss	Not Applicable		--
14	Received Carrier Power	-90.0 dbm	+4.3 db -2.9 db	--
15	Carrier APC Noise BW ($2B_{LO}$ = 20 cps)	+13.0 db	+0.5 db -0.5 db	Figure 4.1.4-3
	CARRIER PERFORMANCE – TRACKING (One-Way)			
16	Threshold SNR in $2B_{LO}$	9.0 db	------	Figure 4.1.4-3
17	Threshold Carrier Power	-148.0 dbm	+1.6 db -0.9 db	--
18	Performance Margin	+58.0	+5.2 db -4.5 db	--
	CARRIER PERFORMANCE – Tracking (Two-Way)			
19	Threshold SNR in $2B_{LO}$	Not Applicable		
20	Threshold Carrier Power			
21	Performance Margin			

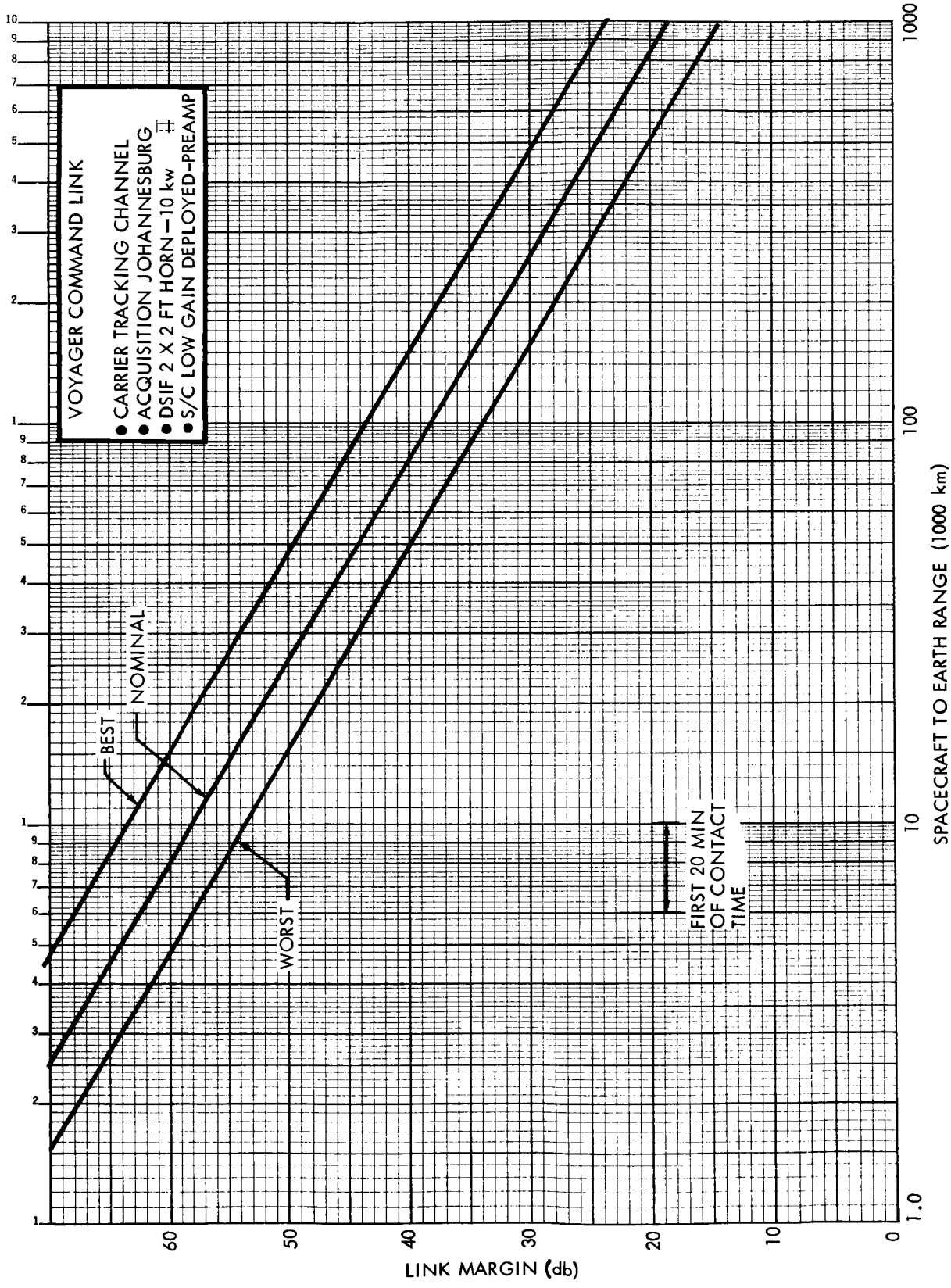

Figure 4.1.4-38:

TELECOMMUNICATION DESIGN CONTROL TABLE 4.1.4-26

PROJECT: VOYAGER DATE

CHANNEL: Earth-Spacecraft, Command Link PAGE 1 of 2

MODE: Cruise; S/C: Low Gain Antenna, Preamp; DSIF: 85 ft.,10 kw

NO.	PARAMETER	VALUE	TOLERANCE	SOURCE
1	Total Transmitter Power	+70.0 dbm	+0.5, -0.0 db	Table 4.1.4-2
2	Transmitting Circuit Loss	-0.4 db	+0.1, -0.1 db	Table 4.1.4-2
3	Transmitting Antenna Gain	+51.0 db	+1.0, -0.5 db	Table 4.1.4-2
4	Transmitting Antenna Pointing Loss	-0.0 db	+0.0, -0.1 db	Table 4.1.4-2
5	Space Loss @ 2115 Mc R = 1.56×10^8 km	-262.7 db	--	
6	Polarization Loss	-0.0 db	+0.2, -0.2 db	Table 4.1.4-5
7	Receiving Antenna Gain	+1.0 db	+1.0, -0.0 db	Section 4.1.4.1
8	Receiving Antenna Pointing Loss	(Included in 7		
9	Receiving Circuit Loss	-1.5 db	+0.4, -0.5 db	Figure 4.1.4-1
10	Net Circuit Loss	-212.6 db	+2.7, -1.4 db	---
11	Total Received Power	-142.6 dbm	+3.2, -1.4 db	---
12	Receiver Noise Spectral Density (N/B) T System 704^{+203}_{-65} °K	-170.1 dbm	+1.1, -0.4 db	Table 4.1.4-3
13	Carrier Modulation Loss	-1.8 db	+0.3, -0.5 db	Figure 4.1.4-3
14	Received Carrier Power	-144.4 dbm	+3.5, -1.9 db	
15	Carrier APC Noise BW ($2B_{LO}$=20 cps)	+13.0 db	+0.5, -0.5 db	Figure 4.1.4-3
	CARRIER PERFORMANCE – TRACKING (One-Way)			
16	Threshold SNR in $2B_{LO}$	+9.0 db	--	Figure 4.1.4-3
17	Threshold Carrier Power	-148.1 dbm	+1.6, -0.9 db	---
18	Performance Margin	+3.7 db	+4.4, -3.5 db	---
	CARRIER PERFORMANCE – TRACKING (Two-Way)			
19	Threshold SNR in $2B_{LO}$	NOT APPLICABLE		
20	Threshold Carrier Power			
21	Performance Margin			

TELECOMMUNICATION DESIGN CONTROL TABLE 4.1.4-26

PROJECT: Voyager DATE
CHANNEL: Earth-Spacecraft, Command PAGE 2 of 2
MODE: Cruise; S/C: Low Gain Antenna, Preamp; DSIF: 85 Feet, 10 KW

NO.	PARAMETER	VALUE	TOLERANCE	SOURCE
	CARRIER PERFORMANCE – DATA			
22	Threshold SNR in $2B_{LO}$	+9.0 db		Figure 4.1.4-3
23	Threshold Carrier Power	-148.1 dbm	+1.6 -0.9 db	
24	Performance Margin	3.7 db	+4.4 -3.5 db	
	DATA CHANNEL			
25	Modulation Loss	-4.8 db	+0.6 -0.8 db	Figure 4.1.4-3
26	Received Data Subcarrier Power	-147.4 dbm	+3.8 -2.2 db	
27	Bit Rate (1/T)	0.0 db		
28	Required ST/N/B	+18.0 db	+1.2 -0.0 db	Figure 4.1.4-3
29	Threshold Subcarrier Power	-152.1 dbm	+2.3 -0.4 db	
30	Performance Margin	+4.7 db	+4.2 -4.5 db	
	SYNC CHANNEL	Not Applicable		
31	Modulation Loss			
32	Received Sync Subcarrier Power			
33	Sync APC Noise BW($2B_{LO}$ =			
34	Threshold SNR in $2B_{LO}$			
35	Threshold Subcarrier Power			
36	Performance Margin			

COMMENTS:

(1) While the spacecraft is maneuvering the receiving antenna pointing loss increases by $-1.0\ ^{+1.0}_{-0.0}$ db. To obtain margins during maneuver periods, subtract 1.0 db from the above nominal margin and add 1.0 db to the positive tolerance.

(2) If 100 kw is used at DSIF, the nominal margins increase by +10 db.

of the mission. The carrier margin on the data channel is graphed in Figure 4.1.4-39 for the normal cruise and low-gain maneuver periods.

During maneuvers, the performance differs from the normal cruise phase because of possible low-gain antenna pointing losses. Normally, the low-gain antenna orientation is such that the Earth is always within the +1.0-decibel gain toroid. In a maneuver, the antenna can become aligned so that gain in the direction of Earth drops by as much as -1.0 decibel. The receiving antenna pointing loss is -1.0 decibel under nominal and worst case conditions with a +1.0-decibel favorable tolerance. As indicated on the graph, performance margins for the nominal and worst-case conditions are 1.0-decibel lower than for the normal cruise phase. Under these conditions, the command link reaches grey-out at 1.38×10^8 kilometers with the 10 kilowatt transmitter. This link configuration is not normally used past the second midcourse maneuver at 100 days after injection when the nominal margin is +17.0 decibels. Under emergency conditions such as high-gain antenna failures, the 100-kilowatt DSIF transmitter can be used to extend the grey-out range to 4.36×10^8 kilometers, well beyond the end of the mission.

Earth - Spacecraft Command Link, Cruise and Orbit; Spacecraft:High-Gain Antenna, Transponder; DSIF:85 foot,10-kilowatt--After activation of the high-gain antenna for telemetry transmission at 2×10^7 kilometers, the high-gain antenna provides command reception also for the remainder of the mission. In the normal cruise phase, the performance differs from the low-gain antenna mode in four areas associated with the high-gain

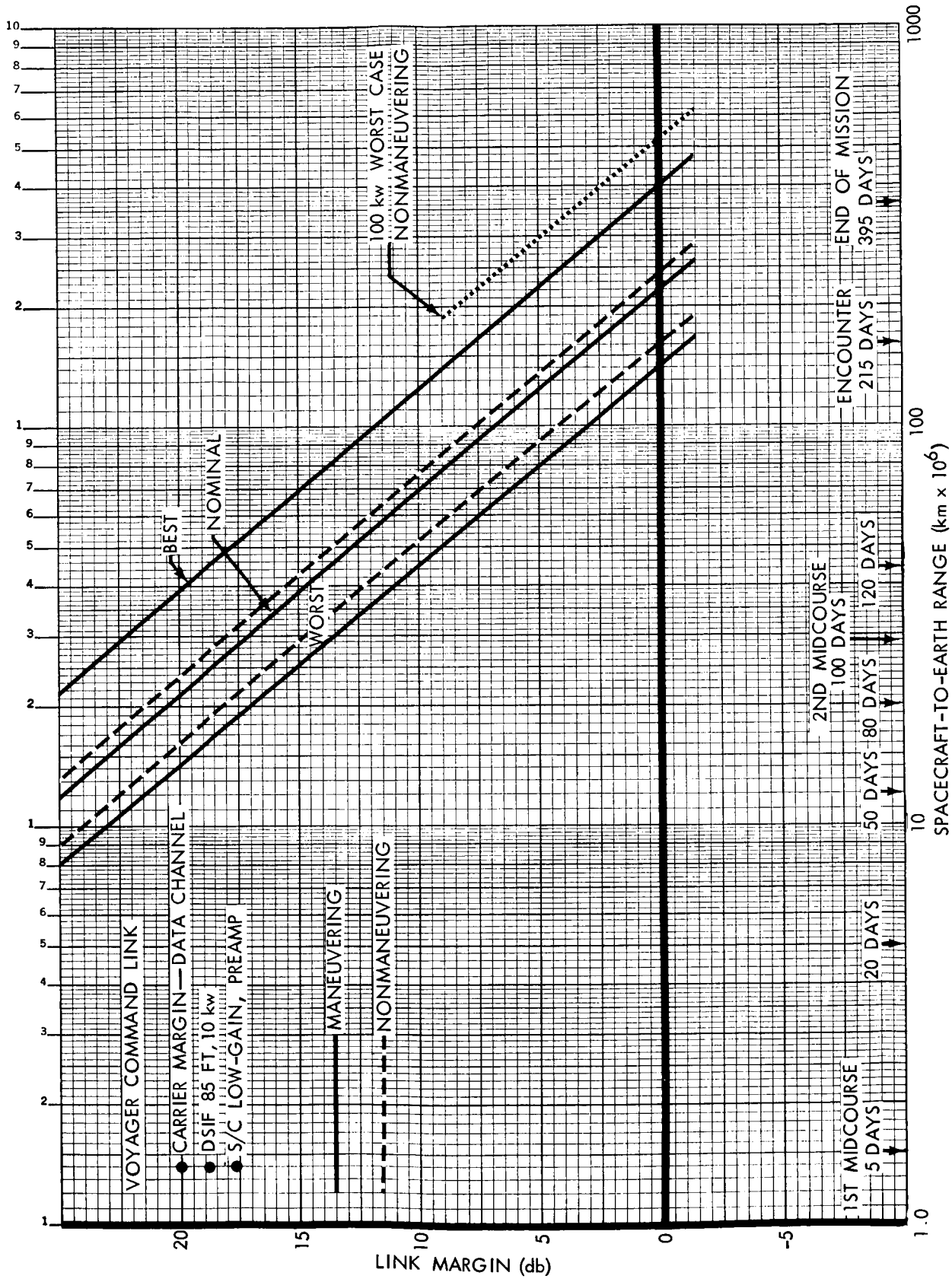

Figure 4.1.4-39:

antenna: gain, pointing loss, receiving-circuit loss, and system noise spectral density. The gain of the 8 by 12 foot antenna at 2115 megacycles is 32.1 decibels with tolerances of +2.0 decibels and -0.0 decibel. The antenna pointing coordinates are updated periodically to keep the pointing loss between 0.0 decibel and -1.0 decibel; the value used in the analysis is -0.5 ± 0.5 decibel. The rf circuitry between the antenna and the transponder receivers introduces nominal losses of -3.1 decibel with tolerances of +0.5 decibel and -1.2 decibel, as explained in Figure 4.1.4-1. The system noise temperature is 2767°K nominally; high and low extremes are 3553° K and 2149°K.

The high-gain command mode provides a carrier performance margin of +19.2 decibel at the end of the mission, with tolerances of +6.5 decibel and -4.1 decibel, as shown in Table 4.1.4-27 and Figure 4.1.4-40. The margin is 25.3 decibel higher, or +44.5 decibels, at 2×10^7 kilometers when the high-gain antenna is activated. The nominal data performance margin is +27.7 decibel, and the sync performance margin is +20.2 decibel at the end of the mission.

4.1.4.4 Turn-Around Ranging Link

Link Parameter Derivation--A link calculation for the turn-around ranging system has been included to indicate the performance at a desired operating range of at least 800,000 kilometers. This calculation considers both the uplink and downlink because the received signal at the spacecraft is corrupted by receiver noise before being retransmitted. For the uplink, it is assumed that command data will not be transmitted

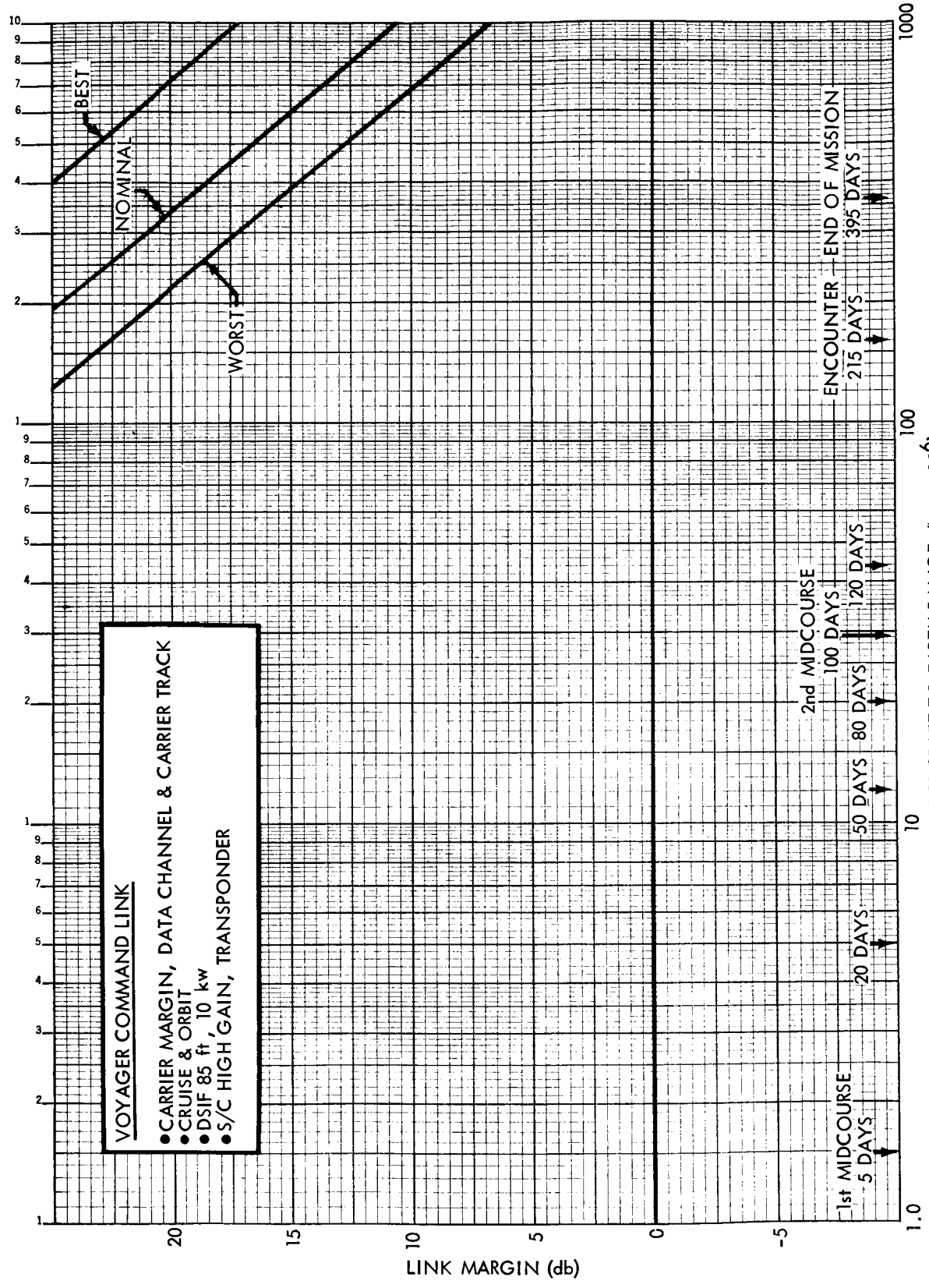

Figure 4.1.4-40.

TELECOMMUNICATION DESIGN CONTROL TABLE 4.1.4-27

PROJECT: VOYAGER DATE

CHANNEL: EARTH-SPACECRAFT,COMMAND LINK PAGE 1 of 2

MODE: CRUISE AND ORBIT: S/C HIGH GAIN, TRANSPONDER;DSIF: 85 FT. 10KW

NO.	PARAMETER	VALUE	TOLERANCE	SOURCE
1	Total Transmitter Power	+ 70.0 dbm	+ 0.5 - 0.0 db	Table 4.1.4-2
2	Transmitting Circuit Loss	- 0.4 db	+ 0.1 - 0.1 db	Table 4.1.4-2
3	Transmitting Antenna Gain	+ 51.0 db	+ 1.0 - 0.5 db	Table 4.1.4-2
4	Transmitting Antenna Pointing Loss	- 0.0 db	+ 0.0 - 0.1 db	Table 4.1.4-2
5	Space Loss	-270.3 db	-	
6	@ 2115 Mc R = 3.69×10^8 km Polarization Loss	- 0.0 db	+ 0.0 - 0.1 db	Table 4.1.4-5
7	Receiving Antenna Gain	+ 32.1 db	+ 2.0 - 0.0 db	Section 4.1.4.1
8	Receiving Antenna Pointing Loss	- 0.5 db	+ 0.5 - 0.0 db	Section 4.1.4.1
9	Receiving Circuit Loss	- 3.1 db	+ 0.5 - 1.2 db	Figure 4.1.4-1
10	Net Circuit Loss	-191.2 db	+ 4.1 - 2.0 db	
11	Total Received Power	-121.1 dbm	+ 4.6 - 2.0 db	
12	Receiver Noise Spectral Density (N/B) T System 2767 $^{+786}_{-618}$ °K	-164.2 dbm	+ 1.1 - 1.1 db	Table 4.1.4-4
13	Carrier Modulation Loss	- 1.8 db	+ 0.3 - 0.5 db	Figure 4.1.4-3
14	Received Carrier Power	-123.0 db	+ 4.9 - 2.5 db	
15	Carrier APC Noise BW ($2B_{LO}$ = 20 cps	13.0 db	+ 0.5 - 0.5 db	Figure 4.1.4-3
	CARRIER PERFORMANCE - TRACKING (One-Way)			
16	Threshold SNR in $2B_{LO}$	9.0 db	-	Figure 4.1.4-3
17	Threshold Carrier Power	-142.2 dbm	+ 1.6 - 1.6 db	
18	Performance Margin	+ 19.2 db	+ 6.5 - 4.1 db	
	CARRIER PERFORMANCE - TRACKING (Two-Way)			
19	Threshold SNR in $2B_{LO}$	NOT APPLICABLE		
20	Threshold Carrier Power			
21	Performance Margin			

TELECOMMUNICATION DESIGN CONTROL TABLE 4.1.4-27

PROJECT: Voyager — DATE
CHANNEL: Earth-Spacecraft. Command Link — PAGE 2 of
MODE: Cruise and Orbit; S/C High Gain. Transponder; DSIF: 85 Feet 10 KW

NO.	PARAMETER	VALUE	TOLERANCE	SOURCE
	CARRIER PERFORMANCE- DATA			
22	Threshold SNR in $2B_{LO}$	9.0 db		Figure 4.1.4-3
23	Threshold Carrier Power	-142.2 dbm	+1.6 -1.6 db	
24	Performance Margin	+19.2 db	+6.5 -4.1 db	
	DATA CHANNEL			
25	Modulation Loss	-4.8 db	+0.6 -0.8 db	Figure 4.1.4-3
26	Received Data Subcarrier Power	-126.0 dbm	+5.2 -2.8 db	
27	Bit Rate (1/T)	0.0 db		
28	Required ST/N/B	-18.0 db	+1.2 -0.0 db	Figure 4.1.4-3
29	Threshold Subcarrier Power	-146.2 dbm	+2.3 -1.1 db	
30	Performance Margin	20.2	+6.3 -5.1 db	
	SYNC CHANNEL			
31	Modulation Loss	Not	Applicable	
32	Receiver Sync Subcarrier Power			
33	Sync APC Noise BW($2B_{LO}$ =			
34	Threshold SNR in $2B_{LO}$			
35	Threshold Subcarrier Power			
36	Performance Margin			

COMMENTS:

(1) While the spacecraft is maneuvering the receiving antenna pointing loss increases by $-1.0\ ^{+1.0}_{-0.0}$ db. To obtain margins during maneuver periods, subtract 1.0 db from the above nom inal margin and add 1.0 db to the positive tolerance.

(2) If 100 kw is used at DSIF, the nominal margins increase by +10 db.

simultaneously with the ranging signal. For the downlink, it is assumed that the ranging signal will be transmitted simultaneously with the spacecraft telemetry Mode 1 data only, to assure minimum degradation of either signal.

All of the parameters except the modulation losses have already been described in detail in Sections 4.1.4.1, 4.1.4.2, and 4.1.4.3 and are referenced in Tables 4.1.4-28 and 4.1.4-29.

Uplink Modulation Loss--An uplink modulation index of 1.20 radians peak has been assumed and is consistent with JPL Memo TM 3361-64-1.

a) Carrier Modulation Loss - For this condition, the modulation loss for the carrier tracking loop is:

$$\frac{Pc}{Pt} = \cos^2\phi$$

where ϕ_r = 1.2 radians $\pm$ 5 percent

Inerefore, $\frac{Pc}{Pt}$ = -8.8 decibel $^{+1.2}_{-1.5}$

b) Ranging Channel Modulation Loss

The modulation loss for the ranging signal is:

$$\frac{Pr}{Pt} = \sin^2 \phi_r = -0.6 \text{ decibel } ^{+0.2}_{-0.2}$$

Downlink Modulation Loss--The modulation indices selected for the ranging signal in conjunction with the Mode 1 telemetry data are:

Mode 1 Sync Channel - ϕ_s = 0.35 radian peak $\pm$ 10 percent

Mode 1 Data Channel - ϕ_d = 1.28 radians peak $\pm$ 10 percent

Ranging Data Channel - ϕ_r = 0.47 radian peak $\pm$ 9 percent

TELECOMMUNICATION DESIGN CONTROL TABLE 4.1.4-28 DATE

PROJECT: VOYAGER PAGE 1 of 2

CHANNEL: Earth-Spacecraft Ranging Link

MODE: Cruise: S/C:Low Gain, Preamp: DSIF:85 ft, 10 KW

NO.	PARAMETER	VALUE	TOLERANCE	SOURCE
1	Total Transmitter Power	+70.0 dbm	+0.5, -0.0 db	Table 4.1.4-2
2	Transmitting Circuit Loss	-0.4 db	+0.1, -0.1 db	Table 4.1.4-2
3	Transmitting Antenna Gain	+51.0 db	+1.0, -0.5 db	Table 4.1.4-2
4	Transmitting Antenna Pointing Loss	0.0 db	+0.0, -0.1 db	Table 4.1.4-2
5	Space Loss	-217.0 db	-----	---
6	2115 $\pm$5 MC $R = 8 \times 10^5$km Polarization Loss	0.0 db	+0.2, -0.2 db	Table 4.1.4-5
7	Receiving Antenna Gain	+1.0 db	+1.0, -0.0 db	Section 4.1.4.1
8	Receiving Antenna Pointing Loss	Included in Item 7		---
9	Receiving Circuit Loss	-1.5 db	+0.4,-0.5 db	Figure 4.1.4-1
10	Net Circuit Loss	-166.9 db	+2.7, -1.4 db	---
11	Total Received Power	-96.9 dbm	+3.2, -1.4 db	
12	Receiver Noise Spectral Density (N/B)	-170.0 dbm	+1.1, -0.4 db	Table 4.1.4-3
13	T System = $725\ ^{+201}_{-\ 62}\ ^{\circ}K$ Carrier Modulation Loss (1.20 RAD Peak)	-8.8 db	+1.2, -1.5 db	Section 4.1.4.1
14	Received Carrier Power	-105.7 dbm	+4.4, -2.9 db	--
15	Carrier APC Noise BW ($2B_{LO}$ = 20 cps)	+13.0 db	+0.5, -0.5 db	Figure 4.1.4-3
	CARRIER PERFORMANCE – TRACKING (One-Way)			
16	Threshold SNR in $2B_{LO}$	+9.0 db	-----	Figure 4.1.4-3
17	Threshold Carrier Power	-148.0 dbm	+1.6, -0.9 db	--
18	Performance Margin	+42.3 db	+5.3, -4.5 db	--
	CARRIER PERFORMANCE – TRACKING (Two-Way)			
19	Threshold SNR in $2B_{LO}$	+9.0 db	----	Figure 4.1.4-3
20	Threshold Carrier Power	-148.0 dbm	+1.6, -0.9 db	--
21	Performance Margin	+42.3 db	+5.3, -4.5 db	---

TELECOMMUNICATION DESIGN CONTROL TABLE 4.1.4-28

PROJECT: Voyager
CHANNEL: Earth-Spacecraft Ranging Link
MODE: Cruise: S/C Low-Gain, Preamp; DSIF: 85 ft. 10 KW

DATE
PAGE 2 of 2

NO.	PARAMETER	VALUE	TOLERANCE	SOURCE
	CARRIER PERFORMANCE- RANGING			
22	Threshold SNR in $2B_{LO}$	+9.0 db	----	Figure 4.1.4-3
23	Threshold Carrier Power	-148.0 dbm	+1.6 -0.9 db	
24	Performance Margin	+42.3 db	+5.3 -4.5 db	
	DATA CHANNEL - RANGING			
25	Modulation Loss (1.2 RAD Peak)	-0.6 db	+0.2 -0.2 db	Section 4.1.4.4
26	Received Data Subcarrier Power	-97.5 dbm	+3.4 -1.6 db	
27	Noise Bandwidth (BM - 2.2mc)	+63.5 db	+0.7 -0.6 db	Section 4.1.4.4
28	Required ST/N/B			
29	Noise Power	-106.5 dbm	+1.8 -1.0 db	
30	Output SNR	+9.0 db	+4.4 -3.4 db	
	SYNC CHANNEL			
31	Modulation Loss	Not	Applicable	
32	Receiver Sync Subcarrier Power			
33	Sync APC Noise BW($2B_{LO}$ =			
34	Threshold SNR in $2B_{LO}$			
35	Threshold Subcarrier Power			
36	Performance Margin			

COMMENTS:

TELECOMMUNICATION DESIGN CONTROL TABLE 4.1.4-29

PROJECT: VOYAGER DATE

CHANNEL: Spacecraft-Earth Ranging and Telemetry Link, Mode 1 PAGE 1 OF 3

MODE: Cruise; S/C Low-Gain, 50 watts; DSIF: 85 ft., Maser

NO.	PARAMETER	VALUE	TOLERANCE	SOURCE
1	Total Transmitter Power	+47.0 dbm	+2.0, -0.0 db	Section 4.1.4.1
2	Transmitting Circuit Loss	-2.6 db	+0.5, -1.3 db	Figure 4.1.4-1
3	Transmitting Antenna Gain	+1.0 db	+1.0, -0.0 db	Section 4.1.4.1
4	Transmitting Antenna Pointing Loss	0.0 db	+0.0, -0.0 db	Section 4.1.4.1
5	Space Loss @ 2295 Mc R = 8 x 10^5 km	-217.7 db	+0.0, -0.0 db	
6	Polarization Loss	0.0 db	+0.1, -0.1 db	Table 4.1.4-5
7	Receiving Antenna Gain	+53.0 db	+1.0, -0.5 db	Table 4.1.4-2
8	Receiving Antenna Pointing Loss	0.0 db	+0.0, -0.1 db	Table 4.1.4-2
9	Receiving Circuit Loss	-0.2 db	+0.1 -0.0 db	Table 4.1.4-2
10	Net Circuit Loss	-166.5 db	+2.7, -2.0 db	
11	Total Received Power	-119.5 dbm	+4.7, -2.0 db	
12	Receiver Noise Spectral Density (N/B)	-182.1 dbm	+0.9, -0.5 db	Table 4.1.4-2
13	T System 45^{+10}_{-5} °K Carrier Modulation Loss	-5.7 db	+1.2, -1.2 db	Section 4.1.4.4
14	Received Carrier Power	-125.2 dbm	+5.9, -3.2 db	
15	Carrier APC Noise BW ($2B_{LO}$= 12 cps	+10.8 db	+0.0, -0.5 db	Figure 4.1.4-3
	CARRIER PERFORMANCE - TRACKING (One Way)			
16	Threshold SNR in $2B_{LO}$	+9.0 db	----	Figure 4.1.4-1
17	Threshold Carrier Power	-162.3 dbm	+0.9, -1.0 db	
18	Performance Margin	+37.1 db	+6.9, -4.1 db	
	CARRIER PERFORMANCE - TRACKING (Two Way)			
19	Threshold SNR is $2B_{LO}$	+9.0 db	----	Figure 4.1.4-3
20	Threshold Carrier Power	-162.3 dbm	+0.9, -1.0 db	
21	Performance Margin	+37.1 db	+6.9, -4.1 db	

TELECOMMUNICATION DESIGN CONTROL TABLE 4.1.4-29

PROJECT: VOYAGER DATE

CHANNEL: Spacecraft-Earth Ranging and Telemetry Link, Mode 1 PAGE 2 of 3

MODE: Cruise; S/C Low-Gain, 50 watts; DSIF 85 ft., Maser

NO.	PARAMETER	VALUE	TOLERANCE	SOURCE
	CARRIER PERFORMANCE Ranging			
22	Threshold SNR in $2B_{LO}$	+9.0 db	----	TM 3361-64-1
23	Threshold Carrier Power	-162.3 dbm	+0.9, -1.0 db	
24	Performance Margin	+37.1 db	+6.9, -4.1 db	
	DATA CHANNEL			
25	Modulation Loss	(See next page)		
26	Received Data Subcarrier Power			
27	Bit Rate (1/T)			
28	Required ST/N/B			
29	Threshold Subcarrier Power			
30	Performance Margin			
	SYNC CHANNEL Ranging (Clock)			
31	Modulation Loss P_{clock}/P_{trans}	-23.6 db	+1.6, -2.3 db	TM 3361-64-1
32	Receiver Clock Subcarrier Power	-143.1 dbm	+6.3, -4.3 db	
33	Clock APC Noise BW($2B_{LO}$ = 0.8 cps)	-1.0 db	+0.0, -1.0 db	TM 3361-64-1
34	Threshold SNR in $2B_{LO}$	+6.0 db	----	
35	Threshold Subcarrier Power	-177.1 dbm	+0.9, -1.5 db	
36	Performance Margin	+34.0 db	+7.8, -5.2 db	

COMMENTS:

TELECOMMUNICATION DESIGN CONTROL TABLE 4.1.4-29

PROJECT: VOYAGER DATE

CHANNEL: Spacecraft-Earth Ranging and Telemetry Link, Mode 1 PAGE 3 of 3

MODE: Cruise; S/C Low-Gain, 50 watts; DSIF:85 ft. Maser

NO.	PARAMETER	VALUE	TOLERANCE	SOURCE
	CARRIER PERFORMANCE Mode 1 Data			
22	Threshold SNR in $2B_{LO}$	+15.0 db	----	Figure 4.1.4-3
23	Threshold Carrier Power	-156.3 dbm	+0.9, -1.0 db	
24	Performance Margin	+31.1 db	+6.9, -4.1 db	
	DATA CHANNEL Mode 1 Data			
25	Modulation Loss	-4.3 db	+0.7, -0.9 db	Section 4.1.4.4
26	Received Data Subcarrier Power	-123.8 dbm	+5.4, -2.9 db	
27	Bit Rate (1/T) (22-2/9 bits/sec)	+13.5 db	----	
28	Required ST/N/B	+7.6 db	+0.5, -0.5 db	Figure 4.1.4-3
29	Threshold Subcarrier Power	-161.0 dbm	+1.4, -1.0 db	
30	Performance Margin	+37.2 db	+6.4, -4.3 db	
	SYNC CHANNEL			
31	Modulation Loss	-14.6 db	+1.8, -1.9 db	Section 4.1.4.4
32	Receiver Sync Subcarrier Power	-134.1 dbm	+6.5, -3.9 db	
33	Sync APC Noise BW($2B_{LO}$ = 0.5 cps)	-3.0 db	+0.4, -0.4 db	Figure 4.1.4-3
34	Threshold SNR in $2B_{LO}$	+14.0 db	+0.5, -0.5 db	Figure 4.1.4-3
35	Threshold Subcarrier Power	-171.1 dbm	+1.8, -1.4 db	
36	Performance Margin	+37.0 db	+7.9, -5.7 db	

COMMENTS:

The modulation indices shown above for Mode 1 telemetry data are identical to those previously derived in Section 4.1.4.2. The ranging-signal phase deviation of 0.47 radian was chosen in an attempt to achieve threshold operation simultaneously for all channels; i.e., tracking, ranging, sync, and data. Although the above choices of modulation indices are not optimum, the techniques described in Section 4.1.4.2 could be applied to achieve the desired results.

The modulation losses for each channel are:

1) Carrier Modulation Loss:

$$\frac{P_c}{P_t} = J_0^2(\phi_d)\cos^2\phi_s\cos^2\phi_r$$

$$\frac{P_c}{P_t} = (-4.1 \text{ db } {}^{+0.9}_{-0.9}) + (-0.6 \text{ db } {}^{+0.1}_{-0.1}) + (-1.0 \text{ db } {}^{+0.2}_{-0.2})$$

$$\therefore \quad \frac{P_c}{P_t} = -5.7 \text{ decibel } {}^{+1.2}_{-1.2}$$

2) Mode 1 Data Channel Modulation Loss:

$$\frac{P_d}{P_t} = 2J_1^2(\phi_d)\cos^2\phi_s\cos^2\phi_r$$

$$\frac{P_d}{P_t} = (-2.7 \text{ db } {}^{+0.4}_{-0.6}) + (-0.6 \text{ db } {}^{+0.1}_{-0.1}) + (-1.0 \text{ db } {}^{+0.2}_{-0.2})$$

$$\therefore \quad \frac{P_d}{P_t} = -4.3 \text{ decibel } {}^{+0.7}_{-0.9}$$

3) Mode 1 Sync Channel Modulation Loss:

$$\frac{P_s}{P_t} = J_0^2(\phi_d)\cos^2\phi_r\sin^2\phi_s$$

$$\frac{P_s}{P_t} = \left(-4.1 \text{ db } {}^{+0.9}_{-0.9}\right) + \left(-1.0 \text{ db } {}^{+0.2}_{-0.2}\right) + \left(-9.5 \text{ db } {}^{+0.7}_{-0.8}\right)$$

$$\therefore \quad \frac{P_s}{P_t} = -14.6 \text{ decibel } {}^{+1.8}_{-1.9}$$

4) Ranging Channel Modulation Loss--The modulation loss for this channel is defined as the ratio of the power in the DSIF received clock channel to the total received signal. In order to evaluate this loss, it is necessary to determine the ranging power to the total transmitter power [P (limiter output) / P (transmitted)], the limiter suppression factor [P(ranging)/P(limiter output)], and the transmitted clock to total ranging channel power [P(clock)/P(ranging)]. The total modulation loss is equal to the sum of the above components or P (clock)/P (transmitted).

The component P(limiter output)/P(transmitted) is the fraction of the total transmitted power in the sidebands produced by the ranging signal at the video limiter output of the spacecraft's ranging unit. Using the modulation indices quoted earlier, this loss is determined from the following expression:

$$\frac{P_r}{P_t} = J_o^2 (\phi_d) \cos^2 \phi_s \sin^2 \phi_r$$

$$\frac{P_r}{P_t} = (-4.1 \text{ db } {}^{+0.9}_{-0.9}) + (-0.6 \text{ db } {}^{+0.1}_{-0.1}) + (-6.9 \text{ db } {}^{+0.6}_{-0.8})$$

$$\therefore \quad \frac{P_r}{P_t} = -11.6 \text{ decibel } {}^{+1.6}_{-1.8}$$

Using the uplink ranging signal-to-noise ratio of +9.0 decibels ${}^{+4.4}_{-3.4}$ (Table 4.1.4-28), the limiter suppression loss for a hard limiter, whose

input is a ranging signal and Gaussion noise, can be obtained from Figure 4.1.4-41.

Hence,

$$\frac{P\ (\text{ranging})}{P\ (\text{limiter output})} = 0 \text{ decibel } {}^{+0}_{-0.5}$$

The remaining component, P(clock)/P(ranging), is assumed to be -12.0 decibel as stated in JPL Memo TM 3361-64-1.

Thus, the total modulation loss:

$$\frac{P(\text{clock})}{P(\text{transmitted})} = (-11.6 \text{ decibel}^{+1.6}_{-1.8}) + (0.0 \text{ decibel}^{+0}_{-0.5}) + (-12.0 \text{ decibel}^{+0}_{-0})$$

$$\frac{P(\text{clock})}{P(\text{transmitted})} = -23.6 \text{ decibel}^{+1.6}_{-2.3}$$

Supporting Analysis

Ranging Threshold--A threshold signal-to-noise ratio in $2B_{LO}$ of 6 decibel has been used for the ranging clock loop. Assuming the loop has been designed for a threshold of 0 decibel in $2B_{LO}$ of 0.8 cps, the corresponding signal-to-noise ratio in $2B_L$ was estimated to be 4.3 decibels. Hence, the loop phase error (σ) is:

$$\sigma^2 = \left(\frac{N}{S}\right)_{2B_L} = \frac{1}{2.67} = 0.374 \text{ radian}^2$$

$\therefore \sigma = -.61$ radian = 35 degrees (rms)

Thus, the probability of loss of lock $\left[P\ (\sigma > |90^\circ|) \right]$ is 5×10^{-3}.

Acquisition Analysis--For a 6-decibel signal-to-noise ratio in the ranging code tracking loop, the total acquisition time will be on the

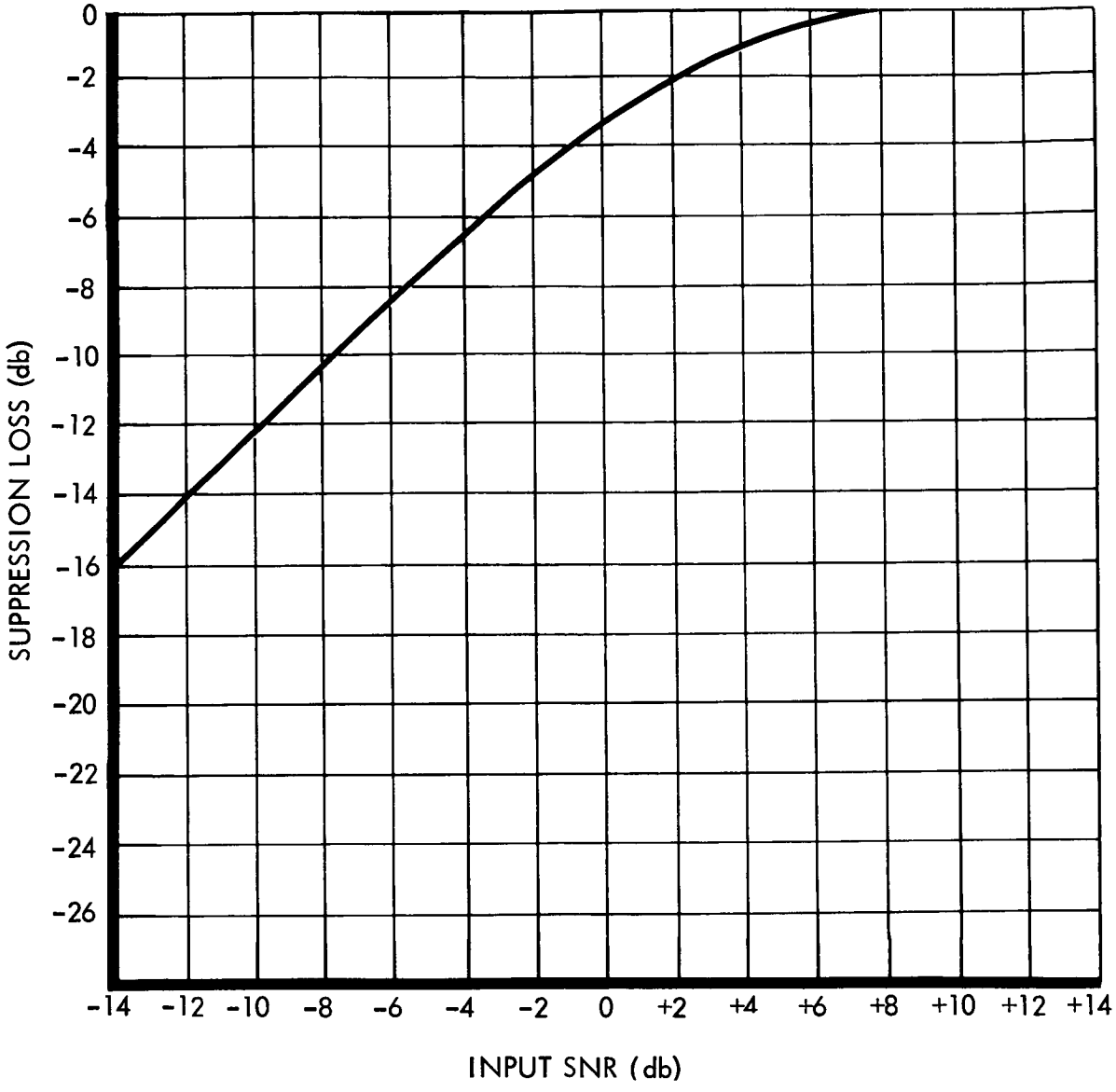

Figure 4.1.4-41: Ranging Signal Suppression Loss For a Hard Limiter Whose Input is a Ranging Signal and Gaussian Noise

order of 330 seconds for the complete code with a 10^{-3} probability of false sync. This appears to be an acceptable acquisition time. A complete acquisition analysis has been made and is contained in Philco Report WDL-TR-2531, "Mars Mission Communication Analysis."

Earth - Spacecraft Ranging Link, Cruise; Spacecraft: Low-Gain Antenna, Preamplifier; DSIF: 85-foot Antenna, 10 Kilowatts--The performance of this link is analyzed in Table 4.1.4-28. In this mode, the DSIF transmitter is modulated with a PN range code sequence only; no commands are transmitted during a range code word transmission period. The carrier and ranging modulation losses and tolerances were described above in "Link Parameter Derivations". The bandwidth required for turn-around range code transmission is 2.2 Mc/s, and the noise power is -106.5 dbm with tolerances of +1.8 decibel and -1.0 decibel. The communication distance used in computing the space loss is 8×10^5 kilometers, the desired operating range.

Spacecraft - Earth Ranging and Telemetry Link, Mode 1, Cruise; Spacecraft: Low-Gain Antenna, 50-Watt Transmitter; DSIF: 85-foot Antenna, Maser--In turn-around ranging, the ranging code is modulated on the spacecraft carrier with the Mode 1 data and the sync subcarriers. As shown previously, the ranging modulation loss is $-11.6\ ^{+1.6}_{-1.8}$ decibel, and the ranging threshold signal-to-noise ratio is 6.0 decibels. The loop bandwidth for the ranging clock loop is 0.8 cps in the nominal and best case, and 1.0 cps in the worst case. The design control table for this mode has been prepared as Table 4.2.4-29. Ranging channel performance is graphed in Figure 4.1.4-42, which shows grey-out to occur at 21 days or 5.3×10^6 kilometers.

It is possible to extend the grey-out distance for the turn-around ranging unit by using the spacecraft high-gain antenna and/or the 100-kilowatt transmitter. The 100-kilowatt transmitter improves the uplink output signal-to-noise ratio by 10 decibels, while the high-gain antenna offers 33.3 decibels improvement in downlink antenna gain and 31.1-decibel improvement in uplink gain. Although neither case was evaluated in detail, it was estimated that grey-out range can be extended almost to encounter by using both the high-gain antenna and the 100-kilowatt DSIF transmitter.

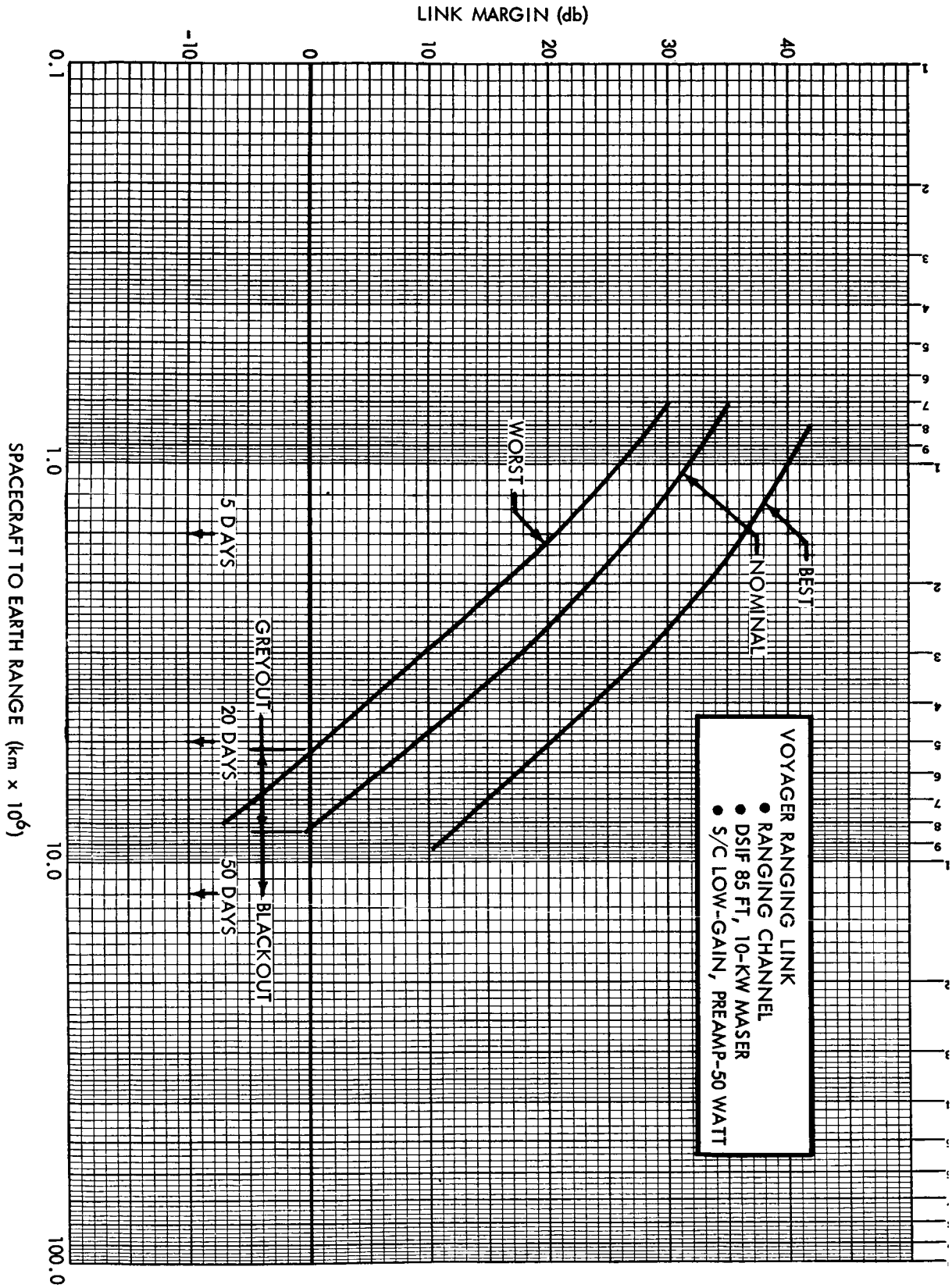

Figure 4.1.4-42:

4.1.5 Spacecraft Reliability Analysis

This section summarizes the reliability analysis performed on the preferred telecommunications system configuration. The reliability parameters for the system are presented for the basic functions performed during the mission and according to hardware delineation. A reliability mathematical model of the functional flow is presented in conjunction with mission time requirements derived from the mission profile.

Reliability Analysis Results--The reliability assessment for the total telecommunication functional capability of the preferred design is estimated at P_s (t) = 0.8416 for a mission time of t = 5880 hours. Comparison of the requirements and estimates by telecommunication subsystem are as follows:

Nomenclature	Time Estimate t: hours	Probability $P_s(t)$
Telecommunications Systems	5880	0.8416
Spacecraft Radio Subsystem	5880	0.9738
Spacecraft Relay Radio Subsystem	217	0.9945
Telemetry and Data Storage Subsystem	5880	0.8833
Antenna Subsystem	5880	0.9838

The reliability parameters are delineated in tabular form in Figure 4.1.5-1 according to both function and subsystem. The preferred configuration is also shown in the same figure in a reliability functional flow format that identifies the redundancy implemented and the subsystem partitioning. Note in Figure 4.1.5-1 that the reliabilities of the cruise science, capsule, and planetary data functions are higher than engineering data. The

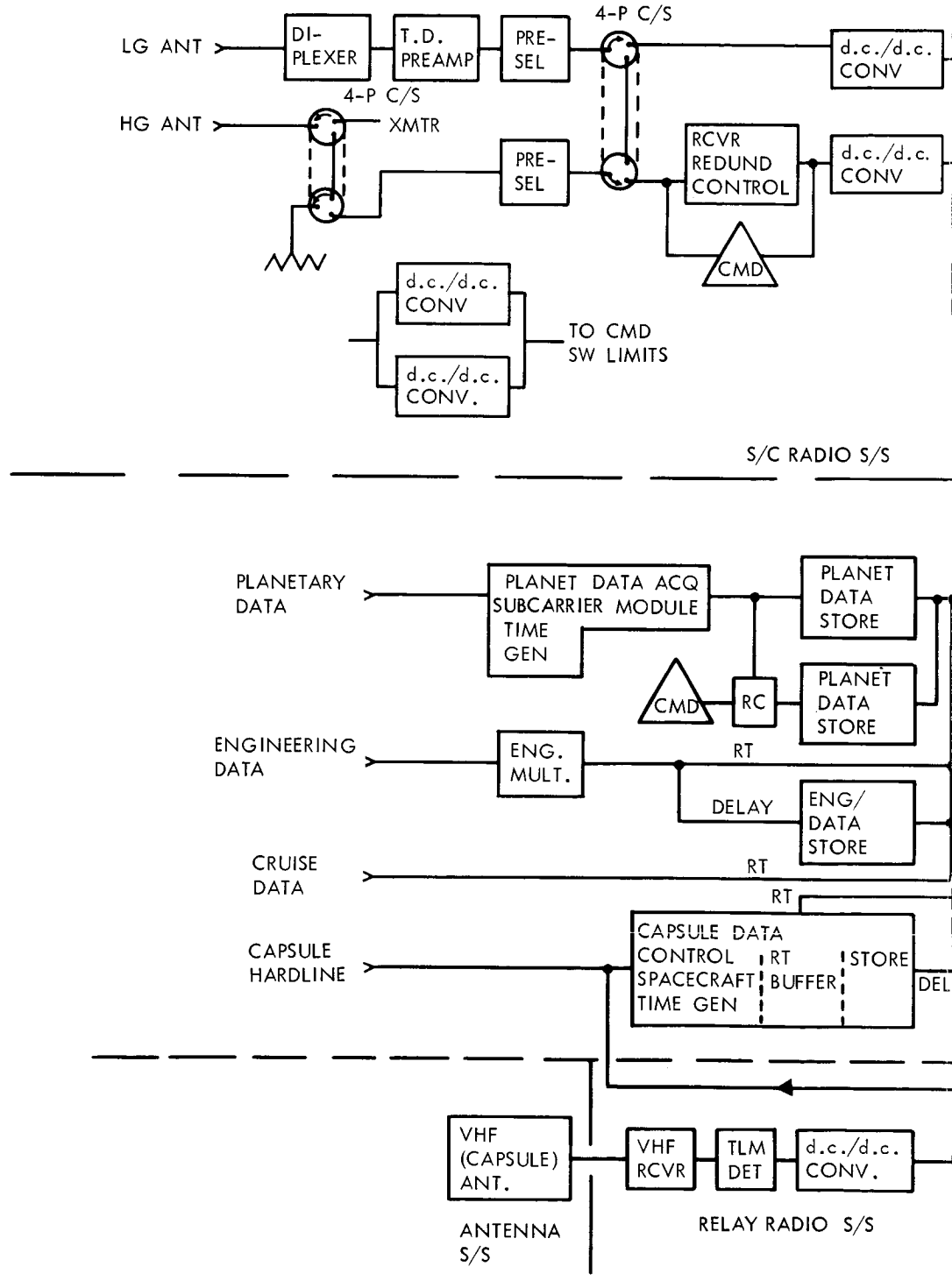
LG ANT
DI-PLEXER
T.D. PREAMP
PRE-SEL
4-P C/S
d.c./d.c. CONV
HG ANT
4-P C/S
XMTR
PRE-SEL
RCVR REDUND CONTROL
d.c./d.c. CONV
CMD
d.c./d.c. CONV
d.c./d.c. CONV.
TO CMD SW LIMITS
S/C RADIO S/S
PLANETARY DATA
PLANET DATA ACQ SUBCARRIER MODULE TIME GEN
PLANET DATA STORE
CMD
RC
PLANET DATA STORE
ENGINEERING DATA
ENG. MULT.
RT
DELAY
ENG/ DATA STORE
CRUISE DATA
RT
RT
CAPSULE HARDLINE
CAPSULE DATA CONTROL SPACECRAFT TIME GEN
RT BUFFER
STORE
DEL
VHF (CAPSULE) ANT.
VHF RCVR
TLM DET
d.c./d.c. CONV.
ANTENNA S/S
RELAY RADIO S/S

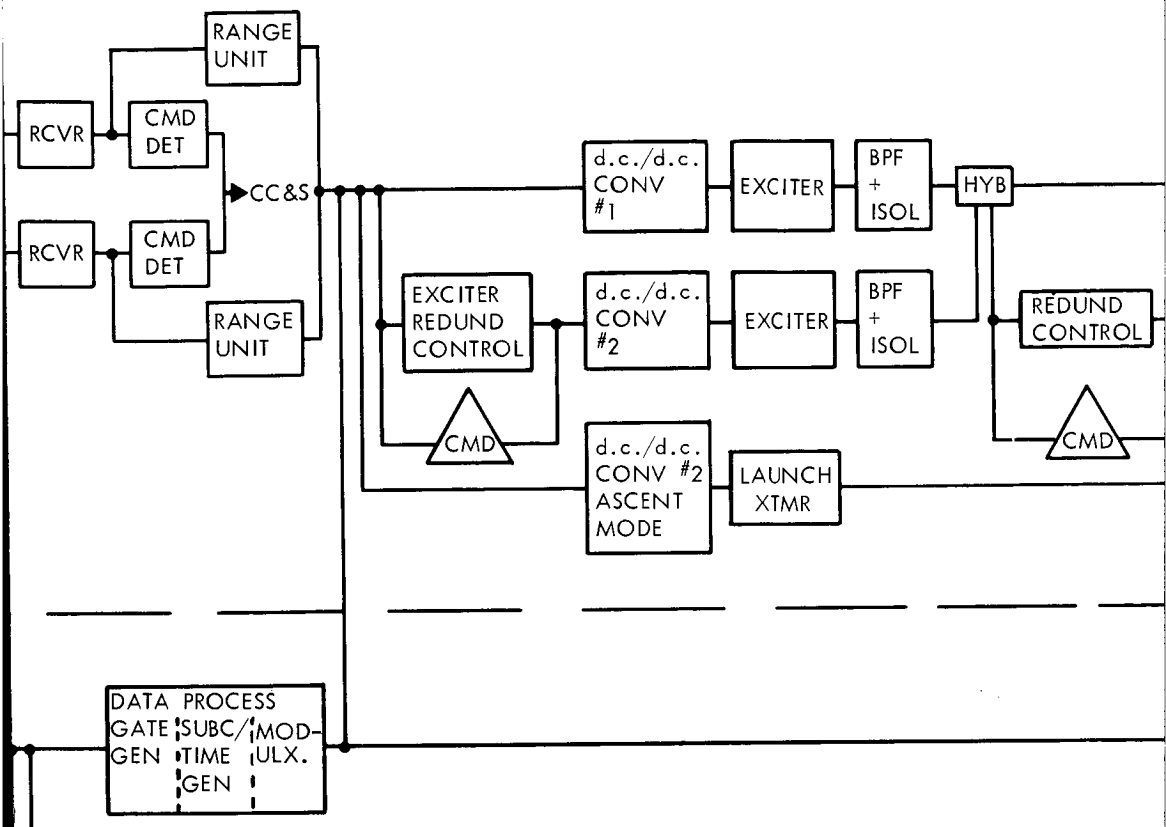

Summary Table Of Preferred Design
Functional Reliabilities Spacecraft
Telecommunications System

FUNCTION	RADIO SPACECRAFT	RELAY RADIO SPACECRAFT	TLM & DATA SPACECRAFT	ANTENNA SPACECRAFT	T S
Command	0.9947			0.9866	
Ranging	0.9744			0.9997	
Telemetry	0.9873	0.9988	0.8849	0.9864	
Telemetry Subfunction					
Capsule RT	0.9873	0.9988	0.9637	0.9864	
Sto	0.9873	0.9988	0.9636	0.9864	
Engr Rt	0.9873		0.9675	0.9867	
Sto	0.9873		0.9674	0.9867	
Cruise Rt	0.9873		0.8994	0.9867	
Planetary	0.9873		0.9648	0.9867	
Subsystem Totals	0.9810	.9998	0.8849	0.9864	
Subsystem Totals *	0.9738	.9945	0.8833	0.9838	
	Requirement Allocation				

* With Mission Environmental Stress Factors

Figure 4.1.5-1:

2

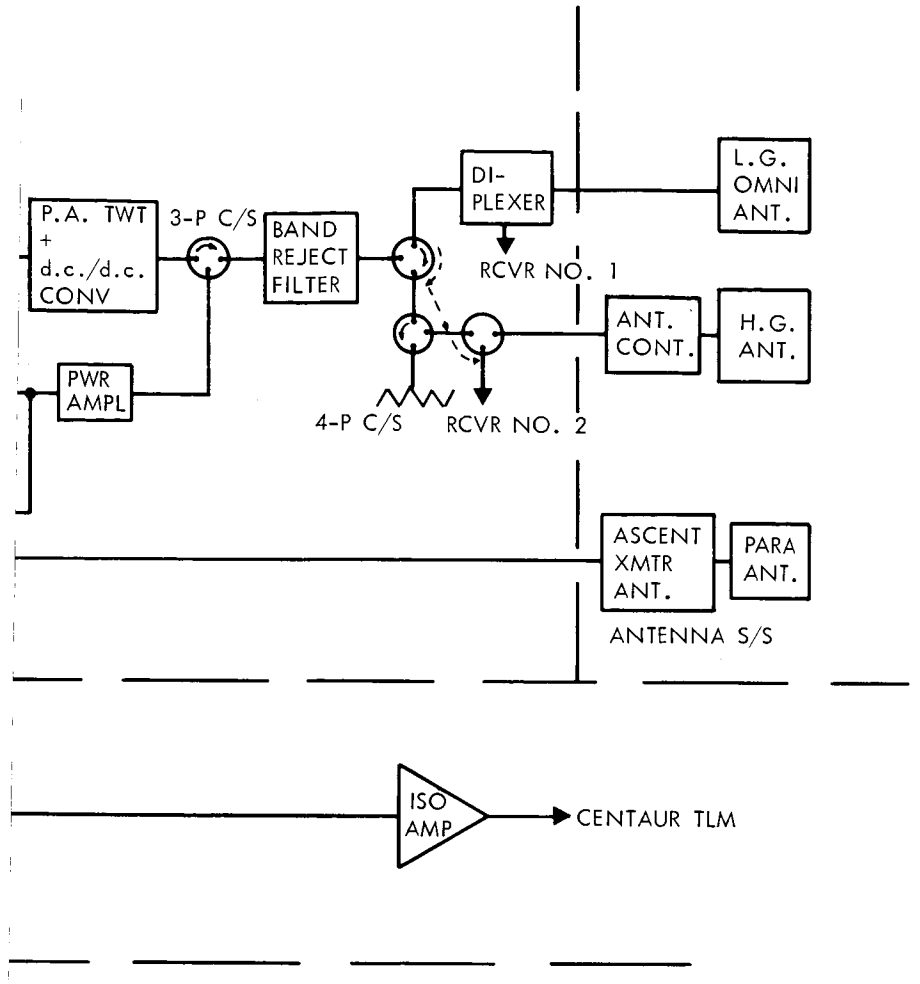

OTALS YSTEM
).9813
).9741
).8608
).9374
).9373
).9425
).9424
).8761
).9399
0.8554
0.8416
0.905

Spacecraft Telecommunications System Reliability Model

reliability estimates are based on a parts count, design analysis, and the part failure rates as defined in the "Voyager 1971 Program Reliability Analysis and Prediction Standard," D2-23834-1, Revision A.

The redundancy allowed in the preferred design has been conservative to prevent excessive switching and redundancy control complexity. Delineation of the mission reliability goals according to criticality, inherent reliability, and backup of specific functions in conjunction with basic reliability improvements of parts, materials, and further design mechanization trades is a major area for further investigation.

Redundancy Considerations--The telecommunication preferred design has the following redundancy:

1) Standby command receiver, command detector, and ranging unit
2) Standby exciter
3) Standby power amplifier
4) Standby planetary tape recorder
5) Subcomponent redundancy in the analog gates of the engineering data analog multiplexer.

Subsystem Reliability Summary--The following paragraphs summarize the reliability assessments of each telecommunications subsystem. For details of the analysis refer to D2-82724-1, "Voyager Reliability."

Radio Subsystem Reliability Assessment--The preferred spacecraft radio subsystem reliability model is shown in Figure 4.1.5-2. The reliability of the radio subsystem has been estimated at $P_s(t) = 0.9738$ for 5880 hours operation.

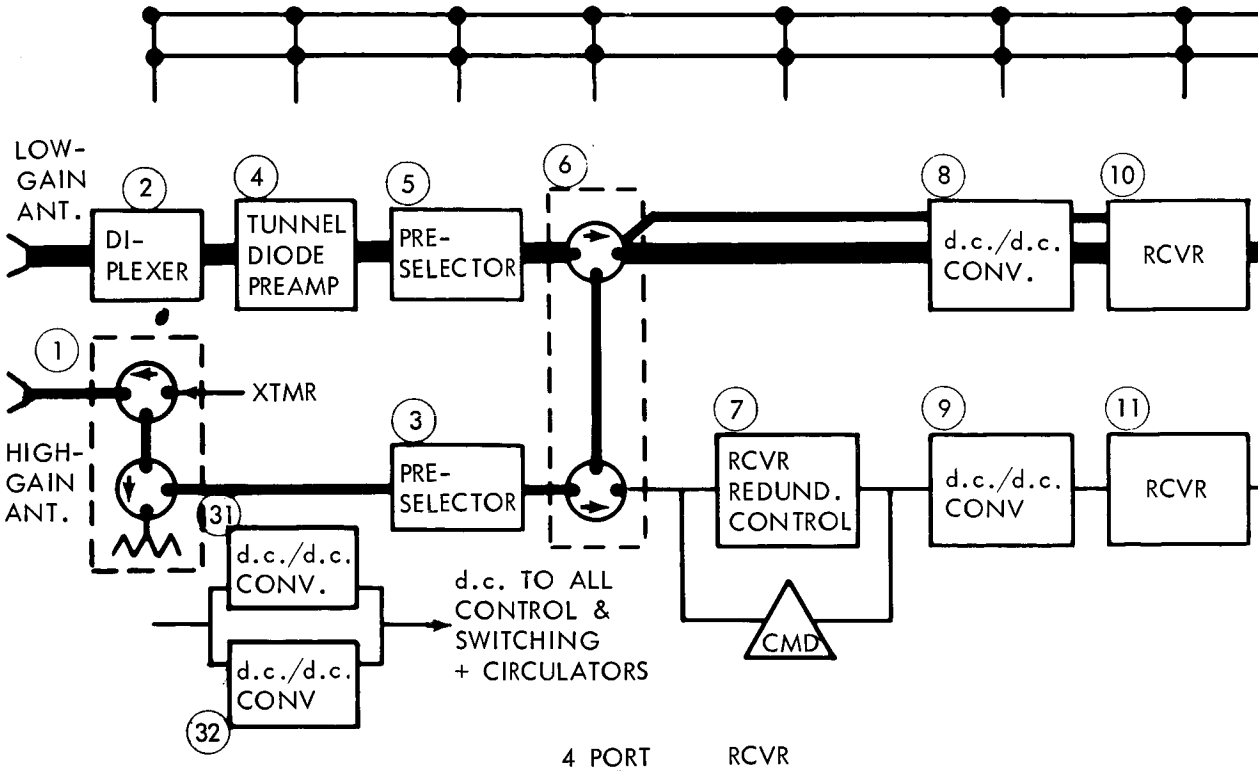

	DI-PLEXER	TDA	PRE-SELECTOR	4 PORT CIRC SW	RCVR REDUND CONTROL	d.c./d.c. CONV	RCVR
FAILURES: λ	10	95.1	7	42.2	200	85	1285
MISSION TIME: t	5880	5880	3480	5880	5880	5880	5880
λ t	0.0006	0.0056	0.00021	0.0025	0.0118	0.0050	0.0756
P_s (t)	0.9994	0.9944	0.99979	0.9975	0.9883	0.9950	0.9272

	4 PORT CIRC SW	d.c./d.c. CONV	REDUND. d.c./d.c. CONV. 31,32		CMD		REDUND. 8, 10, 12, 14
FAILURES: λ	42.2	82					89.12
MISSION TIME: t	5880	5880	5880				5880
λ t	0.0025	0.0048	0.0000231				0.00524
P_S (t)	0.9975	0.9952	0.9999769		0.99		0.99476

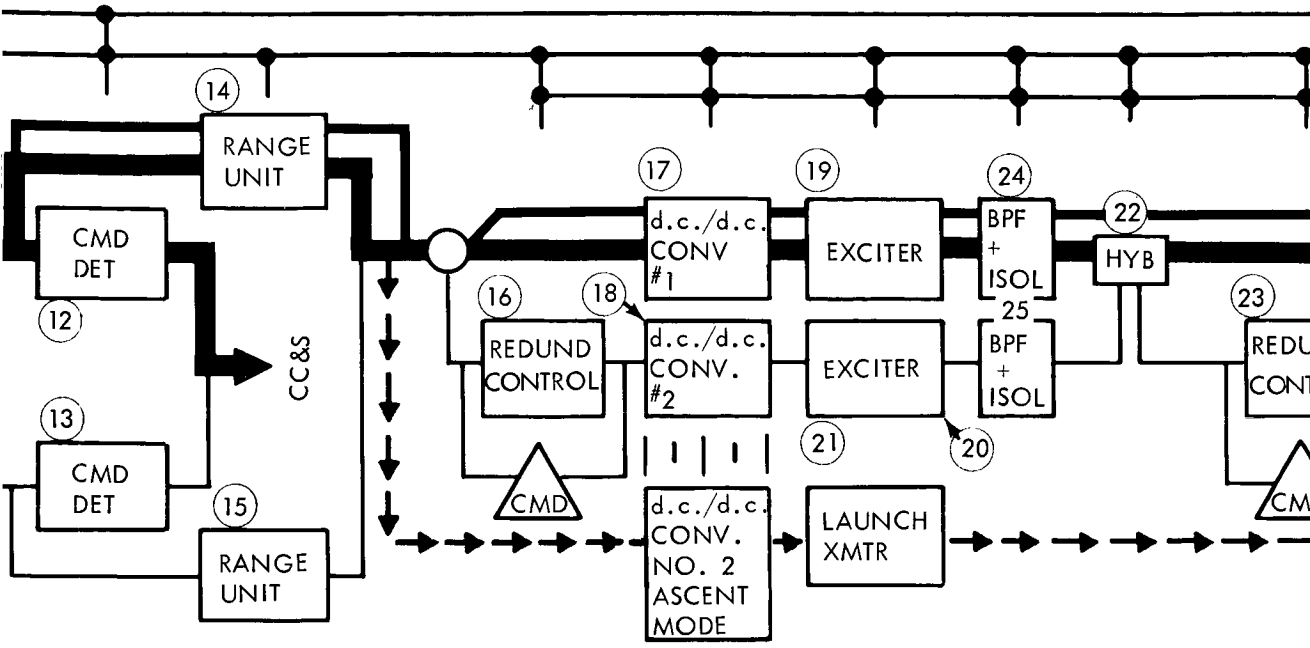

CMD DET	RANGE UNIT	REDUND. CONTROL	d.c./d.c. CONV	EXCITER	BPF + ISOL	HYBRID	RED CO
243	65	182	82	278.2	30	20	
5880	240	5760	5760	5760	5760	5760	5
0.0143	0.0002	0.0105	0.0048	0.0160	0.0017	0.0012	0.
0.9858	0.9998	0.9896	0.9952	0.9841	0.9983	0.9988	0

				LAUNCH XTMR	REDUND. 17, 19, 24		
				291.9	7.99		
				120	5760		
				0.0004	0.00046		
				0.9996	0.99954		

RADIO SUBSYSTEM RELIABILITY SUMMARY TABLE

Subsystem Single Thread	$P_S(t) = 0.7854$
Preferred Design	$P_S(t) = 0.9810$
Subsystem With Environmental Stress Factors	$P_S(t) = 0.9738$
FUNCTIONS	
Command To CC&S	$P_S(t) = 0.9947$
Telemetry Transmission	$P_S(t) = 0.9873$
Ranging	$P_S(t) = 0.9744$

Fig

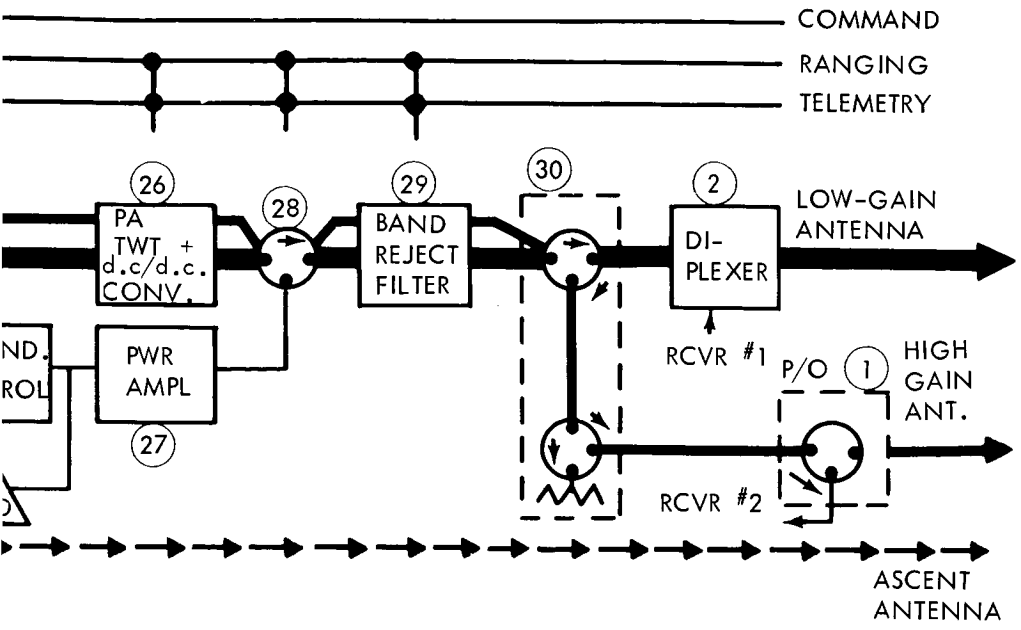

UND. NTROL	PWR AMPL	3 PORT CIRC SW	BAND REJECT FILTER	4 PORT CIRC SW	
82	2092	21.1	10	42.2	FAILURES/10^8 HRS
'60	5760	5760	5760	5760	HOURS
)105	0.1205	0.0012	0.0006	0.00243	
9896	0.8865	0.9988	0.9994	0.99757	

	REDUND PWR AMPL
	118.6
	5760
	0.00683
	0.99317

FLOW CODE

ON-LINE FUNCTIONAL FLOW TO L.G. UTILIZATION

H.G. ANT. UTILIZATION ON-LINE FLOW

ASCENT TRANSMIT ON-LINE MODE

ıre 4.1.5-2: Spacecraft Radio Subsystem Reliability Model

Spacecraft Relay Radio Subsystem Reliability--The single-thread reliability model for the relay radio subsystem is shown in Figure 4.1.5-3. The current estimate of reliability is $P_s(t) = 0.9838$ for $t = 217$ hours. The preferred design does not have redundancy in the relay radio subsystem. The overall telecommunications reliability goal can be most effectively addressed by reliability improvements to the highest risk subsystems for a given weight penalty. The relay radio subsystem in terms of its complexity and functional requirements does not warrant redundancy until detail reliability improvement mechanization is addressed in the high-complexity subsystems.

Spacecraft Telemetry and Data Storage Subsystem--The reliability model for the telemetry and data storage subsystem is shown in Figure 4.1.5-4.

The table in Figure 4.1.5-4 is a summary of the estimates according to function for the preferred redundant configuration. The current estimate of reliability is $P_s(t) = 0.8833$ for 5880 hours. Redundancy improvements resulted in an overall improvement of 1.65 in the subsystem reliability. The weak links were in the engineering multiplexer encoder component (digital multiplexer subcomponent) planetary recorder, and the subcarrier timing generator. Additional system-level reliability trades must be accomplished in Phase IB to determine the degree of redundancy that should be incorporated in this subsystem. Several alternative mechanizations are described in Boeing Document D2-82709-2.

Spacecraft Antenna Subsystem--The reliability model for the antenna subsystem is shown in Figure 4.1.5-3 with functional delineations, reliability parameters, the mathematical model, and the mission times.

RELAY RADIO SUBSYSTEM

ANTENNA SUBSYSTEM

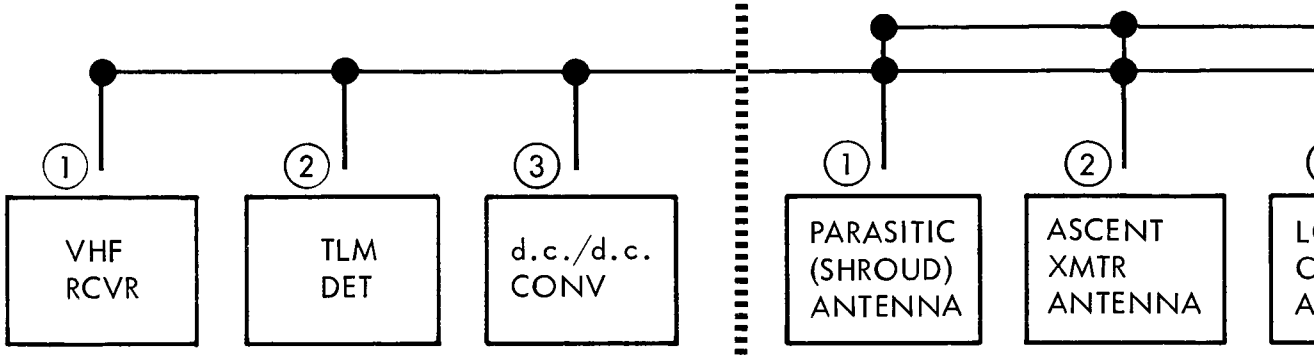

	VHF RCVR	TLM DET	d.c./d.c. CONV
FAILURES λ	318	163	85.4
MISSION TIME: t	217	217	217
λt	0.00069	0.00035	0.00019
P_S (t)	0.99931	0.99965	0.99981

	PARA ANT.	ASCENT ANT.
FAILURES: λ	50	25
MISSION TIME: t	0.06	120
λt	0.00000003	0.00003
P_S (t)	0.99999997	0.99997

ANTENNA MODES

MODES:	1	2	3	4	5	6	CAP TLM	CMD	RAN	TLM
Launch/Ascent	+	+					+		+	+
Cruise/Lo-Gain			+				+	+	+	+
Cruise/Hi-Gain				+	+		+	+		+
Plan. Orbit				+	+			+		+
Capsule Relay										
Post-Sep				+	+	+	+			
Post-Land				+	+	+	+			

RELAY RADIO MODES

Bit Rate	Attenuate High	Attenuate Low	Mode
High	+	+	P-Sep (192 HOURS)
Low		+	P-Land (25 HOURS)

1

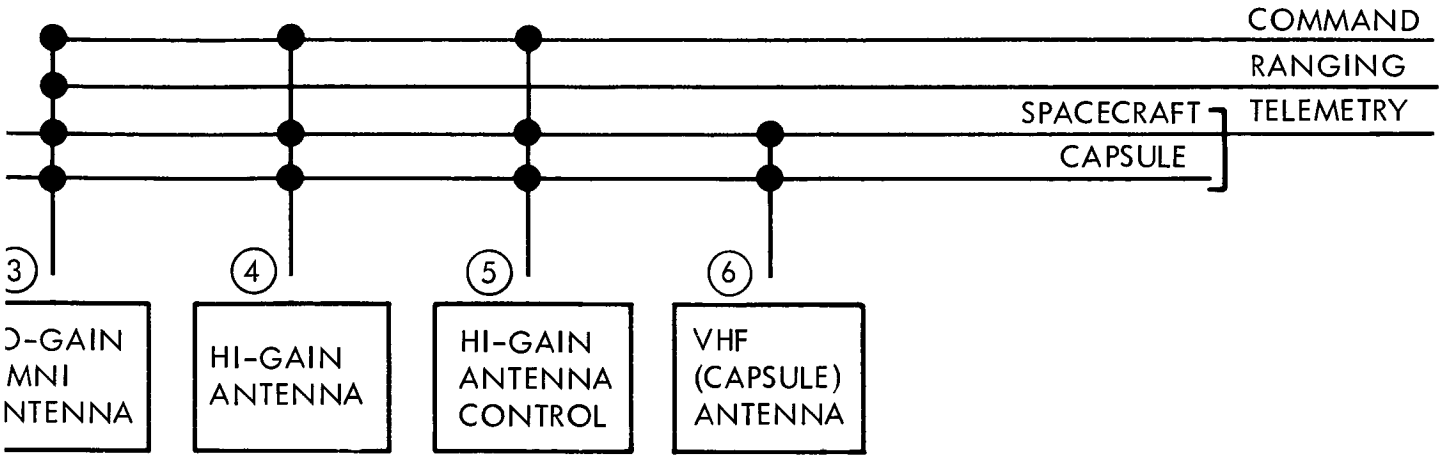

LO-GAIN ANT.	HI-GAIN ANT.	ANT. CONTROL	VHF ANT.	
130	44	250	119	$F/10^8$ hrs
2376	3480	3480	217	HOURS
0.00313	0.0015	0.0087	0.00023	
0.99687	0.9985	0.9913	0.99977	

RELIABILITY SUMMARY TABLE

tenna Subsystem P_S (t)

)system Single Thread - $P_S(t) = P_1P_2P_3P_4P_5P_6 = 0.9866$

mmand Single Thread - $P_S(t) = P_3P_4P_5P_6 = 0.9866$

emetry Single Thread - $P_S(t) = P_1P_2P_3P_4P_5P_6 = 0.9866$

)ging Single Thread - $P_S(t) = P_3$ (240 hr) = 0.9997

ay Radio Subsystem

)gle Thread - $P_S(t) = P_1P_2P_3 = 0.9988$

al with Environmental
ess Factors $P_S(t) = 0.9945$

{ Total with environmental stress factors is $P_S(t) = 0.9838$

Figure 4.1.5-3: Spacecraft Antenna & Relay Radio Subsystems Reliability Model

2

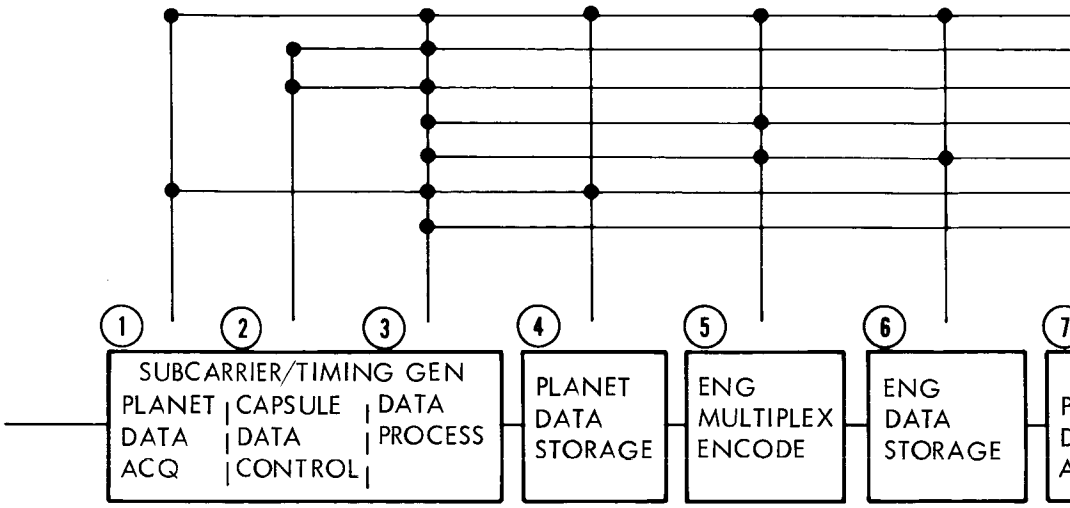

	PLANET DATA ACQ	CAP DATA CONT	DATA PROC	PLANET DATA STORE	ENG MULT/ENC	CRU/ENG DATA STORE	P D A
FAILURES: λ	300	40	288.2	2791	2250	1537	
MISSION TIME: t	720	5160	5880	720	5880	6	
λ t	0.0022	0.0021	0.0169	0.0201	0.1323	0.00009	
$P_s(t)$	0.9978	0.9979	0.9832	0.9801	0.8761	0.99991	

REDUNDANT ⟶ (STANDBY)* (QUAD GATES)*

FAILURES: λ	80.55	1239.6
MISSION TIME: t	720	5880
λ t	0.00058	0.072888
$P_s(t)$	0.99942	0.92960

TEL

FUN NO
TOTAL S
TOTAL SU MISSION STRESS FA
ENGIN REAL DELAY
PLANET
CAPSUL REAL DELAY
CRUISE REAL

*(4) STANDBY COMPONENT REDUNDANCY
(5) SUBCOMPONENT: QUAD ANALOG GATES

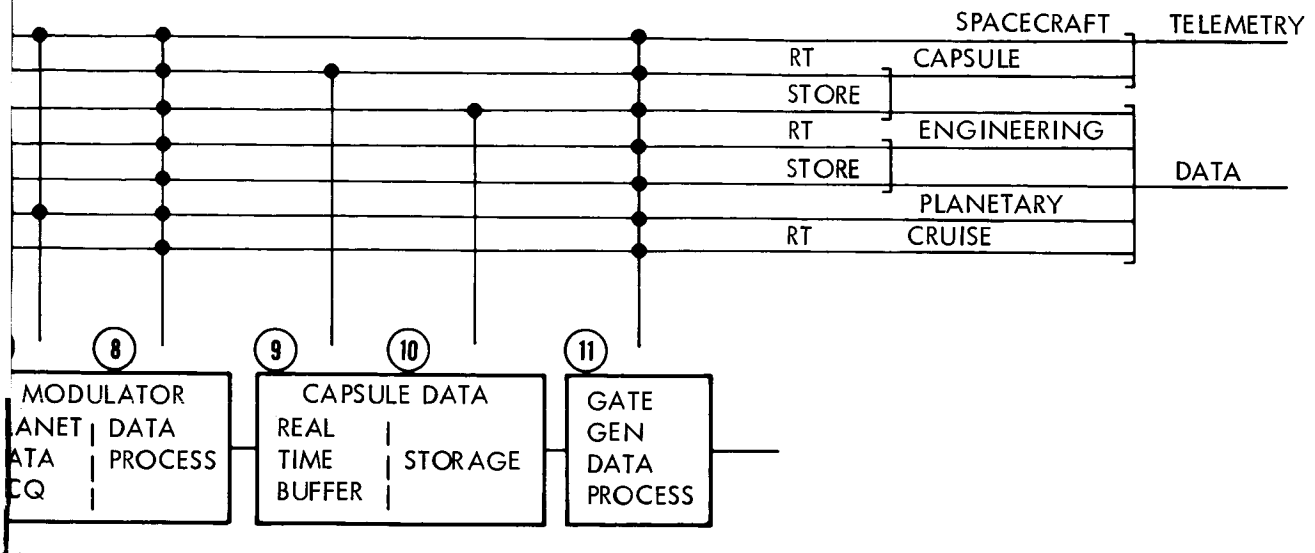

ANET ATA CQ	DATA PROC	REAL TIME	STORE	GATE GEN	
9.2	23.6	217	1537	250	$F/10^8$ HRS
720	5880	5160	6	5880	HOURS
00007	0.0014	0.0112	0.00009	0.0147	
99993	0.9986	0.9889	0.99991	0.9854	

EMETRY AND DATA STORAGE SUBSYSTEM RELIABILITY SUMMARY

CTIONAL ENCLATURE	PROBABILITY OF SUCCESS ESTIMATES		MISSION TIME t HOURS
	SINGLE THREAD	REDUNDANT*	
BSYSTEM	$P_S(t) = 0.8177$	$P_S(t) = 0.8849$	5880
SYSTEM WITH ENVIRONMENTAL CTORS		$P_S(t) = 0.8833$	
ERING DATA ME ED	 0.8476 0.8476	 0.8994 0.8993	 5880 5880/6
RY DATA	0.9461	0.96476	720
DATA ME D	 0.9637 0.9636	 NOT APPLICABLE NOT APPLICABLE	 5160 5160/6
CIENCE ME	 0.9675	 0.8994	 5880

Figure 4.1.5-4: Spacecraft Telemetry & Data Storage Subsystem — Reliability Model

An estimate of $P_s(t) = 0.9839$ has been calculated for the preferred design.

Environmental Hazards--The major reliability hazards in the antenna subsystem are environmental stresses and multipactor effects.

1) Environmental Hazard--The retention of pointing accuracy after being subjected to the environmental stresses of boost, maneuvers, and Mars orbital injection is a basic problem that will require concentrated attention in design and test.

2) Multipactor Hazard--In rf systems incorporating rf power levels in the order of 25-30 watts or greater at UHF/S-band frequencies, consideration must be given to possible multipactor phenomenon and its effects. Testing programs are required in conjunction with a design review of rf hardware to determine if the equipment may be susceptible to the multipactor effect.

CONTENTS

4.2 ELECTRICAL POWER

4.2.1 Scope

The power subsystem provides electrical energy from a solar array and from secondary storage batteries for operation of spacecraft subsystems during the various phases and maneuvers of the mission. The major elements of the electrical power subsystem are shown in a simplified block diagram, Figure 4.2-1. These same major elements are shown in the isometric of Figure 4.2-2 as they relate to the spacecraft configuration. A subsystem with a total weight of 457 pounds results from this preliminary design. The Electrical Power Subsystem is designed to perform the functions highlighted on the accompanying Mission Sequences Matrix.

Investigation was made of electrical power requirements for the 1971 through 1977 Voyager missions. A solar/photovoltaic/battery system was verified as the optimum choice for the Voyager mission. The solar array design employs N on P solar cells to provide 396 watts to the spacecraft loads from 236 square feet of panel area. Wiring of the solar panels has been arranged to minimize magnetic interference.

A silver-cadmium battery, rated at 2460 watt hours capacity, is arranged in 3 identical sections of 38 cells each. The conservative battery design is intended to support up to 2.9 hours of predicted off-Sun operation (occultation during Mars orbit) with sufficient reserve capacity to handle unscheduled extensions of such periods. Battery size and circuit operation have been chosen such that the mission can be successfully completed with any two of the three battery sections operating.

Basic power regulation is accomplished by redundant series switching regulators within the electrical power subsystem, with supplemental power

Figure 4.2-1: Electrical Power Subsystem Simplified Functional Diagram

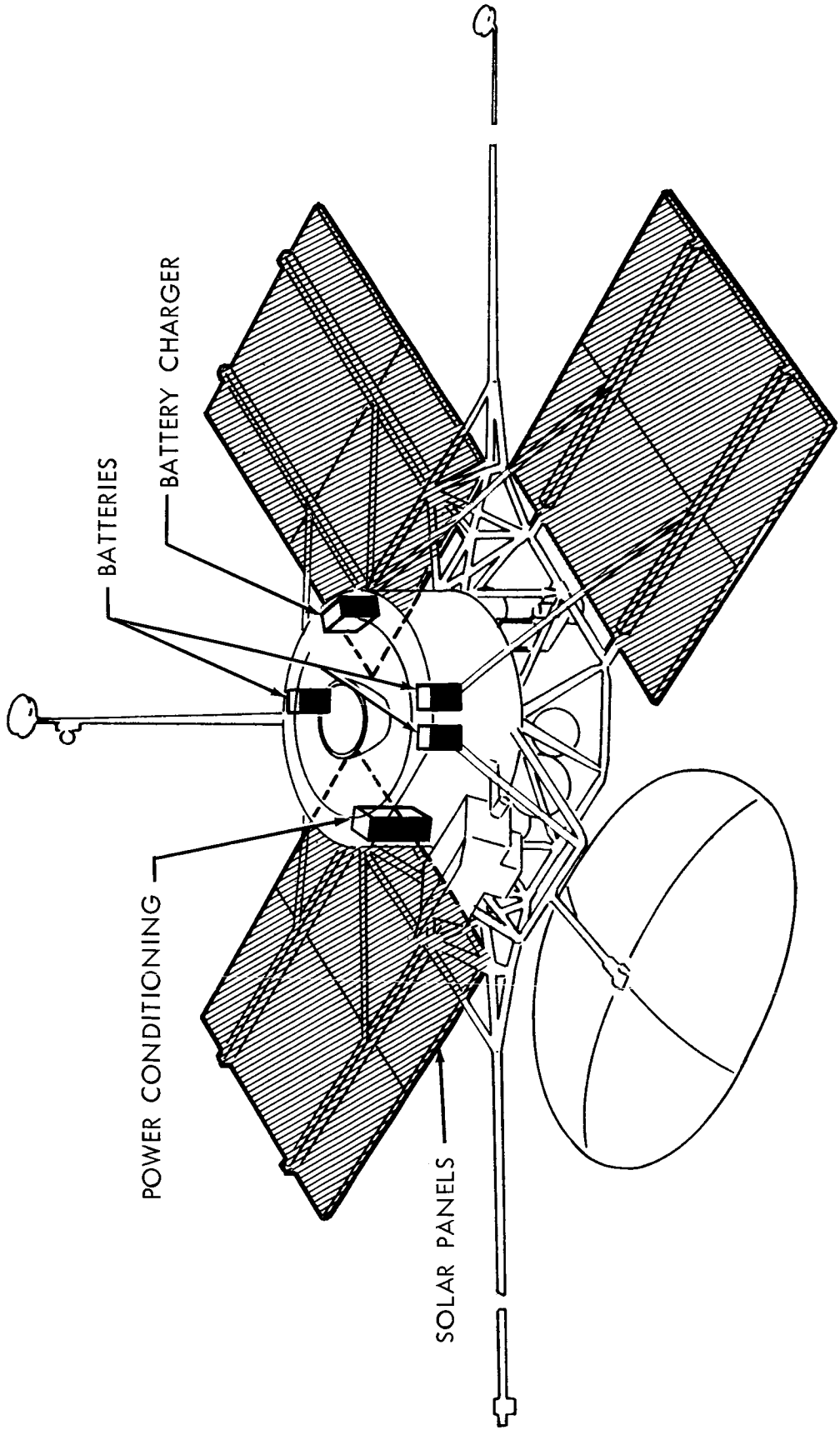

Figure 4.2-2: Electrical Power Subsystem

1.0
PRELAUNCH
AT ETR

GROUND COMPLEX (MOS, LOS, & DSN)	OPERATIONAL READINESS TEST, S/C-DSN COMPATIBILITY TEST SCHED & COORD ETR ACTIVITIES C/O & SUPPORT MOS (DSN ONLY) LOAD CC&S WITH FLIGHT PROGRAM
SPACECRAFT TELECOMMUNICATIONS	SUBSYSTEM C/O & STATUS MONITORING
CENTRAL COMPUTER & SEQUENCER (CC&S)	A) SUBSYSTEM C/O & STATUS B) COMMAND OTHER SUBSYSTEMS FOR C/O & STATUS MONITORING C) READY ALL SUBSYSTEMS FOR LAUNCH D) LOAD CC&S WITH FLIGHT PROGRAM
ATTITUDE REFERENCE SUBSYSTEM AUTOPILOT SUBSYSTEM REACTION CONTROL SUBSYSTEM (RCS)	SUBSYSTEM C/O & STATUS MONITORING
MIDCOURSE CORRECTION PROPULSION SYSTEM ORBIT INJECTION PROPULSION SYSTEM	SUBSYSTEM C/O & STATUS MONITORING
ELECTRICAL POWER SUBSYSTEM	SUBSYSTEM C/O & STATUS MONITORING
S/C STRUCTURE SUBSYSTEM S/C MECHANISMS SUBSYSTEM INSTALLATION CABLES & TUBING	SUBSYSTEM C/O & STATUS MONITORING
TEMPERATURE CONTROL SUBSYSTEM	SUBSYSTEM C/O & STATUS MONITORING SPACECRAFT COOLING SUPPLIED BY CENTAUR
PYROTECHNIC SUBSYSTEM	SUBSYSTEM C/O & STATUS MONITORING
SCIENCE EXPERIMENTS (GFE)	SUBSYSTEM C/O & STATUS MONITORING S/C MAGNETIC MAPPING (FAT)
DATA AUTOMATION EQUIPMENT (GFE)	

2.0 LAUNCH & INJECTION (INCLUDES COUNTDOWN)	3.0 ACQUISITION
MOS/LOS A) COMMAND LIFTOFF B) TRACK VEHICLE DURING BOOST C) SUPPLY FLIGHT COMMANDS (AS REQ) D) RECEIVE & ANALYZE DATA FROM DSN S/C & BOOSTER E) STANDBY ON ALERT F) COMMUNICATE WITH ETR CHANGE FROM MOS/LOS TO DSN CONTROL ON INJECTION INTO TRANSMARS ORBIT A) PROVIDE SFOF/DSIF WITH ANTENNA DSN SEARCH DATA B) RECEIVE ANTENNA SEARCH DATA C) SEARCH FOR & ACQUIRE S/C D) ESTABLISH & VERIFY CONTROL OF S/C E) TRACK S/C (1-WAY) F) RECEIVE & ANALYZE ENGRG DATA	DSN A) MONITOR BOOSTER SEPARATION B) MONITOR SOLAR PANEL DEPLOYMENT C) MONITOR ANTENNA DEPLOYMENT D) PROVIDE COMMANDS TO BACK UP CC&S AS REQUIRED E) TRACK S/C F) REC DATA G) MONITOR SCIENCE DEPLOYMENT DSN H) MONITOR & VERIFY ACQUISITION OF SUN I) MONITOR & VERIFY ACQUISITION OF CANOPUS J) COMMAND REACQUISITION OF CANOPUS (AS REQD) K) MONITOR S/C TRAJECTORY L) UPDATE CC&S TRAJECTORY PARAMETERS FOR PITCH, YAW, & ROLL M) COMPUTE CC&S PITCH, YAW, & ROLL POLARITY
A) TRANSMIT ENGINEERING DATA VIA CENTAUR TELEMETRY B) TRANSMIT ENGINEERING DATA VIA LOW POWER LAUNCH EXCITER C) RECEIVE POWER FROM F/P	A) TRANSMIT ENGINEERING DATA B) RECEIVE POWER FROM F/F C) RECEIVE VIA LOW-POWER LAUNCH EXCITER DETECT & SEND TO CC&S COMMAND SIGNALS FROM EARTH D) TRANSMIT CELESTIAL REFERENCE ACQUISITION TO DSN E) TRANSMIT VERIFICATION OF DEPLOYMENT OF SOLAR PANELS, ANTENNAS, ETC TO EARTH F) TWO-WAY TRACKING
PROVIDE BACKUP COMMANDS AS REQUIRED	A) COMMAND SIGNALS TO PYROTECHNICS & MECH TO DEPLOY • SOLAR PANELS • HIGH-GAIN ANTENNA • VHF ANTENNA • LOW-GAIN ANTENNA • SCIENCE BOOM B) SWITCH ON GYROS & SELECT MODES C) ENABLE SUN-SENSOR ROLL AND PITCH CONTROL D) RECEIVE SUN PRESENCE SIGNAL E) TURN ON CANOPUS TRACKER F) SWITCH ROLL CONTROL TO CANOPUS SENSOR G) ACTIVATE MAGNETOMETER (CALIBRATION ROLL) H) RECEIVE CANOPUS PRESENCE OUTPUT SIGNAL I) TRANSMIT VERIFICATION TO TELE-COMMUNICATION SUBSYSTEM (CANOPUS & SUN PRESENCE) J) PERFORM COMMAND FUNCTIONS FOR CANOPUS OVERRIDE AS REQUIRED K) BACKUP COMMANDS AS REQUIRED
A) ATTITUDE REFERENCE — GYROS OFF DURING LAUNCH B) AUTOPILOT — OFF C) RCS — OFF	A) RECEIVE CC&S COMMAND SWITCH ON GYROS, RCS, & AUTOPILOT B) DAMP ROTATION C) YAW & PITCH SPACECRAFT TO ACQUIRE SUN D) RELAY SUN ACQUISITION SIGNAL TO CC&S E) TURN ON CANOPUS SENSOR, ROLL 360° TO CALIBRATE MAGNETOMETER F) ROLL TO ACQUIRE CANOPUS & PROVIDE STAR MAP G) RELAY ACQUISITION SIGNAL (CANOPUS) TO CC&S H) PERFORM CANOPUS OVERRIDE ROLL MANEUVER AS REQUIRED
A) PROVIDE ENGRG DATA FOR TELECOMUNICATIONS SUBSYSTEM B) PROVIDE BATTERY POWER TO: • TELECOMMUNICATIONS SUBSYSTEM • CC&S • ATTITUDE REFERENCE SUBSYSTEM • AUTOPILOT SUBSYSTEM	A) PROVIDE POWER TO PYROTECHNIC SUBSYSTEMS FOR SQUIB FIRINGS B) PROVIDE POWER TO MECHANISMS C) ACTIVATE SOLAR POWER SYSTEM AFTER SUN ACQUISITION (AUTOMATIC) D) TRANSMIT "VOLTAGE SATISFACTORY" SIGNAL TO CC&S E) PROVIDE POWER TO: • TELEMETRY • CC&S • TEMPERATURE CONTROL • AUTOPILOT
A) PROVIDE PHYSICAL SUPPORT FOR ALL EQUIPMENT B) PROVIDE ATTACHMENT FOR CAPSULE C) SUPPORT FLT CAPSULE	A) PROVIDE PHYSICAL SUPPORT FOR ALL EQUIPMENT B) DRIVE SOLAR PANELS TO LIMIT STOPS C) PROVIDE OUT & LOCK SIGNALS TO TELEMETRY D) DRIVE HIGH-GAIN ANTENNA TO OPERATING POSITION & LOCK E) DRIVE VHF & OMNI ANTENNAS TO OPERATING POSITION & LOCK F) DRIVE MAGNETOMETER BOOM TO OPERATING POSITION & LOCK G) SUPPORT FLT CAPSULE
A) PROVIDE HEAT SINK COOLING CAPABILITY UP TO SHROUD JETTISON B) TEMPERATURE CONTROL AFTER SHROUD JETTISON	PROVIDE TEMPERATURE CONTROL
	RECEIVE SQUIB FIRING SIGNALS FOR DEPLOYMENT OF: • SOLAR PANEL • MAGNETOMETER BOOM • LOW-GAIN ANTENNA • HIGH-GAIN ANTENNA • VHF ANTENNA
	A) CALIBRATE MAGNETOMETER DURING S/C ROLL B) CALIBRATE OTHER SCIENCE INSTR AS REQUIRED

REPEAT UP TO FOUR TIMES

4.0 INTERPLANETARY CRUISE

DSN
A) TRACK S/C
B) RECEIVE & DISPLAY SCIENCE & ENGINEERING DATA
C) MONITOR S/C & CAPSULE STATUS
D) PROCESS DATA ON EARTH TO OBTAIN GUIDANCE COMMANDS (STORED COMMANDS & START TIMES)

A) PROVIDE ROLL TURN
B) PROVIDE YAW TURN
C) PROVIDE MIDCOURSE
D) PROVIDE INITIATE M
E) RECEIVE VERIFICATIO
- DEGREES OF YAW
- THRUST DURATION
- REACQUISITION O

F) TRACK SPACECRAFT

A) TRANSMIT ENGINEERING & SCIENCE DATA VIA DATA MODE NO. 2 (OPTIONAL MODE NO. 3)
B) TRANSMIT CAPSULE ENGINEERING DATA
C) TRANSMIT CONE-ANGLE SETTINGS (CANOPUS TO EARTH)
D) EXERCISE & CALIBRATE HIGH-GAIN ANTENNA T ± 40 DAYS
E) SWITCH FROM LOW-GAIN TO HIGH-GAIN ANTENNA T + 80 DAYS
F) PROVIDE RANGING SIGNAL TO A MAX. RANGE OF 8.0×10^6 KM (NOMINAL)
G) SWITCH TRANSMISSION FROM LAUNCH EXCITER TO TWT POWER AMPLIFIER AND DATA MODE NO. 2

A) RECEIVE ROLL & YAW
B) RECEIVE ANTENNA PO
C) RECEIVE MOTOR BURI
D) RECEIVE INITIATE M
E) SWITCH TO DATA MO
F) RELAY VERIFICATION
G) STORE AND/OR TRAN
TRANSMIT ENGINEER
TO DSN (MODE 2)

A) COMMAND TELECOMMUNICATION TO DATA MODE NO. 2
B) COMMAND CRUISE SCIENCE ON (WARMUP) — SCIENCE INSTRUMENTS
C) COMMAND DATA RECORDERS ON
D) COMMAND TWTA ON
E) SWITCH CANOPUS ANGLE AS REQUIRED
F) INITIATE CRUISE SCIENCE DATA ACQUISITION
G) COMMAND TELECOMMUNICATION CHANGE FROM OMNI TO HIGH-GAIN ANTENNA
H) UPDATE HIGH-GAIN ANTENNA POSITION (AS REQUIRED)
I) COMMAND TELECOMMUNICATIONS — CHANGE DATA TRANSMISSION RATES
J) COMMAND RECALIBRATION OF SCIENCE ELEMENTS AS REQUIRED
K) BACKUP COMMANDS AS REQUIRED

A) COMMAND TELECOMM
B) RECEIVE TRAJECTOR
C) SWITCH GYROS TO R
D) COMMAND ANGULAR
E) RECEIVE GYRO SIGN
F) SWITCH ATTITUDE R
G) ARM PROPULSION S
H) PROVIDE COMMAND
I) RECEIVE ACCELEROM
J) DISARM PROPULSIO
K) COMMAND REVERSE
L) COMMAND REACQUI
M) COMMAND AUTOPILO
N) BACKUP COMMANDS

A) UPDATE CANOPUS CONE ANGLE ON COMMAND
B) SWITCH AUTOPILOT TO CRUISE MODE
C) MAINTAIN S/C ATTITUDE TO CELESTIAL REFERENCES DURING CRUISE

A) SWITCH TO GYRO CO
B) ROLL S/C AND VERIF
C) YAW S/C AND VERIF
D) AUTOPILOT — PROVI
TO TVC DURING MOT
E) TURN ON ACCELERO
F) PROVIDE ACCELERA
TO CC&S
G) TURN OFF ACCELERO

MIDCOURSE PROPULSIO

A) ARM PRESSURIZATI
B) ARM PROPELLANT FE
C) FIRE PROGRAMMED
D) SHUT DOWN ENGINE
E) ISOLATE PROPELLAN
F) ISOLATE PRESSURIZ

A) PROVIDE CONDITIONED SOLAR ELECTRICAL POWER TO:
- TELEMETRY
- CC&S
- ATTITUDE REF
- AUTOPILOT
- TEMPERATURE CONTROL
- SCIENCE
- CAPSULE

B) CHARGE BATTERIES

A) PROVIDE CONDITI
- TELEMETRY
- CC&S
- AUTOPILOT
- ATTITUDE REFERE
- REACTION CONTR
- PROPULSION
- TEMPERATURE C
- PYROTECHNIC
- CAPSULE

A) SUPPORT S/C ASSEMBLIES
B) SUPPORT S/C COMPONENTS
C) MAINTAIN ADEQUATE ALIGNMENT BETWEEN COMPONENTS
D) PROVIDE ACCEPTABLE STATIC & DYNAMIC LOAD ENVIRONMENTS
E) SUPPORT FLIGHT CAPSULE

A) SUPPORT S/C ASSE
B) SUPPORT S/C COMI
C) MAINTAIN ADEQUA
D) PROVIDE ACCEPTA
E) SUPPORT FLIGHT C

PROVIDE TEMPERATURE CONTROL

PROVIDE TEMPERATURE

A) REMOVE PROPULSI
B) PROVIDE IGNITION
C) INHIBIT PROPULS

A) RECEIVE CRUISE SCIENCE "ON" COMMAND
B) ACQUIRE CRUISE SCIENCE DATA
C) TRANSFER CONDITIONED DATA TO DAE
D) RECEIVE POWER FROM E/P
E) RECALIBRATE SCIENCE EXPERIMENTS AS REQUIRED

A) RECEIVE CC&S CO
B) TURN OFF CRUISE

A) RECEIVE DAE "ON" COMMAND
B) PROCESS & TRANSFER DATA TO TM

5.0 INTERPLANETARY TRAJECTORY CORRECTION

6.0 S/C CAPSULE SEPARATION

MAGNITUDE & DIRECTION
MAGNITUDE & DIRECTION
MOTOR BURN DURATION AND ΔV
ANEUVER SEQUENCE COMMAND
ON OF CORRECTION MANEUVER
& ROLL

CELESTIAL REFERENCES

A) INITIATE PRESEPARATION SEQUENCE
B) RECEIVE CAPSULE STATUS DATA
C) COMMAND SEPARATION
D) VERIFY CAPSULE PROGRAM
E) VERIFY SEPARATION
F) TRACK CAPSULE & SPACECRAFT

TURN COMMAND & RELAY TO CC&S
SITIONING DATA & RELAY TO CC&S
DURATION AND & ΔV RELAY TO CC&S
ANEUVER COMMAND & RELAY TO CC&S
DE NO. 1 (FOR LATE MIDCOURSE MANEUVERS)
OF CORRECTION MANEUVER TO DSN
MIT ENGINEERING DATA TO DSN (MODE 3)
NG (SPACECRAFT & CAPSULE) + CRUISE SCIENCE

A) RECEIVE PRESEPARATION SEQUENCE COMMANDS & RELAY TO CC&S
B) SWITCH TO DATA MODE NO. 2
C) TRANSMIT CAPSULE ENGRG DATA TO DSN
D) RECEIVE SEPARATION COMMAND FROM DSN & ROUTE TO CC&S
E) STORE AND/OR TRANSMIT ENGINEERING DATA TO DSN (MODE 3)
TRANSMIT ENGINEERING (SPACECRAFT & CAPSULE) + CRUISE SCIENCE TO DSN (MODE 2)

UNICATION TO DATA MODE NO. 1
CORRECTION PARAMETERS
ATE CONTROL
MANEUVER
ALS & SUM FOR ANGULAR MANEUVERS
FERENCE TO AUTOPILOT SUBSYSTEM
YSTEM
TO INITIATE ATTITUDE MANEUVER & ΔV MANEUVER
ETER SIGNALS & INTEGRATE FOR ΔV MANEUVER
N SYSTEM
ANGULAR MANEUVER
RE CELESTIAL REFERENCES
T SELECTION CONTROL
AS REQUIRED

A) LOAD CAPSULE WITH 5 OR MORE COMMANDS
B) COMMAND CAPSULE SEQUENCING
C) COMMAND TELECOMM SWITCH TO DATA MODE NO. 1
D) COMMAND GYROS ACTIVATE (CAPSULE)
E) COMMAND GYROS ESTABLISH POLARITY (CAPSULE)
F) COMMAND GYROS TO ATTITUDE CONTROL MODE (CAPSULE)
G) COMMAND DATA TAPE RECORDER OFF
H) COMMAND CAPSULE ACTIVATE ENTRY SCIENCE
I) COMMAND CAPSULE ACTIVATE TELECOMM & VERIFY RADIO LINK (VHF)
J) SELECT T/M MODE FOR TRANSMISSION OF CAPSULE DATA
K) COMMAND:
BIOBARRIER SEPARATION
S/C ORIENT TO SEPARATION ATTITUDE
ELECTRICAL CONNECTION SEPARATION
VERIFY SEPARATION
L) COMMAND REORIENT S/C & REACQUIRE CELESTIAL REFERENCES
M) BACKUP COMMANDS AS REQUIRED
N) RECEIVE S/C ORIENTATION PARAMETERS

NTROL
Y
/
DE COMMAND
OR BURN
METERS
TION DATA

METER

H) YAW BACK TO ORIGINAL ATTITUDE & VERIFY
I) REACQUIRE SUN (FINE SUN SENSOR) & VERIFY
J) ROLL TO ORIGINAL ATTITUDE
K) LOCK ON CANOPUS & VERIFY
L) SWITCH AUTOPILOT FROM GYRO CONTROL TO CELESTIAL REF CONTROL

A) SWITCH TO GYRO CONTROL
B) PERFORM ROLL TURN & VERIFY
C) PERFORM YAW TURN & VERIFY
D) MAINTAIN ATTITUDE DURING SEPARATION
E) PERFORM YAW TURN (INVERSE TO C) & VERIFY
F) PERFORM ROLL TURN (INVERSE TO B) & VERIFY
G) REACQUIRE CELESTIAL REFERENCES
H) RETURN TO CELESTIAL REFERENCE ATTITUDE CONTROL MODE

N SYSTEM

ON SYSTEM (FIRE SQUIB VALVE)
ED SUBSYSTEM (FIRE SQUIB VALVE)
ENGINES (OPERATE SOLENOID VALVE)

T FEED SUBSYSTEM
ATION SUBSYSTEM

NED SOLAR OR BATTERY POWER TO:

NCE
OL

ONTROL

A) PROVIDE CONDITIONED SOLAR OR BATTERY POWER TO:
- T/M
- CC&S
- AUTOPILOT
- ATTITUDE REF
- REACTION CONTROL
- TEMPERATURE CONTROL
- PYROTECHNICS
- CAPSULE

MBLIES
ONENTS
E ALIGNMENT BETWEEN COMPONENTS
LE STATIC & DYNAMIC LOAD ENVIRONMENTS
APSULE

A) SUPPORT S/C ASSEMBLIES
B) SUPPORT S/C COMPONENTS
C) MAINTAIN ADEQUATE ALIGNMENT BETWEEN COMPONENTS
D) PROVIDE ACCEPTABLE STATIC & DYNAMIC LOAD ENVIRONMENTS
E) SUPPORT FLIGHT CAPSULE

CONTROL

PROVIDE TEMPERATURE CONTROL

ON SYSTEM INHIBIT

ON SYSTEM

A) RECEIVE SIGNAL TO REMOVE CAPSULE SEPARATION INHIBIT
B) RECEIVE SIGNAL TO FIRE CAPSULE UMBILICAL SEPARATION
C) RECEIVE SIGNAL TO FIRE BIOBARRIER REMOVAL
D) RECEIVE SIGNAL TO FIRE CAPSULE SEPARATION
E) RECEIVE SIGNAL FOR SEPARATION INHIBIT

MAND "CRUISE SCIENCE OFF"
CIENCE

A) RECEIVE CC&S COMMAND "CRUISE SCIENCE OFF"
B) TURN OFF CRUISE SCIENCE

7.0 FLIGHT CAPSULE TRAJECTORY DEFLECTION

9.0 FLIGHT CAPSULE CRUISE

10.0 FLIGHT CAPSULE ENTRY

8.0 FLIGHT S/C CRUISE

A) TRANSMIT ORBIT INJECTION PARAMETERS
- ROLL MAGNITUDE & DIRECTION
- YAW MAGNITUDE & DIRECTION
- MOTOR BURN START TIME

B) TRACK FLIGHT SPACECRAFT
C) RECEIVE, REDUCE & DISPLAY SCIENCE & ENGINEERING DATA
D) PROVIDE COMMANDS TO BACK UP CC&S AS REQUIRED

A) RECEIVE, DECODE, & DIS
B) RELAY UPDATED ORBIT IN
C) PROVIDE COMMAND TO IN
D) PROVIDE BACKUP COMMA
E) TRACK S/C
F) VERIFY ORBIT INSERTION

A) RECEIVE ROLL & YAW TURN MAGNITUDE & DIRECTION COMMAND & RELAY TO CC&S
B) RECEIVE ANTENNA POSITIONING DATA & RELAY TO CC&S
C) RECEIVE MOTOR-BURN START TIME, RELAY TO CC&S
D) RECEIVE CAPSULE DATA, CONDITION & RELAY TO GROUND
E) TRANSMIT FLIGHT SPACECRAFT ENGINEERING, CAPSULE ENGRG, & SCIENCE DATA TO GROUND VIA MODE 2

A) UPDATE ROLL-TURN MAGN
B) UPDATE YAW-TURN MAGN
C) UPDATE MOTOR-BURN ST
D) UPDATE INITIATE MANEU
E) SWITCH TO DATA MODE N
F) REACQUIRE EARTH AFTER
G) RELAY VERIFICATION OF

A) COMMAND SWITCH TO DATA MODE NO. 2
B) COMMAND CANOPUS CONE ANGLE SETTING
C) COMMAND ANTENNA STEP (AS REQUIRED)
D) RECEIVE ORBIT INJECTION PARAMETERS
E) PROVIDE SIGNAL TO PYRO & MECHANISMS TO DEPLOY SCAN PLATFORM (CRUISE SCIENCE T/M OFF) & SWITCH TO DATA MODE NO. 1
F) SWITCH ON DATA RECORDER-COMMAND TELECOMMUNICATIONS RECEIVE CAPSULE DATA
G) BACKUP COMMANDS AS REQUIRED

A) UPDATE STORED ROLL, P
B) UPDATE STORED VELOCIT
C) INITIATE MANEUVER SEQ
D) COMMAND ORIENTATION
E) COMMAND THRUST FOR C
F) COMMAND RETURN TO CR
G) BACKUP COMMANDS AS

A) SWITCH TO GYRO CONTRO
B) PROVIDE ROLL TO PROPE
C) YAW TO PROPER ATTITUD
D) AUTOPILOT – PROVIDE C
E) TURN ON ACCELEROMETER
F) PROVIDE ACCELEROMETE
G) TURN OFF ACCELEROMETE
H) YAW BACK AFTER MOTOR
I) ACQUIRE SUN & VERIFY
J) ROLL BACK TO PROGRAM
K) ACQUIRE CANOPUS & VE
L) SWITCH AUTOPILOT FRO

A) UPDATE CANOPUS CONE ANGLE ON COMMAND
B) SWITCH AUTOPILOT TO CRUISE MODE
C) MAINTAIN S/C ATTITUDE TO CELESTIAL REFERENCES DURING CRUISE

ORBIT INSERTION ENGINE

A) ARM TVC
B) ARM IGNITER
C) FIRE MOTOR & PROVID
D) TERMINATE THRUST (M

A) PROVIDE CONDITIONED SOLAR ELECTRICAL POWER TO:
- T/M
- CC&S
- AUTOPILOT
- ATTITUDE REF
- REACTION CONTROL
- TEMPERATURE CONTROL

B) CHARGE BATTERIES

A) PROVIDE CONDITIONED S
- TELEMETRY
- CC&S
- ATTITUDE REFERENCE
- AUTOPILOT
- TEMPERATURE CONTR
- PULSE TO PYROTECH
- PULSE TO PROPULS

A) SUPPORT S/C ASSEMBLIES
B) SUPPORT S/C COMPONENTS
C) MAINTAIN ADEQUATE ALIGNMENT BETWEEN COMPONENTS
D) PROVIDE ACCEPTABLE STATIC & DYNAMIC LOAD ENVIRONMENTS
E) DRIVE SCAN PLATFORM TO DEPLOYED POSITION & LOCK

A) SUPPORT S/C ASSEMBL
B) SUPPORT S/C COMPONE
C) MAINTAIN ADEQUATE A
D) PROVIDE ACCEPTABLE

PROVIDE TEMPERATURE CONTROL

PROVIDE TEMPERATURE CO

RECEIVE SQUIB FIRING SIGNAL FOR UNLATCHING OF SCAN PLATFORM

A) RECEIVE & EXECUTE C
PROPULSION ENGINE
B) RECEIVE & EXECUTE S
C) RECEIVE & EXECUTE C
STOP
D) RECEIVE & EXECUTE

A) RECEIVE CRUISE SCIENCE "ON" COMMAND
B) ACQUIRE CRUISE SCIENCE DATA
C) TRANSFER CONDITIONED DATA TO DAE
D) RECEIVE POWER FROM EIP
E) RECALIBRATE SCIENCE EXPERIMENTS AS REQUIRED

SCIENCE OFF DURING C

A) RECEIVE DAE "ON" COMMAND
B) PROCESS & TRANSFER DATA TO TM

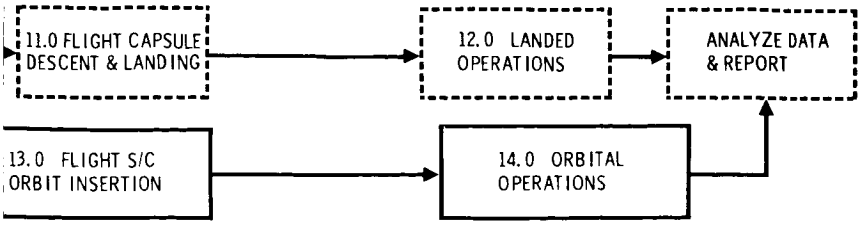

LAY ENGINEERING DATA ECTION PARAMETERS ETIATE INSERTION MANEUVER NDS TO CC&S AS REQUIRED	A) RECEIVE, DECODE, & DISPLAY SCIENCE DATA B) RECEIVE AND ANALYZE ENGINEERING DATA C) TRACK S/C D) RECEIVE & DISPLAY CAPSULE DATA E) PROVIDE DATA FOR ORBITAL TRIM (IF REQUIRED) F) RECEIVE VERIFICATION OF ORBITAL TRIM MANEUVER G) TERMINATE MISSION
TUDE & DIRECTION COMMAND & RELAY TO CC&S TUDE & DIRECTION COMMAND & RELAY TO CC&S RT TIME & RELAY TO CC&S ER & RELAY TO CC&S 2 OR 5A AS REQUIRED OLL TURNS & MOTOR BURN ANEUVERS	A) TRANSMIT SCIENCE & ENGINEERING DATA VIA DATA MODES 5 AND 6 B) RECORD ENGINEERING & SCIENCE DATA AS COMMANDED C) RECEIVE, STORE & RELAY CAPSULE DATA ON COMMAND (MODES 5 AND 6) D) RECEIVE & RELAY DATA FOR ORBIT TRIM IF REQUIRED
CH, & YAW MAGNITUDE & SIGN MAGNITUDE ENCE F S/C TO INJECTION ATTITUDE BIT INSERTION TISE ATTITUDE EQUIRED	A) COMMAND ORBITAL TRIM MANEUVERS (IF REQUIRED) B) SWITCH DATA MODES AS NECESSARY C) RECEIVE ANY ORBITAL OPERATION CHANGES & SEQUENCES D) COMMAND POSITIONING OF SCIENCE SCAN PLATFORM E) SWITCH ON ORBITAL SCIENCE F) SELECT RECORDED SCIENCE READOUT TO TELECOMMUNICATIONS G) BACKUP COMMANDS AS REQUIRED H) STORE DATA FOR ORBIT TRIM (IF REQUIRED) I) TERMINATE MISSION ON COMMAND (IF REQUIRED)
ATTITUDE & VERIFY ROLL & VERIFY MMAND TO TVC DURING MOTOR BURN DATA TO CC&S URN ED ATTITUDE FY GYRO – CONTROL TO CELESTIAL REFERENCE CONTROL	A) MAINTAIN S/C ATTITUDE TO CELESTIAL REFERENCES B) SWITCH AUTOPILOT TO GYRO CONTROL DURING OCCULTATION C) REACQUIRE CELESTIAL REFERENCES FOLLOWING OCCULTATION D) REORIENT S/C FOR ORBITAL TRIM MANEUVER USING GYRO CONTROL E) PROVIDE TVC DURING ENGINE FIRING F) REACQUIRE CELESTIAL REFERENCES FOLLOWING MANEUVERS G) UPDATE CANOPUS CONE ANGLES ON COMMAND
THRUST & TVC FOR BURNS TO DEPLETION)	MIDCOURSE A) ARM PRESSURIZATION & PROPELLANT FEED SUBSYSTEMS B) PROVIDE THRUST (FIRE PROGRAMMED ENGINES) FOR ORBIT TRIM IF REQUIRED C) TERMINATE THRUST ON COMMAND D) ISOLATE PROPELLANT FEED SUBSYSTEM E) ISOLATE PRESSURIZATION SUBSYSTEM
AR OR BATTERY POWER TO: UBSYSTEM L CS	A) PROVIDE CONDITIONED SOLAR OR BATTERY POWER TO: • TELEMETRY • CC&S • ATTITUDE REFERENCE SUBSYSTEM • AUTOPILOT • TEMPERATURE CONTROL • STRUCTURES & MECHANISMS • SCIENCE
SS TS GNMENT BETWEEN COMPONENTS ATIC & DYNAMIC LOAD ENVIRONMENTS	A) SUPPORT S/C ASSEMBLIES B) SUPPORT S/C COMPONENTS C) MAINTAIN ADEQUATE ALIGNMENTS BETWEEN COMPONENTS D) PROVIDE ACCEPTABLE STATIC AND DYNAMIC LOAD ENVIRONMENTS E) POSITION SCAN PLATFORM
ROL	PROVIDE TEMPERATURE CONTROL
MAND SIGNAL TO REMOVE INHIBIT FOR AL FOR PROPULSION ENGINE START MAND SIGNAL FOR PROPULSION ENGINE AL FOR PROPULSION INHIBIT	
INSERTION	A) TURN ON ORBITAL SCIENCE INSTRUMENTS B) ACQUIRE ORBITAL SCIENCE DATA C) TRANSFER CONDITIONED DATA TO DAE D) RECALIBRATE SCIENCE EXPERIMENTS AS REQUIRED
	A) RECEIVE DAE "ON" COMMAND B) PROCESS & TRANSFER DATA TO TM

Mission Sequences Matrix

conditioning being accomplished within each using subsystem. Power control and conditioning equipment provides for switching of solar array and batteries, automatic operation of battery charging regulation, and raw d.c. power and provision of 2400 cps power for operation of the science subsystem. Automatic failure sensing and switching of redundant regulators and inverters is provided together with capability for override control by Earth command.

Requirements and Constraints--Sections 1 and 2 of this volume include the general requirements and constraints governing the selection and optimization of the electrical power subsystem. The load requirements and principal unique constraints which influence the design of the power system are presented herewith.

General--The principal constraints which have a significant influence on the optimization of the preferred power subsystem are:

1) Power sources shall be solar cells and secondary batteries.
2) Battery wet life shall be limited to two years to account for the time from manufacturing through end of mission.
3) The solar array design shall satisfy performance requirements with a minimum solar flux of 46.7 watts/ft^2 (50 mw/cm^2).
4) The secondary battery shall have a capacity sufficient to supply power when sunlight is not available as specified by the mission profile, Figure 4.2-3.
5) The radiation environment at Mars shall be considered, conservatively, as equivalent to the Earth's radiation field.
6) Subsystem reliability shall be 0.999 for 5880 hours of operation.

PHASE CORRESPONDING TO SECTION 3.3		DURATION MINUTES
2.16	LIFTOFF + SEP	2.4
2.18	BURN S-IVB	8.2
2.20	BURN CENTAUR	2.3
2.21	EARTH ORBIT	2.5
2.22	BURN CENTAUR	4.8
3.1	TO 3.3 DEPLOY PANEL	5
3.5	SOLAR ACQ	5
3.7	ACQ SOLAR PWR	
3.8	CANOPUS ACQ & VERIFY	
4.2	COAST	
4.3	UPDATE CANOPUS	
4.4	TRANS E&S	
4.5	ACQ. CRUISE SCIENCE	
5.1	INIT CORRECTION	
5.2	ROLL	4
5.2	VERIFY	5
5.2	PITCH	15
5.2	VERIFY	5
5.3	BURN	10
5.3	VERIFY	5
5.4	PITCH	15
5.4	VERIFY	5
5.4	ROLL + VERIFY	4+5
4.1B	RET TO CRUISE	
4.3B	UPDATE CANOPUS	
4.7	CHG BIT RATE	
5.1B	INITIATE CORR	
5.2B	ROLL	4
5.2B	VERIFY	5
5.2B	PITCH	15
5.2B	VERIFY	5
5.3B	BURN	10
5.3B	VERIFY	5
5.4B	PITCH	15
5.4B	VERIFY	5
5.4B	ROLL	4+5
4.1C	RET TO CRUISE	
4.3C	UPDATE CANOPUS	
4.5C	SW TO HIGH GAIN	

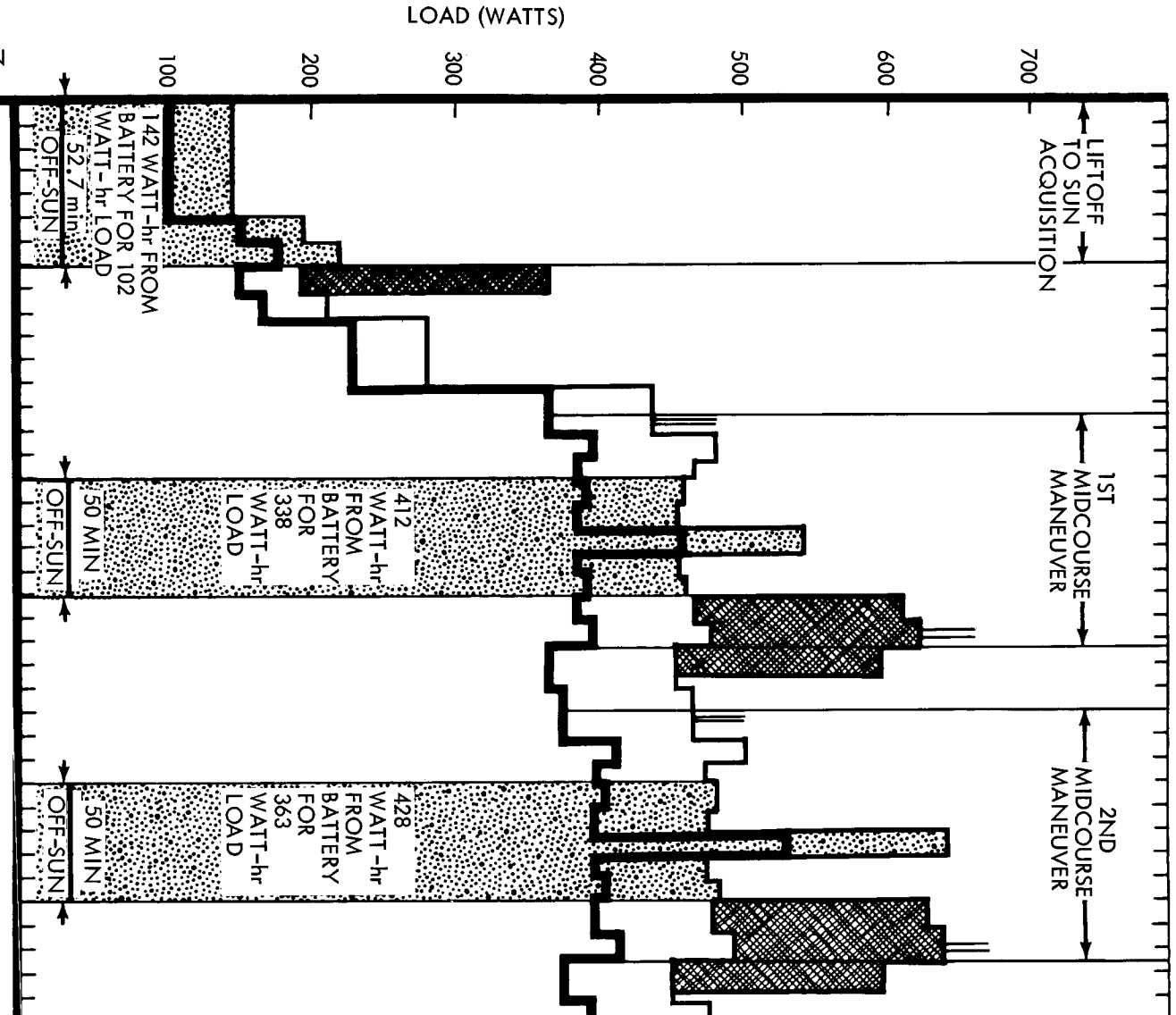

5.1C	INITIATE CORR	
5.2C	ROLL	15
5.2C	REACQ EARTH	12
5.2C	VERIFY ROLL	11
5.2C	YAW	15
5.2C	VERIFY	11
5.3C	BURN	10
5.3C	VERIFY	11
5.4C	YAW	15
5.4C	REACQ SUN	11
5.4C	ACQUIRE CANOPUS	
5.4C	ACQUIRE EARTH	12
5.4C	VERIFY CANOPUS	
4.1D	RET TO CRUISE	
4.3D	UPDATE CANOPUS	
4.5D	UPDATE HIGH GAIN	
4.6D	CHG BIT RATE	
6.1	PWR TO CAPSULE	
6.3	TRANS CAPSUEE DATA	
6.4	PREP FOR BARRIER SEP	
6.5	COMMAND SEPARATION	
6.6	SEP & VERIFY	
6.7	ROLL, ACQ & VERIFY	
6.7	PITCH, ACQ & VERIFY	26
6.8	COMMAND CAPSULE SEP	6
6.9	BRK ELECT CONN	2
6.10	SEPARATE	2
6.11	VERIFY	12
6.12	PITCH, ACQ & VERIFY	26
6.13	ROLL, ACQ & VERIFY	
6.14	RECORD OR RELAY DATA	
8.1	ESTAB S/C CRUISE	
8.3	TERM CRUISE SCIENCE	
8.4	RECEIVE ENG SCIENCE	
8.5	RECORD SCIENCE DATA	
8.6	REC VHF SIG FROM CAPS	
13.3	ROLL	15
13.3	ACQUIRE EARTH	13
13.3	VERIFY	12
13.3	PITCH, ACQ, & VERIFY	40
13.3	YAW & VERIFY	27
13.4	BURN	3
13.4	ACQ EARTH	17
13.4	VERIFY	12
13.5	YAW + FAIL MODE	67
13.5	ACQUIRE SUN	4-6

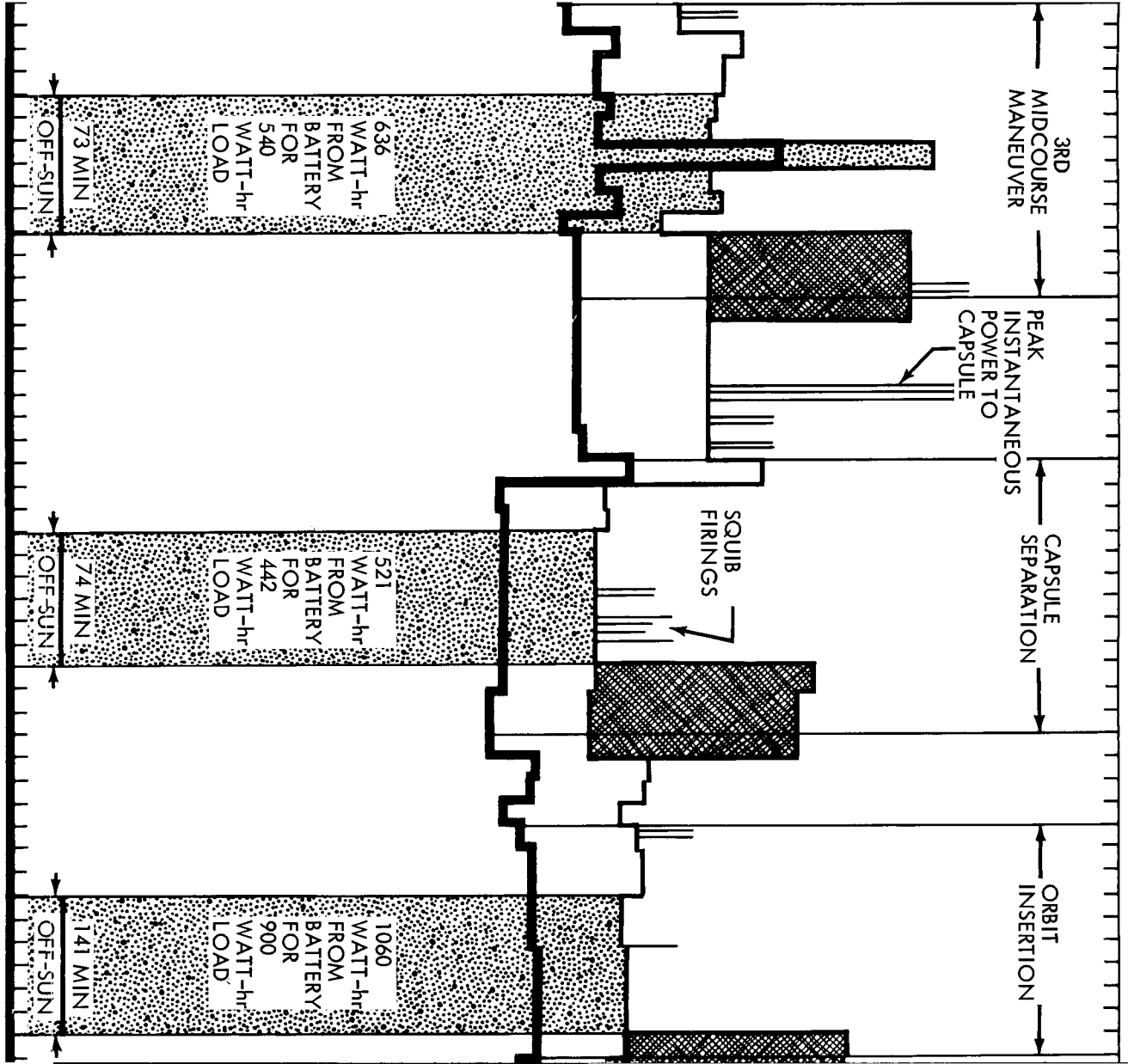

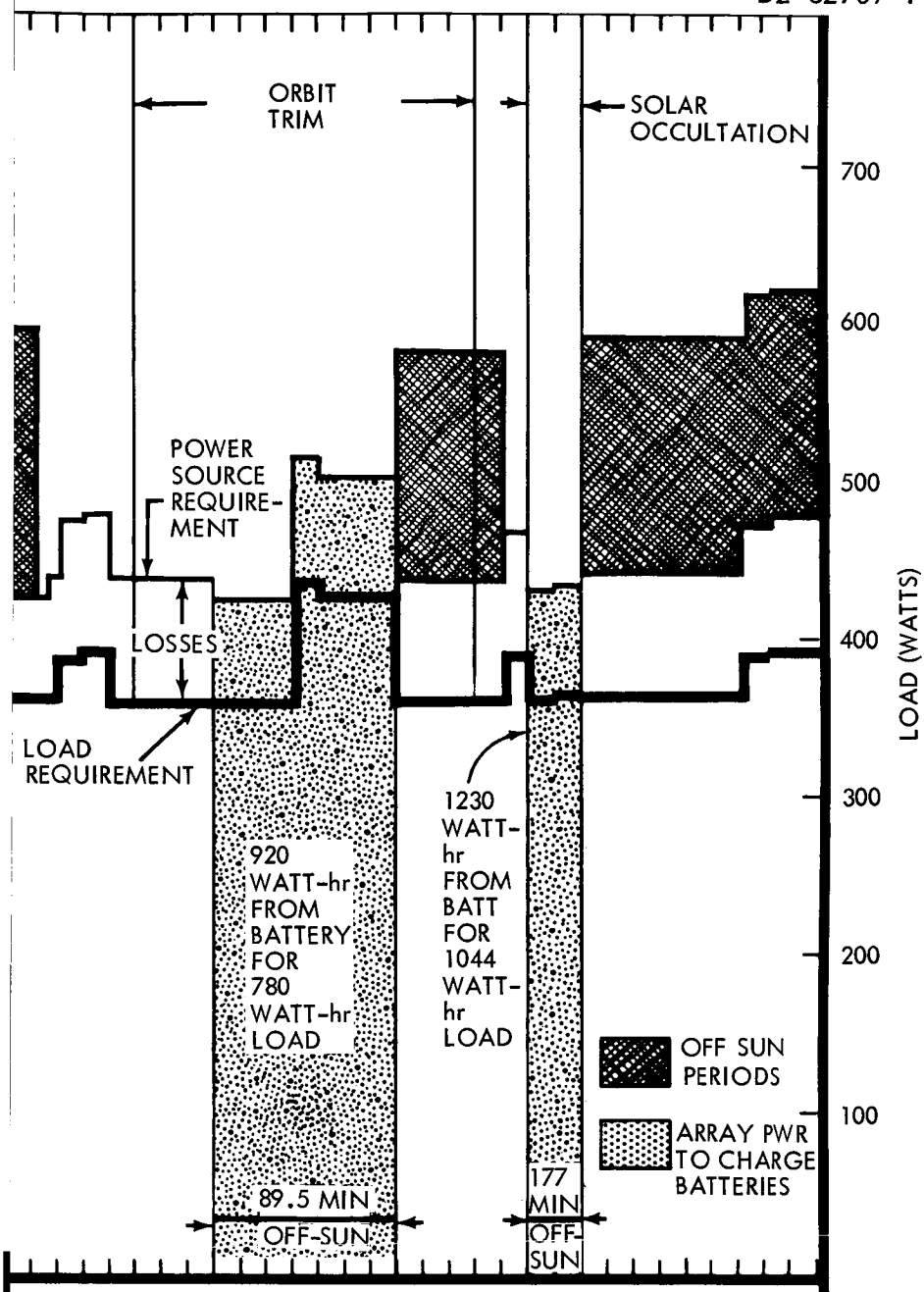

14.2	COAST	15
14.3	POSITION SCAN PLATE	13
14.4	ACQ SCIENCE DATA	12
14.5	TRANS SCIENCE DATA	5-1/2
14.6	RECEIVE SCIENCE DATA	17
14.7	ROLL	12
14.7	ACQ EARTH	15
14.7	VERIFY	29
14.7	PITCH	15
14.7	ACQUIRE EARTH	12
14.7	VERIFY	
14.7	TRIM BURN	
14.7	ACQUIRE EARTH	
14.7	VERIFY	
14.7	YAW	
14.7	ACQUIRE VER	
14.7	ACQUIRE CANOPUS	
14.7	VERIFY	
14.8	REPEAT 14.3-14.6	
14.8	ORBIT	162
14.9	SUN OCCULTATION	15
14.9.1	SUN ACQ	13
14.9.2	ACQ CANOPUS	12
14.9.3	VERIFY	15
14.9.4	ACQ EARTH	12
14.9.4	VERIFY	13
14.9.4	ACQ CANOPUS	
14.9.5	BATT CHARGE AT 14.9.2	
14.8	REPEAT 14.3-14.6	
14.11	TV PART OF ORBIT	
14.12	NON-TV	

Figure 4.2-3: Load Profile Plus Source Profile

7) Provision shall be made for telemetry measurements to provide status information on subsystem performance.

8) Provision shall be made for onboard logic to bypass malfunctioning components wherever practicable.

9) Provision shall be made for ground command override of critical functions.

Power and Energy Requirements--Voyager power and energy requirements may be classified into three major categories:

1) Major power blocks;

2) Power and energy quantity;

3) Power quality.

Major Power Blocks--There are certain natural divisions of the requirements into blocks of power which influence the general layout of the power system. Some of these divisions of power requirements are indicated in the load tables and the load profiles. The divisions of power requirements according to the following tabulation have been utilized during the various stages of development leading to the final power system configuration.

Logical Division	Example Load Blocks
Function	Telecommunications, Science
Type of Power	d.c., 400 cps a.c., 2400 cps a.c., Various voltage levels
Quality	Wide voltage regulation, Close voltage regulation
Reliability of Service	(Determine requirements for redundancy such as voltage regulators)
Mission Phase and Power Source	Phase 2.16 Battery Power Only Phase 4.50 Solar Power Only

Power and Energy Quantity--In defining the power level and duty cycle for the Voyager loads, several iterations have been made to establish applicable power quantities. The final requirements are defined in the following tables and figures:

1) Table 4.2-1, Extract of Computer Load Table showing total power distribution loads, losses and off-Sun energy.
2) Table 4.2-2, Extract of Computer Load Table showing total power demanded by each subsystem at each phase of the mission.
3) Figure 4.2-3, Load Profile showing Power vs. Time during the 116 functional phases into which the mission is divided. Losses, battery requirements, and battery charge requirements are shown explicitly in the profile.

A digital computer (IBM 7094) program, was applied to process load requirements data for rapid reduction to load profiles. Use of the computer makes frequent updating of the load profile practical. Tables 4.2-1 and 4.2-2 are extracts from load tables determined from a computer run. The complete tables include the data arranged according to the 116 phases of the mission which are described in detail in Section 3.3. In future design phases of the Voyager program the digital computer program will be extended to calculate thermal watts in each piece of equipment to provide rapid updating of thermal balance calculations.

The load profile provides the principal basis for sizing of the solar array and battery. The solar array must supply the loads, battery charging requirements, and losses indicated in Figure 4.2-3. During off-Sun periods, indicated by shaded areas, the battery must supply the corresponding loads and losses.

Power Quality--Power quality is defined for the Voyager power system in terms of tolerances by the loads and electrical circuits on the following parameters:

1) Steady-state and transient voltage regulation;

2) Steady-state and transient frequency regulation;

3) Frequency modulation and voltage modulation;

4) Alternating current waveform;

5) Conducted and radiated electro-interference.

The power quality requirements will eventually result in a detailed power quality specification for the power sources, conditioning equipment, and also on loads which may have a significant influence on power quality factors such as waveform and electro-interference level.

Requirements for regulated and unregulated power have been established to meet the power quality demands of the spacecraft loads.

4.2.2 Applicable Documentation

Reference No.

1)	Voyager Spacecraft AgO-Cd Battery Specification	EOS Spec. 613847
2)	Voyager Spacecraft Electrical Power Subsystem Solar Array Electrical Design Considerations	EOS-V-1044
3)	Voyager Spacecraft-Electrical Power Subsystem Circuit Schematics	EOS-V-1034
4)	Voyager Spacecraft Electrical Power Subsystem-Solar Array Structural Drawings	EOS-V-1041
5)	Voyager Spacecraft Electrical Power Subsystem OSE/Spacecraft Interface Table	EOS-V-1042
6)	Voyager Spacecraft Electrical Power Subsystem Reliability Analysis	EOS-V-1043

Table 4.2-1: EXTRACT FROM A LOAD TABLE SHOWING TOTALS OF ALL SUBSYSTEM LOADS

(Also Losses in Power Subsystem, Source Power to Supply Loads and Losses, Watt Hours Off-Sun, and Cumulative Watt Hours)

Phase Number Corresponding to Section 3.3	Time of Phase (Minutes)	Watts Required at Load	Watts Lost In Power Subsystem	Watts Required at Panel	Watt-Hours If Off-Sun	Cumulative Off-Sun Watt-Hours
14.7 Trim Burn	5.5	400.4000	54.87550	455.2755	367.04670	2727.616
14.7 Acq. Ear	17.0	340.4000	51.87550	392.2755	98.13732	2825.753
14.7 Verify	12.0	340.4000	51.87550	392.2755	68.08000	2893.833
14.7 Yaw	15.0	340.4000	51.87550	392.2755	85.10000	2978.933
14.7 Acq. & Ver.	29.0	340.4000	51.87550	392.2755	0.	2978.933
14.7 Acq. Canopus	15.0	340.4000	51.87550	392.2755	0.	2978.933
14.7 Verify	12.0	360.4000	52.87550	413.2755	0.	2978.933
14.8 Repeat 143-146		372.0000	55.48850	427.4885	0.	2978.933
14.8 Orbit		394.5000	62.88350	457.3835	0.	2978.933

Table 4.2-2: EXTRACT OF LOAD TABLE SHOWING TOTALS FOR EACH SUBSYSTEM

Phase Number Corresponding to Section 3.3	Time of Phase (Minutes)	Attitude Reference & Autopilot. Regulated d.c.	Propulsion. Unregulated d.c.	Telecommunication. Regulated d.c.	Science. 2.4 k.c.	Thermal Control. Unregulated d.c.	CC&S. Regulated d.c.
14.7 Trim Burn	5	66.50000	60.000	183.4000	20.50000	5.000000	65.000
14.7 Acq. Earth	17	66.50000	0.	183.4000	20.50000	5.000000	65.000
14.7 Verify	12	66.50000	0.	183.4000	20.50000	5.000000	65.000
14.7 Yaw	15	66.50000	0.	183.4000	20.50000	5.000000	65.000
14.7 Acq. & Ver.	29	66.50000	0.	183.4000	20.50000	5.000000	65.000
14.7 Acq. Can.	15	66.50000	0.	183.4000	20.50000	5.000000	65.000
14.7 Verify	12	66.50000	0.	183.4000	20.50000	25.000000	65.000
14.8 Repeat 14.3		49.50000	0.	205.0000	27.50000	25.000000	65.000
14.8 Orbit		49.50000	0.	205.0000	75.00000	0.000000	65.000

4.2.3 Functional Description

The subsystem shown in diagrammatic form by Figure 4.2-4 is described in the following subsections:

1) Briefly describes each major component (Section 4.2.3.1);
2) Reviews significant and electrical characteristics (Section 4.2.3.2);
3) Describes operational modes (Section 4.2.3.3);
4) Develops transfer functions for the subsystem and the major components (Section 4.2.3.4);
5) Reviews optimization studies by which the subsystem was developed (Section 4.2.3.5).

4.2.3.1 Component and Description

The major components of the subsystem are identified in simplified form in Figure 4.2-4 and in greater detail in EOS drawing 614068 (Reference 3).

Component	Quantity
Solar Panel	3
Battery	3
Power Switch and Logic Assembly	1
Battery Charger and Failure Sense Unit	3
Booster Converter and Sharing Sense Unit	1
Series Switcning d.c./d.c. Regulator	4
d.c./a.c. Inverter	2
d.c. Failure Sensing Unit	2
a.c. Failure Sensing Unit	1

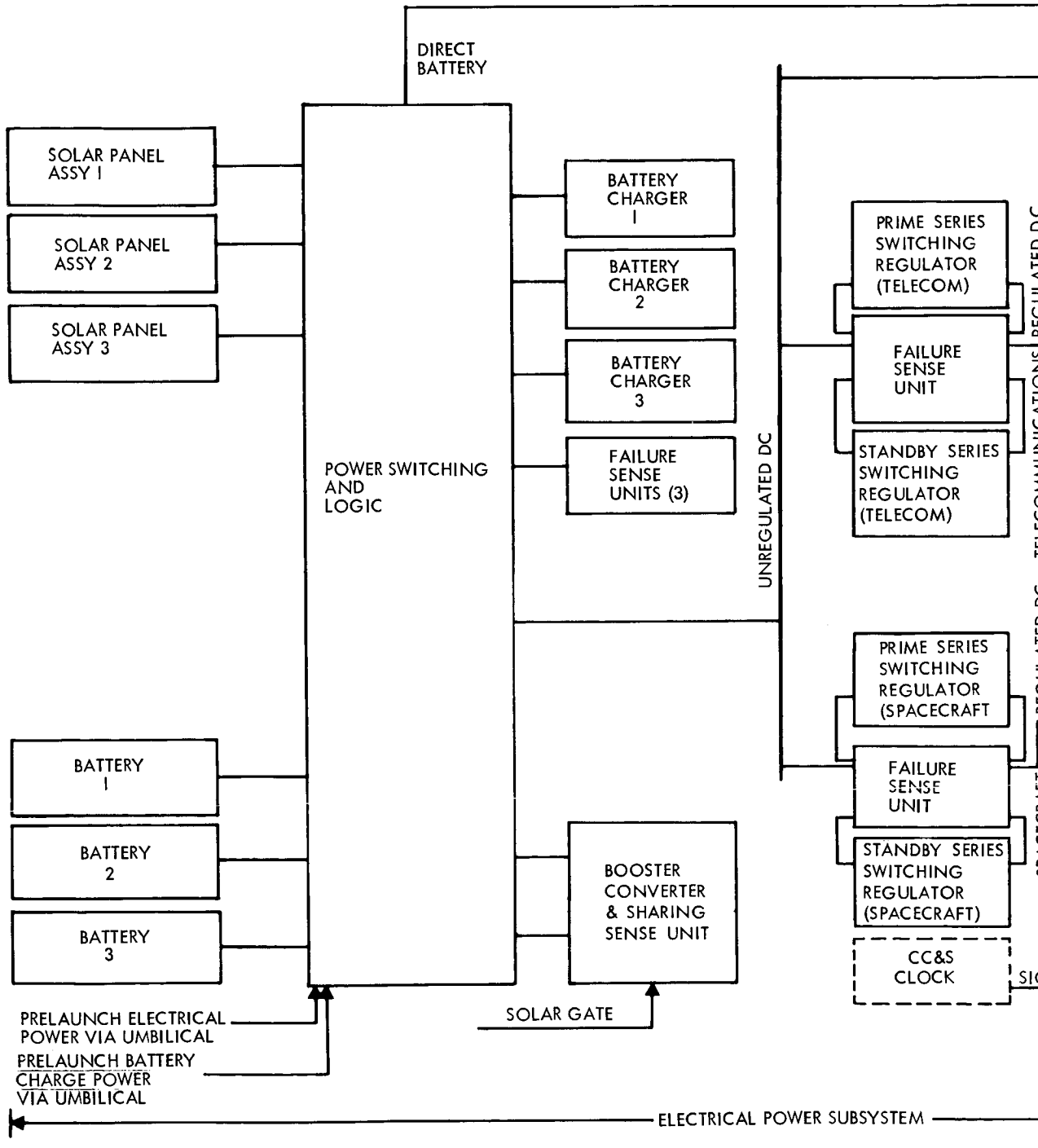
DIRECT BATTERY
SOLAR PANEL ASSY 1
SOLAR PANEL ASSY 2
SOLAR PANEL ASSY 3
POWER SWITCHING AND LOGIC
BATTERY CHARGER 1
BATTERY CHARGER 2
BATTERY CHARGER 3
FAILURE SENSE UNITS (3)
UNREGULATED DC
PRIME SERIES SWITCHING REGULATOR (TELECOM)
FAILURE SENSE UNIT
STANDBY SERIES SWITCHING REGULATOR (TELECOM)
PRIME SERIES SWITCHING REGULATOR (SPACECRAFT
FAILURE SENSE UNIT
STANDBY SERIES SWITCHING REGULATOR (SPACECRAFT)
CC&S CLOCK
BATTERY 1
BATTERY 2
BATTERY 3
BOOSTER CONVERTER & SHARING SENSE UNIT
SOLAR GATE
PRELAUNCH ELECTRICAL POWER VIA UMBILICAL
PRELAUNCH BATTERY CHARGE POWER VIA UMBILICAL
ELECTRICAL POWER SUBSYSTEM

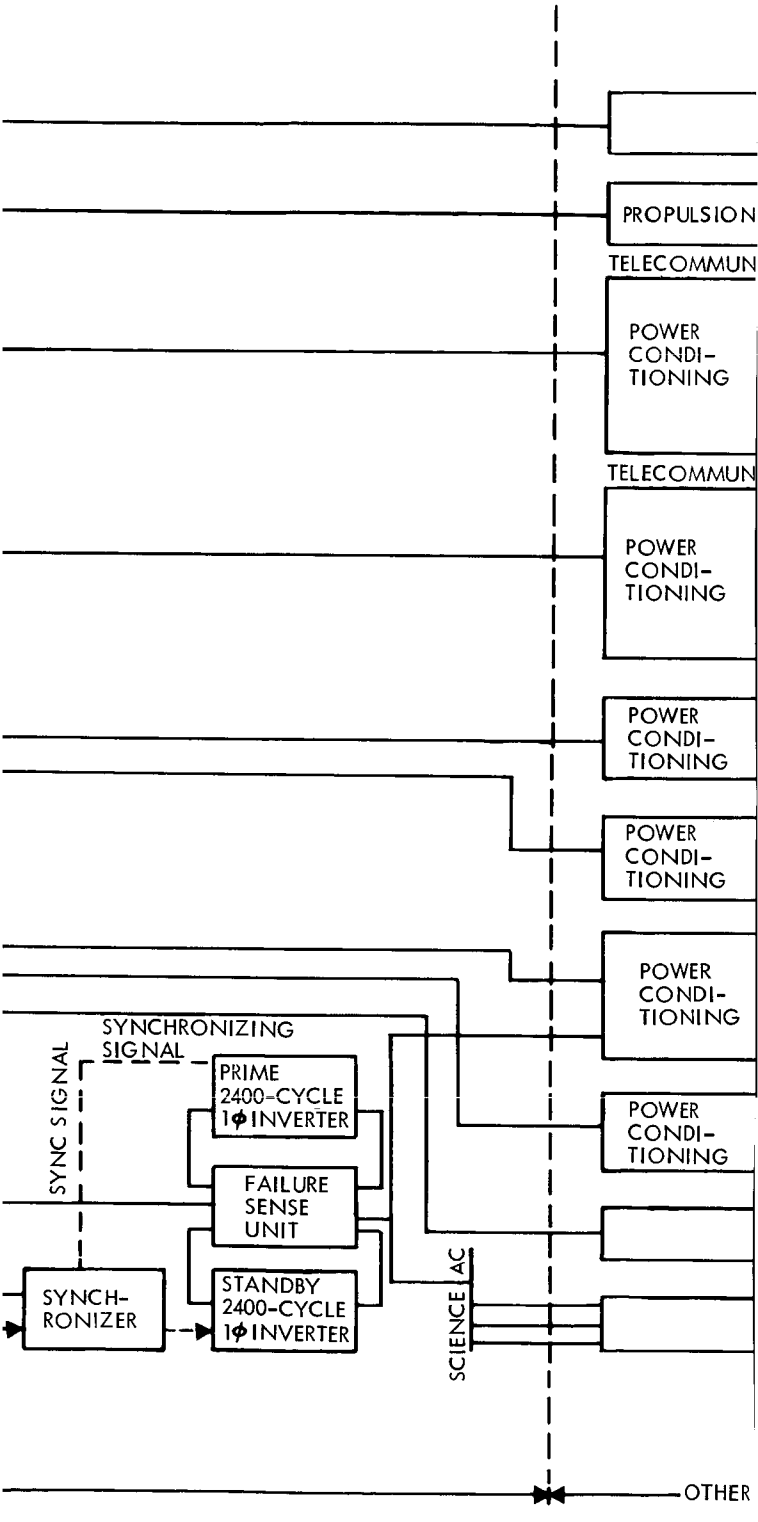
PROPULSION
TELECOMMUN
POWER CONDI-TIONING
TELECOMMUN
POWER CONDI-TIONING
POWER CONDI-TIONING
POWER CONDI-TIONING
POWER CONDI-TIONING
POWER CONDI-TIONING
SYNCHRONIZING SIGNAL
SYNC SIGNAL
PRIME 2400-CYCLE 1φ INVERTER
FAILURE SENSE UNIT
STANDBY 2400-CYCLE 1φ INVERTER
SYNCH-RONIZER
SCIENCE AC
OTHER

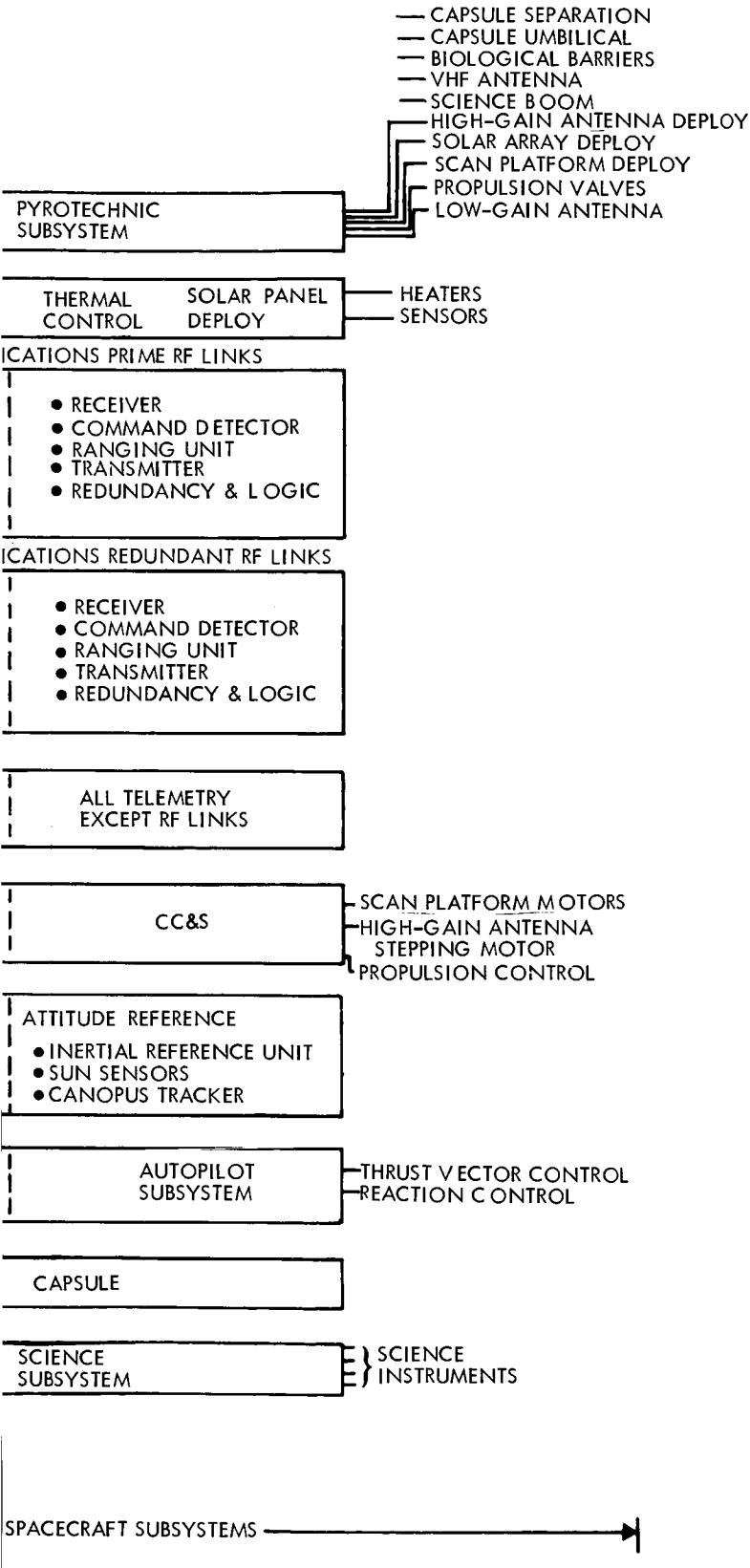

Figure 4.2-4: Functional Diagram of Electrical Power Subsystem

The solar array, consisting of three panels of two structural sections, converts the incident solar energy to electrical power for the spacecraft. Each panel is composed of eight independent electrical sections to minimize the effect of degradation or failure in one section.

Power during off-Sun phases of the mission or during peak load occurrences is provided by three silver-cadmium (AgO-Cd) batteries.

Power from the solar array and batteries are summed through a diode logic network in the power switching and logic (PS&L). A switch for selecting external (operational support equipment) or internal (batteries/solar array) power is also provided in the PS&L.

The battery chargers provide recharge control during Sun-oriented phases of the mission.

The booster converter and sharing sense unit ensures that normal system operation will be resumed upon reacquisition of the Sun after maneuvers or orbital occultation. Normal system operation occurs when all loads are supplied by the solar panel and no power is drained from the batteries in a sharing mode. The unit supplies a periodic, short voltage pulse to ensure operation in the high-voltage region of the solar panel I-V curve (see Section 4.2.13).

Two independently regulated d.c. busses provide power to the telecommunications subsystem and to the remainder of the spacecraft. A standby or redundant unit is provided for each of the two prime regulators.

The d.c./a.c. inverter provides a.c. regulated power to the attitude reference and science subsystems.

The failure-sense units provide detection and switching functions to disconnect a failed regulator or inverter and connect the redundant unit.

The synchronizer provides an accurate base frequency reference for the d.c./a.c. inverters.

4.2.3.2 Significant Electrical Characteristics

Solar array characteristics are:

1)	Nominal operating output voltage near Earth:	60 volts
2)	Nominal operating output voltage--Mars Orbit:	65 volts
3)	Peak output voltage--Mars orbit:	100 volts
4)	Maximum power near Earth (55°C):	1910 watts
5)	Maximum power Mars encounter (-2°C):	994 watts
6)	Maximum power end of mission (-18°C):	685 watts
7)	Maximum power at 50 mw/cm^2 (-24°C):	664 watts
8)	Solar-cell efficiency at air mass = zero, 140 mw/cm^2, (28°C):	11 percent
9)	Sun orientation required (for rated performance):	$\pm$5 degrees

Battery characteristics are:

1)	Cell voltage--end of discharge:	1.0 volts
2)	Cell voltage--end of charge:	1.5 volts
3)	Battery voltage--end of discharge:	38 volts
4)	Battery voltage--end of charge:	58 volts

5)	Nominal load voltage range:	40-46 volts
6)	Maximum battery capacity of one unit (system total = 3):	820 watt-hours

Power-conditioning equipment characteristics are:

1)	Series-switching d.c./d.c. regulator	
	a) Input Voltage:	37 to 100 v.d.c.
	b) Output Voltage:	35 v.d.c. ± 1%*
	c) Power Rating,Normal Operation:	205 watts
	(1) Design Maximum:	400 watts
	(2) Peak Capability (10 milliseconds)	700 watts
	d) Nominal Efficiency at 205 watts:	90%
2)	Inverter 2400 Cycle, Single Phase, square wave	
	a) Input Voltage:	35 v.d.c. ± 1%
	b) Output Voltage:	50 volts rms ± 3%
	c) Power Rating	
	(1) Nominal:	75 watts
	(2) Maximum:	120 watts
	d) Nominal Efficiency at 75 watts:	85%

4.2.3.3 Operational Modes

Prelaunch--During prelaunch activities, power is supplied to the power subsystem from operational support equipment (OSE). Spacecraft power-conditioning equipment operates at all times. Just prior to launch,

*NOTE: Voltage tolerance at user subsystem is ±5% to account for connector and line-voltage drops.

power is switched from external ground power to the spacecraft batteries. A load profile for all mission phases is shown in Figure 4.2-3.

Launch to Solar Acquisition--During the launch-to-solar-acquisition phase, spacecraft electrical power is provided by the spacecraft storage batteries.

Cruise--During normal cruise phases of the mission, all power is provided by the solar array except that the pyrotechnic subsystem is supplied by the battery. All power conditioning equipment is energized with the exception of the standby redundant equipment. The battery is kept fully charged by means of the charger/booster assembly. Capsule power (intermittent 200 watts peak) is supplied by the 35 volt d.c./d.c. regulators as indicated on the electrical system functional block diagram.

Midcourse Maneuver, Flight Capsule Deployment and Encounter--During midcourse maneuvers the battery charger is disabled. Raw power is available from spacecraft batteries.

Orbit Phase--During the orbit phase, the power subsystem will operate as in the cruise phase except that during the occulted portion raw power will be supplied by the spacecraft batteries and during the sunlit portion the solar array will supply all spacecraft power and battery recharge power.

4.2.3.4 System and Component Transfer Functions

Mathematical models have been developed for the various components of the electrical power system. These component models are based on test data and on applicable equivalent circuits and associated descriptive equations and transfer functions. The component models have voltage and current signal interfaces identified. A technique is used for simple interconnection (paralleling) of multiple power sources and load blocks that is compatible with analog simulation and readily adaptable to changes in system configuration.

Since the single cell power sources are modular (series and parallel buildup of cells or small modules) the basic single cell structure of the sources has been represented and then series and parallel configuration conversion factors are used for system connection.

Simplified models of distribution, and power conditioning and regulating equipment, have been developed. Each basic block has input and output voltage and current signals for system connection. Internal relationships between these terminal quantities include an adequate representation of the basic control law and an approximate representation of constant and variable losses.

Mathematical models of the various system components and the transfer functions relating the various terminal quantities are presented in the sections of the report devoted to a description of the respective components.

Figure 4.2-5, which shows the basic structure of the Voyager power system mathematical model, illustrates the component paralleling technique and the general signal interconnection between the transfer functions of the various system components. All symbols are defined in Table 4.2-3.

Steady-state analog computer runs have been made of the simple system illustrated in Figure 4.2-6. The transfer functions of the solar cell and battery are derived in the following sections. The computer results shown in Figure 4.2-7 demonstrate the performance of the electrical power subsystem illustrated in Figure 4.2-6. The computer analysis will be used in the various phases of the Voyager program on a continuing basis to compare both dynamic and steady-state performance of applicable configurations.

Transfer Functions of Solar Array--A mathematical model has been developed that simulates the electrical characteristics of a solar array. Figure 4.2-8 is a block diagram showing the internal representation of the solar cell with the various transfer functions between the external signal quantities. The model uses experimentally derived coefficients to determine the change in I-V characteristics of the array as temperatures and intensity change. The model shown in Figure 4.2-8 has been compared to other techniques of deriving I-V curves and, over the range of expected temperatures and intensities, appears to accurately simulate the change in array characteristics. Further work will be done in Phase IB to ensure that all experimental coefficients and approaches are correct. The main advantage of the approach illustrated in Figure 4.2-8 over the more

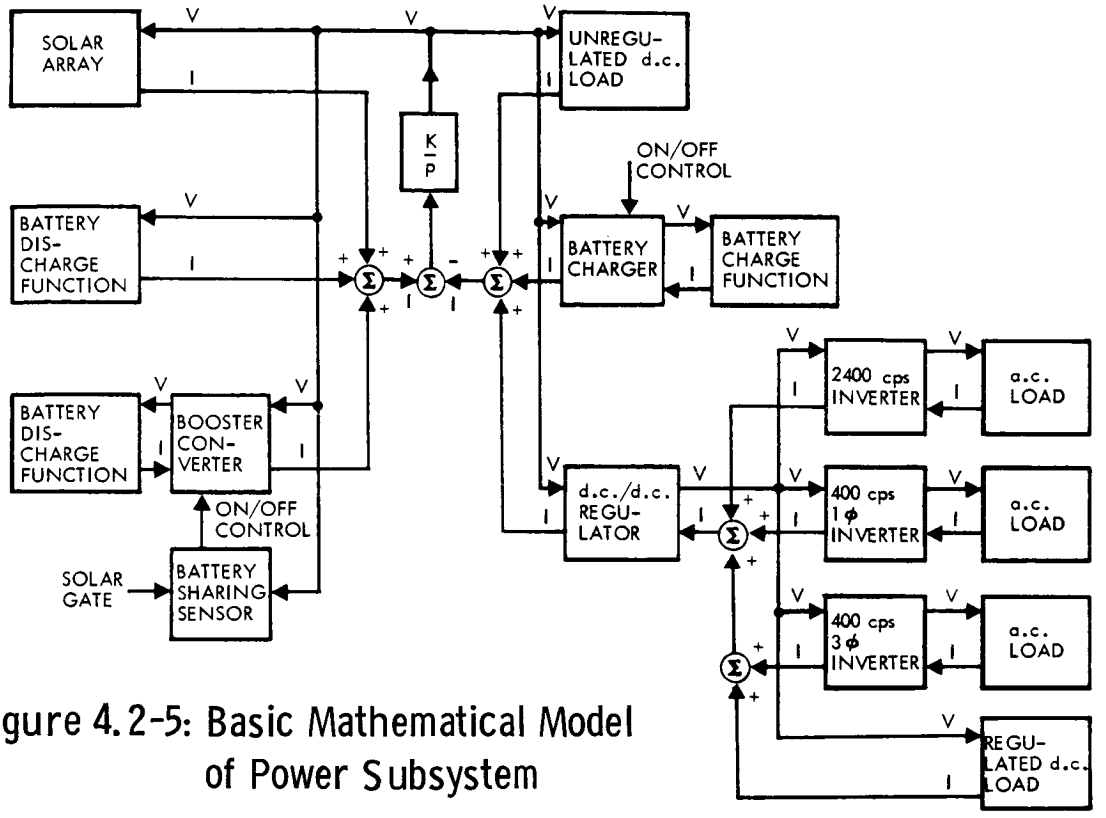

Figure 4.2-5: Basic Mathematical Model of Power Subsystem

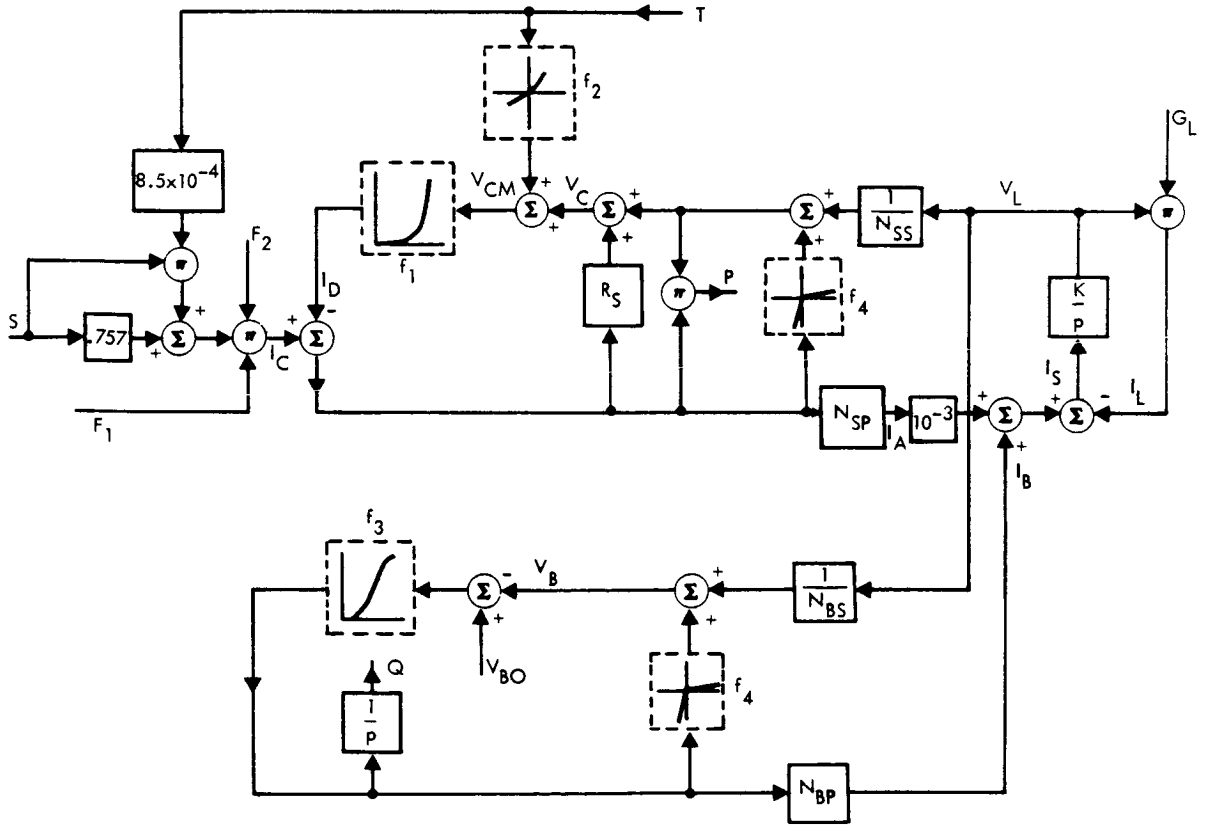

Figure 4.2-6: Mathematical Model of Solar-Cell/Battery/Load

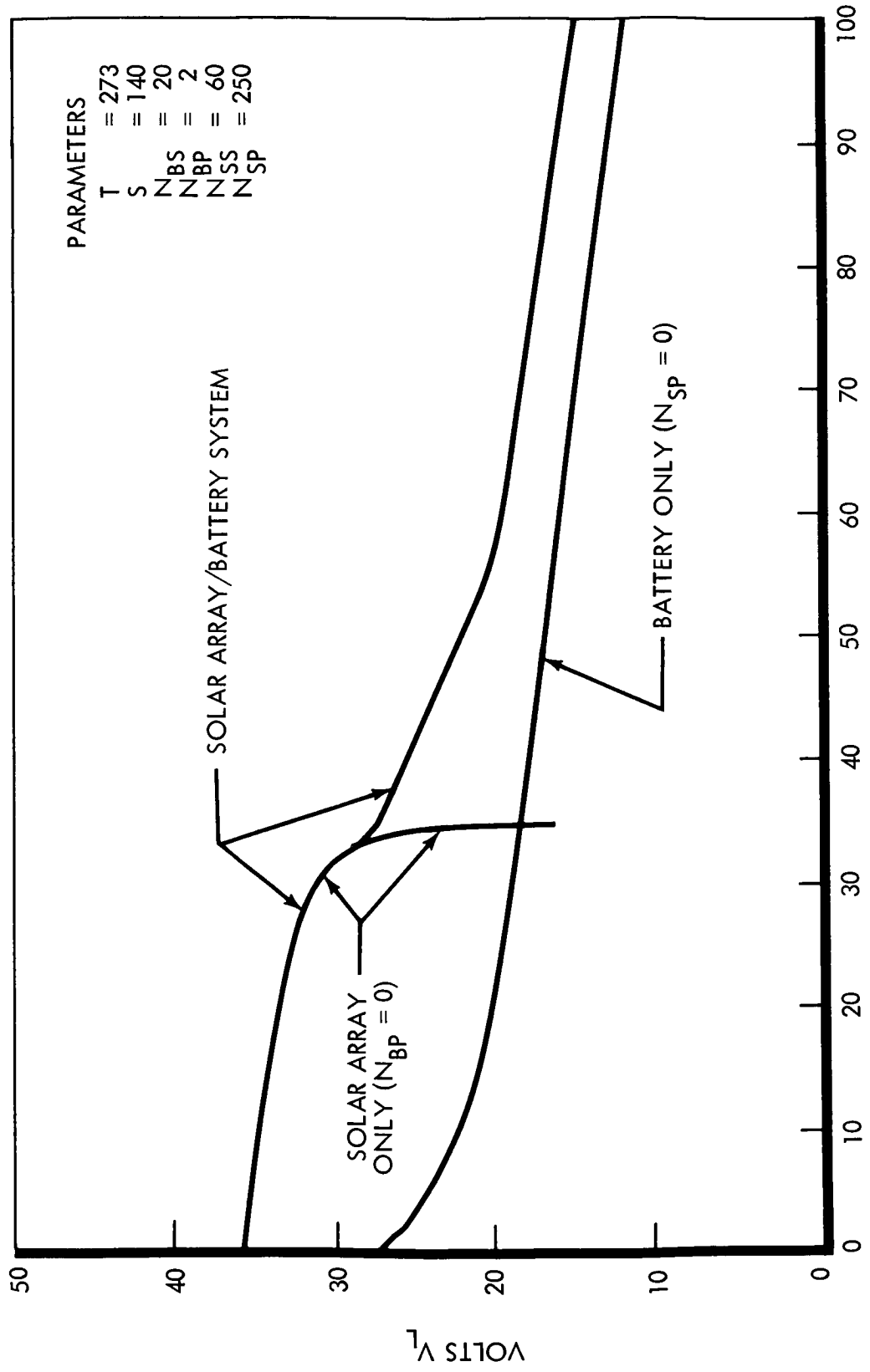

Figure 4.2-7: Volt-Ampere Characteristics System of Figure 4.2-6 Analog Computer X-Y Plot

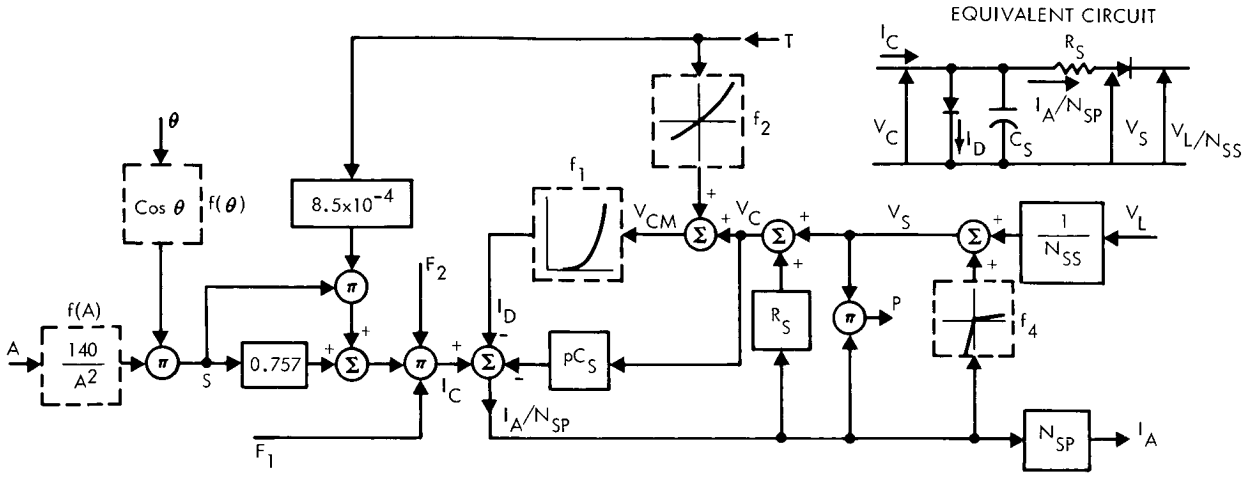

SYMBOLS

A = DISTANCE FROM SUN (astronomical units)
C_S = SINGLE-CELL CAPACITANCE (farads x 10^3)
f_1 = I_D VS V_{CM} BASE FUNCTION (Figure 4.2-8)
f_2 = TEMPERATURE FUNCTION (Figure 4.2-8)
f_4 = BLOCKING DIODE FUNCTION (per-cell basis)
F_1 = DEGRADATION FACTOR (per-unit)
F_2 = DESIGN FACTOR (per-unit)
I_A = SOLAR ARRAY CURRENT (ma)
I_C = SINGLE-CELL CURRENT-GENERATOR (ma)
I_D = SINGLE-CELL DIODE JUNCTION CURRENT (ma)
N_{SS} = NUMBER CELLS IN SERIES
N_{SP} = NUMBER CELLS IN PARALLEL
P = SINGLE-CELL POWER (mw)
p = DERIVATIVE OPERATOR, d/dt
R_S = SINGLE-CELL RESISTANCE (ohms x 10^{-3})
S = SOLAR INTENSITY (mw/cm^2)
T = CELL TEMPERATURE (°K)
V_C = DIODE JUNCTION VOLTAGE (volts)
V_{CM} = MODIFIED JUNCTION VOLTAGE (volts)
V_L = ARRAY VOLTAGE (volts)
V_S = CELL VOLTAGE (volts)
θ = ORIENTATION ANGLE (degrees)

Figure 4.2-8: Detailed Mathematical Model of Solar Cell

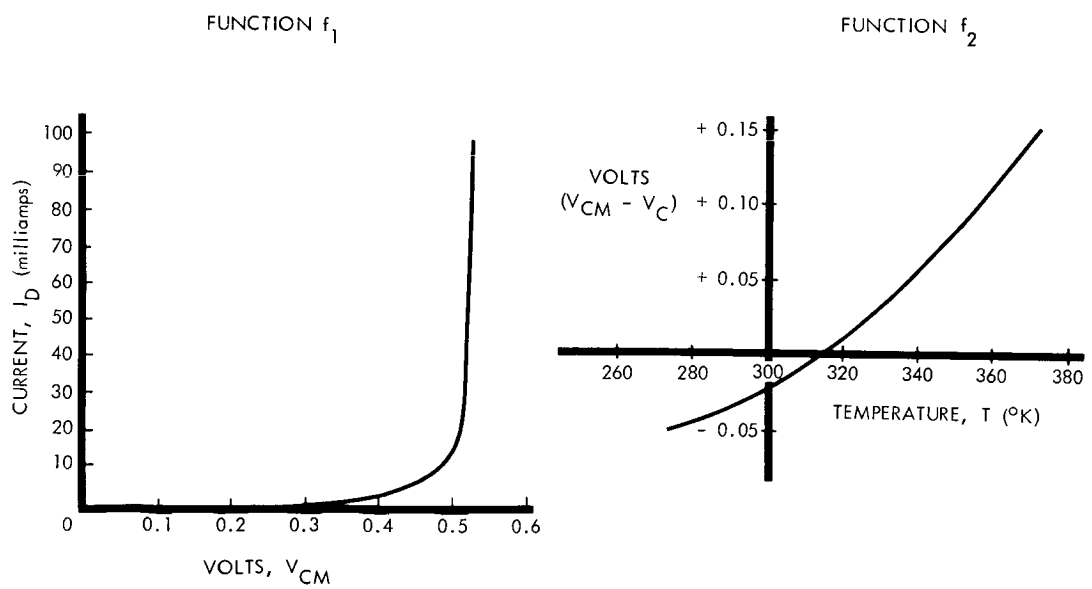

Figure 4.2-9: Solar Cell Functions

Table 4.2-3: DEFINITION OF SYMBOLS

List of Symbols

A	Distance from Sun (astronomical units)
C_B	Equivalent capacitance
C_S	Single-cell capacitance (farads x 10^3)
f_1	I_D vs V_{CM} base function
f_2	Temperature function
f_3	Battery charge/discharge function
f_4	Blocking diode function
f_B	Blocking and series loss function
f_S	Feedback-control saturation function
$f(T_B)$	Temperature compensation function
f_V	Voltage control function
G_A	Feedback-control gain
$G_C(p)$	Feedback-control stabilizing function
G_L	Load conductance (mhos)
G_S	Shunt loss conductance
I	General current signal
I_o	Output current
I_A	Solar-array current (ma)
I_B	Total battery current
I_C	Single-cell current generator (ma)
I_D	Single-cell diode junction current (ma)
I_i	Input current
I_L	Load current (amps)
K_B	Boost transformation factor
K/p	Current balance integrating control

Table 4.2-3: (Cont.)

K_T	Ideal voltage and current total transformation factor
N_{BP}	Number of battery cells in parallel
N_{BS}	Number of battery cells in series
N_{SP}	Number of solar cells in parallel
N_{SS}	Number of solar cells in series
θ	Orientation angle (deg.)
p	Derivative operator d/dt
P	Single-cell power (mw)
Q	Ampere hours charged or discharged
R	Feedback-control reference
R_S	Single-cell resistance (ohms x 10^{-3})
S	Solar intensity (mw/cm^2)
T	Cell temperature (^oK)
T_B	Battery temperature
V	General voltage signal
V_i	Input voltage
V_o	Output voltage
V_{BO}	Battery no-load voltage
V_C	Diode junction voltage (volts)
V_{CM}	Modified junction voltage (volts)
V_L	Bus voltage (volts)
V_S	Solar cell voltage (volts)
V_B	Battery cell voltage (volts)

traditional I-V curve translation techniques (originated by Zautendyke) is that it can be integrated more readily into the overall system analog model.

The following are some significant facts and the principal assumptions which are the basis for the representation shown in Figure 4.2-8.

1) The basic electrical circuit shown in Figure 4.2-8 is used as an equivalent form.

2) Test data on a 2-by-2 centimeter RCA 8-mil silicon N/P solar cell was used to determine the functional relationships in a sample model and to verify the model by analog simulation. Conversion to array voltage and current is accomplished through the factor N_{SS} (cells in series) and N_{SP} (cells in parallel).

3) Diode junction current I_D is a function of solar-cell temperature and diode voltage: $I_D = f_d(V_c,T)$. Test data on the cells indicated in 2) above was plotted to show this functional relationship. The following explicit form approximation was found to fit the data with good accuracy:

$$f_d(V_c,T) \quad f_1(V_c + f_2(T))$$

Functions f_1 and f_2 are shown in Figure 4.2-9 and are indicated in the representation of Figure 4.2-8.

4) Current-generator current I_c is a function of solar-cell light intensity, S, and temperature T: $I_c = f_{s1}(S,T)$. The following explicit form approximation was found to fit the test data with good accuracy:

$$f_{s1}(S,T) \quad S\ F_1\ F_2\ f_{s2}\ (T)$$

where: $f_{s2}(T) = 8.5 \times 10^{-4}\ T + 0.757$

Analog computer runs were made to verify the solar cell simulation for various solar intensities and temperatures. Typical results of the computer run for the sample chosen are shown in Figure 4.2-10.

In the model shown, series resistance was chosen as a constant. The effect on voltage is not accounted for at present in the model but will be investigated in later models.

Transfer Function of Battery--Mathematical models have been developed that simulate the electrical characteristics of a secondary battery in the charge and discharge modes. Figure 4.2-11 is a block diagram showing the internal representation of a battery with the various transfer functions between the external signal quantities. The following assumptions are the basis for the representation shown in Figure 4.2-11.

1) Test data on a 3 ampere-hour Yardney silver cadmium (AgO-Cd) cell was used to determine the steady-state functional relationships in the model. Conversion to battery voltage and current is accomplished through the factors N_{BS} (cells in series) and N_{BP} (cells in parallel).

2) The battery transfer characteristic f_3 can in general be expressed as a function of several variables:

$$I_B = f_3\left[(V_{BO} - V_B),\ T_B,\ Q_O,\ \bar{H}\right]$$

where T_B = Battery temperature

Q_O = State-of-charge

H = Charge/Discharge cycle history

A typical function f_3 in Figure 4.2-12 was evaluated from the test data of a (AgO-Cd) cell for a fully charged condition at normal room ambient temperature.

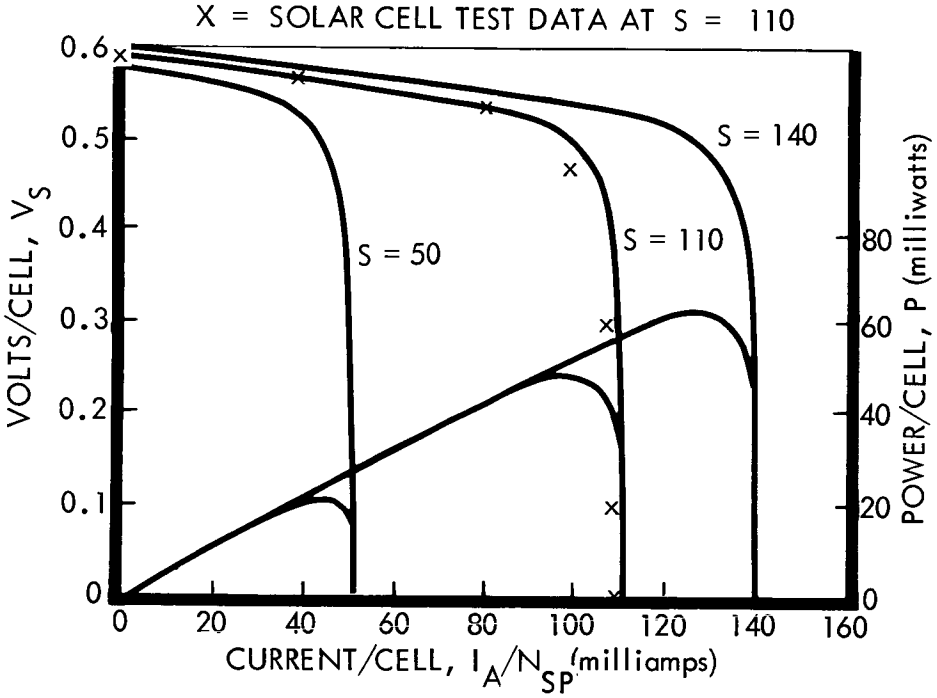

Volt-Ampere and Power Characteristics —
Solar Cell Model of Figure 4.2-8
T = 273°K (Analog Computer X-Y Plot)

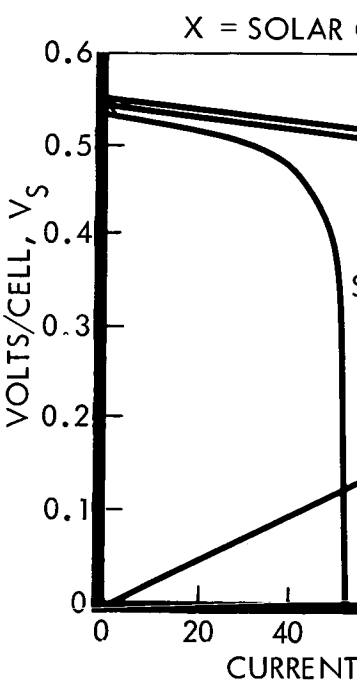

Volt-Am
Solar C
T = 313

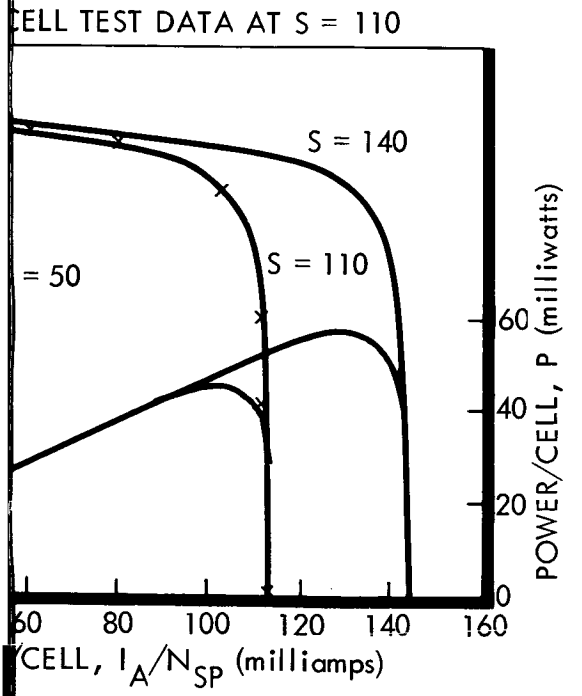

pere and Power Characteristics—
ll Model of Figure 4.2-8
K (Analog Computer X-Y Plot)

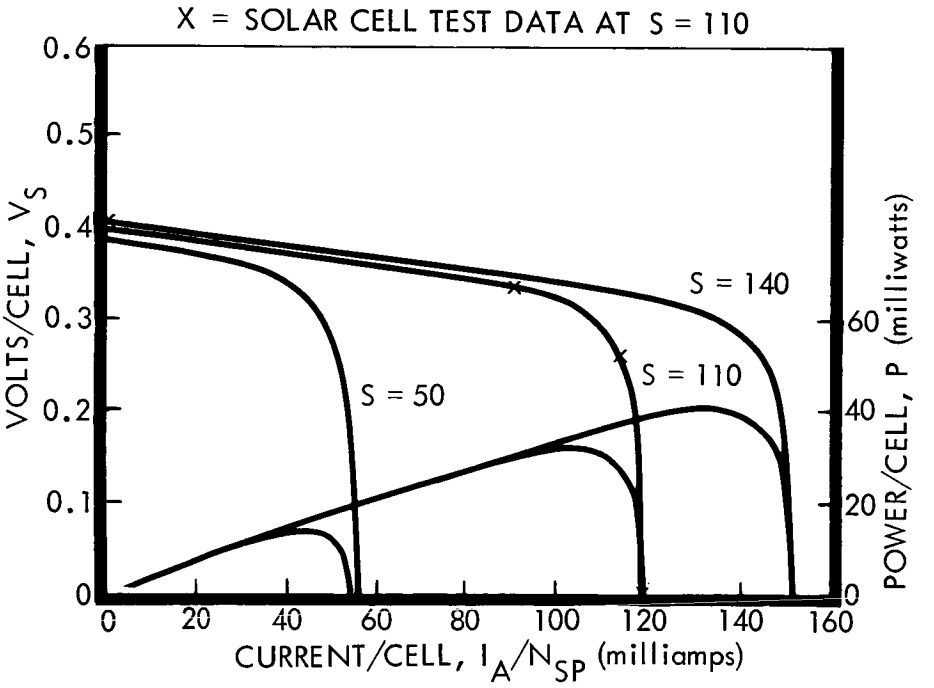

Volt-Ampere and Power Characteristics —
Solar Cell Model of Figure 4.2-8
T = 373°K (Analog Computer X-Y Plot)

Figure 4.2-10: Typical Computer Runs

2

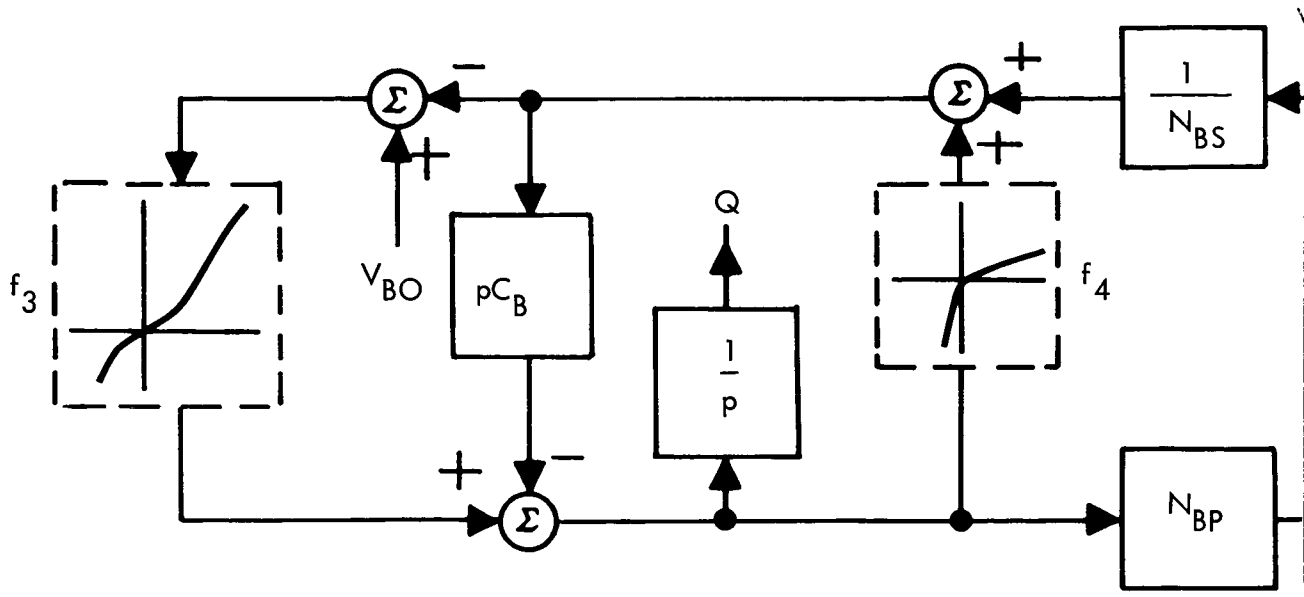

DISCHARGE MODEL

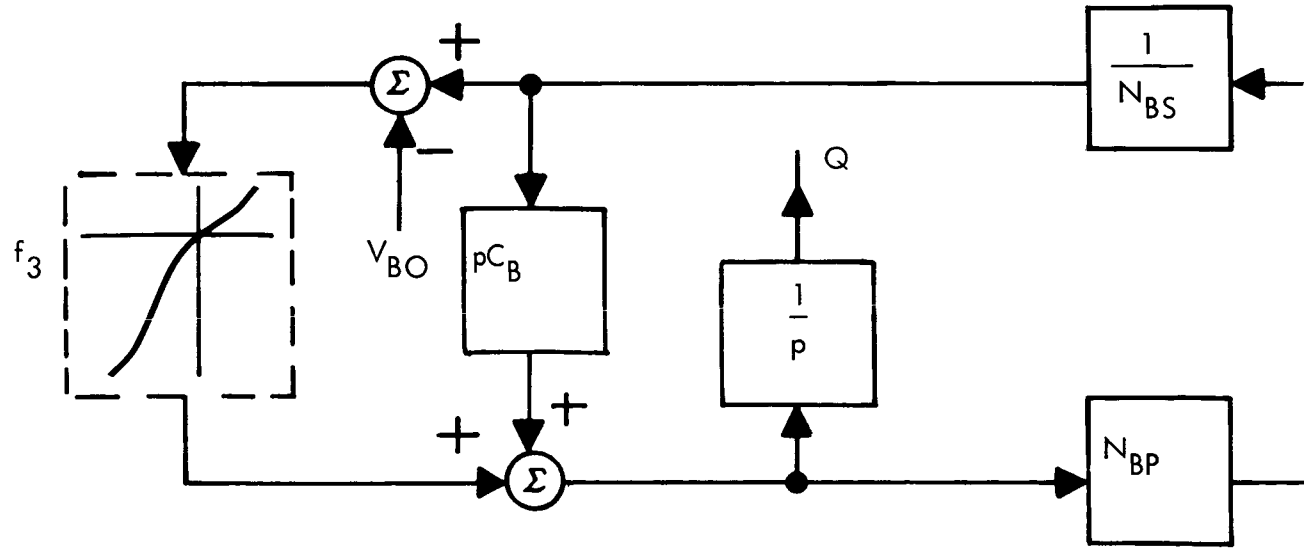

CHARGE MODEL

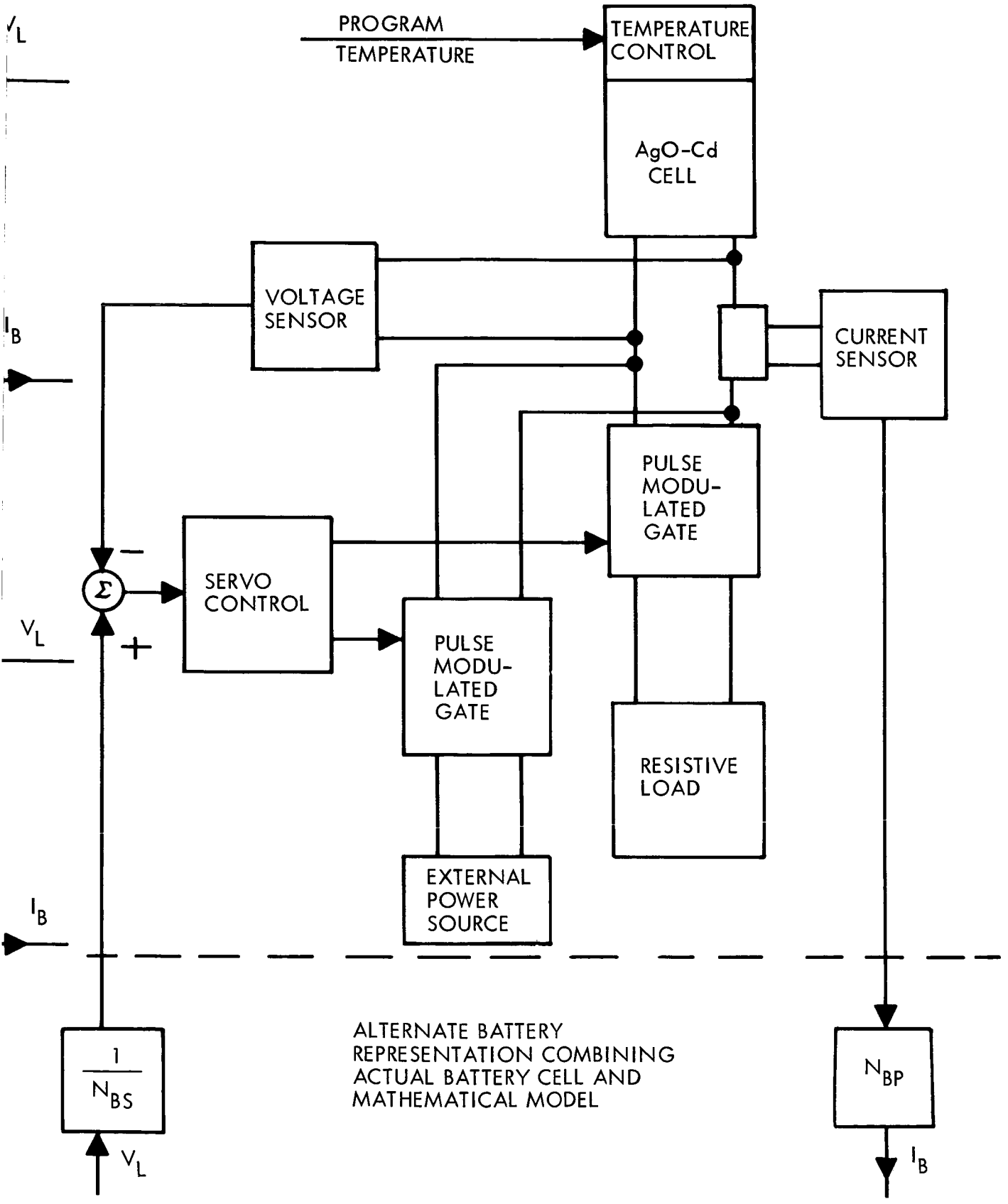

Figure 4.2-11: Battery Models

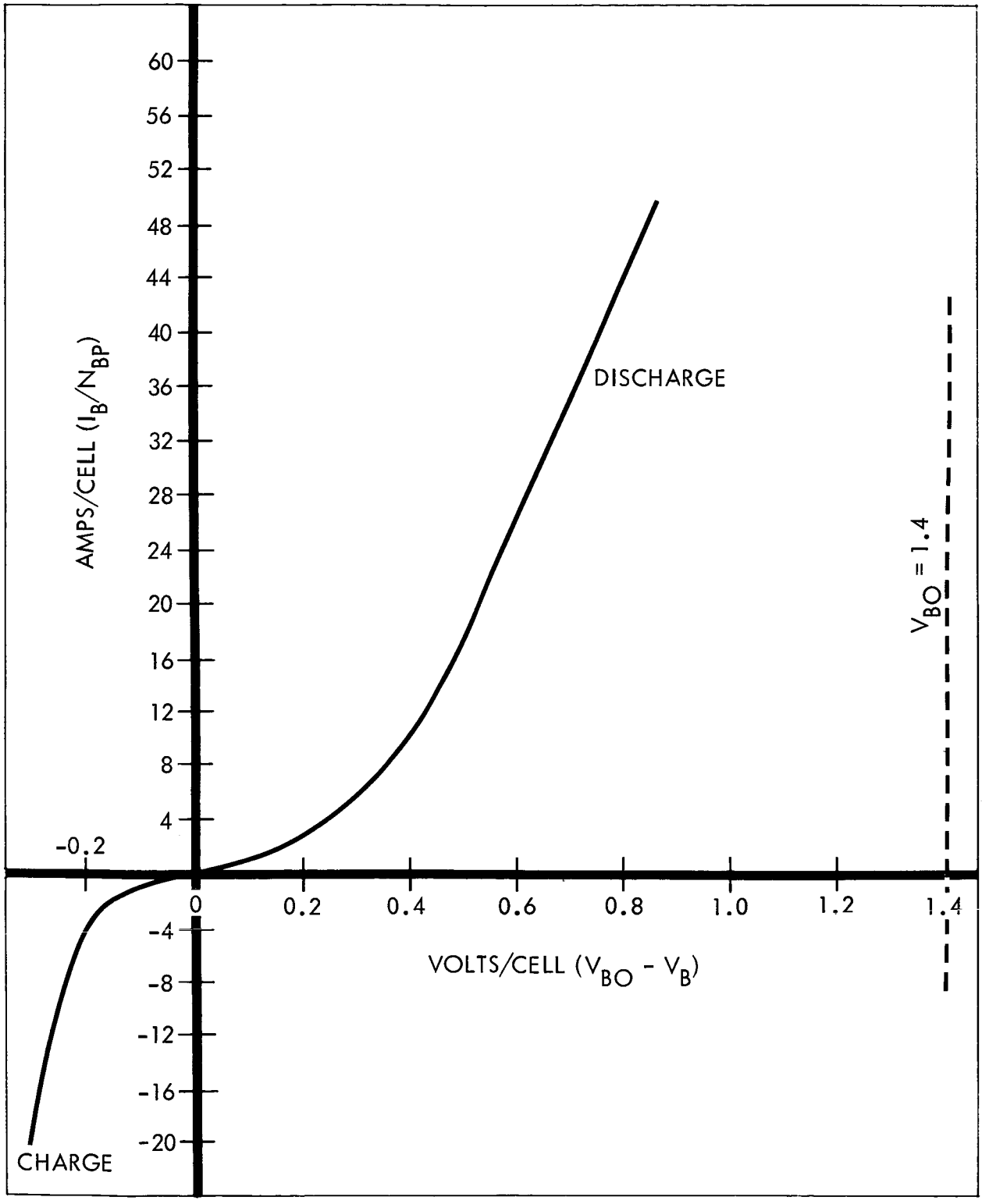

Figure 4.2-12: Battery Function f_3

3) The dynamic representation of a battery is complicated by the fact that both the equivalent dissipative elements and energy storage (capacitance and inductance) elements are non-linear. From a frequency-response standpoint there are both frequency-dependent and amplitude-dependent nonlinearities. Because of the relatively complex nature of battery dynamics, only a simplified dynamic representation to account for the relatively large battery capacitance effect has been included in the model of Figure 4.2-11.

Also shown in Figure 4.2-11 is an alternate arrangement in which the actual AgO-Cd cell is employed in conjunction with the mathematical model. This method of representation provides greater accuracy of battery-transfer-function simulation and provides for programming variation of battery temperature and state of charge. The alternate method employs a servoamplifier that adjusts actual battery charge and discharge conditions to match actual battery voltage and mathematical model voltage. This arrangement will also provide an accurate dynamic representation of the battery for a dynamic analysis of the solar-cell/battery system in real time on the analog computer.

Transfer Functions of Power Conditioning Equipment--Simplified mathematical models have been developed for the d.c./d.c. converter regulator, battery charger, battery booster, and inverters. The following assumptions are the basis for the simplified representations shown in Figure 4.2-13.

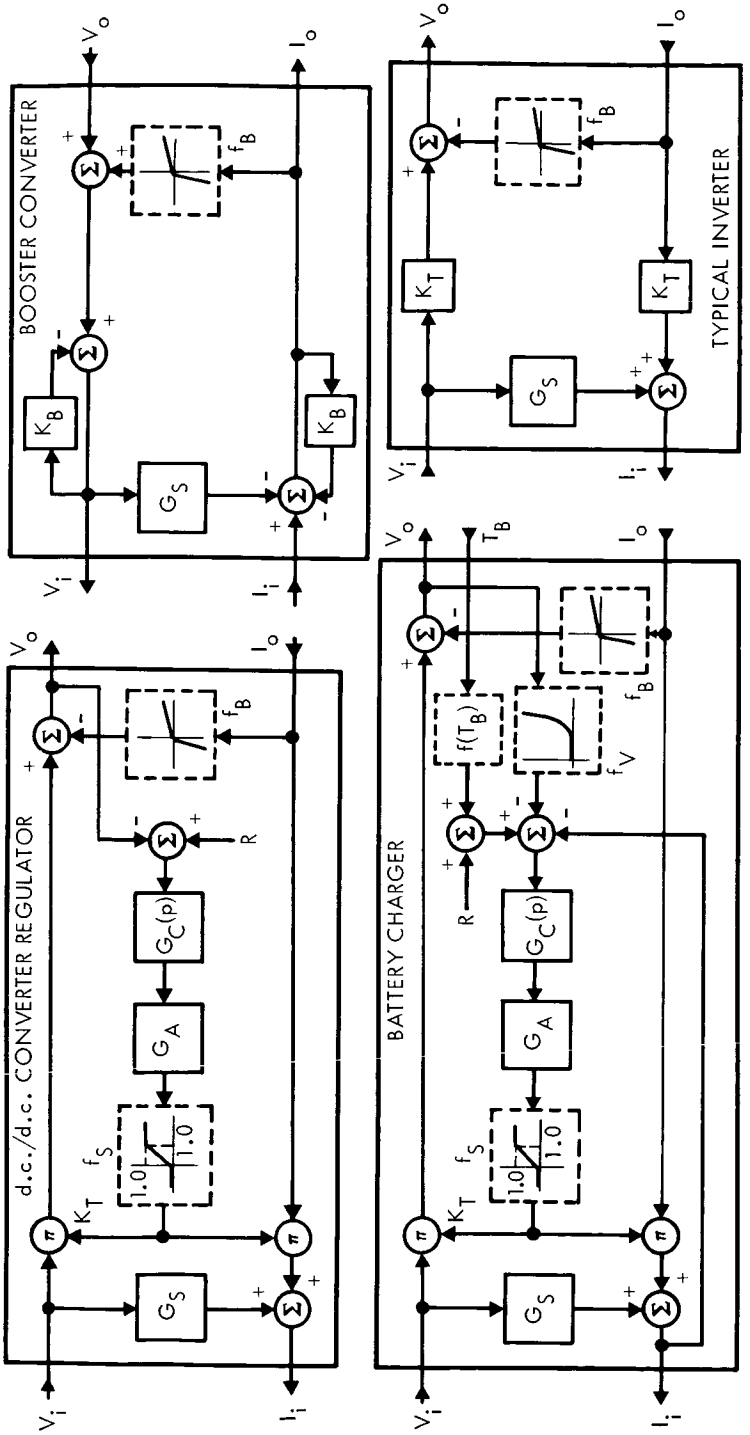

Figure 4.2-13: Transfer Functions of Conversion and Regulating Equipment

1) The power losses in the equipment are represented by a loss that is a function of input voltage plus a loss that is a function of output current.

2) In the representation of the basic control law relating the terminal quantities, the dynamics associated with the frequencies of the pulse modulation mode of control is neglected.

3) The representations are in terms of general parameters showing the proposed form of the transfer functions without quantitative values.

4.2.3.5 Subsystem Design Optimization Studies

Top-level trade studies described in D2-82709-2, Section 4.2, lead to the selection of a basic electrical power subsystem concept. However, many lower-level trade studies or design optimizations are needed to establish details of the mechanization. These design optimizations are contained in this section and cover the following subjects:

1) Selection of subsystem regulated d.c. voltage;

2) Power distribution to telecommunications and central computer and sequencer;

3) Power distribution for science subsystem;

4) Power switching and logic configuration;

5) Prevention of solar array and battery sharing mode;

6) Method of applying redundancy.

Selection of Subsystem Regulated d.c. Voltage--Selection of the regulated d.c. voltage level is illustrated in Figure 4.2-14 and is based primarily on operating ranges of the battery and solar panel, and weight and reliability of the electrical power subsystem. A high bus voltage is

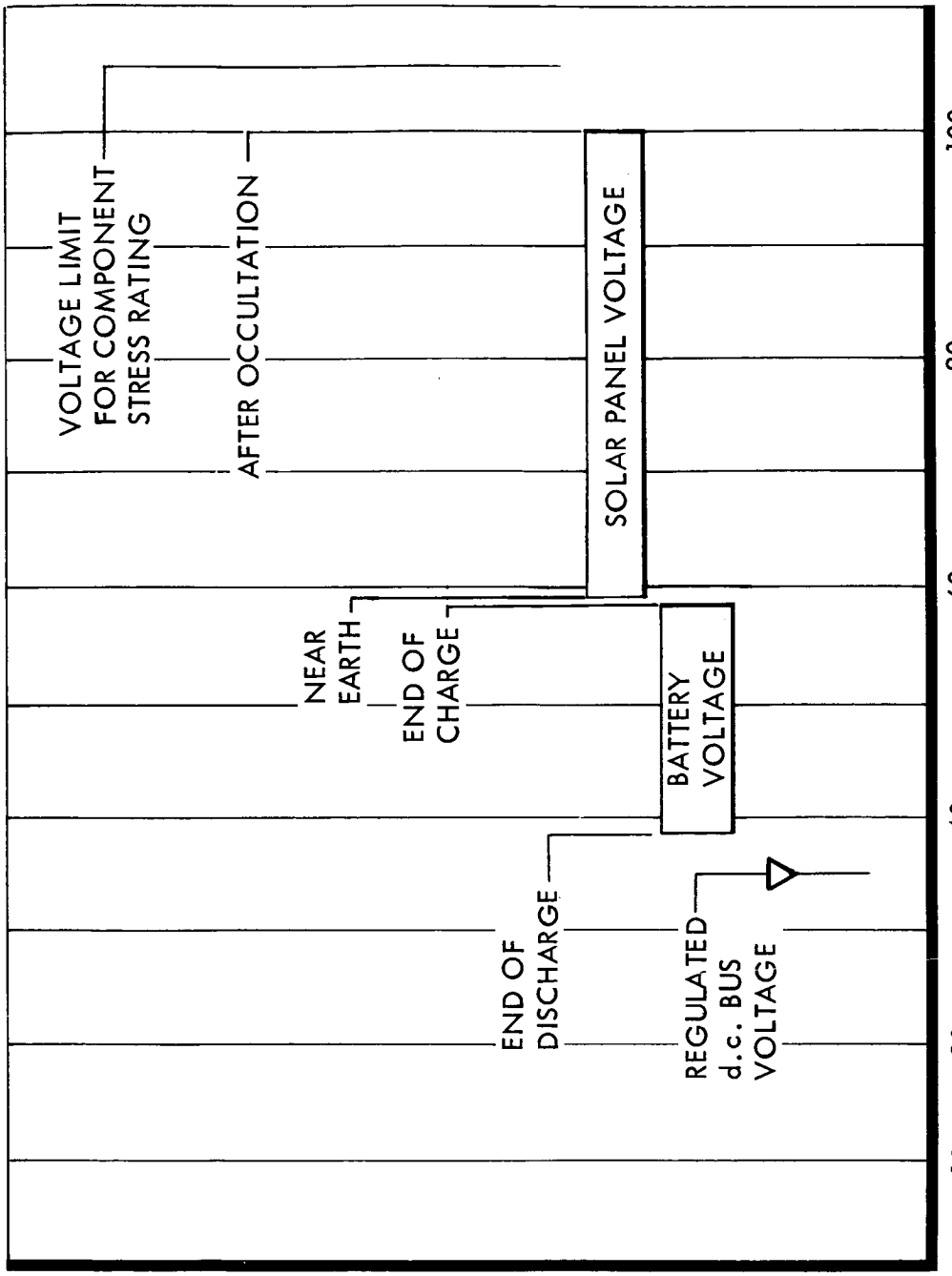

Figure 4.2-14: Subsystem Voltage Relationships

desirable to keep current levels low and minimize component and wire weight. Also, high impedance levels lead to easier filtering (both ripple and RFI) and lower currents tend to minimize magnetic fields.

As shown in Figure 4.2-14, the maximum unregulated bus voltage from the solar panel is established at some level below the maximum stress level of the solid-state components in the series regulator.

For a transistor with a V_{CEX} rating of 150 volts (typical) at a voltage stress rating of 70 percent, the maximum source voltage must be limited to about 100 volts. Assuming worst-case conditions at Mars with an array temperature of -180°C (exiting shadow), a solar intensity of 65 mw/cm^2 (just after encounter) and an array voltage of 100 volts, the array voltage at Earth will be 58 volts (at 140 mw/cm^2, 55°C, and a load power of 500 watts).

The unregulated bus voltage must be higher than the voltage needed to charge the battery. This sets the solar-array minimum operating voltage, which must be equal to or greater than the terminal voltage of the fully charged battery (58 volts).

The regulated system bus must be less than the end-of-discharge plateau voltage of the battery (38 volts for the preferred configuration).

To be compatible with the battery and solar-panel limits, the regulated bus system was chosen at 35 v.d.c. The primary factor in limiting the

voltage to a maximum of 35 v.d.c. is the high panel voltage during Mars orbit occurring just after occultation. (See Section 4.2.9, Figure 4.2-19)

Power Distribution to Telecommunications and Central Computer and Sequencer--

Transmission of data to Earth is the primary purpose of the spacecraft. If one or more spacecraft functions fail, the return of engineering data to Earth to enable analysis and malfunction identification is of extreme importance. Preservation of the ability to transmit commands to the spacecraft in an effort to correct or work around the malfunction is of equal importance. Each subsystem involved in the transmission of data to Earth or the reception and execution of commands is designed to achieve maximum probability of maintaining these vital functions. Interactions between subsystems are not allowed to influence the operations of data transmission and command reception.

The telecommunication and CC&S subsystems have had features incorporated to support the concept outlined above.

Two alternate approaches were considered: supply power from a common regulated d.c. bus or supply power from a separate regulated bus.

The second alternate was selected after an analysis of failure modes and effects. System weight is increased by the addition of primary and standby series-switching d.c./d.c. regulators and the associated d.c. failure sensing unit.

1) Two series-switching d.c./d.c. regulators = 12.8 pounds

2) One d.c. failure sensing unit = 1.7 pounds

The failure modes and effects analysis follows. Only failure modes producing system difficulty are discussed.

Supply from Common Regulator--A short-circuit condition in any equipment supplied by the regulator will cause failure of the primary regulator and ultimately of the standby unit unless the fault clears itself. Power to telecommunications and CC&S will be degraded or fail completely.

A serious overload in any equipment powered from the regulator might degrade performance.

A noisy or oscillatory condition in another subsystem (for example, the autopilot) might cause degraded telecommunication or CC&S performance because of electrical interference feeding through the power circuits.

Supply from Separate Regulator--Noise occurring in equipment connected to the Spacecraft Bus (Figure 4.2-4) is effectively filtered and prevented from interfering with telecommunications by the isolation inherent in the regulators.

A serious overload or short circuit in the Spacecraft Bus might cause the spacecraft regulator to fail and permit the unregulated bus voltage to drop low enough to draw power from the batteries. In such a case, the d.c. resistance of the regulator sensing elements will limit the

current, and the voltage will not fall below the second plateau level of the battery. This voltage is within the rated input range of the telecommunication regulator; therefore, normal operation of the telecommunication and CC&S subsystems will continue.

Power Distribution Science Subsystem--Most of the electrical power distributed by the power subsystem is in the form of regulated d.c. at 35 volts. Regulated 2.4-kilocycle a.c. at 50 volts rms is distributed to the science subsystem. The reasons for this choice are discussed in the following paragraph.

The many science experiments will be conceived and designed by a relatively large number of individuals and organizations throughout the country. Power distributed should be in a form that can be readily converted by the user and must present the least amount of interface problems. A standard square-wave a.c. voltage fulfills this requirement better than a standard d.c. voltage. The a.c. voltage can be easily converted by a transformer-rectifier unit and regulated by a simple voltage regulator (if required). On the other hand, d.c. voltage must be converted by a more complex d.c./d.c. converter.

Many of the experimenters on the Voyager program have built equipment for the Mariner IV spacecraft. Because Mariner IV used 2.4-kilocycle, 50-volt-rms alternating current, these persons have already gained experience with its use.

A secondary consideration in the selection of the form of the distributed power is overall system efficiency. The total power required by the science subsystem is about 75 watts; however, each experiment item will require lower power levels--down to 1 watt. At these low power levels, the efficiency of d.c./d.c. converters is typically 65 percent because of the relatively high fixed power losses. Transformer-rectifiers, on the other hand, can maintain efficiencies up to 90 percent. Including the efficiency of the power-subsystem 2.4-kilocycle inverter, the resultant efficiency is 77 percent for a.c. distribution compared to 65 percent for d.c. distribution.

Power Switching and Logic Configuration--Power switching and logic (PS&L) designs in the past Ranger and Mariner vehicles have used passive logic diodes to perform the isolation and switching functions of the input power sources. An alternate design was considered for Voyager using active silicon-controlled rectifiers (SCR) in the battery leads and passive diodes in the solar-array leads. This allows a higher regulated bus voltage for the same solar-array voltage as the passive logic design. The advantage of a higher bus voltage will be weighed against a reduced reliability to determine the selected design. (Active SCR'S in the solar-array leads provide no operational advantage. Consequently, they will not be considered as an alternate approach.)

During normal cruise mode, the input raw bus voltage is determined by the intersection of the solar array and load I-V characteristics. With the passive diode PS&L, this voltage level is always higher than the

battery voltage and, consequently, the battery isolation diode is reverse-biased. The battery can be charged only to a voltage level less than the raw bus voltage or battery-charging power will be delivered to the load. The end-of-charge voltage level of the battery is therefore established at the normal solar-array operating voltage (about 58 v d.c.). This establishes the end-of-discharge voltage at 38 v d.c. using the AgO-Cd battery.

Consequently, the minimum regulated output voltage is established at 35 v d.c. (to allow voltage drops through the PS&L, wiring, and series-switching regulator).

For the active SCR design, the battery can be charged to a higher voltage than the raw bus voltage because the SCR need not be operating.

If the system load increases to a value greater than the power capability of the solar array, raw bus voltage will drop. At a preset voltage level (near the maximum power voltage), the SCR will be turned on to connect the battery to the bus. When the load returns to normal, the bus voltage will rise and disconnect the battery from the line as in the passive-diode circuit.

For the SCR system, the beginning-of-discharge voltage rather than the end-of-charge voltage is set at the normal solar-array voltage of 58 v.d.c. Therefore, the end-of-discharge voltage is 44 v.d.c. rather than 38 v d.c., and the regulated system voltage can be 41 rather than 35 v d.c.

The following table illustrates the difference in system parameters for each configuration.

	VC Max	VD Max	No. of Cells	VD Min	System Input Voltage Range	System Regulated Output Volt.
Diode Logic	58.0	50	38	38	38 to 100	35 v d.c.
SCR	62.3	58	44	44	44 to 100	41 v d.c.

VC max = end-of-charge voltage VD max = beginning-of-discharge voltage

V_D min = end-of-discharge voltage

The higher system regulated output voltage would reduce system currents, resultant magnetic fields, and wire sizes.

A comparative reliability analysis (Reference 6) was performed to indicate the relative reliabilities of each alternate configuration for 5880 hours of operation. The definition of failure for each configuration was "loss of more than two panel electrical section diodes or loss of more than one battery diode." The results are as follows:

1) Diode logic R = 0.999998

2) SCR logic R = 0.99872

A considerably lower reliability is noted for the SCR logic relative to the diode logic PS&L; this results because the active circuitry must be

included to operate the SCR's. In addition to the above, the reliability of the battery used with the SCR system will be reduced because a greater number of cells is required (44 compared to 38) to achieve operating voltage. (Note: An alternate to increasing the battery voltage when using the SCR PS&L would be to reduce the solar-array voltage. However, the advantage gained in raising the regulated system voltage would then be lost.)

Advantages of the use of an active SCR circuit are:

1) Reduced input voltage range of the systems, (44 to 100 rather than 38 to 100 v d.c.);
2) Higher regulated d.c. bus voltage (41 rather than 35 v d.c., assuming no change in the solar-panel voltage).

Advantages of the diode logic circuit are:

1) Reduced circuit complexity and greater reliability;
2) Lower number of series battery cells and therefore increased battery reliability.

The diode logic circuit has been selected for the preferred design because of its lower complexity and demonstrated reliability in the Ranger and Mariner spacecraft.

Prevention of Solar Array and Battery Sharing Mode

Whenever the input I-V characteristics curve of the power subsystem intersects the battery I-V curve at a current greater than the solar-

array current and also intersects the solar-array I-V curve at a voltage greater than the battery voltage, power sharing between the solar array and the battery can occur. This is an unnecessary condition that would eventually deplete the energy stored in the battery.

The preferred design of the power subsystem uses a booster converter to prevent the unnecessary sharing. Other methods are possible. The following discussion compares the various approaches.

Four configurations are evaluated (see also Figure 4.2-15):

1) Booster converter;

2) Capacitor discharge;

3) Separate battery;

4) Increased solar-array size (overcapacity).

A discussion of solar-array overcapacity to prevent sharing appears in Appendix B of EPD 250 and references contained in that document.

The first three configurations essentially apply a voltage (pulse) to the unregulated bus; this voltage is equal to or greater than the solar-array maximum power voltage to transfer from the battery-sharing mode. The fourth configuration increases the array size so that only one intersection with the load characteristics can occur; thus battery sharing cannot occur.

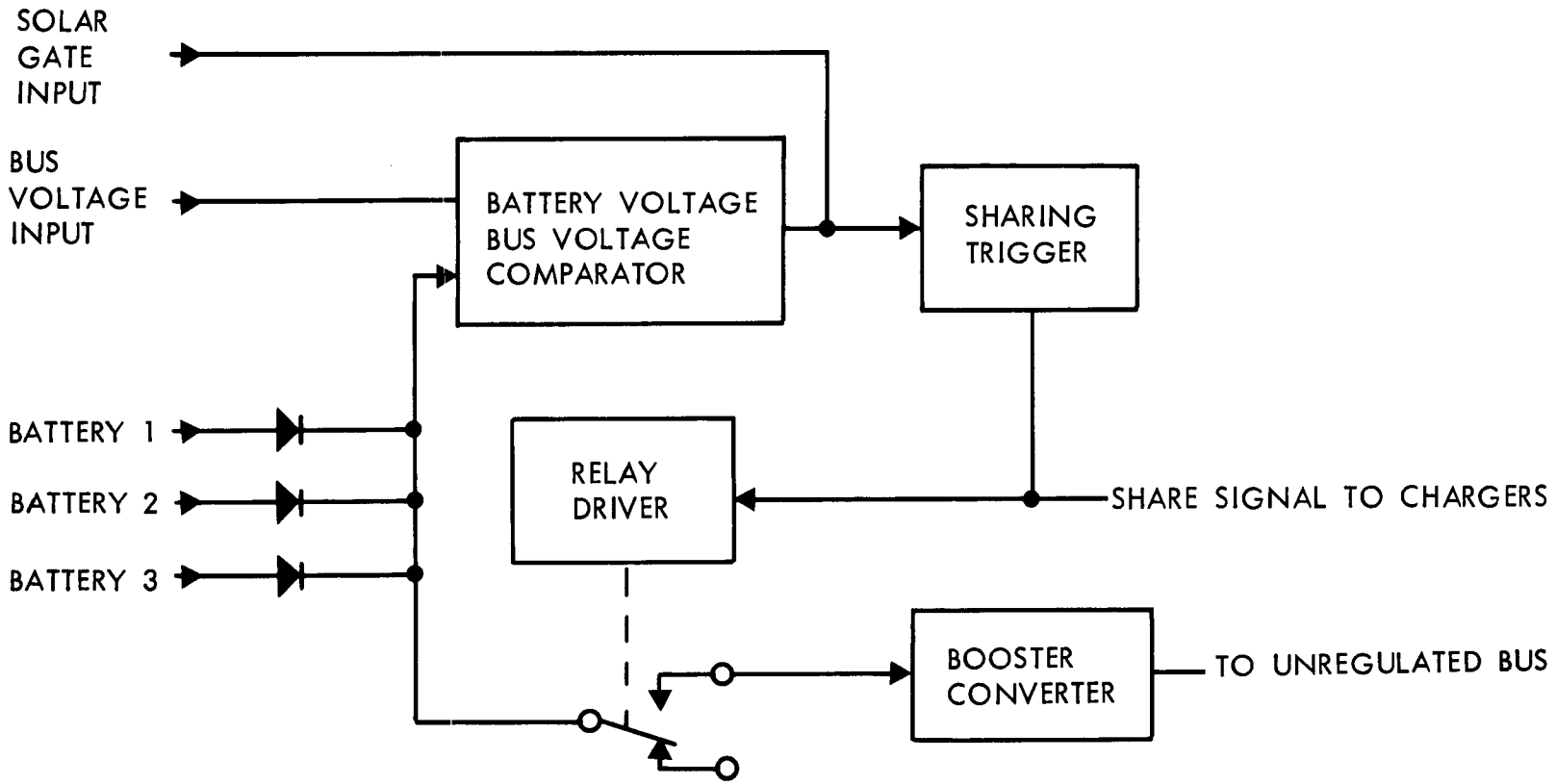

Booster Converter

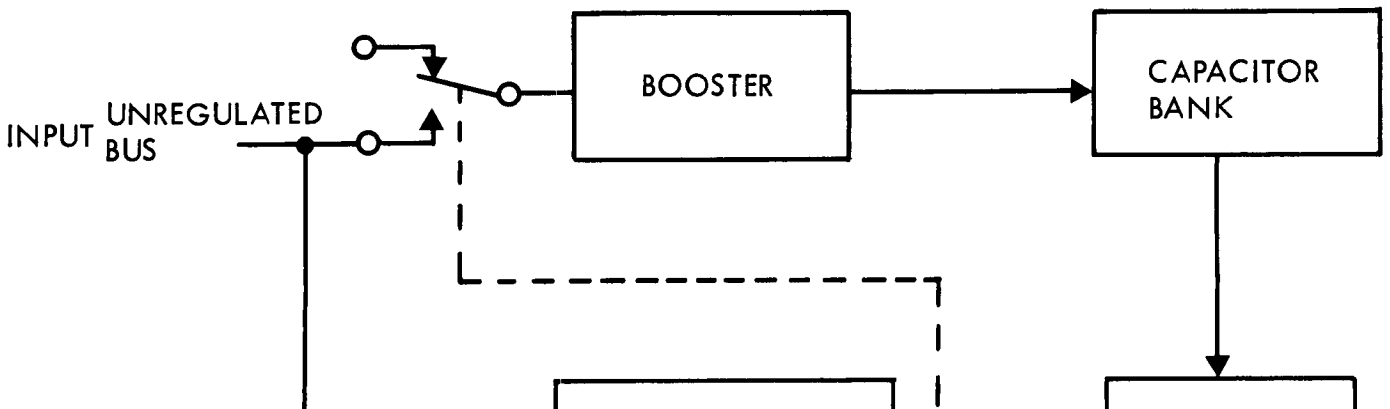

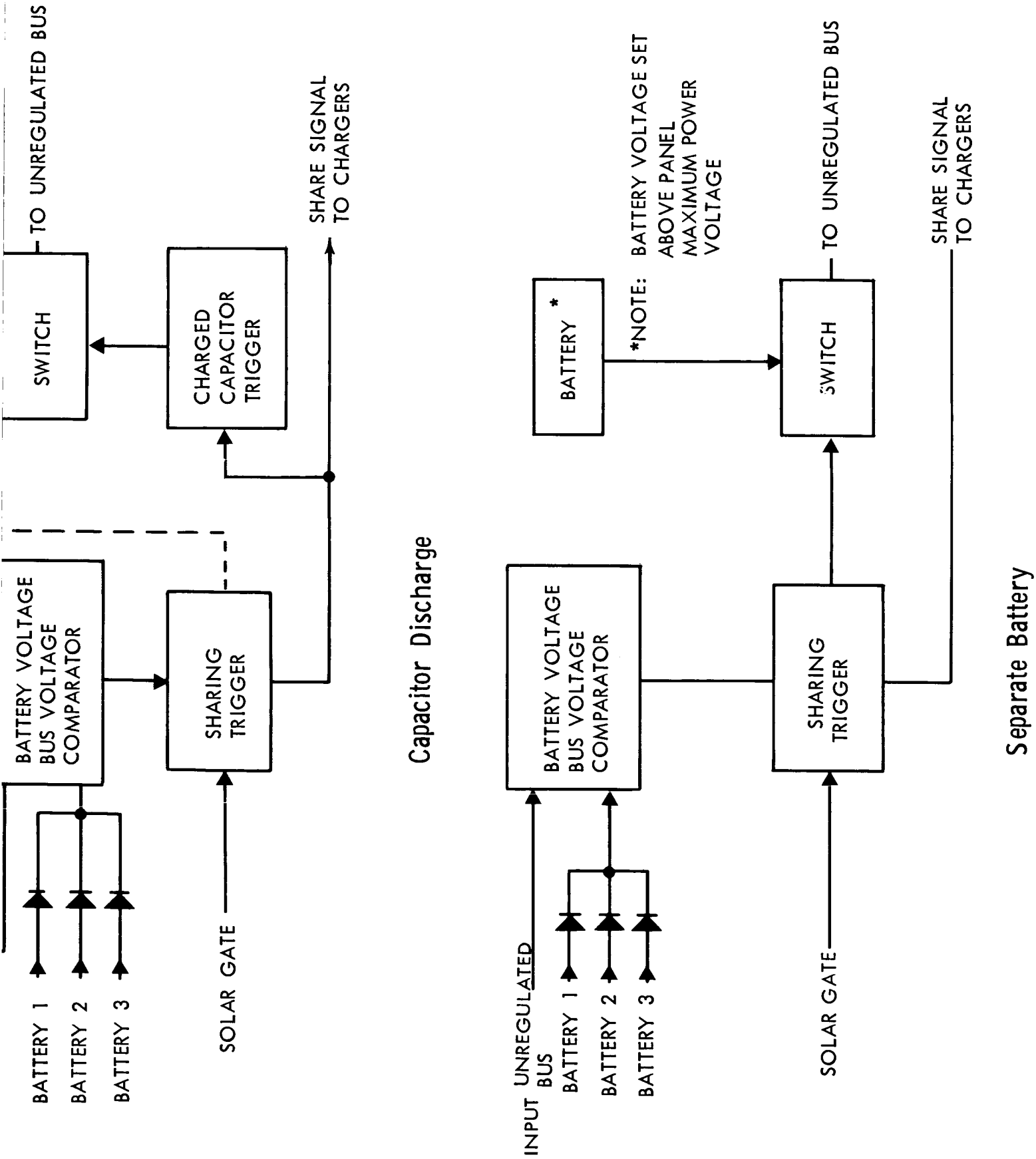

Figure 4.2-15: Solar Panel/Battery Powersharing Mechanization

The following weight estimates were computed for each alternate:

1) Booster converter--1.46 pounds (due to converter circuitry);

2) Capacitor discharge--4.19 pounds (primarily due to capacitor weight);

3) Separate battery--9.66 pounds;

4) Solar-array overcapacity--140 pounds (weight of additional array size).

Reliability--The results of a reliability analysis on each configuration are as follows (see Reference 6

1) Booster converter R = 0.9959

2) Capacitor discharge R = 0.9947

3) Separate battery R = 0.9767

4) Oversize solar array R > 0.9999

The second, third, and fourth configurations have an advantage in that they do not depend on the spacecraft battery charge state for operation. The first (booster converter) will not operate from a completely discharged spacecraft battery; however, it was selected as the preferred design. Its weight and reliability advantages more than compensate for the probability that operation with a completely discharged battery will occur.

Method of Applying Redundancy--Analysis shown in Reference 6, shows the need for redundancy. The method by which redundancy is applied (e.g., passive or failure-sensing switching), is a function of reliability considerations and the practicality of the method. The following paragraphs discuss various methods by which the necessarily

redundant components might be implemented.

Five alternate configurations for mechanizing the redundancy of the series-switching regulator are shown in Figure 4.2-16. Figures 4.2-16a through c show examples of standby redundancy; Figures 4.2-16d and e show operational redundancy.

The configuration in Figure 4.2-16a uses two identical series-switching regulators in which the first unit normally operates continuously in the power subsystem. Regulator 2 is the redundant unit; it is switched onto the line if the first unit fails. Failure of the first unit is detected by a failure-sensing unit that initiates the switching action.

The system shown in Figure 4.2-16b is identical to that shown in Figure 4.2-16a except that a surge-current limiter is inserted in the line to limit the current due either to a short circuit or to switching (such as input capacitor charging).

The system in Figure 4.2-16c uses two identical regulators which are parellel connected. Normally, Regulator 1 is operational whereas Regulator 2 is disabled by low-level drive-circuitry control. If Regulator 1 fails, the drive circuitry for Regulator 2 is activated to make the regulator operational.

The system in Figure 4.2-16d uses two identical regulators whose outputs are summed through diodes; both regulators operate continuously. Each

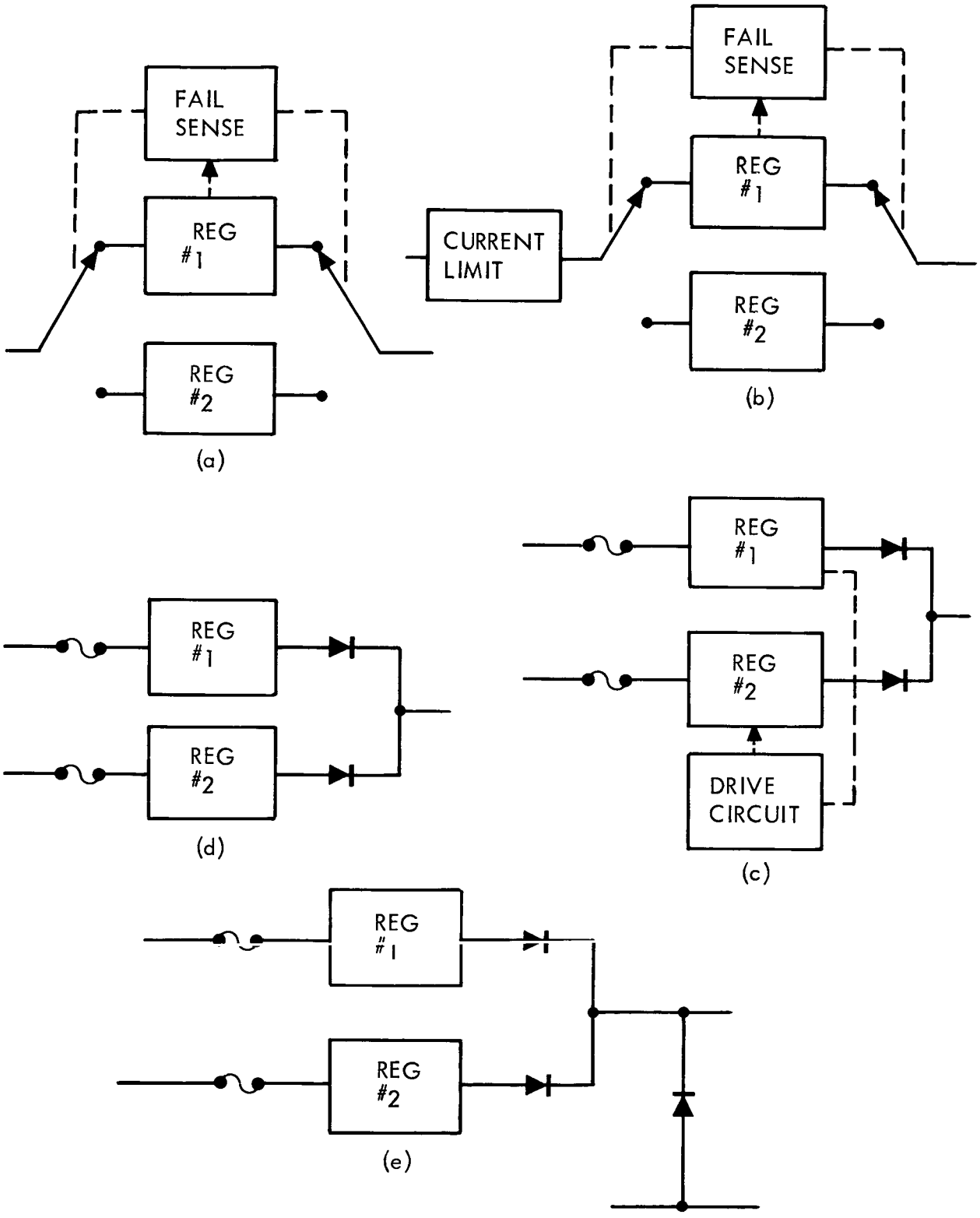

Figure 4.2-16: Application of d.c./d.c. Regulator Redundancy

regulator is capable of supplying the full load demand; if one fails, the second continues to operate.

Figure 4.2-16e shows a variation of the system shown in Figure 4.2-16d. A high-voltage failure would cause the zener diode (set at a voltage somewhat higher than the normal regulated voltage), to draw excessive currents; this in turn will cause the fuse of the faulting regulator to open the circuit. The second regulator will then continue normal operation.

Comparisons are made between each pair of alternates with respect to reliability, safety, performance, and weight.

The predicted reliability of each redundant configuration was calculated on the basis of the number of parts to provide the redundancy (Reference 6).

Configuration	Reliability
Figure 4.2-16a	0.99995
Figure 4.2-16b	0.99945
Figure 4.2-16c	0.99998
Figure 4.2-16d	0.99992
Figure 4.2-16e	0.99982

The significant differences in the calculated values result from: (1) the system in Figure 4.2-16b uses current limiter in series with the configuration for short-circuit protection, and (2) the system in Figure

4.2-16e uses voltage clamp on the output to prevent failure propagation to the load if the operating regulator fails.

The safety to be discussed here is the effect that a failed regulator might have on components in the power subsystem and overall spacecraft that could be damaged by high output voltage. One failure mode within the voltage regulator is a short circuit across the main switching transistor or a failure of the regulating circuitry that would cause an increase in the output voltage of the regulator. In the systems shown in Figures 4.2-16a, b, and c, a failure in the high-voltage mode would be sensed by the failure-sensing unit, which would then initiate switching. However, a switching delay would cause a momentary high voltage at the output terminals.

A short circuit of the main switching transistor of the system shown in Figure 4.2-16c would cause a continuous high voltage at the output terminals. The same condition could result in the system shown in Figure 4.2-16d. The system shown in Figure 4.2-16e has overvoltage-limiting by virtue of a power zener diode (or equivalent device) that would clamp the voltage to a safe value and hold it there until the failure cleared itself or the input fuse to the failed unit opened.

Output-voltage regulation of the systems shown in Figures 4.2-16a, b, and c would not be degraded by including redundancy. However, the output-voltage regulation of the systems shown in Figures 4.2-16d and e would be degraded by diodes in series with the outputs of each regulator.

This would result in an increased output voltage variation under load of about 0.5 volt or 1.5 percent in a 35-volt-d.c. system.

The efficiency of the system shown in Figures 4.2-16a and c are not degraded (except the small amount of power required by the failed-sensing and switching units). The system shown in Figure 4.2-16b will have a lower efficiency because the series current limiter is added to the system. This will result in a reduced system efficiency (overall) of about 2 percent. The system shown in Figures 4.2-16d and e would also have a reduced efficiency because diodes are connected in series with the output leads. This will produce a reduced overall efficiency of about 2.5 percent.

The following table shows the weight of each configuration and the change in total subsystem weight (relative to the preferred design) where the effects of a changed system efficiency are also included.

Configuration	Component Weight (Pounds)	Total Subsystem Weight Change (Pounds)
Figure 4.2-16a	13.8	0
Figure 4.2-16b	14.0	8
Figure 4.2-16c	13.0	0
Figure 4.2-16d	12.8	10
Figure 4.2-16e	12.8	10

Based primarily on reliability, performance, and weight, the configuration shown in Figure 4.2-16a (standby redundancy with failure-mode sensing and switching) has been selected as the preferred design. However, the problems of high voltage output under certain failure modes and surge currents during switching are not completely resolved by application of this system. These problems must be solved before the flight system is chosen.

A similar analysis has been performed on applying redundancy to the 2.4-kilocycle a.c. inverter. Like the d.c. regulator, the results of the analysis are that the preferred design is a standby redundant inverter with failure-sensing and switching units.

4.2.4 Interface Definitions

Inputs--The interfaces are summarized in Figure 4.2-17.

1) From the launch complex, the power subsystem receives:
   a) External electrical power to operate the spacecraft during prelaunch checkout. This power will be in the form of a 40- to 50-volt-nominal d.c. voltage with a current capability of supporting the maximum normal spacecraft load requirements;
   b) External monitoring capability and controlled power to keep the spacecraft batteries fully charged;
   c) External-to-internal power-control signals to actuate the power switching relay in the spacecraft PS&L. A positive indication of external-to-internal power-switching relay mode is provided.

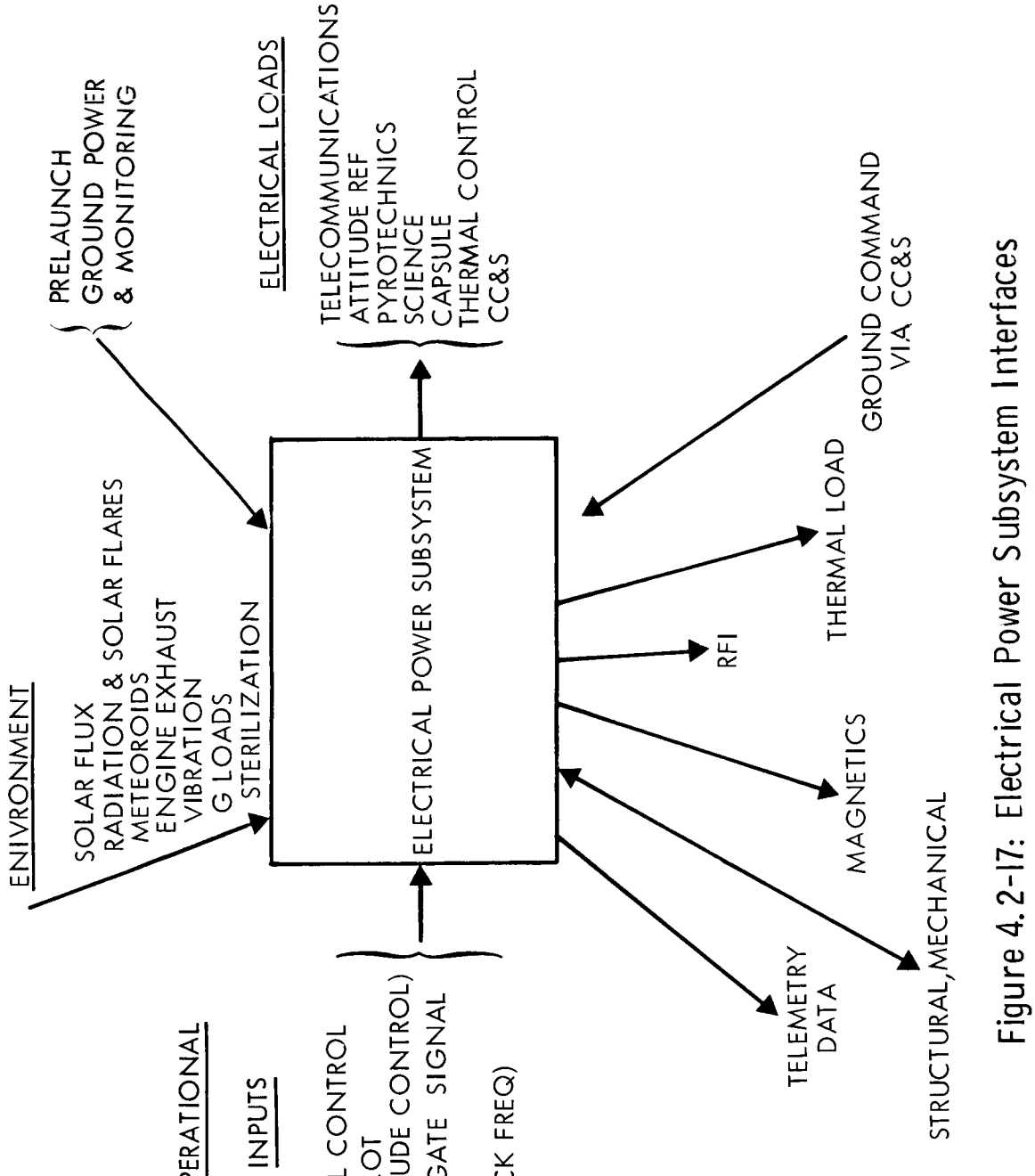

Figure 4.2-17: Electrical Power Subsystem Interfaces

2) From the spacecraft, the power subsystem receives:

   a) From the central computer and sequencer (CC&S) a stable, accurate square wave to synchronize the d.c./a.c. inverter frequencies of the power subsystem;

   b) From the CC&S, inputs to control subsystem functions required at different times in the mission.

Outputs From the Power Subsystem--The power subsystem sends to the launch complex OSE a number of indications and measurements for prelaunch monitoring of power subsystem performance. Specific measurements to be made are indicated in Reference 5, Telemetry measurement outputs are shown in Section 3.7 of this volume. The flight data measurement points are shown in Figure 4.2-18.

The power subsystem provides power to the following:

1) Telecommunication Subsystem

   Voltage = 35 volts d.c.

   Regulation = ±5 percent

   Average load = 195 watts

   Maximum load = 216 watts

2) Attitude Control Subsystem

   Voltage = 35 volts d.c.

   Regulation = ±5 percent

   Average load = 48 watts

   Maximum load = 66 watts

   Voltage = 50v rms square wave

   Regulation = ±5 percent

   Rise & Fall Times = 5±4 micro sec.

   Frequency = 2.4 kilocycles

   Average load = 2 watts

   Maximum load = 2 watts

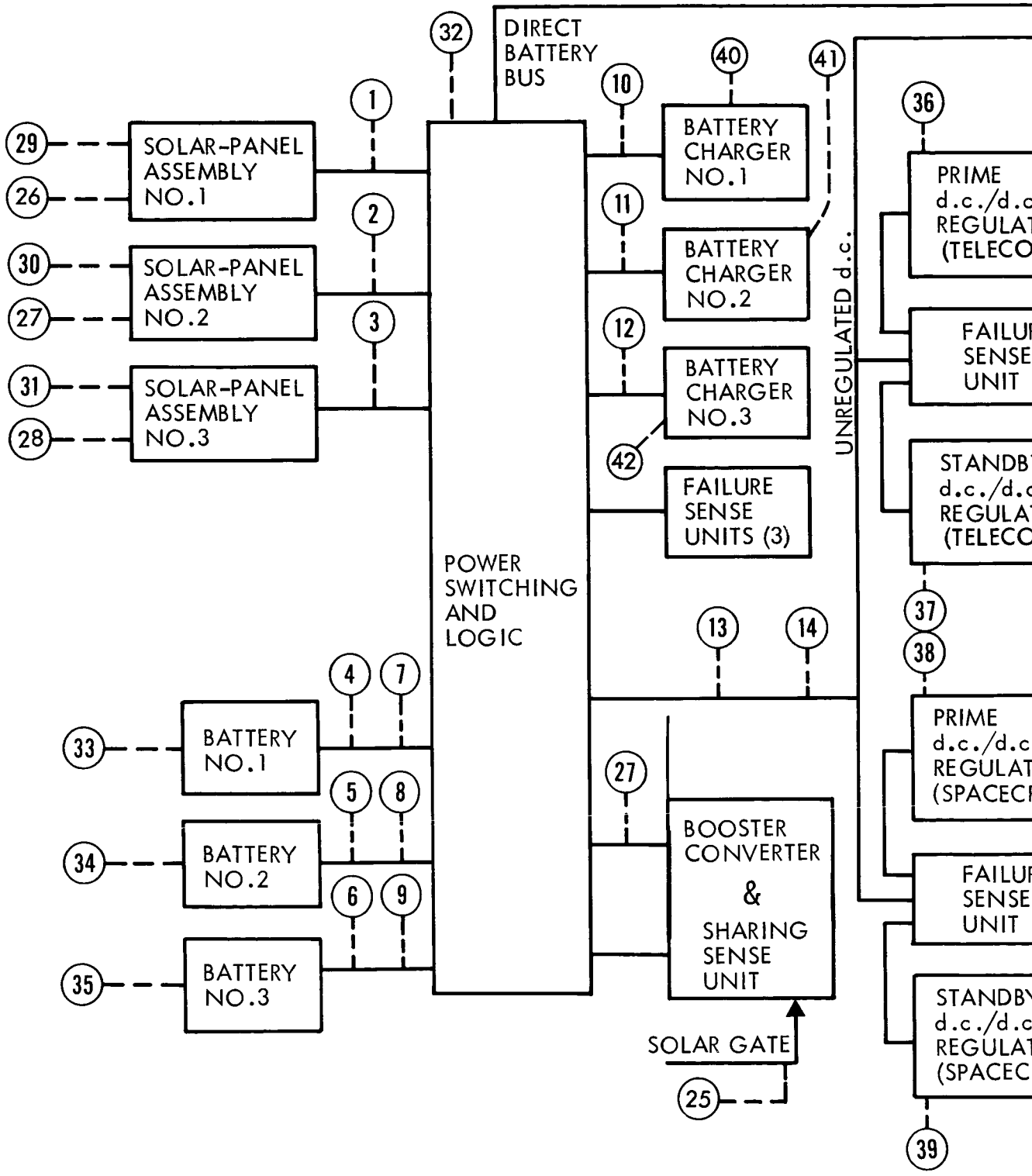
DIRECT BATTERY BUS
32
1
2
3
29
26
30
27
31
28
SOLAR-PANEL ASSEMBLY NO.1
SOLAR-PANEL ASSEMBLY NO.2
SOLAR-PANEL ASSEMBLY NO.3
POWER SWITCHING AND LOGIC
10
11
12
42
40
41
BATTERY CHARGER NO.1
BATTERY CHARGER NO.2
BATTERY CHARGER NO.3
FAILURE SENSE UNITS (3)
UNREGULATED d.c.
36
PRIME d.c./d.c REGULAT (TELECO
FAILU SENSE UNIT
STANDB d.c./d.c REGULA (TELECC
37
38
PRIME d.c./d.c REGULAT (SPACEC
FAILU SENSE UNIT
STANDB d.c./d.c REGULA (SPACEC
39
13
14
4
7
5
8
6
9
33
34
35
BATTERY NO.1
BATTERY NO.2
BATTERY NO.3
27
BOOSTER CONVERTER & SHARING SENSE UNIT
SOLAR GATE
25

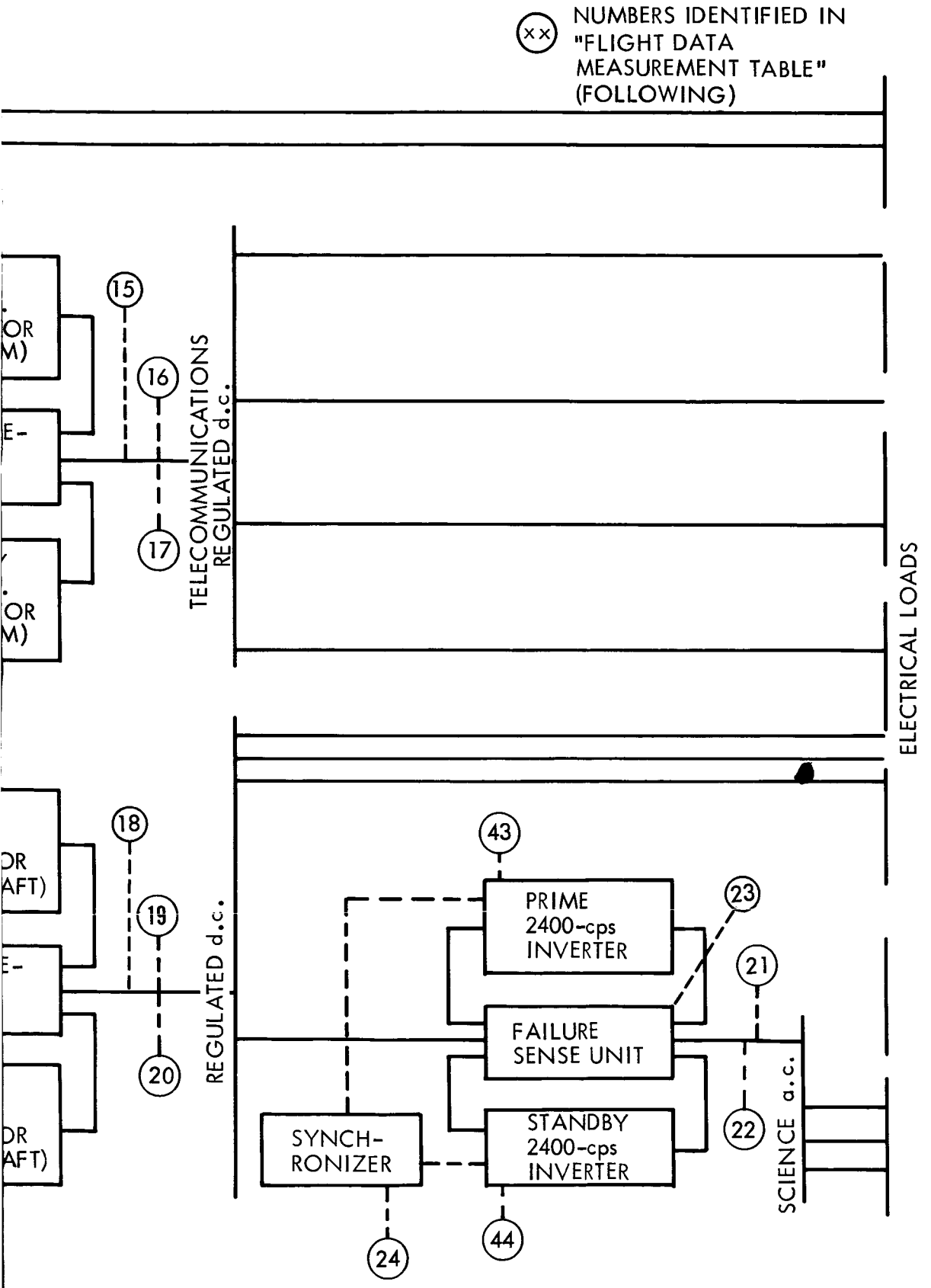

Figure 4.2-18: Electrical-Power-Subsystem Flight-Data Measurement Points

3) CC&S

Voltage = 35 volts d.c.

Regulation = ±5 percent

Average load = 65 watts

Maximum load = 65 watts

4) Thermal Control Subsystem

Voltage = 37 to 100 v.d.c.

Average load = 77 watts

Maximum load = 81 watts

5) Science Subsystem

Voltage = 50 volts rms square wave

Regulation = ±5 percent

Rise and fall times = 5 ±4 microseconds

Frequency = 2400 cps

Average load = 43 watts

Maximum load = 98 watts

Power factor of the 2.4-kilocycle loads = 0.95 or greater

6) Pyrotechnic Subsystem

Voltage = 40 to 51 v.d.c.

Average load = 0 watts

Peak load = 780 watts, 50 ms max. per event

7) Flight Capsule

Voltage = 35 volts d.c.

Regulation = ±5 percent

Average load = (The mission specification states no average load requirement. Up to 200 watts is available on a continuous basis)

Maximum load = 200 watts peak instantaneous

Flight Data Measurement List--The following table shows flight data measurements.

Iden.	Measurement	Unit
1.	Solar Panel 1 Current	Amp
2.	Solar Panel 2 Current	Amp
3.	Solar Panel 3 Current	Amp
4.	Battery B1 Voltage	Volts
5.	Battery B2 Voltage	Volts
6.	Battery B3 Voltage	Volts
7.	Battery B1 Discharge	Amp
8.	Battery B2 Discharge	Amp
9.	Battery B3 Discharge	Amp
10.	Battery B1 Charge	Amp
11.	Battery B2 Charge	Amp
12.	Battery B3 Charge	Amp
13.	Unregulated d.c. Bus Current	Amp
14.	Unregulated d.c. Bus Voltage	Volt
15.	Telecommunications Regulator Output	Amps
16.	Telecommunications Regulator Output	Volts
17.	Telecommunications Regulator Output	Ripple
18.	Spacecraft Regulator Output	Amps
19.	Spacecraft Regulator Output	Volts
20.	Spacecraft Regulator Output	Ripple
21.	2400 cps Inverter Output	Amps
22.	2400 cps Inverter Output	Volts
23.	2400 cps Inverter Frequency Lock	Discrete

Iden.	Measurement	Unit
24	Synchronizer Frequency Lock	Discrete
25	Solar Gate	Discrete
26	Solar Panel 1 Temp (Outboard)	^{o}F
27	Solar Panel 2 Temp (Outboard)	^{o}F
28	Solar Panel 3 Temp (Outboard)	^{o}F
29	Solar Panel 1 Temp (Inboard)	^{o}F
30	Solar Panel 2 Temp (Inboard)	^{o}F
31	Solar Panel 3 Temp (Inboard)	^{o}F
32	PS&L Temp	^{o}F
33	Battery 1 Temp	^{o}F
34	Battery 2 Temp	^{o}F
35	Battery 3 Temp	^{o}F
36	Telecommunications Regulator (Prime) Temp	^{o}F
37	Telecommunications Regulator (Standby) Temp	^{o}F
38	Spacecraft Regulator (Prime) Temp	^{o}F
39	Spacecraft Regulator (Standby) Temp	^{o}F
40	Charger 1 Temp	^{o}F
41	Charger 2 Temp	^{o}F
42	Charger 3 Temp	^{o}F
43	2400 cps Inverter (Prime) Temp	^{o}F
44	2400 cps Inverter (Standby) Temp	^{o}F
45	Relay Status--Booster Converter	Discrete
46	Relay Status--Charger 1	Discrete
47	Relay Status--Charger 2	Discrete
48	Relay Status--Charger 3	Discrete
49	Relay Status--Telecomm. Reg. Fail Sense	Discrete
50	Relay Status--Spacecraft Reg. Fail Sense	Discrete
51	Relay Status--2400 cps Fail Sense	Discrete

Thermal Interface--Table 4.2-4 lists the thermal output and operating temperature range of the power subsystem components:

Table 4.2-4: THERMAL INTERFACES

Item	Nominal Load Heat Output (watts)	Peak Load Heat Output (watts)	Temp Range Allowable (^{o}F)
Series Switching d.c./d.c. Regulator (Telecomunications & CC&S)	29	31	14 to 167
Series Switch d.c./d.c. Regulator (other loads)	15	17	14 to 167
PS&L	29	35	14 to 167
Battery Charger Assembly (during charge)	21	35	14 to 167
Battery Charger Assembly (during float charge)	4		14 to 167
Synchronizer	1		14 to 167
D.c. Failure-Sensing Unit	1.5		14 to 167
A.c. Failure-Sensing Unit	1		14 to 167
Battery Assembly (during charge)	2.8		40 to 110
Battery Assembly (during discharge)	25		40 to 110

Mechanical Interfaces--Table 4.2-5 lists the size and volume of each component of the electrical power subsystem

Table 4.2-5: MECHANICAL INTERFACES

Item	Size (in.)	Volume (cu in.)
D.c./d.c. Regulator (4)	6 by 6 by 4 (ea)	144 (ea)
D.c. Failure Sense Unit (2)	6 by 6 by 3	108
D.c./a.c. 2400-cps inverter (2)	6 by 6 by 2(ea)	72 (ea)
A.c. Failure Sense Unit (1)	6 by 6 by 3	108
Battery Charger Failure-Sensing Assembly (1)	6 by 6 by 3	108
Synchronizer (1)	6 by 6 by 1	36
PS&L (1)	6 by 6 by 3	108
Booster Converter Share Sense	6 by 6 by 2	72
AgO-Cd Batteries (3)	6 by 8 by 14.25 (ea)	685 (ea)
Solar Panels (3)*	83.3 sq ft (ea)	

*The solar panel mechanical attachments are defined in Section 4.2.9, (Figure 4.2-23).

Electrical Power Subsystem External Commands--See Table 4.2-6.

Table 4.2-6: COMMANDS LIST

Item No.	Function	Source
1	Internal Battery On	LCE
2	Internal Battery Off	LCE
3	Switch to Standby Telecommunications Regulator	CC&S
4	Switch to Prime Telecommunication Regulator	
5	Switch to Standby Spacecraft Regulator	
6	Switch to Primary Spacecraft Regulator	
7	Switch to Standby 2400-cps Inverter	
8	Switch to Primary 2400-cps Inverter	
9	Battery Charger 1--Off	
10	Battery Charger 1--Reset	
11	Battery Charger 2--Off	
12	Battery Charger 2--Reset	
13	Battery Charger 3--Off	
14	Battery Charger 3--Reset	
15	Battery Sharing Booster--Inhibit	
16	Solar Gate--On--Override	

4.2.5 Performance

Power outputs to each subsystem were listed in Section 4.2.4. Additional information on each output form is listed below.

1) Unregulated d.c.--

Voltage range while on battery: 37 to 50 volts;

Voltage range while on panels (temperature, steady-state): 57 to 66 volts;

Voltage range while on panels (low temperature just after occultation): 80 to 100 volts for 10 minutes;

Voltage range during battery sharing: 37 to 50 volts.

2) Regulated 35 volts d.c.--

Regulation: $\pm$5 percent;

Ripple: 200 mv p-p;

Spikes: 1500 mv p-p.

3) Regulated 2.4 kc a.c.--

Amplitude: 50 v rms squarewave;

Regulation: $\pm$5 percent;

Rise and Fall Times: 5 ± 4 microseconds;

Frequency tolerance (normal): $\pm$0.01 percent;

Frequency tolerance (clock failure): $\pm$2 percent;

Frequency tolerance (synchronizer failure): $\pm$5 percent.

The maximum power available for abnormal operation of user subsystems is limited by the maximum continuous power rating of the conditioning equipment, the available solar-array power, and the available battery-stored energy.

The maximum continuous rating of the conditioning equipment is:

1) 400 watts for the d.c./d.c. series switching mode regulators;

2) 120 watts for the d.c./a.c. 2.4 kc inverter.

The maximum available solar-array power depends on the time in the mission profile that power is needed. Figure 4.2-20 in section 4.2.9 shows the available power versus time after launch.

The energy stored in the three batteries at full charge is 2460 watt-hours.

Predicted Reliability--Overall power subsystem predicted reliability is 0.9969. All reliability considerations are discussed in detail in Reference 6. A summary of the results is shown below.
where predicted mission reliabilities are indicated for functional outputs, each component, telemetry information, and overall mission functional requirements (without T/M) with and without the synchronizer.

1) Functional Output--

Telecommunications d.c.	0.9965
Capsule d.c.	0.9965
Science Payload a.c.*	0.9951
Unregulated d.c. to Thermal Control, Propulsion. Pyrotechnics and Solar Panel Deployment Actuation	0.9965

2) Functional Block

Solar Array	0.99999

*Assumes that power synchronizer is required for satisfactory operation.

	PS&L	0.99990
	Booster and Share Sense	0.99838
	Battery and Charger Configuration (2 of 3)	0.99979
	Synchronizer	0.99817
	D.c. Regulators No. 1 and 2 (Redundant)	0.99993
	D.c. Regulators No. 3 and 4 (Redundant)	0.99993
	D.c./a.c. Inverters No. 1 and 2 (Redundant)	0.99999
3)	Telemetry Point	
	Solar panel current	0.99961
	Battery Discharge Current	0.99952
	Unregulated Bus	0.99710
	Unregulated Bus Voltage	0.99683
	Battery Voltage (each)	0.99962
	Battery Charge I (each)	0.99962
	Regulator input current, each redundant pair	0.99960
	Regulator output current, each redundant pair	0.99957
	Inverter voltage redundant pair	0.99993
	Inverter current redundant pair	0.99993
4)	Overall Subsystem(not including Telemetry Points)	
	Including Synchronizer	0.9969
	Excluding Synchronizer	0.9988

Functional Reliability--Power subsystem reliability will be ensured by including redundant functions as discussed below.

Solar Array--The total solar array is divided into 24 electrically isolated sections. Each solar array section is connected to the raw power bus through blocking diodes in such a way that no reverse current will flow into a defective or degraded solar array section. Complete failure of one electrical section of the solar array will reduce the available power by less than 5 percent.

Stored Energy--The energy-storage system is composed of three electrically independent and isolated batteries. Any two of the batteries can carry the total power subsystem load during the portions of the mission requiring battery energy. Although the energy-storage system will not normally be needed except during launch, maneuvers, and dark periods of the orbit, it will be kept fully charged and on-line. Thus it is always ready as a backup for the solar panels.

Redundant Frequency Source--The power subsystem includes its own oscillator to be used in case of failure of the clock frequency from the CC&S. Each d.c./a.c. inverter will continue to operate even in the absence of a clock or oscillator signal.

Redundant d.c./d.c. Regulators--Two redundant d.c./d.c. regulators are carried in a standby condition and can be connected to the system should the operating d.c./d.c. regulators fail. Switchover is based on onboard detection of over- or undervoltage of the operating regulator. Ground command backup is also provided.

Redundant d.c./a.c. Main 2400-cps Inverter--A redundant d.c./a.c. inverter is carried in a standby condition and can be connected to the system should the primary d.c./a.c. inverter fail. Switchover is based on onboard detection of out-of-tolerance output/input voltage ratio of the operating inverter. Ground command backup is also provided.

Redundant Batteries/Chargers--Each of the three silver-cadmium batteries is charged by a separate charger circuit thereby providing full redundancy for the secondary power source. In addition to the onboard detection of battery/charger failure or degradation, ground command backup is also provided.

Telecommunications and CC&S Power Distribution--Separate redundant d.c./d.c. regulators are included to provide a regulated d.c. bus separate from the remaining spacecraft loads. This has been done to minimize the effect on the telecommunications and CC&S subsystems caused by a load fault in other spacecraft subsystems.

Failure Modes and Effects Analysis--Table 4.2-7 is a failure modes and effects analysis summary which includes failure of the power subsystem components.

Reliability of Power-Conditioning Equipment--The predicted reliability of each module presented below is based on a total mission time of 5880 hours. Refer to Section 6.0"Reliability," of this report and Reference 6 for detailed reliability analysis and calculations.

FUNCTIONAL UNIT	FUNCTION	FAILURE MODES	EFFECT ON POWER SUBSYSTEM	EFFECT ON POWER SUBSYSTEM OUTPUT
2400-cps Inverter No.1	Provides Regulated 2400-cps Square Wave to the Science Subsystem	1) Short or Open	1.1 Failure Sense Unit Will Initiate Swtiching to No.2 Inverter	1.1 A 10-ms Loss of 2400-cps Power Will Occur
		2) Failure of Synchronizing Circuit	2.1 None	2.1 Reduced Accuracy of Frequency (2400-cps ±5 Percent)
2400-cps Inverter No.2	Provides Regulated 2400-cps Square Wave to Science Subsystem if No.1 Has Failed	1) Short	1.1 Overload of d.c. Bus Resulting in Loss of All d.c. Power Except Telecommunications and CC&S 1.2 Overload of d.c./d.c. Regulator Causing It to Fail	1.1 Loss of All Spacecraft Power Except Telecommunications and CC&S
		2) Open	2.1 None	2.1 Loss of 2400-cps Output
		3) Failure of Synchronizing Circuit	3.1 None	3.1 Reduced Accuracy of Frequency (2400-cps ±5 Percent)
Inverter Failure-Sense Unit	Provides Sensing of 2400-cps Output and Initiates Switching to No.2 Inverter if No.1 Output/Input Voltage Ratio Exceeds Low Limit	1) Sensing Circuit Fails	1.1 Initiates Switching From No.1 to No.2 Inverter 2.1 No.1 or No.2 Inverter Will Remain On-Line	1.1 A 10-ms Loss of 2400-cps Power Will Occur 2.1 None (if On-Line Inverter is Operative)
d.c./d.c. Regulator No.1 and No.3	Provides Regulated d.c. Power to All Power Subsystems and Some Spacecraft Subsystems	1) Short, Open, or Loss of Regulation	1.1 Failure-Sense Unit Will Initiate Switching to No.2 Regulator 1.2 A 10-ms Loss of Power Will Occur	1.1 A 10-ms Loss of Power Will Occur
d.c./d.c. Regulator No.2 and No.4	Provides Regulated d.c. Power if No.1 or No.3 Fails	1) Short to Ground	1.1 Loss of Some System Power	1.1 Loss of Some System Power
		2) Short from Input	2.1 Will Provide Unregulated Output From 37 to 70 v.d.c. (Depending on Load and Solar Intensity)	2.1 d.c. Output Voltage Will Vary From +5 Percent to +100 Percent of Normal 2.2 a.c. Output Voltage Will Vary From +5 Percent to +100 Percent of Normal

	Regulator Failure-Sense Unit (Note 2)	Provides Sensing of Regulated d.c. Output and Initiates Switching to No.2 Regulator if No.1 Output Exceeds High or Low Limit. Similar With Regulators 3 and 4	1) Sensing-Circuit Fails	1.1 Initiates Switching From No.1 to No.2 Regulator. Similarly With Regulators 3 and 4. 1.2 A 10-ms Loss of Power Will Occur	1.1 A 10-ms Power Loss Will Occur
			2) Switching Function Fails	2.1 No.1 or No.3 Regulator Will Remain On-Line	2.1 None (If On-Line Regulator is Operative)
	Charger/Booster Assembly (Note 3)	Provides Battery-Charging Function and Battery-Sharing Mode Correction	1) Charger Shorts or Charges at an Excessively High Rate	1.1 Failure-Sense Unit Will Initiate Switching to Off Condition	1.1 None
			2) Charger Opens	2.1 Battery Charging Ceases	2.1 (Same as 1.1)
			3) Unequal Charging Rate on Each of the 3 Batteries	3.1 One or More Batteries May Be Undercharged or Overcharged 3.2 One or More Batteries May Fail	3.1 Reduction in Maximum Operation Time in Dark Periods 3.2 (Same as 3.1)
			4) Failure-Sense Unit Fails	4.1 No.1, No.2, or No.3 Charger Will Remain On-Line	4.1 None (If Charger is Operative)
			5) Booster Converter Shorts	5.1 Booster-Converter Fuse Opens (Battery Sharing May Occur)	5.1 Battery Will Be Depleted and All Voltages Will Be Low After a Period of Time (If Sharing Mode Exists)
			6) Booster Converter Opens	6.1 Battery Sharing May Occur	6.1 (Same as 5.1)
			7) Sharing Sense Circuitry Fails	7.1 (Same as 6.1)	7.1 (Same as 5.1)
8	PS&L	Receives All Raw Input Power and Distributes to Power Subsystem	1) One or More Panel Diodes Open	1.1 Reduction in Power Input	1.1 None (Depending on Load, Solar Distance, and Number of Failed Diodes)
			2) One or More Solar-Panel Diodes Short	2.1 Small Battery Drain Will Occur During Dark Periods	2.1 None if Short to Substrate has not Developed
			3) One Battery Diode	3.1 Loss in Use of One Battery	3.1 None - if Diode Opens
			4) Two Battery Diodes	4.1 Loss in Use of Two Batteries	4.1 Reduced Dark Time Capability
			5) One or More Battery Diodes Short	5.1 Battery(ies) Will Charge Continuously During Sun-Orientation Times	5.1 None (If Battery(ies) Do Not Fail)
	Solar Panels	Provide Raw Power From Sunlight to Power Subsystem	1) Short in One Section	1.1 None (If Major Degradation of Total Array Has Not Occurred)	1.1 None (If Major Degradation of Total Array Has Not Occurred)
			2) Short in Two Sections	2.1 Same as 1.1	2.1 Same as 1.1
			3) Short in 3 or	3.1 Proportional Reduc-	3.1 Proportional Reduc-

			Input 3.2 Battery Charging Rate Reduced	Power at or Near Mars Apheleon 3.2 Reduction of Maximum Operating Time in Dark Periods
		4) Excess Radiation	4.1 (Same as 3.1)	4.1 (Same as 3.1)
Batteries	a) Provide Raw Power During Dark Periods of Mission b) Provide Energy to Prevent Battery Sharing Operation When Sufficient Solar Power Is Available	1) Failure of 1 Battery	1.1 Charging and Usage of Failed Battery Will Be Discontinued	1.1 None
		2) Failure of 2 Batteries	2.1 Charging and Usage of Failed Batteries Will Be Discontinued	2.1 Reduction of Maximum Operating Time in Dark Periods
Synchronizer	Provide Synchronizing Signals to Power Subsystem Inverters	1) Loss of Input Clock Frequency	1.1 Internal Oscillator Will Provide a Frequency Accuracy of ±2 Percent	1.1 a.c. Outputs Frequency Accuracy Reduced to ±2 Percent
		2) Loss of Synchronizing Outputs	2.1 a.c.-Inverter Internal Oscillators Provide Frequency Accuracy of ±5 Percent	2.1 a.c.-Output Frequency Accuracy Reduced to ±5 Percent 2.2 Increase in Noise From Frequency Beating on All Outputs

Note 1: Switching from one inverter to another can also be accomplished by ground command.

Note 2: Switching from one regulator to another can also be accomplished by ground command.

Note 3: Switching by ground command can accomplish:

a) Start- or stop-charging;
b) Switch from one charger to another;
c) Activate battery-sharing mode converter.

The predicted reliability of the power switch and logic unit is 0.999998. The bulk of the circuitry in the PS&L are associated with telemetry monitoring points which do not directly effect system operation. A discussion of the isolating diodes for the solar array and batteries appears also in Reference 6 of Section 4.2.2. The external/internal power switch to be used has redundant contact sets, which eliminate the majority of the contact cumulative failure rate. Therefore, the probability of supplying unregulated d.c. to the subsystem is degraded only very slightly by the PS&L.

The reliability of the series-switching regulator as a unit by itself is 0.99419. This regulator, however, is used in a redundant configuration in the power subsystem and as such has an overall reliability of 0.999995.

The 2.4-kilocycle inverter reliability is similarly affected by the system redundant connection. The unit alone has a reliability of 0.99796 and system reliability of 0.99999.

The battery-charger/battery reliability is 0.9979. Since the battery reliability of 0.98 is less than that of the basic charger, the battery-charger/battery combination reliability does not increase with redundant charger configurations.

The synchronizer reliability is 0.99934. It should be noted that a synchronizer failure will not cause a system failure because of the "free running" capability incorporated in the 2.4-kilocycle inverter.

The d.c. failure sense unit has a reliability figure of 0.99784. while the a.c. failure sense unit reliability is 0.99683.

4.2.6 Physical Characteristics

The physical characteristics of the electrical power subsystem are summarized in Table 4.2-8.

Table 4.2-8: SIGNIFICANT PHYSICAL CHARACTERISTICS

1) Solar Array	
Physical Characteristics	
Area - Planform	241 sq ft
Area - Substrate Surface	236 sq ft
Area - Solar Cell Mounting	209.8 sq ft
Cell Active Area	199 sq ft
Panels Per Array	3
Major Structural Sections Per Panel	2
Structural Subsections Per Panel	4
Electrical Sections Per Structural Subsystem Section	2
Weight - Panels with Strut	238 lbs
Weight - Mechanical Attachments	46 lbs
Total	284 lbs

Solar Cells	
Size	2 x 2 cm
Thickness	0.012 in
Weight	0.32 gms
Cells per Submodule (A)	5
Cells per Submodule (B)	6
No. of Strings per Electrical Section	3
No. of Cells in Series per String	123
Total Cells per Array	48,708
Cell Type	N on-P Silicon
2) Battery (One Unit, Total of 3)	
Type - Silver-Oxide/Cadmium	(AgO-Cd) Sealed
Case Size	16 x 8 x 6 in
Battery Volume	650 cu in
Weight	41 lbs
Cells per Battery	38

3) Power Conditioning Equipment

Component	Number Reqd.	Size(in)	Volume(cu in)	Weight each(lbs)	Total Weight(lbs)
Series Switching d.c./d.c. Regulator	4	6x6x4	144	6.4	25.6
SSR Failure Sense Unit	2	6x6x3	108	2.0	4.0
2.4-kc Inverter	2	6x6x2	72	2.0	4.0
Inverter Failure Sense Unit	1	6x6x3	108	1.7	1.7
Battery Charger/ Failure Sense Unit	3	6x6x3	108	3.0	9.0
Synchronizer	1	6x6x1	36	1.0	1.0
Booster Converter & Share Sense	1	6x6x2	72	1.5	1.5
PS&L	1	6x6x3	108	3.2	3.2
Total Weight					50.0

4) Subsystem Total Weight(pounds)

Solar Array	284
Batteries	123
Power Conditioning Electronics	50
Total Weight	457

4.2.7 Safety Considerations

4.2.7.1 Equipment Safety

Subsystem Electronic Equipment--The power subsystem electronic equipment can be damaged by the application of excessively high input voltages. The input power supplies used during testing will have both maximum-voltage and maximum-current limiting protection devices.

Hardline monitors will all have current-limiting isolation resistors built within the submodules to prevent equipment damage due to external short circuits.

As much as possible, a different connector pin arrangement and/or size will be used on each submodule and OSE/power subsystem interface connections. This will prevent inadvertent interchange of components.

All power subsystem test equipment will incorporate out-of-tolerance alarm detectors that will indicate a malfunction immediately after it occurs.

Appropriate handling fixtures and equipment will be used for each equipment item to minimize the possibility of handling damage and control the environment (e.g. humidity) while in storage.

Solar Panels--The solar panels are very delicate due to the use of very thin aluminum material to minimize weight. The delicate nature

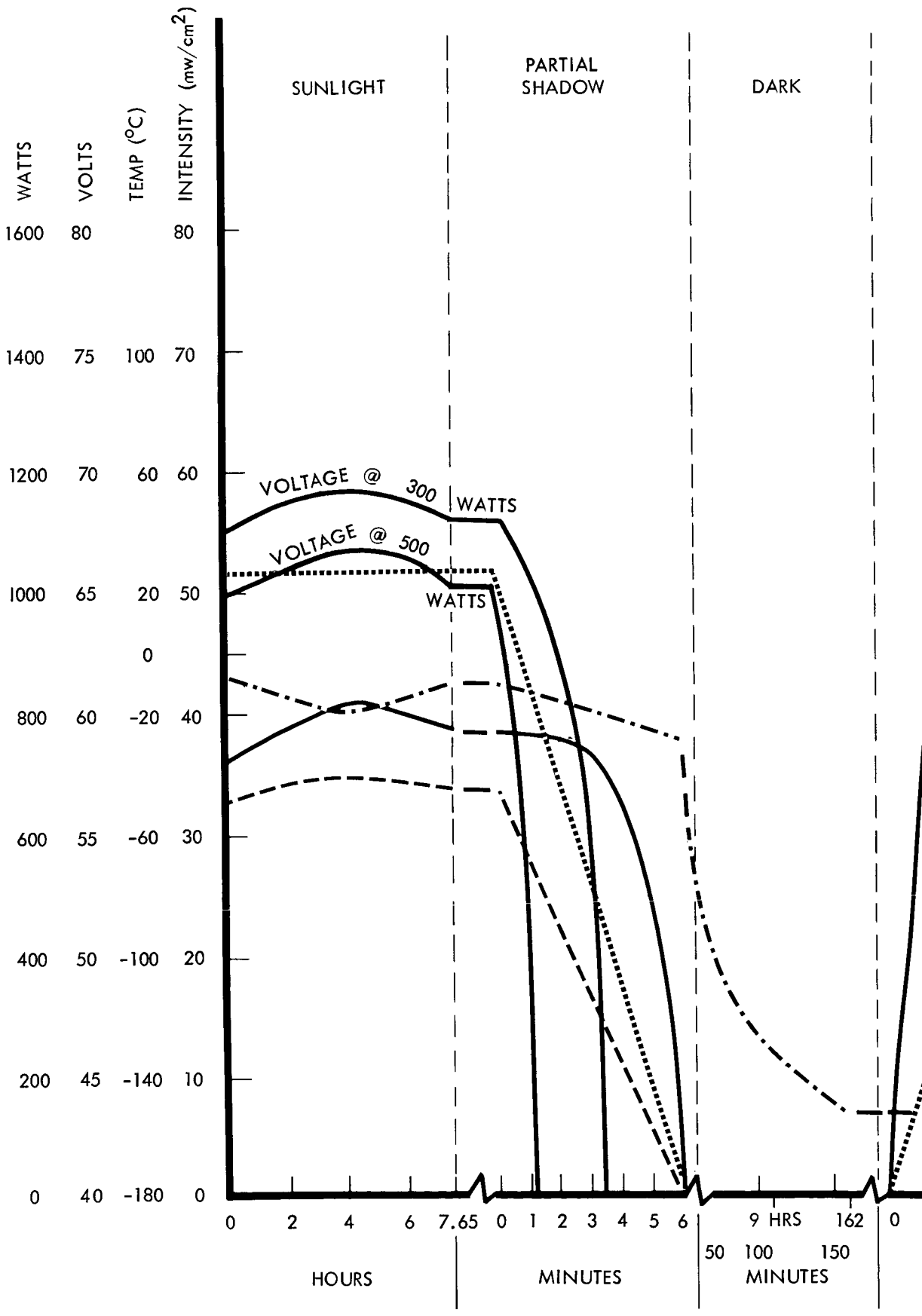
SUNLIGHT
PARTIAL SHADOW
DARK
WATTS
VOLTS
TEMP (°C)
INTENSITY (mw/cm²)
1600 80 80
1400 75 100 70
1200 70 60 60
1000 65 20 50
0
800 60 -20 40
600 55 -60 30
400 50 -100 20
200 45 -140 10
0 40 -180 0
VOLTAGE @ 300
WATTS
VOLTAGE @ 500
WATTS
0 2 4 6 7.65 0 1 2 3 4 5 6 9 HRS 162 0
50 100 150
HOURS
MINUTES
MINUTES

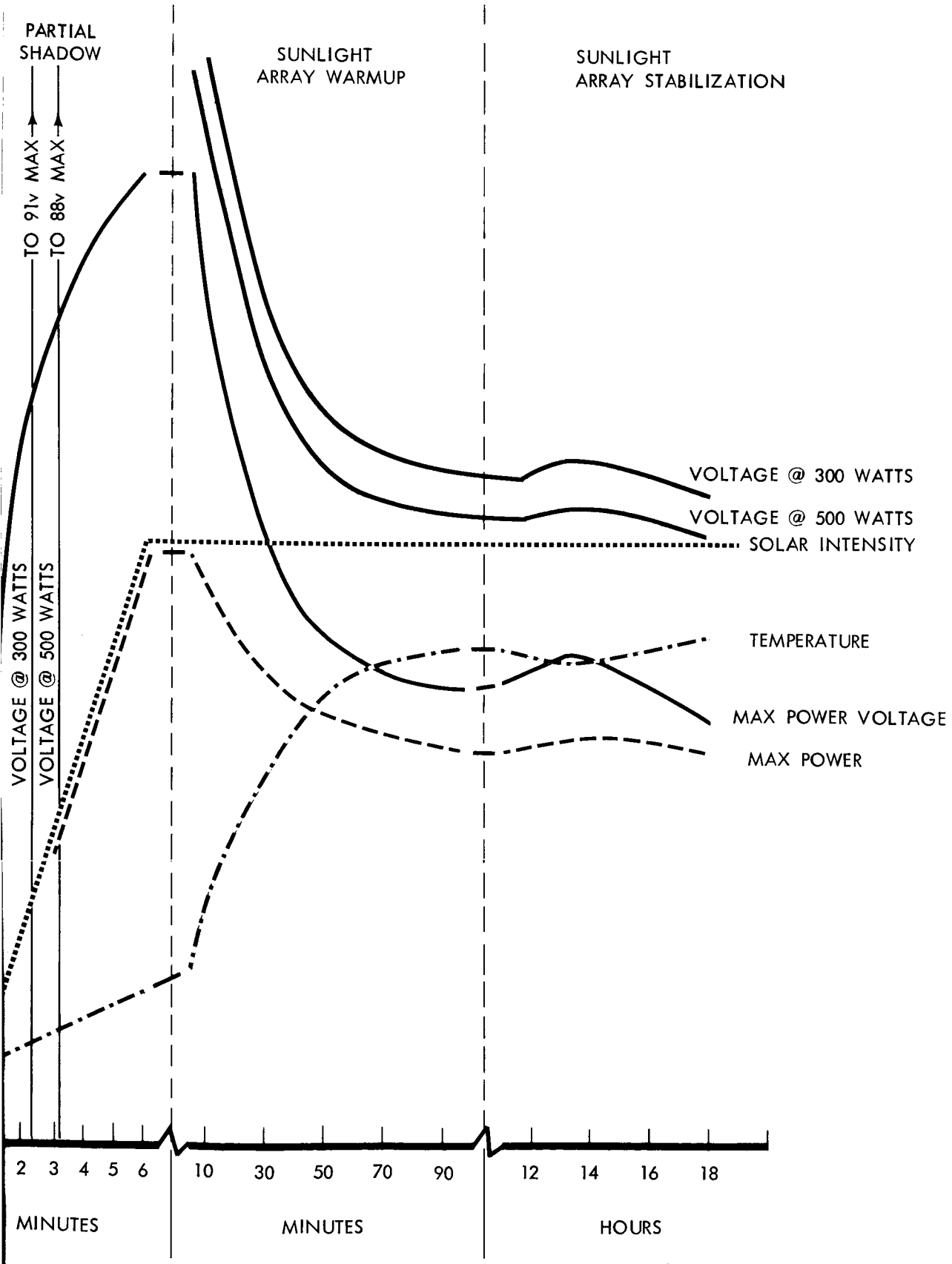

Figure 4.2-21: Typical Array Performance Profile During One Orbit at End of Mission

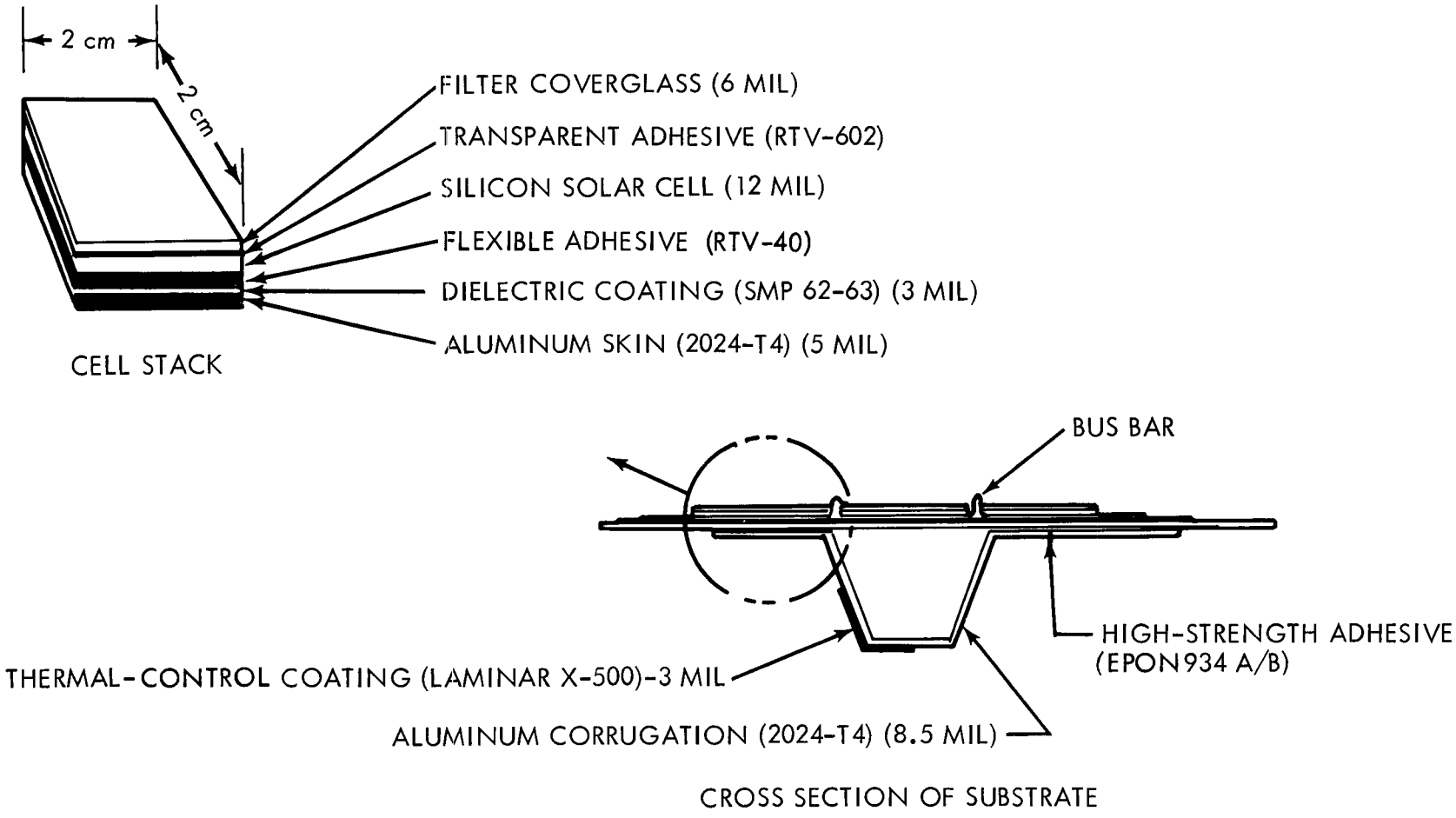

Figure 4.2-22: PHOTOVOLTAIC SOLAR-ARRAY AND SUBSTRATE

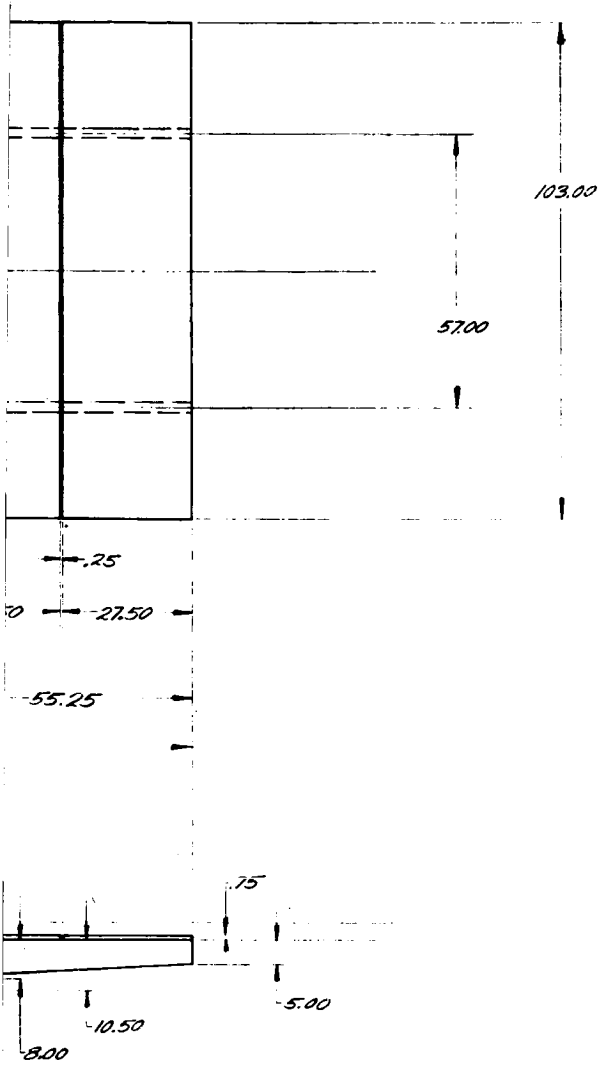

NO. OF CELLS – 123 SERIES
– 396 PARALLEL
– 48708 TOTAL
PANEL AREA – 241.41 FT² TOTAL
SUBSTRATE AREA – 236.04 FT² TOTAL

)TE: DIMENSIONS IN INCHES

Figure 4.2-23: Spacecraft Model 945-6026
Solar-Panel Envelope

6-voltage strings, 123 cells long. There are three 5-cell submodule strings and three 6-cell submodule strings per structural subsection. The 6-voltage strings are further divided into 2 electrically-isolated sections composed of 3 strings each.

Array performance requirements are based on an Earth-space panel voltage greater than 58 volts for battery charging and an end-of-mission power of 620 watts.

K Factors--The array characteristics are based on an extrapolated solar cell I/V curve with degrading modifications known as "K", or contingency, factors. The "K" factors of Table 4.2-9 are used in the design calculations.

Table 4.2-9: "K" FACTORS

	Degradation Factor	Factor
K_a	0.99	Instrumentation errors in panel measurements
K_b	0.98	Error of cell measurement
K_c	0.98	Non-isothermal panel temperature in space
K_d	0.975	Allowance for accuracy of Table Mountain California sunlight measurements
K_e	0.98	Solar Constant Variation and ± 5 degree panel misalignment
K_1	0.956	RMS value of K_a, K_b, K_c, K_d, K_e
K_2	0.95	Coverglass Loss
K_3	0.97	Mismatch and assembly loss
K_4	0.90	Safety Factor

	Degradation Factor	Factor
K_5	1.00 at launch 0.82 at encounter 0.720 at end of mission	Radiation Degradation
K_t	0.793 at launch 0.650 encounter 0.571 at end of mission	Total array degradation $K_1 \times K_2 \times K_3 \times K_4 \times K_5$

The "K" factors are divided into those which can be "averaged" in RMS fashion and those which are straight multiples. The factor "K_t" can be used to calculate solar cell efficiency on the panel; other calculations, such as panel area, must take into account such items as operation off of maximum power point. For the preferred design, an extra 5 percent degradation is added to account for off-maximum power operation.

Other sources of degradation, such as meteoroid damage, random cell, failure, and retro-rocket exhaust impingement are adequately covered by the 10 percent safety factor, K_4.

Following is a brief discussion of the key degradation factors.

RMS Losses, K_1--RMS losses result from uncertainties in the measurement of quantities affecting panel performance. The RMS factors have been used by JPL and other organizations and are considered relatively standard. However, the degradation due to non-isothermal conditions (K_c), in the solar array cannot be taken from measurements and must be derived by calculation (the 2% K_c was calculated by assuming worst-case at Mars).

Coverglass Loss, K_2--The 5 percent is a conservative estimate of coverglass loss and is considered standard in the solar panel industry.

Mismatch and Assembly Loss, K_3--Experience in assembling and matching solar cells and modules on Ranger, Mariner, and other programs indicates that careful practices can hold these losses below 3 percent. These practices include uniform soldering procedures (such as the use of a tunnel oven), careful cleaning and clean room conditions, categorization and matching of cell and submodule currents at several points on the I-V curve (at short-circuit as well as at the operating point), assembly of circuits prior to laydown on the panel, use of bus bar material with very low resistivity, and other techniques. Attempting to compensate temperature variations with different output cells is felt not to be practical.

Solar cells will be bought with a detailed procurement specification for close control, and then categorized by making measurements of voltage and current output. Matching of cells is extremely important in maintaining panel output and will be accomplished by using the cells sorted as described above.

Radiation Environment, K_5--The two basic types of particulate radiation considered for K_5 are the solar flares and the Mars trapped radiation belt. The solar flare intensity is based on the mission specification, page 80. The spectral distribution is based on the power law from $dI/dE=KE^{-n}$ and the mission specification, where I is solar flare

intensity, E is proton energy, and K and n are constants. Based on the above, $I = 7.7 \times 10^{12} E^{-1.95}$ protons/cm^2 -year for 1971. Present radiation measurements apply for 1.A.U. It is possible to estimate by scaling of R^{-2} for the implied special continuity where R is the Sun distance. This is the basis used for the solar flare radiation intensity for the Voyager Mission.

A radiation environment equivalent to Earth's has been assumed for Mar's trapped radiation (see section 2.2). The trapped radiation is assumed to consist of both protons and electrons. It is necessary to adjust the electrons to the equivalent of protons by $\frac{\emptyset e}{3000} = \emptyset p$ for calculation (see reference 2 for further detail).

Micrometeoroid Effects--Limited tests have shown that micrometeoroids larger than about 10^{-3} to 10^{-2} gms are required to open-circuit a solar cell/cover glass combination. Smaller particles will only pit the glass or the N/P junction, or at most crack the device, and the cell will continue to provide power at a reduced level. Pitting will only cause a fractional active-area loss. Calculations based on the mission model show that there will be a total of 74 hits from particles larger than 10^{-4} gms during the total mission, resulting in a maximum possible-power-degradation of 6 percent assuming total cell destruction for the 10^{-4} gms particle. If only area reduction occurs from all impacts, there will be a maximum area loss of 0.037 percent, which assumes pitting that does not diffuse the light but completely blocks it. Therefore, the safety factor of 10 percent should adequately cover the chance of micrometeoroid damage.

Factors K_1, K_2, K_3, K_4 and K_5 can be multiplied together to arrive at K_t, (in contrast to taking an average or RMS value). Since they now represent factors which can be assumed (e.g. the 10 percent safety factor) or calculated from experience (e.g., measurement of coverglass loss).

Calculation of Array Area--From the load profile and by using the K factor and battery information, the solar array area is calculated as shown in detail in reference 2.

4.2.9.2 Structural and Mechanical Description

The array consists of the substrate and cell stack (Figure 4.2-22) that attach to the ladder truss frame. The mechanisms comprise pyrotechnic pin-puller latches, motor-driven deployment devices, and deployed position latches.

Design Objectives--The design objectives and requirements for developing the array structure and mechanisms were: that the structure survive the loading conditions, including a 2.2-g retromaneuver (design factor of 5 g's); that it have a deployed first resonance of 2 cps or greater (the panel is designed to 4 cps to allow for system spring that cannot be absorbed without a detailed design of such items as hinges, etc.); that in a space environment, the structure must be capable of withstanding thermal stress from the retroengine exhaust plume and Mars occultations; and that surface temperatures during transit and orbit do not degrade cell performance.

Description--Figures 4.2-24 through 4.2-29 depict the structural and mechanical arrangements that fulfill the design objectives and requirements. The substrate is a dielectric-insulated (SMP 62/63) aluminum (2024-T4) and skin-stiffened by spanwise aluminum (2024-T4) corrugations. The skin is bonded to the corrugation by a high-strength, high-temperature epoxy (Epon 934 A/B) adhesive. The substrate is designed for strength in the stowed-position environment. The substrate bolts (titanium screws into Stainless Steel A-286 nut inserts) through an aluminum (2024-T4) Z-section into the frame chordwise members and through shear and thermal clips into the spanwise spars. During launch, each section of the spar is supported as a pin-ended beam. When deployed, the complete spar is supported at midspan by the support strut. The chord-frame members are designed for strength during the boost lateral loading conditions, and the spar members are frequency designed for the deployed condition. Individual sections of the spar were checked for strength during boost when not supported as pin-ended beams. The frame truss members are composed of aluminum (6061-T6) T-sections and tubes that are joined by welding. All structural members were checked for maximum allowable displacement due to dynamic and static loading conditions to ensure clearance between themselves and the spacecraft nose-fairing dynamic envelope. Each structural member was designed to ensure separation of resonant frequencies to avoid dynamic coupling.

The panel sections tie to the spacecraft and to each other through machined aluminum (6061-T6) latches that contain pyrotechnic pin pullers. The latch and panel hinges are designed to resist forces due to

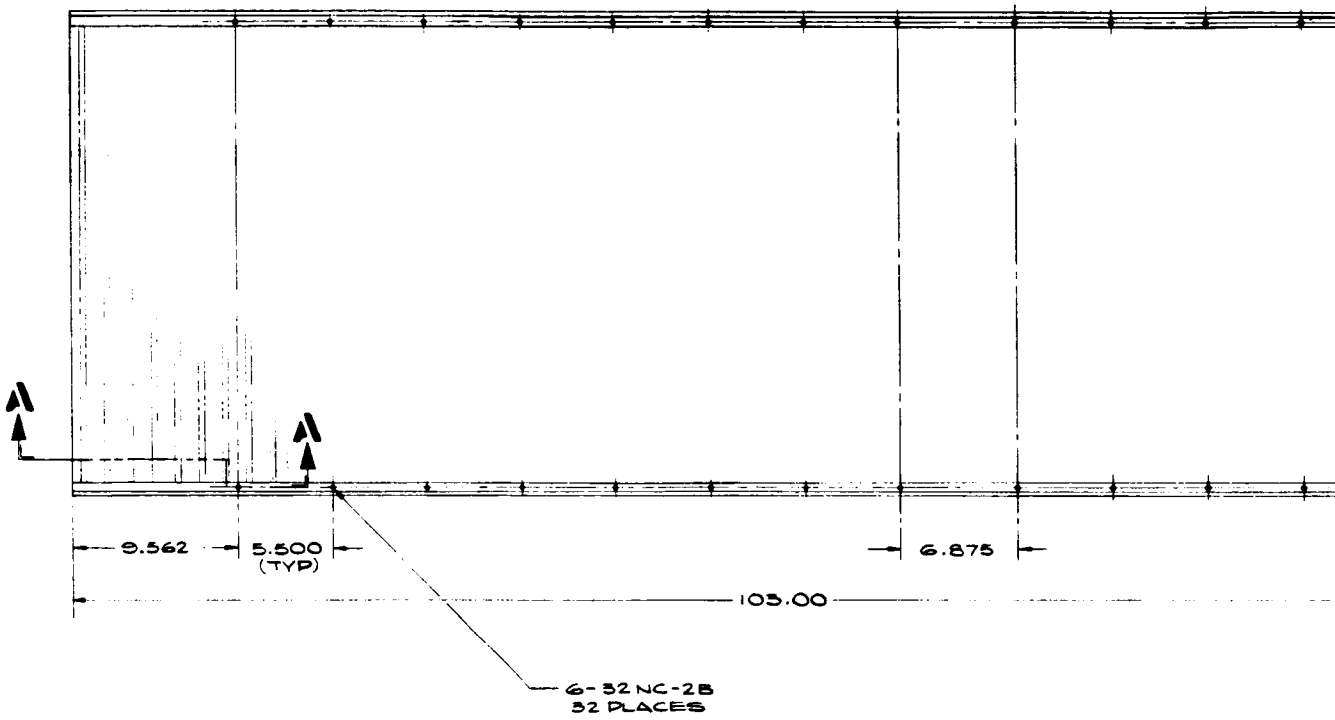

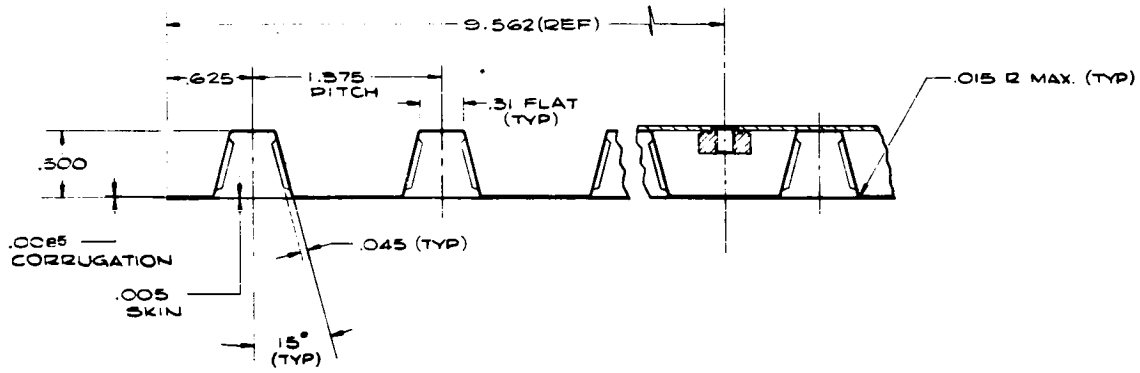

SECTION A-A
SCALE 2/1

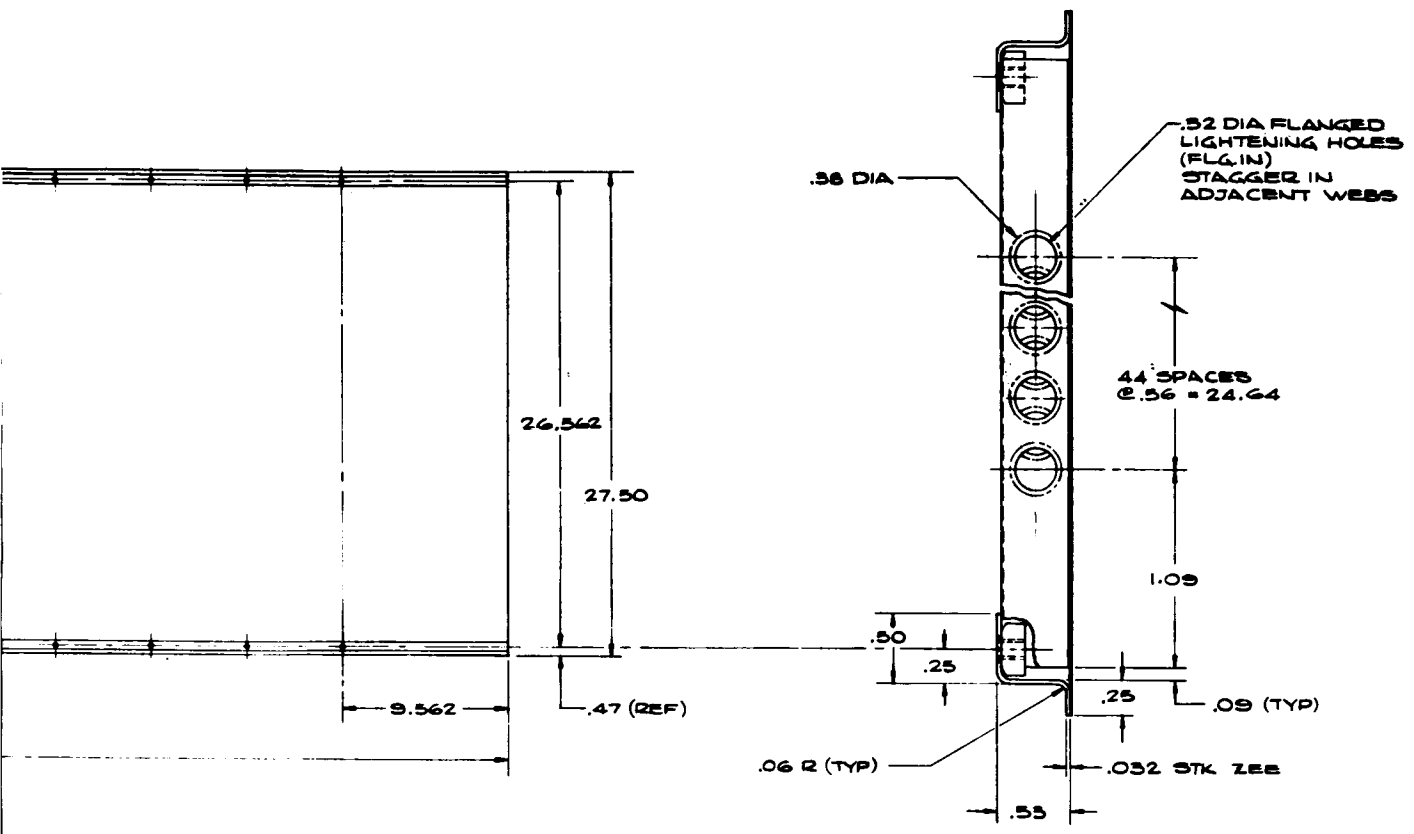

NOTES: UNLESS OTHERWISE SPECIFIED
1. ALL PARTS TO BE BONDED WITH EPOXY RESIN

NOTE: DIMENSIONS IN INCHES

Figure 4.2-24: Spacecraft Model 945-6016 Number 5 Substrate Assembly

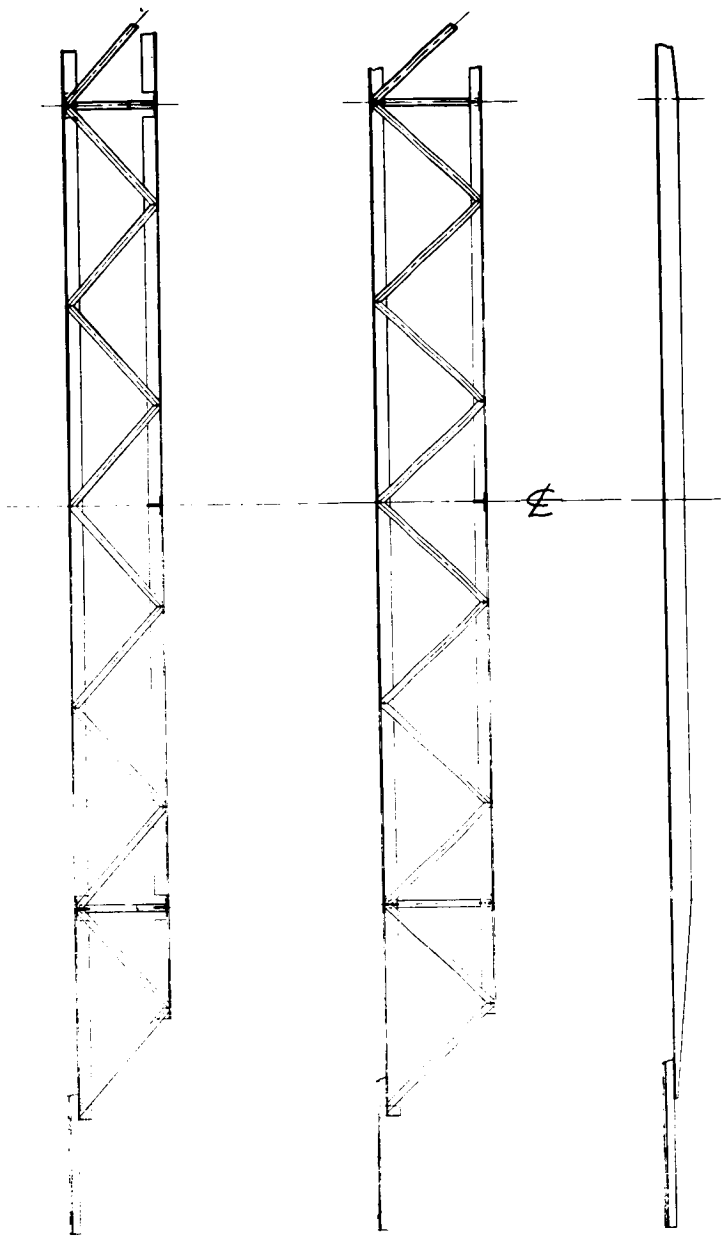

SECTION B-B VIEW C-C

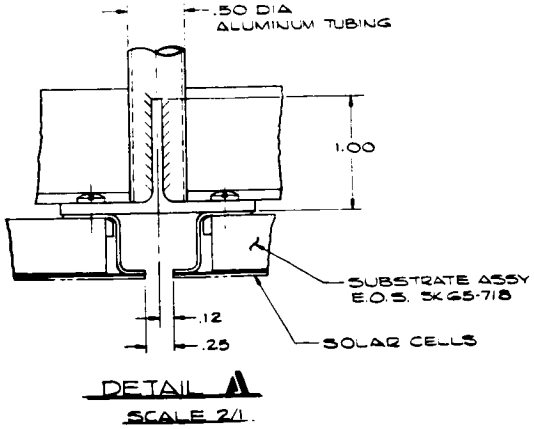

DETAIL A
SCALE 2/1

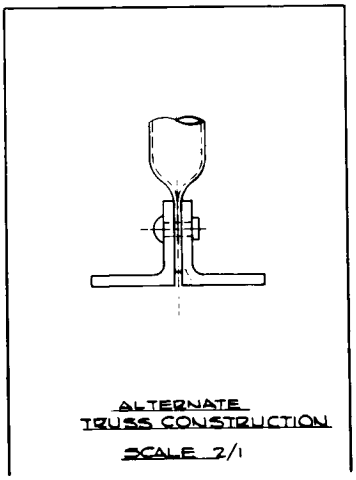

ALTERNATE
TRUSS CONSTRUCTION
SCALE 2/1

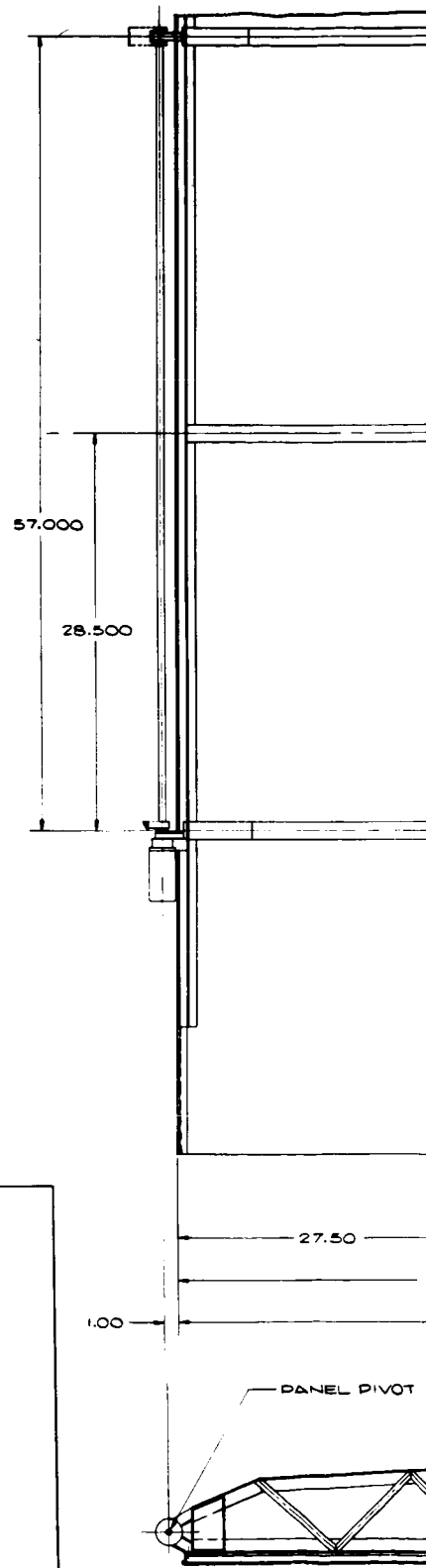

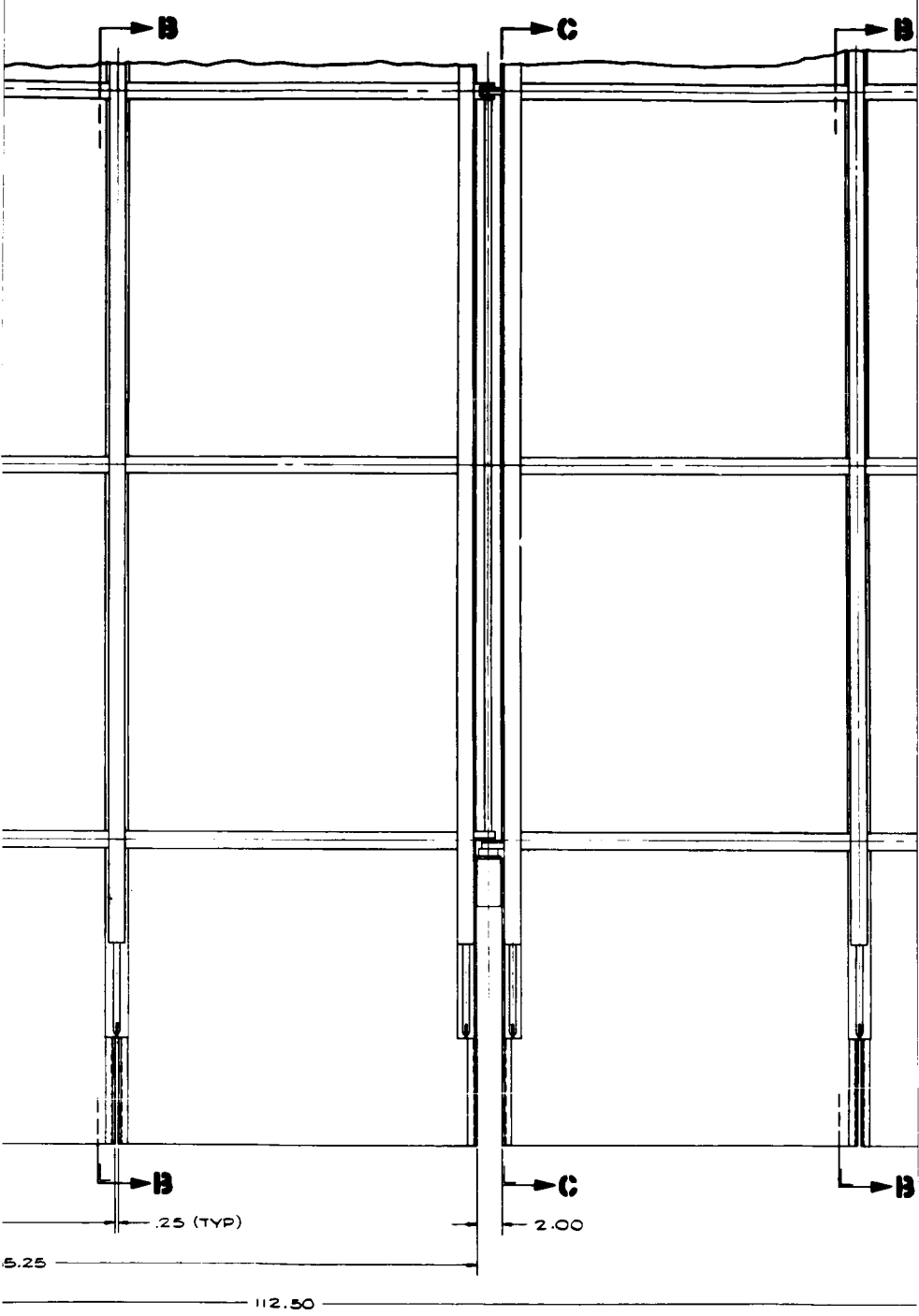

NOTE: DIMENSIC

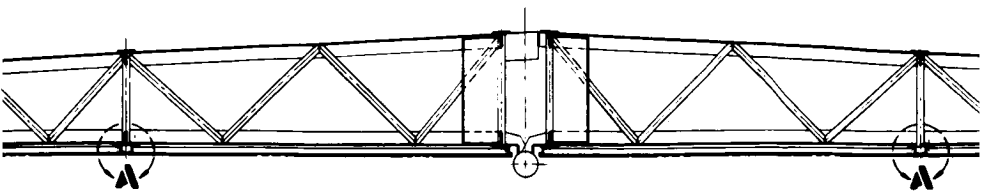

2

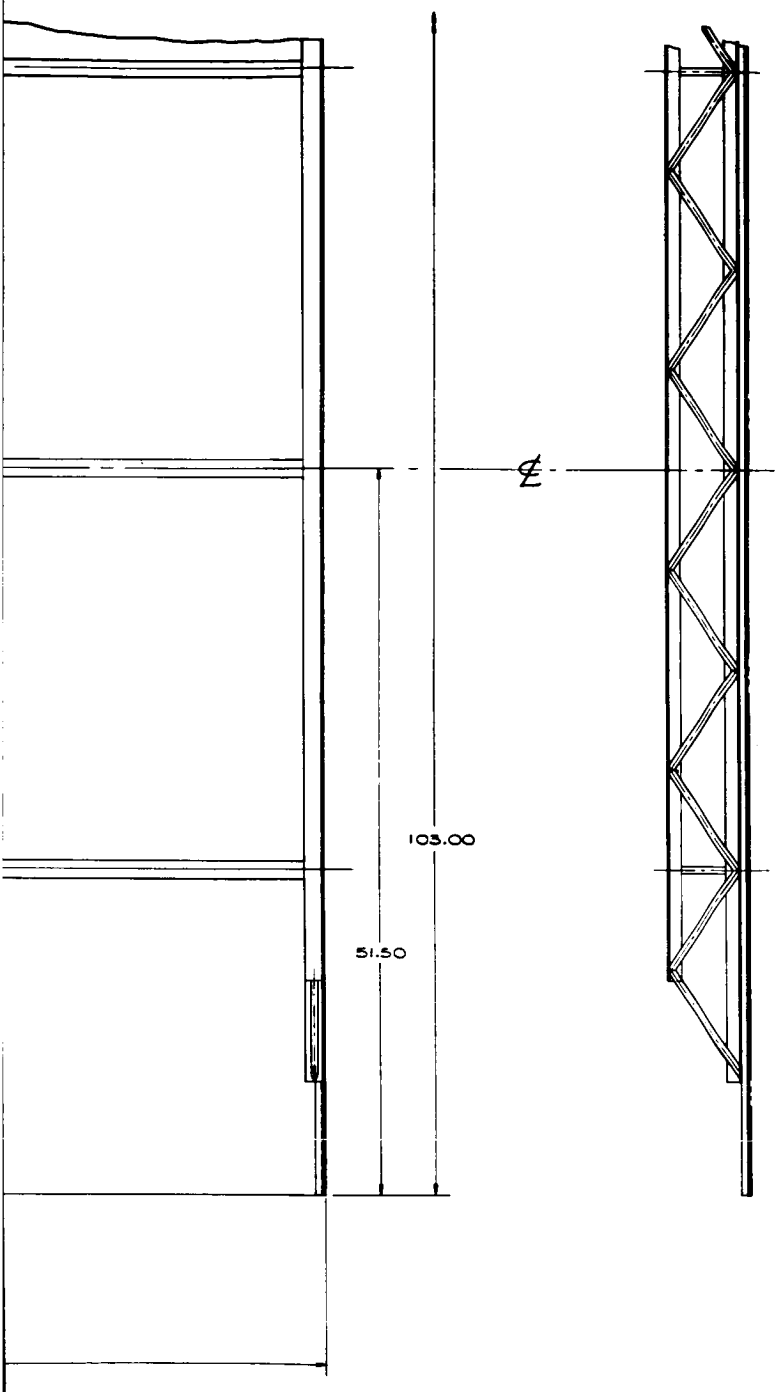

)NS IN INCHES

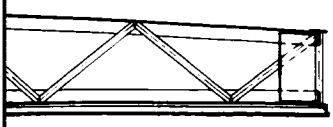

Figure 4.2-25: Spacecraft Model 945-6026 Solar Panel 1 General Arrangement

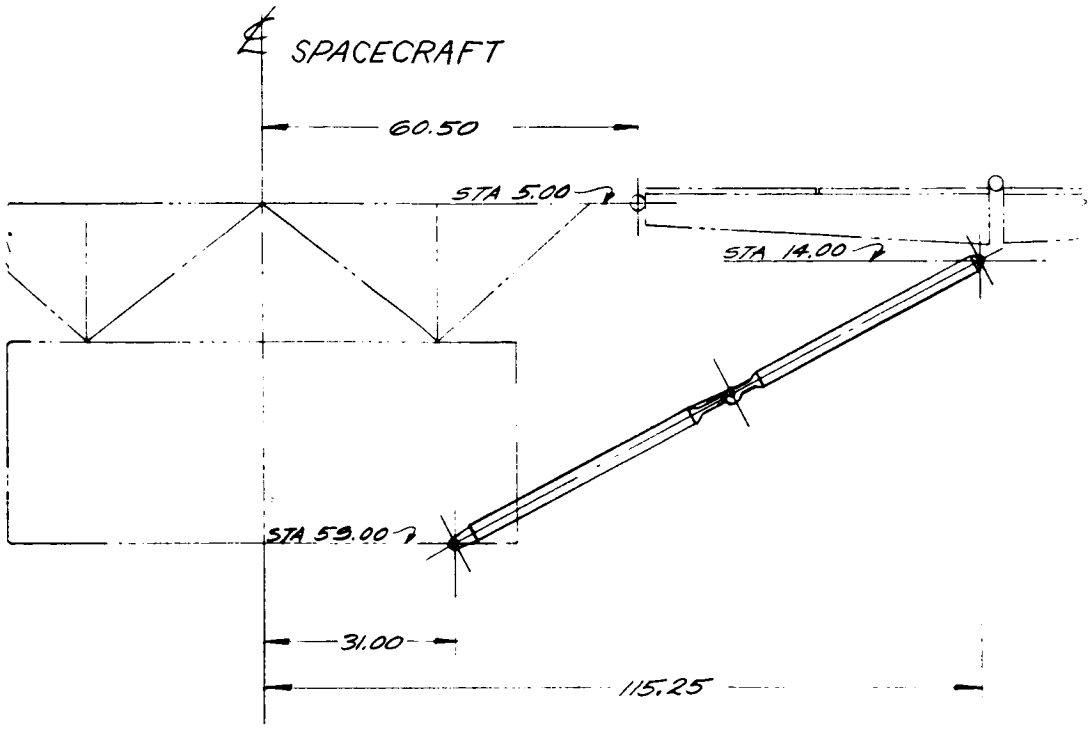

STRUT - EXTENDED
SCALE 1/20

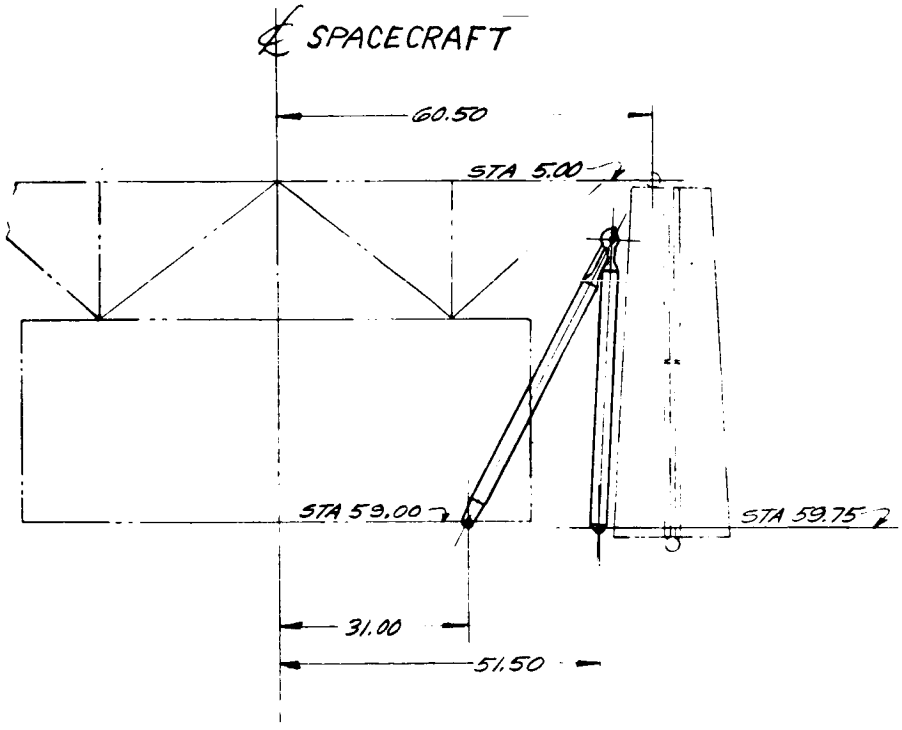

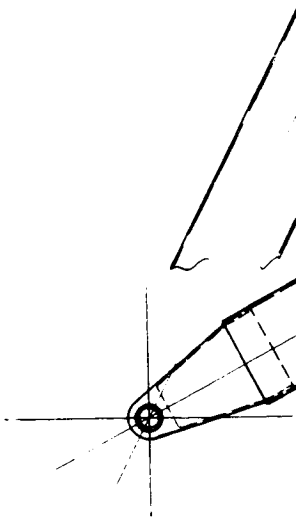

STRUT - FOLDED
SCALE 1/20

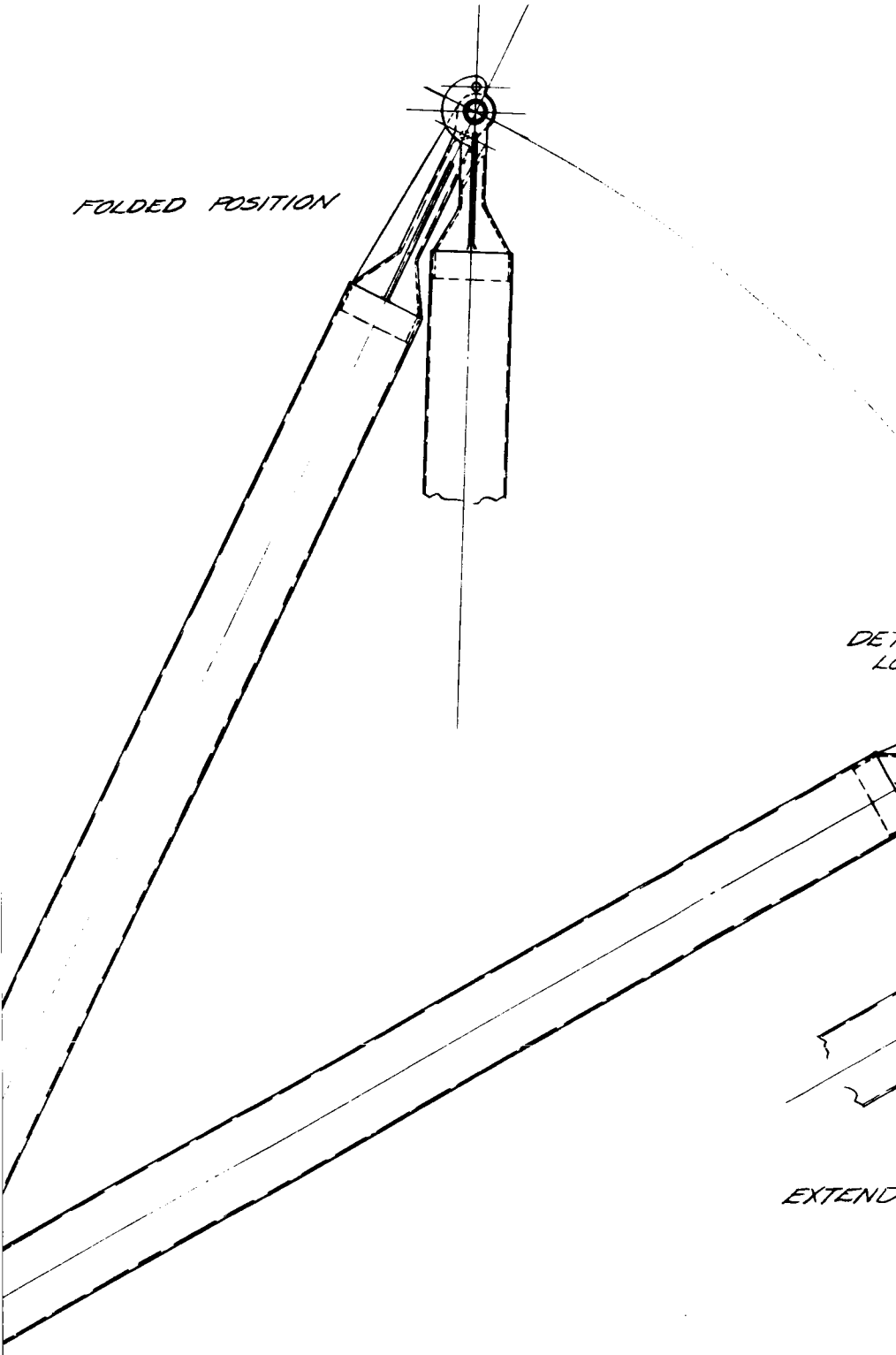

NOTE: DIMEN

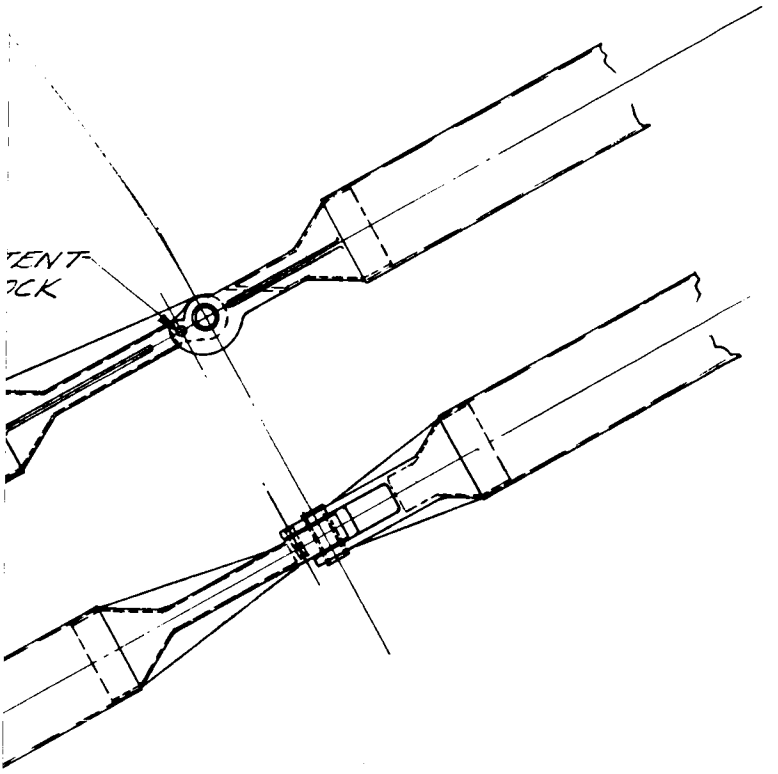

ED POSITION

NSIONS IN INCHES

Figure 4.2-26: Spacecraft Model 945-6026 Panel Strut

℄ SPACECRAFT

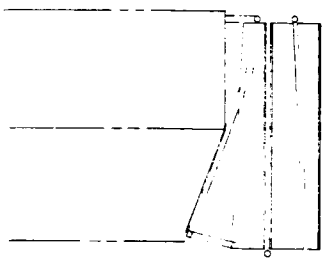

STOWED CONFIGURATION

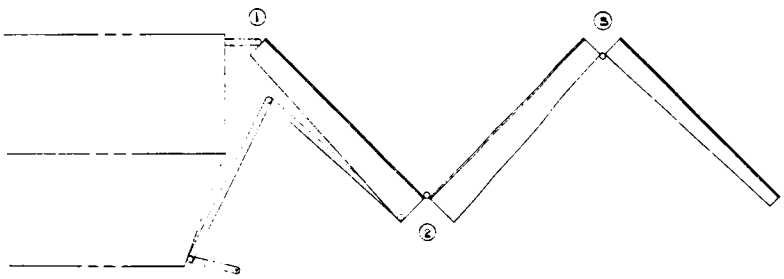

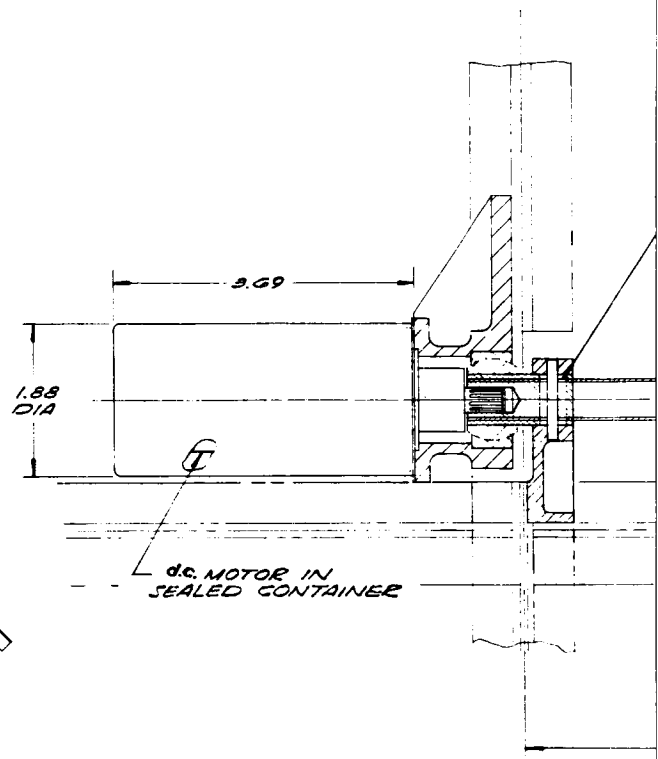

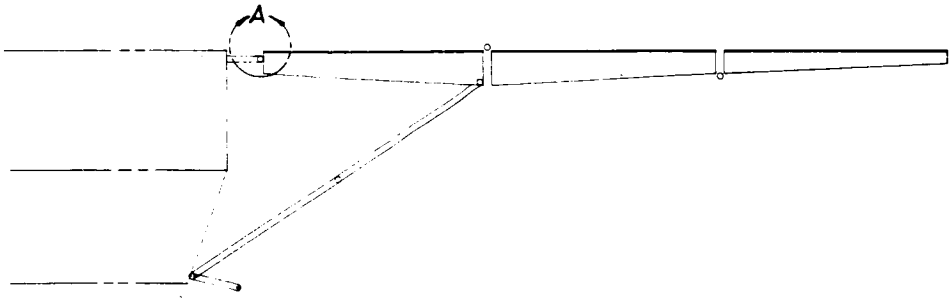

DEPLOYED CONFIGURATION

ELECTRIC MOTOR AND GEAR DRIVE PROVIDING UNIFORM MOTION ALLOWING PANELS TO BE DE-PLOYED AS SHOWN

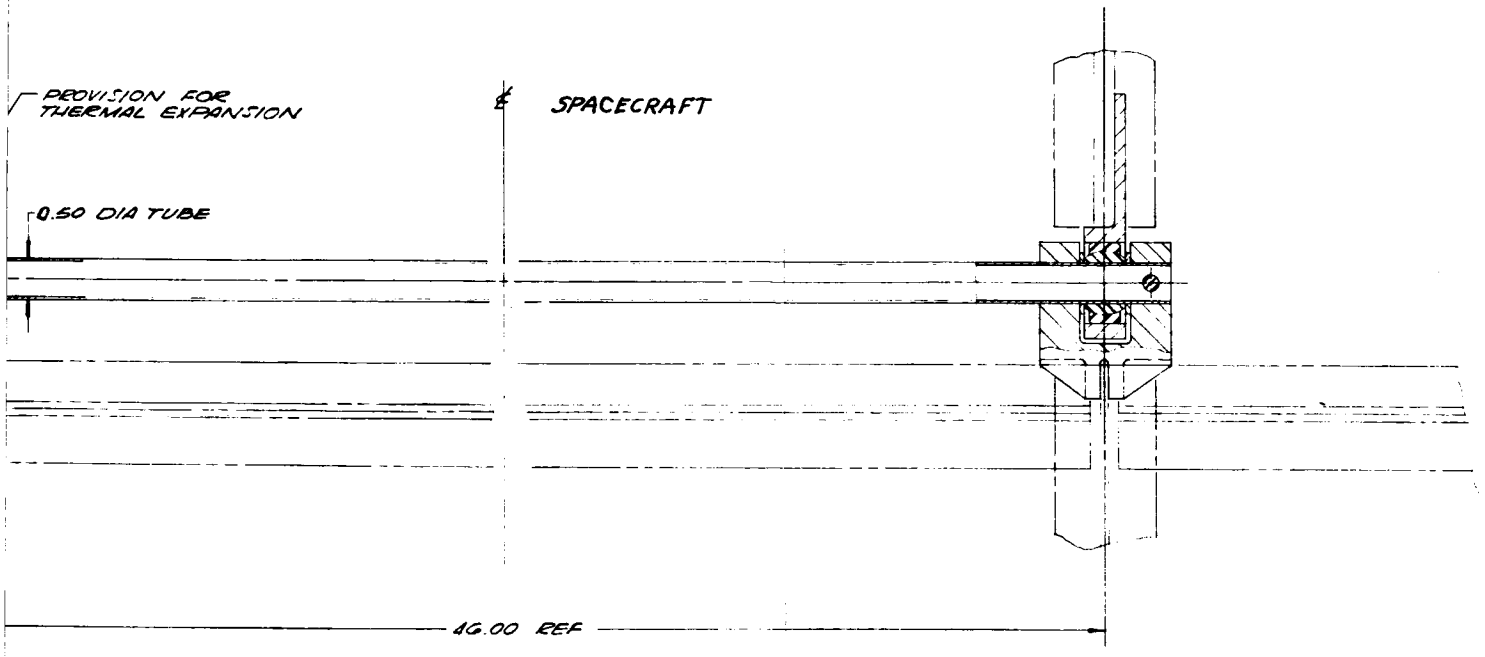

DETAIL A
(TYP 3 PLACES)

Figure 4.2-27: Spacecraft Model 945-6016 Panel Deployment Mechanism

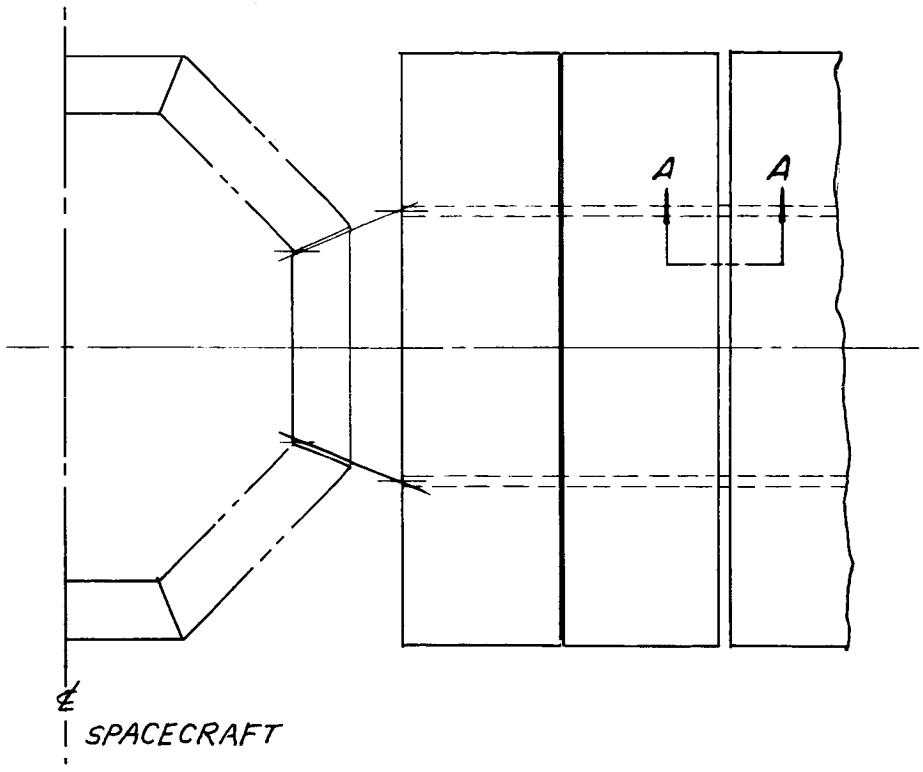
A
A
℄
SPACECRAFT

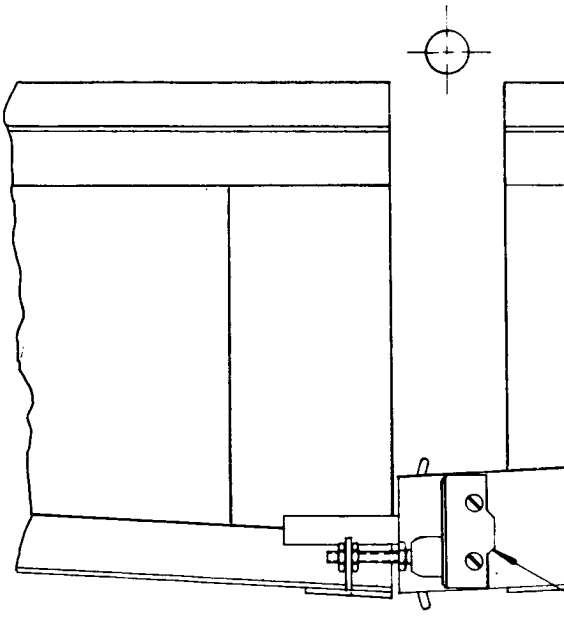

SECTION A-A
SCALE 1/1
TYP 4 PLACES

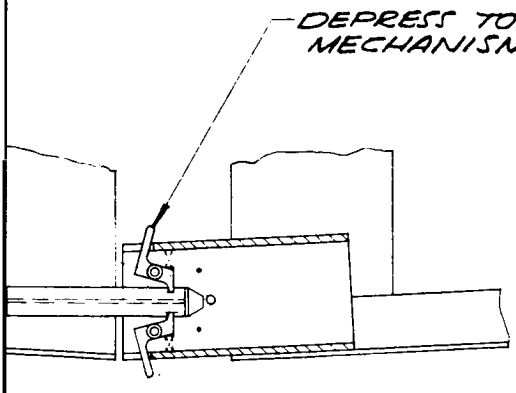

SECTION B-B

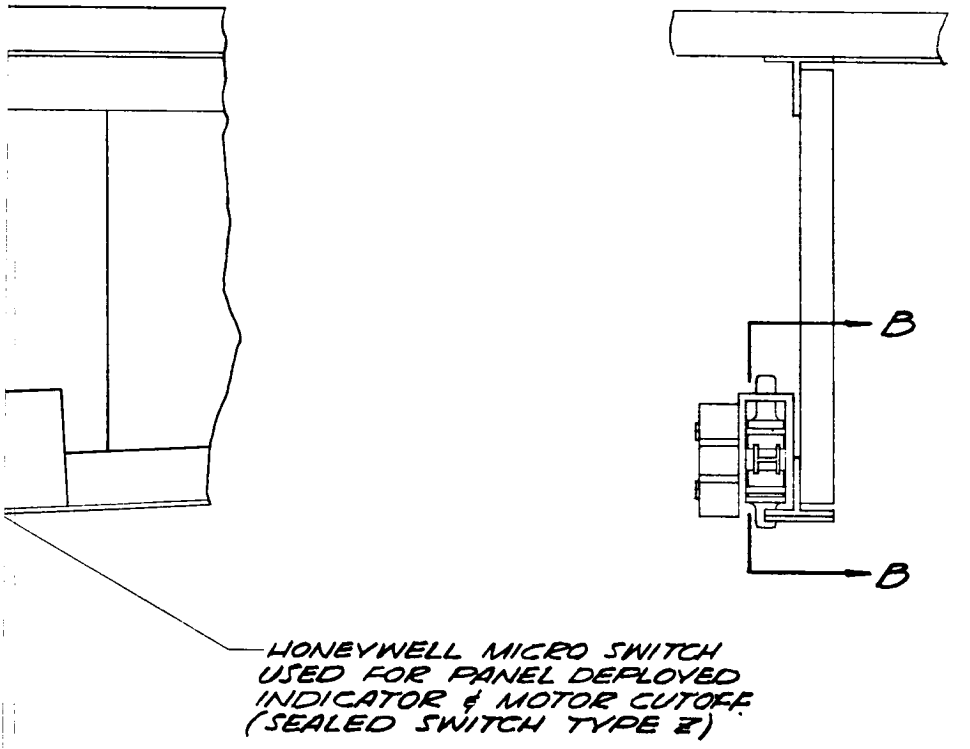

Figure 4.2-28: Spacecraft Model 945-6016
Panel Latches (Deployed) 3

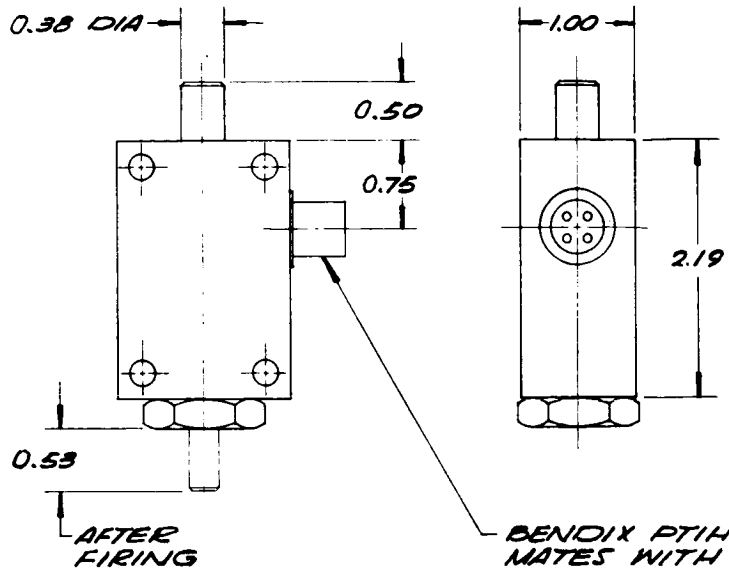

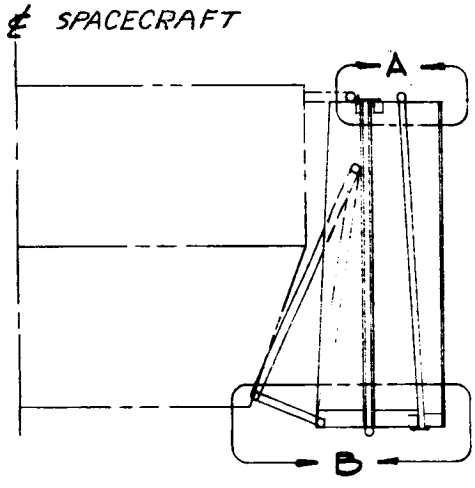

LATCH PIN, ASSY
SCALE - 1/1
MFGR - CONAX
BUFFALO, N.Y.
(SIMILAR TO 1808004)

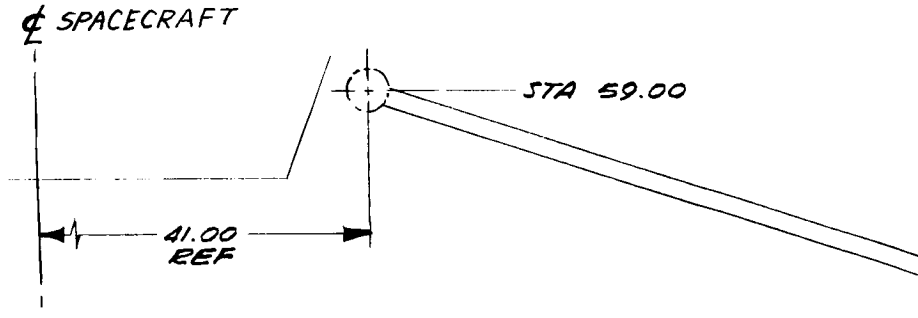

NOTE: DIMENSIONS IN INCHES

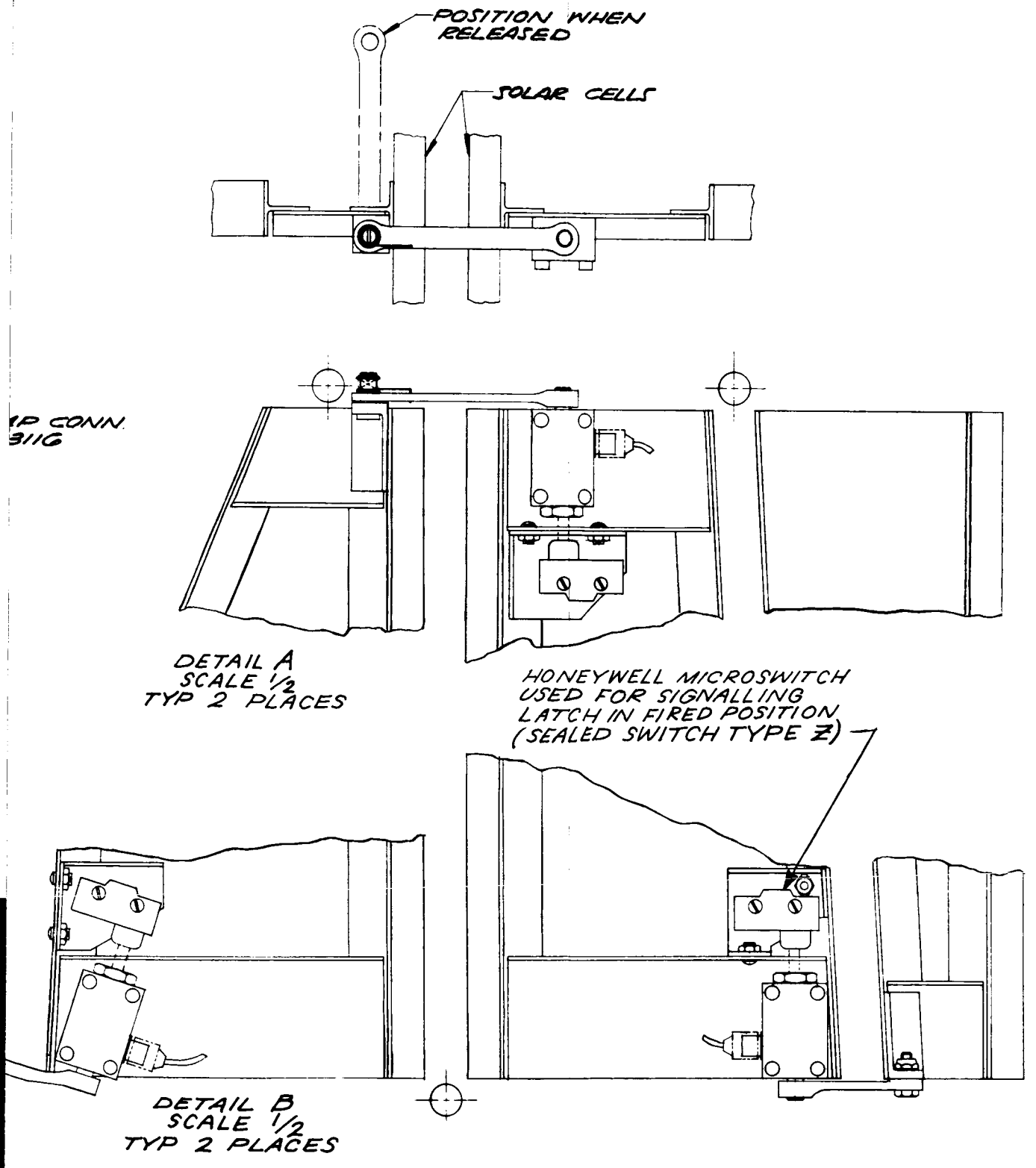

Figure 4.2-29: Spacecraft Model 945-6016
Panel Latches — Stowed

lateral and torsional load conditions. The longitudinal forces are resisted by the hinges. The pin pullers are single-squib double-bridgewire devices (produced by Conax Corporation) that meet the JPL mission specification document requirements. The preferred deployment device is a d.c. motor and gearhead similar to a motor produced by Globe Electrical Industries, designated Type M, sized to an output torque of 30 in.-lb for flexing the cable bundles and overcoming hinge friction. The motor gearhead is sealed in a nitrogen-gas-filled canister and is capable of being space-qualified. The magnetic properties of this system will be determined by testing. If found magnetically unacceptable, the alternate design (torsion-bar vane damper) is available (see Figure 4.2-54). The preferred deployment device has a relatively constant speed for varying load to correctly deploy (in 30 seconds) the panel section to avoid damaging the array or contact with other structural members. The deployed-position latches are designed to rigidly (no backlash) connect the panel-fold sections and to resist, along with the hinges, forces produced by the retromaneuver loading condition. The high-strength parts are made of titanium, and brackets and housings of aluminum (6061-T6) machined parts.

Operational Sequence--The operational sequence of array deployment starts after Earth-orbit injection, at which time a sequence of firing commands is sent to the pin-puller squibs that release the two sections of the panel from themselves and the spacecraft. Next, current is fed to the d.c. drive motors. As the panel structural sections reach the full-deployment position, they trip microswitches that shut

down the motors. The support struts are not electrically driven, but are extended through the action of the panel deployment. When the sections are fully extended, latches engage and tie each section together and lock the strut. The panel stays in this configuration for the remainder of the mission. For ground checkout, the panels can be retracted without being disassembled.

The array structural design has growth potential by adding another structural section. This addition can be made without structural redesign of the existing panels. Table 4.2-10 presents the array weight for various configurations: (1) three panels with two fold sections (present design), (2) three panels with three fold sections, (3) two panels with three fold sections, and (4) two panels with four fold sections.

Table 4.2-10: ARRAY-CONFIGURATION WEIGHT COMPARISON

ITEM	Spacecraft Configuration 945-6026		Spacecraft Configuration 945-6016	
	(1) 2-Fold Panel (lb)	(2) 3-Fold Panel (lb)	(3) 3-Fold Panel (lb)	(4) 4-Fold Panel (lb)
Photovoltaics	92.0	138.0	92.0	122.8
Substrate	69.5	104.2	69.5	92.7
Frame	53.8	84.8	56.5	83.0
Strut	22.5	22.5	14.0	15.0
Mechanisms	46.2	69.2	46.2	61.5
Total	284.0	418.7	278.2	375.0
Array Area (ft^2)	241.41	364.26	242.84	324.74
EOS Envelope Dwg No.	D-614100	D-614105	D-614107	D-614108

Note: First column data is for selected design.

Physical Characteristics and Performance Parameters--Table 4.2-11 lists the physical characteristics (weight and area) of the solar array.

Table 4.2-11: PHYSICAL CHARACTERISTICS -- SOLAR ARRAY

Photovoltaics, Secondary Cabling etc.	91.99 lb	92.0 lb
Mechanisms		
Hinges and Motor Drive	23.58	
Pyrotechnic Release Devices	13.93	
Deploy Latches	8.17	
	45.70 lb	45.7 lb
Array Structures		
Fasteners	0.50 lb	
Substrate	69.51	
Frame	53.78	
Struts (Hinges and Latch)	22.51	
	146.30 lb	146.3 lb
Solar Array Weight		284.0 lb
Array Substrate Area	236.0 sq ft	
Platform Area	241.4 sq ft	
Array Specific Weight	1.18 lbs/sq ft	

Table 4.2-12 lists such performance parameters as fundamental frequency, maximum deflections, critical stress or load, and margin of safety for the array.

Table 4.2-12: PERFORMANCE PARAMETERS -- SOLAR ARRAY

ITEM (Principal Strength Member)	CONFIGURATION	FUNDAMENTAL FREQUENCY (cps)	MAXIMUM DEFLECTION (inches)	MAXIMUM STRESS ($lb/in.^2$)	MARGIN OF SAFETY
Substrate (Spanwise Direction)	Boost	82.1	0.1045	18,000	0.13
	Deployed	82.1	0.0093	small	high
Substrate (Chordwise Frame)	Boost	62.8	0.2096	20,550	0.85
	Deployed	62.8	0.0178	small	high
Array (Spar Frame)	Boost	50.2	0.0039	9480	0.46
	Deployed	4.2	0.5620	11,800	0.17
Strut	Deployed	36.0	N.A.	1050	high

Table 4.2-13 lists the physical characteristics and performance parameters for the array mechanisms. The motor characteristics are shown in Figure 4.2-30.

Table 4.2-13: PHYSICAL AND PERFORMANCE CHARACTERISTICS--ARRAY MECHANISMS

ITEM	PARAMETER OR CHARACTERISTICS
Motor	
Power	24 watts for 30 seconds total (4 watts/motor)
Weight (Including container)	1.36 lb/motor
No. Regulators per Spacecraft	6
Pyrotechnic Pin Puller	
Wt of Pyrotechnic	1.16 lb/latch
Input Watts (avg.)	2 watts
Input Watts (peak)	50 watts
Dissipated Power (Avg)	2 watts
Peak Power Duty	100 milliseconds
Primary Power Source	Unregulated d.c. Bus

External and Internal Loads--The array structure was analyzed using generalized static and dynamic internal load curves. These curves were developed from the design load conditions presented in JPL Document No. 45 and the following estimate of orbit-injection limit loads: (1) engine

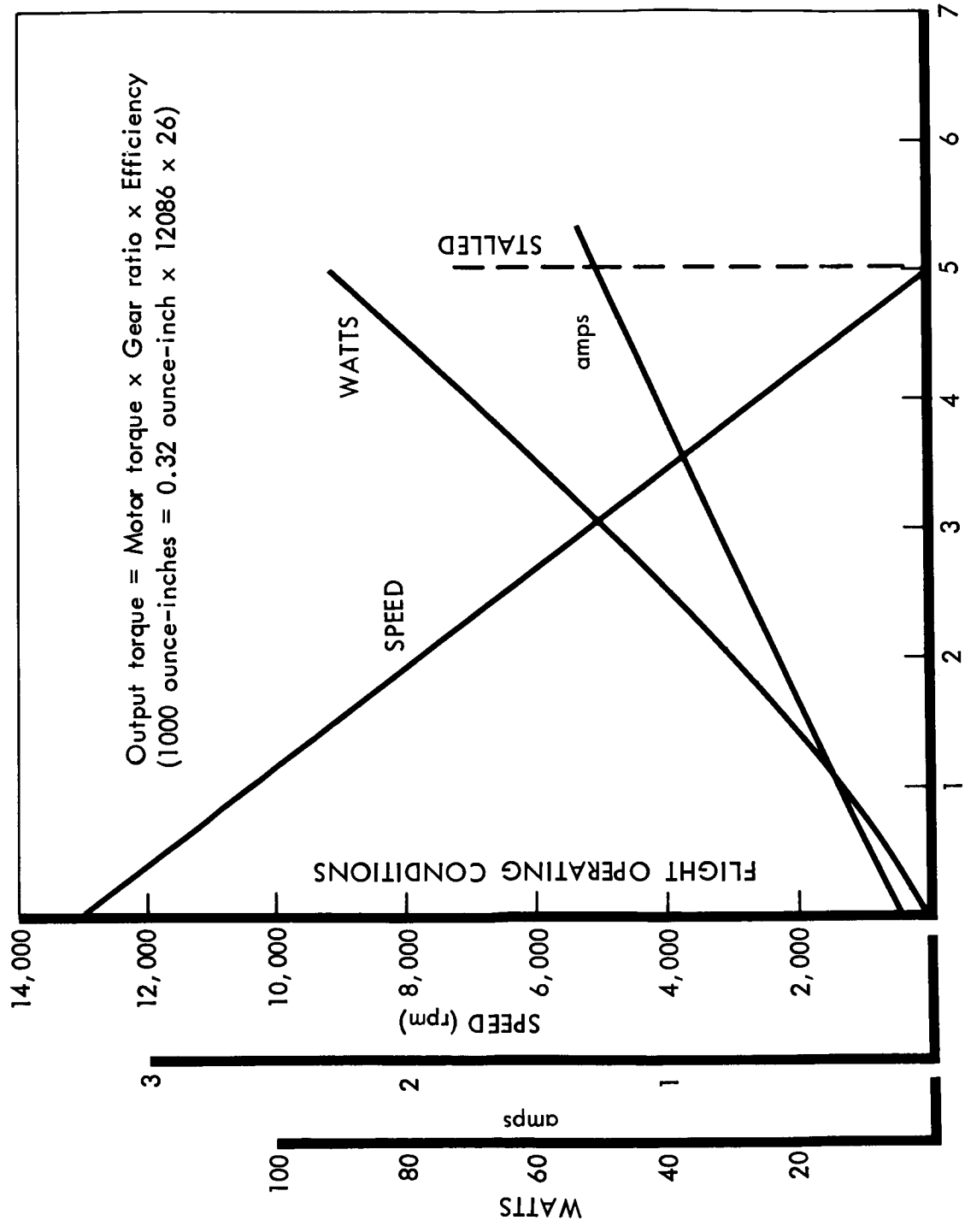

Figure 4.2-30: Motor Charateristics

ignition of 4 g's static longitudinal direction (includes a dynamic modification of 1.82); (2) engine burnout 3 g's static longitudinal direction; (3) engine cutoff-3 g's static longitudinal direction. The procedure was to rationalize a set of external load conditions at the solar-panel, spacecraft interface, and then to apply the external loads to the solar-panel structure to determine internal loads, bending moments and shears. The solar-panel structures were considered to be composed of four major structural elements: the main spars, chord-frame structure, the corrugated substrate, and the support strut. One of the primary design criteria is that these elements be dynamically decoupled, which allows each element to be treated independently as a simple beam (or column).

The design-load conditions are defined at the spacecraft-adapter launch-vehicle-adapter mechanical interface. Preliminary analysis of configurations similar to the preferred spacecraft design indicates that all significant spacecraft cantilever resonances will be below 30 cps. The first resonances of the spar and substrate in the stowed configuration have been predicted to be at 50 and 82 cps. Coincident amplification in the spacecraft and solar-panel structure is not expected. Therefore, the loads defined at the spacecraft-adapter, launch-vehicle-adapter interface are not considered to be amplified or attenuated by the spacecraft structure.

The loading conditions that produce the largest internal loads were reduced to constants to be used in entering the generalized load curves (Table 4.2-14). An ultimate factor of safety of 1.25 is included. For

conditions where both static and dynamic loads are specified, the resulting bending moments (or shear) from the static and dynamic loads are added. The dynamic magnification factors (Q) of the frame (spar) and substrate (based on vibration tests on a prototype solar panel shown in Figure 4.2-31) have been taken to be 20 and 45.

Table 4.2-14: CONSTANTS FOR GENERALIZED LOAD CURVES

LOADING CONDITIONS		STATIC a	DYNAMIC $\ddot{\delta}_s$	DYNAMIC Q
1	Substrate	1.25	0.625 g	45
	Frame	1.25	0.625 g	20
2 Boost Configuration	Substrate	1.25	0.938 g	45
	Frame	1.25	0.938 g	20
3	Substrate	0	1.25 g	45
	Frame	0	1.25 g	20
4	Substrate	0	0	0
	Frame	0	0	
Deployed Configuration	Substrate	5 & -3.75	0	
	Frame	5 & -3.75	0	
	Strut	5 & -3.75	0	

Generalized spar and rib load curves that present deflection, shear, and maximum bending moments for both static and dynamic loading have been developed for the following support conditions:

1) Chordwise Structure: Overhanging uniform beam with two pinned supports, each symmetrical about the beam midspan;

2) Chordwise Structure: Same as Item 1, but with each support clamped;

3) Spanwise Structure: Overhanging uniform beam with two pinned supports, one located at the inboard hinge and the other located outboard of the hinge.

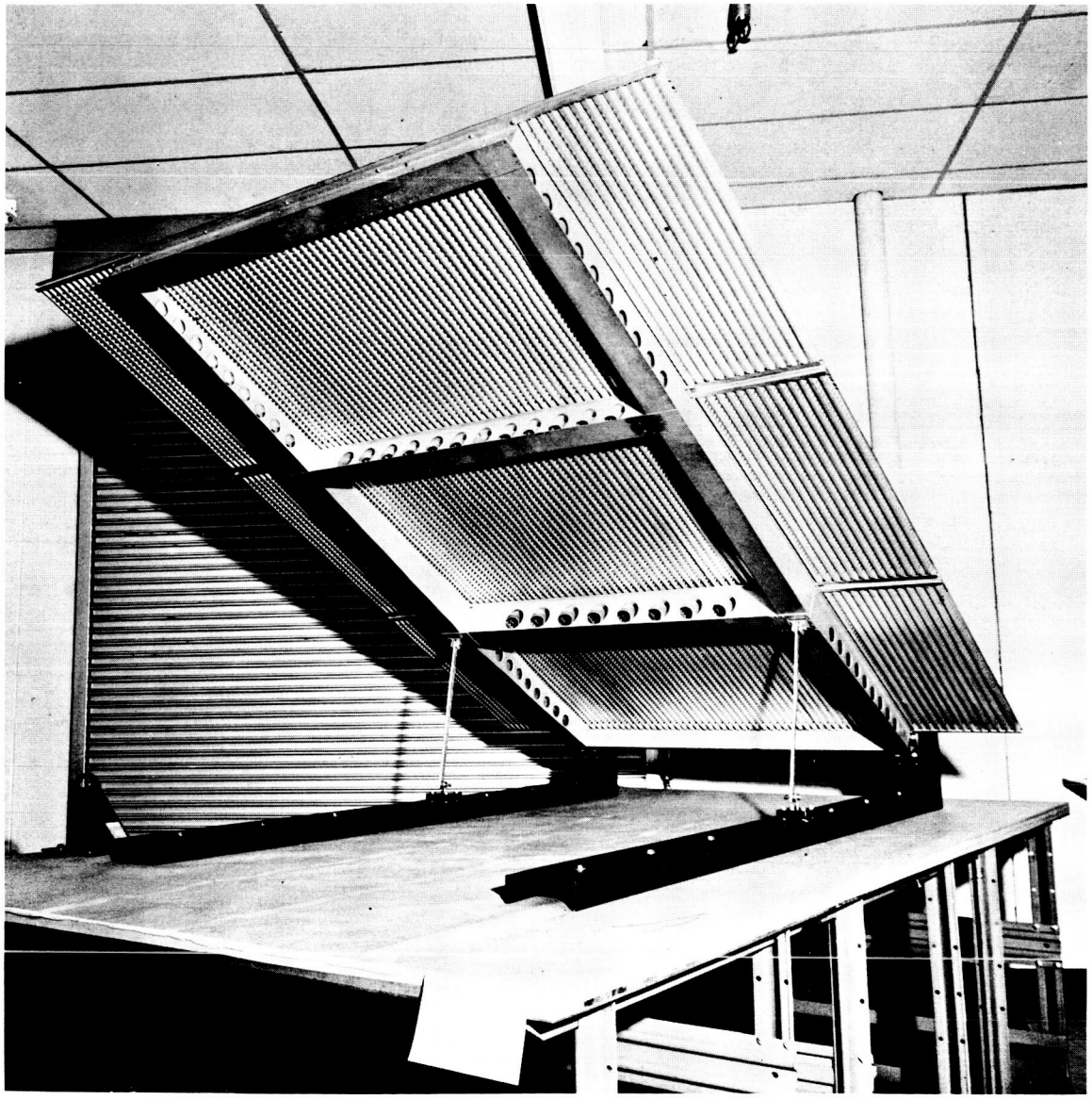

Figure 4.2-31: Prototype Solar Panel

The spar first-mode dynamic bending moment curve is presented in Section 4.2.9.5 (Figure 4.2-50).

Thermal Effects--Determination of panel temperatures involves panel structural and electrical design, thermal control of the spacecraft, and the positioning of other subsystems and science payload.

Detailed thermal calculations of the preferred design panel were accomplished along with selection of thermal coatings discussed later in this section. Significant numbers resulting from the analysis are:

1) Average solar absorptance/thermal emittance ratio = 0.48
2) Equilibrium temperatures (see Figure 4.2-32) (Sun-oriented):
   a) Earth (140 mw/cm^2) = 55^{o}C;
   b) Mars at encounter (65 mw/cm^2) = -2^{o}C;
   c) Mars at end of life (50 mw/cm^2) = -18^{o}C;
3) Transient temperatures (see Figure 4.2-33):
   a) Minimum panel temperature after Mars occultation of 2.9 hr (50 mw/cm^2) = -170^{o}C;
   b) Maximum panel temperature due to retromotor exhaust plume = 60^{o}C.
4) Temperature gradients:
   a) Top to bottom of substrate = 3^{o}C ΔT;
   b) Chordwise (see Figure 4.2-34) (centerline to edge) at Mars = 7^{o}C ΔT;
   c) Spanwise (see Figure 4.2-35) (from end to end) at Mars = 7^{o}C ΔT;

Figure 4.2-32 shows the change in average panel equilibrium temperature as the intensity of solar radiation decreases during transit to Mars. Figure 4.2-33 shows the predicted transient behavior of the average solar-panel temperature during a Mars orbit. Figures 4.3-34 and 4.3-35 show the expected temperature distribution throughout the solar panel for a solar intensity of 50 mw/cm^2. All data assumes a Sun-facing panel.

Typical temperature-dependent data for the thermal emittance of the black-paint coating for the bottom surface is included in the calculations. In addition, available experimental data on filter cover and dielectric material emissivity and absorptivity is also included. The effects of radiative interraction with the spacecraft and with Earth and Mars have been accounted for in these calculations. The detailed temperature distributions in Figures 4.2-34 and -35 account for the interaction with the solar-panel frame and the Spacecraft Bus. A detailed calculation of the temperature gradients through the substrate, including corrugations, has shown that the total temperature difference between the top and bottom panel surfaces does not exceed $3^{o}C$ for the highest-intensity solar radiation.

The transient changes in the solar-panel temperatures will occur during launch, midcourse maneuver, retropropulsion, and solar occultation in the Mars orbit. The panel temperature will rise $10^{o}C$ due to Mars albedo and infrared radiation when, at orbit perigee, the back of the panel directly faces the bright side of Mars.

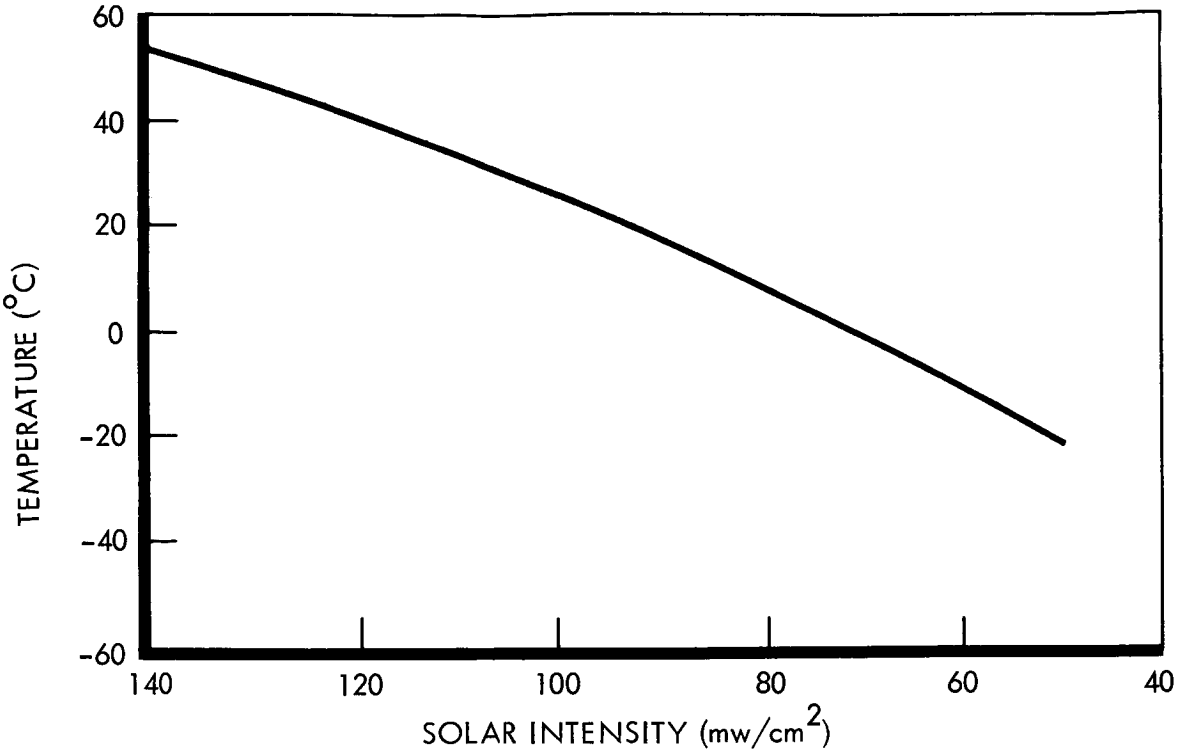

Figure 4.2-32: Average Solar-Panel Temperature During Transit

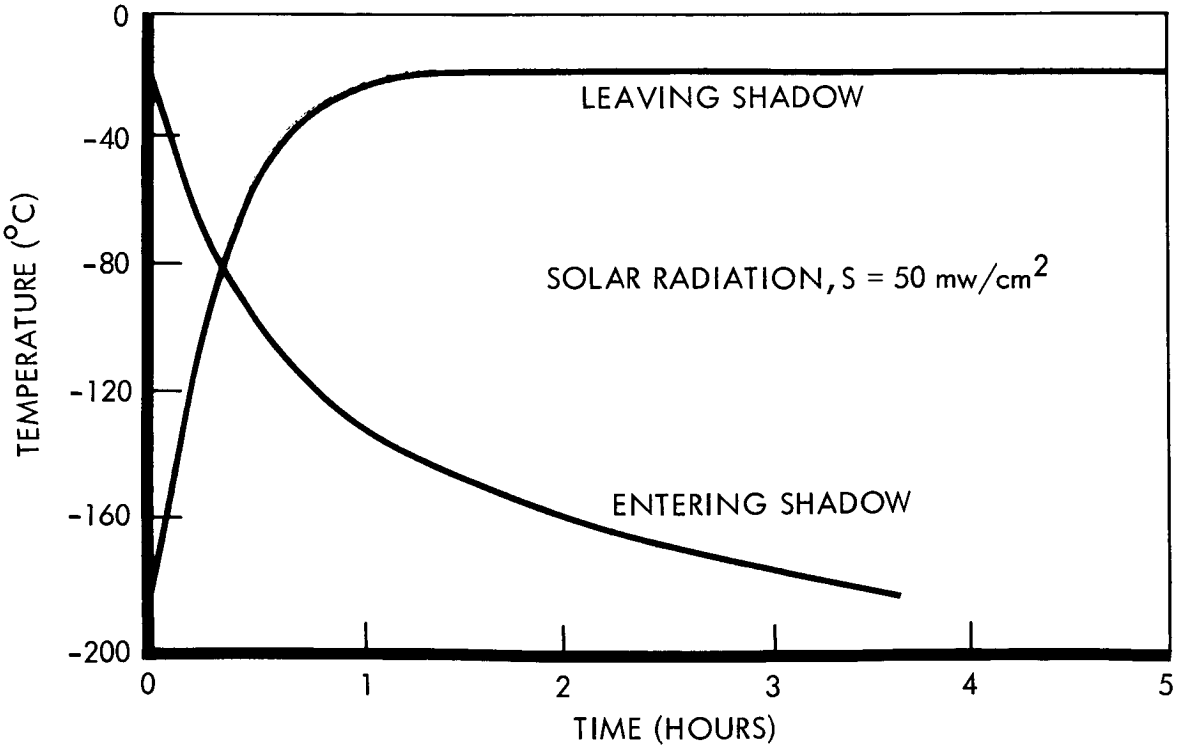

Figure 4.2-33: Voyager Solar-Panel Temperature at Mars During Solar Occultation

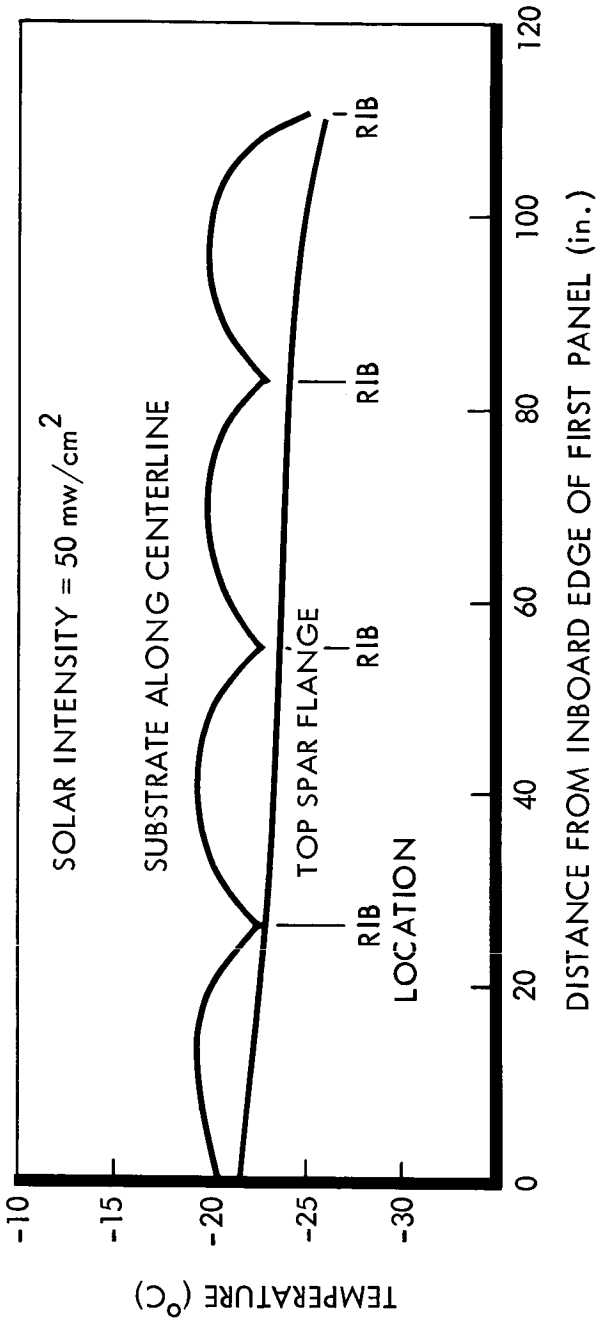

Figure 4.2-34: Spanwise Solar-Panel Temperature – Distribution at Mars

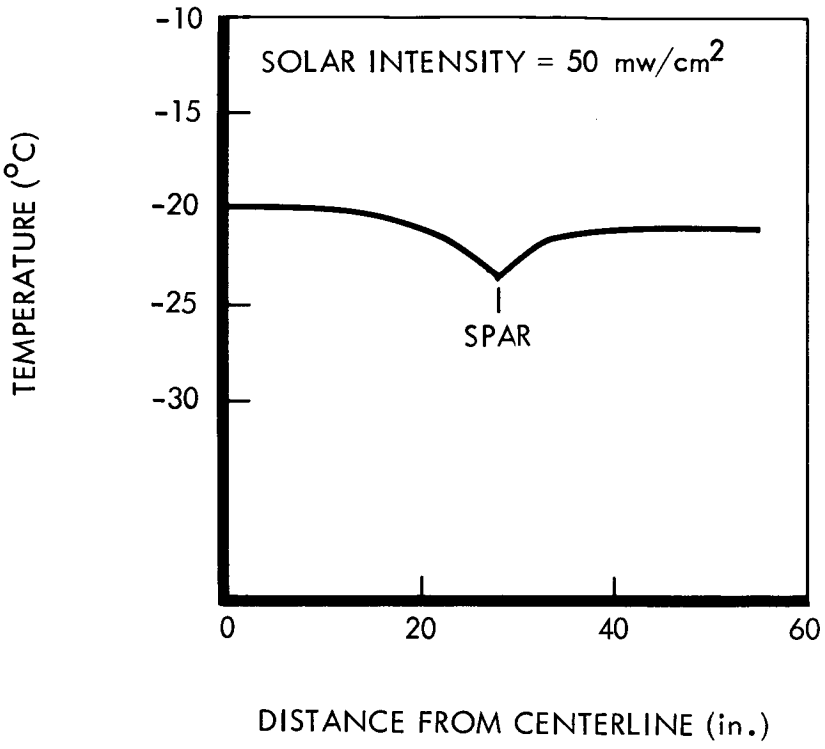

Figure 4.2-35: Chordwise Solar-Panel Temperature Distribution at Mars

A study of the transient behavior of the panel-temperature distribution during the start and finish of solar occultation in Mars orbit indicates that the temperature differences throughout the panel can be large if no direct thermal paths between the substrate and spar cap are incorporated in the design. For this reason, in the preferred design all top chord members of the frame structure will be thermally connected to the local substrate back surface.

Figure 4.2-36 presents the temperature response of the substrate and spanwise truss frame after emergence from the Mars shadow. To illustrate the severity of this problem, when no direct thermal paths are provided, the model employed was selected such that the gradient between these two elements would be as low as possible. The model allowed heat flow from the substrate to the spar cap by conduction only, through zero resistance joints at each chordwise member. Both elements were assumed to be initially at -156.6°C. Then, to determine the spar cap response, a step increase in substrate temperature at zero time of 150°C was imposed. The substrate was allowed to respond as an infinite plate receiving solar energy in a stepwise fashion.

Surface spectral coatings and geometric parameters (view factor) of the solar panels will affect spacecraft thermal control. The thermal emittance of all surfaces of the solar panel will be near 0.785, so that the longitudinal location of the solar panels on the spacecraft is relatively unimportant in this respect. The view factors from the panel to the spacecraft are largest in regions close to the spacecraft walls; thus, temperatures decrease in the outboard direction. Thermal interactions

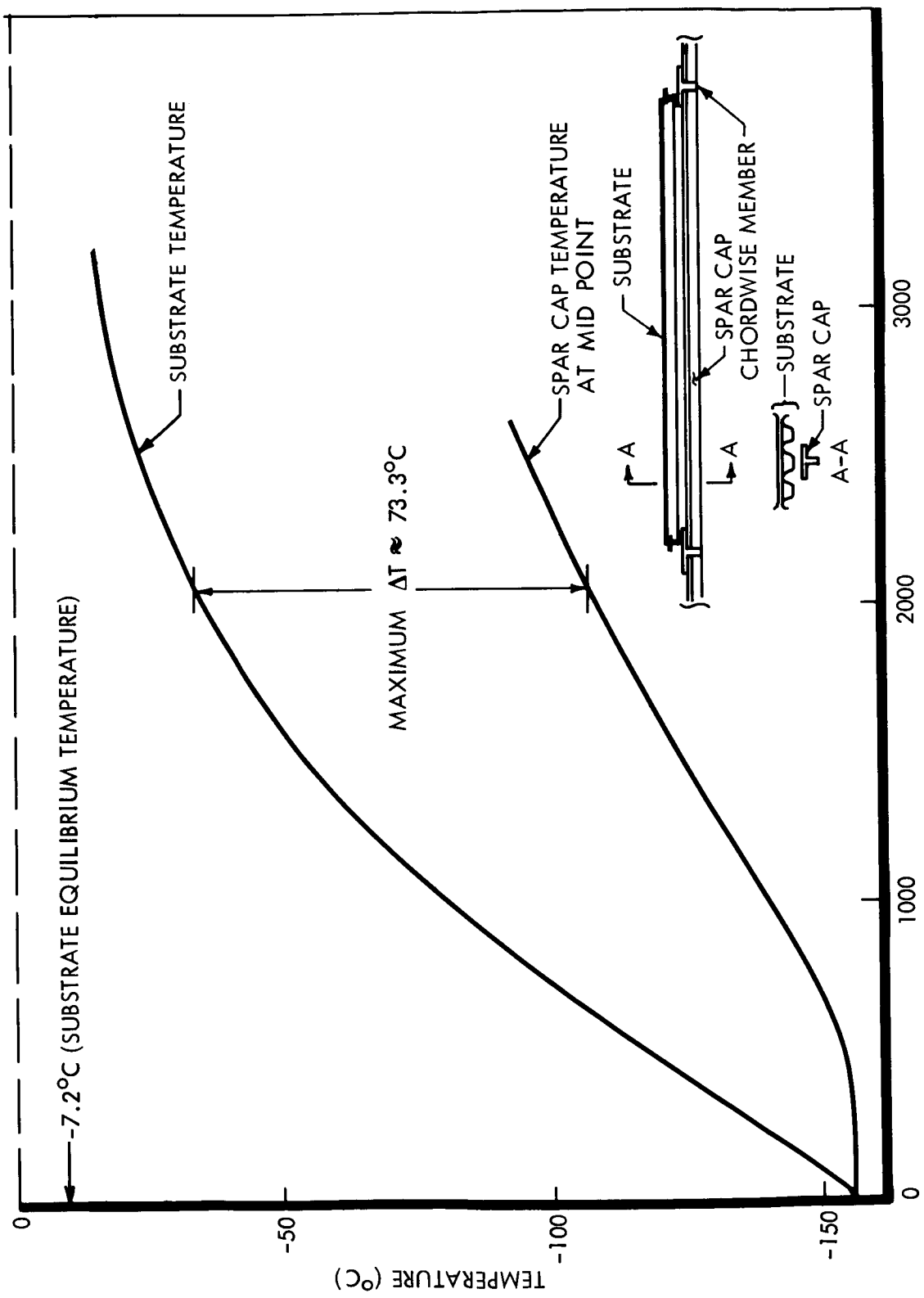

Figure 4.2-36: Solar-Panel Temperature Response at Emergence from Mars Shadow

between the panel and spacecraft have been found to be negligible for distances greater than one wall height away from the spacecraft.

It does not appear that the presence of the capsule will significantly affect solar-panel design. If radiators from RTG power supplies in the capsules were placed directly facing the solar panels, they will decrease the solar array output during part of the transit phase. However, during this phase, the higher solar intensity will provide an adequately high power output.

Aluminum and magnesium are desirable materials for the substrate because of their high thermal-conductivity-to-density ratio. To maximize joint conductance values, the thickness of nonmetallic materials, such as adhesives and dielectrics, are minimized. The supporting frame structure, if good thermal contact is provided, will act as a radiation shield through blockage and as a radiation fin. Spars with open webs, such as a truss, or members of very short height reduce temperature gradients and thermal stress in and out of the plane of the panel. Thermal stresses between the panel substrate and supporting frame are also minimized by using aluminum for both the substrate and frame and by providing good conduction paths through attachment joints.

Although preliminary analytical values have been obtained for the temperature distribution in frame-supported solar panels, thermal tests will

be run in a vacuum chamber with prototype assemblies. These tests will ensure that joint conductance values are realistic and that local temperature variations do not seriously degrade solar-cell performance in space.

4.2.9.3 Reliability

The reliability of the solar array exceeds 0.99999 based on calculations assuming random open-cell failures due to environment such as micrometeoroide and isolation-diode failures and the 10 percent safety factor allowance that has been incorporated in the K factors. Details of calculations are contained in Reference 6.

4.2.9.4 Electrical Design Optimization

Solar Cells--The selection of a solar cell will affect the weight, area, reliability and cost of the panel and also determine the amount of degradation of the solar-array electrical performance during a space mission. The preferred solar cell will have the following characteristics: N-P, 2x2 cm, silicon, 11 percent at AM=0,28°C, 12-mils thick; standard-type solderless sintered Ti-Ag cell contacts; and base resistivity of 10 ohm-cm.

Solar Cell Type--Only the N P and P N silicon solar cells can be seriously considered at this time. The other types such as hetero-junction cells, GaAs cells and dendritic cells, are still in the research and development stages and little or no flight performance data is available for them.

The N P silicon is presently superior to the P N cell in availability and radiation tolerance. The chief advantage of the P N cell is a better voltage coefficient for low-temperature operation. Primarily because of radiation resistance and availability, the N P cell was selected.

Solar Cell Size--The 2 by 2 centimeter cell has been selected for the following reasons: proven flight performance, reduction in panel weight and area resulting from a better packing factor, lower cost, excellent availability, reduced assembly handling, and reduced testing.

In the comparison of the weight advantages between the various size solar cells (1x2 cm, 2x2 cm, and 3x3 cm) larger cells reduce solder, bus bar material, and wiring requirements but the total reduction is small. An advantage of using larger cells is the decrease in panel area, caused by an improvement of area utilization by eliminating some intercell spaces.

Cost savings of perhaps 60 to 70 percent are possible through the use of 2-by-2-centimeter cells over 1 by 2 centimeters, based on experience in purchasing cells, during the past two years.

Reliability analysis made in this study, Reference 6, shows the dependence of reliability on the number of cells. A small increase in panel reliability occurs when using the smaller cells due to the increased redundancy. This is offset by the increase in soldering operations and assembly and test handling of a larger number of smaller cells for a panel of the same power level.

Assembly time and costs are reduced with the use of larger cells because of less cell handling and testing. Also, the reduced handling and assembly time decreases the chances of damage to the panel during assembly.

Solar-cell Efficiency--Cells with efficiencies ranging from 9 percent (AM=0) to 13 percent (AM=0) have been considered. The cell efficiency of 11 percent (AM=0) has been selected.

The price of a cell is a direct function of its efficiency. Cell manufacturers estimate that maximum efficiencies over the next 2 to 10 years will be between 11 percent and 13 percent (AM=0). A maximum efficiency of about 11 percent (AM=0) is realizable in reasonable quantities. Figure 4.2-37 is a cost comparison of present cells.

The use of a high-efficiency cell results in a significant savings in panel weight and panel area as shown in Figure 4.2-38a. Although the panel weight and area decrease with increasing cell efficiency, the total panel costs still increase as seen in Figure 4.2-38b.

Contacts--The standard type of cell contact with solderless Ti-Ag metallic plating has been selected for the Voyager panel because of its present availability, proven flight performance, and lightweight characteristics.

The use of sintered Ti-Ag solderless contacts is an important consideration since it provides a uniformly flat surface for bonding the filter cover glass to the cell. Flat surfaces permit the use of a minimum amount of adhesive. In addition, the lack of solder humps on the back side of the cell reduces the amount of adhesive needed to bond the cell to the substrate, and reduces the chances of the solder contacts shorting through the insulation to the substrate.

Thickness--The solar-cell thicknesses that were evaluated range from 20 mils to 4 mils. The thickness of 12 mils has been selected for the

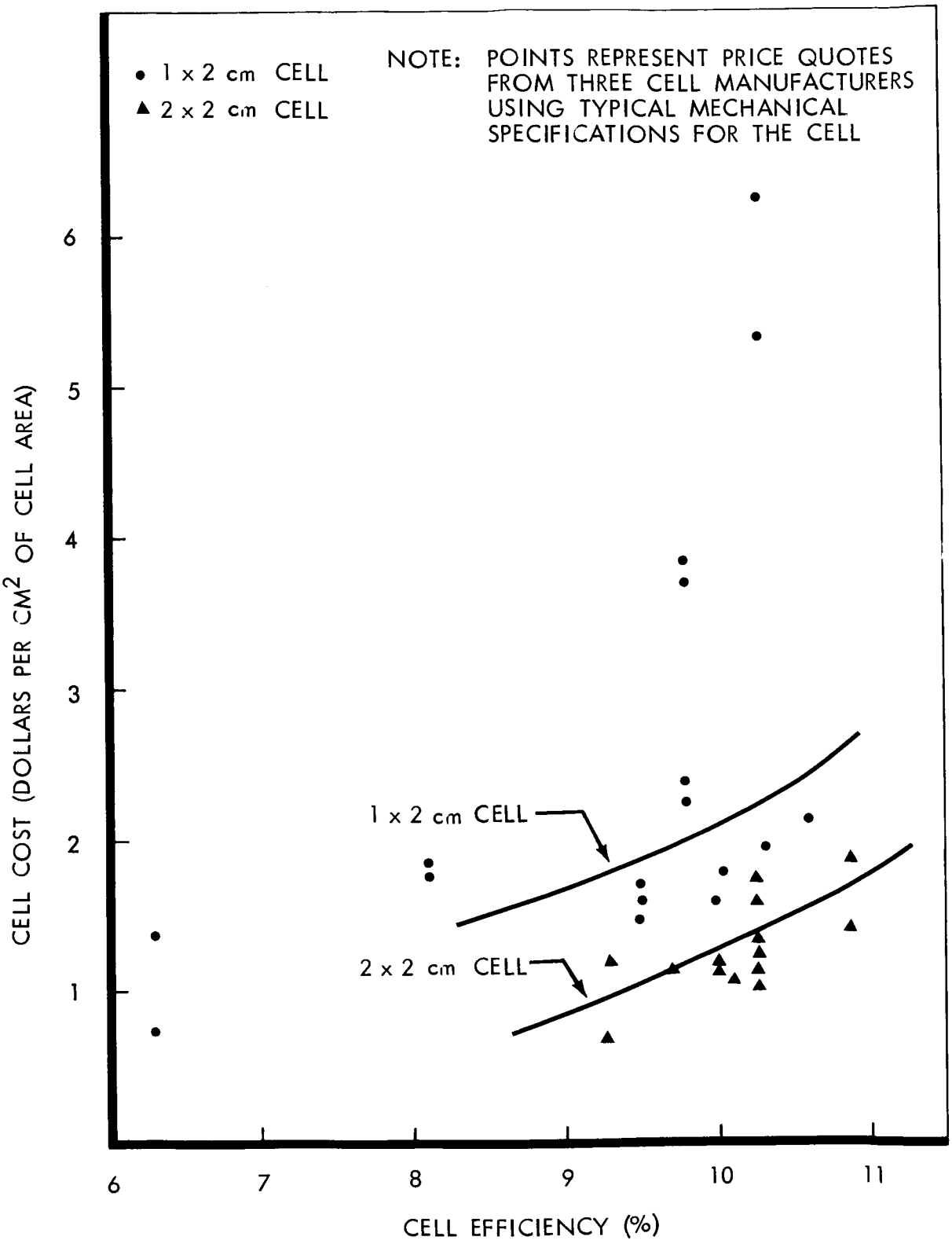

Figure 4.2-37: Solar-Cell Cost Comparison

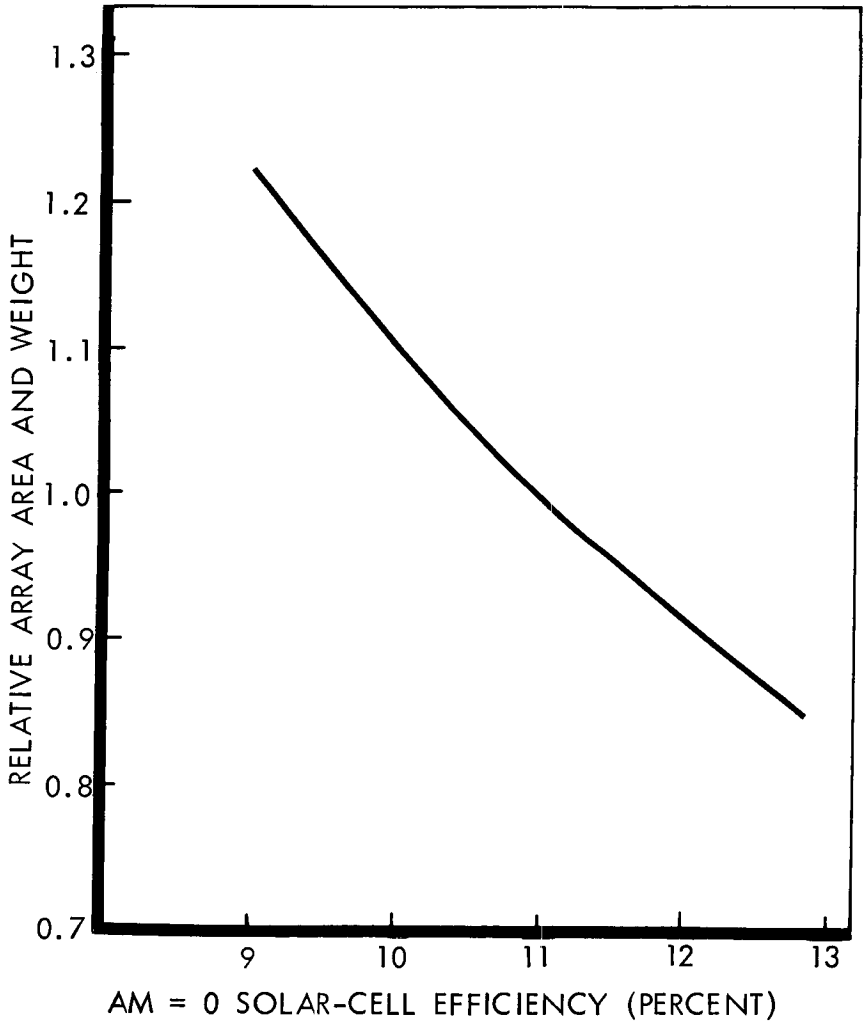

Figure 4.2-38a: Array Weight and Area vs Cell Efficiency for Constant Output Power

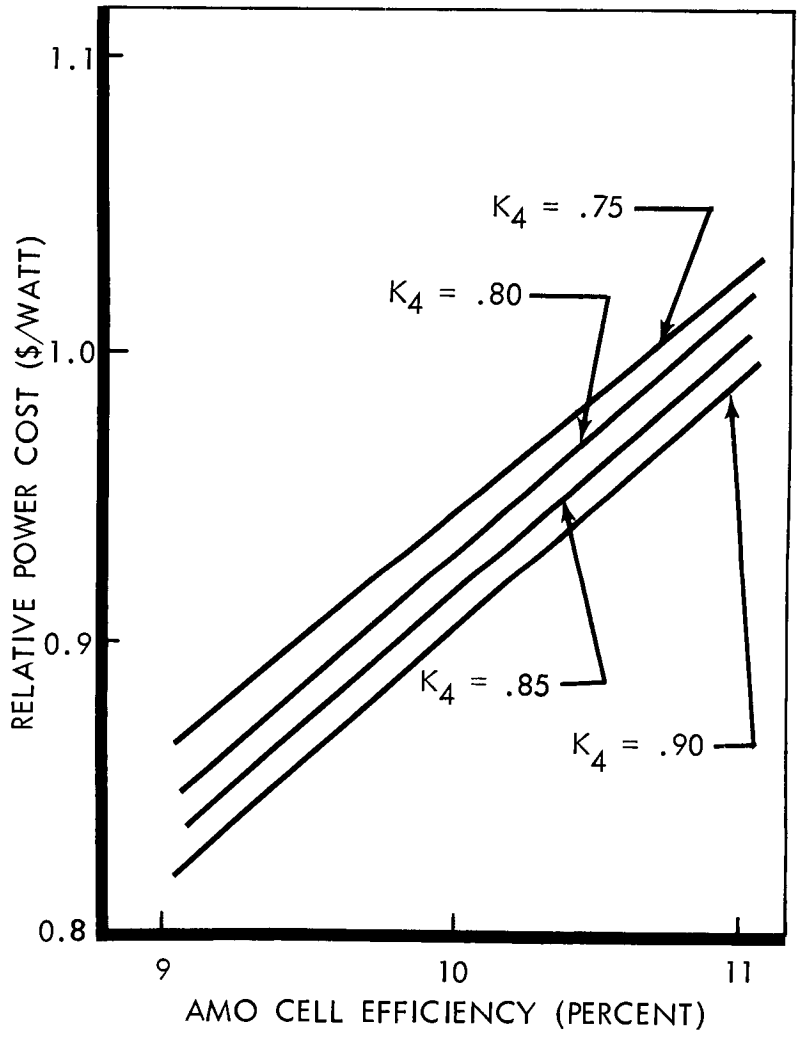

Figure 4.2-38b: Relative Power Cost of Solar Array for Various Packing Factors (K_4)

following reasons: optimum panel weight, good availability, strong enough to minimize handling damage during assembly, and present fabrication techniques may be used. The relationship between cell thickness and panel weight is shown in Figure 4.2-39.

Decreasing the cell thickness reduces both the cell weight and, after a certain point, the cell efficiency. This decrease in conversion efficiency can result in a larger and, therefore, heavier panel. Calculations, made on a typical configuration, show that a 12-mil cell, 11 percent (AM=0) will result in a 273.9-pound panel while a panel with 8-mil cells weighs 275.9 pounds, and a panel with 20-mil cells weighs 291.1 pounds. In addition, the 8-mil-cell panel requires a 4.8 percent area increase over the 12-mil-cell due to reduced efficiency. The thinner cells are more fragile to manufacture, assemble and test.

It is expected that there will be insufficient flight data on cells thinner than 12 mils before the component freeze date of July 1966. There are indications that the thinner cells may have a higher radiation resistance, but there is not enough experimental evidence at the present time to permit evaluation. If this radiation resistance does exist, the thinner cells may be considered for later updating of the Voyager panels.

Base Resistivity--A cell base resistivity of 10 ohm-cm has been selected for its better radiation tolerance, availability and proven flight performance. Lower base resistivity cells have higher maximum power voltage and are theoretically more efficient at low illumination levels

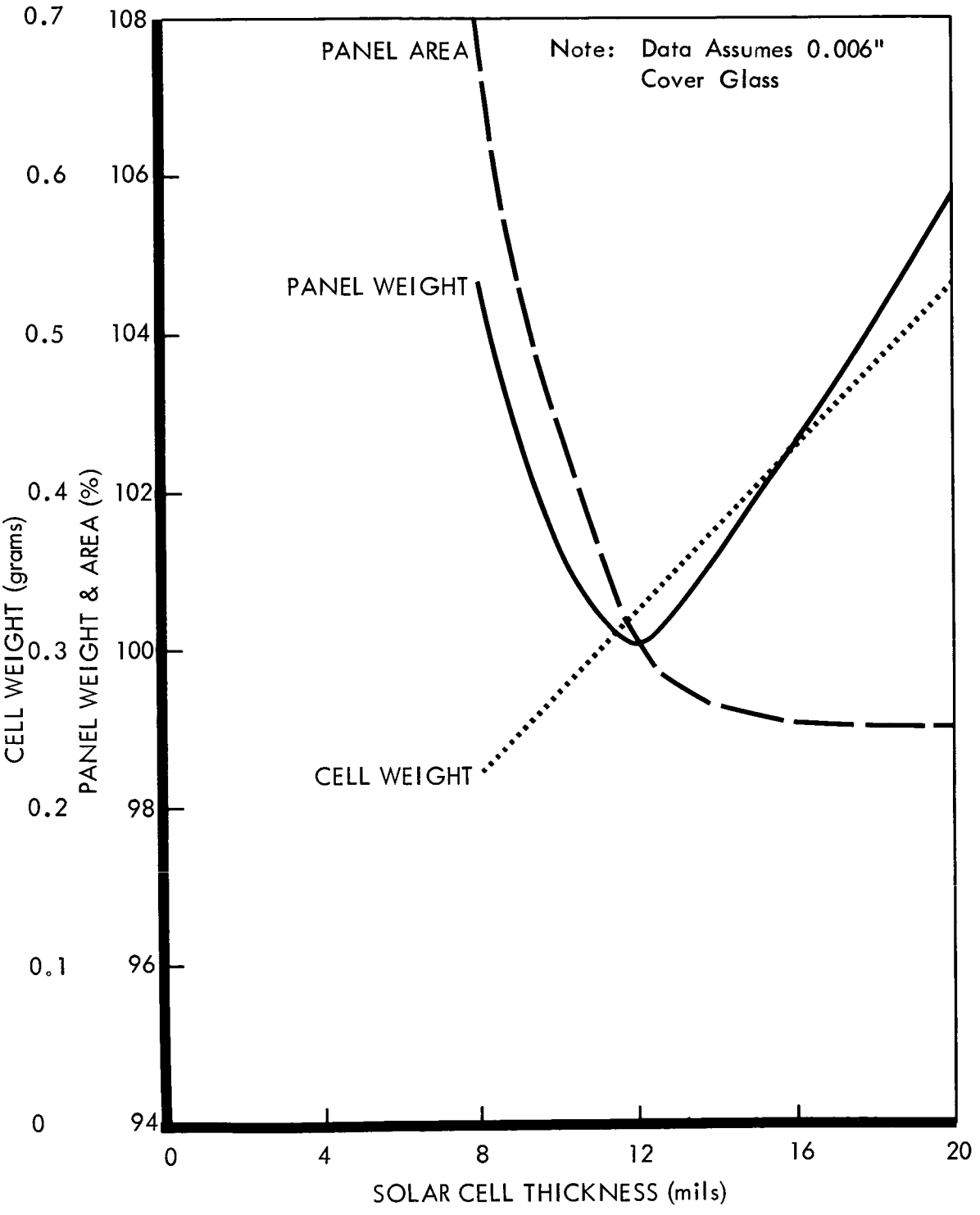

Figure 4.2-39: Solar-Cell Thickness Trades

but the higher radiation resistance is considered more important in the relatively unknown environment of solar flares.

Cover Glass and Cover Glass Attachment--The active surface on a solar cell is covered with a glass cover. This cover protects the cell's active surface from erosion, radiation, micrometeoroid bombardment, assembly, and handling damage, as well as providing a good thermal emission surface. The cover glass is bonded to the active surface of the solar cell by a transparent adhesive. The cover glass and adhesive must withstand physical handling and space environment, and have good thermal transmission properties. This section discusses the selection of the cover material, thickness, filtering, and attachment methods.

There are four basic types of cover glasses that are used for solar cell protection; 0211 microsheet (soda lime glass), 7940 fused silica (quartz), synthetic sapphire, and an integrated cell coating. Corning 7940 fused silica has been selected on the basis of high radiation tolerance, good thermal emission and transmission characteristics, reasonable cost, lighter-weight material, proven flight performance. Cover materials are compared in Table 4.2-15.

Results of several studies show that fused silica is superior to microsheet in a radiation environment. The microsheet tends to darken under strong radiation. The thermal characteristics of fused silica are essentially the same as those of microsheet. Sapphire has a significantly lower emissivity than that of glass or fused silica, and is primarily used only for radiation damage protection. The lower-density fused

silica is 5 percent lighter than microsheet and only 20 percent higher in cost than microsheet (in large quantities).

Cover glass may be obtained in thicknesses ranging from 6 to 60 mils. The glass thickness of 6 mils was selected for the lowest panel weight for the required performance of a 13-month mission based on a 28 percent power loss in the radiation flux, satisfactory handling safety during assembly, and Ranger and Mariner experience.

The performance of a solar cell in a radiation environment is directly related to the thickness of the cover protecting it (Figure 4.2-40a). Figures 4.2-40b and 4.2-40c show the power degradation resulting from the accumulated radiation of solar flares (1971) and various radiation belts at Mars for 6-mil and 60-mil cover glass. The relative panel weight for various thicknesses (Figure 4.2-41) based on the radiation protection afforded by fused silica, shows that the 6-mil cover permits the lightest panel for use in an Earth-equivalent radiation environment.

The preferred spectral filtering for the cover glass will include an anti-reflective and a 0.415-micron spectral cutoff blue reflective coating. This filtering will provide an 8.5 percent increase in cell performance over a bare cell while safeguarding the adhesive from the long term degrading effects of ultraviolet. A red cutoff coating, which is commonly used to further cool the cells by reflecting the unusable infrared light, will not be necessary. The panels are already operating at a low-temperature thermal equilibrium as a result of the low

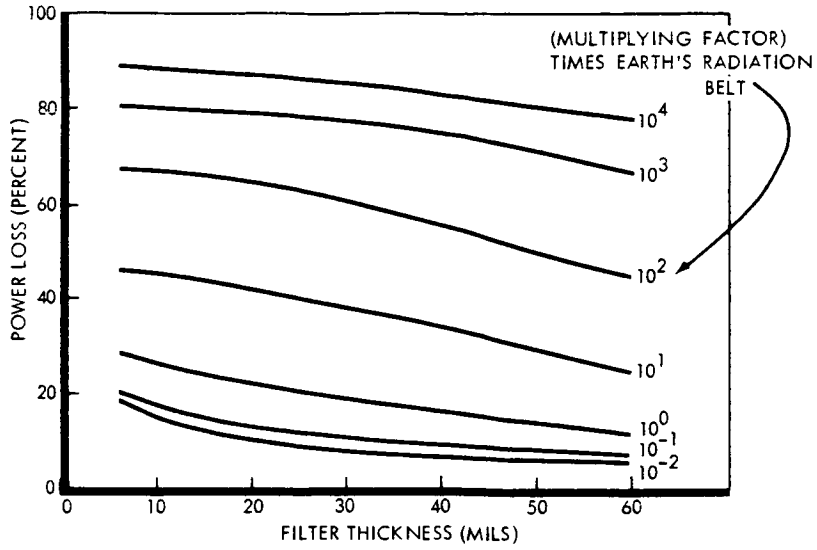

Figure 4.2-40a: Power Degradation vs Coverglass Thickness for Various Radiation Levels

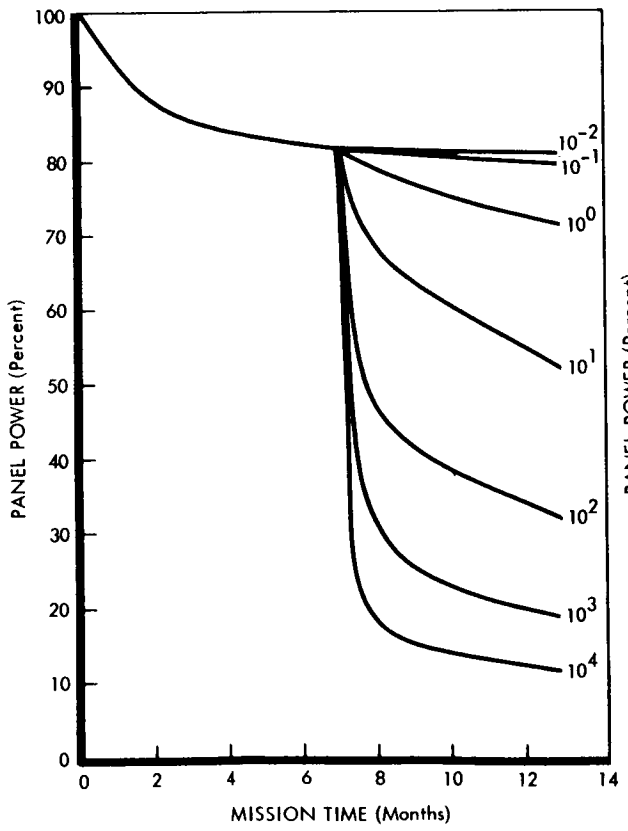

Figure 4.2-40b: Panel Power Degradation Using 6-MIL Coverglass for Various Mars Radiation Belts

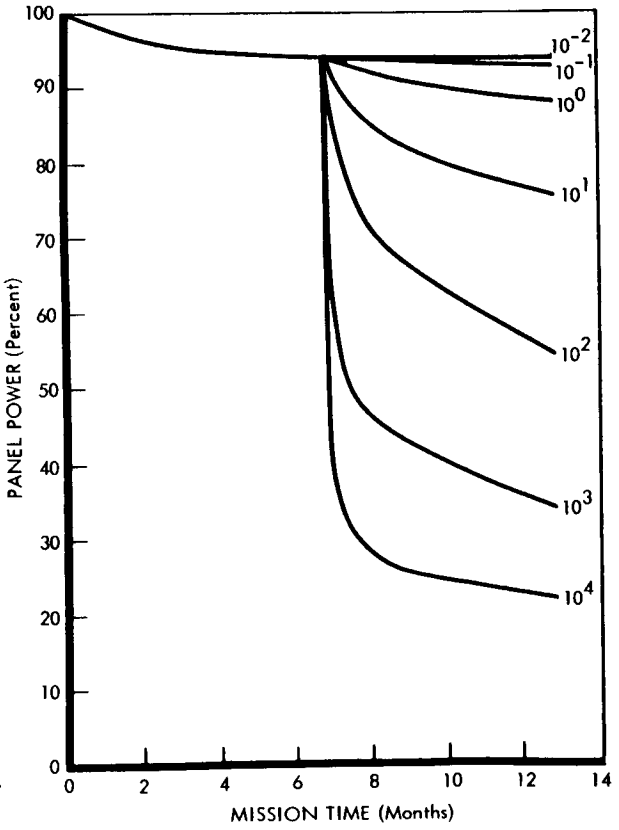

Figure 4.2-40c: Panel Power Degradation Using 60-MIL Coverglass for Various Mars Radiation Belts

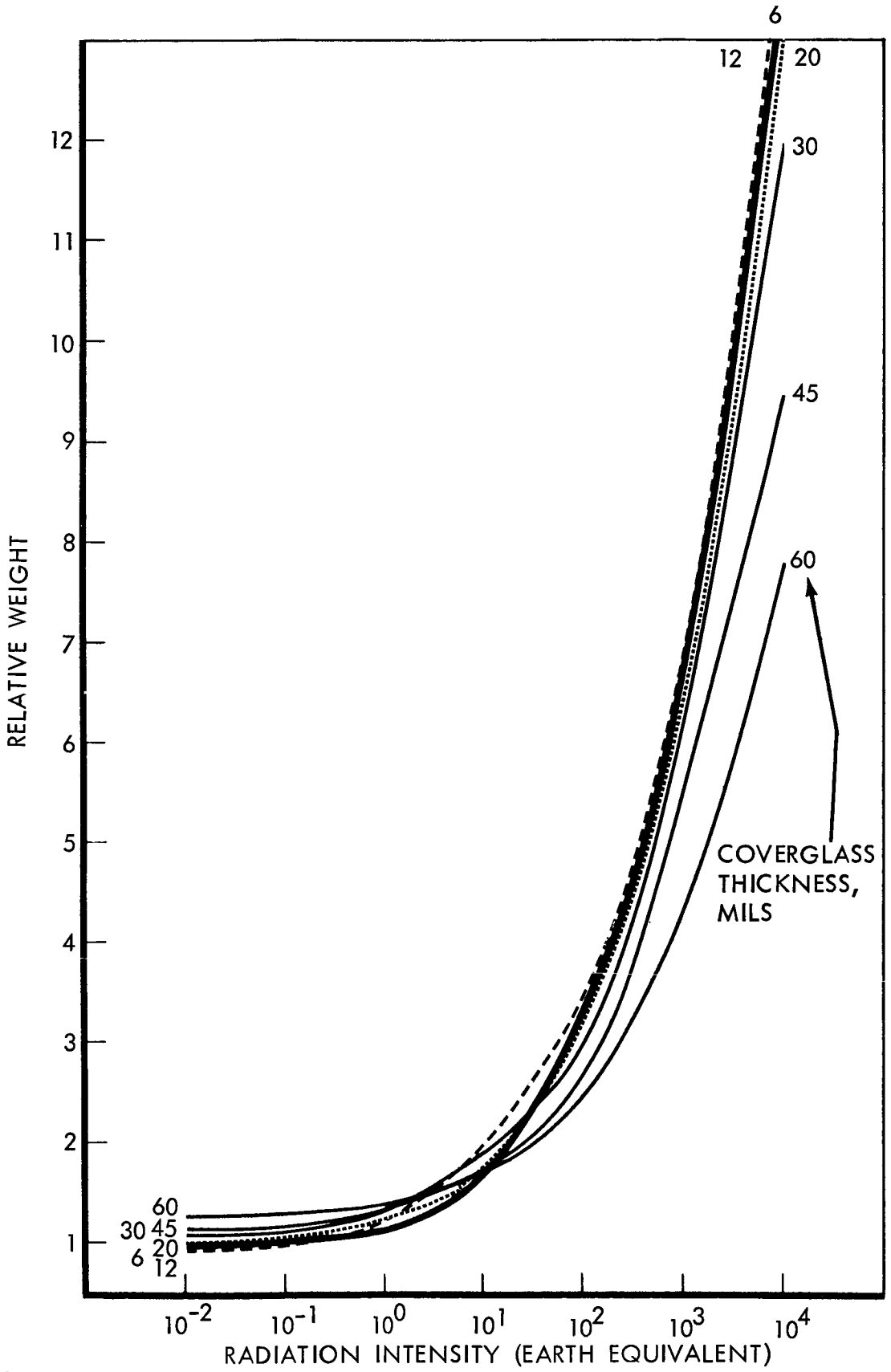

Figure 4.2-41: Relative Panel Weights For Various Coverglasses For Equivalent Power

Table 4.2-15: COVER MATERIAL COMPARISON

	Percent Change in Transmittance at Wavelengths (Microns)					
	4.6 MEV Protons Total Dose of $4 \times 10^{11} p/cm^2$			1 MEV Electrons Total Dose of $10^{16} e/cm^2$		
	0.5	0.6	0.7	0.5	0.6	0.7
1) Microsheet (6 mil) Corning 0211	3.4	1.1	1.1	5.6	3.3	2.2
2) Microsheet (6 mil) Corning 0211 with A-R coating & "Blue filter"	5.2	2.1	1.1	7.3	5.1	4.2
3) Fused silicon (30 mil) Corning 7940	No change					
4) Fused silicon (20 mil) Corning 7940 with A-R coating & "Blue filter"	No change			1.1	2.2	1.1

illumination levels. The addition of red filter would increase the cover cost with less than 1 percent increase in power capability.

The cover adhesive RTV-602 has been selected for the attachment of the cover glass since it has been space qualified. The RTV-602 has been used extensively in similar applications on Ranger and Mariner.

Submodule Design and Attachment--There are two basic methods of connecting cells into a submodule; series or parallel. The parallel submodule has been selected for the following reasons:

1) The opening of one cell in a parallel submodule in a voltage string will not destroy the usefulness of the total string;
2) Repair of a parallel submodule is simpler than repairing a shingle;
3) The flat alignment of a parallel submodule with the substrate requires less bonding adhesive and provides a better thermal transfer to the substrate;
4) Stress relief between cells is possible.

The use of large parallel cell submodules within an electrical section provides increased electrical performance and, therefore, reliability if damage occurs to one or more cells within the section. The present Voyager submodule designs for the study consist of 5 and 6 cells. This choice is based on a reasonable compromise of the mechanical considerations of submodule handling, available panel dimension, and maximum power performance.

Figure 4.2-42a compares the I/V (Curve A) of a 5-cell undamaged submodule with a submodule with one cell open (Curve B). This results in a decrease in the current supplied by the total submodule. When the damaged submodule is added in series with the normal submodules, a marked effect is shown in the total of I/V curve of the string (Figure 4.2-42b). This figure compares the normal I/V curve of a series voltage string 5 cells wide (Curve C) with the effect of a one cell loss on that string (Curve D). Further investigation is required in order to determine the reliability and panel dimension relationships for a larger number of cells in parallel.

Silver-plated molybdenum has been selected for the bus bars on the submodules because of its relatively close coefficient of thermal expansion to silicon and its nonmagnetic properties. The similarity of the coefficient is important because of the low panel temperatures during occulation. Molybdenum solar cell bus bars are being used on several space programs, such as Relay and IMP, and are finding increased application. Submodules with molybdenum have been temperature cycled from 20°C to -180°C with no apparent damage. Nonmagnetic silver-plated molybdenum has been extensively tested, including peeling and soldering tests. (See Reference 2 for additional information.)

The submodules will be mounted to the substrate with RTV-40 adhesive. This adhesive has been used extensively with submodules on many spacecraft. Evaluation tests will continue as the mission environment is further defined.

Electrical Layout and Interconnections--An electrical section is a relatively large group of interconnected submodules that is electrically isolated from other sections of the panel. It is advantageous to have

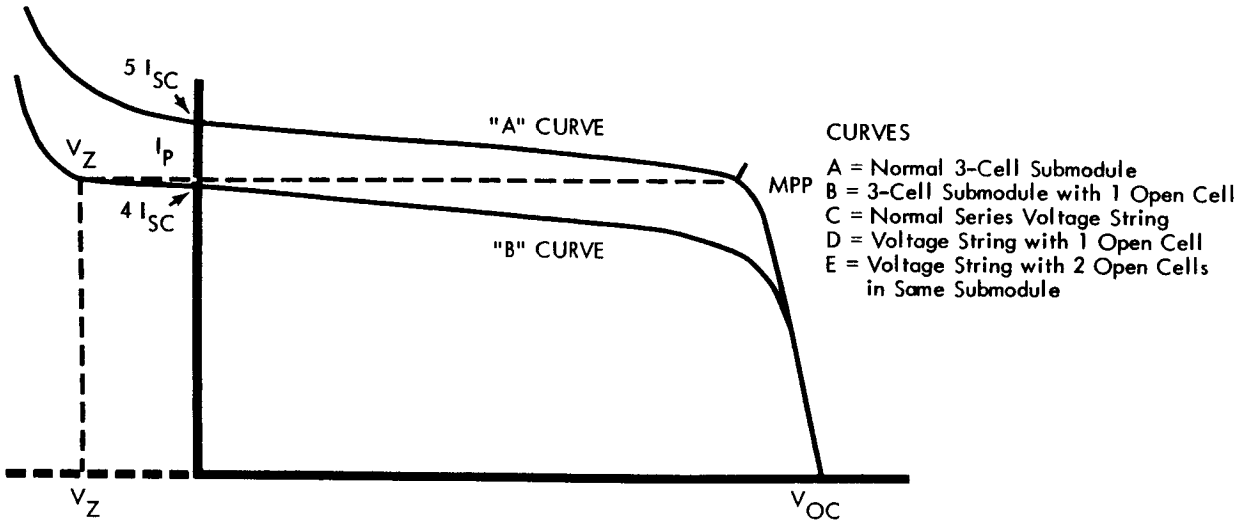

Figure 4.2-42a: 5 Cell Submodule I/V Curve

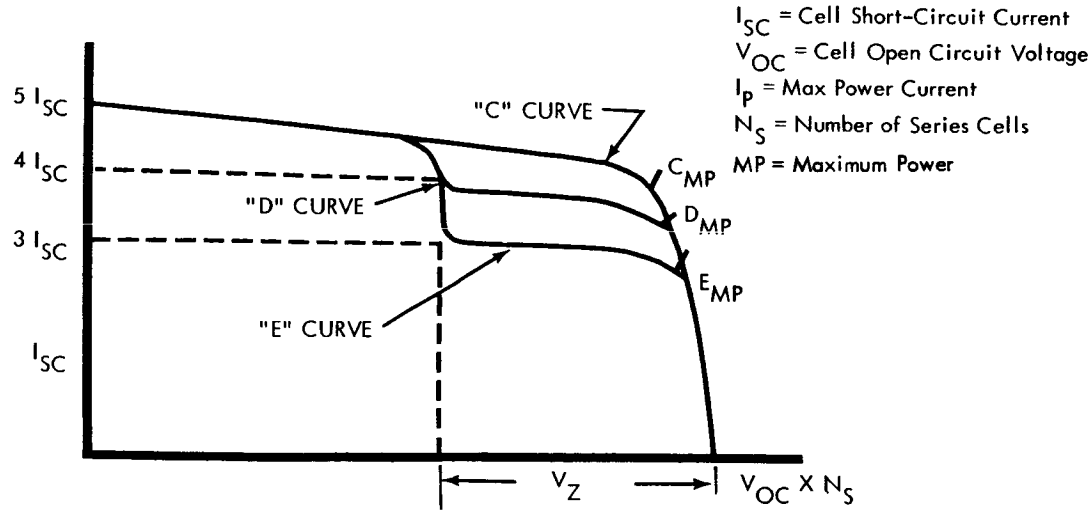

Figure 4.2-42b: Voltage String I/V Curve

a large number of electrically isolated sections to reduce the amount of interaction between damaged cells or shorts and the remaining portion of the panel. It is also advantageous to keep the number of electrical sections to a minimum to reduce wiring complexity and the number of components such as isolation diodes and connectors.

On the basis of reliability and weight, the Voyager solar array will be divided into 24 electrically isolated sections, resulting in two electrical sections per structural section, and permitting a convenient assembly breakdown. Two complete electrical sections can be destroyed without loss of system power. The submodules within a section are interconnected at equipotential points at three separate locations.

Cell Layout and Harnessing--The layout of the cells on the substrate is governed by best use of available area, minimum magnetic field, ease of wiring, modular panel construction, and relatively constant temperature environment.

The preferred design will use the 123-cell series string which fits into the 103-inch dimension of the panel. This arrangement minimizes complexity in series connecting the submodules and reduces the effect of temperature gradients. Magnetic fields are effectively reduced by reversing the polarity of adjacent voltage strings.

Computor calculations indicate that a 15^{o}C temperature gradient across a panel, will cause less than 0.5 percent power loss.

The magnetic field generated by the current flow through the solar cells must be considered in the layout of the cells. Based on an approximate relationship for the magnetic flux density ($B = \frac{200\ I}{r}$ gamma), the limit of 1 gamma at 10 feet is exceeded when the current through a single cell voltage string exceeds 0.015 ampere. The maximum current that a single string of cells can produce is 0.119 ampere when the panel is short circuited at Earth space. If the series string of cells are oriented to allow the current in each string to flow in the same direction, the magnetic fields would be additive and the limit would be exceeded. Therefore, series strings of submodules must be laid in opposing directions to reduce the magnetic effects. Based on this string layout of opposing polarities, calculations are made to determine the maximum magnetic field. The worst-case conditions would occur during maximum current flow through the cells (at Earth space). The maximum density will occur in the plane of the panel perpendicular to the current flow. Calculations of two series strings composed of five-cell and six-cell submodules show that a maximum magnetic flux density of less than 2.0 gamma will occur at the 10-foot point under short circuit conditions. At actual operating conditions the flux density will be less than 0.5 gamma.

An alternate method presently being used on satellites, such as IMP, uses an insulated silver mesh between the cells and the substrate. The current passes through the series cell string in one direction and is jumpered to the wire mesh. The spacing between the wire mesh and the cells is very small, which reduces the overall magnetic effect. The earlier calculation indicates that this technique will not be required for this mission.

4.2.9.5 Structural/Mechanical Design Optimization

Selection of the Array Planform--The array design begins with a definition of its planform dimensions. The total area is determined from the electrical power requirements to meet the needs of the spacecraft. The dimensions of this array are a function of fixed incremental cell dimensions, substrate width limitations imposed by cell application techniques, envelope restriction placed on the array by the spacecraft, nose fairing, and capsule.

Figure 4.2-43 presents four schemes for the arrangement of the panel substrate area. Scheme 1 and 2 show the difference if the series string are run span or chordwise with respect to the panel structure; they have aspect ratios of 0.956 to 1.07 (aspect ratio is defined as the panel length divided by its width). Schemes 3 and 4 are for a 0.592 and 2.38 aspect ratio. It is shown in this section that an aspect ratio of unity will give the lightest panel. Further, the restriction placed on the panel width by the spacecraft limits the maximum width to less than 120 inches and the fold section length to less than 60 inches.

The solar array planform is selected on weight, interface restrictions of the cell and the array maximum allowable envelope.

To better understand panel weight and how it is affected by aspect ratio, a trade study for four array areas was instigated early in the program. Figure 4.2-44 presents the conclusion that for large panel areas, an aspect ratio of one will give the minimum weight. (Note that the weight presented does not include mechanisms and fitting weights.) Weight increase

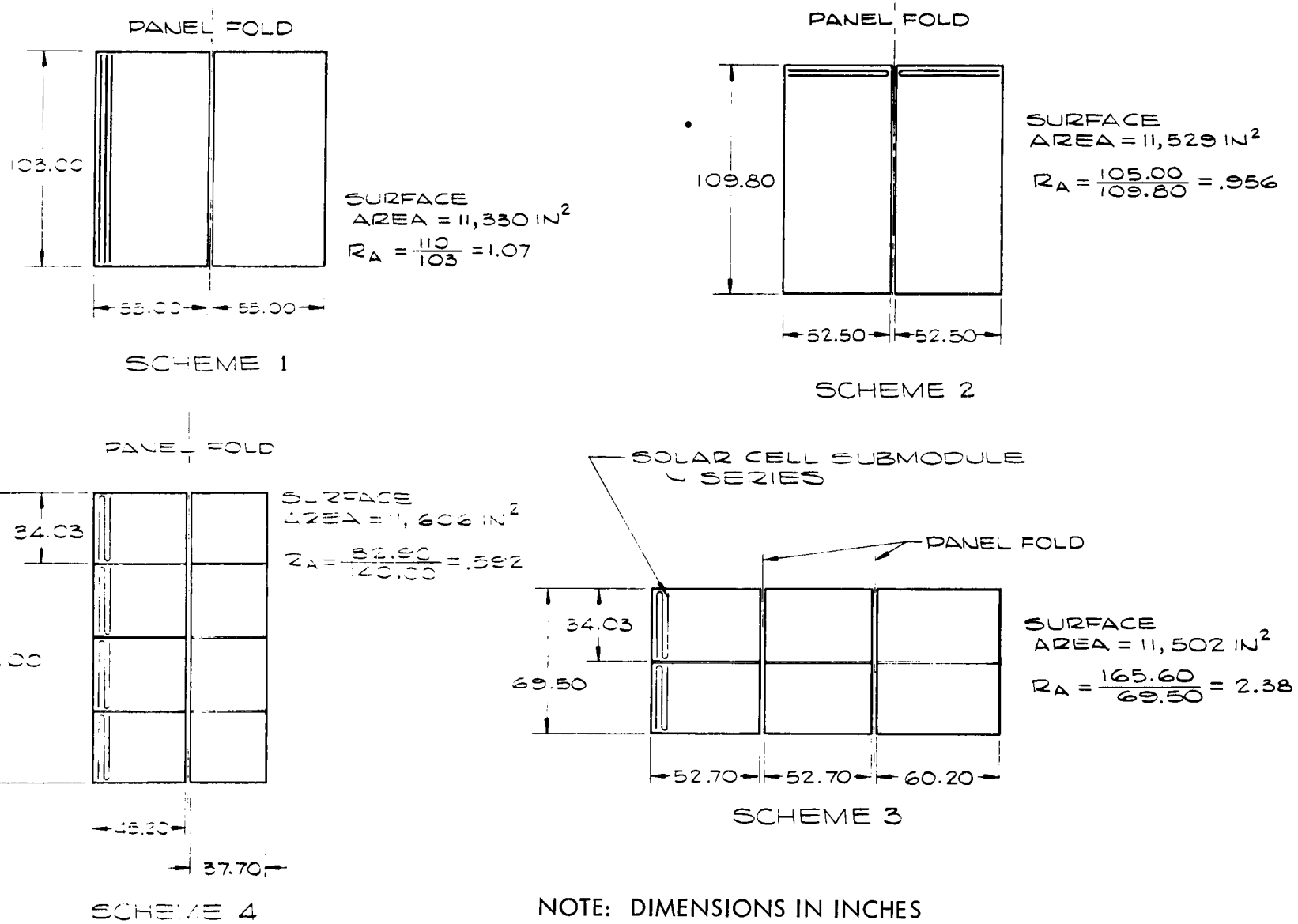

Figure 4.2-43: Solar Panel Planform Configurations

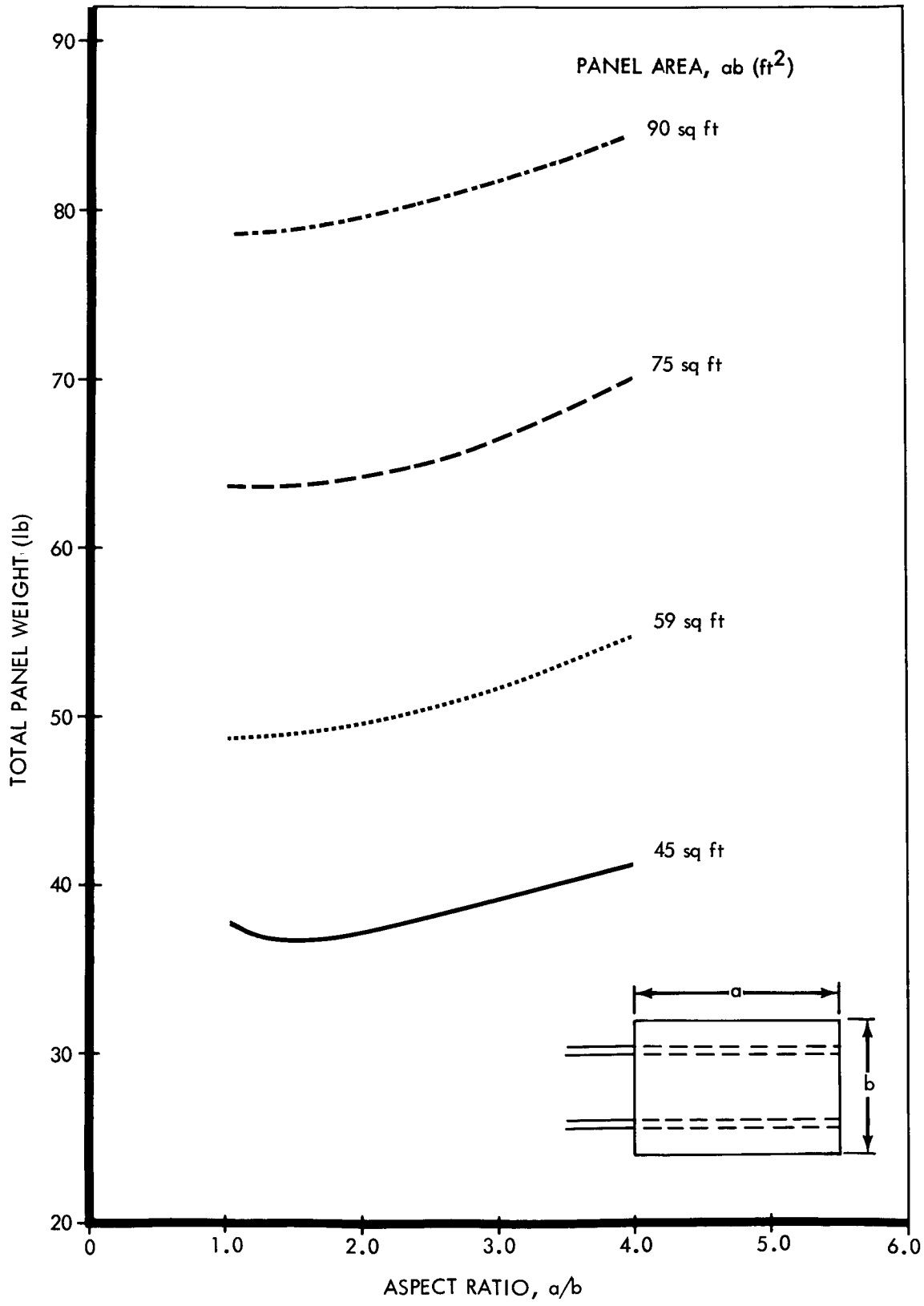

Figure 4.2-44: Weight versus Aspect Ratio

with aspect ratio is not significant, however, until the aspect ratio is greater than 2.5.

Cell patterns were also studied to determine the effect on the planform. The basic building block is the cell submodule, which includes the additional dimensional requirements for spacing and tolerance. The submodule length is defined as the series string width. Using series string width and length, a submodule block/bar chart (3-cell submodule is used as an example) can be developed, as shown in Figure 4.2-45.

Other factors affecting the cell layout are simplicity of interconnections, substrate width limitations, and panel substrate modular concepts. If a solar array is to be composed of mechanical divisions of smaller size than a panel, each of the substrate modules should be uniform in size to facilitate manufacturing, reduce the number of spare substrate sections required, and the number of items to be qualified. A 3-foot wide substrate is the limit that can be safely celled due to the requirement that personnel must reach across this dimension to work on the substrate surface. Packaging efficiency is the last factor that affects the selection of a panel planform. This is a ratio that indicated cell surface area to substrate surface area. It is a function of spacing between individual cells and spacing between submodules, but primarily it is affected by the areas left uncelled for the printed circuit boards or wire bundles that interconnect cells. This area is kept at a minimum by locating interconnections at the panel perimeter or on its centerline.

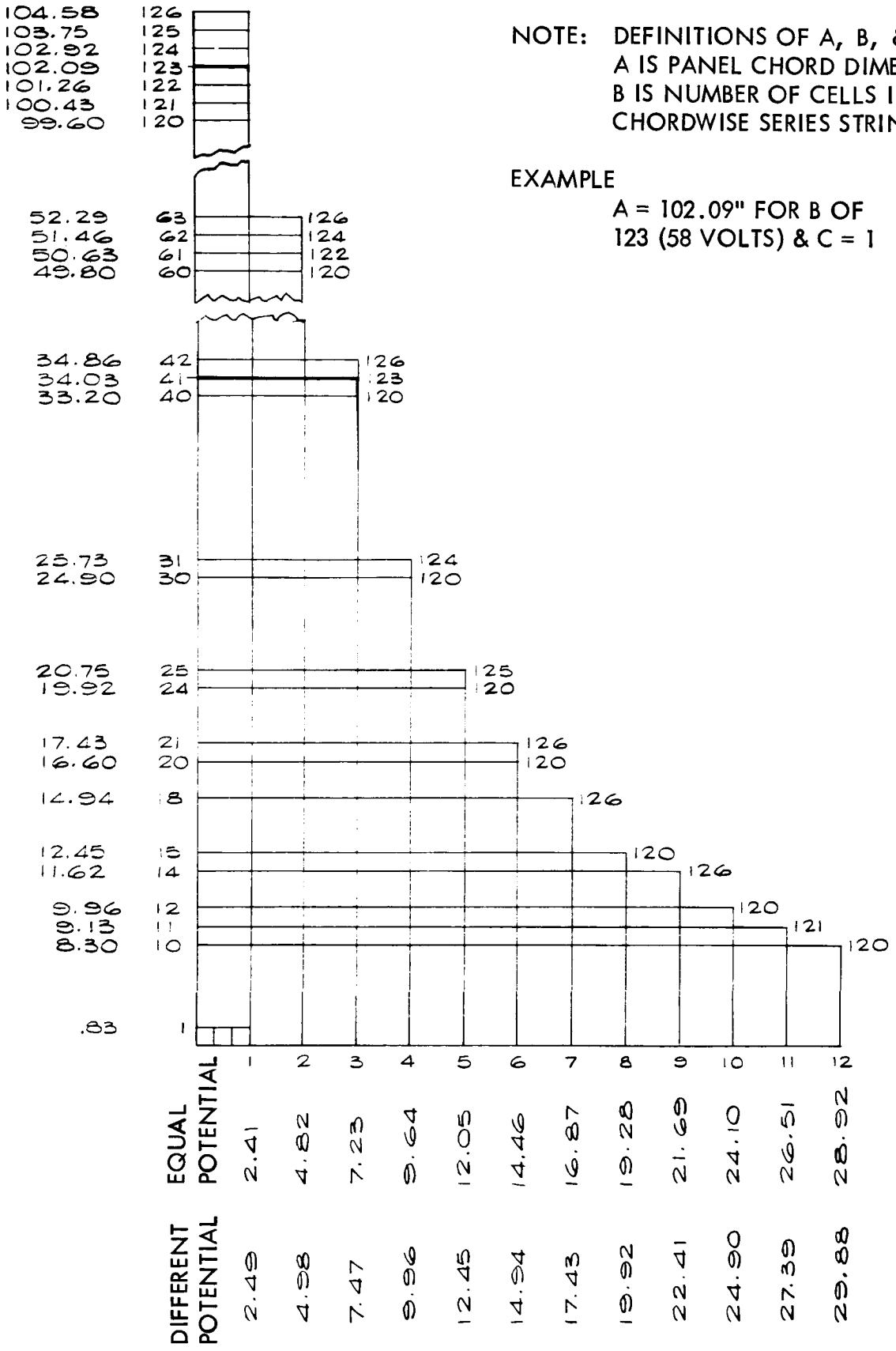

NOTE: DEFINITIONS OF A, B, & C V
A IS PANEL CHORD DIMENSIO
B IS NUMBER OF CELLS IN SE
CHORDWISE SERIES STRINGS

EXAMPLE

A = 102.09" FOR B OF
123 (58 VOLTS) & C = 1

'ALUES:
)N (INCHES) REQUIRED;
RIES; C IS NUMBER OF
(3 CELLS WIDE)

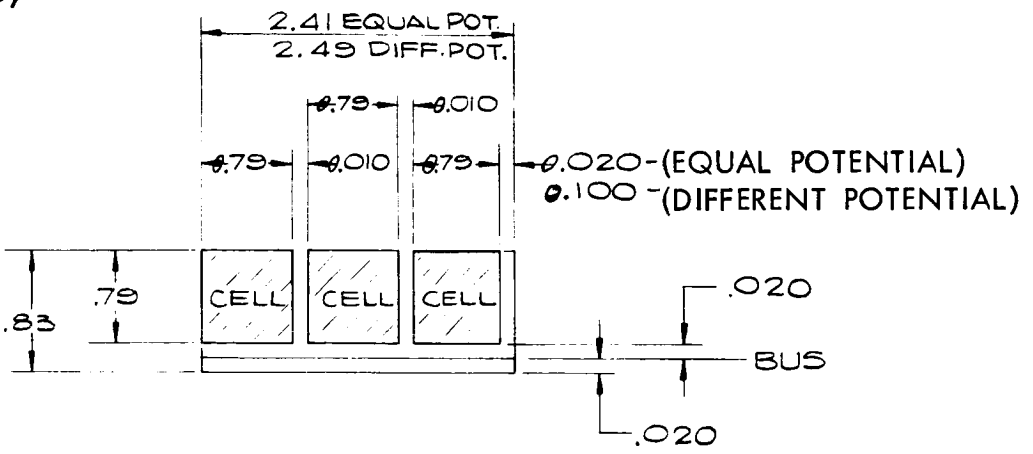

SUBMODULE

NOTE: DIMENSIONS IN INCHES

Figure 4.2-45: Spacecraft Model 945-6026 Cell Submodule and Series Planform

The second step in the solar array design is to mate these different aspect ratio planforms to a particular spacecraft configuration. Envelope restrictions are placed on the planform in its stowed position by clearances between the spacecraft and the nose fairing; the separation plane and the capsule bacterial shroud.

The selection of Scheme 1 for the planform for the panels was based on envelope restrictions and weight. Scheme 4 exceeded the 120-inch width restriction and Scheme 3 had an aspect ratio of the magnitude where weight increase becomes significant. Scheme 2 required some 200 square inches of additional area and did not meet the module restrictions imposed on the substrate without additional area and weight increases.

Substrate Design and Structural Arrangement--The solar panel substrate consists of an adhesive-bonded assembly of spanwise 2024-T4 aluminum corrugations, 0.0085-inch thick and 27.5 inches long, covered with 0.005-inch thick 2024-T4 skin, upon which the solar cells are mounted, as shown in Figure 4.2-22. This assembly is adhesive-bonded along its inboard and outboard edges to a chordwise zee section, 103-inches long, which is bolted to the chordwise ribs of the frame. All lateral (chordwise) loads on the panel are carried inboard in shear by the substrate face sheet. Shear continuity between the face sheet and the spar cap is maintained by continuously riveting a shear panel between the corrugation and the spar cap. This shear panel also provides thermal continuity between the substrate and the spar.

The substrate is designed to support the solar cells, wiring, and its own weight during boost, transit and orbit insertion. It must be rigid enough to enforce a definite separation of its fundamental frequency from that of the supporting frame structure. The substrate must also provide adequate temperature relief for the solar cells. The critical loading condition for the substrate is 1.25 g sinusoidal input, applied normal to the substrate, and magnified by a factor of 45. This is shown as condition 3 of Table 4.2-14 as presented in Section 4.2.9.2. Two classes of substrate were investigated, the plate and the simple beam. The plate was represented by an aluminum honeycomb sandwich, while the beams were aluminum corrugations and face sheets. The honeycomb has equal strength in both the spanwise and chordwise direction. However, when supported by a ladder-type frame it behaves like a plate only adjacent to the frame. Midway between spars the honeycomb is a simple beam, supported by each rib. The honeycomb is 4.7 pounds heavier (0.02 psf) than the corrugations and has a solar cell operating temperature $3^{o}C$ higher.

The aluminum corrugations can be considered a form of orthotropic plate with plate stiffness very large in one direction as compared to the direction at 90 degrees. The skin-covered corrugation is treated as a simple beam. The corrugations were examined to determine whether spanwise or chordwise orientation would be lightest. When the orientation is spanwise the corrugations are 27.5-inches long and easily formed. The frame ribs must be extended beyond the spares to the edges of the panel to provide support for the corrugations. Hence, the corrugations are light and stiff while the frame weight increases.

If the corrugation orientation is chordwise, the corrugations are 103-inches long and attach directly to the spars. Frame ribs are not required to support the corrugations, and hence can be made lighter. This trade was examined for three chordwise lengths and is shown in Figures 4.2-46 and -47. Figure 4.2-46 shows that there is little weight difference for 0.50 deep corrugations when the ratio of spanwise dimension to chordwise length is 0.30 or less. For ratios of 0.50 or greater the chordwise orientation is lightest by a significant amount. The preferred panel design is shown at $D/L = 0.27$. Figure 4.2-47 is a cross plot of Figure 4.2-46 for three corrugation depths. Because weight differences between the two orientations is small, the spanwise direction is selected because of the manufacturing advantages in forming the shorter corrugations.

The use of 0.005-inch thick skin and 0.0085-inch corrugations can be accomplished by chemically milling 0.015-inch sheets of 2024-T4 prior to forming. Sheets of heat-treated aluminum are not manufactured in the 0.003 to 0.015-inch thick range. Thus, the usage of heat treated aluminum alloys to save weight requires additional manufacturing steps. Sheets will be chemically milled in large lots and panel stock selected individually for fabrication. This technique was used in the manufacture of the prototype panel shown in Figure 4.2-31.

Experience on Ranger and Mariner programs showed that fabrication and handling of large aluminum panels composed of 0.002 and 0.003-inch thick sheets was extremely difficult and necessitated frequent repairs. Therefore, the minimum gage for substrate sheet is set at 0.005 inches.

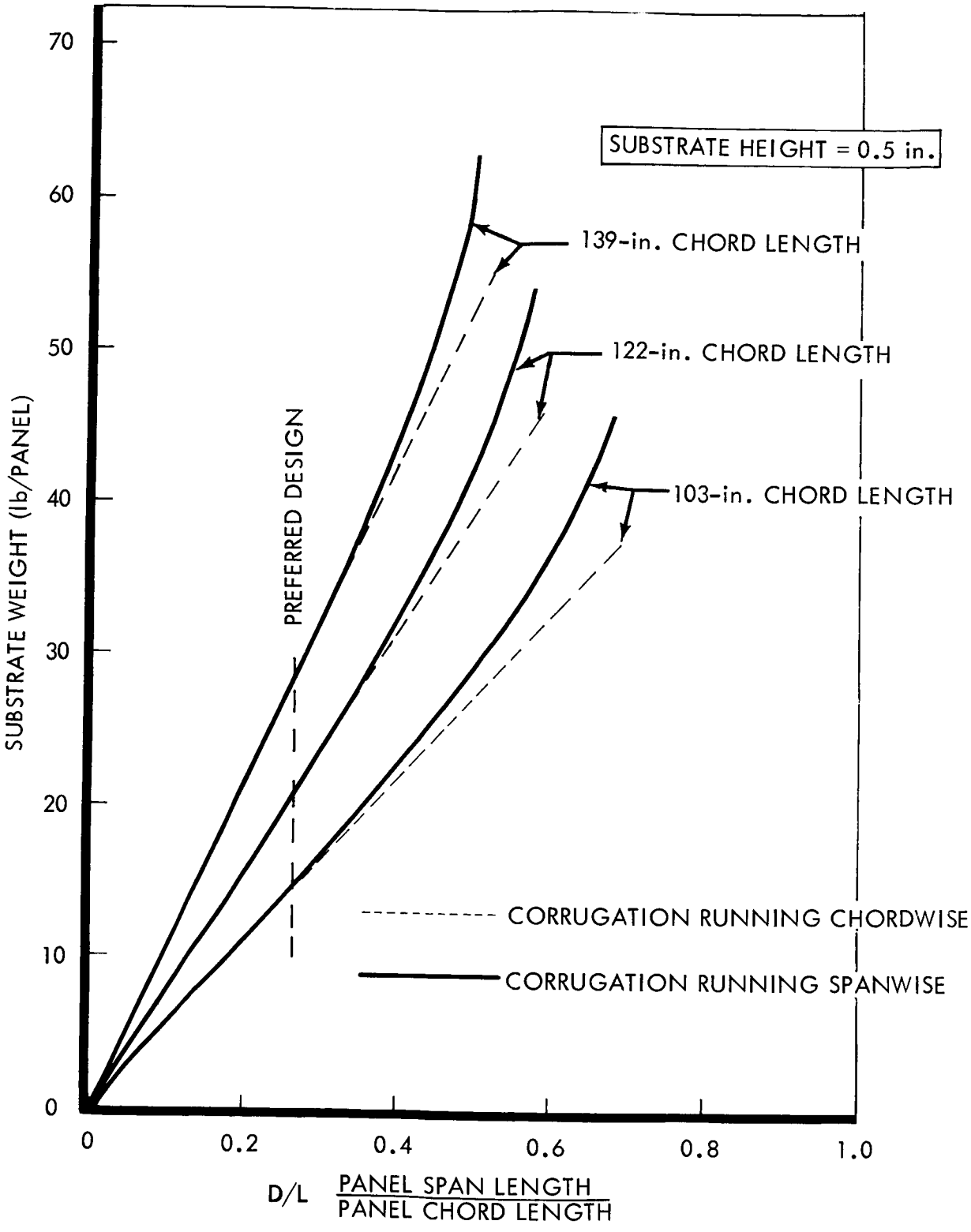

Figure 4.2-46: Substrate Weight vs Corrugation Direction

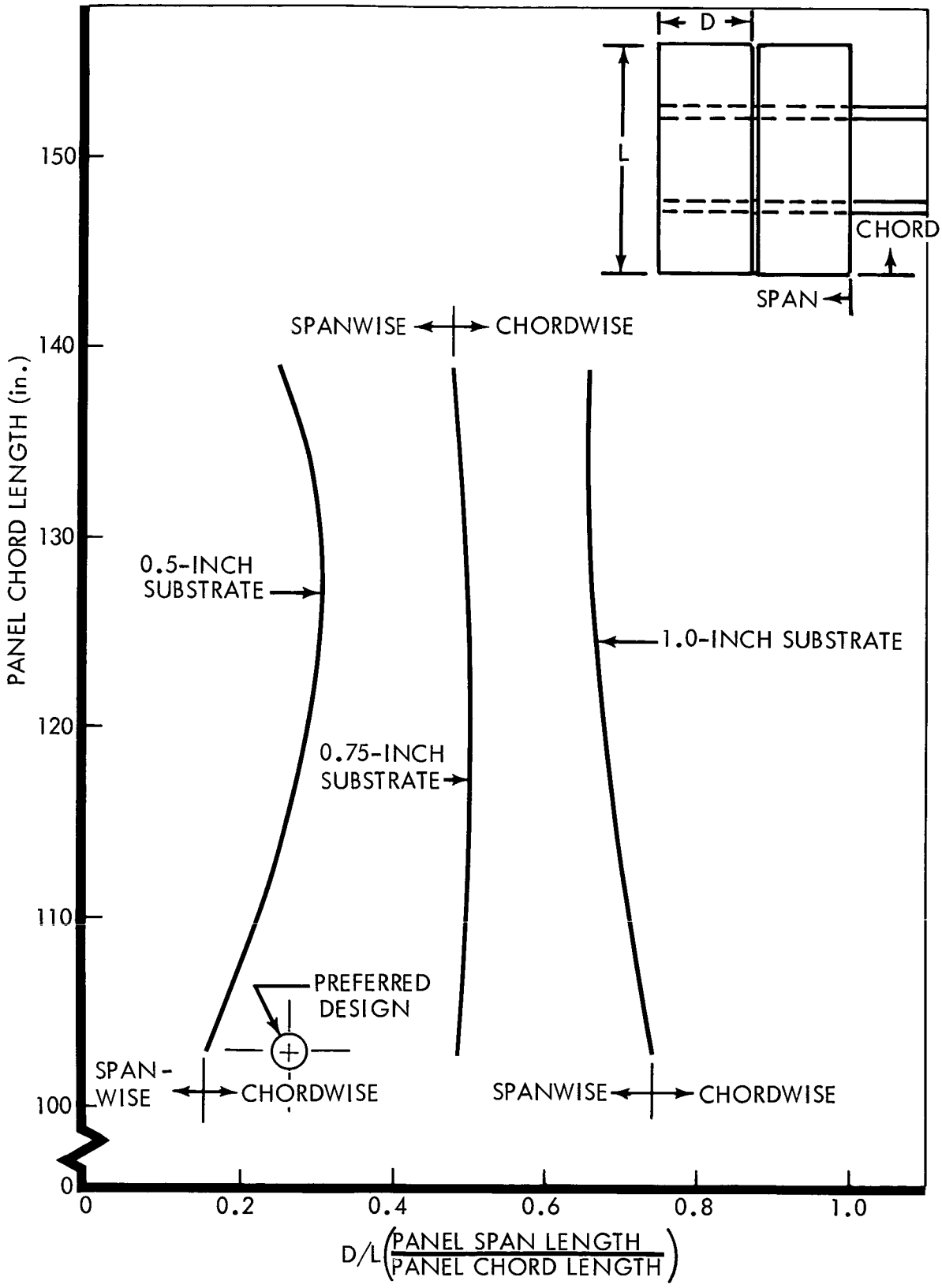

Figure 4.2-47: Preferred Direction of Substrate Corrugations

Spanwise 2024-T4 aluminum corrugations, covered with 2024-T4 aluminum sheet, was selected for the preferred design because of lightweight, manufacturing simplification, and proven reliability in the space environment, as demonstrated by Ranger and Mariner, which used this design approach.

Frame Design and Structural Arrangement--The solar panel structural frame consists of a welded 6061-T6 aluminum space truss having two spanwise spars and six chordwise ribs, as shown in Figure 4.2-25. The spars are spaced 57 inches apart, (55 percent of chord), with their inboard hinges located at points of rigid support on the spacecraft lower structure. Three ribs are located in each section of the panel, one at each end (55.25 inches apart), and one midway between them. These ribs support the spanwise corrugations and provide lateral support for the spars. This interlocking matrix of deep spars and ribs produces a rigid frame design.

When deployed, each spar is supported at its midspan by a 6061-T6 tubular strut, which folds in half for stowage, as shown in Figure 4.2-26. All torsional loads in the frame are carried in differential bending by each spar. The truss frame was selected because of its light weight and high stiffness, when compared to the I beam or box beam.

The frame is designed to support the substrate during boost, transit, and orbit insertion. It is designed to have a first cantilever bending frequency of 2 cps or greater, to avoid dynamic coupling with the autopilot

during transit and orbit insertion. The frame provides sufficient structural flexibility and thermal paths to prevent damage to the substrate during firing of the orbit insertion engine and during emergence from Mars occultation. The frame is designed to carry a third section should future electrical power requirements demand it.

Three alternate beam designs were considered for the ladder frame. These were the I beam, box beam, and truss beam. Figure 4.2-48 shows the I beam and box beam and Figure 4.2-49 shows a truss section built to demonstrate concept and capabilities. Because concept selection is dependent on the magnitude of the applied load, it is necessary to first determine the rib, spar, and strut member loads.

Figure 4.2-50 shows how spar internal bending moment due to vibratory loads is affected by strut attachment location. It is seen that the moment is zero when the support is located at 67.5 percent of span. For static loads, the moment is minimized when the support is located at 70.7 percent of span. Figure 4.2-51 shows how the panel first cantilever bending frequency is affected by strut attachment location and by strut stiffness. The upper curve ($K_s' = \infty$) refers to a spar with rigid supports. The lower curves relate to spars with flexible support struts. The selected strut location at 50 percent of span is seen to provide essentially rigid support to the panel. Maximum panel stiffness is attained when the spar is supported at 73.6 percent of span.

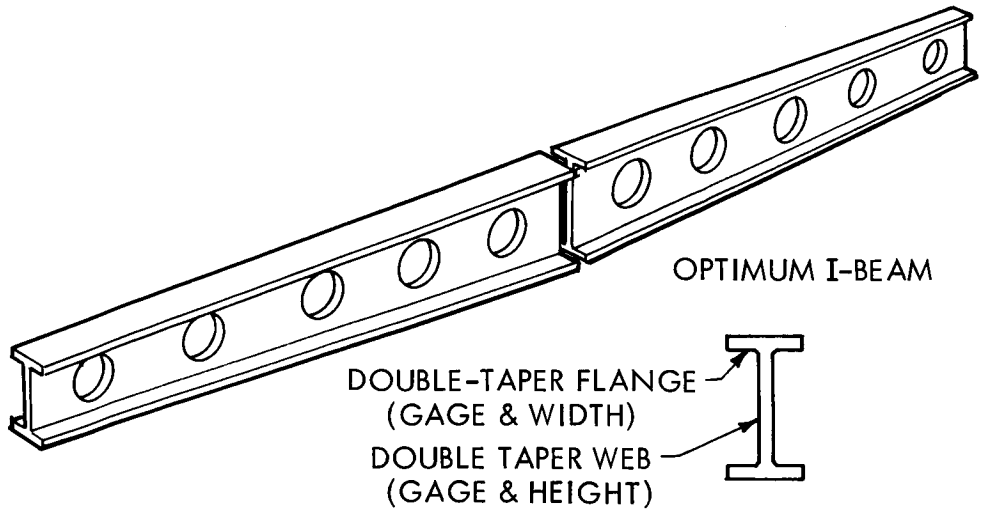

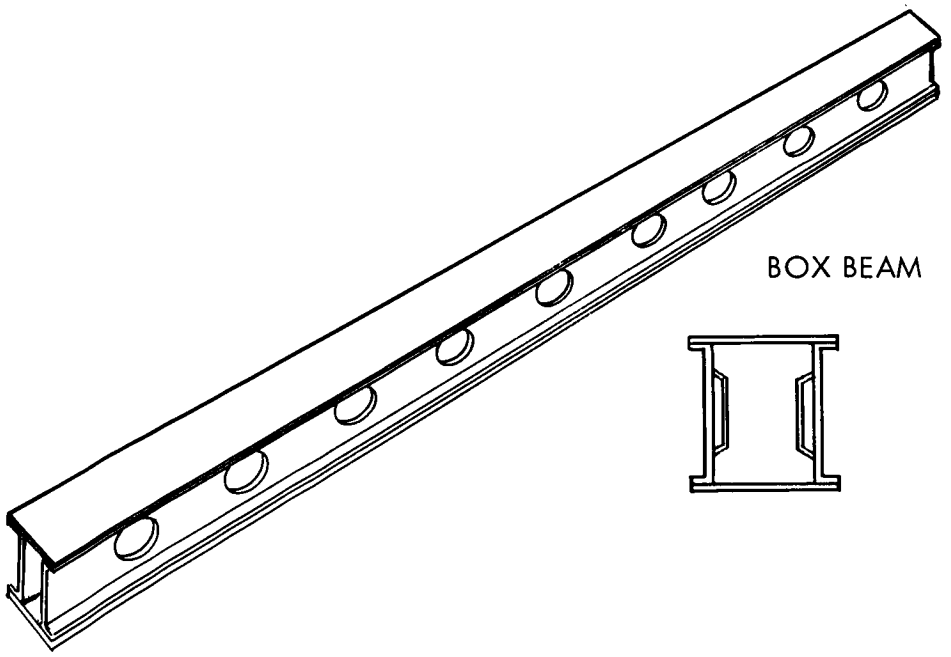

Figure 4.2-48: Frame – Member Concepts

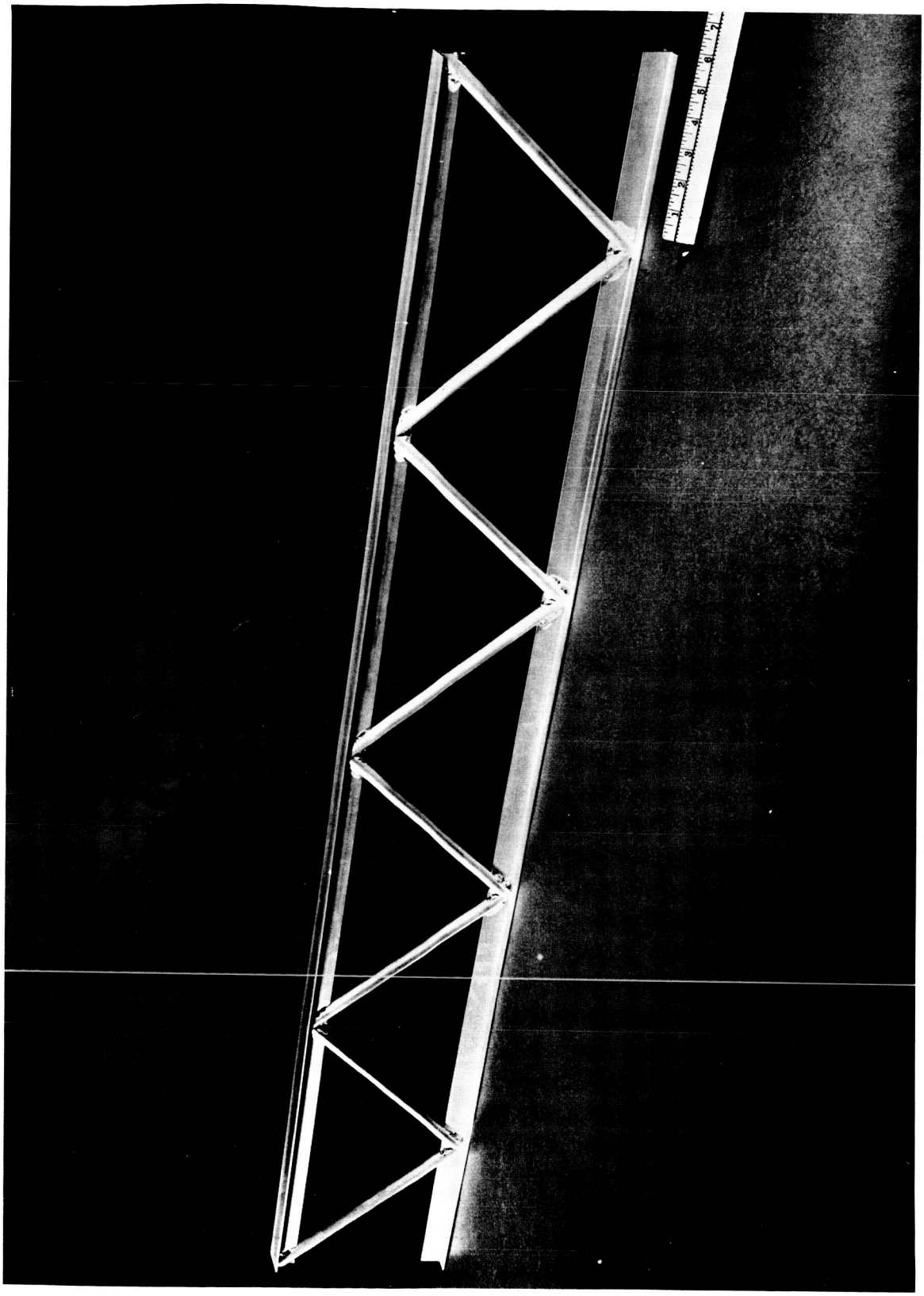

Figure 4.2-49: Truss Frame

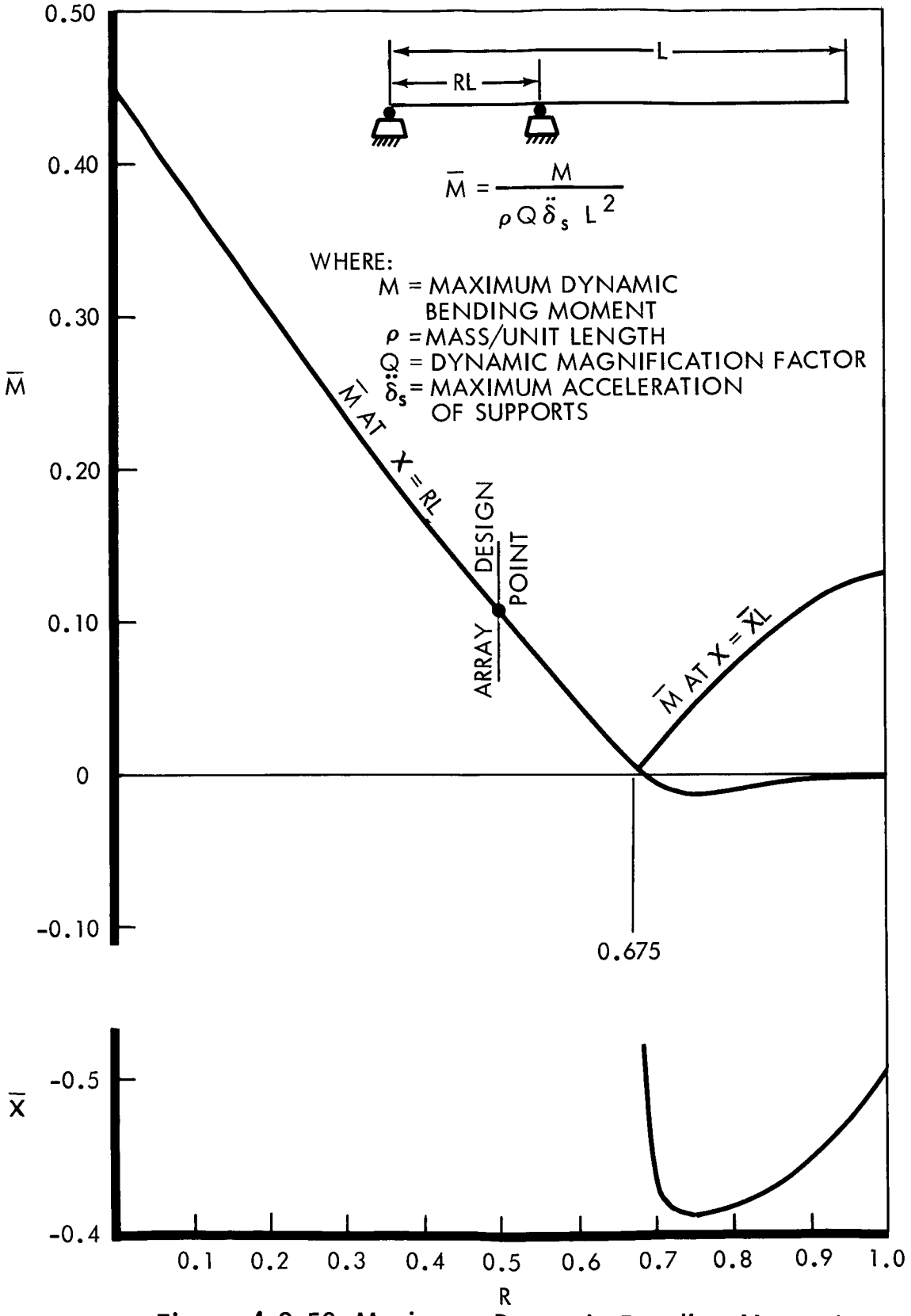

Figure 4.2-50: Maximum Dynamic Bending Moment

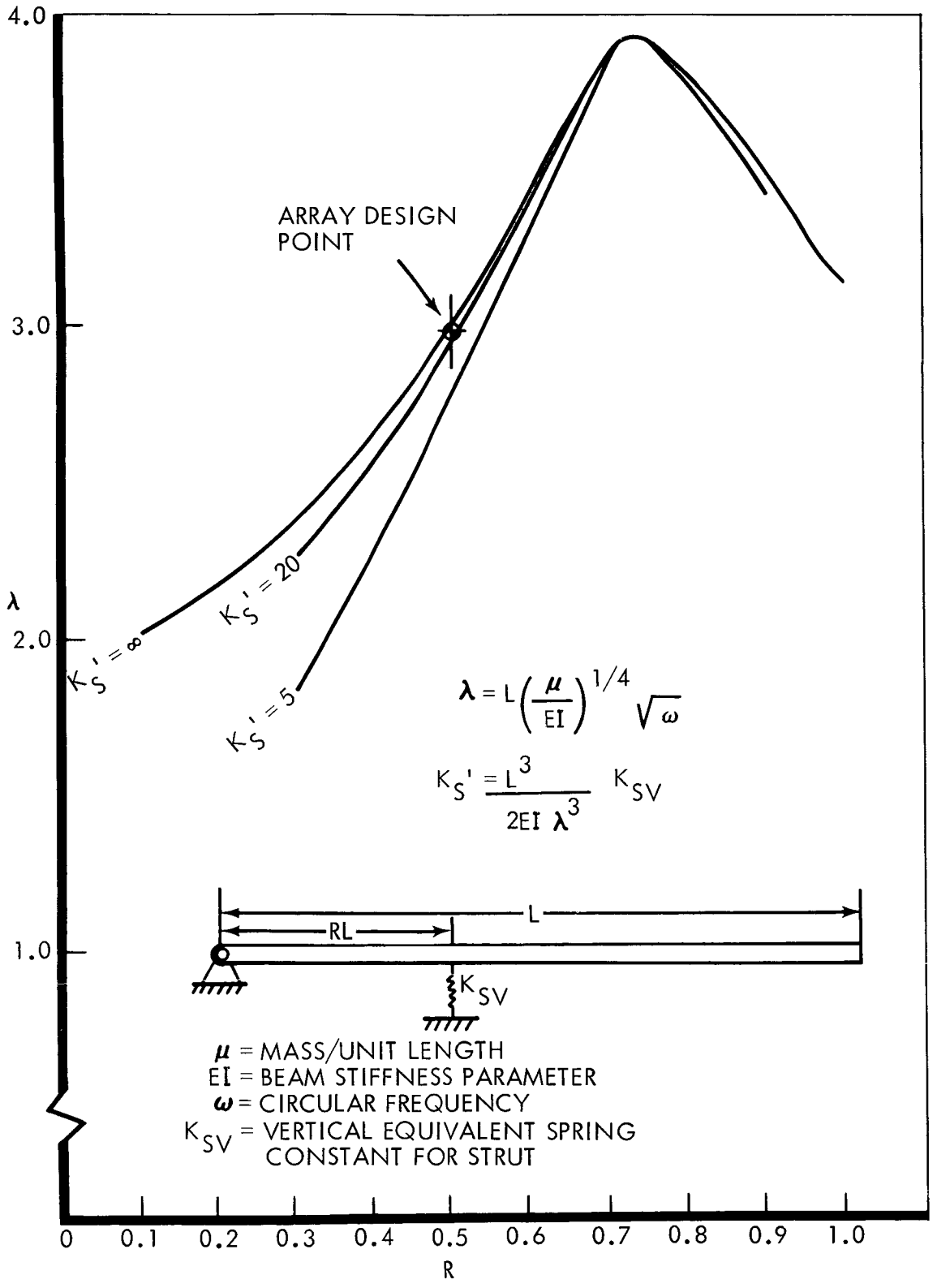

Figure 4.2-51: Fundamental Frequency vs Support Position for Varying Strut Stiffness

In this figure the K_s' is a generalized spring stiffness, λ is the generalized panel strut frequency and R is the ratio of strut location to panel length. Ksv is an effective spring constant coefficient for the strut, where:

$$Ksv = \frac{AE}{L} \sin^2 \phi$$

A=strut cross section area

E=strut meterial modulus

L=strut length

ϕ=angle of strut to panel

Figures 4.2-50 and -51 show that spar loads are minimized and stiffnesses maximized by locating the strut attachment at about 70 percent of span. However, when the weight of the strut was also considered, it was found that the minimum weight arrangement is at 50 percent of span; the selected location for the two section panel. Because stowage requirements prevent locating the attach point further outboard than the end of the inboard section, the strut will be located at 33 percent of span if a three-section panel is required in the future.

With the strut location determined, a spar maximum bending moment of 9610-inch-pounds for the three section panel and 2790-inch-pounds for the two-section panel was calculated for the 2.2 g orbit insertion maneuver (Ultimate Design Factor = 5 g). Figures 4.2-52 and -53 show the variation in spar weight/inch of length versus spar depth for the two-section and three-section panel respectively. The spars are assumed to be untapered. The weight versus depth curves for the I beam, box beam, and truss beam are shown for various panel frequencies and the

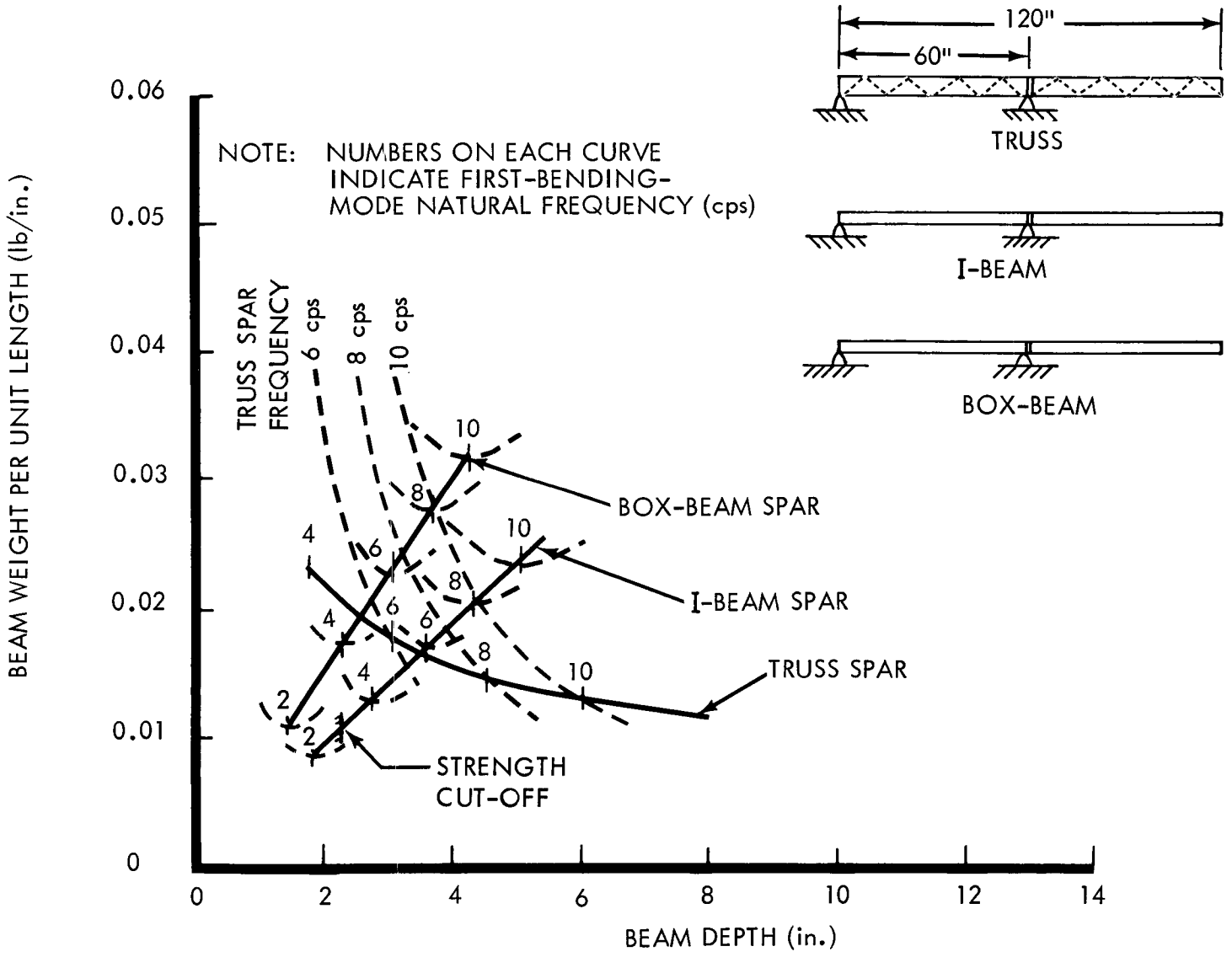

Figure 4.2-52: Beam Weight Comparison – Two-Section Panel, Configuration 945-6026

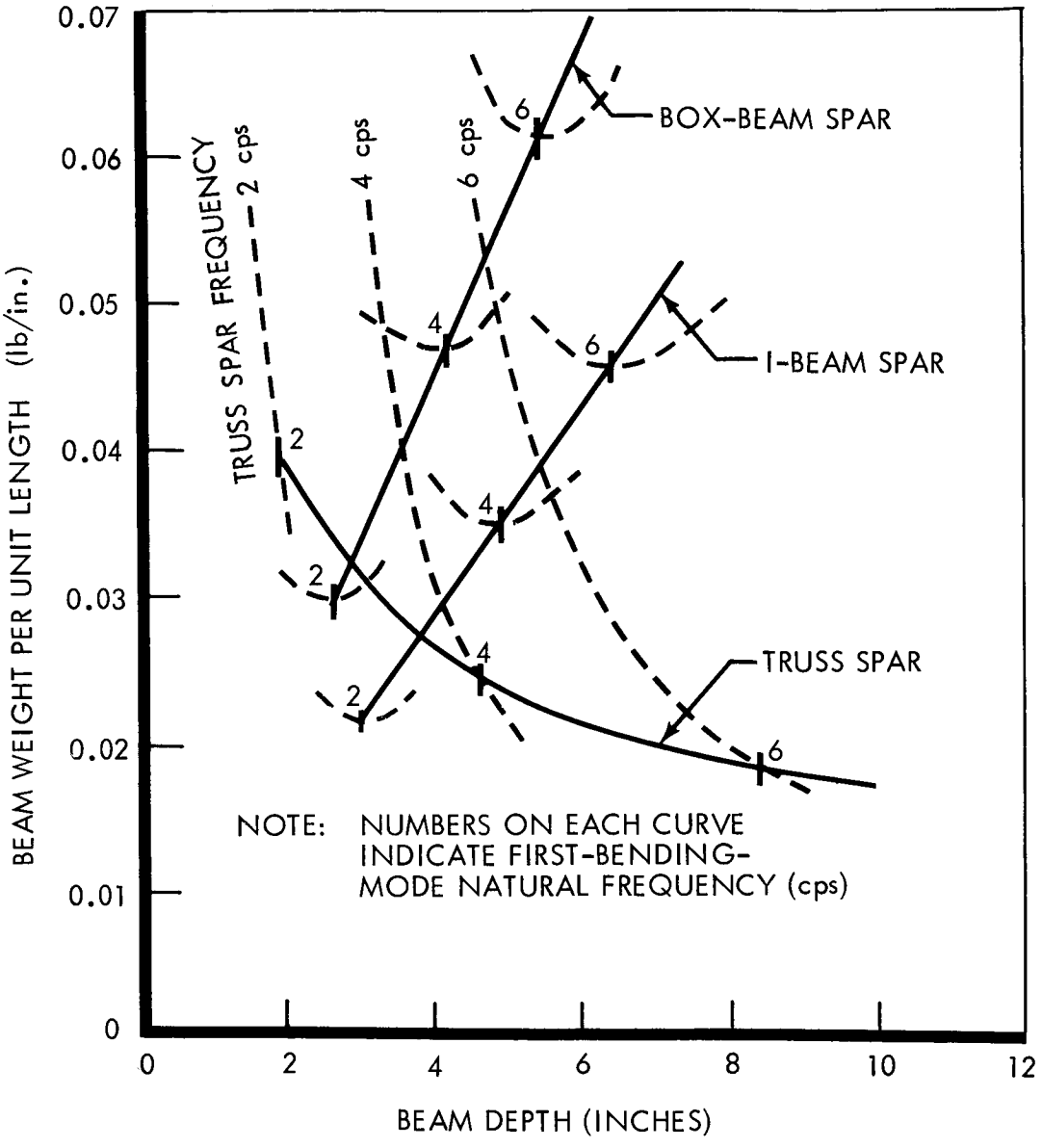

Figure 4.2-53: Beam Weight Comparison — Three-Section Panel, Configuration 945-6016

locus of their minimum points drawn. The I and box beams are stiffness designed, while the truss beam curve represents the strength design cut-off for each truss stiffness design curve. The trussbeam therefore is limited only by depth and not by frequency. It is seen that, for the two-section panel, the I beam is somewhat lighter than the truss and considerably shallower in depth. However, for the three-section panel, upon which the design is based, the strength designed truss is 4.3 pounds lighter than the I beam. In addition the truss is 8-inches deep and provides a 6 cps panel frequency (if untapered) compared to the 3-inch-deep I beam, which provide 2 cps.

Generalized rib design loads were calculated for both static and vibratory load conditions for a number of spar spacings, as discussed in the internal loads section. Minimum loads in the ribs occur when the spars are spaced at 55 percent of the chord. This spacing coincided with the spacing of the four flight capsule attachment points, and hence, the location of the spacecraft primary structure. Boost vibration loads are critical for the ribs.

The beam concepts were also compared for cost and producibility. The I beam can be built by extruding and chemical milling to final size or by riveting, spot welding, or adhesive bonding the flanges and web together. Cost will be low for builtup beams, but high for one-piece tapered beams, which are machined.

The box beam is assembled by spot welding, riveting, and adhesive bonding. Because the box beam is made up from a set of simple elements and assembled by established methods, its structural reliability is high. Box beams are realily assembled into more complex structures and their large, flat surfaces permit easy attachment for substates, cables and other equipment.

Trusses can be built of open members such as rods, tees, angles, etc., or of closed tubes. The open sections are readily welded, adhesive bonded, or riveted. A thermal advantage of the truss section is realized through minimum blockage of the substrate to deep space.

The truss by itself is statically determinant so that temperature gradients do not induce thermal stresses. Tubular truss members are vented by leaving the ends unsealed or by drilling small holes in the walls.

The minimum weight structural arrangement is selected for the panel frame. It consists of a spar and rib ladder frame of truss construction with spars spaced at 55 percent of chord and spar support struts located at 50 percent of span.

Structural Material and Fastening Techniques--The structural material and the associated fastening techniques used in the design of the array structural members must adhere to constraints and requirements similar to those defined for the rest of the spacecraft structure.

The structural materials considered for the substrate of the solar panel have different requirements from those for the main supporting frame. The substrate design is governed by the strength of foil-thin sheets and how they are joined. The cell-side surface of the substrate must be electrically insulated with a dielectric either an an integral part of the structure or coated on. Because of the detrimental effect of heat on adhesives, thermal sterilization, if required, can be an important consideration in substrate material selection.

The frame is an open-web structure comprised of members meeting in small regions of contact. Joint reliability is the main problem in materials considered for the frame.

Unalloyed beryllium was considered for the material for the frame. Magnesium (AZ31B and ZE10A) sheet and extrusions were considered as material for the entire solar-panel structure. Reinforced plastics and clear plastic (epoxy fiberglass mylar) sheets were evaluated from the cell-side skin and possibly for the corrugations of the substrate. Aluminum and mylar honeycomb were considered for part of the substrate structural system. Aluminum alloys were considered for both the substrate and the frame.

The choice of methods of joining either governs, or is governed by the choice of parent material(s). The methods and materials of joining considered for the substrate were brazing with Alcoa brazing sheet, elastomers for visco elastic bonding, spot-welding and bonding with

high-strength adhesives. The candidates for assembly of the frame were riveting, spot welding, adhesive bonding, brazing, and arc welding.

Due to the modular planform of the preferred array and the nature of the loads, beryllium was not used because the small savings in weight did not appear worth the dollar cost and fabrication uncertainties necessary to develop a beryllium substrate. The decision to use beryllium in the spars is ruled out at this time due to the apparent development required to perfect mechanical joining techniques.

Magnesium does not appear to have an advantage except in its bulk. For essentially the same strength, stiffness, and weight as aluminum, a magnesium unit has twice as much volume. That is particularly advantageous in castings for fittings where somewhat thicker sections are required.

Reinforced plastics and plastic sheet were considered for the cell-side skin of the substrate structure. The skin structure and dielectric could be combined into one with the increased electrical reliability of preventing cell-shorts to substrate. Because of large weight disadvantages, as opposed to small increased reliability, the plastic skins are not the preferred design.

Aluminum alloys are preferred materials for both the substrate and the frame because of their great range of strength, the many usable forming and joining techniques, availability, and cost. Alloys can be selected that will not suffer significant properties loss when exposed to sterilization temperatures. Aluminum alloys can be welded, formed, bonded, and welded.

Visco-elastic adhesives (epoxy polyamides) were considered for joining techniques between the corrugations and the face skin. These materials have relatively high energy absorbtion capability and will increase the structural damping in the design. This will lower the dynamic gains and, therefore, decrease the structural cross-sectional area required. The adhesives were not preferred in this design because of the lack of qualifying data for this application.

Spot welding was evaluated for joining these large foil-gage panels. Spot welding techniques must be improved before this process can be used on very thin sheets. Spot welding would impart some damping into the corrugated panel. However, with the thin gages used in the substrate design and the problems associated with the burnthrough, this joining technique was rejected.

Riveting was considered for assembling the frame. However, riveting increases structural damping in the frame, and adds additional weight in the form of rivet heads, gusset plates, and fittings. These factors must be balanced against any weight savings due to reduction in dynamic gain.

Spot welding was considered for joining the frame for the same reasons as riveting. There would not be the weight of the rivet heads involved for spot welding.

Brazing of the frame was considered when the 5-foot-long truss sections were planned. Brazing is a reliable, lightweight method of assembly.

It would require well-designed jigs and careful removal of the flux, but properly designed braze joints would provide adequate strength.

Tungsten-inert-gas (TIG) welding is a reliable, established method of joining aluminum. It is as lightweight as brazing.

The preferred material for the substrate is 2024-T4 aluminum sheet. 7075-T6 and 6061-T6 were considered as backup alloys. Both backup alloys will be penalized in strength if heat-soak sterilization processes are required.

The preferred material for the frame is extrusions of 6061. This is a weldable nonheat-treatable alloy that retains its strength during welding. The endurance limit of 6061 is 20,000 psi. The backup alloy for the frame is 2219.

The materials preferred for assembly of the substrate are the Epon epoxy adhesives. For example 934 A/B, 914, and 929. These adhesives will tolerate thermal sterilization. The recommended welding wires for the frame are 4043 for use with 6061, and 2319 for the backup alloy 2219.

Thermal Control Coatings--The efficiency of solar cells decreases as temperature increases. To minimize the number of cells required, and subsequently the mass of the solar-panel assembly, it is desirable to maintain the solar panels at the lowest possible temperatures.

Thermal coatings are necessary on both sides of a solar panel to reduce equilibrium temperatures. Solar cells with coverglasses provide this protection for one side. Black paint suitable for vacuum conditions is used to coat the back of the panel.

There are many coatings that might be selected for the lower surface of the solar panel. These coatings include several types of paints, plastics, oxide deposits, and surface treatments such as anodizing. Because nearly all of these coatings have high infrared thermal emissivities (near 3.9) the selection of material is usually based on mechanical properties and space-proven reliability.

Anodic coatings, such as the Boeing barrier-layer coating and Boeing HS-1 coating, show promise because of their integral nature and their tolerance to simulated space environment. Silicone paints, enamels, and oxide deposits are easily applied; however, none of these have the reliable performance considered to be the pacing consideration in the selection of thermal-control coatings. Mariner IV used Laminar X-500 with no apparent degradation during the mission.

Laminar X-500, a black polyurethane material manufactured by Magna Coating and Chemical Corporation, has been selected as the preferred coating for the bottom of the solar-panel assembly. This material is relatively easy to apply, is readily available at a reasonable coat, and is space proven. This material cures at room temperature but can withstand the temperature levels proposed in sterilization processes without degradation. It has excellent stability under thermal cycling.

The thermal emissivities of black coatings vary between batches. In order to control emissivity, it will be necessary to measure the emissive properties of the actual material before application.

Dielectric Insulation--The solar cells and their bus bars and interconnection leads that bond to the panel surface must be electrically insulated from the metallic substrate. The insulation material must exhibit specified dielectric strengths and resistances and be compatible to cell application and defective-cell removal techniques.

Methods for achieving an insulated substrate are generally divided into two approaches: surface coatings, anodizing, and adhesive banded plastics; and replacing the metallic substrate by a nonmetallic substrate skin. The dielectrics considered were: (1) a spray-on polyamide based coating (SMP 62/63), (2) anodizing the aluminum skin (Hardaze process), (3) adhesive-bonded plastic or epoxy fiberglass (H-film), and (4) replacing the aluminum skin with a mylar-epoxy-fiberglas skin.

Anodize coatings offer a minimum-weight insulation but were not selected because process parameters were not considered compatible with the design. The mylar skin was rejected by a weight comparison because of the thickness required to achieve skin strength and difficulty in using soldering irons near the mylar.

The SMP 62/63, manufactured by Western States Lacquers Co., has been selected as the preferred insulation coating. This material has been successfully used on Mariner IV. The H-film method is an alternate.

Array Mechanism--The primary objective of the mechanism is to deploy the panel sections so that the array or surrounding structures are not damaged. The selected mechanism should be reliable, have highest power-weight ratio, and be simple to install and operate. The electric motor drive is preferred because speed control is inherent in its design. This will ensure a controlled panel deploy. It is also the lightest of the considered systems.

When stowed, the panel sections are parallel and remain so until released for the deployment sequence. The release devices should be simple, easy to install, be able to accept shear loads imposed during launch environment, and have short response times.

When deployed, the cantilever structure is subjected to vibrational loadings at engine ignition. Latches on each panel section restrain the ensuing moments, allowing the loads to be transmitted from section to section, ensuring rigidity.

Array Mechanisms Considered--In arriving at the preferred design, alternative approaches were considered that together with the proposed electric motor concept, are discussed in the text.

For convenience, the different approaches are identified as follows: Figure 4.2-54: Torsion bar or spring with speed control dampers, Figure 4.2-27: Electric motor drive, Figure 4.2-55: Sliding module panel array, Figure 4.2-56: Scissors or "lazy-tong" configuration, Figure 4.2-57: Bourdon helical-torque transmitter.

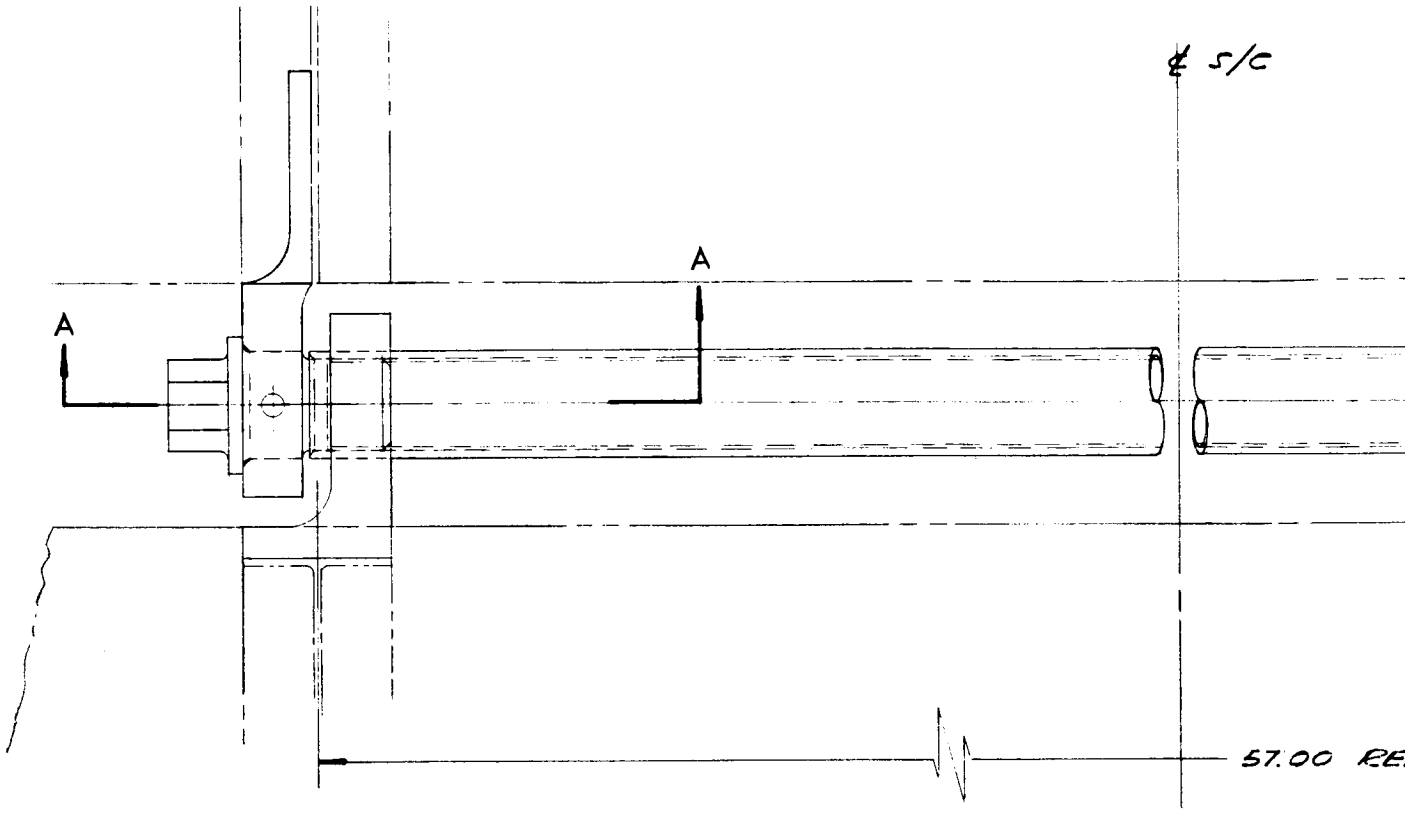
℄ S/C
A
A
57.00 RE

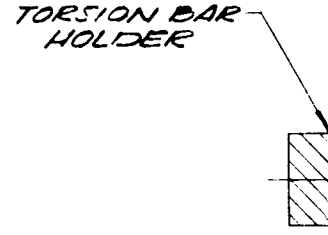
TORSION BAR
HOLDER

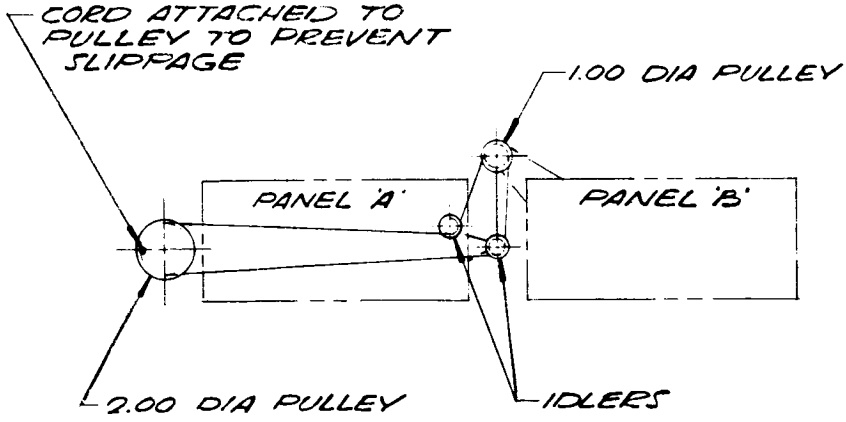
CORD ATTACHED TO
PULLEY TO PREVENT
SLIPPAGE
1.00 DIA PULLEY
PANEL 'A'
PANEL 'B'
2.00 DIA PULLEY
IDLERS

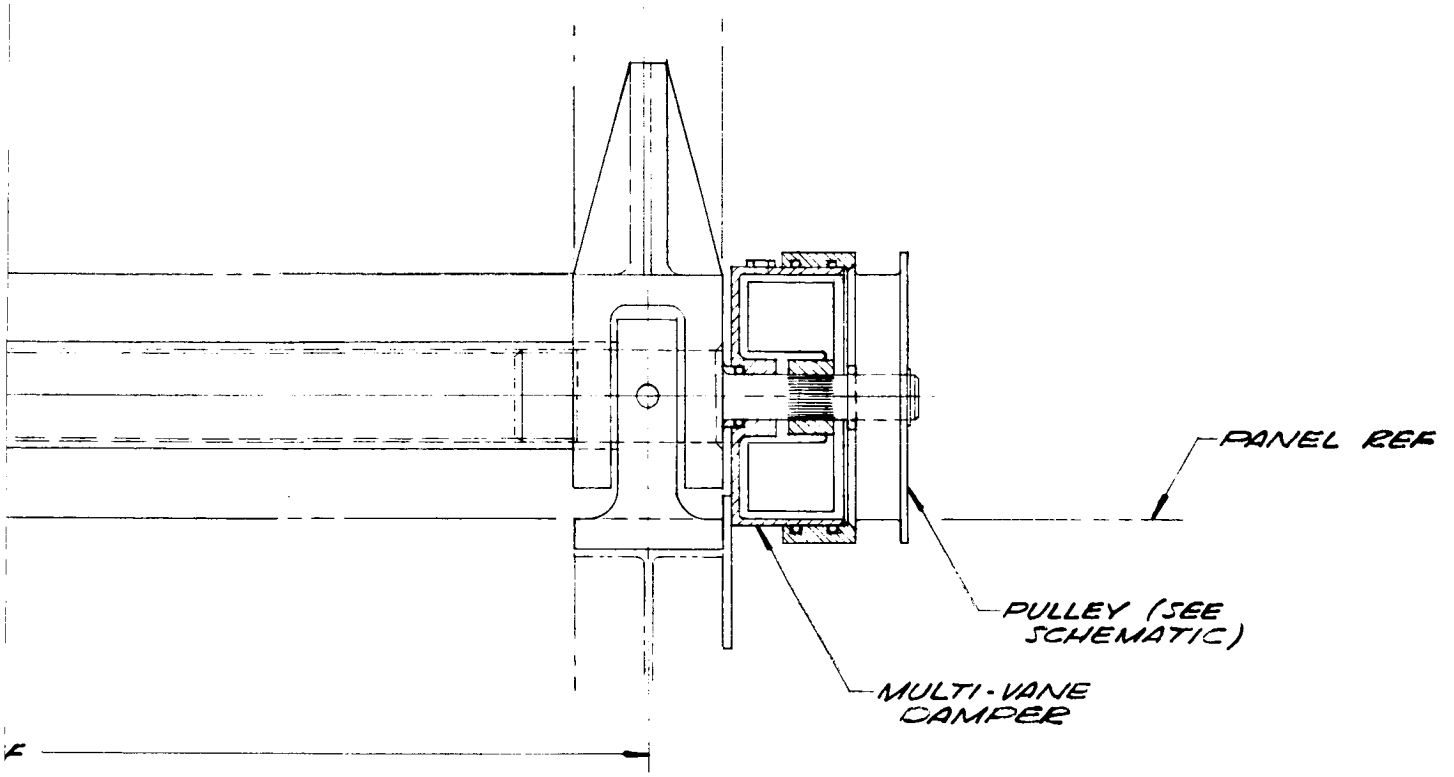

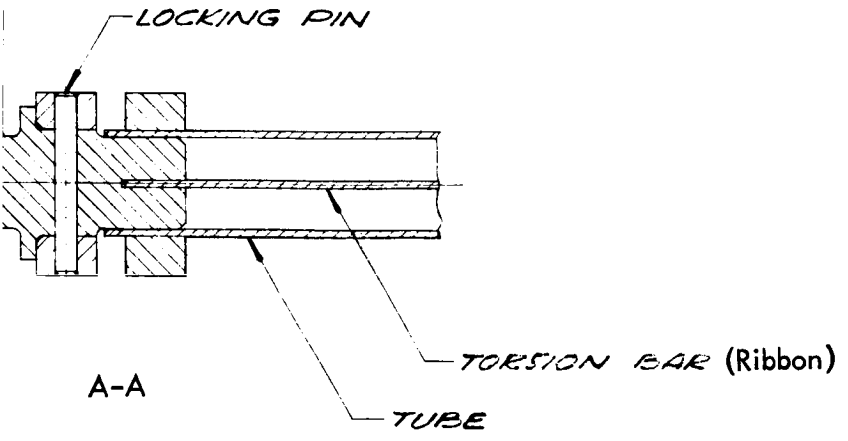

1. Dimensions in inches
2. See dwg #61411b Rev A of reference (4)

Figure 4.2-54: Spacecraft Model 945-6026
Alternate Panel Deployment Mechanism

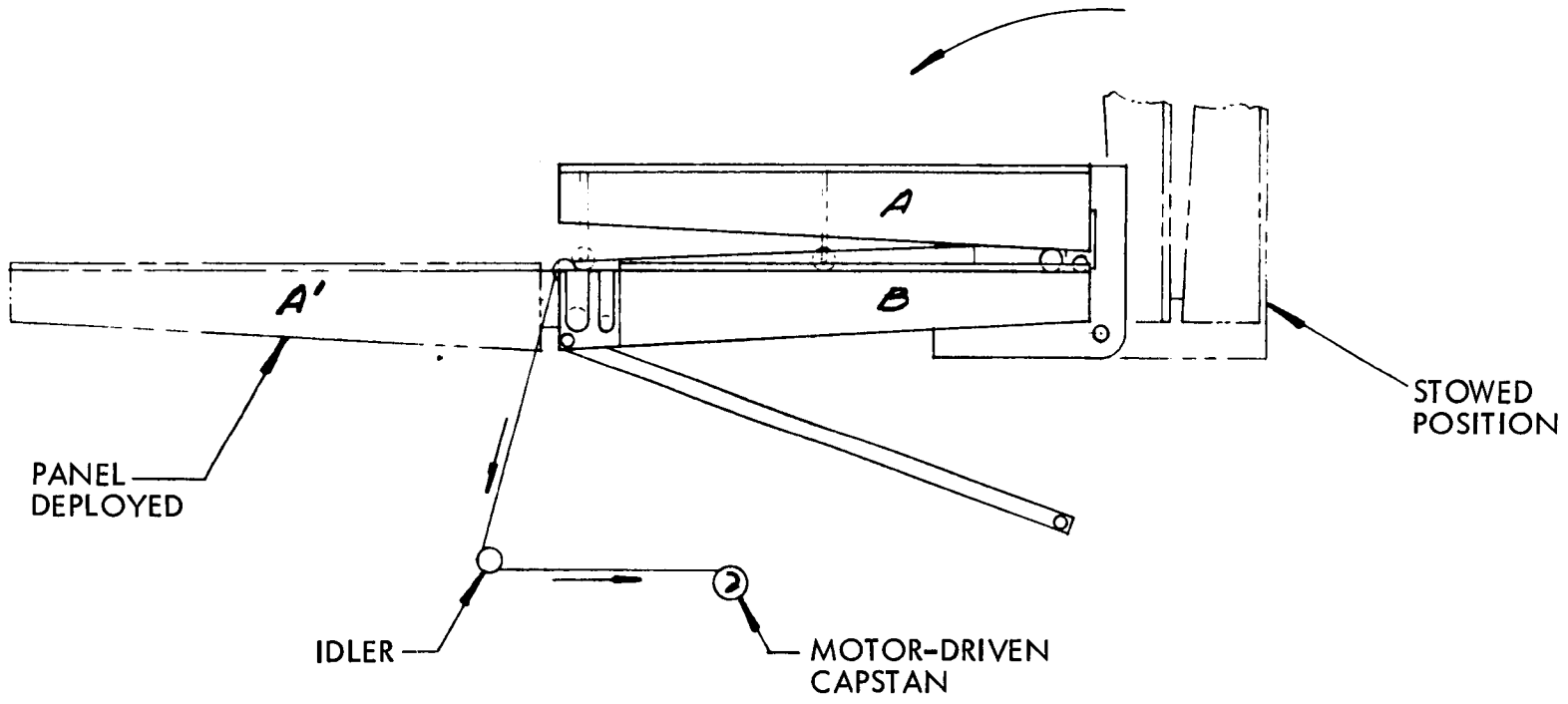

Note on System Operation:
Motor Deploys Panel A by Rotation of capstan, which winds up nylon cord and slides roller-mounted Panel A into the deployed position. When extended. Guides on Panel A enter selected slots on Panel B to allow movement into Position A for locking.

Figure 4.2-55: Spacecraft Model 945-6026 Panel Deployment Mechanism

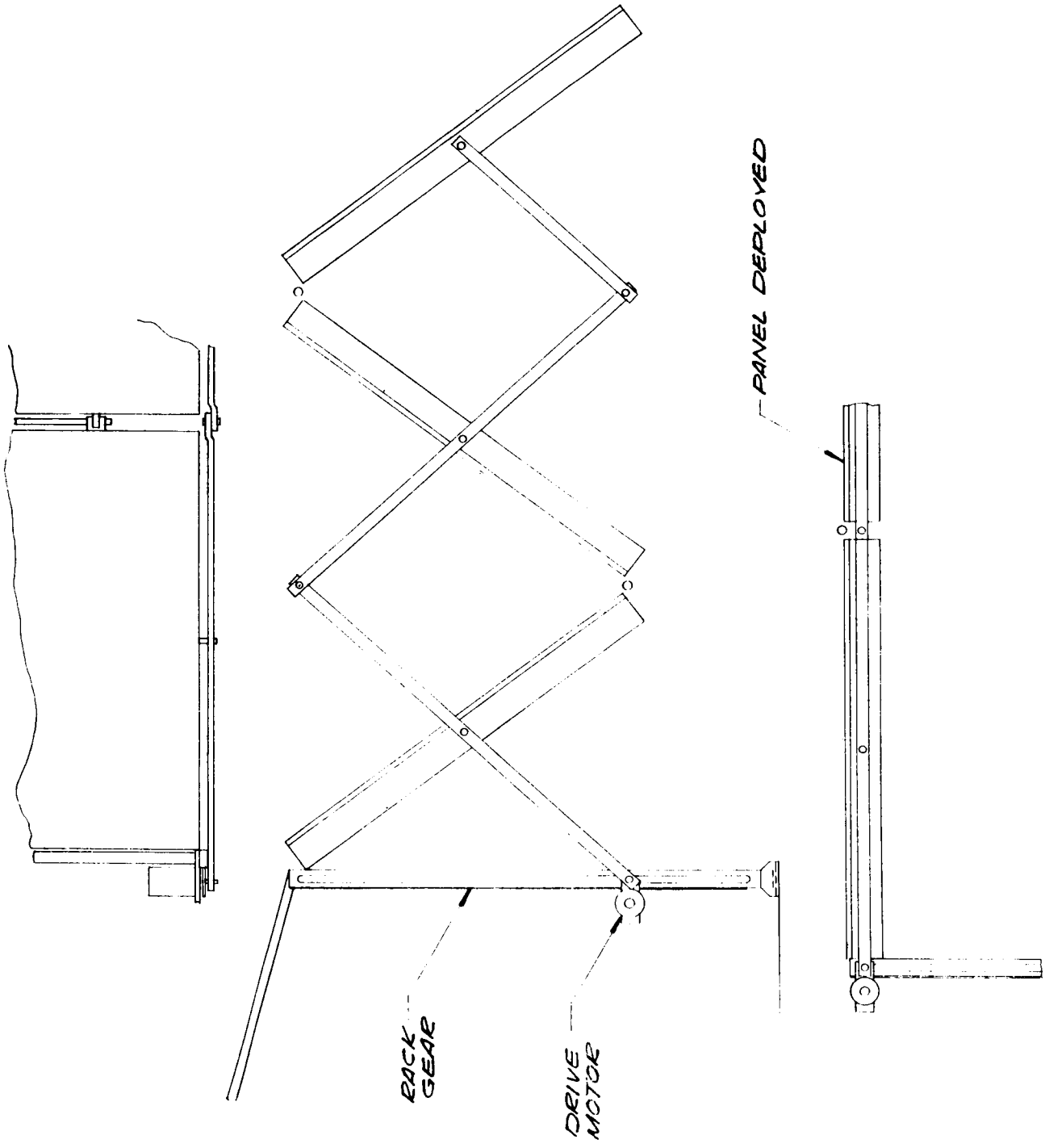

Figure 4.2-56: Spacecraft Model 945-6016 Alternate Panel Deployment Mechanism

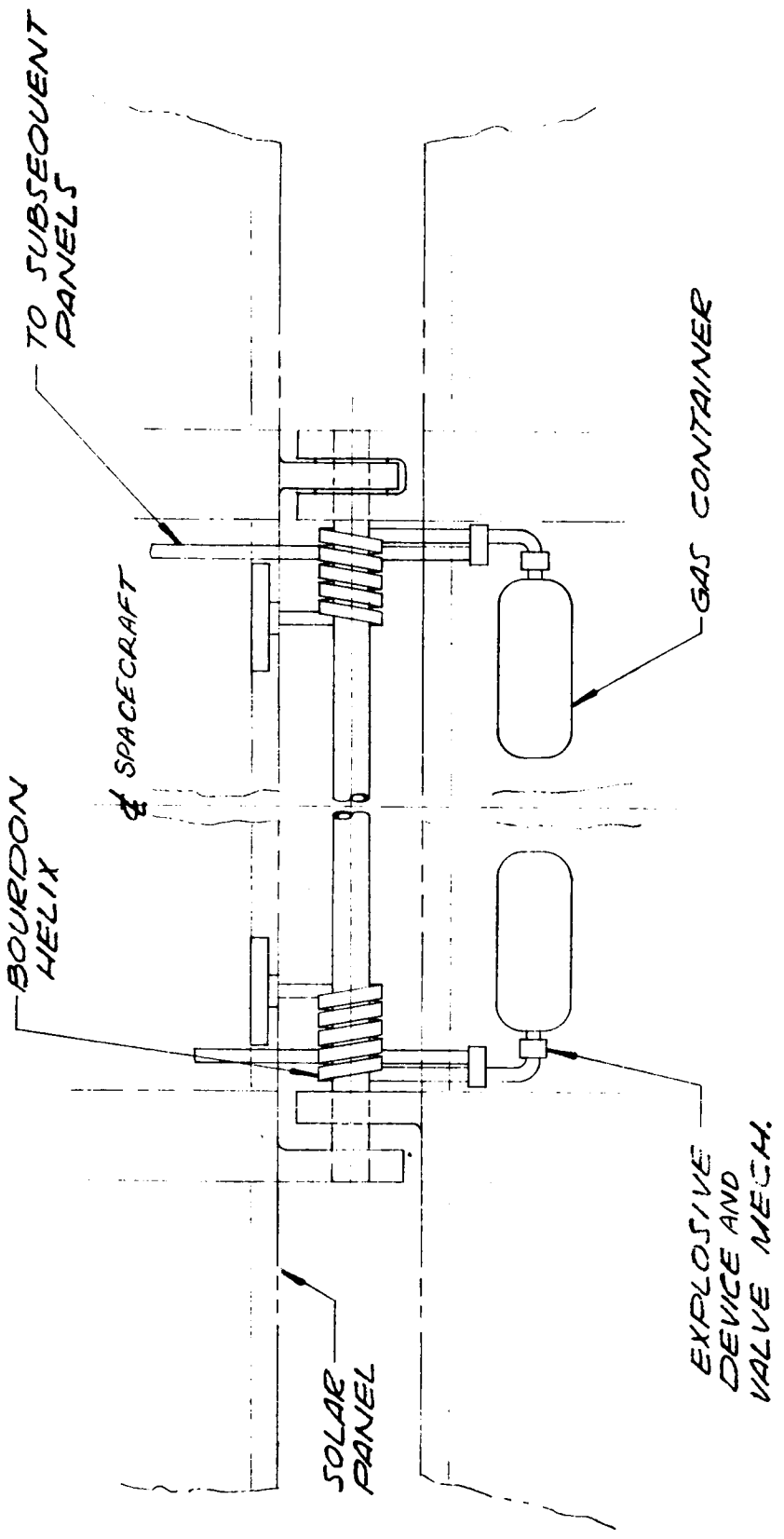

Figure 4.2-57: Spacecraft Model 945-6016 Alternate Panel Deployment Mechanism

The pyrotechnic pin puller was the primary selection as a release device. An alternate was a variation in the form of an explosive bolt.

To maintain a high strength-to-weight ratio, latch mechanisms are desinged to resist vibrational loads in shear planes.

To provide maximum stability and effectiveness, the latches are positioned on the panel spares away from the hinge point.

The reliability of the various deployment mechanisms were evaluated against the stress developed in component members, minimum number of parts, ability for repeatable ground testing without deterioration, and state-of-the-art development. The torsion-bar device is less reliable because of the high stresses in the bar necessary to develop required torques. The slide-and-scissors approach requires a larger number of components. The Bourdon helical device requires development work to bring it up to the state-of-the-art of the other concepts.

Reliability procedures are well established for the pyrotechnic device since an equivalent design has successfully been flown on the Mariner and Ranger spacecrafts. The deploy-latch designs were traded against complexity.

Safety of the pyrotechnic device is satisfied by using shorting plugs on the squibs and adequately sealing them so that products of combustion are self-contained inside the pin puller.

The performance of the deployment devices are traded on torque produced per weight of unit, envelope required, and electrical power required.

In determining the performance of the devices, it is necessary to define deployment angle or distance, time for deployment, and power source. During the development of the array, the requirements have changed from a single section with a deployment angle of less then 90 degrees, to a multisection array with deployment angles of 90 and 180 degrees. For efficiency, it is necessary to deploy the panels as quickly as possible to reduce the drain on the spacecraft batteries. A deployment time of 30 seconds does not introduce high inertia forces in the structure, allows sufficient delay time for cable alignment, and provides an efficient deployment when the spacecraft is in orbit. Having established these parameters, it is possible to evaluate the torque weight ratio per pound of material of the five systems:

Torson bar:	300/6.8	= 118 oz-in/lb.
Electric motor:	1000/3.85	= 260 oz-in/lb.
Sliding module:	1000/6.5	= 154 oz-in/lb.
Scissors:	1000/5.64	= 178 oz-in/lb.
Bourdon tube:	600/5.25	= 115 oz-in/lb.

The electric motor produces the most torque per pound.

Torsion Bar--The most difficult problem with the torsion-bar mechanism is obtaining a low spring constant in a given volume of material without imposing excessive shear stresses due to the high initial torques. The limitation is in having to develop a minimum of 30 lb-in. of torque just before full deployment to straighten the array power cables. With the excess of 20 lb-in. of torque at the moment of panel release, it is necessary to provide a damping mechanism as shown in Figure 4.2-54.

Electric Motor--Deployment by motor does not have limitations with regard to deployment angles. By sealing the motor in a container, problems resulting from high frictional wear on the armature are reduced. Also the motor produces the best power-to-weight ratio of the devices considered. One of the original schemes for motor deployment was to use synchronous motors from 400-cps supply with percise speed control, but this was changed to comply with availability of d.c. from battery source. While the d.c. motor does not give a constant speed because of the large relative load of the gear box, the final drive shaft can be considered reasonably constant. With suitable gear ratios to deploy 90 and 180 degrees, in the same time span, uniform deployment can be expected.

Sliding Module--Deployment time would be longest with this sliding array by a factor of 3 over the other approaches, as the single motor deploys each of the three sections in turn. In principle, the mechanism consists of a single motor acting as a capstan, with a chord (attached by separate latches to the various panel sections in turn) it deploys the array into a stepped cantilever. This scheme was eventually discarded because of difficulty in providing a structural strut for the complete array when fully deployed, and for ineffective backing of the sections.

Scissors--The scissors concept is sound, and with only one drive motor the power drain would be small. But the mechanism requires structural complexity at the spacecraft, and could affect the Canopus sensor. Solving these problems increases the weight and complexity.

Bourdon Tube--Although consideration was given to a Bourdon-tube scheme within the torque range and deployment angles, there is nothing currently being manufactured.

The weight evaluation contributed to the selection of the type of drive. When the deployment function is complete, these items are nonfunctional, becoming simply excess weight and therefore, a penalty. However, the deployment function has to be completely effective and reliable. For example, in the case of the torsion-bar system, to get sufficient torque in the system at the completion of 180 degrees, the initial stored energy exceeds actual requirements by 66 percent. This excess must be suitably damped, as indicated in Figure 4.2-54, which increases the system weight.

The following list compares mechanism-weight per panel section:

Item	Weight (lb.)
Torsion bar:	6.8
Electric motor:	3.85
Sliding module:	6.5
Scissors:	5.64
Bourdon tube:	5.25

The electric motor is lightest.

The alternates considered for both deployment and latching, with the exception of the electric motor, will not produce or contain a magnetic field since they can all be constructed of nonferrous metals. In the case of the d.c. motor, the field system is constructued from

permanent magnet material but has a closed-loop magnetic path that reduces exterior magnetic flux to a minimum.

The pin-puller-release device was selected after considering the following parameters: Safety from combustion products, reliability, simplicity of operation, functional requirements of the structure for force equalization during launch mode, short response times, and ground-station testing for effectiveness.

The deployed latches should be automatic, reliable, have structural integrity and rigidity, be lightweight, and be capable of withstanding repeated testing without impaired efficiency.

The d.c. motor-drive deployment device is the preferred prime mover of the solar array because of minimum weight and maximum torque per pound.

4.2.10 Battery--Component Functional Description

A sealed silver oxide-cadmium battery system has been shown to have the best overall compatibility with mission requirements of the candidates evaluated. The characteristics of the silver oxide-cadmium battery are summarized in Table 4.2-16.

Table 4.2-16: BATTERY CHARACTERISTICS

Property	Mission Requirement	AgO-Cd Capability
Energy density	high	20 wh/lb at 75% depth
Cycle life*	200 cycles	200+ cycles at 75% 300 cycles at 50% depth
Stand life	19 months	24+ months (at 80°F max)
Operational temperature range	60-110°F (estimated)	40-110°F
Thermal sterilizability	24+ hours at 110-120°F (tentative)	presently not feasible
Magnetic	nonmagnetic	nonmagnetic

*See Vol. D2-82709-2, Section 4.2.

The circuit diagram of the battery is shown in Reference 1, dwg 614117.

The cells in each battery are made of multiple silver and cadmium electrodes connected electrically in parallel within the cell container. Each cell contains an oxygen recombination electrode. The electrodes are separated by multiple layers of separator material that serve to hold the electrolyte, prevent mechanical contact of the individual electrodes that would result in internal shorts, and prevent the migration of active material from their respective electrodes that also could cause internal cell shorts.

The electrolyte within the cells consists of concentrated potassium hydroxide in the range of 30-45 percent by weight. Individual cells of this electrochemical system operate at a second discharge plateau voltage of approximately 1.05 volts. Therefore, to make a nominal 40-volt battery for the Voyager Mission, it will be necessary to use 38 cells electrically connected in series. The battery will be composed of individual cells that are electrically connected in series during the assembly of the battery by means of bus bars. This will enable a pre-checkout, screening and selection of individual cells prior to battery assembly. The cells and battery will be wired to an external electrical connector to provide for connections and monitoring of individual cell voltages.

In addition, the battery will contain three temperature-transducers implanted within it to monitor battery temperature for OSE, T/M, and to be used as a feedback to the "end of charge" voltage control.

The battery will also incorporate diodes in the OSE charging outputs to prevent accidental short-circuit of the battery through the ground-support loop.

Three identical batteries are electrically connected in parallel in the proposed system, operating at 50 percent discharge depth during off-Sun in orbital cycling. Two of these batteries will operate during orbit at 75 percent discharge depth and can sustain the mission if one battery fails. All three batteries will be used in parallel; after use, the batteries will automatically be recharged from the solar array. When

full charge is reached, the battery will be maintained on a float condition to keep the capacity at full charge. The load levels and operating conditions for both power delivery phases are given in Table 4.2-17. Typical voltage/time plots are shown in Figures 4.2-58 and 4.2-59 for orbital operation on three batteries (50% discharge) and two batteries (75% discharge).

Table 4.2-17: POWER DELIVERY LOAD LEVELS

	Mission Requirement	2 Batteries-- Operating (data per battery)	3 Batteries-- Operating (data per battery
Orbit Injection Maneuver			
Watts	453	227	151
Discharge Time (hours)	2.33	2.33	2.33
Watt hours	1060	530	353
Ampere hours	28	14	9.6
% depth	--	65	43
Orbit Operation (occulted)			
Watts	424	212	141
Discharge Time (hours)	2.9	2.9	2.9
Watts hours	1230	615	410
Ampere hours	32.4	16.2	10.8
% depth	--	75	50

Battery capacity can be calculated from Table 4.2-17 data to be 21.6 ampere hours, equivalent to approximately 820 watt hours at the nominal voltage.

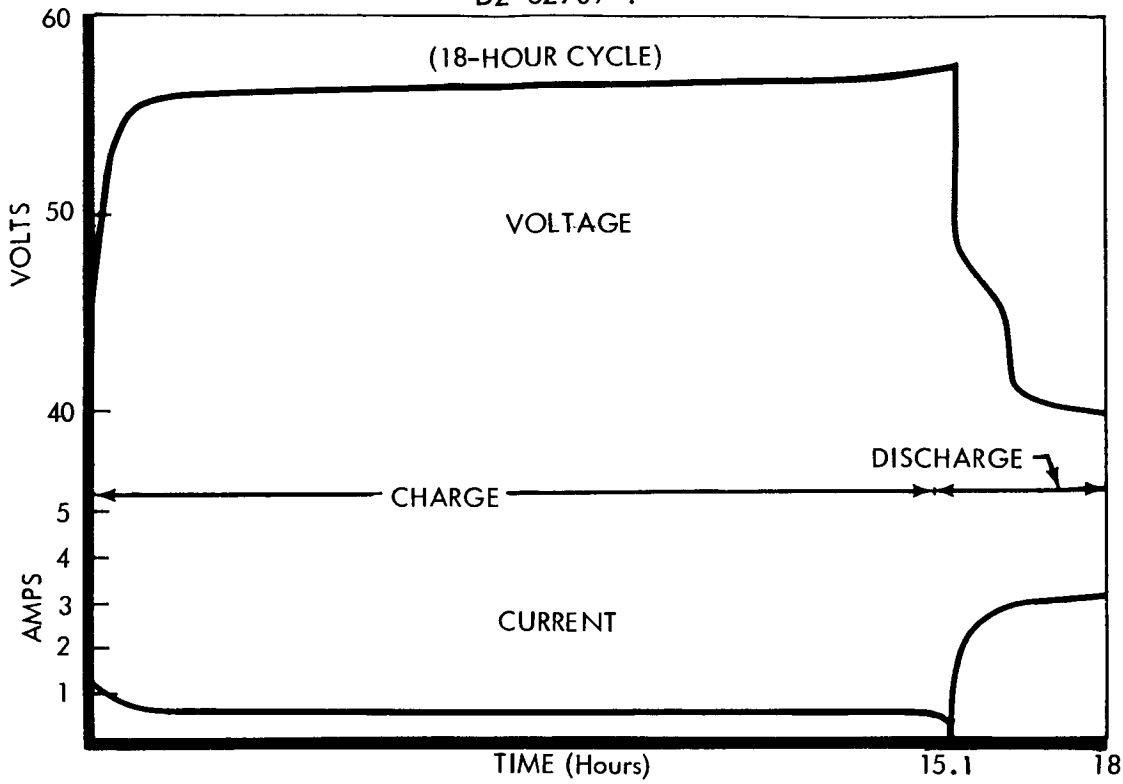

Figure 4.2-58: Projected Performance of AgO-Cd Battery (50-Percent Depth)

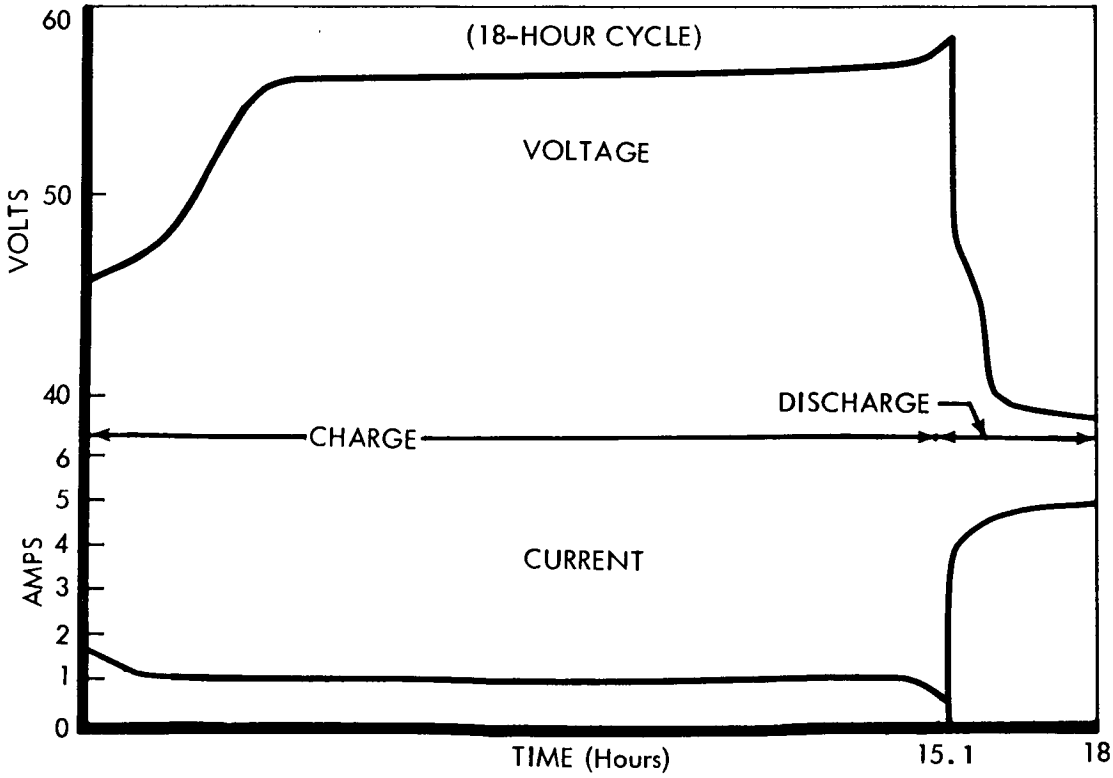

Figure 4.2-59: Projected Performance of AgO-Cd Battery (75-Percent Depth)

Battery characteristics include:

1) Inputs--Charge voltage: 45-58 volts;

2) Outputs--Open circuit voltage, full charge: 54 volts;

Open citcuit voltage, partially discharged: 44 volts;

Load voltage: 38-51.5 volts;

Nominal voltage: 40 volts;

3) Thermal--Heat rejection during discharge: 8 watts each;

Heat rejection during charge: 1 watt each;

4) Weight--41 pounds each;

5) Volume--650 in^3 each.

4.2.10.1 Reliability

Although only limited data is available on silver-cadmium batteries under operational conditions similar to those of the Voyager batteries, these data indicate the following:

1) The exponential form for predicted reliability cannot be utilized using simple mean cycle-to-failure information.

2) Careful screening and testing can result in a very narrow distribution of cycles-to-failure and the achievement of a battery whose mean cycles-to-failure is ten to one-hundred times the anticipated mission.

3) Operational usage support is added to the concept that a very low failure rate can be achieved for this type of battery during its design life and that a normal distribution of failures can be expected as the design life is exceeded.

4) The exponential distribution of failures does not appear to be applicable.

5) Mechanisms of failure are obviously affected by operational usage, i.e., temperature, depth of discharge, cycle rate, etc. However, the relationship to quantitative reliability statements cannot presently be established. In addition, specific design characteristics are expected to greatly affect these relationships.

Ultimate achievement of battery reliability will be obtained through utilization of proven design techniques, a thorough development test program, effective process controls during fabrication, and an intensive inspection and screening system.

An individual battery reliability of 0.98 for the entire mission has been assumed for the purposes of overall mission reliability estimation. It is felt that this number may be somewhat pessimistic based on the operational usage and the foregoing discussions.

4.2.10.2 Design Optimization

Design Parameters--To base comparative studies and understand battery capabilities, performance and parameter data were established. The individual electrode reactions during charge, over-charge, discharge, and over-discharge that occur in this battery system are presented in Figures 4.2-60 and -61. The cell voltages presented are typical values actually obtained. This picture of the individual cell reaction is useful in obtaining an understanding of the electrical performance parameters and different voltage levels of the system. The gassing conditions must be guarded against to insure the prevention of excessive pressure build-ups within individual cells in the battery.

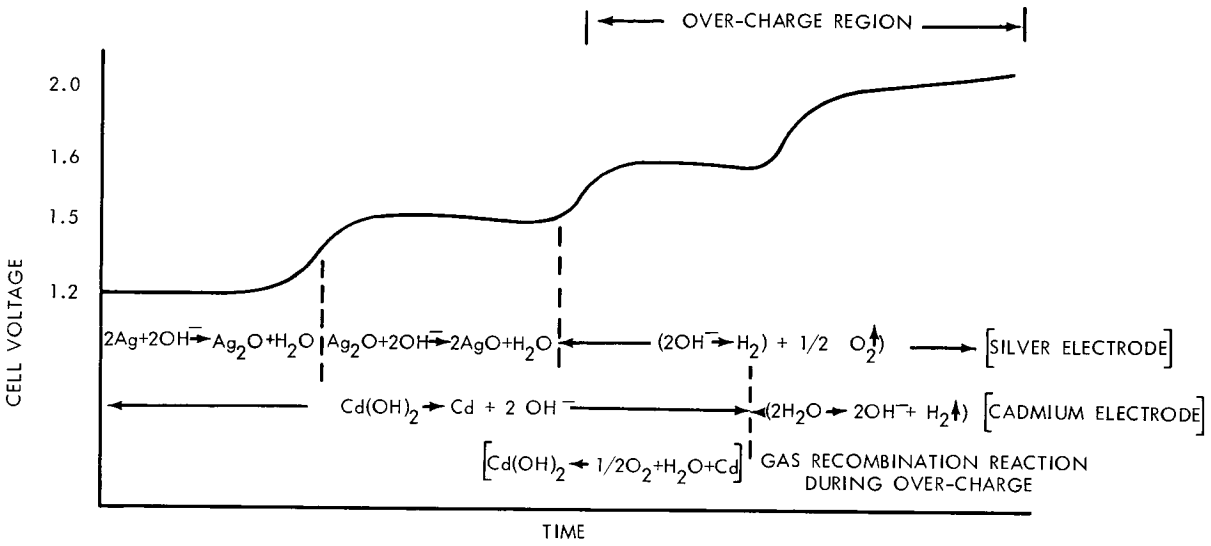

Figure 4.2-60: Step Reactions During Charge Of AgO-Cd Single Cell

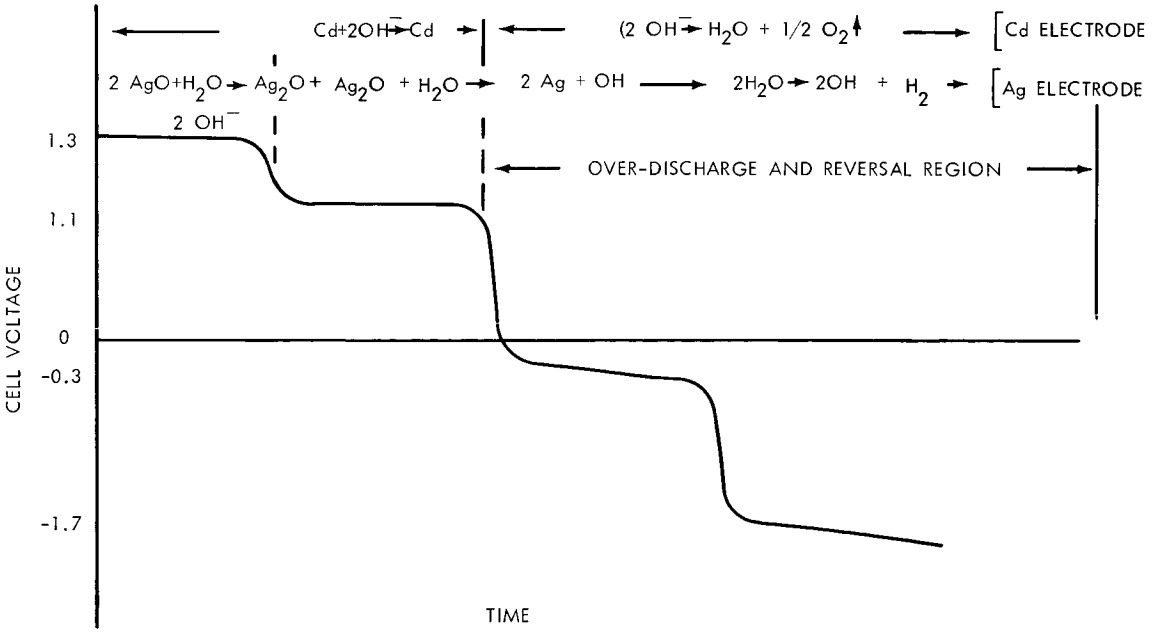

Figure 4.2-61: Step Reactions During Discharge Of Ago-Cd Single Cell

To establish the weight allotment for the battery, a survey of the energy density capability of this type of battery was made. Figure 4.2-62 represents a compilation of various manufacturers' data, calculations, and projections for watt-hour/pound output as a function of battery capacity.

Similar information is also plotted in Figure 4.2-63 for watt-hour/in^3 versus battery capacity. These curves are for medium rates of discharge and moderate ranges of temperature of the type required for Voyager.

Battery Hybrid Combination--The data presented in D2-82709-2, Section 4.2, indicate that it is possible to use a two-battery system, one battery to provide supplemental power during the injection maneuvers, and the other to supply power for the orbit phase. If the injection energy required is greater than the orbit energy, a hybrid system can reduce the overall battery package weight.

A primary sealed silver-zinc battery was considered to augment and make up the energy difference for the orbit injection maneuver as opposed to using an oversized silver-cadmium battery. The silver-zinc system is capable of higher energy densities when used as a primary battery, and is adequate if lifetimes are less than one year.

To illustrate the weight advantage of a combined-battery systems approach, Figure 4.2-64 was prepared. The figure shows the sum of the weights of a silver-zinc and a silver-cadmium battery when the maneuvering energy is higher than the orbit energy as compared to the silver-cadmium battery

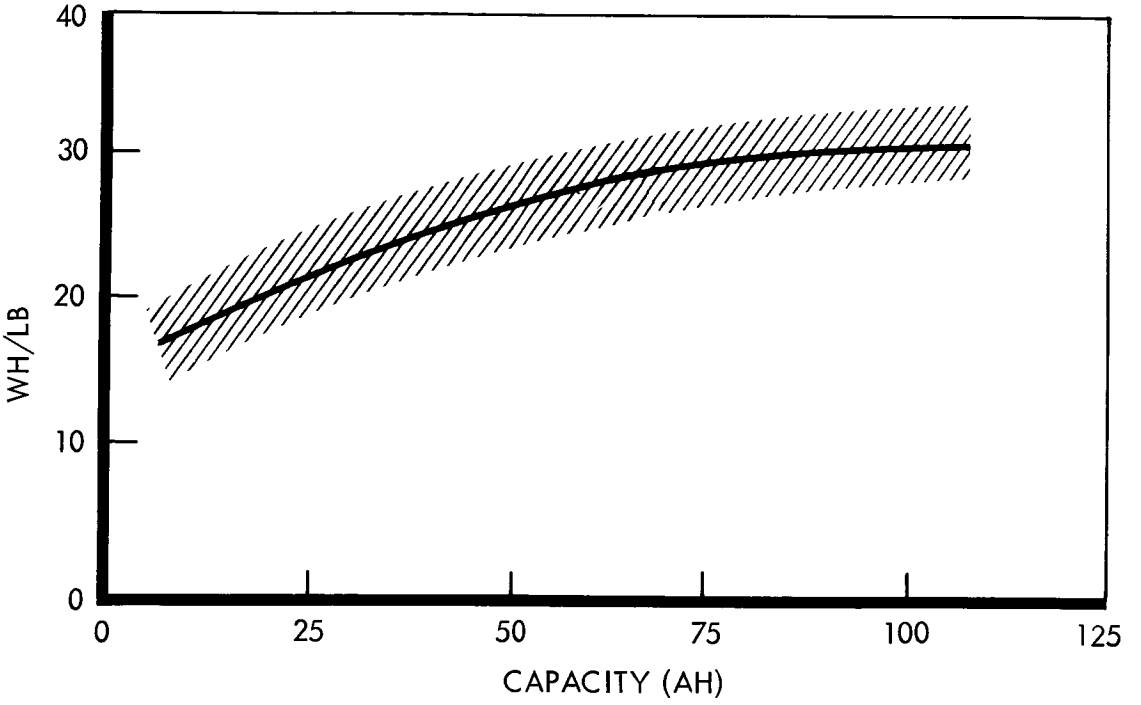

Figure 4.2-62: WH/LB Capability of AgO-Cd Batteries as Function of Capacity— Medium Rate

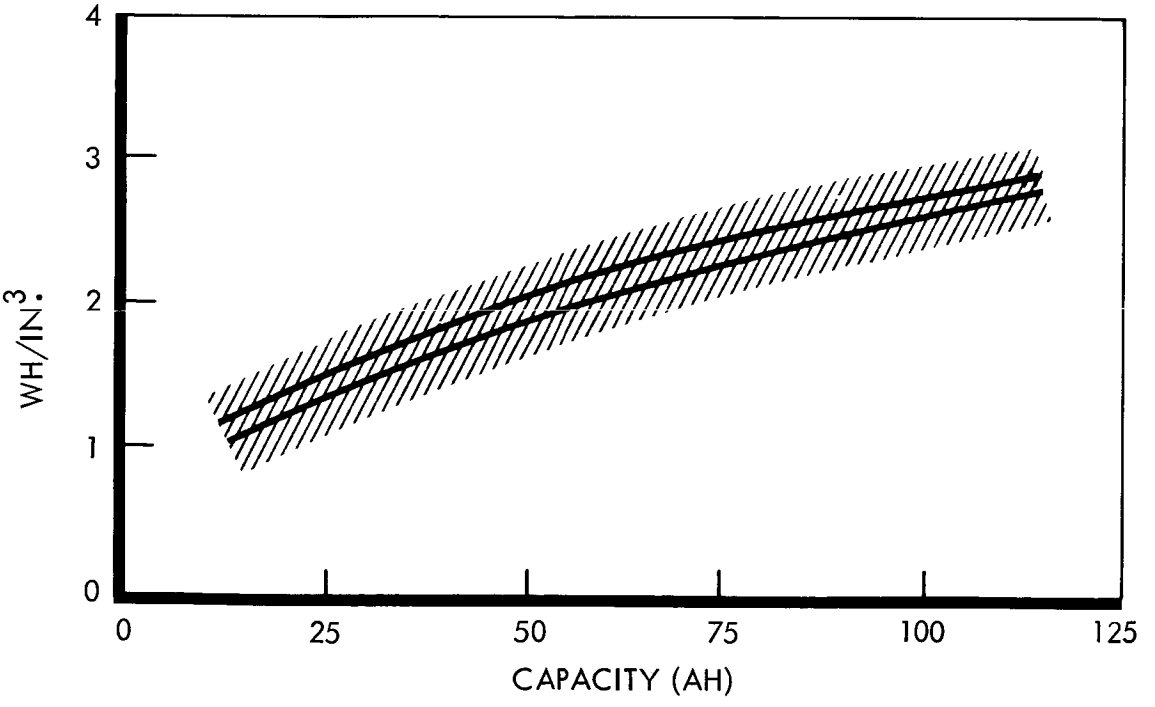

Figure 4.2-63: WH/IN.^{3} of AgO-Cd Batteries as Function of Capacity — Medium Rate

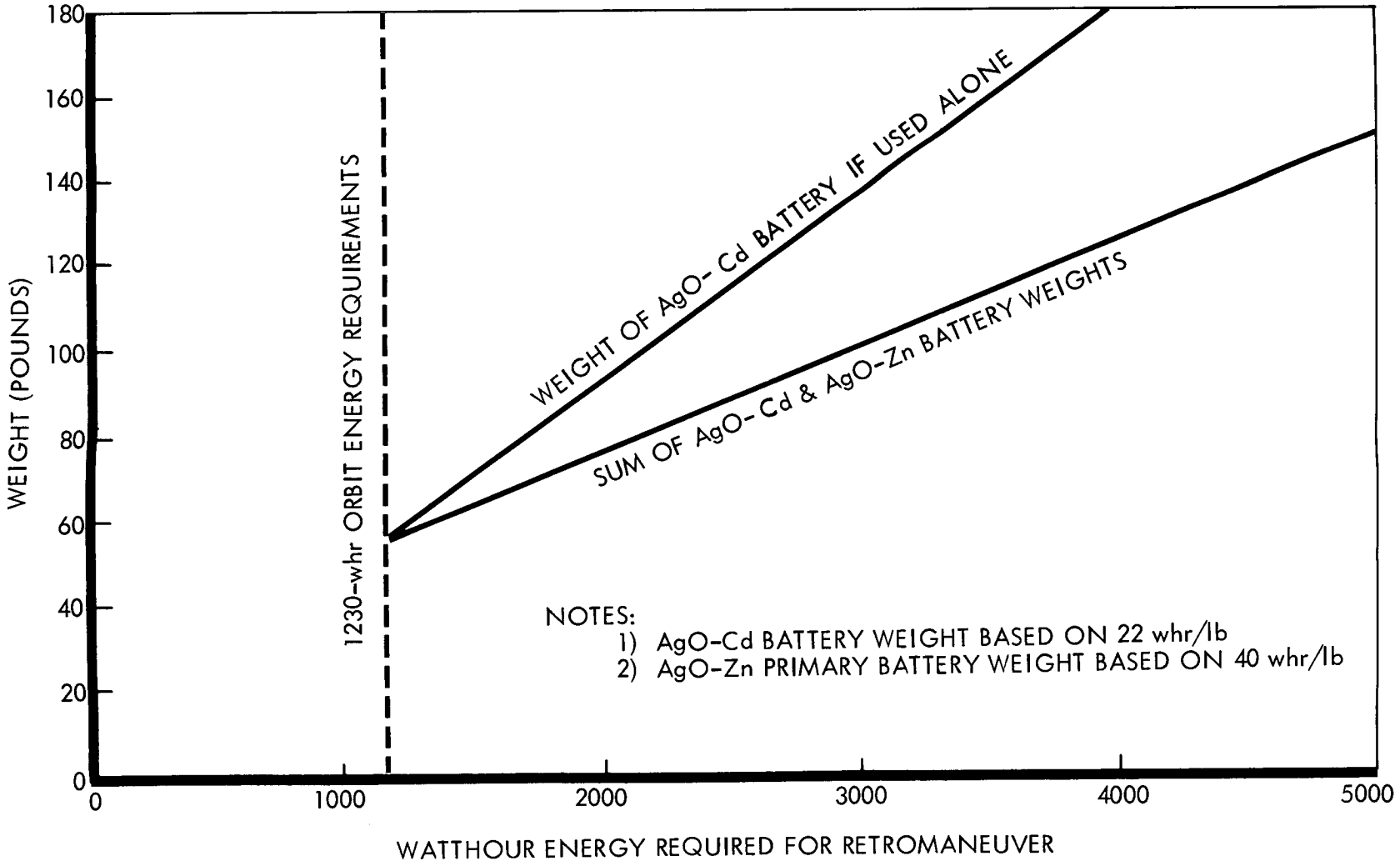

Figure 4.2-64: Comparison of Hybrid Battery Systems for Peak Loads

weight alone. This curve was prepared as a function of progressively-increasing watt-hour energy requirements for the injection maneuver. The requirement for the orbit portion was frozen at 1230 watt-hours; basis for the weights of each of the systems was 40 watt-hours per pound for silver-zinc (as a primary battery), and 22 watt-hours per pound for the silver-cadmium battery. As an example of the weight savings possible, if the maneuver energy requirement was twice the orbit energy requirement, a savings of 27 pounds would result by the use of the hybrid system.

Based on the assumed mission requirements, the orbit energy is higher than the maneuver energy, and the hybrid battery system is not justified. In addition, the complexity of using two different battery systems can only be justified if substantial weight savings are possible.

Silver-Oxide Cadmium Battery Subsystem--Based on the tradeoffs shown in Section 4.2 of D2-82709-2 and the discussion on hybrid systems above, the silver-oxide cadmium battery will be used for the mission. A further analysis was made to determine the best method to achieve a high reliability system with redundancy, if necessary, at minimum weight.

Consideration was given to: one silver-cadmium battery operating at different depths of discharge; batteries operating in parallel such that if one battery fails, the remaining units would still be capable of performing the entire mission; and the use of batteries containing additional cells in series with failure diode protection across each cell such that as the cell failed, the diodes would shunt current past it to enable the remaining cells in the series string to continue to operate.

The total battery package weights, based on a 1230 watt-hour mission requirement are shown in Table 4.2-18.

The watt-hours-per-pound obtainable at 100 percent depth of discharge were based on Figure 4.2-62. The use of one battery at 75 percent depth, which is the maximum depth that can be considered for multiple cycling operation (D2-82709-2, Section 4.2), provides the lightest weight package. This represents a relatively unreliable package since failure of any one of the cells in the series stack will render the battery inoperable. A second alternative use of one battery at a shallower (50 percent) depth of discharge was considered. This enables a more reliable mode of cycling operation but it still exhibits the weakness that if a single cell in the stack has been assembled or manufactured improperly it could render the entire battery and power system useless.

The next consideration was the use of two parallel batteries, either one capable of performing the entire mission. This appraoch would provide rather shallow depths of discharge in normal use and provides for an individual cell or battery failure prior to the completion of the mission. However, the total weight for the two complete batteries is considered excessive, so, another alternative was considered using 3 batteries in parallel, two of which would be capable of performing the mission if one failed. The three-battery system would result in a total-package weight of approximately 123 pounds. The package weight as a function of number of batteries is presented in Figure 4.2-65.

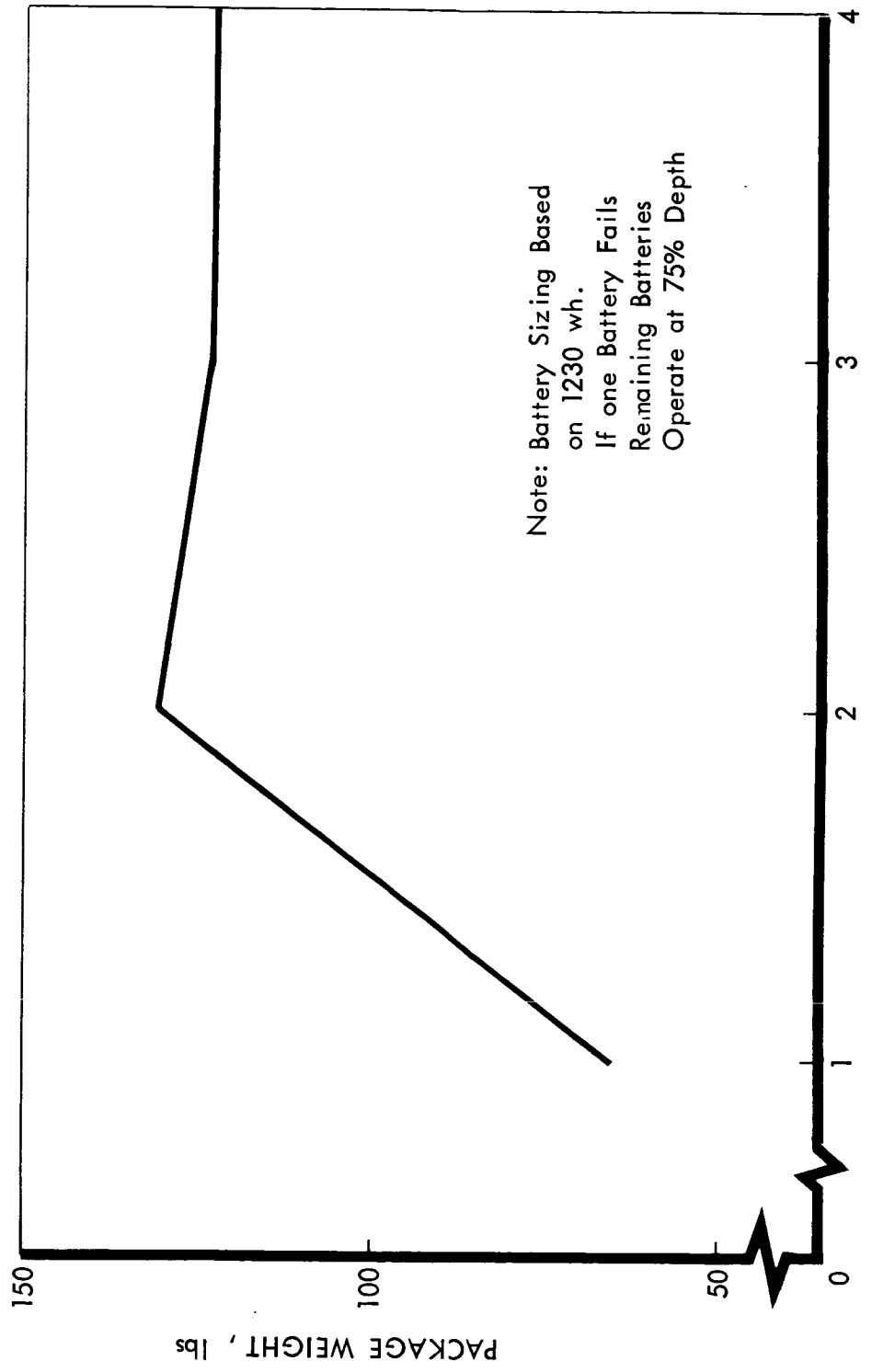

Figure 4.2-65: Multiple Battery Weight as a Function of Number of Batteries

Table 4.2-18: ALTERNATE BATTERY APPROACHES

Approach	Depth of Discharge Normal (%)	Depth of Discharge After One Battery Failed (%)	Actual Battery Capacity (A.H.)	W.H./lb at 100% Depth	W.H./lb/ Cycle Normal Use	Individual Battery Weight (lbs)	Package Weight (lbs)
One Battery	75	-	43	25	18.7	65.7	65.7
One Battery	50	-	65	27	13.5	91	91
Two parallel batteries	37.5	75	43	25	9.4	65.7	131.4
Three parallel batteries	50	75	21.6	20	10	41	123
Four parallel batteries	56	75	14.3	18	10.1	30.5	122
One battery, 3 extra cells plus diode protection	50	-	65	27	13.5	103	103
	60	-	54	26	15.6	90	90

Since battery failures occur on an individual cell basis, the ideal method of achieving increased reliability would be to shunt individual cells in a series-connected battery as the individual cell failures occur. Pursuing this line of thinking, a single battery may be used containing, for example, three extra cells electrically connected across each cell, such that if a failure condition of a cell occurs the current would be shunted past the cell. Associated with the use of this scheme would be the necessity that the spacecraft power conditioning equipment be operable over a wider range of voltages (greater than 38 to 100 volts) since a number of cell failures could be encountered resulting in approximately a 1.5 volt drop in battery terminal voltage per cell failure.

Two depths of discharge for diode battery packages containing three extra cells in series are shown in Table 4.2-18. These weights are based on estimates of diode and heat sink weights in addition to the battery package weight.

Based on the above analysis, the three-battery approach is selected for the Voyager preferred design. This system offers a reasonable package weight with minimum complexity. The use of more than three batteries in parallel does not provide any substantial decrease in weight of the total system.

Charging Techniques--For the orbiting portion of the Voyager mission, the battery subsystem will be charged over a 15.1-hour period, and discharged over a 2.9-hour period, for a total of an 18 hour cycle. The

method by which the energy taken out of the battery during discharge is replaced and the control techniques utilized to prevent overcharge are very critical to assure reliable battery operation. Charge techniques consisting of constant potential charging, constant current charging, and modification of these two methods were considered. For the silver-cadmium battery, it is desirable to charge in such a manner as to minimize gassing at the end of charge. This consideration eliminates the use of a straight constant-potential charging, since very high charge currents can be encountered. Also, it is impractical when charging from solar cells to charge at very high wattages initially, and low wattages toward the end of discharge. This will have the effect of necessitating oversize solar panels. A straight constant current charge is acceptable during the normal charging period, but provision must be made to stop charging when the battery reaches the end of the charge voltage to prevent continuous overcharge. However, if the unit has overcharge capability equivalent to the constant current charging, no problem ensues. Therefore, the most logical compromise is to use a constant or maximum current charge during the initial portion of the charging and then switch to a constant potential mode to prevent excessive overcharge as the battery comes up to voltage. This approach is compatible with spacecraft solar panel capabilities.

Some system advantages can be obtained by allowing higher-power charging at the beginning of charge when the solar panels are cold and operating at higher voltages. This makes best use of the solar power and allows for a tapering of charge current at the end of charge. This condition is

achieved by regulating the input current to the battery charger rather than the output current from the battery charger. For a constant solar array operating voltage, this represents a constant power charge to the batteries. Because of this, the solar array area assigned to battery charging must account only for the average charge rate rather than for a peak charge rate that would otherwise occur toward the end of charge of a constant output current charger (since the end of charge voltage is significantly greater than the beginning of charge voltage). Specifically, this technique constitutes a solar array area savings of 25 percent of that assigned to battery charging, or a savings of 13 square feet based on the Voyager requirements.

Based upon the foregoing considerations, the constant-power charger concept is selected.

4.2.11 Power Switch and Logic--Component Functional Description

The power switch and logic unit (PS&L) accepts power from the spacecraft solar panel sections, the batteries and the external power source (prior to launch) and combines these sources to provide the raw unregulated bus power for the power subsystem. In doing this, it provides proper isolation between the various sources by use of series blocking diodes. Internal/external power switching is accomplished by use of a motor-driven switch. The PS&L also provides a number of voltage and current monitoring circuits for telemetry purposes and monitoring during ground checkout prior to launch. Solar panel, battery, and battery charger performance parameters are measured.

The functional diagram of the PS&L unit is given in Figure 4.2-66. A circuit diagram is provided in Reference 3, drawing No. 614078

4.2.11.1 Performance

When power is available from the solar panels, the battery diodes are back-biased since the solar-panel voltage is higher than the battery voltage. The batteries are isolated from the bus when the solar power is available and may be charged provided that the charging voltage requirement is less than the bus voltage. Batteries are instantly available to provide power during off-Sun periods when solar cells are inactive.

In the battery operating mode, when the solar panels are not illuminated, the bus voltage is equal to the battery voltage (minus diode voltage drops) and the solar-panel diodes become back-biased, thus

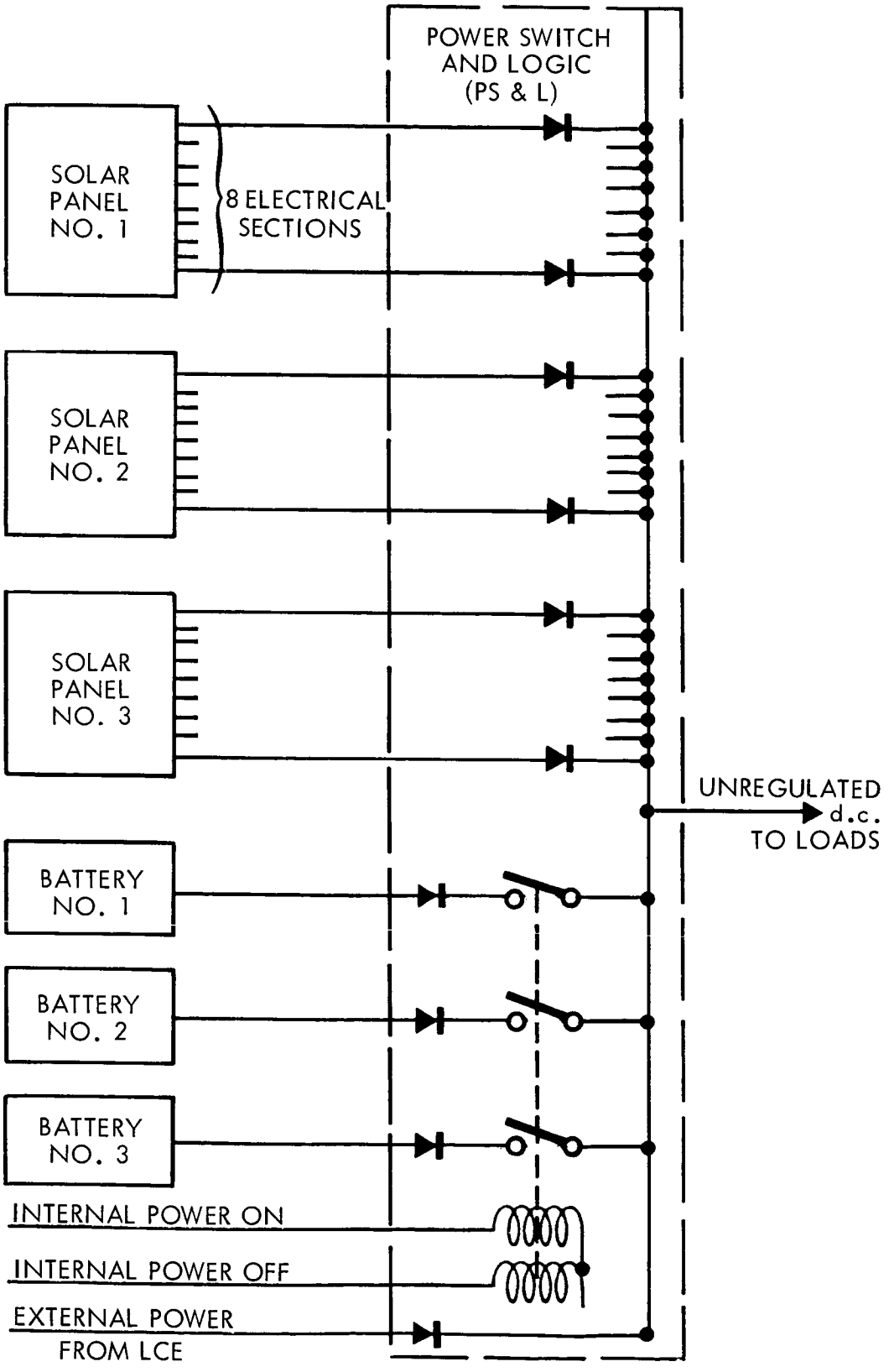

Figure 4.2-66: Power Switch & Logic Schematic

isolating solar panels from the system bus. Separate isolating diodes are provided to connect the batteries to the pyrotechnic bus.

The PS&L provides for telemetry monitoring of solar panel current, battery charge and discharge currents, battery voltage and the unregulated bus voltage and current.

The electrical inputs to the PS&L are d.c. voltage from each solar panel section; d.c. voltage from each of 3 batteries; and external power switching commands. The outputs are: raw d.c. voltage; hardline OSE monitors for raw d.c. voltage and current; temperature-sensor output; pyrotechnic power; and telemetry monitor. Input power lines will be isolated from return lines by use of eight different connectors. Connector pin requirements are as follows:

		Pins	
		Available	Used
1)	3 solar panel inputs	21	16
2)	Battery and external power inputs	35	29
3)	Input power returns	47	39
4)	Raw D.C. output	16	11
5)	Raw D.C. output return	16	11
6)	Telemetry and hardline outputs	45	37

The PS&L efficiency under maximum load conditions is 98.5 percent when operating on solar panels and 98.0 percent when using batteries. An efficiency of 95 percent was used in calculating power subsystem efficiency.

The PS&L weighs 3.2 pounds, with a space factor of 144 cubic inches (8 x 6 x 3 inches).

4.2.11.2 Design Optimization

Three alternate configurations were considered. Their characteristics are given in Table 4.2-19. The first alternate (preferred design) uses a single diode in each input; the second uses redundant diodes (quads) in each input; and the third uses redundant diodes in the battery input leads only. Alternate 1 uses 27 isolation diodes, the second requires 108 diodes while the third alternate requires 36 diodes.

Table 4.2-19: COMPARISON OF ALTERNATE DESIGNS

Alternate	Calculated Reliability	Efficiency (Panel Power)	Efficiency (Battery Power)	Voltage Drop (Volts)	System Weight Increase Over 1st Alternate (Pounds)
1	0.999998	98.4%	97.2%	1	0
2	0.999999	96.6%	94.8%	2	18
3	0.999999	98.4%	94.8%	2	12

Efficiency and voltage drop characteristic of the PS&L are important in that they affect the overall power system. Voltage drops determine selection of battery voltage and the system regulated voltage whereas, efficiency affects solar-panel and battery-power capabilities and, thus, overall system weight.

The first alternate design (using no redundant isolation diodes) is superior to the other designs in all respects except the calculated

reliability. However, the reliability figure exceeds the value allocated to the PS&L and the same basic design has been successfully operated in the Ranger and Mariner C vehicles. Alternates 2 and 3 were not chosen because of the increased voltage drop, reduced efficiency, and higher weight.

4.2.12 Battery Charger--Component Functional Description

A battery charger assembly is provided to recharge the battery after off-Sun battery energy requirement periods. Battery charging can be accomplished during conditions when the system raw bus voltage is higher than the charging voltage requirement. A functional block diagram is shown in drawing no. 614068 of Reference 3.

The battery charger assembly consists of three charger modules (one for each of the three batteries). The circuit diagram appears in Reference 3, drawing no. 614080.

4.2.12.1 Performance

The charger consists of a transistor switch and a filter driven by a pulsewidth modulator (PWM) that controls energy delivered to the battery. The PWM is controlled by the charger input current and the battery state of charge. Charging current will be limited by the PWM until full charge is reached. The charger then shifts to a regulated voltage mode to maintain full charge. Full charge is determined by sensing battery temperature and voltage. When in the constant-voltage mode, the input current limiting sensor is in operation to prevent excessive battery charging if a partial short develops in the batteries.

The failure sensors in each of the charger modules sense charger or battery failures and produce a signal to increase the charge rate of the other two chargers. Failure parameters monitored are high and low charger input currents and battery voltage. On-off ground commands are included to override battery charging.

The electrical interfaces to the battery charger are: unregulated bus, 37 to 100 volts; regulated bus, 35 v.d.c. 3 watts; battery temperature (resistive), one per battery; charger OFF override command (one per charger); and charger ON override command (one per charger). Total output charge power to the batteries is 118 watts average, 180 watts peak. The thermal and mechanical interface is the 8- by 3-inch mounting surface of each charger module. A connector of 23 pins minimum will be used for the charger modules. The efficiency of the chargers will be about 85 percent. Each charger will dissipate a total of 6.3 watts average during charging. Each battery charger will weigh 3 pounds.

4.2.12.2 Design Optimization

A basic constant power-charging regulator was selected to minimize the solar panel area (refer to Section 4.2.10). An analysis of alternate battery charger arrangements is presented in Table 4.2-20.

Table 4.2-20: COMPARISON OF ALTERNATE DESIGNS

Alternate	Reliability	Efficiency (Percent)	Weight (pounds)	Other
1	0.9956	85	8.98	*
2	0.9953	80	12.95	
3	0.9988	85	19.64	
4	0.9962	85	13.58	
5	0.9979	85	10.55	

*Constant-voltage (float) charging after full charge is not possible because charger is switched from battery to battery.

The first design (Figure 4.2-67a) uses one charger that is switched between the three batteries on a time basis. A redundant charger is activated if the primary unit fails. A battery failure will cause switch-over to the next battery so that the remaining two batteries can be fully charged.

The second design (Figure 4.2-67b) uses a primary charger plus a redundant charger, with a current equalizer for each of the three battery lines. The current equalizers divide the charge equally between the three batteries. When a battery reaches full charge, its equalizer is shifted into a constant-voltage mode while the other batteries continue to be charged at a higher current. A failure sensor actuates redundant switch-over and shuts off the current equalizer of the failed channel.

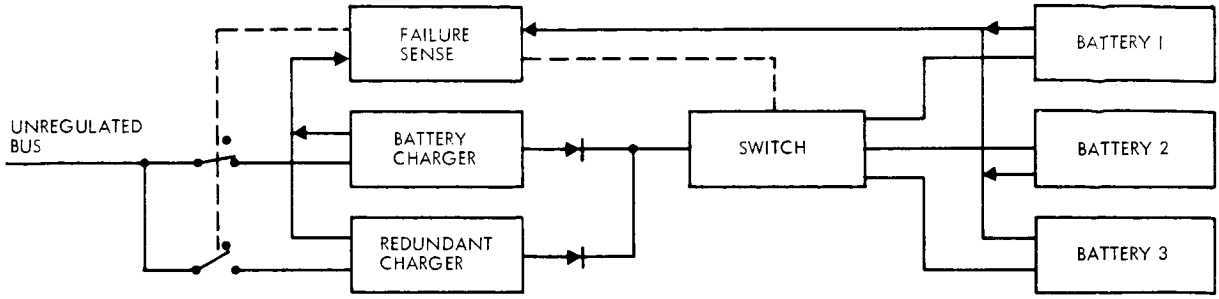

Figure 4.2-67a: Alternate 1

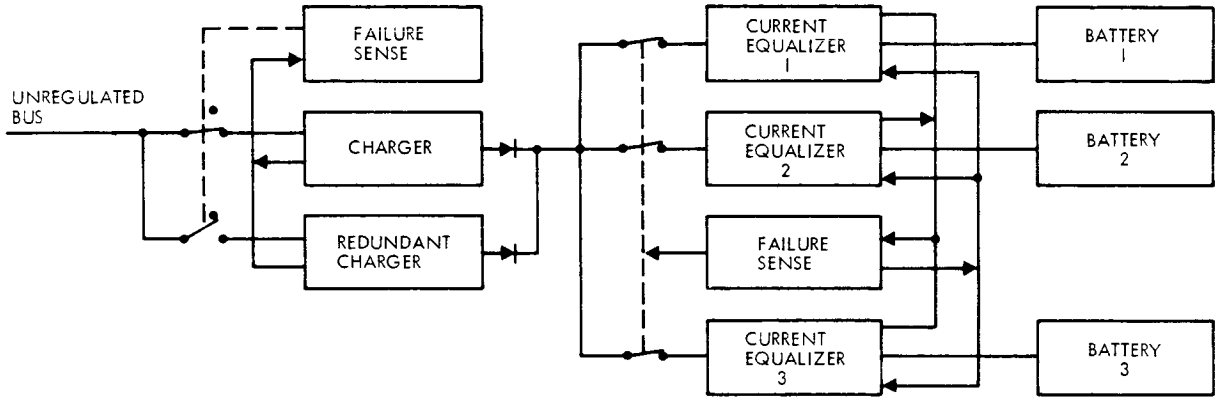

Figure 4.2-67b: Alternate 2

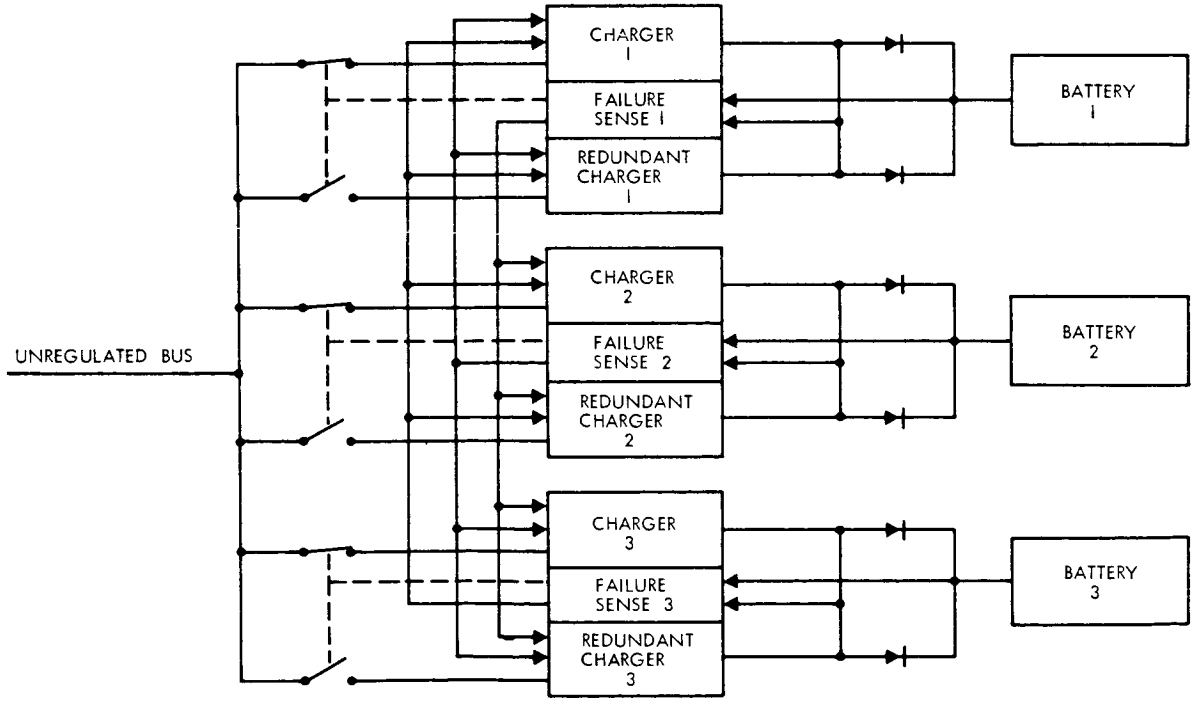

Figure 4.2-67c: Alternate 3

(1)

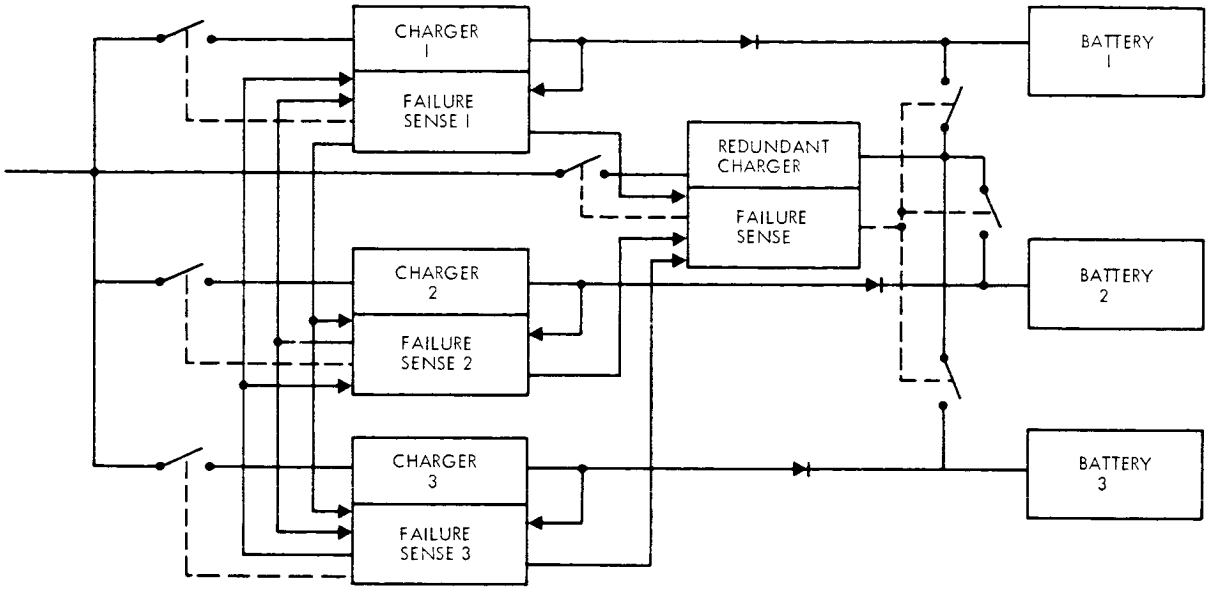

Figure 4.2-67d: Alternate 4

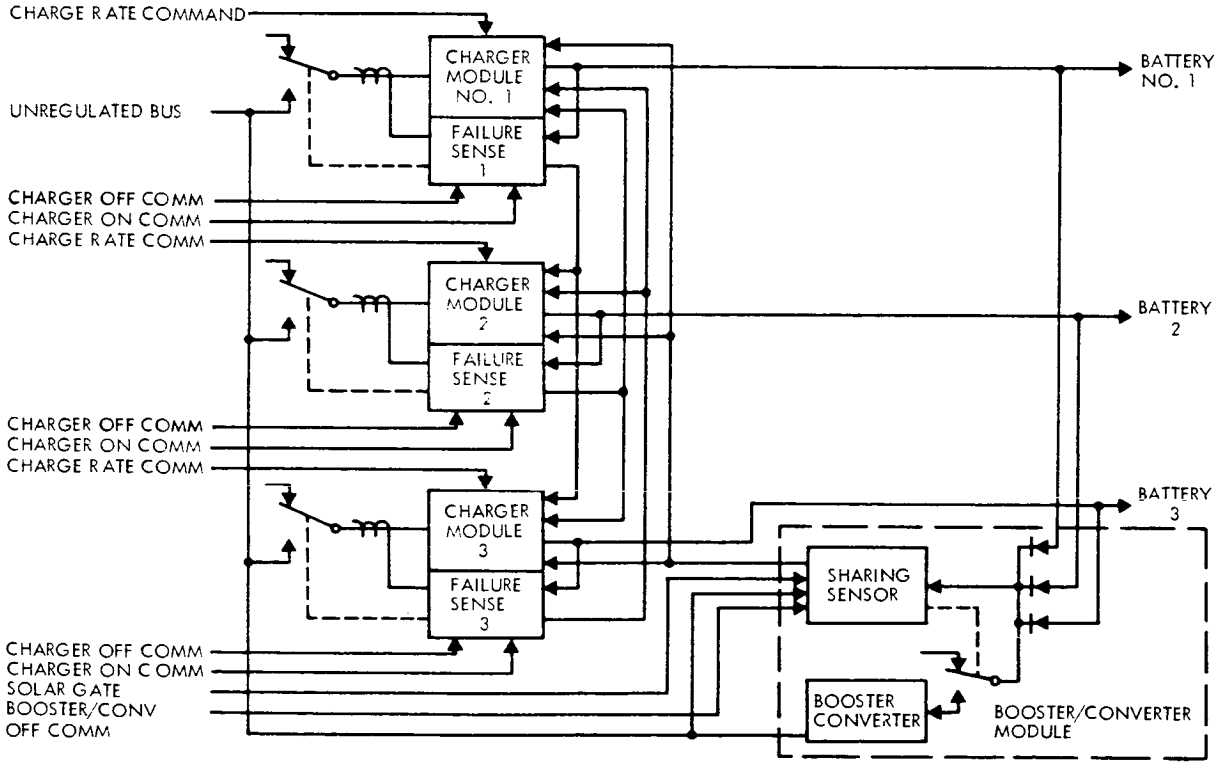

Figure 4.2-67e: Alternate 5

BLOCK DIAGRAMS-ALTERNATE BATTERY CHARGING METHODS

Design 3 (Figure 4.2-67c) uses a charger plus a redundant charger for each battery (six chargers). A charger failure causes redundant switch-over. If a battery fails, its charger is shut off and the charge rate of the other two is increased.

Design 4 (Figure 4.2-67d) uses a charger for each battery, but with a single redundant charger that can be switched in place of any charger that fails. If a battery failure occurs, its channel is turned off by the failure sensor.

Design 5 (Figure 4.2-67e) uses one charger per battery with no redundant chargers. A charger-battery unit can fail without endangering the mission, since two batteries can adequately handle the total load.

The important characteristics of the five charger alternatives are summarized in Table 4.2-20. Alternate 5 has been selected as the preferred design. Only one of the alternates (3) has higher reliability than #5, at the expense of nearly double weight. Alternate 1 has lower reliability and float charging is not possible. Alternate 2 has low reliability and efficiency and is heavy. Alternate 4 has no reliability advantage and is heavier than Number 1, 2 and 5.

4.2.13 Booster Converter--Component Functional Description

An undesirable battery-sharing mode is possible under conditions when adequate power is available from the solar panels to supply all system loads. To sense this condition battery-sharing sensing circuitry is provided. A booster converter is provided to modify the bus voltage

sufficiently to transfer from battery sharing to solar power whenever the battery-sharing sensor dictates.

The battery-sharing sensor and booster converter are shown in a functional block diagram in drawing number 614068 of Reference 3. The circuit diagram is shown in Reference 3, drawing number 614085.

The booster converter module contains a share-sense circuit that determines when battery power is used, stops battery charging, and resets the charger for normal charging when solar-panel power becomes available. When a signal from the Sun-sensor indicates that the solar panels are Sun-oriented, and the share-sensor indicates battery sharing, the booster converter adds power obtained from the battery to the unregulated bus and thus shifts the operating point to the high-voltage, low-current mode.

On and off ground commands are included to override booster converter operation.

The electrical interfaces to the share-sensor and booster converter are: battery power, 100 watts for 10 milliseconds (intermittent); Sun-sensor signal; and booster-converter-off override command.

The thermal and mechanical interface is the 8-by-2-inch mounting surface of the booster converter.

A connector with 21 pins minimum will be used for the booster module.

The booster converter will weigh 1.5 pounds.

4.2.14 Series Switching Regulator--Component Functional Description

The series switching regulator is a closed-loop control system that regulates constant output voltage under conditions of wide input voltage variation and output load variation. The basic regulator consists of a transistor switch and an energy storage network driven by a pulsewidth modulator (PWM). The energy storage network maintains continous power to the load. The pulsewidth is controlled by the PWM, which in turn is controlled by the output voltage level.

The series switching regulator circuit diagram is shown in Reference 3, drawing number 614074.

4.2.14.1 Performance

Capacitors are provided in the regulator to limit output ripple voltage. A "free wheeling" diode circulates load current when the main transistor switch is not conducting. This diode must be an ultrafast type to minimize currents through the switching transistor. A flux oscillator produces a bias voltage to ensure complete saturation of the transistor switch for greater efficiency. A triangular waveform is also produced to set the PWM operating period. An input filter is used to minimize ripple current feedback to the solar panel source.

The series switching regulator will maintain an output of 35 volts d.c. $\pm$1 percent from no load to full load (400 watts). Six hundred

watts can be delivered to the load for short periods of time. It will also handle peak transient loads of 700 watts for 10 milliseconds. The ripple voltage will be less than 400 millivolts (at 35 volts d.c. input) and transient voltages will be less than 1500 millivolts. The regulator will recover to within 10 percent of the half load level within 1 millisecond with a step increase of from half load to full load. Typical efficiencies of the regulator are shown in Figure 4.2-68a. A regulator efficiency of 90 percent was used for system efficiency calculations.

The input voltage range is from 37 to 100 volts d.c. The 35-volt output is monitored by OSE hardlines through a current-limiting resistor. The thermal and mechanical interface of the series switching regulator is the primary submodule mounting surface of 8 by 4 inches. The circuit utilizes 21 pins of a 31-pin (minimum)connector. The regulator measures 8 by 6 by 4 inches and weighs 6.4 pounds.

4.2.14.2 Design Optimization

The three alternate series switching regulators considered (Table 4.2-21) all use a N.P.N. power transistor switch in series with the input with the switching duty cycle controlled to maintain a constant output voltage (Reference 3, drawing numbers 614073, 614074, 614072).

Table 4.2-21: COMPARISON OF ALTERNATE DESIGNS

Alternate	Predicted Reliability	Efficiency (Percent)	Weight (Pounds)
1	0.99420	92	6.1
2	0.99419	90	6.4
3	0.99482	80	6.1

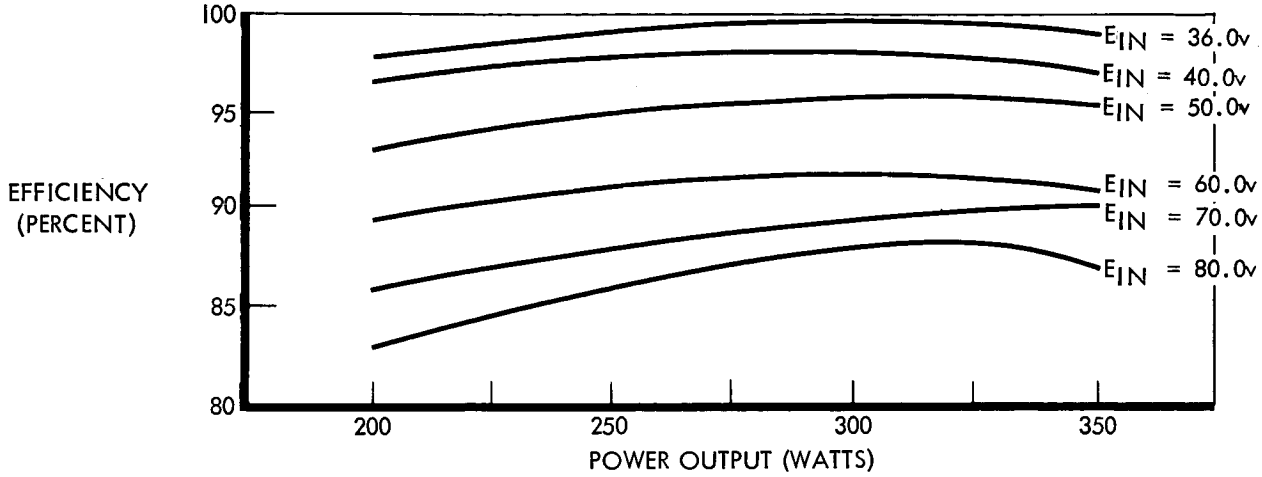

Figure 4.2-68a: Efficiency Vs. Output Power Of Series Switching Regulator

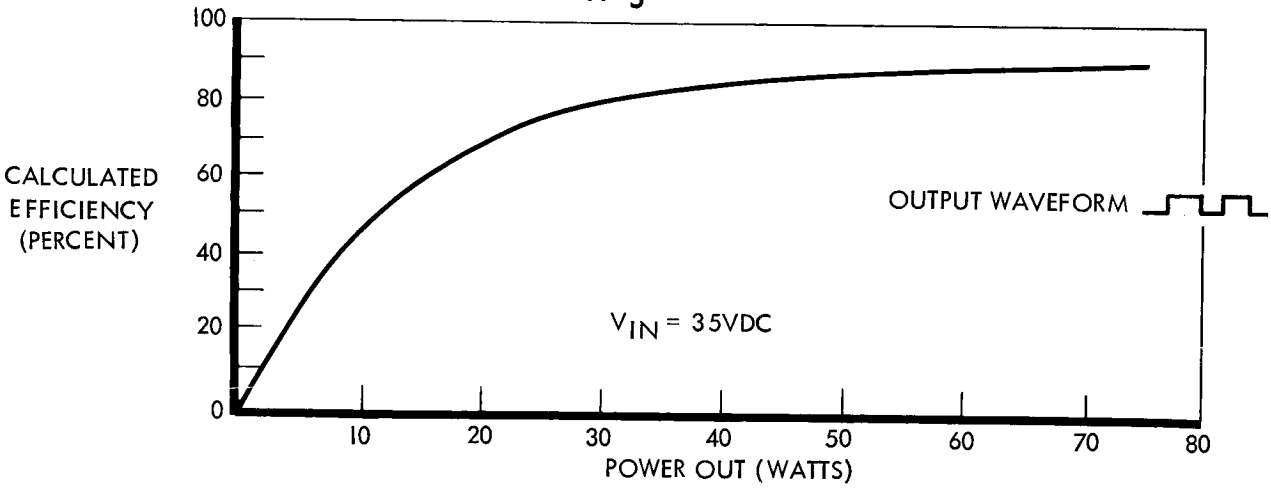

Figure 4.2-68b: 2400-cps Single-Phase Inverter Conversion Efficiency as a Function of Load Power

The first alternate considered uses the transistor switch in the negative lead of the power bus providing an efficient design,but requiring a positive common output lead.

Alternate 2 uses the transistor switch in the positive lead, thereby providing the conventional negative common system. A positive bias voltage is provided to ensure complete saturation of the power transistor during its "on" state.

The switching transistor in Alternate 3 is also placed in the positive lead. In this design, the bias supply is deleted, resulting in a less complex, but lower efficiency unit.

The first alternate design is not recommended for use in the power subsystem because of the serious interface problem and reduced versatility caused by the positive common power system it requires.

The reliability of the third alternate is greater than the second only because of fewer components (no bias supply), but the overall system efficiency suffers. Because of its lower efficiency, an additional 30 to 40 watts would be dissipated, thereby creating an additional load on the thermal control subsystem.

Based on the foregoing analysis, the second alternative is selected for the preferred series switching regulator design.

4.2.15 Inverter-Component Functional Description

A 2400-cps single-phase inverter was selected to supply power to the science subsystem and the attitude reference subsystem. The inverter circuit diagram is in Reference 3, drawing number 614083.

4.2.15.1 Performance

The unit consists of a conventional push-pull type inverter using a linear output transformer to provide the squarewave output. An intermediate-drive transformer provides drive power and has a winding that provides positive feedback to the flux oscillator. The flux oscillator's free-running frequency is determined by the volt-second capability of its square-core transformer and has a freerunning frequency accuracy of $\pm$ 5 percent. An external sync signal will sync the inverter to 0.01 percent accuracy during system operation. The inverter supplies power to two subsystems--the science load requirements are 20 watts during the first trans-Mars cruise, increasing to 75 watts after orbit insertion, and the attitude reference requirement is 2 watts.

The output of the inverter is a 50 volt, $\pm$3 percent, square wave with a rise time of 5, $\pm$ 4, microseconds. The efficiency depends upon load power as shown in Figure 4.2-68b. An efficiency of 85 percent was used for system efficiency calculations. The input power is obtained from the system-35-volt regulated bus.

The thermal and mechanical interfaces are the primary submodule mounting surface which is 2 by 8 inches. The size of the unit is 2 by 8 by 6 inches and weighs 2 pounds.

The circuit will use 11 pins of a 16-pin (minimum) connector.

4.2.15.2 Design Optimization

Two alternate designs (Table 4.2-22) were considered for the 2.4 kc inverter, (Reference 3, drawing numbers 614082 and 614083).

Table 4.2-22: COMPARISON OF ALTERNATE DESIGNS

Alternate	Predicted Reliability	Efficiency (percent)	Weight (pounds)
1	0.99796	88.7	0.70
2	0.99865	90.6	0.63

Alternate 1 is the conventional push-pull type inverter and was derived from the design used in Mariner C. The output components are selected for optimum performance at the 75-watt power level required. A two-transformer-saturable-core oscillator provides the free-running capability of the inverter.

Alternate 2 uses four transistors in a Darlington configuration at the output. This arrangement increases the beta of the output transistor, and thus requires less drive power. The Darlington inverter is driven directly from the saturable-core-oscillator-base-drive transformer, whereas Alternate 1 requires an additional driver stage. The collector of the input transistor is connected to a tap on the output transformer so that it will be capable of driving the output transistor into complete saturation. This is an improvement over conventional Darlington

circuits where the collectors of both transistors are tied together so that complete saturation is unattainable at the output.

There is no appreciable difference of characteristics between the two alternate designs. The conventional push-pull inverter has been selected for the preferred design because this design has been proven on space vehicles.

4.2.16 D. C. Failure Sense Unit--Component Functional Description

The d.c. failure sense unit will sense internal failures and out-of-tolerance conditions of the series switch regulator and switch a standby redundant regulator into operation. The d.c. failure sense unit circuit is shown in Reference 3, drawing number 614071.

4.2.16.1 Performance

Failure sensing is performed by two Schmitt trigger circuits which sense high and low output voltage excursions as an indication of regulator failure modes. When a failure is sensed, redundant unit switching is activated after a time delay. The time delay prevents false transient switchover action. A heavy-duty latching relay is used as the switching device. Other components shown in the schematic (Reference 3,)provide telemetry and OSE monitoring functions for the operating series switching regulator.

The input (raw d.c. voltage) and output (regulated 35 volts d.c.) of the series switching regulator are routed through the switching relay of the unit. An override ground command provides relay reset capability

after redundant switching has occurred. The control circuitry requires 1.5 watts from the unregulated bus. Telemetry signals generated are for regulator input and output currents, regulator output voltage, and a state-of-relay signal.

The mechanical and thermal interface is the 3- by 3- inch primary submodule mounting surface, which is fastened to the case assembly housing. The total unit is 3 by 8 by 6 inches and weighs 2.0 pounds.

Forty-five pins of a 55-pin (minimum) connector will be utilized by the d.c. failure sense unit.

4.2.16.2 Design Optimization

Alternate failure-sensing methods considered were input current sensing and output voltage sensing. Current sensing was discarded early since it will not indicate regulator failures under all system operating conditions. Output voltage sensing of the series switching regulator was selected as the preferred method of failure sensing because it is more reliable and avoids circuit complexity. Schmitt trigger circuits monitor upper and lower limits of the regulator output voltage. Voltage excursions beyond these limits indicate a regulator failure mode.

Switching devices also presented a tradeoff study. Devices considered were semiconductor power switches, motor-driven switches, and latching and nonlatching relays.

The latching relay was selected for the design because it requires the least amount of operating power, weighs less, and minimizes voltage drops presented in series with the voltage regulator.

4.2.17 A.C. Failure Sense Unit--Component Functuional Description

The a.c. failure sense unit will sense internal 2.4-kilocycle inverter failures and out-of-tolerance conditions and perform redundant unit switching. The circuit diagram of the unit is shown in Reference 3, drawing number 614075.

4.2.17.1 Performance

The input (regulated 35 volts d.c.) and output of the 2.4-kilocycle inverter are routed through the switching relay of the unit. An override ground command provides relay reset capability after redundant switching has occurred. The control circuitry requires 1.0 watt from the regulated d.c. bus for operation. Telemetry signals are generated for inverter output voltage and current and a state-of-relay signal.

The mechanical and thermal interface is the 3 by 8 inch primary submodule mounting surface of the unit.

The total unit is 3 by 8 by 6 inches and weighs 1.7 pounds.

Forty-two pins of a 50-pin connector will be utilized.

4.2.17.2 Design Optimization

Many failure sensing schemes were considered, of which the two most promising are discussed below.

Alternate 1 determines a failure by monitoring the ratio of the output voltage to input voltage of the inverter. A differential amplifier, referenced to the 35-volt-d.c. input voltage, senses the inverter output voltage level. Switching to the redundant inverter will occur if the output-to-input voltage ratio is lower than a preset value.

Alternate 2 failure sensing is accomplished by a Schmitt trigger circuit. It initiates redundant switchover when the inverter output voltage drops below a level indicative of an inverter failure. A second trigger circuit gates and activates the voltage sensing circuit only when the inverter d.c. input voltage is above a certain level. Thus, redundant switchover will not occur due to low input voltages, or due to d.c. regulator failure.

Alternate 1 was selected for the preferred design. The main competing characteristic between the two designs is circuit complexity. Alternate 1 uses a single differential amplifier for failure sensing, whereas alternate 2 requires two Schmitt trigger circuits involving 12 more components. Calculated reliabilities of the two designs (of 0.99683, Alternate 1; and 0.99687, Alternate 2) are nearly identical. Weight and performance characteristic differences are also insignificant.

4.2.18 Synchronizer--Component Functional Description

The synchronizer provides synchronizing signals to the 2400 cps inverters to hold close frequency limits (2400 cps ± 0.01 percent).

The synchronizer circuit diagram is shown in Reference 3, drawing number 614067.

4.2.18.1 Performance

The synchronizer receives the 38.4 kilocycle primary clock sync signal from the CC&S and performs the necessary frequency division to produce the sync signals required. It uses JK micrologic binaries to perform the frequency dividing functions. A redundant Colpitts-type oscillator is activated when the primary clock signal is not present or fails.

The synchronizer requires 35 volts d.c., 1 watt for circuit operation. The input clock signal will be 38.4 kilocycles (±0.01 percent), 20 volts peak-to-peak, square wave. The two output sync signals (one for each inverter) will be a 2.4 kilocycle (±2 percent free-running; ±0.01 percent, synchronized) square wave with 4±3 microseconds rise time. Amplitude will be 35 volts peak-to-peak.

The mechanical and thermal interface is the primary submodule mounting surface and is 8 by 1 inches.

The total unit is 1 by 8 by 8 inches and weighs 1 pound.

It will use 15 pins of a 20-pin (minimum) connector.

4.2.18.2 Design Optimization

Several alternate designs were considered to provide the synchronization required. The type of binary circuits used presents one tradeoff consideration, while other alternates represent a tradeoff in the redundant internal oscillator approach.

Table 4.2-23: COMPARISON OF ALTERNATE DESIGNS

Alternate	Reliability	Binary Complexity	Power Losses
1	0.99813	Micrologic	Least Power Loss
2	0.99835	Discrete Component	Most Power Loss
3	0.99934	Micrologic	
4	0.99808	Micrologic	

Alternate 1 (reference 3, drawing number 614076) considers use of micrologic JK binary circuits to perform the frequency dividing function. A redundant oscillator remains "free running" with its output inhibited by the presence of a CC&S clock signal.

Alternate 2 (reference 3, drawing number 614070) is identical to Alternate 1 except that discrete component binaries are used in the former.

Alternate 3 (reference 3, drawing number 614067) utilizes micrologic countdown circuitry, but differs in that an inactive redundant oscillator

is used. Failure or absence of the clock signal causes application of power to the oscillator, which then drives the countdown circuitry to produce the sync signal.

Alternate 4 uses the local oscillator to drive the countdown micrologic binaries with the CC&S clock signal providing the local oscillator with synchronization.

Alternate 3 has been selected for the preferred design. It utilizes micrologic circuitry, which is more desirable than discrete component circuitry because it is less complex, dissipates low power, and weighs less. This alternate design also uses a standby redundant oscillator with true parallel redundancy.

CONTENTS

4.3 SPACECRAFT PROPULSION

Summary--The selected spacecraft propulsion module, shown in Figure 4.3-1, consists of a combined solid-fueled-motor and liquid-monopropellant subsystem. Spacecraft-propulsion predicted reliability is 0.997. The module, which weighs 3500 pounds, satisfies all Voyager mission propulsion requirements through 1977. Propulsion-module performance is summarized in Table 4.3-1. The liquid monopropellant subsystem uses four 50 pound thrust, regulated-pressure-fed, radiation-cooled, hydrazine engines. These engines, which employ the Shell 405 spontaneous decomposition catalyst, are operated in pairs, to provide engine redundancy. Thrust-vector control is accomplished by four jet vanes per engine. A total of 395 pounds of hydrazine is stored in two spherical tanks containing butyl bladders for positive expulsion. Regulated nitrogen gas, drawn from the reaction-control-subsystem gas supply, provides bladder pressurization. Both pressurant and propellant are positively isolated after each firing. The solid-fueled motor provides a 5700-foot-per-second orbit-insertion-velocity increment. The oblate spheroid motor case is fabricated of glass filament and epoxy resin. The partially buried nozzle has an exit-to-throat-area ratio of 73 to 1. The propellant is an aluminized polybutadiene cast in a modified conocyl grain that provides for regressive burning. Total propellant weight is 2306 pounds. The average nominal thrust is 7988 pounds, the maximum acceleration during burn is 2.2 g's. Ignition is provided by an aft-mounted, controlled-pressure, Alclo-iron igniter. Pitch and yaw-thrust-vector control is supplied by secondary injection using Freon 114B2 as the injectant fluid and unregulated nitrogen gas as a pressurant. Roll-thrust-vector control is provided by

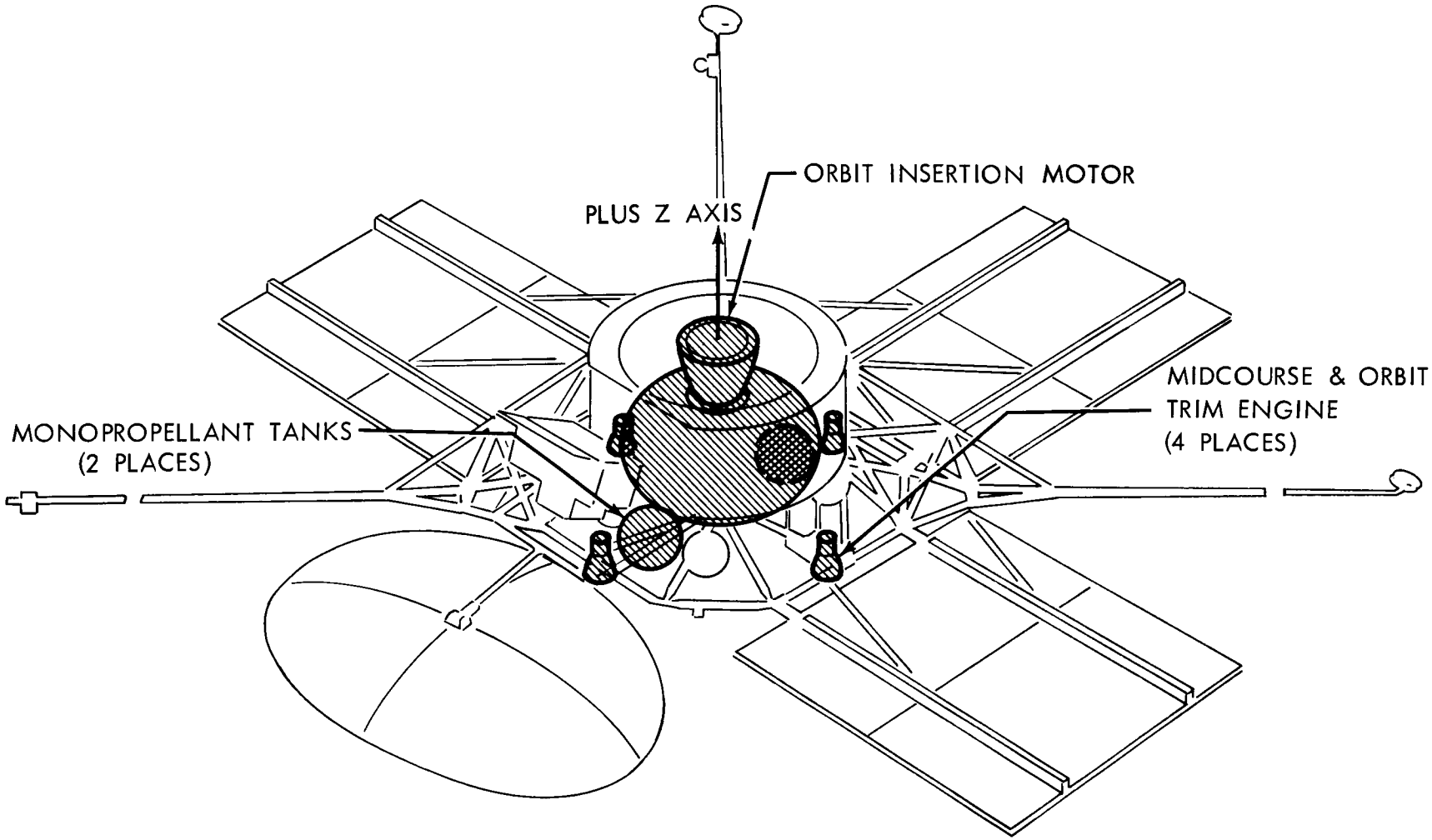

Figure 4.3-1: Propulsion Subsystem

Table 4.3-1: PROPULSION SUBSYSTEM PERFORMANCE PARAMETERS

Propulsion Module	Gross Weight	3,470 lbm
	Contingency	39 lbm
	Maximum allowable	3,500 lbm
	Total inerts	699 lbm
	Contingency	62 lbm
Orbit Insertion Subsystem	Propellant Weight (solid)	2,306 lbm ± .15%, 1σ
	Maximum possible	2,838 lbm (1.)
	Propellant specific impulse (assumed)	300 lbf-sec/lbm
	Total impulse	694,106 lbf-sec ± 0.6%, 3σ
	Thrust, average	7,988 lbf
	Maximum T/W	2.2 lbf/lbm
	Thrust Vector Fluid Weight	61 lbm (2.)
	Thrust Vector Capability	3.0 degrees
	Velocity increment	5700 ft/sec ± .32%
Midcourse Correction and Orbit Trim Subsystem	Propellant Weight (N_2H_4)	395 lbm
	Propellant Specific Impulse	235 lbf-sec/lbm
	Total Impulse	92,825 lbf-sec
	Thrust/per engine	50 lbf ± 1, 3σ
	Maximum T/W (2 engines)	0.0360
	Minimum T/W (2 engines)	0.0128
	Thrust Vector Capability	5 degrees
	Velocity increment (Midcourse)	246 ft/sec (75 m/sec)
	Velocity increment (orbit trim)	328 ft/sec (100 m/sec)
	Minimum Total Impulse Bit (2 engines)	1.0 lbf-sec
	Minimum ΔV (Midcourse)	0.0043 ft/sec ± 10%
	Minimum ΔV (Orbit time)	0.0119 ft/sec ± 10%

Total Propulsion Subsystem predicted reliability = 0.997

1.) Growth capability
2.) Included in inert weight

the reaction-control subsystem. A functional block diagram of the propulsion subsystem is shown in Figure 4.3-2. The module is sterilized to prevent planetary contamination. The Propulsion subsystem is designed to perform the functions highlighted on the accompanying Mission Sequences Matrix.

4.3.1 Scope

The Planetary Vehicle requires propulsion capability for midcourse corrections to remove or reduce trajectory dispersions and perform required trajectory biasing. Additional capability is required for inserting the Flight Spacecraft into orbit around Mars and subsequent orbit trimming.

This section presents a functional description of the preferred Spacecraft Propulsion design. The process leading to selection of this design, supporting trade studies and analyses are described in Boeing Document D2-82709-2, Section 4.3.

4.3.2 Applicable Documents

1) Aerojet General Corporation, "Voyager Retropropulsion Motor Program, Phase IA Report, A Proposal to The Boeing Company," Proposal SNP-65564-2 as amended, Division of General Tire, Sacramento, California, June 1965 (Unclassified).

2) Aerojet General Corporation, "Voyager Retropropulsion Motor Program, Phase IA Report, Confidential Supplement to, A Proposal to The Boeing Company," Proposal SNP-65564-2, Division of General Tire, Sacramento, California, June, 1965 (Confidential).

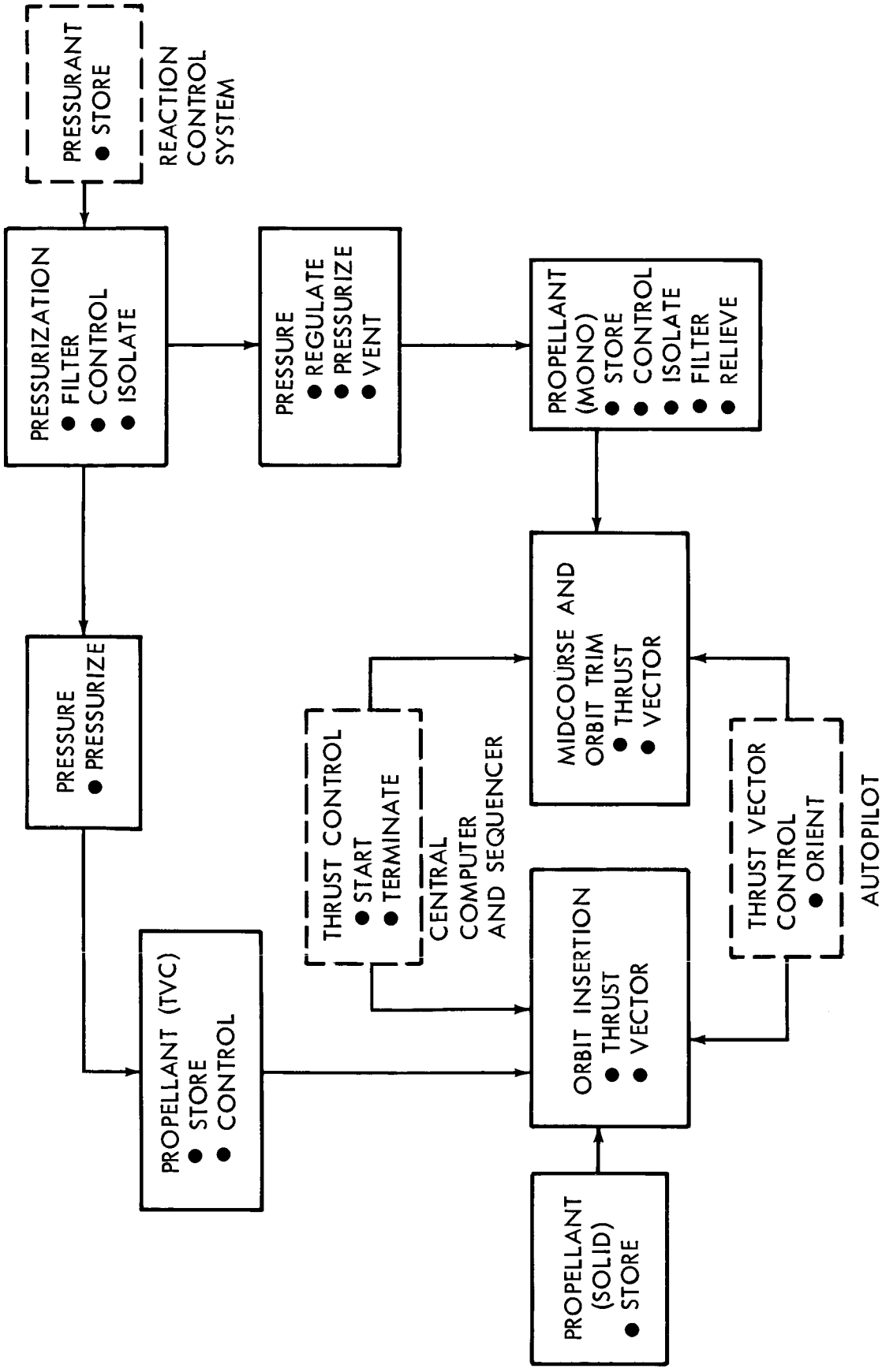

Figure 4.3-2: Propulsion Subsystem Functional Diagram

	1.0 PRELAUNCH AT ETR	2.0 LAUNCH & INJECTION (INCLUDES COUNTDOWN)
GROUND COMPLEX (MOS, LOS, & DSN)	OPERATIONAL READINESS TEST, S/C-DSN COMPATIBILITY TEST SCHED & COORD ETR ACTIVITIES C/O & SUPPORT MOS (DSN ONLY) LOAD CC&S WITH FLIGHT PROGRAM	MOS/LOS A) COMMAND LIFTOFF B) TRACK VEHICLE DURING BOOST C) SUPPLY FLIGHT COMMANDS (AS REQ) D) RECEIVE & ANALYZE DATA FROM S/C & BOOSTER E) STANDBY ON ALERT F) COMMUNICATE WITH ETR CHANGE FROM MOS/LOS TO D ON INJECTION INTO TRANSM DSN A) PROVIDE SFDF/DSIF WITI B) RECEIVE ANTENNA SEARC C) SEARCH FOR & ACQUIRE D) ESTABLISH & VERIFY CO E) TRACK S/C (1-WAY) F) RECEIVE & ANALYZE ENGI
SPACECRAFT TELECOMMUNICATIONS	SUBSYSTEM C/O & STATUS MONITORING	A) TRANSMIT ENGINEERING DATA VIA CENTAUR TELEMETRY B) TRANSMIT ENGINEERING DATA VIA LOW POWER LAUNCH EXCITER C) RECEIVE POWER FROM E/P
CENTRAL COMPUTER & SEQUENCER (CC&S)	A) SUBSYSTEM C/O & STATUS B) COMMAND OTHER SUBSYSTEMS FOR C/O & STATUS MONITORING C) READY ALL SUBSYSTEMS FOR LAUNCH D) LOAD CC&S WITH FLIGHT PROGRAM	PROVIDE BACKUP COMMANDS AS REQUIRED
ATTITUDE REFERENCE SUBSYSTEM AUTOPILOT SUBSYSTEM REACTION CONTROL SUBSYSTEM (RCS)	SUBSYSTEM C/O & STATUS MONITORING	A) ATTITUDE REFERENCE — GYROS OFF DURING LAUNCH B) AUTOPILOT — OFF C) RCS — OFF
MIDCOURSE CORRECTION PROPULSION SYSTEM ORBIT INJECTION PROPULSION SYSTEM	SUBSYSTEM C/O & STATUS MONITORING	
ELECTRICAL POWER SUBSYSTEM	SUBSYSTEM C/O & STATUS MONITORING	A) PROVIDE ENGRG DATA FOR TELECOMUNICATIONS SUBSYSTEM B) PROVIDE BATTERY POWER TO: • TELECOMMUNICATIONS SUBSYSTEM • CC&S • ATTITUDE REFERENCE SUBSYSTEM • AUTOPILOT SUBSYSTEM
S/C STRUCTURE SUBSYSTEM S/C MECHANISMS SUBSYSTEM INSTALLATION CABLES & TUBING	SUBSYSTEM C/O & STATUS MONITORING	A) PROVIDE PHYSICAL SUPPORT FOR ALL EQUIPMENT B) PROVIDE ATTACHMENT FOR CAPSULE C) SUPPORT FLT CAPSULE
TEMPERATURE CONTROL SUBSYSTEM	SUBSYSTEM C/O & STATUS MONITORING SPACECRAFT COOLING SUPPLIED BY CENTAUR	A) PROVIDE HEAT SINK COOLING CAPABILITY UP TO SHROUD JETTISON B) TEMPERATURE CONTROL AFTER SHROUD JETTISON
PYROTECHNIC SUBSYSTEM	SUBSYSTEM C/O & STATUS MONITORING	
SCIENCE EXPERIMENTS (GFE)	SUBSYSTEM C/O & STATUS MONITORING S/C MAGNETIC MAPPING (FAT)	
DATA AUTOMATION EQUIPMENT (GFE)		

REPEAT UP TO

3.0 ACQUISITION

4.0 INTERPLANETARY CRUISE

+ CONTROL 'S ORBIT ANTENNA DATA C ROL OF S/C DATA	DSN A) MONITOR BOOSTER SEPARATION B) MONITOR SOLAR PANEL DEPLOYMENT C) MONITOR ANTENNA DEPLOYMENT D) PROVIDE COMMANDS TO BACK UP CC&S AS REQUIRED E) TRACK S/C F) REC DATA G) MONITOR SCIENCE DEPLOYMENT DSN H) MONITOR & VERIFY ACQUISITION OF SUN I) MONITOR & VERIFY ACQUISITION OF CANOPUS J) COMMAND REACQUISITION OF CANOPUS (AS REQD) K) MONITOR S/C TRAJECTORY L) UPDATE CC&S TRAJECTORY PARAMETERS FOR PITCH, YAW, & ROLL M) COMPUTE CC&S PITCH,YAW,&ROLL POLARITY	DSN A) TRACK S/C B) RECEIVE & DISPLAY SCIENCE & ENGINEERING DATA C) MONITOR S/C & CAPSULE STATUS D) PROCESS DATA ON EARTH TO OBTAIN GUIDANCE COMMANDS (STORED COMMANDS & START TIMES)	A) B) C) D) E) F)
	A) TRANSMIT ENGINEERING DATA B) RECEIVE POWER FROM E/P C) RECEIVE VIA LOW-POWER LAUNCH EXCITER DETECT & SEND TO CC&S COMMAND SIGNALS FROM EARTH D) TRANSMIT CELESTIAL REFERENCE ACQUISITION TO DSN E) TRANSMIT VERIFICATION OF DEPLOYMENT OF SOLAR PANELS, ANTENNAS, ETC TO EARTH F) TWO-WAY TRACKING	A) TRANSMIT ENGINEERING & SCIENCE DATA VIA DATA MODE NO. 2 (OPTIONAL MODE NO. 3) B) TRANSMIT CAPSULE ENGINEERING DATA C) TRANSMIT CONE-ANGLE SETTINGS (CANOPUS TO EARTH) D) EXERCISE & CALIBRATE HIGH-GAIN ANTENNA T + 40 DAYS E) SWITCH FROM LOW-GAIN TO HIGH-GAIN ANTENNA T + 80 DAYS F) PROVIDE RANGING SIGNAL TO A MAX. RANGE OF 8.0×10^6 KM (NOMINAL) G) SWITCH TRANSMISSION FROM LAUNCH EXCITER TO TWT POWER AMPLIFIER AND DATA MODE NO. 2	A) B) C) D) E) F) G)
	A) COMMAND SIGNALS TO PYROTECHNICS & MECH TO DEPLOY • SOLAR PANELS • HIGH-GAIN ANTENNA • VHF ANTENNA • LOW-GAIN ANTENNA • SCIENCE BOOM B) SWITCH ON GYROS & SELECT MODES C) ENABLE SUN-SENSOR ROLL AND PITCH CONTROL D) RECEIVE SUN PRESENCE SIGNAL E) TURN ON CANOPUS TRACKER F) SWITCH ROLL CONTROL TO CANOPUS SENSOR G) ACTIVATE MAGNETOMETER (CALIBRATION ROLL) H) RECEIVE CANOPUS PRESENCE OUTPUT SIGNAL I) TRANSMIT VERIFICATION TO TELE-COMMUNICATION SUBSYSTEM (CANOPUS & SUN PRESENCE) J) PERFORM COMMAND FUNCTIONS FOR CANOPUS OVERRIDE AS REQUIRED K) BACKUP COMMANDS AS REQUIRED	A) COMMAND TELECOMMUNICATION TO DATA MODE NO. 2 B) COMMAND CRUISE SCIENCE ON (WARMUP) — SCIENCE INSTRUMENTS C) COMMAND DATA RECORDERS ON D) COMMAND TWTA ON E) SWITCH CANOPUS ANGLE AS REQUIRED F) INITIATE CRUISE SCIENCE DATA ACQUISITION G) COMMAND TELECOMMUNICATION CHANGE FROM OMNI TO HIGH-GAIN ANTENNA H) UPDATE HIGH-GAIN ANTENNA POSITION (AS REQUIRED) I) COMMAND TELECOMMUNICATIONS — CHANGE DATA TRANSMISSION RATES J) COMMAND RECALIBRATION OF SCIENCE ELEMENTS AS REQUIRED K) BACKUP COMMANDS AS REQUIRED	A) B) C) D) E) F) G) H) I) J) K) L) M) N)
	A) RECEIVE CC&S COMMAND SWITCH ON GYROS, RCS, & AUTOPILOT B) DAMP ROTATION C) YAW & PITCH SPACECRAFT TO ACQUIRE SUN D) RELAY SUN ACQUISITION SIGNAL TO CC&S E) TURN ON CANOPUS SENSOR, ROLL 360 TO CALIBRATE MAGNETOMETER F) ROLL TO ACQUIRE CANOPUS & PROVIDE STAR MAP G) RELAY ACQUISITION SIGNAL (CANOPUS) TO CC&S H) PERFORM CANOPUS OVERRIDE ROLL MANEUVER AS REQUIRED	A) UPDATE CANOPUS CONE ANGLE ON COMMAND B) SWITCH AUTOPILOT TO CRUISE MODE C) MAINTAIN S/C ATTITUDE TO CELESTIAL REFERENCES DURING CRUISE	A) B) C) D) E) F) G)
			M) A) B) C) D) E) F)
	A) PROVIDE POWER TO PYROTECHNIC SUBSYSTEMS FOR SQUIB FIRINGS B) PROVIDE POWER TO MECHANISMS C) ACTIVATE SOLAR POWER SYSTEM AFTER SUN ACQUISITION (AUTOMATIC) D) TRANSMIT "VOLTAGE SATISFACTORY" SIGNAL TO CC&S E) PROVIDE POWER TO: • TELEMETRY • CC&S • TEMPERATURE CONTROL • AUTOPILOT	A) PROVIDE CONDITIONED SOLAR ELECTRICAL POWER TO: • TELEMETRY • CAPSULE • CC&S • ATTITUDE REF • AUTOPILOT • TEMPERATURE CONTROL • SCIENCE B) CHARGE BATTERIES	A
	A) PROVIDE PHYSICAL SUPPORT FOR ALL EQUIPMENT B) DRIVE SOLAR PANELS TO LIMIT STOPS C) PROVIDE OUT & LOCK SIGNALS TO TELEMETRY D) DRIVE HIGH-GAIN ANTENNA TO OPERATING POSITION & LOCK E) DRIVE VHF & OMNI ANTENNAS TO OPERATING POSITION & LOCK F) DRIVE MAGNETOMETER BOOM TO OPERATING POSITION & LOCK G) SUPPORT FLT CAPSULE	A) SUPPORT S/C ASSEMBLIES B) SUPPORT S/C COMPONENTS C) MAINTAIN ADEQUATE ALIGNMENT BETWEEN COMPONENTS D) PROVIDE ACCEPTABLE STATIC & DYNAMIC LOAD ENVIRONMENTS E) SUPPORT FLIGHT CAPSULE	A B C D E
	PROVIDE TEMPERATURE CONTROL	PROVIDE TEMPERATURE CONTROL	P
	RECEIVE SQUIB FIRING SIGNALS FOR DEPLOYMENT OF: • SOLAR PANEL • MAGNETOMETER BOOM • LOW-GAIN ANTENNA • HIGH-GAIN ANTENNA • VHF ANTENNA		A B C
	A) CALIBRATE MAGNETOMETER DURING S/C ROLL B) CALIBRATE OTHER SCIENCE INSTR AS REQUIRED	A) RECEIVE CRUISE SCIENCE "ON" COMMAND B) ACQUIRE CRUISE SCIENCE DATA C) TRANSFER CONDITIONED DATA TO DAE D) RECEIVE POWER FROM E/P E) RECALIBRATE SCIENCE EXPERIMENTS AS REQUIRED	A B
		A) RECEIVE DAE "ON" COMMAND B) PROCESS & TRANSFER DATA TO TM	

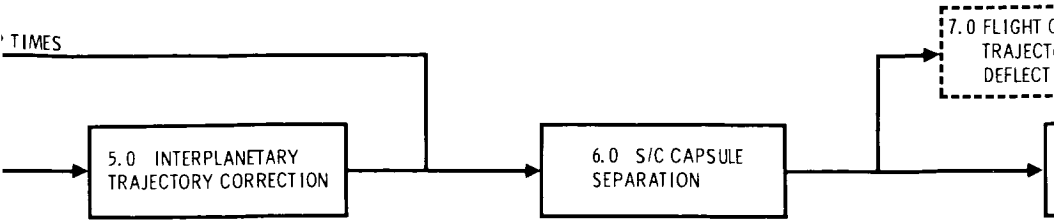

E ROLL TURN MAGNITUDE & DIRECTION E YAW TURN MAGNITUDE & DIRECTION E MIDCOURSE MOTOR BURN DURATION AND ΔV E INITIATE MANEUVER SEQUENCE COMMAND E VERIFICATION OF CORRECTION MANEUVER REES OF YAW & ROLL JST DURATION QUISITION OF CELESTIAL REFERENCES SPACECRAFT	A) INITIATE PRESEPARATION SEQUENCE B) RECEIVE CAPSULE STATUS DATA C) COMMAND SEPARATION D) VERIFY CAPSULE PROGRAM E) VERIFY SEPARATION F) TRACK CAPSULE & SPACECRAFT	A) TRANSMIT ORBIT • ROLL MAGNITU • YAW MAGNITU • MOTOR BURN B) TRACK FLIGHT SI C) RECEIVE, REDUC D) PROVIDE COMMA
E ROLL & YAW TURN COMMAND & RELAY TO CC&S E ANTENNA POSITIONING DATA & RELAY TO CC&S E MOTOR BURN DURATION AND & ΔV RELAY TO CC&S E INITIATE MANEUVER COMMAND & RELAY TO CC&S H TO DATA MODE NO. 1 (FOR LATE MIDCOURSE MANEUVERS) VERIFICATION OF CORRECTION MANEUVER TO DSN AND/OR TRANSMIT ENGINEERING DATA TO DSN (MODE 3) MIT ENGINEERING (SPACECRAFT & CAPSULE) + CRUISE SCIENCE I (MODE 2)	A) RECEIVE PRESEPARATION SEQUENCE COMMANDS & RELAY TO CC&S B) SWITCH TO DATA MODE NO. 2 C) TRANSMIT CAPSULE ENGRG DATA TO DSN D) RECEIVE SEPARATION COMMAND FROM DSN & ROUTE TO CC&S E) STORE AND/OR TRANSMIT ENGINEERING DATA TO DSN (MODE 3) TRANSMIT ENGINEERING (SPACECRAFT & CAPSULE) + CRUISE SCIENCE TO DSN (MODE 2)	A) RECEIVE ROLL & TO CC&S B) RECEIVE ANTENN C) RECEIVE MOTOR- D) RECEIVE CAPSUL E) TRANSMIT FLIGH SCIENCE DATA T
AND TELECOMMUNICATION TO DATA MODE NO. 1 /E TRAJECTORY CORRECTION PARAMETERS H GYROS TO RATE CONTROL AND ANGULAR MANEUVER /E GYRO SIGNALS & SUM FOR ANGULAR MANEUVERS H ATTITUDE REFERENCE TO AUTOPILOT SUBSYSTEM ROPULSION SYSTEM DE COMMAND TO INITIATE ATTITUDE MANEUVER & ΔV MANEUVER /E ACCELEROMETER SIGNALS & INTEGRATE FOR ΔV MANEUVER M PROPULSION SYSTEM AND REVERSE ANGULAR MANEUVER AND REACQUIRE CELESTIAL REFERENCES AND AUTOPILOT SELECTION CONTROL IP COMMANDS AS REQUIRED	A) LOAD CAPSULE WITH 5 OR MORE COMMANDS B) COMMAND CAPSULE SEQUENCING C) COMMAND TELECOMM SWITCH TO DATA MODE NO. 1 D) COMMAND GYROS ACTIVATE (CAPSULE) E) COMMAND GYROS ESTABLISH POLARITY (CAPSULE) F) COMMAND GYROS TO ATTITUDE CONTROL MODE (CAPSULE) G) COMMAND DATA TAPE RECORDER OFF H) COMMAND CAPSULE ACTIVATE ENTRY SCIENCE I) COMMAND CAPSULE ACTIVATE TELE-COMM & VERIFY RADIO LINK (VHF) J) SELECT T/M MODE FOR TRANSMISSION OF CAPSULE DATA K) COMMAND: BIOBARRIER SEPARATION S/C ORIENT TO SEPARATION ATTITUDE ELECTRICAL CONNECTION SEPARATION VERIFY SEPARATION L) COMMAND REORIENT S/C & REACQUIRE CELESTIAL REFERENCES M) BACKUP COMMANDS AS REQUIRED N) RECEIVE S/C ORIENTATION PARAMETERS	A) COMMAND SWIT B) COMMAND CANO C) COMMAND ANTE D) RECEIVE ORBIT E) PROVIDE SIGNA (CRUISE SCIENC F) SWITCH ON DAT RECEIVE CAPSU G) BACKUP COMMA
H TO GYRO CONTROL /C AND VERIFY /C AND VERIFY ILOT — PROVIDE COMMAND DURING MOTOR BURN ON ACCELEROMETERS DE ACCELERATION DATA ES OFF ACCELEROMETER H) YAW BACK TO ORIGINAL ATTITUDE & VERIFY I) REACQUIRE SUN (FINE SUN SENSOR) & VERIFY J) ROLL TO ORIGINAL ATTITUDE K) LOCK ON CANOPUS & VERIFY L) SWITCH AUTOPILOT FROM GYRO CONTROL TO CELESTIAL REF CONTROL	A) SWITCH TO GYRO CONTROL B) PERFORM ROLL TURN & VERIFY C) PERFORM YAW TURN & VERIFY D) MAINTAIN ATTITUDE DURING SEPARATION E) PERFORM YAW TURN (INVERSE TO C) & VERIFY F) PERFORM ROLL TURN (INVERSE TO B) & VERIFY G) REACQUIRE CELESTIAL REFERENCES H) RETURN TO CELESTIAL REFERENCE ATTITUDE CONTROL MODE	A) UPDATE CANOPI B) SWITCH AUTOP C) MAINTAIN S/C
E PROPULSION SYSTEM RESSURIZATION SYSTEM (FIRE SQUIB VALVE) ROPELLANT FEED SUBSYSTEM (FIRE SQUIB VALVE) ROGRAMMED ENGINES (OPERATE SOLENOID VALVE) DOWN ENGINE E PROPELLANT FEED SUBSYSTEM E PRESSURIZATION SUBSYSTEM		
IDE CONDITIONED SOLAR OR BATTERY POWER TO: EMETRY SS OPILOT ITUDE REFERENCE ACTION CONTROL OPULSION MPERATURE CONTROL ROTECHNIC PSULE	A) PROVIDE CONDITIONED SOLAR OR BATTERY POWER TO: • T/M • CC&S • AUTOPILOT • ATTITUDE REF • REACTION CONTROL • TEMPERATURE CONTROL • PYROTECHNICS • CAPSULE	A) PROVIDE COND • T/M • CC&S • AUTOPILOT • ATTITUDE RE • REACTION C • TEMPERATUR B) CHARGE BATTER
ORT S/C ASSEMBLIES ORT S/C COMPONENTS TAIN ADEQUATE ALIGNMENT BETWEEN COMPONENTS IDE ACCEPTABLE STATIC & DYNAMIC LOAD ENVIRONMENTS ORT FLIGHT CAPSULE	A) SUPPORT S/C ASSEMBLIES B) SUPPORT S/C COMPONENTS C) MAINTAIN ADEQUATE ALIGNMENT BETWEEN COMPONENTS D) PROVIDE ACCEPTABLE STATIC & DYNAMIC LOAD ENVIRONMENTS E) SUPPORT FLIGHT CAPSULE	A) SUPPORT S/C A B) SUPPORT S/C C C) MAINTAIN ADE D) PROVIDE ACCE E) DRIVE SCAN PL
TEMPERATURE CONTROL	PROVIDE TEMPERATURE CONTROL	PROVIDE TEMPERA
VE PROPULSION SYSTEM INHIBIT IDE IGNITION IIT PROPULSION SYSTEM	A) RECEIVE SIGNAL TO REMOVE CAPSULE SEPARATION INHIBIT B) RECEIVE SIGNAL TO FIRE CAPSULE UMBILICAL SEPARATION C) RECEIVE SIGNAL TO FIRE BIOBARRIER REMOVAL D) RECEIVE SIGNAL TO FIRE CAPSULE SEPARATION E) RECEIVE SIGNAL FOR SEPARATION INHIBIT	RECEIVE SQUIB FI OF SCAN PLATFORI
VE CC&S COMMAND "CRUISE SCIENCE OFF" OFF CRUISE SCIENCE	A) RECEIVE CC&S COMMAND "CRUISE SCIENCE OFF" B) TURN OFF CRUISE SCIENCE	A) RECEIVE CRUIS B) ACQUIRE CRUI C) TRANSFER CON D) RECEIVE POWE E) RECALIBRATE S
		A) RECEIVE DAE " B) PROCESS & TR

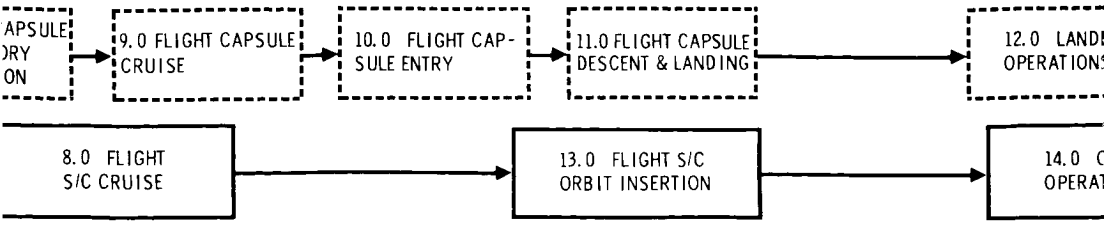

INJECTION PARAMETERS DE & DIRECTION DE & DIRECTION START TIME ACECRAFT & DISPLAY SCIENCE & ENGINEERING DATA NDS TO BACK UP CC&S AS REQUIRED	A) RECEIVE, DECODE, & DISPLAY ENGINEERING DATA B) RELAY UPDATED ORBIT INJECTION PARAMETERS C) PROVIDE COMMAND TO INITIATE INSERTION MANEUVER D) PROVIDE BACKUP COMMANDS TO CC&S AS REQUIRED E) TRACK S/C F) VERIFY ORBIT INSERTION	A) RECEIVE, DECODE, & DISPLAY SCIE B) RECEIVE AND ANALYZE ENGINEERIN C) TRACK S/C D) RECEIVE & DISPLAY CAPSULE DATA E) PROVIDE DATA FOR ORBITAL TRIM F) RECEIVE VERIFICATION OF ORBITAL G) TERMINATE MISSION
AW TURN MAGNITUDE & DIRECTION COMMAND & RELAY POSITIONING DATA & RELAY TO CC&S BURN START TIME, RELAY TO CC&S DATA, CONDITION & RELAY TO GROUND SPACECRAFT ENGINEERING, CAPSULE ENGRG, & GROUND VIA MODE 2	A) UPDATE ROLL-TURN MAGNITUDE & DIRECTION COMMAND & RELAY TO CC&S B) UPDATE YAW-TURN MAGNITUDE & DIRECTION COMMAND & RELAY TO CC&S C) UPDATE MOTOR-BURN START TIME & RELAY TO CC&S D) UPDATE INITIATE MANEUVER & RELAY TO CC&S E) SWITCH TO DATA MODE NO. 2 OR 5A AS REQUIRED F) REACQUIRE EARTH AFTER ROLL TURNS & MOTOR BURN G) RELAY VERIFICATION OF MANEUVERS	A) TRANSMIT SCIENCE & ENGINEERING B) RECORD ENGINEERING & SCIENCE DA C) RECEIVE, STORE & RELAY CAPSULE D) RECEIVE & RELAY DATA FOR ORBIT T
CH TO DATA MODE NO. 2 PUS CONE ANGLE SETTING INA STEP (AS REQUIRED) INJECTION PARAMETERS L TO PYRO & MECHANISMS TO DEPLOY SCAN PLATFORM E TIM OFF) & SWITCH TO DATA MODE NO. 1 RECORDER-COMMAND TELECOMMUNICATIONS E DATA NDS AS REQUIRED	A) UPDATE STORED ROLL, PITCH, & YAW MAGNITUDE & SIGN B) UPDATE STORED VELOCITY MAGNITUDE C) INITIATE MANEUVER SEQUENCE D) COMMAND ORIENTATION OF S/C TO INJECTION ATTITUDE E) COMMAND THRUST FOR ORBIT INSERTION F) COMMAND RETURN TO CRUISE ATTITUDE G) BACKUP COMMANDS AS REQUIRED	A) COMMAND ORBITAL TRIM MANEUVE B) SWITCH DATA MODES AS NECESSAR C) RECEIVE ANY ORBITAL OPERATION D) COMMAND POSITIONING OF SCIENC E) SWITCH ON ORBITAL SCIENCE F) SELECT RECORDED SCIENCE READOU G) BACKUP COMMANDS AS REQUIRED H) STORE DATA FOR ORBIT TRIM (IF RE I) TERMINATE MISSION ON COMMAND
	A) SWITCH TO GYRO CONTROL B) PROVIDE ROLL TO PROPER ATTITUDE & VERIFY ROLL C) YAW TO PROPER ATTITUDE & VERIFY D) AUTOPILOT – PROVIDE COMMAND TO TVC DURING MOTOR BURN E) TURN ON ACCELEROMETER F) PROVIDE ACCELEROMETER DATA TO CC&S G) TURN OFF ACCELEROMETER H) YAW BACK AFTER MOTOR BURN I) ACQUIRE SUN & VERIFY J) ROLL BACK TO PROGRAMMED ATTITUDE K) ACQUIRE CANOPUS & VERIFY L) SWITCH AUTOPILOT FROM GYRO – CONTROL TO CELESTIAL REFERENCE CONTROL	
S CONE ANGLE ON COMMAND LOT TO CRUISE MODE TTITUDE TO CELESTIAL REFERENCES DURING CRUISE		A) MAINTAIN S/C ATTITUDE TO CELEST B) SWITCH AUTOPILOT TO GYRO CONT C) REACQUIRE CELESTIAL REFERENCES D) REORIENT S/C FOR ORBITAL TRIM M E) PROVIDE TVC DURING ENGINE FIRI F) REACQUIRE CELESTIAL REFERENCES G) UPDATE CANOPUS CONE ANGLES ON
	ORBIT INSERTION ENGINE A) ARM TVC B) ARM IGNITER C) FIRE MOTOR & PROVIDE THRUST & TVC D) TERMINATE THRUST (MOTOR BURNS TO DEPLETION)	MIDCOURSE A) ARM PRESSURIZATION & PROPELL B) PROVIDE THRUST (FIRE PROGRAMM IF REQUIRED C) TERMINATE THRUST ON COMMAND D) ISOLATE PROPELLANT FEED SUBSYS E) ISOLATE PRESSURIZATION SUBSY
ITIONED SOLAR ELECTRICAL POWER TO: NTROL CONTROL IES	A) PROVIDE CONDITIONED SOLAR OR BATTERY POWER TO: • TELEMETRY • CC&S • ATTITUDE REFERENCE SUBSYSTEM • AUTOPILOT • TEMPERATURE CONTROL • PULSE TO PYROTECHNICS • PULSE TO PROPULSION	A) PROVIDE CONDITIONED SOLAR OR • TELEMETRY • CC&S • ATTITUDE REFERENCE SUBSYSTE • AUTOPILOT • TEMPERATURE CONTROL • STRUCTURES & MECHANISMS • SCIENCE
SSEMBLIES OMPONENTS UATE ALIGNMENT BETWEEN COMPONENTS TABLE STATIC & DYNAMIC LOAD ENVIRONMENTS ATFORM TO DEPLOYED POSITION & LOCK	A) SUPPORT S/C ASSEMBLIES B) SUPPORT S/C COMPONENTS C) MAINTAIN ADEQUATE ALIGNMENT BETWEEN COMPONENTS D) PROVIDE ACCEPTABLE STATIC & DYNAMIC LOAD ENVIRONMENTS	A) SUPPORT S/C ASSEMBLIES B) SUPPORT S/C COMPONENTS C) MAINTAIN ADEQUATE ALIGNMENTS D) PROVIDE ACCEPTABLE STATIC AND ENVIRONMENTS E) POSITION SCAN PLATFORM
URE CONTROL	PROVIDE TEMPERATURE CONTROL	PROVIDE TEMPERATURE CONTROL
ZING SIGNAL FOR UNLATCHING A	A) RECEIVE & EXECUTE COMMAND SIGNAL TO REMOVE INHIBIT FOR PROPULSION ENGINE B) RECEIVE & EXECUTE SIGNAL FOR PROPULSION ENGINE START C) RECEIVE & EXECUTE COMMAND SIGNAL FOR PROPULSION ENGINE STOP D) RECEIVE & EXECUTE SIGNAL FOR PROPULSION INHIBIT	
E SCIENCE "ON" COMMAND SE SCIENCE DATA DITIONED DATA TO DAE FROM E/P CIENCE EXPERIMENTS AS REQUIRED	SCIENCE OFF DURING ORBIT INSERTION	A) TURN ON ORBITAL SCIENCE INSTR B) ACQUIRE ORBITAL SCIENCE DATA C) TRANSFER CONDITIONED DATA TO D) RECALIBRATE SCIENCE EXPERIME
ON" COMMAND ANSFER DATA TO TM		A) RECEIVE DAE "ON" COMMAND B) PROCESS & TRANSFER DATA TO T

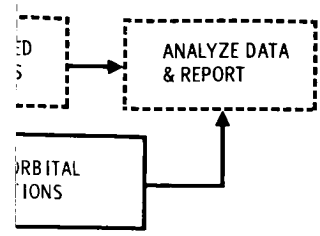

E DATA
DATA

F REQUIRED)
TRIM MANEUVER

DATA VIA DATA MODES 5 AND 6
TA AS COMMANDED
ATA ON COMMAND (MODES 5 AND 6)
RIM IF REQUIRED

RS (IF REQUIRED)
Y
CHANGES & SEQUENCES
E SCAN PLATFORM

T TO TELECOMMUNICATIONS

QUIRED)
(IF REQUIRED)

AL REFERENCES
DL DURING OCCULTATION
FOLLOWING OCCULTATION
ANEUVER USING GYRO CONTROL
G
FOLLOWING MANEUVERS
COMMAND

ANT FEED SUBSYSTEMS
ED ENGINES) FOR ORBIT TRIM

TEM
STEM

BATTERY POWER TO:

M

BETWEEN COMPONENTS
DYNAMIC LOAD

MENTS

DAE
NTS AS REQUIRED

M

Mission Sequences Matrix

3) Rocket Research Corporation, "Monopropellant Hydrazine Propulsion Subsystems for the Voyager Spacecraft," Proposal 65-P-147, Seattle, Washington, June 30, 1965.

4) Military Specification, MIL-P-26536B, "Propellant, Hydrazine," 13 March 1964.

4.3.3 Functional Description

The functional description of the Spacecraft Propulsion module covers (1) the liquid-monopropellant midcourse and orbit-trim subsystem and (2) the orbit-insertion solid-fueled motor. The functional descriptions include in order of presentation: subsystem-description, schematic, functional-block-diagram, logic-diagram, operational-sequence, and key-performance characteristics.

4.3.3.1 Functional Description--Midcourse and Orbit-Trim Propulsion Subsystem

Description--The mechanization of the midcourse and orbit-trim propulsion subsystem is shown in Figure 4.3-3. A list of components is provided in Table 4.3-2. Key subsystem components include engines, tanks and bladders, regulators, and valving. There are four 50-pound constant-thrust, radiation-cooled, regulated-gas pressure-fed, hydrazine-monopropellant engines. Shell 405 catalyst is used for hydrazine spontaneous decomposition. Unlimited restart capability is thus provided. Four jet vanes per engine and actuators are provided for two-axis thrust-vector control up to 5 degrees on each chamber. The hydrazine is stored in two spherical titanium tanks mounted as shown in Figure 4.3-4. These tanks contain 395

MISSION SEQUENCE	PROPULSION SEQUENCE	FUNCTION
PRELAUNCH	LAUNCH	
LAUNCH AND INJECTION		
ACQUISITION		
INTERPLANETARY CRUISE		
INTERPLANETARY TRAJECTORY CORRECTION	1ST MIDCOURSE CORRECTION	ACTIVATE PRESSURIZATI ACTIVATE PROPELLANT FIRE PROGRAMMED ENG SHUT DOWN ENGINES ISOLATE PROPELLANT FE ISOLATE PRESSURIZATIO
INTERPLANETARY CRUISE		
INTERPLANETARY TRAJECTORY CORRECTION	2ND MIDCOURSE CORRECTION	SAME AS FOR 1ST MIDC CORRECTION
INTERPLANETARY CRUISE		
INTERPLANETARY TRAJECTORY CORRECTION	3RD MIDCOURSE CORRECTION	SAME AS FOR 1ST MIDC CORRECTION
INTERPLANETARY CRUISE	4TH COAST	
INTERPLANETARY TRAJECTORY CORRECTION	4TH MIDCOURSE CORRECTION (IF REQUIRED)	ACTIVATE PRESSURIZATI ACTIVATE PROPELLANT FIRE PROGRAMMED ENG SHUT DOWN ENGINES ISOLATE PROPELLANT FE ISOLATE PRESSURIZATIO
S/C CAPSULE SEPARATION		
FLIGHT SPACECRAFT CRUISE		
FLIGHT SPACECRAFT ORBIT INSERTION	MARS ORBIT INSERTION	ACTIVATE PRESSURIZATI FIRE MOTOR ISOLATE PRESSURIZATIC
ORBITAL OPERATIONS	ORBIT TRIM	ACTIVATE PRESSURIZATI ACTIVATE PROPELLANT FIRE PROGRAMMED ENG SHUT DOWN ENGINES ISOLATE PROPELLANT FE ISOLATE PRESSURIZATIO

Table

	ACTION	
ON SUBSYSTEM FEED SUBSYSTEM INES ED SUBSYSTEM N SUBSYSTEM	FIRE TWO NC SQUIB VALVES FIRE ONE NC SQUIB VALVE ACTUATE TWO SOLENOID VALVES DEACTIVATE TWO SOLENOID VALVES FIRE ONE NO SQUIB VALVE FIRE TWO NO SQUIB VALVES	
OURSE	SAME AS 1ST MIDCOURSE CORRECTION	
OURSE	SAME AS 1ST MIDCOURSE CORRECTION	
ON SUBSYSTEM FEED SUBSYSTEM INES ED SUBSYSTEM N SUBSYSTEM	FIRE TWO NC SQUIB VALVES FIRE TWO NC SQUIB VALVES ACTIVATE TWO SOLENOID VALVES DEACTIVATE TWO SOLENOID VALVES ACTIVATE ONE SOLENOID VALVE ACTIVATE ONE SOLENOID VALVE	
		FU
ON SUBSYSTEM N SUBSYSTEM	ACTIVATE ONE SOLENOID VALVE AND FIRE TWO NC SQUIB VALVES FIRE TWO SQUIBS ACTIVATE ONE SOLENOID VALVE AND FIRE TWO N.O. SQUIB VALVES	ACTIVATE PRESS FIRE MOTOR ISOLATE PRESSU
ON SUBSYSTEM FEED SUBSYSTEM INES ED SUBSYSTEM N SUBSYSTEM	ACTIVATE ONE SOLENOID VALVE ACTIVATE ONE SOLENOID VALVE ACTIVATE TWO SOLENOID VALVES DEACTIVATE TWO SOLENOID VALVES ACTIVATE ONE SOLENOID VALVE ACTIVATE ONE SOLENOID VALVE	ACTIVATE PRESSU ACTIVATE PROPE FIRE PROGRAMME SHUT DOWN ENG ISOLATE PROPELL ISOLATE PRESSUR

2

4.3-3: Spacecraft-Propulsion Flight Operational Sequence

IF 4TH MIDCOURSE CORRECTION
NOT REQUIRED

NCTION	ACTION
JRIZATION SUBSYSTEM	FIRE FOUR NC SQUIB VALVES FIRE TWO SQUIBS
RIZATION SUBSYSTEM	ACTIVATE ONE SOLENOID VALVE AND FIRE TWO N.O. SQUIB VALVES
RIZATION SUBSYSTEM .LANT FEED SUBSYSTEM :D ENGINES ;INES ANT FEED SUBSYSTEM IZATION SUBSYSTEM	ACTIVATE ONE SOLENOID VALVE FIRE TWO NC SQUIB VALVES ACTIVATE TWO SOLENOID VALVES DEACTIVATE TWO SOLENOID VALVES ACTIVATE ONE SOLENOID VALVE ACTIVATE ONE SOLENOID VALVE

pounds of hydrazine. Butyl bladders are used for positive-displacement propellant expulsion. A combination of regulators, squib-actuated valves, and solenoid-actuated valves are used for pressurization and propellant feed. This valving network provides positive isolation of both pressurant and propellant after each midcourse-engine firing. An additional isolation leg is provided for the backup midcourse and orbit-trip maneuvers. Pressurization-gas storage is common with the reaction-control subsystem. Fifteen pounds of nitrogen pressurant are required for midcourse, orbit-trim and orbit insertion TVC. All pressurant and propellant lines are welded or brazed to minimize leakage.

The midcourse-propulsion subsystem is assembled as a submodule and installed in the spacecraft in modular form. The four monopropellant engines are positioned symmetrically around the orbit-insertion motor with their nozzle exhausts directed parallel to the spacecraft centerline and along the minus Z axis. The midcourse-propulsion subsystem is fully sterilized. The hardware and the propellants are sterilized independently by heat soaking. Propellant loading is accomplished under aseptic conditions.

Functional Block Diagram--A functional block diagram of the midcourse-correction and orbit-trim-propulsion subsystem is shown in Figure 4.3-5. Key interfaces are indicated. A detailed definition of interfaces is provided in Section 4.3.4.

Logic Diagram--A diagram illustrating the control logic of the monopropellant subsystem is shown in Figure 4.3-6.

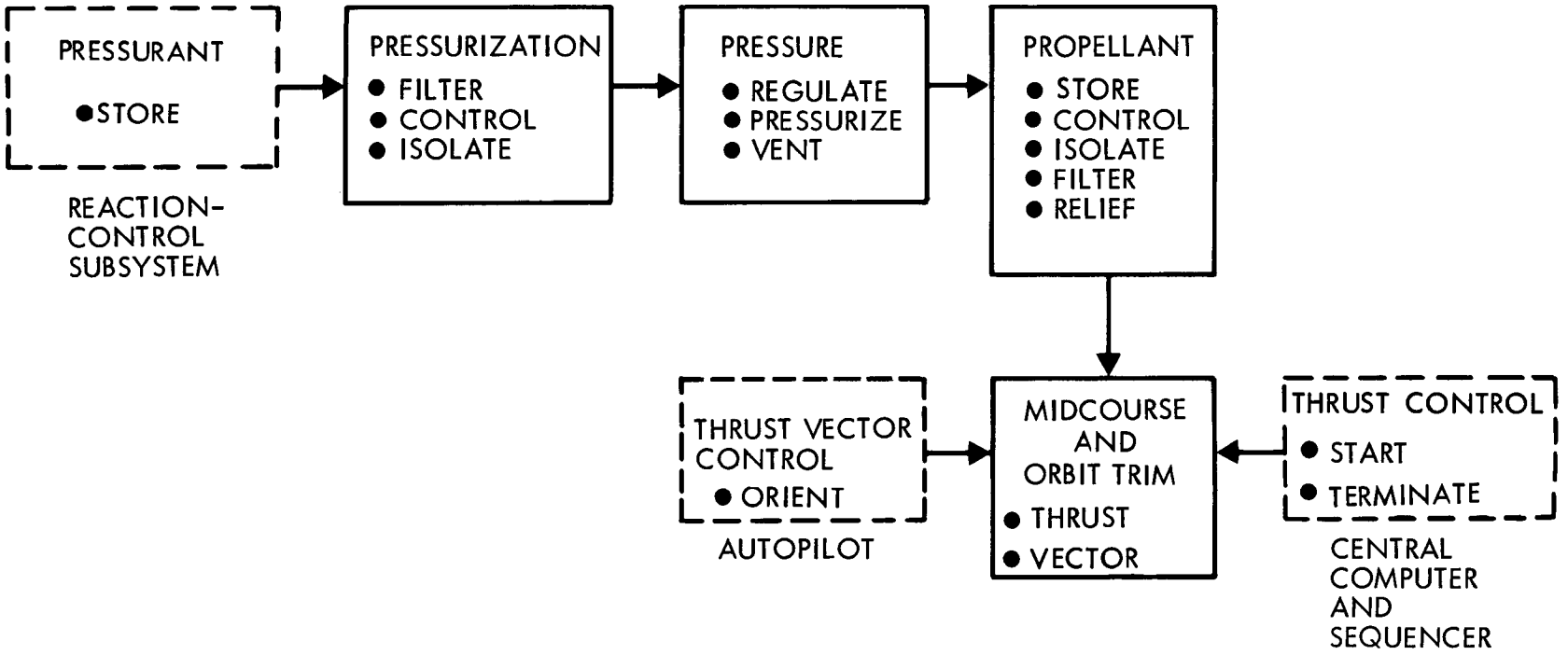

Figure 4.3-5: Monopropellant Midcourse and Orbit-Trim Subsystem — Functional Block Diagram

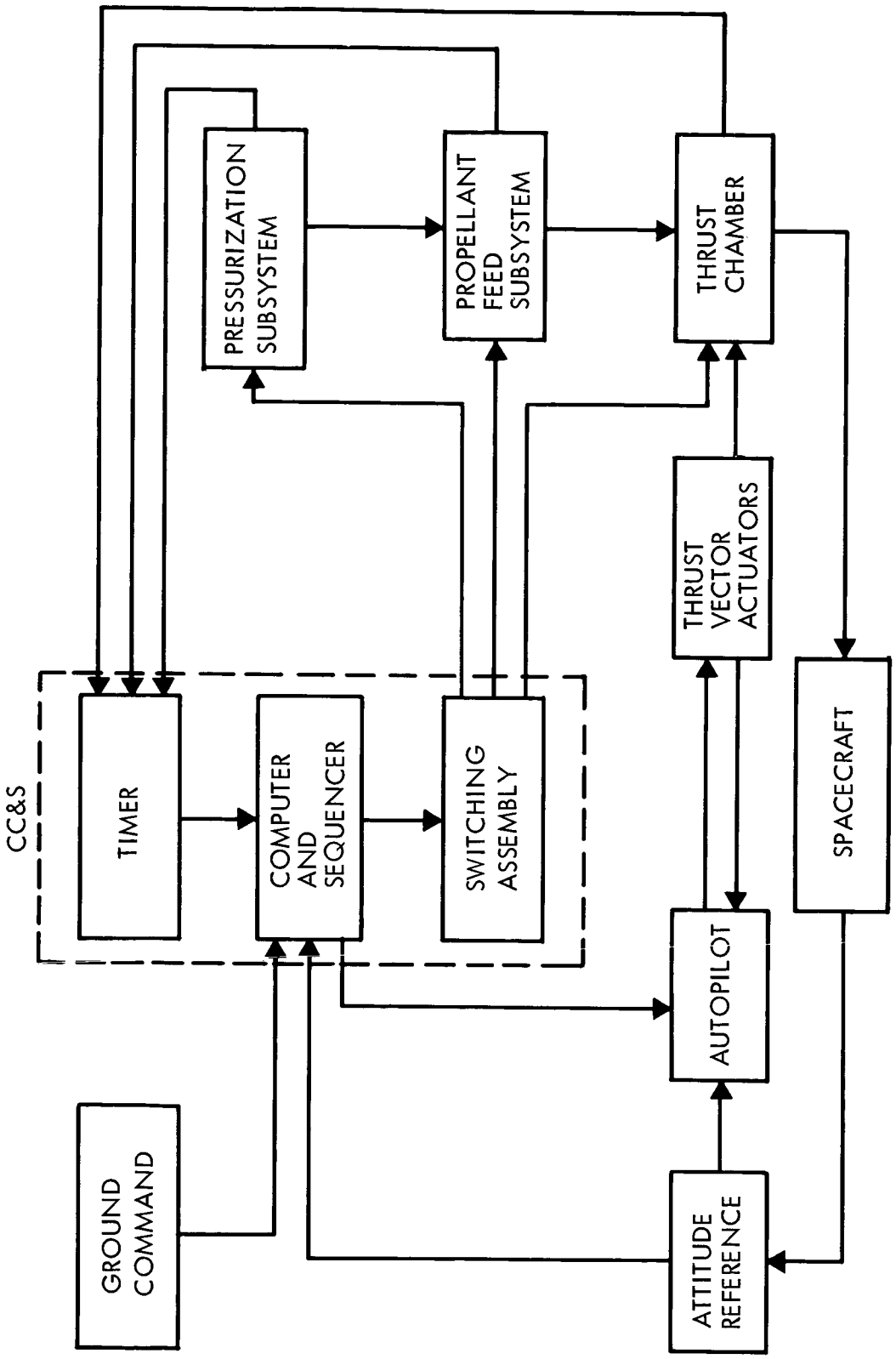

Figure 4.3-6: Monopropellant Midcourse and Orbit-Trim Subsystem — Logic Diagram

to the normally open nitrogen- and propellant-isolation squib valves. The valves close and isolate the nitrogen and propellant systems.

Performance Characteristics--Pertinent performance characteristics presented in this section include engine, jet-vane, pressurization-subsystem, malfunction detection system, and overall monopropellant performance. Other key performance parameters and physical characteristics are provided in Sections 4.3.5 and 4.3.6.

Engines--Monopropellant-engine-performance characteristics are shown in Table 4.3-4. The following performance characteristics, including thrust, specific impulse, start and shutdown impulse, size, and weight, are design specifications for the required new monopropellant engine. These engine characteristics are based on those of similar engines that are currently being designed and tested under NASA Contract NAS7-372. The monopropellant engine envelope is shown in Figure 4.3-7. The effect of initial catalyst-bed temperature on pressure-rise-delay time is shown in Figure 4.3-8. These pressure-rise-delay times are of particular significance for minimum-velocity-increment midcourse maneuvers following long coast periods, as delay times will vary by a factor of five within the allowable subsystem -temperature-control limits. Engine thrust chamber and nozzle surface temperatures at various axial stations are presented in Figure 4.3-9.

Engine exhaust plume characteristics that affect spacecraft thermal balance are shown in Figure 4.3-10.

Table 4.3-4: ENGINE DATA SHEET

Designation	
Potential Manufacturers	Rocket Research Corp. Walter Kidde
Status	New Development Required
Propellants	Hydrazine Monopropellant
Engine Thrust, Vacuum	50 LBF
Engine Specific Impulse, Vac.	235 LBF - sec/LBM
Expansion Ratio A_e/A_t	50
Exit Area	9.43 sq. in.
Chamber Pressure	150 PSIA
Start Time Impulse	20 ms on to first rise 200 ms first rise to 90% cold
Shutdown Time and Impulse	5 ms off to first drop 100 ms first drop to 10%
Minimum Total Impulse Bit	.5 lb-sec 7ms pulse width
Throttle Ratio	None
Restart Capability	Multiple
Burn Time	982
Ignition	Spontaneous catalyst
Cooling	Radiation
Weight, Dry	2.5 LBM 2.6 LBM for jet vanes
Size Length	5.72 in.
Size Diameter	3.5 in.
Thrust Vector Type	Jet vanes
Thrust Vector Angle	5° effective
Thrust Vector Rate	
Thrust Vector Acceleration	
Fuel Inlet Pressure	260 psi nominal

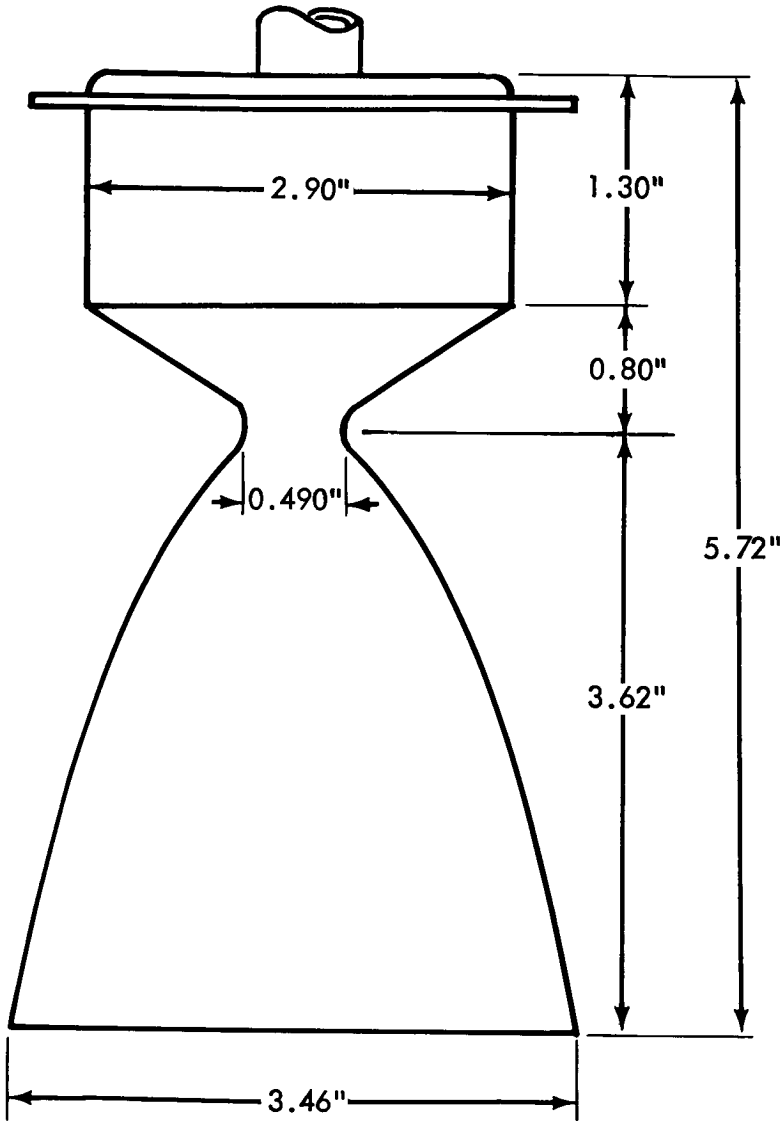

Figure 4.3-7: 50-LBF Monopropellant Hydrazine Engine (ε = 50:1)

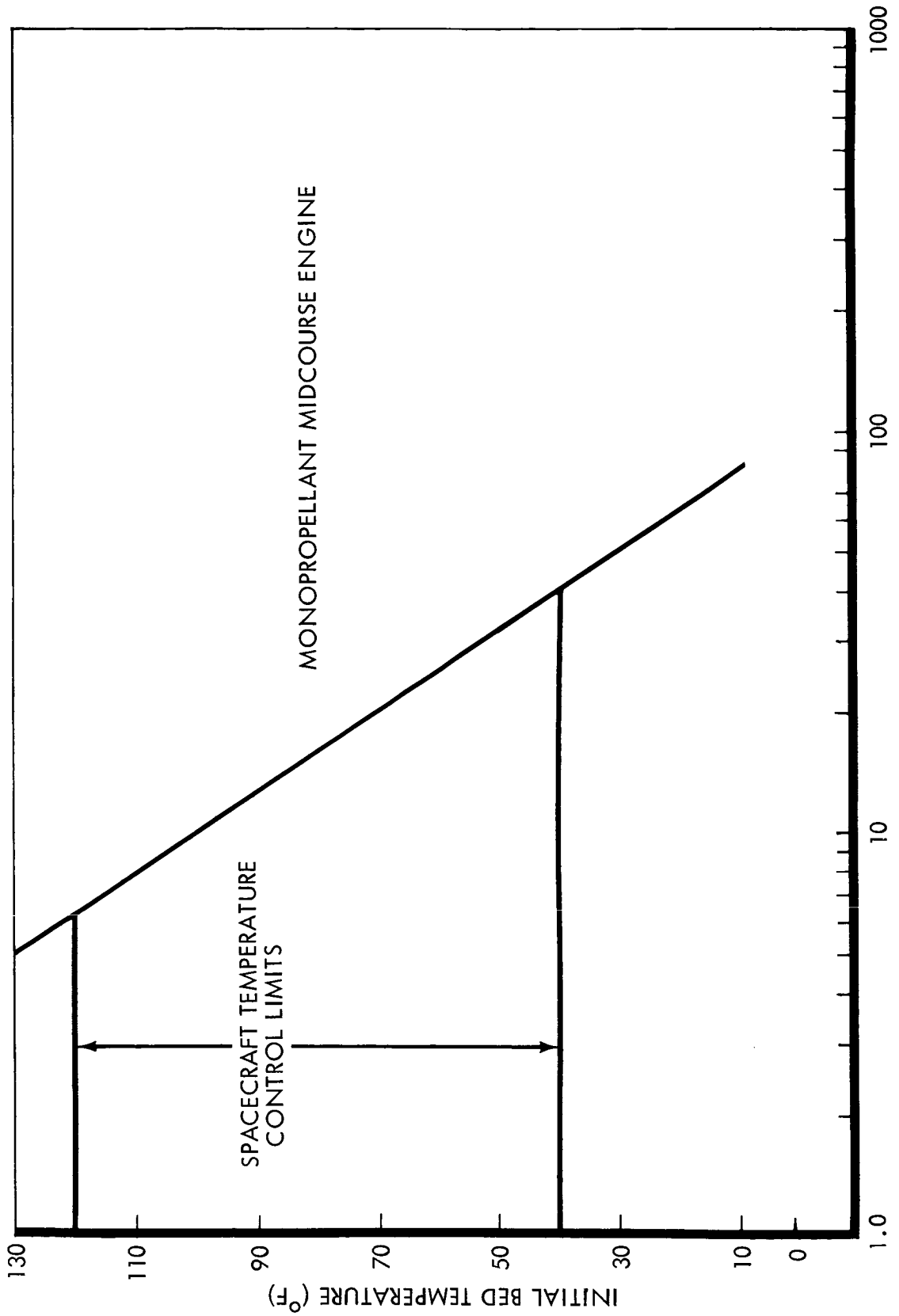

Figure 4.3-8: Pressure-Rise Delay Time Versus Initial Catalyst Bed Temperature

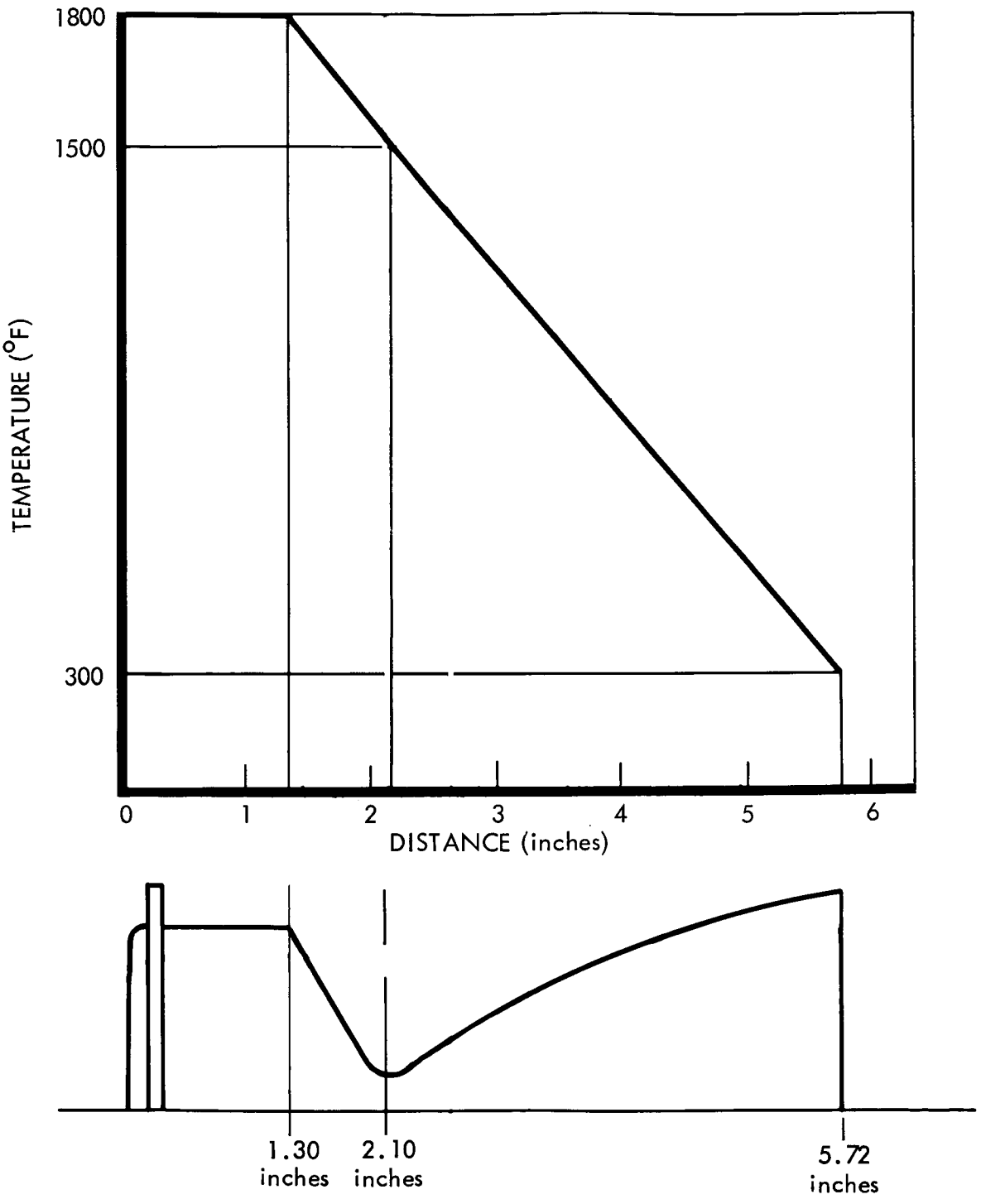

Figure 4.3-9: Thrust Chamber & Nozzle External Temperatures — Monopropellant Engine

ε - Expansion Ratio
θ_e - Nozzle Exit Angle
γ - Specific Heats Ratio
M - Mach Number
P - Pressure
T - Temperature
$(\ )_c$ - Chamber Condition
$(\ )_e$ - Nozzle Exit Condition

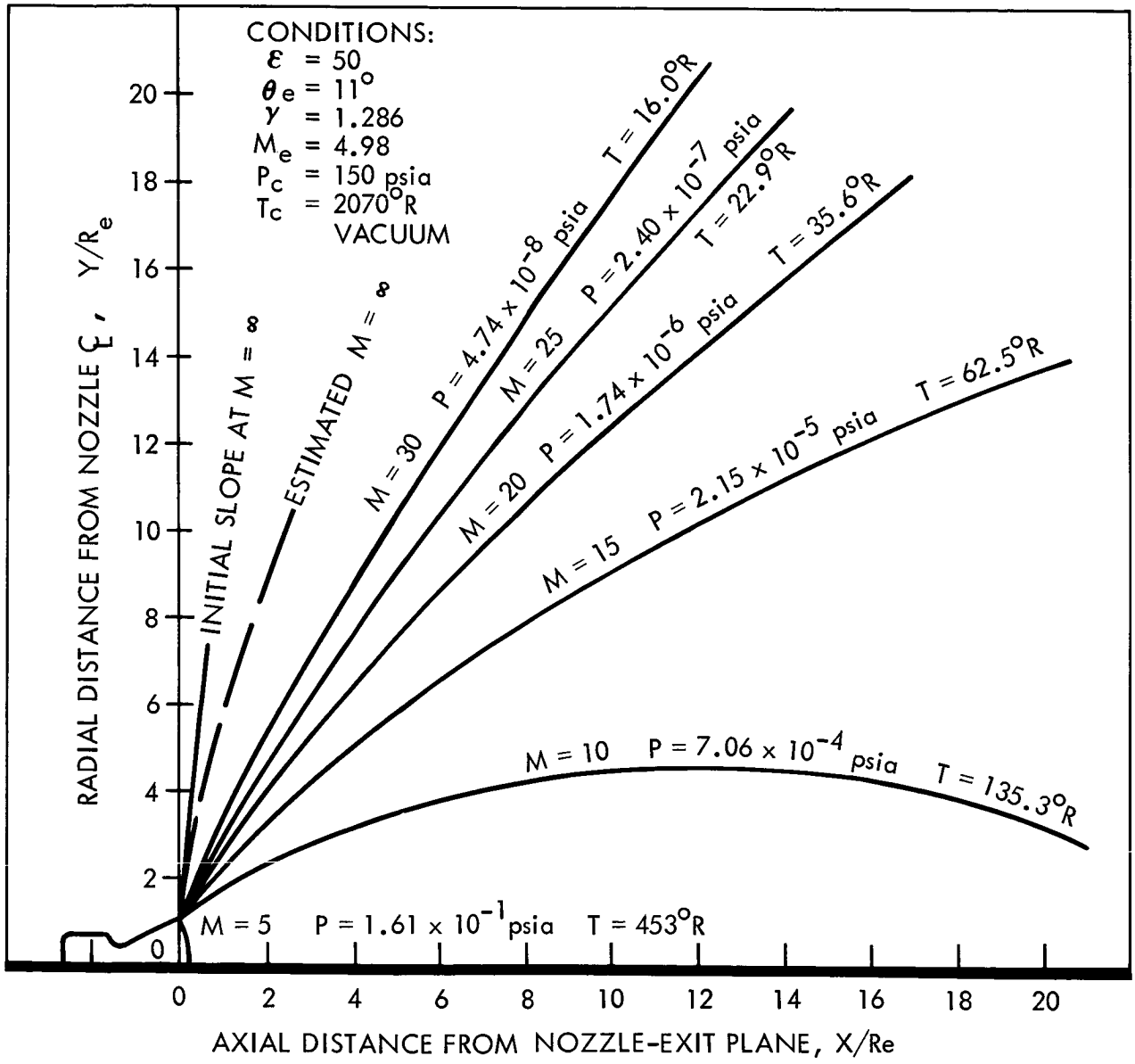

Figure 4.3-10: Monopropellant Engine Exhaust-Plume Definition

Jet vanes--A jet-vane-performance curve showing thrust deflection for a given vane deflection is given in Figure 4.3-11. Vane performance is based on vane lift and drag data from JPL Specification MC-4-610A.

Pressurization--The pressurization subsystem for the midcourse and orbit-trim propellant consists of nitrogen pressurant supplied by the reaction control system from four interconnected storage tanks. Each tank contains 15 pounds of nitrogen at an initial nominal pressure of 3500 psia. Fifteen pounds of the 60-pound total nitrogen capacity are allocated to the propulsion subsystem. The scheduled allotment for the various pressurization functions is:

Four midcourse operations (total)	7.0 pounds
One orbit-insertion thrust-vector-control operation	4.0 pounds
One orbit-trim operation	4.0 pounds

As shown in Figure 4.3-3, the pressurization subsystem consists of isolation valving for midcourse and orbit-trim propulsion and orbit-insertion thrust-vector-control. The midcourse and orbit-trim propulsion pressurization system is regulated and includes propellant-tank relief valves for overpressurization protection. Orbit-insertion thrust-vector-control liquid secondary injection is accomplished by an unregulated blowdown system.

The midcourse pressurization subsystem pressures (in pounds per square inch absolute) are:

Storage pressure, initial (RCS)	3500
Regulator inlet pressure, nominal	3500 to 1000
Regulator outlet pressure, nominal	264
Propellant tank pressure, nominal	264
Relief valve cracking pressure, nominal	310

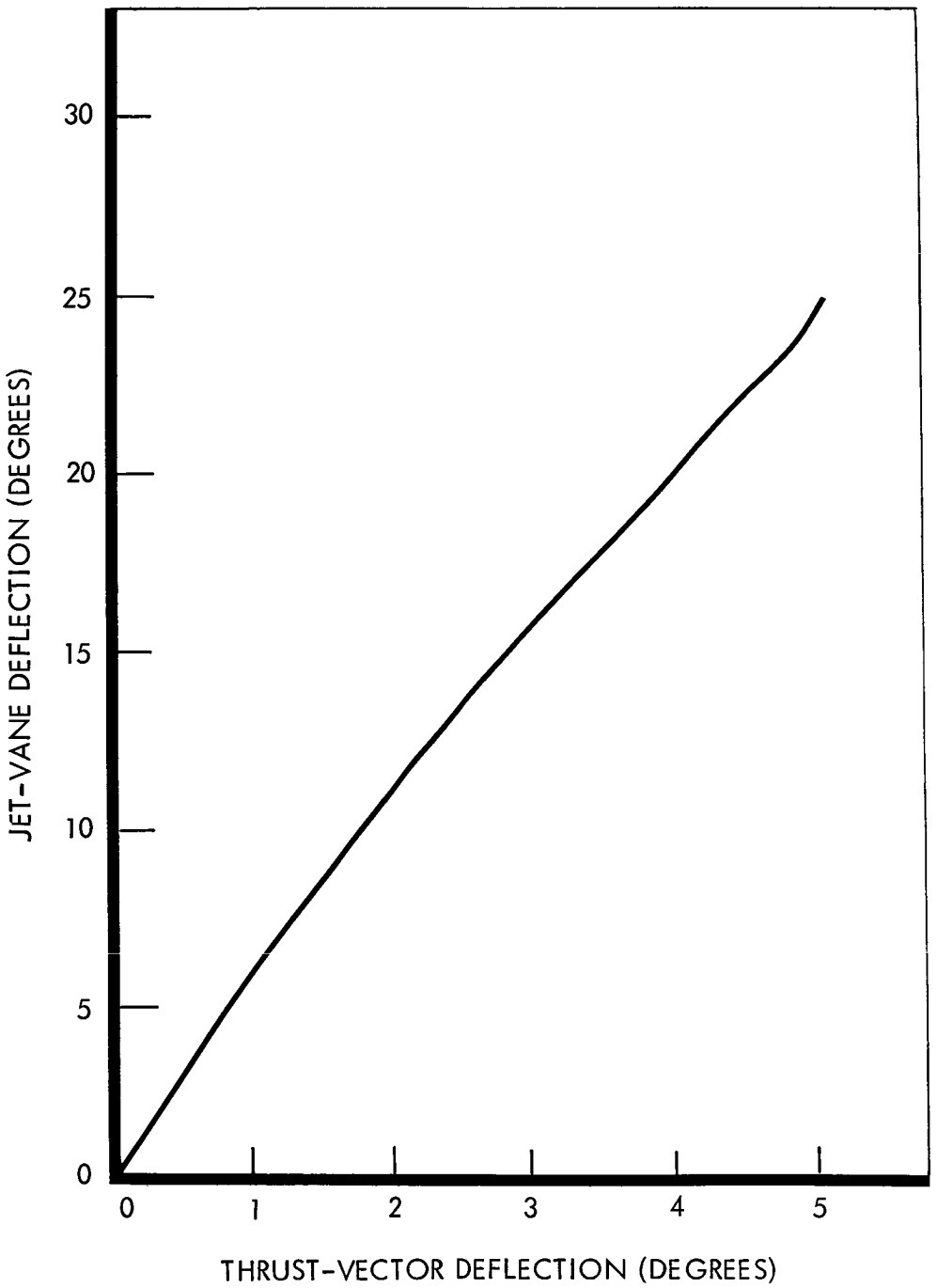

Figure 4.3-11: Jet-Vane Deflection Vs Thrust-Vector Deflection

The orbit-insertion thrust-vector-control pressurization subsystem pressures (in pounds per square inch absolute) are:

Initial N_2 supply and thrust-vector-control tank pressure	1500
Final N_2 supply and thrust-vector-control tank pressure	1330

Midcourse-propulsion pressurization and propellant-feed-system component characteristics are summarized in Table 4.3-5.

Malfunction Detection System--A redundant set of midcourse and orbit trim engines is provided to achieve high reliability. Utilization of this backup mode hinges on a single and highly reliable Malfunction Detection System (MDS). The MDS consists of triply redundant pressure transducers mounted on each of the two primary monopropellant engines utilized for normal operations. The signals from the pressure transducers are fed into a MDS signal conditioner which compares pressure transducer will not result in an engine-out signal. If both engines register full pressure readings, the system is functioning normally. A zero pressure reading on both engines indicates that the normally-closed squib valve in the propellant leg (see Figure 4.3-3) failed to open. The MDS signal conditioner then signals the CC&S to command the firing of a normally-closed squib in the next available propellant leg. Unequal pressure readings from the primary engine set indicate engine malfunction. The MDS signal conditioner then signals the CC&S to fire both normally-open squib valves in the propellant line leading to the primary set. This set is consequently positively isolated for the remainder of the mission. Subsequent midcourse and orbit trim maneuvers are then accomplished by the redundant engine set.

[1] NO.	COMPONENT	PRESSURE - psia						
		OPERATING NOMINAL	DESIGN MAXIMUM	PROOF	DESIGN ULTIMATE	CRACK-ING	LOCK-UP	RESE
RCS	PRESSURANT TANK	1500 to 3500	4075	5100	8960			
12	N_2 FILTER	↑	↑	↑	↑			
15	N.O. SQUIBS							
10	N.C. SQUIBS							
19	N.C. SQUIBS							
20	N.O. SOLENOID							
12	N_2 FILTERS	↓	↓	↓	↓			
6	N_2 CHECKOUT	1500 to 3500	4075	5100	8960			
9	REGULATOR OUTLET	264	313	392	689		274	
9A	REGULATOR INLET	1500 to 3500	4075	5100	8960			
11	RELIEF VALVE	264	313	392	689	309 ± 4		295 ±
6	N_2 CHECKOUT	264	↑	↑	↑			
7,8	N_2H_4 TANKS AND BLADDERS	264						
6	N_2H_4 FILL	262						
6	N_2H_4 CHECKOUT	↑						
5	N.O. PROPELLANT SQUIBS							
4	N.C. PROPELLANT SQUIBS							
18	N.C. PROPELLANT SQUIBS	↓						
14	N.O. PROPELLANT SOLENOID	262						
3	FILTERS	260						
13	N.O. PROPELLANT SQUIBS	260	↓	↓	↓			
17	N.C. PROPELLANT SOLENOID	260	313	392	689			

[1] Refers to no. of Figure 4.3-3 and Table 4.3-2 [2] 60 watts continuous during engine operation (per v

Table 4.3-5:

ΔT	ΔP (psia)	TEMPERATURE (°F) MEDIA	TEMPERATURE (°F) OPERATING AMBIENT	MEDIA	MEDIA FLOW RATE (lb/sec) NOMINAL	MEDIA FLOW RATE (lb/sec) MAXIMUM	MAX. ALLOWABLE LEAKAGE (scc-hr-N_2) INTERNAL	MAX. ALLOWABLE LEAKAGE (scc-hr-N_2) EXTERNAL	POWER NO FIRE	POWER ALL FIRE
	NEGLIGIBLE	0-120	40-120	N_2				0		
								0.04		
							10^{-6} [3]	0.08 [4] 0.04 [3]	1 AMP 1 WATT	10 AMP 5 MS
							0	0.04 [4] 0.08 [3]		5 AMP 5 MS
								0.04 [4] 0.08 [3]	1 AMP 1 WATT	10 AMP 5 MS
								1		
								0.04		
				N_2				0.05 [5]		
				N_2H_4			10			
								1		
10	NEGL.							10		
		0-120						0.05 [5]		
	2	40-120			0.112 to 0.85			0.8/TANK		
	NEGLIGIBLE				0.425 to 0.85			0.05 [5]		
								0.05 [5]		
							10^{-6} [3]	0.08 [4] 0.04 [3]	1 AMP 1 WATT	5 AMP 5 MS
					0.425 to 0.85			0.04 [4] 0.08 [3]		5 AMP 5 MS
					0.112 to 0.85			0.04 [4] 0.08 [3]	1 AMP 1 WATT	10 AMP 5 MS
					0.425 to 0.85			1		
	2							0.04		
	0						10^{-6} [3]	0.08 [4] 0.04 [3]	1 AMP 1 WATT	10 AMP 5 MS
	0	40-120	40-120	N_2H_4	0.425 to 0.85			1		

lve) [3] After firing (closed) [4] Before firing [5] Capped

(2)

Voyager Midcourse-Propulsion-Pressurization and Propellant-Feed-System Characteristics

MICRON FILTRATION		PORTS		SYSTEM	REMARKS
OPERATIONAL	NOMINAL	ABSOLUTE	SIZE	TYPE		
				BRAZE	PRESSURIZATION	
	5	20				
60 WATT MS						
					PRESSURIZATION	
					PROPELLANT FEED	
60 WATT MS						
	5	20				
2				BRAZE	PROPELLANT FEED	

(3)

The simplicity of the MDS is due to (i) utilization of two normally-closed squib valves in paralllll on each pressurization leg, and (ii) utilization of two regulators in parallel which are designed to fail only in the closed position.

Monopropellant Subsystem--Pertinent subsystem performance parameters, including total impulse, impulse duration, and propellant weight, are given in Table 4.3-6. Midcourse-correction total impulse was based on the maximum initial gross weight of 7800 pounds and a velocity increment of 75 meters per second. Orbit-trim total impulse was based on a maximum initial gross weight of 2939 pounds and a velocity increment of 100 meters per second. Initial gross weight for orbit trim was calculated for a worst case situation where all orbit insertion thrust-vector-control freon injectant was inserted into orbit.

Table 4.3-6: MIDCOURSE CORRECTION AND ORBIT TRIM PROPULSION SUBSYSTEM PERFORMANCE PARAMETERS

Maneuver	Total Impulse (pound-second)	Engines Burn Time seconds	Propellant Weight (pounds)
Midcourse Correction (4)	58,725	588	255
Orbit Trim	34,100	341	140

4.3.3.2 Functional Description--Orbit-Insertion-Propulsion Subsystem The following is a functional description of the solid-fueled motor orbit-insertion-propulsion subsystem.

Description--The orbit-insertion solid-fueled motor is shown in Figure 4.3-12. The motor has an ovaloid glass-filament epoxy-resin case. The major diameter is 50.58 inches and the case length is 35.2 inches from the face of the forward boss to the face of the aft boss. From the face of the forward boss to the end of the exit cone, the motor length is 55.56 inches. The motor, with an average thrust of 7988 pounds, provides an orbit-insertion-velocity increment of 5700 feet per second. Total motor weight, exclusive of the thrust-vector-control system, is 2578 pounds. Propellant weight (exclusive of thrust-vector-control) is 2306 pounds, which results in a mars fraction μ, of 0,896. Solid-fueled motor data is presented in Table 4.3-7. Major motor components are: propellant, case, igniter, safe and arm device, nozzle, liner and insulation, and thrust-vector-control.

Propellant--The selected propellant, ANB-3066, is in production for the Minuteman Wing VI second-stage motor. This propellant meets all performance and structural requirements. It is an aluminized-carboxyl terminated-polybutadiene propellant of which over 4,000,000 pounds have been produced. The vacuum delivered specific impulse, with an expansion ratio, ϵ, of 73 (contoured nozzle), is assumed to be 300 pounds (force)-second per pound (mass). Propellant burning rate is 0.21 inch per second at 500 psia. Physical properties exceed the most stringent structural requirements at all operational temperatures by a factor of 1.5. The propellant is nondetonable; it is rated as a Class 2 explosive hazard.

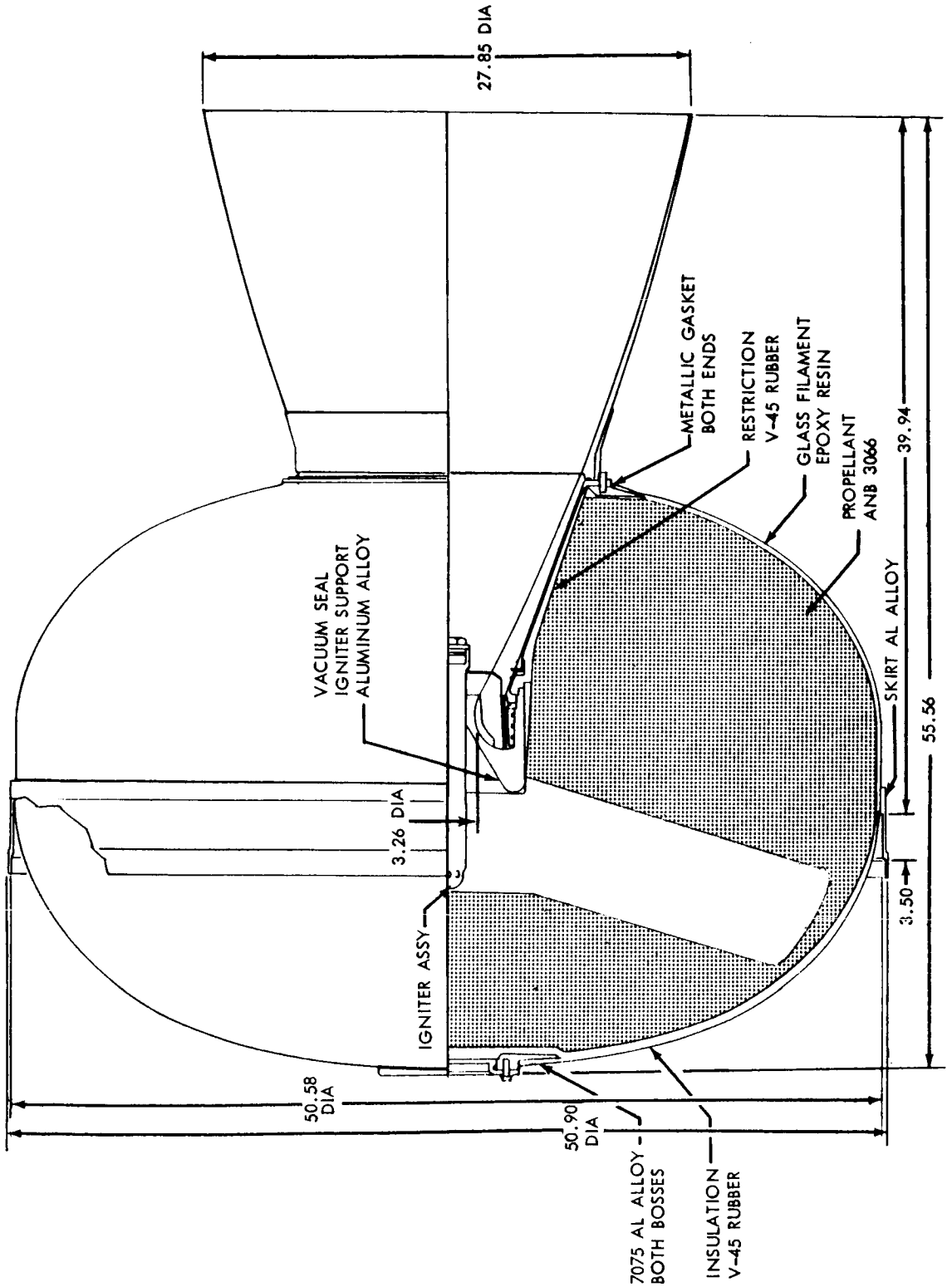

Figure 4.3-12: Orbit Insertion Solid Motor

Table 4.3-7. SOLID RETRO DATA SHEET

Designation	
Potential Manufacturer(s)	Aerojet General, Inc. Thiokol Chemical Corp.
Status	New Development Required
Propellant	Aluminized Polybutadiene Solid
Motor Thrust Vacuum (Avg)	7988 lbf
Motor Specific Impulse	300 lbf-sec/lbm (assumed)
Expansion Ratio	73/1
Exit Area	610 sq. in.
Chamber Pressure (Avg)	500 (psia)
Ignition Delay Time (Time to 90%)	70 M/sec
Restart Capability	None
Burn Time	90 sec
Ignition	Alclo-iron igniter
Cooling	Ablation
Weight	
Inerts (Excluding TVC)	272 lbm*
Propellant	2306 lbm
TVC	108 lbm
Size	
Length	55.56 in.
Diameter	50.58 in.
Thrust Vector	
Type	Freon 114B2 Secondary Injection
Angle	3° Max.
Rate	40 cps

*Add 33 lb for titanium case

Grain Design--The grain for the proposed motor is a modified conocyl design. This design has been successfully demonstrated on the Skybolt missile. The proposed grain configuration permits a relatively thick web (18 inches) for a motor of this size, and results in a regressive thrust time trace and near constant vehicle inertial load. Since the propellant face next to the submerged portion of the nozzle is not a burning surface, the propellant gives thermal protection to the nozzle interior surface during firing.

The conocyl slot in the grain reduces propellant strains during temperature cycling, thus increasing motor environmental capability.

Case--The oblate spheroidal chamber is fabricated from Owens-Corning S-994 glass filament roving impregnated with Shell 56-68 epoxy resin. This material is now used in manufacturing Polaris A-3 first-stage chambers which have a recorded reliability of 100%. The nominal wall thickness at the equator is 0.07 inch based on a maximum expected operating pressure of 737 psia. The chamber weight is 73 pounds. The motor is aligned and attached to the spacecraft by means of an aluminum stub skirt that is secondarily bonded to the motor equator. Thrust loads for the proposed motor are relatively low for a motor diameter of 50.58 inches. Consequently, bonding stresses imposed in securing the skirt to the chamber are less than 100 pounds per square inch. To ensure high reliability, the fabrication methods and quality-control procedures will be those used and proven during the development and production of the Polaris A-3 first-stage motor. Elliptical forward and aft fiberglass domes of identical shape are used on both the Polaris and Minuteman

missiles. (Titanium can be substituted for fiberglass but results in a 30-pound weight penalty.) A 4-inch cylindrical insert, provided between the forward and aft domes, allows for loading 532 additional pounds of propellant. This growth capability can be used without a case redesign, for future missions with higher energy requirements than the 1971 and 1973 Mars opportunities and for missions to other planets.

Igniter and Safe and Arm Device--The main propellant charge is ignited by a lightweight Alclo-iron igniter located in the nozzle throat. The charge is held in place by the motor vacuum seal. Alclo-iron igniters have been used on Genie, Sparrow, Improved Tartar, Skybolt, and Polaris A2 and A3 missiles. An aft-ending mounting technique is used. It has been successfully demonstrated on motors ranging from 40 to 120 inches in diameter. Ignition is initiated by two dual-bridgewire squibs. Good correlation between predicted and actual ignition transients has been achieved using this system.

Safety is provided by a safe and arm device. The output of both igniter squibs are blocked in the safe position by misalignment of a pressure-sealed blocking rotor. The squibs are each shorted. The firing circuit is open until the unit is armed by remote actuation. A safety pin must be removed before arming. It cannot be removed while arming power is applied. Manual insertion of the pin disarms the device. A pressure switch detects normal or inadvertant initiation of a squib. The safe and arm device weighs approximately 3.0 pounds.

Nozzle--The selected nozzle relies on Minuteman Wing VI second-stage nozzle design, materials, and fabrication technology. Minuteman uses a submerged fixed nozzle with a tungsten throat, molybdenum support ring, titanium and steel supporting structures, and a silica-phenolic exit cone extension. The Minuteman design is now in production and has been successfully tested both statically and in flight more than 30 times. Nozzle design consists of a submerged, molded entrance section, a nonerod-ing tungsten throat insert, a molybdenum support ring, an ablative primary exit cone insert, steel and titanium structural members, and a silica-phenolic ablative exit cone extension. Experience with Alcor motors indicates that thrust misalignment can be held within 0.001 radian angular alignment and 0.010 inches lateral displacement. The nozzle throat area is 8.35 square inches and the exit area is 610 square inches resulting in an expansion ratio of 73. The overall weight of the Voyager retro thrust motor nozzle is 101 pounds.

Insulation--Motor internal insulation is a silica-loaded nitrile rubber. This insulation has demonstrated reliable operation on the Minuteman and Polaris programs. At the major diameter of the conocyl slot, where the insulation is exposed for nearly the full duration of the firing, the insulation is 0.60 inch thick. At the minor diameter of the ovaloid chamber, where the insulation is not exposed until after 45 seconds of motor firing, the insulation is 0.30 inch thick. The insulation then tapers to 0.03 inch at the aft boss where it is not exposed until the end of the firing. Insulation thicknesses were calculated for a 50-degree rise in case temperature during firing and a maximum postfiring outside case temperature of 250°F.

Secondary Injection Thrust Vector Control--Orbit-insertion thrust-vector-control is maintained by a Freon-114B2 secondary-injection system. Sixty-one pounds of injectant are stored in a 24-inch major diameter toroidal tank surrounding the nozzle-exit cone. Four hydraulic servo-actuated injector valves are mounted at 90-degree intervals around the nozzle periphery at the 40 percent expansion ratio plane. High-pressure nitrogen from the main supply forces the injectant out of the toroidal tank. A butyl-rubber expulsion bladder in the toroidal tank separates the liquid and gas.

At engine ignition, squib valves open and high-pressure nitrogen forces Freon into the injection valves. The injectors are not filled prior to this time so that injector-position checkout can be performed with a minimum of ground support equipment. Burst discs between the Freon tank and injectors prevent Freon leakage prior to operation. Freon is used for ground checkout and is retained in the actuation line under pressure. A pressure indicator provides indication that the system is in a flight-ready condition. As the thrust vector control injectors are actuated, the Freon is ejected from the storage tank through the injector nozzles, as required. After solid motor burnout, the excess Freon leaves the vehicle through a non-propulsive flight drain.

Mechanization of the secondary-injection thrust-vector-control subsystem is depicted in Figure 4.3-13. A list of components is provided in Table 4.3-8. This subsystem is similar to those used on Polaris A2, Minuteman Wing VI second-stage, HiBEX, and Sprint first-stage missiles.

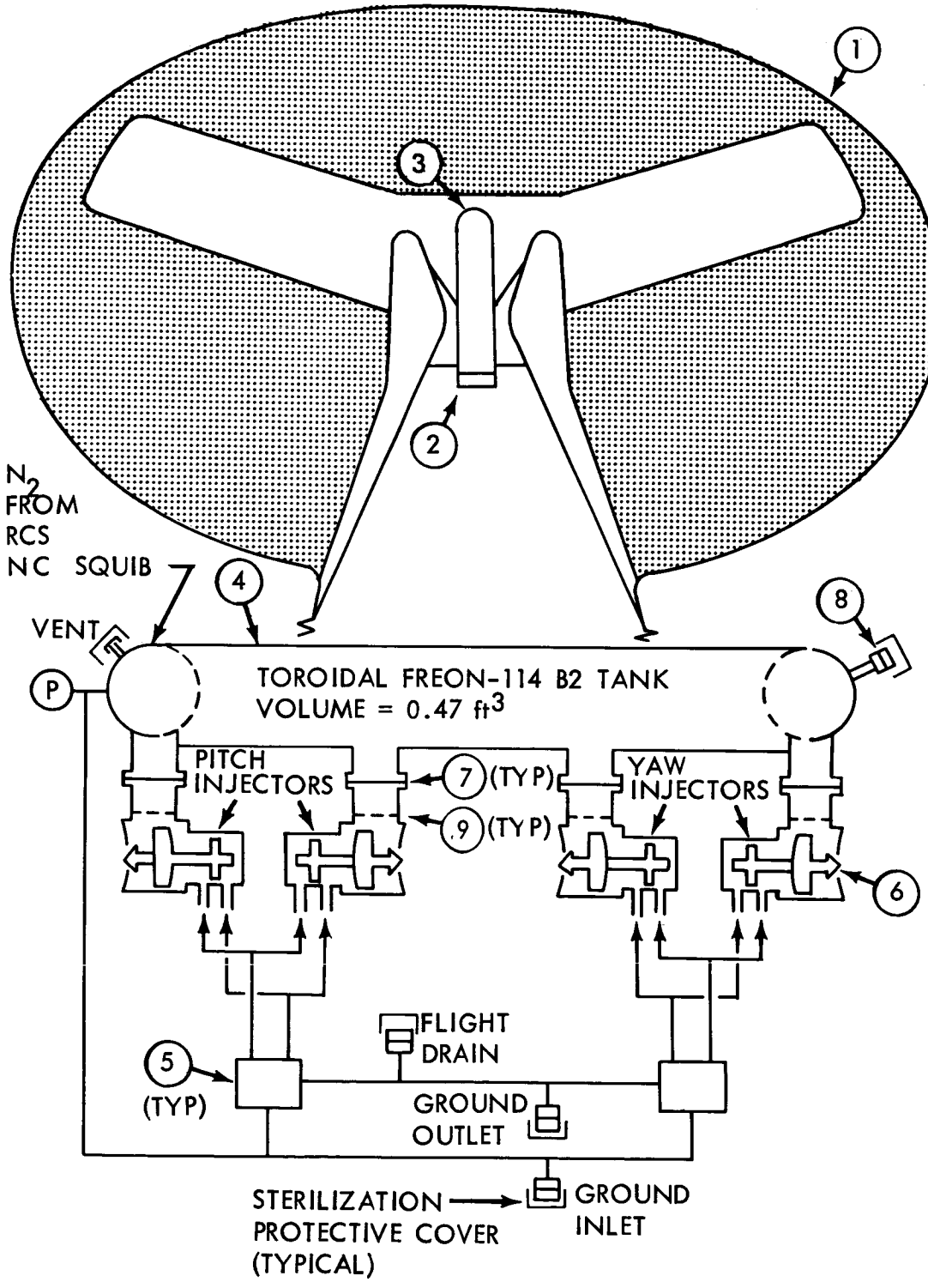

Figure 4.3-13: Orbit-Insertion TVC Schematic

Table 4.3-8: COMPONENTS LIST		
ORBIT INSERTION MOTOR AND TVC		
ITEM	QTY	NAME
1	1	Solid Motor
2	1	Safe and Arm
3	1	Igniter
4	1	Injectant Tank
5	4	Servo Valve
6	4	Injectant Valve
7	4	Burst Disk
8	1	Valve Cap and Fill
9	4	Filter Screens

The orbit-insertion-propulsion-subsystem hardware (including the solid propellant) and its fluids will be sterilized independently by the heat soak technique. Sterile fluids will be loaded under aseptic conditions.

Functional Block Diagram--A functional block diagram of the orbit-insertion-propulsion subsystem is given in Figure 4.3-14. This block diagram, in conjunction with the midcourse- and orbit-trim propulsion-subsystem block diagram in Figure 4.3-5, comprises the Spacecraft-Propulsion block diagram.

Logic Diagram--A diagram illustrating the control logic of the orbit-insertion-propulsion subsystem is shown in Figure 4.3-15. This diagram, in conjunction with the midcourse and orbit-trim-propulsion logic diagram in Figure 4.3-6, comprises the Spacecraft-Propulsion logic diagram.

Operational Sequence--The operational sequence for the orbit-insertion propulsion subsystem is included in Table 4.3-3.

Performance Characteristics--Pertinent performance characteristics for the orbit-insertion-propulsion subsystem include solid-motor, thrust-vector-control, and subsystem performance. Other performance parameters and physical characteristics are provided in Sections 4.3.5 and 4.3.6.

Solid Motor--The orbit-insertion solid-fueled-motor performance characteristics are shown in Table 4.3-9. Solid-fueled-motor vacuum thrust and chamber-pressure time traces are provided in Figure 4.3-16.

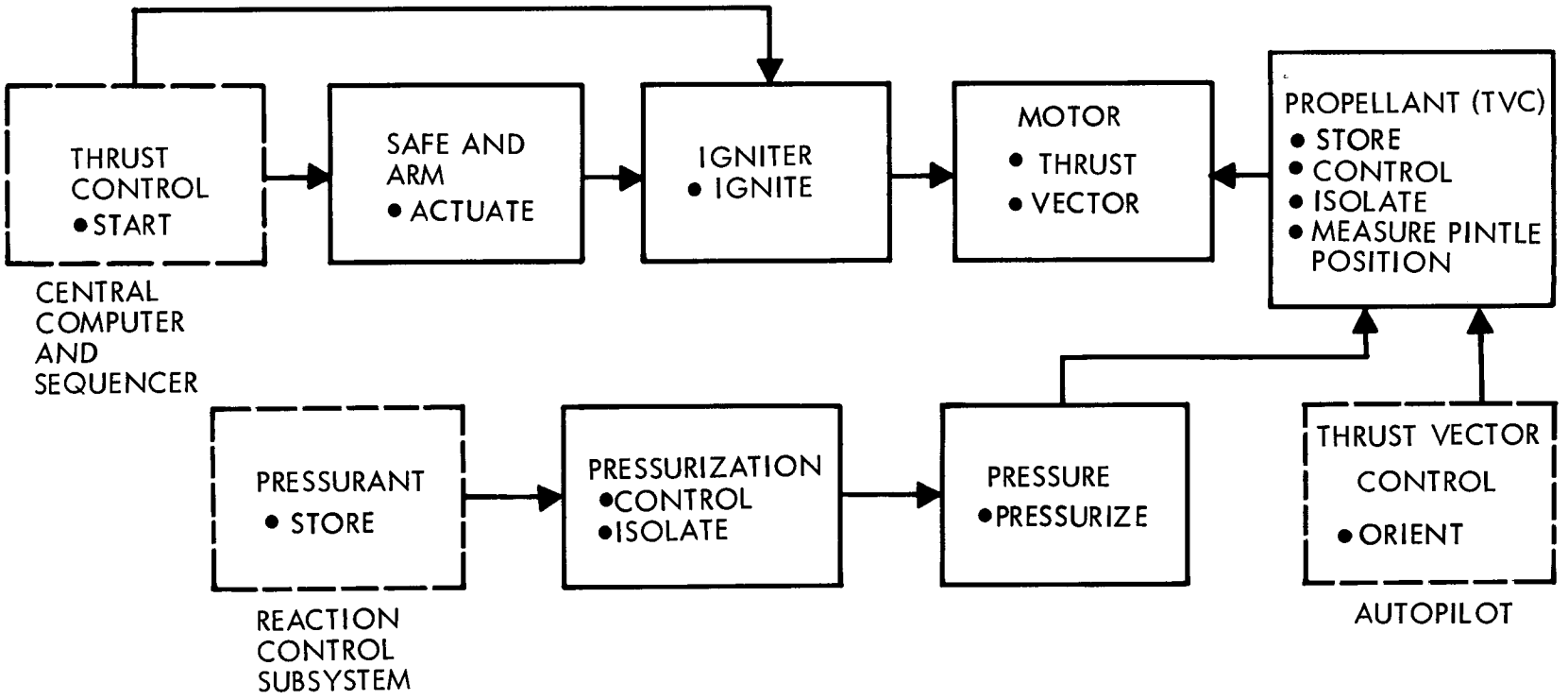

Figure 4.3-14: Functional Block Diagram — Solid Insertion Motor

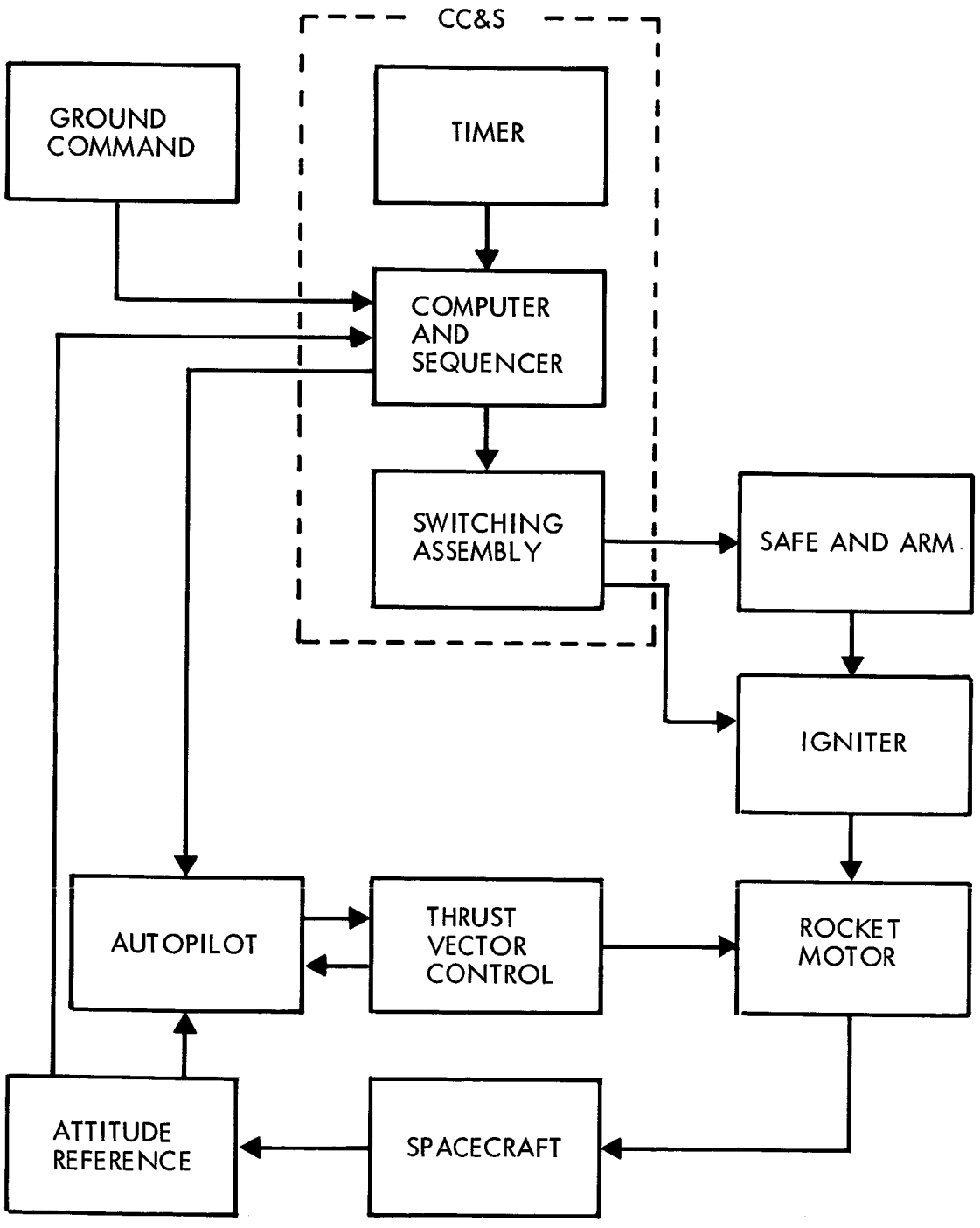

Figure 4.3-15: Logic Diagram — Solid Retro Motor

Table 4.3-9: Propellant Properties — Elliptical Solid-Propellant Retro Motor

Performance	
Delivered Vacuum I_{sp} (lbf-sec/lbm) (assumed)	300
Average Thrust (lbf)	7988
Maximum Thrust (lbf)	10700
Average Chamber Pressure (psia)	500
Maximum Chamber Pressure (psia)	670
Propellant Ballistic Properties	
Burning Rate at 500 psia (in./sec)	0.21
Burning Rate Exponent	0.27
Density ($lbm/in.^3$)	0.064
Mass Flow Coefficient (lbm/lbf-sec)	0.00627
Design Data	
Throat Area ($in.^2$)	8.35
Exit Area ($in.^2$)	610
Expansion Ratio	73
Nozzle Configuration	contoured
Volumetric Loading (percent)	89.9
Physical Properties	
(77°F and Strain Rate of 0.74 in./min/in.)	
Modulus (psi)	392
Strain at Maximum Stress (%)	49
Max. Stress (psi)	88
Burning Rate Characteristics	

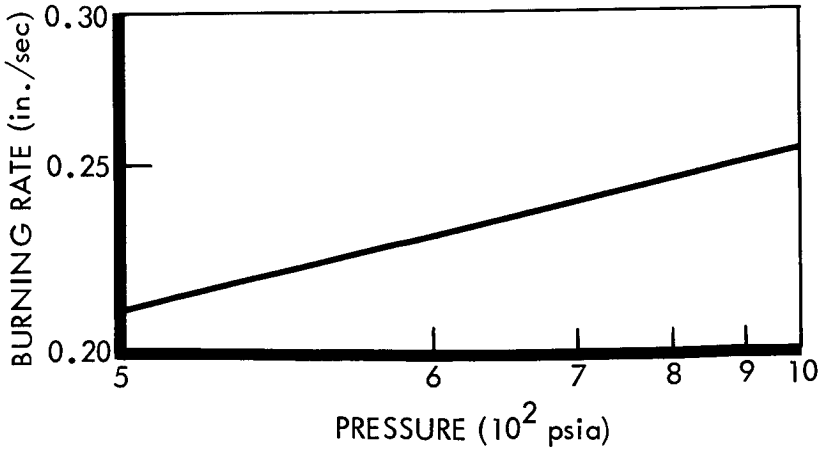

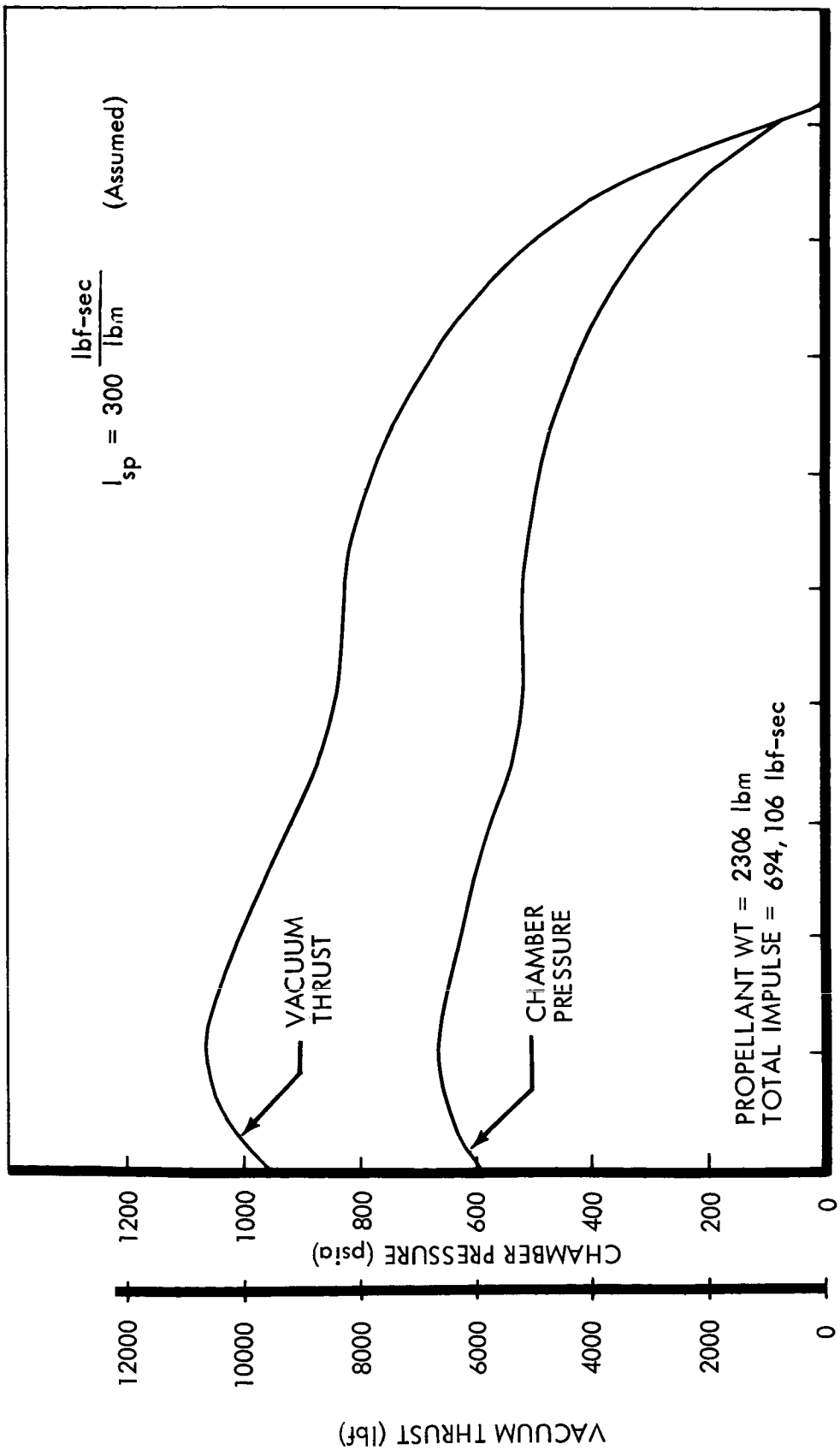

Figure 4.3-16: Solid-Propellant-Motor Performance Data

Thrust Vector Control--The thrust vector control duty cycle, shown in Figure 4.3-17, is based on a vehicle maximum-lateral-center-of-gravity offset of 0.15 inch and a conservative installed motor nominal-thrust-vector angularity of 0.25 degree. The minimum distance between the thrust vector trumion point during secondary injection and the spacecraft center-of-gravity during burning is 20 inches. The thrust-vector-control valves are sized for a maximum deflection angle of 3 degrees which is adequate for quickly stabilizing the vehicle following retro thrust ignition. The secondary injection system will operate at pressures between 1300 and 1500 psi unregulated. Between 3 and 4 pounds of nitrogen from the reaction-control-system nitrogen supply (60 pounds total) are required for secondary injection pressurization.

Subsystem Performance--The orbit insertion propulsion subsystem performance is presented in Table 4.3-1.

4.3.4 Interface Definition

Interfaces for midcourse, orbit trim, and the orbit-insertion-propulsion subsystems are defined below. These interfaces fall into two categories, Flight Spacecraft equipment and operational support equipment.

4.3.4.1 Midcourse and Orbit Trim Propulsion Subsystem

Interfaces with spacecraft equipment include power, CC&S, autopilot, and telemetry as shown in Figure 4.3-18. Thrust-vector-control interfaces with the autopilot, thermal interaction of the engine with spacecraft thermal balance, mechanical interfaces with structure, as well as interfaces with telemetry, power, CC&S and the reaction control subsystem are listed in Table 4.3-10.

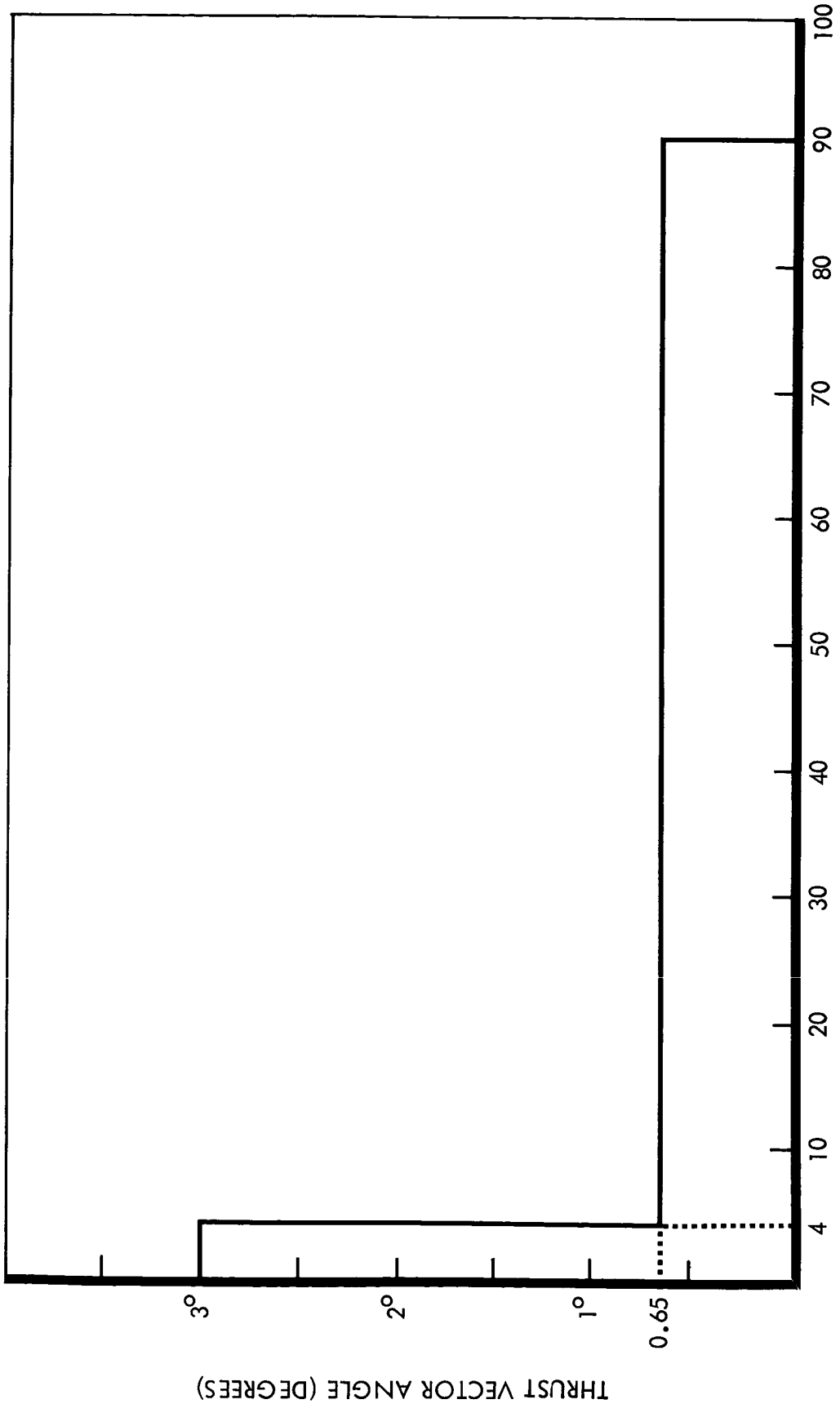

Figure 4.3-17: Solid Retro Secondary Injection Duty Cycle

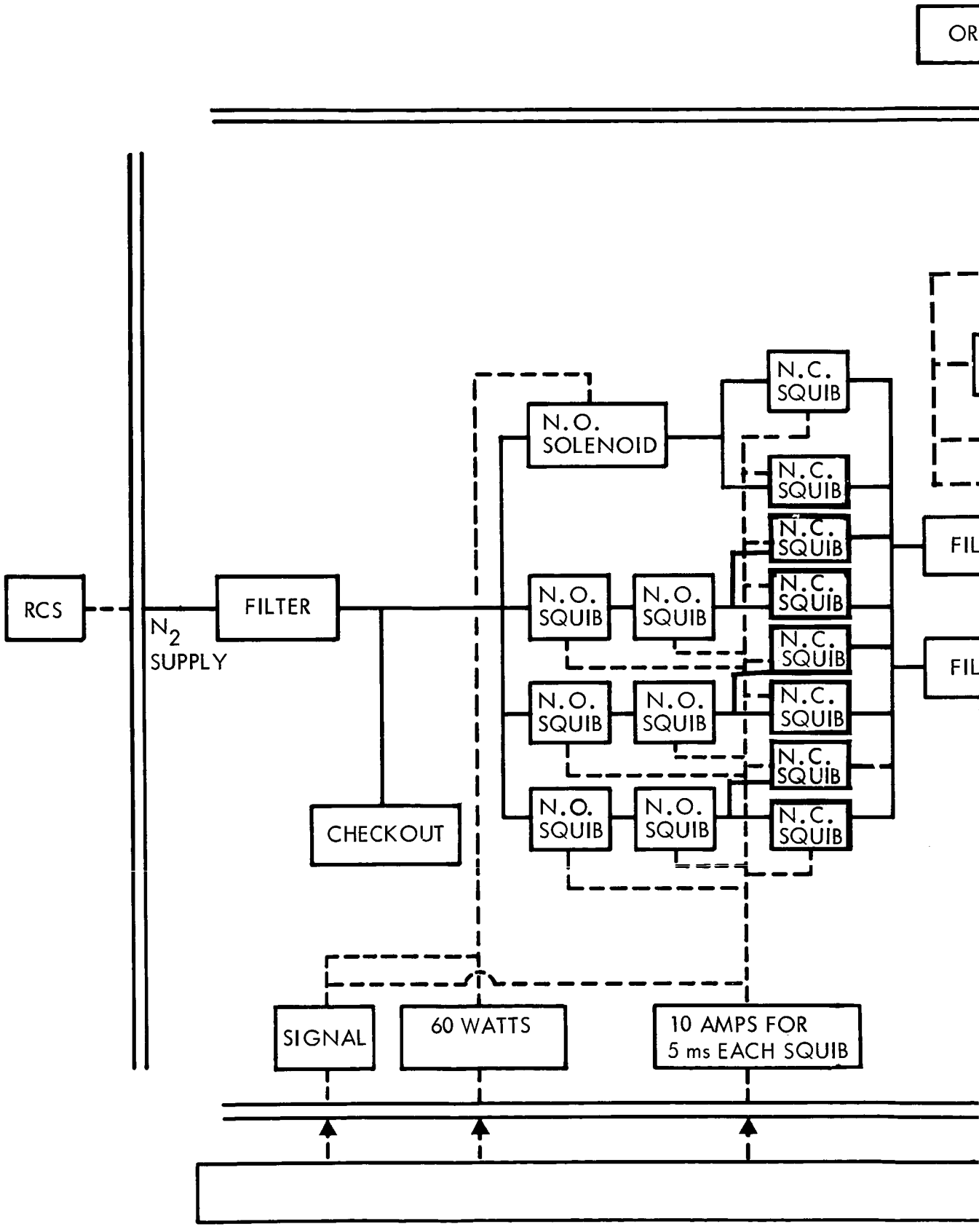
OR
N.C. SQUIB
N.O. SOLENOID
N.C. SQUIB
N.C. SQUIB
FIL
RCS
FILTER
N.O. SQUIB
N.O. SQUIB
N.C. SQUIB
N.C. SQUIB
FIL
N_2 SUPPLY
N.C. SQUIB
N.O. SQUIB
N.O. SQUIB
N.C. SQUIB
N.C. SQUIB
CHECKOUT
N.O. SQUIB
N.O. SQUIB
N.C. SQUIB
SIGNAL
60 WATTS
10 AMPS FOR 5 ms EACH SQUIB

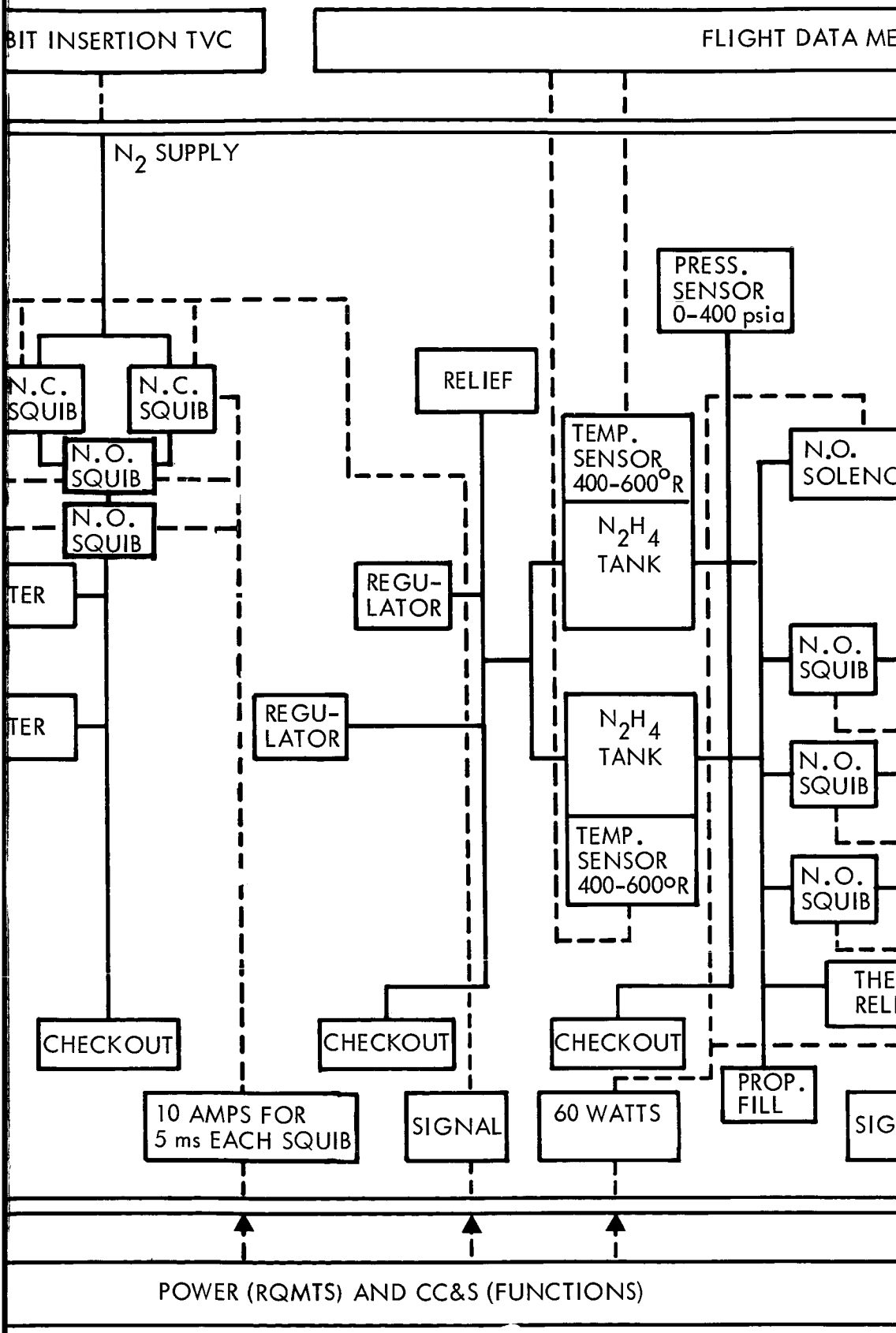
BIT INSERTION TVC
FLIGHT DATA ME
N_2 SUPPLY
PRESS. SENSOR 0-400 psia
N.C. SQUIB
N.C. SQUIB
N.O. SQUIB
N.O. SQUIB
RELIEF
TEMP. SENSOR 400-600°R
N_2H_4 TANK
N.O. SOLENC
TER
REGU-LATOR
N.O. SQUIB
TER
REGU-LATOR
N_2H_4 TANK
N.O. SQUIB
TEMP. SENSOR 400-600°R
N.O. SQUIB
THE REL
CHECKOUT
CHECKOUT
CHECKOUT
PROP. FILL
10 AMPS FOR 5 ms EACH SQUIB
SIGNAL
60 WATTS
SIG
POWER (RQMTS) AND CC&S (FUNCTIONS)

Figure 4.3-18:

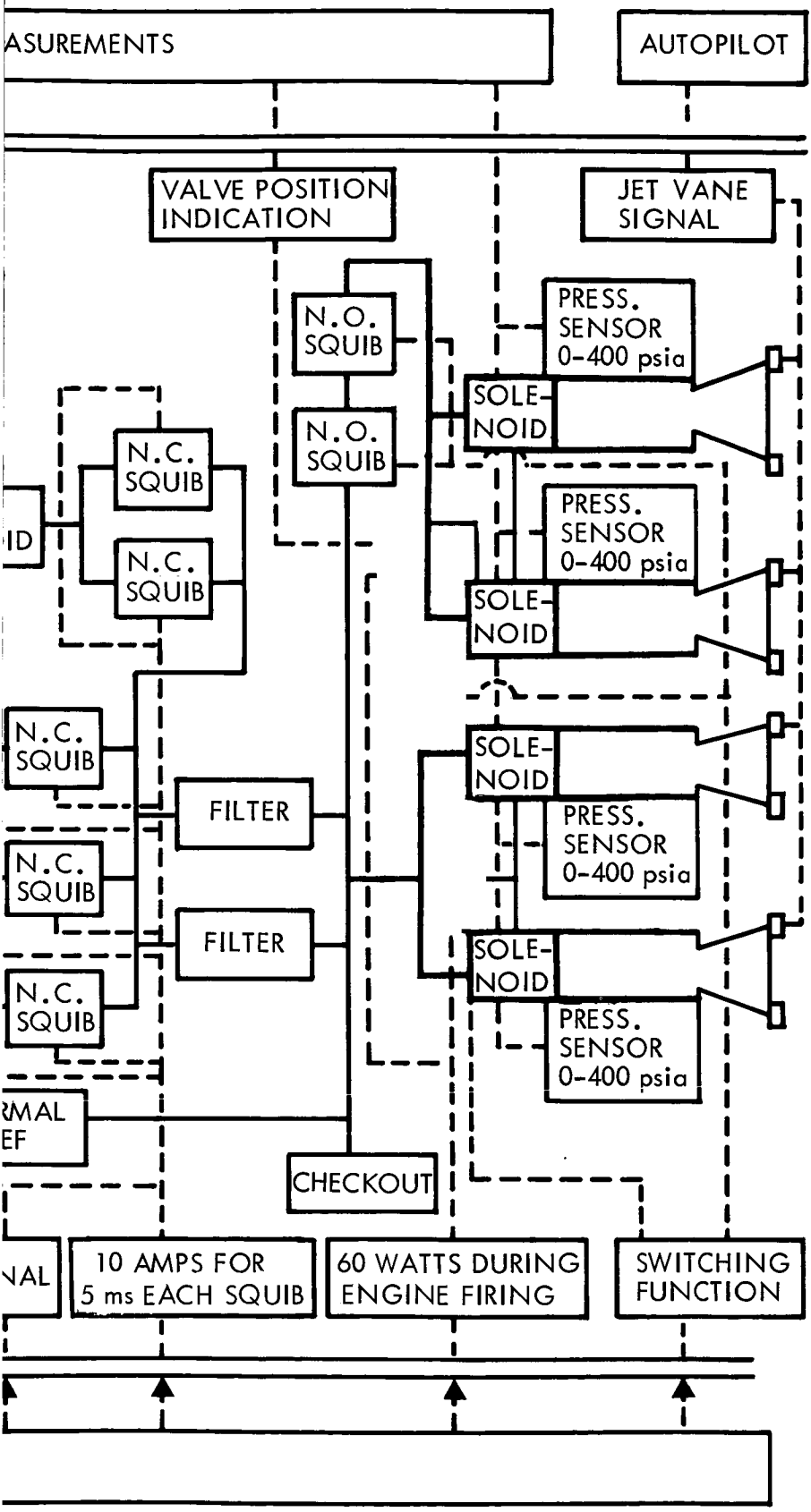

Midcourse and Orbit Trim Subsystem Interfaces with Telemetry, CC&S, Power, and Autopilot

Table 4.3-10: MIDCOURSE AND ORBIT TRIM PROPULSION SUBSYSTEM INTERFACES WITH SPACECRAFT

FLIGHT DATA MEASUREMENT	NUMBER
1) Pressure Sensors - 0 to 400 psia	(9)
2) Propellant Tank Temperature Sensors 400 to 600 ^{o}R	(2)
3) Valve Position Indicators	(2)

POWER AND CC&S

1) N.O. Squib Valves - 10 amps for 5 M.S. Min. (Isolation and Malfunction)	(13)
2) N.C. Squib Valves - 10 amps for 5 M.S. Min. (Isolation and Malfunction)	(5)
3) Solenoid Valves, 60 Watt, 28 Volts (Engine and Isolation)	(6)

MECHANICAL

1) Propulsion Modul to Structure Attach Points and Solid Motor Attach

2) Power Receptacle(s)

3) Telemetry Receptacle(s)

4) Jet Vane Power Receptacle

5) Midcourse Propulsion to RCS N_2 Supply Joint

ATTITUDE CONTROL

(Actual Connection Listed Under Mechanical)

1) Actuation Input to Jet Vane Actuators of 4 Midcourse Engines

2) N_2 Supply to Midcourse Propulsion System Pressurization

THERMAL CONTROL

Temperature Control Requirements for Monopropellant (40-120^{o}F)

CC&S

1) Midcourse Engine Firing Selection

2) Midcourse Engine Malfunction Switching Selection (Pressure Transducers)

Interfaces with Operational Support Equipment include propulsion system test and checkout, pressurization, and propellant servicing as shown in Figure 4.3-19. A tabulation of these interfaces is shown in Table 4.3-11.

4.3.4.2 Orbit-Insertion-Propulsion Subsystem

The interfaces with spacecraft equipment include power, CC&S, telemetry, thermal control, Autopilot, and Operational Support Equipment. These are shown in Figure 4.3-20, tabulated in Table 4.3-12, and discussed below.

Power, CC&S, and Telemetry--The solid-propellant orbit-insertion motor will require electrical power for five functions: 1) Safe-arm device actuation; 2) Igniter squibs firing; 3) Actuation of normally closed squib valves in the thrust-vector-control system; 4) Signalling the thrust-vector-control servo valves; and 5) Supplying power to the thrust-vector-control injector valve pintle position indicators.

Thermal--The temperature of the solid-fueled motor will be maintained between +30°F and +90°F by the thermal control unit. During and after firing, the spacecraft is thermally protected from both the hot case, nozzle, and exhaust plume.

Autopilot--Thrust vector control commands to the servo-valves originate in the autopilot.

Operational Support Equipment--Interfaces between the orbit-insertion-propulsion subsystem and the operational support equipment include: 1) Ordnance Test Unit; 2) Propulsion System Test Unit; 3) Propellant Servicing Unit (Freon); 4) Solid Motor Alignment Unit; and 5) Solid Motor Transporter. These interfaces are listed in Table 4.3-12.

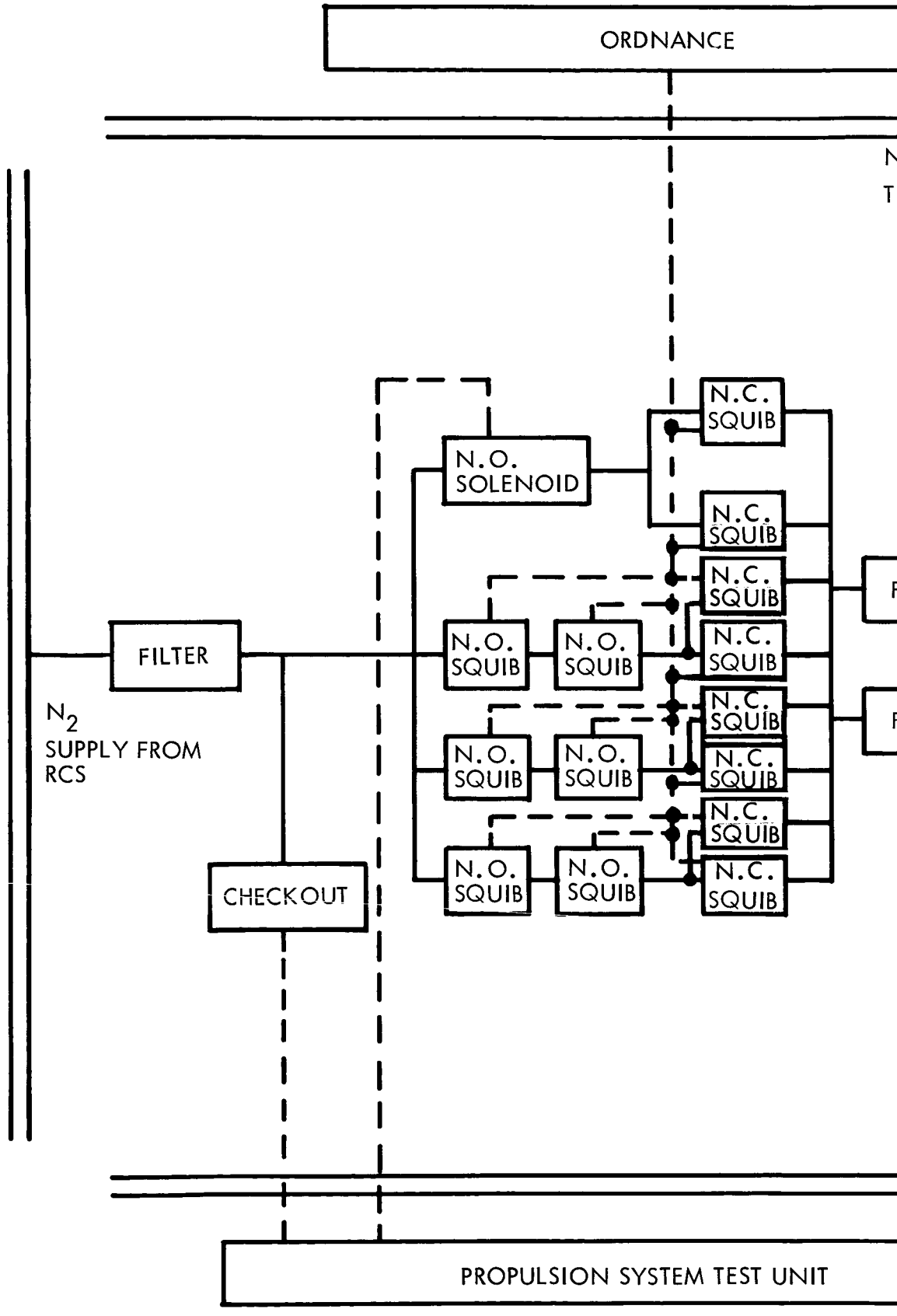
ORDNANCE
N.C. SQUIB
N.O. SOLENOID
N.C. SQUIB
N.C. SQUIB
FILTER
N.O. SQUIB
N.O. SQUIB
N.C. SQUIB
N.C. SQUIB
N_2 SUPPLY FROM RCS
N.O. SQUIB
N.O. SQUIB
N.C. SQUIB
N.C. SQUIB
CHECKOUT
N.O. SQUIB
N.O. SQUIB
N.C. SQUIB
PROPULSION SYSTEM TEST UNIT

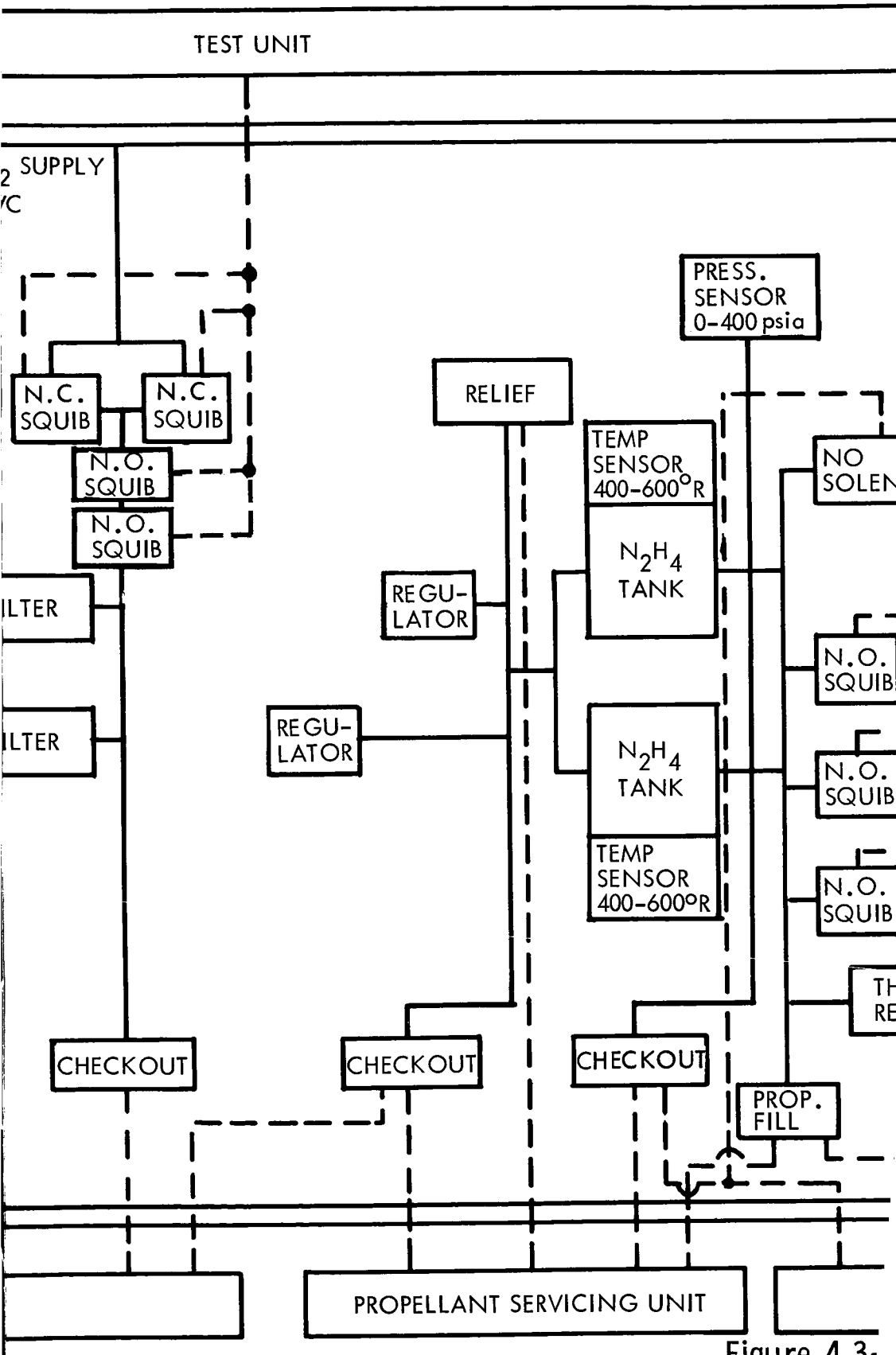
TEST UNIT
SUPPLY
N.C. SQUIB
N.C. SQUIB
N.O. SQUIB
N.O. SQUIB
ILTER
ILTER
PRESS. SENSOR 0-400 psia
RELIEF
TEMP SENSOR 400-600°R
N_2H_4 TANK
REGU-LATOR
REGU-LATOR
N_2H_4 TANK
TEMP SENSOR 400-600°R
NO SOLEN
N.O. SQUIB
N.O. SQUIB
N.O. SQUIB
CHECKOUT
CHECKOUT
CHECKOUT
PROP. FILL
PROPELLANT SERVICING UNIT

Figure 4.3-

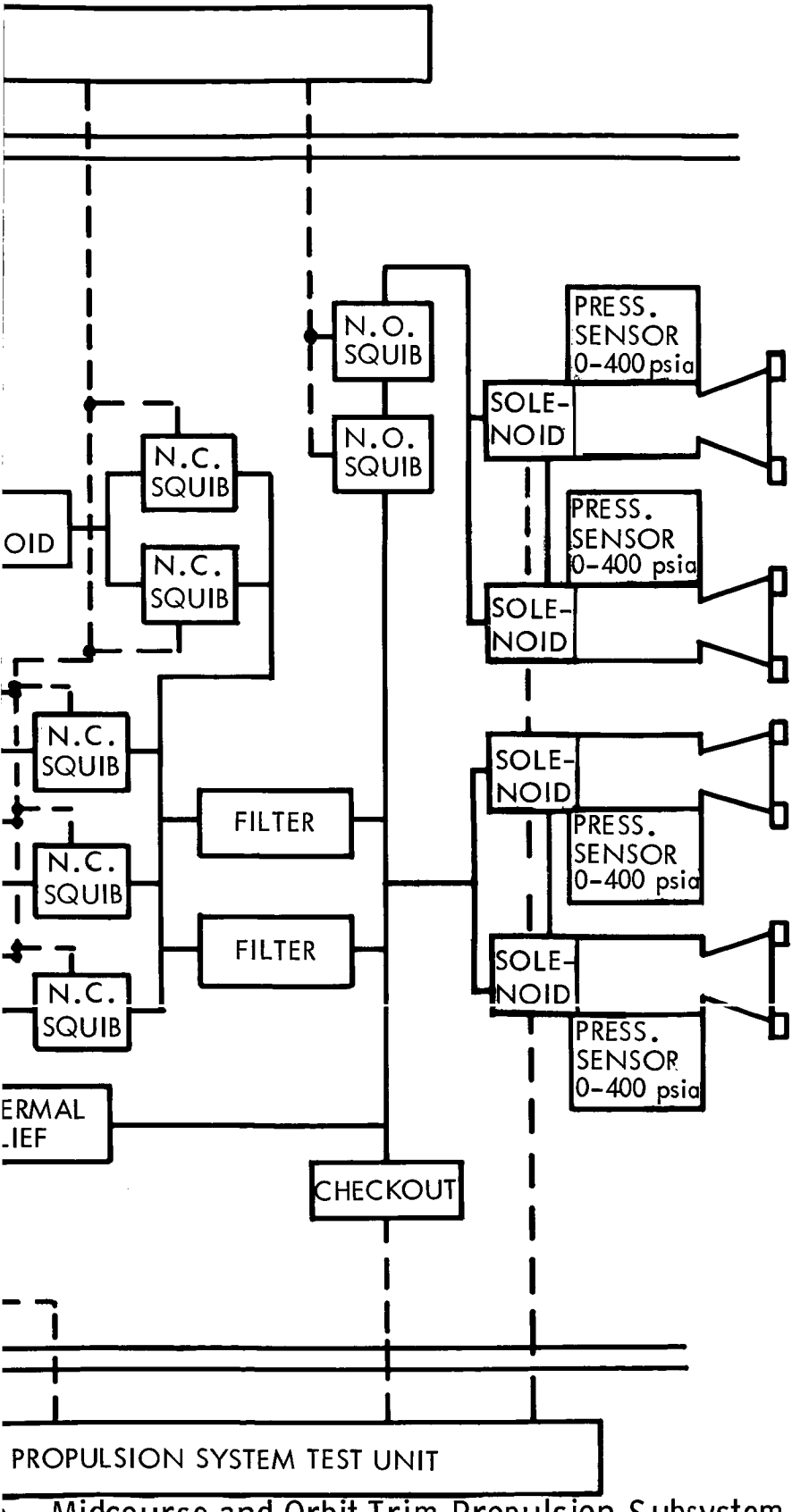

). Midcourse and Orbit Trim Propulsion Subsystem Interfaces with Operational Support Equipment

Table 4.3-11: MIDCOURSE AND ORBIT TRIM PROPULSION SUBSYSTEM INTERFACES WITH OPERATIONAL SUPPORT EQUIPMENT

PROPULSION SYSTEM TEST UNIT	NUMBER
1) Solenoid Actuation	(4)
2) Feed System Leak Check Equipment	
3) Pressurization System Leak Check Equipment	
4) Regulator Checkout	
PROPELLANT SERVICING	
1) N_2H_4 Fill and Vent	
2) N_2H_4 Tank Pre-Pressurization	
ORDNANCE TEST UNIT	
1) Squib Continuity Checkout (Midcourse Engine)	(24)
FLUSH PURGE AND DRY	
1) N_2H_4 Feed System	
SPECIAL TOOLS	

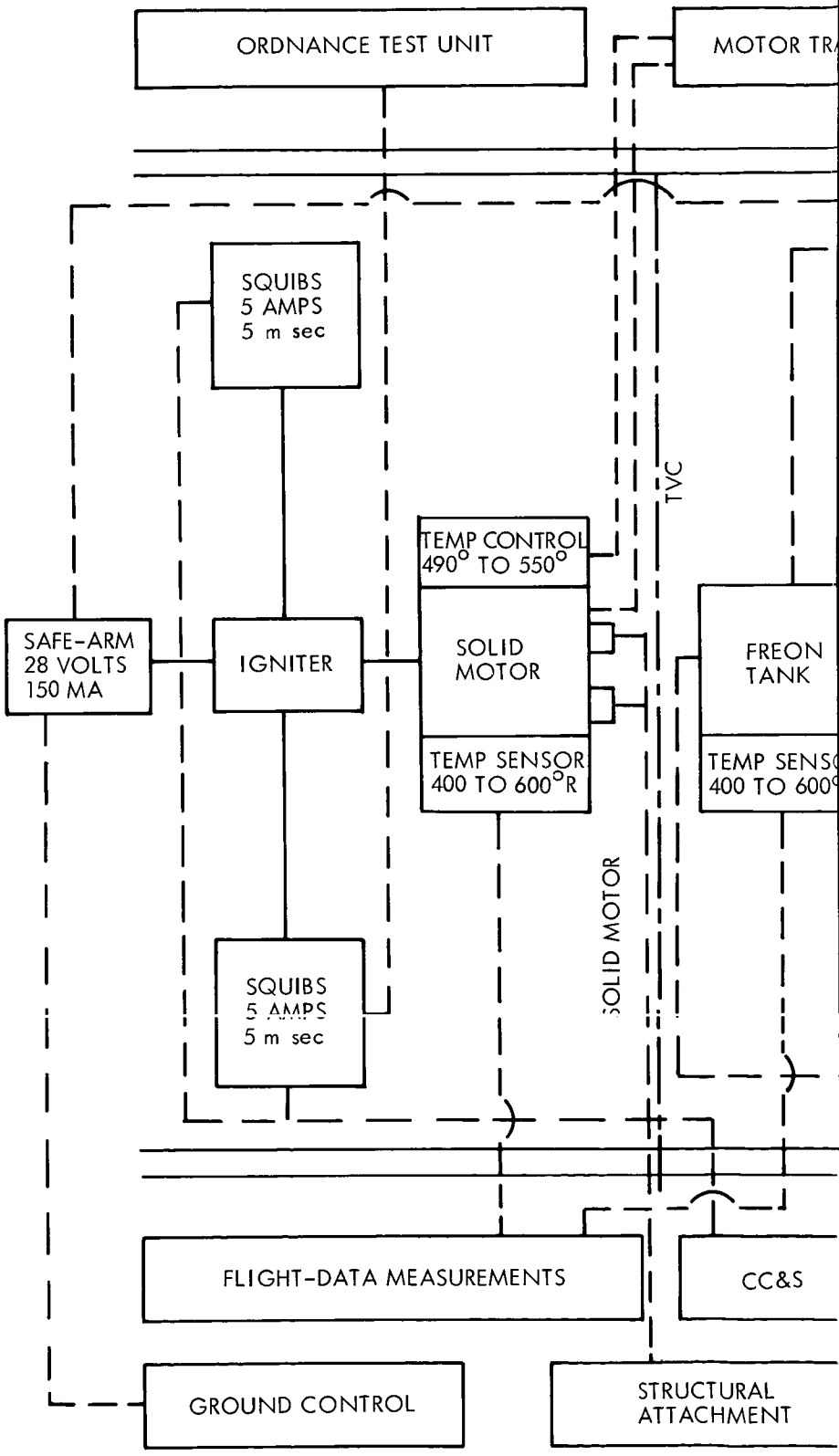
ORDNANCE TEST UNIT
MOTOR TR
SQUIBS
5 AMPS
5 m sec
TVC
TEMP CONTROL
490° TO 550°
SAFE-ARM
28 VOLTS
150 MA
IGNITER
SOLID
MOTOR
FREON
TANK
TEMP SENSOR
400 TO 600°R
TEMP SENS
400 TO 600°
SQUIBS
5 AMPS
5 m sec
SOLID MOTOR
FLIGHT-DATA MEASUREMENTS
CC&S
GROUND CONTROL
STRUCTURAL
ATTACHMENT

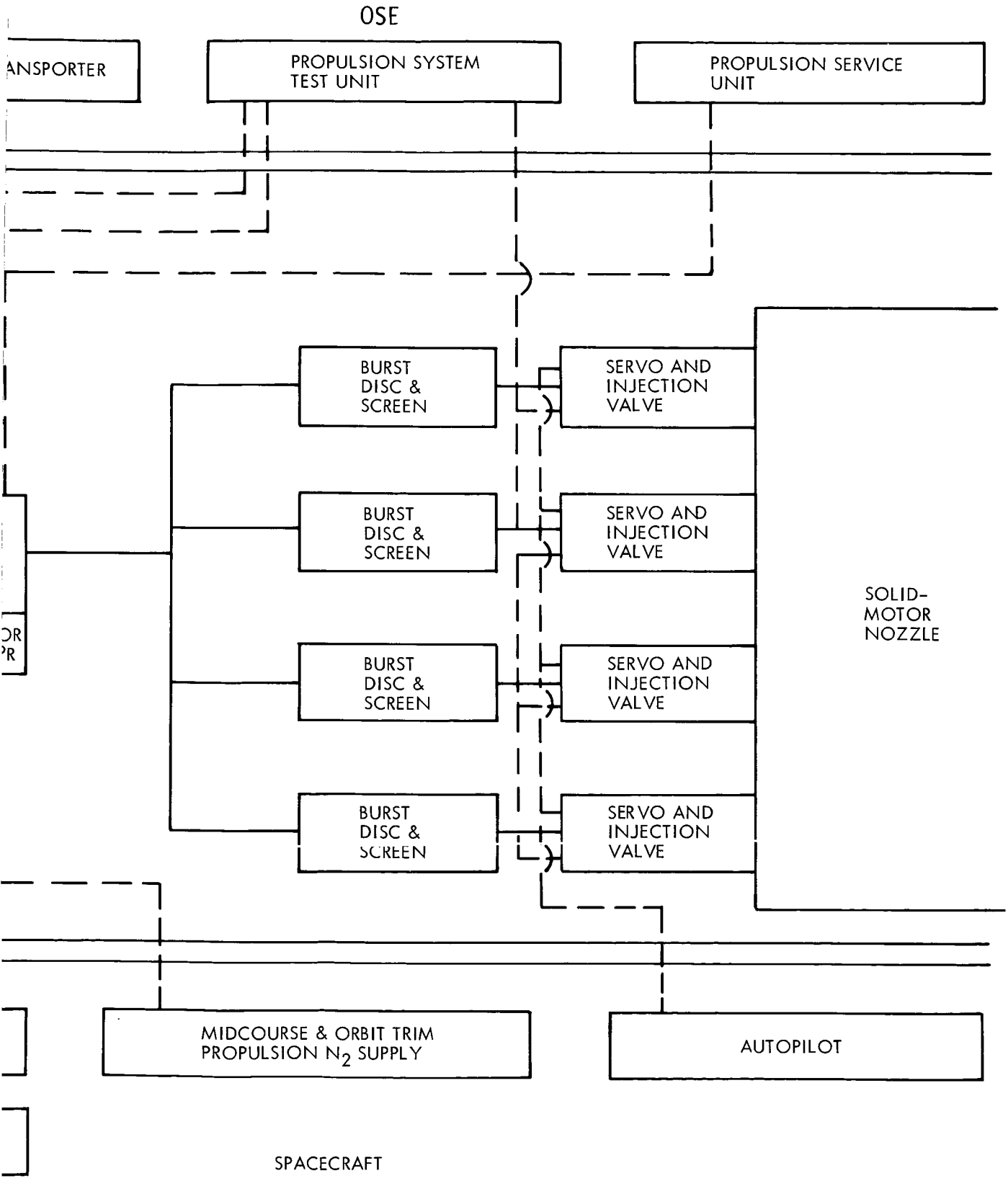

Figure 4.3-20: Orbit Insertion Propulsion Subsystem — O.S.E. Interface Diagram

Table 4.3-12: ORBIT INSERTION PROPULSION SUBSYSTEM INTERFACES WITH SPACECRAFT AND O.S.E.

SPACECRAFT FLIGHT DATA MEASUREMENTS	NUMBER
1) Solid Motor Temperature Sensor	(1)
2) Freon Tank Temperature Sensor	(1)
CC&S POWER	
1) Solid Motor Ignition Squibs - 5 Amps, 5 ms per Squib	(2)
GROUND CONTROL	
1) Solid Motor Safe & Arm Device - 28 Volts, 150 M.A.	(1)
MECHANICAL	
1) TVC to Midcourse Propulsion Subsystem-Joint	(1)
2) TVC to Autopilot~Servo Power Receptical	(1)
ATTITUDE CONTROL (Actual Connection Listed under Mechanical)	
1) Actuation Input to Solid Motor TVC Servo	
THERMAL CONTROL	
1) Temperature Control Requirements for Solid Motor (30^{o} to 90^{o}F)	
O.S.E. PROPULSION SYSTEM TEST UNIT	
1) Solid Motor Safe & Arm Elect Checkout	
2) TVC Freon Tank Leak Checkout	
3) TVC Servo Valve Actuation Checkout	
MOTOR TRANSPORTER	
1) Transportation Requirements	
2) Thermal Control ~30 to 90^{o}F	
PROPULSION SERVICE UNIT	
1) TVC Freon Fill & Drain	
ORDANCE TEST UNIT	
1) Solid Motor Ignition Squib Electrical Continuity Checkout - 1 Amp - 1 Watt	

4.3.5 Performance Parameters

The propulsion subsystem performance parameters discussed below include subsystem reliability, tolerances, sensitivity, and transients. Table 4.3-1 summarizes the propulsion subsystem performance parameters.

4.3.5.1 Reliability

The predicted reliability of the propulsion subsystem is 0.9973. This prediction is a result of the high reliability of the orbit-insertion solid-fueled motor and the selective redundancy provided in the design of the midcourse and orbit-trim subsystem.

Solid Subsystem--The reliability of the solid motor, subsequent to an intensive development program, is predicted to be 0.9995 for this size motor and application. The secondary fluid-injection system reliability is improved by isolating it from the remainder of the subsystem prior to orbit insertion. This decreases the time that Freon tankage is exposed to high-pressure nitrogen gas. Burst disks are provided to seal the reservoir outlet ports and minimize Freon leakage.

Monopropellant Subsystem--The high reliability of the midcourse and orbit-trim subsystem is based on simplicity and redundancy. Positive isolation of pressurant from propellant, and propellant from engine-inlet solenoid valves minimizes leakage. One leg of series-mounted one-way squib valves is available for each of the three midcourse correction firings. On the gas side, each leg consists of two

normally closed dual-squib valve for isolation prior to engine operation; and two normally open squib valves in series for positive shutoff after engine operation. On the propellant side, one normally closed and one normally open squib valve are provided for isolation prior to and after engine use. The backup midcourse maneuver and any orbit trim maneuver are expected to take place within a relatively short time. Therefore, a solenoid valve in series with two parallel normally closed squib valves is considered compatible with minimum leakage design. Dual filters in parallel are supplied to prevent squib valve particles from reaching the regulators and engine-inlet solenoids. Dual regulators which can only fail in the closed position, are provided for redundancy. A nonpropulsive relief valve is provided downstream of the regulators to prevent overpressurization of the propellant tankage.

The isolation valving downstream of the propellant tanks follows the same philosophy as above. The engines are operated in pairs. If one of the pair experiences a malfunction, both engines will be shutdown and isolated. The other pair is then brought into operation. A thermal relief valve is provided to permit expansion of the propellant trapped between the isolation valves and the engine inlet valves. The butyl bladders have been proven in previous monopropellant systems and have exhibited excellent reliability. The monopropellant engines, operating at relatively low pressures and temperatures, have high reliability.

4.3.5.2 Tolerances

Pertinent propulsion subsystem and component tolerances are listed in Table 4.3-13.

Table 4.3-13: PROPULSION SUBSYSTEM TOLERANCES

Item	Value	Tolerance	Confidence
Weight			
Propulsion Subsystem Weight	3470 LB	±0.1%	3 σ
Orbit Insertion Subsystem Weight	2686 LB	±0.1%	3 σ
Midcourse and Orbit Trim Subsystem Weight	784 LB	±0.1%	3 σ
Solid Motor Weight	2578 LB	±0.1%	3 σ
Solid Propellant Weight	2306 LB	±0.15%	1 σ
N_2H_4 Propellant Weight	395 LB	±0.1LB	3 σ
Performance			
Solid Motor			
Total Impulse	694,106 LB-Sec	±.6%	3 σ
N_2H_4 Subsystem Total Impulse	98,825 LB-Sec	±1.2%	3 σ
Solid Motor Thrust (Ave)	7988 LB	±4%	3 σ
N_2H_4 Engine Thrust (Each)	50 LB	±1 LB	3 σ
Minimum Midcourse	0.0043 Ft/Sec	±10%	3 σ
Minimum Orbit Trim	0.0119 Ft/Sec	±10%	3 σ
Orbit Insertion	5700 Ft/Sec	±0.32%	1 σ
Solid Motor Is (Assumed)	300 Sec	±.32%	3 σ
N_2H_4 Engine Is (Assumed)	235 Sec	±2.8 Sec	3 σ

4.3.5.3 Propulsion Subsystem Sensitivity Coefficients

Sensitivity coefficients (exchange ratios, trade factors) describing startburn or burnout weight variations as a function of specific impulse variations are given in Table 4.3-14. Coefficients are based on propulsion subsystem nominal weight breakdown values given in Table 4.3-15. Contingency allowances are incorporated as spacecraft inert weight.

4.3.5.4 Transients

The thrust-time transients associated with the monopropellant and solid systems are described in the following paragraphs.

Midcourse and Orbit Trim Propulsion Subsystem--A typical thrust-time trace for a hydrazine monopropellant engine is depicted in Figure 4.3-21. This figure is based on estimated cold catalyst bed response times for a 50 pound thrust engine. Engine catalyst bed and propellant temperatures are assumed to be at 70^{o}F. These transients are summarized below:

Item	Time
Start Transient	
Signal to First Indication of Pressure Rise	20 milliseconds
Signal to 90 percent Thrust	200 milliseconds
Cutoff Transient	
Signal to First Indication of Thrust Decay	5 milliseconds
Signal to 10 percent Thrust	100 milliseconds

Table 4.3-14: PROPULSION SUBSYSTEM SENSITIVITY COEFFICIENTS

CONDITION	SENSITIVITY COEFFICIENT	UNITS	MIDCOURSE CORRECTION	ORBIT INSERTION	ORBIT TRIM
Constant Startburn Mass	$\frac{\partial M_{BO}}{\partial I_s}$	$\frac{\text{LBM}}{\frac{\text{LBF}}{\text{LBM/SEC}}}$	1.035	5.732	0.5201
Constant Burnout Mass	$\frac{\partial M_{SB}}{\partial I_s}$	$\frac{\text{LBM}}{\frac{\text{LBF}}{\text{LBM/SEC}}}$	-1.106	-10.19	-0.5617
Constant Startburn and Burnout Mass	$\frac{\partial(\Delta V)}{\partial I_s}$	$\frac{\text{FT/SEC}}{\frac{\text{LBF}}{\text{LBM/SEC}}}$	1.047	19.0	1.395

Table 4.3-15: PROPULSION SUBSYSTEM
MISSION DUTY CYCLE WEIGHT AND PERFORMANCE BREAKDOWN

MANEUVER	WEIGHT STATUS	WEIGHT (lbm)	SPECIFIC IMPULSE I_s (lbf-sec/lbm)	VELOCITY (m/sec)
Midcourse Correction	Startburn	7800		
	Propellant	255	235 (Assumed)	75
	Burnout	7545		
(Capsule Separation)	(Capsule)	(2300)		
Orbit Insertion	Startburn	5245		
	Propellant	2306	300 (Assumed)	1740
	Burnout	2939		
Orbit Trim	Startburn	2939		
	Propellant	127	235 (Assumed)	100
	Burnout	2812		
In-Orbit	Contingencies: Monoprop. (13) Inerts (70) (Titanium case for Solid Motor (30)	113		
	Assigned Prop. Inerts	699		
	Spacecraft and Science Payload	2000		

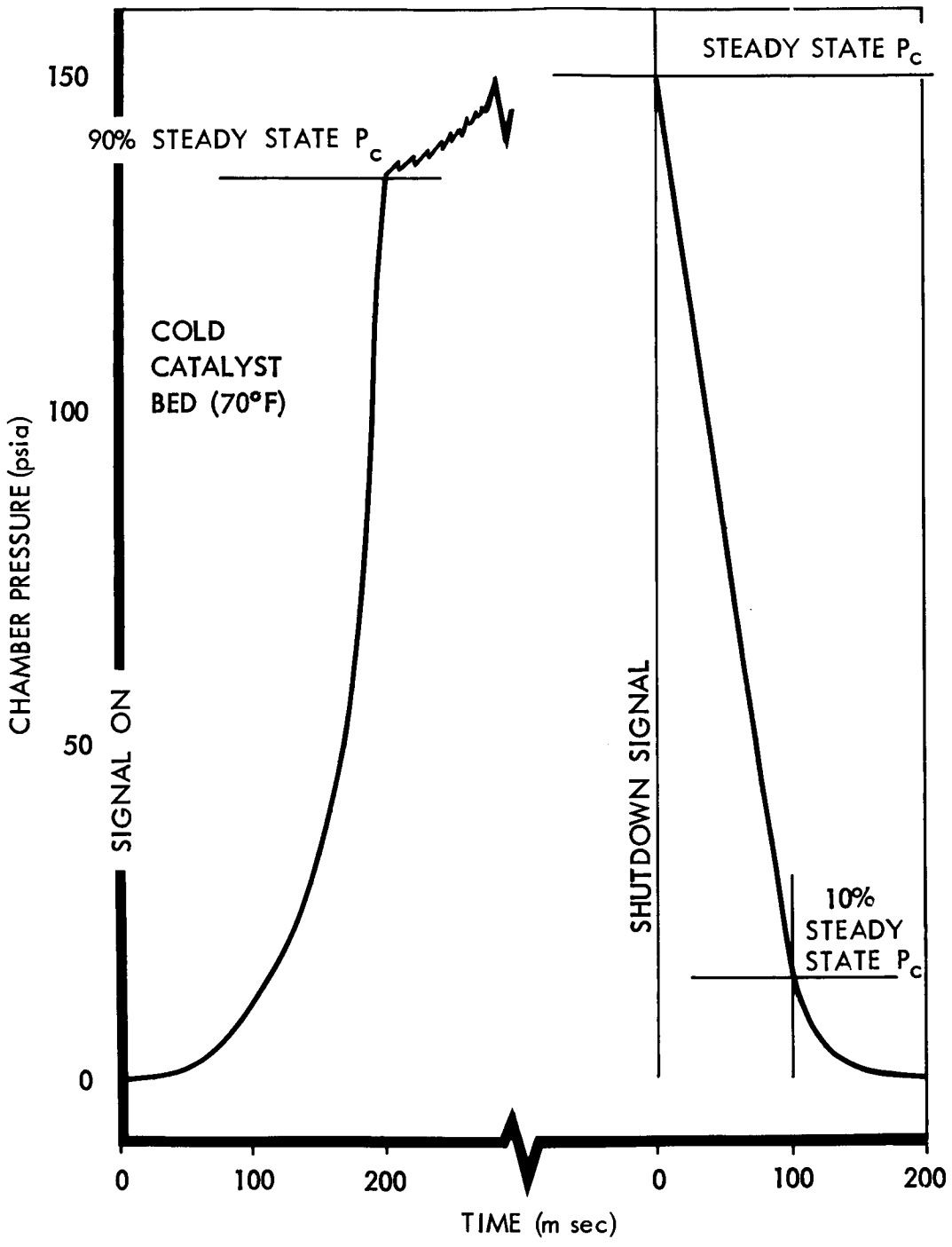

Figure 4.3-21:Monopropellant-Hydrazine-Engine Transient Performance

Orbit Insertion Propulsion Subsystem--The estimated start transient thrust-time trace for the orbit-insertion motor is shown in Figure 4.3-22. Motor and propellant temperature is assumed to be 70°F.

The thrust-vector-control system dynamics are presented in Section 4.6.

4.3.5.5 Midcourse Maneuver Velocity Errors

Midcourse correction maneuver errors occur primarily because of component, instrumentation, and subsystem operating tolerances. These errors consist of burntime dependent errors, burntime independent errors, and transient errors. Timed engine control is sensitive to all of these errors. Figure 4.3-23 shows the normalized 3-sigma velocity error of the midcourse propulsion subsystem for timed engine control. Timer errors are not included. Desired error limits included in this figure represent 1 percent velocity errors (1 sigma) for all maneuvers greater than 1 meter per second. For maneuvers less than 1 meter per second, a 3-sigma boundary of 10 percent is prescribed. Accelerometer-controlled engine operation removes the effects of all errors occurring prior to signalled engine cutoff. The error under these conditions results from fixed shutoff errors. This error is shown in Figure 4.3-23 exclusive of accelerometer errors and failure circumstances. The magnitude of accelerometer-controlled engine errors is very small. In actuality, accelerometer errors will dominate.

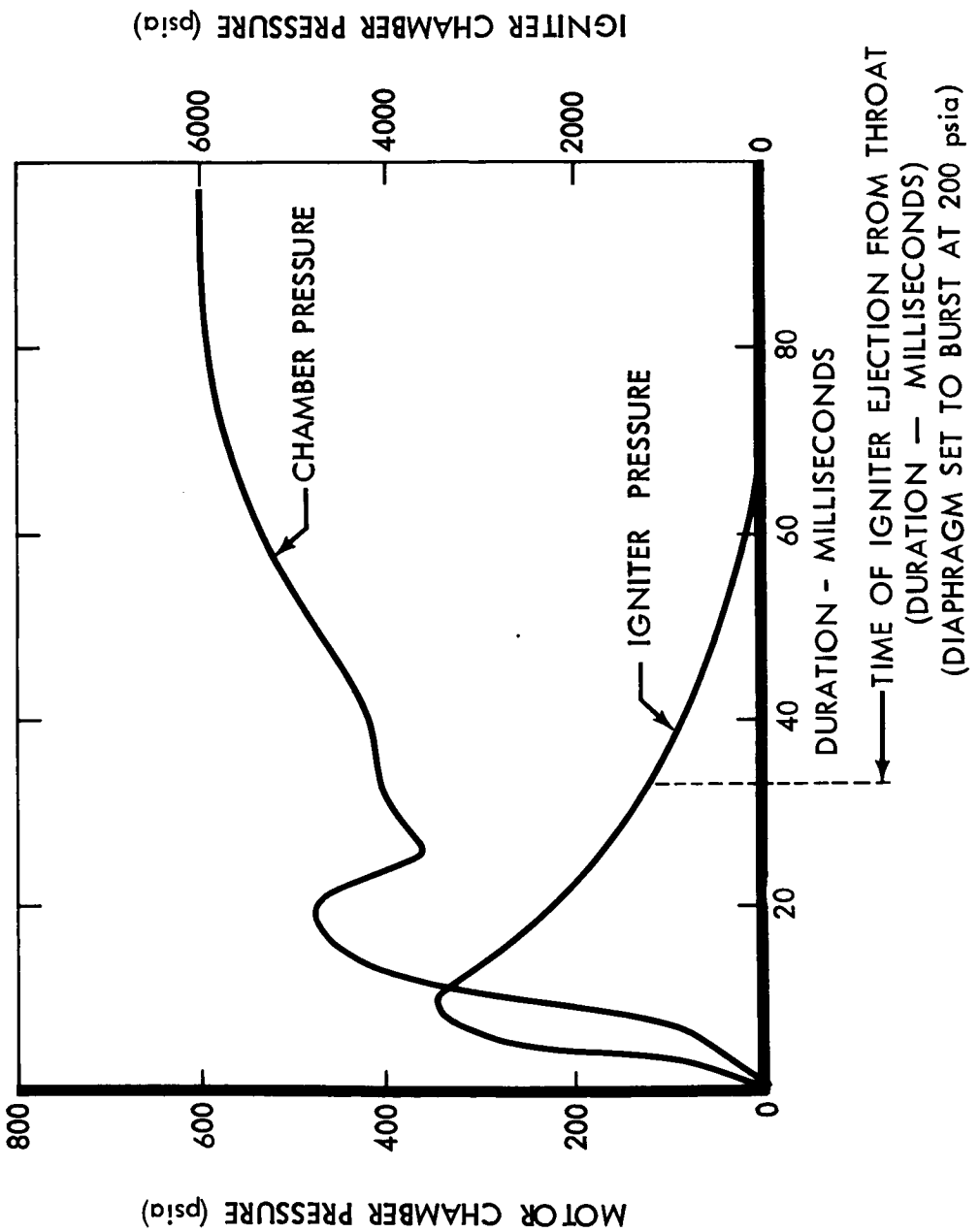

Figure 4.3-22: Ignition Transient — Voyager Retropropulsion Motor

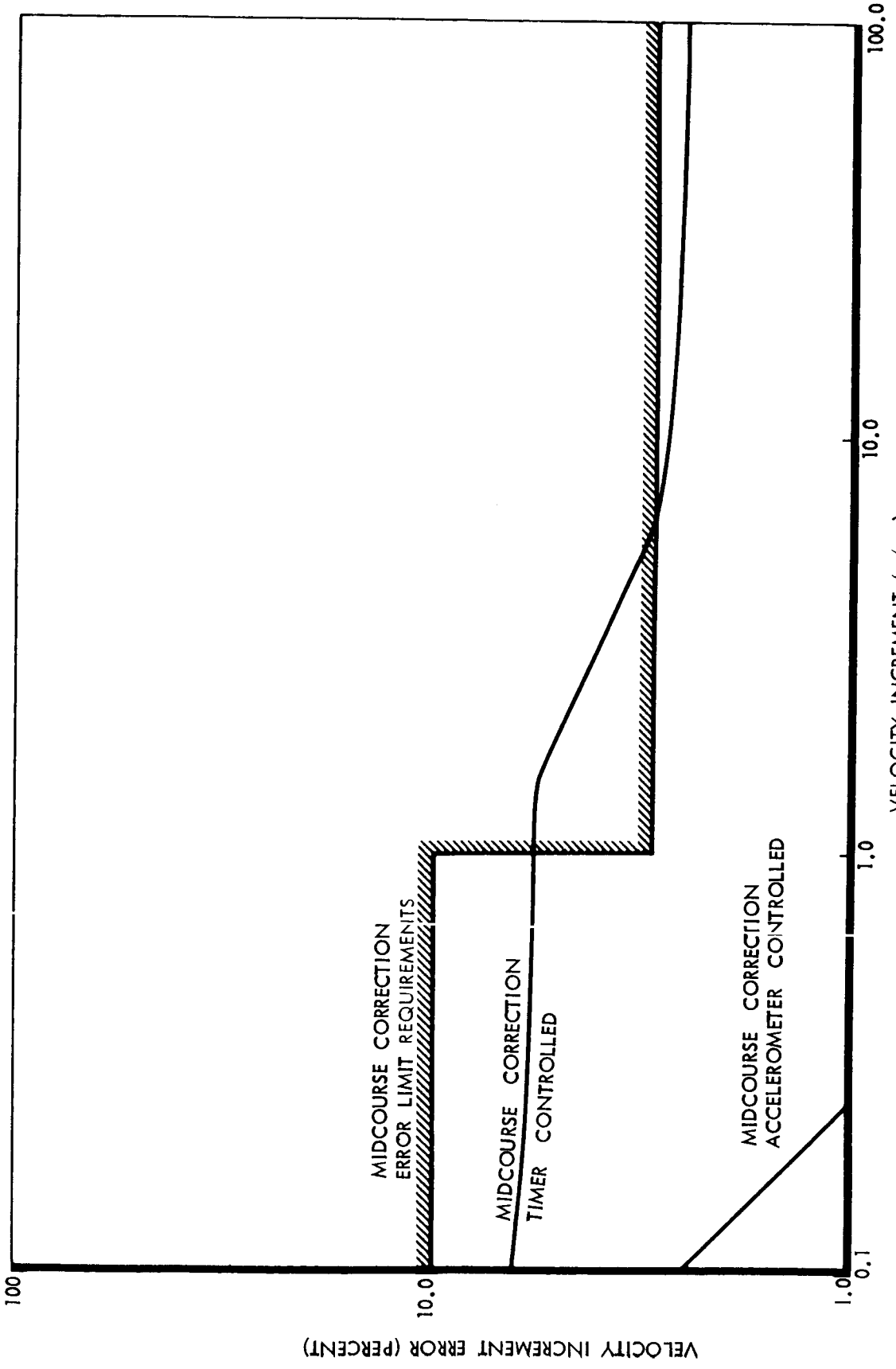

Figure 4.3-23: Percent ΔV Error vs Midcourse Propulsion System ΔV

4.3.6 Physical Characteristics and Constraints

This section defines the following for the propulsion subsystem: 1) Module weight; 2) Module configuration envelope; 3) Subsystem power consumption; 4) Subsystem temperature requirements; and 5) Subsystem constraints. Volume and dimensions of subsystem components were provided in Sections 4.3.2 and 4.3.3. Subsystem environment during operations is specified in Section 4.4.1.

4.3.6.1 Weight

Module installation gross weight is 3500 pounds. A detailed module weight statement is given in Table 4.3-16.

4.3.6.2 Envelope

Propulsion module envelope is shown in Figure 4.3-4.

4.3.6.3 Power

Propulsion subsystem power consumption is summarized in Table 4.3-17.

4.3.6.4 Temperatures

Propulsion subsystem environmental temperatures during shipping, storage, and operations are given in Table 4.3-18.

4.3.6.5 Constraints

1) The module must be capable of imparting to a 7800-pound Planetary Vehicle a maximum velocity increment of 75 meters per second for fulfillment of maximum expected midcourse maneuver requirement.

Table 4.3-16: WEIGHT STATEMENT - PROPULSION SUBSYSTEM

	Weight, Pounds
Solid Rocket Motor Inerts - Orbit Insertion	272
O.I. Motor T.V.C. Provisions	108
Liquid Rocket Engine - Orbit Insertion	---
O.I. Engine T.V.C. Provisions	---
Liquid Rocket Engine - Midcourse Corrections	12
M.C. Engine T.V.C. Provisions	10
Liquid Propellant Tankage	26
Liquid Propellant Expulsion Provisions	10
Liquid Propellant Plumbing	24
Pressurant Tankage	*
Pressurant Plumbing	16
Heat Shield - O.I. Motor/Engines	32
Heat Shield - M.C. Engines	20
Insulation Blanket - Solid Motor Chamber	8
Thermal Shrouds and Louvers	11
Structural Support - Solid Rocket Motor	30
Structural Support - Liquid Rocket Engines, Tankage	53
Meteoroid Shielding	42
Wire Harness	10
Nitrogen Gas - Propellant Tank Pre-charge	---
Nitrogen Gas - Stored in Pressurant Tankage	*
Liquid Propellant Residuals Allowance	15
Weight Contingency	100**
INSTALLATION INERT WEIGHT	799
Liquid Propellant ***	395
Solid Propellant	2306
INSTALLATION GROSS WEIGHT	3500

* Incorporated into Reaction Control Subsystem
** Includes 30 pound allowance for possible change from fiberglass to titanium solid motor case.
***Includes 3% contingency for effect of Jet Vane Deflection on specific impluse.

Table 4.3-17

PROPULSION SUBSYSTEM POWER REQUIREMENTS

Mission Sequence	Propulsion Subsystem Operation	Power Requirements
1st Midcourse	1. Activate Pressurization Subsystem - two N.C. Squib	20 amp, 5 M.S.
	2. Activate Propellant Feed Subsystem - One N.C. Squib	10 amp, 5 M.S.
	3. Fire Programmed M.C. Engines - Two Solenoid continuous during engine operation	120 watts max.
	4. Isolate Propellant Feed Subsystem - One N.O. Squib	10 amp, 5 M.S.
	5. Isolate Pressurization Subsystem - Two N.O. Squibs	20 amp, 5 M.S.
2nd Midcourse	Same as 1st Midcourse	Same as 1st M.C.
3rd Midcourse	Same as 1st Midcourse	Same as 1st M.C.
4th Midcourse (if required)	1. Activate Pressurization Subsystem - Two N.C. Squibs	20 amp, 5 M.S.
	2. Activate Propellant Feed Subsystem - Two N.C. Squibs	20 amp, 5 M.S.
	3. Fire Programmed Engines - Two solenoid valves continuous during engine operation	120 watts max
	4. Isolate Propellant Feed Subsystem - One solenoid duration of latching operation	60 watts max
	5. Isolate Pressurization Subsystem - One solenoid duration of latching operation	60 watts max.
Mars Orbit Insertion	1. Activate Pressurization Subsystem - One solenoid duration of latching operation	60 watts max
	plus two N.C. Squibs	20 amps, 5 M.S.
	2. Fire Motor - two ignition Squibs	10 amps, 5 M.S.
	3. Isolate Pressurization Subsystem - One solenoid Plus two N.O. Squibs	60 watts max. 20 amp, 5 M.S.

Table 4.3-17 (cont.)

Mission Sequence	Propulsion Subsystem Operation	Power Requirements
Orbit Trim	1. Activate Pressurization Subsystem - One latching solenoid	60 watts max
	2. Activate Propellant Feed Subsystem - One latching solenoid	60 watts max
	3. Fire Programmed Engines - two solenoid valves continuous during engine operation	120 watts max
	4. Isolate Propellant Feed Subsystem - One solenoid duration of latching operation	60 watts max
	5. Isolate Pressurization Subsystem - One solenoid duration of latching operation	60 watts max

Table 4.3-18: ENVIRONMENTAL TEMPERATURES

Midcourse Correction Subsystem	
Operational environmental temperatures	
Pressurization system Propellant and propellant supply system Engine and jet vanes	+40° to +120°F
Storage environmental temperatures	
Pressurization system Propellant and propellant supply system Engine and jet vanes	+40° to +120°F
Shipping environmental temperatures	
Pressurization system Propellant supply system	-65° to +125°F
Engine and jet vanes Propellant	+40° to +120°F
Orbit Insertion Subsystem	
Operational environmental temperatures	
Solid propellant motor Thrust vector propellant Thrust vector hardware	+30° to +90°F
Storage environmental temperatures	
Solid propellant motor Thrust vector propellant Thrust vector hardware	+30° to +90°F
Shipping environmental temperatures	
Solid propellant motor Thrust vector propellant Thrust vector hardware	+30° to +90°F

2) The module will be capable of delivering a minimum midcourse correction velocity increment of 0.100 meter per second to a 7800-pound Planetary Vehicle to an accuracy of 0.010 meter per second.

3) The module will be capable of imparting to a 5500-pound flight spacecraft a fixed velocity increment of 5700 feet per second for fulfillment of orbit insertion maneuver requirement to an accuracy of 20 feet per second.

4) The module will be capable of imparting to a 2939-pound spacecraft a maximum velocity increment of 100 meters per second for fulfillment of the maximum expected orbit trim maneuver.

5) The module will be capable of a total of six monopropellant subsystem ignitions and thrust terminations for fulfillment of the maximum expected number of midcourse maneuvers and orbit trim.

6) The midcourse and orbit trim maneuver ignitions and engine operations must be accomplished in a vacuum environment under zero gravity conditions.

7) The preflight to launch ambient temperature range at the propulsion module will be $+40^{\circ}$ to $+90^{\circ}$F.

8) The propulsion module temperature limits from time of launch through termination of the mission will be from $+40^{\circ}$ to $+90^{\circ}$F.

9) The module must be capable of vacuum environment storage in excess of 395 days without causing any deleterious effect on the flight spacecraft attitude control or performance.

10) The midcourse and orbit-trim rocket engine nominal steady state vacuum thrust with four jet vanes deflected through 10 degrees will be no greater than 52.5 pounds and no less than 47.5 pounds per engine.

11) The vacuum specific impulse on which propellant load and velocity increment capability are to be determined will be 235.

4.3.7.1 Fire

The following three elements must be present for a fire to occur; heat, oxidizer, and fuel. The elimination of any of these elements will preclude the danger of fire. In the elimination process, factors to be considered during propellant servicing, subsystem checkout, and propellant transfer are as follows.

Propellant Servicing and Subsystem Checkout--1) Proper grounding to certified ground stake; 2) Proper placement and tagging of squib shorting plugs; and 3) Avoidance of sparks from tooling.

Propellant Transfer (Storage Container to OSE)--1) Proper common bond and grounding; and 2) Proper tooling for making connections.

Propellant Transfer (OSE to Propulsion Subsystem)--1) Proper grounding; 2) Proper tooling; and 3) No smoking in operation area.

4.3.7.2 Explosion

The same factors considered for prevention of fire apply for prevention of explosions. In addition, consideration should be given to barricades of sufficient mass to decrease the effect of an explosion, should one occur.

4.3.7.3 Toxicity

Factors to be considered in eliminating toxicity effects are: 1) Minimization of spills and leaks; 2) Use of impermeable protection clothing and self-contained breathing apparatus for personnel; 3) frequent sampling of air in proximity of propulsion subsystem; 4) periodic examination of

personnel, and 5) Instruction of personnel in hygienic procedures and basic first aid.

4.3.8 Design Verification Testing Requirements

The preferred Spacecraft Propulsion design uses concepts, components, and materials that rely on existing experience and available technology. To further increase confidence in the selected propulsion subsystem, design verification and testing are proposed. These tests could and should be conducted prior to the July 1966 design freeze date.

4.3.8.1 Solid Rocket

All materials and components proposed on the preferred design have demonstrated their required high reliability on production programs. However, the reliable operation of these components, when integrated into a full-scale oblate spheroid or very short cylindrical motor with a conocyl grain design, has not been demonstrated. In addition, heat sterilization and space aging effects on the solid motor need to be more clearly defined. To resolve those questions, the following design verification test program is proposed.

Propellant--The critical item in development of a heat sterilizable solid motor is the propellant. Nonaluminized propellants have been successfully heat-sterilized. Aluminized propellants have not fully demonstrated this capability. A 5 percent aluminum polybutadiene formulation, cut into 6 by 8 by 0.5 inch slabs, has successfully completed heat cycle sterilization. The preferred design propellant containing 16 percent aluminum is presently undergoing sterilization. However, it is expected that some reformulation of the propellant composition will be required to achieve a reliable, high-performance, sterilizable propellant.

They are off-the-shelf, aluminized, high-performance formulations that have better high-temperature capabilities than the preferred design propellant. This formulation, though it has not been as widely used as the preference propellant, can be considered as a backup.

Consequently, it is proposed that:

1) Several samples of aluminized propellants be heat-cycle sterilized, and;
   a) The physical properties of the sterilized propellants be determined.
   b) Two of the most promising samples be cast into approximately eight subscale motors and then static fired. Measurements on exhaust plume thermal radiation intensities will be conducted simultaneously with this and all other firing tests as discussed in Section 4.4.1.
2) Four additional subscale motors containing the sterilized propellant will be cast and stored under a simulated space environment.
   a) After 4 and 8 months, two of these motors will be removed and static fired.
   b) Janaf specimens will also be stored for physical properties evaluation.

Motor--Two heavyweight (steel) motors identical, or similar, to the proposed design will be built and fired (the domes from an existing motor of approximately 50 inch diameter will be used if possible). The first motor will be fired in an altitude chamber. This motor will be used to demonstrate the ballistic properties and structural compatibility of the design. The second motor will be heat-cycle sterilized and then statically fired.

4.3.8.2 Secondary Injection Thrust-Vector-Control

The proposed freon secondary injection Thrust-Vector-Control system is patterned from the Minuteman and HiBEX missile designs. No new concepts or materials are proposed.

4.3.8.3 Monopropellant Subsystem

Design verification tests prior to the July 1966 freeze date is required in two areas, catalyst qualification and subsystem sterilization.

Catalyst Qualification--The development and qualification of the Shell 405 spontaneous catalyst is essential for the Voyager mission. The requirement for the several operations of the midcourse and orbit-trim propulsion engines requires that a simple and reliable means for restarting an engine after long shutdown periods be provided.

The qualification program for this catalyst should be completed prior to July 1966. At the present stage of development, there is confidence within the industry that the catalyst will fulfill all requirements. However, all possible operating conditions have not yet been explored. Items of interest in establishing qualification are:

1) Long-term storage in high vacuum, solar radiation, and nuclear radiation
2) Exposure of the catalyst to micrometeoroid bombardment
3) Determination of cold- and hot-bed engine transients under extremes of propellant and hardware temperatures, propellant pressures, propellant quality, propellant flow rate, and ambient temperature
4) Determination of the effects of temperature extremes on catalyst structural integrity

5) Development of optimum propellant injection and catalyst bed packing

6) Determination of the effects of growth propellants on catalyst performance.

It is recommended that the catalyst be fully characterized prior to July 1966 by subjecting it to a comprehensive qualification program.

Subsystem Sterilization--Sterilization of the monopropellant subsystem must be accomplished. Methods to accomplish sterilization of both propellant and hardware without degradation of performance or reliability must be determined. Such methods must be inexpensive and capable of being accomplished rapidly. Two problem areas are apparent at the present time, the propellant and squib valves. Alternate means of sterilization to the specified heat cycle should be fully explored. Trades must be established for terminal propellant heat-cycle sterilization versus offsite heat-cycle sterilization with aseptic loading. Effects of heat-cycle sterilization on valve squibs must be fully investigated.

It is proposed that such a sterilization program be completed prior to the July 1966 design-freeze date.

CONTENTS

4.4 ENGINEERING MECHANICS

This section contains a functional description of the preferred designs and design methods for the following subsystems:

1) Temperature control subsystem;

2) Packaging and cabling;

3) Structure subsystem;

4) Mechanisms subsystem;

5) Pyrotechnic subsystem;

6) Weights, center of gravity, and moments and products of inertia.

In each of the first five sections, the following detail is included:

1) Scope;

2) Applicable documents;

3) Functional description;

4) Interface definition;

5) Performance parameters;

6) Physical characteristics and constraints;

7) Safety considerations;

8) Test requirements to meet the July 1966 design freeze.

4.4.1 Temperature Control Subsystem

4.4.1.1 Summary

The temperature control subsystem maintains components within prescribed temperature limits and provides a reasonable margin for uncertainties and off-design situations. Simple, proven techniques are used, resulting in high reliability and ease of testing to prove the design. A

functional flow diagram for the temperature control subsystem is shown in Figure 4.4-1. Specific design information is summarized in Table 4.4-1.

Internal equipment, which includes packaged subsystems and associated bus structure, relies on internally developed heat and space-facing louvers for control. Louvers open to expose the exterior equipment-package surfaces that function as radiator surfaces. Temperature uniformity is enhanced by grouping equipment for well-distributed heat loads and by providing good thermal coupling of components. Electric heaters are provided for backup control through ground command, because the most probable failures will result in low temperatures. Analysis shows all internal equipment radiator surface temperatures are held between 50 and 80°F, except the traveling wave tube amplifier package which operates at temperatures up to 110°F.

Propulsion-module temperature control is independent of the internal equipment system, relying on a solar shield for insulation from the Sun and conventional space-facing louvers to regulate excess heat. Insulation reduces the thermal effects of engine firing, and electric heaters commanded from the ground provide backup control.

Temperature of the boom-mounted equipment, solar panels, and the science payload is also controlled independently, primarily by surface coatings and insulation. Specular surfaces are used on some exterior components, but have been carefully limited to locations where reflection problems will not arise.

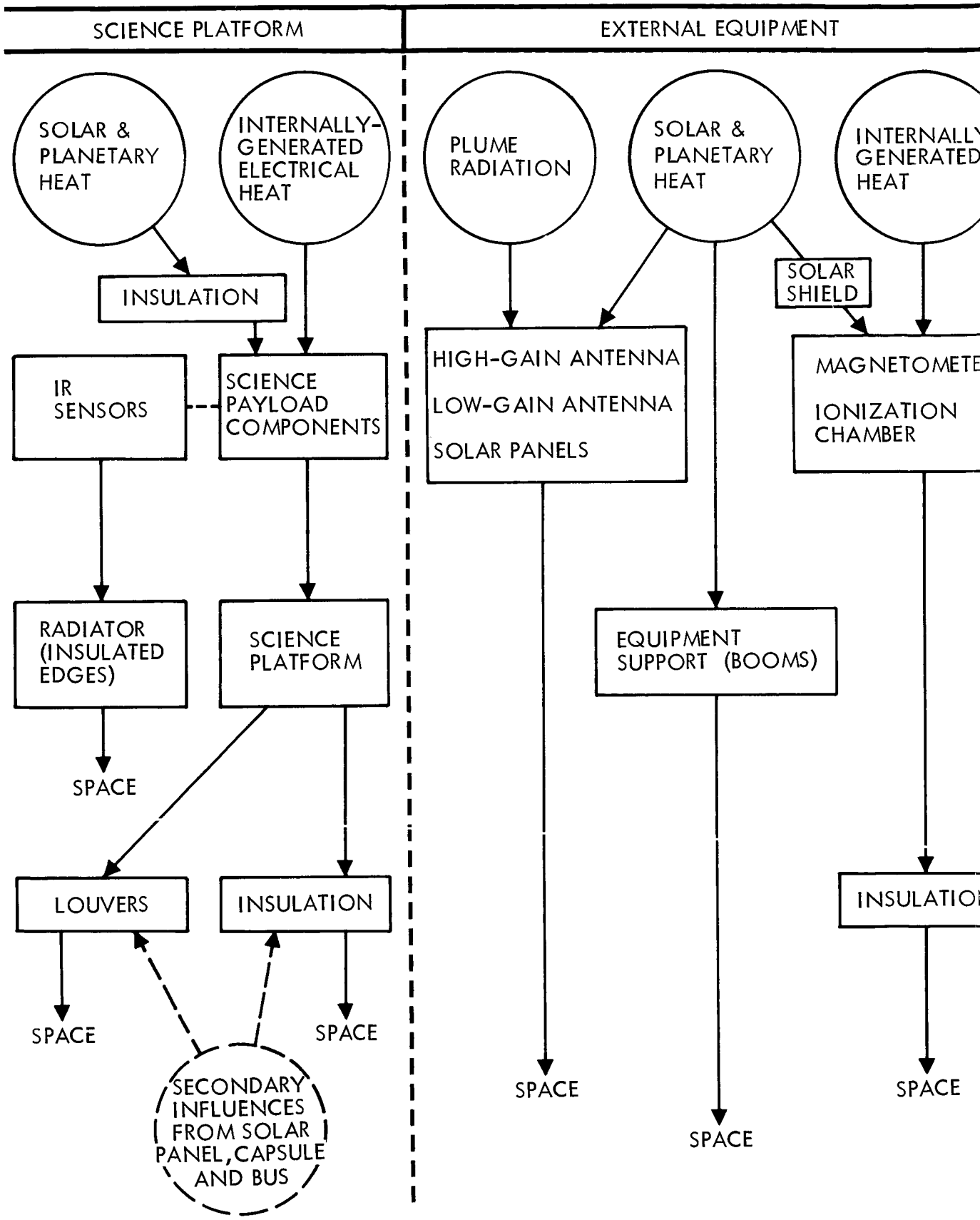
SCIENCE PLATFORM
EXTERNAL EQUIPMENT
SOLAR & PLANETARY HEAT
INTERNALLY-GENERATED ELECTRICAL HEAT
PLUME RADIATION
SOLAR & PLANETARY HEAT
INTERNALLY GENERATED HEAT
INSULATION
SOLAR SHIELD
IR SENSORS
SCIENCE PAYLOAD COMPONENTS
HIGH-GAIN ANTENNA
LOW-GAIN ANTENNA
SOLAR PANELS
MAGNETOMETE
IONIZATION CHAMBER
RADIATOR (INSULATED EDGES)
SCIENCE PLATFORM
EQUIPMENT SUPPORT (BOOMS)
SPACE
LOUVERS
INSULATION
INSULATIO
SPACE
SPACE
SECONDARY INFLUENCES FROM SOLAR PANEL, CAPSULE AND BUS
SPACE
SPACE
SPACE

(1)

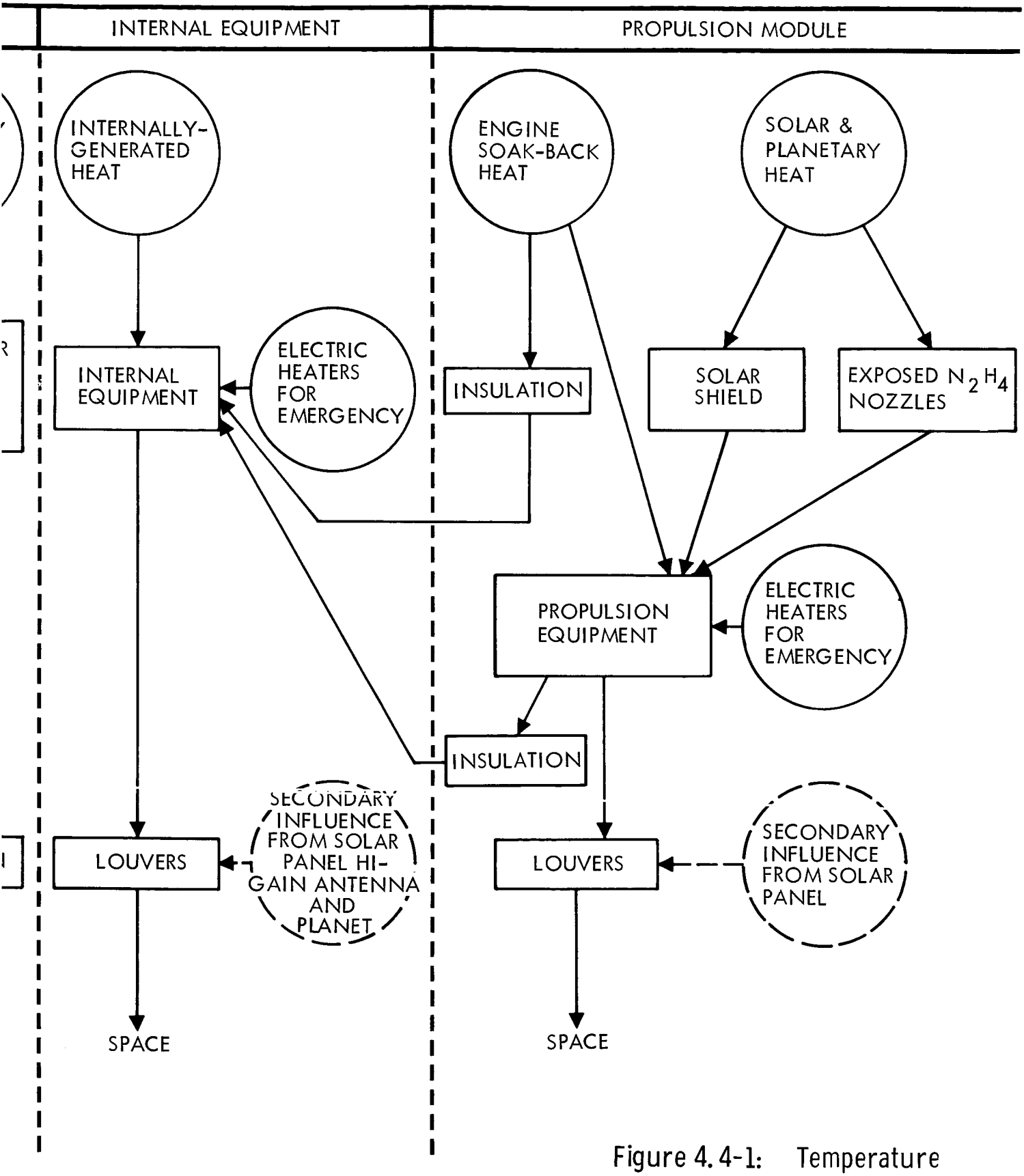

Figure 4.4-1: Temperature Control Functional Diagram

TABLE 4.4-1: PREFERRED TEMPERATURE CONTROL SYSTEM

LOCATION	ITEM	DESCRIPTION
Internal Equipment	Packaging	Large groupings--radiator on space-facing side; black anodize on package cases.
	Mounting	Back side, close-bolt spacing, indium foil used for maximum joint thermal conductance.
	Louvers	25 sq ft.-specular-aluminum-finish, spiral bimetallic actuators; radiatively coupled; teflon bearings.
	Radiator (under louvers)	Exterior with thermal white paint (B-1056 coating), initial α_s/ϵ_{ir} = 0.22/0.90.
	Electric Heaters	Resistance-wire heaters, if necessary, with thermostatic switches; emergency mode by ground control; unregulated power is used.
	Wire Harnesses	Selectively insulated.
	Insulation	Aluminized mylar insulation from capsule and from propulsion module.
	Temperature Instrumentation	Up to 18 temperature and 10 louver-position transducers.
Propulsion Module	Louvers	1.6-ft^2, specular-aluminum-finish, spiral bimetallic actuators; radiatively coupled; teflon bearings.
	Combination Radiator/ Meteoroid Bumper (under louvers)	Exterior with laminar X-500 black paint.
	Electric Heaters	Resistance wire heaters, with thermostatic switches. Emergency mode by ground control. Unregulated power is used.
	Solid-Engine Heat Shield	Composite titanium, Q-felt, metal foil, and aluminized mylar.

TABLE 4.4-1: PREFERRED TEMPERATURE CONTROL SYSTEM (CONT.)

LOCATION	ITEM	DESCRIPTION
Propulsion Module (Cont.)	Hydrazine-Engine Heat Shields	Composite titanium, Q-felt, and aluminized mylar.
	Solar Shield	Aluminized mylar layers--aluminum exterior with Laminar X-500 black paint.
	Temperature Instrumentation	Up to 12 temperature transducers.
External Equipment	High-Gain Antenna	Concave-surface paint with α/ϵ = 0.7; convex-surface specular aluminum; specular boom exterior.
	Low-Gain Antenna and Boom	Specular-exterior insulated joint; laminar X-500 black paint on boom exterior.
	Magnetometer	Multilayer-insulation solar shield; specular boom exterior.
	Solar Panel	Solar cell interference coating, Laminar X-500 black back side.
	Ion-Chamber	Multiplyer-insulation solar shield.
	Temperature Instrumentation	Up to six temperature transducers.
Scan Platform	Platform Deck	Insulate from external cover; internal heat generation from equipment and heaters; laminar X-500 black paint on radiator exterior; conventional louvers.

An important concern with solar panels and boom-mounted equipment is radiant heating from the solid-engine plume. This problem was solved primarily by developing a configuration that minimizes exposure to the plume and confines exposure to the backside surfaces that are least sensitive; and secondarily, by selecting an engine with a high-expansion-ratio nozzle.

All of the temperature-control methods selected use space-proven concepts and materials, thus minimizing developmental testing. However, because temperature control of a large spacecraft involves complex interaction between many elements, model testing will be required to ensure proper subsystem operation. The effects of this interaction have been minimized by isolating major thermal-control areas and by designing individual electronic assemblies as thermal entities, wherever practical.

4.4.1.2 Scope

The temperature-control subsystem is designed to maintain all component parts within acceptable temperature limits throughout all mission phases. The subsystem includes such components as insulation, heat shields, louvers, surface coatings, and electric heaters. Also involved are design aspects, such as good structural heat paths, good thermal coupling between components, and distribution of equipment for relatively even heat generation. The Engineering Mechanics subsystems are designed to perform the functions highlighted on the accompanying Mission Sequences Matrix.

	1.0 PRELAUNCH AT ETR	2.0 LAUNCH & INJECTION (INCLUDES COUNTDOWN)
GROUND COMPLEX (MOS, LOS, & DSN)	OPERATIONAL READINESS TEST, S/C-DSN COMPATIBILITY TEST SCHED & COORD ETR ACTIVITIES C/O & SUPPORT MOS (DSN ONLY) LOAD CC&S WITH FLIGHT PROGRAM	MOS/LOS A) COMMAND LIFTOFF B) TRACK VEHICLE DURING BOOST C) SUPPLY FLIGHT COMMANDS (AS REQ) D) RECEIVE & ANALYZE DATA FROM S/C & BOOSTER DSN E) STANDBY ON ALERT F) COMMUNICATE WITH ETR CHANGE FROM MOS/LOS TO ON INJECTION INTO TRAN A) PROVIDE SFOF/DS IF DSN SEARCH DATA B) RECEIVE ANTENNA SE C) SEARCH FOR & ACQU D) ESTABLISH & VERIFY E) TRACK S/C (1-WAY) F) RECEIVE & ANALYZE
SPACECRAFT TELECOMMUNICATIONS	SUBSYSTEM C/O & STATUS MONITORING	A) TRANSMIT ENGINEERING DATA VIA CENTAUR TELEMETRY B) TRANSMIT ENGINEERING DATA VIA LOW POWER LAUNCH EXCITER C) RECEIVE POWER FROM E/P
CENTRAL COMPUTER & SEQUENCER (CC&S)	A) SUBSYSTEM C/O & STATUS B) COMMAND OTHER SUBSYSTEMS FOR C/O & STATUS MONITORING C) READY ALL SUBSYSTEMS FOR LAUNCH D) LOAD CC&S WITH FLIGHT PROGRAM	PROVIDE BACKUP COMMANDS AS REQUIRED
ATTITUDE REFERENCE SUBSYSTEM AUTOPILOT SUBSYSTEM REACTION CONTROL SUBSYSTEM (RCS)	SUBSYSTEM C/O & STATUS MONITORING	A) ATTITUDE REFERENCE — GYROS OFF DURING LAUNCH B) AUTOPILOT — OFF C) RCS — OFF
MIDCOURSE CORRECTION PROPULSION SYSTEM ORBIT INJECTION PROPULSION SYSTEM	SUBSYSTEM C/O & STATUS MONITORING	
ELECTRICAL POWER SUBSYSTEM	SUBSYSTEM C/O & STATUS MONITORING	A) PROVIDE ENGRG DATA FOR TELECOMUNICATIONS SUBSYSTEM B) PROVIDE BATTERY POWER TO: • TELECOMMUNICATIONS SUBSYSTEM • CC&S • ATTITUDE REFERENCE SUBSYSTEM • AUTOPILOT SUBSYSTEM
S/C STRUCTURE SUBSYSTEM S/C MECHANISMS SUBSYSTEM INSTALLATION CABLES & TUBING	SUBSYSTEM C/O & STATUS MONITORING	A) PROVIDE PHYSICAL SUPPORT FOR ALL EQUIPMENT B) PROVIDE ATTACHMENT FOR CAPSULE C) SUPPORT FLT CAPSULE
TEMPERATURE CONTROL SUBSYSTEM	SUBSYSTEM C/O & STATUS MONITORING SPACECRAFT COOLING SUPPLIED BY CENTAUR	A) PROVIDE HEAT SINK COOLING CAPABILITY UP TO SHROUD JETTISON B) TEMPERATURE CONTROL AFTER SHROUD JETTISON
PYROTECHNIC SUBSYSTEM	SUBSYSTEM C/O & STATUS MONITORING	
SCIENCE EXPERIMENTS (GFE)	SUBSYSTEM C/O & STATUS MONITORING S/C MAGNETIC MAPPING (FAT)	
DATA AUTOMATION EQUIPMENT (GFE)		

REPEAT UF

	3.0 ACQUISITION	4.0 INTERPLANETARY CRUISE
) DSN CONTROL SMARS ORBIT /ITH ANTENNA URCH DATA RE S/C CONTROL OF S/C NGRG DATA	DSN A) MONITOR BOOSTER SEPARATION B) MONITOR SOLAR PANEL DEPLOYMENT C) MONITOR ANTENNA DEPLOYMENT D) PROVIDE COMMANDS TO BACK UP CC&S AS REQUIRED E) TRACK S/C F) REC DATA G) MONITOR SCIENCE DEPLOYMENT DSN H) MONITOR & VERIFY ACQUISITION OF SUN I) MONITOR & VERIFY ACQUISITION OF CANOPUS J) COMMAND REACQUISITION OF CANOPUS (AS REQD) K) MONITOR S/C TRAJECTORY L) UPDATE CC&S TRAJECTORY PARAMETERS FOR PITCH, YAW, & ROLL M) COMPUTE CC&S PITCH, YAW, & ROLL POLARITY	DSN A) TRACK S/C B) RECEIVE & DISPLAY SCIENCE & ENGINEERING DATA C) MONITOR S/C & CAPSULE STATUS D) PROCESS DATA ON EARTH TO OBTAIN GUIDANCE COMMANDS (STORED COMMANDS & START TIMES)
	A) TRANSMIT ENGINEERING DATA B) RECEIVE POWER FROM E/F C) RECEIVE VIA LOW-POWER LAUNCH EXCITER DETECT & SEND TO CC&S COMMAND SIGNALS FROM EARTH D) TRANSMIT CELESTIAL REFERENCE ACQUISITION TO DSN E) TRANSMIT VERIFICATION OF DEPLOYMENT OF SOLAR PANELS, ANTENNAS, ETC TO EARTH F) TWO-WAY TRACKING	A) TRANSMIT ENGINEERING & SCIENCE DATA VIA DATA MODE NO. 2 (OPTIONAL MODE NO. 3) B) TRANSMIT CAPSULE ENGINEERING DATA C) TRANSMIT CONE-ANGLE SETTINGS (CANOPUS TO EARTH) D) EXERCISE & CALIBRATE HIGH-GAIN ANTENNA T + 40 DAYS E) SWITCH FROM LOW-GAIN TO HIGH-GAIN ANTENNA T + 80 DAYS F) PROVIDE RANGING SIGNAL TO A MAX. RANGE OF 8.0×10^6 KM (NOMINAL) G) SWITCH TRANSMISSION FROM LAUNCH EXCITER TO TWT POWER AMPLIFIER AND DATA MODE NO. 2
	A) COMMAND SIGNALS TO PYROTECHNICS & MECH TO DEPLOY • SOLAR PANELS • HIGH-GAIN ANTENNA • VHF ANTENNA • LOW-GAIN ANTENNA • SCIENCE BOOM B) SWITCH ON GYROS & SELECT MODES C) ENABLE SUN-SENSOR ROLL AND PITCH CONTROL D) RECEIVE SUN PRESENCE SIGNAL E) TURN ON CANOPUS TRACKER F) SWITCH ROLL CONTROL TO CANOPUS SENSOR G) ACTIVATE MAGNETOMETER (CALIBRATION ROLL) H) RECEIVE CANOPUS PRESENCE OUTPUT SIGNAL I) TRANSMIT VERIFICATION TO TELECOMMUNICATION SUBSYSTEM (CANOPUS & SUN PRESENCE) J) PERFORM COMMAND FUNCTIONS FOR CANOPUS OVERRIDE AS REQUIRED K) BACKUP COMMANDS AS REQUIRED	A) COMMAND TELECOMMUNICATION TO DATA MODE NO. 2 B) COMMAND CRUISE SCIENCE ON (WARMUP) — SCIENCE INSTRUMENTS C) COMMAND DATA RECORDERS ON D) COMMAND TWTA ON E) SWITCH CANOPUS ANGLE AS REQUIRED F) INITIATE CRUISE SCIENCE DATA ACQUISITION G) COMMAND TELECOMMUNICATION CHANGE FROM OMNI TO HIGH-GAIN ANTENNA H) UPDATE HIGH-GAIN ANTENNA POSITION (AS REQUIRED) I) COMMAND TELECOMMUNICATIONS — CHANGE DATA TRANSMISSION RATES J) COMMAND RECALIBRATION OF SCIENCE ELEMENTS AS REQUIRED K) BACKUP COMMANDS AS REQUIRED
	A) RECEIVE CC&S COMMAND SWITCH ON GYROS, RCS, & AUTOPILOT B) DAMP ROTATION C) YAW & PITCH SPACECRAFT TO ACQUIRE SUN D) RELAY SUN ACQUISITION SIGNAL TO CC&S E) TURN ON CANOPUS SENSOR, ROLL 360 TO CALIBRATE MAGNETOMETER F) ROLL TO ACQUIRE CANOPUS & PROVIDE STAR MAP G) RELAY ACQUISITION SIGNAL (CANOPUS) TO CC&S H) PERFORM CANOPUS OVERRIDE ROLL MANEUVER AS REQUIRED	A) UPDATE CANOPUS CONE ANGLE ON COMMAND B) SWITCH AUTOPILOT TO CRUISE MODE C) MAINTAIN S/C ATTITUDE TO CELESTIAL REFERENCES DURING CRUISE
	A) PROVIDE POWER TO PYROTECHNIC SUBSYSTEMS FOR SQUIB FIRINGS B) PROVIDE POWER TO MECHANISMS C) ACTIVATE SOLAR POWER SYSTEM AFTER SUN ACQUISITION (AUTOMATIC) D) TRANSMIT "VOLTAGE SATISFACTORY" SIGNAL TO CC&S E) PROVIDE POWER TO: • TELEMETRY • CC&S • TEMPERATURE CONTROL • AUTOPILOT	A) PROVIDE CONDITIONED SOLAR ELECTRICAL POWER TO: • TELEMETRY • CAPSULE • CC&S • ATTITUDE REF • AUTOPILOT • TEMPERATURE CONTROL • SCIENCE B) CHARGE BATTERIES
	A) PROVIDE PHYSICAL SUPPORT FOR ALL EQUIPMENT B) DRIVE SOLAR PANELS TO LIMIT STOPS C) PROVIDE OUT & LOCK SIGNALS TO TELEMETRY D) DRIVE HIGH-GAIN ANTENNA TO OPERATING POSITION & LOCK E) DRIVE VHF & OMNI ANTENNAS TO OPERATING POSITION & LOCK F) DRIVE MAGNETOMETER BOOM TO OPERATING POSITION & LOCK G) SUPPORT FLT CAPSULE	A) SUPPORT S/C ASSEMBLIES B) SUPPORT S/C COMPONENTS C) MAINTAIN ADEQUATE ALIGNMENT BETWEEN COMPONENTS D) PROVIDE ACCEPTABLE STATIC & DYNAMIC LOAD ENVIRONMENTS E) SUPPORT FLIGHT CAPSULE
	PROVIDE TEMPERATURE CONTROL	PROVIDE TEMPERATURE CONTROL
	RECEIVE SQUIB FIRING SIGNALS FOR DEPLOYMENT OF: • SOLAR PANEL • MAGNETOMETER BOOM • LOW-GAIN ANTENNA • HIGH-GAIN ANTENNA • VHF ANTENNA	
	A) CALIBRATE MAGNETOMETER DURING S/C ROLL B) CALIBRATE OTHER SCIENCE INSTR AS REQUIRED	A) RECEIVE CRUISE SCIENCE "ON" COMMAND B) ACQUIRE CRUISE SCIENCE DATA C) TRANSFER CONDITIONED DATA TO DAE D) RECEIVE POWER FROM E/P E) RECALIBRATE SCIENCE EXPERIMENTS AS REQUIRED
		A) RECEIVE DAE "ON" COMMAND B) PROCESS & TRANSFER DATA TO TM

TO FOUR TIMES

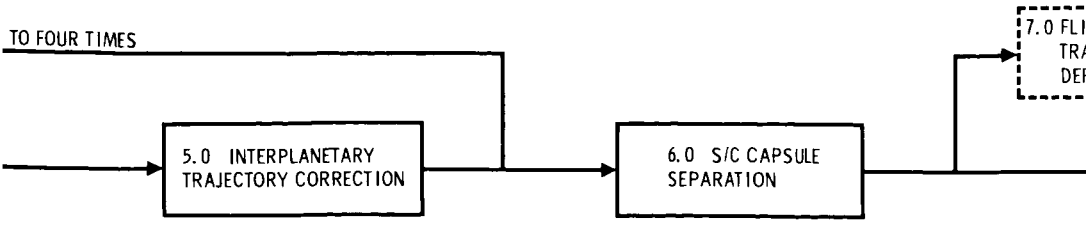

A) PROVIDE ROLL TURN MAGNITUDE & DIRECTION B) PROVIDE YAW TURN MAGNITUDE & DIRECTION C) PROVIDE MIDCOURSE MOTOR BURN DURATION AND ΔV D) PROVIDE INITIATE MANEUVER SEQUENCE COMMAND E) RECEIVE VERIFICATION OF CORRECTION MANEUVER • DEGREES OF YAW & ROLL • THRUST DURATION • REACQUISITION OF CELESTIAL REFERENCES F) TRACK SPACECRAFT	A) INITIATE PRESEPARATION SEQUENCE B) RECEIVE CAPSULE STATUS DATA C) COMMAND SEPARATION D) VERIFY CAPSULE PROGRAM E) VERIFY SEPARATION F) TRACK CAPSULE & SPACECRAFT	A) TRANSMI • ROLL • YAW • MOTO B) TRACK FI C) RECEIVE D) PROVIDE
A) RECEIVE ROLL & YAW TURN COMMAND & RELAY TO CC&S B) RECEIVE ANTENNA POSITIONING DATA & RELAY TO CC&S C) RECEIVE MOTOR BURN DURATION AND & ΔV RELAY TO CC&S D) RECEIVE INITIATE MANEUVER COMMAND & RELAY TO CC&S E) SWITCH TO DATA MODE NO. 1 (FOR LATE MIDCOURSE MANEUVERS) F) RELAY VERIFICATION OF CORRECTION MANEUVER TO DSN G) STORE AND/OR TRANSMIT ENGINEERING DATA TO DSN (MODE 3) TRANSMIT ENGINEERING (SPACECRAFT & CAPSULE) + CRUISE SCIENCE TO DSN (MODE 2)	A) RECEIVE PRESEPARATION SEQUENCE COMMANDS & RELAY TO CC&S B) SWITCH TO DATA MODE NO. 2 C) TRANSMIT CAPSULE ENGRG DATA TO DSN D) RECEIVE SEPARATION COMMAND FROM DSN & ROUTE TO CC&S E) STORE AND/OR TRANSMIT ENGINEERING DATA TO DSN (MODE 3) TRANSMIT ENGINEERING (SPACECRAFT & CAPSULE) + CRUISE SCIENCE TO DSN (MODE 2)	A) RECEIVE TO CC&S B) RECEIVE C) RECEIVE D) RECEIVE E) TRANSMI SCIENCE
A) COMMAND TELECOMMUNICATION TO DATA MODE NO. 1 B) RECEIVE TRAJECTORY CORRECTION PARAMETERS C) SWITCH GYROS TO RATE CONTROL D) COMMAND ANGULAR MANEUVER E) RECEIVE GYRO SIGNALS & SUM FOR ANGULAR MANEUVERS F) SWITCH ATTITUDE REFERENCE TO AUTOPILOT SUBSYSTEM G) ARM PROPULSION SYSTEM H) PROVIDE COMMAND TO INITIATE ATTITUDE MANEUVER & ΔV MANEUVER I) RECEIVE ACCELEROMETER SIGNALS & INTEGRATE FOR ΔV MANEUVER J) DISARM PROPULSION SYSTEM K) COMMAND REVERSE ANGULAR MANEUVER L) COMMAND REACQUIRE CELESTIAL REFERENCES M) COMMAND AUTOPILOT SELECTION CONTROL N) BACKUP COMMANDS AS REQUIRED	A) LOAD CAPSULE WITH 5 OR MORE COMMANDS B) COMMAND CAPSULE SEQUENCING C) COMMAND TELECOMM SWITCH TO DATA MODE NO. 1 D) COMMAND GYROS ACTIVATE (CAPSULE) E) COMMAND GYROS ESTABLISH POLARITY (CAPSULE) F) COMMAND GYROS TO ATTITUDE CONTROL MODE (CAPSULE) G) COMMAND DATA TAPE RECORDER OFF H) COMMAND CAPSULE ACTIVATE ENTRY SCIENCE I) COMMAND CAPSULE ACTIVATE TELE-COMM & VERIFY RADIO LINK (VHF) J) SELECT T/M MODE FOR TRANSMISSION OF CAPSULE DATA K) COMMAND: BIOBARRIER SEPARATION S/C ORIENT TO SEPARATION ATTITUDE ELECTRICAL CONNECTION SEPARATION VERIFY SEPARATION L) COMMAND REORIENT S/C & REACQUIRE CELESTIAL REFERENCES M) BACKUP COMMANDS AS REQUIRED N) RECEIVE S/C ORIENTATION PARAMETERS	A) COMMA B) COMMA C) COMMA D) RECEIVE E) PROVID (CRUISE F) SWITCH RECEIVE G) BACKUP
A) SWITCH TO GYRO CONTROL B) ROLL S/C AND VERIFY C) YAW S/C AND VERIFY D) AUTOPILOT — PROVIDE COMMAND TO TVC DURING MOTOR BURN E) TURN ON ACCELEROMETERS F) PROVIDE ACCELERATION DATA TO CC&S G) TURN OFF ACCELEROMETER H) YAW BACK TO ORIGINAL ATTITUDE & VERIFY I) REACQUIRE SUN (FINE SUN SENSOR) & VERIFY J) ROLL TO ORIGINAL ATTITUDE K) LOCK ON CANOPUS & VERIFY L) SWITCH AUTOPILOT FROM GYRO CONTROL TO CELESTIAL REF CONTROL	A) SWITCH TO GYRO CONTROL B) PERFORM ROLL TURN & VERIFY C) PERFORM YAW TURN & VERIFY D) MAINTAIN ATTITUDE DURING SEPARATION E) PERFORM YAW TURN (INVERSE TO C) & VERIFY F) PERFORM ROLL TURN (INVERSE TO B) & VERIFY G) REACQUIRE CELESTIAL REFERENCES H) RETURN TO CELESTIAL REFERENCE ATTITUDE CONTROL MODE	A) UPDATE B) SWITCH C) MAINTA
MIDCOURSE PROPULSION SYSTEM A) ARM PRESSURIZATION SYSTEM (FIRE SQUIB VALVE) B) ARM PROPELLANT FEED SUBSYSTEM (FIRE SQUIB VALVE) C) FIRE PROGRAMMED ENGINES (OPERATE SOLENOID VALVE) D) SHUT DOWN ENGINE E) ISOLATE PROPELLANT FEED SUBSYSTEM F) ISOLATE PRESSURIZATION SUBSYSTEM		
A) PROVIDE CONDITIONED SOLAR OR BATTERY POWER TO: • TELEMETRY • CC&S • AUTOPILOT • ATTITUDE REFERENCE • REACTION CONTROL • PROPULSION • TEMPERATURE CONTROL • PYROTECHNIC • CAPSULE	A) PROVIDE CONDITIONED SOLAR OR BATTERY POWER TO: • T/M • CC&S • AUTOPILOT • ATTITUDE REF • REACTION CONTROL • TEMPERATURE CONTROL • PYROTECHNICS • CAPSULE	A) PROVID • T/M • CC&S • AUTO • ATTI • REAC • TEMP B) CHARGE
A) SUPPORT S/C ASSEMBLIES B) SUPPORT S/C COMPONENTS C) MAINTAIN ADEQUATE ALIGNMENT BETWEEN COMPONENTS D) PROVIDE ACCEPTABLE STATIC & DYNAMIC LOAD ENVIRONMENTS E) SUPPORT FLIGHT CAPSULE	A) SUPPORT S/C ASSEMBLIES B) SUPPORT S/C COMPONENTS C) MAINTAIN ADEQUATE ALIGNMENT BETWEEN COMPONENTS D) PROVIDE ACCEPTABLE STATIC & DYNAMIC LOAD ENVIRONMENTS E) SUPPORT FLIGHT CAPSULE	A) SUPPOR B) SUPPOR C) MAINTA D) PROVID E) DRIVE
PROVIDE TEMPERATURE CONTROL	PROVIDE TEMPERATURE CONTROL	PROVIDE TE
A) REMOVE PROPULSION SYSTEM INHIBIT B) PROVIDE IGNITION C) INHIBIT PROPULSION SYSTEM	A) RECEIVE SIGNAL TO REMOVE CAPSULE SEPARATION INHIBIT B) RECEIVE SIGNAL TO FIRE CAPSULE UMBILICAL SEPARATION C) RECEIVE SIGNAL TO FIRE BIOBARRIER REMOVAL D) RECEIVE SIGNAL TO FIRE CAPSULE SEPARATION E) RECEIVE SIGNAL FOR SEPARATION INHIBIT	RECEIVE SC OF SCAN P
A) RECEIVE CC&S COMMAND "CRUISE SCIENCE OFF" B) TURN OFF CRUISE SCIENCE	A) RECEIVE CC&S COMMAND "CRUISE SCIENCE OFF" B) TURN OFF CRUISE SCIENCE	A) RECEIVE B) ACQUIR C) TRANSF D) RECEIVE E) RECALI
		A) RECEIV B) PROCES

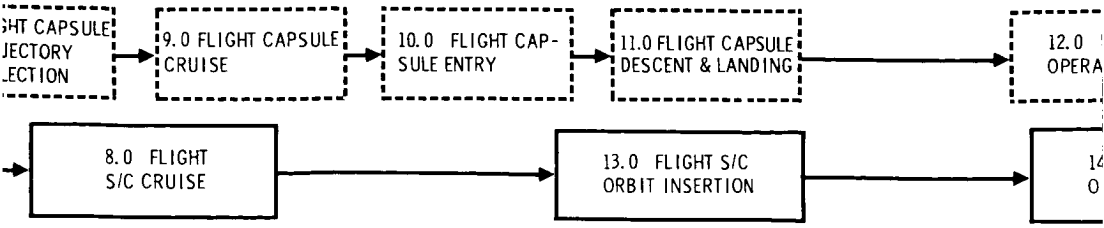

ORBIT INJECTION PARAMETERS AGNITUDE & DIRECTION AGNITUDE & DIRECTION BURN START TIME IGHT SPACECRAFT REDUCE & DISPLAY SCIENCE & ENGINEERING DATA COMMANDS TO BACK UP CC&S AS REQUIRED	A) RECEIVE, DECODE, & DISPLAY ENGINEERING DATA B) RELAY UPDATED ORBIT INJECTION PARAMETERS C) PROVIDE COMMAND TO INITIATE INSERTION MANEUVER D) PROVIDE BACKUP COMMANDS TO CC&S AS REQUIRED E) TRACK S/C F) VERIFY ORBIT INSERTION	A) RECEIVE, DECODE, & DISPLA B) RECEIVE AND ANALYZE ENGI C) TRACK S/C D) RECEIVE & DISPLAY CAPSUL E) PROVIDE DATA FOR ORBITAL F) RECEIVE VERIFICATION OF C G) TERMINATE MISSION
OLL & YAW TURN MAGNITUDE & DIRECTION COMMAND & RELAY NTENNA POSITIONING DATA & RELAY TO CC&S OTOR-BURN START TIME, RELAY TO CC&S APSULE DATA, CONDITION & RELAY TO GROUND FLIGHT SPACECRAFT ENGINEERING, CAPSULE ENGRG, & ATA TO GROUND VIA MODE 2	A) UPDATE ROLL-TURN MAGNITUDE & DIRECTION COMMAND & RELAY TO CC&S B) UPDATE YAW-TURN MAGNITUDE & DIRECTION COMMAND & RELAY TO CC&S C) UPDATE MOTOR-BURN START TIME & RELAY TO CC&S D) UPDATE INITIATE MANEUVER & RELAY TO CC&S E) SWITCH TO DATA MODE NO. 2 OR 5A AS REQUIRED F) REACQUIRE EARTH AFTER ROLL TURNS & MOTOR BURN G) RELAY VERIFICATION OF MANEUVERS	A) TRANSMIT SCIENCE & ENGIN B) RECORD ENGINEERING & SCI C) RECEIVE, STORE & RELAY CA D) RECEIVE & RELAY DATA FOR
) SWITCH TO DATA MODE NO. 2) CANOPUS CONE ANGLE SETTING) ANTENNA STEP (AS REQUIRED) ORBIT INJECTION PARAMETERS SIGNAL TO PYRO & MECHANISMS TO DEPLOY SCAN PLATFORM SCIENCE T/M OFF) & SWITCH TO DATA MODE NO. 1 N DATA RECORDER-COMMAND TELECOMMUNICATIONS CAPSULE DATA COMMANDS AS REQUIRED	A) UPDATE STORED ROLL, PITCH, & YAW MAGNITUDE & SIGN B) UPDATE STORED VELOCITY MAGNITUDE C) INITIATE MANEUVER SEQUENCE D) COMMAND ORIENTATION OF S/C TO INJECTION ATTITUDE E) COMMAND THRUST FOR ORBIT INSERTION F) COMMAND RETURN TO CRUISE ATTITUDE G) BACKUP COMMANDS AS REQUIRED	A) COMMAND ORBITAL TRIM M B) SWITCH DATA MODES AS NE C) RECEIVE ANY ORBITAL OPER D) COMMAND POSITIONING OF E) SWITCH ON ORBITAL SCIEN F) SELECT RECORDED SCIENCE G) BACKUP COMMANDS AS REC H) STORE DATA FOR ORBIT TRI I) TERMINATE MISSION ON CO
	A) SWITCH TO GYRO CONTROL B) PROVIDE ROLL TO PROPER ATTITUDE & VERIFY ROLL C) YAW TO PROPER ATTITUDE & VERIFY D) AUTOPILOT – PROVIDE COMMAND TO TVC DURING MOTOR BURN E) TURN ON ACCELEROMETER F) PROVIDE ACCELEROMETER DATA TO CC&S G) TURN OFF ACCELEROMETER H) YAW BACK AFTER MOTOR BURN I) ACQUIRE SUN & VERIFY J) ROLL BACK TO PROGRAMMED ATTITUDE K) ACQUIRE CANOPUS & VERIFY L) SWITCH AUTOPILOT FROM GYRO – CONTROL TO CELESTIAL REFERENCE CONTROL	
ANOPUS CONE ANGLE ON COMMAND AUTOPILOT TO CRUISE MODE N S/C ATTITUDE TO CELESTIAL REFERENCES DURING CRUISE		A) MAINTAIN S/C ATTITUDE TO B) SWITCH AUTOPILOT TO GYR C) REACQUIRE CELESTIAL REFE D) REORIENT S/C FOR ORBITAL E) PROVIDE TVC DURING ENGI F) REACQUIRE CELESTIAL REFE G) UPDATE CANOPUS CONE ANG
	ORBIT INSERTION ENGINE A) ARM TVC B) ARM IGNITER C) FIRE MOTOR & PROVIDE THRUST & TVC D) TERMINATE THRUST (MOTOR BURNS TO DEPLETION)	MIDCOURSE A) ARM PRESSURIZATION & P B) PROVIDE THRUST (FIRE PRO IF REQUIRED C) TERMINATE THRUST ON COM D) ISOLATE PROPELLANT FEED E) ISOLATE PRESSURIZATION
CONDITIONED SOLAR ELECTRICAL POWER TO: ILOT IDE REF ION CONTROL RATURE CONTROL BATTERIES	A) PROVIDE CONDITIONED SOLAR OR BATTERY POWER TO: • TELEMETRY • CC&S • ATTITUDE REFERENCE SUBSYSTEM • AUTOPILOT • TEMPERATURE CONTROL • PULSE TO PYROTECHNICS • PULSE TO PROPULSION	A) PROVIDE CONDITIONED SO • TELEMETRY • CC&S • ATTITUDE REFERENCE SU • AUTOPILOT • TEMPERATURE CONTROL • STRUCTURES & MECHAN • SCIENCE
S/C ASSEMBLIES S/C COMPONENTS N ADEQUATE ALIGNMENT BETWEEN COMPONENTS ACCEPTABLE STATIC & DYNAMIC LOAD ENVIRONMENTS CAN PLATFORM TO DEPLOYED POSITION & LOCK	A) SUPPORT S/C ASSEMBLIES B) SUPPORT S/C COMPONENTS C) MAINTAIN ADEQUATE ALIGNMENT BETWEEN COMPONENTS D) PROVIDE ACCEPTABLE STATIC & DYNAMIC LOAD ENVIRONMENTS	A) SUPPORT S/C ASSEMBLIES B) SUPPORT S/C COMPONENTS C) MAINTAIN ADEQUATE ALIGN D) PROVIDE ACCEPTABLE STAT ENVIRONMENTS E) POSITION SCAN PLATFORM
MPERATURE CONTROL	PROVIDE TEMPERATURE CONTROL	PROVIDE TEMPERATURE CONTR
JIB FIRING SIGNAL FOR UNLATCHING ATFORM	A) RECEIVE & EXECUTE COMMAND SIGNAL TO REMOVE INHIBIT FOR PROPULSION ENGINE B) RECEIVE & EXECUTE SIGNAL FOR PROPULSION ENGINE START C) RECEIVE & EXECUTE COMMAND SIGNAL FOR PROPULSION ENGINE STOP D) RECEIVE & EXECUTE SIGNAL FOR PROPULSION INHIBIT	
CRUISE SCIENCE "ON" COMMAND CRUISE SCIENCE DATA R CONDITIONED DATA TO DAE POWER FROM EIP RATE SCIENCE EXPERIMENTS AS REQUIRED	SCIENCE OFF DURING ORBIT INSERTION	A) TURN ON ORBITAL SCIENC B) ACQUIRE ORBITAL SCIENC C) TRANSFER CONDITIONED D D) RECALIBRATE SCIENCE EX
DAE "ON" COMMAND & TRANSFER DATA TO TM		A) RECEIVE DAE "ON" COMMA B) PROCESS & TRANSFER DA

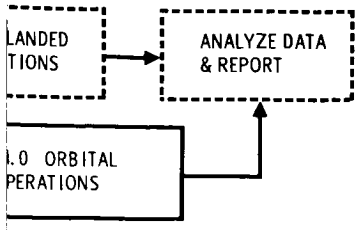

T SCIENCE DATA
EERING DATA

E DATA
TRIM (IF REQUIRED)
BITAL TRIM MANEUVER

EERING DATA VIA DATA MODES 5 AND 6
ENCE DATA AS COMMANDED
PSULE DATA ON COMMAND (MODES 5 AND 6)
ORBIT TRIM IF REQUIRED

ANEUVERS (IF REQUIRED)
CESSARY
ATION CHANGES & SEQUENCES
SCIENCE SCAN PLATFORM
CE
READOUT TO TELECOMMUNICATIONS
QUIRED
M (IF REQUIRED)
MMAND (IF REQUIRED)

CELESTIAL REFERENCES
) CONTROL DURING OCCULTATION
RENCES FOLLOWING OCCULTATION
TRIM MANEUVER USING GYRO CONTROL
NE FIRING
RENCES FOLLOWING MANEUVERS
GLES ON COMMAND

ROPELLANT FEED SUBSYSTEMS
OGRAMMED ENGINES) FOR ORBIT TRIM

MAND
SUBSYSTEM
SUBSYSTEM

LAR OR BATTERY POWER TO:

BSYSTEM

SMS

MENTS BETWEEN COMPONENTS
IC AND DYNAMIC LOAD

OL

INSTRUMENTS
E DATA
ATA TO DAE
REMENTS AS REQUIRED

VID
TA TO TM

Mission Sequences Matrix

5

4.4.1.3 Applicable Documents

1) "Thermal Control Mars Orbiting Mission", Boeing Document D2-23525-6, October 1964.

2) "Analysis of Movable Louvers for Temperature Control", J. A. Plamondon, JPL Technical Report No. 32-555, January 1, 1964.

4.4.1.4 Functional Description

Functional Diagram --Figure 4.4-1 is a functional flow diagram of the preferred temperature control subsystem. The major subsystem groups are the internal bus equipment, the external bus equipment, propulsion module, and the planet-scan platform. To a large extent, these major groups are thermally isolated from each other. These subsystem groups are shown in Figure 4.4.-2

Design Philosophy--The design philosophy for developing the temperature control subsystem was to use simple, proven techniques that allowed for uncertainties, off-design conditions, and limited failures; and to design the system for tests that would definitely prove its performance. Temperature-control and packaging-design concepts permit versatility in relocating equipment. Some of the measures taken to implement this philosophy were:

1) Equipment was required to function properly over a temperature range significantly broader than the maximum range predicted for operation;

2) The internal equipment, propulsion module, and planet-scan platform were thermally isolated from each other to allow for independent development of systems not functionally connected;

Figure 4.4-2: Temperature Control Subsystem

3) The placement of equipment considered temperature requirements, power loads, and duty cycles so that heat loads would be well distributed, thus reducing dependence on controls;

4) Dependence on thermally white coatings for thermal control was minimized because of degradation effects and testing limitations;

5) The subsystem was designed so that a single failure of a temperature control component would not significantly degrade thermal performance.

Internal Bus Equipment--The internal bus thermal-control equipment employs conventional louvers as the basic mode of control. Black paint is used on the equipment boxes to maximize radiative coupling, and low-absorptivity paint (initial α_s/ϵ_{IR} = 0.22/0.9) is used on the radiator surface behind the louvers to minimize the effects of solar heating during space maneuvers. When high thermal conductance across joints is required, indium foil is placed under the equipment mount flanges, based on the experimental design data shown in Figure 4.4-3. Multilayered aluminized mylar is used to thermally isolate equipment from the propulsion module and the capsule. Electric heaters with ground command control are used selectively as a backup for failure. Unregulated power is used with the heaters.

The traveling wave tube amplifier (TWTA) is the largest single source of heat. It requires the rejection of approximately 100 watts (thermal). Effective cooling of the TWTA has been achieved using the combined techniques of:

1) Designing the TWTA internally for good conduction along critical paths;

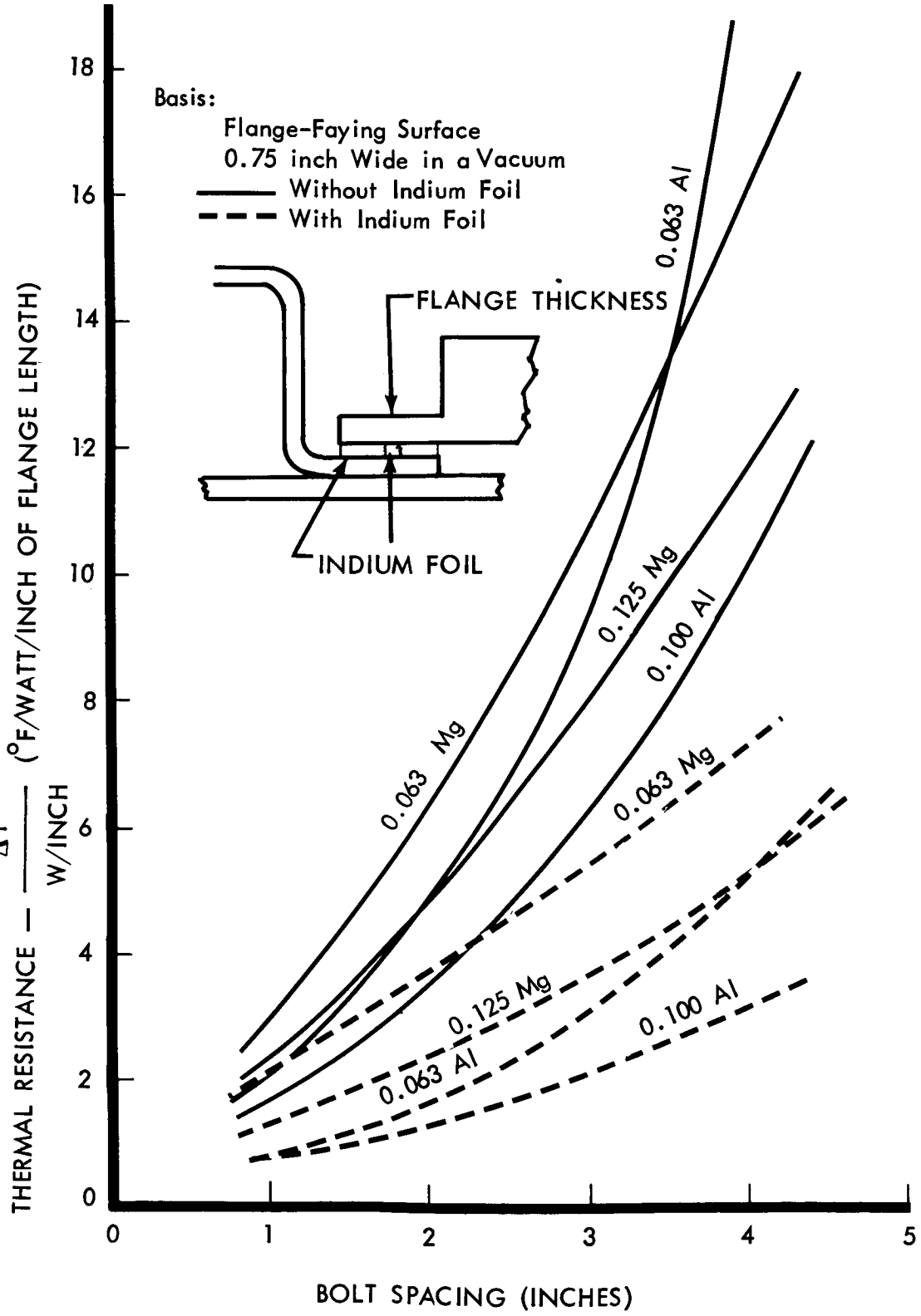

Figure 4.4-3: Thermal Resistance Of Bolted Flange Joints

2) Using tapered radiation fins for removal of most of the heat;

3) Mounting the TWTA directly to the radiator;

4) Locating the TWTA near low-heat producers (see Section 3.10 of Volume A).

Conventional louvers with specular aluminum surfaces, spiral bimetallic actuators with radiative coupling, and teflon bearings are employed. The influence of heat from the solar panels on the louvers reduces their heat-dissipating efficiency by approximately 25 percent at Earth, compared with 100-percent dissipating capability in Mars orbit. Consequently, the louvers are designed to slightly favor the open position (equipment temperatures higher than average) near Earth to maximize modulating capability over the rest of the mission. The main departure from conventional practice is the possible use of actuators with a new bimetal combination that minimizes magnetic problems. Table 4.4-2 shows the suitable nonmagnetic bimetallic combinations. To verify that this design has the desired control response, a thermalvacuum test is planned for completion before July 1966.

External Equipment--Solar shields, insulation, surface-coatings, and electric heaters are the major techniques used to control external-equipment temperatures. The high-gain antenna is coated on the concave surface to give an $\alpha_S/\epsilon_{IR} = 0.7$, which will provide a temperature of approximately 70°F at encounter to match preflight test conditions as closely as possible.

Analysis of the booms and other external equipment shows that specular surfaces are generally preferred for temperature control because

TABLE 4.4-2: SUITABLE NONMAGNETIC BIMETALLIC COMBINATIONS
(In order of desirability)

Material Combinations	Thermal Coefficient of Expansion μin/in/^{o}C
1) Most aluminum alloys* + platinum-tungsten alloy	(22-24)/(4.6-8.9)
2) Most aluminum alloys* + titanium-chrome alloy	(22-24)/8
3) Beryllium-copper + platinum-tungsten alloy	18/(4.6-8.9)
4) Most aluminum alloys* + palladium alloy	(22-24)/9
5) Beryllium-copper + titanium-chrome alloy	18/8

*Aluminum alloys 2024-T4 or 6061-T6 would be very suitable

NOTE: Iron, cobalt, and nickel must be avoided in all alloys

COMMENT: The order and combinations of choice depends mainly on the thermal coefficients involved, but also the space environmental stability of the materials and ductility was considered.

(1) differential expansion is minimized on the high- and low-gain antennas, (2) angular deflection is minimized on the magnetometer boom, (3) heat losses are reduced on body-mounted equipment, (4) low-temperature problems with internal electrical leads are minimized, and (5) a small weight saving is achieved. However, to minimize possible reflection problems, black paint will be used wherever its use might be acceptable. Specular surfaces were, therefore, limited to locations where reflection problems could not arise, and to locations where thermal problems would otherwise be significant. These problem locations include: the magnetometer boom, which has a chemically brightened, lightly sandblasted surface to maintain angular deflection within tolerance; and the micrometeoroid detectors which have specular surfaces to minimize heat loss.

Low-thermal-conductance joints are used to attach exterior components, with teflon spacers used for movable joints and textolite spacers for rigid joints. Exceptions are the plasma probe, the trapped-radiation detector, the ion detector, and the micrometeoroid detectors, which are body-mounted and depend on conduction from the structure for proper temperature control.

Multilayer insulation has been used selectively throughout the spacecraft, with a preference for aluminized mylar. In the solar shield, the exterior of the multilayer insulation is covered with black-painted aluminum sheet, except near the hydrazine engines where a titanium exterior is used. Polished titanium is also used for the solid propellant engine heat shield.

Propulsion Module--Temperature control of the propulsion module is independent of other equipment control systems. The system relies on a solar shield to insulate from the Sun, and on conventional spaceviewing louvers to regulate excess heat that penetrates the shield. Most of the heat leak across the shield occurs via the four hydrazine engine nozzles; consequently, there is a trade between louver area, thermal conductance of the combustion chamber to plumbing and supports, and the amount of nozzle protrusion outside the shield. A low-conductance, recessed engine design approach was selected that results in a large temperature drop across the engine and minimizes the control range on the louvers. Additional temperature control features in the propulsion module are insulation to contain the effects of engine firing and electric heaters commanded from the ground for backup control.

Planet-Scan Platform--Temperature control for the planet-scan components is provided primarily by conduction to the equipment mounting deck, which in turn is controlled by exterior louvers of conventional design. Multilayer insulation and internal heat generation are also used. rs

4.4.1.5 Interface Definition

Electrical Interfaces--Electric heaters are employed in the thermal control system for emergency heating. The heaters are controlled from Earth through the CC&S.

Instrumentation--About 41 transducers are used to sense temperatures throughout the spacecraft. Of these, about six operate through the ground umbilical link for prelaunch monitoring, and the remaining transducers function through the telemetry system.

Mechanical--Louvers are the only mechanical thermal control devices on the Spacecraft Bus. The louvers are actuated by spirally wound bimetallic elements that are thermally coupled by radiation to the radiators.

Structural--High thermal conductance is desired in mounting equipment to the structure. This need is satisfied in some instances by close bolt spacing, and in other cases by the use of indium foil beneath the mounting flanges. Joints requiring low thermal conductance typically will use textolite spacers for rigid joints and teflon spacers for movable joints. Requirements for meteoroid protection must also be met, imposing the need for either thick radiator surfaces or radiator surfaces protected by meteoroid bumpers.

Optical--Surface finishes used for temperature control on exterior surfaces will not interfere with the Canopus sensor or science devices. Specular exterior surfaces have therefore been limited to locations where reflection problems do not arise and where thermal problems would otherwise be significant. Specular surfaces are used on louvers, the magnetometer boom, the high gain antenna boom, and the micrometeoroid detectors.

Magnetic--It is desired that ferromagnetic components not be used in the temperature-control subsystem, and development of new bimetallic actuator elements for louver control is required.

Configuration--The major constraints on the configuration are:

1) Components must have adequate protection from exhaust-plume heating of the solid propellant engine;
2) Overall layout must permit thermal isolation of the internal equipment, propulsion module, and planet-scan platform;
3) Equipment louvers must have a high veiw factor to space ($F \geqslant$ about 0.6). On the launch pad, the louvers must be exposed sufficiently to permit circulation of ground cooling air.

4.4.1.6 Temperature-Control Performance Parameters

Detailed thermal analyses have been made to determine if the design is adequate and to control the design in any problem areas. These analyses show that temperatures are maintained within their limits and that system performance is not highly sensitive to changes in equipment duty cycles, spacecraft maneuvers, or space environmental effects. Results of these analyses verify that the basic thermal control concepts are sound and that performance will be adequate. A summary of critical temperature requirements is given in Section 3.3.

Temperature predictions of representative equipment are summarized in Table 4.4-3 and Figures 4.4-4 through 4.4-12. These analytical results

are based on equipment power duty cycles expected in flight with an analytical model consisting of 252 nodes, 420 solid conductors, and 130 radiation conductors. Radiation shape factors, external heat loads, and the final transient temperature analyses, were determined by computer solution.

As noted in Table 4.4-3, the highest temperatures on an overall spacecraft basis occur during cruise near Earth when power is high and the secondary heating influences of the solar panels are maximum. The hottest condition anticipated locally is during an early midcourse correction maneuver which could possibly result in direct exposure of the louvers to the Sun. When this occurs, the pitch axis (in line with the two opposing solar panels) will be directed toward the general vicinity of the Sun. Therefore, it will be possible to minimize misorientation effects by equipment distribution so the mass-to-power ratio is higher in these two zones than the spacecraft average. Figure 4.4-4 gives temperature histories during a worst-case maneuver, and shows that about 100 minutes of exposure to the Sun will be acceptable near Earth, whereas exposures longer than 2 hours can be endured at Mars insertion.

The coldest overall temperatures for the spacecraft occur during occultation in Mars orbit. Typical performance data are shown in Figures 4.4-5 and 4.4-6. Analytical results show that internal equipment is only slightly affected by occultation, and therefore performance of external components is the main concern. Analyses have been conducted for typical conditions in Mars orbit. However, performance for all components for worst-case conditions has not been determined.

Table 4.4-3: TEMPERATURE ANALYSIS SUMMARY

	TEMPERATURE (°F)		
	CRUISE AT	CRUISE AT	MARS ORBIT AT
COMPONENT	EARTH	MARS	ACQUISITION
Ultraviolet Spectrometer	69	53	53
Radio Transponder	68	54	53
Radio	70	58	58
Diplexer Switches	67	52	51
Data Storage and Electronics	71	58	57
Telemetry	75	52	51
Inertial Reference Unit	62	55	55
CC&S	83	76	76
Canopus Sensor	66	60	60
Beacon	62	55	55
Regulator	73	66	66
Infrared Spectrometer Electronics	68	61	61
Plasma Instruments	75	68	68
Charger Booster	60	53	53
2400-Cycle Inverters	59	52	52
Battery	83	68	67
Solar Panels	110	10	-275 to +40
Hydrazine Tank	82	59	59
Micrometeorid Detectors	47	30	30

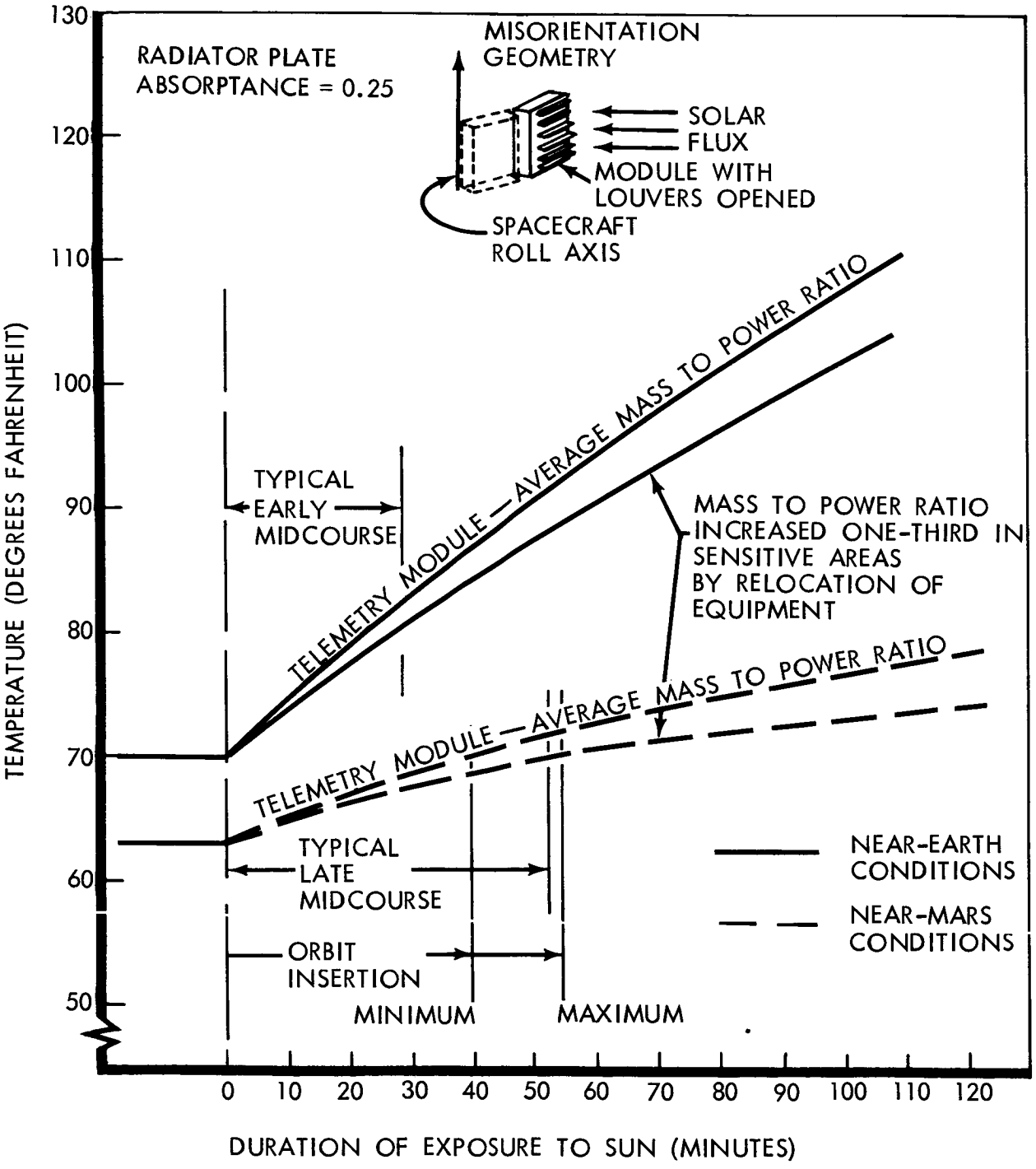

Figure 4.4-4: Equipment Heating During Misorientation

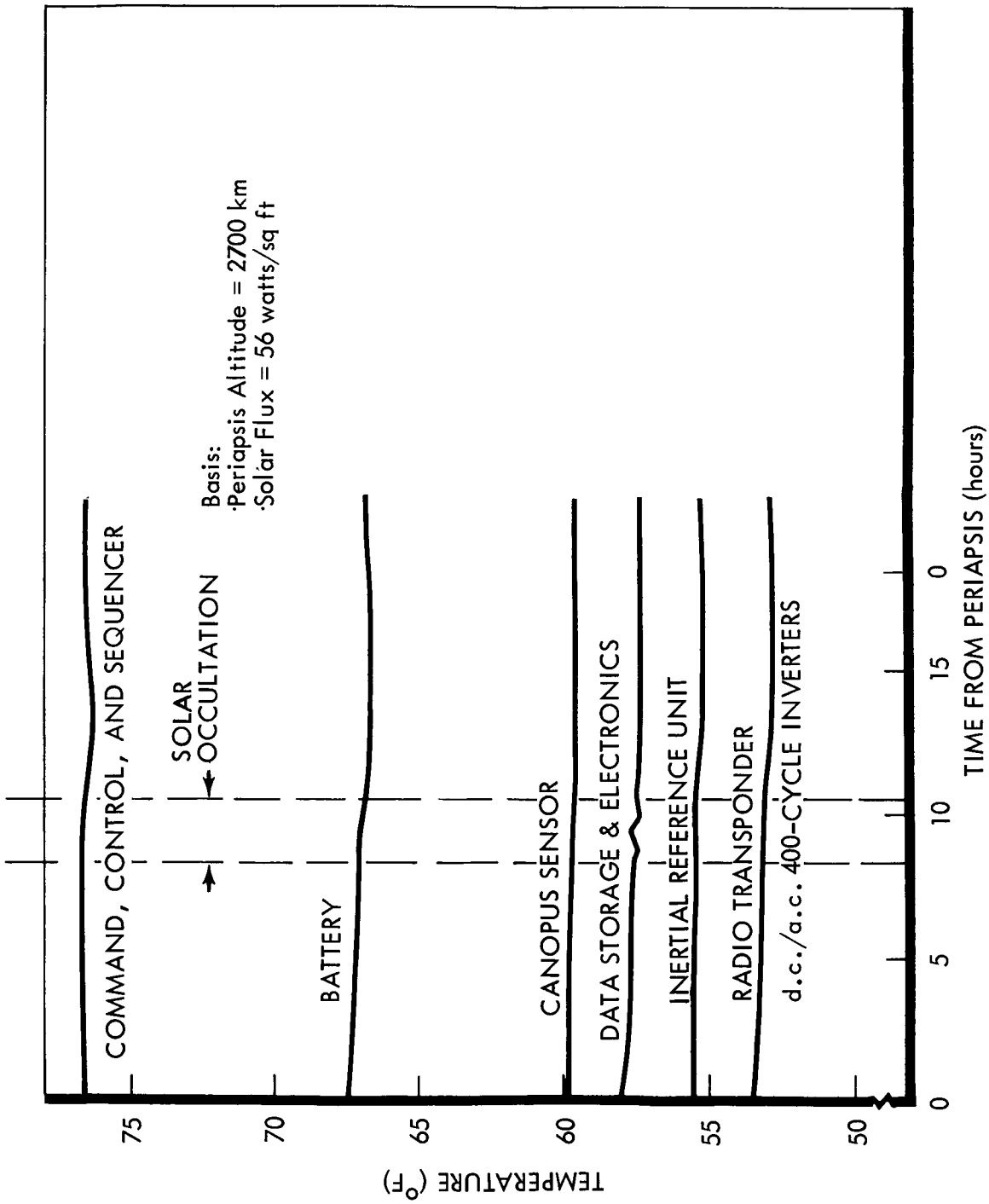

Figure 4.4-5: Internal Equipment Temperatures In Mars Orbit

Basis:

- Louver Concept
- Mars Scanner and IR Spectrometer on Same Radiator Plate
- Periapsis Altitude = 2700 km
- Solar Flux = 56.5 watts per sq ft
- TV Operating Limits = 14 to 131°F
- Mars Scanner Limits = -40 to -4°F
- IR Spectrometer Limits -110 to +50°F

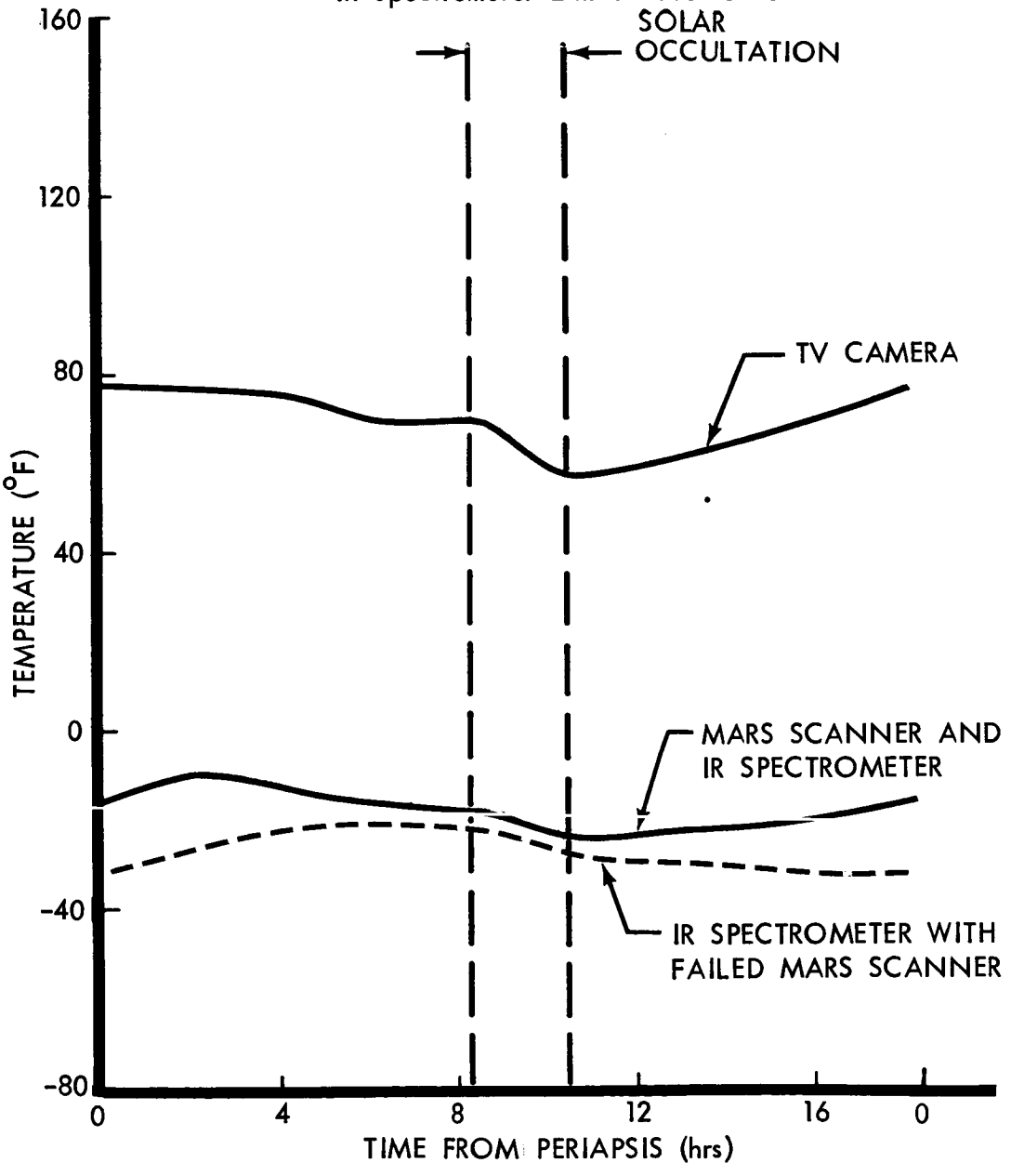

Figure 4.4-6: Temperature Analysis Of Planet Scan Platform During Occulting Mars Orbit

Temperature predictions of the traveling-wave-tube amplifier are shown in Figure 4.4-7. Radiator thickness was varied in these analyses. The temperatures shown are those resulting if the radiator thickness is 0.24 inch.

Temperature predictions for the solid-propellant engine during insertion into Mars orbit are given in Figure 4.4-8. Propellant case temperature is noted to be relatively low (225°F maximum) and presents no unusual problems with soakback heating of the hydrazine or cold-gas-system components.

An important concern with solar panels and boom-mounted equipment is radiant heating from the solid-propellant-engine plume. Temperature predictions of plume heating appear in Figure 4.4-9; as shown, configuration and engine-design choices have been effective in reducing plume heating effects to tolerable levels. Nevertheless, because experimental justification of the analytical plume heating rates is not available, it is planned that an experimental program be undertaken on plume heating, as discussed in Section 4.4.1.9.

Analysis of the magnetometer boom at Mars acquisition with the lightly sandblasted surface shows a temperature of 110°F, and a deflection of about 0.5 degree due to the small temperature gradients. By comparison, a black-painted boom was calculated to operate at -15°F with a deflection of about 3.0 degrees due to temperature gradients. It is seen, therefore, that the sandblasted surface meets the requirement of less than 1-degree

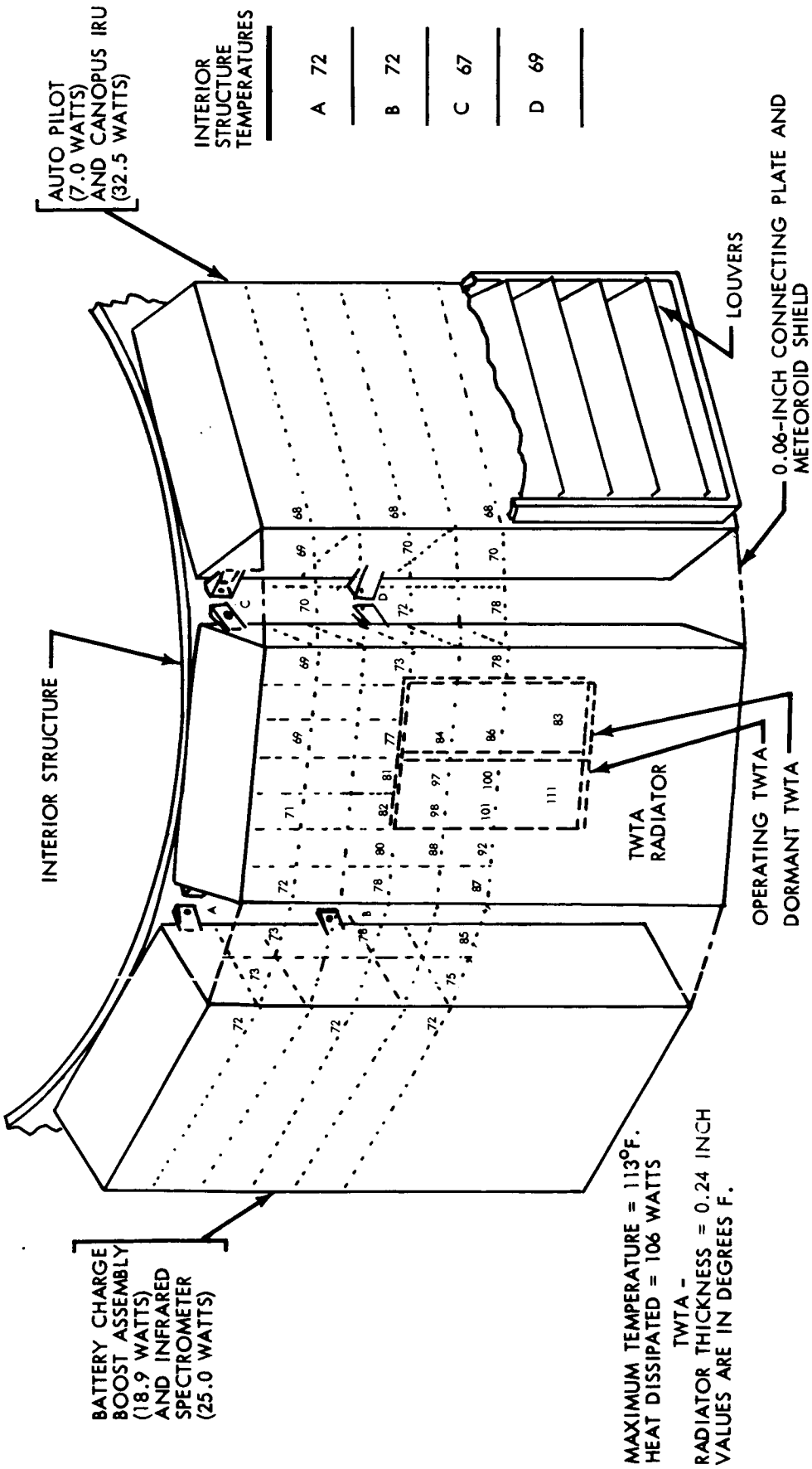

Figure 4.4-7: Telecommunications TWTA Thermal Analysis

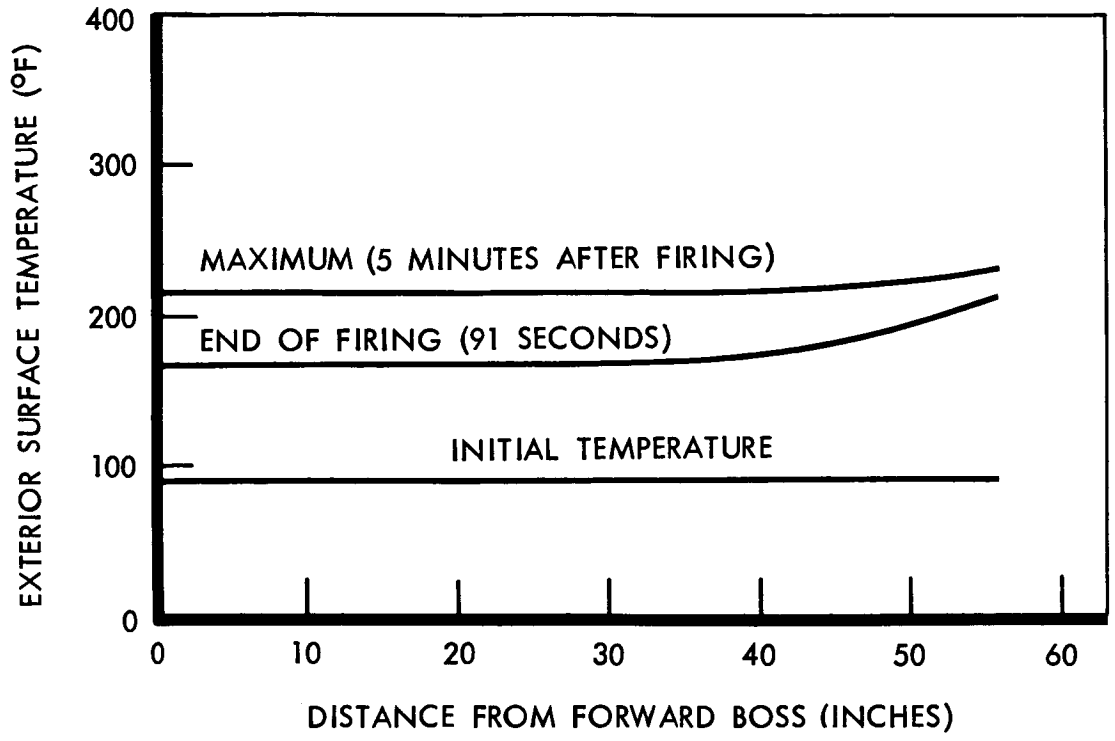

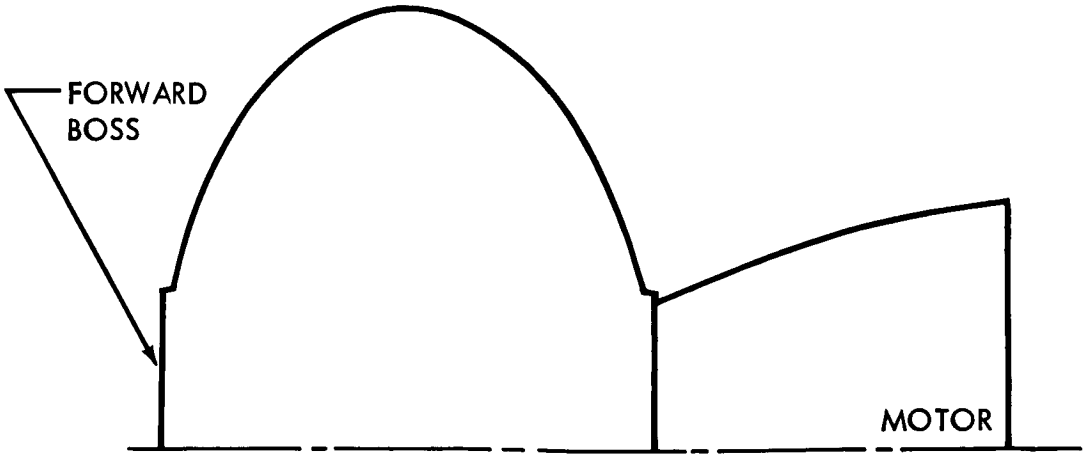

Figure 4.4-8: Orbit Insertion Motor Temperatures

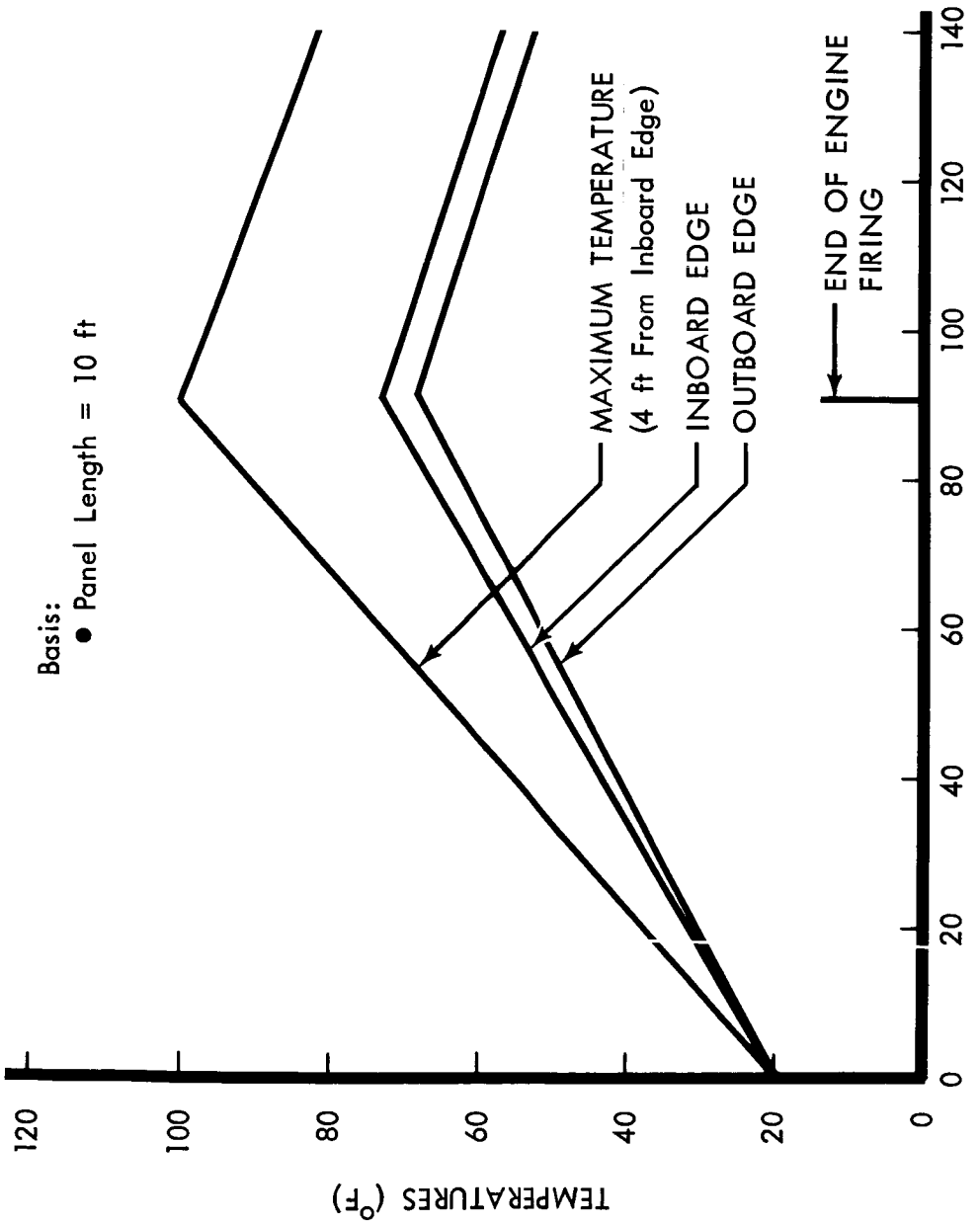

Figure 4.4-9: Effect Of Plume Radiation On Solar Panel Temperature

deflection, whereas the black surface does not. Parametric performance data on boom temperatures and deflections are given in Section 4.0 of Volume B.

Figure 4.4-10 shows typical temperature distributions on the high-gain antenna at the start of the mission and 173 days later. Analyses of antenna deflections resulting from these temperature gradients show that antenna performance will be acceptable; typical deflections are expected to be about 0.15 inch. Analyses of plume heating effects on the high-gain antenna show that the temperature increase will be about $30^{o}F$, which is acceptable.

Typical temperature histories on the solar panels are shown in Figures 4.4-9, 4.4-11, and 4.4-12. Temperatures are noted to be about $110^{o}F$ at the start of the mission, decaying to about $-20^{o}F$ at the end of the mission, with temperature dips to $-275^{o}F$ during occultation in Mars orbit.

Figure 4.4-6 shows typical temperatures occuring within the planet-scan platform during Mars orbit; components are held within their tolerance. Comparison of the louver and radiator concepts showed that the louver system could adjust effectively to some component failures, whereas the radiator system had limited capability in this respect.

Electric Power Usage--The design philosophy on power usage is that a minimum number of electric heaters be used for thermal control, particularly during occultation in Mars orbit when little power is

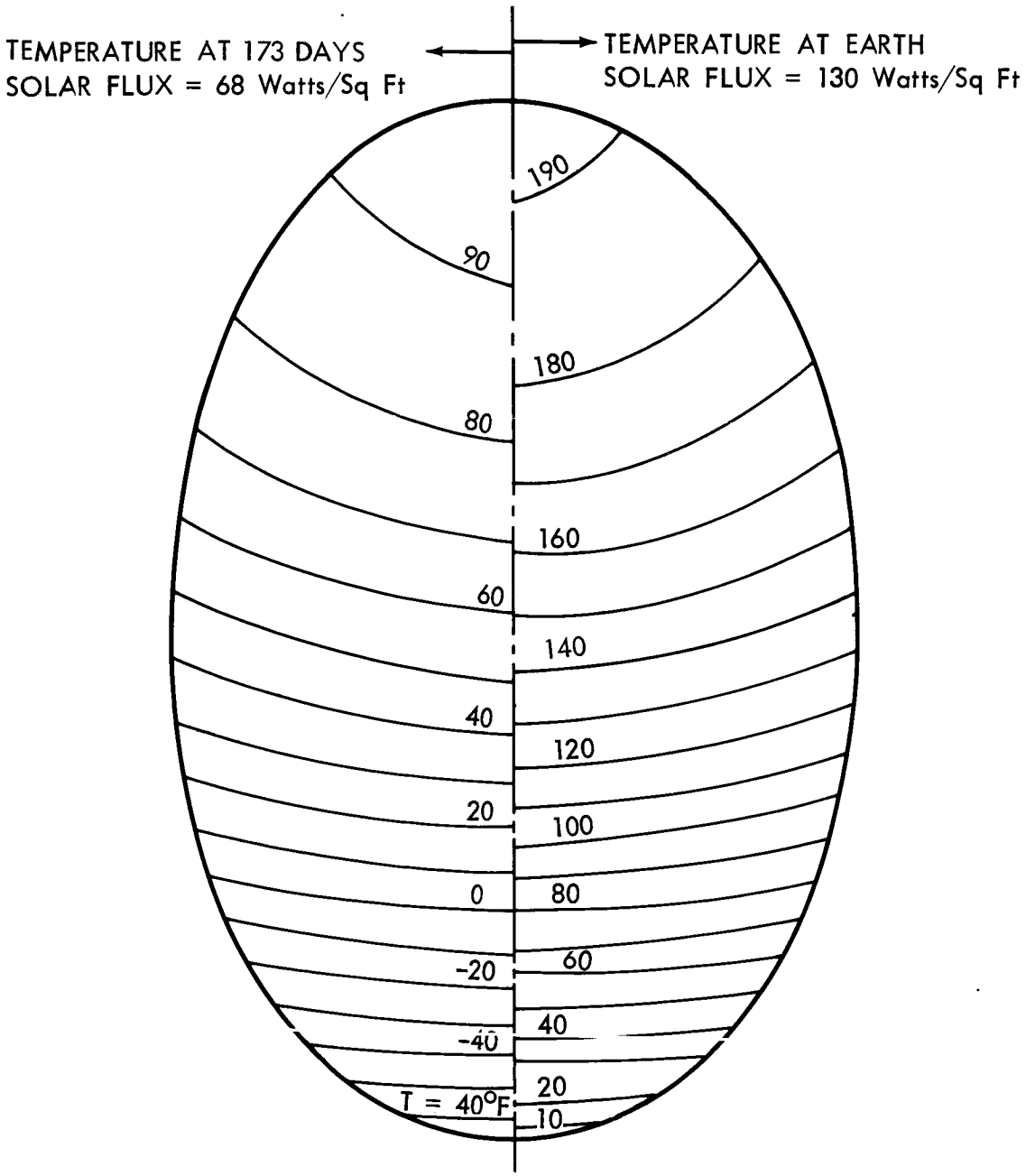

Basis:

True View
Ratio, Solar Absorptance/Emittance = 0.7
Angle to Sun = 40°
Focal Length/Major Diameter = 0.35
Adiabatic Back
4-mil Sheets

Figure 4.4-10: High-Gain-Antenna Temperatures

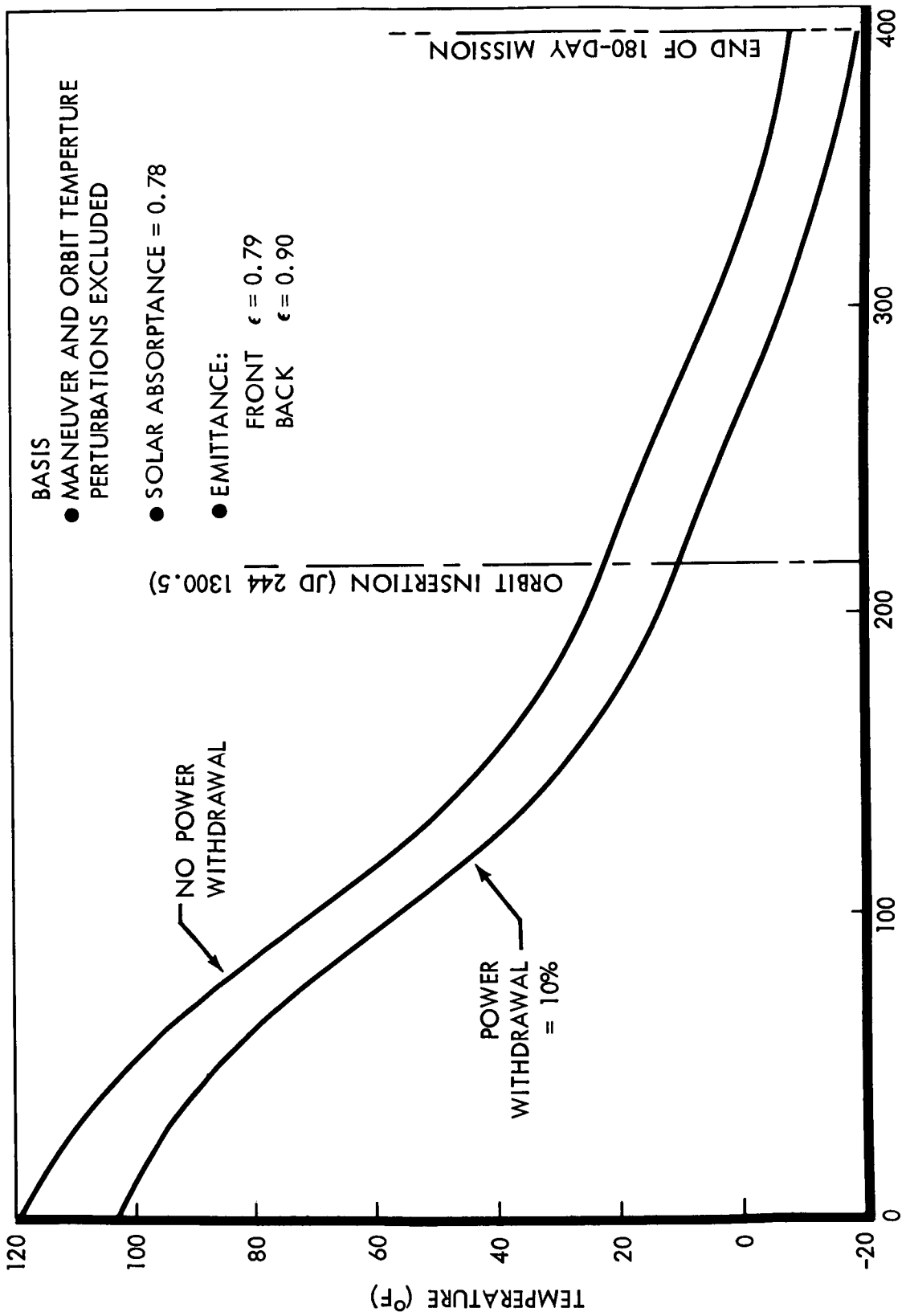

Figure 4.4-11: Solar Panel Temperature

Basis:
Solar Absorptance = 0.78
Emittance = 0.90
Energy Withdrawal = 10%
Solar/Flux = 63 watts/sq ft
Periapsis Altitude = 2700 km

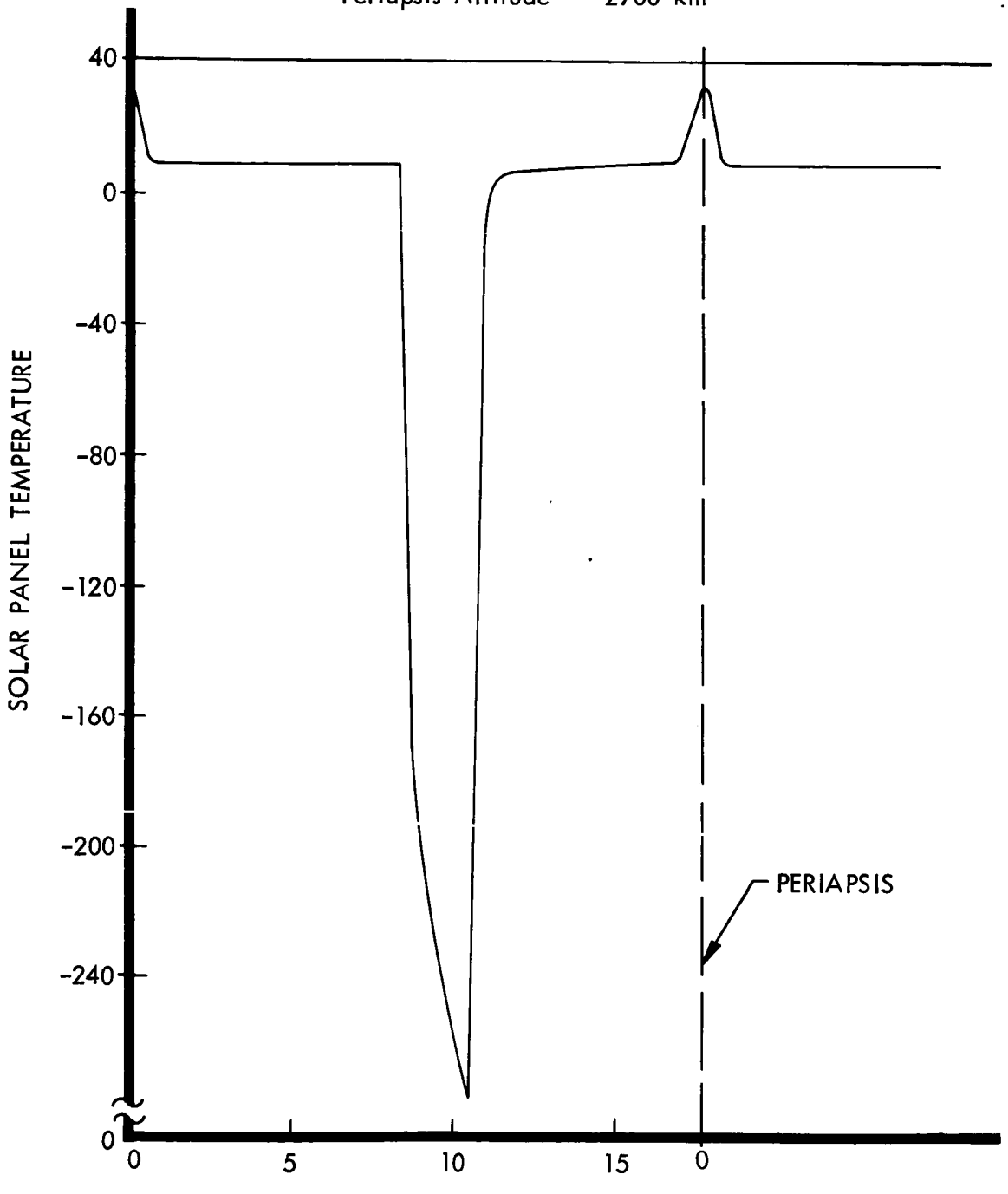

Figure 4.4-12: Solar Panel Temperature In Occulting Mars Orbit

available. In the event operation of electrical heaters (in a backup mode) are necessary, they will require up to 40 watts; this is tabulated in greater detail in Section 4.2. Heater power requirements are generally highest during the latter part of the mission when the least solar radiation is available. Heater power requirements also increases somewhat when equipment power levels are low.

Failure Analysis--Louvers are the temperature-control items most subject to failure. Failure rates are expected to be low, however, because of design simplicity. Worst-case conditions are louvers failing to open near Earth, and louvers failing to close near Mars. Both types of failures are compensated in part by reaction of adjacent louvers and by the good thermal coupling achieved in the packaging and arrangement of equipment. Estimates of the effects of louver failures on equipment temperatures show that failure of two adjacent louvers should be tolerable but that failure of three adjacent louvers probably will not be tolerable. Electric heater systems are also subject to failure. Analysis of these systems shows that shorting, open circuiting, and switching problems will be of greater concern than failure of heaters and temperature sensors.

Problem Areas--Radiant heating of external bus components by the solid-propellant-engine exhaust plume is considered to be the major thermal-control problem. This is a problem not because of heating rates, which are low enough, but because of the difficulty of verifying the design by test. Because plume-heating data depend heavily on analysis, an experimental plume heating investigation is planned as discussed in Section 4.4.1.8.

A second problem is temperature control of the science payload. Though the concepts analyzed are reasonable and show satisfactory performance, it is recognized that design of the package can be severely constrained by unique design features of science payload items. As a consequence, definition of the thermal constraints and design of the planet-scan platform should be concurrent with that of the rest of the spacecraft so temperature-control provisions can be optimized for the science payload.

An additional problem is in the design of a bimetal louver actuator with a minimum magnetic effect. Manufacture of nonmagnetic actuators is feasible, but they do not appear to be commercially available. Therefore questions on performance of a new actuator element must be resolved and the conclusions weighed against the penalties of using the conventional elements.

4.4.1.7 Physical Characteristics and Restraints

Specific design information is summarized in Table 4.4-1. A weight of 36 pounds is estimated for the temperature-control system. Power usage can be up to 40 watts with all ground options used. Internal-equipment radiator temperatures are controlled by the system within the range of 50 to 80°F, and other equipment is controlled within its individual tolerance limits. The system was designed specifically for the 1971 mission, but performance will be satisfactory for the 1973 mission.

4.4.1.8 Safety

Operation of the spacecraft outside the tolerable temperature range introduces the possibility of damage to components, which could be

injurious to personnel or equipment. If out-of-tolerance environmental temperatures occur before launch, there is sufficient instrumentation and time to allow for detection and corrective action. Failure of the nitrogen tank could be explosive, but will not occur until temperatures exceed at least 220°F. Gas buildup in batteries is also temperature-dependent and can cause an explosive failure. Overheating of the freon system before launch will not cause tank rupture because this system is not pressurized until after launch.

4.4.1.9 Development and Testing Before July 1966

Radiant heating of solar panels and boom-mounted equipment is based on analytically derived plume heating rates. A program is required to provide experimental justification of these analyses. A direct confirmation test with a flight engine will not be possible in this time period, so a test by inference is required using available solid-propellant chambers and high-expansion nozzles in an altitude chamber.

Testing of conventional louvers will be required to establish the level of magnetic interference. If interference exists, development of new actuators will be required and will include verification testing.

4.4.2 Packaging and Spacecraft Cabling

Summary--Electronic packaging is the technology of assembling parts into functional assemblies that meet the requirements and constraints of a program. Packaging covers subassembly and installation of electronic components and parts within an assembly. Cabling covers the electrical interconnection of these assemblies.

There are 19 assemblies located in the equipment compartment. These are arranged and designed to meet the Flight Spacecraft temperature-control, center-of-gravity, and subsystem functional requirements. The preferred assembly installation is shown in Figure 4.4-13 and consists of an assembly attached to the structure by standard spaced bolts at the backside (i.e., the side toward the spacecraft centerline). The arrangement facilitates balancing the spacecraft and is consistant with other important constraints such as minimum cable length (for reducing weight and power loss and for minimizing EMI effects) and uniform thermal distribution.

The temperature control louver installation is structurally independent of the assemblies. The louvers are installed in standard panel sections to accommodate two standard louver sizes. The panels are mounted on the spacecraft using shear pins at the lower bulkhead and pin joints at the upper bulkhead as illustrated. This arrangement mounts the panels independently of one another allowing removal of one panel at a time for access.

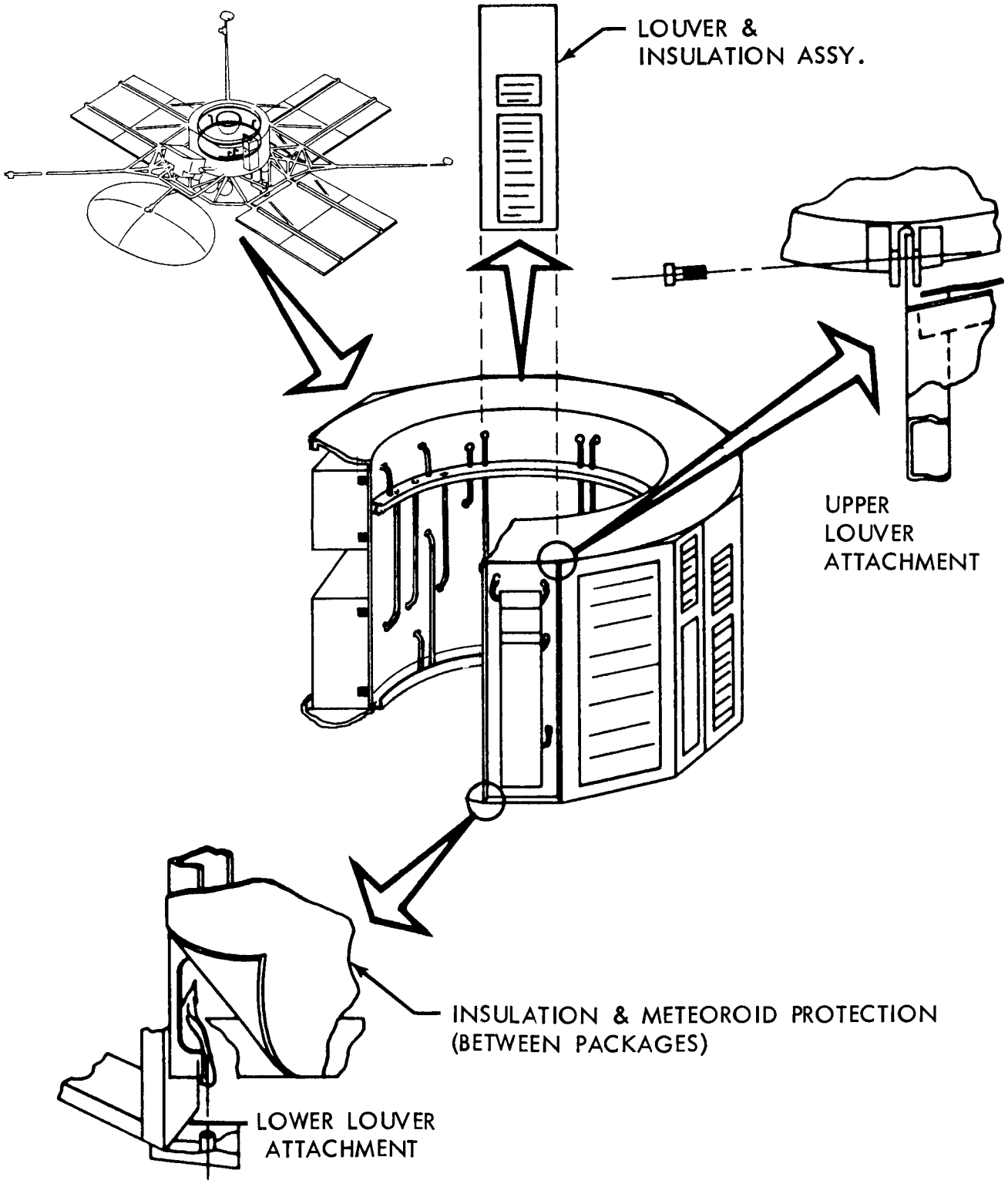

Figure 4.4-13: Packaging and Cabling Subsystem

The package assemblies are standard in cross section and vary in dimension along the spacecraft Z axis to meet the volume-and heat-dissipation requirements. Each package has a standard 8-inch radial dimension (perpendicular to radiating surface) and either an 8- or 16-inch circumferential dimension.

Electronic subsystems are interconnected with the Spacecraft's power and signal wiring harnesses. These harnesses are supported in cable trays that are routed along the inboard edge of the spacecraft equipment compartment. Interconnections between the spacecraft harnesses and the electronic packages are made with NAS 1599 connectors.

Unique requirements imposed on Voyager packaging are those for thermal control in an occulting orbit, meteoroid protection, and extended-duration exposure to high vacuum. The thermal stability of the package is maintained by conducting internally generated heat from its source to a space radiating surface on the package. Meteoroid protection is provided by using a meteoroid bumper on the front of each package. The bumper will break up the meteoroids; the residue is then stopped by an internal structure member. Survival in a high-vacuum is ensured by the control and selection of parts and material, and by potting, coating, and sealing electronic subassemblies and connectors.

4.4.2.1 Spacecraft Assembly Installation

Scope--This section covers description of the functions and physical characteristics of the installation of the subsystem assemblies into the spacecraft. The preferred arrangement of the assemblies is presented.

Functional Description--The preferred installation is supported by the Flight-Spacecraft primary structure and enclosed by the thermal shields, meteoroid bumpers, and louvers. Each assembly is independent and self-contained, providing its own protection from electromagnetic interference, flight environment, and ground handling. The assembly chassis are provided with means of attaching handles to facilitate installation and removal. Assemblies which require precise alignment are provided with guide pins. The assemblies are equipped with test connectors that are readily accessible when the equipment is mounted on the spacecraft.

Interface Definition--The spacecraft package assembly interfaces are defined below.

Thermal--There are two thermal interfaces: the heat radiating surface that faces dark space, and the heat conducting areas joining the assemblies to the primary structure.

The side of the assembly facing dark space radiates heat through louvers that are controlled by the temperature of the radiating surface. The side of the assembly opposite the heat radiating surface is joined to the primary structure to provide a heat path for transfer of heat to other assemblies and to the primary structure.

Mechanical--Electrical, electronic and miscellaneous equipment is supported by structure integral with the radiating surface. The assembly uses a minimum number of fasteners to the primary structure. The radiating surfaces of the assemblies protect the packaged equipment from meteoroid damage.

Electrical--The interface between the spacecraft assembly and the spacecraft cabling is through a miniaturized manually installed connector. The assembly protects the packaged equipment from electrostatic charges developed during flight by distributing them through a common ground.

Magnetic--The quasi-static magnetic properties of the package design must be held to within the required limits during the mission. Equipment and wiring will be physically located such that the magnetic fields will be minimized.

Performance--The performance requirements for assemblies are derived from constraints imposed by uniform packaging and from consequences of subsystem functional requirements. The environmental requirements are particularly important.

Size--The assembly size is 8 inches along the vehicle radial demension, either 8 or 16 inches on vehicle circumferential dimension, and of variable height along the spacecraft Z axis as required to suit specific volume and thermal control need.

Weight--The maximum assembly weight is limited to about 50 pounds. It is determined primarily by equipment installation, handling,and personnel safety considerations.

All assemblies are provided with a device (e.g., guide pins) to prevent the package from slipping or falling when the last holddown bolt is

removed. This device is used to prealign the package fasteners to facilitate installation.

Thermal Balance--Thermal balance depends on heat rejection through radiating to space. The electronic packages operate through a temperature range of 30 to 100°F. With this differential, radiation between assemblies will not be a major factor. The radiator area of each assembly is sized according to the amount of heat generated in the equipment and the capability to dissipate by radiation approximately 0.2 watt per square inch. This radiation capability is modified by the view angle and the position of the thermal control louvers.

Physical Characteristics and Constraints--The volume available for spacecraft equipment is 47 cubic feet. Nineteen assemblies are supported on the equipment wall. The assembly support structure adds a small amount to the spacecraft weight; however, this technique facilitates mounting and demounting assemblies. The shear web of the cylindrical section is stabilized by vertical parallel stiffeners approximately 5 inches apart, to which the assemblies are fastened. This arrangement also facilitates proper center-of-gravity positioning and adjacent grouping of those assemblies that have many connectors.

The back-mounted assembly installation shown in Figure 4.4-14 provides separate heat paths for conducting heat to or from adjacent assemblies or structure and to the radiating face. The package is a single assembly that is easy to handle, test, and check out. It is attached by fasteners at the back located in a standard hole pattern which can, however, be

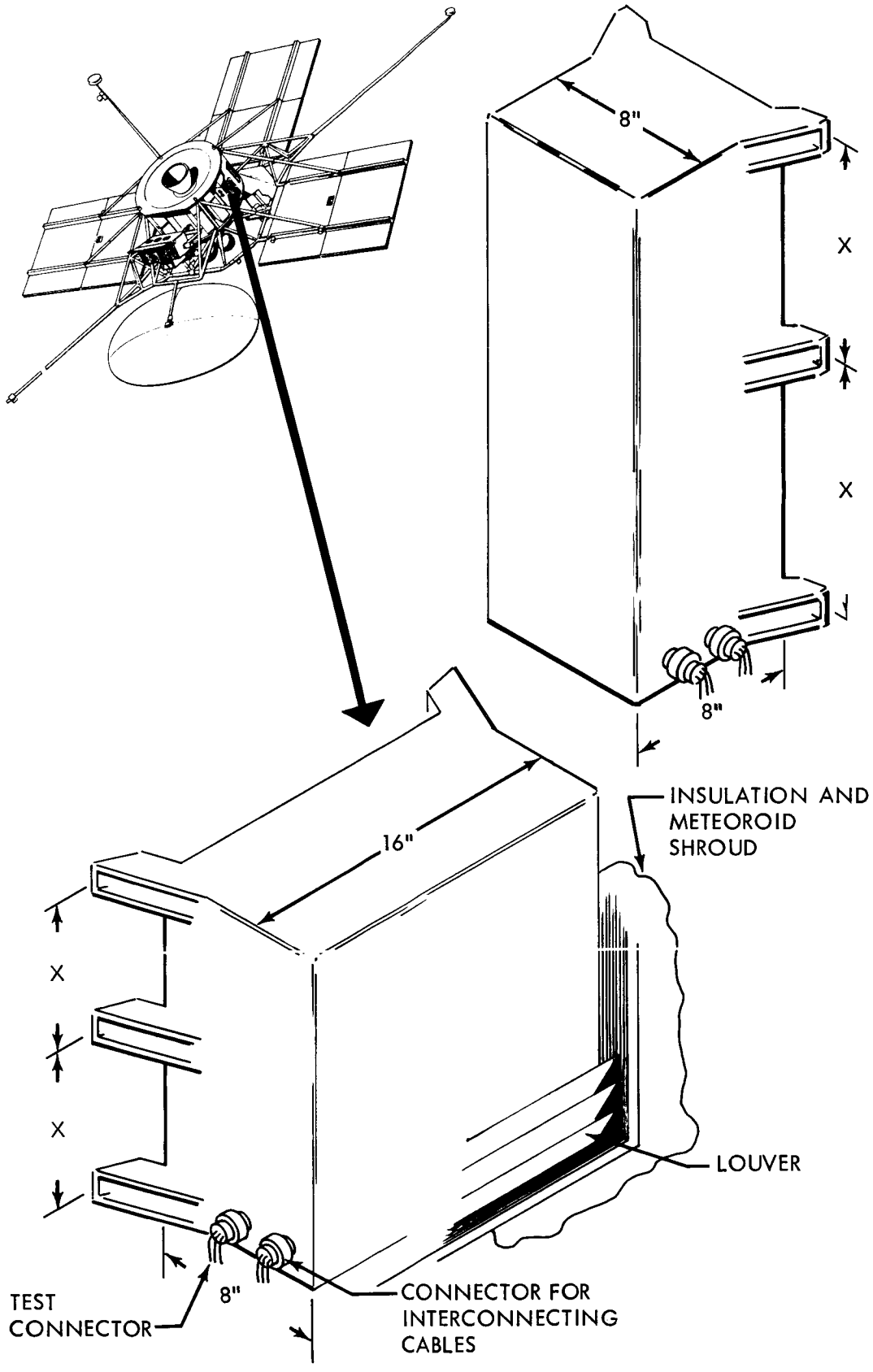

Figure 4.4-14: Back Mounted Package

varied to change the heat conduction path to or from the structure and adjacent assemblies. The radiating surface faces dark space and heat radiated is controlled by the size of the radiating surface and louvers and by locating high heat dissipation assemblies uniformly within the spacecraft. Each package has one standard radial (perpendicular to radiating face) dimension, 8 inches. There are two standard dimensions, 8 and 16 inches, in the circumferential direction (parallel to the radiating face) and the third dimension along the spacecraft "Z" axis is variable to match the standard attachment hole pattern and meet the requirement of the packaged equipment for heat radiation. This installation simplifies the package design by separating the conduction and radiation requirements so the package can be designed to satisfy each requirement independently.

During midcourse guidance, when the spacecraft experiences transient thermal loads resulting in increased stress in the primary structure, the equipment support structure expands or contracts uniformly in radial direction from the spacecraft Z axis, thus equipment alignment is maintained within required tolerances.

4.4.2.2 Spacecraft Cabling and Harness

This section provides a functional description of the spacecraft cable and harness subsystem.

Scope--The electrical design consideration includes the control of magnetic and electrostatic interference, power losses, voltage drop in conductors, and insulation electrical characteristics. In addition, consideration is given to the mechanical aspects of insulation strength;

thermal protection; meteoroid protection; nuclear radiation; vibration; sterilization; and support and accessibility during construction, rework, adjustment, and test. The peculiar effects of space environment upon all components and materials is considered.

Applicable Documents--

AFMT SO-2	Air Force Missile Test Center Pamphlet, "General Range Safety Plan"
Boeing Document D2-23036	"Electro-Interference, Class II Research: Application of Computer Techniques to System-Interference Analysis 93.1.1"

Functional Description--The wire and cable harness is separated into two assemblies held rigidly with cable clamps fastened to the harness trays. Power and signal harnesses are separated. The harness trays are attached to the inside of the equipment panel as shown in Figure 4.4-13 and serve as structural members. The harness breakouts are routed through grommeted holes in the harness tray and held rigidly to the panel stiffeners. The forward harness tray assembly provides routing for low-power signals whereas the aft tray will contain electrical power harness and pyrotechnic cables.

This tray arrangement provides a minimum flexing of the cables and harness during installation and maintenance. Plugin connectors (miniature circular Type NAS 1599) are easily aligned to ensure straight, free engagement of the contacts and allow visual inspection to assure good electrical contact.

Interface Definition--The cable and harness subassemblies provide the following:

1) Electrical connections between assembly installations (shown in the Functional Block Diagram Figure 3.10-3) are indicated in Figure 4.4-15 which identifies those spacecraft subsystems that interface with the cables and harness.
2) Signal isolation from electromagnetic interference.
3) Mechanical strength to withstand induced vibration and the effects of ground handling.
4) Standardized ground-return techniques.

Physical Characteristics and Constraints--The diameter of the forward and aft harness assemblies will not exceed 1.5 and 1 inch, respectively. The total weight of both harness assemblies will not exceed 100 pounds.

The major constraints associated with design of cable and harness subassemblies are electromagnetic interference (conducted, radiated), and magnetic fields resulting from direct-current loops.

Electromagnetic interference--The electromagnetic control techniques have been reviewed and the installation will comply with Eastern Test Range (ETR) Radio Communication Instruction (RCI) No. 30-29 requirements.

The design guidelines used to minimize electromagnetic interference for cable harnesses are:

Figure 4.4-15: CABLE AND HARNESS INTERFACE

Spacecraft Subsystems	Capsule	Propulsion	Science Payload	Telecommunications	Attitude Reference	Autopilot	Reaction Control	CC&S	Electric Power	Mechanisms	Temperature Control	Pyrotechnics
Capsule								X				X
Propulsion						X		X	X			X
Science Payload				X					X			
Spacecraft Bus												
Telecommunications			X		X	X	X	X	X	X		
Attitude Reference				X		X		X	X			
Autopilot		X		X	X		X	X	X			
Reaction Control				X		X		X				
CC&S	X	X		X	X	X	X		X	X	X	X
Electrical Power		X	X	X	X	X		X		X	X	X
Mechanisms				X				X	X			X
Temperature Control								X	X			
Pyrotechnics	X	X						X	X	X		

secured to the package structure.

Electronic parts or modular units are mounted on a thermal-structure. The structure supports and protects the components while carrying away internally generated heat by conduction. Figure 4.4-16(b) shows a typical interleaved cordwood module subassembly, with the modules interconnected on a printed wiring board.

Electronic subassemblies are mechanically attached to a supporting case by positive fasteners. These fasteners provide both mechanical support and a low-loss thermal connection. An alternate packaging configuration will use a compression technique that eliminates the external case, thus reducing total package weight and improving thermal efficiency.

Sub assemblies are interconnected in the above configurations by: Printed wiring techniques using multilayer circuits or flexible printed wiring and by cabling techniques listed in Figure 4.4-18.

Internally generated heat is carried along the thermal structure and is finally radiated to space. The radiating face is the outboard surface of the package with respect to the spacecraft longitudinal centerline. Both the thermal structure and the radiating face of the subassembly are sized to efficiently remove the heat from the components. The temperature ranges of the faces are defined in Section 3.3.

PRINTED CIRCUIT BOARD ASSEMBLY

SINGLE-SIDED BOARD	LOW-DENSITY DISCRETE PARTS	DISCRETE HEAT SINK
DOUBLE-SIDED CIRCUIT BOARD	LOW-DENSITY DISCRETE PARTS	
	LOW-DENSITY CORDWOOD MODULES	
	HIGH-DENSITY INTEGRATED CIRCUITS	COMPOSI HEAT SIN
MULTILAYER CIRCUITRY	HIGH-DENSITY CORDWOOD MODULES	COMPOSI HEAT SIN
CORDWOOD MODULARIZED ASSEMBLY	CORDWOOD-WELDED CONSTRUCTION	
	CORDWOOD-SOLDERED CONSTRUCTION	

USED ON	HANDLING & STORAGE CONTROL	CIR	
		CIRCUITRY PRINTING	ETCH
MINUTEMAN WS 133A	BAC 5760 BAC 5485	BAC 5760	BAC
DYNA SOAR X-20	—	BAC 5762	BAC
MINUTEMAN SECURITY SYST	BAC 5799	BAC 5799	BAC
MINUTEMAN FORCE MODERNIZATION	BAC 5828	BAC 5762	BAC
LUNAR ORBITER	D2-100338-1	BAC 5762	BAC
LUNAR ORBITER	D2-100338-1	BAC 5762	BAC
LUNAR ORBITER	D2-100338-1	—	—
MINUTEMAN FORCE MODERNIZATION	BAC 5828	BAC 5760	BAC
HiBEX	BAC 5485	—	—

CUIT-BOARD FABRICATION				CIRCUIT-BOARD AS		
IING	BOARD LAMI- NATION	MACHINING	PLATING	PARTS INST	CONNEC- TOR INST	BO HE SIN
5760	—	BAC 5760	BAC 5746	BAC 5760	BAC 5760	—
5762	—	—	BAC 5761	BAC 5123	—	—
5799	—	BAC 5799	—	BAC 5799	BAC 5799	—
5760	—	BAC 5760	—	BAC 5828	BAC 5828	—
5762	D2-100462-1	BAC 5762	BAC 5028	BAC 5123	BAC 5029	D2-10
5762	D2-100462-1	BAC 5762	BAC 5028	BAC 5123	BAC 5029	D2-10
-	—	—	BAC 5728	BAC 5123	—	—
5760	—	BAC 5760	—	BAC 5828	BAC 5828	—
-	—	—	—	BAC 5123	—	—

SY		JOINING				
ND AT IK	CORD-WOOD INSTALL	FLOW-SOLDER	PLANAR PULSE SOLDER	HAND SOLDER	CROSS-WIRE WELDING	PLAN BRAZ
-	—	BAC 5760	—	—	—	—
-	—	—	—	BAC 5052	—	—
-	—	BAC 5760	—	BAC 5052	—	—
-	BAC 5828	BAC 5760	BAC 5828	—	—	—
1462-1	—	—	BAC 5029	—	—	—
1462-1	BAC 5123	BAC 5760	—	BAC 5052	—	—
-	—	—	—	—	BAC 5909	—
-	—	BAC 5760	—	—	—	—
-	—	—	—	BAC 5052	—	—

4

AR ING	ENCAPSULATION		WIRING HARNESS & CONNECTOR ASSEMBLY
	POTTING	COATING	
-	—	BAC 5760	BAC 5550
	—	BAC 5747	BAC 5157
-	—	—	BAC 5154
-	BAC 5828	BAC 5828	BAC 5117
-	—	BAC 5747	BAC 5120
-	BAC 5512	BAC 5747	BAC 5155
			BAC 5162
			CONNECTOR POTTING
			WIRE-HARNESS FABRICATION
			IN-PROCESS ELECTRICAL TESTING
			ELECTRICAL BONDING
			CRIMPED ELECTRICAL CONNECTION
			HEAT SHRINKAGE MATERIALS
			ELECTRICAL CONNECTOR ASSY
	BAC 5512	—	
	BAC 5828	—	
	BAC 5512	—	

The radiating surface of the package also acts as a meteroroid bumper. When meteoroids collide with the radiating surface or bumper, they are broken up, and the residue is stopped by the package's internal structure. This meteoroid protection scheme is shown in three sketches in Figure 4.4-19.

Interface Definition--The spacecraft interfaces are defined in terms of the assemblies. These interfaces are listed in Section 4.4.2.1 and are detailed in the individual subsystem descriptions.

Physical Characteristics and Constraints--Voyager electronic packages are lightweight, high-density packages using miniature low-power electronics wherever possible. The specific packaging design for each electronic assembly will be selected based on applicable JPL packaging requirement specifications and the related experience and status of qualified processes of the industry-team member.

Management control of the design is implemented through use of the approved parts lists, packaging guides, material and process specifications, and the pertinent preliminary design and critical design reviews. Each subcontractor and industry-team member will use his own developed and proven techniques, subject to Boeing approval for compliance with requirements.

The package designs will be verified with worst-case analyses for which computer programs are available. Fabrication will be accomplished in shops employing clean-room environments as required. Proven

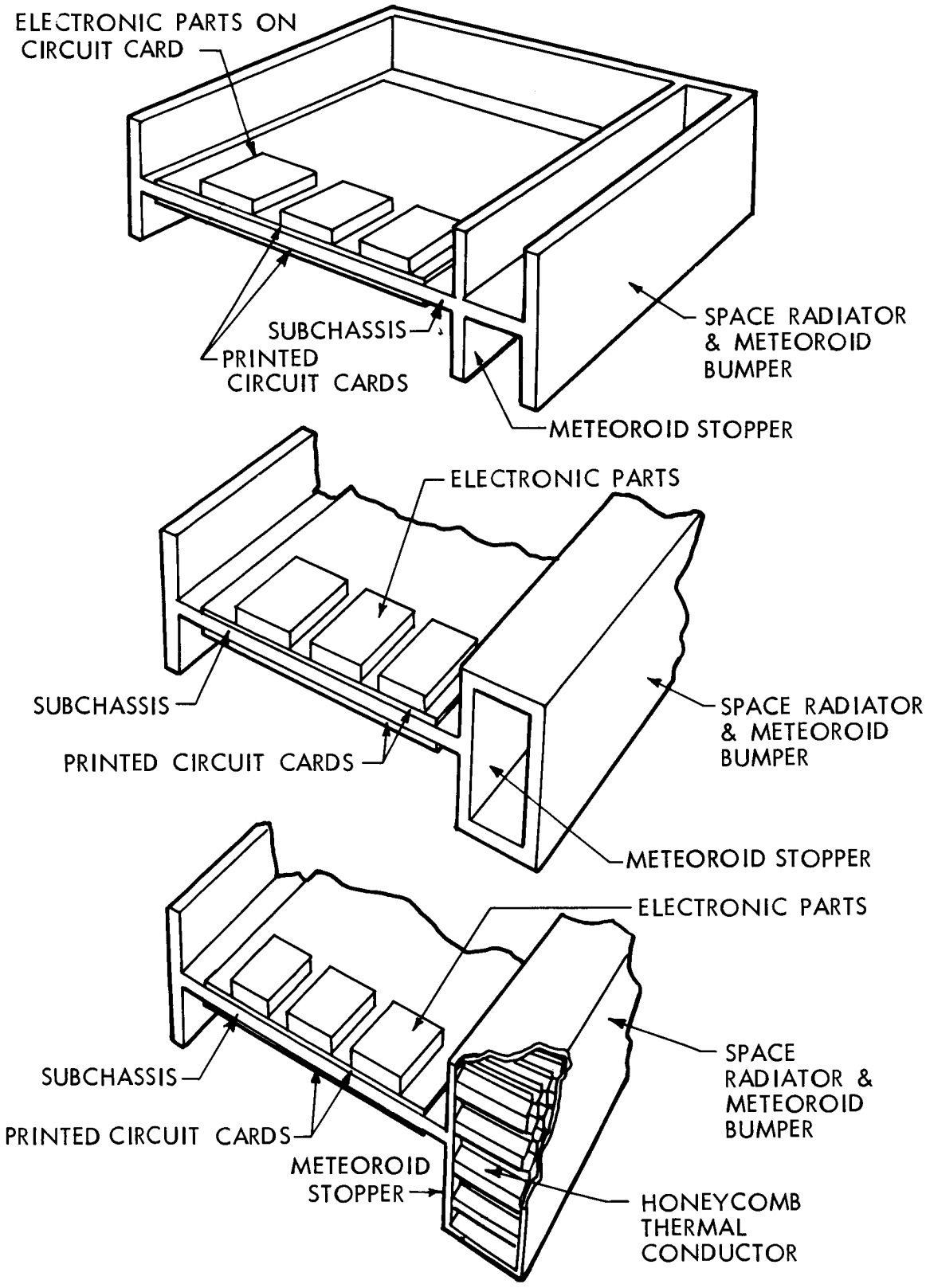

Figure 4.4-19: Electronic Package Meteoroid Protection

processes will be used. Existing processes have been screened on a preliminary basis for Voyager applications. The process application matrix chart shown in Figure 4.4-18 relates several typical packaging techniques (i.e. single-sided boards, cordwood modules, etc.) to the approved and qualified process specifications that are in existence and use.

Figure 4.4-20 shows the relationship between packaging concepts and some of the important missile and space programs on which The Boeing Company has had prime responsibility for packaging the electronic system. The chart summarizes experience in the required technologies and indicates the preferred methods for solving the most important and critical packaging problems for Voyager. Previous experience is indicated with the technique or approach that is chosen for Voyager packaging. For example, in the thermal control category, the conduction plus radiation cooling technique is being used on the Lunar Orbiter. A minor variation is planned for Voyager in that primary thermal control is achieved through direct radiation to space from the heat-producing package rather than a common cold plate. This variation necessitates a subsequent reduction of parts density in order to achieve the necessary amount of radiating area. Voyager part densities will consequently be about 40 percent lower than that of the Lunar Orbiter flight programmer. While this reduction imposes no thermal penalty, the ratio of package supporting structure weight to electronic parts weight increases.

APPLICABLE EXPERIENCE / PROGRAM	THERMAL CONTROL TECHNIQUE	METEOROID PROTECTION	MAGNETIC EMANATION CONTROL	PARTS SELECTION & APPLICATION	CARD ASSY METHOD	FABRICATION PROCESSES CARDS	MODULE ASSY METHOD
MARINER 'C' (JPL)	CONDUCTION + RADIATION	INHERENT STRUCTURE PROTECTION	N A	PREFERRED PARTS LIST	POINT-TO-POINT HAND SOLDER	ONE & TWO SIDED ETCHED WIRING BOARDS	
LUNAR ORBITER (BOEING)	CONDUCTION + RADIATION	INHERENT STRUCTURE PROTECTION	N A	HIGH RELIABILITY PARTS	PULSE SOLDER & HAND SOLDER	TWO-SIDED ETCHED WIRING BOARD BOND TO HEAT SINK	WELDED CORDWOOD - ENCAPSULATED
MINUTEMAN GROUND SUPPORT EQPMT (BOEING)	FORCED CONVECTION	N A	N A	HI-REL	FLOW SOLDER	ONE-SIDED EWB	SOLDERED CORDWOOD - CONFORMAL COATED
VOYAGER (BOEING)	CONDUCTION + RADIATION MASS	DOUBLE-WALL METEOROID	ELIMINATE MAGNETIC MATERIALS	HI-REL	PULSE SOLDER & HAND SOLDER	TWO-SIDED EWB BOND TO HEAT SINK	WELDED CORDWOOD ENCAPSULATED
TOPIC -SPACE VEHICLE PROGRAMMER (BOEING RESEARCH)	CONDUCTION + FORCED CONVENTION	N A	N A	PREFERRED PARTS LISTS	PULSE SOLDER & HAND SOLDER	CLEARANCE HOLE MULTILAYER WIRING BOARD	N A
HiBEX FLIGHT ELECT (BOEING)	CONDUCTION + HEAT SINK	N A	N A	COMMERCIAL QUALITY	HAND SOLDER	ONE-SIDED EWB	SOLDERED CORDWOOD - ENCAPSULATED

Figure 4.4-20: Packaging Technology Status

The structural and thermal designs proposed for Voyager subassemblies are based on previous experiences on the Lunar Orbiter program. Figures 4.4-21 and 4.4-22 are graphs that show typical thermal and vibrational responses of Lunar Orbiter type subassemblies that are proposed for Voyager. The maximum expected temperature rise between a solid-state integrated circuit and the edge of its supporting structure is 10^{o} F. An additional 10 degree rise will result if an overall packaging structural enclosure is imposed in the thermal circuit. The vibrational response of a typical Lunar Orbiter solid state integrated circuit card indicates a resonance at 210 cps with a "Q" input multiplier of 8. These characteristics can be improved if necessary for the Voyager packaging by use of appropriate stiffening, foaming, or structural damping of subassemblies.

Meteoroid protection of the assemblies is a necessity because of the prolonged Voyager mission. The shroud-type of protection scheme used on other programs cannot be employed since each package must directly view dark space to radiate heat. An integral structural web of material that functions as both heat radiator and meteoroid bumper is included on each package. The weight efficiency of the design is optimized by evaluating the spacing between the meteoroid shields versus the total weight gain of the system because of increased spacing. This analysis is shown in Figure 4.4-23.

The optimum shield spacing for this design is 0.7 to 0.8 inch. At that spacing, the weight penalty for the evaluated design is 0.83 pound per square foot of protection.

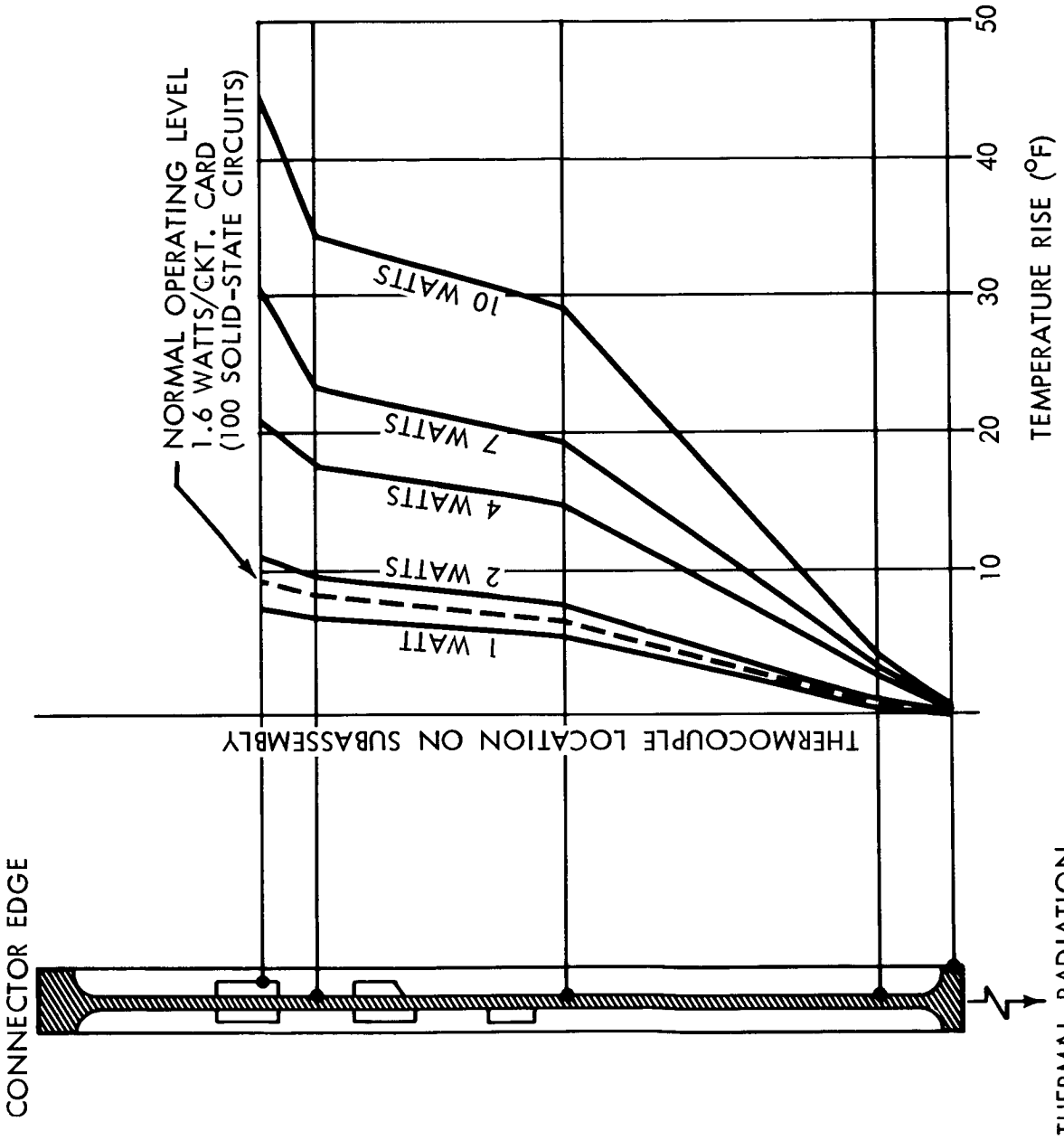

Figure 4.4-21: Thermal Data for Solid-State Integrated-Circuit Subassembly

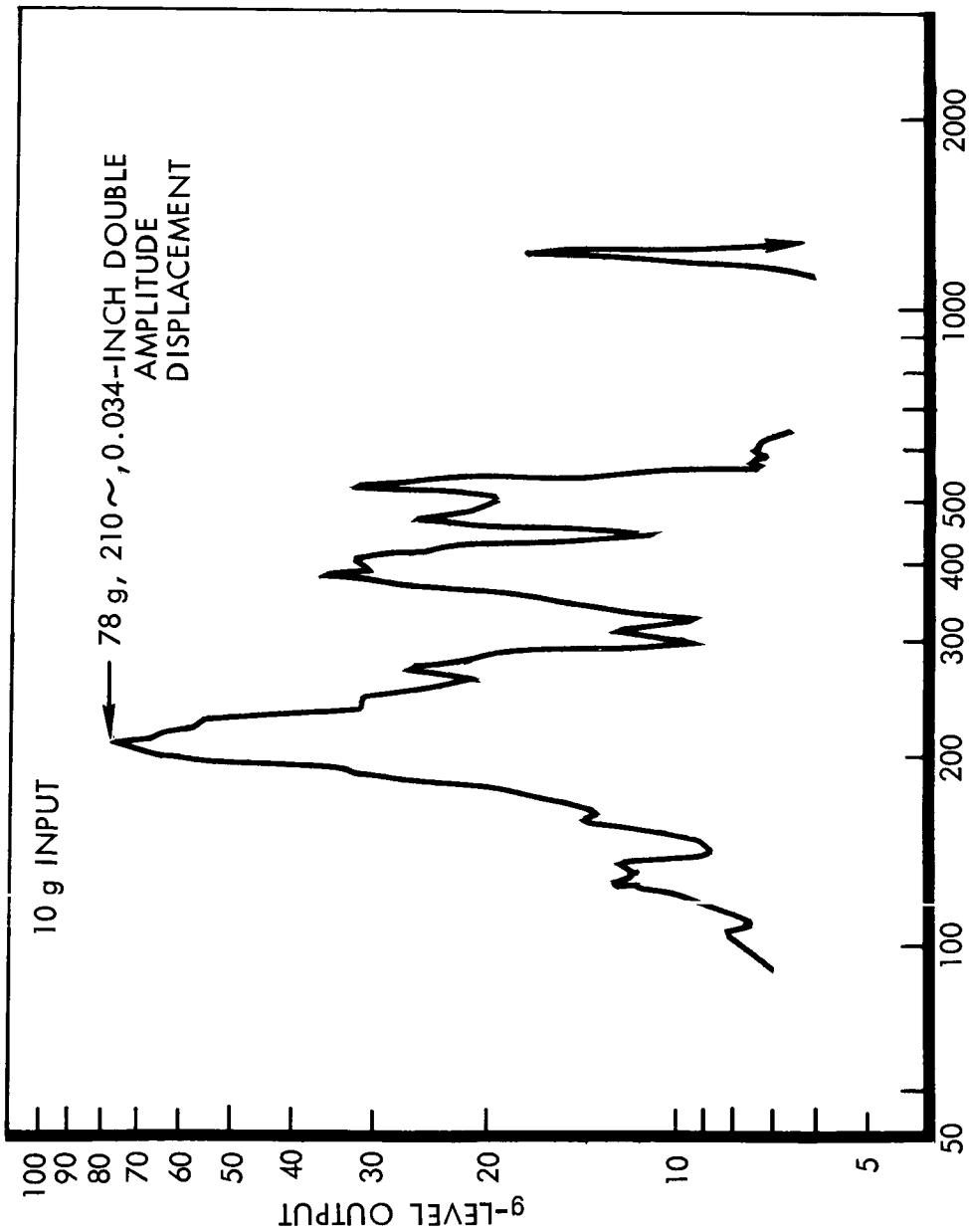

Figure 4.4-22: Frequency Response — Solid State Integrated Circuit Subassembly (Lunar Orbiter)

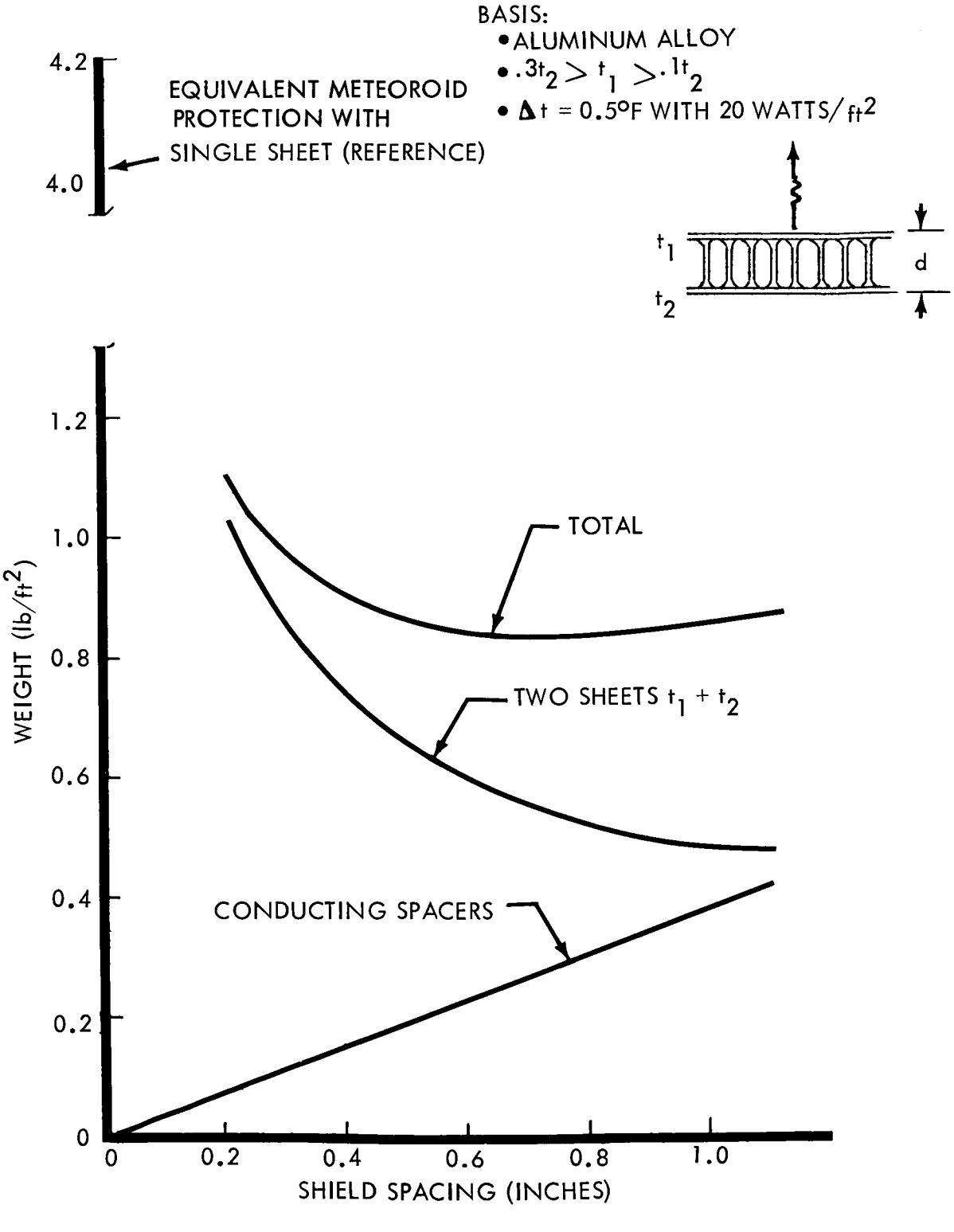

Figure 4.4-23: Radiating Meteoroid Shield

4.4.3 Spacecraft Structure

The primary spacecraft structure (Figure 4.4-24) supports all major elements of the Planetary Vehicle, including the Flight Capsule, the propulsion module, and the Spacecraft Science Payload. An additional function of the primary structure is to provide thermal load paths between many of the electronic assemblies, thereby helping to stabilize temperatures. It consists of two major assemblies--the equipment support structure and the lower support structure. The equipment support structure (Figure 4.4-25) is a magnesium cylinder, supported at top and bottom by a magnesium ring frame. Four machined aluminum truss longerons are located between the top and bottom ring, 90° apart. These longerons support the Flight Capsule and also transfer equipment loads to the lower support structure. The lower support structure is a welded titanium tube truss which attaches to the Centaur adapter, and supports all appendages.

The solar panel substrates consist of corrugated aluminum covered by flat sheets. These, in turn, are supported by welded truss-type aluminum ribs and spars. The low-gain-antenna booms are magnesium tubes of constant diameter, and the magnetometer boom is a linearly tapered aluminum tube. The high-gain antenna is an aluminum honeycomb shell of parabolic cross section.

Minimum weight considerations dominate the selection of structural arrangement, member cross section, material, and manufacturing processes. Titanium is selected for the trusswork. Aluminum alloys are selected for capsule support fittings and the magnetometer boom. Magnesium alloys are chosen for the ring frames, cylindrical shell, and antenna booms.

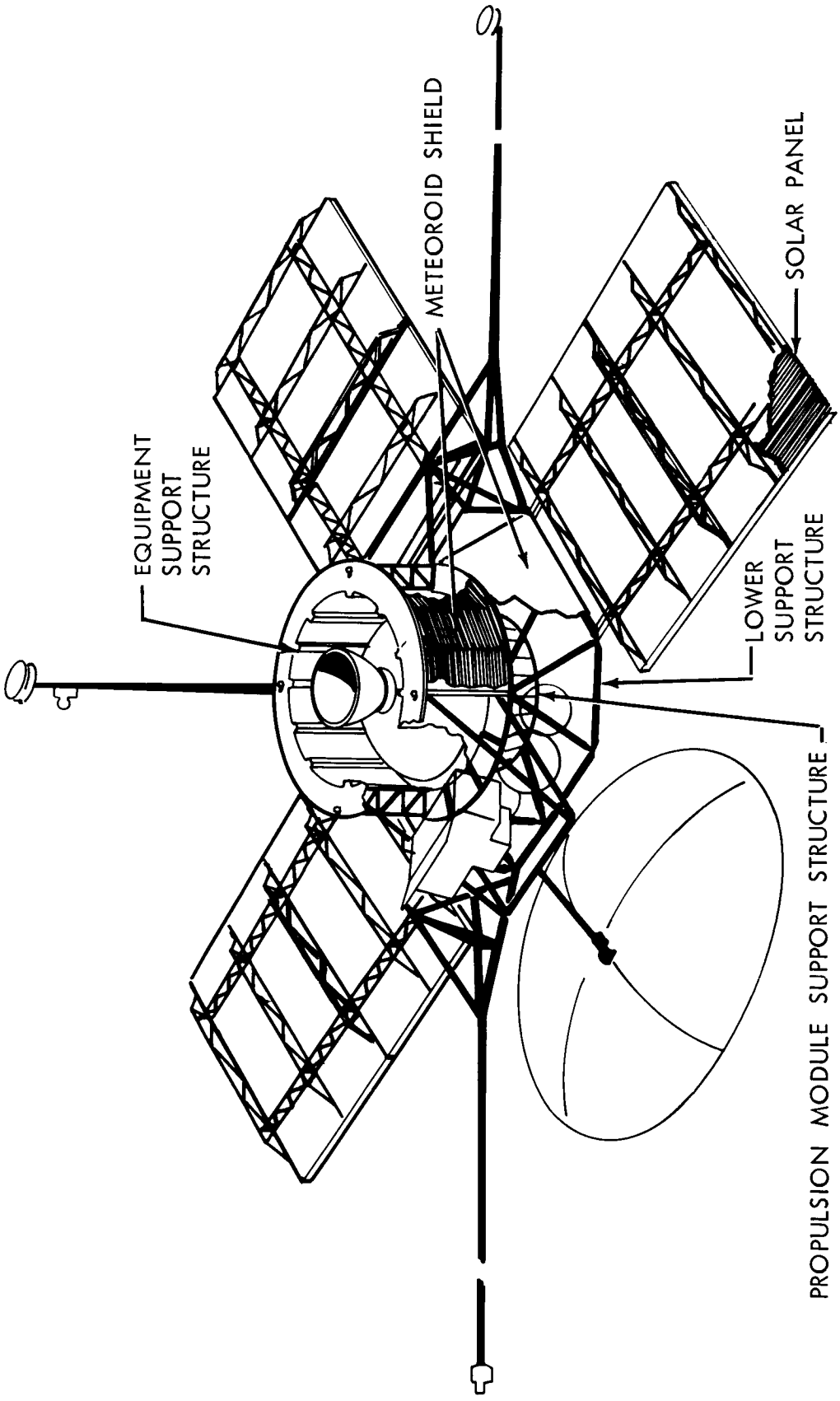

Figure 4.4-24: Structure Subsystem

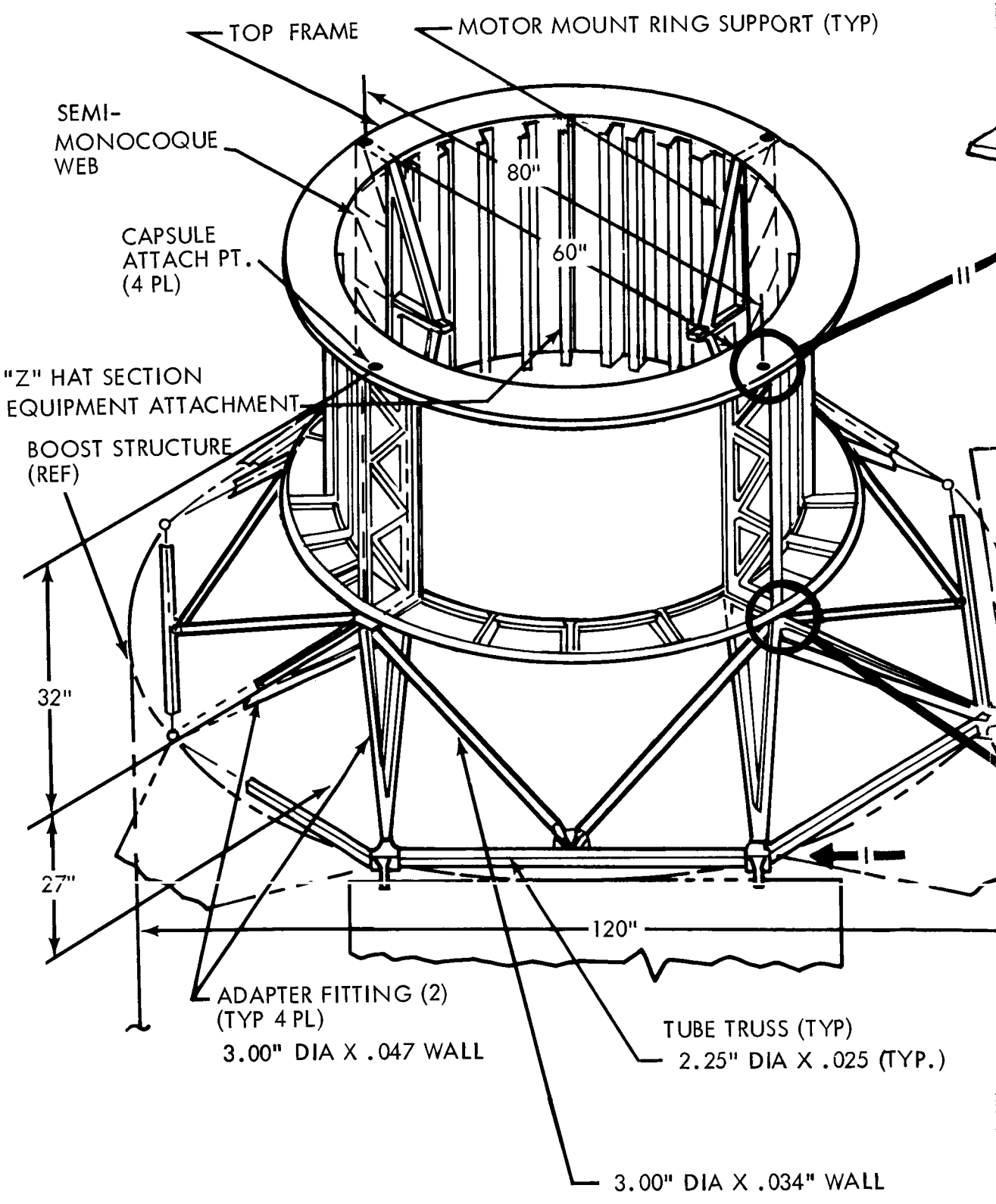
TOP FRAME
MOTOR MOUNT RING SUPPORT (TYP)
SEMI-
MONOCOQUE
WEB
80"
60"
CAPSULE
ATTACH PT.
(4 PL)
"Z" HAT SECTION
EQUIPMENT ATTACHMENT
BOOST STRUCTURE
(REF)
32"
27"
120"
ADAPTER FITTING (2)
(TYP 4 PL)
3.00" DIA X .047 WALL
TUBE TRUSS (TYP)
2.25" DIA X .025 (TYP.)
3.00" DIA X .034" WALL

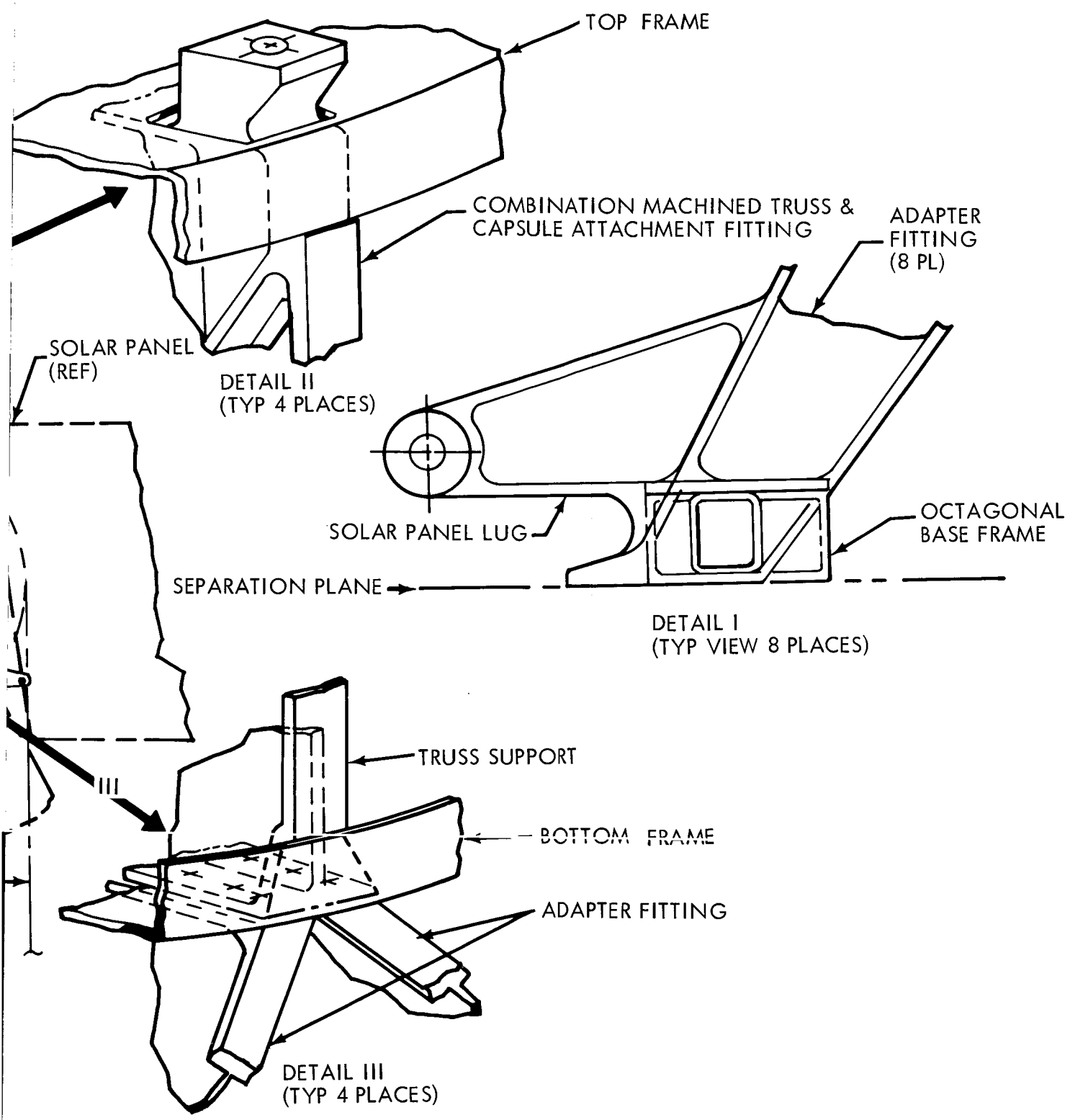

Figure 4.4-25: Primary Structure Module

All of the structural members discussed above are considered fully developed insofar as Voyager applications are concerned.

4.4.3.1 Applicable Documents

1) D2-82729-1, "Structural Load Analysis and Test Data for Phase IA Study";

2) D2-82729-2, "Internal Loads and Analysis of Structure for Phase IA Study";

3) D2-82734-1, "Materials and Processes for Voyager--Phase IA."

4.4.3.2 Functional Description

The spacecraft structural design is primarily influenced by the boost vibration loads applied to the spacecraft and to the 4500-pound Flight Capsule to be used in the 1975 and 1977 missions. The axial, shear, and moment design ultimate loads at the Centaur adapter for this configuration are 118,020 pounds, 60,810 pounds, and 6.58×10^6 inch-pounds, respectively--the latter two acting simultaneously.

Designs of the propulsion module and inboard members of the truss longeron are based on the boost vibration loads applied to the 3500-pound propulsion system to be used in the 1971 and 1973 mission configurations. The maximum axial, shear, and moment design ultimate loads (at the Centaur adapter) are 107,120 pounds, 48,300 pounds, and 3.98×10^6 inch-pounds, respectively--the latter two acting simultaneously. As can be readily seen, the boost vibration loads play a large part in design of the primary structure and stowed appendages. Second in importance are the orbit-

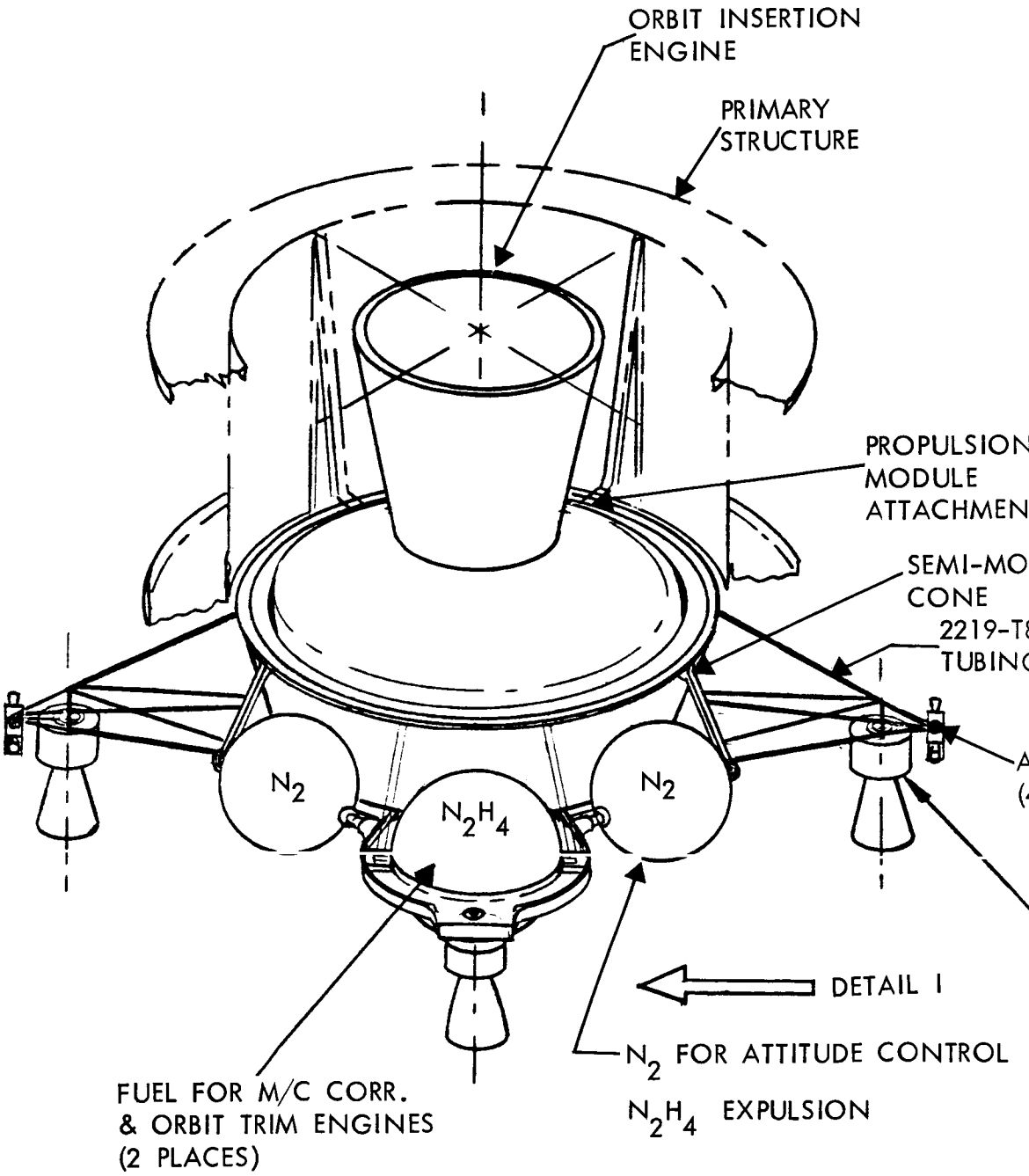
ORBIT INSERTION ENGINE
PRIMARY STRUCTURE
PROPULSION MODULE ATTACHMEN
SEMI-MO CONE
2219-T8 TUBIN
N_2
N_2H_4
N_2
DETAIL I
N_2 FOR ATTITUDE CONTROL
N_2H_4 EXPULSION
FUEL FOR M/C CORR. & ORBIT TRIM ENGINES (2 PLACES)

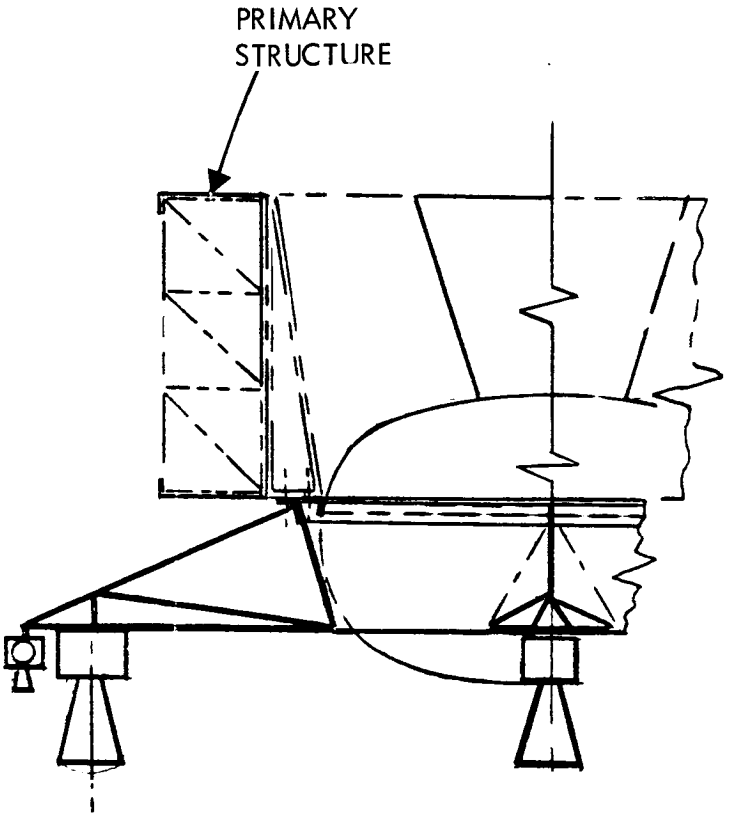

T

NOQUE

351

TTITUDE CONTROL
PLACES)

M/C CORRECTION
& ORBIT TRIM
ENGINE
(4 PLACES)

Figure 4.4-26: Propulsion Module Structure

difference is small between 2219-T851, 6Al-4V, and AZ80A-T5 for these relatively long lightly loaded members, with 2219-T851 being the lightest.

Meteoroid shielding protects the exposed equipment package surface area. Shielding consists of an aluminum bumper greater than 0.006-inch thick spaced approximately 1.0 inch outside the 0.060-inch thermal radiator. Shielding is also added around the lower surface and sides of the propulsion module. This shield consists of a 0.006-inch-thick aluminum foil on the outside of the 1.0-inch-thick insulation blanket and a 0.018-inch-thick aluminum sheet on the inside face. This shield covers a surface area of 143 square feet.

Solar panel structure functional description is presented in Section 4.2 of this document.

The magnetometer boom is required to support the magnetometer during boost (stowed position), transit, and orbit insertion. The boom structure must be sufficiently rigid so that vibration at its natural frequency will not degrade the capability of the autopilot and reaction control subsystem to maintain the desired attitude of the spacecraft. The boom length must be such as to position the magnetometer at least three spacecraft diameters away from the spacecraft, with an alignment maintained within 1 degree. The boom structure is constrained to stow within the Launch Vehicle nose fairing with a minimum of joints and mechanisms. It must minimize the moment of inertia about the spacecraft major axes and minimize weight.

The magnetometer boom is a foldable cantilever beam of 320-inch length that supports a 1-pound magnetometer at its tip (Figure 4.4-27). The beam consists of a linearly tapered round tube, 6.0 inches in diameter at the inboard hinge point and 2.0 inches at the tip. The base of the boom is attached at a hinge fitting on a tubular truss extension from the bus primary structure. The boom is fabricated from aluminum alloy 6061-T6 tubing. The folding mechanism consists of two hinges and one latch. When stowed, the midhinge point is supported by the VHF antenna support structure. The outboard section is secured to the base section of the boom for support.

The VHF and low-gain-antenna support structures are similar to the magnetometer boom except that their overall lengths are less and therefore tapering is not necessary. The untapered tube also doubles as a wave guide.

The paraboloidal high-gain antenna is made of a 0.5-inch-deep honeycomb sandwich. It is supported at the center on a fitting that extends back axially from the antenna to a pitch pivot motor shaft. The pitch pivot motor is mounted on a tube that is an extension of the yaw pivot motor shaft. These are stepping motors that provide moment, torque, and shear paths for the structure mounted on their shaft. The yaw pivot motor is mounted on a tubular frame that uses a torque tube, a beam, and a strut. The frame attaches to the top and bottom of the bus structure on each side of the science scan platform. The frame folds up alongside the bus for stowage. Auxiliary struts stabilize the folded frame and antenna center. The high-gain antenna and supports are shown in Figure 4.4-28.

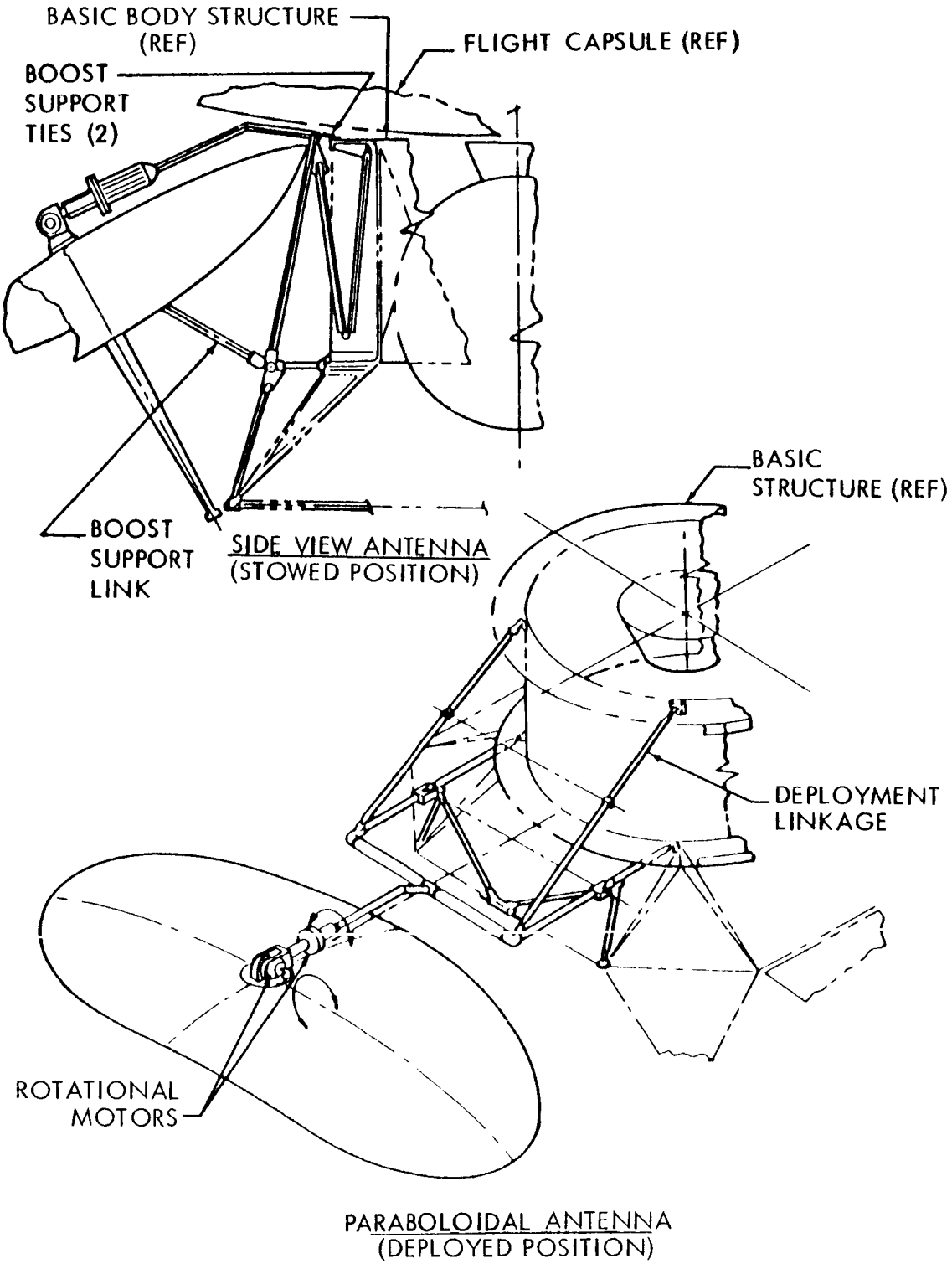

Figure 4.4-28: High-Tain Antenna Deployment and Pointing Mechanism

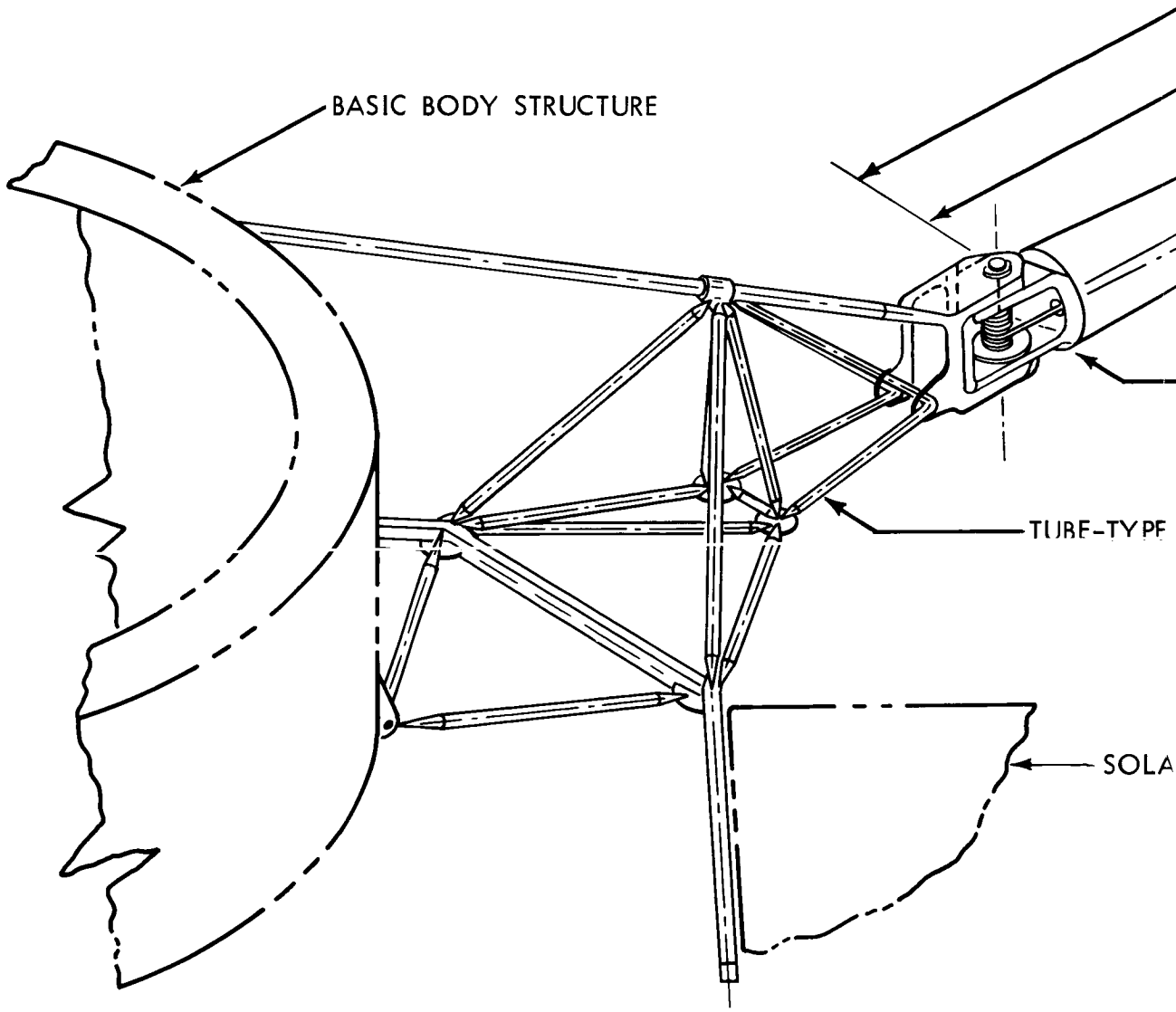
BASIC BODY STRUCTURE
TUBE-TYPE
SOLA

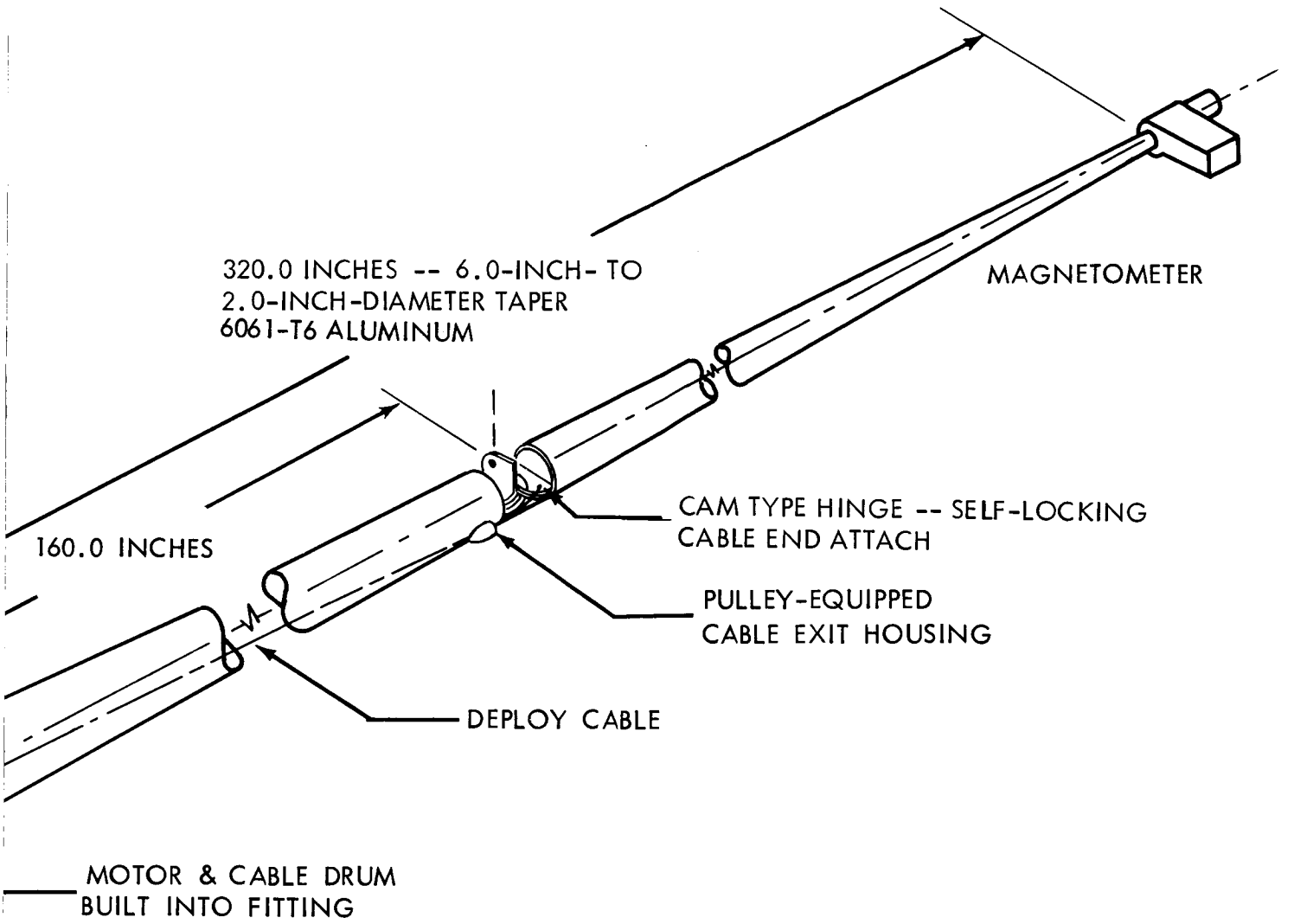

TRUSS

R PANELS (REF)

Figure 4.4-27: Magnetometer Boom Installation

Round tubing was used throughout this structure to obtain high stiffness and strength with limited depth. The arrangement of members was dictated by available clearances between the antenna and the science scan platform. All members are of titanium alloy. This material is most efficient for struts and gives maximum stiffness for members of limited depth. With this arrangement the antenna will not deflect more than 0.75 degree (± 0.75 degree) during firing of the orbit insertion engine.

4.4.3.3 Interface Definition

The major interfaces of the primary structure of the spacecraft consist of the four-point attachment to the Flight Capsule sterilization canister and the eight-point attachment to the Centaur adapter. A bolted field joint is used at the top of the spacecraft to connect the spacecraft adapter to the Flight Capsule sterilization canister. The adapter and canister are released from the spacecraft, after the launch of the Flight Capsule, by releasing a single tension band clamping four V-block clamps. A similar field joint and release system with eight clamps is used at the spacecraft-to-Centaur interface.

Two interfaces exist within the spacecraft primary structure. The first is the assembly joint between the equipment support structure and the lower support structure. This joint consists of four 5/8-inch diameter titanium bolts, acting in double shear. The second is the joint between the propulsion module and the equipment support structure. The propulsion module is attached with four 7/16-inch diameter titanium bolts.

Four solar-panel-to-Spacecraft interfaces exist at each solar panel. These consist of two hinge fittings, which are integral with the Centaur attach fittings, and two support-strut fittings, which are integral with the truss longeron at the top of the equipment support structure.

In addition, two interfaces exist at each antenna boom and at the magnetometer boom. These consist of the hinge and latch for each, and the latch for the boom-tip when stowed.

The equipment-to-primary-structure interface exists at the equipment support structure cylinder. Equipment modules are bolted to the vertical stiffeners of the cylinder. All cabling is attached to the inner and outer face of the cylinder. Thermal control louvers interface with the top and bottom frame of the equipment support structure.

4.4.3.4 Performance Parameters

The load-carrying structure weighs 250 pounds, and can support a 4500-pound capsule together with a 500-pound propulsion subsystem, or a 2300-pound capsule in conjunction with a 3500-pound propulsion subsystem. The primary structure carries a 250-pound science payload and 1500 pounds of nonstructural spacecraft weight.

Future electric power growth is provided by designing the solar panel support fittings to carry the loads imposed by an added solar panel section. Structural reliability is attained by efficient designs, requiring simple and direct construction processes, conservative dynamic magnification factors, and realistic safety factors on design

loads, redundant (multiple path) structural arrangements, proven stress analysis techniques, minimum guaranteed structural material mechanical properties, and the use of space-proven materials. Since sufficient statistical information is not available on structures exposed to the design environment to calculate reliability, the structural reliability of the primary structure is assumed to be 0.999 or the basis of history.

The meteoroid shielding around the equipment gives a no-penetration probability of 0.9914 for a 30-day orbit, and 0.960 for a 180-day orbit. Shielding around the propulsion module, as described in Section 4.4.3.2, produces a probability of no penetration of the propulsion system tankage of 0.997 during transit. During orbit, the hydrazine tanks will be empty. The probability of not penetrating the N_2 tanks in orbit exceeds 0.9999. Properties of the tank materials (annealed titanium) are such that if the tank is penetrated, the N_2 gas will leak out without an explosion.

4.4.3.5 Physical Characteristics

Weight--The weight of the structural subsystem is listed below. These weights include the primary structure, secondary structure, propulsion module structure, and meteoroid shielding.

Equipment Compartment		251.6
Compartment Cylindrical Shell	68.7	
Compartment Vertical Truss	20.2	
Upper Support Ring	15.3	
Lower Support Ring	46.1	

Lower Support Truss	101.3	
Secondary Support Structure		121.6
High-Gain Antenna Supports	2.0	
Low-Gain Antenna Supports	5.9	
VHF Antenna Supports	5.9	
Science Boom	23.1	
Science-Boom Supports	11.7	
Scan Platform	24.0	
Scan Platform Supports	8.7	
Solar-Panel Attach Structure	8.0	
Equipment Attach Structure	12.0	
Meteoroid Shielding	20.3	
Propulsion Compartment		124.6
Motor-Support Assembly	30.5	
Tank-Support Assembly	33.1	
Engine-Support Assembly	7.2	
Miscellaneous Supports and Fasteners	4.8	
Meteoroid Shielding	49.0	
		497.8

Accessibility, Maintainability, and Versatility--Complete accessibility to all propulsion and equipment is provided. Access to each equipment module is accomplished from the outside periphery of the equipment compartment by removing quick-disconnect insulation blankets and louvers. The insulation blanket is attached with mechanically interlocking tape. The louvers are attached by two quick-disconnect fasteners at the top and two shear pins at the bottom of each panel. The panel may be lifted

out after disconnecting the fasteners. Maintainability of the equipment is achieved by providing ample hand clearance for all electrical disconnects. After unbolting the attaching bolts, modules may be lifted from the compartment. Heavier equipment packages have inserts for handles. The truss design of the lower support structure provides access to the propulsion module. The orbit insertion engine can be removed from the spacecraft without removing the entire propulsion module. Similarly, each tank and midcourse engine can be removed independently from the spacecraft. Versatility, as applied to the spacecraft structure, refers to the adaptability to accept new equipment configurations. The modular concept of electronic packaging, attitude control, and propulsion subsystems provides versatility within the allowable strength of the support structure. Should heavier equipment be required for future missions, critical structure could be reinforced or replaced.

4.4.3.6 Safety Considerations

The propulsion and attitude control pressure vessels are primarily designed for personnel safety. High hazard factors and annealed titanium are combined to produce a tough structural design. Should an internal crack grow through the tank well after a long period of pressurization, there would be no explosive failure of the tank, only gas leakage.

Tanks will be assembled and pressurized in a hazardous-assembly area before installing the spacecraft on the Launch vehicle.

4.4.3.7 Development Testing Prior to July 1966

Minimum development testing is required for the structural subsystem.

Testing, confined largely to structural elements, will consist of:

1) Material properties tests

2) Structural element static tests

3) Joint heat conductance tests

4) Meteoroid penetration tests

Test data will be used to support the spacecraft structural design.

4.4.4 Mechanisms Subsystems

Voyager spacecraft mechanisms are categorized as (1) those that perform the function of deployment only; (2) those that perform the function of intermittent positioning or pointing; (3) those required to position louvers in response to thermal inputs; and (4) those required for separation. These mechanisms are located as shown in Figure 4.4-29.

The first category includes those mechanisms required for deploying the VHF antenna, the low-gain antenna, the high-gain antenna, the magnetometer boom, and the solar panels. The two antenna mechanisms involve simple deployment requiring a single hinging element that is rotated 135 degrees in the deployment cycle. Vinson actuators, which are essentially dashpot-snubbed springs, were selected as the deployment mechanisms for both because of their self-sufficiency and controllable rate of extension. Deployment of the high-gain antenna is accomplished by a combination of Vinson actuators, a torsion spring and a damper. The magnetometer boom is a two-section folded boom with parallel hinge axes. The inner and outer sections rotate 135 degrees and 180 degrees respectively, during the deployment cycle. The Vinson actuator was selected for deployment of the boom inner section, and a cable and fixed quadrant rotate the outer section into position. Locking is accomplished by driving spring-actuated tapered pins into matching tapered holes. The solar panels are discussed in Section 4.2 of this document.

Mechanisms in the second category are used to point the high-gain antenna and the planet-scan platform, and position the planet scan platform optics cover. A d.c. digital motor coupled with a harmonic drive was selected

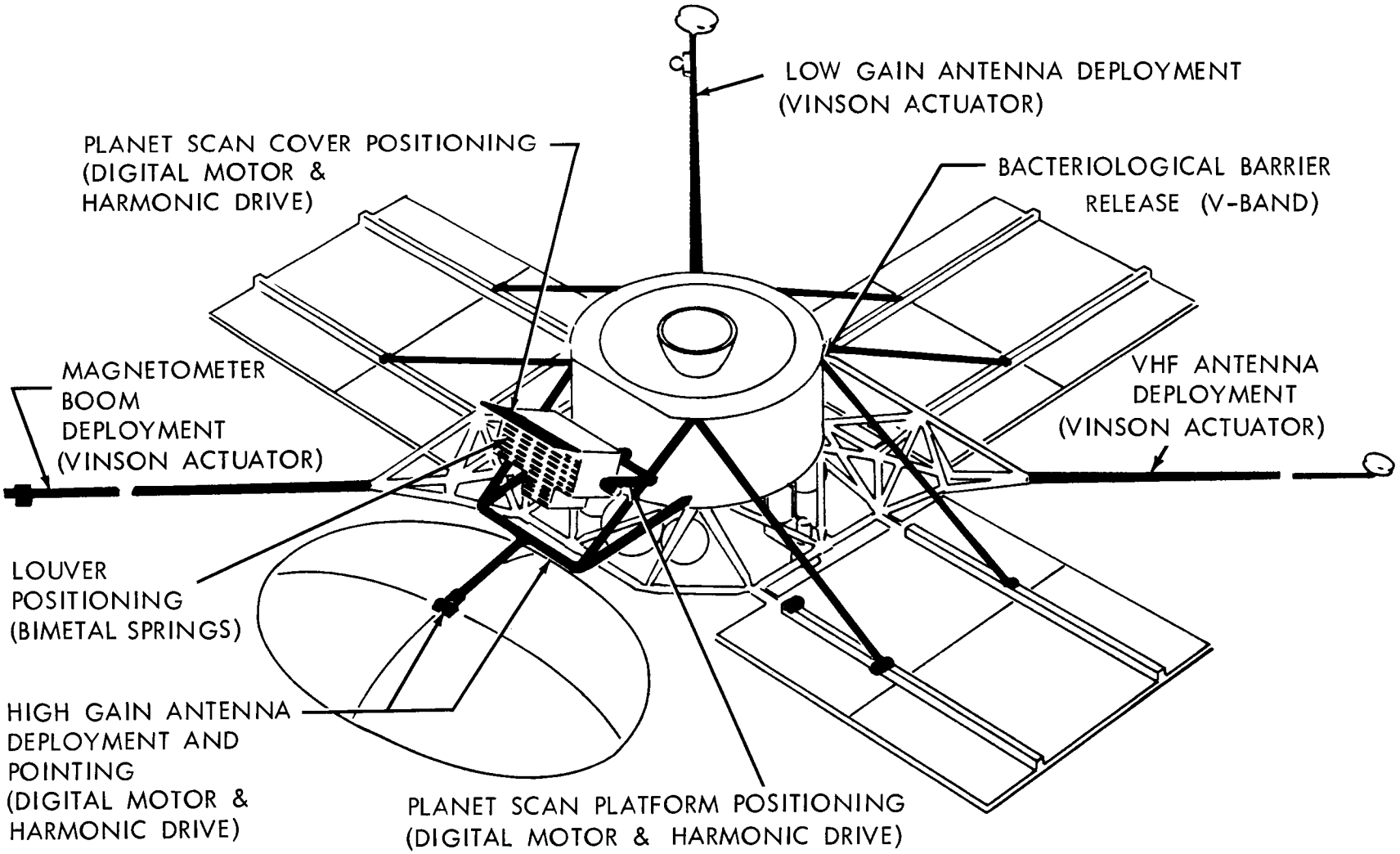

Figure 4.4-29: Mechanisms Subsystem

as the drive mechanism because of high reliability (0.99998), high gear ratio with no backlash, low friction loss, and capability for hermetic sealing. This drive mechanism is being used on the NASA Lunar Orbiter.

The temperature-sensing and louver control mechanism uses a bimetallic spring that was selected on the basis of its simplicity, light weight, and proven use on Mariner C.

The mechanism in the fourth category performs the function of releasing the portion of the sterilization canister that remains with the spacecraft after separation of the capsule. A V-band employing two pyrotechnic devices (each with dual igniters), was selected on the basis of low probability of failure (1×10^{-10}) in a synchronized release.

All mechanisms selected employ space-proven components but design conservatism requires that the large mechanisms for deployment and actuation of the high-gain antenna and planet-scan platform be tested before the development freeze date of July 1966.

4.4.4.1 Deployment Mechanisms for VHF-Omni Antenna Boom and Low-Gain-Antenna Booms

Applicable Documentation--Boeing Design Specification 10-72077, "Actuator, Linear, Spring Loaded, Hydraulically Damped," is applicable to the Vinson actuator mentioned in this section.

Functional Description--These mechanisms are required to rotate one-piece booms 135 degrees in a plane normal to the hinge axis. The booms are locked in their stowed positions by single retainer pins and released by a dual-squib pyrotechnic pin pullers. The booms are then deployed by Vinson actuators operating on bell cranks. The actuators are driven by helical coil springs and each incorporates an oil damper to control the deployment rate so as to prevent boom damage. Spring-actuated tapered pins rigidly lock the booms in their deployed positions and operate switches that generate telemetry signals when the booms are locked. The hinge axes incorporate rotary connectors that are parts of the coaxial lines leading to the antennas. The units weigh 3.05 pounds.

Interface Definition--The following interfaces are required for these mechanisms:

1) Two electrical impulses of 3 amperes each from two separate circuits must be supplied by the programmer to fire one dual-squib pin puller to release an antenna boom.
2) Two electrical leads to a boom lock position indicator suitable for signal voltages are required to signal telemetry that the boom is locked.

Performance--Oscillatory limitation is the only performance requirement affecting these mechanisms. The boom hinge and lock mechanisms will not contribute to the oscillatory frequency of the boom, thus they have no effect on performance parameters.

Safety Considerations--To prevent inadvertant firing of the boom squibs, the boom-release-pin pullers are protected by safety switches in the pyrotechnic firing circuit. The no-fire amperage of the pin-puller pyrotechnic squib is 2.0 amperes as defined in Section 4.4.5 of this document.

Test and Instrumentation--Testing is necessary to ensure that the boom will deploy when the hinge mount is subject to thermal distortion. When subjected to a load-producing distortion of the hinge axes equivalent to that predicted for maximum thermal distortion at the time of deployment in space, the mechanism shall demonstrate the ability to deploy and lock the antenna boom while the latter is supported in a simulated zero-g environment.

Other than the switch that indicates that the boom has been deployed and locked, no instrumentation is required.

4.4.4.2 Magnetometer-Boom Deployment Mechanism (Figure 4.4.4-25)

Functional Description--The mechanism rotates a two-section boom in a plane perpendicular to the two parallel hinge axes; the inner and outer boom sections rotate 135 degrees and 180 degrees respectively in the deployment cycle. The boom is locked in the stowed position by four retainer pins that are released by dual-squib pyrotechnic pin pullers. The inner section is deployed by a Vinson actuator, and the outer section is positioned simultaneously by a fixed quadrant and a static cable. The Vinson actuator controls the deployment rate to prevent damage to the boom.

Spring-actuated tapered pins rigidly lock the boom sections at the hinge joints when the sections reach their deployed positions and operate switches that signal the telemetry system when the boom is locked.

Interfaces--The interfaces required to support this mechanism are as follows:

1) Two electrical impulses of 5 amperes each from two separate circuits must be supplied by the programmer to fire four dual-squib pyrotechnic pin pullers.
2) Two electrical leads suitable for signal voltages connect to each of the two boom-lock-position indicators to indicate that the boom is locked.

Performance--The following performance requirements are applicable to this mechanism:

1) Rigidity of the boom hinge and lock mechanism shall be sufficient to produce no significant effect on the oscillatory frequency of the boom.
2) When properly supported and balanced to simulate a zero-g condition, the boom deployment mechanism will be able to repeatedly position the magnetometer mounting platform within 0.25 degree about any of three axes parallel to the spacecraft X, Y and Z axes.
3) When the spacecraft is not maneuvering or thrusting for ΔV correction, rotation of the magnetometer with respect to the X, Y, and Z axes due to beam deflection (during operation of the attitude control system) shall not exceed 0.75 degree.

Safety Considerations--To prevent inadvertant firing of the boom squibs, the boom-release-pin puller is protected by a safety switch in the pyrotechnic firing circuit. The no-fire amperage of the pyrotechnic squib in the pin-puller is 2.0 amperes as defined in Section 4.4.5.

Test and Instrumentation--Testing is necessary to ensure boom deployment when the hinge mount is subjected to thermal distortion. When subjected to a load-producing distortion of the hinge axes equivalent to that predicted for maximum thermal distortion at time of deployment in space, the mechanism shall demonstrate the ability to deploy and lock the antenna boom while the latter is supported in a simulated zero-g environment.

Other than the switches that indicate that the boom has been deployed and locked, no instrumentation is required.

4.4.4.3 Solar-Panel Deployment Mechanism

This mechanism is described in Section 4.2

4.4.4.4 High-Gain-Antenna Deployment and Pointing Mechanism

(Figure 4.4-30)

Functional Description--The paraboloidal antenna is stowed in the near-inverted position and locked in place by several retainer pins that anchor support links to the spacecraft structure. The pins are released by firing dual-squib pyrotechnic pin-pullers at each pin location. The antenna is then partially deployed by four Vinson actuators that drive the deployment links. Braking is integral with the actuators. The deployment

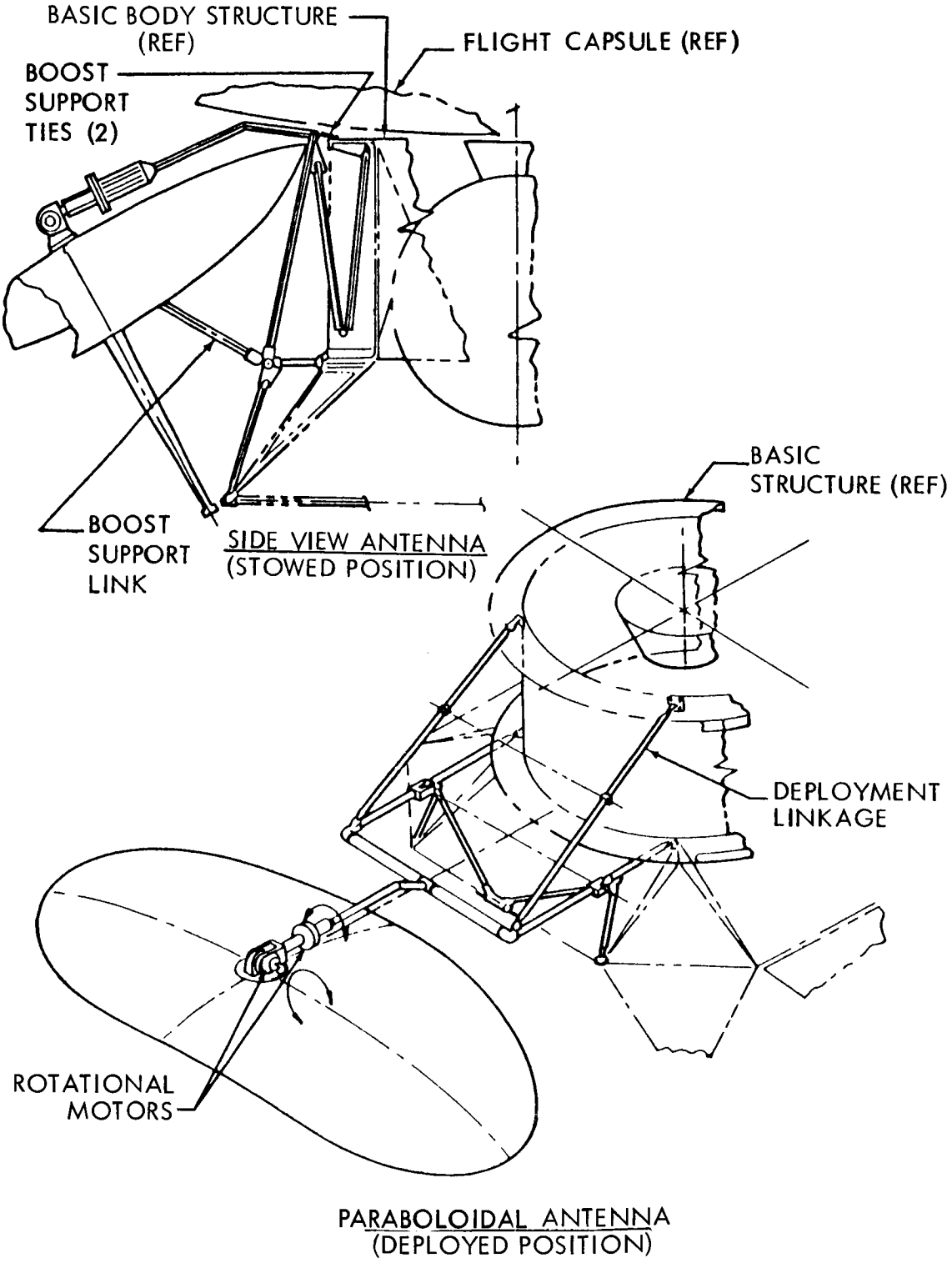

Figure 4.4-30: High-Gain Antenna Deployment and Pointing Mechanism

linkage is rigidly locked by spring-drive tapered pins. Deployment is completed by rotating the antenna support boom into position; this rotation is accomplished by the torsion spring and damper mechanism.

In the deployed position, one rotational axis of the antenna is parallel to the Y axis of the spacecraft. The reasons for selecting this orientation are discussed in detail in Section 4.1.9.

Both the deployment and scanning drive units employ stepping (digital) motors that have the advantages of: automatic internal locking ability to serve as incremental position encoders and no electrical power required during the holding phase. Their light weight (9 ounces) also influenced selection.

The harmonic drive unit was selected for the gearing head because it has the advantages of compactness, high reduction ratio with minimal gearing, low friction loss, and essentially zero backlash. A gear ratio of 205:1 was selected for the harmonic drive, and a 36 degree stepper increment for the digital motor. This combination permits driving the antenna about either axis in stepped increments of 0.175-degree, and produces a pointing error no greater than $\pm$5.3 seconds of arc. Under continuous stepping impulse, the motor will drive the antenna at speeds in excess of five times the rate of 0.2-degree per second required during spacecraft maneuvering periods.

The motor and drive are combined in one unit that is hermetically enclosed except for the harmonic gear spline which is designed for operation

in space environments. The combined unit contains a heater to keep the internal temperature within the range of -40 to +80 degrees F. The unit also houses pressure and temperature transducers that connect electrically to the telemetry circuit.

For rotation about its Y axis, the antenna rotates about the axis of a large-diameter tube that provides wide-span bearing support. Rotation about its X axis is provided by a single gimbal. In each case, sleeve bearings are mounted in spheres in order to give the bearing 2 degrees of freedom and prevent bearing drag or seizure due to thermal distortion of the bearing housing. This arrangement also provides bearing redundance, thus improving the total reliability. To achieve low friction and minimum deterioration, the bearing surfaces of both the sphere and its internal sleeve bearing will be made from teflon impregnated material.

Interface Definition--The following interfaces are required:

1) Connectors and cabling to transmit two electrical impulses of 5 amperes each to two different circuits from the programmer for firing four dual-squib pin pullers.
2) Four two-wire electrical connectors and cables are required for connecting the deploy-lock-position indicators to the telemetry system.
3) One four-wire electrical connector and cable is required for carrying power to each digital motor from the d.c. power supply.
4) One 13-wire electrical connector and cable is required for connecting the encoder to the programmer.
5) One four-wire electrical connector and cable is required to connect each temperature transducer (in each of two drive units) to the telemetry system.

6) One four-wire electrical connector and cable is required to connect each pressure transducer (in each of two drive units) to the telemetry system.

7) A two-wire electrical connector and cable is required to connect each thermal control heating element (in each of two drive units) to the d.c. power supply.

Performance--To meet the established spacecraft maneuvering rates and pointing accuracy requirements, the antenna deployment and pointing system must:

1) Rotate the antenna at rates in excess of 0.2-degree per second about each of two axes.

2) Position the antenna in increments less than 0.2-degree about each axis.

3) Position the antenna electrical axis within 0.1-degree of the spacecraft Z axis after the deployment cycle is completed.

Physical Characteristics--The following characteristics pertain to this mechanism:

1) Weight: 11.3 pounds (Drive mechanism only)

2) Power Requirements:

Positioning -- 50 watts d.c. power in 50-millisecond pulses at a maximum rate of 25 pulses per second to each antenna drive motor, but not simultaneously.

Temperature Control -- 1 watt of d.c. power for power supply drive unit heater element.

Safety Considerations--The only item for safety considerations is protection of the deployment release pin-puller. This is accomplished by a safety switch to the pyrotechnic firing circuit.

Test and Instrumentation--Testing is necessary to ensure that the antenna will deploy when the hinge mount is subjected to thermal distortion. When subjected to a load that produces distortion of the hinge axes equivalent to that predicted for maximum thermal distortion at time of deployment in space, the mechanism will demonstrate the ability to deploy and lock the antenna linkage in a simulated zero-g environment.

Tests will be conducted to demonstrate that the deployment mechanism will repeatedly position the antenna to meet the requirements of the performance parameters previously noted.

Other than the four switches which indicate that the antenna is deployed and locked, no instrumentation is required.

4.4.4.5 Planetary-Scan-Platform Positioning Mechanism
(Figure 4.4-31)

Functional Description--The scan platform consists of a science-instrument mounting plate that is driven by two electro-mechanical units about two perpendicular axes.

The science-instrument mounting plate is a flat bed measuring 25 by 33 inches designed to accommodate the science-instrument package defined in

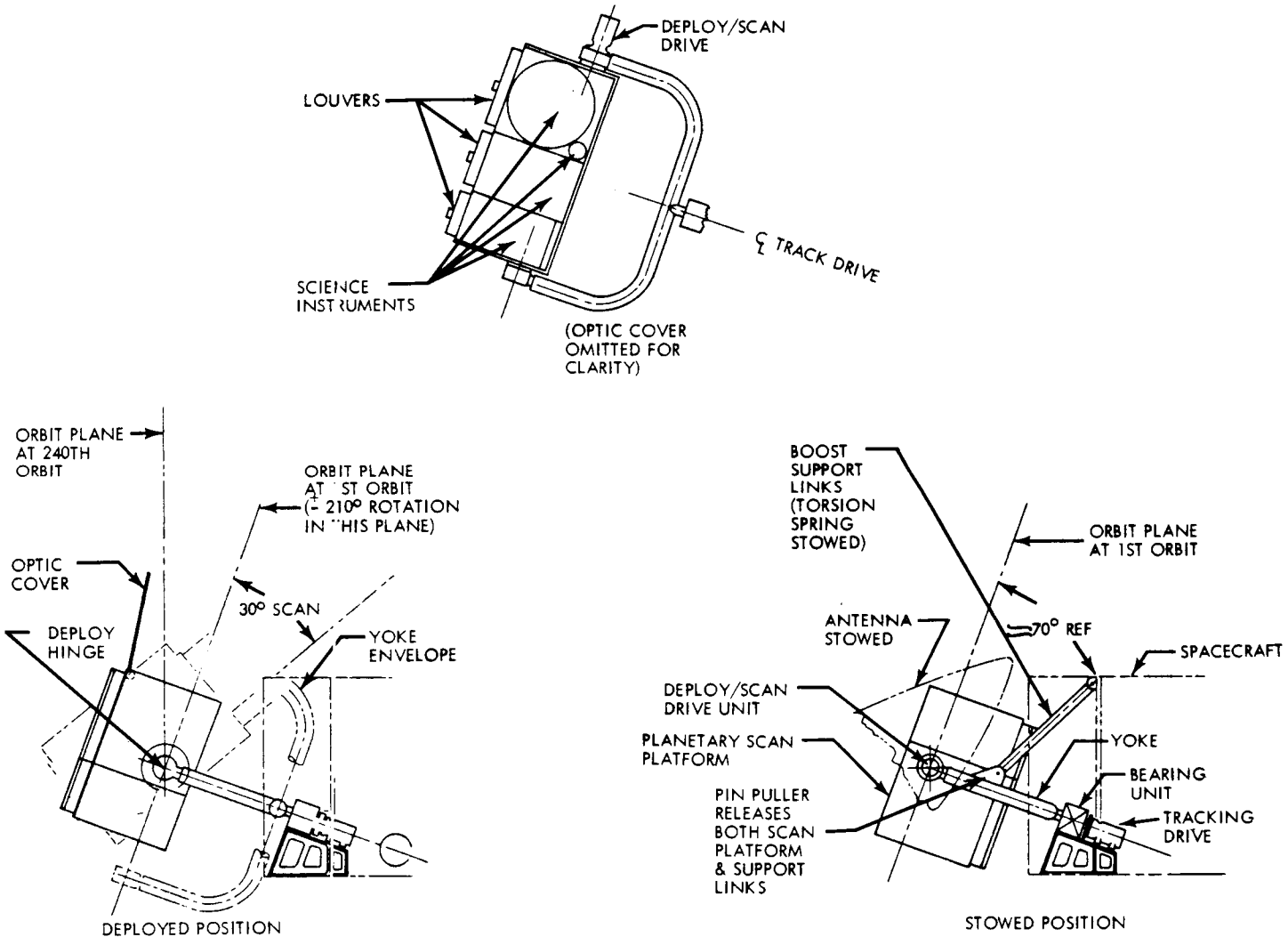

Figure 4.4-31 : PLANETARY-SCAN PLATFORM DEPLOYMENT AND POINTING MECHANISM

Section 4.5 of this document. The mounting plate functions as a radiator from which the heat emittance is controlled by a set of louvers mounted beneath the plate. The louver mechanism is described in Section 4.4.4.7. The platform is supported in a gimbal mount that permits scanning up to 30 degrees on each side of the orbit plane. The gimbal mount in turn rotates 360 degrees about its support post to permit pointing at any point in the orbit plane.

The science platform is supported in the stowed position by two links that attach to the spacecraft. Two locking pins attach the links to the gimbal mount. The locking pins also anchor the platform to the gimbal mount to provide support to the platform during boost. The locking pins are released by pyrotechnic pin pullers, and the platform is then free to rotate.

The platform is rotated 180 degrees about its scan axis for deployment into position for scanning along the track. The stowed position of the scan platform also permits rotating the platform 180 degrees about the tracking axis to position the platform in the plane of the initial orbit. This redundant mode of positioning permits deployment and tracking in the preselected orbit plane should the scanning drive unit become inoperable. However, no scanning or updating of the orbit plane position is possible in this redundant mode.

Rotation of the scan platform about the tracking axis has been restricted to $\pm$180 degrees (0 to -360 degrees from stowed position) to alleviate

problems associated with wire-bundle routing and flexing. The motion provides full pointing coverage in the orbit plane and simplifies the programming and position reporting problems.

The scanning and tracking drive units are of the same type selected for the high-gain antenna (Section 4.4.4.4), employing a digital motor coupled with a harmonic drive. To meet the more exacting requirements of the science instruments, however, a lower gear ratio is required. A gear ratio of 410:1 was chosen for the harmonic drive and combined with a 36-degree-increment stepper motor. This combination permits driving the scan platform about both the scan and tracking axes in increments of 0.088-degree per step, and produces a theoretical pointing error of only 2.65 minutes of arc.

The motor and drive unit are combined into one unit that is hermetically enclosed except for the harmonic gear spline that is designed for operation in space environments. The combined unit contains a heater element to keep the internal temperature within the range of -40 to +80°F. The unit also houses pressure and temperature transducers that connect electrically to the telemetry circuit.

For rotation about its track axis, the platform rotates about the axis of a large-diameter tube that provides wide-span bearing support. Rotation about the scan axis is provided by a single gimbal with its axis on the axial centerline of the track axis drive. In each case, sleeve-type bearings are mounted in spheres. This arrangement provides the bearing with 2 degrees of freedom and prevents bearing drag or seizure due to thermal distortion of the bearing housing. It also provides bearing redundancy,

thereby further improving the total reliability. The bearing surfaces of both the sphere and its internal sleeve bearing will be made of teflon impregnated material to achieve low friction and minimum deterioration.

Interface Definition--The following interfaces are required:

1) Connectors and cables to transmit four 5-ampere electrical impulses (two each from two different circuits) for firing two dual-squib pin-pullers.
2) One four-wire electrical connector and cable is required to carry power to each digital motor from the d.c. power supply.
3) One thirteen-wire connector and cable is required to connect the shaft transducer on each drive unit to both the programmer and the telemetry system.
4) One four-wire connector and cable is required to connect the temperature transducer in each drive unit to the telemetry system.
5) One four-wire connector and cable is required to connect the pressure transducer in each drive unit to the telemetry system.
6) One two-wire connector and cable is required to connect the thermal control heating element in each drive unit to d.c. power.

Performance--The drive unit will be capable of driving the scan platform in increments of 0.088 degree, $\pm$0.001 degree.

Physical Characteristics--The two significant physical characteristics are weight and power requirements:

1) Weight: 11.5 pounds not including the gimbal mount supporting the platform.

2) Power Requirements:

Positioning -- 50 watts of d.c. power in 50-millisecond pulses at a maximum rate of 25 pulses per second to each drive motor simultaneously.

Temperature Control -- 1 watt of d.c. power to provide temperature control in the drive unit.

Safety Considerations--The only item for safety consideration is protection of the deployment release pin puller. This is accomplished by a safety switch in the pyrotechnic firing circuit.

Test Instrumentation--Testing is required to ensure that the platform will operate when the platform mount is subjected to thermal distortion. When subjected to a load-producing distortion of the pivot axes equivalent to that predicted for maximum thermal distortion in space, the mechanism will demonstrate the ability to rotate the scan platform about both axes. The platform may be supported to simulate a zero-g condition during the test.

No special instrumentation is required for this mechanism.

4.4.4.6 Planetary-Scan-Optics Cover Mechanism

Functional Description--This mechanism consists of a one-piece cover that is rotated a minimum of 100 degrees against a stop to fully expose the science systems optics. The cover is rotated by a d.c. digital motor coupled to a harmonic-drive-type gearhead, both housed in a single hermatically sealed unit. Initially, the cover is locked in the closed position

by a mechanical detent that is integral with the stepper motor. Activation by the spacecraft programmer causes the motor to rotate the cover to the open position. The cover is positioned by having the programmer send the required number of pulses to the digital motor. The mechanical detent then retains the cover position.

A redundant mode of operation is incorporated by including torsion spring and pyrotechnic pin puller. The torsion spring is wound as the motor drives the cover closed. The pin puller disconnects the drive motor from the cover shaft, allowing the torsion spring to drive the cover to the open position should the motor become incapacitated.

Interfaces--The following interfaces are required:

1) Connectors and cables to transmit from the telemetry system two 5-ampere electrical impulses, (one each from two difference circuits) for firing the dual-squib pin-puller.
2) One four-wire electrical connector and cable is required to provide power to the digital motor from the d.c. power supply.
3) One two-wire electrical connector and cable is required for connecting the pressure transducer to the telemetry system.
4) One two-wire electrical connector and cable is required for connecting the temperature transducer to the telemetry system.
5) A two-wire connector and cable is required for connecting the position transducer in the motor to the programmer.
6) One two-wire electrical connector and cable is required for connecting the thermal control heating element in the drive motor to the d.c. power supply.

Performance--This mechanism shall have a reliability no less than 0.9999.

Physical Characteristics--The only significant physical characteristics of this mechanism are as follows:

1) Weight: 0.8 pounds

2) Power Requirements: Cover operation -- Approximately 15 watts of d.c. power for 5 seconds for each operation.
Temperature control-- 1 watt of d.c. power.

Safety Considerations--The only item for safety consideration is the protection of the cover-emergency-release-pin puller. This protection is provided by a safety switch in the pyrotechnic firing circuit.

4.4.4.7 Louver Operating Mechanism

Functional Description--Each louver blade is supported by a longitudinal shaft which in turn is supported by teflon bearings at each end. Differential expansion of a bimetallic spring attached to each shaft forces the blade to rotate. Individual response characteristics can be achieved in each louver by adjusting the spring position on each shaft. Further information appears in Section 4.4.1 of this document.

4.4.7.4 Interfaces

The only interfaces applicable to this mechanism are the various sources of heat discussed in Section 4.4.1 of this document.

Performance--The bimetallic-torsion-spring performance requirements are defined in Section 4.4.1 of this document.

Physical Characteristics and Constraints--Weight and volume are the only significant physical characteristics for this mechanism. Each spring weighs 0.025 pound and its installed volume is represented by a cylinder 1.5 inches in diameter and 0.25-inch deep.

Tests--The only tests considered necessary are those required to demonstrate that each louver blade satisfactorily responds to thermal inputs within its thermal operating envelope.

4.4.4.8 Capsule and Bacteriological Barrier Separation Mechanism

Functional Description--The capsule and integral bacteriological barrier are attached to the Spacecraft Bus by a tension band. The band is made in two halves that are bolted together when the band is attached. For release, dual-squib pyrotechnic cutters sever each band-half at its midpoint, thereby releasing the barrier. Separation velocity is imparted to the barrier by springs mounted at the attachment points. A switch actuated by departure of the barrier conveys this information to telemetry.

Interfaces--The interfaces include the following:

1) Connectors and cables for transmitting four 5-ampere electrical impulses (two each from two different circuits) for firing two dual-squib band cutters.
2) A two-wire electrical connector and cable is required to connect the separation indicator switch to the telemetry system.

Performance--To ensure separation of the capsule or the barrier, the release mechanism shall have a failure rate no greater than 1×10^{-10}.

Physical Characteristics--The only significant physical characteristic is the weight -- 3.2 pounds. This figure includes the separation devices, the separation springs, and their supports.

Safety Considerations--Safety considerations are limited to protection of the tension-band-cutter pyrotechnics. This is accomplished by a safety switch in the pyrotechnic firing circuit.

4.4.5 Pyrotechnic Subsystem

The pyrotechnic subsystem will provide individual programmed applications of spacecraft unregulated battery power for the purpose of initiating (firing) spacecraft pyrotechnic devices (squibs) and will provide protection against the inadvertent firing of those devices. Application of power is accomplished through the CC&S assembly as shown in Figure 4.4-32

The squibs are used for unlatching the mechanisms that deploy stowed articles, and for capsule-spacecraft separation, propulsion pressurization valve operation, solid-engine ignition, propulsion regulator valve actuation, liquid-propellant valve operation, TVC pressurization valve operation, and biological barrier removal.

The squibs are identified as a part of the particular subsystem in which they are installed. These devices are indicated in Figure 4.4-32 for reference purposes although they are not a part of the pyrotechnic subsystem. The function of controlling the application of power to the squibs including timing, sequencing, and fire command signals is performed by the central computer and sequencer (CC&S) subsystem control assembly (see Section 4.8). The functions of arming the pyrotechnic subsystem, inhibiting application of power, and the actual application of power to the squib bridgewires are performed by the pyrotechnic subsystem which is a portion of the CC&S switching assembly (see Section 4.8).

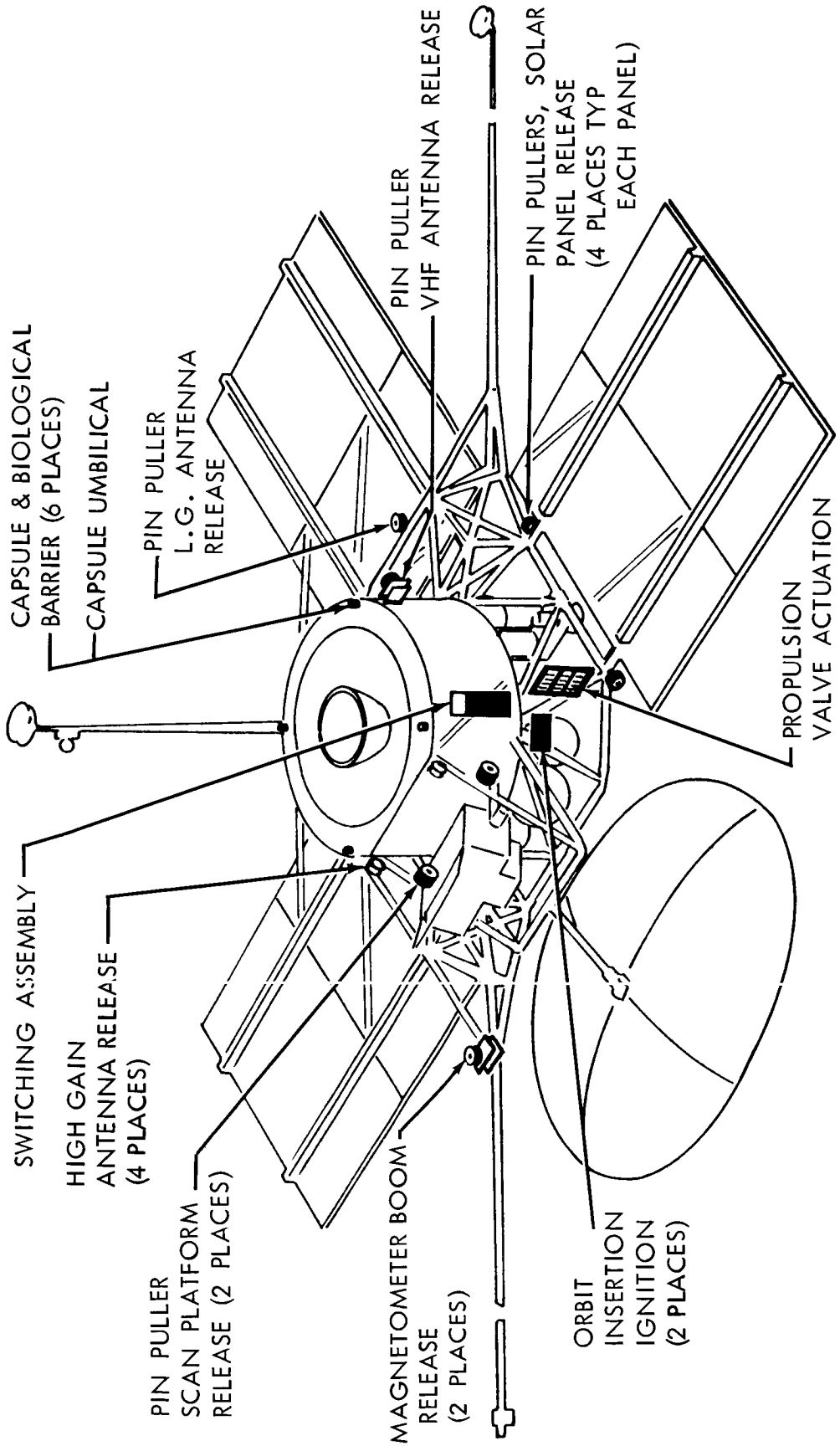

Figure 4.4-32: Pyrotechnics Subsystem

The major components of the pyrotechnic subsystem are an arming switch, a signal amplifier, inhibit switches, and power-transistor firing switches. The subsystem controls the firing of 114 separate bridgewires.

The CC&S switching assembly squib firing circuitry is identical in design to that of the NASA Lunar Orbiter and employs redundant, solid-state circuits. Arming of the subsystem is commanded and verified before launch through the umbilical connection. The electrical design requirements conform to the provisions of AFTRP 80-2, "General Range Safety Plan," Volume I.

Primary and first backup commands for firing the squibs are provided by the stored program of the CC&S control assembly. A second backup command, initiated on the ground, may be sent at any time via the telecommunications command link.

4.4.5.2 Applicable Document

AFTRP 80-2, "General Range Safety Plan," Volume 1.

4.4.5.3 Functional Description

The pyrotechnic subsystem functions include the boom, antenna, and science platform deployment; Capsule-spacecraft separation; propulsion pressurization valve operation; TVC system; pressurization valve operation; propellant valve operation; propulsion regulator selection; and biological barrier removal. A schematic diagram of the subsystem is shown in Figure 4.4-33.

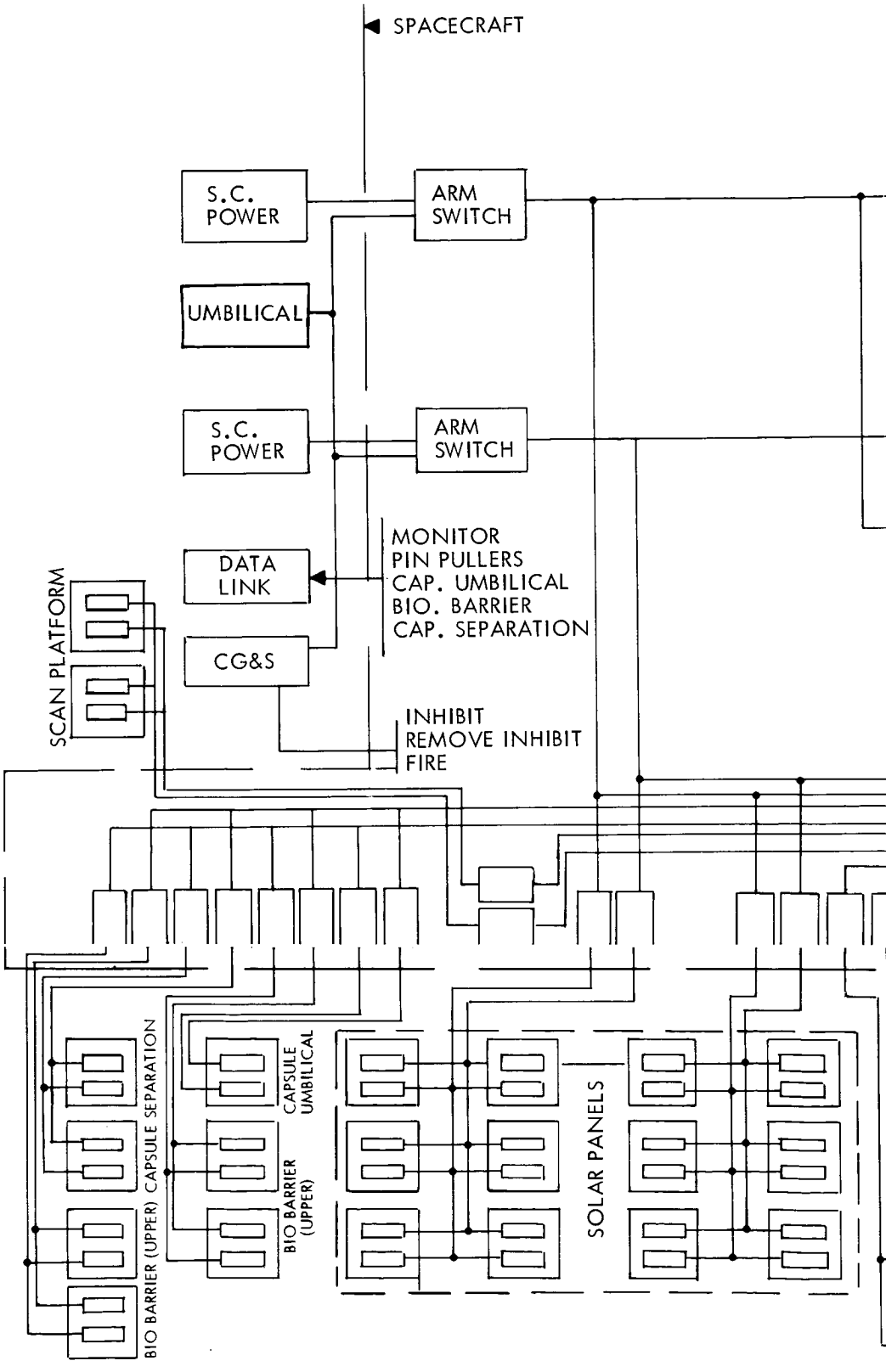
SPACECRAFT
S.C. POWER
ARM SWITCH
UMBILICAL
S.C. POWER
ARM SWITCH
MONITOR
PIN PULLERS
CAP. UMBILICAL
BIO. BARRIER
CAP. SEPARATION
DATA LINK
CG&S
INHIBIT
REMOVE INHIBIT
FIRE
SCAN PLATFORM
BIO BARRIER (UPPER)
CAPSULE SEPARATION
CAPSULE UMBILICAL
BIO BARRIER (UPPER)
SOLAR PANELS

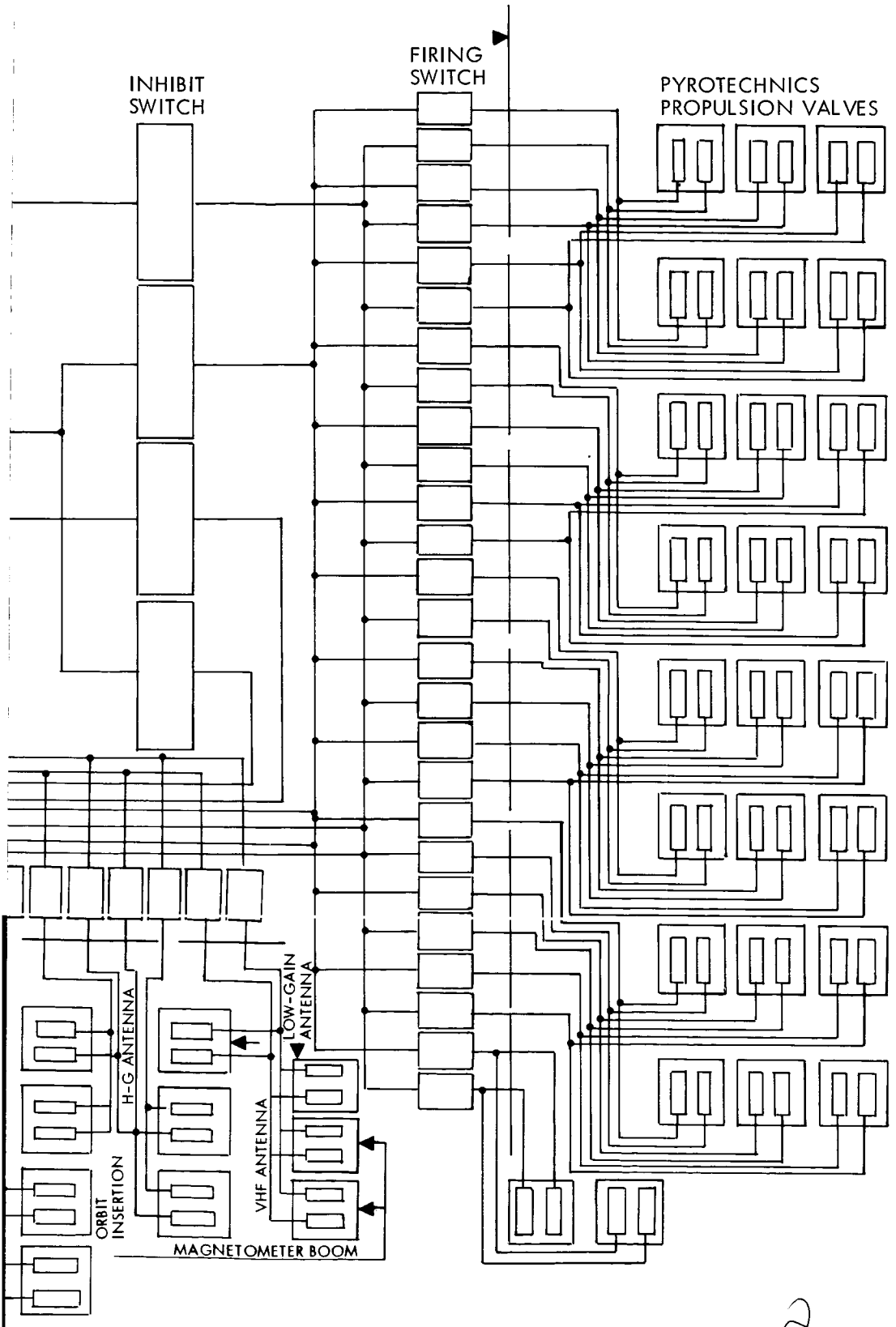

Figure 4.4-33: Functional Schematic — Pyrotechnic Subsystem

Power for the subsystem is supplied by the electrical Power Subsystem batteries. Signals to remove inhibit, fire, and add inhibit are provided by the CC&S subsystem. The squibs shall contain the following features in addition to the requirements of AFTRP 80-2:

1) All squibs will contain two bridgewires for redundancy, except that pin pullers may contain two one-bridgewire squibs.
2) All pyrotechnic devices will use one-piece bodies terminating in an integral connector shell.
3) All pyrotechnic devices will be capable of withstanding 1 ampere/1 watt for 5 minutes without firing or degrading performance. The 1 ampere/1 watt condition will be applied to both bridgewires simultaneously.
4) The pyrotechnic device will provide continuous shielding between firing-lead and device and shall ensure that the shield circuit is completed before contact is made with connector pins.
5) Exploding bridgewire devices will not be used.
6) Squibs will be nonrupturing and will provide positive gas containment.
7) Electrical system design will consider each squib as a dead short after firing.
8) Squibs installed in propulsion subsystem valves will be capable of performing the intended function after exposure to the combined space environments for a period of 1 year.

The CC&S subsystem will control pyrotechnic safety and, on command, will select and fire the proper squib.

The subsystem will be maintained in the safe condition by the arming switch until commanded (via the umbilical) into the armed condition before launch. The armed condition is verified through umbilical monitoring. Closure of the arming switch completes the circuit between the electrical power subsystem battery bus and the CC&S switching assembly. The CC&S switching assembly will then complete the squib-firing circuit upon stored commands, or backup real-time ground-originated commands, through the CC&S control assembly.

The propulsion subsystem, planet-scan platform and cover release, the capsule-spacecraft separation, and the capsule biological-barrier- release squibs used during the late stages of the mission are further protected by an inhibit switch. The inhibit switch must be activated before the closing of the solid-state firing switch to fire these pyrotechnic devices.

Latch Actuation -- Latch pyrotechnics are those used to release and actuate deployed articles after booster separation. The primary signal for firing latch pyrotechnics will be timed, originated, and sequenced by the CC&S with backup signals as required, first by the CC&S and then by ground command.

Input requirements are arming-switch actuation, CC&S actuation, spacecraft power, inhibit command, remove-inhibit command, and fire-pyrotechnics command. The output signals are firing signals to squibs and instumentation signals.

Command signals, inhibit switches, firing switches, electrical circuitry,

and the bridgewires in the squib are all redundant. Pin pullers may have additional redundancy by using two single-bridgewire squibs.

Inhibit Control -- The inhibit control is a latching relay for the mid-course engines, the orbit insertion engine, planet-scan platform and cover, and the capsule and capsule biological barrier separation squibs. It will be switched to the conductive state by the CC&S.

Firing Control - The power control consists of a solid-state switching transistor. It will be switched to the conductive state by the CC&S.

4.4.5.4 Interface Definition

Input Signals Required

1) Command(via umbilical)to activate arming switch before launch(CC&S).
2) Spacecraft unregulated battery power applied directly to the arming switch.
3) Stored command- and ground-originated command signals to actuate solar-panel latches as backup to the primary stored command.
4) Ground-originated command signal to actuate the low-gain- antenna boom latch as backup to stored command.
5) Ground-originated command signal to actuate the VHF-antenna boom latch as backup to the stored command.
6) Ground-originated command signal to actuate the magnetometer boom latches as backup to the stored command.
7) Ground-originated command signal to actuate high-gain-antenna latches

8) Ground-originated command signal to actuate scan-platform latches as backup to the stored command.

9) Command signal to remove propulsion inhibit for first midcourse engine start-stop series.

10) Command signal for first midcourse engine start.

11) Command signal for first midcourse engine stop.

12) Command signal for propulsion inhibit.

13) Command signal to remove propulsion inhibit for second midcourse engine start-stop series.

14) Command signal for second midcourse engine start.

15) Command signal for second midcourse engine stop.

16) Command signal for propulsion inhibit.

17) Command signal to remove propulsion inhibit for third midcourse engine start-stop series.

18) Command signal for third midcourse engine start.

19) Command signal for third midcourse engine stop.

20) Command signal for propulsion inhibit.

21) Command signal to remove propulsion inhibit for orbit insertion. sequence.

22) Command signal for orbit insertion TVC pressurization.

23) Command signal for propulsion inhibit.

24) Command signal to remove propulsion inhibit for orbit trim.

25) Command signal for orbit-trim-engine start.

26) Command signal for propulsion inhibit.

27) Command signal to remove propulsion inhibit for backup regulator selection.

28) Command signal to fire backup regulator selection.

29) Command signal for propulsion inhibit.

30) Command signal to remove propulsion inhibit for midcourse engine isolation.

31) Command signal for midcourse engine isolation.

32) Command signal for propulsion inhibit.

33) Command signal to remove capsule separation inhibit.

34) Command signal to fire capsule-spacecraft umbilical separation.

35) Command signal to fire upper-biological-barrier removal.

36) Command signal to fire capsule separation.

37) Command signal to fire lower-biological-barrier removal.

38) Command signal for separation inhibit.

Output Signals--Pyrotechnic firing signals will be provided to do each of the following:

1) First start midcourse engines (four circuits)

2) First stop midcourse engines (six circuits)

3) Second start midcourse engines (four circuits)

4) Second stop midcourse engines (six circuits)

5) Third start midcourse engines (four circuits)

6) Third stop midcourse engines (six circuits)

7) Fourth start midcourse engines (eight circuits)

8) Start orbit insertion TVC pressurization (4 circuits)

9) Ignite orbit insertion motor (four circuits)

10) Select backup regulator (six circuits)

11) Isolate midcourse engines (four circuits)

12) Fire magnetometer boom release (four circuits)

10) The minimum time between firing of two successive midcourse start-stop series is 1 minute.

11) The minimum time between the stop signal for any midcourse engine series and release of high-gain-antenna latches is 1 minute.

12) The minimum time between biological barrier removal and capsule separation is 1 minute.

13) The minimum time between capsule separation and planet-scan platform release is 1 day.

4.4.5.7 Safety

Safety of the subsystem and associated pyrotechnic components during assembly, checkout and prelaunch activities will be ensured by the arming switch and by connecting pyrotechnic devices as late as possible in the assembly using procedures and support equipment specifically approved for use with ordnance. All circuits will be designed in accordance with AFTRP 80-2, "General Range Safety Plan," Volume 1.

4.4.5.8 Testing

The Lunar Orbiter pyrotechnic subsystem will be fully qualified by July 1966. Since the preferred design is identical in concept to the Lunar Orbiter, no development testing will be required other than that identified for the CC&S in Section 4.8. This testing will include breadboard-circuit evaluation during Phase IB.

4.4.6 Mass Properties

4.4.6.1 Summary Weight Statement and Weight Allocations

	Allocated Weights	Current Weights
Spacecraft Bus		
Spacecraft Telecommunications	207	207
Attitude Reference Subsystem	51	51
Autopilot Subsystem	11	11
Reaction Control Subsystem	212	212
Central Computer & Sequencer Subsystem	58	58
Electric Power Subsystem	457	457
Spacecraft Structure Subsystem	373	373
Spacecraft Mechanisms Subsystem	59	59
Temperature Control Subsystem	36	36
Pyrotechnic Subsystem	(incl. in CC&S)	
Instl. Cables/Harness Assemblies	100	100
Weight Contingency--Bus	--	186
TOTAL SPACECRAFT BUS	1564	1750
Spacecraft Propulsion Installation		
Midcourse Correction Prop. Subsystem	(508)	(508)
Rocket Engine System	22	22
Propellant System Inerts	75	75
Pressurization Plumbing	16	16
Hydrazine--Usable	395	395
Orbit-Insertion-Prop. System	(2686)	(2686)
Rocket Engine, Solid--Inerts	272	272
Thrust Vector Control Unit	108	108
Solid Propellant--Usable	2306	2306
Spacecraft Struct--Prop. Inst	(125)	(125)
Temperature Control--Prop. Inst	(71)	(71)
Inst. Cables/Harness--Prop. Inst	(10)	(10)
Weight Contingency--Prop. Inst	(--)	(100)
Contingency	--	62
Contingency--Fiberglass-to-Ti Eng Case	--	38
TOTAL PROPULSION INSTALLATION	3400	3500
Spacecraft Science Payload		
Science Payload Instrumentation	195	195
Science Payload--Data Automation	55	55
TOTAL SCIENCE PAYLOAD	250	250
Flight Capsule System	2300	2300
Separated Planetary Vehicle	7514	7800

NOTE: For detail weights refer to Section 3.4.

CONTENTS

4.5 SPACE SCIENCE

4.5.1 Scope

The orderly improvement of knowledge in science and technology is the primary purpose of the Voyager Program. Therefore, the Flight Spacecraft carries into an orbit around Mars a complement of scientific experiments embodied in 250 pounds of instruments and data automation equipment (DAE). The Science Payload will be designed to perform the functions highlighted on the accompanying Mission Sequences Matrix.

Definition of the Science payload and DAE for Voyager will be the responsibility of JPL and NASA Headquarters. The flight hardware will be provided as GFE to the spacecraft contractor. Thus, a detailed examination of the Science payload was properly excluded from this contract. However, in order to understand the impact of the Science payload on the rest of the spacecraft and its subsystems, many proposed experiments have been investigated and their interfaces have been defined. A specific group of experiments has been chosen as a "representative payload". As an indication of the detailed examination performed on each of these experiments, a typical experiment (mapping) has been chosen and is discussed to show items which must be considered in the experiment/spacecraft trade-offs and interfaces. The Science Payload will be designed to perform the functions highlighted on the accompanying Mission Sequences matrix.

Figure 4.5-1 shows typical possible instrument locations in the current preferred spacecraft design. In addition to transporting the Science Payload, the spacecraft provides it with 100 watts of power; orientation and stability as reported by the autopilot; attitude control and scan-platform engineering data; and, most important, transmission of the scientific data (up to 50,000 bits per second).

	1.0 PRELAUNCH AT ETR	2.0 LAUNCH & INJECTION (INCLUDES COUNTDOWN)
GROUND COMPLEX (MOS, LOS, & DSN)	OPERATIONAL READINESS TEST, S/C-DSN COMPATIBILITY TEST SCHED & COORD ETR ACTIVITIES C/O & SUPPORT MOS (DSN ONLY) LOAD CC&S WITH FLIGHT PROGRAM	MOS/LOS A) COMMAND LIFTOFF B) TRACK VEHICLE DURING BOOST C) SUPPLY FLIGHT COMMANDS (AS REQ) D) RECEIVE & ANALYZE DATA FROM S/C & BOOSTER DSN E) STANDBY ON ALERT F) COMMUNICATE WITH ETR CHANGE FROM MOS/LOS ON INJECTION INTO TRA A) PROVIDE SFOF/DS IF DSN SEARCH DATA B) RECEIVE ANTENNA S C) SEARCH FOR & ACQ D) ESTABLISH & VERIF E) TRACK S/C (1-WAY) F) RECEIVE & ANALYZE
SPACECRAFT TELECOMMUNICATIONS	SUBSYSTEM C/O & STATUS MONITORING	A) TRANSMIT ENGINEERING DATA VIA CENTAUR TELEMETRY B) TRANSMIT ENGINEERING DATA VIA LOW POWER LAUNCH EXCITER C) RECEIVE POWER FROM F/P
CENTRAL COMPUTER & SEQUENCER (CC&S)	A) SUBSYSTEM C/O & STATUS B) COMMAND OTHER SUBSYSTEMS FOR C/O & STATUS MONITORING C) READY ALL SUBSYSTEMS FOR LAUNCH D) LOAD CC&S WITH FLIGHT PROGRAM	PROVIDE BACKUP COMMANDS AS REQUIRED
ATTITUDE REFERENCE SUBSYSTEM AUTOPILOT SUBSYSTEM REACTION CONTROL SUBSYSTEM (RCS)	SUBSYSTEM C/O & STATUS MONITORING	A) ATTITUDE REFERENCE — GYROS OFF DURING LAUNCH B) AUTOPILOT — OFF C) RCS — OFF
MIDCOURSE CORRECTION PROPULSION SYSTEM ORBIT INJECTION PROPULSION SYSTEM	SUBSYSTEM C/O & STATUS MONITORING	
ELECTRICAL POWER SUBSYSTEM	SUBSYSTEM C/O & STATUS MONITORING	A) PROVIDE ENGRG DATA FOR TELECOMUNICATIONS SUBSYSTEM B) PROVIDE BATTERY POWER TO: • TELECOMMUNICATIONS SUBSYSTEM • CC&S • ATTITUDE REFERENCE SUBSYSTEM • AUTOPILOT SUBSYSTEM
S/C STRUCTURE SUBSYSTEM S/C MECHANISMS SUBSYSTEM INSTALLATION CABLES & TUBING	SUBSYSTEM C/O & STATUS MONITORING	A) PROVIDE PHYSICAL SUPPORT FOR ALL EQUIPMENT B) PROVIDE ATTACHMENT FOR CAPSULE C) SUPPORT FLT CAPSULE
TEMPERATURE CONTROL SUBSYSTEM	SUBSYSTEM C/O & STATUS MONITORING SPACECRAFT COOLING SUPPLIED BY CENTAUR	A) PROVIDE HEAT SINK COOLING CAPABILITY UP TO SHROUD JETTISON B) TEMPERATURE CONTROL AFTER SHROUD JETTISON
PYROTECHNIC SUBSYSTEM	SUBSYSTEM C/O & STATUS MONITORING	
SCIENCE EXPERIMENTS (GFE)	SUBSYSTEM C/O & STATUS MONITORING S/C MAGNETIC MAPPING (FAT)	
DATA AUTOMATION EQUIPMENT (GFE)		

REPEAT UP

) DSN CONTROL MARS ORBIT ITH ANTENNA IRCH DATA RE S/C CONTROL OF S/C NGRG DATA	DSN A) MONITOR BOOSTER SEPARATION B) MONITOR SOLAR PANEL DEPLOYMENT C) MONITOR ANTENNA DEPLOYMENT D) PROVIDE COMMANDS TO BACK UP CC&S AS REQUIRED E) TRACK S/C F) REC DATA G) MONITOR SCIENCE DEPLOYMENT DSN H) MONITOR & VERIFY ACQUISITION OF SUN I) MONITOR & VERIFY ACQUISITION OF CANOPUS J) COMMAND REACQUISITION OF CANOPUS (AS REQD) K) MONITOR S/C TRAJECTORY L) UPDATE CC&S TRAJECTORY PARAMETERS FOR PITCH, YAW, & ROLL M) COMPUTE CC&S PITCH, YAW, & ROLL POLARITY	DSN A) TRACK S/C B) RECEIVE & DISPLAY SCIENCE & ENGINEERING DATA C) MONITOR S/C & CAPSULE STATUS D) PROCESS DATA ON EARTH TO OBTAIN GUIDANCE COMMANDS (STORED COMMANDS & START TIMES)
	A) TRANSMIT ENGINEERING DATA B) RECEIVE POWER FROM E/P C) RECEIVE VIA LOW-POWER LAUNCH EXCITER DETECT & SEND TO CC&S COMMAND SIGNALS FROM EARTH D) TRANSMIT CELESTIAL REFERENCE ACQUISITION TO DSN E) TRANSMIT VERIFICATION OF DEPLOYMENT OF SOLAR PANELS, ANTENNAS, ETC TO EARTH F) TWO-WAY TRACKING	A) TRANSMIT ENGINEERING & SCIENCE DATA VIA DATA MODE NO. 2 (OPTIONAL MODE NO. 3) B) TRANSMIT CAPSULE ENGINEERING DATA C) TRANSMIT CONE-ANGLE SETTINGS (CANOPUS TO EARTH) D) EXERCISE & CALIBRATE HIGH-GAIN ANTENNA T + 40 DAYS E) SWITCH FROM LOW-GAIN TO HIGH-GAIN ANTENNA T + 80 DAYS F) PROVIDE RANGING SIGNAL TO A MAX. RANGE OF 8.0×10^6 KM (NOMINAL) G) SWITCH TRANSMISSION FROM LAUNCH EXCITER TO TWT POWER AMPLIFIER AND DATA MODE NO. 2
	A) COMMAND SIGNALS TO PYROTECHNICS & MECH TO DEPLOY • SOLAR PANELS • HIGH-GAIN ANTENNA • VHF ANTENNA • LOW-GAIN ANTENNA • SCIENCE BOOM B) SWITCH ON GYROS & SELECT MODES C) ENABLE SUN-SENSOR ROLL AND PITCH CONTROL D) RECEIVE SUN PRESENCE SIGNAL E) TURN ON CANOPUS TRACKER F) SWITCH ROLL CONTROL TO CANOPUS SENSOR G) ACTIVATE MAGNETOMETER (CALIBRATION ROLL) H) RECEIVE CANOPUS PRESENCE OUTPUT SIGNAL I) TRANSMIT VERIFICATION TO TELE-COMMUNICATION SUBSYSTEM (CANOPUS & SUN PRESENCE) J) PERFORM COMMAND FUNCTIONS FOR CANOPUS OVERRIDE AS REQUIRED K) BACKUP COMMANDS AS REQUIRED	A) COMMAND TELECOMMUNICATION TO DATA MODE NO. 2 B) COMMAND CRUISE SCIENCE ON (WARMUP) — SCIENCE INSTRUMENTS C) COMMAND DATA RECORDERS ON D) COMMAND TWTA ON E) SWITCH CANOPUS ANGLE AS REQUIRED F) INITIATE CRUISE SCIENCE DATA ACQUISITION G) COMMAND TELECOMMUNICATION CHANGE FROM OMNI TO HIGH-GAIN ANTENNA H) UPDATE HIGH-GAIN ANTENNA POSITION (AS REQUIRED) I) COMMAND TELECOMMUNICATIONS — CHANGE DATA TRANSMISSION RATES J) COMMAND RECALIBRATION OF SCIENCE ELEMENTS AS REQUIRED K) BACKUP COMMANDS AS REQUIRED
	A) RECEIVE CC&S COMMAND SWITCH ON GYROS, RCS, & AUTOPILOT B) DAMP ROTATION C) YAW & PITCH SPACECRAFT TO ACQUIRE SUN D) RELAY SUN ACQUISITION SIGNAL TO CC&S E) TURN ON CANOPUS SENSOR, ROLL 360 TO CALIBRATE MAGNETOMETER F) ROLL TO ACQUIRE CANOPUS & PROVIDE STAR MAP G) RELAY ACQUISITION SIGNAL (CANOPUS) TO CC&S H) PERFORM CANOPUS OVERRIDE ROLL MANEUVER AS REQUIRED	A) UPDATE CANOPUS CONE ANGLE ON COMMAND B) SWITCH AUTOPILOT TO CRUISE MODE C) MAINTAIN S/C ATTITUDE TO CELESTIAL REFERENCES DURING CRUISE
	A) PROVIDE POWER TO PYROTECHNIC SUBSYSTEMS FOR SQUIB FIRINGS B) PROVIDE POWER TO MECHANISMS C) ACTIVATE SOLAR POWER SYSTEM AFTER SUN ACQUISITION (AUTOMATIC) D) TRANSMIT "VOLTAGE SATISFACTORY" SIGNAL TO CC&S E) PROVIDE POWER TO: • TELEMETRY • CC&S • TEMPERATURE CONTROL • AUTOPILOT	A) PROVIDE CONDITIONED SOLAR ELECTRICAL POWER TO: • TELEMETRY • CAPSULE • CC&S • ATTITUDE REF • AUTOPILOT • TEMPERATURE CONTROL • SCIENCE B) CHARGE BATTERIES
	A) PROVIDE PHYSICAL SUPPORT FOR ALL EQUIPMENT B) DRIVE SOLAR PANELS TO LIMIT STOPS C) PROVIDE OUT & LOCK SIGNALS TO TELEMETRY D) DRIVE HIGH-GAIN ANTENNA TO OPERATING POSITION & LOCK E) DRIVE VHF & OMNI ANTENNAS TO OPERATING POSITION & LOCK F) DRIVE MAGNETOMETER BOOM TO OPERATING POSITION & LOCK G) SUPPORT FLT CAPSULE	A) SUPPORT S/C ASSEMBLIES B) SUPPORT S/C COMPONENTS C) MAINTAIN ADEQUATE ALIGNMENT BETWEEN COMPONENTS D) PROVIDE ACCEPTABLE STATIC & DYNAMIC LOAD ENVIRONMENTS E) SUPPORT FLIGHT CAPSULE
	PROVIDE TEMPERATURE CONTROL	PROVIDE TEMPERATURE CONTROL
	RECEIVE SQUIB FIRING SIGNALS FOR DEPLOYMENT OF: • SOLAR PANEL • MAGNETOMETER BOOM • LOW-GAIN ANTENNA • HIGH-GAIN ANTENNA • VHF ANTENNA	
	A) CALIBRATE MAGNETOMETER DURING S/C ROLL B) CALIBRATE OTHER SCIENCE INSTR AS REQUIRED	A) RECEIVE CRUISE SCIENCE "ON" COMMAND B) ACQUIRE CRUISE SCIENCE DATA C) TRANSFER CONDITIONED DATA TO DAE D) RECEIVE POWER FROM E/P E) RECALIBRATE SCIENCE EXPERIMENTS AS REQUIRED
		A) RECEIVE DAE "ON" COMMAND B) PROCESS & TRANSFER DATA TO TM

0 FOUR TIMES

7.0 FLIGH
TRAJE
DEFLE

5.0 INTERPLANETARY TRAJECTORY CORRECTION

6.0 S/C CAPSULE SEPARATION

I) PROVIDE ROLL TURN MAGNITUDE & DIRECTION J) PROVIDE YAW TURN MAGNITUDE & DIRECTION K) PROVIDE MIDCOURSE MOTOR BURN DURATION AND ΔV L) PROVIDE INITIATE MANEUVER SEQUENCE COMMAND M) RECEIVE VERIFICATION OF CORRECTION MANEUVER • DEGREES OF YAW & ROLL • THRUST DURATION • REACQUISITION OF CELESTIAL REFERENCES N) TRACK SPACECRAFT	A) INITIATE PRESEPARATION SEQUENCE B) RECEIVE CAPSULE STATUS DATA C) COMMAND SEPARATION D) VERIFY CAPSULE PROGRAM E) VERIFY SEPARATION F) TRACK CAPSULE & SPACECRAFT	A) TRANSMIT OF • ROLL MAGI • YAW MAGN • MOTOR BU B) TRACK FLIGH C) RECEIVE, RE D) PROVIDE CO
A) RECEIVE ROLL & YAW TURN COMMAND & RELAY TO CC&S B) RECEIVE ANTENNA POSITIONING DATA & RELAY TO CC&S C) RECEIVE MOTOR BURN DURATION AND & ΔV RELAY TO CC&S D) RECEIVE INITIATE MANEUVER COMMAND & RELAY TO CC&S E) SWITCH TO DATA MODE NO. 1 (FOR LATE MIDCOURSE MANEUVERS) F) RELAY VERIFICATION OF CORRECTION MANEUVER TO DSN G) STORE AND/OR TRANSMIT ENGINEERING DATA TO DSN (MODE 3) TRANSMIT ENGINEERING (SPACECRAFT & CAPSULE) + CRUISE SCIENCE TO DSN (MODE 2)	A) RECEIVE PRESEPARATION SEQUENCE COMMANDS & RELAY TO CC&S B) SWITCH TO DATA MODE NO. 2 C) TRANSMIT CAPSULE ENGRG DATA TO DSN D) RECEIVE SEPARATION COMMAND FROM DSN & ROUTE TO CC&S E) STORE AND/OR TRANSMIT ENGINEERING DATA TO DSN (MODE 3) TRANSMIT ENGINEERING (SPACECRAFT & CAPSULE) + CRUISE SCIENCE TO DSN (MODE 2)	A) RECEIVE ROL TO CC&S B) RECEIVE ANT C) RECEIVE MOT D) RECEIVE CAP E) TRANSMIT FL SCIENCE DAT
A) COMMAND TELECOMMUNICATION TO DATA MODE NO. 1 B) RECEIVE TRAJECTORY CORRECTION PARAMETERS C) SWITCH GYROS TO RATE CONTROL D) COMMAND ANGULAR MANEUVER E) RECEIVE GYRO SIGNALS & SUM FOR ANGULAR MANEUVERS F) SWITCH ATTITUDE REFERENCE TO AUTOPILOT SUBSYSTEM G) ARM PROPULSION SYSTEM H) PROVIDE COMMAND TO INITIATE ATTITUDE MANEUVER & ΔV MANEUVER I) RECEIVE ACCELEROMETER SIGNALS & INTEGRATE FOR ΔV MANEUVER J) DISARM PROPULSION SYSTEM K) COMMAND REVERSE ANGULAR MANEUVER L) COMMAND REACQUIRE CELESTIAL REFERENCES M) COMMAND AUTOPILOT SELECTION CONTROL N) BACKUP COMMANDS AS REQUIRED	A) LOAD CAPSULE WITH 5 OR MORE COMMANDS B) COMMAND CAPSULE SEQUENCING C) COMMAND TELECOMM SWITCH TO DATA MODE NO. 1 D) COMMAND GYROS ACTIVATE (CAPSULE) E) COMMAND GYROS ESTABLISH POLARITY (CAPSULE) F) COMMAND GYROS TO ATTITUDE CONTROL MODE (CAPSULE) G) COMMAND DATA TAPE RECORDER OFF H) COMMAND CAPSULE ACTIVATE ENTRY SCIENCE I) COMMAND CAPSULE ACTIVATE TELE-COMM & VERIFY RADIO LINK (VHF) J) SELECT T/M MODE FOR TRANSMISSION OF CAPSULE DATA K) COMMAND: BIOBARRIER SEPARATION S/C ORIENT TO SEPARATION ATTITUDE ELECTRICAL CONNECTION SEPARATION VERIFY SEPARATION L) COMMAND REORIENT S/C & REACQUIRE CELESTIAL REFERENCES M) BACKUP COMMANDS AS REQUIRED N) RECEIVE S/C ORIENTATION PARAMETERS	A) COMMAND S B) COMMAND C C) COMMAND A D) RECEIVE ORI E) PROVIDE SI (CRUISE SC F) SWITCH ON RECEIVE CA G) BACKUP CO
A) SWITCH TO GYRO CONTROL B) ROLL S/C AND VERIFY C) YAW S/C AND VERIFY D) AUTOPILOT — PROVIDE COMMAND TO TVC DURING MOTOR BURN E) TURN ON ACCELEROMETERS F) PROVIDE ACCELERATION DATA TO CC&S G) TURN OFF ACCELEROMETER H) YAW BACK TO ORIGINAL ATTITUDE & VERIFY I) REACQUIRE SUN (FINE SUN SENSOR) & VERIFY J) ROLL TO ORIGINAL ATTITUDE K) LOCK ON CANOPUS & VERIFY L) SWITCH AUTOPILOT FROM GYRO CONTROL TO CELESTIAL REF CONTROL	A) SWITCH TO GYRO CONTROL B) PERFORM ROLL TURN & VERIFY C) PERFORM YAW TURN & VERIFY D) MAINTAIN ATTITUDE DURING SEPARATION E) PERFORM YAW TURN (INVERSE TO C) & VERIFY F) PERFORM ROLL TURN (INVERSE TO B) & VERIFY G) REACQUIRE CELESTIAL REFERENCES H) RETURN TO CELESTIAL REFERENCE ATTITUDE CONTROL MODE	A) UPDATE CAN B) SWITCH AU C) MAINTAIN
MIDCOURSE PROPULSION SYSTEM A) ARM PRESSURIZATION SYSTEM (FIRE SQUIB VALVE) B) ARM PROPELLANT FEED SUBSYSTEM (FIRE SQUIB VALVE) C) FIRE PROGRAMMED ENGINES (OPERATE SOLENOID VALVE) D) SHUT DOWN ENGINE E) ISOLATE PROPELLANT FEED SUBSYSTEM F) ISOLATE PRESSURIZATION SUBSYSTEM		
A) PROVIDE CONDITIONED SOLAR OR BATTERY POWER TO: • TELEMETRY • CC&S • AUTOPILOT • ATTITUDE REFERENCE • REACTION CONTROL • PROPULSION • TEMPERATURE CONTROL • PYROTECHNICS • CAPSULE	A) PROVIDE CONDITIONED SOLAR OR BATTERY POWER TO: • T/M • CC&S • AUTOPILOT • ATTITUDE REF • REACTION CONTROL • TEMPERATURE CONTROL • PYROTECHNICS • CAPSULE	A) PROVIDE C • T/M • CC&S • AUTOPIL • ATTITUD • REACTIO • TEMPERA B) CHARGE BA
A) SUPPORT S/C ASSEMBLIES B) SUPPORT S/C COMPONENTS C) MAINTAIN ADEQUATE ALIGNMENT BETWEEN COMPONENTS D) PROVIDE ACCEPTABLE STATIC & DYNAMIC LOAD ENVIRONMENTS E) SUPPORT FLIGHT CAPSULE	A) SUPPORT S/C ASSEMBLIES B) SUPPORT S/C COMPONENTS C) MAINTAIN ADEQUATE ALIGNMENT BETWEEN COMPONENTS D) PROVIDE ACCEPTABLE STATIC & DYNAMIC LOAD ENVIRONMENTS E) SUPPORT FLIGHT CAPSULE	A) SUPPORT S B) SUPPORT S C) MAINTAIN D) PROVIDE A E) DRIVE SCA
PROVIDE TEMPERATURE CONTROL	PROVIDE TEMPERATURE CONTROL	PROVIDE TEMP
A) REMOVE PROPULSION SYSTEM INHIBIT B) PROVIDE IGNITION C) INHIBIT PROPULSION SYSTEM	A) RECEIVE SIGNAL TO REMOVE CAPSULE SEPARATION INHIBIT B) RECEIVE SIGNAL TO FIRE CAPSULE UMBILICAL SEPARATION C) RECEIVE SIGNAL TO FIRE BIOBARRIER REMOVAL D) RECEIVE SIGNAL TO FIRE CAPSULE SEPARATION E) RECEIVE SIGNAL FOR SEPARATION INHIBIT	RECEIVE SQUI OF SCAN PLAT
A) RECEIVE CC&S COMMAND "CRUISE SCIENCE OFF" B) TURN OFF CRUISE SCIENCE	A) RECEIVE CC&S COMMAND "CRUISE SCIENCE OFF" B) TURN OFF CRUISE SCIENCE	A) RECEIVE CI B) ACQUIRE C C) TRANSFER D) RECEIVE PI E) RECALIBRA
		A) RECEIVE D B) PROCESS

CAPSULE TORY TION → 9.0 FLIGHT CAPSULE CRUISE → 10.0 FLIGHT CAPSULE ENTRY → 11.0 FLIGHT CAPSULE DESCENT & LANDING → 12.0 LAN OPERATIO

8.0 FLIGHT S/C CRUISE → 13.0 FLIGHT S/C ORBIT INSERTION → 14.0 OPER

BIT INJECTION PARAMETERS ITUDE & DIRECTION TUDE & DIRECTION N START TIME SPACECRAFT BCE & DISPLAY SCIENCE & ENGINEERING DATA MANDS TO BACK UP CC&S AS REQUIRED	A) RECEIVE, DECODE, & DISPLAY ENGINEERING DATA B) RELAY UPDATED ORBIT INJECTION PARAMETERS C) PROVIDE COMMAND TO INITIATE INSERTION MANEUVER D) PROVIDE BACKUP COMMANDS TO CC&S AS REQUIRED E) TRACK S/C F) VERIFY ORBIT INSERTION	A) RECEIVE, DECODE, & DISPLAY S B) RECEIVE AND ANALYZE ENGINEE C) TRACK S/C D) RECEIVE & DISPLAY CAPSULE DA E) PROVIDE DATA FOR ORBITAL TR F) RECEIVE VERIFICATION OF ORBI G) TERMINATE MISSION
& YAW TURN MAGNITUDE & DIRECTION COMMAND & RELAY NNA POSITIONING DATA & RELAY TO CC&S R-BURN START TIME, RELAY TO CC&S ULE DATA, CONDITION & RELAY TO GROUND GHT SPACECRAFT ENGINEERING, CAPSULE ENGRG, & TO GROUND VIA MODE 2	A) UPDATE ROLL-TURN MAGNITUDE & DIRECTION COMMAND & RELAY TO CC&S B) UPDATE YAW-TURN MAGNITUDE & DIRECTION COMMAND & RELAY TO CC&S C) UPDATE MOTOR-BURN START TIME & RELAY TO CC&S D) UPDATE INITIATE MANEUVER & RELAY TO CC&S E) SWITCH TO DATA MODE NO. 2 OR 5A AS REQUIRED F) REACQUIRE EARTH AFTER ROLL TURNS & MOTOR BURN G) RELAY VERIFICATION OF MANEUVERS	A) TRANSMIT SCIENCE & ENGINEER B) RECORD ENGINEERING & SCIENC C) RECEIVE, STORE & RELAY CAPSU D) RECEIVE & RELAY DATA FOR ORB
ITCH TO DATA MODE NO. 2 ANOPUS CONE ANGLE SETTING TENNA STEP (AS REQUIRED) IT INJECTION PARAMETERS NAL TO PYRO & MECHANISMS TO DEPLOY SCAN PLATFORM NCE T/M OFF) & SWITCH TO DATA MODE NO. 1 ATA RECORDER-COMMAND TELECOMMUNICATIONS SULE DATA MANDS AS REQUIRED	A) UPDATE STORED ROLL, PITCH, & YAW MAGNITUDE & SIGN B) UPDATE STORED VELOCITY MAGNITUDE C) INITIATE MANEUVER SEQUENCE D) COMMAND ORIENTATION OF S/C TO INJECTION ATTITUDE E) COMMAND THRUST FOR ORBIT INSERTION F) COMMAND RETURN TO CRUISE ATTITUDE G) BACKUP COMMANDS AS REQUIRED	A) COMMAND ORBITAL TRIM MANE B) SWITCH DATA MODES AS NECES C) RECEIVE ANY ORBITAL OPERATI D) COMMAND POSITIONING OF SC E) SWITCH ON ORBITAL SCIENCE F) SELECT RECORDED SCIENCE REA G) BACKUP COMMANDS AS REQUI H) STORE DATA FOR ORBIT TRIM (I I) TERMINATE MISSION ON COMM
OPUS CONE ANGLE ON COMMAND OPILOT TO CRUISE MODE /C ATTITUDE TO CELESTIAL REFERENCES DURING CRUISE	A) SWITCH TO GYRO CONTROL B) PROVIDE ROLL TO PROPER ATTITUDE & VERIFY ROLL C) YAW TO PROPER ATTITUDE & VERIFY D) AUTOPILOT – PROVIDE COMMAND TO TVC DURING MOTOR BURN E) TURN ON ACCELEROMETER F) PROVIDE ACCELEROMETER DATA TO CC&S G) TURN OFF ACCELEROMETER H) YAW BACK AFTER MOTOR BURN I) ACQUIRE SUN & VERIFY J) ROLL BACK TO PROGRAMMED ATTITUDE K) ACQUIRE CANOPUS & VERIFY L) SWITCH AUTOPILOT FROM GYRO – CONTROL TO CELESTIAL REFERENCE CONTROL	A) MAINTAIN S/C ATTITUDE TO CEL B) SWITCH AUTOPILOT TO GYRO C C) REACQUIRE CELESTIAL REFEREN D) REORIENT S/C FOR ORBITAL TR E) PROVIDE TVC DURING ENGINE F F) REACQUIRE CELESTIAL REFEREN G) UPDATE CANOPUS CONE ANGLES
	ORBIT INSERTION ENGINE A) ARM TVC B) ARM IGNITER C) FIRE MOTOR & PROVIDE THRUST & TVC D) TERMINATE THRUST (MOTOR BURNS TO DEPLETION)	MIDCOURSE A) ARM PRESSURIZATION & PROP B) PROVIDE THRUST (FIRE PROGR IF REQUIRED C) TERMINATE THRUST ON COMMA D) ISOLATE PROPELLANT FEED SUB E) ISOLATE PRESSURIZATION SU
NDITIONED SOLAR ELECTRICAL POWER TO: T REF CONTROL TURE CONTROL TERIES	A) PROVIDE CONDITIONED SOLAR OR BATTERY POWER TO: • TELEMETRY • CC&S • ATTITUDE REFERENCE SUBSYSTEM • AUTOPILOT • TEMPERATURE CONTROL • PULSE TO PYROTECHNICS • PULSE TO PROPULSION	A) PROVIDE CONDITIONED SOLAR • TELEMETRY • CC&S • ATTITUDE REFERENCE SUBSY • AUTOPILOT • TEMPERATURE CONTROL • STRUCTURES & MECHANISM • SCIENCE
C ASSEMBLIES C COMPONENTS DEQUATE ALIGNMENT BETWEEN COMPONENTS CEPTABLE STATIC & DYNAMIC LOAD ENVIRONMENTS PLATFORM TO DEPLOYED POSITION & LOCK	A) SUPPORT S/C ASSEMBLIES B) SUPPORT S/C COMPONENTS C) MAINTAIN ADEQUATE ALIGNMENT BETWEEN COMPONENTS D) PROVIDE ACCEPTABLE STATIC & DYNAMIC LOAD ENVIRONMENTS	A) SUPPORT S/C ASSEMBLIES B) SUPPORT S/C COMPONENTS C) MAINTAIN ADEQUATE ALIGNME D) PROVIDE ACCEPTABLE STATIC ENVIRONMENTS E) POSITION SCAN PLATFORM
RATURE CONTROL	PROVIDE TEMPERATURE CONTROL	PROVIDE TEMPERATURE CONTROL
FIRING SIGNAL FOR UNLATCHING ORM	A) RECEIVE & EXECUTE COMMAND SIGNAL TO REMOVE INHIBIT FOR PROPULSION ENGINE B) RECEIVE & EXECUTE SIGNAL FOR PROPULSION ENGINE START C) RECEIVE & EXECUTE COMMAND SIGNAL FOR PROPULSION ENGINE STOP D) RECEIVE & EXECUTE SIGNAL FOR PROPULSION INHIBIT	
UISE SCIENCE "ON" COMMAND RUISE SCIENCE DATA ONDITIONED DATA TO DAE WER FROM F/P TE SCIENCE EXPERIMENTS AS REQUIRED	SCIENCE OFF DURING ORBIT INSERTION	A) TURN ON ORBITAL SCIENCE I B) ACQUIRE ORBITAL SCIENCE D C) TRANSFER CONDITIONED DAT D) RECALIBRATE SCIENCE EXPE
E "ON" COMMAND TRANSFER DATA TO TM		A) RECEIVE DAE "ON" COMMAND B) PROCESS & TRANSFER DATA

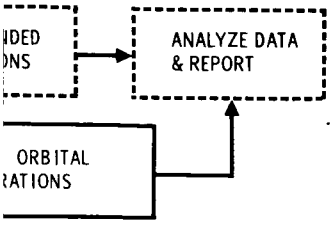

IENCE DATA
ING DATA
TA
M (IF REQUIRED)
AL TRIM MANEUVER

NG DATA VIA DATA MODES 5 AND 6
E DATA AS COMMANDED
KE DATA ON COMMAND (MODES 5 AND 6)
T TRIM IF REQUIRED

UVERS (IF REQUIRED)
SARY
ON CHANGES & SEQUENCES
IENCE SCAN PLATFORM

DOUT TO TELECOMMUNICATIONS
ED
F REQUIRED)
AND (IF REQUIRED)

STIAL REFERENCES
NTROL DURING OCCULTATION
ES FOLLOWING OCCULTATION
M MANEUVER USING GYRO CONTROL
IRING
ES FOLLOWING MANEUVERS
ON COMMAND

ELLANT FEED SUBSYSTEMS
AMMED ENGINES) FOR ORBIT TRIM

ID
SYSTEM
SYSTEM

OR BATTERY POWER TO:

STEM

NTS BETWEEN COMPONENTS
AND DYNAMIC LOAD

STRUMENTS
ATA
, TO DAE
IMENTS AS REQUIRED

O TM

Mission Sequences Matrix

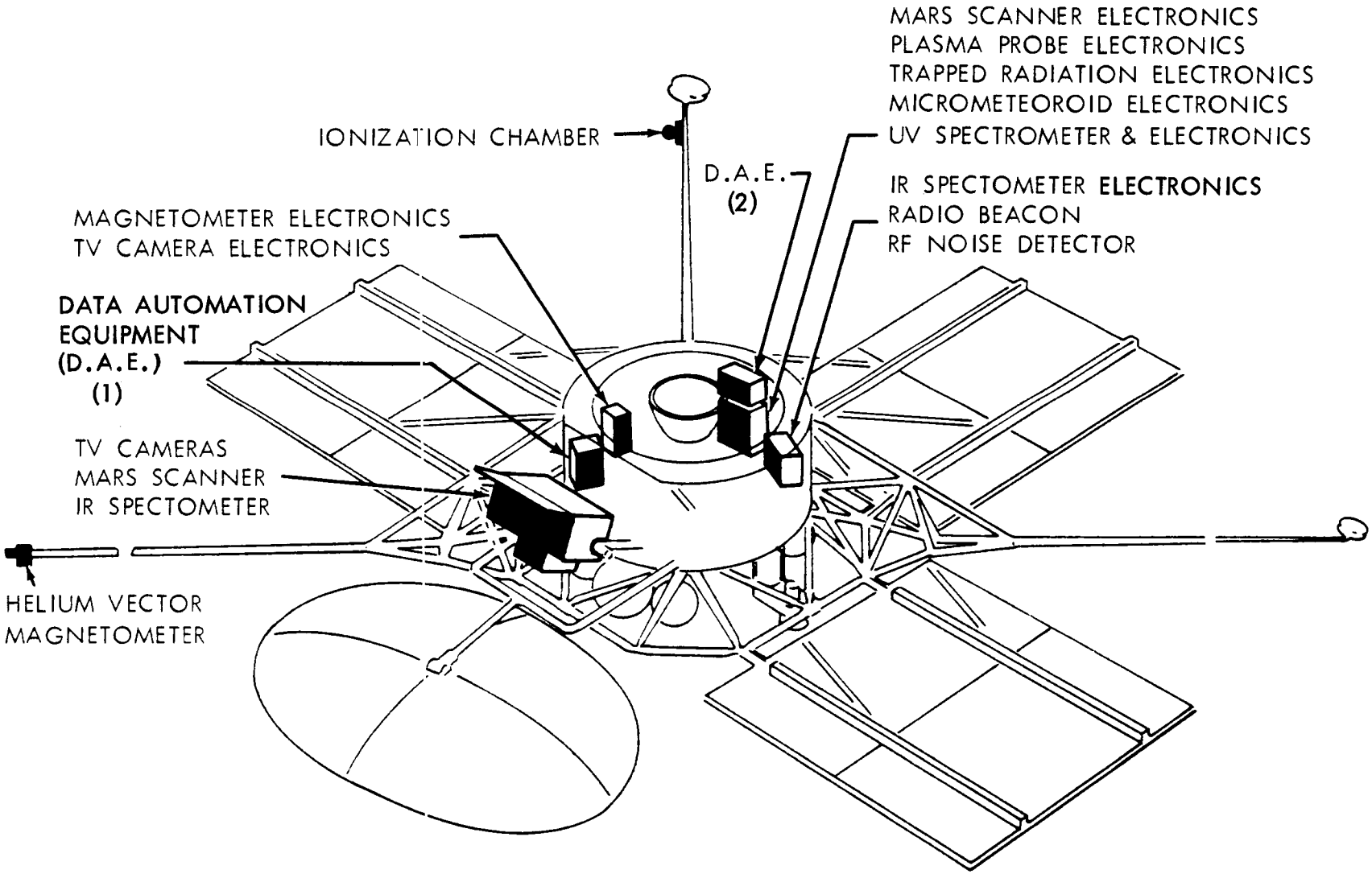

Figure 4.5-1: Space Science

MARS ORBIT		INTERPLANETARY
Mapping Cameras		Magnetometer
IR Scanner	Scan Platform	Plasma
IR Spectrometer		Van Allen Radiation
RF Occultation		Meteoroids
UV Spectrometer	Body-Mounted	Galactic Cosmic Ray
RF Noise		

These typical experiments are within the present instrument technology; some are even spaceflight proven.

4.5.4 Interface Definition

Space science experiments exercise constraints on the Voyager Program, on the Mission 1971 (1969), on the Spacecraft Bus, on spacecraft operations, on spacecraft support and test equipment, and on several Spacecraft Subsystems. A few of the more important, yet typical, constraints include:

1) Schedule of science-experiment availability;

2) Magnetic cleanliness for the magnetometer experiment;

3) Orbit selection for mapping;

4) Data modes.

4.5.4.1 Instrumentation

In the terms of the mission specifications, the space science instrumentation characteristics are summarized in table 4.5-1 and compared with a representative payload.

Table 4.5-1: SPACE SCIENCE INSTRUMENT SUMMARY

	Weight		Power		Volume	
	A	B	A	B	A	B
			W	W		
Primary Sensors (Scan)	90	90	15	9	5	4.6
Primary Sensors (Body)	40	34	10	16	2	2.2
Remote Electronic Hardware	65	40	50	50	1	0.7
Data Automation Equipment	55	55	25	25	1	1.0
TOTAL	250	219	100	95	9	8.5

A = "Voyager 1971 Mission Guidelines" B = "Preferred Design"

4.5.4.2 List of Experiments

The characteristics, requirements, and performance of REAL instruments for each experiment are defined in Table 4.5-2. Their specifications are defined in detail in 1) and 2) in Section 4.5.2 above.

Although none of these specific instruments are as yet selected nor committed, and although improvements will probably be developed, these data do provide a comprehensive technical foundation for a configuration specifically designed to be universally adaptable to whatever experiments are ultimately selected within the limitations of the specifications.

4.5.4.3 Magnetometrics

To develop the foregoing interfaces, a detailed assessment has been made of the magnetics and mapping interrelationships with the spacecraft and mission design.

		TELEVISION SUBSYSTEM
OPTICAL		NO STRAY LIGHT INTO THE OPTICS OF EITHER TV CAMERA IS TOLERABLE DURING NORMAL OPERATIONS TV OPTICS MUST BE PROTECTED AGAINST MICROMETEOROID DAMAGE DURING CRUISE PHASE.
MECHANICAL		BOTH CAMERAS MOUNT ON PLANET SCAN PLATFORM AND VIEW OF EACH CAMERA MUST BE UNOBSTRUCTED THROUGH 210 DEGREES OF SCAN. WHEN SCAN PLATFORM IS DEPLOYED IN THE OPERATIONAL POSITION THE ORIENTATION OF THE TV CAMERAS WITH RESPECT TO THE S/C AXES SHALL BE KNOWN. WITHIN 0.1 DEGREE. WIDE ANGLE TV CAMERA TO BE BORE-SIGHTED WITH RESPECT TO S/C + Z AXIS.
ELECTRICAL	INPUT	-50 V RMS, 2400 CPS SQUARE WAVE FROM S/C POWER. FRAME COMMAND LINE START COMMAND LINE STOP COMMAND READOUT COMMAND AGC SIGNAL LEVEL (MULTIPLEXER COMMAND) TARGET VOLTAGE (MULTIPLEXER COMMAND) PLANET-IN-VIEW SIGNAL (REDUNDANT)
	OUTPUT	ENGINEERING TEMPERATURE TO ENG. MUX ENCODER SIGNALS TO DATA AUTOMATION EQUIPMENT: DIGITAL PICTURE "ZEROES" DIGITAL PICTURE "ONES" PLANET-IN-VIEW SIGNAL MULTIPLEXED DIGITAL OUTPUT AAC LOGIC 1 AAC LOGIC 2 AAC LOGIC 3 FILTER AND SHUTTER POSITION
RF REQUIREMENTS	SENSOR	SENSORS AND ELECTRONICS WILL BE DESIGNED TO MEET THE CLASS II RFI REQUIREMENTS AS A MINIMUM OF JPL SPEC. 30236-ETS-A.
	ELECTRONICS	
THERMAL	SENSOR	THE SUBSYSTEM SHALL BE CAPABLE OF OPERATING OVER THE TEMPERATURE RANGE ATTAINABLE BY SPACECRAFT TEMPERATURE CONTROL.
	ELECTRONICS	DESIGN FOR THERMAL INDEPENDENCE FROM S/C. SEE STATEMENT UNDER HELIUM VECTOR MAGNETOMETER.
RADIOACTIVE OR NUCLEAR RADIATION	SENSOR	DESIGN OF ASSOCIATED CIRCUITRY WILL MINIMIZE EFFECTS OF RADIATION.
	ELECTRONICS	SINCE LOCATED IN BUS COMPARTMENT, RADIATION EFFECTS ANTICIPATED CONSISTENT WITH CC&S AND TELEMETRY.
MAGNETIC		DESIGN SHOULD CONFORM TO THE MINIMUM USE OF MAGNETIC MATERIALS REQUIREMENT OF JPL SPEC. 31252.

MARS SCANNER	IR SPECTROMETER	DUAL FREQUENCY RADIO EXPERIMENT
LOOKS IN SAME DIRECTION AS TV CAMERAS, (I.E., TOWARD MARS NADIR), NORMAL TO SURFACE UP TO 30° DEVIATIONS USEABLE. COOLING RADIATOR MUST POINT AWAY FROM SUN AND MARS.	POINTS TO MARS NADIR NEARLY NORMAL DESIRED (UP TO 45° DEVIATION AT SURFACE USEABLE. BORE SIGHTED WITHIN 0.1% OF TV CAMERA.	ANTENNA DIRECTED WITH MAJOR LOBE TOWARD EARTH AT TIME OF IMMERSION IN AND EMERSION FROM MARS SHADOWS.
MOUNTS RIGIDLY ON STABLE PLATFORM WITH TV CAMERAS AND IR SPECTROMETER. A CONSTANT VELOCITY AND ALTITUDE DESIRABLE	MOUNTS ON TV CAMERA PLATFORM. SENSORS SHOULD BE THERMALLY ISOLATED FROM ELECTRONICS AND OTHER HEAT SOURCES. MIRRORS AND GRATING MUST BE PROTECTED AGAINST LAUNCH SHOCK.	MOUNTED ON SPACECRAFT BODY IN ELECTRONICS COMPARTMENT.
POWER ON/OFF SELECT MS MODE START MS MEASUREMENT STOP MS MEASUREMENT SCAN AMPLITUDE 1 SCAN AMPLITUDE 2 SCAN AMPLITUDE 3 SCAN POSITION 1 SCAN POSITION 2 SCAN POSITION 3 SCAN POSITION 4 SCAN POSITION 5 INSTRUMENT SETTING UPDATE.	POWER ON/OFF CALIBRATE START SCAN STOP SCAN	POWER ON/OFF
FOUR ANALOG CHANNELS TO DAE, ± 6 V DC. MAXIMUM CURRENT 1 MICROAMP. COMPATIBLE WITH NASA - JPL SIGNAL CONVERTER FOR MARINER C, MS SENSOR TEMPERATURE MEASUREMENT TO ENG. MUX ENCODER CALIBRATION COMMAND.	5 CHANNELS - ANALOG ± 5 VOLTS TO DAE GRATING POSITION PBS OUTPUT DATA PBSE OUTPUT DATA SI OUTPUT DATA GRATING POSITION IR SENSOR TEMP. MEASUREMENT TO ENG MUX ENCODER.	6 OUTPUTS, ± 5 V, ANALOG. CHANNEL 1 ±5V ANALOG PHASE DATA CHANNEL 1 ± 5V ANALOG AMPLITUDE DATA CHANNEL 2 ±5V ANALOG PHASE DATA CHANNEL 2 ±5V ANALOG AMPLITUDE DATA CHANNEL 2 ±5V ANALOG ±5V ANALOG ±5V ANALOG TEMPERATURE MEASUREMENT TO ENG. MUX ENCODER
SENSORS AND ELECTRONICS WILL BE DESIGNED TO MEET THE CLASS II RFI REQUIREMENTS AS A MINIMUM OF JPL SPEC. 30236-ETS-A.	SENSORS AND ELECTRONICS WILL BE DESIGNED TO MEET THE CLASS II RFI REQUIREMENTS AS A MINIMUM OF JPL SPEC. 30236-ETS-A.	NO INTERFERING R.F. EMISSION FROM ORBITER WITHIN ONE OCTAVE OF SELECTED TEST FREQUENCIES SENSORS AND ELECTRONICS WILL BE DESIGNED TO MEET THE CLASS II RFI REQUIREMENTS AS A MINIMUM OF JPL SPEC 30236-ETS-A.
ACCEPTS CIS-MARTIAN AND TRANS-MARTIAN SPACE ENVIRONMENT. MUST BE THERMALLY WELL ISOLATED FROM ELECTRONICS AND OTHER VEHICLE HEAT SOURCES.	ISOLATED FROM HEAT SOURCES. COOLED BY CRYOGENICS, RADIATION OR ACTIVE MEANS TO -120°C (PBSE SENSOR).	SEE STATEMENT FOR TV.
ACCEPTS CIS-MARTIAN AND TRANS-MARTIAN SPACE ENVIRONMENT. SEE STATEMENT UNDER TV AND MAGNETOMETER	SEE STATEMENT UNDER TV AND MAGNETOMETER	SEE STATEMENT UNDER TV AND MAGNETOMETER
NOT SENSITIVE TO ANTICIPATED LEVELS. DESIGN TO MINIMIZE EFFECTS. NOT SENSITIVE TO ANTICIPATED LEVELS. WILL BE CONSISTENT WITH CC&S AND TELEMETRY.	SENSOR AND ELECTRONICS WILL BE CHANGED TO MINIMIZE EFFECTS OF ANY RADIATION.	NO PROBLEMS IN CIS-MARTIAN OR TRANS-MARTIAN SPACE.
DESIGN SHOULD CONFORM TO MINIMUM USE OF MAGNETIC MATERIALS REQUIREMENT, JPL SPEC. 31252	DESIGN SHOULD CONFORM TO MINIMUM USE OF MAGNETIC MATERIALS REQUIREMENT, JPL SPEC. 31252	VEHICLE FIELDS BELOW 1 GAMMA DESIRED DESIGN SHOULD CONFORM TO MINIMUM USE OF MAGNET MATERIALS REQUIREMENT, JPL SPEC. 31252

ULTRA VIOLET SPECTROMETER	MARS RF NOISE DETECTOR
MUST POINT AT SUN WHEN MEASUREMENTS ARE TAKEN.	NONE
MOUNTED ON SPACECRAFT BUS OR SUN-TRACKER ASSEMBLY.	ANTENNAS MOUNTED OUTSIDE THE VEHICLE MUST SNAP OPEN AFTER THE SPACECRAFT IS INJECTED INTO ORBIT THROUGH THE EARTH'S ATMOSPHERE. DEHAVILAND ROD CONCEPT POSSIBLE.
POWER ON/OFF UPDATE SLIT ANGLE.	POWER ON/OFF
1 ANALOG OUTPUT, ± 5V FROM PHOTOCELL UV SENSOR TEMPERATURE MEASUREMENT	5 ANALOG CHANNELS, 0-5V CH 1 SIGNAL OUTPUT CH 2 SIGNAL OUTPUT CH 3 SIGNAL OUTPUT CH 4 SIGNAL OUTPUT CH 5 SIGNAL OUTPUT ELECTRONICS TEMPERATURE MEASUREMENT.
SENSORS AND ELECTRONICS WILL BE DESIGNED TO MEET THE CLASS II RFI REQUIREMENTS AS A MINIMUM OF JPL SPEC. 30236-ETS-A.	NO TROUBLE ANTICIPATED FROM UHF SOURCES. NO TROUBLE ANTICIPATED FROM UHF SOURCES. SENSORS AND ELECTRONICS WILL BE DESIGNED TO MEET THE CLASS II RFI REQUIREMENTS AS A MINIMUM OF JPL SPEC. 30236-ETS-A.
MARINER C SPECIFICATION. SEE STATEMENT UNDER TV	$\leq$ 300°C.
SEE STATEMENT UNDER TV AND MAGNETOMETER	SEE STATEMENT UNDER TV AND MAGNETOMETER
NOT DETERMINED.	NOT SENSITIVE
NOT DETERMINED.	< 10 RAD/HOUR
DESIGN SHOULD CONFORM TO MINIMUM USE OF MAGNETIC MATERIALS REQUIREMENT, JPL SPEC. 31252	DESIGN SHOULD CONFORM TO MINIMUM USE OF MAGNETIC MATERIALS REQUIREMENT, JPL SPEC. 31252

HELIUM VECTOR MAGNETOMETER EXPERIMENT	PLASMA INSTRUMENT
N/A	SENSOR MOUNTED SO THAT THE NORMAL TO THE COLLECTOR "LOOKS OUT" TOWARD THE SUN BUT 10 DEGREES FROM SPACECRAFT -TO-SUN LINE
THE MAGNETOMETER SENSOR IS LOCATED ON A NONFERROMAGNETIC BOOM APPROXIMATELY 34 FEET IN LENGTH SO THAT PERTURBATION BY MAGNETIC-MATERIALS AND FIELDS OF THE SPACECRAFT IS MINIMIZED. ORIENTATION OF EACH AXIS OF THE MAGNETOMETER SENSOR RELATIVE TO SPACECRAFT MUST BE KNOWN TO WITHIN ONE DEGREE. ONE SENSOR AXIS SHALL BE PARALLEL TO THE SPACECRAFT AXIS TO WITHIN ONE DEGREE.	RIGID MOUNT OF PLASMA CUP AT A POINT ABOVE OR IN FRONT WHERE ANY PLASMA SHEATH BUILT UP AROUND THE VEHICLE IS MINIMIZED.
POWER ON/OFF CALIBRATION "ON" PULSE CALIBRATION "OFF" PULSE	POWER ON/OFF READOUT COMMAND STEPPING CLOCK PULSE.
ENGINEERING TEMPERATURE MEASUREMENT TO ENGINEERING MULTIPLEXER ENCODER. THREE DATA OUTPUTS (ONE FOR EACH AXIS) TO DAE. Z - AXIS OUTPUT Y - AXIS OUTPUT X - AXIS OUTPUT	VOLTAGES OR CURRENTS FROM 32 CHANNELS PROPORTIONAL TO PARTICLE FLUXES. SIGNAL INDICATING DIRECTION OF RELATIVE MOTION. TEMPERATURE - MEASUREMENT
- GOLD FLASHING FOR RF SHIELDING SEE STATEMENT UNDER TV AND MAGNETOMETER	ISOLATION FROM LARGE VOLTAGE VARIATIONS.
SEE STATEMENT UNDER TV AND MAGNETOMETER - USUAL PRECAUTIONS ONLY ARE NEEDED. SEE STATEMENT UNDER TV	USUAL ISOLATION FROM LARGE RFI. GENERATES RATHER LARGE VOLTAGE PULSES OF SQUARE WAVES OF FREQUENCY APPROXIMATELY 1400 CPS WHICH MUST BE KEPT AWAY FROM OTHER SYSTEMS.
DESIGN TO BE THERMALLY INDEPENDENT.	$<$ 100°C
ELECTRONICS - ASSOCIATED ELECTRONICS ARE LOCATED IN THE REMOTE ELECTRONICS HARDWARE COMPARTMENT IN THE SPACECRAFT BUS FOR THE PURPOSE OF MAINTAINING THEM WITHIN THE OPERATING TEMPERATURE DESIGN LIMITS.	(INSIGNIFICANT HEAT GENERATED) SEE STATEMENT UNDER TV AND MAGNETOMETER
OPERATES OUT ON BOOM AND NO RADIATION EFFECTS ANTICIPATED FROM RTG IN THE CAPSULE.	ELECTRONS 10^9 CM^{-2} SEC^{-1} ABOVE 40 KEV PROTRONS ALPHAS$<10^8$ CM^{-2} SEC^{-1} ABOVE 40 KEV
- SINCE LOCATED IN BUS COMPARTMENT - RADIATION EFFECTS CONSISTENT WITH CC&S TELEMETRY ANTICIPATED.	DOSE RATES $\leq$ 10 RAD/HR.
CHANGE IN SPACECRAFT MAGNETIC FIELD TO BE HELD TO $\leq$ 1.0 GAMMA AT SENSOR. MUST BE MAGNETICALLY ISOLATED FROM SPACECRAFT BUS.	WILL CAUSE FLUCTUATING FIELDS WITH AMPLITUDE 10G, FREQUENCY 1400 CPS NEARBY. ENVIRONMENT REQUIREMENT: 1. VEHICLE MAGNETIC MOMENT WHERE μ = MIN PARTICLE MOMENTUM TO BE DETECTED X 4 (RADIUS OF VEHICLE)^2 = 2/3 X 10^6 GAUSS-CM^3 = 2/3 X 10^{-4} WEBER-M. = 50 AMP-TURN/METER 2. MAGNITUDE OF LOCAL MAGNETIC FLUCTUATIONS CAUSED BY VEHICLE MIN. PARTICLE MOMENTUM TO BE DETECTED (RADIUS OF VEHICLE) 0.2 GAUSS

TRAPPED RADIATION DETECTOR	MICROMETEOROID DETECTOR
NONE	NONE
MOUNTED TO LOOK IN A 30° CONE ONE OF A PAIR OF GEIGER COUNTERS AND ONE OF A PAIR OF SOLID STATE DETECTORS IN SUN DIRECTION AND THE SAME FOR ANTI-SUN DIRECTION.	MOUNT SENSOR OUTSIDE VEHICLE WITH PLATE APPROXIMATELY PERPENDICULAR TO DIRECTION OF VEHICLE TRAVEL.
500 VDC MEASUREMENT 8VDC MEASUREMENT 78VDC MEASUREMENT 500V CURRENT MEASUREMENT 75V CURRENT MEASUREMENT 8V CURRENT MEASUREMENT POWER ON/OFF.	POWER ON/OFF CALIBRATE SIGNAL READOUT COMMAND MEASURE +12VDC MEASURE +3VDC MEASURE -7VDC MEASURE +12V CURRENT MEASURE +3V CURRENT MEASURE -7V CURRENT
A SEQUENCE OF FIVE WORDS CONSISTING OF EIGHT BITS. GM #1 OUTPUT SIGNAL GM #2 OUTPUT SIGNAL COMPARATOR OUTPUT SIGNAL SS #1 OUTPUT SIGNAL SS #2 OUTPUT SIGNAL TEMPERATURE MEASUREMENT	2 ANALOG SIGNALS (FRONT AND BACK) GIVING MOMENTUM OF EACH IMPACT. FRONT GATE ANALOG SIGNAL BACK GATE ANALOG SIGNAL SENSOR TEMPERATURE MEASUREMENT
SENSORS AND ELECTRONICS ARE RELATIVELY INSENSITIVE TO RF NOISE. SENSORS AND ELECTRONICS WILL BE DESIGNED TO MEET THE CLASS II RFI REQUIREMENTS AS A MINIMUM OF JPL SPEC 30236-ETS-A.	NONE SEE STATEMENT UNDER TV AND MAGNETOMETER NONE SENSORS AND ELECTRONICS WILL BE DESIGNED TO MEET THE CLASS II RFI REQUIREMENTS AS A MINIMUM OF JPL SPEC. 30236-ETS-A.
SENSORS AND ELECTRONICS WILL BE DESIGNED TO MEET THE CLASS II RFI REQUIREMENTS AS A MINIMUM OF JPL SPEC. 30236-ETS-A.	SENSORS AND ELECTRONICS WILL BE DESIGNED TO MEET THE CLASS II RFI REQUIREMENTS AS A MINIMUM OF JPL SPEC. 30236-ETS-A.
SENSORS AND ELECTRONICS WILL BE DESIGNED TO MEET THE CLASS II RFI REQUIREMENTS AS A MINIMUM OF JPL SPEC. 30236-ETS-A.	SENSORS AND ELECTRONICS WILL BE DESIGNED TO MEET THE CLASS II RFI REQUIREMENTS AS A MINIMUM OF SPL SPEC. 30236-ETS-A
	NOT SPECIFIED
NO PROBLEM	< 10 RAD/HR
DESIGN SHOULD CONFORM TO MINIMUM USE OF MAGNETIC MATERIALS REQUIREMENT, JPL SPEC. 31252	DESIGN SHOULD CONFORM TO MINIMUM USE OF MAGNETIC MATERIALS REQUIREMENT, JPL SPEC. 31252

Table 4.5-2: Typical Science Experiments Requirements and Performance Data — for 1971 Voyager Spacecraft

IONIZATION CHAMBER EXPERIMENT	DATA AUTOMATION EQUIPMENT	
NONE	NOT APPLICABLE	OPTICAL
MOUNT OUTSIDE AND SEVERAL FEET AWAY FROM NEARBY MASSES TO MINIMIZE EFFECTS OF SECONDARIES. BASE CIRCUIT AND PRE-AMPLIFIER SHOULD BE MOUNTED ADJACENT TO CHAMBER.	THE DAE IS PHYSICALLY LOCATED IN THE SPACECRAFT BUS.	MECHANICAL
POWER ON/OFF.	CRUISE (RT) POWER: 50V RMS, 2400 CPS SQUARE WAVE. 1 - 8 BIT PARALLEL, 30 DISCRETES, 14 ANALOG; 32 DATA PULSE TRAINS, 5 CLOCK FREQUENCIES.	INPUT ELECTRICAL
SINGLE CHANNEL OF RANDOM PULSES UP TO 10 PULSES PER SECOND. SIGNAL GROUND. PREAMPLIFIER TEMPERATURE MEASUREMENT 310 VDC MEASUREMENT.	95 DISCRETES, 9 DATA PULSE TRAINS	OUTPUT
NONE	NONE	SENSOR RF REQUIREMENTS
USUAL SHIELDING PRECAUTIONS. USE RFI REQUIREMENTS. SEE STATEMENT UNDER TV AND MAGNETOMETER	ELECTRONICS - SHOULD BE DESIGNED TO MEET RFI REQUIREMENTS OF JPL SPECIFICATION 30236-ETS-A.	ELECTRONICS
SENSORS AND ELECTRONICS WILL BE DESIGNED TO MEET THE CLASS II RFI REQUIREMENTS AS A MINIMUM OF JPL SPEC. 30236-ETS-A.		SENSOR THERMAL
	ELECTRONICS - SHALL BE CAPABLE OF OPERATING WITHIN THE TEMPERATURE RANGE ATTAINABLE BY SPACECRAFT TEMPERATURE CONTROL	ELECTRONICS
ON-BOARD PENETRATING RADIATION FLUXES (ESPECIALLY ELECTRONS: E > 1/2 MEV); $\leq 30\ CM^{-2}\ SEC^{-1}$	ELECTRONICS - DESIGN OF CIRCUITRY TO BE SUCH AS TO MINIMIZE THE EFFECTS OF EXTERNAL RADIATION. SEE MC-3-120A, PARAGRAPH 1.1	SENSOR RADIOACTIVE OR NUCLEAR RADIATION
DOSE RATE $\leq$ 10 RAD/HOUR		ELECTRONICS
OBSERVE USUAL PRECAUTIONS IN CONSTRUCTION OF ELECTRICAL PART OF EXPERIMENT TO MAINTAIN MAGNETIC CLEANLINESS OF SPACECRAFT.	DESIGN TO CONFORM TO THE MINIMUM USE OF MAGNETIC MATERIALS REQUIREMENT. SEE MC-3-120A, PARAGRAPH 1.2.2	MAGNETIC

ENVIRONMENTAL		SPACECRAFT MOTION OR VIBRATION MUST BE CONTROLLED TO MINIMIZE CAMERA POINTING ERRORS.
PERFORMANCE PARAMETERS RELIABILITY		$\lambda_s = 37.9 \times 10^{-6}\ hr^{-1}$ PER SENSOR. $\lambda_e = 41.8 \times 10^{-6}\ hr^{-1}$ PER ELECTRONICS
SENSITIVITY		0.0075 FT-CANDLE-SECONDS AT THRESHOLD S/N RATIO FOR HIGH CONTRAST PICTURES. FILTER LOSSES ARE NOT INCLUDED.
DYNAMIC RANGE		64:1 ILLUMINATION WITH AUTOMATIC VIDEO GAIN CONTROL.
RESOLUTION		TV #1: A SURFACE AREA OF 35 x 35 KM 200M RES. @ 2 KM ALT. TV #2: COVER A SINGLE AREA OF 350 x 350 KM @ 2 KM RES. @ 2 KM ALT.
SENSOR RESPONSE		EXPOSURE TIME VARIABLE FROM .01 to 0.5 SECONDS.
SIGNAL CHARACTERISTICS		SIZE 500 ELEMENTS X 500 LINES ON A 0.44" X 0.44" FORMAT FIELD OF VIEW: CAMERA #1: 1.35° COVERAGE ANGLE; CAMERA #2: 5° MAX COVERAGE ANGLE.
BIT RATE		50,000 BITS PER SECOND TO DAE, ALTERNATELY, 1 PICTURE EVERY 2 MINUTES FOR EACH SYSTEM.
PHYSICAL CHARACTERISTICS AND CONSTRAINTS WEIGHT	SENSOR	SENSOR #1 - 23 POUNDS SENSOR #2 - 20 POUNDS
	ELECTRONICS	ELECTRONICS #1 - 8 POUNDS ELECTRONICS #2 - 8 POUNDS
VOLUME	SENSOR	SENSOR #1 - 10" X 15" X 25" SENSOR #2 - 3" D X 15"
	ELECTRONICS	ELECTRONICS #1 3 - 6" X 6" X 2", 2 - 6" X 6" X 1" ELECTRONICS #2 3 - 6" X 6" X 2", 2 - 6" X 6" X 1"
POWER	SENSOR ELECTRONICS	SENSORS #1, #2 - 1 WATT EACH ELECTRONICS #1, #2 - 9 WATTS EACH
OPERATING TEMPERATURE LIMITS (SELF CONTROLLED)	SENSORS	-20°C to +40°C
	ELECTRONICS	-10°C to +70°C
NON-OPERATING TEMPERATURE LIMITS	SENSORS	-50°C to +100°C
	ELECTRONICS	-40°C to +125°C
SAFETY CONSIDERATIONS		NO SPECIAL CARE NEEDED

SHOCK PROTECTION DURING BOOST.	PROTECT OPTICS FROM LAUNCH SHOCKS	MARINER C. SPECIFICATION. DESIGN TO MINIMIZE SHOCK.
$\lambda = 9.6 \times 10^{-6}$ HR^{-1} (SENSORS AND ELECTRONICS) $\lambda = 20.0 \times 10^{-6}$ HR^{-1} (OPTICS AND MECHANICAL)	λ (OPTICS AND MECHANICAL) = 10.0×10^{-6} HR^{-1}. λ (PHOTOSURF. & ELECT.) = 27.7×10^{-5} HR^{-1}.	$\lambda = 31.6 \times 10^{-6}$ HR^{-1}.
THERMAL RESOLUTION: 2° @ 260°K VISUAL RESOLUTION: 0.5% OVER ALBEDO 0 TO 30%. H_2O ABSORPTION RESOLUTION: 1% OVER RANGE 0 TO 6%.	NOT AVAILABLE.	20 MICROVOLTS/METER
NOT SPECIFIED	1.7 - 2.4 MICRONS, 3.1-4 MICRONS, 5.1-6.6 MICRONS	NOT SPECIFIED
SPATIAL: 0.4 X 0.4 MILLIRADIANS (VISUAL) 0.8 X 3.2 MILLIRADIANS (WATER VAPOR) 0.8 X 0.8 MILLIRADIANS (THERMAL) THERMAL 2° @ 260°K	> 0.06 MICRONS	NOT SPECIFIED
(SAMPLE RATE 1.25 STRIPS/SECOND). ELECTRONIC BAND PASS: - VISUAL ALBEDO 280 CPS; H_2O VAPOR 34 CPS THERMAL BAND 139 CPS	20 CPS.	NOT SPECIFIED
S/N 9.7×10^4 FOR .01 ALBEDO INCREMENT. 2.6 FOR 1% H_2O ABSORPTION. 6.2 FOR 2° THERMAL CHANGE.	S/N PBS >100 PBSE≈100	NOT SPECIFIED
3440 PER STRIP. 4330 PER SECOND. (NEAR PERIAPSIS ONLY)	4×10^4 ORBIT	4×10^3/ORBIT
20 LBS.	27 LBS.	2.7 LBS.
2 LBS.	ELECTRONICS 7 LBS COOLING 3.5 LBS	
14" D X 15" 7" X 7" X 3"	15" X 14" X 8" 8" X 8" X 6"	CROSSED TUBULAR EXTENSIBLE RODS, DIPOLES, 8" AND 3 FT LENGTH 7" X 7" X 6"
3.7 W	1 W	1.6 WATTS TOTAL
-20° TO -40°C (NORMAL RANGE -40C PBS DETECTOR, BY SELF-CONTAINED RADIANT COOLING.) MARINER C SPEC. ENVIRONMENT	-120°C to 0°C 0°C TO +50°C COOLING SYSTEM 0°C TO +50°C	-150°C TO +125°C 0°C TO +50°C
NOT SPECIFIED	-150°C TO +40°C -70°C TO +125°C COOLING: -70°C TO +125°C	-150°C TO +125°C -50°C TO +125°C
NO SPECIAL HAZARDS.	CARE IN INSTALLING AND TESTING PYROTECHNIC DEVICES USED TO REMOVE PROTECTIVE SUPPORTS AND TO IMPLEMENT OPERATION.	NO SPECIAL REQUIREMENTS.

MARINER C SPECIFICATION.	STANDARD MARINER SPECIFICATION
λ (PHOTOSURFACE & ELECTRONICS) = 27.7×10^{-6} HR^{-1} λ (OPTICS & MECH.) = $10.0 \times 10^{-6} HR^{-1}$	$\lambda = 3.5 \times 10^{-6} HR^{-1}$.
NOT SPECIFIED	20 MICROVOLTS/METER
10^6	10^5
0.03 ANGSTROMS @ 1216°A (VARIABLE)	NOT SPECIFIED
1000 - 4000 ANGSTROMS (OR SELECTED BANDS)	20 CPS/CHANNEL
NOT SPECIFIED	S/N 100
2.4×10^6/ORBIT	200 BITS/SEC
20 LBS.	———
3.0 LBS.	2.3 LBS.
9" X 10" X 20" 8" X 8" X 2"	ROD ANTENNAS 75' AND 30' LONG. EXTENDED 6" X 3" X 3"
2 W 10 W	2 W
MARINER C SPECIFICATION. -50°F TO +150°F	MARINER C SPECIFICATION
MARINER C SPECIFICATION	NOT SPECIFIED
NO SPECIAL REQUIREMENTS.	NO HAZARDS

DESIGN TO MEET EARTH, SPACE ENVIRONMENTS	MARINER C SPECIFICATION
$\lambda = 14.3 \times 10^{-6} HR^{-1}$	$\lambda = 12.7 \times 10^{-6} HR^{-1}$
$\pm$ 0.25 GAMMA PER AXIS	TYPICALLY 2 MV RMS OUTPUT/10^7 PARTICLES EM^{-2} SEC^{-1}
$\pm$ 360 GAMMA	ENERGY 30EV to 10 KEV FLUX 30^7 TO 10" CM^{-2} SEC^{-1}
NOT SPECIFIED.	ENERGY $\pm$ 10% FLUX $\pm$ 10^7 CM^{-2} SEC^{-1} DIRECTION OF RELATIVE MOTION WITHIN 5°
5 CPS MAX^M	1 CHANNEL MEASUREMENT/SEC.
NOT SPECIFIED	S/N 0.2 TO 5000.
24 BITS/SAMPLE 1 SAMPLE/MINUTE CAPABILITY WITH READINGS TO BE MADE CONTINUOUSLY THROUGHOUT CRUISE PHASE AND ORBITING PHASE.	NECESSARY TO CORRELATE PLASMA PROBE READINGS WITH MAGNETIC FIELD MEASUREMENT. (6 BITS/MEASUREMENT) (32 CHANNELS) (3 SEGMENTS) (2 POLARITY) + 10 BIT/RELATIVE VELOCITY /20 MIN $\cong$ 1 BIT/SEC ~ $3(10^4)$/ORBIT
$\leq$ 1 LB.	5 LB.
< 5 LBS.	2 LB.
3" D X 5" 2 - 6" X 6" X 2"	10" D X 4" 3 - 6" X 6" X 1"
0.3 W 4.7 W	0.1 WATTS .4 WATTS
40°C TO 55°C -10°C TO +65°C	< 100°C (-10°C TO + 80°C) -10°C TO 50°C
-40°C TO +65°C = -40°C TO +65°C	$\leq$ 300°C < 50°C
NONE	DO NOT OPERATE HIGH VOLTAGE SQUARE WAVE GENERATOR UNTIL OUTSIDE OF EARTH ATMOSPHERE.

MARINER C SPECIFICATION	SEE MARINER C SPEC.
$\lambda = 5.94 \times 10^{-6} HR^{-1}$	$\lambda = 2.1 \times 10^{-6} HR^{-1}$
$E_e > 40$ KEV $E_a > 1.0$ MEV	MOMENTUM $\leq 10^{-5}$ DYNE-SECOND
10^6 CM^{-2} SEC^{-1}	0 TO 10^{-4} CM^{-2} SECOND^{-1}
NONE SPECIFIED	±20% IN MOMENTUM
NONE SPECIFIED	NOT SPECIFIED
NONE SPECIFIED	NOT SPECIFIED
NONE SPECIFIED	5 BITS/HOUR (RANDOM BITS GENERATED BY PARTICLE IMPACTS)
1 POUND	1 POUND
1 POUND	0.2 POUND
1/2" X 3" X 5" 3 - 1/2" X 3" X 5"	1" X 10" X 10" 2" X 3" X 3"
0.1 W 0.9 W	0.01 W 0.2 W
SOLID STATE DETECTOR 20° + 5°C -10°C TO +50°C	< 200°C -10°C TO + 50°C
-20°C TO +100°C -20°C TO +100°C	< 200°C < 50°C
NOT SPECIFIED	NO HAZARD

MARINER C SPECIFICATION	LIFE REQUIREMENT OF OPERATING AND STORAGE AS A VACUUM 250 EARTH DAYS	ENVIRONMENTAL
RELIABILITY $\lambda = 11.9 \times 10^{-6}$ OPERATING TIME: 10^{-4} HOUR^{-1} (CAN BE DESTROYED BY MICROMETEOROID PENETRATION) DORMANT TIME: 10^{-5} HOUR^{-1}	RELIABILITY - = 8.42×10^{-6} HR^{-1} (REAL TIME) = 13.2×10^{-6} HR^{-1} (NON REAL TIME)	PERFORMANCE PARAMETERS RELIABILITY
~1 PULSE/ (5×10^5 MINIMUM IONIZING PARTICLES INCIDENT) SENSITIVE TO PROTONS: >10 MEV. ELECTRONS: >1/2 MEV: α : > 40 MEV	NOT SPECIFIED	SENSITIVITY
10 ION CM^{-3} ATM^{-1} TO 1000 ION CM^{-3} ATM^{-1}	NOT SPECIFIED	DYNAMIC RANGE
$\pm$0.5%	NOT SPECIFIED	RESOLUTION
1 MEASUREMENT/(37 SECOND SAMPLING INTERVAL)	NOT SPECIFIED	SENSOR RESPONSE
S/N > 100/1	NOT SPECIFIED	SIGNAL CHARACTERISTICS
(5 BITS/MEASUREMENT) (12 MEASUREMENT/HR.) (18 HR/ORBIT) = 10^3 BITS/ORBIT (THIS RATE IS REDUCED BY A FACTOR OF 12 OUTSIDE THE MARS MAGNETOSPHERE.	TELEMETRY FOR APPROXIMATELY FIRST 10% OF MISSION TMY BIT RATE 33 1/3 BPS, the BALANCE AT 8 1/3 BPS. NOMINAL TOTAL BITS - ON TAPE MACHINE DURING 144 SECONDS FRAME IS 516,168.	BIT RATE
1.2 POUND	N/A	PHYSICAL CHARACTERISTICS AND CONSTRAINTS SENSOR WEIGHT
0.2 POUND	ELECTRONICS - 55 POUNDS	ELECTRONICS
5"D SPHERE + 2"D X 4"	ELECTRONICS 1 FT^3	SENSOR ELECTRONICS VOLUME
10^{-10} WATTS 0.3 WATTS	ELECTRONICS - 25 W	SENSOR ELECTRONICS POWER
-50°C TO +125°C -10°C TO 50°C	-10°C TO 80°C	SENSOR ELECTRONICS OPERATING TEMPERATURE LIMITS (SELF CONTROLLED)
$\leq$300°C < 50°C	-55°C TO +125°C	SENSORS ELECTRONICS NON-OPERATING TEMPERATURE LIMITS
NO HAZARDS	NO SPECIAL	SAFETY CONSIDERATIONS

During flight the magnetics measurement experiment would require:

1) Magnetometer calibration by current injection into each of the orthogonal Helmholtz coil balancers;
2) Vehicle rotation in two orthogonal planes (after Mars trajectory injection, midcourse correction, capsule separation, and Mars orbit) to determine spacecraft magnetic bias at the magnetometer;
3) Range switching of the helium magnetometer to prevent saturation. (The present unit has a range of $\pm$ 350, which may be extended incrementally to $\pm$ 20,000, if desired.);
4) Mars orbit data sufficient to establish a reference plance and altitude from which a magnetic profile map of the near Mars magnetic field may be constructed.

4.5.4.4 Mapping

The mapping experiment has a very strong interaction with the total spacecraft system. It has been chosen as a typical experiment to describe in this study in enough detail to indicate some of the system consideration involved in incorporating this experiment.

Measured in bits of data returned, the maps of Mars have the most overwhelming importance. Even the purpose of the experiments in orbit are primarily to make images of Mars' surface, particularly from 40 degrees south to 10 degrees north latitude. By the planned repetition of these maps in 30 to 90 days, presence of life might be inferred from seasonal growth, as is suggested in Figure 4.5-3.

Optimizing these images involves most of the orbital parameters and, simultaneously, many of the camera design parameters. These relationships are shown in Figure 4.5-4. The extent of these interfaces necessitate a close coordination between the spacecraft and experiment designer.

Ground Resolution Over Zone of Interest--The static resolution capability of the camera system is a function of its photosurface. Within wide limits, ground-resolution requirements can be achieved when the focal length of the camera lens is designed to provide proper resolution at the desired orbit altitude. However, image motion caused by orbital velocity, vehicle motion within limit cycle, and planetary rotation causes smear that degrades the static resolution capability. Figure 4.5-5 shows the relative contributions of these factors. Figure 4.5-6 shows that for a specific camera system there is an optimum orbit altitude. The two

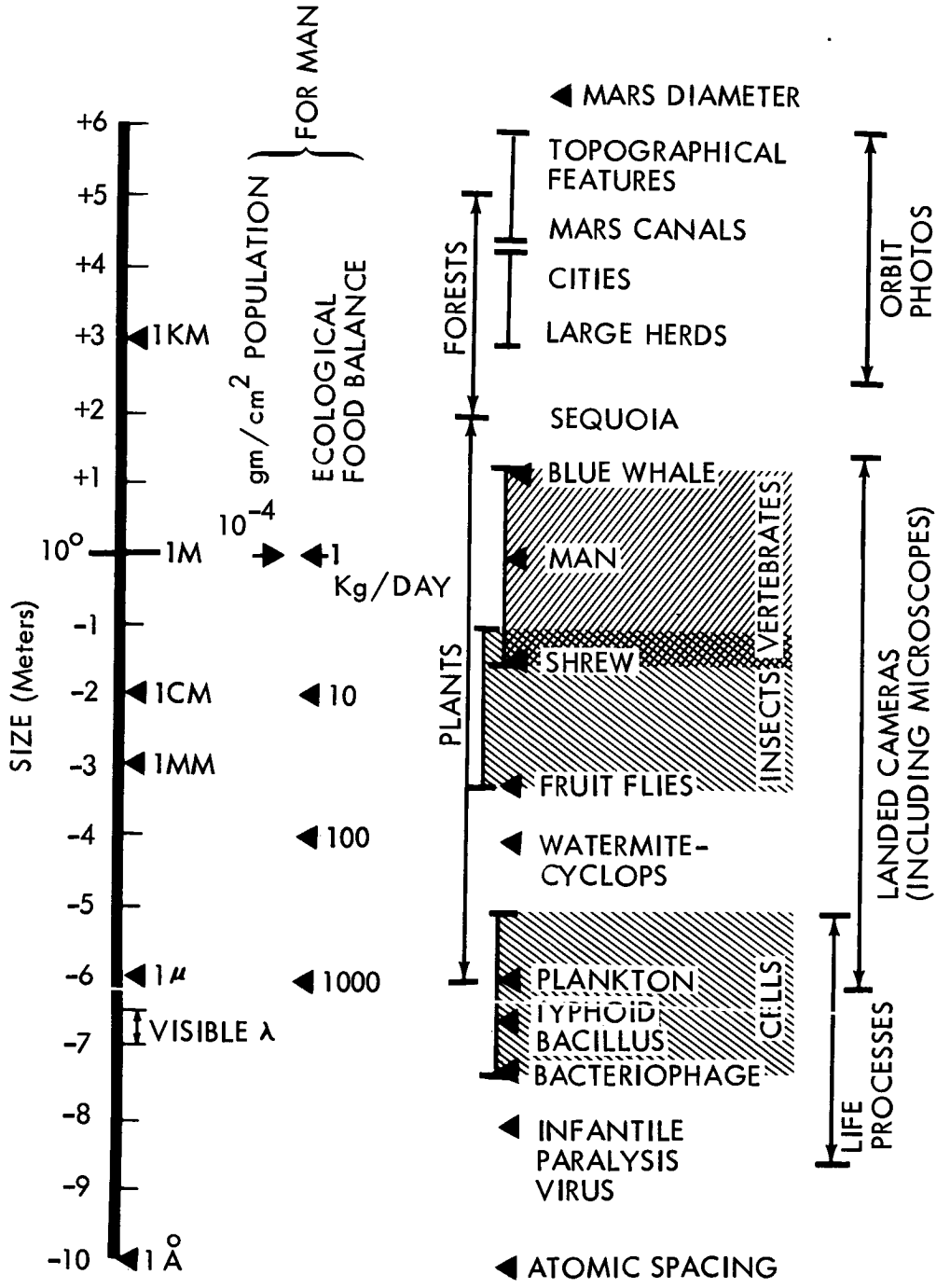

Figure 4.5-3: Size of Biological Phenomena

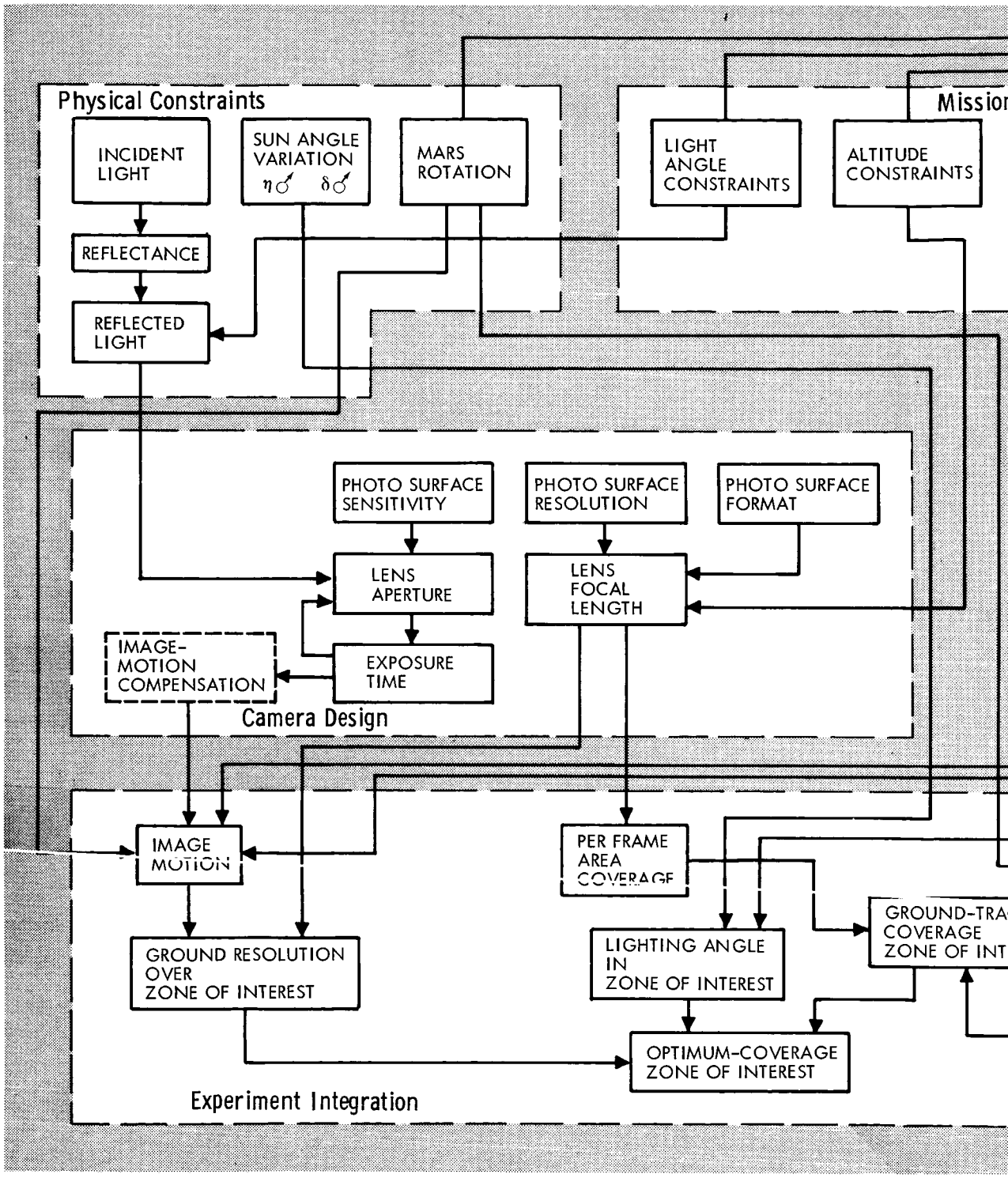
Physical Constraints
Mission
INCIDENT LIGHT
SUN ANGLE VARIATION
MARS ROTATION
LIGHT ANGLE CONSTRAINTS
ALTITUDE CONSTRAINTS
REFLECTANCE
REFLECTED LIGHT
PHOTO SURFACE SENSITIVITY
PHOTO SURFACE RESOLUTION
PHOTO SURFACE FORMAT
LENS APERTURE
LENS FOCAL LENGTH
IMAGE-MOTION COMPENSATION
EXPOSURE TIME
Camera Design
IMAGE MOTION
PER FRAME AREA COVERAGE
GROUND-TRA
COVERAGE
ZONE OF INT
GROUND RESOLUTION OVER ZONE OF INTEREST
LIGHTING ANGLE IN ZONE OF INTEREST
OPTIMUM-COVERAGE ZONE OF INTEREST
Experiment Integration

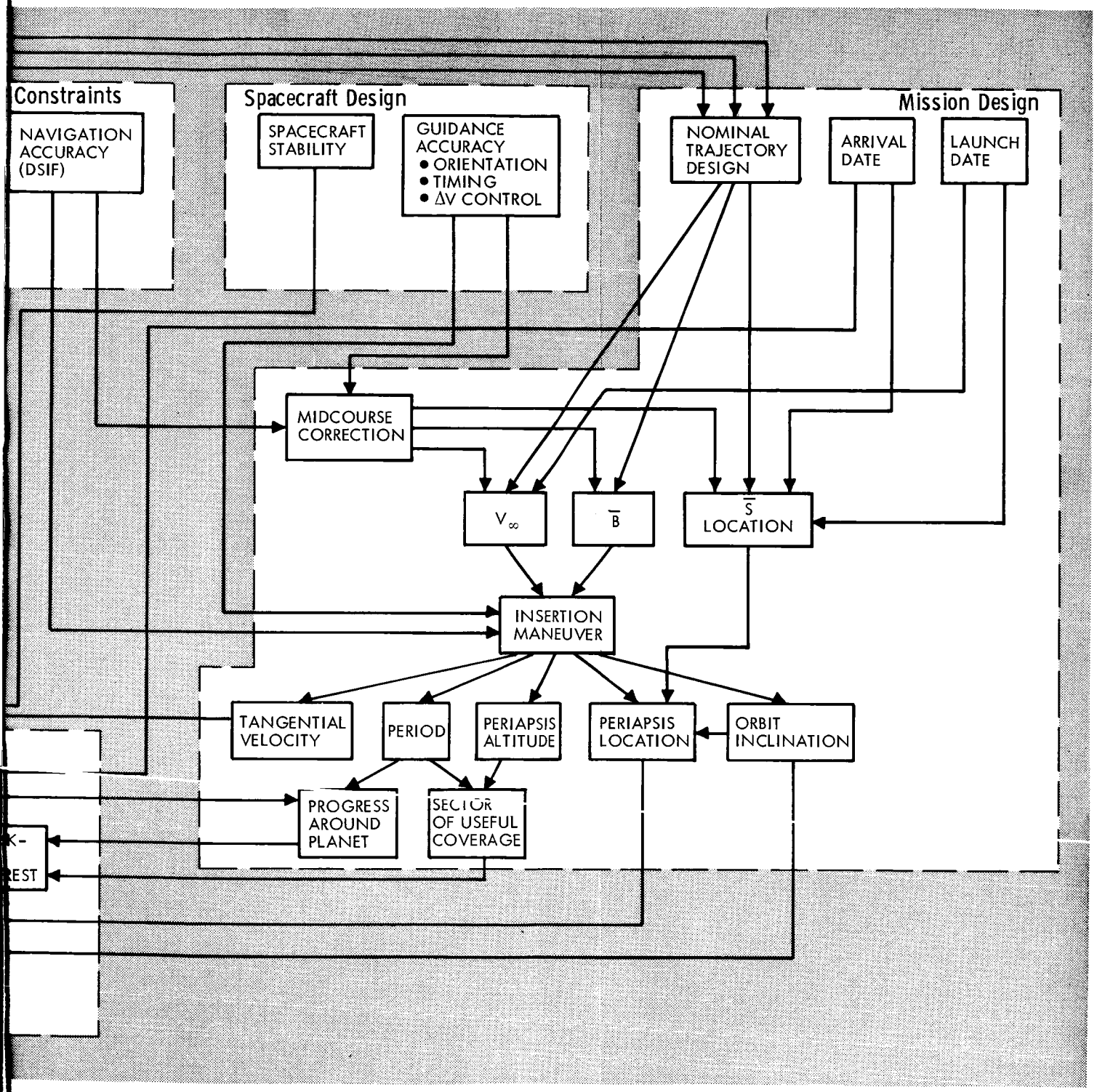

Figure 4.5-4: IMAGING EXPERIMENT PARAMETRIC LOGIC DIAGRAM

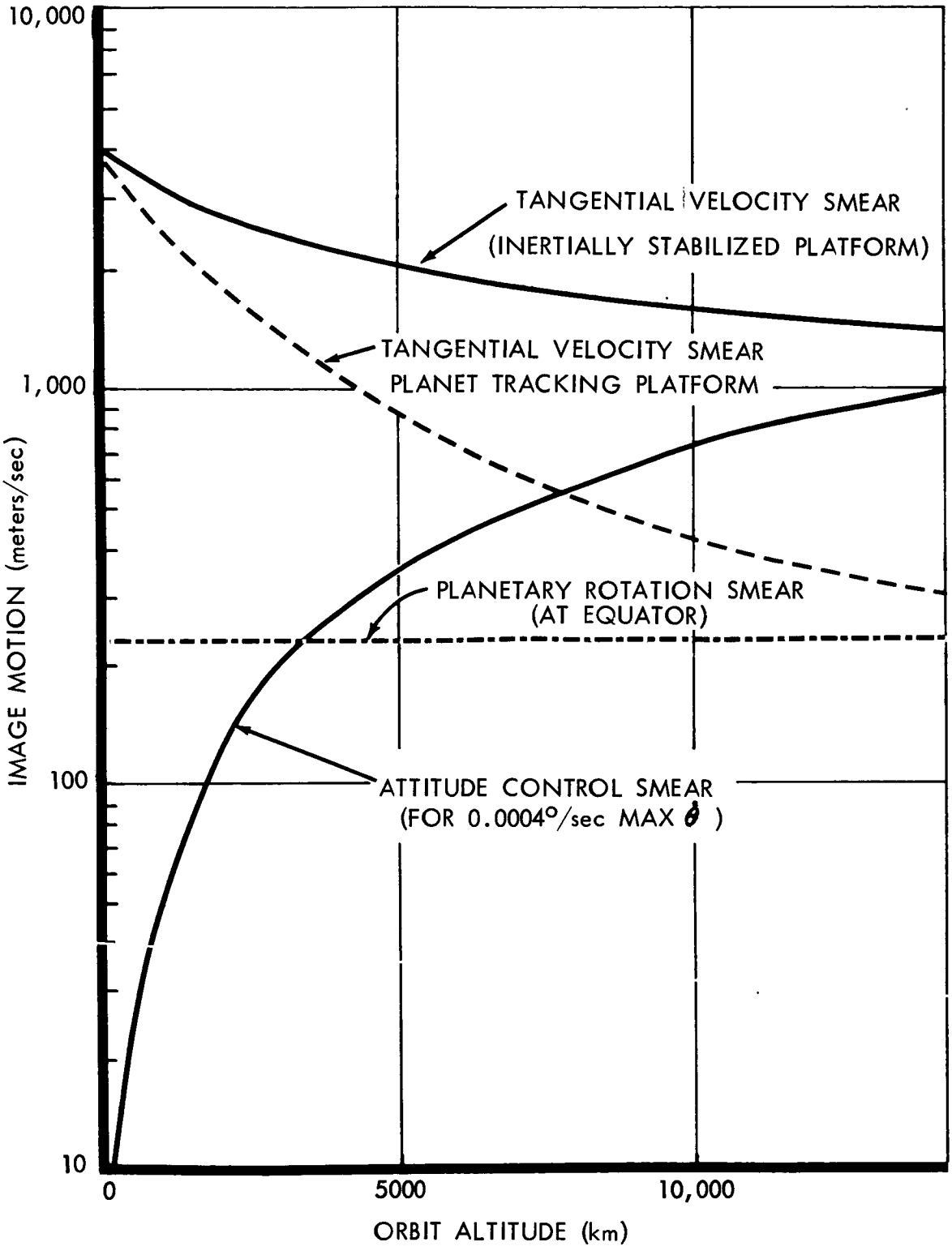

Figure 4.5-5: Image Smear Components

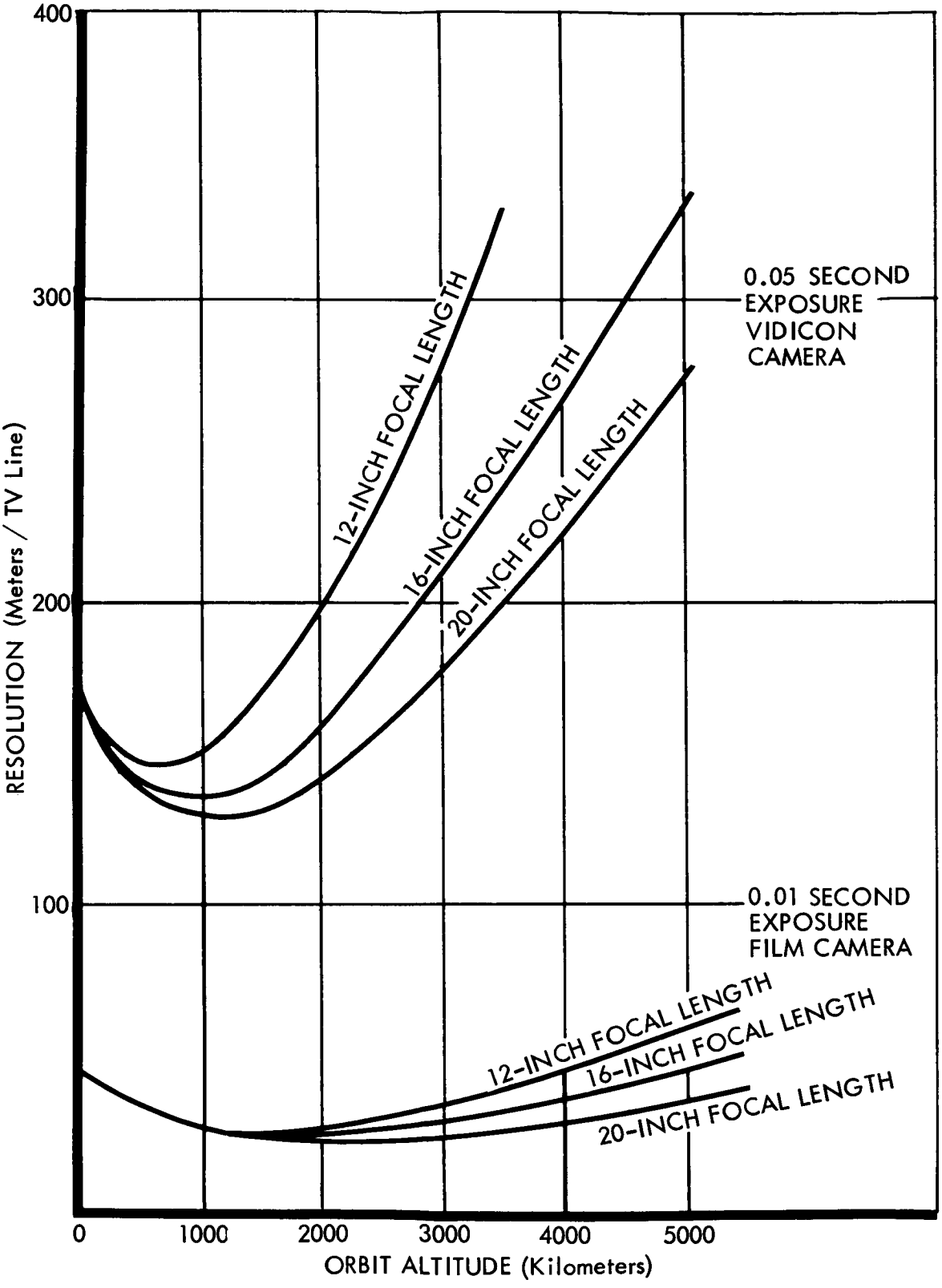

Figure 4.5-6: Resultant Resolution Versus Altitude — Planet Tracking Scan Platform and No IMC

systems used as examples are a typical 400-line vidicon camera system and a high-resolution film camera, such as that used on the Lunar Orbiter.

Ground Track Coverage--The total area coverage capability of the system depends on the per-frame area coverage, the sector of useful coverage, the progress (longitudinal spacing between adjacent orbits), and the total number of orbits before repetition. The per-frame coverage is determined solely by the spacecraft altitude once the photo-surface dimensions and focal length are selected.

The sector of useful coverage is the portion of the orbit wherein the resolution is satisfactory. Ground resolution, measured in lines per kilometer, decreases as the spacecraft moves away from periapsis. For this discussion it is assumed that the sector of useful coverage is limited at the points where the orbit altitude is two times the periapsis altitude.

To expand coverage of the zone of interest, the periapsis should be centered therein, insofar as possible. Factors influencing its location are:

1) Time of arrival (influences position of $\bar{S}$), Figure 4.5-7;
2) Hyperbolic approach velocity (influences angle between periapsis and $\bar{S}$), Figure 4.5-8;
3) Periapsis altitude (influences angle between periapsis and $\bar{S}$), Figure 4.5-8.

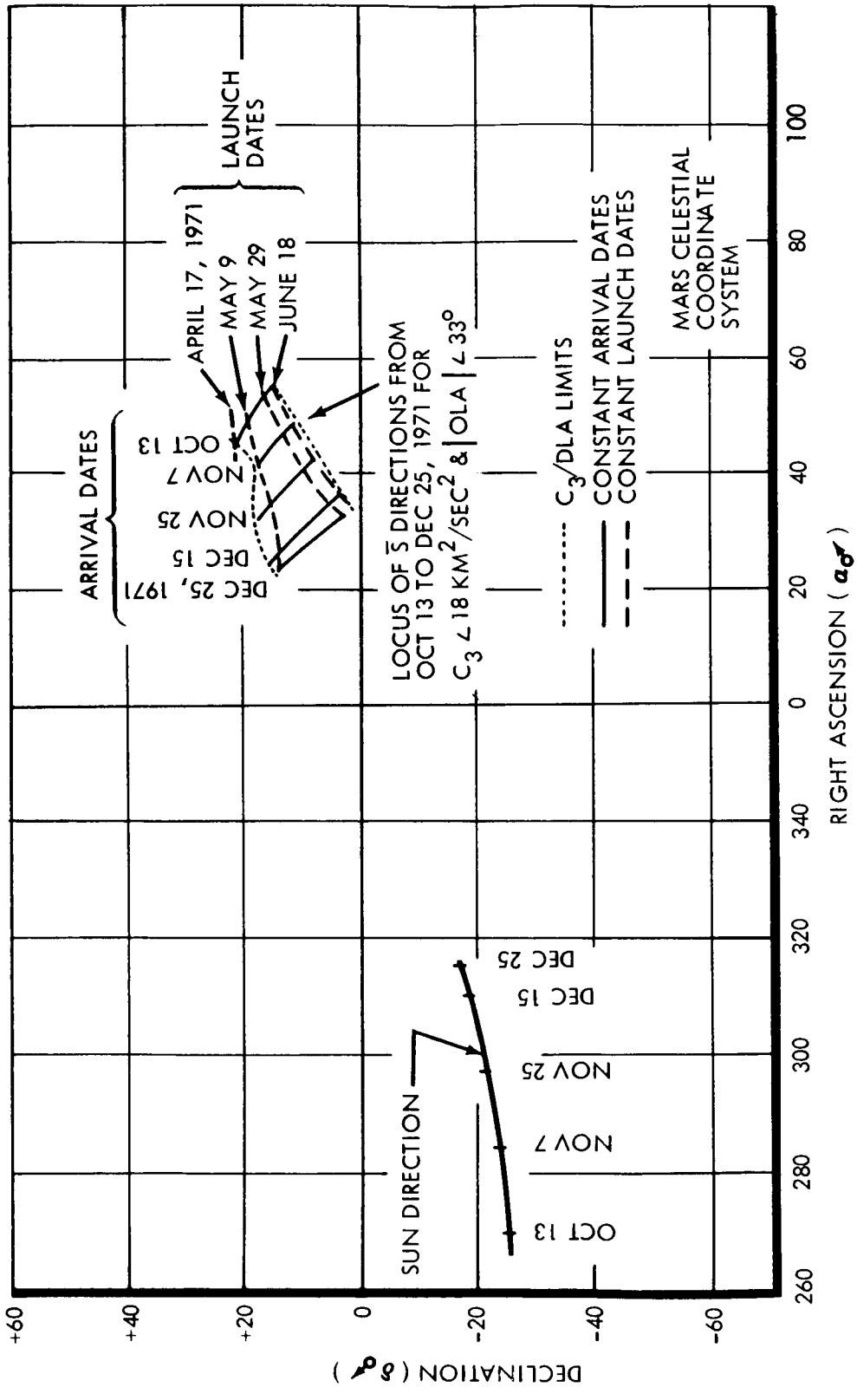

Figure 4.5- 7: Relative Direction of Sun and Approach Asymptote

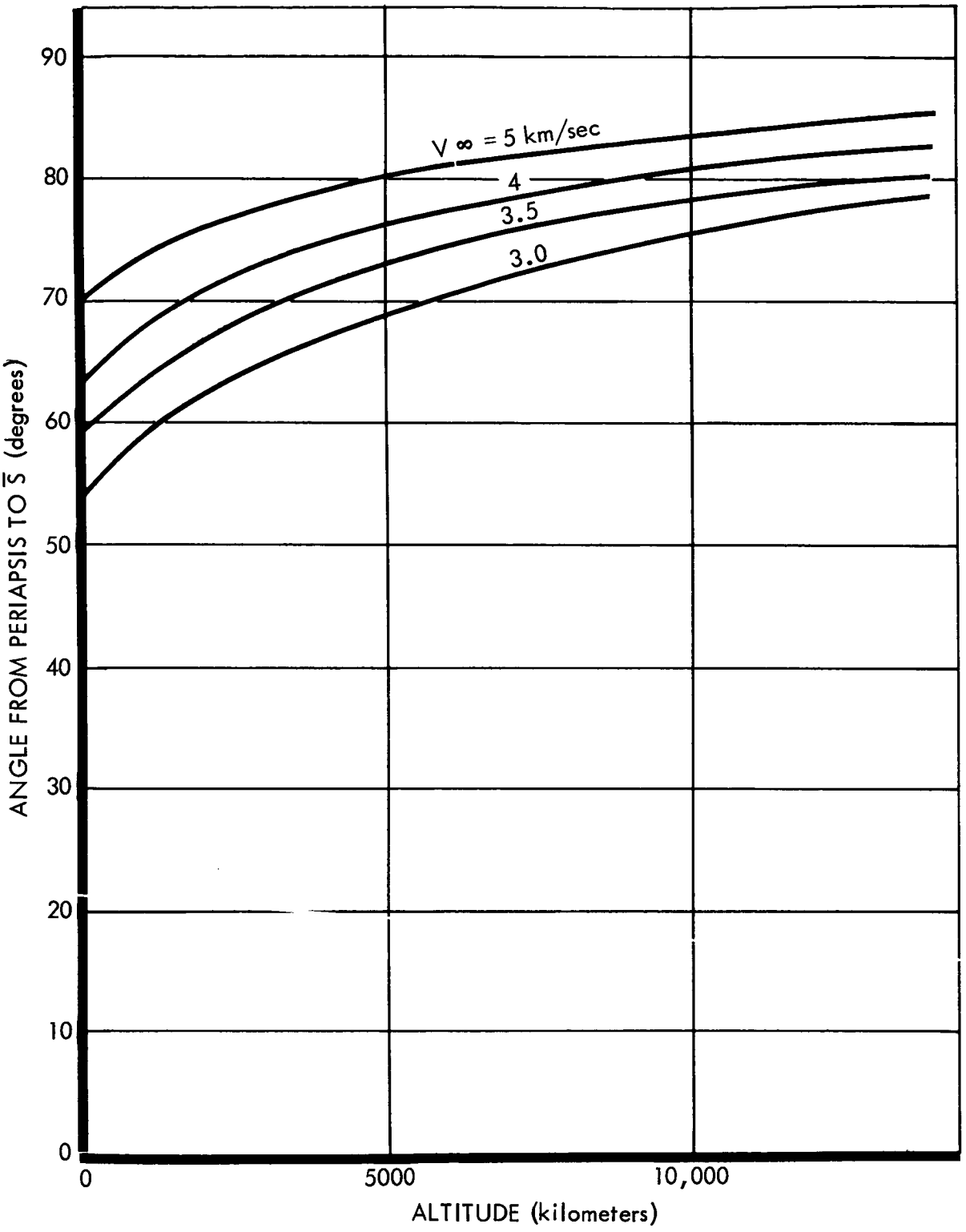

Figure 4.5-8: Effect of Hyperbolic Approach Velocity on Periapsis Location

Figure 4.5-9 shows the location of the sector of useful coverage for arrival dates of October 31, 1971; November 7, 1971; and December 25, 1971. Locations are shown in a Mars-centered celestial coordinate system. (Zero degrees RA is vernal equinox in northern Mars hemisphere.)

As the spacecraft passes through the sector of useful coverage on successive orbits, successive ground tracks are traced out over the surface of Mars. Per the mission guidelines, these ground tracks should progress uniformly around the surface of Mars, returning to the same general area within a period of 30 to 90 days (See Figure 4.5-10). The progress (the change in longitude between adjacent ground tracks) is a compromise between the desirability of obtaining continuous coverage and the requirement to return to the original area in the desired period of time. The orbit period would be adjusted to be nearly, but not exactly some harmonic ratio, such as 1/2, 1/1, 3/4, 5/4, of the planet rotational period. Figure 4.5-11 shows the progress as a function of deviation from the harmonic period. The chosen harmonic ratio is not particularly important to the science subsystem.

Lighting Angle--Figure 4.5-12 shows the relative position of the equiangular Sun lines 10 and 50 degrees above thehorizon on several dates during the potential orbiting mission. Figure 4.5-13 shows a typical orbit as it passes through the zone of good lighting. From a knowledge of the progress of the ground track and the change in lighting angle with time, plots can be made of the actual ground coverage under specific lighting conditions. This is shown in Figure 4.5-14 for a number of orbits.

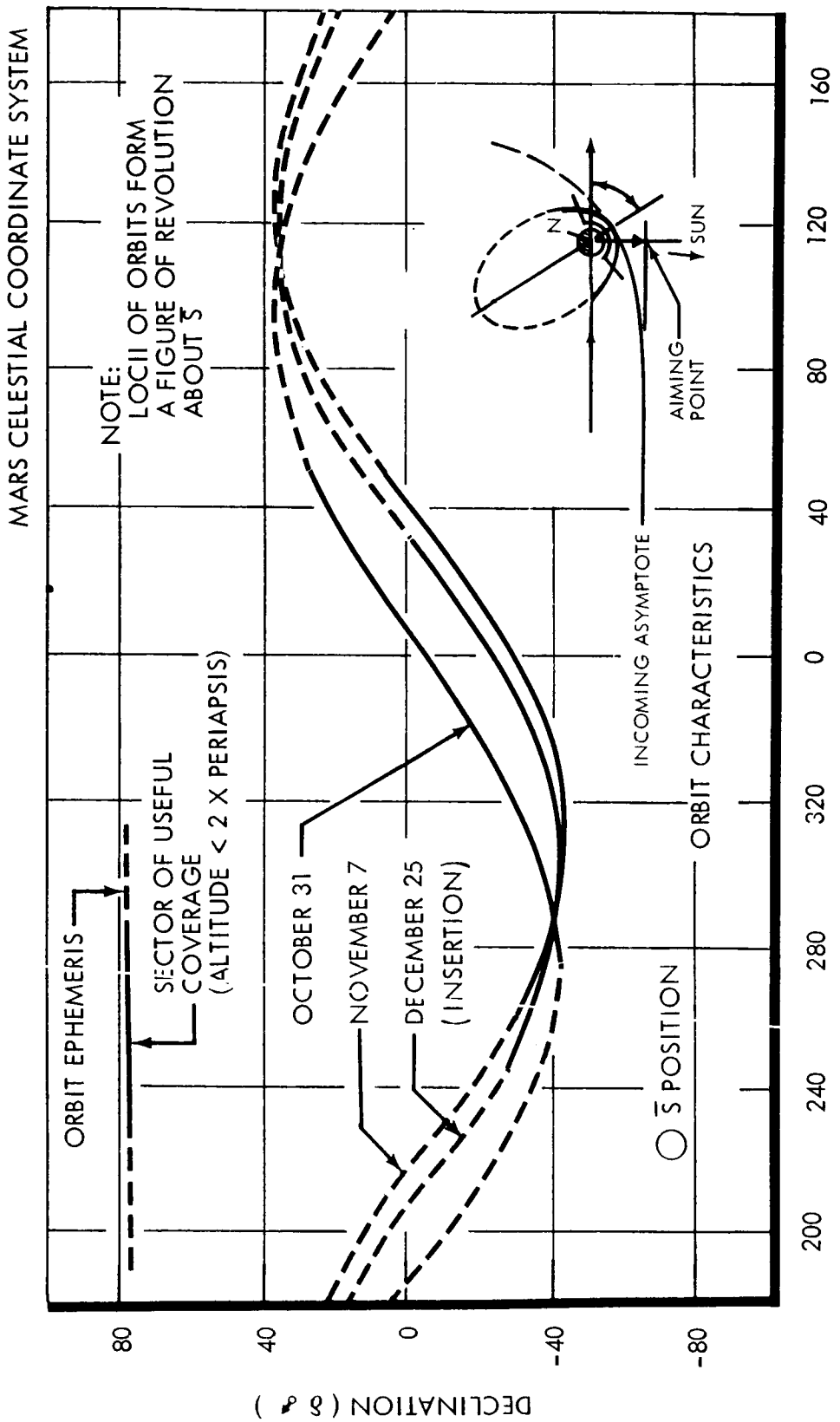

Figure 4.5-9: Sector of Useful Coverage — 40° Orbits

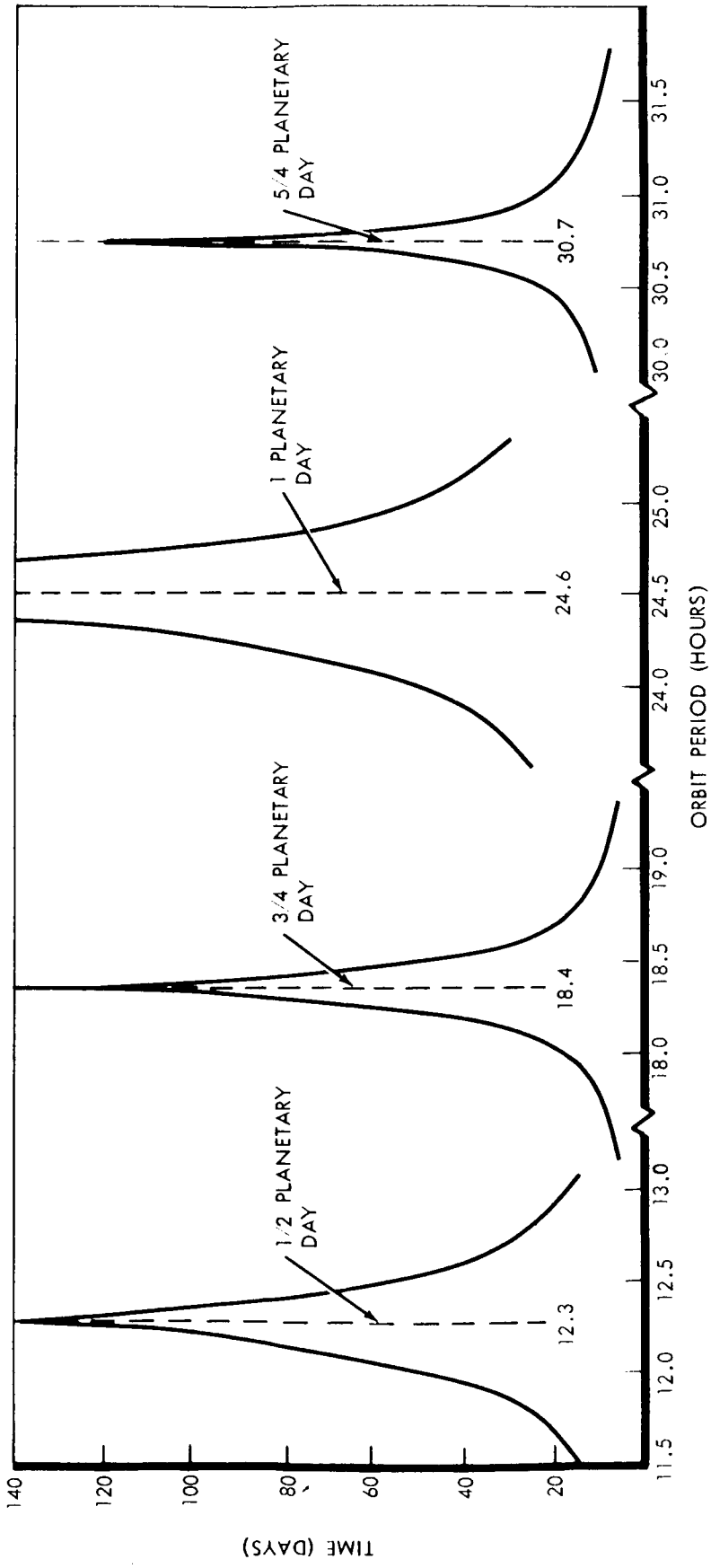

Figure 4.5-10: Orbit Period versus Time to Return

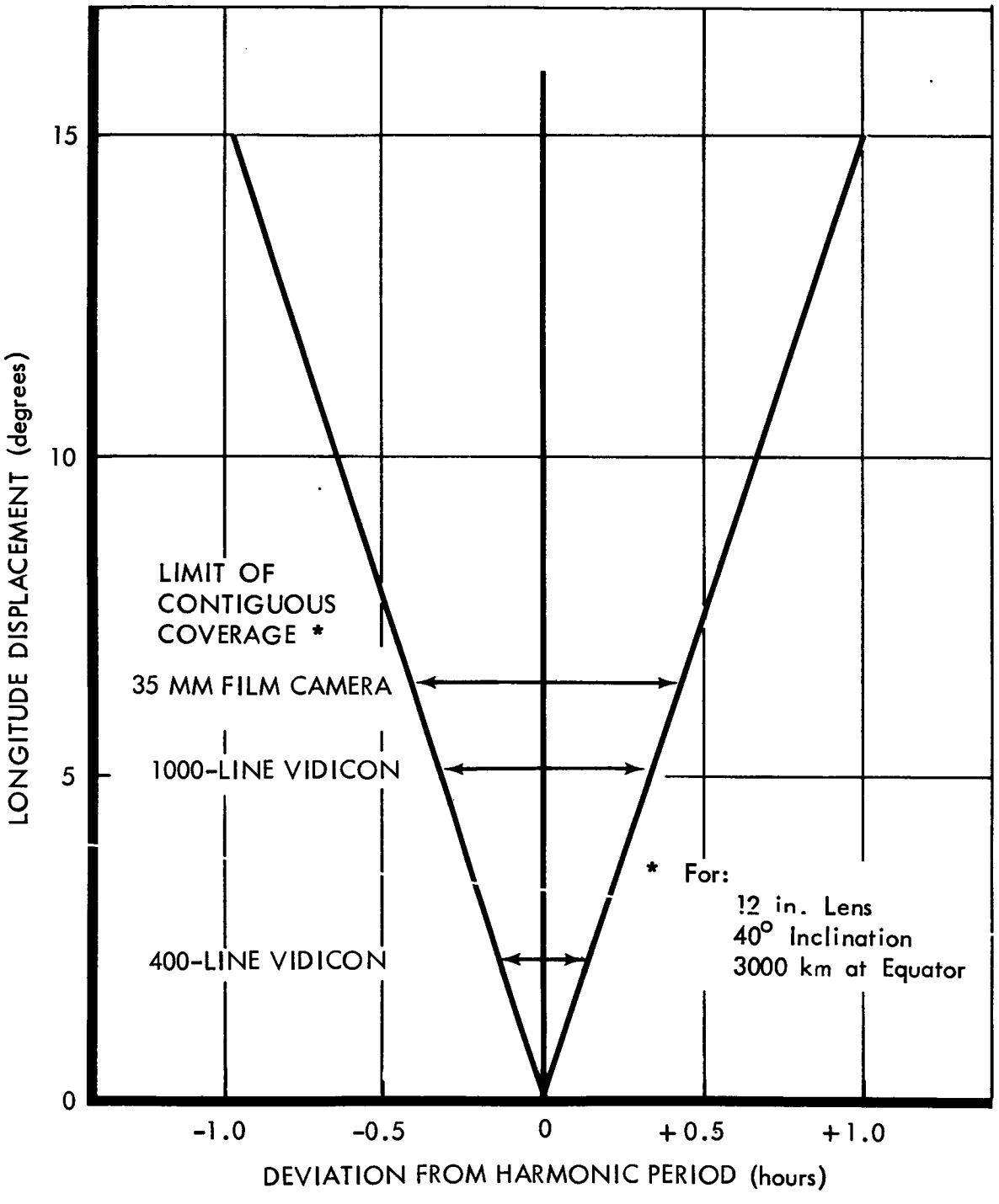

Figure 4.5-11: Progress of Ground Track versus Deviation From Harmonic Period

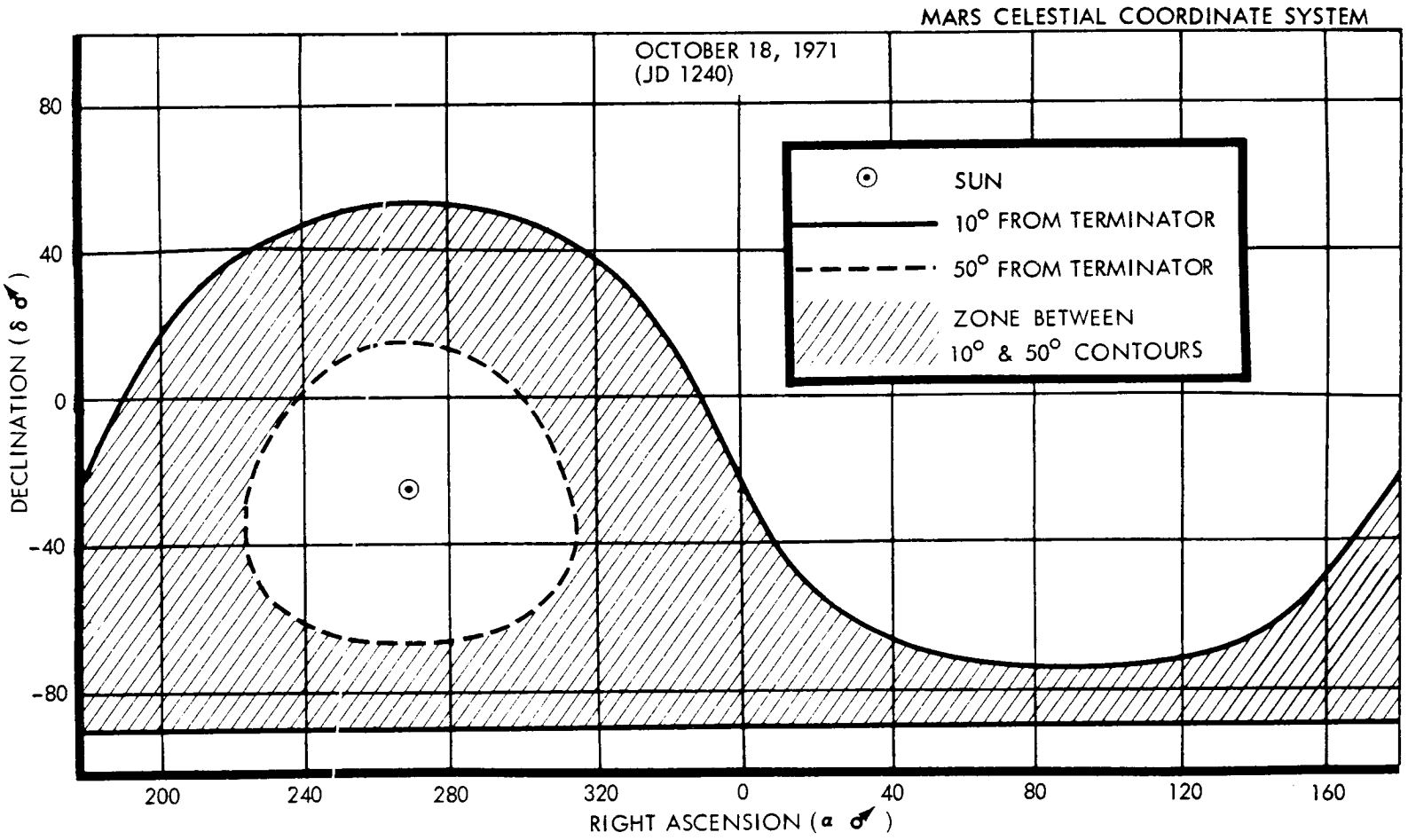
MARS CELESTIAL COORDINATE SYSTEM
OCTOBER 18, 1971
(JD 1240)
SUN
10° FROM TERMINATOR
50° FROM TERMINATOR
ZONE BETWEEN
10° & 50° CONTOURS
80
40
0
-40
-80
DECLINATION (δ ♂)
200
240
280
320
0
40
80
120
160
RIGHT ASCENSION (α ♂)

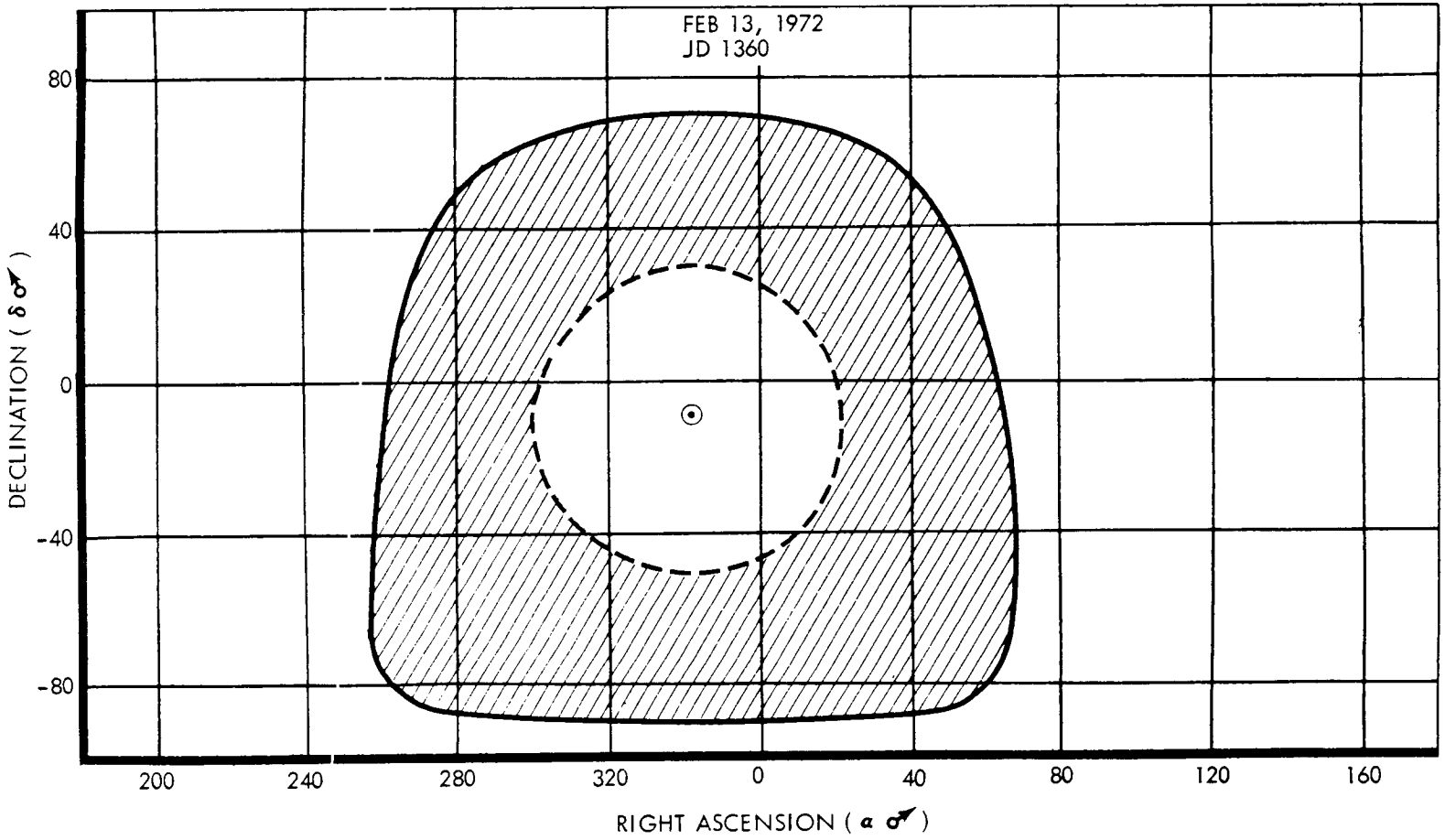
FEB 13, 1972
JD 1360
80
40
0
-40
-80
DECLINATION (δ ♂)
200
240
280
320
0
40
80
120
160
RIGHT ASCENSION (α ♂)

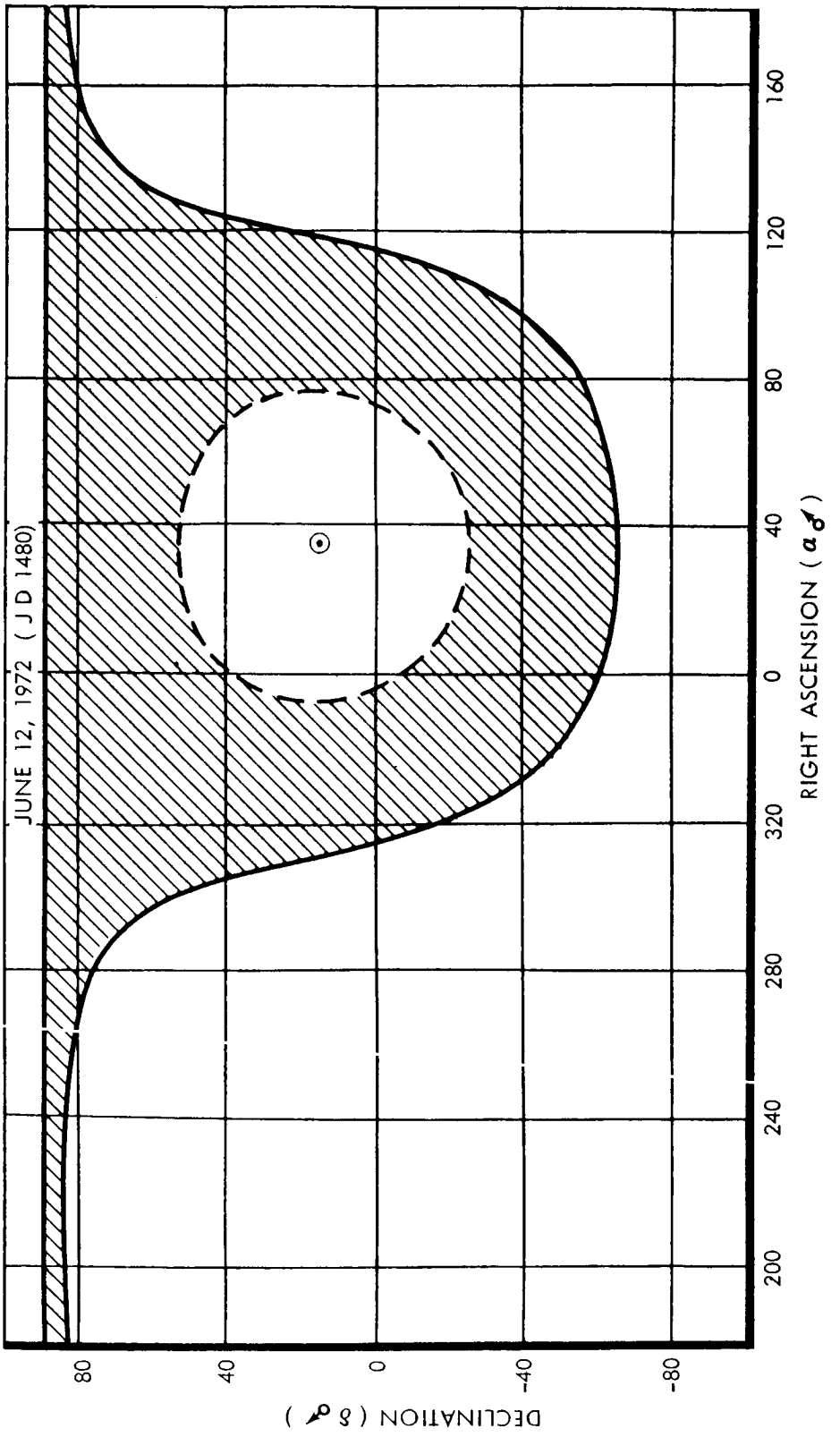

Figure 4.5-12: Light-Angle Contours

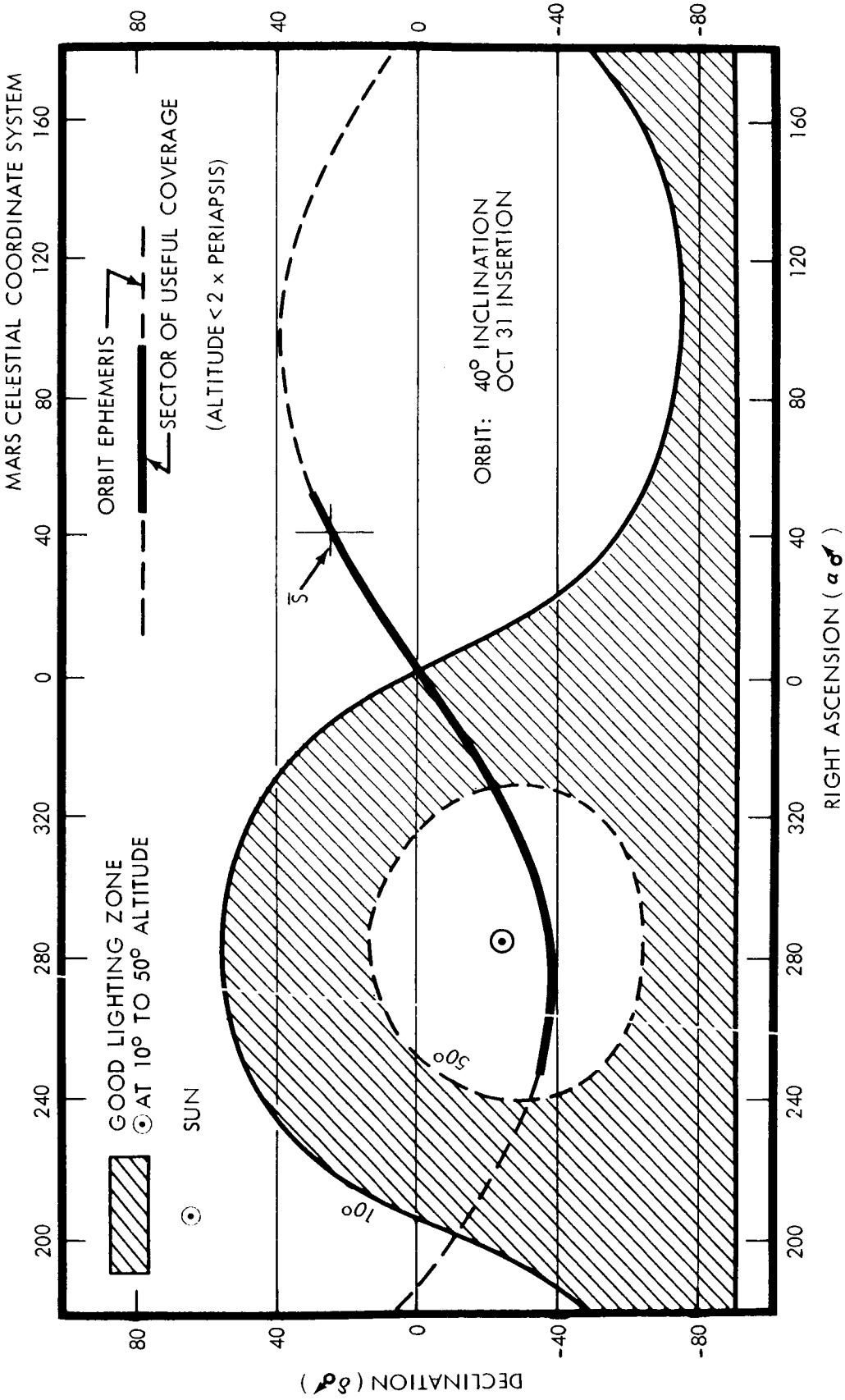

Figure 4.5-13: Sector of Useful Coverage in Good Lighting on October 31, 1971

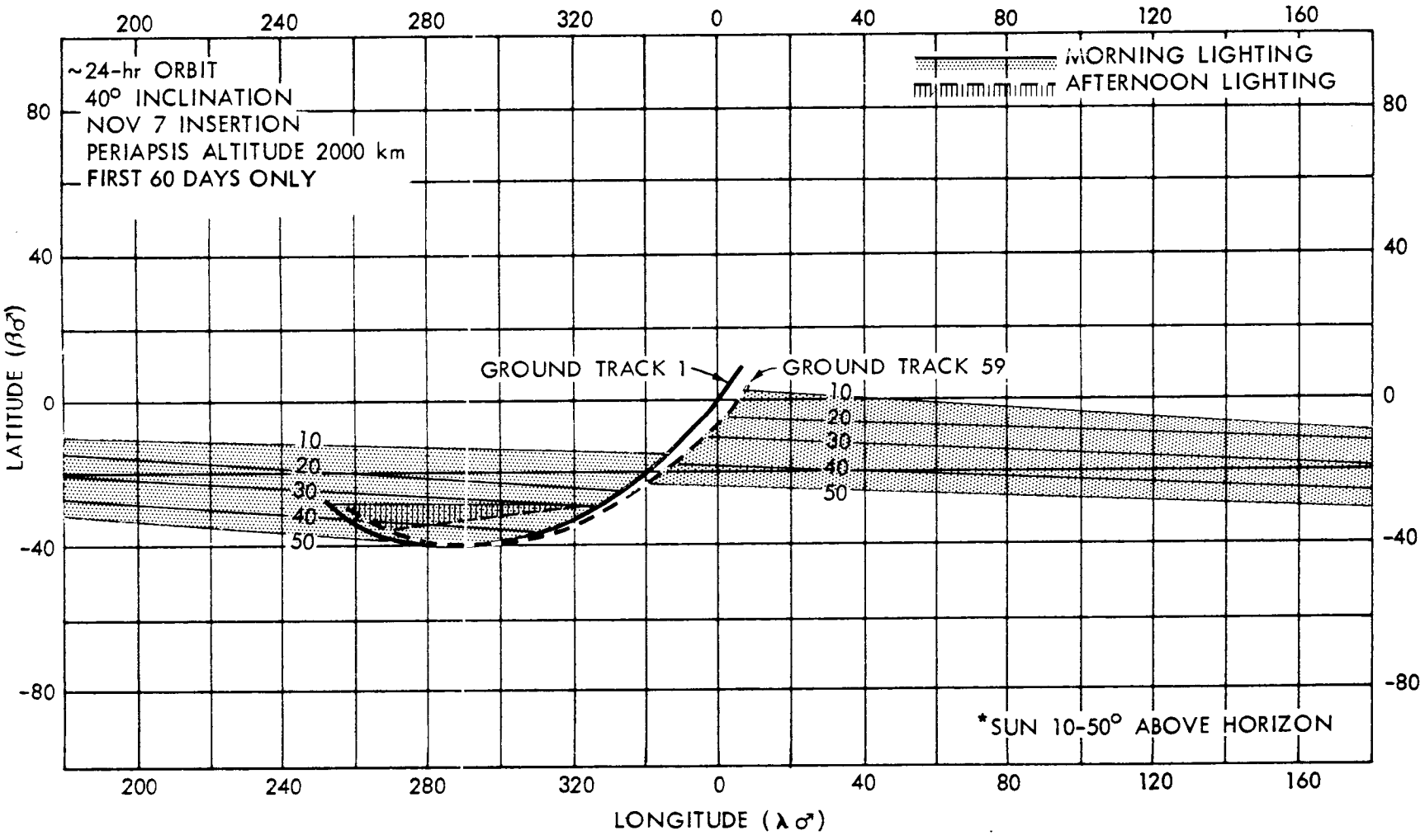
~24-hr ORBIT
40° INCLINATION
NOV 7 INSERTION
PERIAPSIS ALTITUDE 2000 km
FIRST 60 DAYS ONLY
MORNING LIGHTING
AFTERNOON LIGHTING
GROUND TRACK 1
GROUND TRACK 59
10
20
30
40
50
*SUN 10-50° ABOVE HORIZON
LATITUDE (β♂)
LONGITUDE (λ♂)
200
240
280
320
0
40
80
120
160
80
40
0
-40
-80

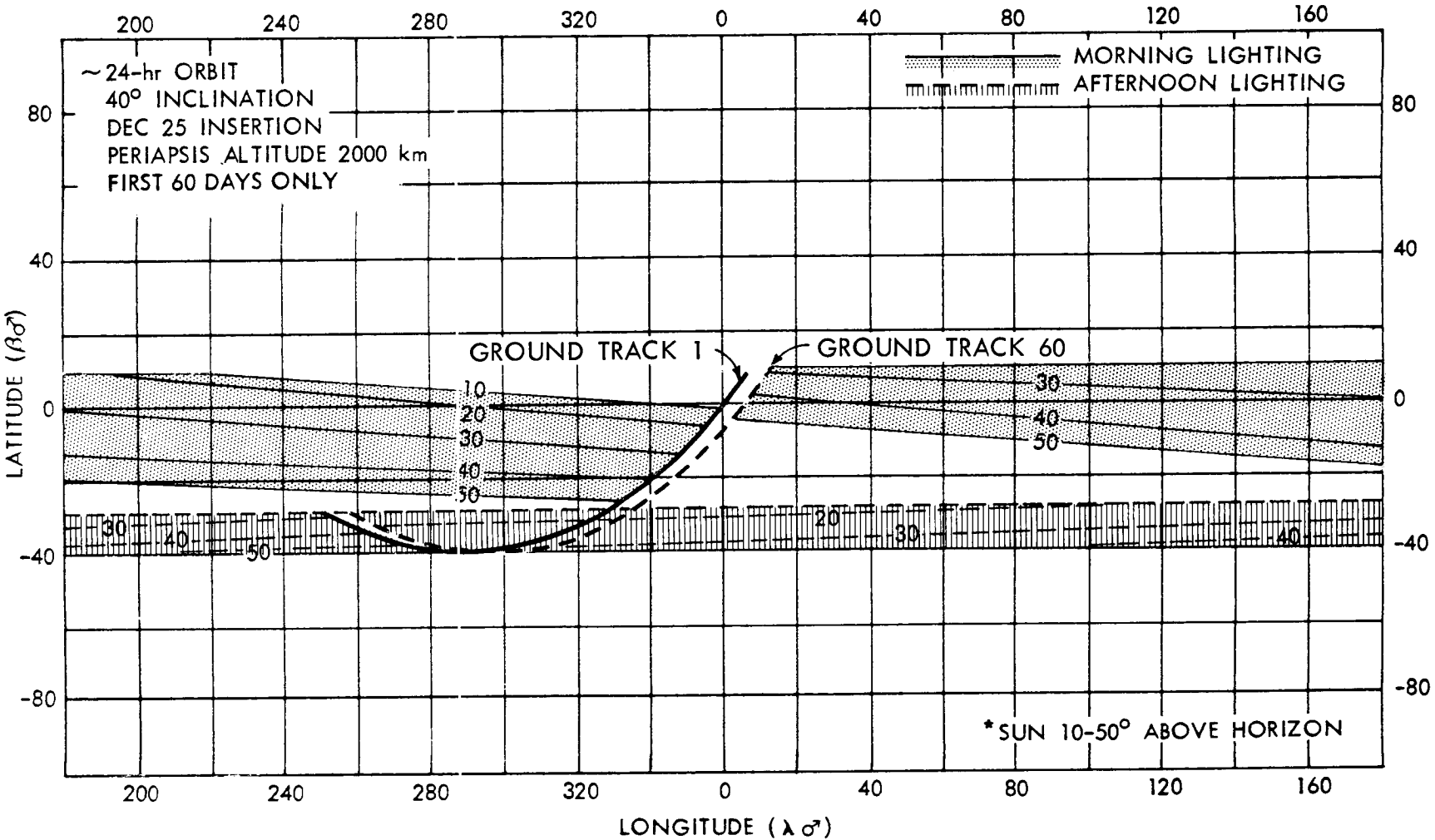
~24-hr ORBIT
40° INCLINATION
DEC 25 INSERTION
PERIAPSIS ALTITUDE 2000 km
FIRST 60 DAYS ONLY
MORNING LIGHTING
AFTERNOON LIGHTING
GROUND TRACK 1
GROUND TRACK 60
10
20
30
40
50
*SUN 10-50° ABOVE HORIZON
LATITUDE (β♂)
LONGITUDE (λ♂)
200
240
280
320
0
40
80
120
160
80
40
0
-40
-80

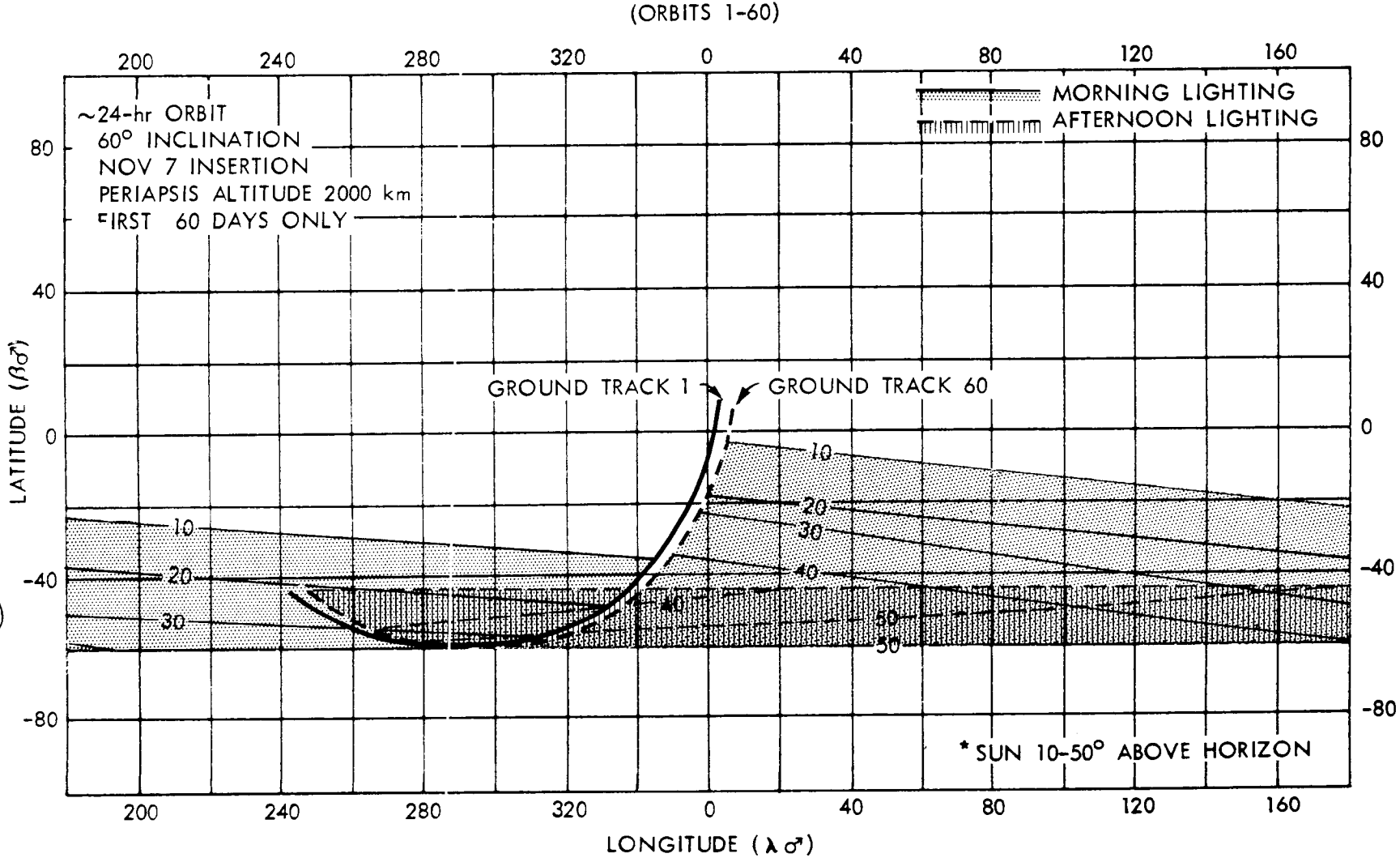
(ORBITS 1-60)
200
240
280
320
0
40
80
120
160
~24-hr ORBIT
60° INCLINATION
NOV 7 INSERTION
PERIAPSIS ALTITUDE 2000 km
FIRST 60 DAYS ONLY
MORNING LIGHTING
AFTERNOON LIGHTING
GROUND TRACK 1
GROUND TRACK 60
10
20
30
40
50
80
40
0
-40
-80
LATITUDE (βσ')
* SUN 10-50° ABOVE HORIZON
LONGITUDE (λσ')

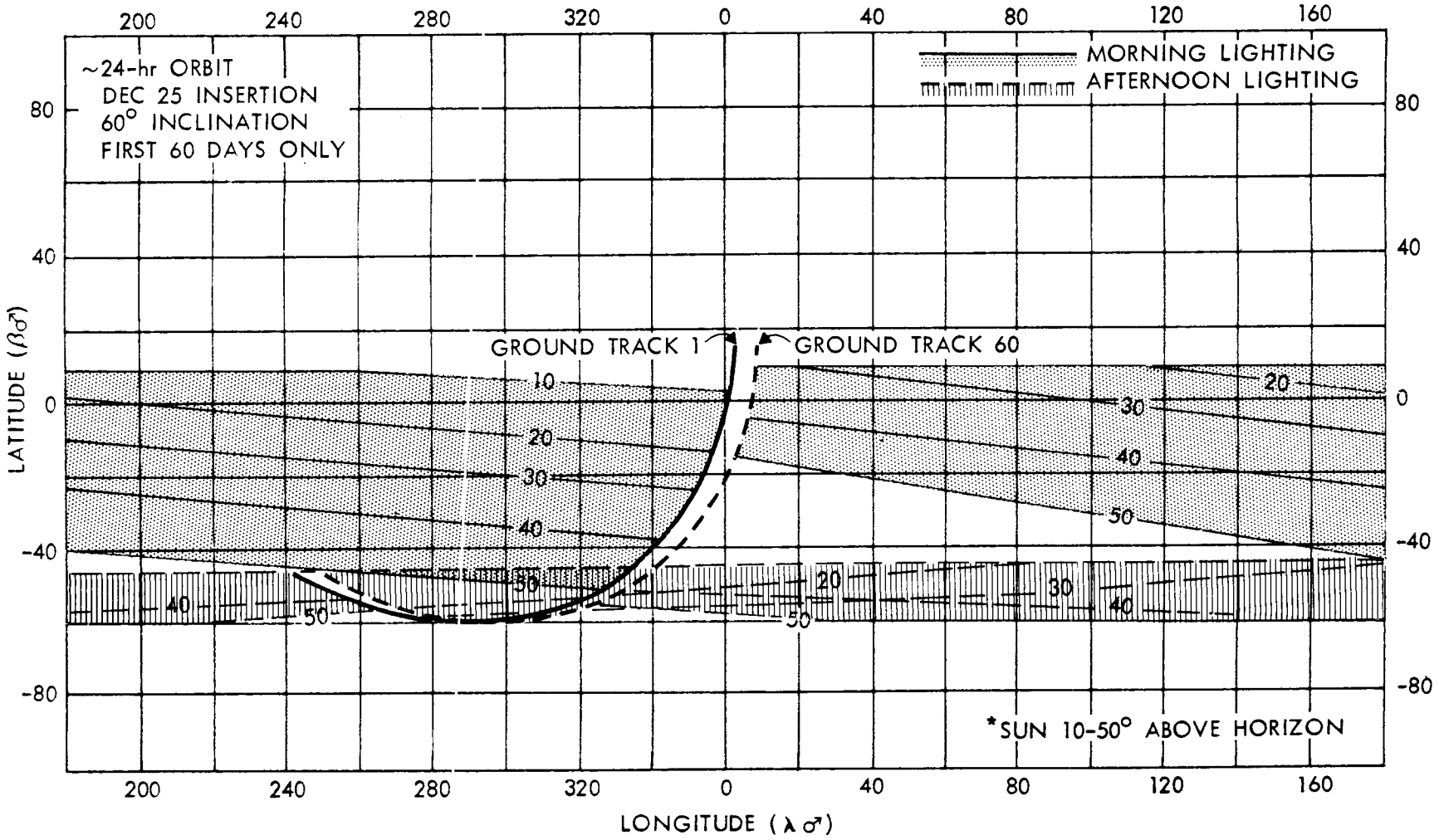
~24-hr ORBIT
DEC 25 INSERTION
60° INCLINATION
FIRST 60 DAYS ONLY
MORNING LIGHTING
AFTERNOON LIGHTING
GROUND TRACK 1
GROUND TRACK 60
10
20
30
40
50
*SUN 10-50° ABOVE HORIZON
LATITUDE (βσ♂)
LONGITUDE (λσ♂)
200
240
280
320
0
40
80
120
160
80
40
0
-40
-80

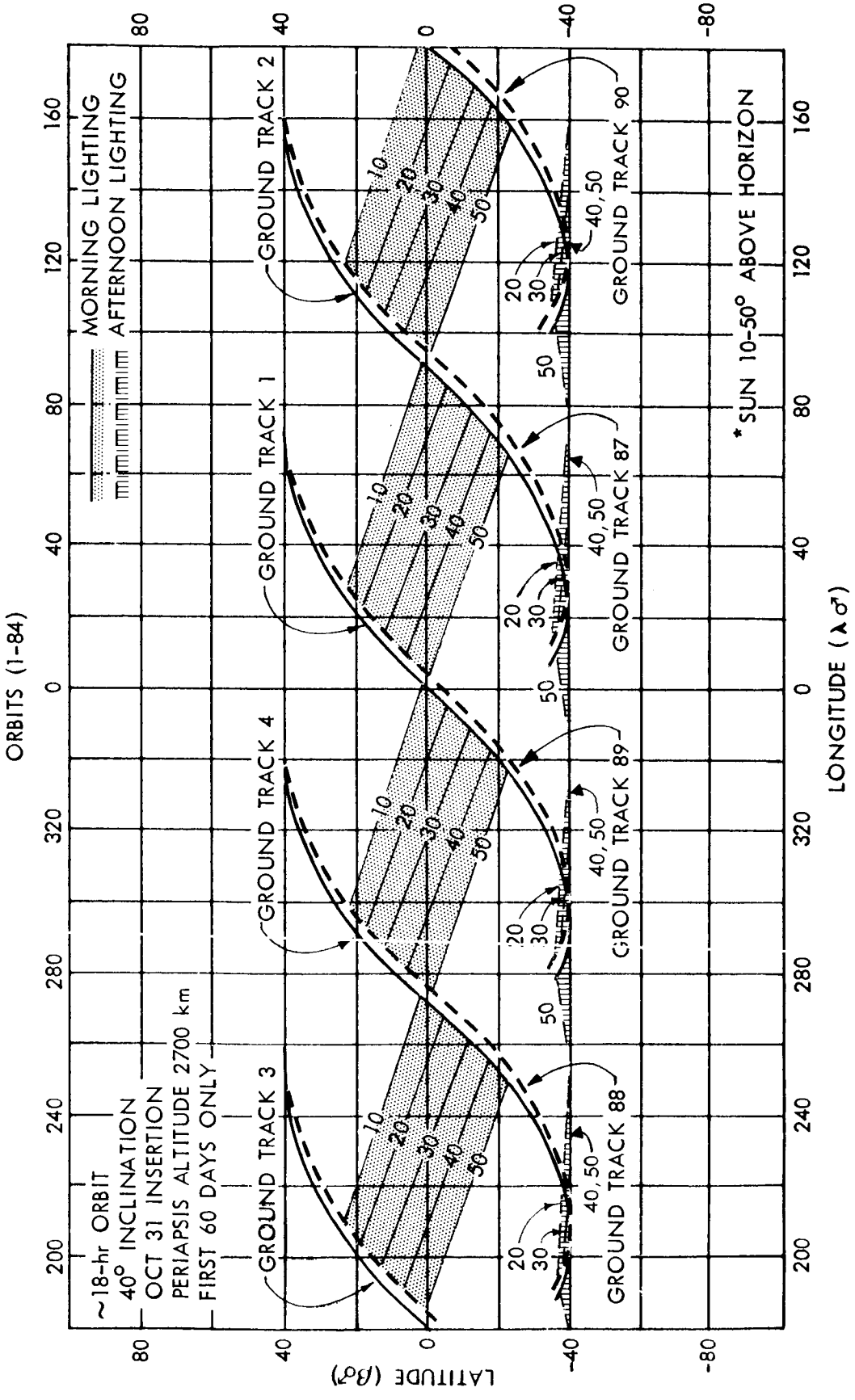

Figure 4.5-14: Surface Coverage in Good Lighting*

Selection of a specific orbit is deliberately avoided pending choice of a camera system and specific mission objectives.

Data Rate Considerations--One of the important choices which must be determined by the experimenters, is that of the data format. Techniques similar to that of Mariner IV represent one method of data selection. Data may be edited on-board in a variety of other ways. The spacecraft system can handle any of these data modes. Currently, the spacecraft can handle data at 50,000 bits per second, the maximum rate planned for the data automation equipment. High redundancy of data in visual image systems allows approximately 2 to 1 saving of bandwidth using conventional electronic compression methods. Images presented by 3 - 4 Roberts modulation techniques look as good as the six-bit digitized original (see item 3 in Section 4.5.2 above), but only a three-bit digitized image. Because program interest is primarily in the scientific utility rather than in the aesthetic quality of the data, a totally different method of treating visual image data has been examined.

A number of methods are available to expand the data-to-earth capability. For example three other image-data editing concepts being used by the photogeologists and lunar petrologists are also of direct interest to Voyager. These create special-purpose isodata maps of:

1) Contour lines drawn through areas of equal brightness--isotonal. (See 4) in Section 4.5.2 above.) This process is developed in Figure 4.5-15.
2) Contour lines drawn through areas of similar texture or roughness--isotextural. (See 5) in Section 4.5.2 above.)

Illustrations from Reference 2
by permission of the author

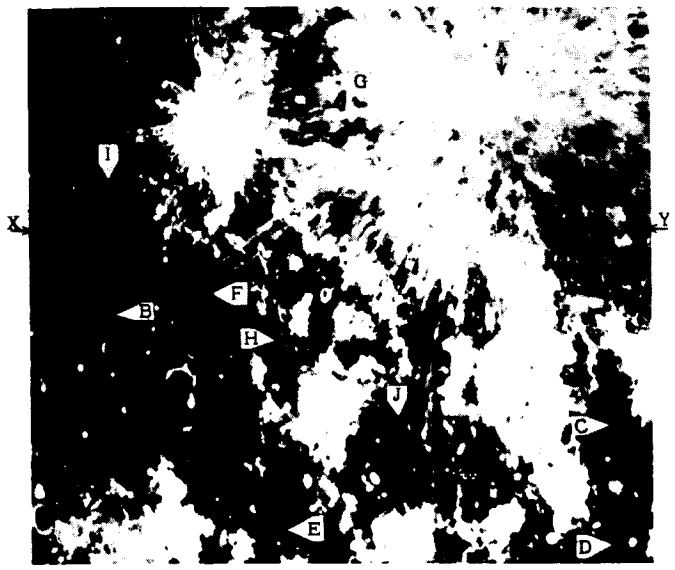

HIGH-CONTRAST ENLARGEMENT
OF FULL-MOON PHOTOGRAPH
OF LANSBERG REGION OF MOON

ISOTONAL MAP OF LANSBERG
REGION OF MOON

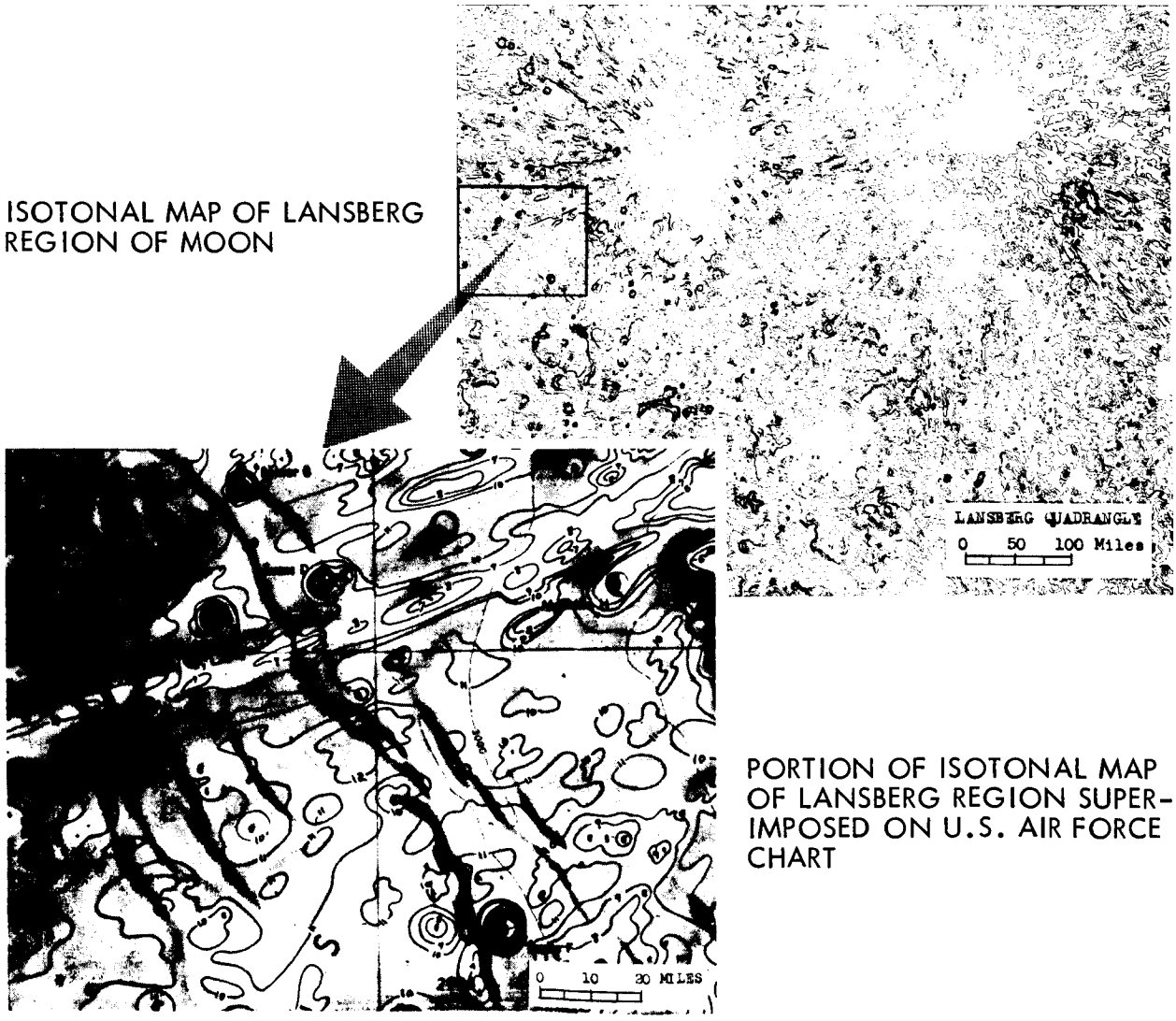

PORTION OF ISOTONAL MAP
OF LANSBERG REGION SUPER-
IMPOSED ON U.S. AIR FORCE
CHART

Figure 4.5-15: Development of Isotonal Map Overlay
for Lansberg Region of Moon

3) Contour lines drawn through areas of equal temperature--isotherms. See 6) in Section 4.5.2 above.) The process is shown in Figures 4.5-16 through 18. Figure 4.5-16 is the control photo.

The majority of raw-image redundancy is removed. As an example of the data compression, consider the isotherm plot of the Copernicus region (Figure 4.5-18) versus the unedited raw 1000-line six-bit video map shot of the area:

1) Video information content = $(1000)^2$ x 6 bits = 6 x 10^6 bits per frame for image data

2) Isotherm Edit:

   a) X and Y coordinates at 20 bits per point

   b) Data level 6 bits per point

      Total 26 bits/point of selected data

   c) Typical data population = 1200 points. This value is determined from actual count of selected data points of material processed by Boeing.

3) Total: 26 x 1200 = 31,200 bits per frame

The iso plots of the Copernicus area have typical, special-interest data density. Therefore, 30,000 to 50,000 bits per frame is considered the special information content. By editing prior to transmission, a relative saving of approximately 200 to 1 can be effected over raw-data transmission.

The impact that pretransmission editing could have on Voyager is:

1) Special-interest scientific data (isotonal, isotextural, isothermal, etc.) edits may be transmitted at a significant bandwidth saving over raw-data transmission.

Figure 4.5-16: Control Photograph for Lunar Thermal Isodata Presentation

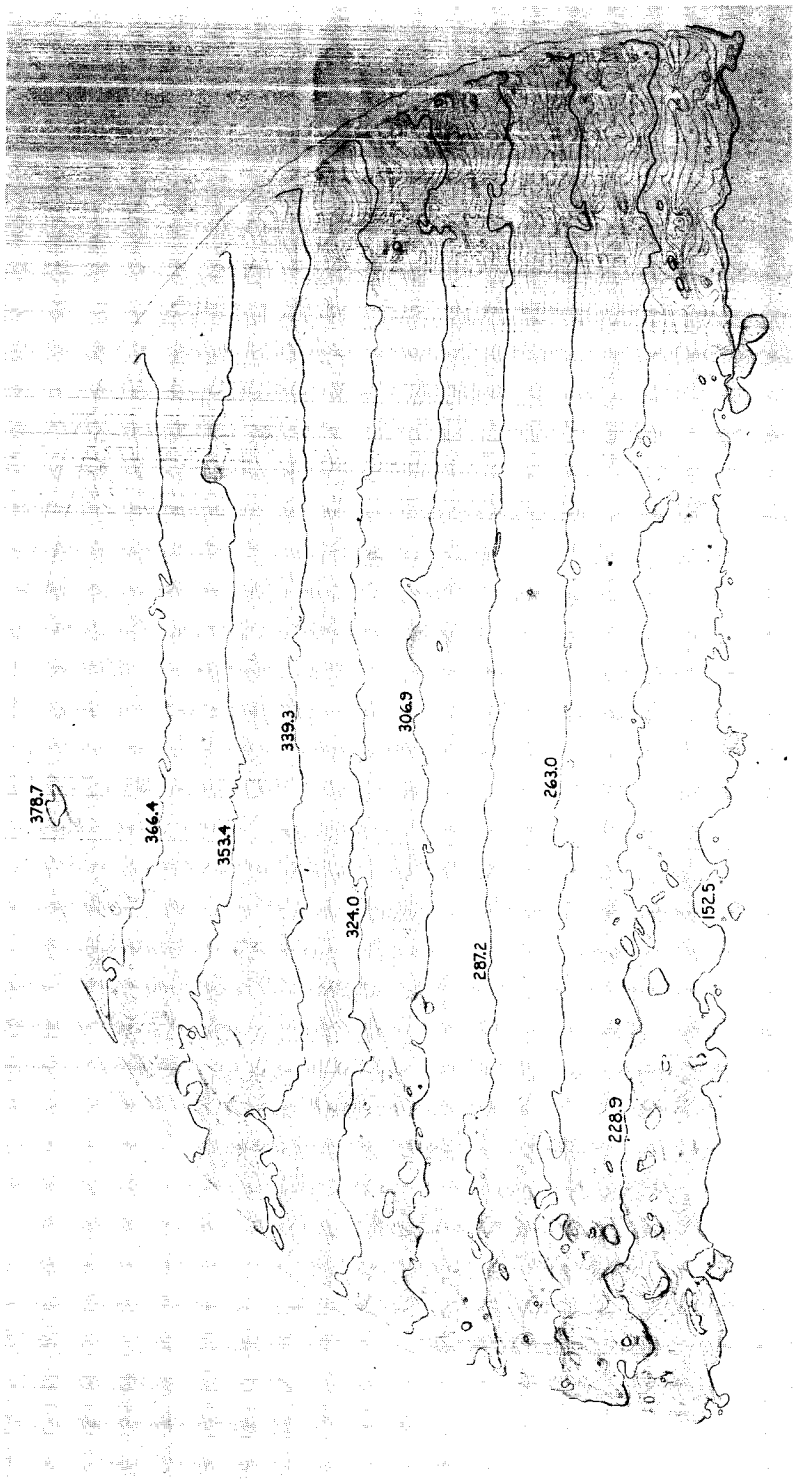

Figure 4.5-17: Example of Isodata Presentation — Lunar-Surface Isotherms Plotted

Figure 4.5-18: Example of Hand-Drawn Isodata Presentation for Copernicus Region of Moon

2) Planetary surface information for much larger areas can be obtained by correlation of the video image frames with the large area coverage shown as isotonal and isotextural data. This allows extrapolation of the video planet surface image into areas not transmitted as full video. The process is shown in Figure 4.5-19.

Such a capability should be incorporated in the DAE rather than the telecommunication subsystem.

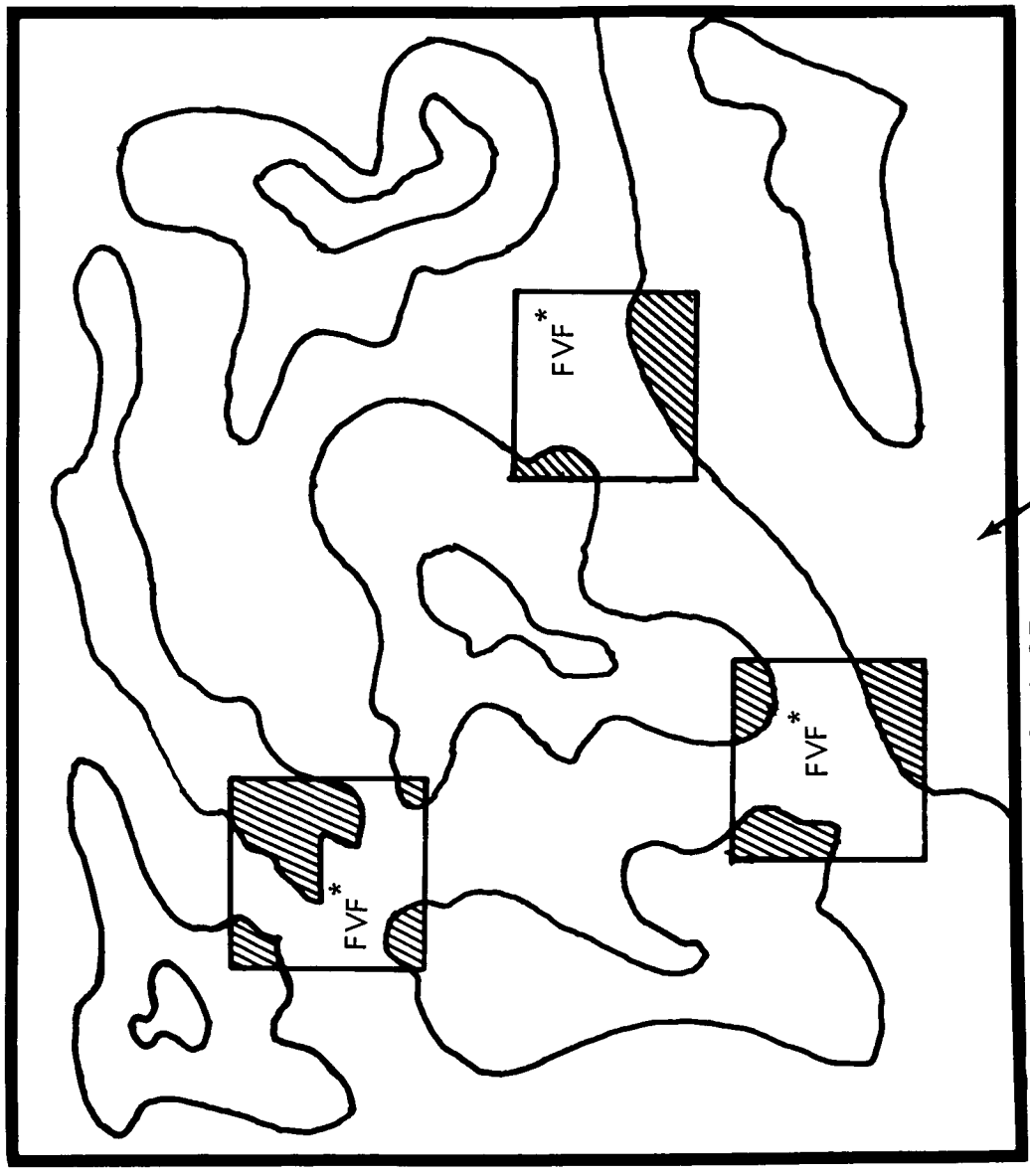

Figure 4.5-19: Isotonal Plot for Data Extrapolation

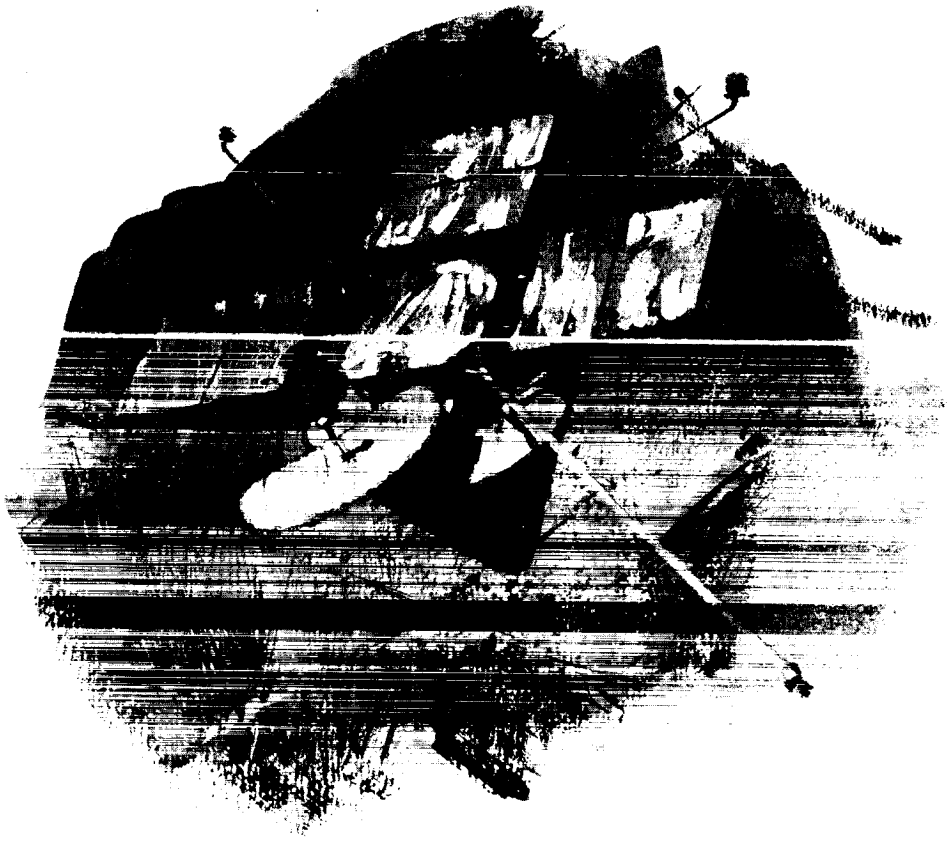

CONTENTS

4.6 ATTITUDE REFERENCE AND AUTOPILOT SUBSYSTEM

Summary

The function of the attitude reference and autopilot subsystem is to provide input signals to the reaction control thruster valves, to the jet vane actuators of the midcourse engines, and to the secondary injection valves of the orbit insertion engine such that the spacecraft attitude, attitude rate, thrust vector alignment and velocity are controlled within specified limits. The subsystem depends upon the central computer and sequencer for commands, integration, comparison, and switching functions. The Attitude Reference and Autopilot subsystem is designed to perform the function highlighted on the accompanying Mission Sequence Matrix.

This preferred subsystem is comprised of celestial reference sensors, an inertial reference unit, and an autopilot which controls both powered and unpowered flight. Celestial reference sensors are space-proven instruments. Two fully redundant Barnes/JPL Canopus trackers, used on Mariner IV, are applied. The Nortronics (Mariner) Sun Sensor is used with a Ball Brothers Sun sensor as backup. The Ball Brothers Sun sensor has been space-proven in the Orbiting Astronomical Observatory Program. The choice of the Ball Brothers unit for backup was made in order to minimize the effects of identical failure modes of identical equipments. The inertial reference unit provides redundant accelerometers and strapdown gyros. The Autonetics free-rotor G-10B gyros were selected for Voyager. Although the G-10B gyro has not been space-proven, it has many advantages over ball-bearing and single-degree-of-freedom gas bearing gyros. These advantages are:

- Proven reliability of the Autonetics free rotor gyro design through

	1.0 PRELAUNCH AT ETR	2.0 LAUNCH & INJECTION (INCLUDES COUNTDOWN)
GROUND COMPLEX (MOS, LOS, & DSN)	OPERATIONAL READINESS TEST, S/C-DSN COMPATIBILITY TEST SCHED & COORD ETR ACTIVITIES C/O & SUPPORT MOS (DSN ONLY) LOAD CC&S WITH FLIGHT PROGRAM	MOS/LOS A) COMMAND LIFTOFF B) TRACK VEHICLE DURING BOOST C) SUPPLY FLIGHT COMMANDS (AS REQ) D) RECEIVE & ANALYZE DATA FROM S/C & BOOSTER DSN E) STANDBY ON ALERT F) COMMUNICATE WITH ETR CHANGE FROM MOS/LO ON INJECTION INTO T A) PROVIDE SFOF/DS DSN SEARCH DAT B) RECEIVE ANTENNA C) SEARCH FOR & AC D) ESTABLISH & VER E) TRACK S/C (1-WA F) RECEIVE & ANALY
SPACECRAFT TELECOMMUNICATIONS	SUBSYSTEM C/O & STATUS MONITORING	A) TRANSMIT ENGINEERING DATA VIA CENTAUR TELEMETRY B) TRANSMIT ENGINEERING DATA VIA LOW POWER LAUNCH EXCITER C) RECEIVE POWER FROM E/P
CENTRAL COMPUTER & SEQUENCER (CC&S)	A) SUBSYSTEM C/O & STATUS B) COMMAND OTHER SUBSYSTEMS FOR C/O & STATUS MONITORING C) READY ALL SUBSYSTEMS FOR LAUNCH D) LOAD CC&S WITH FLIGHT PROGRAM	PROVIDE BACKUP COMMANDS AS REQUIRED
ATTITUDE REFERENCE SUBSYSTEM AUTOPILOT SUBSYSTEM **REACTION CONTROL SUBSYSTEM (RCS)**	SUBSYSTEM C/O & STATUS MONITORING	A) ATTITUDE REFERENCE — GYROS OFF DURING LAUNCH B) AUTOPILOT — OFF C) RCS — OFF
MIDCOURSE CORRECTION PROPULSION SYSTEM ORBIT INJECTION PROPULSION SYSTEM	SUBSYSTEM C/O & STATUS MONITORING	
ELECTRICAL POWER SUBSYSTEM	SUBSYSTEM C/O & STATUS MONITORING	A) PROVIDE ENGRG DATA FOR TELECOMUNICATIONS SUBSYSTEM B) PROVIDE BATTERY POWER TO: • TELECOMMUNICATIONS SUBSYSTEM • CC&S • ATTITUDE REFERENCE SUBSYSTEM • AUTOPILOT SUBSYSTEM
S/C STRUCTURE SUBSYSTEM S/C MECHANISMS SUBSYSTEM INSTALLATION CABLES & TUBING	SUBSYSTEM C/O & STATUS MONITORING	A) PROVIDE PHYSICAL SUPPORT FOR ALL EQUIPMENT B) PROVIDE ATTACHMENT FOR CAPSULE C) SUPPORT FLT CAPSULE
TEMPERATURE CONTROL SUBSYSTEM	SUBSYSTEM C/O & STATUS MONITORING SPACECRAFT COOLING SUPPLIED BY CENTAUR	A) PROVIDE HEAT SINK COOLING CAPABILITY UP TO SHROUD JETTISON B) TEMPERATURE CONTROL AFTER SHROUD JETTISON
PYROTECHNIC SUBSYSTEM	SUBSYSTEM C/O & STATUS MONITORING	
SCIENCE EXPERIMENTS (GFE)	SUBSYSTEM C/O & STATUS MONITORING S/C MAGNETIC MAPPING (FAT)	
DATA AUTOMATION EQUIPMENT (GFE)		

REPEAT UP

	3.0 ACQUISITION	4.0 INTERPLANETARY CRUISE
S TO DSN CONTROL ANSMARS ORBIT F WITH ANTENNA SEARCH DATA UIRE S/C Y CONTROL OF S/C E ENGRG DATA	DSN A) MONITOR BOOSTER SEPARATION B) MONITOR SOLAR PANEL DEPLOYMENT C) MONITOR ANTENNA DEPLOYMENT D) PROVIDE COMMANDS TO BACK UP CC&S AS REQUIRED E) TRACK S/C F) REC DATA G) MONITOR SCIENCE DEPLOYMENT H) MONITOR & VERIFY ACQUISITION OF SUN I) MONITOR & VERIFY ACQUISITION OF CANOPUS J) COMMAND REACQUISITION OF CANOPUS (AS REQD) K) MONITOR S/C TRAJECTORY L) UPDATE CC&S TRAJECTORY PARAMETERS FOR PITCH, YAW, & ROLL M) COMPUTE CC&S PITCH, YAW & ROLL POLARITY	DSN A) TRACK S/C B) RECEIVE & DISPLAY SCIENCE & ENGINEERING DATA C) MONITOR S/C & CAPSULE STATUS D) PROCESS DATA ON EARTH TO OBTAIN GUIDANCE COMMANDS (STORED COMMANDS & START TIMES)
	A) TRANSMIT ENGINEERING DATA B) RECEIVE POWER FROM E/P C) RECEIVE VIA LOW-POWER LAUNCH EXCITER DETECT & SEND TO CC&S COMMAND SIGNALS FROM EARTH D) TRANSMIT CELESTIAL REFERENCE ACQUISITION TO DSN E) TRANSMIT VERIFICATION OF DEPLOYMENT OF SOLAR PANELS, ANTENNAS, ETC TO EARTH F) TWO-WAY TRACKING	A) TRANSMIT ENGINEERING & SCIENCE DATA VIA DATA MODE NO. 2 (OPTIONAL MODE NO. 3) B) TRANSMIT CAPSULE ENGINEERING DATA C) TRANSMIT CONE-ANGLE SETTINGS (CANOPUS TO EARTH) D) EXERCISE & CALIBRATE HIGH-GAIN ANTENNA T + 40 DAYS E) SWITCH FROM LOW-GAIN TO HIGH-GAIN ANTENNA T + 80 DAYS F) PROVIDE RANGING SIGNAL TO A MAX. RANGE OF 8.0×10^6 KM (NOMINAL) G) SWITCH TRANSMISSION FROM LAUNCH EXCITER TO TWT POWER AMPLIFIER AND DATA MODE NO. 2
	A) COMMAND SIGNALS TO PYROTECHNICS & MECH TO DEPLOY • SOLAR PANELS • HIGH-GAIN ANTENNA • VHF ANTENNA • LOW-GAIN ANTENNA • SCIENCE BOOM B) SWITCH ON GYROS & SELECT MODES C) ENABLE SUN-SENSOR ROLL AND PITCH CONTROL D) RECEIVE SUN PRESENCE SIGNAL E) TURN ON CANOPUS TRACKER F) SWITCH ROLL CONTROL TO CANOPUS SENSOR G) ACTIVATE MAGNETOMETER (CALIBRATION ROLL) H) RECEIVE CANOPUS PRESENCE OUTPUT SIGNAL I) TRANSMIT VERIFICATION TO TELECOMMUNICATION SUBSYSTEM (CANOPUS & SUN PRESENCE) J) PERFORM COMMAND FUNCTIONS FOR CANOPUS OVERRIDE AS REQUIRED K) BACKUP COMMANDS AS REQUIRED	A) COMMAND TELECOMMUNICATION TO DATA MODE NO. 2 B) COMMAND CRUISE SCIENCE ON (WARMUP) — SCIENCE INSTRUMENTS C) COMMAND DATA RECORDERS ON D) COMMAND TWTA ON E) SWITCH CANOPUS ANGLE AS REQUIRED F) INITIATE CRUISE SCIENCE DATA ACQUISITION G) COMMAND TELECOMMUNICATION CHANGE FROM OMNI TO HIGH-GAIN ANTENNA H) UPDATE HIGH-GAIN ANTENNA POSITION (AS REQUIRED) I) COMMAND TELECOMMUNICATIONS — CHANGE DATA TRANSMISSION RATES J) COMMAND RECALIBRATION OF SCIENCE ELEMENTS AS REQUIRED K) BACKUP COMMANDS AS REQUIRED
	A) RECEIVE CC&S COMMAND SWITCH ON GYROS, RCS, & AUTOPILOT B) DAMP ROTATION C) YAW & PITCH SPACECRAFT TO ACQUIRE SUN D) RELAY SUN ACQUISITION SIGNAL TO CC&S E) TURN ON CANOPUS SENSOR, ROLL 360 TO CALIBRATE MAGNETOMETER F) ROLL TO ACQUIRE CANOPUS & PROVIDE STAR MAP G) RELAY ACQUISITION SIGNAL (CANOPUS) TO CC&S H) PERFORM CANOPUS OVERRIDE ROLL MANEUVER AS REQUIRED	A) UPDATE CANOPUS CONE ANGLE ON COMMAND B) SWITCH AUTOPILOT TO CRUISE MODE C) MAINTAIN S/C ATTITUDE TO CELESTIAL REFERENCES DURING CRUISE
	A) PROVIDE POWER TO PYROTECHNIC SUBSYSTEMS FOR SQUIB FIRINGS B) PROVIDE POWER TO MECHANISMS C) ACTIVATE SOLAR POWER SYSTEM AFTER SUN ACQUISITION (AUTOMATIC) D) TRANSMIT "VOLTAGE SATISFACTORY" SIGNAL TO CC&S E) PROVIDE POWER TO: • TELEMETRY • CC&S • TEMPERATURE CONTROL • AUTOPILOT	A) PROVIDE CONDITIONED SOLAR ELECTRICAL POWER TO: • TELEMETRY • CAPSULE • CC&S • ATTITUDE REF • AUTOPILOT • TEMPERATURE CONTROL • SCIENCE B) CHARGE BATTERIES
	A) PROVIDE PHYSICAL SUPPORT FOR ALL EQUIPMENT B) DRIVE SOLAR PANELS TO LIMIT STOPS C) PROVIDE OUT & LOCK SIGNALS TO TELEMETRY D) DRIVE HIGH-GAIN ANTENNA TO OPERATING POSITION & LOCK E) DRIVE VHF & OMNI ANTENNAS TO OPERATING POSITION & LOCK F) DRIVE MAGNETOMETER BOOM TO OPERATING POSITION & LOCK G) SUPPORT FLT CAPSULE	A) SUPPORT S/C ASSEMBLIES B) SUPPORT S/C COMPONENTS C) MAINTAIN ADEQUATE ALIGNMENT BETWEEN COMPONENTS D) PROVIDE ACCEPTABLE STATIC & DYNAMIC LOAD ENVIRONMENTS E) SUPPORT FLIGHT CAPSULE
	PROVIDE TEMPERATURE CONTROL	PROVIDE TEMPERATURE CONTROL
	RECEIVE SQUIB FIRING SIGNALS FOR DEPLOYMENT OF: • SOLAR PANEL • MAGNETOMETER BOOM • LOW-GAIN ANTENNA • HIGH-GAIN ANTENNA • VHF ANTENNA	
	A) CALIBRATE MAGNETOMETER DURING S/C ROLL B) CALIBRATE OTHER SCIENCE INSTR AS REQUIRED	A) RECEIVE CRUISE SCIENCE "ON" COMMAND B) ACQUIRE CRUISE SCIENCE DATA C) TRANSFER CONDITIONED DATA TO DAE D) RECEIVE POWER FROM E/P E) RECALIBRATE SCIENCE EXPERIMENTS AS REQUIRED
		A) RECEIVE DAE "ON" COMMAND B) PROCESS & TRANSFER DATA TO TM

TO FOUR TIMES

5.0 INTERPLANETARY TRAJECTORY CORRECTION

6.0 S/C CAPSULE SEPARATION

7.0 FLIGH TRAJ DEFLE

A) PROVIDE ROLL TURN MAGNITUDE & DIRECTION B) PROVIDE YAW TURN MAGNITUDE & DIRECTION C) PROVIDE MIDCOURSE MOTOR BURN DURATION AND ΔV D) PROVIDE INITIATE MANEUVER SEQUENCE COMMAND E) RECEIVE VERIFICATION OF CORRECTION MANEUVER • DEGREES OF YAW & ROLL • THRUST DURATION • REACQUISITION OF CELESTIAL REFERENCES F) TRACK SPACECRAFT	A) INITIATE PRESEPARATION SEQUENCE B) RECEIVE CAPSULE STATUS DATA C) COMMAND SEPARATION D) VERIFY CAPSULE PROGRAM E) VERIFY SEPARATION F) TRACK CAPSULE & SPACECRAFT	A) TRANSMIT C • ROLL MAG • YAW MAG • MOTOR BI B) TRACK FLIG C) RECEIVE, RE D) PROVIDE CO
A) RECEIVE ROLL & YAW TURN COMMAND & RELAY TO CC&S B) RECEIVE ANTENNA POSITIONING DATA & RELAY TO CC&S C) RECEIVE MOTOR BURN DURATION AND & ΔV RELAY TO CC&S D) RECEIVE INITIATE MANEUVER COMMAND & RELAY TO CC&S E) SWITCH TO DATA MODE NO. 1 (FOR LATE MIDCOURSE MANEUVERS) F) RELAY VERIFICATION OF CORRECTION MANEUVER TO DSN G) STORE AND/OR TRANSMIT ENGINEERING DATA TO DSN (MODE 3) TRANSMIT ENGINEERING (SPACECRAFT & CAPSULE) + CRUISE SCIENCE TO DSN (MODE 2)	A) RECEIVE PRESEPARATION SEQUENCE COMMANDS & RELAY TO CC&S B) SWITCH TO DATA MODE NO. 2 C) TRANSMIT CAPSULE ENGRG DATA TO DSN D) RECEIVE SEPARATION COMMAND FROM DSN & ROUTE TO CC&S E) STORE AND/OR TRANSMIT ENGINEERING DATA TO DSN (MODE 3) TRANSMIT ENGINEERING (SPACECRAFT & CAPSULE) + CRUISE SCIENCE TO DSN (MODE 2)	A) RECEIVE RO TO CC&S B) RECEIVE AN C) RECEIVE MO D) RECEIVE CA E) TRANSMIT F SCIENCE DA
A) COMMAND TELECOMMUNICATION TO DATA MODE NO. 1 B) RECEIVE TRAJECTORY CORRECTION PARAMETERS C) SWITCH GYROS TO RATE CONTROL D) COMMAND ANGULAR MANEUVER E) RECEIVE GYRO SIGNALS & SUM FOR ANGULAR MANEUVERS F) SWITCH ATTITUDE REFERENCE TO AUTOPILOT SUBSYSTEM G) ARM PROPULSION SYSTEM H) PROVIDE COMMAND TO INITIATE ATTITUDE MANEUVER & ΔV MANEUVER I) RECEIVE ACCELEROMETER SIGNALS & INTEGRATE FOR ΔV MANEUVER J) DISARM PROPULSION SYSTEM K) COMMAND REVERSE ANGULAR MANEUVER L) COMMAND REACQUIRE CELESTIAL REFERENCES M) COMMAND AUTOPILOT SELECTION CONTROL N) BACKUP COMMANDS AS REQUIRED	A) LOAD CAPSULE WITH 5 OR MORE COMMANDS B) COMMAND CAPSULE SEQUENCING C) COMMAND TELECOMM SWITCH TO DATA MODE NO. 1 D) COMMAND GYROS ACTIVATE (CAPSULE) E) COMMAND GYROS ESTABLISH POLARITY (CAPSULE) F) COMMAND GYROS TO ATTITUDE CONTROL MODE (CAPSULE) G) COMMAND DATA TAPE RECORDER OFF H) COMMAND CAPSULE ACTIVATE ENTRY SCIENCE I) COMMAND CAPSULE ACTIVATE TELE-COMM & VERIFY RADIO LINK (VHF) J) SELECT T/M MODE FOR TRANSMISSION OF CAPSULE DATA K) COMMAND: BIOBARRIER SEPARATION S/C ORIENT TO SEPARATION ATTITUDE ELECTRICAL CONNECTION SEPARATION VERIFY SEPARATION L) COMMAND REORIENT S/C & REACQUIRE CELESTIAL REFERENCES M) BACKUP COMMANDS AS REQUIRED N) RECEIVE S/C ORIENTATION PARAMETERS	A) COMMAND B) COMMAND C) COMMAND D) RECEIVE OF E) PROVIDE S (CRUISE SC F) SWITCH ON RECEIVE CA G) BACKUP CO
A) SWITCH TO GYRO CONTROL B) ROLL S/C AND VERIFY C) YAW S/C AND VERIFY D) AUTOPILOT — PROVIDE COMMAND TO TVC DURING MOTOR BURN E) TURN ON ACCELEROMETERS F) PROVIDE ACCELERATION DATA TO CC&S G) TURN OFF ACCELEROMETER H) YAW BACK TO ORIGINAL ATTITUDE & VERIFY I) REACQUIRE SUN (FINE SUN SENSOR) & VERIFY J) ROLL TO ORIGINAL ATTITUDE K) LOCK ON CANOPUS & VERIFY L) SWITCH AUTOPILOT FROM GYRO CONTROL TO CELESTIAL REF CONTROL	A) SWITCH TO GYRO CONTROL B) PERFORM ROLL TURN & VERIFY C) PERFORM YAW TURN & VERIFY D) MAINTAIN ATTITUDE DURING SEPARATION E) PERFORM YAW TURN (INVERSE TO C) & VERIFY F) PERFORM ROLL TURN (INVERSE TO B) & VERIFY G) REACQUIRE CELESTIAL REFERENCES H) RETURN TO CELESTIAL REFERENCE ATTITUDE CONTROL MODE	A) UPDATE CA B) SWITCH AU C) MAINTAIN
MIDCOURSE PROPULSION SYSTEM A) ARM PRESSURIZATION SYSTEM (FIRE SQUIB VALVE) B) ARM PROPELLANT FEED SUBSYSTEM (FIRE SQUIB VALVE) C) FIRE PROGRAMMED ENGINES (OPERATE SOLENOID VALVE) D) SHUT DOWN ENGINE E) ISOLATE PROPELLANT FEED SUBSYSTEM F) ISOLATE PRESSURIZATION SUBSYSTEM		
A) PROVIDE CONDITIONED SOLAR OR BATTERY POWER TO: • TELEMETRY • CC&S • AUTOPILOT • ATTITUDE REFERENCE • REACTION CONTROL • PROPULSION • TEMPERATURE CONTROL • PYROTECHNIC • CAPSULE	A) PROVIDE CONDITIONED SOLAR OR BATTERY POWER TO: • T/M • CC&S • AUTOPILOT • ATTITUDE REF • REACTION CONTROL • TEMPERATURE CONTROL • PYROTECHNICS • CAPSULE	A) PROVIDE • T/M • CC&S • AUTOPI • ATTITUD • REACTIO • TEMPER B) CHARGE BA
A) SUPPORT S/C ASSEMBLIES B) SUPPORT S/C COMPONENTS C) MAINTAIN ADEQUATE ALIGNMENT BETWEEN COMPONENTS D) PROVIDE ACCEPTABLE STATIC & DYNAMIC LOAD ENVIRONMENTS E) SUPPORT FLIGHT CAPSULE	A) SUPPORT S/C ASSEMBLIES B) SUPPORT S/C COMPONENTS C) MAINTAIN ADEQUATE ALIGNMENT BETWEEN COMPONENTS D) PROVIDE ACCEPTABLE STATIC & DYNAMIC LOAD ENVIRONMENTS E) SUPPORT FLIGHT CAPSULE	A) SUPPORT B) SUPPORT C) MAINTAIN D) PROVIDE A E) DRIVE SCA
PROVIDE TEMPERATURE CONTROL	PROVIDE TEMPERATURE CONTROL	PROVIDE TEMP
A) REMOVE PROPULSION SYSTEM INHIBIT B) PROVIDE IGNITION C) INHIBIT PROPULSION SYSTEM	A) RECEIVE SIGNAL TO REMOVE CAPSULE SEPARATION INHIBIT B) RECEIVE SIGNAL TO FIRE CAPSULE UMBILICAL SEPARATION C) RECEIVE SIGNAL TO FIRE BIOBARRIER REMOVAL D) RECEIVE SIGNAL TO FIRE CAPSULE SEPARATION E) RECEIVE SIGNAL FOR SEPARATION INHIBIT	RECEIVE SIGN OF SCAN PLAT
A) RECEIVE CC&S COMMAND "CRUISE SCIENCE OFF" B) TURN OFF CRUISE SCIENCE	A) RECEIVE CC&S COMMAND "CRUISE SCIENCE OFF" B) TURN OFF CRUISE SCIENCE	A) RECEIVE C B) ACQUIRE C C) TRANSFER D) RECEIVE PI E) RECALIBRA
		A) RECEIVE D B) PROCESS

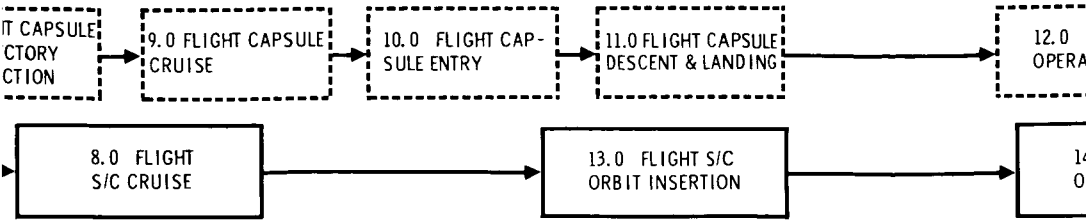

RBIT INJECTION PARAMETERS NITUDE & DIRECTION NITUDE & DIRECTION IRN START TIME IT SPACECRAFT DUCE & DISPLAY SCIENCE & ENGINEERING DATA MMANDS TO BACK UP CC&S AS REQUIRED	A) RECEIVE, DECODE, & DISPLAY ENGINEERING DATA B) RELAY UPDATED ORBIT INJECTION PARAMETERS C) PROVIDE COMMAND TO INITIATE INSERTION MANEUVER D) PROVIDE BACKUP COMMANDS TO CC&S AS REQUIRED E) TRACK S/C F) VERIFY ORBIT INSERTION	A) RECEIVE, DECODE, & DISPL B) RECEIVE AND ANALYZE ENG C) TRACK S/C D) RECEIVE & DISPLAY CAPSU E) PROVIDE DATA FOR ORBITA F) RECEIVE VERIFICATION OF G) TERMINATE MISSION
L & YAW TURN MAGNITUDE & DIRECTION COMMAND & RELAY ENNA POSITIONING DATA & RELAY TO CC&S TOR-BURN START TIME, RELAY TO CC&S PSULE DATA, CONDITION & RELAY TO GROUND LIGHT SPACECRAFT ENGINEERING, CAPSULE ENGRG, & TA TO GROUND V1A MODE 2	A) UPDATE ROLL-TURN MAGNITUDE & DIRECTION COMMAND & RELAY TO CC&S B) UPDATE YAW-TURN MAGNITUDE & DIRECTION COMMAND & RELAY TO CC&S C) UPDATE MOTOR-BURN START TIME & RELAY TO CC&S D) UPDATE INITIATE MANEUVER & RELAY TO CC&S E) SWITCH TO DATA MODE NO. 2 OR 5A AS REQUIRED F) REACQUIRE EARTH AFTER ROLL TURNS & MOTOR BURN G) RELAY VERIFICATION OF MANEUVERS	A) TRANSMIT SCIENCE & ENGI B) RECORD ENGINEERING & SC C) RECEIVE, STORE & RELAY C D) RECEIVE & RELAY DATA FOR
WITCH TO DATA MODE NO. 2 CANOPUS CONE ANGLE SETTING ANTENNA STEP (AS REQUIRED) BIT INJECTION PARAMETERS IGNAL TO PYRO & MECHANISMS TO DEPLOY SCAN PLATFORM IENCE T/M OFF) & SWITCH TO DATA MODE NO. 1 DATA RECORDER-COMMAND TELECOMMUNICATIONS PSULE DATA MMANDS AS REQUIRED	A) UPDATE STORED ROLL, PITCH, & YAW MAGNITUDE & SIGN B) UPDATE STORED VELOCITY MAGNITUDE C) INITIATE MANEUVER SEQUENCE D) COMMAND ORIENTATION OF S/C TO INJECTION ATTITUDE E) COMMAND THRUST FOR ORBIT INSERTION F) COMMAND RETURN TO CRUISE ATTITUDE G) BACKUP COMMANDS AS REQUIRED	A) COMMAND ORBITAL TRIM M B) SWITCH DATA MODES AS NI C) RECEIVE ANY ORBITAL OPE D) COMMAND POSITIONING O E) SWITCH ON ORBITAL SCIEN F) SELECT RECORDED SCIENCE G) BACKUP COMMANDS AS RE H) STORE DATA FOR ORBIT TR I) TERMINATE MISSION ON C
	A) SWITCH TO GYRO CONTROL B) PROVIDE ROLL TO PROPER ATTITUDE & VERIFY ROLL C) YAW TO PROPER ATTITUDE & VERIFY D) AUTOPILOT – PROVIDE COMMAND TO TVC DURING MOTOR BURN E) TURN ON ACCELEROMETER F) PROVIDE ACCELEROMETER DATA TO CC&S G) TURN OFF ACCELEROMETER H) YAW BACK AFTER MOTOR BURN I) ACQUIRE SUN & VERIFY J) ROLL BACK TO PROGRAMMED ATTITUDE K) ACQUIRE CANOPUS & VERIFY L) SWITCH AUTOPILOT FROM GYRO – CONTROL TO CELESTIAL REFERENCE CONTROL	
NOPUS CONE ANGLE ON COMMAND TOPILOT TO CRUISE MODE S/C ATTITUDE TO CELESTIAL REFERENCES DURING CRUISE		A) MAINTAIN S/C ATTITUDE TO B) SWITCH AUTOPILOT TO GYR C) REACQUIRE CELESTIAL REFE D) REORIENT S/C FOR ORBITAL E) PROVIDE TVC DURING ENGI F) REACQUIPE CELESTIAL REFE G) UPDATE CANOPUS CONE AN
	ORBIT INSERTION ENGINE A) ARM TVC B) ARM IGNITER C) FIRE MOTOR & PROVIDE THRUST & TVC D) TERMINATE THRUST (MOTOR BURNS TO DEPLETION)	MIDCOURSE A) ARM PRESSURIZATION & F B) PROVIDE THRUST (FIRE PR IF REQUIRED C) TERMINATE THRUST ON CO D) ISOLATE PROPELLANT FEED E) ISOLATE PRESSURIZATION
ONDITIONED SOLAR ELECTRICAL POWER TO: OT E REF N CONTROL ITURE CONTROL TTERIES	A) PROVIDE CONDITIONED SOLAR OR BATTERY POWER TO: • TELEMETRY • CC&S • ATTITUDE REFERENCE SUBSYSTEM • AUTOPILOT • TEMPERATURE CONTROL • PULSE TO PYROTECHNICS • PULSE TO PROPULSION	A) PROVIDE CONDITIONED S • TELEMETRY • CC&S • ATTITUDE REFERENCE SU • AUTOPILOT • TEMPERATURE CONTROL • STRUCTURES & MECHAN • SCIENCE
/C ASSEMBLIES /C COMPONENTS ADEQUATE ALIGNMENT BETWEEN COMPONENTS CCEPTABLE STATIC & DYNAMIC LOAD ENVIRONMENTS N PLATFORM TO DEPLOYED POSITION & LOCK	A) SUPPORT S/C ASSEMBLIES B) SUPPORT S/C COMPONENTS C) MAINTAIN ADEQUATE ALIGNMENT BETWEEN COMPONENTS D) PROVIDE ACCEPTABLE STATIC & DYNAMIC LOAD ENVIRONMENTS	A) SUPPORT S/C ASSEMBLIES B) SUPPORT S/C COMPONENT C) MAINTAIN ADEQUATE ALIG D) PROVIDE ACCEPTABLE STA ENVIRONMENTS E) POSITION SCAN PLATFOR
ERATURE CONTROL	PROVIDE TEMPERATURE CONTROL	PROVIDE TEMPERATURE CONTR
B FIRING SIGNAL FOR UNLATCHING FORM	A) RECEIVE & EXECUTE COMMAND SIGNAL TO REMOVE INHIBIT FOR PROPULSION ENGINE B) RECEIVE & EXECUTE SIGNAL FOR PROPULSION ENGINE START C) RECEIVE & EXECUTE COMMAND SIGNAL FOR PROPULSION ENGINE STOP D) RECEIVE & EXECUTE SIGNAL FOR PROPULSION INHIBIT	
RUISE SCIENCE "ON" COMMAND RUISE SCIENCE DATA CONDITIONED DATA TO DAE WER FROM E/P TE SCIENCE EXPERIMENTS AS REQUIRED	SCIENCE OFF DURING ORBIT INSERTION	A) TURN ON ORBITAL SCIENC B) ACQUIRE ORBITAL SCIEN C) TRANSFER CONDITIONED D) RECALIBRATE SCIENCE EX
AE "ON" COMMAND & TRANSFER DATA TO TM		A) RECEIVE DAE "ON" COMM B) PROCESS & TRANSFER DA

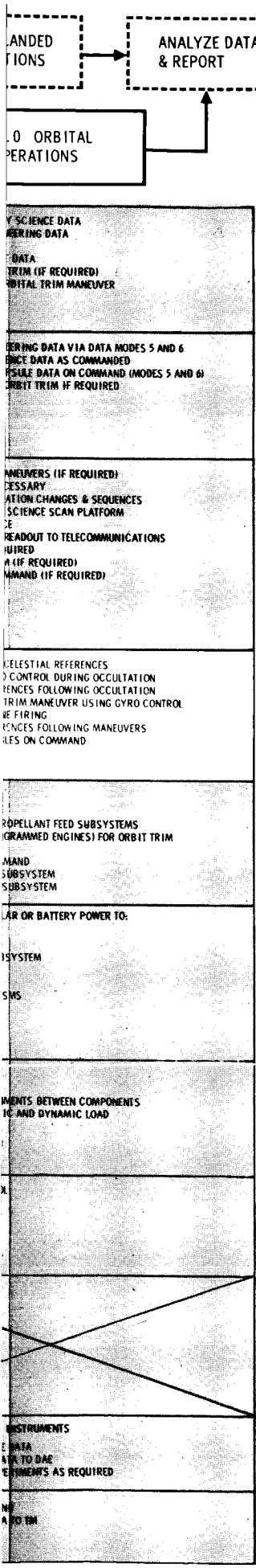

Mission Sequences Matrix

17 million operational hours of the G-6B4,

- No wearout mechanism,
- Low power and weight
- All axis redundancy with the addition of one additional gyro

The primary accelerometer chosen for Voyager is the space-proven Bell IIIB. The Autonetics Electromagnetic Miniature Accelerometer was selected as a redundant unit because of its potentially great reliability, small weight and power, and to avoid use of identical primary and backup units. The two accelerometers are aligned with the thrust axis, and are operated in parallel to measure ΔV. The autopilot is basically an analog device with d.c. amplifiers. It can be switched to operate with the various sensors in rate or limit cycle modes to drive the spacecraft attitude thrusters and propulsion engine thrust vector controls.

4.6.1 System Description

4.6.1.1 Scope

The location of the attitude reference and autopilot subsystem equipment, including the Sun sensor assemblies, is shown in Figure 4.6-1. A brief description of each of the major components is given below.

Inertial Reference Unit, Gyros--Gyros are used to maintain attitude when data from optical sensors is not available, i.e., during occultation and maneuvers. Autonetics G10 gyros were chosen because of the superior reliability exhibited by the two-axis, free-rotor gyro design during more than 17,000,000 hours of Minuteman operational experience. The G10 gyro is a scaled version of the Minuteman G6B gyro and is therefore estimated to have a MTBF of more than 1,000,000 hours.

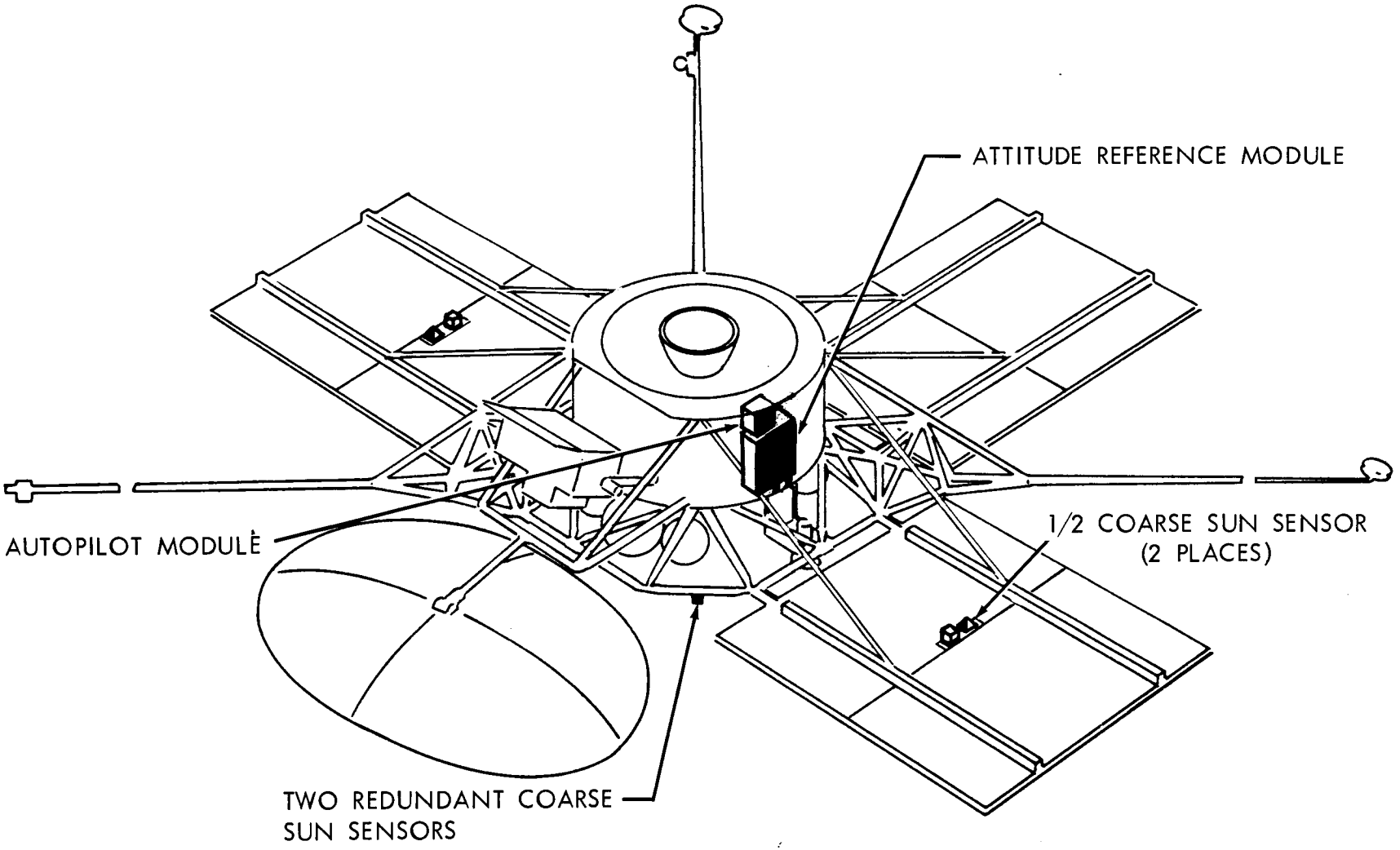

Figure 4.6-1: Attitude Reference and Autopilot Subsystem

Inertial Reference Unit, Accelerometers--Accelerometers are used to sense acceleration during midcourse and orbit-insertion velocity corrections. Output of the accelerometers is integrated in the central computer and sequencer to measure velocity change. For midcourse corrections, ΔV thus measured is compared to commanded value, and acts to terminate thrust when the desired value is achieved. During the orbit-insertion acceleration, the accelerometers provide engineering data for eventual transmittal to the DSIF. Accelerometers selected for Voyager are the Autonetics EMA and the Bell DVM-IIIB, which are more fully described in Section 4.6.2. They are operated in parallel, and backed up by minimum-maximum timer operation for midcourse thrust cutoff.

Canopus Sensor--The Canopus sensor functions to provide roll reference data during the cruise phases of the mission. The JPL-Barnes sensor was selected as both primary and redundant unit for the Voyager spacecraft. A detailed description is given in Section 4.6.3.

Sun Sensor--The Sun sensors provide pitch and yaw information used to orient the roll axis and solar cells toward the Sun. Two basic types of detectors, silicon and cadmium sulfide, were considered. Silicon cell output is a function of light intensity, which causes a change in sensor gain as the spacecraft moves away from the Sun towards Mars. Compensation for this gain change requires a minor increase in system complexity. The output from cadmium sulfide cells will not exhibit this sensor gain change. Ball Brothers silicon and Nortronics cadmium sulfide sensors have operated with no failure on OSO, Mariner, and other programs. Both were selected for use

Table 4.6-2: ATTITUDE REFERENCE AND AUTOPILOT MODES OF OPERATION

PHASE	DESCRIPTION	REQUIREMENT
Initial Acquisition	Damp rotation and then slew in pitch and yaw to acquire Sun. Slew in roll and acquire Canopus: gyro position and rate are employed.	Tumble rate: 3^{o}/Sec Slew Rate: 0.2^{o}/Sec
Cruise	Vehicle attitude is maintained in alignment to Sun and Canopus.	Limit Cycle: $\pm 0.4^{o}$
Maneuver	Reorient vehicle for engine firing. Celestial references are dropped; gyro control is terminated when celestial references are reacquired.	Slew Rate: 0.2^{o}/sec
Inertial Hold (Midcourse)	Gyro rate and position information are used to maintain attitude through appropriate deflection of the jet vanes.	Thrust Vector: held within $\pm 0.2^{o}$ (1σ)
Inertial Hold (Orbit Insertion)	Gyro rate and position information are used to maintain pitch and yaw through actuation of the secondary injection valves with roll control maintained by the reaction jets.	Thrust Vector: held within $\pm 0.6^{o}$ (1σ)
Mars Orbit (Scanning Experiment)	Gyro/optical limit cycle Attitude error information is supplied with rate stabilization signals being provided by the gyros.	Attitude Hold: $\pm 0.2^{o}$ Rate Limit 0.01^{o}/sec
Occultation	Vehicle attitude is maintained with reference to the Sun and Canopus during periods of occultation.	Attitude Hold: $\pm 0.4^{o}$ for a maximum of 2.5 hours

1.0 PRELAUNCH

A. Subsystem checkout & status monitoring

2.0 LAUNCH & INJECTION

Attitude Reference

A. Initial status — gyros off duri
B. Receive electrical power IR
C. Provide engineering data to cations subsystem

4.0 INTERPLANETARY CRUISE

A. Update Canopus cone angle on command
B. Maintain spacecraft attitude to celestial references during cruise

5.0 INTERPLANETARY TRAJEC

A. Switch to gyro control
B. Roll spacecraft and verify
C. Yaw spacecraft and verify
D. Turn on accelerometers
E. Autopilot — provide comman
F. Provide acceleration data to
G. Turn off accelerometer
H. Yaw back to original attitud
I. Reacquire Sun (fine Sun sens
J. Roll to original attitude
K. Lock on Canopus and verify
L. Switch from gyro control to

8.0 FLIGHT SPACECRAFT CRUISE

A. Update Canopus cone angle on command
B. Maintain spacecratt attitude to celestial reference during cruise

13.0 FLIGHT SPACECRAFT OR

A. Switch to gyro control
B. Provide pitch to proper attit
C. Yaw to proper attitude and
D. Autopilot — provide comman
E. Yaw back after motor burn
F. Acquire Sun and verify
G. Roll back to programmed att
H. Acquire Canopus and verify
I. Switch autopilot from gyro c reference control

Table 4.6-3: Mission Sequence — Attitude Reference & Autopilot Subsystem

g boost

elecommuni-

TORY CORRECTION

to TVC during motor burn
CC&S

e and verify
r) and verify

celestial reference control

IT INSERTION

de and verify roll
erify
to TVC during Motor burn

tude

ntrol to celestial

3.0 ACQUISITION

A. Receive CC&S command. Switch on gyros. Damp Rotation
B. Gyro control — yaw & pitch to acquire Sun
C. Relay Sun acquisition signal to CC&S
D. Turn on Canopus sensor (autopilot control)
E. Roll to acquire Canopus
F. Relay acquisition signal (Canopus) to CC&S
G. Perform Canopus override roll maneuver as required

6.0 SPACECRAFT CAPSULE SEPARATION

A. Switch to gyro
B. Perform roll turn and verify
C. Perform yaw and turn and verify
D. Maintain attitude during separation
E. Perform yaw turn (inverse to C) and verify
F. Perform roll turn (inverse to B) and verify
G. Reacquire celestial references
H. Return to celestial reference attitude control mode

14.0 ORBITAL OPERATIONS

A. Maintain spacecraft attitude to celestial reference
B. Switch autopilot to gyro control during occultation
C. Reacquire celestial references following occultation
D. Reorient spacecraft for orbital trim maneuver using gyro control
E. Provide TVC during engine firing
F. Reacquire celestial references following maneuvers
G. Update Canopus cone angles on command
H. Select reduced dead band on command

4.6.1.2 Applicable Documentation

1) JPL Document No. 45, V-MA-004-14-03, "Preliminary Voyager 1971 Mission Specification," 1 May 1965

2) JPL Project Document No. 46, V-MA-004-002-14-03, "Voyager 1971 Mission Guidelines," 9 May 1965

3) General Errata, JPL Project Document No. 45 and JPL Project Document No. 46

4) "Boeing Baseline Subsystem Description," CS 2-5533-V-24

5) Boeing Document No. VIE-2, "Voyager Spacecraft Objectives, Requirements, and Constraints"

6) Boeing Document No. D2-106051-3, "Voyager System Engineering 1971 Flight Spacecraft Functional Description"

7) Boeing Document No. D2-106200, "Administrative Requirements Voyager Spacecraft Systems"

8) JPL Document No. 683MA

9) Boeing Document No. 2-4461-0-267

10) Boeing Document No. D2-23834-1, "Voyager 1971 Program - Reliability Analysis and Prediction Standards"

11) JPL Specifications MC-1-110 through MC-4-610A, Mariner C Spacecraft Design Book

12) Autonetics Report T5-1161.1/3061A, "Voyager Attitude Reference and Autopilot Subsystems Investigations"

13) JPL Specification 30236-ETS-A, "RF Interference Control for Spacecraft and Ground Control Equipment"

4.6.1.3 Functional Description

During flight the spacecraft is maintained at certain angular orientations, or is rotated at prescribed angular rates through the application of appropriate torques. During unpowered flight, these torques are obtained by the expulsion of gas through nitrogen thrusters. During the midcourse rocket motor firing, stabilizing torques are obtained by the positioning of jet vanes, which deflect the rocket exhaust. For orbit injection, the solid-rocket thrust is deflected through the secondary injection of Freon into the rocket nozzle. It is the function of the autopilot subsystem to supply the proper actuating signals to these torque producing devices. To do this, the autopilot subsystem makes use of spacecraft attitude and rate information from the attitude reference subsystem. Figure 4.6-2 is a block diagram that shows the operational features and functional interfaces of these two subsystems and the torque-producing elements.

During the cruise portions of the mission, proper orientation is achieved through application of the attitude error signal from a Sun sensor to the pitch and yaw cold-gas jets after appropriate conditioning by the autopilot. A roll attitude reference is required to complete the definition of a spacecraft orientation for accurate pointing of the high-gain antenna. This is provided by a star tracker with an output signal that is proportional to the deviation of Canopus from the boresight line of the sensor.

During the periods of midcourse-correction and orbit-injection engine firings and the attitude maneuvers that precede and follow them, the

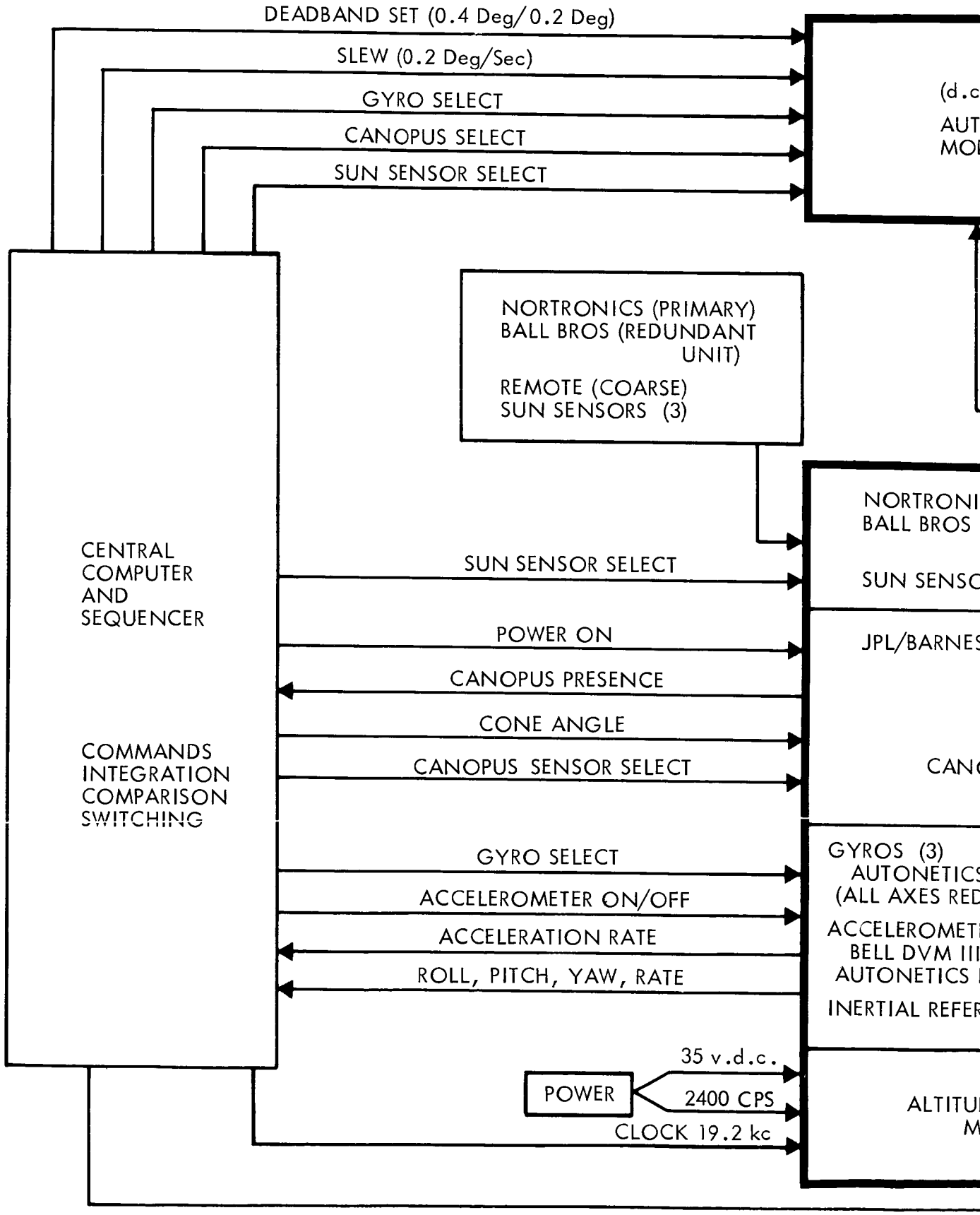
DEADBAND SET (0.4 Deg/0.2 Deg)
SLEW (0.2 Deg/Sec)
GYRO SELECT
CANOPUS SELECT
SUN SENSOR SELECT
(d.c
AUT
MOI
NORTRONICS (PRIMARY)
BALL BROS (REDUNDANT UNIT)
REMOTE (COARSE)
SUN SENSORS (3)
NORTRONI
BALL BROS
SUN SENSC
CENTRAL
COMPUTER
AND
SEQUENCER
SUN SENSOR SELECT
POWER ON
CANOPUS PRESENCE
CONE ANGLE
CANOPUS SENSOR SELECT
JPL/BARNES
CANC
COMMANDS
INTEGRATION
COMPARISON
SWITCHING
GYRO SELECT
ACCELEROMETER ON/OFF
ACCELERATION RATE
ROLL, PITCH, YAW, RATE
GYROS (3)
AUTONETICS
(ALL AXES RED
ACCELEROMETI
BELL DVM III
AUTONETICS
INERTIAL REFER
35 v.d.c.
POWER
2400 CPS
CLOCK 19.2 kc
ALTITU
M

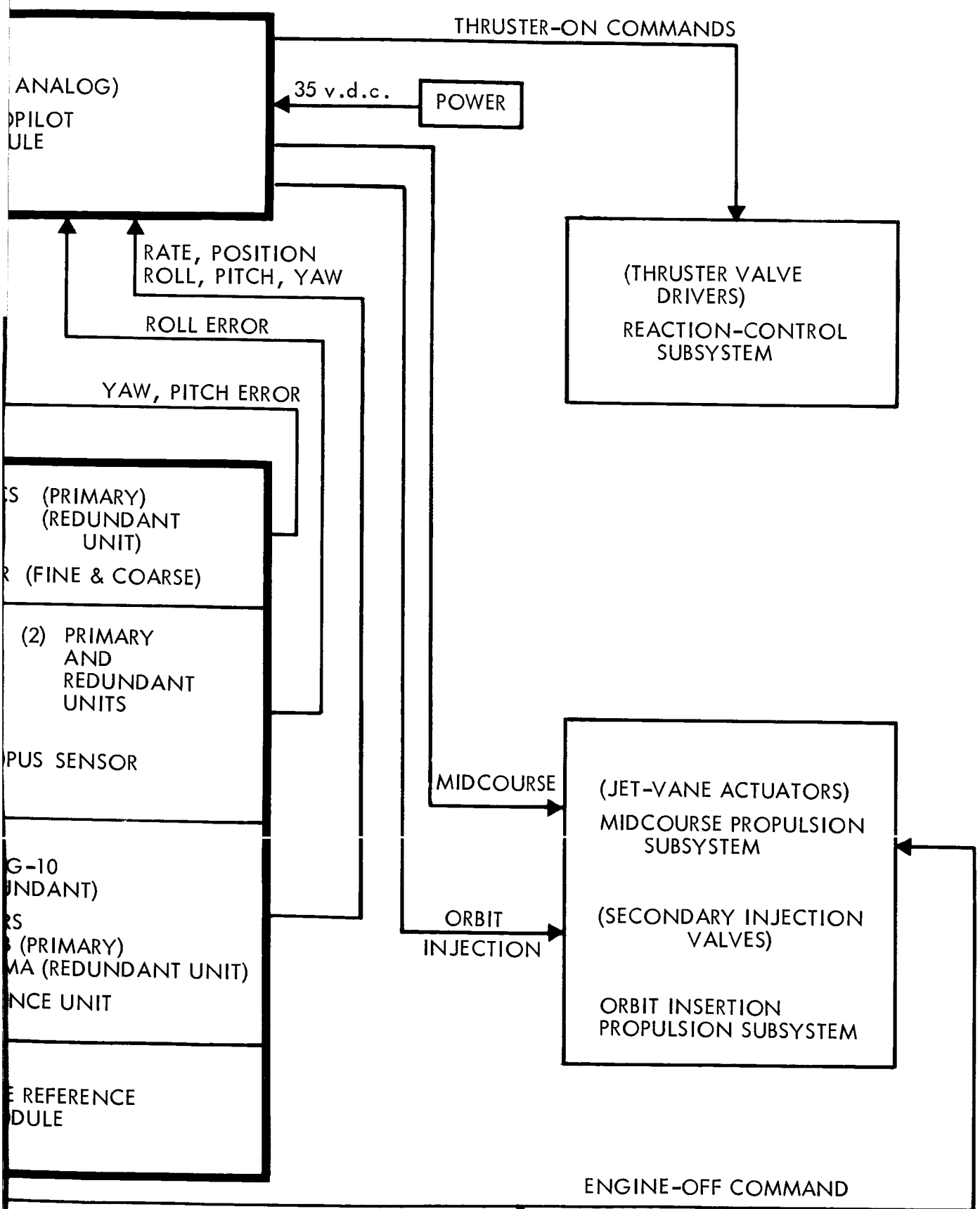

Figure 4.6-2: Attitude Reference and Autopilot Subsystem

gyros in the inertial reference unit (IRU) provide the attitude information. This type of operation is also used during periods of Sun occultation.

To minimize propellant consumption during the long cruise periods, efficient (minimum impulse) limit-cycle operations are desired. For this purpose a rate feedback signal is derived by integrating the electrical on-time of the jets. For undisturbed limit-cycle operation, the switching amplifier is designed to turn off before the minimum design pulse-width of 20 milliseconds has elapsed.

The autopilot subsystem accepts the attitude and rate signals from the attitude reference subsystem and sequential slew commands from the CC&S. These signals are conditioned and applied to the appropriate torque producing devices to achieve the desired spacecraft attitude response.

Because of the on-off operation, which is characteristic of the cold-gas jets, the proportional (or analog) attitude error signals are conditioned by the autopilot subsystem to turn on the jets at a predetermined and variable threshold level. The jet vanes and the secondary injection valves are proportional devices, and therefore, the operation is identical to that of a simple second-order positioned servo system.

Mission Phase-Control Mode Relationships--The application of various control modes to the mission phases are shown in Table 4.6-4. The mission

phases are listed in terms of the control modes required for each vehicle axis. Note that most of the basic control modes are required for more than one mission phase. Descriptions and diagrams of the available control modes follow:

Table 4.6-4: MISSION PHASE - CONTROL MODE RELATIONSHIPS

	CONTROL MODE		
MISSION PHASE	PITCH	YAW	ROLL
Sun Acquisition	Sun Acquisition	Sun Acquisition	Rate Stabilization
Canopus Acquisition	Sun Acquisition	Sun Acquisition	Slew, Canopus Acquisition
Cruise	Cruise	Cruise	Cruise
Maneuver to Thrust Attitude, Capsule Separation Attitude	Inertial Hold	Slew, Inertial Hold	Slew, Inertial Hold
Midcourse Thrust	Midcourse TVC	Midcourse TVC	Inertial Hold
Orbit Insertion Thrust	Orbit Insertion TVC	Orbit Insertion TVC	Inertial Hold
Return to Cruise Attitude	Slew, Inertial Hold, Sun Acquisition, Cruise	Slew, Inertial Hold, Sun Acquisition, Cruise	Slew, Inertial Hold, Canopus Acquisition, Cruise
Sun Occultation	Inertial Hold	Inertial Hold	Cruise
Canopus Occultation	Cruise	Cruise	Inertial Hold

Rate Stabilization Mode (Roll)--In this mode the position loop is opened on the vehicle roll axis and no roll attitude information is fed into the switching amplifier (Figure 4.6-3). The switching amplifier is thus actuated by only the vehicle attitude rate signal from the gyro and causes the roll jets to be turned on, thereby reducing the roll rate to the dead zone limit. This condition is maintained until another control mode is initiated.

Sun Acquisition Mode (Pitch and Yaw)--This operational mode satisfies the requirements of both initial rate stabilization and Sun acquisition for the pitch and yaw axis. The pitch and yaw axis switching amplifiers receive vehicle rate information from the gyros and position information from limiter circuits in series with the Sun sensor output signals (Figure 4.6-4). The vehicle thus maneuvers about these axes in the proper directions until the Sun-sensor signals enter the proportional range of the limiter circuits. The switching amplifiers now receive proportional information from the Sun sensor mixed with the rate signals from the gyros. The jets are operated to reduce the drift rates to limit cycle rates. When the vehicle roll axis is thereby properly aligned, a Sun-acquisition detector enables the slew mode to be established for roll search of Canopus.

Canopus Acquisition Mode (Roll)--The Canopus acquisition mode follows a roll "slew mode," which brings Canopus into the field of view of the Canopus sensor. As noted by the similarity between Figure 4.6-4 and

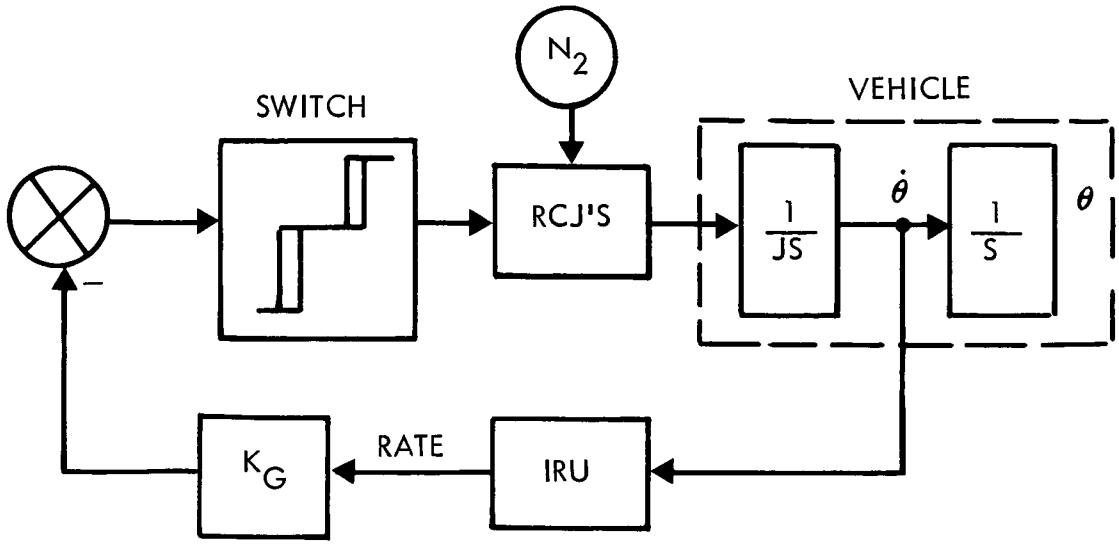

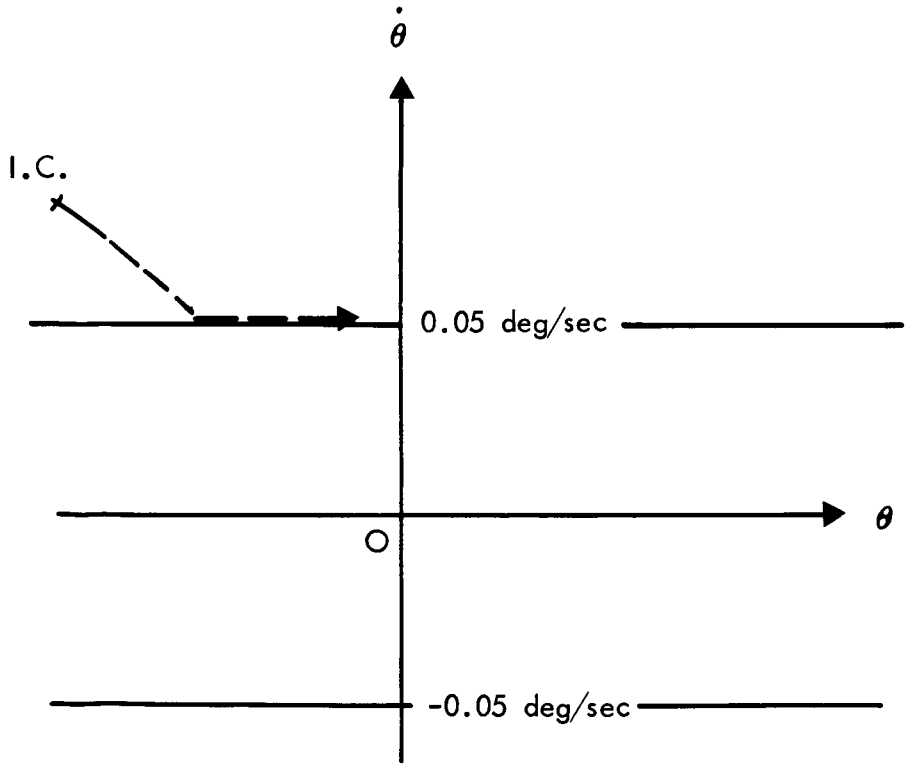

DEADZONE: $\dot{\theta} = \pm 0.05$ deg/sec

INITIAL CONDITIONS: $|\dot{\theta}_o| \leq 3$ deg/sec $|\theta_o| \leq 180$ deg

Figure 4.6-3: Rate-Stabilization Mode (Roll)

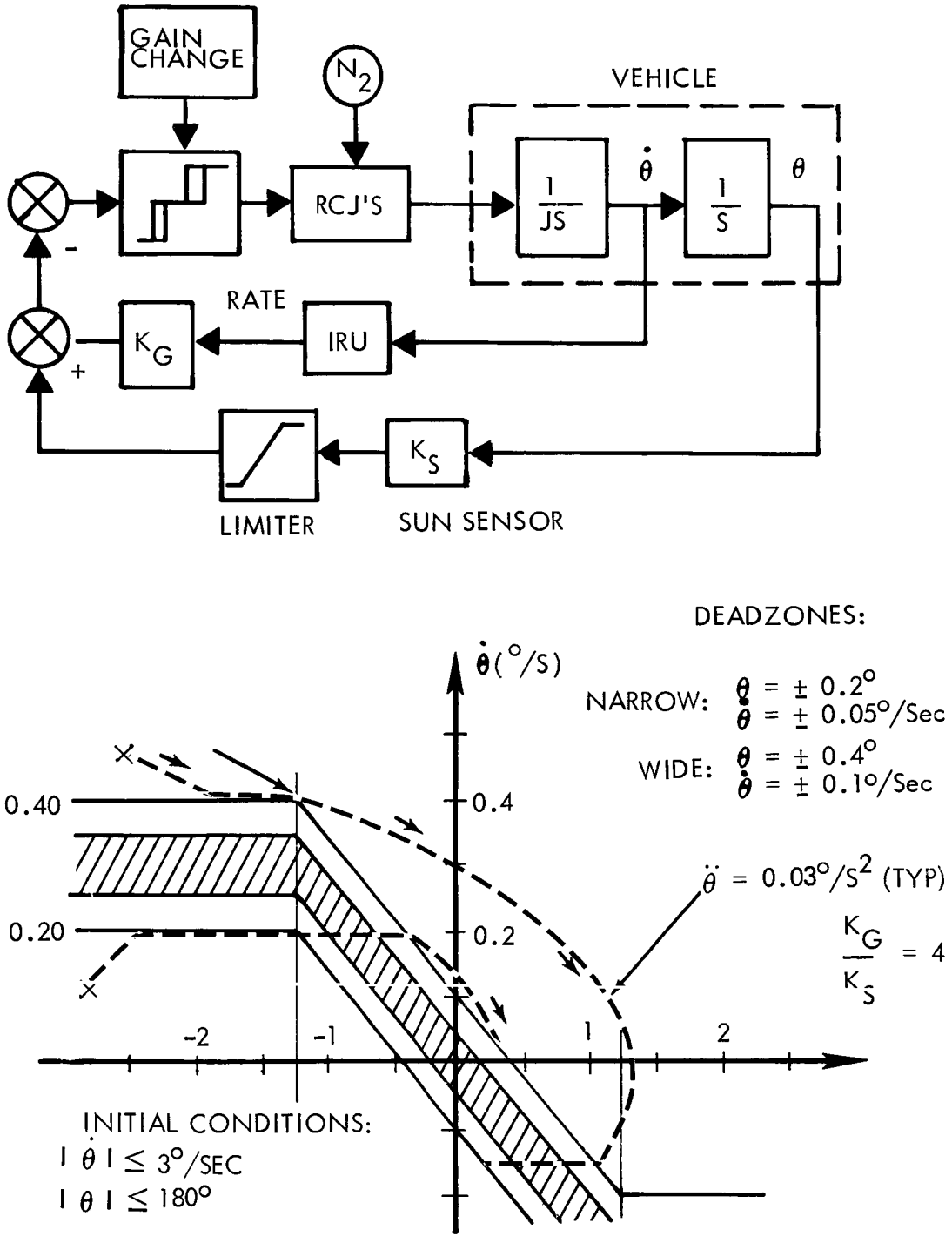

Figure 4.6.-4: Sun Acquisition Mode (Pitch and Yaw)

Figure 4.6-5 the operational feature of this mode is identical to the Sun-acquisition mode, except that Canopus is identified by magnitude.

Cruise Mode (All Axes)--In the cruise mode, three-axis attitude stabilization is maintained by optical sensor error signals operating the gas jets via the autopilot subsystem. Minimum-impulse, limit-cycle operation is achieved with a derived-rate feedback signal obtained by approximate integration of the electrical on-time of the reaction control thruster (Figure 4.6-6).

Slew Mode (Attitude Maneuver)--The jets are controlled by the switching amplifiers in response to the difference between a commanded attitude rate signal and the spacecraft rate as indicated by the gyro rate-output signals (Figure 4.6-7). Predetermined attitude commands are entered in a "windup" register. During slew, the gyro output counts down the "windup" register. A similar maneuver in the opposite direction is used to realign the vehicle to cruise orientation.

Inertial Hold Mode--The cold-gas jets are pulsed by the switching amplifiers in response to the mixed inertial attitude error and rate signals from the gyros. The result is to stabilize the vehicle attitude and rate about the orientation which exists at the initiation of this mode of control (Figure 4.6-8).

Midcourse Thrust Vector Control Mode--This control mode uses four monopropellant 50-pound thrust engines, with each engine having four independent jet vanes and actuators for thrust vector control. Two engines are

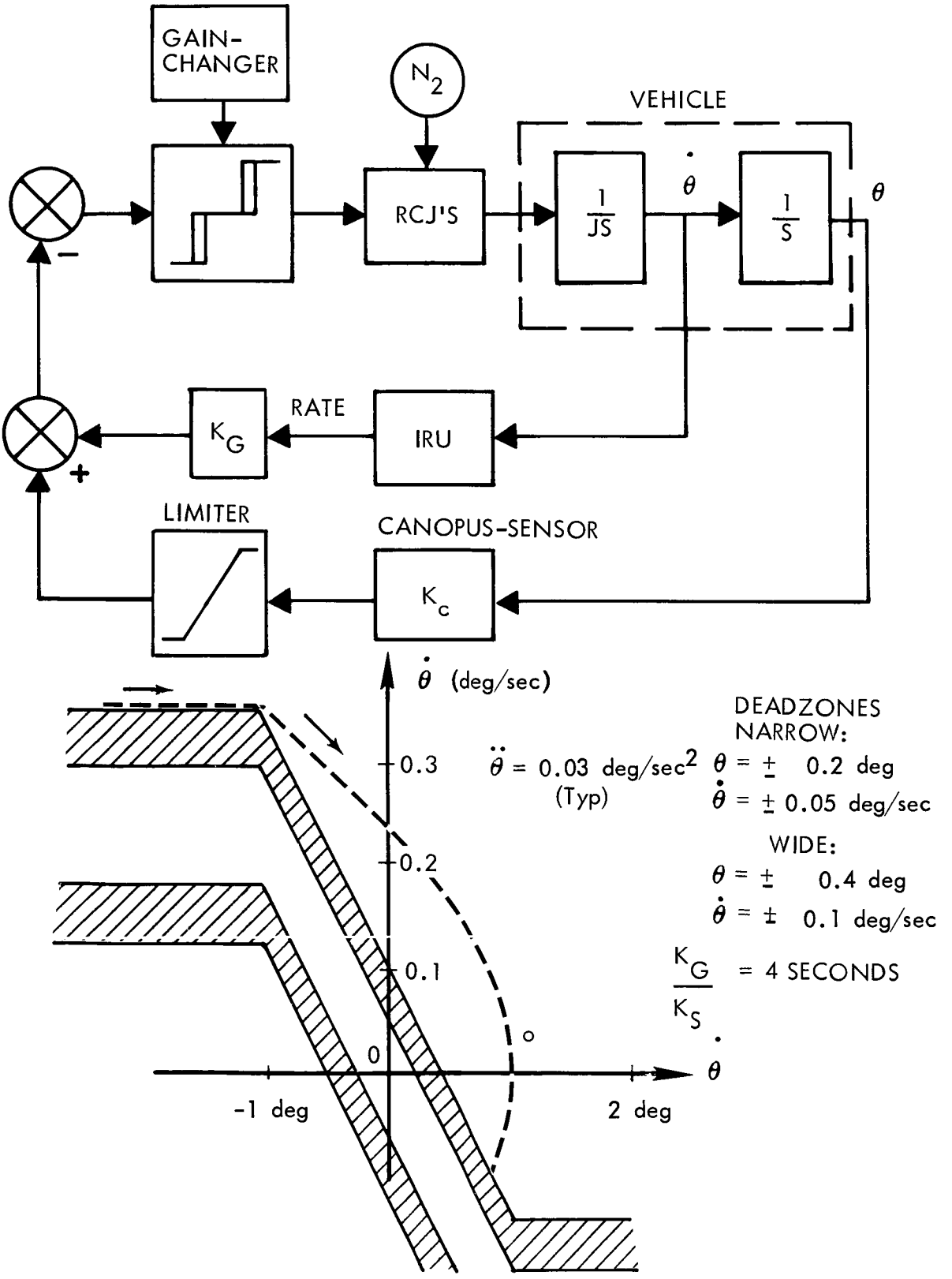

Figure 4.6.-5: Canopus Acquisition Mode (Roll)

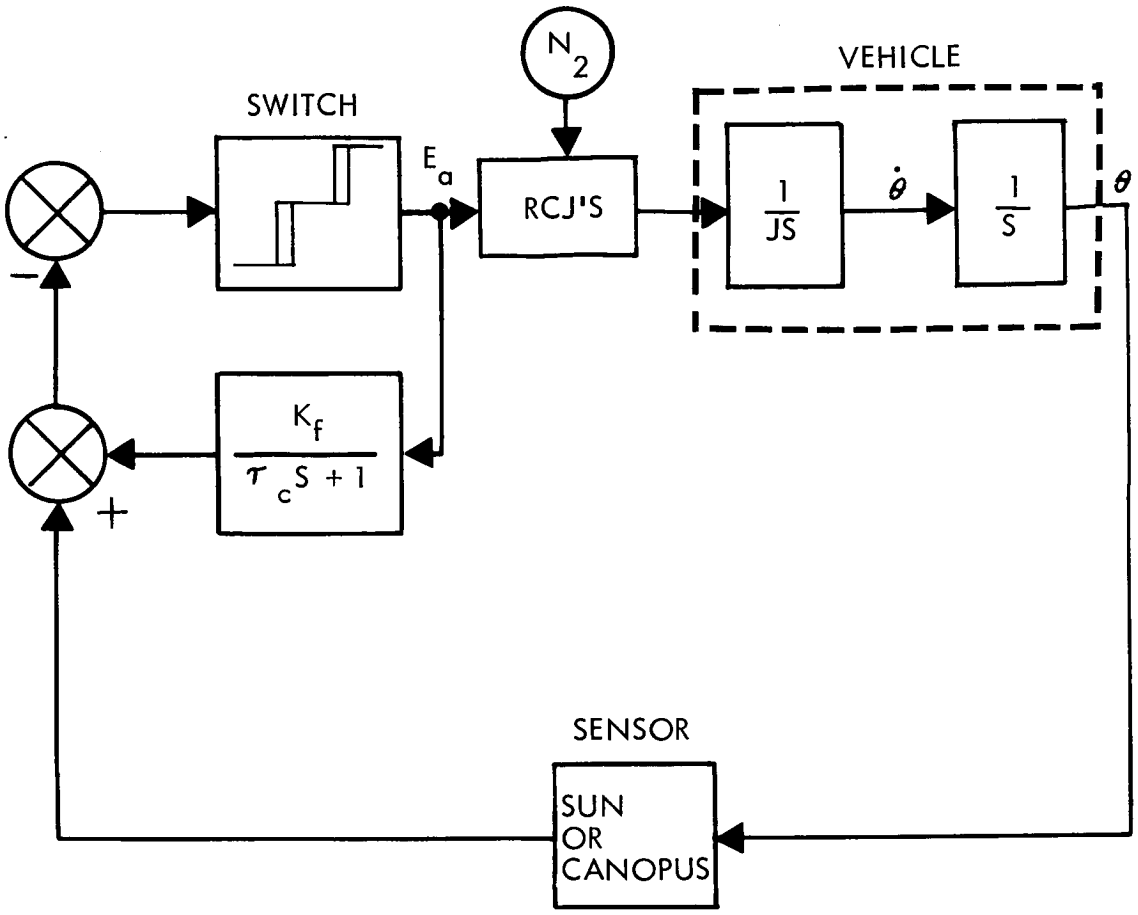

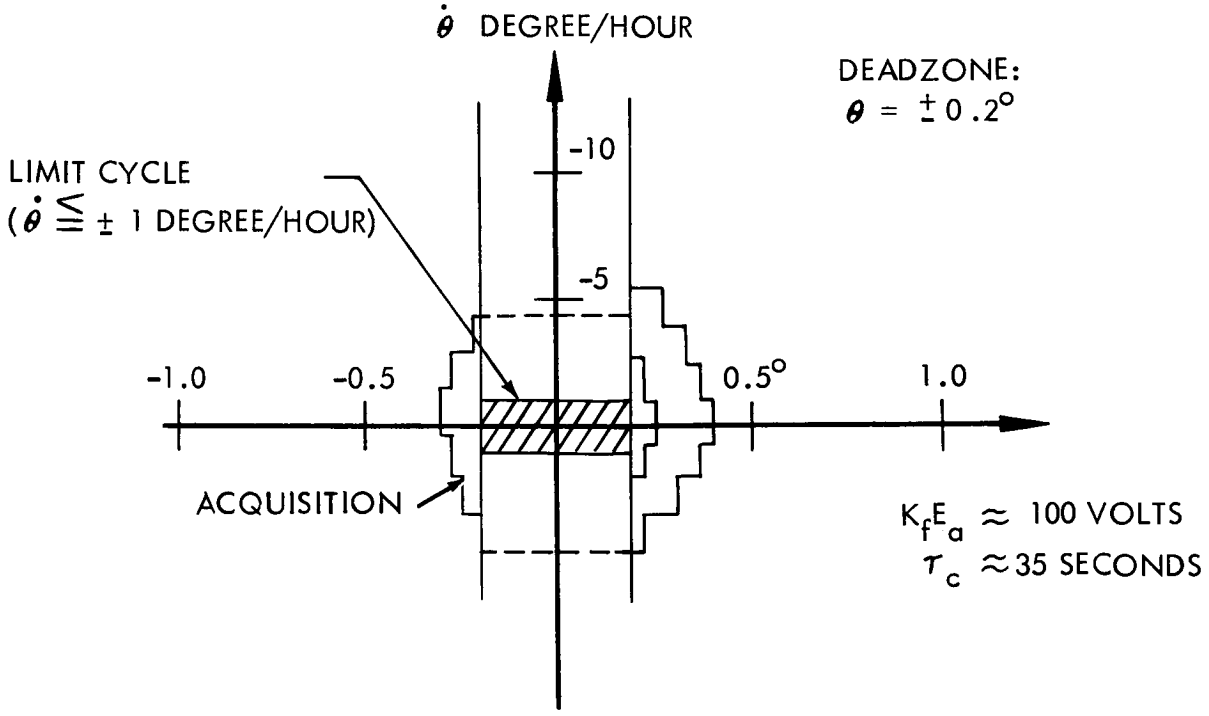

Figure 4.6-6: Cruise Mode

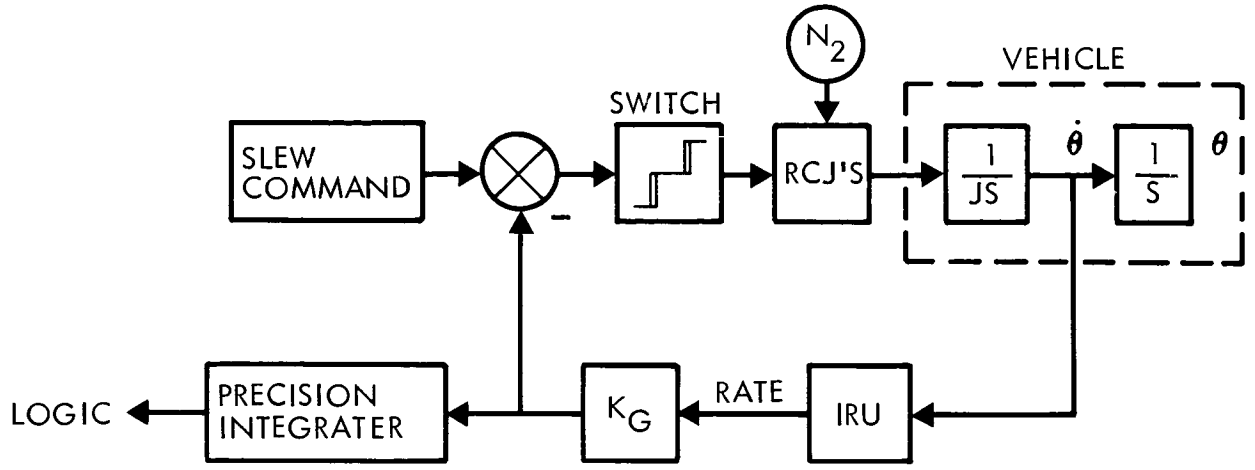

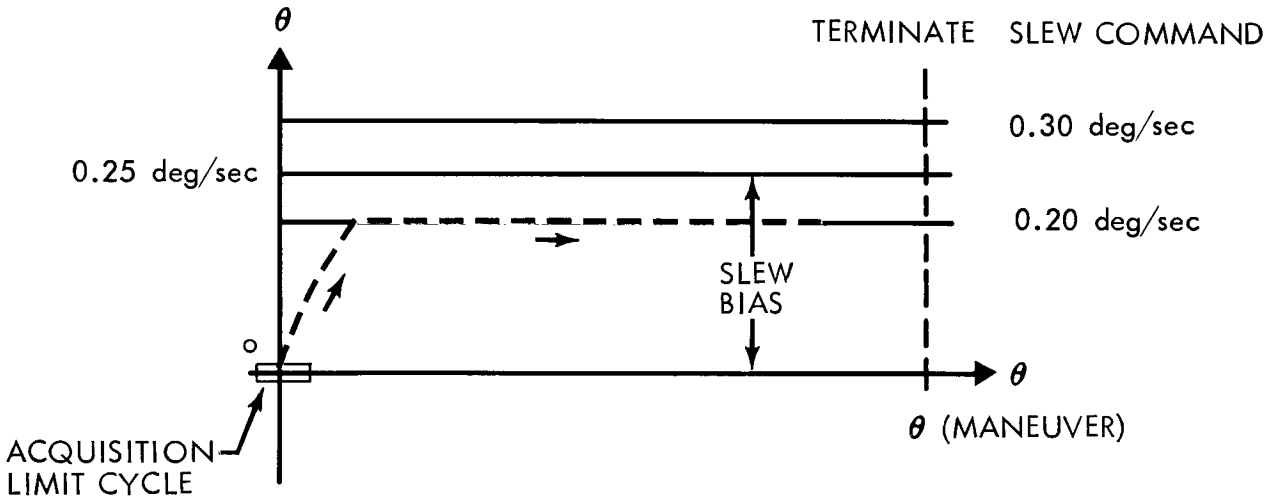

DEADZONE: $\dot{\theta} = \pm$ 0.05 deg/sec ABOUT $\pm$ 0.25 deg/sec

MANEUVER: $\theta = \pm$ 180 deg

INITIAL CONDITIONS: ACQUISITION LIMIT CYCLE $\left(\begin{array}{l}|\dot{\theta}| \leq 5 \text{ deg/hr} \\ |\theta| \leq 0.2 \text{ deg}\end{array}\right)$

Figure 4.6-7: Slew Mode

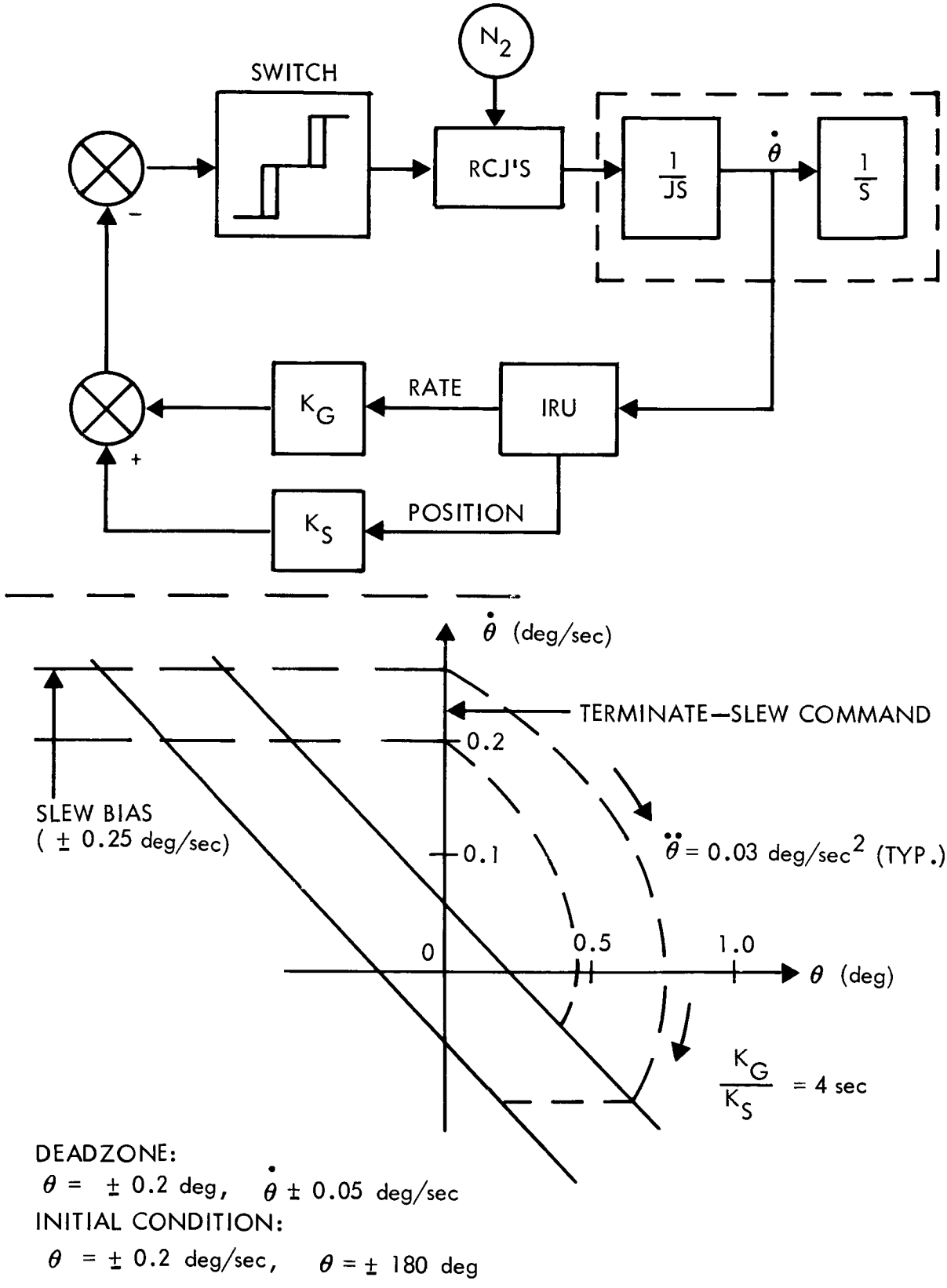

Figure 4.6-8: Inertial Hold Mode

used at a time and the jet vanes on these engines are used to provide control about all three axes. The other two engines provide an identical redundant mode. A functional block diagram of the system appears in Figure 4.6-9. An example of the system performance is shown in Figure 4.6-10.

Orbit Insertion Thrust Vector Control Mode--Pitch and yaw thrust vector control is provided by fluid injection into the exhaust stream of the solid-propellant orbit-insertion engine. Pintle valves for controlling the rate of fluid injection are controlled by hydraulic servos. A functional block diagram of this system is shown in Figure 4.6-11. An example of the system performance is shown in Figure 4.6-12. Roll control is provided by activating both sets of reaction control jets.

4.6.1.4 Interfaces

Optical/Mechanical--The Canopus and Sun sensors require unobstructed fields of view. In addition, shielding must be provided to block out sunlight reflections from other parts of the spacecraft. The attitude reference module has optical interfaces with alignment fixtures since prisms on the sensors are provided to aid in alignment with the module precision-mount surfaces. The mechanical interface of the autopilot with the spacecraft is not critical except for support and thermal requirements.

Thermal--As a design goal, semiconductor junction temperatures will be kept below 600 degrees R. Analysis of the module thermal characteristics will be carried out using digital simulations of thermal equivalent

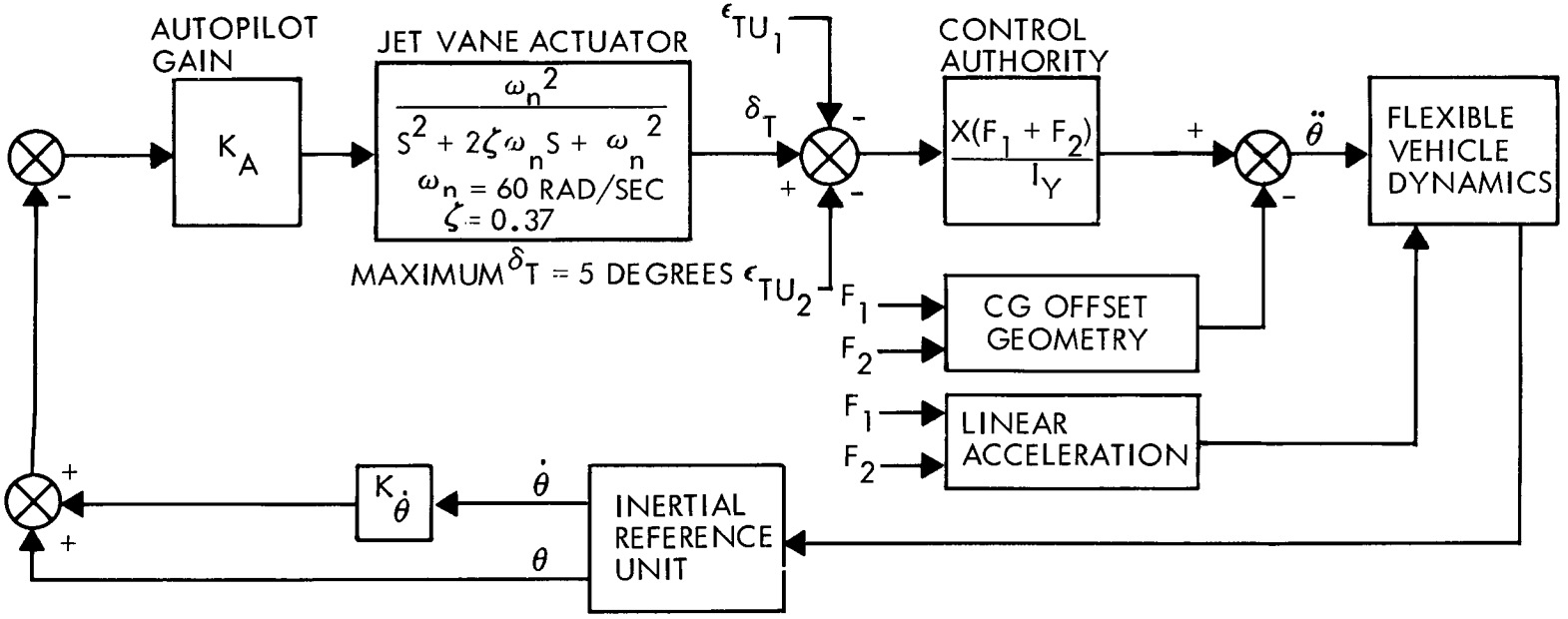

PITCH (OR YAW) AXIS: MONOPROPELLANT ENGINES WITH JET VANES

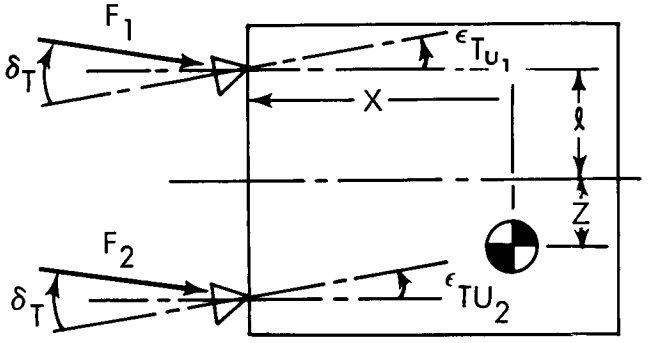

THRUST ALIGNMENT GEOMETRY

3σ TOLERANCES

ϵ_{TU} = THRUST ALIGNMENT UNCERTAINTY
= ± 0.5 DEGREE
Z = VEHICLE CG OFFSET UNCERTAINTY
= ± 0.10 INCH
3% VARIATION IN NOMINAL THRUST LEVELS

ROLL CONTROL

SAME CONTROL SYSTEM AS FOR PITCH OR YAW

Figure 4.6.-9: Thrust Vector Autopilot — Midcourse Correction

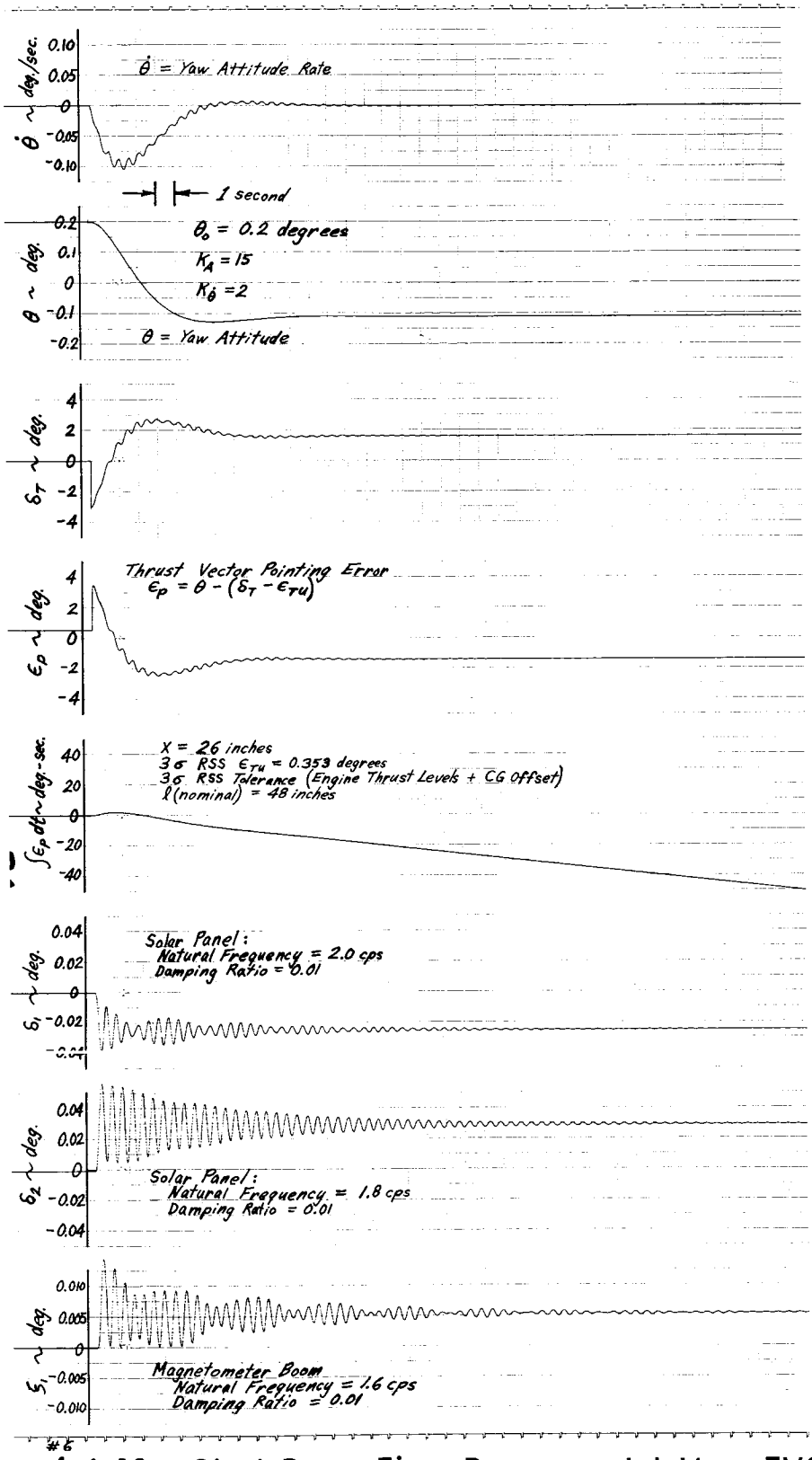

Figure 4.6-10: Start-Burn Time Response Jet Vane TVC — Midcourse Correction

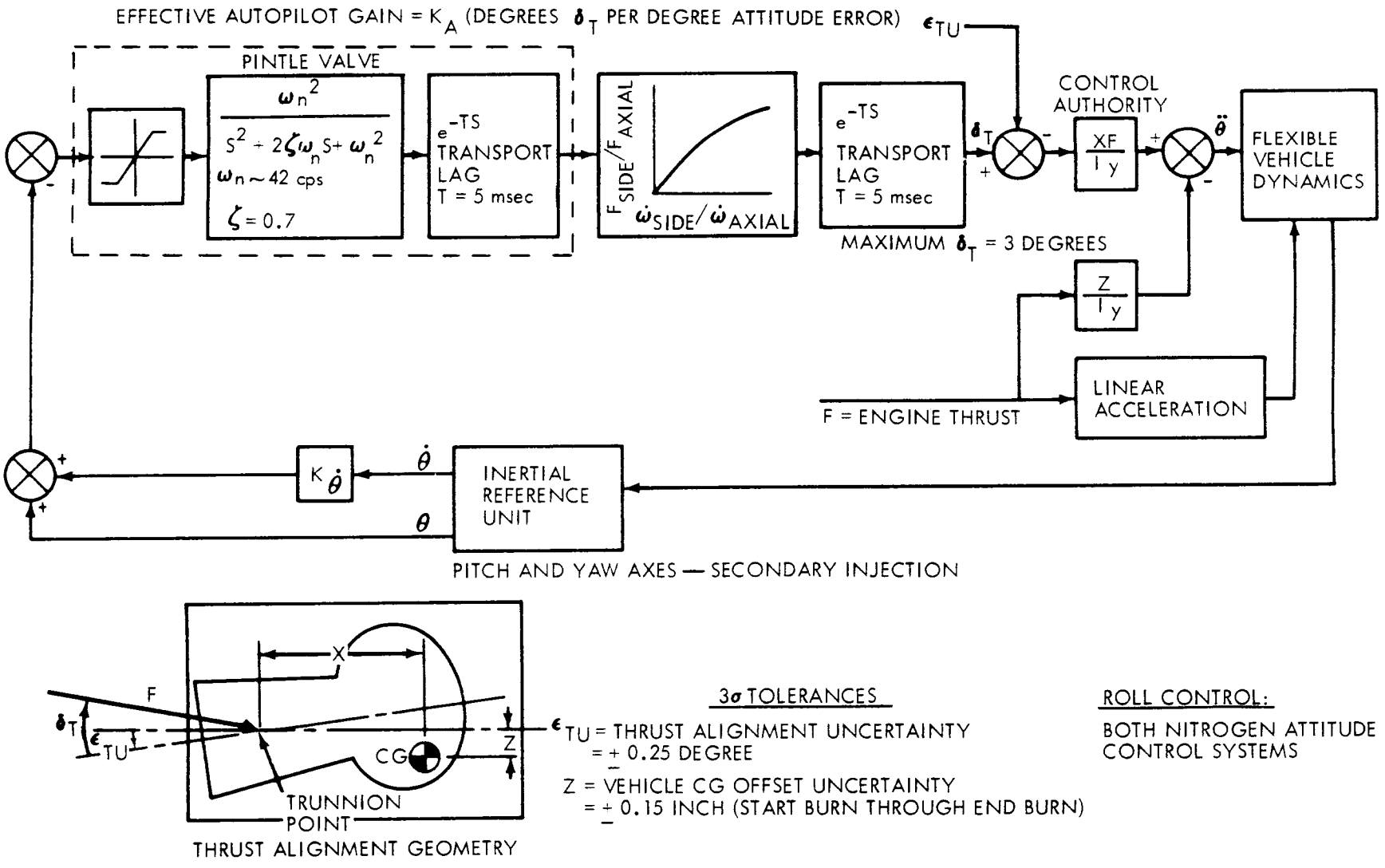

Figure 4.6.-11: Thrust Vector Autopilot — Orbit Insertion

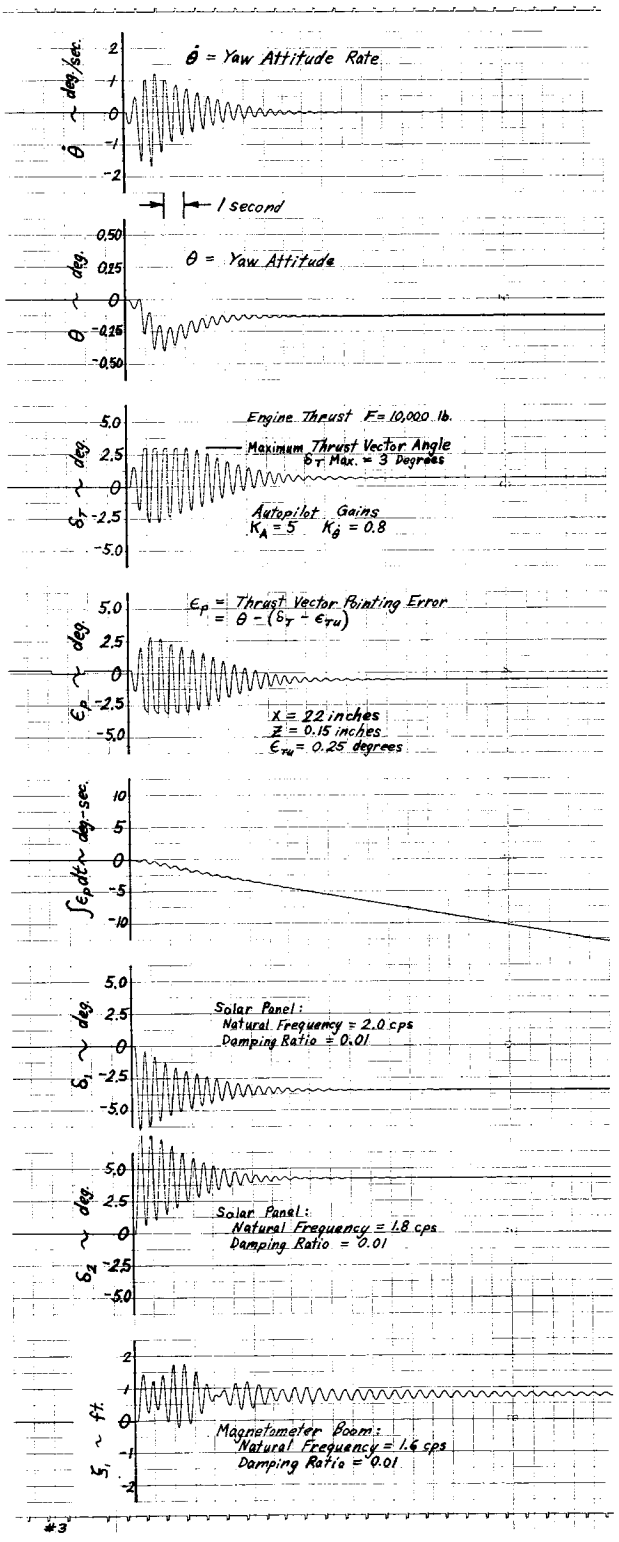

Figure 4.6-12: Start-Burn Time Response Secondary Injection TVC — Orbit Insertion

circuits. To account for the dynamic characteristics of the louver system and solar occultation effects, simulation will include time-varying solution capability.

Electronics are packaged in a configuration so each card substrate acts as its own radiator. The substrate is in the form of a T-section, the upper T-surface acting as the radiator. These cards are then inserted into the module frame and locked in with low thermal impedance card locks.

Electrical, Signals--A list of the electrical signal interfaces is given in Table 4.6-5. Included in this list are the CC&S, telemetry, and OSE interfaces.

Electrical, Power Requirements--Each module in the attitude reference and autopilot subsystem will utilize power provided by the power supply subsystem as indicated in Table 4.6-6. Other voltages required will be inverted from the +35 volts d.c. supply. The flyback transformer scheme of power inversion will be used in which a pulse width modulated transistor switch drives a flyback transformer.

Magnetic Flux Attenuation--Radiated magnetic flux from the electronic modules will be reduced to the required levels by means of two design approaches: careful design of magnetic components to prevent flux generation and shielding and shorting band techniques to attenuate residual radiated flux. Permanent magnets will be carefully designed to be stable

Table 4.6-5a: ATTITUDE REFERENCE SYSTEM INTERFACE LIST

No.	Function	Signal Characteristics Type	Level	Usage Functional Conn. From	To	OSE Conn.	TM 71
1	Pri. Sun Sen., Pitch, Fine Error	Analog	1 v/deg ±5% 5v max			X	
2	Pri. Sun Sen., Yaw, Fine Error	Analog	1 v/deg ±5% 5v max			X	
3	Pri. Sun Sen., Pitch Coarse Error					X	
4	Pri. Sun Sen., Yaw Coarse Error					X	
5	Sec. Sun Sen., Pitch, Fine Error		6 v/deg 6v max			X	
6	Sec. Sun Sen., Yaw, Fine Error	Analog	6 v/deg 6v max			X	
7	Sec. Sun Sen., Pitch, Coarse Error					X	
8	Sec. Sun Sen., Yaw, Coarse Error					X	
9	Sun Sensor, Pitch Error	Analog	±2.5 v		A/P		X
10	Sun Sensor, Yaw Error				A/P		X
11	Select Sec. Sun Sen.	Discrete	+6 vd.c.(T) Ovdc(F)	CC&S			X
12	Sun Sen. Acquisition	Discrete	+6 vd.c.(T) Ovdc(F)		A/P, CC&S		X
13	Pri. Sun Sen. Acquisition	Discrete	+6 vd.c.(T) Ovdc(F)			X	
14	Sec. Sun Sen. Acquisition	Discrete	+6 vd.c.(T) Ovdc(F)			X	
15	Canopus Power On			CC&S			
16	Can. Pitch Gimbal Increment	Discrete	0 to +6v	CC&S			
17	Can. Pitch Gimbal Decrement	Discrete	+6 vdc(T) Ovdc(F)		CC&S		
18	Can. Pitch Gimbal Angle	Analog					X
19	Activate Sun Shutters	Discrete		Sun Sen			
20	Activate Sun Shutters	Discrete		CC&S			
21	Canopus Sen. Pri. Power	DC Power	+35v	Pwr SS			
22	Pri. Canopus Sen. Power	2400 cps(sq wave)	50v	Pwr SS			
23	Select Sec. Canopus Sensor	Discrete	0 to +6v	CC&S			
24	Canopus Acquisition	Discrete			CC&S		X
25	Canopus Roll Error	Analog	±3 v (max)		A/P		X
26	Canopus Sen. Star Magnitude	Analog	+9 v (max)				X
27	Pri. Canopus Sen. Power On	Discrete				X	
28	Sec. Canopus Sen. Power On	Discrete				X	
29	Pri. Canopus Sen.	Discrete	0 to +6 v			X	
30	Sec. Canopus Sen. Acquisition	Discrete	0 to +6 v			X	

Table 4.6-5a: ATTITUDE REFERENCE SYSTEM INTERFACE LIST (Cont'd)

No.	Function	Signal Characteristics Type	Level	Usage Functional Conn. From	To	OSE Conn.	TM 71
31	Mon. Pri. Canopus Sen. Roll Error	Analog	±3 v (max)			X	
32	Mon. Sec. Canopus Sen. Roll Error	Analog	+3 v			X	
33	Mon. Pri. Canopus Sen. Star Magnitude	Analog	9 v (max)			X	
34	Mon. Sec. Canopus Sen. Star Magnitude	Analog	9 v (max)			X	
35	IRV Instrument Block Temp.	Analog	0 to +1 v				X
36	IRV Input Power, +35 v	d.c.	+35 v	Pwr Sub. S			
37	IRV Input Power, 614.6 kc	a.c.	NA	CC&S			
38	IRV Input Power, 2.4 kc	a.c.	NA	Pwr Sys			
39	IRV Pwr Supply 1 +12 v d.c.	d.c.	+12 v			X	
40	IRV Pwr Supply 2 +12 v d.c.	d.c.	+12 v			X	
41	IRV Pwr Supply 3 +12 v d.c.	d.c.	+12 v			X	
42	Roll Gyro Select	Discrete		CC&S			
43	Pitch Gyro Select	Discrete	0 to +6 v	CC&S			
44	Yaw Gyro Select	Discrete		CC&S			
45	Roll Gryo Sel Verify	Discrete					X
46	Pitch Gyro Sel Verify	Discrete	0 to +5 v				X
47	Yaw Gyro Sel Verify	Discrete					X
48	Roll Gyro θ Output	Analog		A/P			
49	Pitch Gyro θ Output	Analog	0 to ±4 v	A/P			
50	Yaw Gryo θ Output	Analog		A/P			
51	Roll Gyro θ Rate Output	Analog		A/P			X
52	Pitch Gyro θ Rate Output	Analog		A/P			X
53	Yaw Gyro θ Rate Output	Analog		A/P			X
54	Roll Gyro "A" O Output	Analog	±4 v				X
55	Roll Gyro "A" O Output	Analog	±4 v				X
56	Pitch Gyro "A" O Output	Analog	±4 v				X
57	Pitch Gyro "B" O Output						X
58	Yaw Gyro "A" O Output						X
59	Yaw Gyro "B" O Output	Analog	±4 v				X
60	Roll Gyro Spin Motor	Discrete	6 v d.c.				X
61	Pitch Gyro Spin Motor	Discrete	0 to +6 v				

Table 4.6-5a: ATTITUDE REFERENCE SYSTEM INTERFACE LIST (Cont'd)

No.	Function	Signal Characteristics Type	Level	Usage Functional Conn From	To	OSE Conn	TM 71
62	Yaw Gyro Spin Motor	Discrete	0 to +6 v				X
63	Roll Gyro Digital Output				CC&S		
64	Pitch Gyro Digital Output				CC&S		
65	Yaw Gyro Digital Output				CC&S		
66	Roll Gyro Dias Input	Pulse 2 kc (max)		CC&S			
67	Roll Gyro Bias Input			CC&S			
68	Pitch Gyro Bias Input	Pulses	0 to +6 v	CC&S			
69	Pitch Gyro Bias Input	1.2	0 to +6 v	CC&S			
70	Yaw Gyro Bias Input			CC&S			
71	Yaw Gyro Bias Input	Pulses		CC&S			
72	Roll Gyro Range	Discrete		CC&S			
73	Pitch Gyro Range	Discrete	0 to +5 v	CC&S			
74	Yaw Gyro Range	Discrete		CC&S			
75	Reset Register	Discrete	0 to +4 v	CC&S			
76	EMA Acc. "+" Acceleration Output	Pulses	0 to +4 v		CC&S	X	
77	EMA Acc. "-" Acceleration Output	100 cps (max)			CC&S	X	
78	Bell Acc. + Output		0 to +6 v		CC&S	X	
79	EMA DC Amp. Output	100 cps (max)	Sawtooth on 4.5vd.c.				X
80	Bell DC Amp. Output	Analog	N/A				X
81	EMA Pickoff Output	20 kc	6 mv/mr				
82	EMA Precision Clock	2 kc (pulses)	0 to +4 v			X	
83	Bell Bias Input Check	d.c. Current	4 ma			X	
84	EMA Bias Input Check	d.c. Current	4 ma			X	
85	Accel. Power On	Discrete	+6v d.c.(T) Ovd.c. (F)	CC&S			
86	Bell Accel. Output	Pulses	0 to +6 v d.c.		CC&S	X	

Table 4.6-5b: AUTOPILOT INTERFACE

No.	Function	Signal Characteristics Type	Signal Characteristics Level	Usage Functional Conn From	Usage Functional Conn To	Usage OSE Conn	Usage TM 71
1	Select Sun Sen #1 (P&Y)	Discrete	True (-12 vd.c.), False (+6 vd.c.)	CC&S			
2	Select Canopus Sen #1 (R)						
3	Select IRV Gyro Rate (P)						
4	Select IRV Gyro Rate (Y)						
5	Select IRV Gyro Rate (R)						
6	Select Derived Rate (P)						
7	Select Derived Rate (Y)						
8	Select Derived Rate (R)						
9	Select IRV Pos (P)						
10	Select IRV Pos (Y)						
11	Select IRV Pos (R)						
12	Select Pitch Slow Rate (+)						
13	Select Pitch Slow Rate (-)						
14	Select Yaw Slow Rate (+)						
15	Select Yaw Slow Rate (-)						
16	Select Roll Slow Rate (+)						
17	Select Roll Slow Rate (-)						
18	Select TVC Pitch						
19	Select TVC Yaw						
20	Select TVC Roll						
21	Select N2 Thrusters #1						
22	Select N2 Thrusters #2						
23	Select Dead Band (P&Y)						
24	Select Dead Band (R)	Discrete	True (-12 vd.c.), False +6 vd.c.)	CC&S			
25	Sun Sensor (P)	Analog	+6 vd.c. to -6vd.c. 2 v/deg	Sun Sen			
26	Sun Sensor (Y)		+6 vd.c. to -6v.d.c.2 v/deg	Sun Sen			
27	Canopus Sensor (R)		+6 vd.c. to -6vd.c. 2 v/deg	Can Sen			
28	Gyro Position (P)		+6 vd.c. to -6vd.c. 2 v/deg	IRU			
29	Gyro Rate (P)						
30	Gyro Position (Y)						

Table 4.6-5b: AUTOPILOT INTERFACE (Cont'd)

No.	Function	Signal Characteristics Type	Level	Usage Functional Conn From	To	OSE Conn	TM 71
31	Gyro Rate (Y)	Analog	+6 vd.c. to -6vd.c. 2 v/deg	IRU			
32	Gyro Position (R)						
33	Gyro Rate (R)						
34	Tri Safe Amp. Output #1	Analog	± 6 v d.c.			X	
45	Tri Safe Amp. Output #9	Analog	± 6 v d.c.			X	
46	Tri Safe Power Supply #1	Analog	± 12 v d.c. + 6 v d.c.			X	
52	Tri Safe Power Supply #6	Analog	± 12 v d.c. + 6 v d.c.			X	
53	Feedback Pot (+ Excitation) #1	Analog	+ 12 v d.c.		Prop.Sys.		
54	Feedback Pot (- Excitation) #1		- 12 v d.c.				
83	Feedback Pot (+ Excitation) #16		+ 12 v d.c.		Prop.Sys.		
84	Feedback Pot (- Excitation) #16		- 12 v d.c.		Prop.Sys.		
85	Feedback Signal #1		0 - 12 v d.c.	Prop.Sys.		X	
100	Feedback Signal #16		0 - 12 v d.c.			X	
101	Jet Vane Actuator (+) #1		0 - 33 v d.c.		Prop.Sys.		
102	Jet Vane Actuator (-) #1		0 - 33 v d.c.				
131	Jet Vane Actuator (+) #16		0 - 33 v d.c.				
132	Jet Vane Actuator (-) #16	Analog	0 - 33 v d.c.				
133	Jet Vane Actuator C.T. #1	-	Ground	Prop.Sys.			
148	Jet Vane Actuator C.T. #16	-	Ground	Prop.Sys.			
149	(+) Pitch Solenoid #1	Discrete	Open(+35vd.c.)Close(1.5vd.c.)		React Cont		X
150	(-) Pitch Solenoid #1						X
151	(+) Yaw Solenoid #1						X
152	(-) Roll Solenoid #1				React Cont		X
153	(+) Roll Solenoid #1						X

Table 4.6-5b: AUTOPILOT INTERFACE (Cont'd)

No.	Function	Signal Characteristics Type	Level	Usage Functional Conn. From	To	OSE Conn.	TM 71
154	(+) Roll Solenoid #1	Discrete	Open(+35vd.c.)Close(1.5vd.c)		React Cont		X
155	(-) Roll Solenoid #1						X
156	(-) Roll Solenoid #1						X
157	(+) Pitch Solenoid #2						X
158	(-) Pitch Solenoid #2						X
159	(+) Yaw Solenoid #2						X
160	(-) Yaw Solenoid #2						X
161	(+) Roll Solenoid #2						X
162	(+) Roll Soelnoid #2						X
163	(-) Roll Solenoid #2						X
164	(-) Roll Solenoid #2	Discrete	Open(+35vd.c.)Close(1.5vd.c.)		React Cont		X

Table 4.6-6: POWER SUPPLY SUMMARY FOR ATTITUDE REFERENCE AND FLIGHT CONTROL SUBSYSTEMS

POWER INPUT IN WATTS

	Attitude Reference Module		Autopilot Module		
			+35 v d.c. (Signal Power)	+35 v d.c. (Valves and Solenoids)	
	35 v d.c.	2400 cps		Average	Maximum
Prelaunch, Launch, and Injection	0	2	0	0	0
Postseparation Stabilization	28.9	2	12	28	28
Sun Acquisition	28.9	2	12	14	28
Canopus Acquisition	32.5	2	12	28	56
Interplanetary Cruise	32.5	2	10	0	56
Midcourse Maneuver	32.5	2	15	32	64
Orbit Insertion	32.5	2	15	59.2	59.2
Mars Orbit	32.5	2	10	0	56

under varying magnetic transients, to permit effective cancellation of residual d.c. flux.

Noise Pickup and Electrointerference--The effects of electrointerference will be reduced by: control of grounding methods, transient suppression devices, shielding, wire and cable routing, and component packaging. A separation will be made between signal-type and power-type grounds. Chassis and box cover bending will provide low-impenance current paths for any field-induced current that may be generated.

Wires carrying audio signals will be shielded and the shield insulated to maintain isolation from any chassis or structure ground at all points but one. Internal wiring of the modules will be routed to avoid formation of circuit loops and ground loops. Required separation will be determined by the signal involved. The JPL specification 30236-ETS-A will be used as a guideline. (Reference 13 of Section 4.6.1)

Radiation--Depending on the mission profile, the flux values from the Mars trapped radiation and solar-flare event protons are expected to be too low to cause permanent displacement damage to electronics. Dose rates are also low enough to neglect bulk ionization effects (photocurrents) in semiconductors.

An area of concern that has received considerable attention is the phenomenon of surface ionization per TelStar experience. The effect apparently arises from ionization of the gas in the device in question and the

subsequent reaction of these gas ions with the device surface. This reaction induces surface inversion layers that alter junction characteristics. Devices irradiated under bias exhibit this effect much more strongly than the devices that are not biased. It has been found that: 1) surface passivation, 2) evacuation of the devices, 3) screening tests at 8.5×10^5 radians per hour for 1 minute (equivalent to at least 3 months in orbit) are effective in reducing problems from this source.

NASA space labs in Greenbelt, Maryland, indicate that the screening procedure is quite effective. They point out that a transistorized encoder (UK-1 Satellite), is still operating after 3 years in near-Earth orbit. Both NASA and Battelle (who are performing a radiation test program for NASA) feel that the most severe Earth orbit from a radiation standpoint will not cause sufficient permanent or surface damage to integrated circuits or fast transistor devices, based on a 3-year electron exposure, to make them inoperative. However, a 3-year proton exposure would be borderline on a surface-effect basis.

4.6.1.5 Performance Parameters

Subsystems performance parameters are defined as those parameters which the subsystem measures, i.e., attitude angle with respect to some celestial reference, attitude angle rate, and velocity changes along the true thrust line through the vehicle. The worth of these performance parameters is most accurately described in terms of the measurement errors.

A summary table of attitude errors is given in Table 4.6-7; and a summary of the EMA error analysis for midcourse maneuvers is given in Table 4.6-7A. The accelerometers can be used to monitor the insertion maneuver to provide engineering data with an accuracy of 0.2 percent.

System Reliability--The predicted reliability for the selected attitude references and autopilot subsystem is in Table 4.6-1 discussed earlier. The reliability block diagram for this system is shown in Figure 4.6-13. Detailed parts counts and substantiation of these failure rates and mission reliability numbers appear in the Voyager reliability document, D2-82724-1.

4.6.1.6 Physical Characteristics and Constraints

The attitude reference and autopilot subsystem is organized into modules that are discussed below.

Autopilot Module--As shown in Figure 4.6-14, the electronics for the autopilot control subsystem is packaged in a single module whose dimensions are 8 inches wide, 8 inches long, and 10 inches high. The module will contain six electronic cards of the metal-substrate configuration.

Attitude Reference Module--This module, shown in Figure 4.6-15, contains the inertial reference unit, two Canopus trackers, which comprise the Canopus tracker unit, and the redundant fine Sun sensors and their associated electronics. The Canopus tracker unit, the fine Sun sensors, and

Error Source	Error Description Breakdown		
Inertial Sensors (G10 Gyros)	Mechanical Misalignment of Sensitive Axes with Vehicle:		
	Drift During Inertial Hold: *		Random (0.01
			Bias (0.1°/hr
			Temp. (0.005
	Drift During Thrust: **	g - Sensitive	0.2
			0.3
		g^2 - Sensitive	9.6
			1.6
	Gyro Nonorthogonality: +		
Optical Sensors (Barnes JPL Ball Bros.)	Mechanical Misalignment of Sensitive Axis with Vehicle:		Sun Sensor
			Canopus S
	Null Offset (Mechanical, Internal, and Electrical):		Sun Sensor
			Canopus S
	Sensing Accuracy:		Sun Sensor
			Canopus S
Initial Condition	Limit-Cycle Attitude:		
	Switching Amplifier Null Offset:		
Maneuver Control	Gyro Torquer Scale Factor (330 ppm): +		
	CC&S Control Quantization:		

*Based on 100-Minute Third Midcourse Correction and 70-Minute Orbit Injection Ma
10°F Temp Change

**2-Minute, 2-g Thrust

+ 100-Degree Maneuvers, pitch and roll

Note: Caluculation based on typical maneuvers. See section 3-8 for maximum

Table 4.6-7: Attitude Error Summary

	Third Midcourse Maneuver (35 degrees)			Orbit Insertion (35 degrees)			Midcourse Error Totals (3σ) (degrees)	Insertion Error Totals (3σ) (degrees)
	Pitch	Yaw	Roll	Pitch	Yaw	Roll		
	0.05	0.05	0.05	0.05	0.05	0.05		
5°/hr)	0.025	0.025	0.025	0.018	0.018	0.018		
)	0.250	0.250	0.250	0.18	0.18	0.18		
°/hr/°F)	0.08	0.08	0.08	0.06	0.06	0.06		
°/hr/g	—	—	—	—	—	—		
°/hr/g	—	—	—	—	—	.033		
°/hr/g^2	—	—	—	.013	.013	.013		
°/hr/g^2	—	—	—	.002	.002	—		
	0.10	0.08	0.10	0.10	0.08	0.10	0.463	0.340
	0.08	0.08	0	0.11	0.11	0		
ensor	0	0	0.04	0	0	0.04		
	0.025	0.025	0	0.032	0.032	0		
ensor	0	0	0.025	0	0	0.025		
	0.005	0.005	0	0.007	0.007	0		
ensor	0	0	0.10	0	0	0.10	0.162	0.196
	0.15	0.15	0.15	0.20	0.20	0.20		
	0.03	0.03	0.03	0.04	0.04	0.03	0.265	0.354
	0.033	0	0.033	0.033	0	0.033		
	0.01	0	0.01	0.01	0	0.01	0.049	0.049

euvers,

aneuver time

Table 4.6-7A: EMA ERROR BUDGET (3σ)

(FINAL MIDCOURSE MANEUVER, ΔV = 1 fps)

	Acceleration Error (g's)	Velocity Error (fps)	Allowable Velocity Error (fps)
I. Proportional Errors			
Bias:			
Magnitude*	7×10^{-5}	5.4×10^{-3}	
Temperature Coefficient (3×10^{-5}g/°F)	9×10^{-5}	1.65×10^{-3}	
Noise	3×10^{-5}	$.55 \times 10^{-3}$	
Vibration (150 ppm/g)	4×10^{-7}	$.01 \times 10^{-3}$	
Scale Factor:			
Precision (1500 ppm)	8×10^{-5}	1.47×10^{-3}	
Stability (90 day, 300 ppm)	1.6×10^{-5}	$.29 \times 10^{-3}$	
Linearity (150 ppm/g)	4×10^{-7}	$.01 \times 10^{-3}$	
Temperature Coefficient (150 ppm/°F)	2.4×10^{-5}	$.44 \times 10^{-3}$	
*Trimmed to within 7×10^{-5}g prior to maneuver		5.9×10^{-3}	0.03
II. Nonproportional Errors			
Quantization Error	------	0.01	0.1
Total RSS Error		0.011	0.1

Average acceleration = 0.013g

Temperature deviation = 3°F

Time of thrust = 2.4 seconds

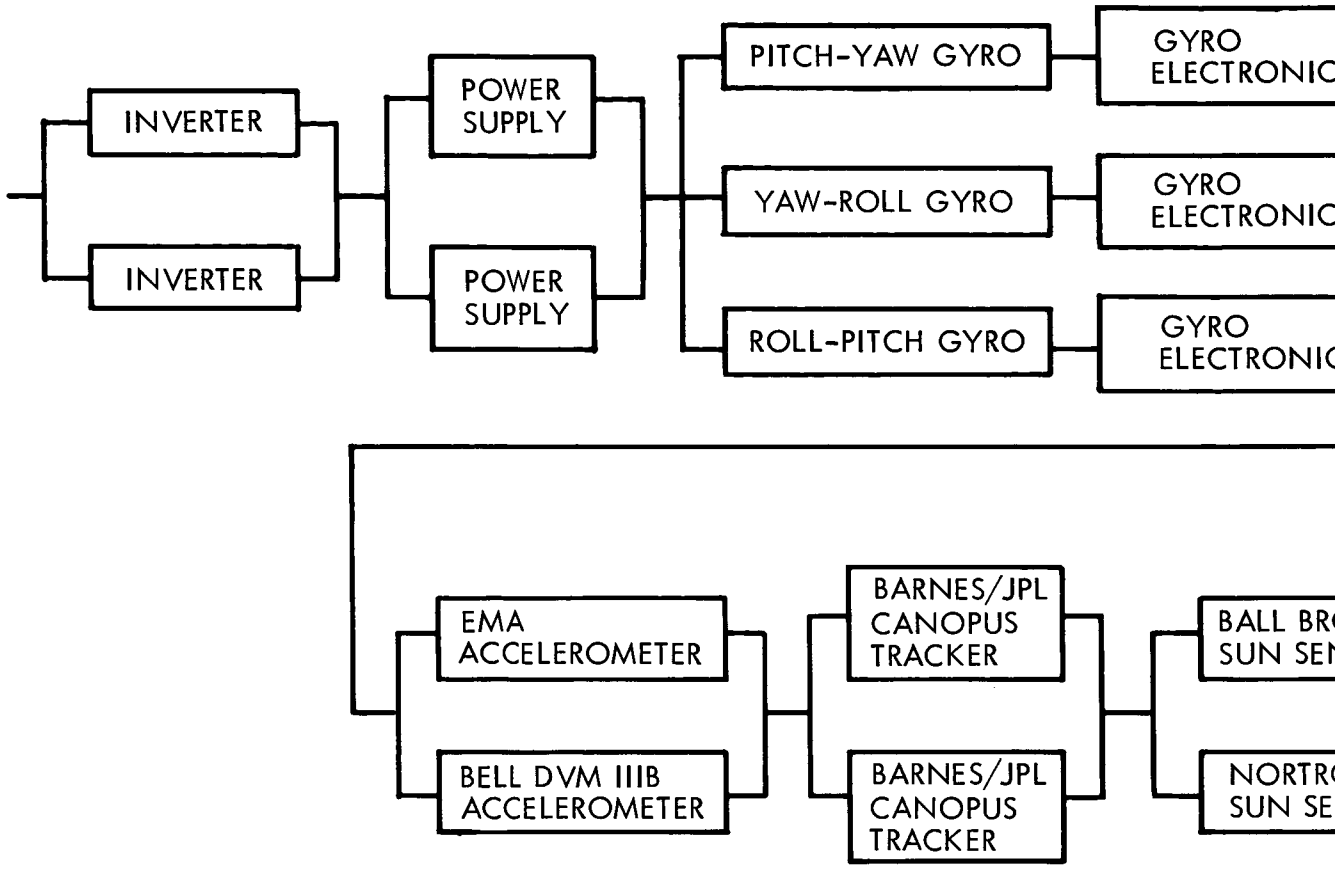
INVERTER
INVERTER
POWER SUPPLY
POWER SUPPLY
PITCH-YAW GYRO
YAW-ROLL GYRO
ROLL-PITCH GYRO
GYRO ELECTRONIC
GYRO ELECTRONIC
GYRO ELECTRONIC
EMA ACCELEROMETER
BELL DVM IIIB ACCELEROMETER
BARNES/JPL CANOPUS TRACKER
BARNES/JPL CANOPUS TRACKER
BALL BR
SUN SEN
NORTR
SUN SE
ATTITUDE R

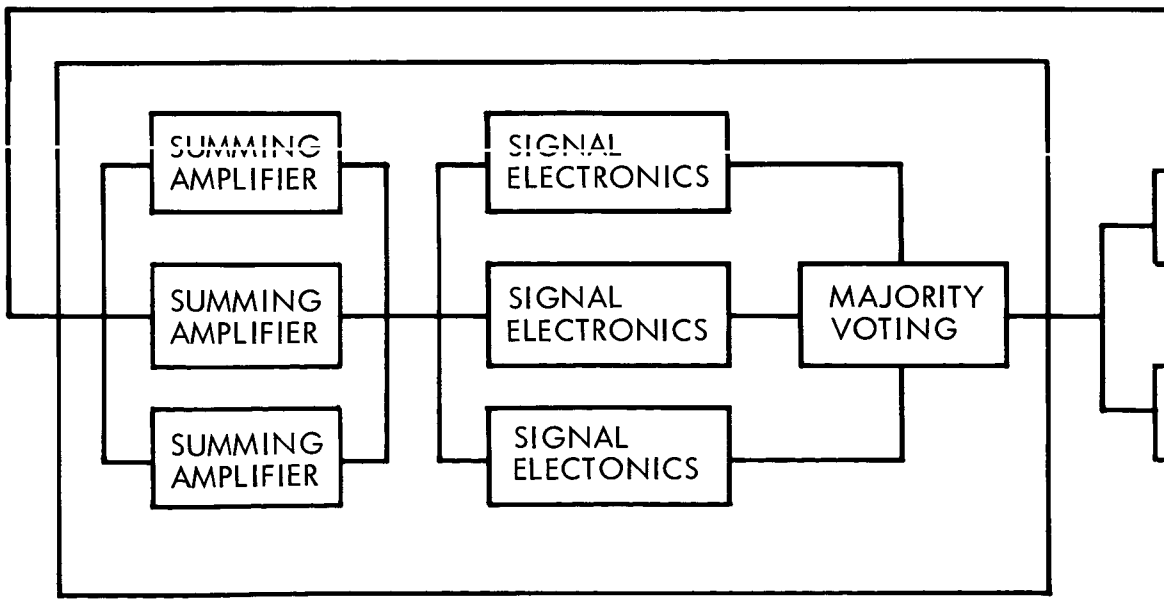
SUMMING AMPLIFIER
SUMMING AMPLIFIER
SUMMING AMPLIFIER
SIGNAL ELECTRONICS
SIGNAL ELECTRONICS
SIGNAL ELECTONICS
MAJORITY VOTING

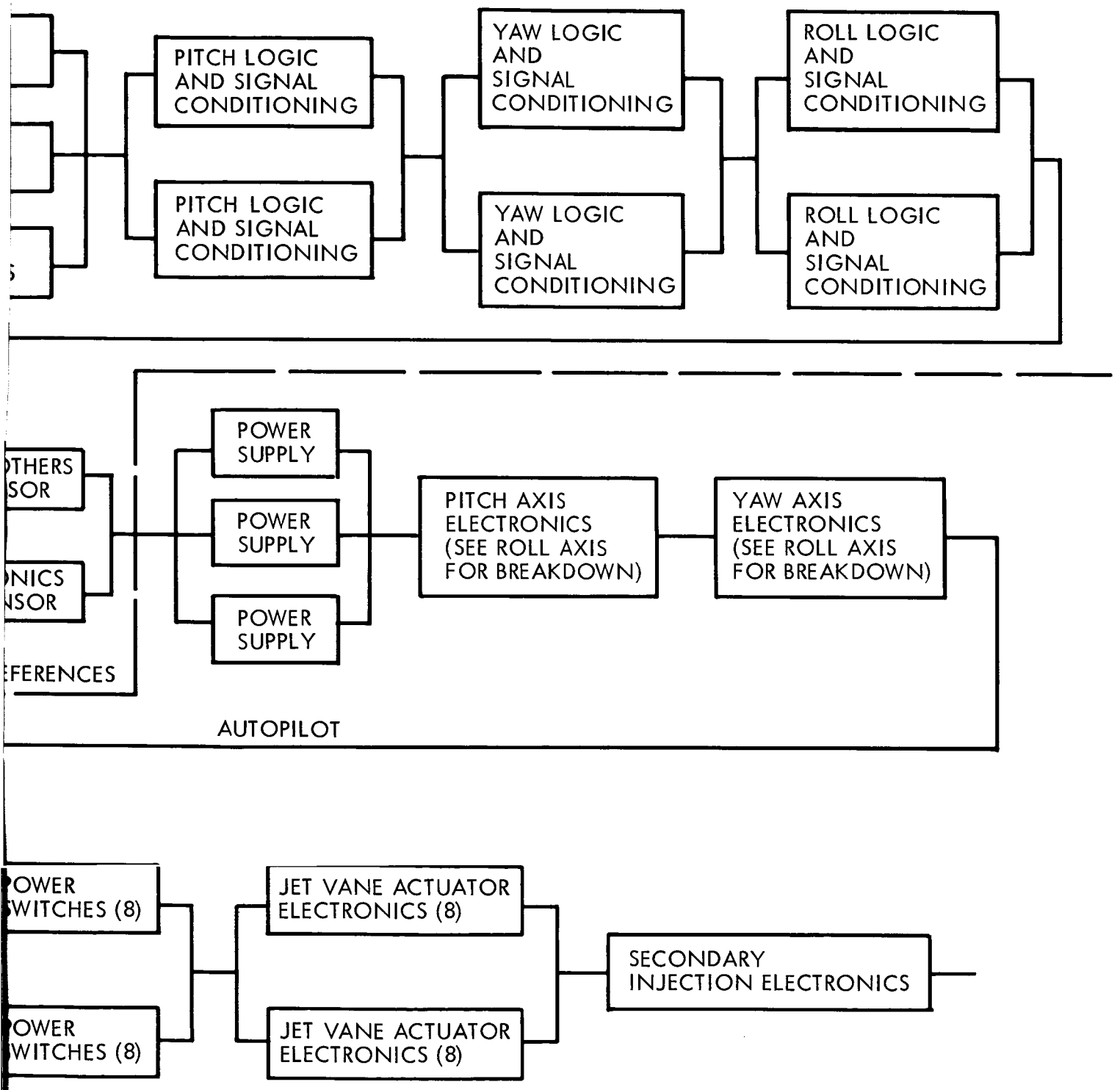

Figure 4.6-13: Attitude References and Autopilot — Reliability

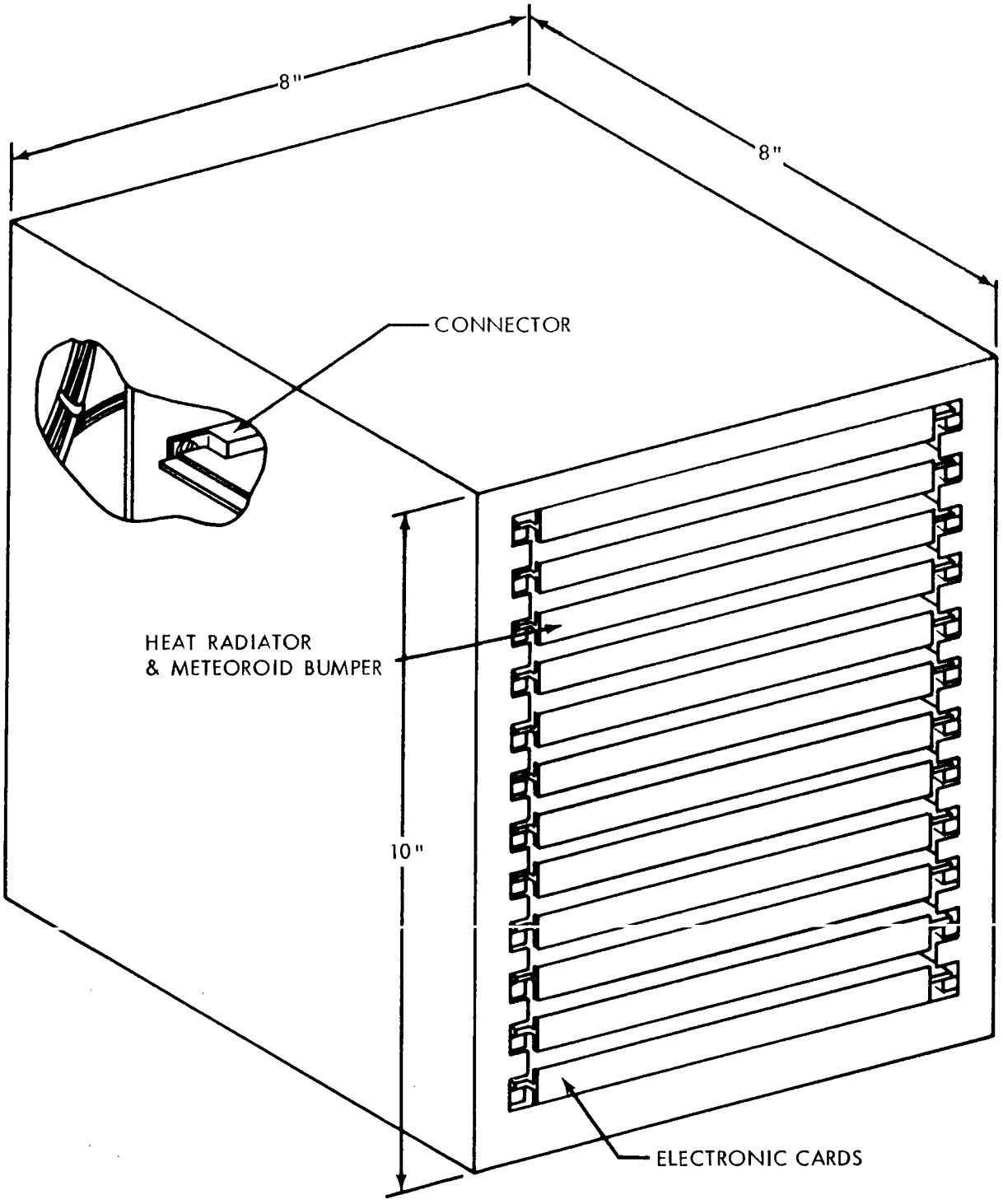

Figure 4.6-14: Cards Fitted into Module

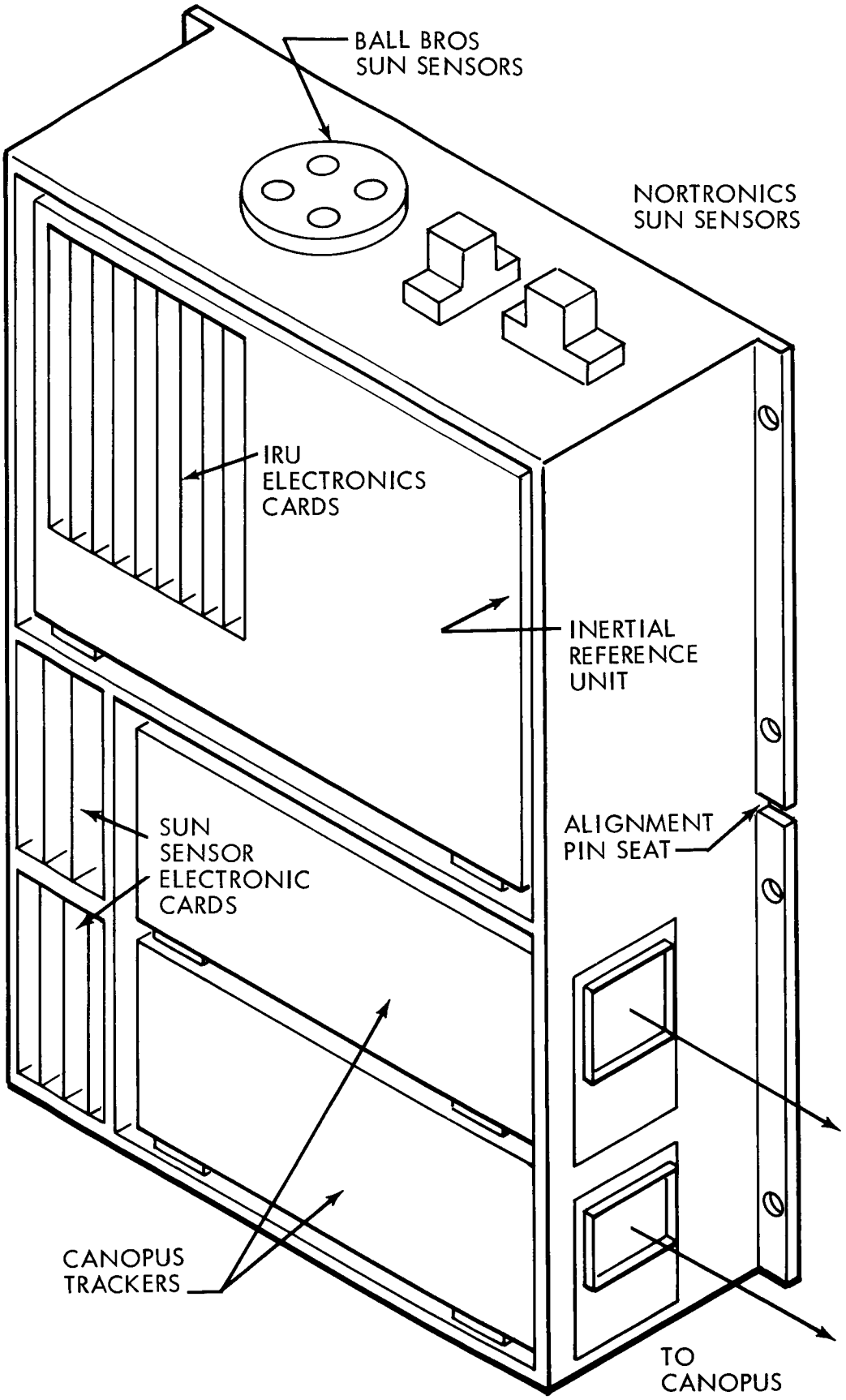

Figure 4.6-15: Attitude Reference Module

the inertial reference unit are integrated into a single module to simplify problems of interalignment and alignment to the spacecraft. They are aligned to each other to within 0.01 degree within the module, and the module is aligned to the spacecraft to within 0.05 degree.

Inertial Reference Unit--The inertial reference unit contains three gyros, two accelerometers, and the required electronics for operation of these inertial instruments. For additional description, see Section 4.6.2. Figure 4.6-16 shows the gyro-accelerometers block-mounted in one end of the box, and the electronic cards plugged into the other end of the box. Alignment buttons are provided on the top of the box for mounting to the module structure.

Canopus Sensors, Sun Sensors, and Electronics--The two Canopus sensors are mounted in the module structure as shown in Figure 4.6-15. For additional discussion see Section 4.6.3. They are cocked to one side at an angle of 14 degrees to provide clearance of the optical paths to Canopus with respect to the high-gain antenna on the spacecraft. The electronics for the Canopus sensors will be packaged inside the envelopes of the sensors themselves. The fine Sun sensors will be mounted on top of the module structure on alignment buttons. The two redundant coarse Sun sensors for the dark side of the spacecraft will each be divided, mounted on two separate 7-by 3-by 2 inch assemblies, and located on the spacecraft structure as single assemblies. The electronics for all of the Sun sensors and the redundant switching control electronics for the Canopus sensors and the Sun sensors are packaged in the space behind the

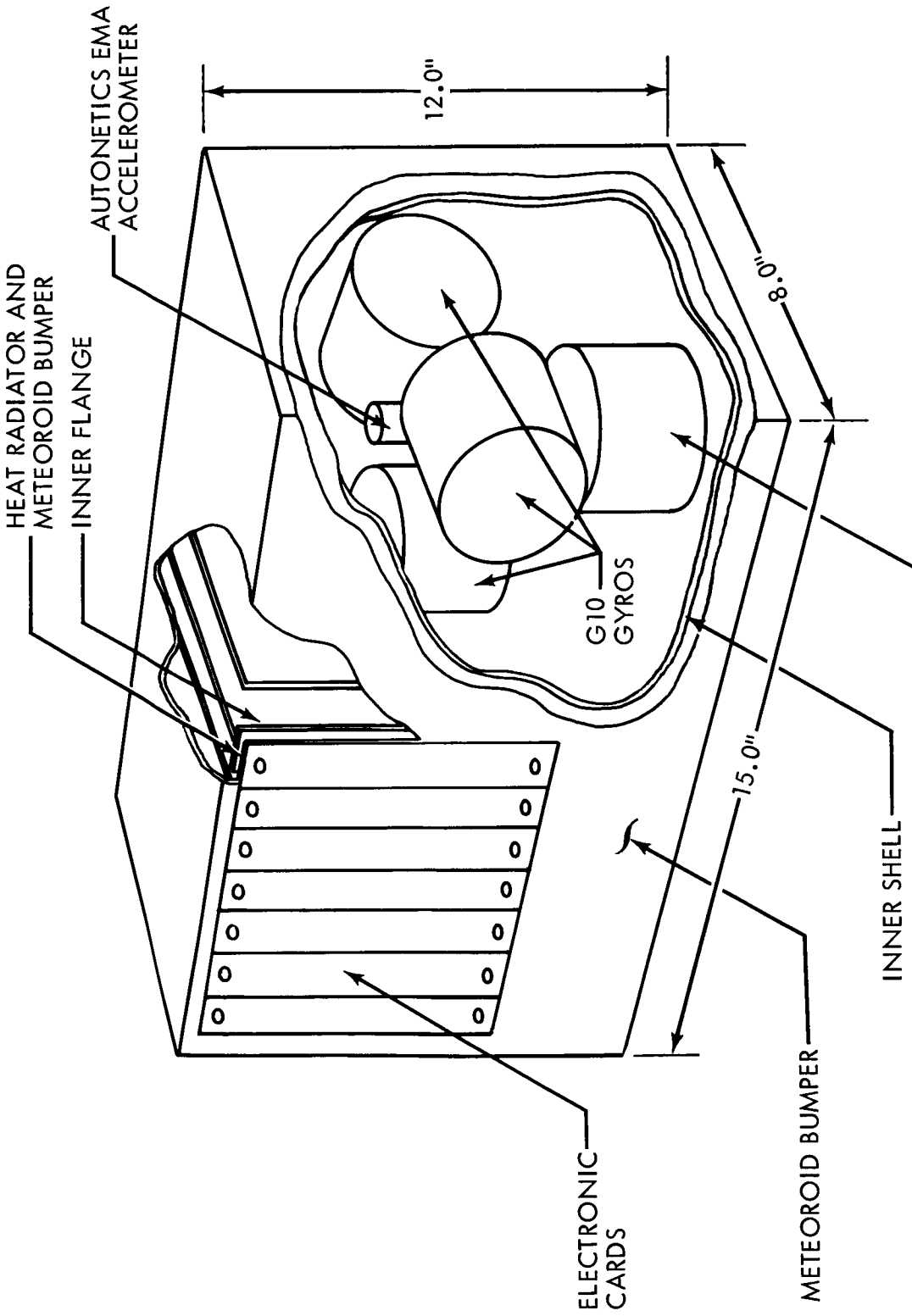

Figure 4.6.-16: Inertial Reference Unit

Canopus sensors. The gyro reference axes, the Canopus sensors axes, and the Sun sensor axes will be precision aligned to an accuracy of 0.01 degree. The entire attitude reference module will be removable from the spacecraft without disturbing the relative alignment of the instruments.

Weight and Volume Summary--The weights and volumes of the electronic modules are summarized in Table 4.6-8.

Packaging and Interconnection Concepts, Standard Card Packaging--Standard electronic cards will be used. Figure 4.6-18 shows a cross section of the metal-substrate printed circuit boards used. Metal-substrate board technology has two advantages: (1) high thermal conductivity of aluminum; and (2) ruggedness and resistance to deflection in a vibration and shock environment.

Component short circuit to the aluminum is avoided because of the double layer of insulators. Electronic parts mounted on the metal-substrate boards will be attached by soldering to contact pads on the surface of the board using temperature-controlled lap soldering techniques of the Improved Minuteman program. The metal-substrate boards will be made so the aluminum core has, integrally attached to it, a heat-radiating and meteoroid-bumper flange. This flange will face and radiate directly into open space. Behind this flange will be an inner flange to stop scatter from the meteoroid bumper. Power transistors and other high-power-dissipating elements required in the electronics will be mounted on the

Table 4.6-8: VOLUME AND WEIGHT SUMMARY--

ATTITUDE REFERENCE AND FLIGHT CONTROL SUBSYSTEM

SUBSYSTEM	WEIGHT (lbs)	DIMENSIONS (in.)	VOLUME (cu. in.)
ATTITUDE REFERENCE MODULE			
Inertial Reference Unit	21.7		
Canopus-Sensor Unit	13.5		
Sun-Sensor Unit	2.5		
Structures, Harness, and Connectors	11.9		
TOTAL	49.6	16 x 8 x 24	3105.6
AUTOPILOT MODULE			
Electronics	6.0		
Structures, Harness, and Connectors	5.0		
TOTAL	11.0	8 x 8 x 10	640
REMOTE SUN SENSORS			
1 - Sun Side	0.5		
2 - Dark Side	1.0		
TOTAL	1.5	3 (3 x 7 x 2)	126

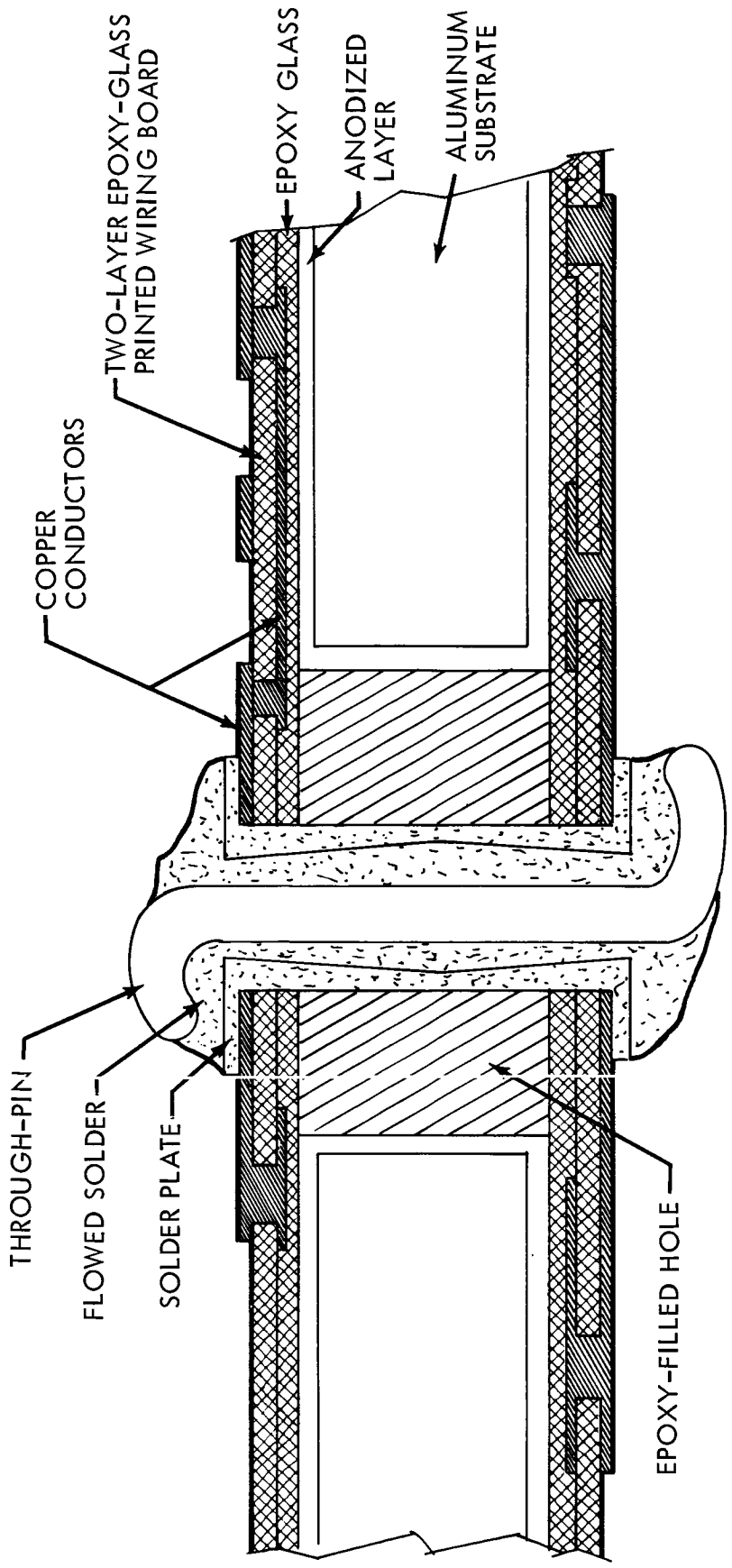

Figure 4.6-18: Cross Section of Metal Substrate Board

metal-substrate boards in direct contact with the hard-anodized aluminum substrate by designing cutout holes in the laminated-epoxy, glass-printed, wiring board.

Electronic Parts and Circuits--Full use will be made of the array of highly reliable parts in the approved Voyager parts list. This includes miniature and microminiature discrete components, hybrid thin-film circuits, and integrated circuits. The use of these different techniques will be predicated on the nature of the electronic functional requirements, particularly in the interest of maximizing reliability.

Each circuit design will be subjected to computer functional analysis. The most advanced method and the one to be used on the Voyager program is SCAN (System for Computer Analysis). SCAN was the evolutionary outgrowth of earlier programs and was used on the Improved Minuteman system.

4.6.1.7 Safety Consideration

The equipment is not hazardous to personnel except for the high-voltage (1800 volts) section of the Canopus sensors. This section is enclosed and will be properly marked with warning signs. The attitude reference module weighs over 40 pounds; therefore, special ground handling equipment will be required.

4.6.1.8 Test Programs

The components of the attitude reference and autopilot subsystems will be tested both separately and as a complete breadboard unit under simulated

space conditions using an air bearing space-simulation platform complete with cold-gas-jet torquers. This testing will be completed by July 1966 for the parts of the subsystem not presently space-proven. If necessary for scheduling reasons, initial testing of Sun-sensing and Canopus-sensing operations will be conducted using simulated Sun and Canopus sensors to verify the acquisition mechanizations. Tests will be based on best knowledge at that time of the final Voyager configuration and dynamics.

Proof of the redundancy mechanizations will be shown through failure simulation for each component. Performance dynamics will be measured for the types of failures possible, based on analysis of the failure modes.

The effects of hard vacuum and radiation will be measured on non-space-proven parts and hardware by detailed testing. Hard-vacuum environment will be applied to items to be proven, their temperature will be varied, and the effects on individual performance will be determined. This will be translated into net effect on system performance. Nuclear-radiation tests involving continuous high-intensity gamma radiation may be performed in this phase to evaluate the extent of surface ionization problems in active circuitry.

In addition to the tests indicated above, Autonetics requested authorization to place a piggyback payload on a satellite in early 1966. This payload will include two G10 strapdown gyros and an EMA accelerometer and

associated electronics. Output signals will be telemetered and compared against other references onboard. A relatively long period in orbit is planned for this flight, with the Autonetics components continuously activated.

4.6.2 IRU

The IRU includes the accelerometer unit and the gyro unit.

4.6.2.1 Accelerometers

Scope--The accelerometer unit contains the accelerometers and all supporting electronics necessary to generate pulse signals to the CC&S representing velocity increments.

Applicable Documentation--The following documents apply:

1) Bell Model DVM IIIB
   a) Autonetics Industry Survey, 73A-V-1
   b) Questionnaire Files on SSGS, 73A-VI-1 and 73A-VIII-1
   c) Bell Report No. 60016-035B, December 1964
2) Autonetics EMA
   a) T4-1265/23, "Accelerometer Digitizing Techniques"
   b) T5-997/32, "Technical Description for A40 Electromagnetic Accelerometer"
   c) T5-983/32, "Miniaturized Servo and Digitizer Electronics"

Functional Description--A block diagram of the Voyager accelerometer unit is shown in Figure 4.6-19. The accelerometer unit includes one Autonetics EMA accelerometer and one Bell DVM IIIB accelerometer.

The accelerometers operate in parallel redundancy, with both operating during all velocity-change maneuvers.

Accelerometers Mechanizations--The Autonetics electromagnetic accelerometer is a single-axis, closed-loop, force-servo type. Although it is

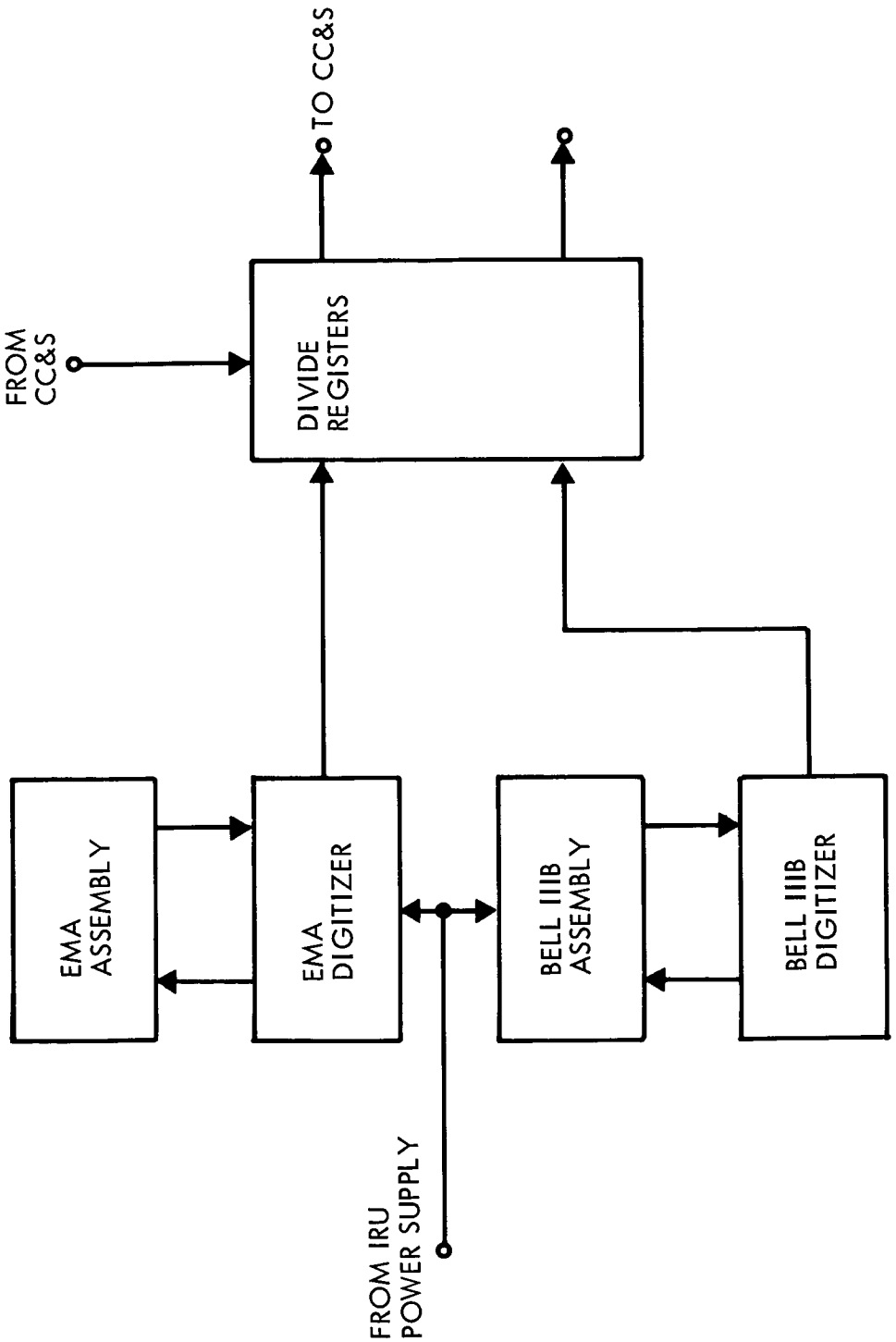

Figure 4.6-19: Accelerometer-Unit Block Diagram

inherently an analog accelerometer, a digital velocity output is obtained when it is combined with current-digitizing components in the force-servo loop.

Figures 4.6-20 and 4.6-21 are exploded views of the EMA. The acceleration-sensing member is a fused silica proof mass that is attached to the accelerometer stators by means of an integral flexure section. The proof mass and the flexure section are made of a single, precisely lapped and etched disk of fused silica.

The pickoff member, which generates an electrical signal in response to the proof mass displacement relative to the stator members, is a capacitance-bridge type, as shown in Figure 4.6-22. The pickoff bridge is excited by a 19.2-kc carrier signal and the output of the bridge is a suppressed carrier signal whose amplitude is proportional to the proof mass displacement. The servo current is fed back to the two forcing coils located in the radial magnetic field of the Invar stator permanent-magnet circuits.

The Bell DVM IIIB consists of an accelerometer sensor packaged with its electronics, plus an analog-to-pulse rate converter as shown in Figures 4.6-23 and 4.6-24. The accelerometer sensor consists of a single-axis magnetically restored pendulum. This restoring force is created by the interaction between a permanent magnetic field generated by magnets attached to the accelerometer housing and an electromagnetic field produced by a current flowing through a forcer coil attached to the pendulum. The forcer-coil current, which is directly proportional to acceleration, is converted to a pulse output in the pulse-rate converter.

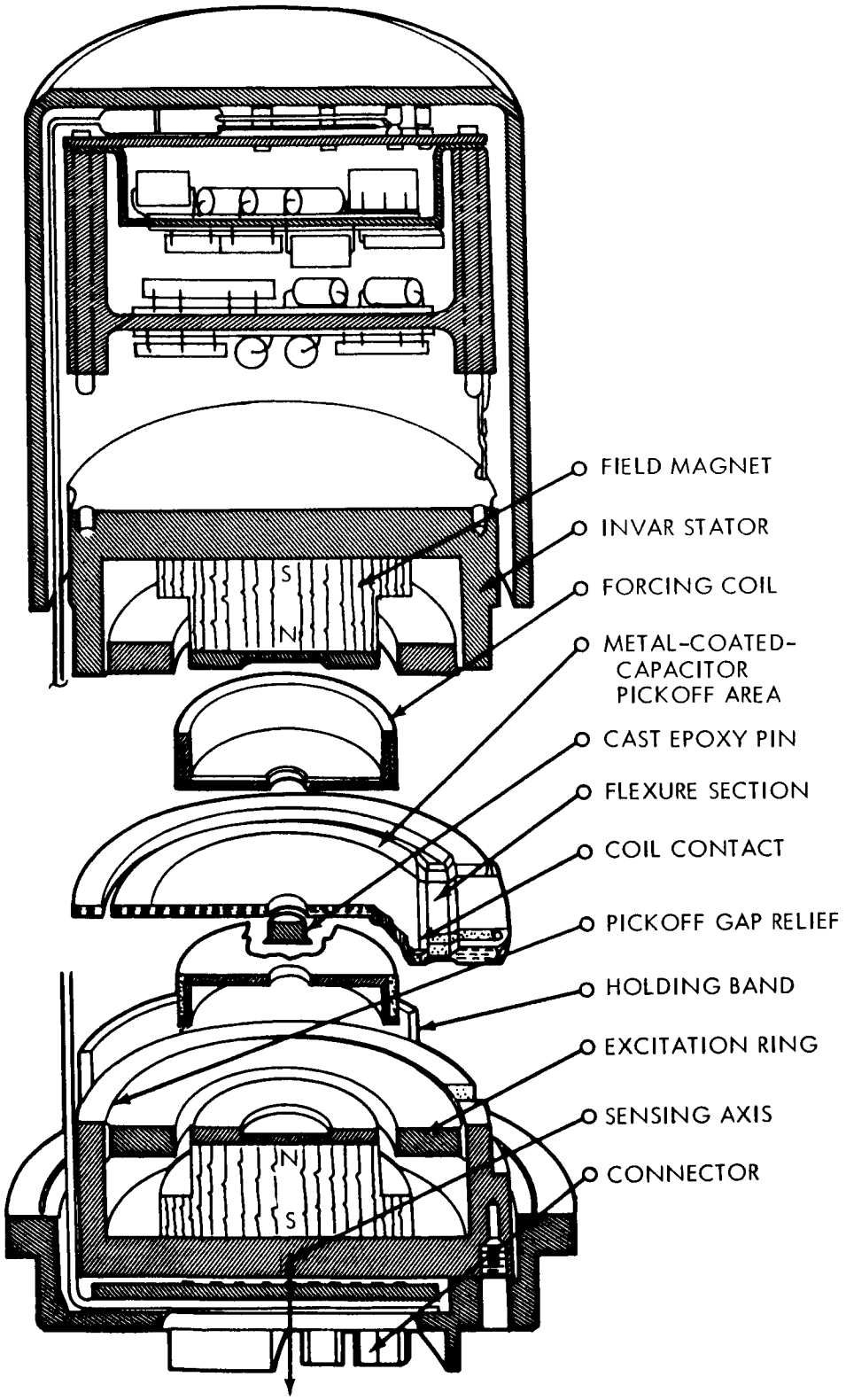

Figure 4.6-20: EMA Cross Section

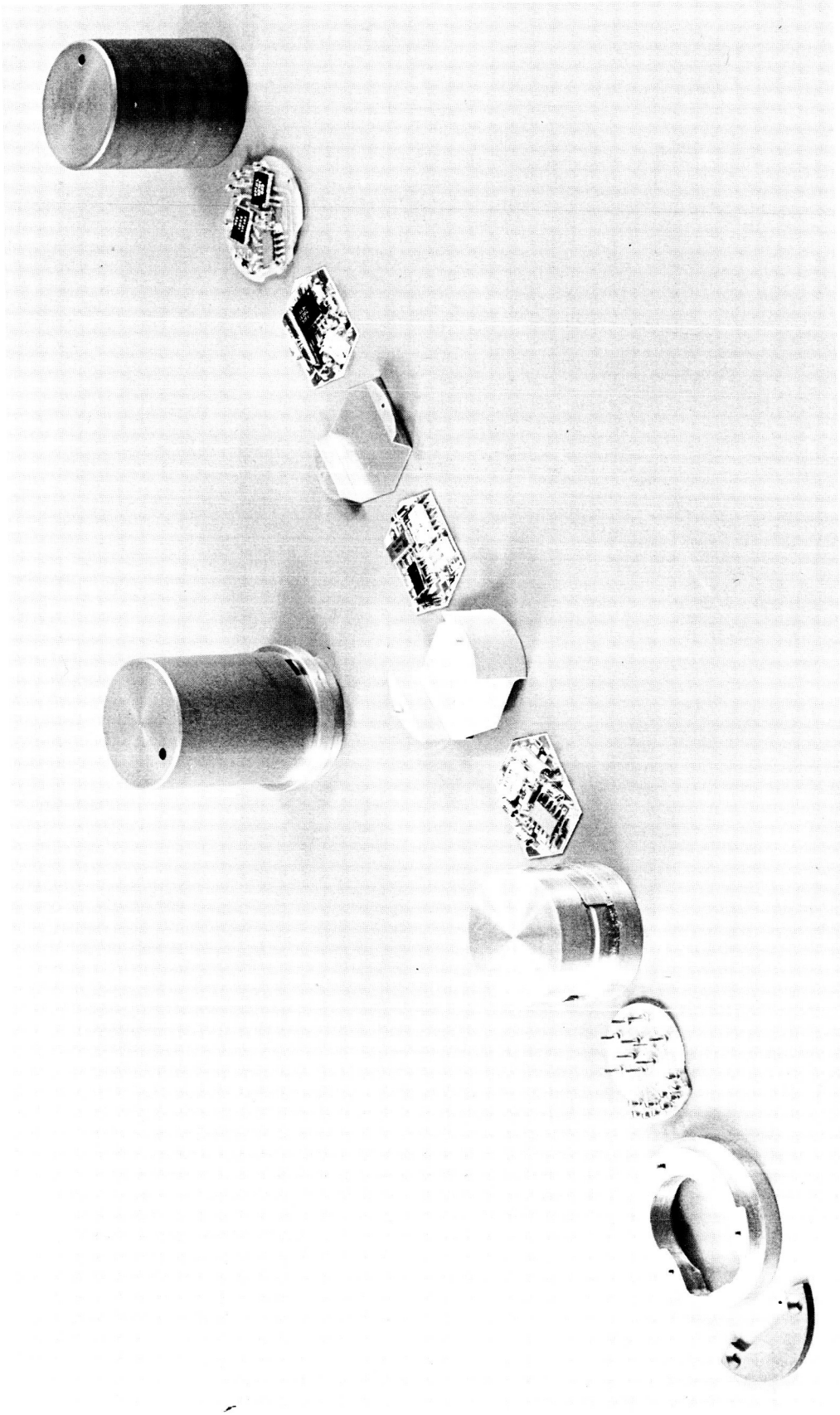

Figure 4.6-21: Autonetic EMA

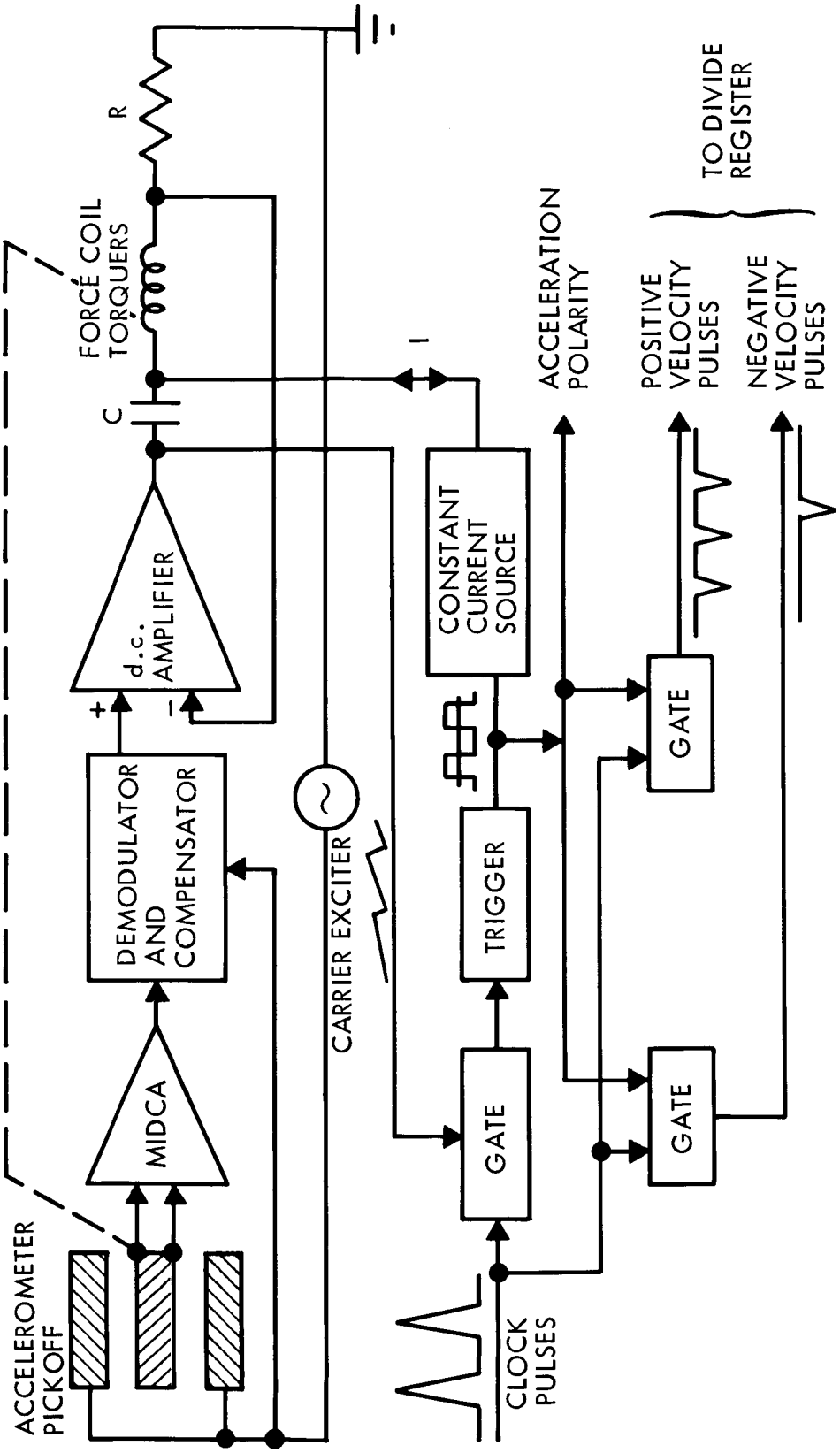

Figure 4.6-22: EMA Block Diagram

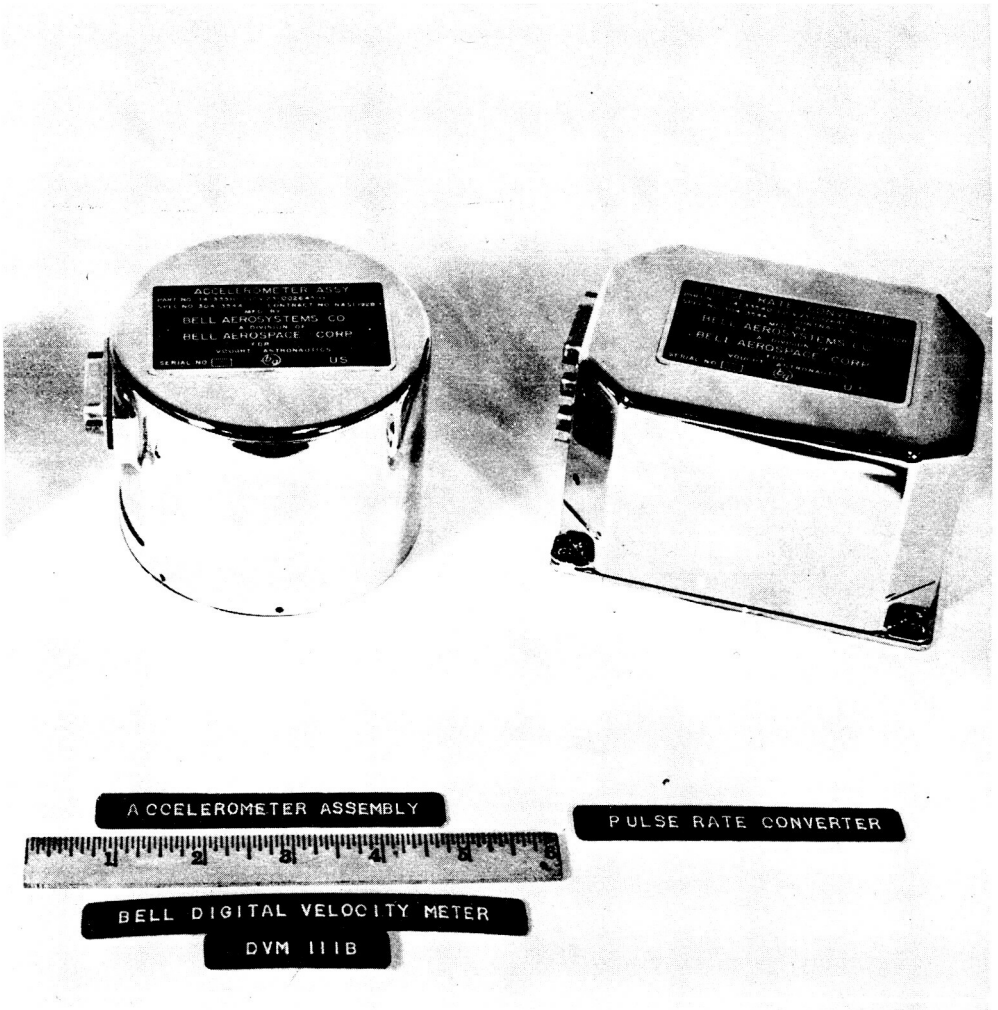

Figure 4.6-23: Bell Digital Velocity Meter DVM 111B

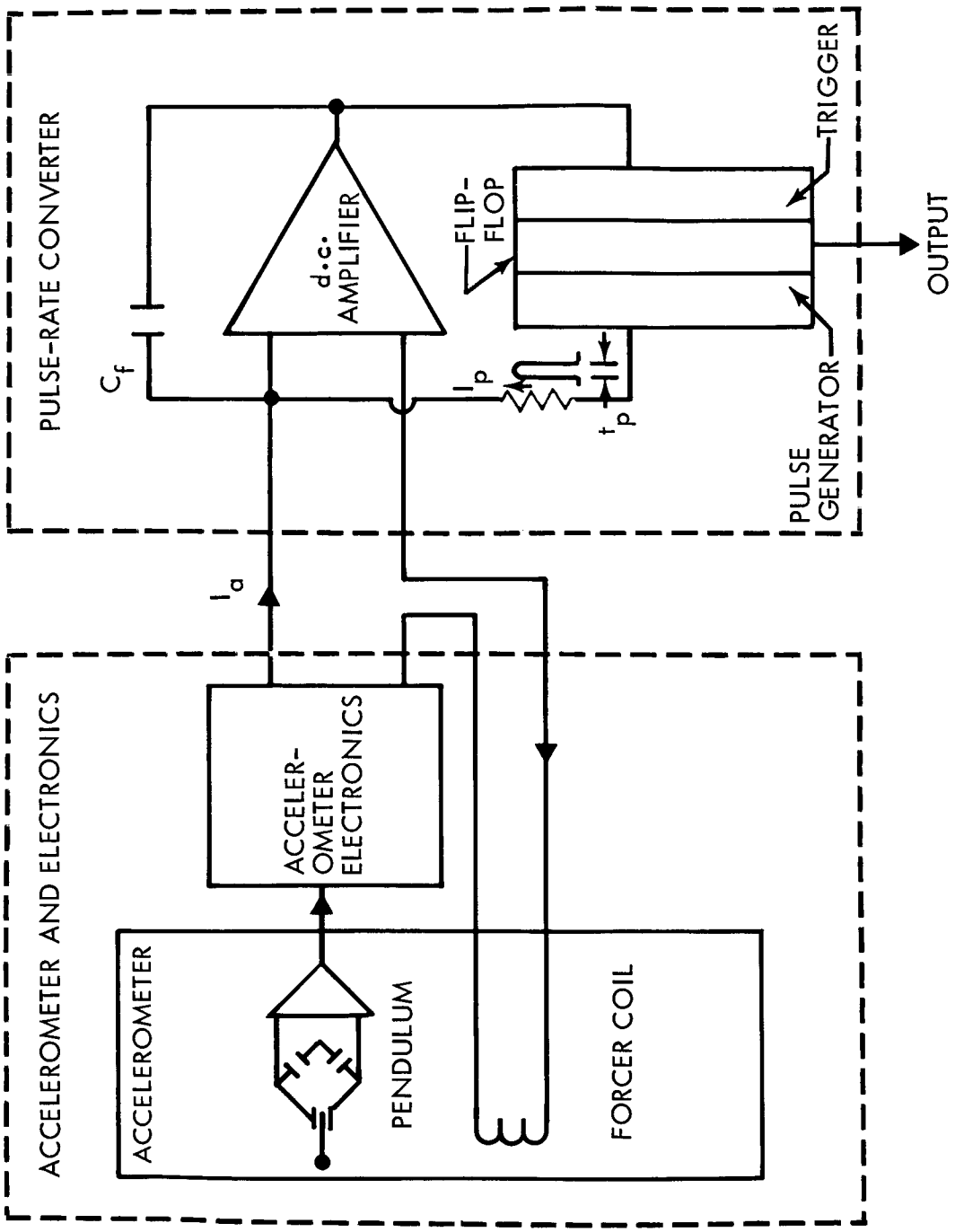

Figure 4.6-24: Block Diagram of Bell DVM-111B

The pendulous mass, consisting of a one-piece circular metallic frame that houses a forcer coil, is suspended from the base plate by insulated beryllium copper springs. This mass is positioned in the radial flux gap of a high-intensity magnetic field, as shown in Figure 4.6-25. A capacitance bridge is used for detecting proof mass position. The accelerometer output is a voltage proportional to the capacitance bridge unbalance.

The accelerometer electronics consists of a 192-kc oscillator for the position pick-off excitation, a preamplifier-demodulator, and a low-drift d.c. amplifier. The pulse-rate converter consists of a low-drift d.c. amplifier integrator, a precision pulse generator, and trigger logic circuitry. Whenever the output of the integrator due to an accelerometer input signal reaches a positive or negative trigger level, a precision-voltage/time-integral pulse is generated and introduced as a current pulse to the forcer coil.

Redundancy--Self-check and redundance are obtained by simultaneously operating both accelerometers and then using time gating in the CC&S to eliminate erroneous thrust-termination signals.

The accelerometers typically fail by sending no pulses or artifically high pulse rates. Ignoring thrust-termination signals until a minimum time has elapsed will eliminate the high-pulse-rate case, and issuing a termination signal after a predetermined maximum time has elapsed will eliminate the no-pulse case. This double time gating selects the good accelerometer if one accelerometer has failed and utilizes lapsed time as a backup if both accelerometers fail.

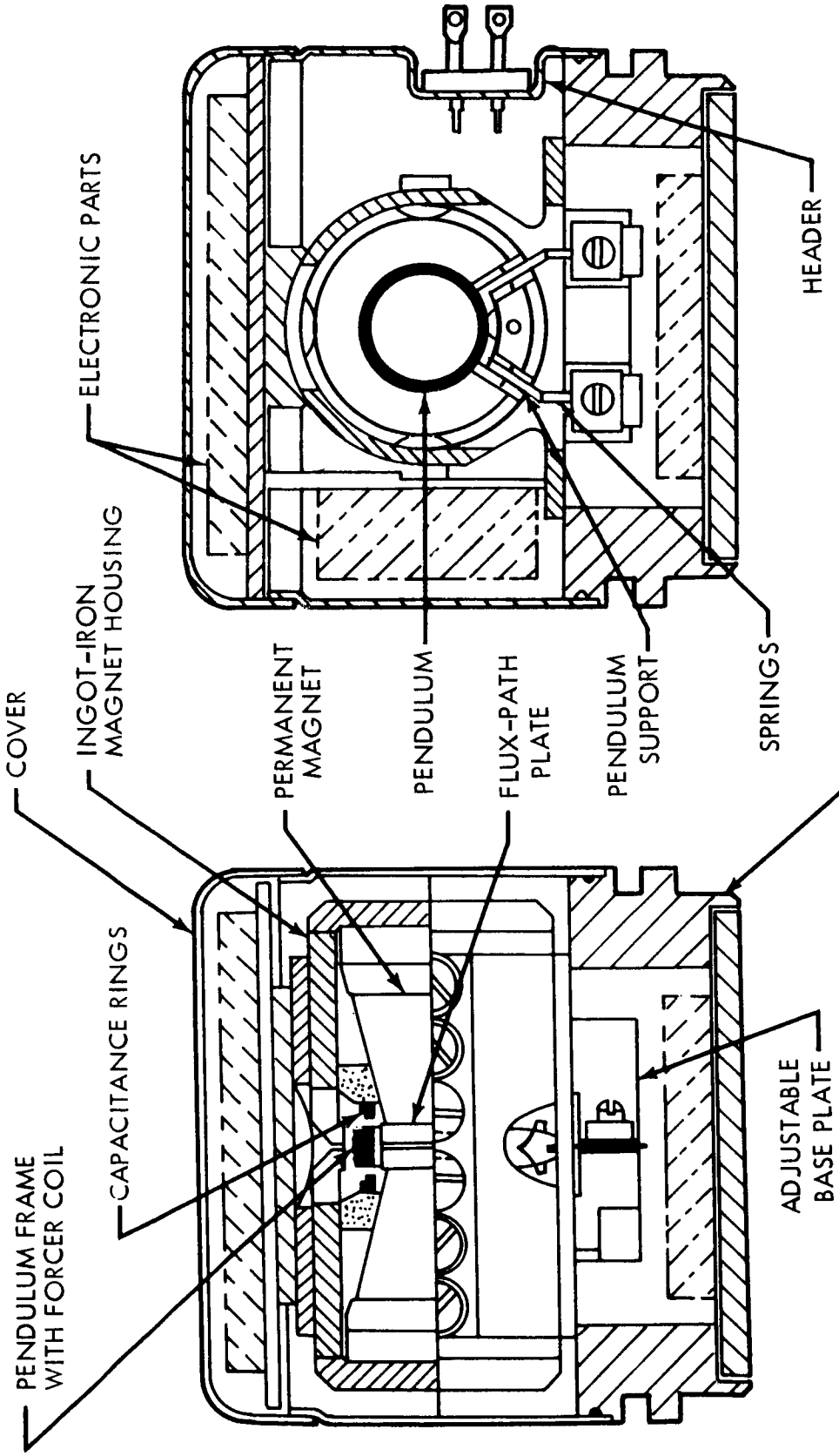

Figure 4.6-25: Bell DVM-III B Sensor

Interfaces--Four types are discussed below.

Signal--Accelerometer interfaces with spacecraft subsystems and OSE are defined in the attitude reference interface list, Table 4.6-5.

Power--The accelerometer unit operates off the IRU power supply, which receives 35-volt d.c. Seventeen watts are required by the accelerometer unit during normal operation. The power requirements are tabulated below.

1)	EMA	0.5 watt maximum
2)	Bell IIIB	
	a) Instrument and electronics	4.5 watts
	b) Required digitizer heater	12.0 watts
	Total	17.0 watts

Thermal--Instruments are mounted on a beryllium block. Conduction is the primary mode of heat transfer through the block. The beryllium block interfaces with a stainless-steel mounting support, which provides a form of thermal insulation. The IRU housing is attached to the spacecraft. Heat generated by the accelerometers is ultimately removed from the spacecraft by thermal radiation through a passive system.

Mechanical--Mechanically, the EMA is clamped to a reference flange on the IRU block. The Bell IIIB is attached to the IRU block by three screws combined with alignment pads.

Performance--The discussions in the following subsections apply.

Performance--(This includes the alignment accuracy of accelerometers with respect to attitude reference box). Table 4.6-9 summarizes the accelerometer performance parameters.

Table 4.6-9: ACCELEROMETER PERFORMANCE

	EMA	BELL DVM IIIB
Acceleration Threshold	2 μg	1 μg
Linearity	50 μg/g	30 up to 0.3 g input 0.01% of input above 0.3 g
Cross-Axis Sensitivity	-	5 μg/g
Cross Coupling	30 ppm/g	10 ppm/g
Scale Factor mismatch (positive to negative)	50 ppm	10 ppm
Scale Factor	0.02 to 0.2 ft/sec/pulse	0.04 to 1.0 ft/sec/pulse
Scale-Factor Stability	0.01%/mo.	0.006%/mo.
Scale-Factor Temp. Sens.	50 ppm/^{o}F	1 ppm/^{o}F (with compensation)
Scale Factor Precision	1:30,000	1:50,000
Bias	Can be adjusted to 70 μg	Can be adjusted to 50 μg
Bias Hysteresis	10 μg	20 μg (repeatability)
Bias Stab. from Turn-on to Turn-on	10 μg	20 μg
Bias Temp. Sens.	10 μg/^{o}F	10 μg/^{o}F
Bias Stab. (short term)	20 μg (per day)	1 μg (per day)
Bias Stab. (long term)	50 μg (90 days)	50 μg (30 days)
Bias Noise (referred to input)	10 μg	-
Vibration Sensitivity	50 μg/g^2 below 20 cps 20 μg/g^2 above 20 cps	3 μg/g^2
Input Axis Alignment w.r.t. ref. surface	1 min	1 min
Input Axis Stability	5 sec (90 days)	-
Input Axis Temp. Sens.	0.1 sec/^{o}F	-

Reliability--As opposed to conventional pendulous accelerometers, the EMA is an extremely simple instrument having no moving parts. Since the EMA has no moving parts or fluid flotation elements, all of the mechanisms that might involve wear, fluid absorption, or leakage are not applicable. The most likely EMA failure modes are concerned with electronic part failure, quartz fracture, and permanent magnet instability. All of these modes are extremely remote. Table 4.6-10 shows a parts-breakdown and failure-rate prediction for both electronic and mechanical parts used in the EMA. Parts failure rates are based on Minuteman failure rates as experienced by Autonetics. Mechanical failure rate has been conservatively estimated to be a fifth of the electronics failure rate. The calculated MTBF for the Bell DVM IIIB is also provided in Table 4.6-10.

Table 4.6-10: ACCELEROMETER RELIABILITY

AUTONETICS EMA:

Total Unit MTBF			990,000 hours MTBF
1)	Instrument		0.45 failures/hour x 10^6
2)	Electronics		0.56
	a) A.c. Amplifier	0.08	
	b) Demodulator	0.08	
	c) D.c. Amplifier	0.05	
	d) Current Limiter	0.23	
	e) Logic and Switching	0.12	

BELL MODEL DVM IIIB:

	Basic Sensor Unit with Pickoff Preamp	Complete Analog Accel with Servo Elec (Model IIIB)	Analog Accelerometer with Pulse Converter (Model DVM IIB)
Calculated MTBF (hours)	35,600	12,500	10,000 hours MTBF

Development Status--Development of the Autonetics EMA was initiated 2.5 years ago in response to a requirement for a small, low-cost accelerometer. During the development period, 27 accelerometers were fabricated. Development testing, in excess of 5000 instrument hours, has been performed including operation in a nuclear-reactor environment.

Eight instruments were delivered to Chance Vought, where they were tested as part of the SLAM program. Six were subjected to and survived the new reactor radiation environment. Holloman AFB has purchased two accelerometers for testing as part of a low-cost navigator program. Two accelerometers are undergoing test on the Autonetics N16 inertial navigator in van test at Boeing-Seattle. The remaining 15 accelerometers have been laboratory-tested. The EMA is presently planned to be part of a piggyback satellite payload in early 1966.

The DVM IIB is a fully developed production instrument. Fifty such complete instruments and over 400 sensors have been built. The DVM IIIB has been fully qualified, flight-proof tested, and delivered for use on the Scout vehicle, Minuteman re-entry vehicle, and the NASA SERT program. The sensor portion of the DVM IIIB has been used on many other space programs such as the Vega, Ranger, Mariner, Agena, and others.

Accelerometer Test Data--The performance of an experimental accelerometer typical of the EMA design is illustrated by the following figures. The acceleration bias versus time (Figure 4.6-26) was obtained with the accelerometer operating and oriented with the sensing axis approximately level. The temperature was controlled at 100°F. The acceleration bias

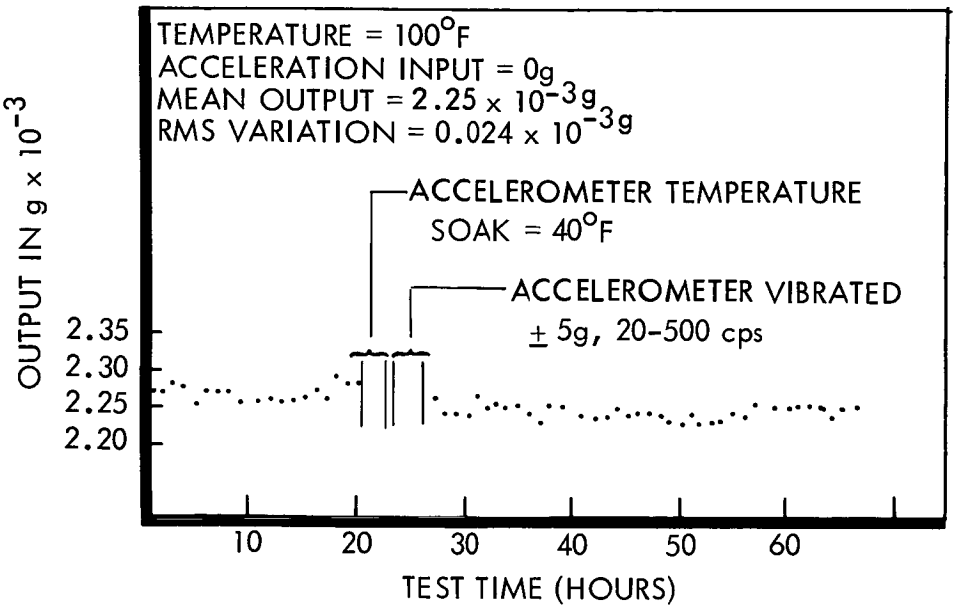

Figure 4.6-26: Bias Change with Time

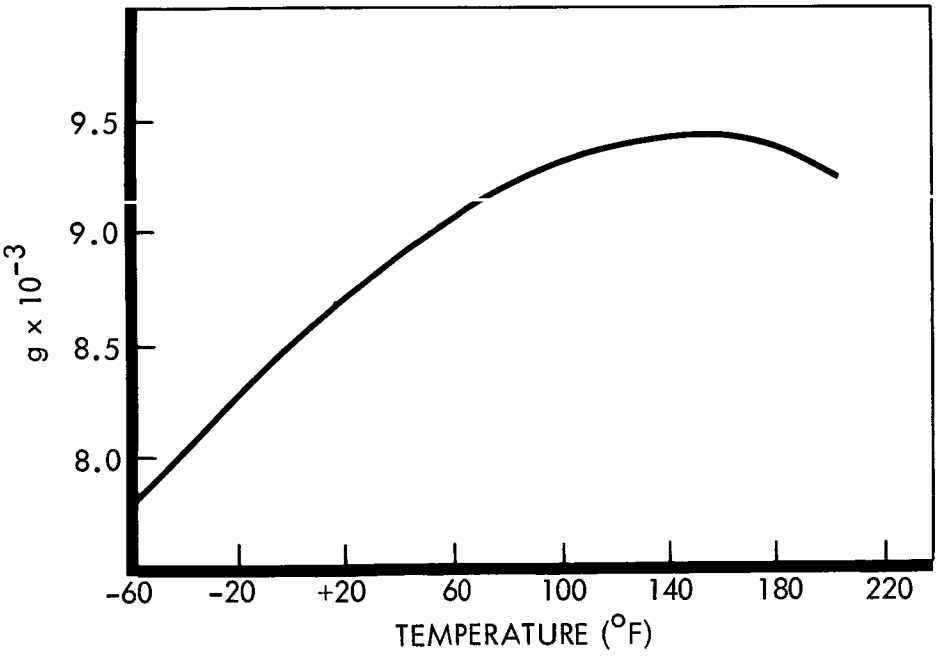

Figure 4.6-27: Bias Change with Temperature

versus temperature (Figure 4.6-27) was also obtained with the accelerometer's sensing axis oriented approximately level.

Physical Characteristics and Constraints--Tables 4.6-11 and 4.6-12A give the physical parameters.

Safety--The accelerometers use no voltages greater than 28 volts d.c.; have no sharp edges; contain no pressure vessels, toxic materials, or other safety hazards; and, therefore, require no special safety considerations.

4.6.2.2 Gyro Unit

Scope--The gyro unit includes the gyros and the electronics necessary to obtain vehicle angular position and rate information for three axes and includes the circuitry necessary for failure detection and switching of the redundant components.

Applicable Documentation--The following documents apply:

1) "Nuclear Radiation Hardened Inertial Reference Study and Evaluation Program," Autonetics EM-263-215
2) "Effects of Nuclear Radiation on Autonetics Type G2K2A Gyro," EM-1263, 22 May 1957
3) "Voyager Design Studies Volume IV, Orbit-Bus Design Part I," AVCO RAD-TR-63-34, 15 October 1963
4) "Inertial Sensors Catalogue," Honeywell ADC-234, April 1963
5) Free Rotor Gyro Acceleration Sensitivity, Autonetics TM-388-68-28, 13 August 1958
6) Inertial Components Development and Techniques, Autonetics ASD-TDR-62-378, April 1962

Table 4.6-11: PHYSICAL CHARACTERISTICS

	AUTONETICS EMA	BELL DVM IIIB
Size	1" dia x 1-3/8" (including servo and digitizer)	4" dia x 3" (sensor and servo only)
		3.5" x 4.94" x 3.0" (digitizer only)
Weight	2-1/2 oz total	35-1/2 oz (sensor and servo only)
		33-1/2 oz (digitizer)
Accel. Range (as desired, up to indicated level)	±20 g	±100 g
Suspension Type	Quartz Flexure	Metal Flexure
Power Required	** +28 volts d.c. 10%	+28 volts d.c. 10%
Power Consumption	0.5 watt	8 watts
		12 watts (digitizer temp. control)

**The accelerometer operates from the gyro supply, which provides:

±10 volts, 1%
±20 volts, 1%
Each Matched to 5%
19.2 kc, 6 volts
2.4 kc, Clock

Table 4.6-12A: PHYSICAL CONSTRAINTS

	BELL DVM IIIB	AUTONETICS EMA
OPERATING		
Acceleration	Rated capacity	Rated capacity
Sinusoidal Vibration	20 to 100 cps, 12 g 100 to 1000 cps, 24 g 1000 to 2000 cps, 9 g	20 to 100 cps, 6 g 100 to 600 cps, 15 g 600 to 2000 cps, 25 g
Random Vibration	7 g rms, 20 to 2000 cps	Not available
Shock	30 g for 11 msec	50 g for 11 msec
Temperature	0 to 160°F	-100 to 200°F
Pressure	Sea level to space	Vacuum to 3 atm
Magnetic	100 gauss	200 oerstedt
Radio Frequency Interference	Meets MIL-I-26600	Meets MIL-I-26600
NONOPERATING		
Shock	30 g, 11 msec	50 g, 11 msec
Temperature	-60 to +200°F	-150 to +300°F
Pressure	Sea level to space	Vacuum to 30 atm
Radiation	Not Available	10^{13} nvt
Humidity, Salt Spray, Fungus, Sand, and Dust	Meets MIL-E-5272C	Meets MIL-E-5272C

Functional Description--A block diagram of the Voyager gyro unit is shown in Figure 4.6-28. The gyro unit consists of three Autonetics G10B free-rotor gyros and support electronics. The gyro unit receives its main power from Voyager ±35 volts d.c. source, 2.4 kilocycles from the power unit and 19.2 kilocycles from the CC&S. A photo of the G10 gyro is shown in Figure 4.6-29.

As shown in Figure 4.6-30, a free-rotor gyro loop consists of a pulse-width-modulated (PWM) servo for each gyro axis, a speed-control servo to minimize the effects due to speed variations, and an up-down counter with a digital/analog converter connected to the outputs of each pulse width modulated servo. All outputs used for control of the vehicle are processed through selection circuitry where commands from the CC&S are carried out. Commands from the CC&S can select any one of the six available gyro axes for use in the autopilot.

Gyro Mechanizations--The Autonetics G10B is a high-reliability two-axis free-roto gyro. For Voyager application, the G10B will be operated in the caged mode and will utilize two torquing levels. The high torquing level, capable of 5 degrees per second will be used for damping of the injection separation rates and the low level torquing (0.3 degree per second) will be used during normal operation for the rest of the mission. The gyroscopic element consists of a simple flywheel rotor. The rotor, spun by means of an induction drivemotor, is supported by a self-lubricating gas bearing. The spherical gas bearing affords the rotor three degrees of angular freedom and permits definition of a spin axis and two displacement axes. Relative displacement between the rotor and

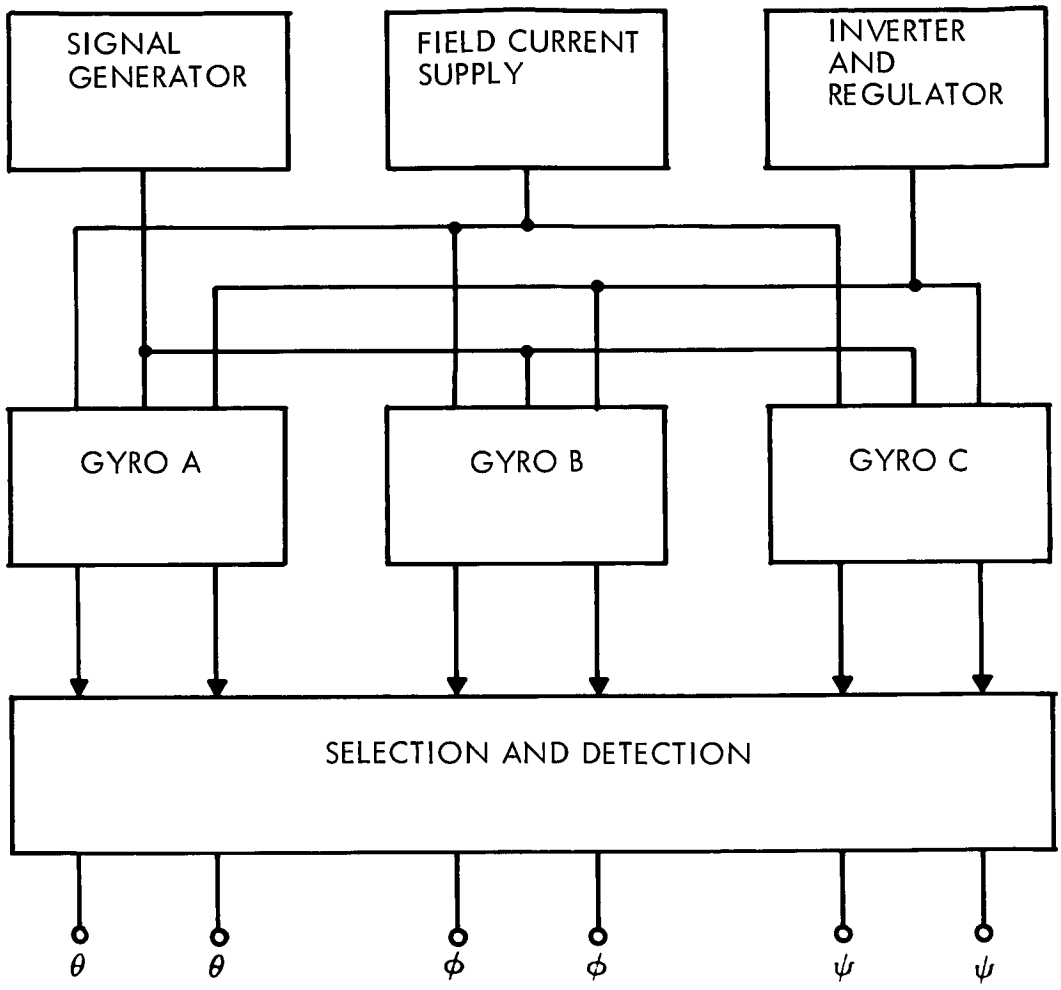

Figure 4.6-28: Gyro-Unit Block Diagram

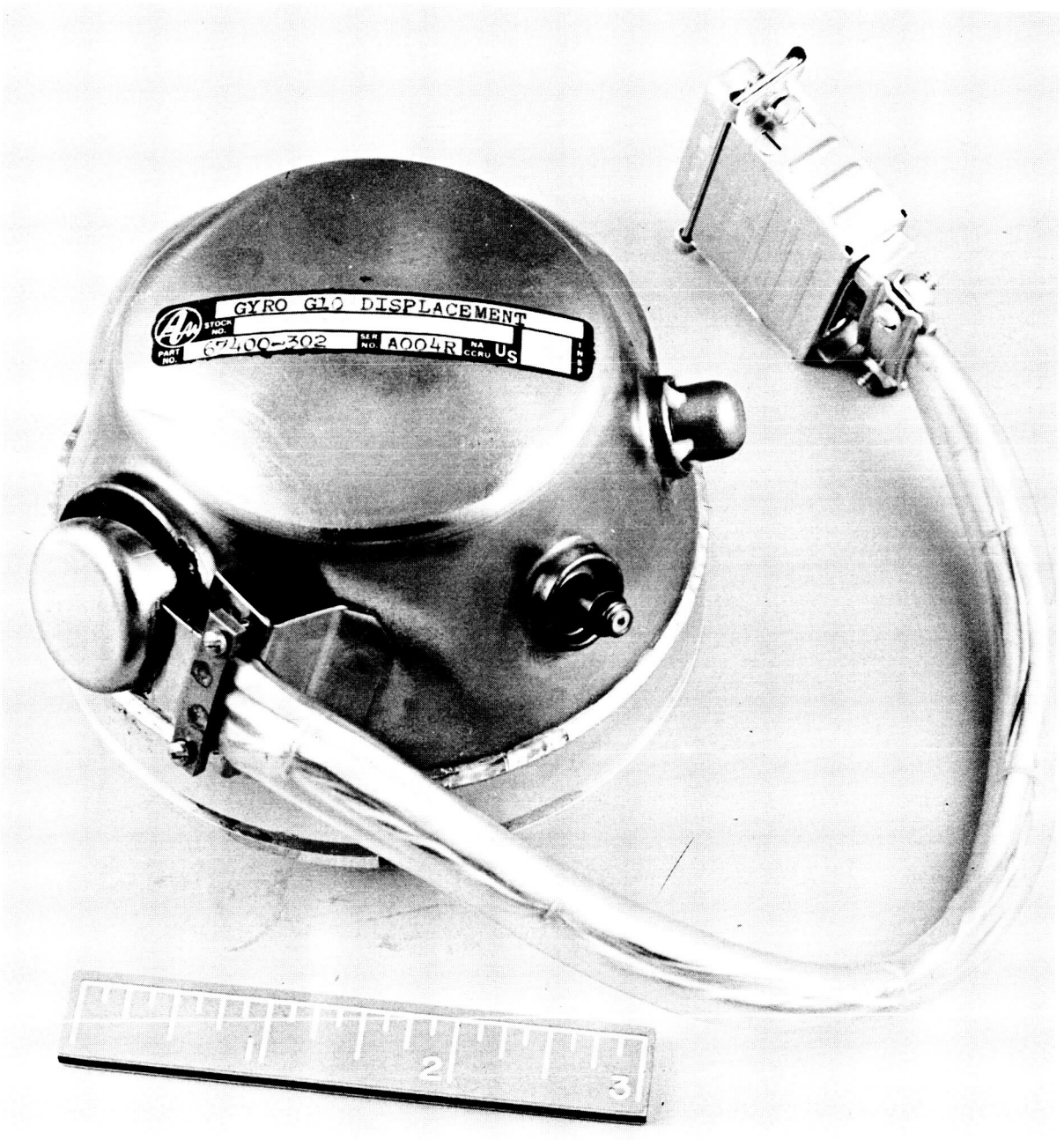

Figure 4.6-29: Autonetics G-10 Gyro

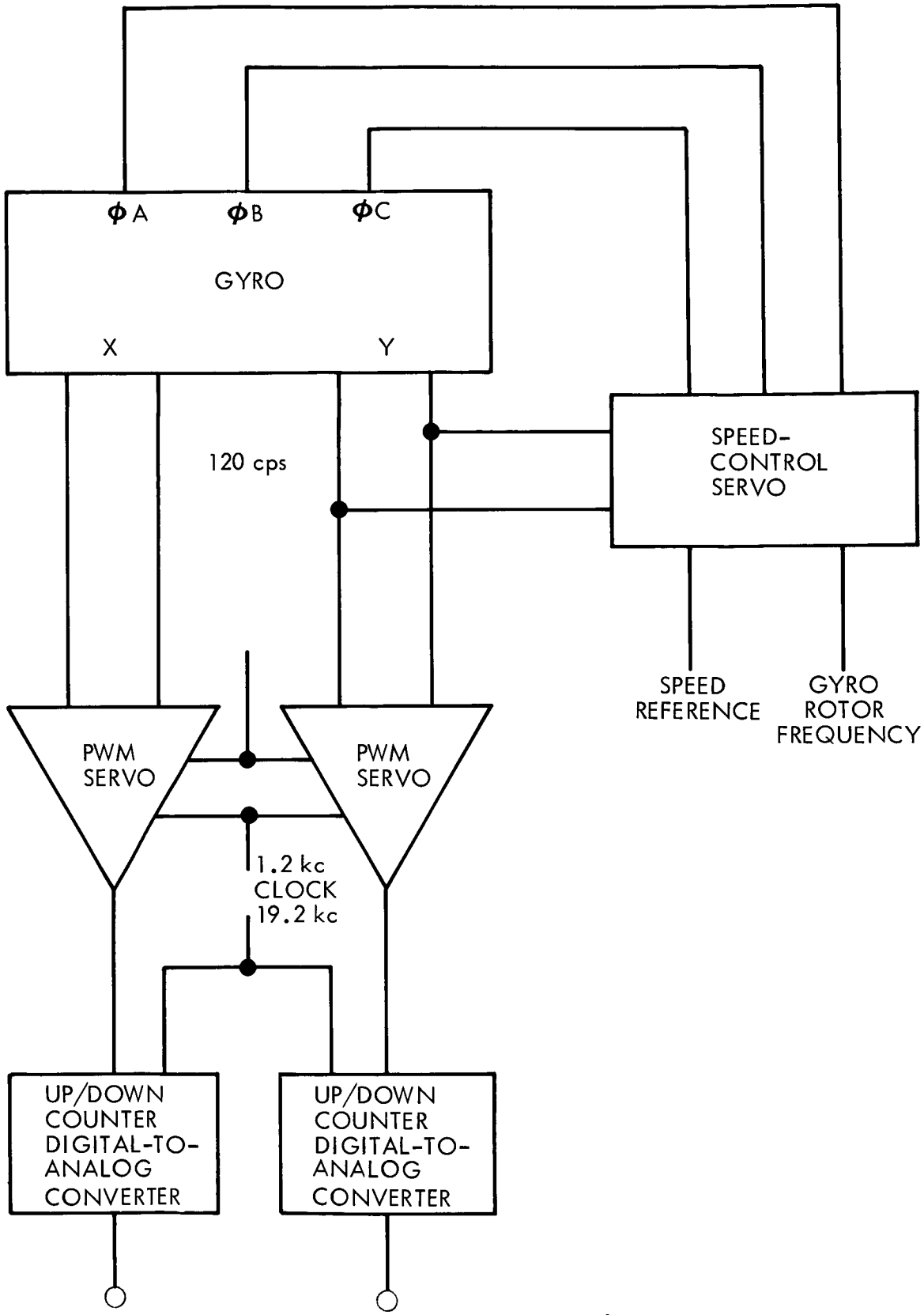

Figure 4.6-30: Gyro Block Diagram

case structure is sensed by a two-axis capacitor pickoff. A four-pole electromagnetic torquer produces attractive forces on a ferrite sleeve attached to the rotor, resulting in controlled gyroscopic precession. A cut-away view of the gyro is shown in Figure 4.6-31.

The speed controller servo system is based on a standard technique used on the Minuteman II systems. The controller uses the gyro pickoff signal, which contains the gyro speed signal generated by eight rotor rim holes passing over special cutouts on the pickoff plate of the gyro. The gyro speed is maintained to the accuracy of the time base used by varying the amplitude of the three-phase quasi-square wave applied to the gyro induction motor.

Figure 4.6-32 shows the mechanization of the PWM servo. The gyro torquer current is pulse-width modulated at 120 revolutions per second but modified by the condition that the current can change polarity only in coincidence with a 1200-pulse-per-second clock pulse applied to the current-switching logic. The logic then sends an "up" pulse to the up-down counting register for the condition of positivie torquer current and a "down" pulse to the register for the condition of negative torquer current and a 1200-pulse-per-second clock pulse.

The outputs of the gyro PWM servos are sent to a simple serial binary up-down register shown in Figure 4.6-33 where the total vehicle angle departure from null can be determined. The total capacity of the register is ± 2 degrees. The digital-to-analog converter is a conventional ladder network consisting of metal-film resistors and low-leakage transistors for the switching

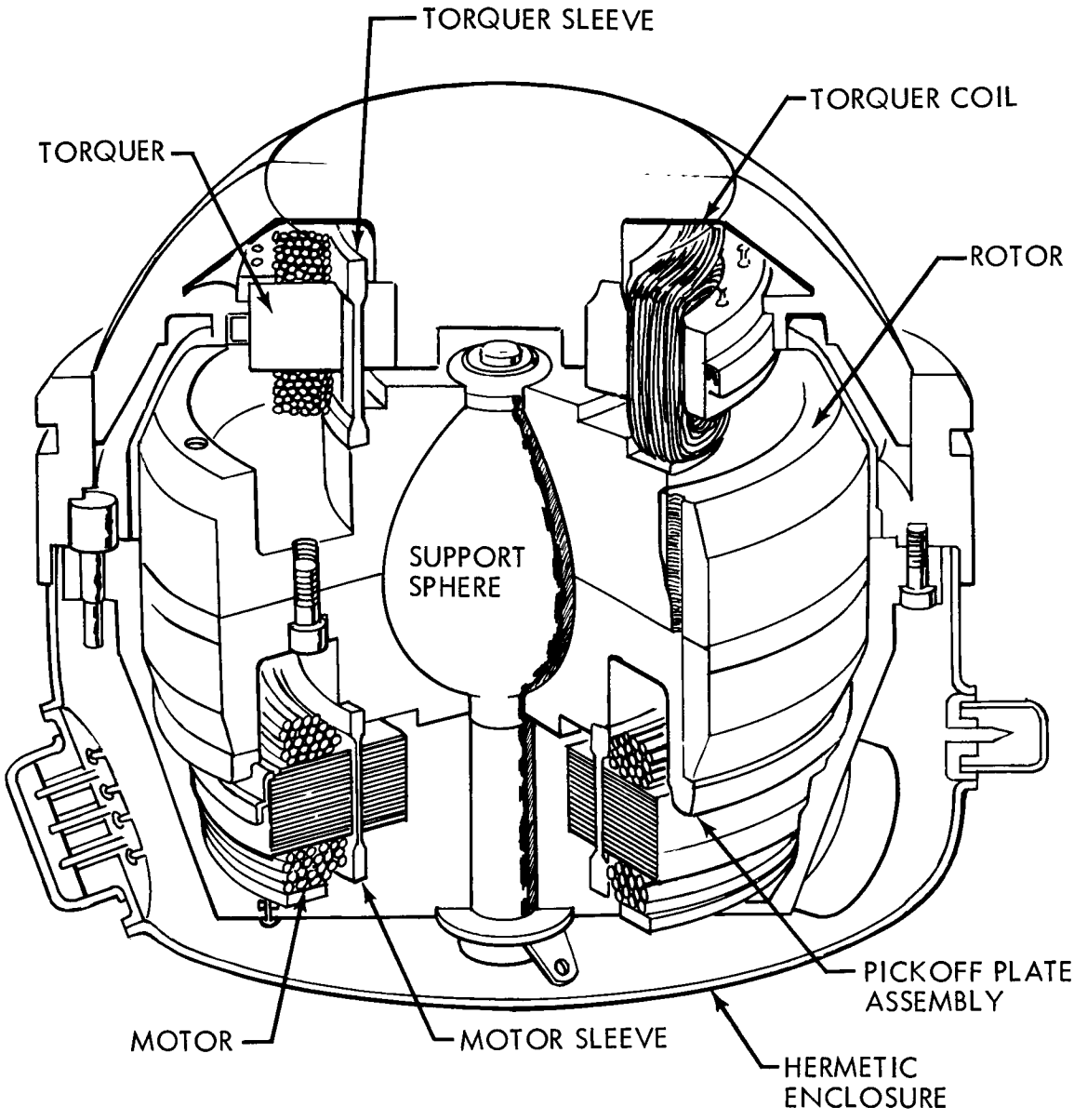

Figure 4.6-31: Autonetics G10 Gyro

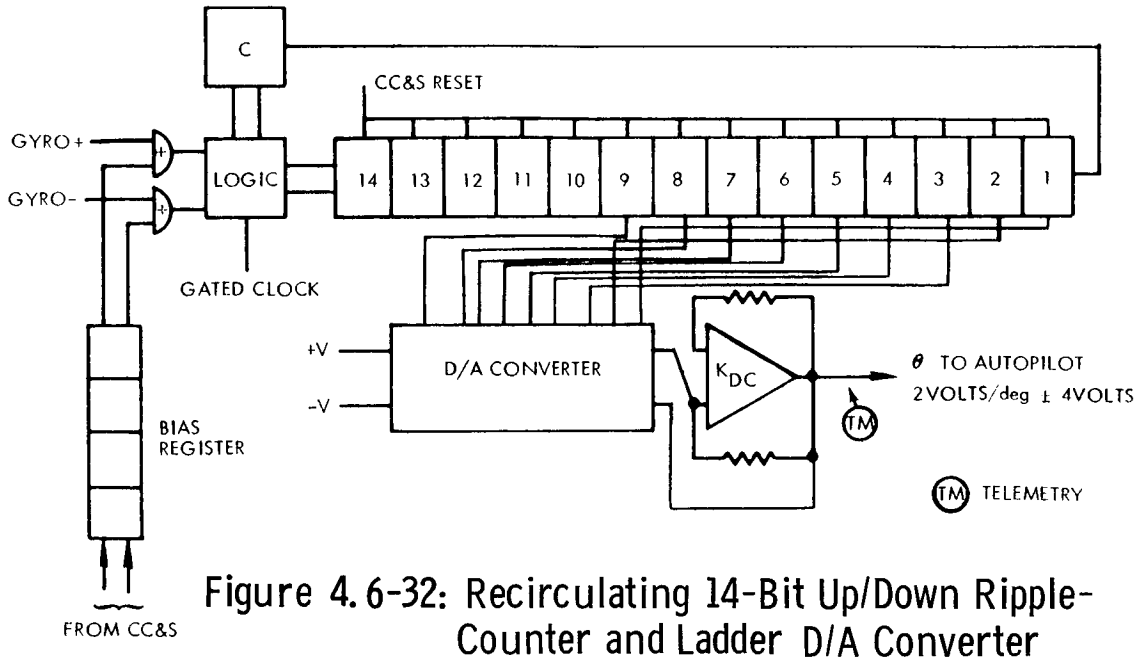

Figure 4.6-32: Recirculating 14-Bit Up/Down Ripple-Counter and Ladder D/A Converter

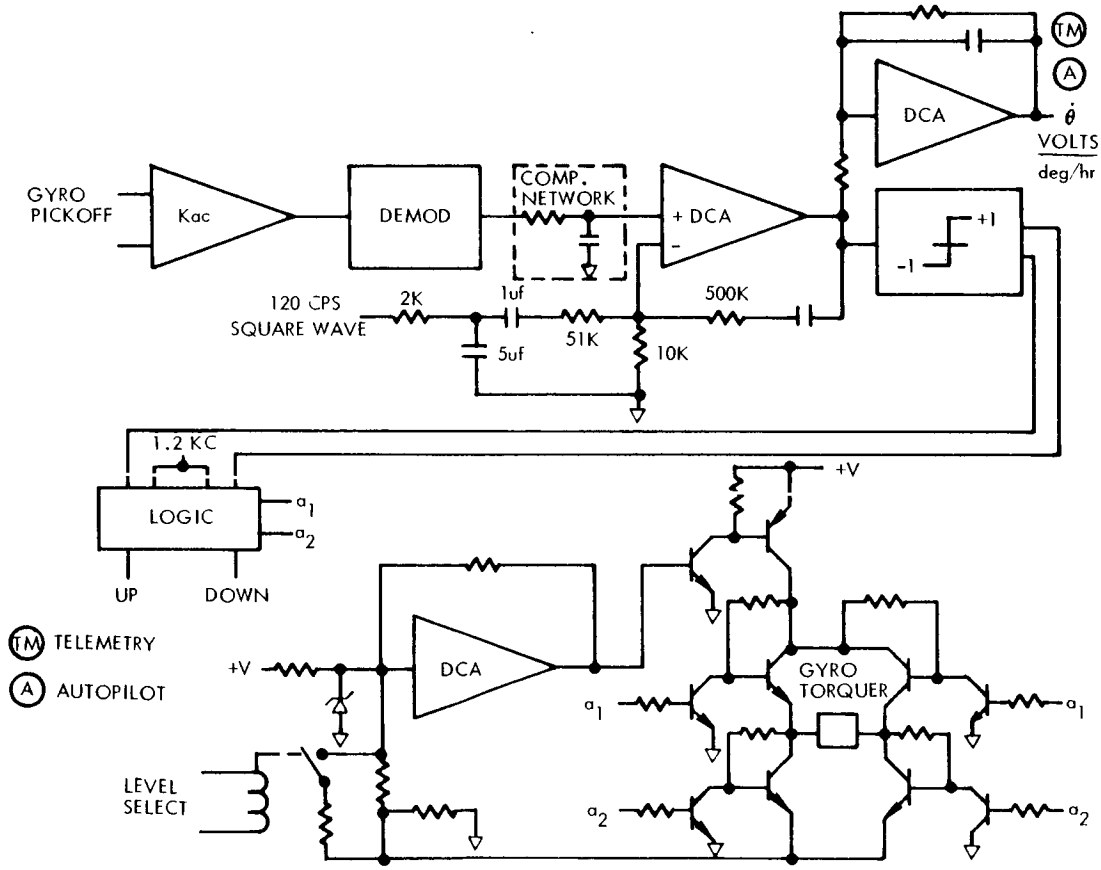

Figure 4.6-33: PWM Servo Mechanization

elements. Data recirculation in the register requires 0.833 millisecond. During this period, no data is available to the digital-to-analog converter. To prevent the d.c. output voltage from varying during this period, a sample and hold circuit is used to decouple the D/A converter from the circulating register.

Included with the up-down counter is a four-bit register that receives information for the CC&S corresponding to gyro bias. This information is read into the up-down counter just prior to a maneuver without destroying the information in the register.

Support Electronics--The support electronics include the signal conditioners, dual inverter and regulator, and the field current supply.

The standard and very efficient (85 percent) flyback regulator-type power supply is used. The principle is that energy is stored in the primary of the transformer through the power switch, then, when the power switch is turned off, the transformer flies back, delivering the stored energy into the various secondary windings, thereby developing the required output voltages. Voltage regulation is accomplished by controlling the "on" time of the power switch.

A constant field for gyro torquing is supplied by the field current supply, which consists of three individual current supplies, one for each gyro.

Redundancy--Figure 4.6-34 shows the redundancy mechanization of the G10 gyro unit. Two modes of detecting gross gyro unit error phenomena are provided. The error modes that will be automatically sensed and corrected for are as follows: input vehicle rates that exceed the torquer capacity of the PWM servos and loss of gyro speed control after the gyro rotor has once obtained speed. The more subtle corrections will be made, based on decisions made by ground control on the basis of telemetry data. The appropriate commands will be issued to the Voyager CC&S.

The analog signal representing average gyro rate will be scaled such that the voltage will be within a given range for normal operation. For excessive rates, greater than or equal to $\pm$ 1000 degrees per hour, this analog signal will initiate a switching sequence that automatically increases the dynamic range of both of the PWM servos on the gyro.

The second detection function provided in the gyro unit monitors three gyro speed signals simultaneously. An analog signal from each gyro speed-control loop will be sent to a ternary switch that can sense rotor speeds both above and below the normal operating speed. If the gyro loses speed control and not regain it within a specified length of time, the sensing circuit will initiate a switching sequence that will remove the gyro motor from the speed controller and place a redundant, fixed-amplitude, three-phase, 400-cycle-per-second quasi-square-wave voltage on the motor.

Commands from the CC&S will be received by the gyro selection circuitry. Three distinct commands will be required to select any axis for presentation

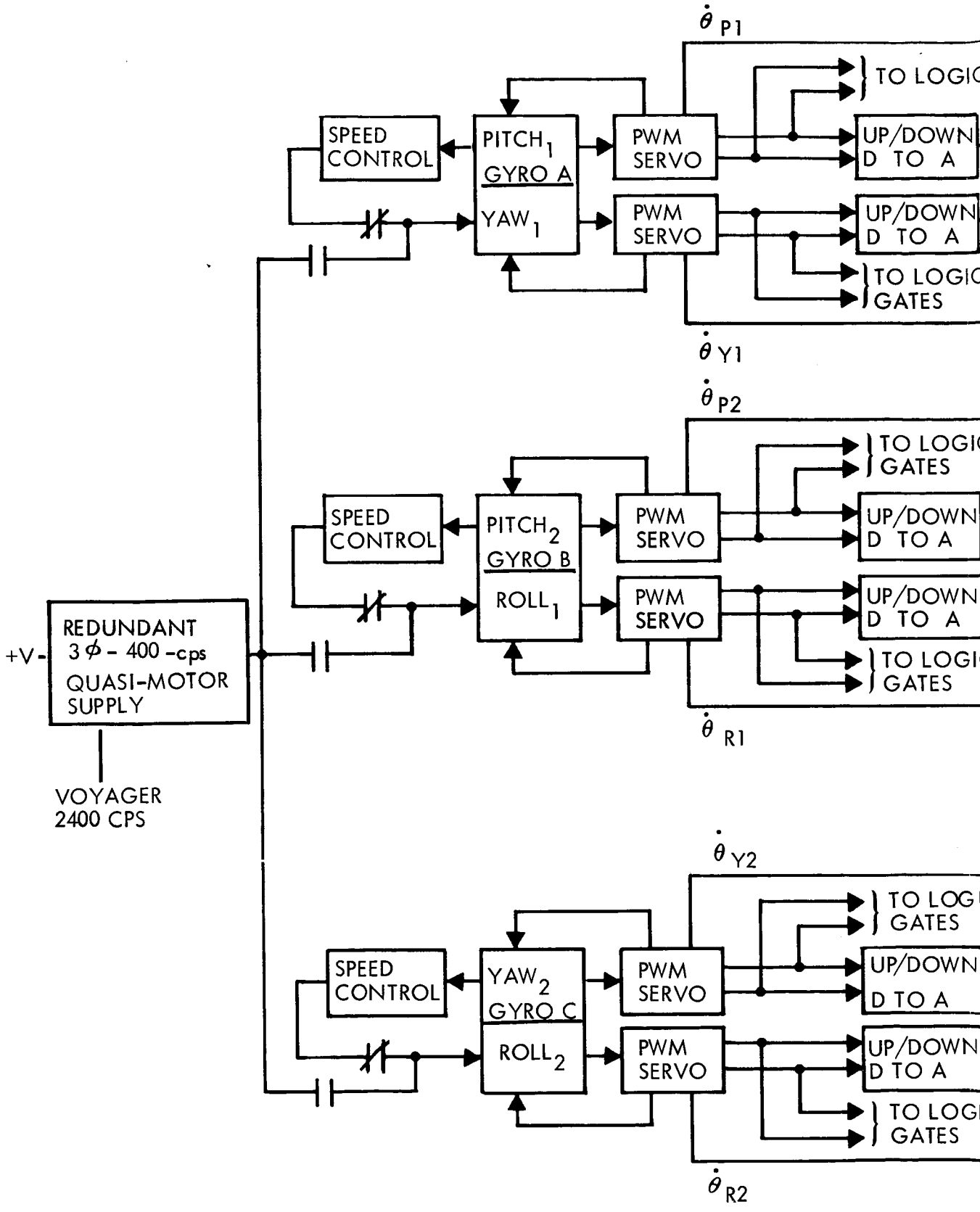
$\dot{\theta}_{P1}$
TO LOGIC
SPEED CONTROL
PITCH$_1$ GYRO A
YAW$_1$
PWM SERVO
PWM SERVO
UP/DOWN D TO A
UP/DOWN D TO A
TO LOGIC GATES
$\dot{\theta}_{Y1}$
$\dot{\theta}_{P2}$
TO LOGIC GATES
SPEED CONTROL
PITCH$_2$ GYRO B
ROLL$_1$
PWM SERVO
PWM SERVO
UP/DOWN D TO A
UP/DOWN D TO A
TO LOGIC GATES
$\dot{\theta}_{R1}$
+V-
REDUNDANT 3 ϕ - 400 -cps QUASI-MOTOR SUPPLY
VOYAGER 2400 CPS
$\dot{\theta}_{Y2}$
TO LOGIC GATES
SPEED CONTROL
YAW$_2$ GYRO C
ROLL$_2$
PWM SERVO
PWM SERVO
UP/DOWN D TO A
UP/DOWN D TO A
TO LOGIC GATES
$\dot{\theta}_{R2}$

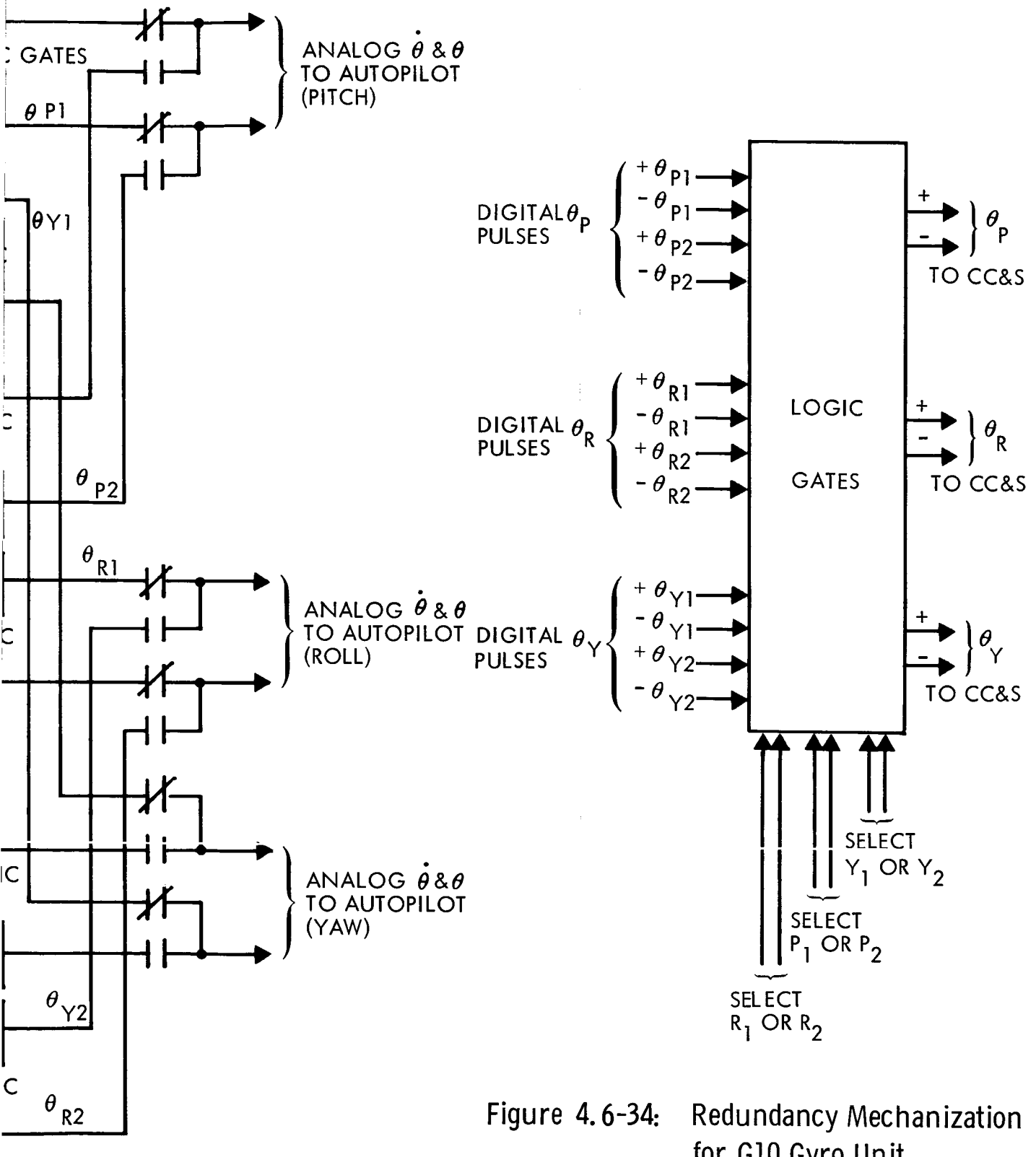

Figure 4.6-34: Redundancy Mechanization for G10 Gyro Unit

to the autopilot. The command to select a given axis also presents, on the proper line, the digital signals to be used by the CC&S during maneuvers.

Interfaces--Four types are discussed below.

Signal--The attitude reference interfaces with the autopilot, CC&S, telemetry and OSE test points are shown in Section 4.6.1.1.

Power (Other Than Reference Signals)--All power consumed in the gyro unit will be from the ±35 volts d.c. supply. This power is required continuously during the entire mission.

		Watts
Gyro motor excitation -	Max. at 16,000°/hr	2.0
	Max. at 1,000°/hr	2.0
Pickoff excitation		
Torquerer	Max. at 16,000°/hr	5.4
	Max. at 1,000°/hr	0.3
PWM Servos		6.0
Speed Controllers		6.0
Frequency Division		1.2
Gyro Selection		3.0
Inverter Regulators		7.9
High Rate		31.5
Low Rate		26.4

Thermal--The power consumed by the primary system is 26.4 watts, of which 2.3 watts is dissipated in the gyro and 24.8 watts in the associated electronics. The three G10B gyros are mounted on a precast beryllium block along with the Bell IIIB and Autonetics EMA accelerometers. The beryllium block is then mounted in the IRU box through stainless steel bushings. It is expected that the temperature of the gyro block will not vary by greater than $10^{o}F$ during the maneuver intervals. Fine thermal compensation will be provided internally to the gyro.

The power dissipated by the gyro electronics will be conducted through the metal substrate to the heat-radiator flanges. Conductive heat transfer to the IRU enclosure will also be used to increase the heat radiating surface.

Mechanical--The three gyros will be mounted on a precast beryllium mounting block such that they form an orthogonal set. The block in turn will be aligned in the instrument section of the attitude reference box.

Gyro Test Data--To reduce power consumption, the free-rotor gyro will be operated at a low rotor speed of 50 revolutions per second as compared to the normal speed of 155 to 240 revolutions per second. This results in a significant reduction in power consumption as shown in Figure 4.6-35.

Concurrently, a dramatic reduction in the random drift rate can be expected as shown in Figure 4.6-36. The reduction in angular momentum would ordinarily degrade performance, but in the case of the free-rotor gyro, this does not occur since the major portions of the random torques

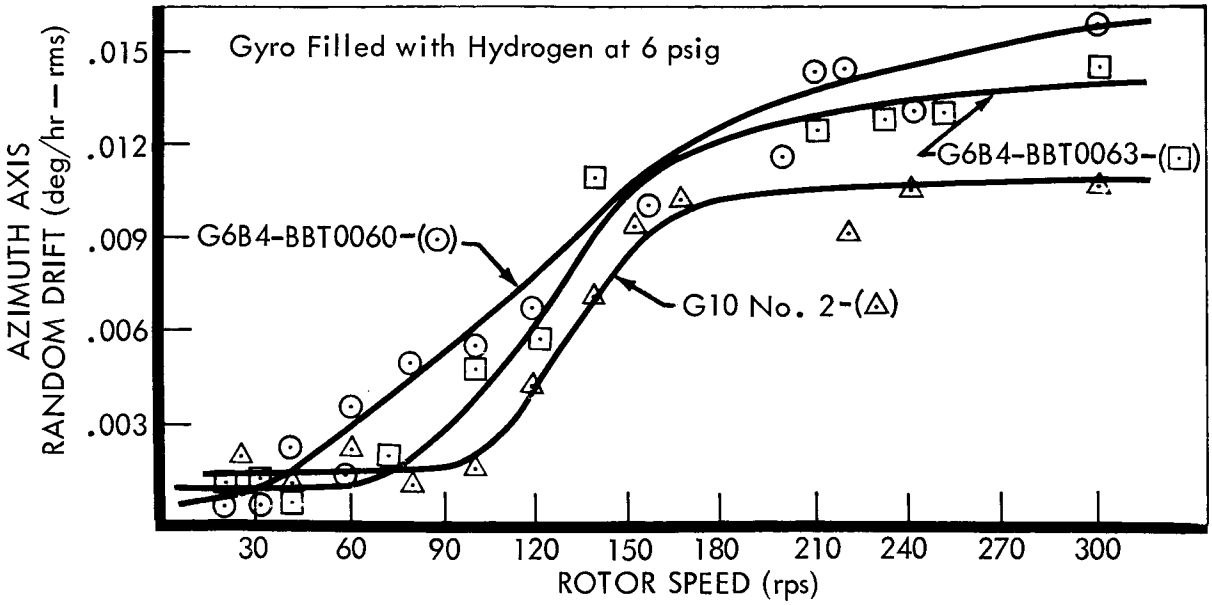

Figure 4.6-35: Slow-Speed Gyro Performance — Azimuth Axis Drift vs Rotor Speed

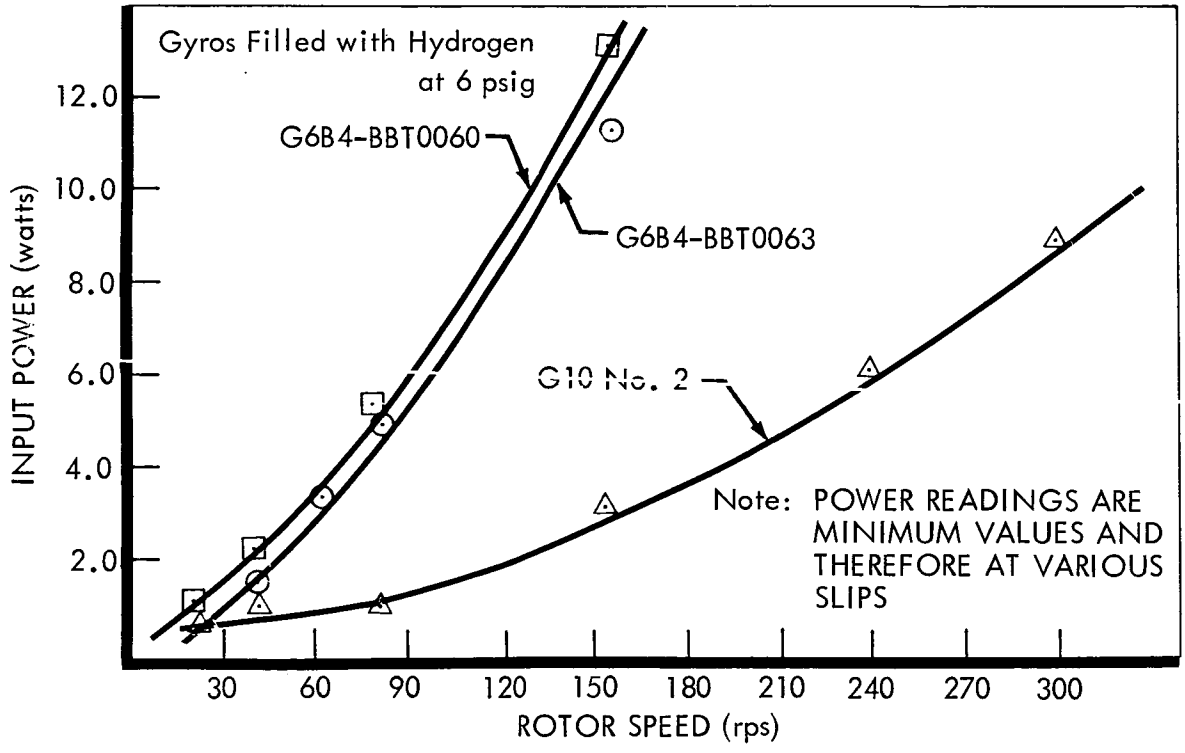

Figure 4.6-36: Slow-Speed Gyro Performance — Power Input vs Rotor Speed

are hydrodynamic in nature and are also reduced with speed. Note that the drift rate is down to 0.0015 degrees per hour at 60 revolutions per second, as compared to 0.01 degrees per hour at normal speed.

Another requirement is that the gyro must maintain good bias stability. Figures 4.6-37 and 4.6-38 are representative values of uncompensated and compensated torquer scale factor and axis alignment temperature sensitivities from a G8 gyro. The uncompensated scale factor and axis alignment sensitivities are -185 ppm/^{o}F and -15.6 seconds of arc/^{o}F, respectively. With compensation resistors installed, the sensitivities are down to 2.1 ppm/^{o}F and -0.11 seconds of arc/^{o}F, respectively.

Tests involving the measurement of a caged, G10 free-rotor gyro in a precession mode were conducted in order to simulate the free-rotor gyro's operation in a strapped down, attitude control configuration, as proposed for the Voyager system. The results indicate the suitability of the free-rotor gyros for the Voyager mission requirements.

The G10 free-rotor gyro was mounted (with spin axis horizontal) on a single axis fluid bearing azimuth drift-test platform stabilized and precessed by a single axis Autonetics SINS gyro. Platform rotation is sensed by the caged G10 gyro and presented at the output of the up-down counter. At the completion of one or more complete limit cycles, the reading of the up-down counter is indicative of the magnitude and direction of the gyro bias error and continued limit cycles provide continuous updating of the gyro bias.

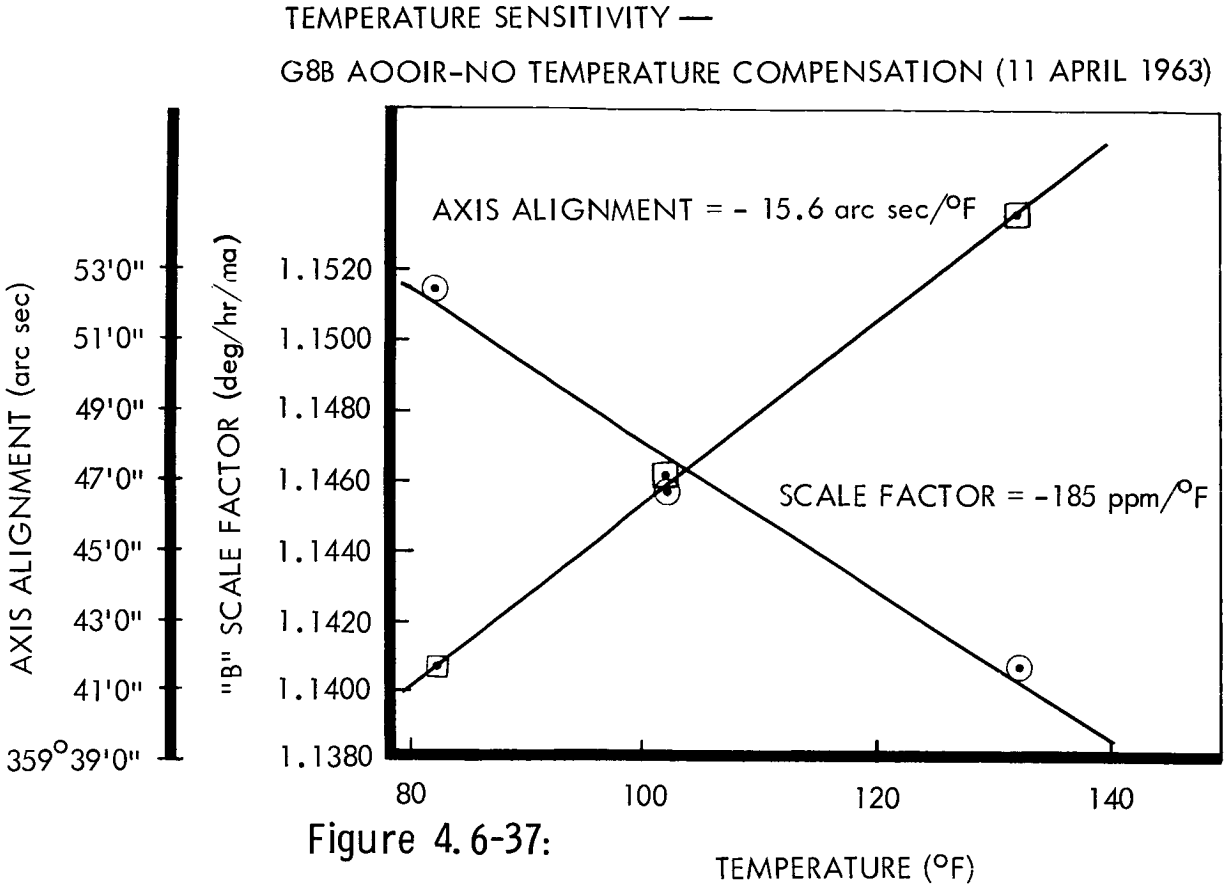

Figure 4.6-37:

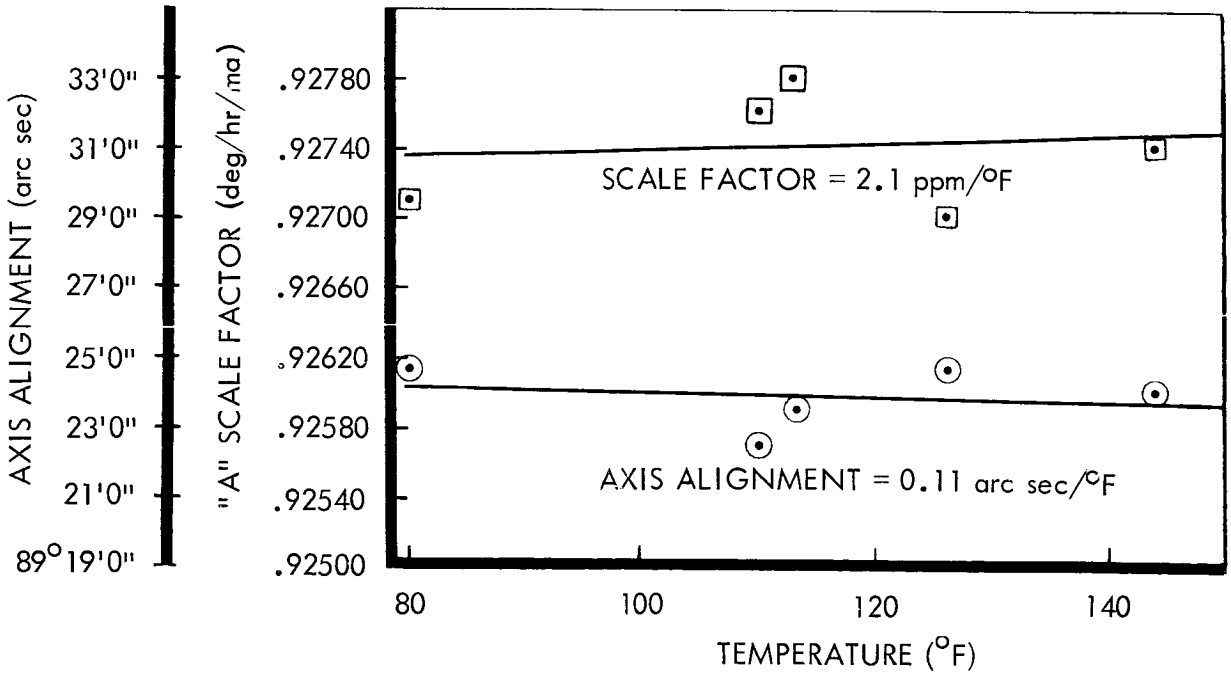

Figure 4.6-38: Gyro Performance — Axis Alignment vs Temperature (Temperature-Compensated)

Typical test results are shown in Figure 4.6-39. Here, the platform was precessed back and forth (in a sawtooth manner), at a rate of 2.33 degrees per hour to a peak to peak angle of 0.8 degrees (simulating the limit cycle expected during the cruise mode). The slope of the integral of the sawtooth wave is due to bias error which was removed by the above repetitious process. Measurements taken at the other output axis of the free-rotor gyro indicated negligible cross axis coupling and nutation frequency excitation (less than 1/2 second).

Two other tests were conducted to determine (1) the ability of the free-rotor gyro to stop a platform rotating at a high angular rate, and (2) the attitude measurement capability of the gyro over a larger angle. For the first test, the table was rotated at 3 degrees per second, simulating tumbling action during the initial-acquisition mode. While the table is rotating, the gyro is turned on and caged. The gyro rate signal is then switched on to detect and stop the platform from rotating. The results of the test show that a rate table rotating at 6 degrees per second is captured by a G10 gyro mounted on it in 2 seconds of time from gyro starting time.

For the second test, the table was rotated by 90 degrees at 0.18 degree per second. After 15 minutes in the inertial-hold mode, the table was rotated back to the original position. The positional output of the gyro is compared with the output of the angular transducer of the rate table. The mean position error obtained from 3 trials of (0^{o}-90^{o}-0^{o}) was 0.048 degree with an rms variation of 0.075 degree. The mean error of a 90 degree turn was 0.024 degree with an rms variation of 0.036 degree.

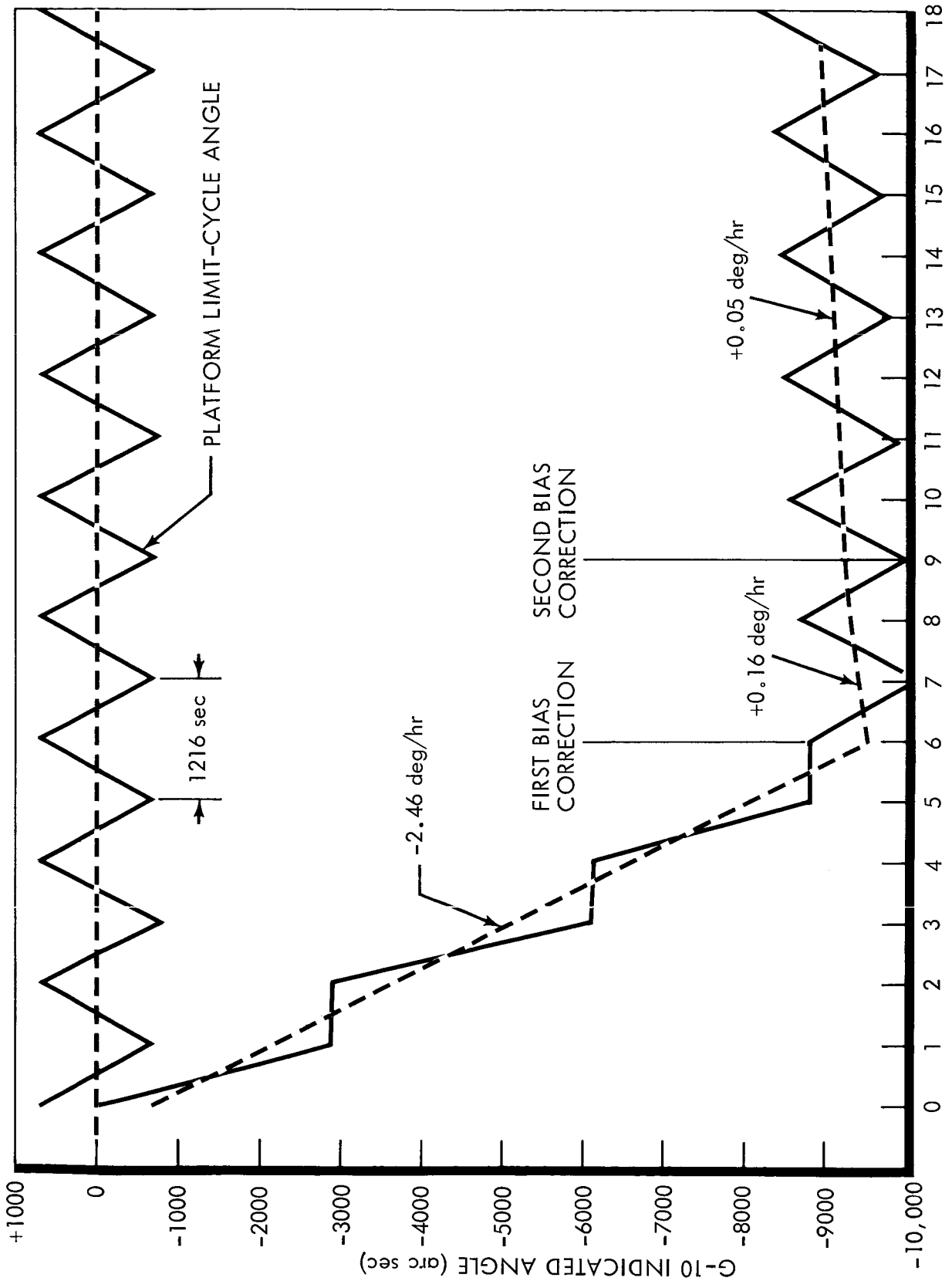

Figure 4.6-39: Limit-Cycle Drift

Gyro Drift Model -The free-rotor gyro drift model for the G10B gyro can be described by the following equation:

$$\phi_1 = N_1 + C A_1 - DA_2 - B A_1 A_3 - E A_2 A_3 + F A_3^2$$

$$\phi_2 = N_2 + C A_2 + DA_1 - B A_2 A_3 + E A_1 A_3 + F A_3^2$$

Where:

1, 2 refer to the input axes,

3 refers to the spin axes

A_1, A_2, and A_3 are the accelerations along the 1, 2, and 3 axes, respectively. The values of error terms are:

C = Drift due to mass unbalance $0.5^\circ/hr/g$

D = Drift due to structural compliance $0.2^\circ/hr/g$

B = Drift due to gas compliance incompressible effects $9.6^\circ/hr/g^2$

E = Drift due to gas compliance compressible effect $1.6^\circ/hr/g^2$

F = Drift due to axial g^2 sensitivity $0.001^\circ/hr/g^2$

N = Nonacceleration dependent drift

The bias of N term of the expression includes the following components:

Compensated	0.5°/hr rms
Random drift (9-min. inverval)	0.005°/hr rms (1σ)
Bias Stability	0.05°/hr rms (1σ)
Temperature Sensitivity	$0.005^\circ/hr/^\circ F$

Torquer scale factor errors such as torquer eccentricity, unbalanced turns, etc., are fully compensated when pulse width modulation is used.

Spin rate coupling will be less than:

Direct coupling	0.002^{o}/hr
Cross coupling	0.02^{o}/hr

The accuracy and ripple of the analog rate are 5 percent and 1 percent, respectively. The analog position errors are $\pm$ 0.03 degrees excluding gyro error sources.

Development Status--The Autonetics G10B free-rotor gyro is the result of extensive experience in the design, development, and production of precision gyros for inertial autonavigators. The design of the G10B gyro is a scaled-down version of the G6B4 free-rotor gyro used in the Minuteman Program. This provides reductions in size, weight, and power consistent with the requirements of space guidance components.

Development of free-rotor gyros began at Autonetics in 1955. The present Minuteman G6B4 is an improved version of the first production Minuteman free-rotor gyro and includes a number of improvements, the most significant being the addition of a welded mu-metal hermetic enclosure to ensure the required reliability of the hermetic seal. Other improvements for greater reliability include a heavier stop bearing and printed-circuit wiring harnesses.

The G6B4 is now produced in quantity for the Minuteman Program with over 2,500 having been manufactured. The G10B gyro was designed to satisfy a need for a smaller, more compact, low-cost instrument that maintains the G6B4 reliability.

The G10B is a small version of the G6B4 gyro produced on the G6B4 production line for the C141 astro-tracker guidance system. This production was stopped by the cancellation of the program, but it is presently being produced for the Elliott Brothers ES inertial guidance system. The G10B gyro is expected to be part of a piggyback satellite payload in early 1966.

Physical Characteristics and Constraints--The physical characteristics are summarized in Table 4.6-12B.

Safety Considerations--The gyro unit weighs less than 25 pounds, uses no voltage greater than 35 volts, has no sharp edges, is not explosive, etc., and, therefore, does not require any special safety considerations.

4.6.3 Canopus Sensor

4.6.3.1 Scope

The Canopus-sensor unit consists of two independent Canopus sensors plus the switching electronics necessary for switching autopilot control from one sensor to the other in case of sensor failure. The preferred trackers are essentially identical to those presently in space on the Mariner IV spacecraft. Due to lack of complete data, however, the unmodified Barnes sensor is described in this section.

4.6.3.2 Applicable Documentation

1) "System Description and Performance of a Canopus Star Tracker," published by Barnes Engineering Company, date unknown.

Table 4.6-12

Gyro Parameters

Rotor moment of inertia - 945 gm - cm^2

Rotor angular momentum - 3.6 x 10^5 gm-cm^2/sec

Size: 3.3 x 3.5 in.

Weight: 2 lbs.

Input Parameters

Pickoff excitation: 20 v ±2% rms
19.2 kc ±1% rms

Gyro motor normal: 5 v rms nominal

Operating voltage: 400 cps ± 0.05% three-phase quasi-square wave. Voltage shall be regulated for rotor speed control.

Start Voltage: 10 v rms nominal 400 cps three-phase quasi-square wave not exceed 5 sec

Gyro motor power normal

Operating: 0.7 watts
Starting: 1.5 watts

Pulse Torquing Signals

Current levels
High Rate: 100 ma
Low rate: 25 ma

Torquer Scale Factor

High Rate: 160°/hr/ma
Low Rate: 40°/hr/ma

Maximum Torquing Rate

High Rate: 16,000°/hr
Low Rate: 1,000°/hr

Torquer Linearity: 0.01%

Environmental Conditions

Storage temperature: -80 to 165°F

Ambient temperature: -65 to 165°F

Acceleration: ± 6g's steady state dc

Magnetic field: 50 gauss

Radiation hardened: Yes

Torques Power Requirements

High rate: 1.8 watts

Low rate: 0.1 watts

Output Signal

Pickoff: 19.2 kc suppressed carrier modulated. Normal near zero-level signal with maximum 100-mv rms. Amplitude of unmodulated speed signal (fundamental frequency 480 cps) shall be 2 ± 0.4 mv peak to peak.

Pickoff scale factor: 500 mv/mr

-10% + 20% (uncompensated)

2) "Proposal for Canopus Tracker," Barnes Engineering Company, BEC-P951, July 1, 1965.

3) JPL Space Programs Summary No. 37-29, Volume VI (July 1, 1964 to August 31, 1964).

4.6.3.3 Functional Description

The preferred configuration for the Canopus tracker is shown in Figure 4.6-40. The subsystem contains two complete Canopus sensors, each with optics, an image-dissector tube, power supplies, signal-processing electronics, and Sun shutter. It also contains two power switches, a Canopus select switch, and two Sun shutter drivers. The Canopus sensor provides roll-error signal with a scale factor of 1 volt per degree. The Canopus switch selects between the two sensors on command from the CC&S and provides the roll error signal to the autopilot.

Barnes Canopus Tracker--Shown in Figure 4.6-41, the Canopus-sensor optics unit is a semisolid Cassegrain Schmidt unit with a focal length of 0.8 inch and a speed of f/0.8. A fiber optics faceplate is used to transfer the focused star image from the flat focal plane of the telescope to the rounded front surface of the image-dissector tube.

A system of baffles is used in front of the telescope to eliminate interference from stray light, such as reflected sunlight from outside the field of view. The baffle assembly consists of a series of apertures around the field of view, each aperture having a razor-sharp edge to minimize reflections from the aperture itself. The length of the baffle is

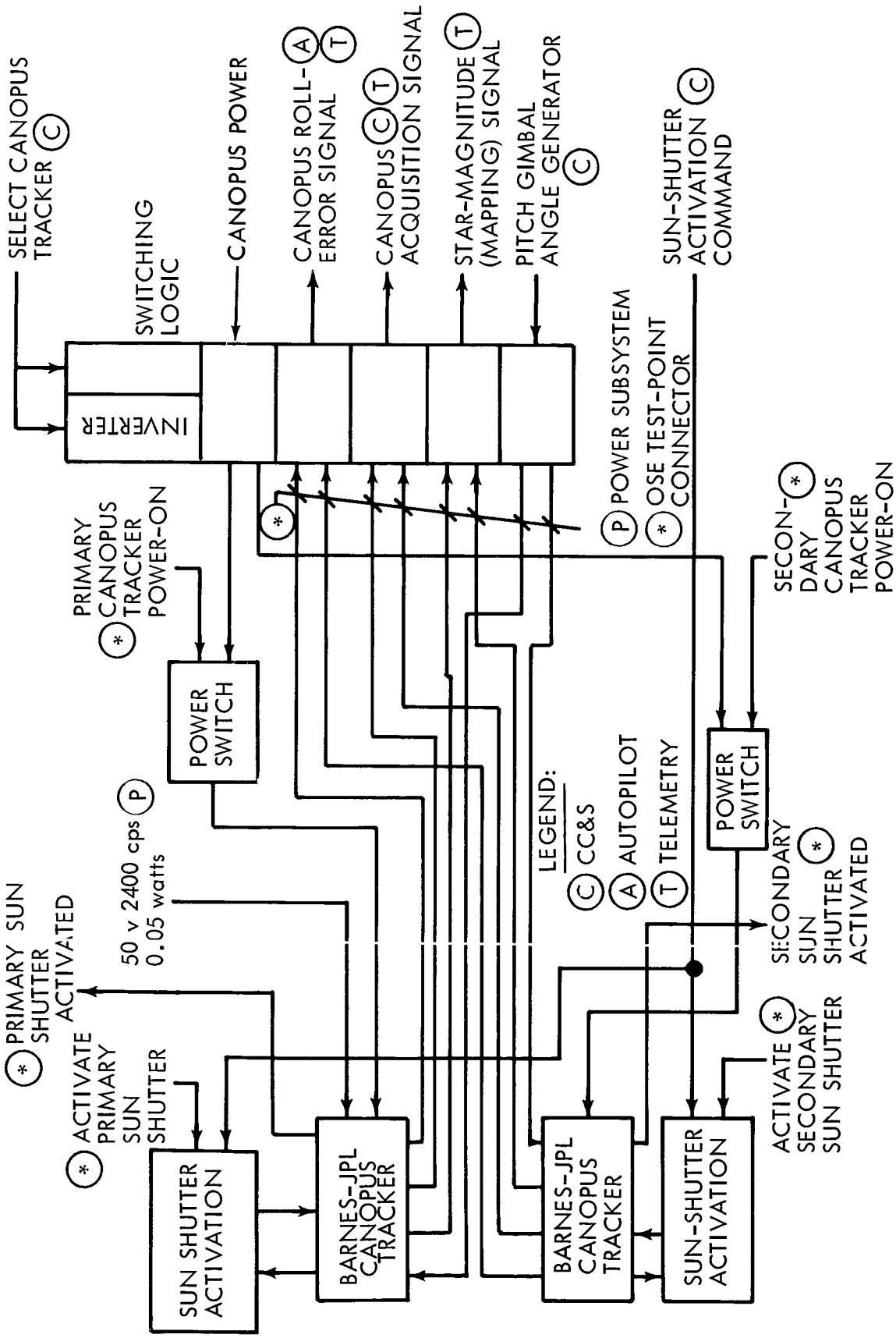

Figure 4.6-40: Canopus Tracker Subsystem

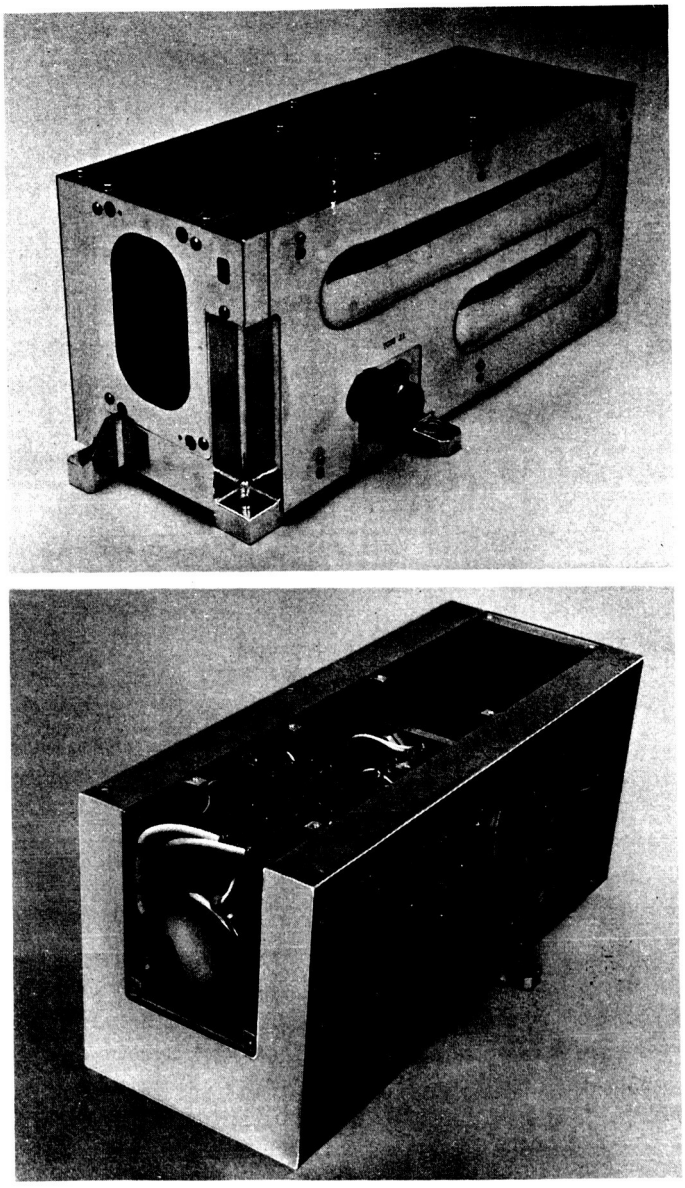

Figure 4.6-41: Barnes Canopus Tracker

dependent on the proximity of reflecting bodies. The baffle will be tailored to the Voyager configuration.

The faceplate of the tube and the telescope focal length define a 32-degree field of view for the sensor. The anode slit, the telescope focal length, and the electron-focusing optics define an instantaneous slit-shaped field of 0.86 degree of 10 degrees. The 10-degree instantaneous field electronically is "gimbaled" to cover the 32-degree field by applying discrete voltages to the appropriate deflection plates.

Five voltage steps provide overlapping coverage of the field. A 1000-cps sinusoidal waveform applied to the other deflection plates causes the instantaneous field to be swept sinusoidally in a direction approximately perpendicular to its long dimension. The sweep amplitude is 4 degrees, peak to peak. Tube-fabrication techniques do not permit precise alignment of the deflection plates and anode slit, so the resulting crosstalk must be compensated electronically.

Sensor Electronics--In addition to the optics and the image-dissector tube, the primary Canopus sensor will consist of the following electronics modules (Figure 4.6-42):

1) A high-gain, wide-bandwidth (500 cps), transistorized, three-stage preamplifier;
2) A high-Q, narrow-bandwidth, temperature-stabilized LC filter (the center frequency is 1000 cps, and the bandwidth is 50 cps);
3) A phase-sensitive half-wave diode demodulator;

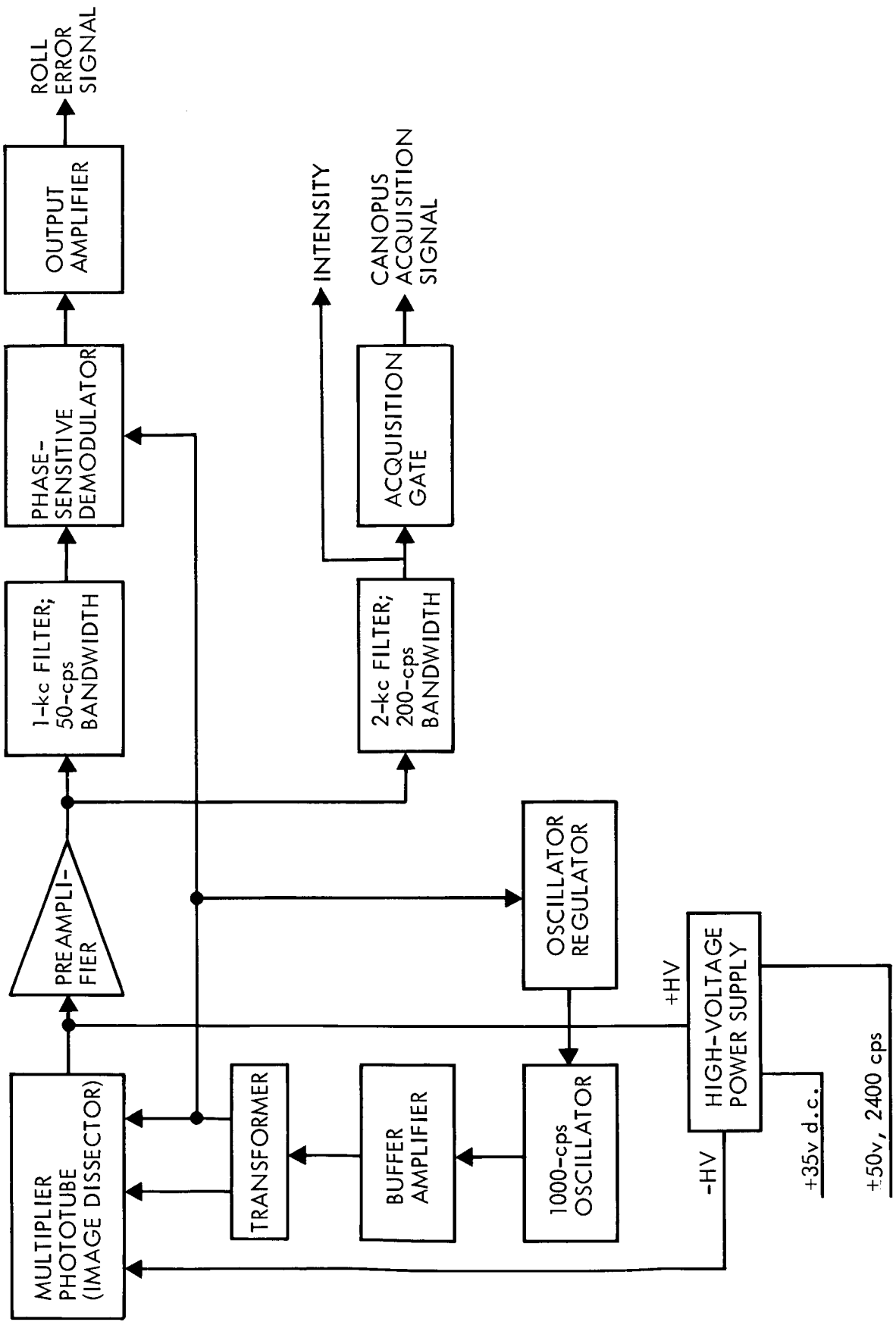

Figure 4.6-42: Barnes Canopus Tracker — Block Diagram

4) A transistorized d.c. amplifier, with a filter to limit ripple and noise (this amplifier provides the roll-error output signal);

5) A medium-bandwidth LC filter with a center frequency of two kc (this filter is in the acquisition-signal-processing loop; the bandwidth is 200 cps);

6) An acquisition circuit consisting of two modified Schmitt triggers in cascade for Canopus magnitude comparison;

7) A conventional, stabilized, LC-tuned circuit 1000-cps oscillator with an AGC loop for amplitude stability;

8) A single-stage buffer amplifier and transformer;

9) An intermediate power supply to convert the +35-volt d.c. primary power into d.c. power to all other modules;

10) A high-voltage control amplifier to generate the -1800 volt d.c. required for the image-dissector-tube photomultiplier.

The acquisition (or recognition) gate consists of two modified Schmitt triggers in cascade. One trigger sets the low acquisition threshold, and the other sets the high threshold. An output discrete is issued only when the signal passed by the medium-band filter is between the two thresholds. This indicates that an object in the brightness range of Canopus is in the field of view of the Canopus sensor.

The sun shutters will be placed outside the baffle assemblies as done on Mariner IV. In case of failure in the closed position, a small squib may be provided to free the view of the sensor, if necessary. Subsequent maneuvering would be carefully planned to avoid any possibility for the sensor being exposed to direct sunlight.

Redundancy Mechanization--A computer redundancy optimization program applied to the Canopus sensor subsystem indicates that two Canopus sensors are required. No analysis was made to select redundant blocks at a level lower than a complete Canopus sensor. Therefore, each sensor is completely independent of the other, including independent power supplies.

Failure will be recognized by ground analysis of telemetered signals from the two Canopus sensors because, at present, there is insufficient information on failure modes to permit confidence to be placed in automatic failure recognition. Therefore, selection of the secondary Canopus sensor will also be ground-based.

A discrete signal from the CC&S will be fed to an inverter, whose outputs ("1" and "0") control the power switches and the output gates of the two sensors. The backup sensor power switch will be biased open in the normal mode, and the output terminals of this sensor shorted to ground by appropriate transistor gates. If the primary sensor fails, a discrete from the CC&S will open the primary power switch, close the secondary power switch, short the primary outputs to ground, and connect the secondary outputs to the autopilot. Independent Sun shutters are provided to protect the two image-dissector tubes from damage due to exposure to direct sunlight. These shutters operate simultaneously, bypassing all redundancy switching circuitry.

4.6.3.4 Characteristics

The important characteristics of the Barnes Canopus trackers are illustrated in Table 4.6-13.

4.6.4 Sun Sensor

4.6.4.1 Scope

The Sun sensor unit consists of two independent Sun sensors, each capable of acquiring the Sun and supplying pointing-error information to the autopilot to permit Sun tracking for attitude reference. Each Sun sensor consists of a fine sensing unit, the output of which is a linear function of the pointing-error and the necessary coarse-sensing units to permit acquisition of the Sun from any initial orientation. A fifth sensing unit provides the necessary control for switching from coarse to fine units.

4.6.4.2 Documentation

Applicable documents are:

1) "Guidance and Attitude Control Sun Sensors for the Mariner II," G. W. Mosenholder and L. F. Schmidt, JPL, Proc. IRIS, October 1963 (Secret).

2) "Flight Acceptance Test Procedure for LOS Sun Sensor," Ball Brothers, 17012, 12 March 1965.

3) "Functional Description of Nortronics Sun Sensors Used for NASA-JPL Ranger and Mariner Space Vehicles," Nortronics Report, NORT 65-360, 16 December 1964.

Table 4.6-13: CANOPUS TRACKER CHARACTERISTICS

Size (one tracker)	11 x 5 x 4.5 inches
Weight (one tracker)	5 pounds
Temperature Range	$-18^{\circ}C$ to $+40^{\circ}C$
Power	2 watts, 35 volts d.c. (each tracker)
Accuracy	0.1°
Total Field of View	$32^{\circ} \times 4^{\circ}$
Scan Field of View	$10^{\circ} \times 4^{\circ}$
Instantaneous Field of View	$10^{\circ} \times 0.86^{\circ}$
MTBF (one tracker)	154,000 hours
Mission Success Probability (redundant trackers)	0.9984
Development Status	Mariner IV Design
Mechanical Alignment	0.01° Roll, 0.1° Yaw and Pitch

4.6.4.3 Functional Description

The preferred configuration of the Sun sensor unit is shown in Figure 4.6-43. The unit will consist of redundant two-axis Sun sensors. The primary (Nortronics) sensor will contain its own a.c./d.c. converter. The backup (Ball Brothers) sensor will contain a signal preamplifier. The unit also contains switches to select coarse or fine sensing and to select between control by primary and by backup sensors. Each Sun sensor will have a gradient of 1 volt per degree about each of two axes (yaw and pitch).

Primary Sun Sensor--The Nortronics Sun sensor will consist of 17 sintered, CdS photoconductive detectors (Clairex type 605) providing 4π steradian, two-axis coverage. The detectors are mounted in housings that provide mechanical support and alignment for the detectors, define the detector fields of view, and provide means for changing illumination as a function of Sun pointing-angle error. Two pairs of detectors are operated as fine sensors--one pair in each axis. The two detectors of a pair are shaded by a mask, or umbrella, so that as direction to the Sun changes the amount of illuminated area of each detector changes (one increasing, the other decreasing) and the ratio of their electrical resistances changes. Since each pair is connected in a bridge-type circuit, the bridge output voltage varies proportionately with the pointing-angle error. Due to the high sensitivity of this bridge arrangement, outputs are sufficiently large to be fed directly to the autopilot.

Six pairs of the detectors are operated as coarse sensors, whereas the fine sensors provide fine control about the Sun sensor null in a small

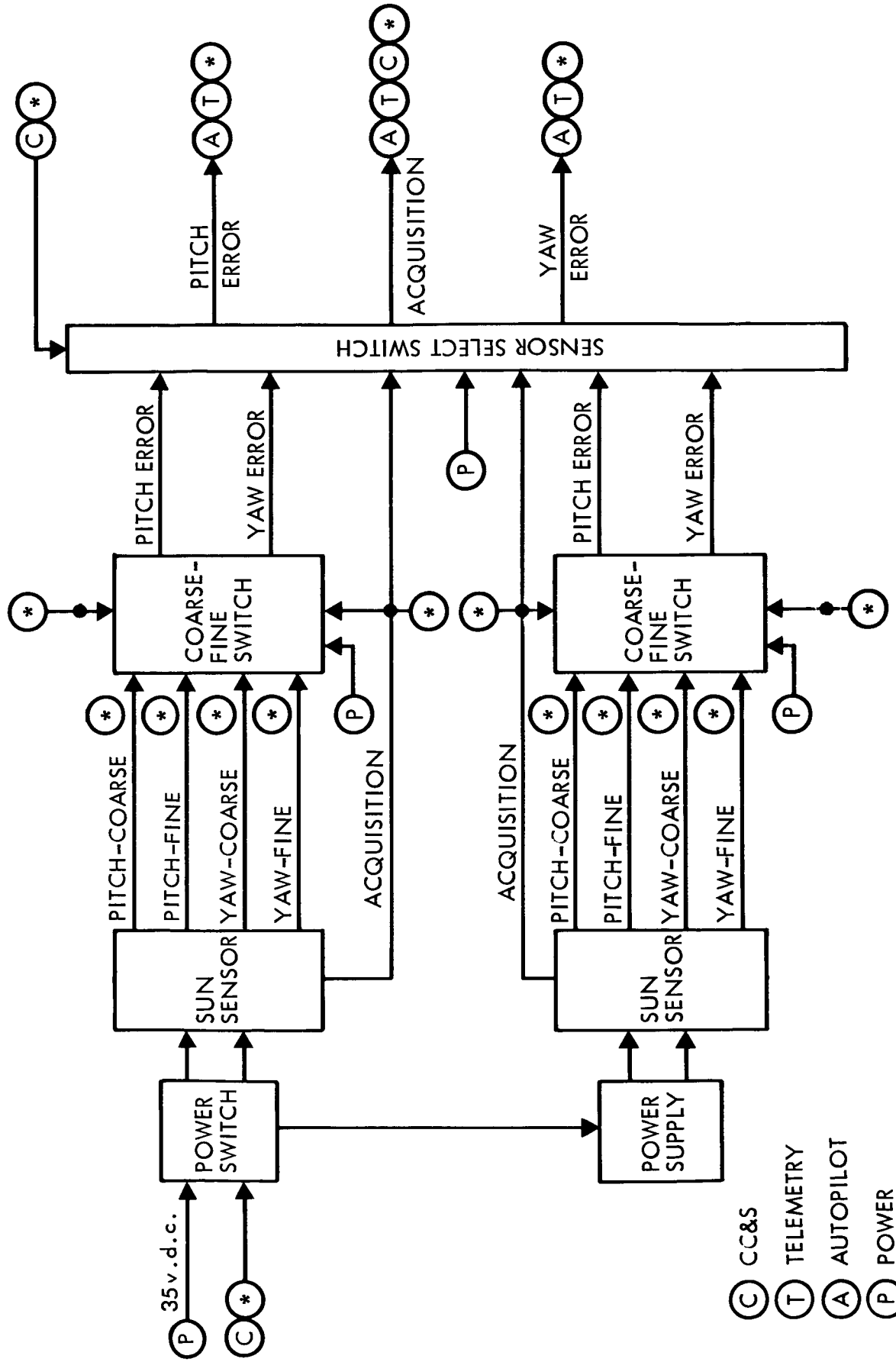

Figure 4.6-43: Sun Sensor Unit

field of view; the coarse sensors provide coarse error information (basically just the sign of the error) over the remainder of the 4π steradians. Two pairs of coarse sensors are aligned with the fine sensors and two pairs of coarse sensors (one pair in each axis) face in the opposite direction. The other two pairs of coarse sensors (one pair in each axis) are aligned to face orthogonally to the fine sensor direction. The coarse sensors are also connected in bridge-type circuits, but only those on the Sun axis are under an umbrella; the coarse sensors facing orthogonally to the fine sensors are unshaded, with the detectors of each pair facing in opposite directions so either (but never both) is illuminated.

One detector operated as a primary acquisition sensor, aligned to the fine sensor field of view, is used to control the switching from the coarse-alignment mode to the fine-alignment mode. There are two null positions in each axis: one is an unstable null at a 180-degree error angle, occurring in the coarse-alignment mode; the other is a stable null at zero-degree error angle, occurring in the fine-alignment mode.

The Ball Brothers FE5A-CE3 Sun tracker consists of a set of 13 silicon photovoltaic cells mounted in housings with various shades, baffles, and lenses. The cells are operated in six pairs, two coarse-sensing pairs and one fine-sensing pair in each axis, plus one "target eye" for sensing presence of the Sun in the field of view of the fine sensors. Electrically, each pair consists of two cells connected as opposing current sources, with the difference current fed to a low-impedance amplifier. Thus, when one cell receives more sunlight than the other, a

Table 4.6-14: SUN SENSOR CHARACTERISTICS

	Primary (Nortronics)	Secondary (Ball)
Accuracy	0.1^{o} - 0.05^{o}	0.02^{o}
Linear Range	$\pm 3^{o}$	$\pm 5^{o}$
MTBF	10^{5} Hours (including electronics)	10^{6} hours (sensor only)
Development Status	Mechanical redesign of Mariner II Sensor	Lunar Orbiter, OSO Sensors (electronics unproven)
Size	(4 Units) $2\frac{1}{2}$x$1\frac{1}{4}$x$1\frac{1}{4}$ in. (1 Unit) $2\frac{1}{2}$x$s\frac{1}{2}$x$1\frac{1}{1}$ in.	(2 Units) 3x3x1 inch (2 Units) 3x$1\frac{1}{2}$x1 inch
Weight (Existing Design)	11 ounces (total)	9 ounces (total, sensors)
Temperature Range	-16^{o}C to $+65^{o}$C	-12^{o}C to $+85^{o}$C
Shock, Vibration	No available information (Operated on Mariner II)	No available information (Operated on OSO)
Radiation Effects	No available information	No available data OSO unaffected Starfish program troubled by radiation Shields are available
Power	600 mw, 50 v, 2400 cps 100 mw, 35 vdc (switches)	400 mw
Mechanical Alignment	Fine: 0.01^{o} Yaw, Pitch; 1^{o} Roll Coarse: 1^{o} All Axes	

craft. The field of view of each Sun sensor is slightly obscured by the other Sun sensor along the horizon of the field of view.

For the dark-side Sun sensors, it is necessary to mechanize the hemispherical field of view through two quarter-sphere fields of view provided by coarse Sun sensors located opposite to each other across the spacecraft. The flight capsule and spacecraft would represent a major obstruction in the field of view of a single-location Sun sensor. Each dark-side Sun-sensor assembly, consisting of a primary (Nortronics) coarse and a redundant secondary (Ball Brothers) sun sensor mounted on a single plate, has a field of view of π steradian (quarter sphere). The fields of view of the two half Sun sensor assemblies are arranged back to back to provide a completely hemispherical dark-side field of view.

4.6.5 Autopilot

4.6.5.1 Scope

The autopilot subsystem provides the actuation signals to the reaction-jet subsystem and propulsion subsystems, based on inputs from the Sun sensor, Canopus sensor, and the inertial reference unit. Mode control of the autopilot is performed by the central computer and sequencer (CC&S).

4.6.5.2 Applicable Documentation

Applicable documents are:

1) Jet Propulsion Laboratory

   a) "Preliminary Voyager 1971 Mission Specification," May 1, 1965;

   b) "Voyager 1971 Mission Guidelines," May 1, 1965

2) The Boeing Company

a) D2-106051-3, "Voyager System Engineering--1971 Flight Spacecraft Functional Description";

4.6.5.3 Functional Description

A functional block diagram of the autopilot subsystem is shown in Figure 4.6-44. Input (attitude reference) and output (reaction jet and propulsion) subsystems are included in the diagram to clarify the operation of the autopilot during the various modes.

Control Modes--The autopilot is required to stabilize the spacecraft during the powered and unpowered phases of flight. The various control modes provided by the autopilot subsystem are keyed to the demands of these flight phases. Six primary modes of control are available through discrete switching from the CC&S. The table in Figure 4.6-44 shows the following switching logic for each of the control modes.

Gyro/Optical Limit Cycle--Attitude error information is supplied by the Sun and Canopus sensors, with rate stabilization signals provided by the gyro subsystem.

Maneuver and Slew--A constant rate command signal is issued to the autopilot from the CC&S. When a given attitude error (stored as a difference between commanded attitude and gyro-derived attitude) approaches zero, the slew command is removed.

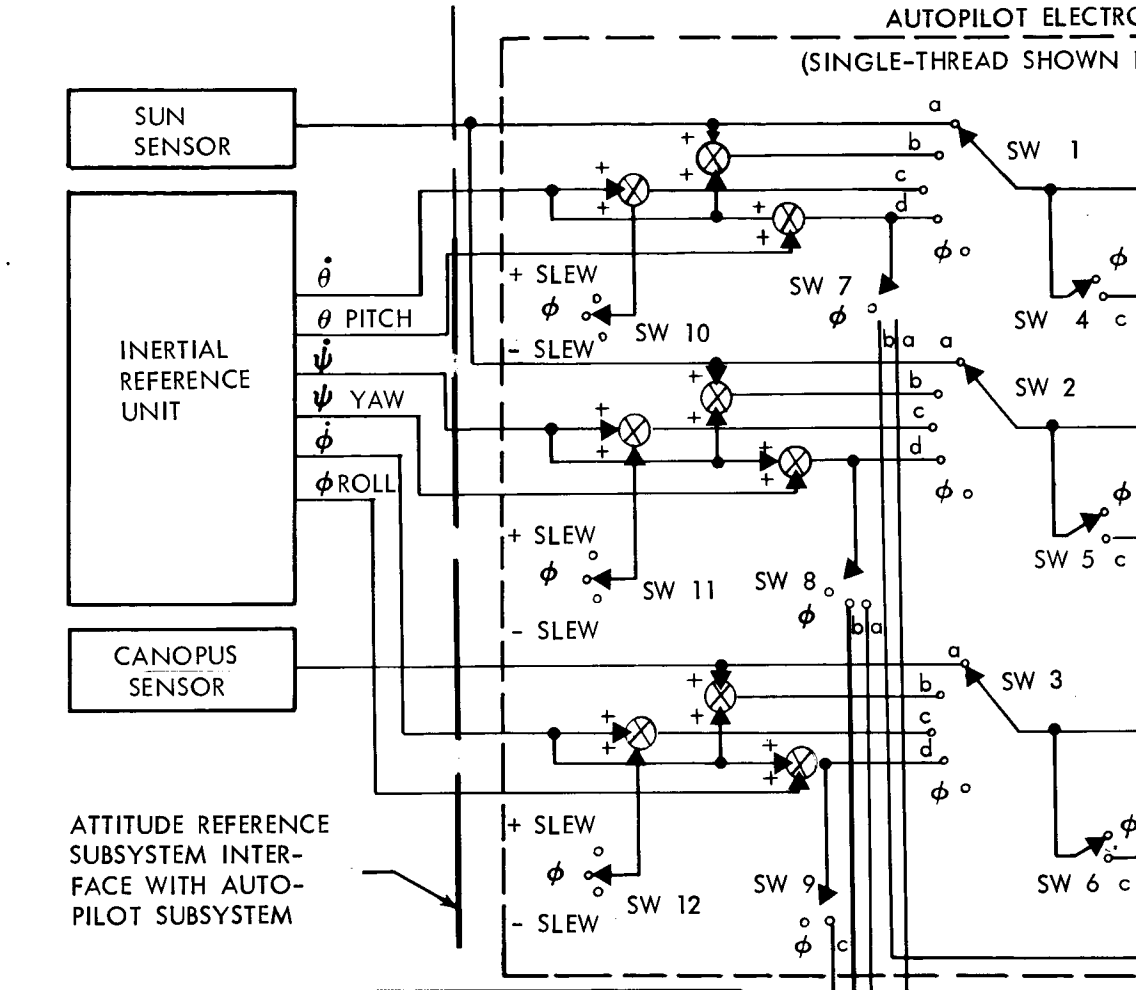

MODE	SW 1 & 2	SW 3	SW 4-6	SW 7 & 8	SW 9	SW 10-12
GYRO/OPTICAL LIMIT CYCLE	b	b	φ	φ	φ	φ
MANEUVER AND SLEW	c	c	φ	φ	φ	+ or -
INERTIAL HOLD (RCJ)	d	d	φ	φ	φ	φ
INERTIAL HOLD - (MIDCOURSE ΔV)	φ	φ	φ	a	c	φ
INERTIAL HOLD - (ORBIT ΔV)	φ	d	φ	b	φ	φ
CRUISE LIMIT CYCLE	a	a	c	φ	φ	φ

1

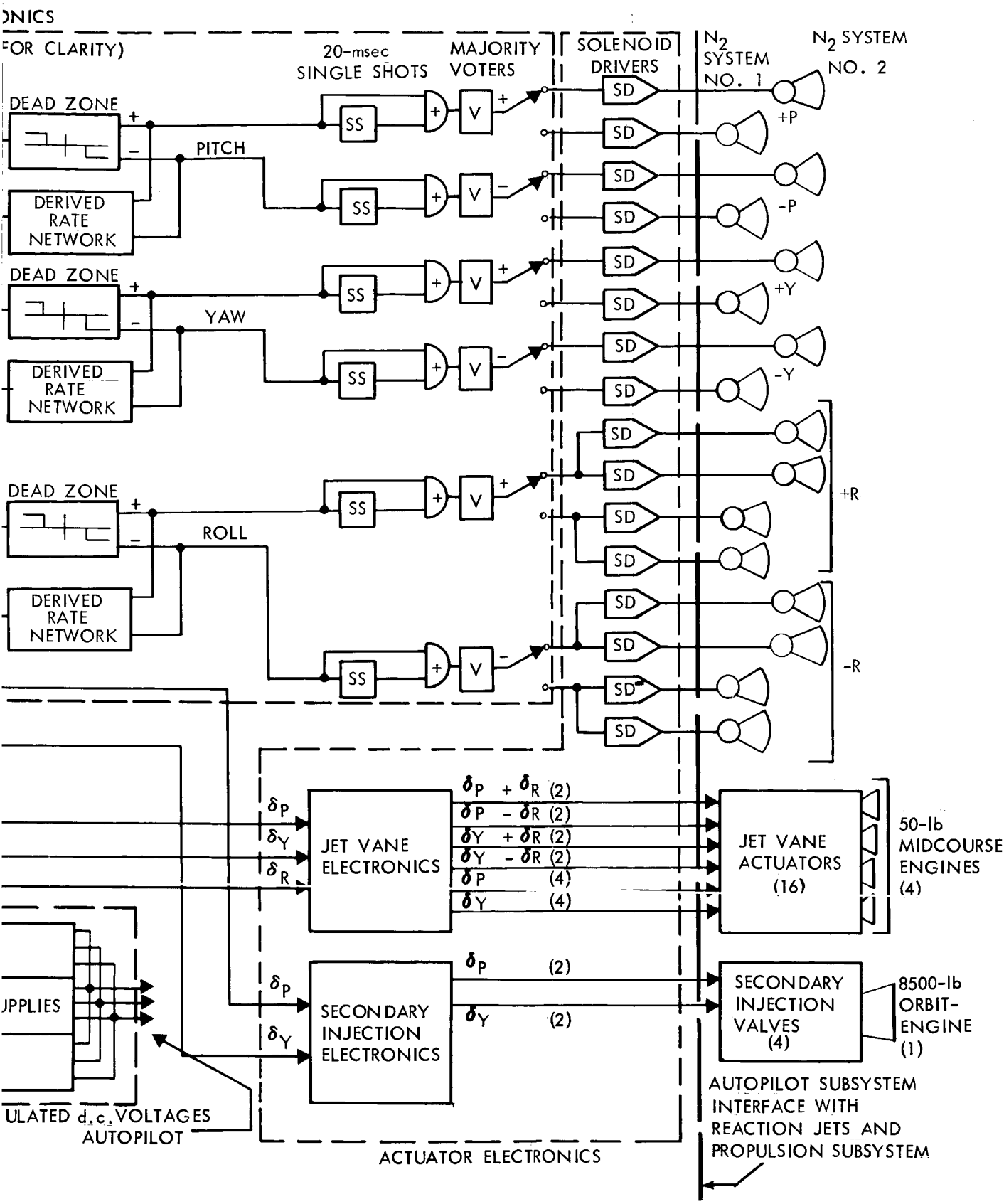

Figure 4.6-44: Autopilot Functional Block Diagram

2

Inertial Hold (using reaction control jets)--Gyro rate and position information is employed to maintain attitude through appropriate actuation of the cold gas reaction jets.

Inertial Hold (midcourse)--Gyro rate and position information is employed to maintain attitude through appropriate deflection of jet vanes operating in the nozzles of the four 50 pound midcourse engines.

Inertial Hold (Insertion)--Gyro rate and position information is employed to maintain pitch and yaw control through activation of secondary injection valves in the 8500 pound engines, with roll control maintained by the reaction jet subsystem.

Cruise Limit Cycle--Vehicle attitude is maintained with reference Sun and Canopus sensors. Stabilization and convergence to a minimum impulse limit cycle is achieved through the use of derived rate logic aroung the switching amplifier.

Mechanization--As shown in Figure 4.6-44, the autopilot subsystem consists of the following subfunctions:

1) The autopilot electronics, which includes the signal switches, signal amplifiers, variable dead-band generators, derived-rate networks, single-shot delays, and the majority voters.
2) The actuator electronics, which includes the solenoid drivers, jet-vane electronics for the midcourse-propulsion jet-vane control, and the secondary-injection electronics for the orbit-injection-engine thrust vector control.

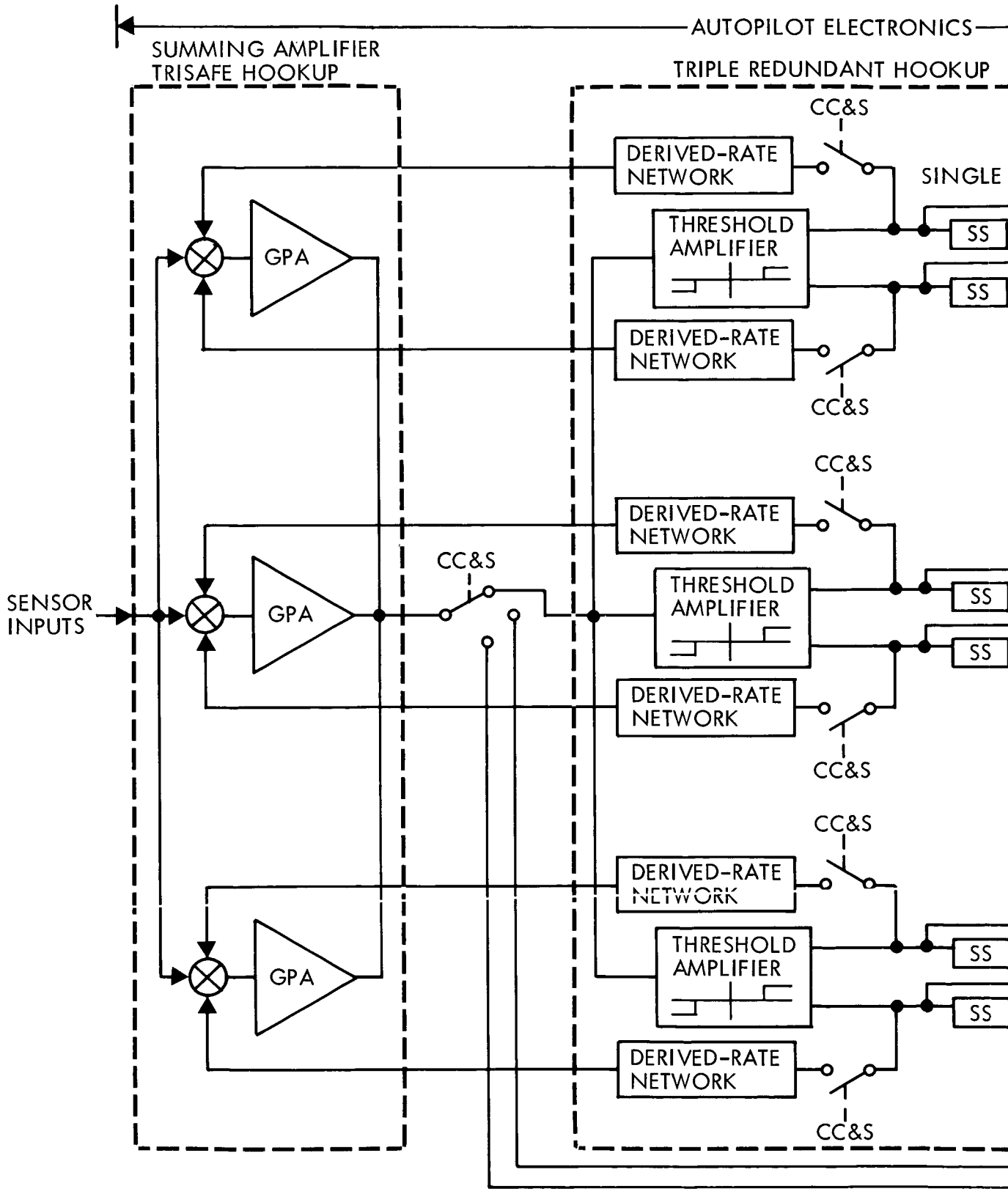
AUTOPILOT ELECTRONICS
SUMMING AMPLIFIER
TRISAFE HOOKUP
TRIPLE REDUNDANT HOOKUP
CC&S
DERIVED-RATE NETWORK
SINGLE
THRESHOLD AMPLIFIER
SS
SS
DERIVED-RATE NETWORK
CC&S
CC&S
DERIVED-RATE NETWORK
CC&S
SENSOR INPUTS
GPA
THRESHOLD AMPLIFIER
SS
SS
DERIVED-RATE NETWORK
CC&S
CC&S
DERIVED-RATE NETWORK
GPA
THRESHOLD AMPLIFIER
SS
SS
DERIVED-RATE NETWORK
CC&S

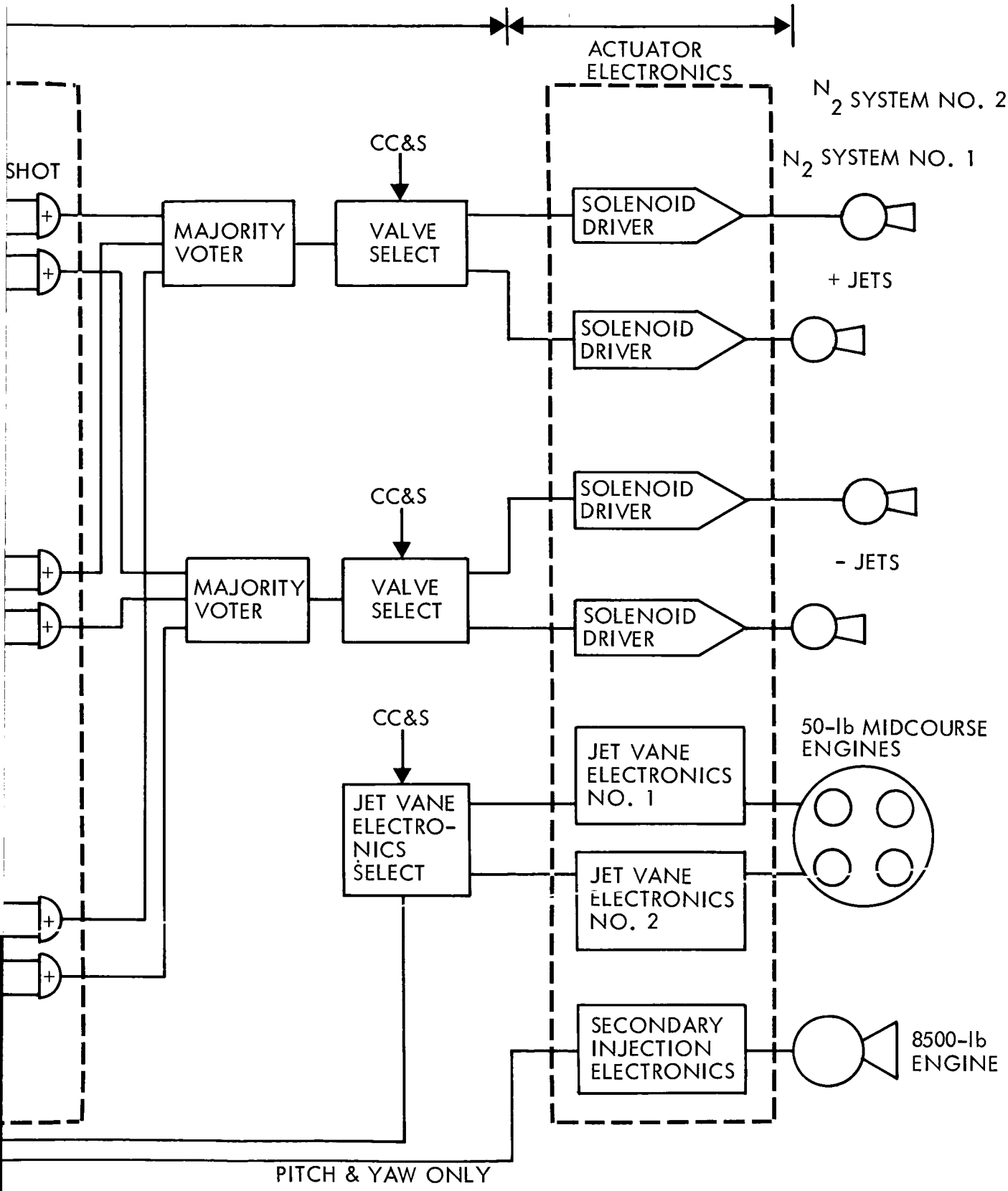

Figure 4.6-45: Voyager Autopilot Redundant Single-Axis

3) The power supplies to furnish power at appropriate voltages and regulated conditions to the electronics listed above.

In the single-axis redundant mechanization (Figure 4.6-45) the summing amplifiers for each axis are connected in a TRISAFE configuration (see Volume 3) followed by a triple-redundant, majority-voting configuration. The redundancy technique applied to the actuator electronics group is discussed in a following paragraph. As shown in the figure, the TRISAFE summing amplifier is time shared between the reaction jet, midcourse, and injection subsystems by CC&S command.

Consider now the operational characteristics of each axis of the autopilot subsystem. A single-thread (i.e., nonredundant version) of the autopilot electronics is shown in Figure 4.6-46 for illustration. When the CC&S commands the cruise mode, the Sun sensor signal is summed with a derived-rate signal and amplified through the pitch and yaw summing amplifier and fed to the pitch and yaw dead-band generators, respectively. The derived-rate signal shuts off the position-error signal (sensor input) before the position error is zero, thus enabling the spacecraft to approach a minimum impulse limit cycle. The delay ensures minimum thrusting time of 20 milliseconds to ensure an efficient gas pulse and to prevent chattering of the valve due to noise on the signal lines. The roll axis is identical, except that the sensor is a Canopus sensor. The output of the triple-redundant pitch (yaw or roll) electronics (6 lines) is connected to two majority-voting circuits (3 lines to each voter as shown in Figure 4.6-45).

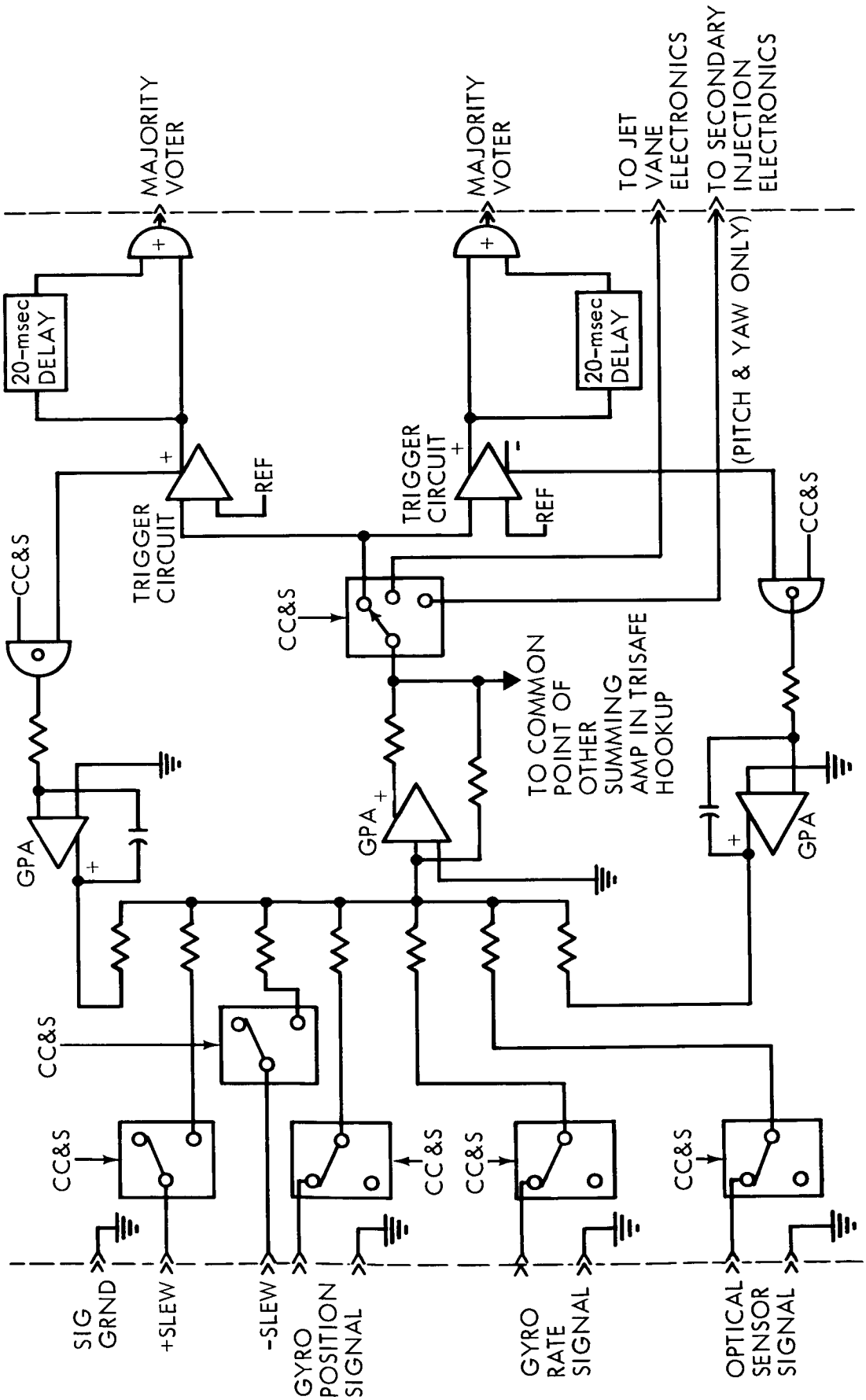

Figure 4.6-46: Autopilot Electronics Block Diagram — Single Thread

The majority-voting circuit and valve-select switch are shown in Figure 4.6-47. The output of this circuit will go the same state as that of any two (or all three) of the inputs. Series-parallel (quad) connection of the diodes is necessary to bring the reliability of the voter and select switch up to requirements. A CC&S command derived from detection circuitry in the propulsion subsystem selects which of the two positive pitch (+P) power switches or two negative pitch (-P) power switches are energized. Combinations of the outputs of the three-axis TRISAFE summing amplifiers are used as position commands to the jet vane electronics (see Figure 4.6-48). Each jet vane torquer is assumed to have a center-tapped winding such that it may be driven by a high-stability differential power amplifier. The actuator has a potentiometer transducer providing position feedback to the signal amplifier.

Figure 4.6-49 illustrates the interface between the jet vane electronics and the jet vane actuators for the four 50-pound thrust midcourse engines. Only one pair (A and C or B and D) of engines will operate at a time; the second pair is to be used as a backup.

The outputs of the pitch and yaw TRISAFE summing amplifier are used as position commands for the secondary-injection jets orbit-insertion engine (see Figure 4.6-50). Potentiometer transducers on each of the two jet controls provide position feedback to the signal amplifiers.

Redundancy--To achieve the apportioned probability of mission success specified for the Voyager autopilot of 0.9996, a composite redundancy philosophy was used. This approach utilizes TRISAFE, triple redundancy

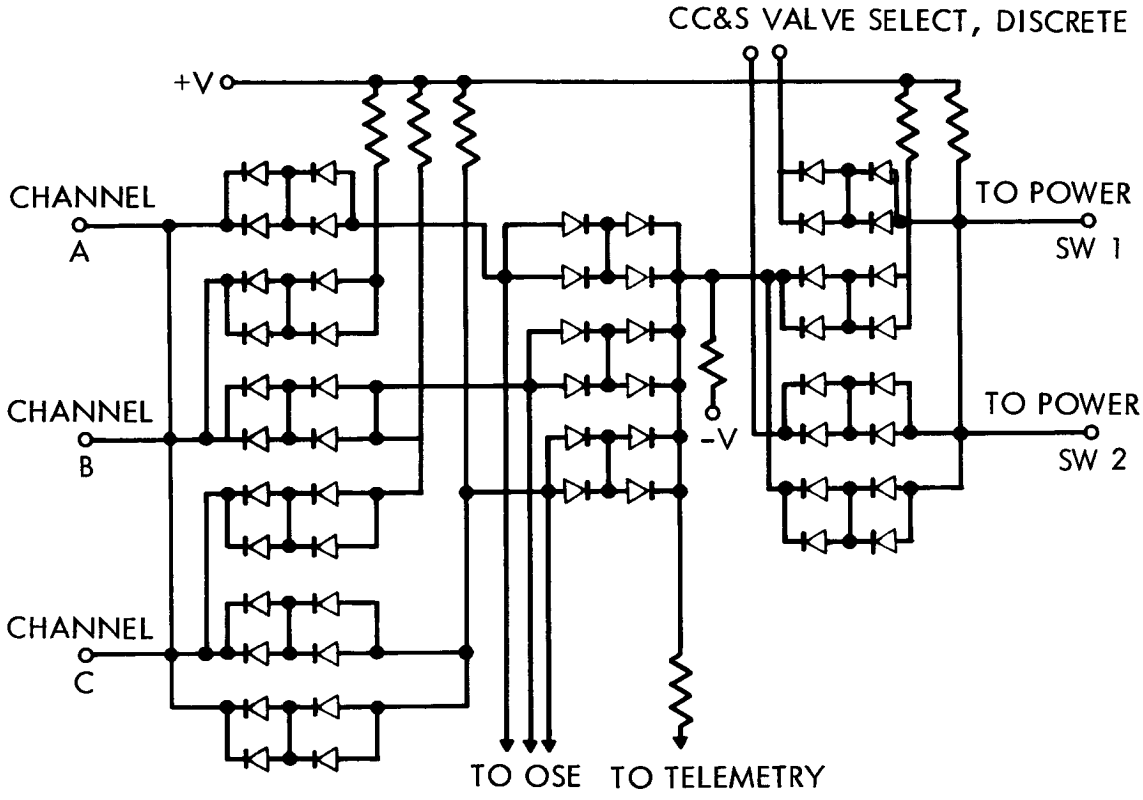

Figure 4.6-47: CC&S Valve Select — Majority Voting Circuit

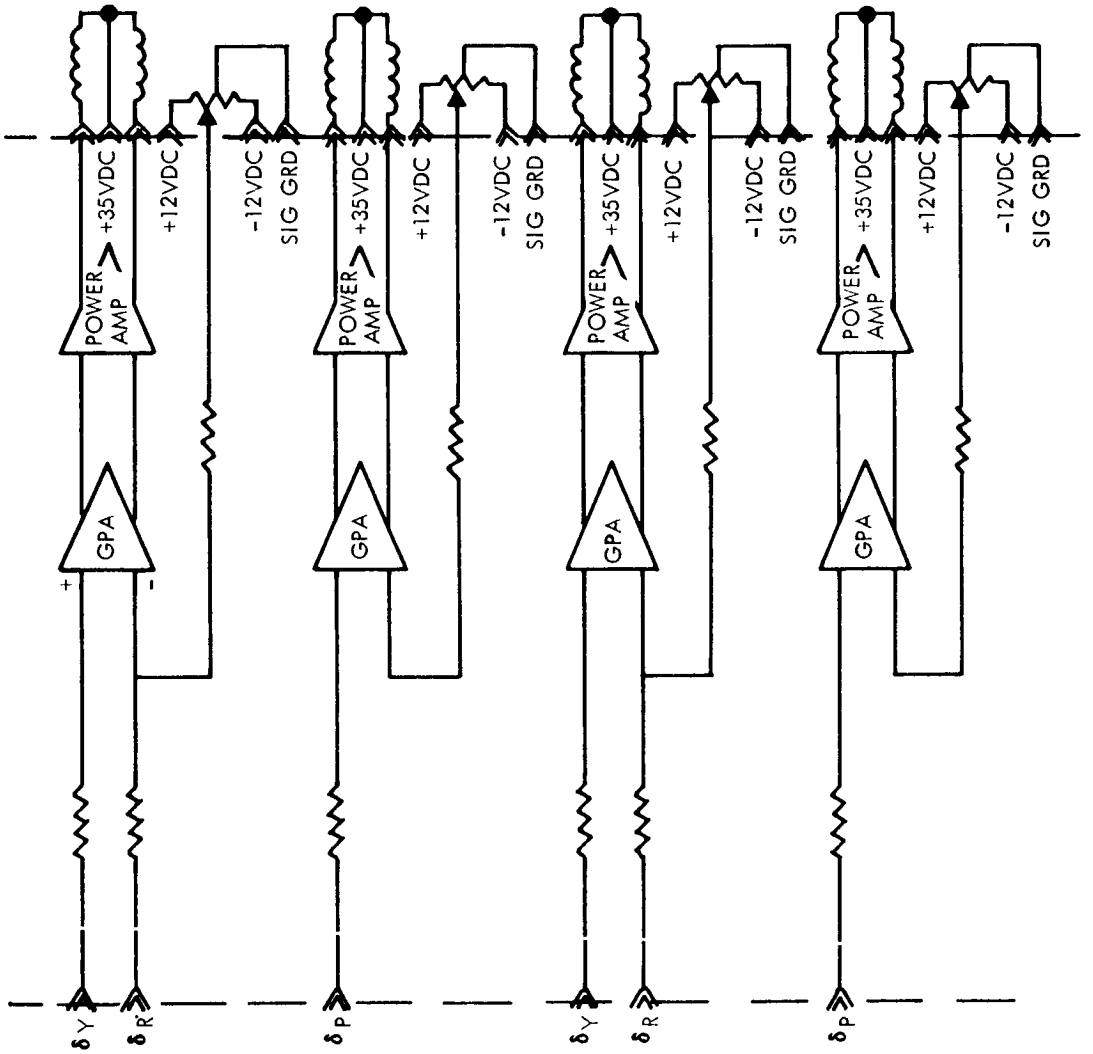

Figure 4.6-48: Jet Vane Actuation Electronics for one Engine

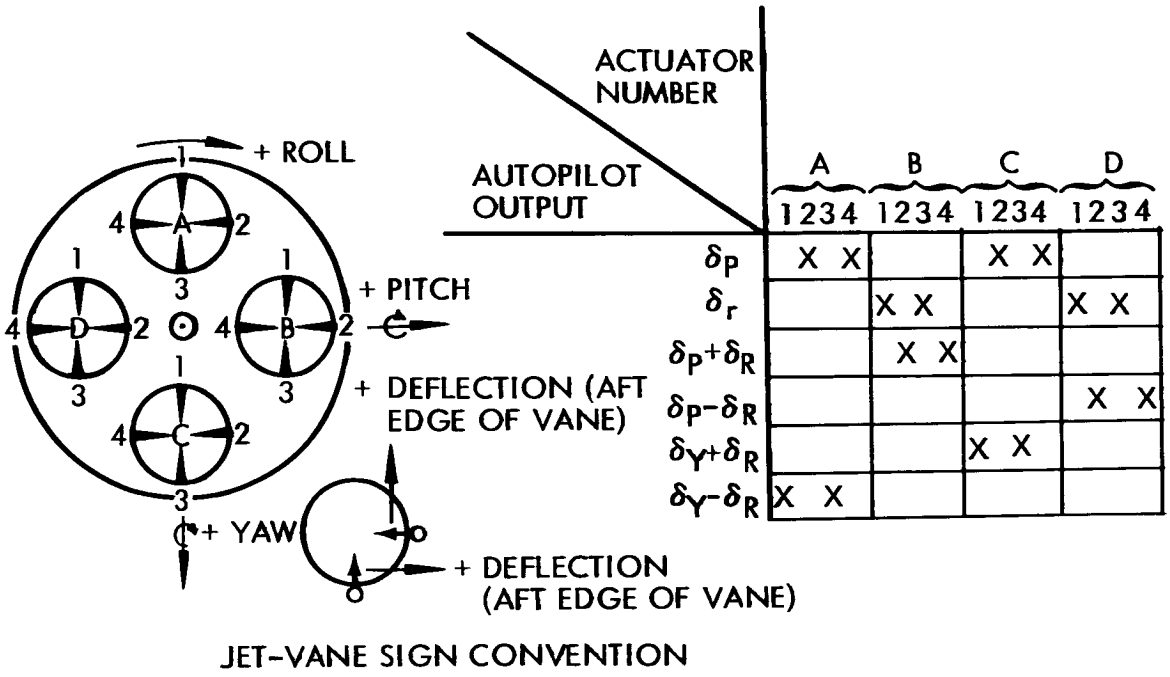

Figure 4.6-49. Midcourse Propulsion System/Autopilot Interface

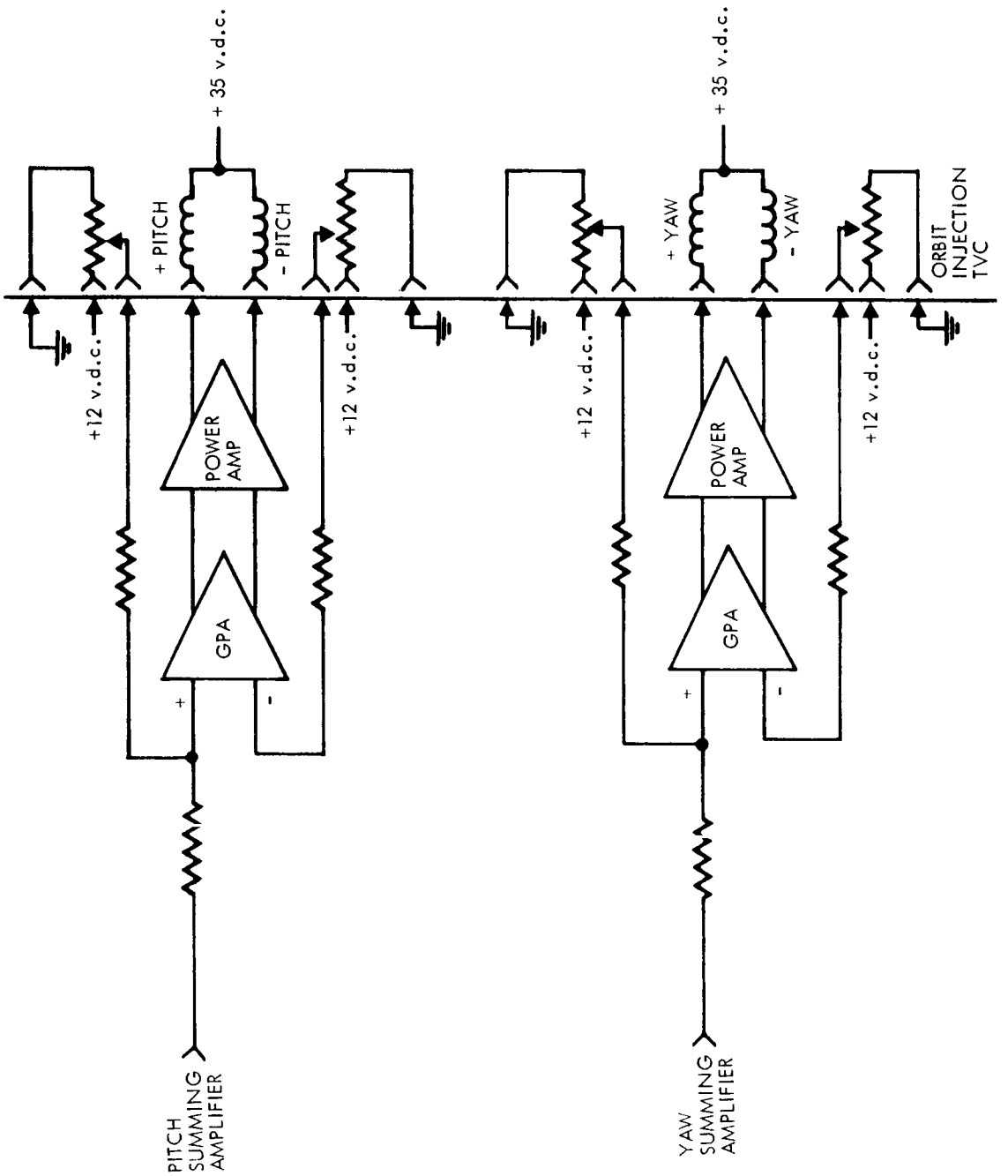

Figure 4.6-50: Secondary Injection Electronics

with majority voting, dual standby redundancy, parallel redundancy, and series-parallel redundancy. The autopilot electronics applies the TRISAFE and majority voting mechanizations for automatically detecting failures.

The preferred configuration of the power switches for the reaction control jets is a single nonredundant power switch for each thruster valve. This configuration is preferred since the switch is 156 times more reliable than the reaction-jet mechanism and also since the reaction jets (including power switches) are to be operated in a parallel-redundant hookup.

Since the jet vanes are also operating in a dual backup mode in a manner similar to the thruster valves, and since the probability of failure of the electronics is approximately 30 times less than that of a jet-vane assembly, a single jet-vane amplifier was used for each vane actuator. Thus, with the vanes operating in a dual backup mode, 16 single-channel jet-vane electronics are required.

In the case of the secondary-injection electronics, there is only one main engine and it has no backup thrust-vector control. Since the electronics is already more reliable than the secondary injection mechanism (0.9999 versus 0.9995) and since, if redundancy were employed triple redundancy would be required to isolate the failure, the single channel of injector electronics was used.

As far as was practical, the autopilot subsystem was considered in single-thread, dual- and triple-redundant arrangements. The range of reliability predictions resulting from these mechanizations was 0.99708 for a single-thread subsystem to 0.999812 for the preferred redundant d.c. analog system. Reliability predictions for a number of different systems are presented in Volume B. It may be noted that most of the system mechanizations met the mission reliability apportionment of 0.9996. Although the preferred system did achieve the highest predicted reliability, reasons other than reliability also supported its selection; namely, it had the least increase in weight, size, and power requirements per unit increase in reliability.

Power Supply--The power supply consists of a transistor inverter followed by a switching-type regulator. The switching regulator is used because of its high efficiency (85 percent). To meet the reliability requirements, the power supply was made redundant. The particular implementation chosen is to connect three individual power supplies in a TRISAFE configuration.

4.6.5.4 Interfaces

Signal Interfaces--Autopilot interfaces with other systems, telemetry, and OSE list points are described in Section 4.6.1.

Power--Power requirements are presented in Table 4.6-15. The assumptions are:

1) The autopilot electronics are on continuously.

Table 4.6-15: Power Breakdown for Preferred System

OPERATION MODE / SUBSYSTEM		AUTOPILOT ELECTRONICS	ACTUATOR ELECTRONICS & LOAD						POWER-SUPPLY DISSIPATION TRISAFE	TOTAL POWER	
			COLD-GAS JETS		JET VANES		SECONDARY INJEC.				
				SOLENOID	VANE ELECT.	ACTUATOR	INJECTION ELECT.	HYDRAULIC CONTROL		ELECTRONIC	LOAD
CRUISE MODE	JETS ON	13.5	4.5	14	0	0	0	0	3	21	14
	JETS OFF	13.5	1	0	0	0	0	0	2	16.5	0
MIDCOURSE-CORRECTION MODE	ACTUATOR OFF	13.5	1	0	4.8	64	0	0	3	21.8	64
	ACTUATOR ON	13.5	1	0	4.8	15	0	0	3	21.8	15
ORBIT-INJECTION MODE	HYDRAUL. ON	13.5	1	0	0	0	1.2	1.2	2.5	18.2	14.2
	OFF	13.5	1	14	0	0	1.2	1.2	2.5	18.2	14.2

NOTE: ALL NUMBERS IN WATTS

2) During the cruise mode:

   a) Two cold gas jets are on at any instant of time;

   b) Backup jets and power switches are off until required for service;

3) During midcourse correction mode:

   a) Two jets (or 8 jet-vane electronics) are on at any instant of time;

   b) Backup jets and electronics are off until required for service.

4) During orbit injection two hydraulic valves are on at any instant of time.

Thermal Interface--The heat resulting from power dissipated within the autopilot module will be conducted to the flange side of the cards through the metal substrate boards. The heat will then be radiated into space by the radiator flanges. The steady-state power dissipation is 13.5 watts; with a radiating surface area of 80 square inches, the surface face heat density is 27 watts per square foot, which can be easily radiated. Transient power dissipation will be absorbed by the thermal mass of the module and radiated from the flanges. The module weight of 11 pounds gives it adequate thermal mass to handle the worst power dissipation transient of 21.8 watts for 60 seconds.

Mechanical Interface--The autopilot module will be mounted to the spacecraft by flanges on the side away from the heat radiators. Alignment of the module is not required.

4.6.5.5 Physical Characteristics

The autopilot subsystem requires six 6-by-8inch plug-in cards. The cards contain two 5.8-by-7-inch two-layer circuit boards. The circuits contained on each card are:

1) Card No. 1--triple-redundant pitch electronics;

2) Card No. 2--triple-redundant roll electronics;

3) Card No. 3--triple-redundant yaw electronics;

4) Card No. 4--triple-redundant power supply;

5) Card No. 5--majority-voting circuit, cold-gas power switches, and secondary-injection electronics;

6) Card No. 6--sixteen jet-vane actuator-drive electronics.

Total volume is 640 cubic inches and the weight is expected to be 11 pounds, of which 5 pounds is wire harnesses, connectors, and module structure.

4.6.5.6 Safety

The autopilot module weighs less than 40 pounds, uses no voltage greater than 35 volts, and therefore requires no special safety considerations.

4.6.5.7 Test Results

A functional simulation of the Voyager autopilot loop has been performed. The operation of the attitude jets, the vehicle dynamics, and dead band control were simulated. The capture of the vehicle after a slewing maneuver is reported on Figure 4.6-51.

The simulation showed successful operation in capturing from a slewing maneuver and in limit cycling after capture. The results of the simulation are described in detail in Autonetics' Report T5-1161.1/3061A, "Voyager Attitude Reference and Autopilot Subsystems Investigation" (Document No. 12 in Section 4.6.1.2).

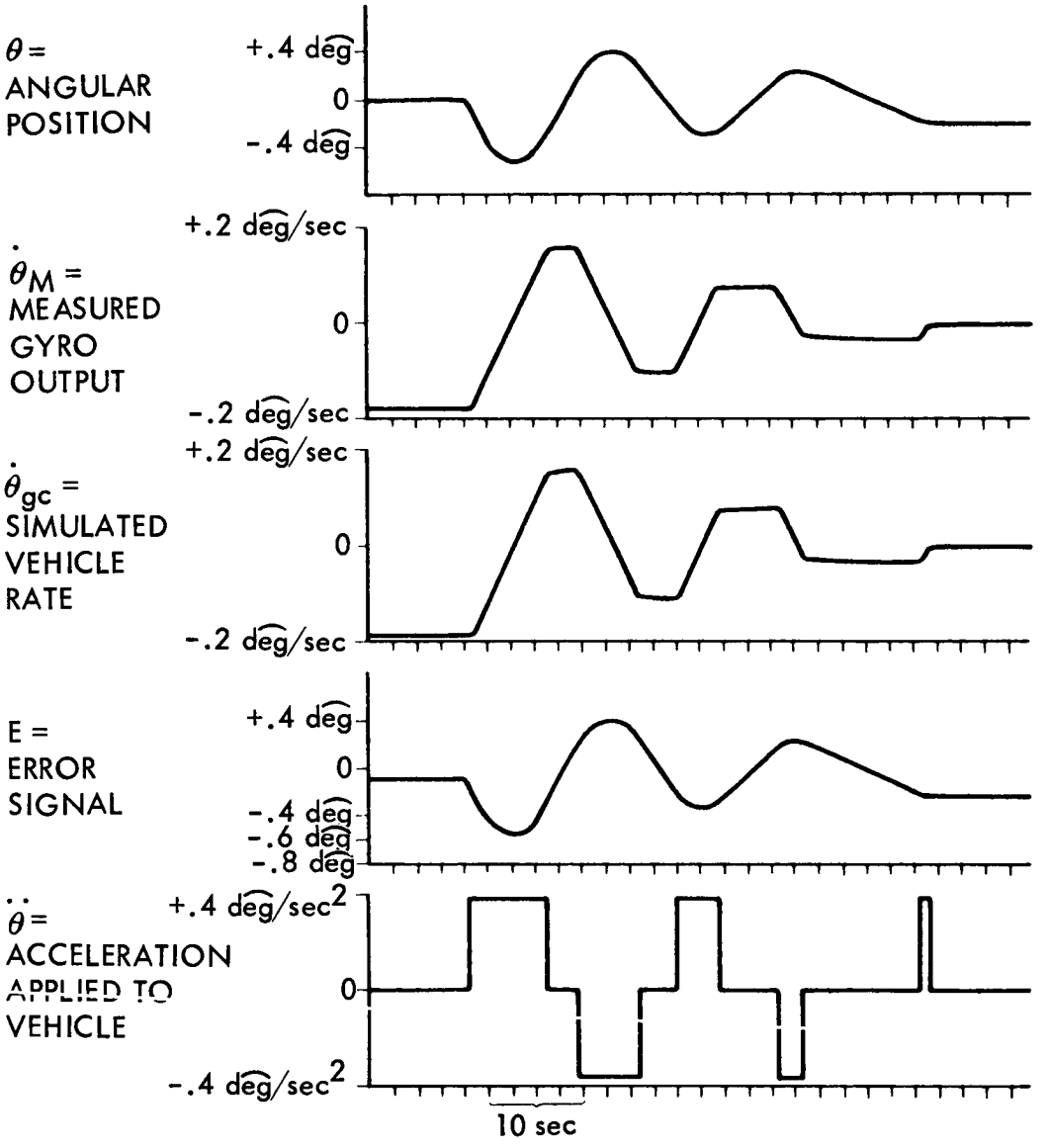

NOTES:

INITIAL SLEWING RATE .18 deg/sec	DEAD ZONE SETTING $\theta_{L.C.}$ = 2 deg
ACCELERATION $\ddot{\theta}$ = .04 deg/sec^2	GAIN RATIO $K\dot{\theta}$ = .5K

Figure 4.6-51: Voyager Autopilot Simulation Results— Capture After Slewing

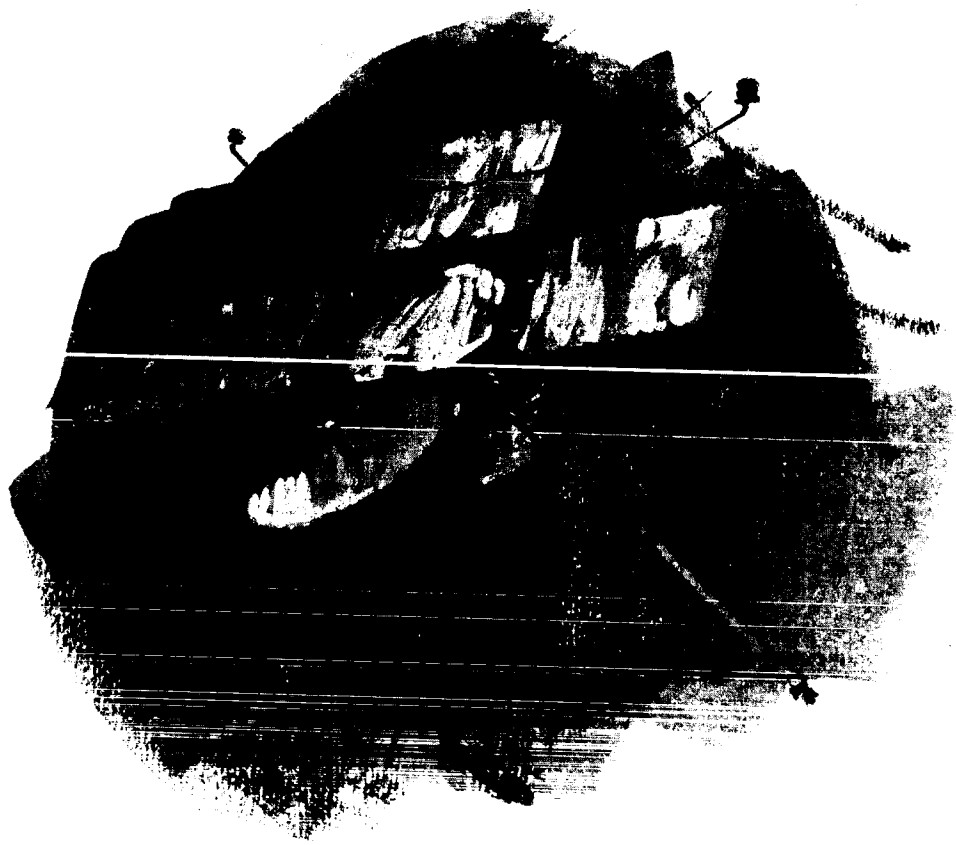

CONTENTS

4.7 REACTION CONTROL SUBSYSTEM

Summary

The reaction control subsystem uses the cold-gas, mass-expulsion concept of reaction control. Control moments are produced by expulsion of nitrogen from 0.25-pound thrusters located on the periphery of the spacecraft body. The thrusters receive commands from the autopilot and are arranged in two completely redundant sets. Selection of one or both of the thruster sets is controlled by the central computer and sequencer (CC&S) by means of solenoid latching valves. Sixty pounds of sterilized nitrogen, of which 15 are reserved for use by the propulsion subsystem as pressurant, are stored at 3500 psia in four tanks. Regulators reduce this pressure to 50 psia for use by the thrusters. A schematic of the subsystem is shown in Figure 4.7-1 and a block diagram in Figure 4.7-2. A summary of key performance parameters is shown in Table 4.7-1.

The Reaction Control Subsystem is designed to perform the functions highlighted on the accompanying mission sequences matrix.

The reaction control subsystem uses proven concepts and components throughout. Nitrogen has seen extensive use in space as a control-system propellant and is clean, stable, and easy to handle. Tanks in the subsystem are made of Ti-6Al-4V annealed titanium with a hazard factor of 2.2 (ultimate) for safety. All connections in the stainless-steel propellant lines are brazed for minimum leakage. Propellant loading is based on a safety factor of two applied to computed impulse requirements. Overall subsystem reliability is 0.9996.

Table 4.7-1: REACTION CONTROL SUBSYSTEM PERFORMANCE PARAMETERS

		Performance	
Subsystem Weight		212 pounds	
Nitrogen Weight		60 pounds*	
Subsystem Reliability		0.9996	
Propellant Storage Pressure		3500 psia @ 70°F	
Thruster System Pressure		50 psia	
Thrust Level		0.25 pounds (all thrusters)	
Number of Propellant Tanks		4	
Total Impulse		3040 pound-seconds	
Specific Impulse		68 seconds	
Moment Arms		53 inches (all axes)	
Angular Accelerations		Transit	Orbit
	Pitch	0.012 $^{o}/s^{2}$	0.044 $^{o}/s^{2}$
	Yaw	0.009 $^{o}/s^{2}$	0.020 $^{o}/s^{2}$
	Roll	0.020 $^{o}/s^{2}$	0.031 $^{o}/s^{2}$

*This includes 15 pounds for propulsion subsystem pressurization requirements.

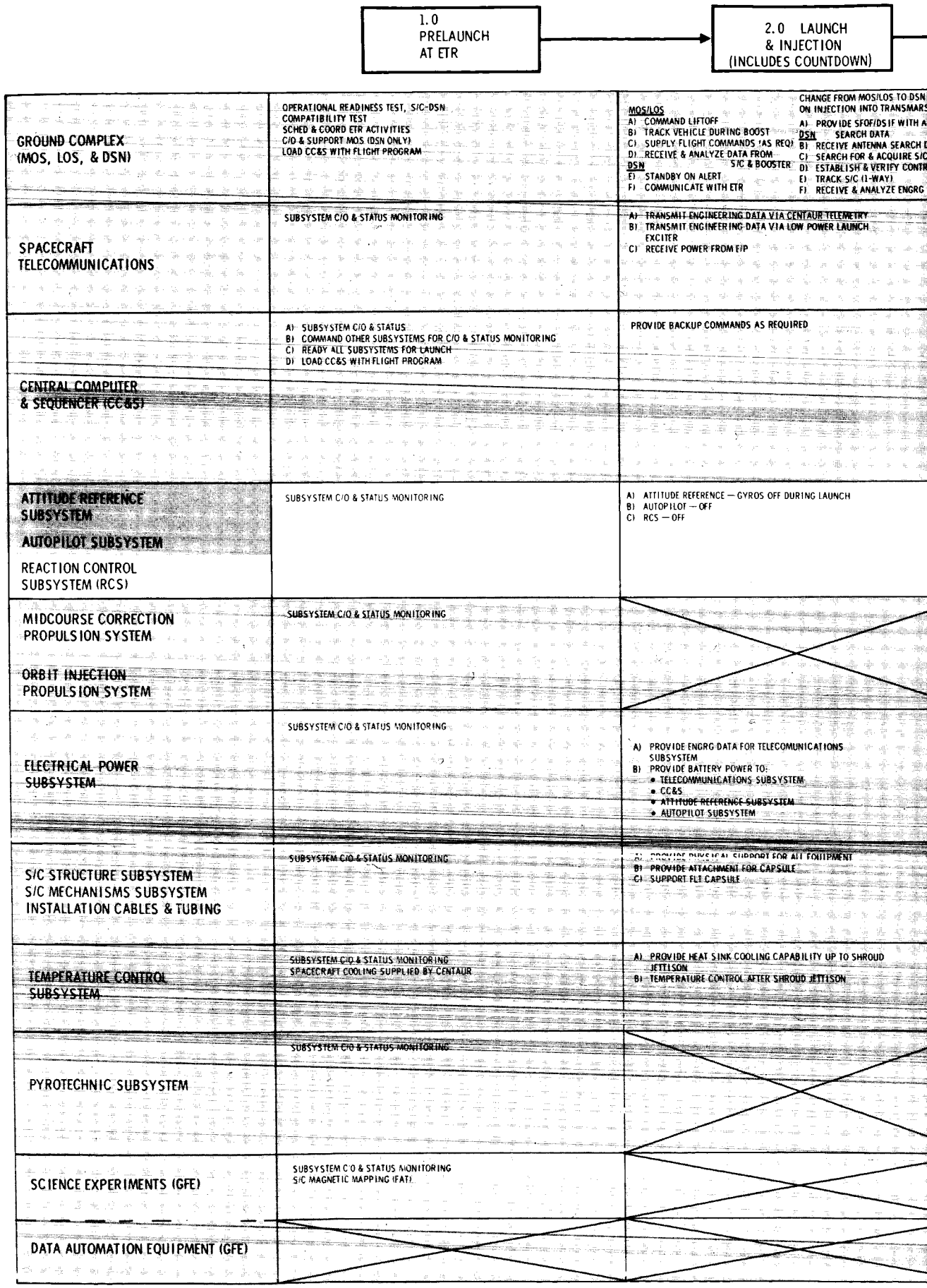
1.0 PRELAUNCH AT ETR
2.0 LAUNCH & INJECTION (INCLUDES COUNTDOWN)
GROUND COMPLEX (MOS, LOS, & DSN)
OPERATIONAL READINESS TEST, S/C-DSN COMPATIBILITY TEST
SCHED & COORD ETR ACTIVITIES
C/O & SUPPORT MOS (DSN ONLY)
LOAD CC&S WITH FLIGHT PROGRAM
MOS/LOS
A) COMMAND LIFTOFF
B) TRACK VEHICLE DURING BOOST
C) SUPPLY FLIGHT COMMANDS (AS REQ)
D) RECEIVE & ANALYZE DATA FROM S/C & BOOSTER
DSN
E) STANDBY ON ALERT
F) COMMUNICATE WITH ETR
CHANGE FROM MOS/LOS TO DSN ON INJECTION INTO TRANSMARS
A) PROVIDE SFOF/DS IF WITH A
DSN SEARCH DATA
B) RECEIVE ANTENNA SEARCH D
C) SEARCH FOR & ACQUIRE S/C
D) ESTABLISH & VERIFY CONTR
E) TRACK S/C (1-WAY)
F) RECEIVE & ANALYZE ENGRG
SPACECRAFT TELECOMMUNICATIONS
SUBSYSTEM C/O & STATUS MONITORING
A) TRANSMIT ENGINEERING DATA VIA CENTAUR TELEMETRY
B) TRANSMIT ENGINEERING DATA VIA LOW POWER LAUNCH EXCITER
C) RECEIVE POWER FROM E/P
CENTRAL COMPUTER & SEQUENCER (CC&S)
A) SUBSYSTEM C/O & STATUS
B) COMMAND OTHER SUBSYSTEMS FOR C/O & STATUS MONITORING
C) READY ALL SUBSYSTEMS FOR LAUNCH
D) LOAD CC&S WITH FLIGHT PROGRAM
PROVIDE BACKUP COMMANDS AS REQUIRED
ATTITUDE REFERENCE SUBSYSTEM
AUTOPILOT SUBSYSTEM
REACTION CONTROL SUBSYSTEM (RCS)
SUBSYSTEM C/O & STATUS MONITORING
A) ATTITUDE REFERENCE — GYROS OFF DURING LAUNCH
B) AUTOPILOT — OFF
C) RCS — OFF
MIDCOURSE CORRECTION PROPULSION SYSTEM
ORBIT INJECTION PROPULSION SYSTEM
SUBSYSTEM C/O & STATUS MONITORING
ELECTRICAL POWER SUBSYSTEM
SUBSYSTEM C/O & STATUS MONITORING
A) PROVIDE ENGRG DATA FOR TELECOMUNICATIONS SUBSYSTEM
B) PROVIDE BATTERY POWER TO:
• TELECOMMUNICATIONS SUBSYSTEM
• CC&S
• ATTITUDE REFERENCE SUBSYSTEM
• AUTOPILOT SUBSYSTEM
S/C STRUCTURE SUBSYSTEM
S/C MECHANISMS SUBSYSTEM
INSTALLATION CABLES & TUBING
SUBSYSTEM C/O & STATUS MONITORING
B) PROVIDE ATTACHMENT FOR CAPSULE
C) SUPPORT FLT CAPSULE
TEMPERATURE CONTROL SUBSYSTEM
SUBSYSTEM C/O & STATUS MONITORING
SPACECRAFT COOLING SUPPLIED BY CENTAUR
A) PROVIDE HEAT SINK COOLING CAPABILITY UP TO SHROUD JETTISON
B) TEMPERATURE CONTROL AFTER SHROUD JETTISON
PYROTECHNIC SUBSYSTEM
SUBSYSTEM C/O & STATUS MONITORING
SCIENCE EXPERIMENTS (GFE)
SUBSYSTEM C/O & STATUS MONITORING
S/C MAGNETIC MAPPING (FAT)
DATA AUTOMATION EQUIPMENT (GFE)

REPEAT UP TO FO

3.0 ACQUISITION

4.0 INTERPLANETARY CRUISE

CONTROL ORBIT ITENNA ATA DL OF S/C DATA	DSN A) MONITOR BOOSTER SEPARATION B) MONITOR SOLAR PANEL DEPLOYMENT C) MONITOR ANTENNA DEPLOYMENT D) PROVIDE COMMANDS TO BACK UP CC&S AS REQUIRED E) TRACK S/C F) REC DATA G) MONITOR SCIENCE DEPLOYMENT DSN H) MONITOR & VERIFY ACQUISITION OF SUN I) MONITOR & VERIFY ACQUISITION OF CANOPUS J) COMMAND REACQUISITION OF CANOPUS (AS REQD) K) MONITOR S/C TRAJECTORY L) UPDATE CC&S TRAJECTORY PARAMETERS FOR PITCH, YAW, & ROLL M) COMPUTE CC&S PITCH, YAW & ROLL POLARITY	DSN A) TRACK S/C B) RECEIVE & DISPLAY SCIENCE & ENGINEERING DATA C) MONITOR S/C & CAPSULE STATUS D) PROCESS DATA ON EARTH TO OBTAIN GUIDANCE COMMANDS (STORED COMMANDS & START TIMES)	A) PRO B) PRO C) PRO D) PRO E) REC • D • T • R F) TRA
	A) TRANSMIT ENGINEERING DATA B) RECEIVE POWER FROM E/P C) RECEIVE VIA LOW-POWER LAUNCH EXCITER DETECT & SEND TO CC&S COMMAND SIGNALS FROM EARTH D) TRANSMIT CELESTIAL REFERENCE ACQUISITION TO DSN E) TRANSMIT VERIFICATION OF DEPLOYMENT OF SOLAR PANELS, ANTENNAS, ETC TO EARTH F) TWO-WAY TRACKING	A) TRANSMIT ENGINEERING & SCIENCE DATA VIA DATA MODE NO. 2 (OPTIONAL MODE NO. 3) B) TRANSMIT CAPSULE ENGINEERING DATA C) TRANSMIT CONE-ANGLE SETTINGS (CANOPUS TO EARTH) D) EXERCISE & CALIBRATE HIGH-GAIN ANTENNA T + 40 DAYS E) SWITCH FROM LOW-GAIN TO HIGH-GAIN ANTENNA T + 80 DAYS F) PROVIDE RANGING SIGNAL TO A MAX. RANGE OF 8.0×10^9 KM (NOMINAL) G) SWITCH TRANSMISSION FROM LAUNCH EXCITER TO TWT POWER AMPLIFIER AND DATA MODE NO. 2	A) REC B) REC C) REC D) REC E) SW F) REL G) STO TRA TO
	A) COMMAND SIGNALS TO PYROTECHNICS & MECH TO DEPLOY • SOLAR PANELS • HIGH-GAIN ANTENNA • VHF ANTENNA • LOW-GAIN ANTENNA • SCIENCE BOOM B) SWITCH ON GYROS & SELECT MODES C) ENABLE SUN-SENSOR ROLL AND PITCH CONTROL D) RECEIVE SUN PRESENCE SIGNAL E) TURN ON CANOPUS TRACKER F) SWITCH ROLL CONTROL TO CANOPUS SENSOR G) ACTIVATE MAGNETOMETER (CALIBRATION ROLL) H) RECEIVE CANOPUS PRESENCE OUTPUT SIGNAL I) TRANSMIT VERIFICATION TO TELECOMMUNICATION SUBSYSTEM (CANOPUS & SUN PRESENCE) J) PERFORM COMMAND FUNCTIONS FOR CANOPUS OVERRIDE AS REQUIRED K) BACKUP COMMANDS AS REQUIRED	A) COMMAND TELECOMMUNICATION TO DATA MODE NO. 2 B) COMMAND CRUISE SCIENCE ON (WARMUP) — SCIENCE INSTRUMENTS C) COMMAND DATA RECORDERS ON D) COMMAND TWTA ON E) SWITCH CANOPUS ANGLE AS REQUIRED F) INITIATE CRUISE SCIENCE DATA ACQUISITION G) COMMAND TELECOMMUNICATION CHANGE FROM OMNI TO HIGH-GAIN ANTENNA H) UPDATE HIGH-GAIN ANTENNA POSITION (AS REQUIRED) I) COMMAND TELECOMMUNICATIONS — CHANGE DATA TRANSMISSION RATES J) COMMAND RECALIBRATION OF SCIENCE ELEMENTS AS REQUIRED K) BACKUP COMMANDS AS REQUIRED	A) CO B) RE C) SW D) CO E) RE F) SW G) AR H) PR I) RE J) DI K) CO L) CO M) CO N) BA
	A) RECEIVE CC&S COMMAND SWITCH ON GYROS, RCS, & AUTOPILOT B) DAMP ROTATION C) YAW & PITCH SPACECRAFT TO ACQUIRE SUN D) RELAY SUN ACQUISITION SIGNAL TO CC&S E) TURN ON CANOPUS SENSOR, ROLL 360° TO CALIBRATE MAGNETOMETER F) ROLL TO ACQUIRE CANOPUS & PROVIDE STAR MAP G) RELAY ACQUISITION SIGNAL (CANOPUS) TO CC&S H) PERFORM CANOPUS OVERRIDE ROLL MANEUVER AS REQUIRED	A) UPDATE CANOPUS CONE ANGLE ON COMMAND B) SWITCH AUTOPILOT TO CRUISE MODE C) MAINTAIN S/C ATTITUDE TO CELESTIAL REFERENCES DURING CRUISE	A) SW B) RO C) YA D) AU TO E) TU F) PR TO G) TU
			MIDCO A) AR B) AR C) FI D) SH E) IS F) IS
	A) PROVIDE POWER TO PYROTECHNIC SUBSYSTEMS FOR SQUIB FIRINGS B) PROVIDE POWER TO MECHANISMS C) ACTIVATE SOLAR POWER SYSTEM AFTER SUN ACQUISITION (AUTOMATIC) D) TRANSMIT "VOLTAGE SATISFACTORY" SIGNAL TO CC&S E) PROVIDE POWER TO: • TELEMETRY • CC&S • TEMPERATURE CONTROL • AUTOPILOT	A) PROVIDE CONDITIONED SOLAR ELECTRICAL POWER TO: • TELEMETRY • CAPSULE • CC&S • ATTITUDE REF • AUTOPILOT • TEMPERATURE CONTROL • SCIENCE B) CHARGE BATTERIES	A) P
	A) PROVIDE PHYSICAL SUPPORT FOR ALL EQUIPMENT B) DRIVE SOLAR PANELS TO LIMIT STOPS C) PROVIDE OFF & LOCK SIGNALS TO TELEMETRY D) DRIVE HIGH-GAIN ANTENNA TO OPERATING POSITION & LOCK E) DRIVE VHF & OMNI ANTENNAS TO OPERATING POSITION & LOCK F) DRIVE MAGNETOMETER BOOM TO OPERATING POSITION & LOCK G) SUPPORT FLT CAPSULE	A) SUPPORT S/C ASSEMBLIES B) SUPPORT S/C COMPONENTS C) MAINTAIN ADEQUATE ALIGNMENT BETWEEN COMPONENTS D) PROVIDE ACCEPTABLE STATIC & DYNAMIC LOAD ENVIRONMENTS E) SUPPORT FLIGHT CAPSULE	A) S B) S C) M D) P E) S
	PROVIDE TEMPERATURE CONTROL	PROVIDE TEMPERATURE CONTROL	PRO
	RECEIVE SQUIB FIRING SIGNALS FOR DEPLOYMENT OF: • SOLAR PANEL • MAGNETOMETER BOOM • LOW-GAIN ANTENNA • HIGH-GAIN ANTENNA • VHF ANTENNA		A) R B) P C)
	A) CALIBRATE MAGNETOMETER DURING S/C ROLL B) CALIBRATE OTHER SCIENCE INSTR AS REQUIRED	A) RECEIVE CRUISE SCIENCE "ON" COMMAND B) ACQUIRE CRUISE SCIENCE DATA C) TRANSFER CONDITIONED DATA TO DAE D) RECEIVE POWER FROM E/P E) RECALIBRATE SCIENCE EXPERIMENTS AS REQUIRED	A) R B) T
		A) RECEIVE DAE "ON" COMMAND B) PROCESS & TRANSFER DATA TO TM	

R TIMES

7.0 FLIGHT CAPS
TRAJECTORY
DEFLECTION

5.0 INTERPLANETARY TRAJECTORY CORRECTION

6.0 S/C CAPSULE SEPARATION

VIDE ROLL TURN MAGNITUDE & DIRECTION VIDE YAW TURN MAGNITUDE & DIRECTION VIDE MIDCOURSE MOTOR BURN DURATION AND ΔV VIDE INITIATE MANEUVER SEQUENCE COMMAND EIVE VERIFICATION OF CORRECTION MANEUVER EGREES OF YAW & ROLL HRUST DURATION EACQUISITION OF CELESTIAL REFERENCES CK SPACECRAFT	A) INITIATE PRESEPARATION SEQUENCE B) RECEIVE CAPSULE STATUS DATA C) COMMAND SEPARATION D) VERIFY CAPSULE PROGRAM E) VERIFY SEPARATION F) TRACK CAPSULE & SPACECRAFT	A) TRANSMIT ORBIT INJEC • ROLL MAGNITUDE & I • YAW MAGNITUDE & D • MOTOR BURN START B) TRACK FLIGHT SPACEC C) RECEIVE, REDUCE & DI D) PROVIDE COMMANDS T
EIVE ROLL & YAW TURN COMMAND & RELAY TO CC&S EIVE ANTENNA POSITIONING DATA & RELAY TO CC&S EIVE MOTOR BURN DURATION AND & ΔV RELAY TO CC&S EIVE INITIATE MANEUVER COMMAND & RELAY TO CC&S ITCH TO DATA MODE NO. 1 (FOR LATE MIDCOURSE MANEUVERS) AY VERIFICATION OF CORRECTION MANEUVER TO DSN RE AND/OR TRANSMIT ENGINEERING DATA TO DSN (MODE 3) NSMIT ENGINEERING (SPACECRAFT & CAPSULE) + CRUISE SCIENCE DSN (MODE 2)	A) RECEIVE PRESEPARATION SEQUENCE COMMANDS & RELAY TO CC&S B) SWITCH TO DATA MODE NO. 2 C) TRANSMIT CAPSULE ENGRG DATA TO DSN D) RECEIVE SEPARATION COMMAND FROM DSN & ROUTE TO CC&S E) STORE AND/OR TRANSMIT ENGINEERING DATA TO DSN (MODE 3) TRANSMIT ENGINEERING (SPACECRAFT & CAPSULE) + CRUISE SCIENCE TO DSN (MODE 2)	A) RECEIVE ROLL & YAW T TO CC&S B) RECEIVE ANTENNA POS C) RECEIVE MOTOR-BURN D) RECEIVE CAPSULE DAT E) TRANSMIT FLIGHT SPA SCIENCE DATA TO GRO
MMAND TELECOMMUNICATION TO DATA MODE NO. 1 E TRAJECTORY CORRECTION PARAMETERS CH GYROS TO RATE CONTROL MAND ANGULAR MANEUVER EIVE GYRO SIGNALS & SUM FOR ANGULAR MANEUVERS TCH ATTITUDE REFERENCE TO AUTOPILOT SUBSYSTEM PROPULSION SYSTEM VIDE COMMAND TO INITIATE ATTITUDE MANEUVER & ΔV MANEUVER EIVE ACCELEROMETER SIGNALS & INTEGRATE FOR ΔV MANEUVER ARM PROPULSION SYSTEM MMAND REVERSE ANGULAR MANEUVER MAND REACQUIRE CELESTIAL REFERENCES MAND AUTOPILOT SELECTION CONTROL UP COMMANDS AS REQUIRED	A) LOAD CAPSULE WITH 5 OR MORE COMMANDS B) COMMAND CAPSULE SEQUENCING C) COMMAND TELECOMM SWITCH TO DATA MODE NO. 1 D) COMMAND GYROS ACTIVATE (CAPSULE) E) COMMAND GYROS ESTABLISH POLARITY (CAPSULE) F) COMMAND GYROS TO ATTITUDE CONTROL MODE (CAPSULE) G) COMMAND DATA TAPE RECORDER OFF H) COMMAND CAPSULE ACTIVATE ENTRY SCIENCE I) COMMAND CAPSULE ACTIVATE TELECOMM & VERIFY RADIO LINK (VHF) J) SELECT T/M MODE FOR TRANSMISSION OF CAPSULE DATA K) COMMAND: BIOBARRIER SEPARATION S/C ORIENT TO SEPARATION ATTITUDE ELECTRICAL CONNECTION SEPARATION VERIFY SEPARATION L) COMMAND REORIENT S/C & REACQUIRE CELESTIAL REFERENCES M) BACKUP COMMANDS AS REQUIRED N) RECEIVE S/C ORIENTATION PARAMETERS	A) COMMAND SWITCH TO B) COMMAND CANOPUS C) COMMAND ANTENNA S D) RECEIVE ORBIT INJECT E) PROVIDE SIGNAL TO F (CRUISE SCIENCE T/M F) SWITCH ON DATA REC RECEIVE CAPSULE DAT G) BACKUP COMMANDS
ICH TO GYRO CONTROL S/C AND VERIFY S/C AND VERIFY PILOT — PROVIDE COMMAND C DURING MOTOR BURN ON ACCELEROMETERS IDE ACCELERATION DATA C&S OFF ACCELEROMETER H) YAW BACK TO ORIGINAL ATTITUDE & VERIFY I) REACQUIRE SUN (FINE SUN SENSOR) & VERIFY J) ROLL TO ORIGINAL ATTITUDE K) LOCK ON CANOPUS & VERIFY L) SWITCH AUTOPILOT FROM GYRO CONTROL TO CELESTIAL REF CONTROL	A) SWITCH TO GYRO CONTROL B) PERFORM ROLL TURN & VERIFY C) PERFORM YAW TURN & VERIFY D) MAINTAIN ATTITUDE DURING SEPARATION E) PERFORM YAW TURN (INVERSE TO C) & VERIFY F) PERFORM ROLL TURN (INVERSE TO B) & VERIFY G) REACQUIRE CELESTIAL REFERENCES H) RETURN TO CELESTIAL REFERENCE ATTITUDE CONTROL MODE	A) UPDATE CANOPUS CON B) SWITCH AUTOPILOT T C) MAINTAIN S/C ATTITU
E PROPULSION SYSTEM RESSURIZATION SYSTEM (FIRE SQUIB VALVE) ROPELLANT FEED SUBSYSTEM (FIRE SQUIB VALVE) PROGRAMMED ENGINES (OPERATE SOLENOID VALVE) DOWN ENGINE TE PROPELLANT FEED SUBSYSTEM TE PRESSURIZATION SUBSYSTEM		
VIDE CONDITIONED SOLAR OR BATTERY POWER TO: ELEMETRY C&S UTOPILOT ATTITUDE REFERENCE REACTION CONTROL PROPULSION TEMPERATURE CONTROL YROTECHNIC APSULE	A) PROVIDE CONDITIONED SOLAR OR BATTERY POWER TO: • T/M • CC&S • AUTOPILOT • ATTITUDE REF • REACTION CONTROL • TEMPERATURE CONTROL • PYROTECHNICS • CAPSULE	A) PROVIDE CONDITION • T/M • CC&S • AUTOPILOT • ATTITUDE REF • REACTION CONTRO • TEMPERATURE CON B) CHARGE BATTERIES
PORT S/C ASSEMBLIES PORT S/C COMPONENTS AINTAIN ADEQUATE ALIGNMENT BETWEEN COMPONENTS VIDE ACCEPTABLE STATIC & DYNAMIC LOAD ENVIRONMENTS PORT FLIGHT CAPSULE	A) SUPPORT S/C ASSEMBLIES B) SUPPORT S/C COMPONENTS C) MAINTAIN ADEQUATE ALIGNMENT BETWEEN COMPONENTS D) PROVIDE ACCEPTABLE STATIC & DYNAMIC LOAD ENVIRONMENTS E) SUPPORT FLIGHT CAPSULE	A) SUPPORT S/C ASSEMI B) SUPPORT S/C COMPO C) MAINTAIN ADEQUATE D) PROVIDE ACCEPTABLE E) DRIVE SCAN PLATFOR
E TEMPERATURE CONTROL	PROVIDE TEMPERATURE CONTROL	PROVIDE TEMPERATURE C
OVE PROPULSION SYSTEM INHIBIT VIDE IGNITION IBIT PROPULSION SYSTEM	A) RECEIVE SIGNAL TO REMOVE CAPSULE SEPARATION INHIBIT B) RECEIVE SIGNAL TO FIRE CAPSULE UMBILICAL SEPARATION C) RECEIVE SIGNAL TO FIRE BIOBARRIER REMOVAL D) RECEIVE SIGNAL TO FIRE CAPSULE SEPARATION E) RECEIVE SIGNAL FOR SEPARATION INHIBIT	RECEIVE SQUIB FIRING OF SCAN PLATFORM
EIVE CC&S COMMAND "CRUISE SCIENCE OFF" N OFF CRUISE SCIENCE	A) RECEIVE CC&S COMMAND "CRUISE SCIENCE OFF" B) TURN OFF CRUISE SCIENCE	A) RECEIVE CRUISE SCI B) ACQUIRE CRUISE SC C) TRANSFER CONDITIO D) RECEIVE POWER FRO E) RECALIBRATE SCIENC
		A) RECEIVE DAE "ON" CO B) PROCESS & TRANSFE

ULE	9.0 FLIGHT CAPSULE CRUISE	10.0 FLIGHT CAPSULE ENTRY	11.0 FLIGHT CAPSULE DESCENT & LANDING	12.0 LANDED OPERATIONS
8.0 FLIGHT S/C CRUISE		13.0 FLIGHT S/C ORBIT INSERTION		14.0 ORB OPERATIO

TION PARAMETERS DIRECTION IRECTION TIME RAFT SPLAY SCIENCE & ENGINEERING DATA O BACK UP CC&S AS REQUIRED		A) RECEIVE, DECODE, & DISPLAY ENGINEERING DATA B) RELAY UPDATED ORBIT INJECTION PARAMETERS C) PROVIDE COMMAND TO INITIATE INSERTION MANEUVER D) PROVIDE BACKUP COMMANDS TO CC&S AS REQUIRED E) TRACK S/C F) VERIFY ORBIT INSERTION	A) RECEIVE, DECODE, & DISPLAY SCIENCE B) RECEIVE AND ANALYZE ENGINEERING DA C) TRACK S/C D) RECEIVE & DISPLAY CAPSULE DATA E) PROVIDE DATA FOR ORBITAL TRIM (IF RE F) RECEIVE VERIFICATION OF ORBITAL TRI G) TERMINATE MISSION
URN MAGNITUDE & DIRECTION COMMAND & RELAY ITIONING DATA & RELAY TO CC&S START TIME, RELAY TO CC&S , CONDITION & RELAY TO GROUND ECRAFT ENGINEERING, CAPSULE ENGRG, & ND VIA MODE 2		A) UPDATE ROLL-TURN MAGNITUDE & DIRECTION COMMAND & RELAY TO CC&S B) UPDATE YAW-TURN MAGNITUDE & DIRECTION COMMAND & RELAY TO CC&S C) UPDATE MOTOR-BURN START TIME & RELAY TO CC&S D) UPDATE INITIATE MANEUVER & RELAY TO CC&S E) SWITCH TO DATA MODE NO. 2 OR 5A AS REQUIRED F) REACQUIRE EARTH AFTER ROLL TURNS & MOTOR BURN G) RELAY VERIFICATION OF MANEUVERS	A) TRANSMIT SCIENCE & ENGINEERING DAT B) RECORD ENGINEERING & SCIENCE DATA C) RECEIVE, STORE & RELAY CAPSULE DATA D) RECEIVE & RELAY DATA FOR ORBIT TRIM
DATA MODE NO. 2 CONE ANGLE SETTING TEP (AS REQUIRED) TION PARAMETERS YRO & MECHANISMS TO DEPLOY SCAN PLATFORM (OFF) & SWITCH TO DATA MODE NO. 1 ORDER-COMMAND TELECOMMUNICATIONS A S REQUIRED		A) UPDATE STORED ROLL, PITCH, & YAW MAGNITUDE & SIGN B) UPDATE STORED VELOCITY MAGNITUDE C) INITIATE MANEUVER SEQUENCE D) COMMAND ORIENTATION OF S/C TO INJECTION ATTITUDE E) COMMAND THRUST FOR ORBIT INSERTION F) COMMAND RETURN TO CRUISE ATTITUDE G) BACKUP COMMANDS AS REQUIRED	A) COMMAND ORBITAL TRIM MANEUVERS B) SWITCH DATA MODES AS NECESSARY C) RECEIVE ANY ORBITAL OPERATION CHA D) COMMAND POSITIONING OF SCIENCE S E) SWITCH ON ORBITAL SCIENCE F) SELECT RECORDED SCIENCE READOUT TO G) BACKUP COMMANDS AS REQUIRED H) STORE DATA FOR ORBIT TRIM (IF REQUI I) TERMINATE MISSION ON COMMAND (IF
E ANGLE ON COMMAND O CRUISE MODE DE TO CELESTIAL REFERENCES DURING CRUISE		A) SWITCH TO GYRO CONTROL B) PROVIDE ROLL TO PROPER ATTITUDE & VERIFY ROLL C) YAW TO PROPER ATTITUDE & VERIFY D) AUTOPILOT – PROVIDE COMMAND TO TVC DURING MOTOR BURN E) TURN ON ACCELEROMETER F) PROVIDE ACCELEROMETER DATA TO CC&S G) TURN OFF ACCELEROMETER H) YAW BACK AFTER MOTOR BURN I) ACQUIRE SUN & VERIFY J) ROLL BACK TO PROGRAMMED ATTITUDE K) ACQUIRE CANOPUS & VERIFY L) SWITCH AUTOPILOT FROM GYRO – CONTROL TO CELESTIAL REFERENCE CONTROL	A) MAINTAIN S/C ATTITUDE TO CELESTIAL B) SWITCH AUTOPILOT TO GYRO CONTROL C) REACQUIRE CELESTIAL REFERENCES FOL D) REORIENT S/C FOR ORBITAL TRIM MANE E) PROVIDE TVC DURING ENGINE FIRING F) REACQUIRE CELESTIAL REFERENCES FOL G) UPDATE CANOPUS CONE ANGLES ON CO
		ORBIT INSERTION ENGINE A) ARM TVC B) ARM IGNITER C) FIRE MOTOR & PROVIDE THRUST & TVC D) TERMINATE THRUST (MOTOR BURNS TO DEPLETION)	MIDCOURSE A) ARM PRESSURIZATION & PROPELLANT B) PROVIDE THRUST (FIRE PROGRAMMED IF REQUIRED C) TERMINATE THRUST ON COMMAND D) ISOLATE PROPELLANT FEED SUBSYSTEM E) ISOLATE PRESSURIZATION SUBSYSTEM
ED SOLAR ELECTRICAL POWER TO: TROL		A) PROVIDE CONDITIONED SOLAR OR BATTERY POWER TO: • TELEMETRY • CC&S • ATTITUDE REFERENCE SUBSYSTEM • AUTOPILOT • TEMPERATURE CONTROL • PULSE TO PYROTECHNICS • PULSE TO PROPULSION	A) PROVIDE CONDITIONED SOLAR OR BAT • TELEMETRY • CC&S • ATTITUDE REFERENCE SUBSYSTEM • AUTOPILOT • TEMPERATURE CONTROL • STRUCTURES & MECHANISMS • SCIENCE
BLIES NENTS ALIGNMENT BETWEEN COMPONENTS STATIC & DYNAMIC LOAD ENVIRONMENTS M TO DEPLOYED POSITION & LOCK		A) SUPPORT S/C ASSEMBLIES B) SUPPORT S/C COMPONENTS C) MAINTAIN ADEQUATE ALIGNMENT BETWEEN COMPONENTS D) PROVIDE ACCEPTABLE STATIC & DYNAMIC LOAD ENVIRONMENTS	A) SUPPORT S/C ASSEMBLIES B) SUPPORT S/C COMPONENTS C) MAINTAIN ADEQUATE ALIGNMENTS BET D) PROVIDE ACCEPTABLE STATIC AND DY ENVIRONMENTS E) POSITION SCAN PLATFORM
ONTROL		PROVIDE TEMPERATURE CONTROL	PROVIDE TEMPERATURE CONTROL
SIGNAL FOR UNLATCHING		A) RECEIVE & EXECUTE COMMAND SIGNAL TO REMOVE INHIBIT FOR PROPULSION ENGINE B) RECEIVE & EXECUTE SIGNAL FOR PROPULSION ENGINE START C) RECEIVE & EXECUTE COMMAND SIGNAL FOR PROPULSION ENGINE STOP D) RECEIVE & EXECUTE SIGNAL FOR PROPULSION INHIBIT	
NCE "ON" COMMAND ENCE DATA ED DATA TO DAE E/P E EXPERIMENTS AS REQUIRED		SCIENCE OFF DURING ORBIT INSERTION	A) TURN ON ORBITAL SCIENCE INSTRUME B) ACQUIRE ORBITAL SCIENCE DATA C) TRANSFER CONDITIONED DATA TO DAE D) RECALIBRATE SCIENCE EXPERIMENTS
MMAND DATA TO TM			A) RECEIVE DAE "ON" COMMAND B) PROCESS & TRANSFER DATA TO TM

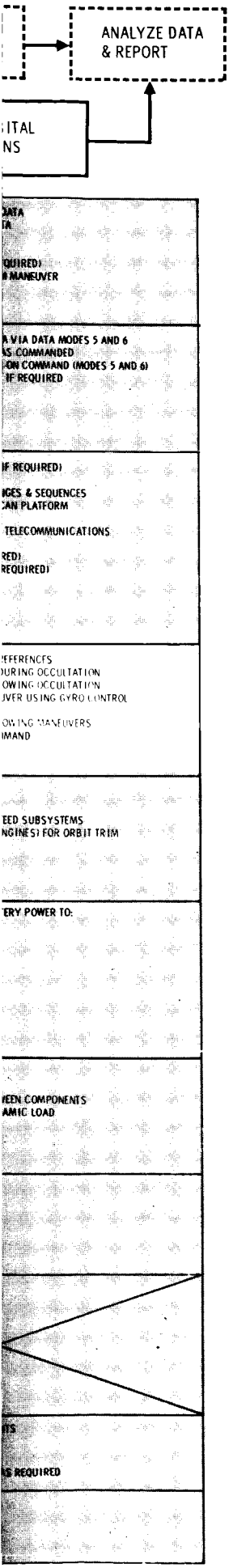

Mission Sequences Matrix

4.7.1 Scope

The reaction control subsystem produces the control moments required for stabilization of unpowered flight. It is the means by which the commands of the autopilot subsystem are translated into spacecraft angular motions for initial vehicle stabilization, acquisition of optical references, limit-cycle operation during cruise, overcoming of disturbance torques, maneuvering for thrusting and capsule separation, roll stabilization during orbit insertion and reacquisitions after occultations. During powered flight the reaction control subsystem is supplanted as the primary control moment source.

The subsystem described here is the preferred configuration that resulted from the study of alternate mechanizations described in D2-82709-2, Section 4.7. The description that follows provides functional as well as hardware and interface information. No new concepts are presented; the reaction control subsystem design is conservative and well-proven.

4.7.2 Applicable Documents

1) JPL Specification MC-4-410A, "Functional Specification, Mariner C. Flight Equipment, Attitude Control Subsystem," 6 December 1963.
2) JPL Technical Report No. 32-663 "Ranger Block III Attitude Control System," 15 November 1964.
3) JPL Engineering Planning Document No. 277 "Mariner Spacecraft Functional Description," 5 May 1965.
4) Boeing Process Specification 5956, "In Place Induction Brazing of Fittings to Tubes," dated 2-1-65.

4.7.3 Functional Description

4.7.3.1 Subsystem Description

The selected concept is a cold-gas nitrogen reaction jet subsystem. The subsystem is activated after solar-panel deployment by the central computer and sequencer selecting one of a set of redundant thrusters through actuation of a solenoid latching valve. Three-axis control is provided by eight 0.25-pound thrusters mounted on the periphery of the spacecraft body. Roll jets are fired in couples to prevent cross-coupling. Pitch and yaw jets are mounted directly on the control axes which are coincident with the principal axes to eliminate cross-coupling. The thrusters receive commands from the autopilot. Fuel consumption during the mission is assessed by monitoring telemetered data from pressure and temperature transducers on the fuel tanks. Thruster valve operation is monitored by a valve switch which detects thruster malfunctions and switches operation to the standby set of thrusters.

As shown in Figure 4.7-2, the nitrogen required for reaction control is combined with the propulsion subsystem pressurant to reduce the number of required tanks.

4.7.3.2 Component Description

Major subsystem components are shown in the schematic diagram of Figure 4.7-2. Component characteristics are summarized in Table 4.7-2 and discussed below.

Table 4.7-2: COMPONENT SUMMARY CHART

COMPONENT	CHARACTERISTICS	DEVELOPMENT
Thruster Assembly	(1) 0.25 lbs thrust (2) 14 watts (3) 50 psia pressure (4) 1.0 scc/hr leakage	Similar units qualified for Ranger and Mariner and will be on Lunar Orbiter
Pressure Regulator	(1) 3500 psia inlet (2) 50 psia outlet (3) 56 psia relief	Similar units will be qualified for Lunar Orbiter
Solenoid Latching Valve	(1) Positive latching (2) 1.0 scc/hr leakage (3) 18 to 30 Vdc	Similar units qualified for OGO
Tank	(1) 15.5 in. O.D. (2) Ti-6Al-4V (3) Safety factor 2.2 (4) 15 lb N_2	Similar units will be qualified for Lunar Orbiter
Fill Valve	3500 psia nominal operating, redundant cap	Similar units will be qualified for Lunar Orbiter
Transducers: Temperature Pressure	-60°F to 160°F 0 to 5,000 psia	Similar units will be qualified for Lunar Orbiter
Quad Check Valve	3500 psia nominal operating	Similar units qualified for Apollo
Filter	(1) 5 microns metal (2) 10 microns non-metal	Similar units will be qualified for Lunar Orbiter
Plumbing	(1) Stainless steel (2) Induction brazed	Similar tubing will be qualified for Lunar Orbiter

Thruster Assembly--Thruster assemblies have been developed or are being developed for use in a cold gas attitude control subsystem for such spacecraft as OSO, OGO, OAO, Ranger, Mariner, Syncom, Surveyor, Lunar Orbiter, Nimbus, and advanced Pioneer. The design embodies a hard-seat valve together with a hermetically sealed, continuous-duty solenoid that requires 14 watts. The nozzle is designed to provide 0.25 pounds of thrust with a chamber pressure of 50 psia. Similar units have been qualified for service at -65°F to 160°F. This thruster will withstand a sterilization temperature of 135°C. Maximum leakage in the de-energized position is 1.0 scc/hr. Four independently operated thruster nozzles and solenoids are incorporated into a common assembly, two roll, and two pitch (or yaw).

Solenoid Latching Valve--A pneumatic shutoff valve incorporates a latching device that will maintain the valving in the last-energized position if electrical power fails. The actuating solenoid and the unlatching solenoid are designed for continuous duty; however, a pulsed voltage input is sufficient to actuate the valve to either the open or closed position. Operating pressure is 3500 psia at 70°F nominally and the units are proof tested to 5000 psia. Environmental temperature range is -65°F to 160°F. Leakage is 1.0 scc/hr.

Pressure Regulator--The pressure regulator is a high-pressure pneumatic device of all-metal construction. Inlet pressure is up to 4000 psia and the regulated outlet pressure is 50 psia. An integral relief valve is set at 6 psia above nominal outlet pressure setting.

Tanks--The four nitrogen storage tanks are 15.50 inches outside diameter and are fabricated of annealed Ti-6Al-4V titantium. The initial gas storage pressure is 3500 psia, nominal, 4,000 psia, maximum. The tanks are designed for an ultimate design pressure of 8800 psia, giving an ultimate factor of safety of 2.2.

Transducers--Temperature and pressure transducers are provided at the tanks to enable telemeter monitoring of these parameters. Propellant quantity and storage environment can thus be detected.

Quad Check Valves--The quad check valves are included in the system such that a leak in either of a pair of tanks will not cause loss of propellent from the other pair.

Fill Valves--Two fill valves are provided to service the nitrogen supply tanks. These valves are manually operated and have an external cap to provide redundant sealing. Both valve and cap are designed for the 4000-psia system pressure.

Filters--Filters are provided downstream of both fill valves. The retention characteristics of the filter element are as follows:

Nominal rating--5 microns;

Absolute rating--10 microns.

Plumbing--All plumbing in the reaction control subsystem is stainless steel. All connections in the plumbing are made with the Aeroquip method of induction brazing to minimize leakage and

maximize cleanliness. Plumbing is sized to meet maximum flow conditions during initial acquisition.

4.7.3.3 Nitrogen Quality

The reaction control subsystem will be charged with filtered dry nitrogen. Particulate matter size will be kept to less than 5 microns for metal particles and 10 microns for nonmetal particles to reduce the possibility of leakage through the hard-seat valves in the regulators or thrusters. To prevent any possibility of the formation of ice in thruster nozzles, dry gas will be used. The dew point will be -95°F to -100°F.

The nitrogen and its entire containment system will be sterilized. A more complete discussion may be found in D2-82709-2, Section 3.4.5.4.

4.7.4 Reliability

The reaction control subsystem features 100 percent redundancy of all components. The propellant storage tanks are in dual, operative, redundancy and isolated by check valves. The remaining portion consists of two, standby-redundant, single-thread arrangements of components.

The failure modes of primary concern are: a jet valve failure to open, a jet valve failure to close, and a leaking valve. Of these, the failed-open valve is the most critical since, if undetected, it can prematurely deplete the propellant supply. A failure mode analysis is shown in Table 4.7-3.

Table 4.7-3: REACTION CONTROL SUBSYSTEM FAILURE MODES

Failure Mode	Subsystem Effect	Spacecraft Effect	Detection and Correction
OPEN JET			
Pitch and Yaw	Opposite jet fires to balance moments resulting in excessive gas flow.	Normal limit-cycle rate exceeded. Vehicle attitude outside deadband.	Primary: Onboard MDS (see text). Secondary: Ground detection (probably satisfactory for early failures only).
Roll	Opposite jets fire; excessive gas flow.	Pitch and yaw coupling (a minor effect). Remains with limit-cycle deadband.	Primary: Onboard MDS. Secondary: Ground detection (probably satisfactory only for early failures).
CLOSED JET			
Pitch and Yaw	Jet does not fire but remains electrically on.	Vehicle attitude outside of deadband limits.	Primary: Onboard MDS. Secondary: Ground detection (will probably require reacquisition).
Roll	Remaining roll jet supplies roll control torque.	Pitch or yaw coupling (minor effect).	Primary: Onboard MDS. Secondary: Ground detection.
LEAKING* JET			
Pitch, Yaw, or Roll	Steady gas flow; small steady disturbance torque; opposite jet pulsing greater than normal; leaking jet pulsing less than normal.	Unsymmetrical limit-cycle operation.	Primary: Ground detection (satisfactory because of low propellant leakage rate).

*Assumes leak is too small to be detected by onboard MDS (valve position indicator)

The primary onboard malfunction detection scheme consists of an electrical switch actuated by the motion of the thrust valve. This will give an indication of the mechanical condition of the valve (open or closed). A disagreement between the switch indication and the electrical input to the valve driver is evidence of one of the following failures: mechanically stuck open or closed valve, a defective solenoid, or a defective driver. The comparison logic causes the standby portion of the subsystem to be activated and the defective section to be isolated.

The calculated mission reliability of the reaction control subsystem is 0.9996. A detailed reliability analysis is contained in Section 6.0.

4.7.5 Interfaces

4.7.5.1 Electrical

From autopilot subsystem: 12 thruster on-off commands (35 volts)

From central computer and sequencer: 4 commands (2 on, 2 off) to solenoid latching valves

To central computer and sequencer: 16 malfunction-detection signals

To Telecommunications: 2 pressure signals; 4 temperature signals.

4.7.5.2 Mechanical

Thruster alignment: $\pm 2^{o}$ to spacecraft axes

4.7.5.3 Thermal

Tanks and lines: +30°F to +110°F

Thrusters: 0° to 165°F

All components: 135°C non-operating (sterilization)

4.7.5.4 Propulsion Subsystem

The reaction control subsystem provides up to 15 pounds of high-pressure nitrogen to the propulsion subsystem for use as propellant tank pressurant.

4.7.5.5 Operational Support Equipment

Propulsion service unit: nitrogen fill and drain;

propulsion system test unit: leak check and valve actuation check

4.7.6 Performance

4.7.6.1 Control Authorities

Angular accelerations and the maneuver rate are selected to minimize reaction-control fuel consumption and yet meet mission requirements. A maneuver rate of 0.2 degrees per second was selected to conserve fuel while ensuring reasonable total times for midcourse, orbit insertion, and capsule separation sequences.

For operational simplicity, one thrust level for all thrusters is selected. The variations in spacecraft moments of inertia thus cause a variation in angular accelerations. The resultant angular accelerations are:

	Transit	Orbit
Pitch	0.012 deg/sec.^{2}	0.044 deg/sec.^{2}
Yaw	0.009 "	0.020 "
Roll	0.020 "	0.031 "

These accelerations represent 0.25-pound thrusters mounted on the spacecraft body with a moment arm of 53 inches.

4.7.6.2 Control Dynamics

Typical cold-gas thruster response characteristics are shown in Figure 4.7-3. The values shown are for an 0.05-pound thruster, but will vary only slightly for the Voyager 0.25-pound units. Also shown on this figure is the duration of the single-shot, which is the minimum electrical on-time of the thruster valve driver. The duration of the single-shot is determined by the maximum time required to achieve full thrust. The purpose of the single-shot is to eliminate valve chatter and to ensure full thrust operation every time the thruster is actuated. No I_{sp} degradation should occur at minimum pulse lengths if full thrust is achieved during each pulse. The exact length of the single-shot is determined after valve characteristics are determined. A conservative 20 milliseconds has been used here and in the autopilot design.

4.7.6.3 Disturbing Torques

The external disturbing torques of interest are caused by gravity gradient, solar pressure, meteorite bombardment, Martian exosphere and electromagnetic emission. Gravity-gradient torques about the

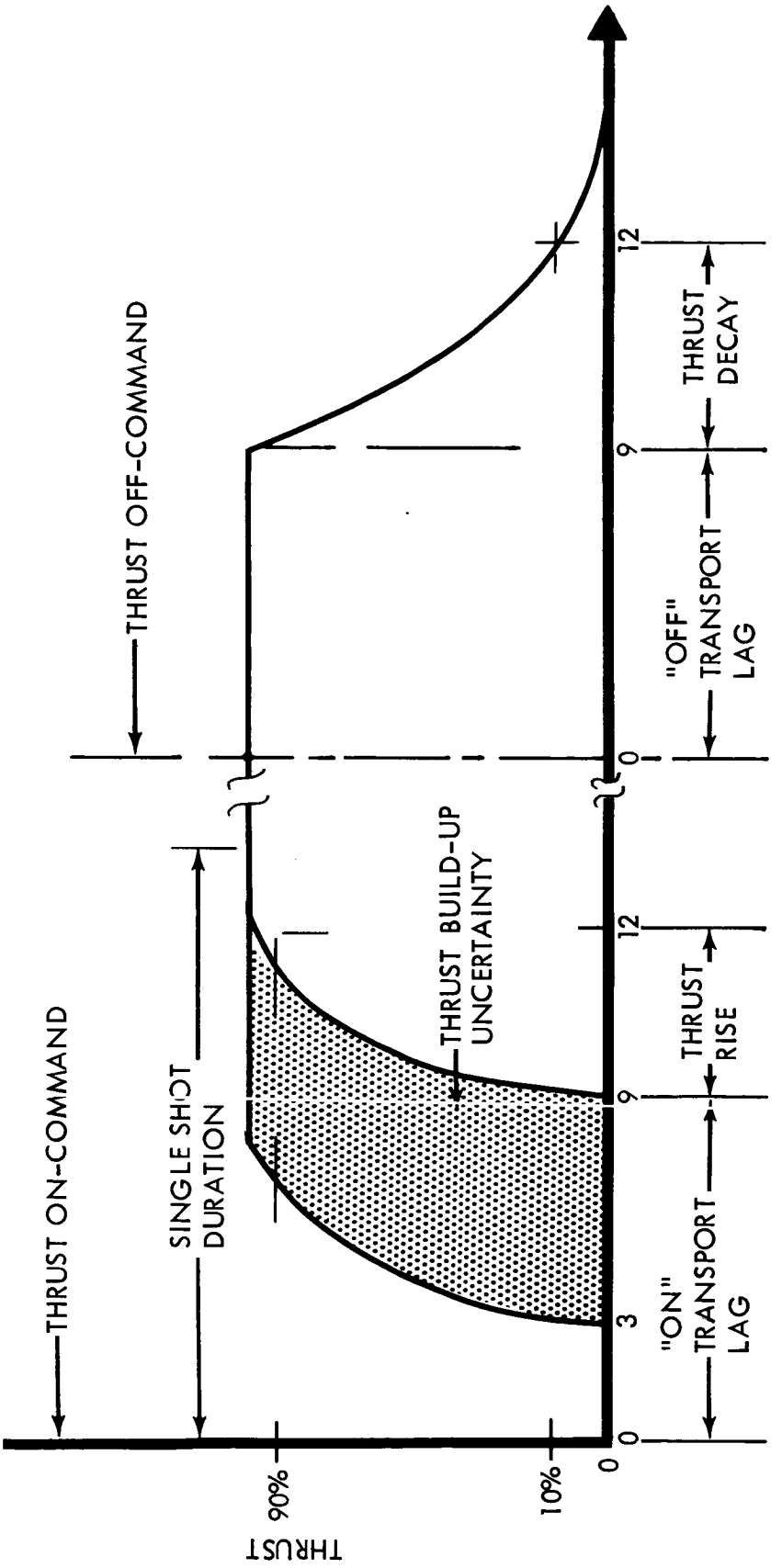

Figure 4.7-3: Thruster Dynamics

spacecraft axes as a function of orbit position relative to periapsis are shown in Figure 4.7-4. Time integration of the area under the curves indicates that the impulse required to compensate for the gravitational torque is 0.4 pound-second per orbit.

Figure 4.7-5 depicts the spacecraft areas exposed to solar pressure forces. An unbalanced area about the pitch axis causes a constant bias torque of 3.6×10^{-6} foot-pounds and an unbalanced area about the yaw axis causes a constant bias torque of 20×10^{-6} foot-pounds.

Since the angular velocity imparted to the spacecraft by a micrometeorite hit is very small, the resulting effect on fuel budget is insignificant and was not considered further. The 50 watts emitted from the high-gain antenna results in a disturbing torque of 0.36×10^{-6} foot-pounds.

The disturbance torques caused by the Martian exosphere have not been calculated in detail. The effect is considerable. Figure 4.7-6 shows an estimate of exospheric drag as a function of time before and after periapsis. A value of 2.5 was used as an average for free-molecular-flow drag coefficient. Compared to solar pressure, the drag values are much higher at periapsis, but 1.5 hours from periapsis fall to values lower than solar pressure. Exact determination of torques involves detailed studies at many points in the orbit and many angles of attack. At present, an allotment of 75 pound-seconds has been allowed in the nitrogen budget for exospheric effects. This is twice the allotment for orbit-phase solar pressure disturbances.

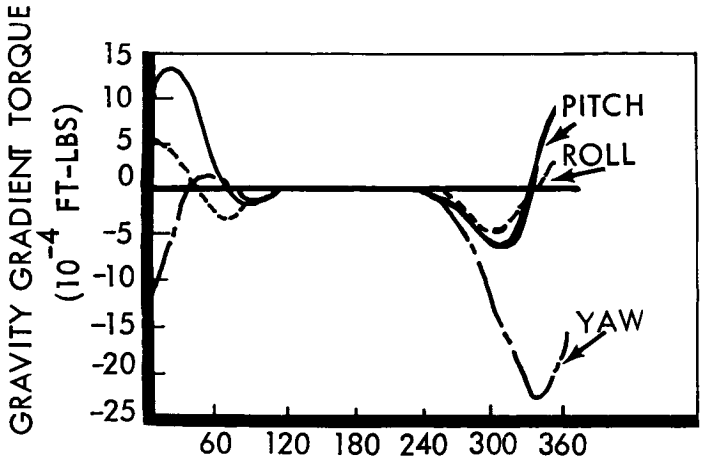

Figure 4.7-4: Gravity Gradient Torque (18-Hour Orbit)

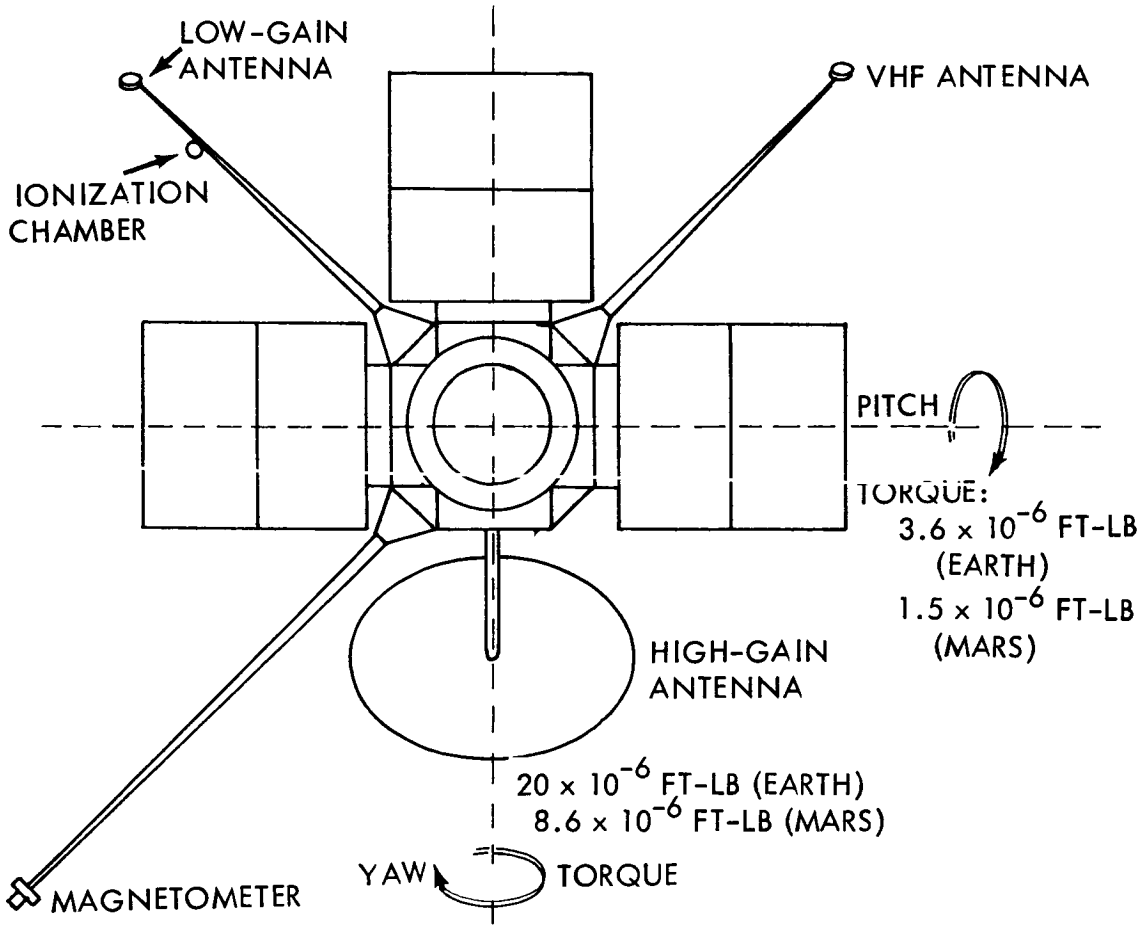

Figure 4.7-5: Solar Pressure Torque

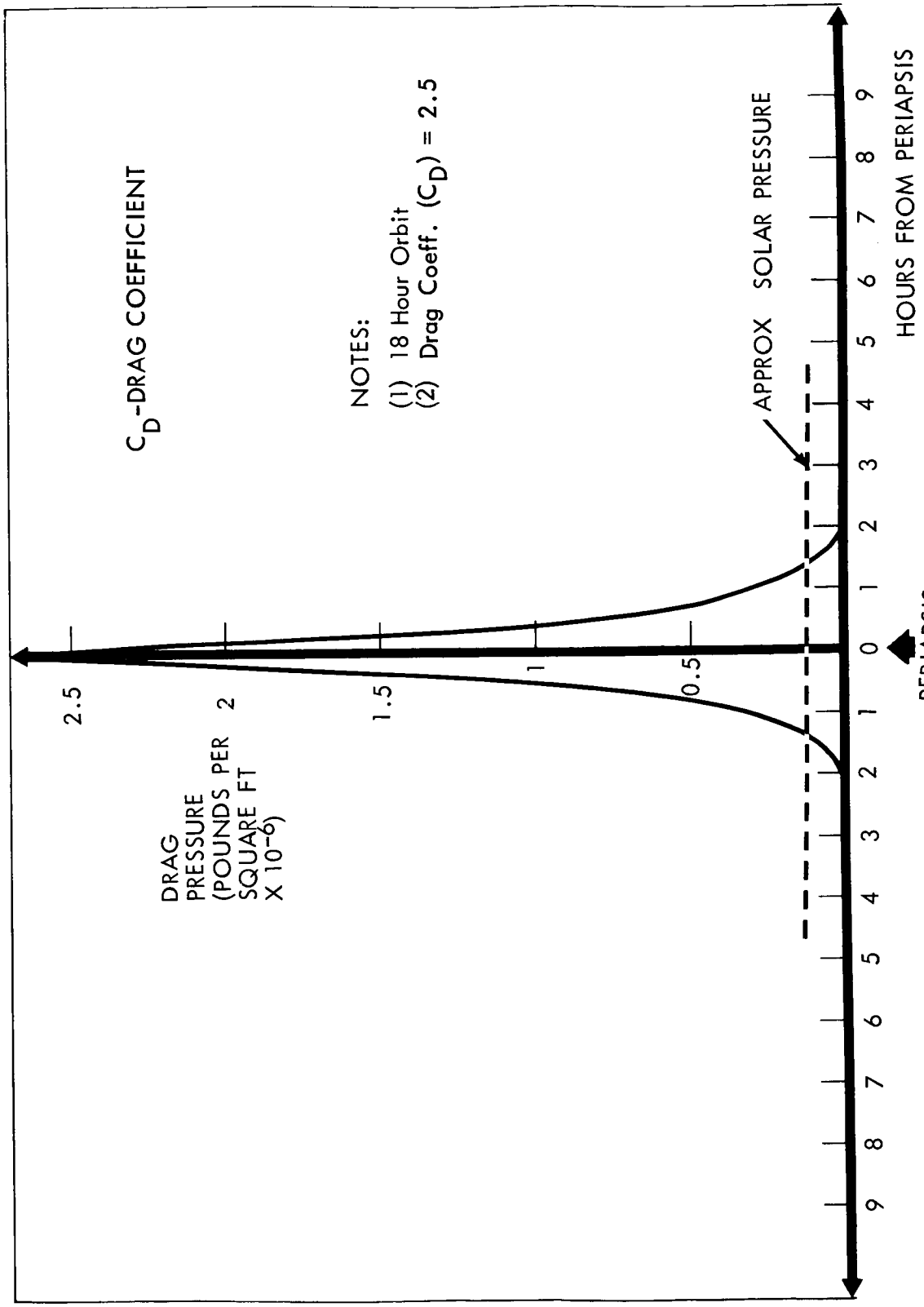

Figure 4.7-6: Martian Exospheric Drag

The internal disturbing torque resulting from movement of the high-gain antenna is considered insignificant. During both the transit and orbit phases, the antenna is stepped only intermittently. Movement of the science platform will probably not affect the fuel budget significantly, but will be accounted for when platform motions are better defined.

4.7.6.4 Fuel Budget

Total impulse requirements of the reaction control subsystem are summarized in Table 4.7-4. A safety factor of 2 is used to arrive at a total requirement of 3040 pound-seconds of impulse.

4.7.7 Physical Characteristics and Constraints

The reaction control subsystem is physically integrated into the propulsion subsystem module, and is installed in and removed from the spacecraft body as a unit with this module. The four 15.5-inch-diameter nitrogen tanks are mounted in pairs symmetrically opposite each other such that propellant use is balanced for minimum disturbance of the spacecraft center of gravity. All check valves, solenoid latching valves, pressure regulators, distribution tees and necessary test points are mounted on a control panel. Reaction-jet thrusters are mounted on the module and there are no separable fittings in the system other than at the fill and test points. The moment arm of the jet thrusters is 53 inches for all axes. The general arrangement of the components is shown in Figure 4.7-1.

Table 4.7-4: FUEL ALLOCATION

Transit	Impulse (lb-sec)	
Initial Acquisition 3°/s separation rate	251.5	
Limit-cycle ±0.4° for 220 days	71.5	
Midcourse Corrections (4) Two deadband closures to ±0.2° One pitch and return rotation Two roll and return rotations "ON" transients (engine) Burn cutoff transients	346.5	
Maneuver for Capsule Separation One deadband closure to ±0.2° One pitch and return rotation Two roll and return rotations 1°/s separation rate	148.3	
Disturbance Torque Solar Pressure	65.0	
Leakage 20 std. cc/hr for 220 days	16.3	
		899
Orbit		
Orbit Insertion and two Trims Two deadband closures to ±0.2° One pitch and return rotation Two roll and return rotations "ON" transients (engine) 40 in-lb roll torque due to swirl	169.37	
Limit-Cycle ±0.2° for 180 days	243.4	
Sun Reacquisitions after Sun Occultations (106) .025°/s	48.3	
Canopus Reacquisitions after Canopus Occultations (30) .025°/s	12.15	
Disturbance Torques Solar pressure Gravity gradient Antenna emission Mars exosphere	133.86	
Leakage 20 std. cc/hr for 180 days	13.6	
		621
Total		1520
Total (safety factor=2)		3040

The total subsystem weight is 212 pounds, including 60 pounds of propellant. Forty-five pounds of this propellant is for reaction control and 15 pounds is for propulsion subsystem pressurization.

Power consumption is 14 watts per thruster. Peak power transients will occur during Sun acquisition (four thrusters on for up to 5 minutes) and during orbit insertion (four thrusters on for 90 seconds at 80 percent duty cycle). Thermal constraints are noted in Section 4.7.5.

4.7.8 Safety

The system uses no hazardous liquids or propellants. Nitrogen being completely inert represents no toxic or fire hazard. The high-pressure storage tanks are designed to a 2.2 factor of safety, burst-pressure/operating-pressure, and are fabricated from annealed Ti-6Al-4V titanium as noted in Section 4.7.3.2.

4.7.9 Development Tests

The nitrogen reaction control system is a thoroughly developed and space-proven concept. No development work on the components of the basic system is required for the 1966 development freeze.

One exception may possibly exist, however. The use of standby thruster redundancy and common tankage requires a highly reliable malfunction detection scheme. A valve position indicator to show the mechanical condition of the valve (open or closed) can serve this purpose, as is shown in D2-82709-2, Section 4.6. It is in the mechanization of this type of device, or of one of the alternate

malfunction detection schemes, that some development testing may be required. No state-of-the-art advances are required since more complex proportional feedback transducers (capacitive or inductive pickoffs, linear potentiometers, and differential transformers) are fully developed.

Testing will take place also to ensure that the nitrogen and portions of the subsystem that it comes in contact with can be properly sterilized.

CONTENTS

4.8 CENTRAL COMPUTER AND SEQUENCER

Summary--The central computer and sequencer provides event timing, sequencing, synchronization, and switching signals for spacecraft control and operation during prelaunch and all mission operations. To meet these requirements, the CC&S must incorporate both data-processing and power-switching circuitry. The design selected utilizes a modified NASA Lunar Orbiter programmer, which is a special purpose, memory-oriented (digital) computer. The equipment consists of two separate functional assemblies--the control assembly containing redundant data processors and the switching assembly providing complete redundancy in all power switching. Switching of all CC&S functions may be accomplished by either ground or onboard command. The CC&S design provides:

1) A reliability of 0.9941 over the mission period of 5880 hours (245 days);
2) A random-access storage capacity of 256 words at 21 bits/word;
3) A timing accuracy for mission control of 1 part in 10^6 over a period of 16 hours;
4) The capability to execute up to 333 different commands.

The system weighs 58 pounds, occupies a volume of 2700 cubic inches, and requires 40 watts of power. The CC&S is located in the spacecraft as shown in Figure 4.8-1.

CC&S stores a preplanned sequence of spacecraft events for directing the mission and accepts changes to that sequence at any time as commanded by mission operations. The number and complexity of Earth-based commands has been minimized by the CC&S design such that only mission variables must be transmitted. Options are

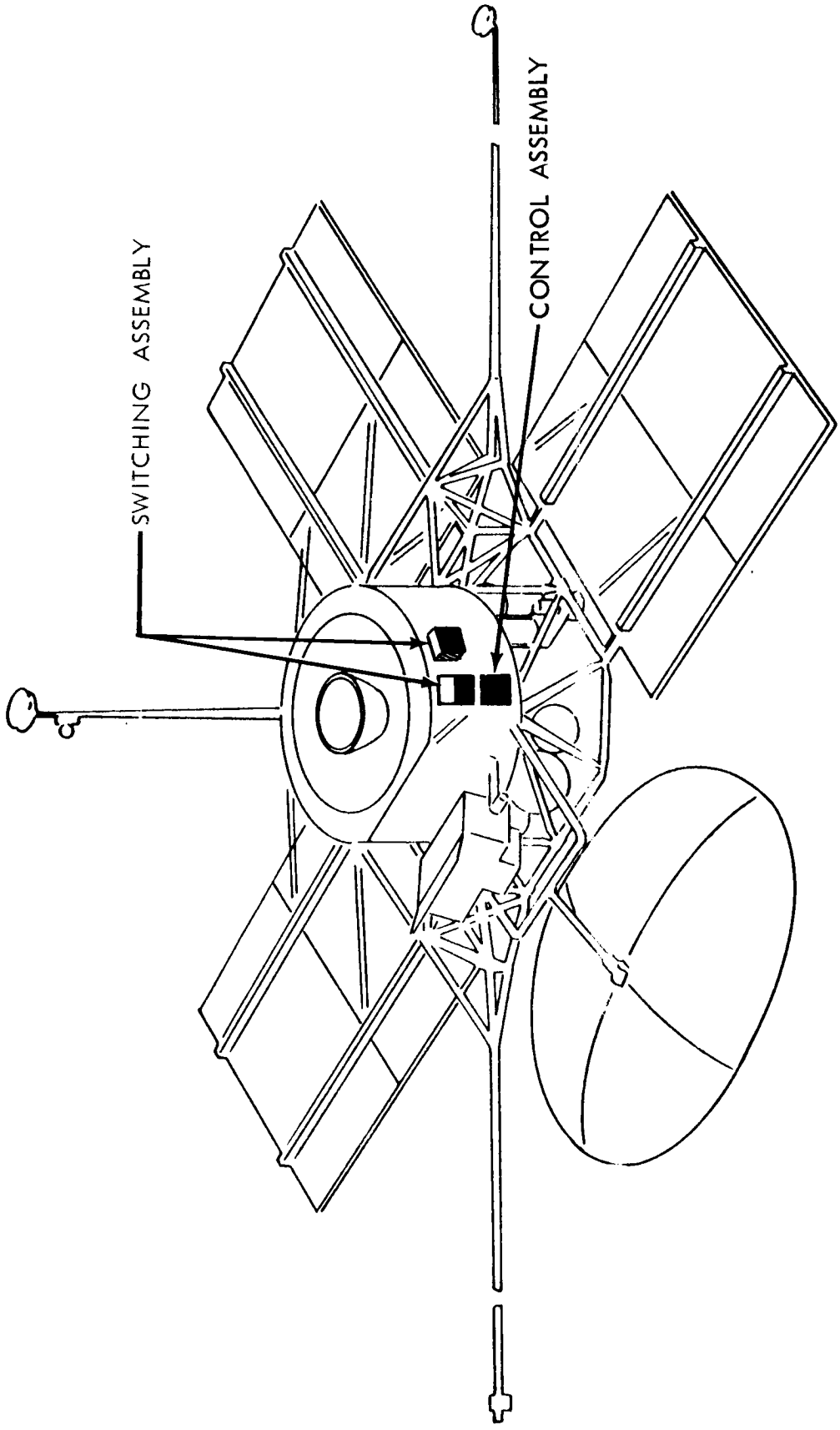

Figure 4.8-1: Central Computer and Sequencer Subsystem

available for many direct commands from mission operations via the DSN. Choices of stored commands, direct commands, and their operational use are based on the logic available from the flight sequence charts found in Section 3.9. Spacecraft events are implemented by issuance of commands from the CC&S to other spacecraft subsystems. The system block diagram is shown in Figure 4.8-2.

Figure 4.8-3 shows the functional units of the CC&S and their interconnection of control, timing, and data transfer paths. At the top of the diagram is the clock generator providing spacecraft time and the ferrite core memory containing the flight program. The command register holds the command word received from the memory for decoding by the output matrix. Centrally shown are the units that perform the arithmetic function of summation of angular and velocity maneuver magnitudes and their comparison with commanded values. Incoming messages from ground control are accepted and validated in the command decoder, mode control register, and input parity checker prior to being executed.

The switching assembly and signal conditioning are used to interface the issuance commands to all spacecraft subsystems. As an example, the flight control switching unit provides the required interfacing with the autopilot. The output matrix decoder unit provides necessary functions for spacecraft subsystems control. The CC&S is the focus for functional control and interfaces within the spacecraft. The interface functions between the CC&S and the spacecraft subsystems are shown in Figure 4.8-4.

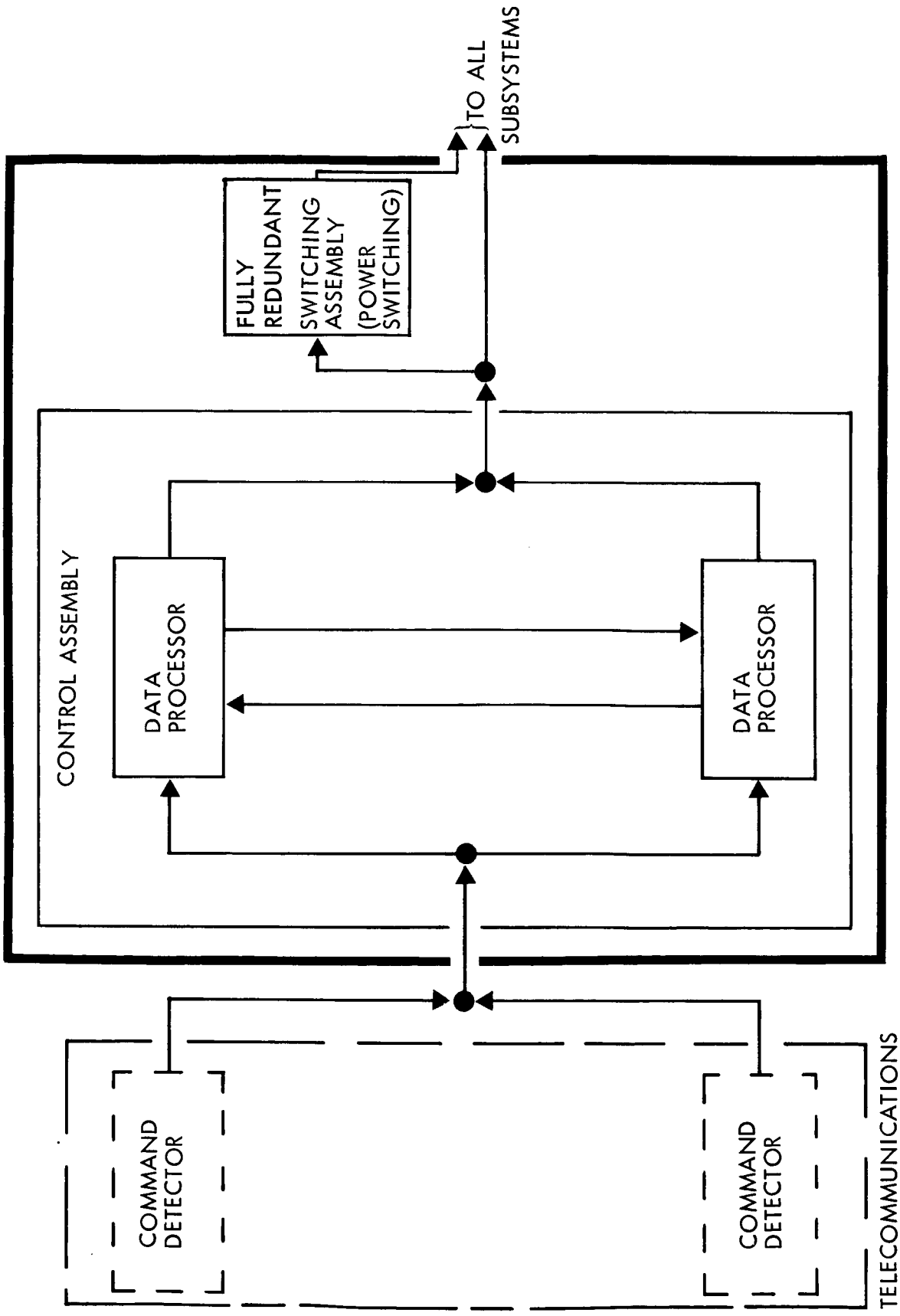

Figure 4.8-2: Central Computer and Sequencer System Block Diagram

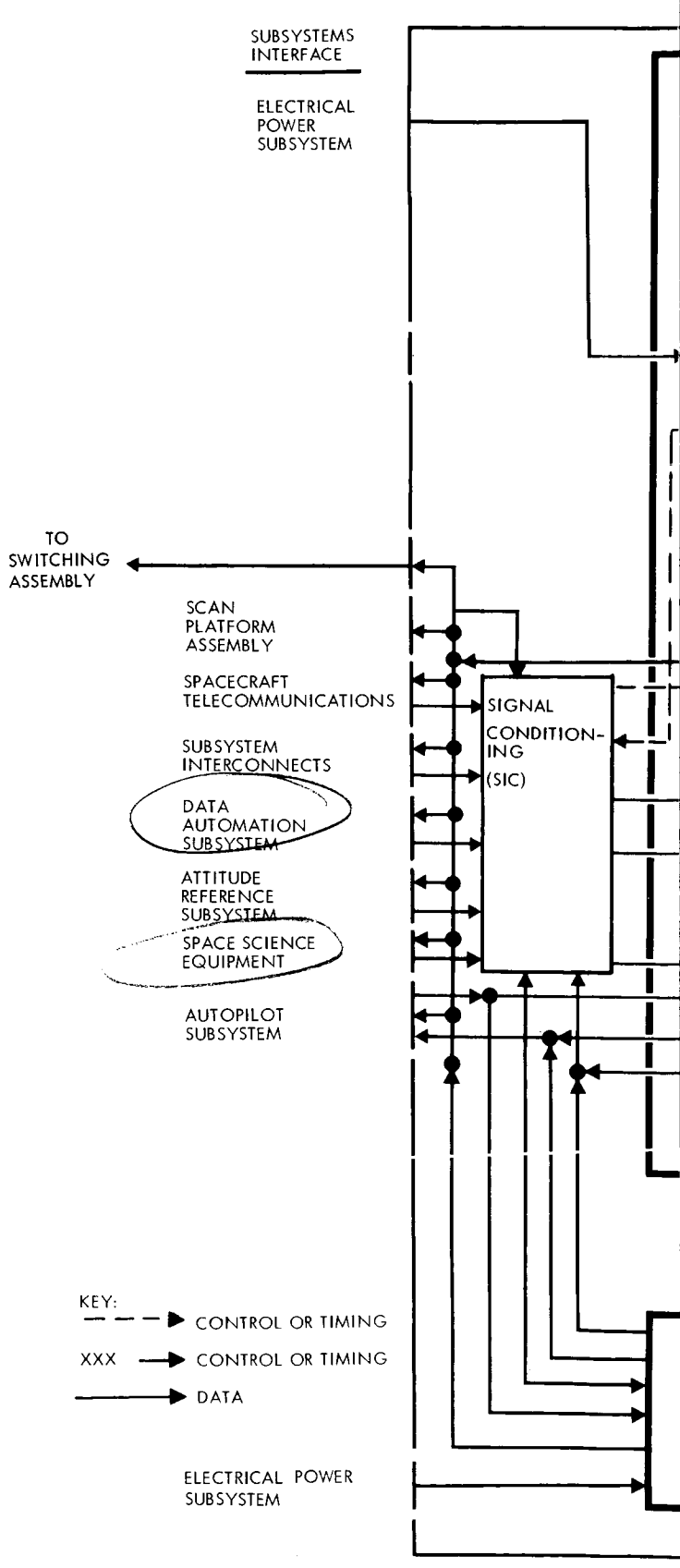
SUBSYSTEMS INTERFACE
ELECTRICAL POWER SUBSYSTEM
TO SWITCHING ASSEMBLY
SCAN PLATFORM ASSEMBLY
SPACECRAFT TELECOMMUNICATIONS
SUBSYSTEM INTERCONNECTS
DATA AUTOMATION SUBSYSTEM
ATTITUDE REFERENCE SUBSYSTEM
SPACE SCIENCE EQUIPMENT
AUTOPILOT SUBSYSTEM
SIGNAL CONDITION-ING (SIC)
KEY:
CONTROL OR TIMING
XXX CONTROL OR TIMING
DATA
ELECTRICAL POWER SUBSYSTEM

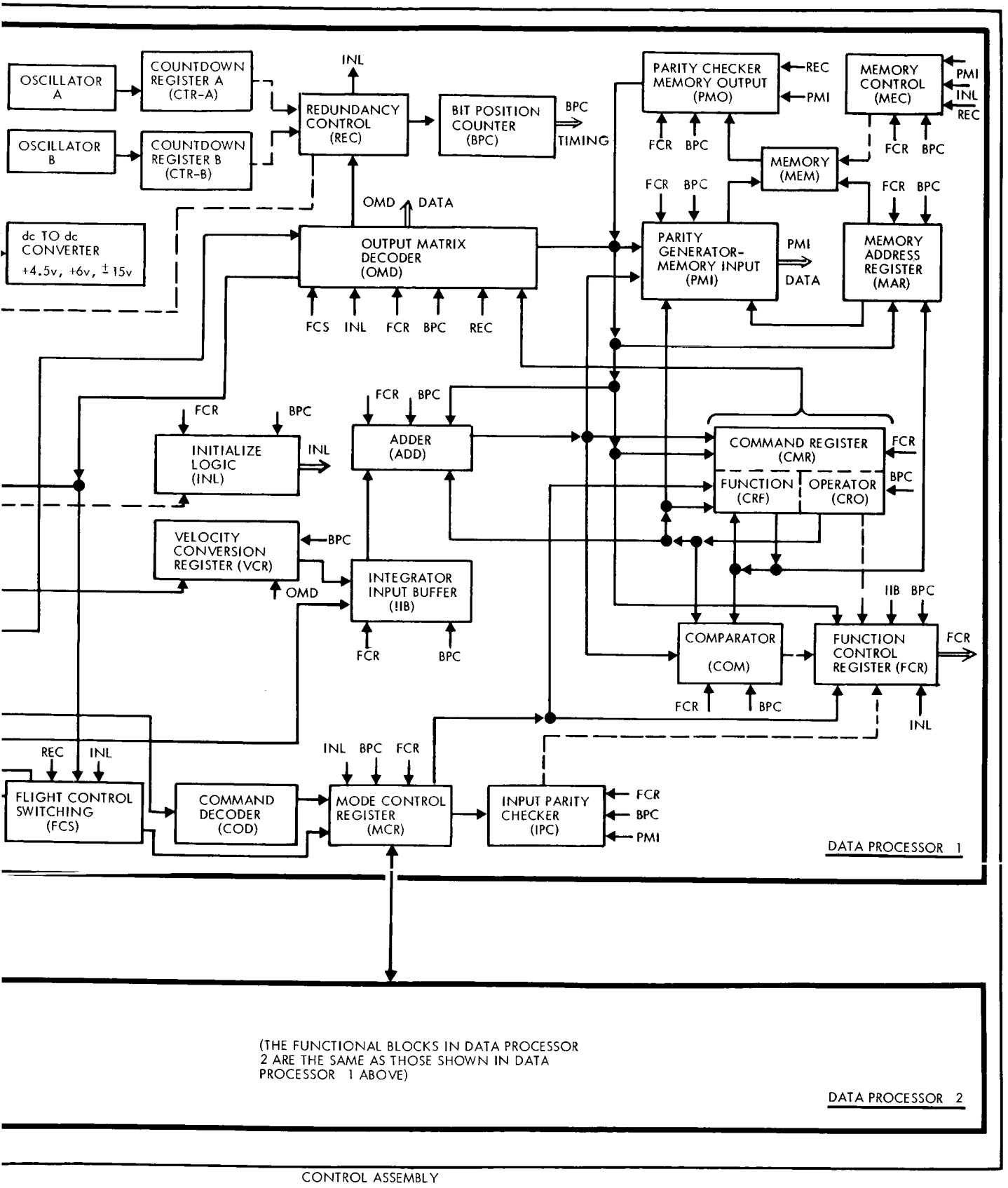

Figure 4.8-3: Central Computor and Sequencer Functional Block Diagram

The CC&S logic has been developed to minimize ground commands and internal storage. The unit functions by storing preset operational routines. These routines are sequenced by both ground commands and by stored commands. Repetitive sequencing by stored commands is accomplished by address modifications. Constant values employed for magnitude comparison are sequentially stored in blocks of addresses so that the repetitive main routine can obtain the proper constants for each maneuver. Any stored word can be modified by insertion of new words transmitted during flight. Command words sent from the ground are first double parity checked and then either stored in the memory or executed immediately (real-time use). They will also be telemetered for ground verification.

The CC&S switching assembly is developed to provide power switching signals requiring high voltage and current outputs. Power switching is required for firing squibs, solenoid drivers, motor drivers, and relay drivers. Low-level signals originating in the control assembly causes the appropriate power switching signal to be issued from the switching assembly to the specific subsystem.

The NASA Lunar Orbiter Programmer is directly applicable to the Voyager CC&S. The development status of this programmer is that it has completed development testing and is currently undergoing reliability testing. It has successfully completed 3 months of thermal vacuum and vibration testing. The system will be space qualified by July 1966. The benefits derived will be an accelerated development of the Voyager CC&S.

4.8.1 Scope

4.8.1.1 Subsystem Identification and Intended Usage

The central computer and sequencer (CC&S) (Figures 4.8-2 and 4.8-3) is the major control element for directing the Voyager spacecraft. The CC&S will execute a preplanned sequence of events stored internally and supplemented by the insertion of mission variables from Mission Operations. Specifically, the CC&S provides sequencing and timing command signals to spacecraft subsystems as directed by the stored flight program or as directed from ground control. It provides the logic implementation to control the magnitude and direction of spacecraft maneuvers. It provides timing signals and pulse trains to other spacecraft subsystems. The Central Computer and Sequencer subsystem is designed to perform the functions highlighted on the Mission Sequences Matrix.

The CC&S issues commands to the following subsystems (Figure 4.8-4):

1) Spacecraft telecommunications;
2) Attitude reference subsystem;
3) Autopilot subsystem;
4) Spacecraft mechanisms subsystem;
5) Temperature-control subsystem;
6) Pyrotechnic subsystem;
7) Midcourse-correction propulsion subsystem;
8) Orbit-injection propulsion subsystem;
9) Science paylod data-automation system;
10) Electrical power subsystem.

	1.0 PRELAUNCH AT ETR	2.0 LAUNCH & INJECTION (INCLUDES COUNTDOWN)
GROUND COMPLEX (MOS, LOS, & DSN)	OPERATIONAL READINESS TEST, S/C-DSN COMPATIBILITY TEST SCHED & COORD ETR ACTIVITIES C/O & SUPPORT MOS (DSN ONLY) LOAD CC&S WITH FLIGHT PROGRAM	MOS/LOS A) COMMAND LIFTOFF B) TRACK VEHICLE DURING BOOST C) SUPPLY FLIGHT COMMANDS (AS REQ) D) RECEIVE & ANALYZE DATA FROM S/C & BOOSTER DSN E) STANDBY ON ALERT F) COMMUNICATE WITH ETR CHANGE FROM MOS/LOS TO ON INJECTION INTO TRANSF A) PROVIDE SFOF/DSIF WI DSN SEARCH DATA B) RECEIVE ANTENNA SEAR C) SEARCH FOR & ACQUIR D) ESTABLISH & VERIFY C E) TRACK S/C (1-WAY) F) RECEIVE & ANALYZE EN
SPACECRAFT TELECOMMUNICATIONS	SUBSYSTEM C/O & STATUS MONITORING	A) TRANSMIT ENGINEERING DATA VIA CENTAUR TELEMETRY B) TRANSMIT ENGINEERING DATA VIA LOW POWER LAUNCH EXCITER C) RECEIVE POWER FROM E/P
CENTRAL COMPUTER & SEQUENCER (CC&S)	A) SUBSYSTEM C/O & STATUS B) COMMAND OTHER SUBSYSTEMS FOR C/O & STATUS MONITORING C) READY ALL SUBSYSTEMS FOR LAUNCH D) LOAD CC&S WITH FLIGHT PROGRAM	PROVIDE BACKUP COMMANDS AS REQUIRED
ATTITUDE REFERENCE SUBSYSTEM AUTOPILOT SUBSYSTEM REACTION CONTROL SUBSYSTEM (RCS)	SUBSYSTEM C/O & STATUS MONITORING	A) ATTITUDE REFERENCE — GYROS OFF DURING LAUNCH B) AUTOPILOT — OFF C) RCS — OFF
MIDCOURSE CORRECTION PROPULSION SYSTEM ORBIT INJECTION PROPULSION SYSTEM	SUBSYSTEM C/O & STATUS MONITORING	
ELECTRICAL POWER SUBSYSTEM	SUBSYSTEM C/O & STATUS MONITORING	A) PROVIDE ENGRG DATA FOR TELECOMMUNICATIONS SUBSYSTEM B) PROVIDE BATTERY POWER TO • TELECOMMUNICATIONS SUBSYSTEM • CC&S • ATTITUDE REFERENCE SUBSYSTEM • AUTOPILOT SUBSYSTEM
S/C STRUCTURE SUBSYSTEM S/C MECHANISMS SUBSYSTEM INSTALLATION CABLES & TUBING	SUBSYSTEM C/O & STATUS MONITORING	A) PROVIDE PHYSICAL SUPPORT FOR ALL EQUIPMENT B) PROVIDE ATTACHMENT FOR CAPSULE C) SUPPORT FLT CAPSULE
TEMPERATURE CONTROL SUBSYSTEM	SUBSYSTEM C/O & STATUS MONITORING SPACECRAFT COOLING SUPPLIED BY CENTAUR	A) PROVIDE HEAT SINK COOLING CAPABILITY UP TO SHROUD JETTISON B) TEMPERATURE CONTROL AFTER SHROUD JETTISON
PYROTECHNIC SUBSYSTEM	SUBSYSTEM C/O & STATUS MONITORING	
SCIENCE EXPERIMENTS (GFE)	SUBSYSTEM C/O & STATUS MONITORING S/C MAGNETIC MAPPING (FAT)	
DATA AUTOMATION EQUIPMENT (GFE)		

REPEAT UP T

SN CONTROL ARS ORBIT H ANTENNA H DATA S/C TROL OF S/C G DATA	DSN A) MONITOR BOOSTER SEPARATION B) MONITOR SOLAR PANEL DEPLOYMENT C) MONITOR ANTENNA DEPLOYMENT D) PROVIDE COMMANDS TO BACK UP CC&S AS REQUIRED E) TRACK S/C F) REC DATA G) MONITOR SCIENCE DEPLOYMENT DSN H) MONITOR & VERIFY ACQUISITION OF SUN I) MONITOR & VERIFY ACQUISITION OF CANOPUS J) COMMAND REACQUISITION OF CANOPUS (AS REQD) K) MONITOR S/C TRAJECTORY L) UPDATE CC&S TRAJECTORY PARAMETERS FOR PITCH, YAW, & ROLL M) COMPUTE CC&S PITCH, YAW, & ROLL POLARITY	DSN A) TRACK S/C B) RECEIVE & DISPLAY SCIENCE & ENGINEERING DATA C) MONITOR S/C & CAPSULE STATUS D) PROCESS DATA ON EARTH TO OBTAIN GUIDANCE COMMANDS (STORED COMMANDS & START TIMES)	
	A) TRANSMIT ENGINEERING DATA B) RECEIVE POWER FROM E/P C) RECEIVE VIA LOW-POWER LAUNCH EXCITER DETECT & SEND TO CC&S COMMAND SIGNALS FROM EARTH D) TRANSMIT CELESTIAL REFERENCE ACQUISITION TO DSN E) TRANSMIT VERIFICATION OF DEPLOYMENT OF SOLAR PANELS, ANTENNAS, ETC TO EARTH F) TWO-WAY TRACKING		A) TRANSMIT ENGINEERING & SCIENCE DATA VIA DATA MODE NO. 2 (OPTIONAL MODE NO. 3) B) TRANSMIT CAPSULE ENGINEERING DATA C) TRANSMIT CONE-ANGLE SETTINGS (CANOPUS TO EARTH) D) EXERCISE & CALIBRATE HIGH-GAIN ANTENNA T + 40 DAYS E) SWITCH FROM LOW-GAIN TO HIGH-GAIN ANTENNA T + 80 DAYS F) PROVIDE RANGING SIGNAL TO A MAX. RANGE OF 8.0×10^6 KM (NOMINAL) G) SWITCH TRANSMISSION FROM LAUNCH EXCITER TO TWT POWER AMPLIFIER AND DATA MODE NO. 2
	A) COMMAND SIGNALS TO PYROTECHNICS & MECH TO DEPLOY • SOLAR PANELS • HIGH-GAIN ANTENNA • VHF ANTENNA • LOW-GAIN ANTENNA • SCIENCE BOOM B) SWITCH ON GYROS & SELECT MODES C) ENABLE SUN-SENSOR ROLL AND PITCH CONTROL D) RECEIVE SUN PRESENCE SIGNAL E) TURN ON CANOPUS TRACKER F) SWITCH ROLL CONTROL TO CANOPUS SENSOR G) ACTIVATE MAGNETOMETER (CALIBRATION ROLL) H) RECEIVE CANOPUS PRESENCE OUTPUT SIGNAL I) TRANSMIT VERIFICATION TO TELE-COMMUNICATION SUBSYSTEM (CANOPUS & SUN PRESENCE) J) PERFORM COMMAND FUNCTIONS FOR CANOPUS OVERRIDE AS REQUIRED K) BACKUP COMMANDS AS REQUIRED		A) COMMAND TELECOMMUNICATION TO DATA MODE NO. 2 B) COMMAND CRUISE SCIENCE ON (WARMUP) — SCIENCE INSTRUMENTS C) COMMAND DATA RECORDERS ON D) COMMAND TWTA ON E) SWITCH CANOPUS ANGLE AS REQUIRED F) INITIATE CRUISE SCIENCE DATA ACQUISITION G) COMMAND TELECOMMUNICATION CHANGE FROM OMNI TO HIGH-GAIN ANTENNA H) UPDATE HIGH-GAIN ANTENNA POSITION (AS REQUIRED) I) COMMAND TELECOMMUNICATIONS — CHANGE DATA TRANSMISSION RATES J) COMMAND RECALIBRATION OF SCIENCE ELEMENTS AS REQUIRED K) BACKUP COMMANDS AS REQUIRED
	A) RECEIVE CC&S COMMAND SWITCH ON GYROS, RCS, & AUTOPILOT B) DAMP ROTATION C) YAW & PITCH SPACECRAFT TO ACQUIRE SUN D) RELAY SUN ACQUISITION SIGNAL TO CC&S E) TURN ON CANOPUS SENSOR, ROLL 360 TO CALIBRATE MAGNETOMETER F) ROLL TO ACQUIRE CANOPUS & PROVIDE STAR MAP G) RELAY ACQUISITION SIGNAL (CANOPUS) TO CC&S H) PERFORM CANOPUS OVERRIDE ROLL MANEUVER AS REQUIRED		A) UPDATE CANOPUS CONE ANGLE ON COMMAND B) SWITCH AUTOPILOT TO CRUISE MODE C) MAINTAIN S/C ATTITUDE TO CELESTIAL REFERENCES DURING CRUISE
	A) PROVIDE POWER TO PYROTECHNIC SUBSYSTEMS FOR SQUIB FIRINGS B) PROVIDE POWER TO MECHANISMS C) ACTIVATE SOLAR POWER SYSTEM AFTER SUN ACQUISITION (AUTOMATIC) D) TRANSMIT "VOLTAGE SATISFACTORY" SIGNAL TO CC&S E) PROVIDE POWER TO: • TELEMETRY • CC&S • TEMPERATURE CONTROL • AUTOPILOT		A) PROVIDE CONDITIONED SOLAR ELECTRICAL POWER TO: • TELEMETRY • CAPSULE • CC&S • ATTITUDE REF • AUTOPILOT • TEMPERATURE CONTROL • SCIENCE B) CHARGE BATTERIES
	A) PROVIDE PHYSICAL SUPPORT FOR ALL EQUIPMENT B) DRIVE SOLAR PANELS TO LIMIT-STOPS C) PROVIDE OUT & LOCK SIGNALS TO TELEMETRY D) DRIVE HIGH-GAIN ANTENNA TO OPERATING POSITION & LOCK E) DRIVE VHF & OMNI ANTENNAS TO OPERATING POSITION & LOCK F) DRIVE MAGNETOMETER BOOM TO OPERATING POSITION & LOCK G) SUPPORT FLT CAPSULE		A) SUPPORT S/C ASSEMBLIES B) SUPPORT S/C COMPONENTS C) MAINTAIN ADEQUATE ALIGNMENT BETWEEN COMPONENTS D) PROVIDE ACCEPTABLE STATIC & DYNAMIC LOAD ENVIRONMENTS E) SUPPORT FLIGHT CAPSULE
	PROVIDE TEMPERATURE CONTROL		PROVIDE TEMPERATURE CONTROL
	RECEIVE SQUIB FIRING SIGNALS FOR DEPLOYMENT OF: • SOLAR PANEL • MAGNETOMETER BOOM • LOW-GAIN ANTENNA • HIGH-GAIN ANTENNA • VHF ANTENNA		
	A) CALIBRATE MAGNETOMETER DURING S/C ROLL B) CALIBRATE OTHER SCIENCE INSTR AS REQUIRED		A) RECEIVE CRUISE SCIENCE "ON" COMMAND B) ACQUIRE CRUISE SCIENCE DATA C) TRANSFER CONDITIONED DATA TO DAE D) RECEIVE POWER FROM E/P E) RECALIBRATE SCIENCE EXPERIMENTS AS REQUIRED
			A) RECEIVE DAE "ON" COMMAND B) PROCESS & TRANSFER DATA TO TM

) FOUR TIMES

5.0 INTERPLANETARY TRAJECTORY CORRECTION

6.0 S/C CAPSULE SEPARATION

7.0 FLIGHT TRAJEC DEFLEC

PROVIDE ROLL TURN MAGNITUDE & DIRECTION PROVIDE YAW TURN MAGNITUDE & DIRECTION PROVIDE MIDCOURSE MOTOR BURN DURATION AND ΔV PROVIDE INITIATE MANEUVER SEQUENCE COMMAND RECEIVE VERIFICATION OF CORRECTION MANEUVER • DEGREES OF YAW & ROLL • THRUST DURATION • REACQUISITION OF CELESTIAL REFERENCES TRACK SPACECRAFT	A) INITIATE PRESEPARATION SEQUENCE B) RECEIVE CAPSULE STATUS DATA C) COMMAND SEPARATION D) VERIFY CAPSULE PROGRAM E) VERIFY SEPARATION F) TRACK CAPSULE & SPACECRAFT	A) TRANSMIT OR • ROLL MAGN • YAW MAGN • MOTOR BU B) TRACK FLIGH C) RECEIVE, RED D) PROVIDE COM
RECEIVE ROLL & YAW TURN COMMAND & RELAY TO CC&S RECEIVE ANTENNA POSITIONING DATA & RELAY TO CC&S RECEIVE MOTOR BURN DURATION AND & ΔV RELAY TO CC&S RECEIVE INITIATE MANEUVER COMMAND & RELAY TO CC&S SWITCH TO DATA MODE NO. 1 (FOR LATE MIDCOURSE MANEUVERS) RELAY VERIFICATION OF CORRECTION MANEUVER TO DSN STORE AND/OR TRANSMIT ENGINEERING DATA TO DSN (MODE 3) TRANSMIT ENGINEERING (SPACECRAFT & CAPSULE) + CRUISE SCIENCE TO DSN (MODE 2)	A) RECEIVE PRESEPARATION SEQUENCE COMMANDS & RELAY TO CC&S B) SWITCH TO DATA MODE NO. 2 C) TRANSMIT CAPSULE ENGRG DATA TO DSN D) RECEIVE SEPARATION COMMAND FROM DSN & ROUTE TO CC&S E) STORE AND/OR TRANSMIT ENGINEERING DATA TO DSN (MODE 3) TRANSMIT ENGINEERING (SPACECRAFT & CAPSULE) + CRUISE SCIENCE TO DSN (MODE 2)	A) RECEIVE ROLL TO CC&S B) RECEIVE ANTE C) RECEIVE MOT D) RECEIVE CAP E) TRANSMIT FL SCIENCE DAT
) COMMAND TELECOMMUNICATION TO DATA MODE NO. 1) RECEIVE TRAJECTORY CORRECTION PARAMETERS) SWITCH GYROS TO RATE CONTROL) COMMAND ANGULAR MANEUVER RECEIVE GYRO SIGNALS & SUM FOR ANGULAR MANEUVERS SWITCH ATTITUDE REFERENCE TO AUTOPILOT SUBSYSTEM) ARM PROPULSION SYSTEM) PROVIDE COMMAND TO INITIATE ATTITUDE MANEUVER & ΔV MANEUVER RECEIVE ACCELEROMETER SIGNALS & INTEGRATE FOR ΔV MANEUVER DISARM PROPULSION SYSTEM) COMMAND REVERSE ANGULAR MANEUVER COMMAND REACQUIRE CELESTIAL REFERENCES) COMMAND AUTOPILOT SELECTION CONTROL) BACKUP COMMANDS AS REQUIRED	A) LOAD CAPSULE WITH 5 OR MORE COMMANDS B) COMMAND CAPSULE SEQUENCING C) COMMAND TELECOMM SWITCH TO DATA MODE NO. 1 D) COMMAND GYROS ACTIVATE (CAPSULE) E) COMMAND GYROS ESTABLISH POLARITY (CAPSULE) F) COMMAND GYROS TO ATTITUDE CONTROL MODE (CAPSULE) G) COMMAND DATA TAPE RECORDER OFF H) COMMAND CAPSULE ACTIVATE ENTRY SCIENCE I) COMMAND CAPSULE ACTIVATE TELE-COMM & VERIFY RADIO LINK (VHF) J) SELECT T/M MODE FOR TRANSMISSION OF CAPSULE DATA K) COMMAND: BIOBARRIER SEPARATION S/C ORIENT TO SEPARATION ATTITUDE ELECTRICAL CONNECTION SEPARATION VERIFY SEPARATION L) COMMAND REORIENT S/C & REACQUIRE CELESTIAL REFERENCES M) BACKUP COMMANDS AS REQUIRED N) RECEIVE S/C ORIENTATION PARAMETERS	A) COMMAND S B) COMMAND C C) COMMAND A D) RECEIVE ORE E) PROVIDE SI (CRUISE SCI F) SWITCH ON RECEIVE CAP G) BACKUP COM
) SWITCH TO GYRO CONTROL) ROLL S/C AND VERIFY) YAW S/C AND VERIFY) AUTOPILOT — PROVIDE COMMAND TO TVC DURING MOTOR BURN TURN ON ACCELEROMETERS PROVIDE ACCELERATION DATA TO CC&S) TURN OFF ACCELEROMETER H) YAW BACK TO ORIGINAL ATTITUDE & VERIFY I) REACQUIRE SUN (FINE SUN SENSOR) & VERIFY J) ROLL TO ORIGINAL ATTITUDE K) LOCK ON CANOPUS & VERIFY L) SWITCH AUTOPILOT FROM GYRO CONTROL TO CELESTIAL REF CONTROL	A) SWITCH TO GYRO CONTROL B) PERFORM ROLL TURN & VERIFY C) PERFORM YAW TURN & VERIFY D) MAINTAIN ATTITUDE DURING SEPARATION E) PERFORM YAW TURN (INVERSE TO C) & VERIFY F) PERFORM ROLL TURN (INVERSE TO B) & VERIFY G) REACQUIRE CELESTIAL REFERENCES H) RETURN TO CELESTIAL REFERENCE ATTITUDE CONTROL MODE	A) UPDATE CAN B) SWITCH AUT C) MAINTAIN S
IDCOURSE PROPULSION SYSTEM) ARM PRESSURIZATION SYSTEM (FIRE SQUIB VALVE)) ARM PROPELLANT FEED SUBSYSTEM (FIRE SQUIB VALVE)) FIRE PROGRAMMED ENGINES (OPERATE SOLENOID VALVE)) SHUT DOWN ENGINE ISOLATE PROPELLANT FEED SUBSYSTEM ISOLATE PRESSURIZATION SUBSYSTEM		
) PROVIDE CONDITIONED SOLAR OR BATTERY POWER TO: • TELEMETRY • CC&S • AUTOPILOT • ATTITUDE REFERENCE • REACTION CONTROL • PROPULSION • TEMPERATURE CONTROL • PYROTECHNICS • CAPSULE	A) PROVIDE CONDITIONED SOLAR OR BATTERY POWER TO: • T/M • CC&S • AUTOPILOT • ATTITUDE REF • REACTION CONTROL • TEMPERATURE CONTROL • PYROTECHNICS • CAPSULE	A) PROVIDE C • T/M • CC&S • AUTOPILO • ATTITUDE • REACTION • TEMPERA B) CHARGE BAT
SUPPORT S/C ASSEMBLIES) SUPPORT S/C COMPONENTS) MAINTAIN ADEQUATE ALIGNMENT BETWEEN COMPONENTS) PROVIDE ACCEPTABLE STATIC & DYNAMIC LOAD ENVIRONMENTS) SUPPORT FLIGHT CAPSULE	A) SUPPORT S/C ASSEMBLIES B) SUPPORT S/C COMPONENTS C) MAINTAIN ADEQUATE ALIGNMENT BETWEEN COMPONENTS D) PROVIDE ACCEPTABLE STATIC & DYNAMIC LOAD ENVIRONMENTS E) SUPPORT FLIGHT CAPSULE	A) SUPPORT SU B) SUPPORT SI C) MAINTAIN A D) PROVIDE AC E) DRIVE SCA
ROVIDE TEMPERATURE CONTROL	PROVIDE TEMPERATURE CONTROL	PROVIDE TEMPE
) REMOVE PROPULSION SYSTEM INHIBIT) PROVIDE IGNITION) INHIBIT PROPULSION SYSTEM	A) RECEIVE SIGNAL TO REMOVE CAPSULE SEPARATION INHIBIT B) RECEIVE SIGNAL TO FIRE CAPSULE UMBILICAL SEPARATION C) RECEIVE SIGNAL TO FIRE BIOBARRIER REMOVAL D) RECEIVE SIGNAL TO FIRE CAPSULE SEPARATION E) RECEIVE SIGNAL FOR SEPARATION INHIBIT	RECEIVE SQUIB OF SCAN PLAT
) RECEIVE CC&S COMMAND "CRUISE SCIENCE OFF") TURN OFF CRUISE SCIENCE	A) RECEIVE CC&S COMMAND "CRUISE SCIENCE OFF" B) TURN OFF CRUISE SCIENCE	A) RECEIVE CR B) ACQUIRE CI C) TRANSFER C D) RECEIVE PO E) RECALIBRA
		A) RECEIVE DA B) PROCESS &

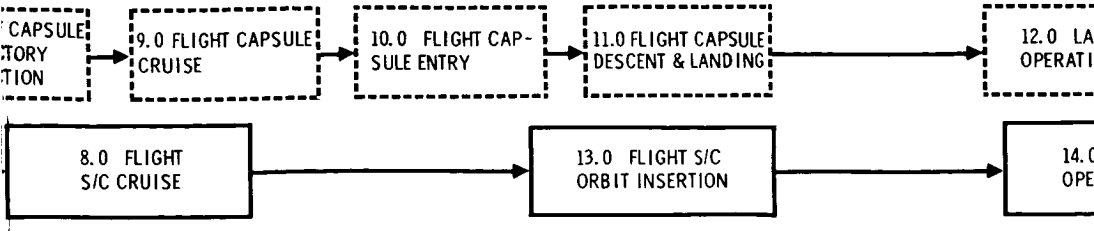

T INJECTION PARAMETERS TUDE & DIRECTION UDE & DIRECTION START TIME SPACECRAFT CE & DISPLAY SCIENCE & ENGINEERING DATA ANDS TO BACK UP CC&S AS REQUIRED	A) RECEIVE, DECODE, & DISPLAY ENGINEERING DATA B) RELAY UPDATED ORBIT INJECTION PARAMETERS C) PROVIDE COMMAND TO INITIATE INSERTION MANEUVER D) PROVIDE BACKUP COMMANDS TO CC&S AS REQUIRED E) TRACK S/C F) VERIFY ORBIT INSERTION	A) RECEIVE, DECODE, & DISPLAY B) RECEIVE AND ANALYZE ENGINEE C) TRACK S/C D) RECEIVE & DISPLAY CAPSULE D E) PROVIDE DATA FOR ORBITAL TR F) RECEIVE VERIFICATION OF ORB G) TERMINATE MISSION
& YAW TURN MAGNITUDE & DIRECTION COMMAND & RELAY NA POSITIONING DATA & RELAY TO CC&S R-BURN START TIME, RELAY TO CC&S LE DATA, CONDITION & RELAY TO GROUND HT SPACECRAFT ENGINEERING, CAPSULE ENGRG, & TO GROUND VIA MODE 2	A) UPDATE ROLL-TURN MAGNITUDE & DIRECTION COMMAND & RELAY TO CC&S B) UPDATE YAW-TURN MAGNITUDE & DIRECTION COMMAND & RELAY TO CC&S C) UPDATE MOTOR-BURN START TIME & RELAY TO CC&S D) UPDATE INITIATE MANEUVER & RELAY TO CC&S E) SWITCH TO DATA MODE NO. 2 OR 5A AS REQUIRED F) REACQUIRE EARTH AFTER ROLL TURNS & MOTOR BURN G) RELAY VERIFICATION OF MANEUVERS	A) TRANSMIT SCIENCE & ENGINEE B) RECORD ENGINEERING & SCIEN C) RECEIVE, STORE & RELAY CAPS D) RECEIVE & RELAY DATA FOR OR
ITCH TO DATA MODE NO. 2 NOPUS CONE ANGLE SETTING ITENNA STEP (AS REQUIRED) IT INJECTION PARAMETERS NAL TO PYRO & MECHANISMS TO DEPLOY SCAN PLATFORM NCE T/M OFF) & SWITCH TO DATA MODE NO. 1 ATA RECORDER-COMMAND TELECOMMUNICATIONS SULE DATA MANDS AS REQUIRED	A) UPDATE STORED ROLL, PITCH, & YAW MAGNITUDE & SIGN B) UPDATE STORED VELOCITY MAGNITUDE C) INITIATE MANEUVER SEQUENCE D) COMMAND ORIENTATION OF S/C TO INJECTION ATTITUDE E) COMMAND THRUST FOR ORBIT INSERTION F) COMMAND RETURN TO CRUISE ATTITUDE G) BACKUP COMMANDS AS REQUIRED	A) COMMAND ORBITAL TRIM MAN B) SWITCH DATA MODES AS NECE C) RECEIVE ANY ORBITAL OPERAT D) COMMAND POSITIONING OF S E) SWITCH ON ORBITAL SCIENCE F) SELECT RECORDED SCIENCE RE G) BACKUP COMMANDS AS REQU H) STORE DATA FOR ORBIT TRIM I) TERMINATE MISSION ON COM
PUS CONE ANGLE ON COMMAND PILOT TO CRUISE MODE C ATTITUDE TO CELESTIAL REFERENCES DURING CRUISE	A) SWITCH TO GYRO CONTROL B) PROVIDE ROLL TO PROPER ATTITUDE & VERIFY ROLL C) YAW TO PROPER ATTITUDE & VERIFY D) AUTOPILOT – PROVIDE COMMAND TO TVC DURING MOTOR BURN E) TURN ON ACCELEROMETER F) PROVIDE ACCELEROMETER DATA TO CC&S G) TURN OFF ACCELEROMETER H) YAW BACK AFTER MOTOR BURN I) ACQUIRE SUN & VERIFY J) ROLL BACK TO PROGRAMMED ATTITUDE K) ACQUIRE CANOPUS & VERIFY L) SWITCH AUTOPILOT FROM GYRO – CONTROL TO CELESTIAL REFERENCE CONTROL	A) MAINTAIN S/C ATTITUDE TO CE B) SWITCH AUTOPILOT TO GYRO C C) REACQUIRE CELESTIAL REFERE D) REORIENT S/C FOR ORBITAL TR E) PROVIDE TVC DURING ENGINE F) REACQUIRE CELESTIAL REFERE G) UPDATE CANOPUS CONE ANGLE
	ORBIT INSERTION ENGINE A) ARM TVC B) ARM IGNITER C) FIRE MOTOR & PROVIDE THRUST & TVC D) TERMINATE THRUST (MOTOR BURNS TO DEPLETION)	MIDCOURSE A) ARM PRESSURIZATION & PRO B) PROVIDE THRUST (FIRE PROG IF REQUIRED C) TERMINATE THRUST ON COMM D) ISOLATE PROPELLANT FEED SU E) ISOLATE PRESSURIZATION SU
DITIONED SOLAR ELECTRICAL POWER TO: REF CONTROL DRE CONTROL ERIES	A) PROVIDE CONDITIONED SOLAR OR BATTERY POWER TO: • TELEMETRY • CC&S • ATTITUDE REFERENCE SUBSYSTEM • AUTOPILOT • TEMPERATURE CONTROL • PULSE TO PYROTECHNICS • PULSE TO PROPULSION	A) PROVIDE CONDITIONED SOLA • TELEMETRY • CC&S • ATTITUDE REFERENCE SUBS • AUTOPILOT • TEMPERATURE CONTROL • STRUCTURES & MECHANIS • SCIENCE
ASSEMBLIES COMPONENTS EQUATE ALIGNMENT BETWEEN COMPONENTS EPTABLE STATIC & DYNAMIC LOAD ENVIRONMENTS PLATFORM TO DEPLOYED POSITION & LOCK	A) SUPPORT S/C ASSEMBLIES B) SUPPORT S/C COMPONENTS C) MAINTAIN ADEQUATE ALIGNMENT BETWEEN COMPONENTS D) PROVIDE ACCEPTABLE STATIC & DYNAMIC LOAD ENVIRONMENTS	A) SUPPORT S/C ASSEMBLIES B) SUPPORT S/C COMPONENTS C) MAINTAIN ADEQUATE ALIGNM D) PROVIDE ACCEPTABLE STATI ENVIRONMENTS E) POSITION SCAN PLATFORM
ATURE CONTROL	PROVIDE TEMPERATURE CONTROL	PROVIDE TEMPERATURE CONTROL
IRING SIGNAL FOR UNLATCHING RM	A) RECEIVE & EXECUTE COMMAND SIGNAL TO REMOVE INHIBIT FOR PROPULSION ENGINE B) RECEIVE & EXECUTE SIGNAL FOR PROPULSION ENGINE START C) RECEIVE & EXECUTE COMMAND SIGNAL FOR PROPULSION ENGINE STOP D) RECEIVE & EXECUTE SIGNAL FOR PROPULSION INHIBIT	
SE SCIENCE "ON" COMMAND HSE SCIENCE DATA NDITIONED DATA TO DAE ER FROM E/P SCIENCE EXPERIMENTS AS REQUIRED	SCIENCE OFF DURING ORBIT INSERTION	A) TURN ON ORBITAL SCIENCE B) ACQUIRE ORBITAL SCIENCE C) TRANSFER CONDITIONED DA D) RECALIBRATE SCIENCE EXP
"ON" COMMAND RANSFER DATA TO TM		A) RECEIVE DAE "ON" COMMA B) PROCESS & TRANSFER DAT

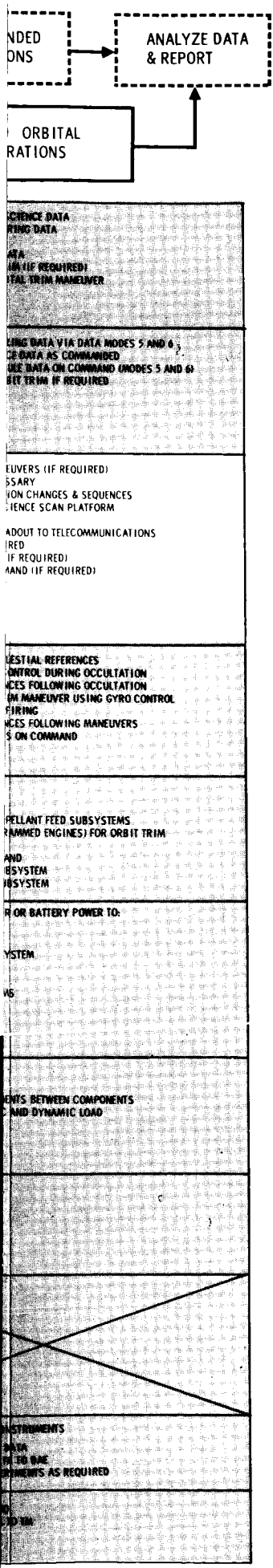

Mission Sequences Matrix

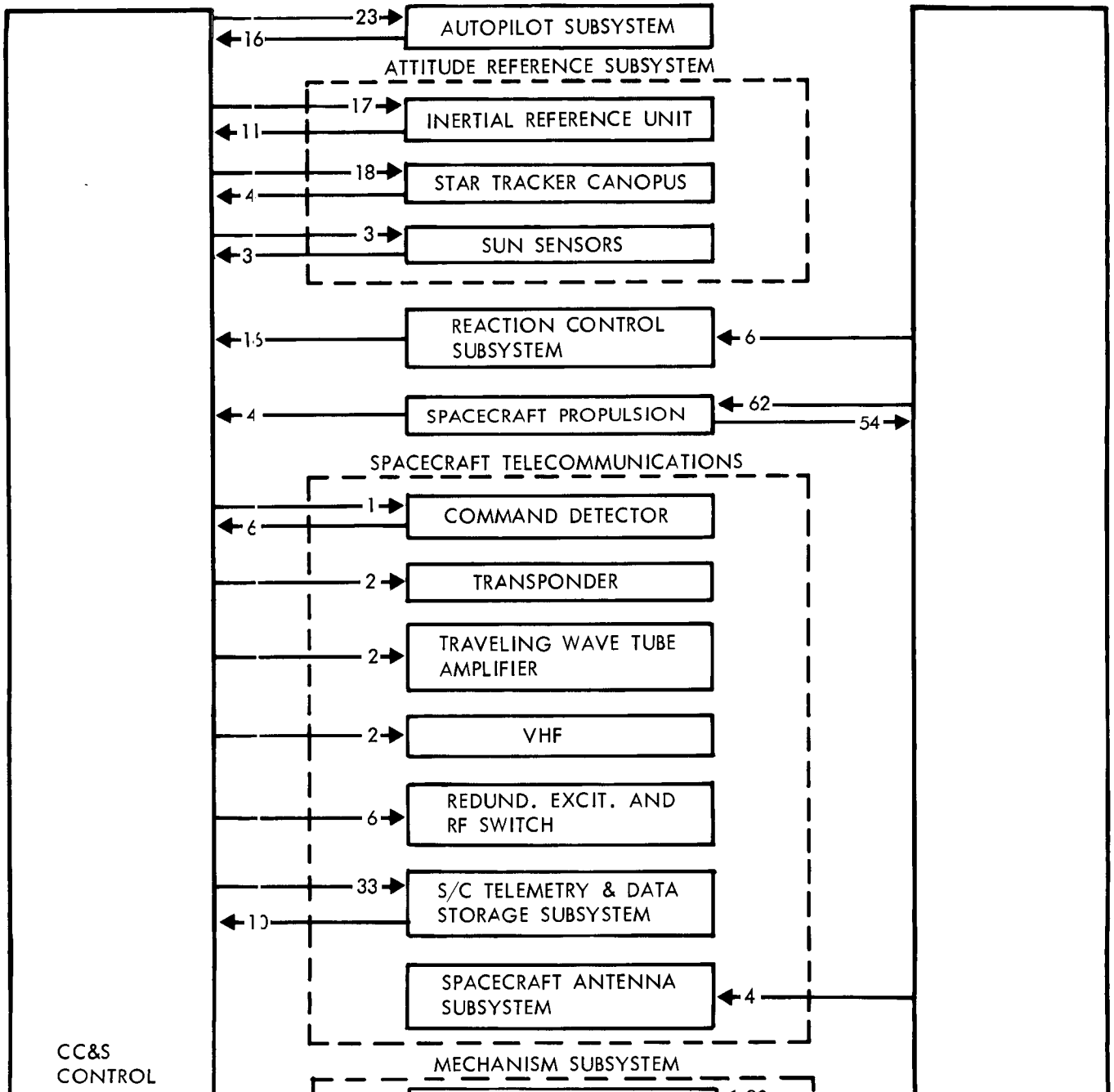
AUTOPILOT SUBSYSTEM
23
16
ATTITUDE REFERENCE SUBSYSTEM
INERTIAL REFERENCE UNIT
17
11
STAR TRACKER CANOPUS
18
4
SUN SENSORS
3
3
REACTION CONTROL SUBSYSTEM
15
6
SPACECRAFT PROPULSION
4
62
54
SPACECRAFT TELECOMMUNICATIONS
COMMAND DETECTOR
1
6
TRANSPONDER
2
TRAVELING WAVE TUBE AMPLIFIER
2
VHF
2
REDUND. EXCIT. AND RF SWITCH
6
S/C TELEMETRY & DATA STORAGE SUBSYSTEM
33
10
SPACECRAFT ANTENNA SUBSYSTEM
4
CC&S CONTROL
MECHANISM SUBSYSTEM

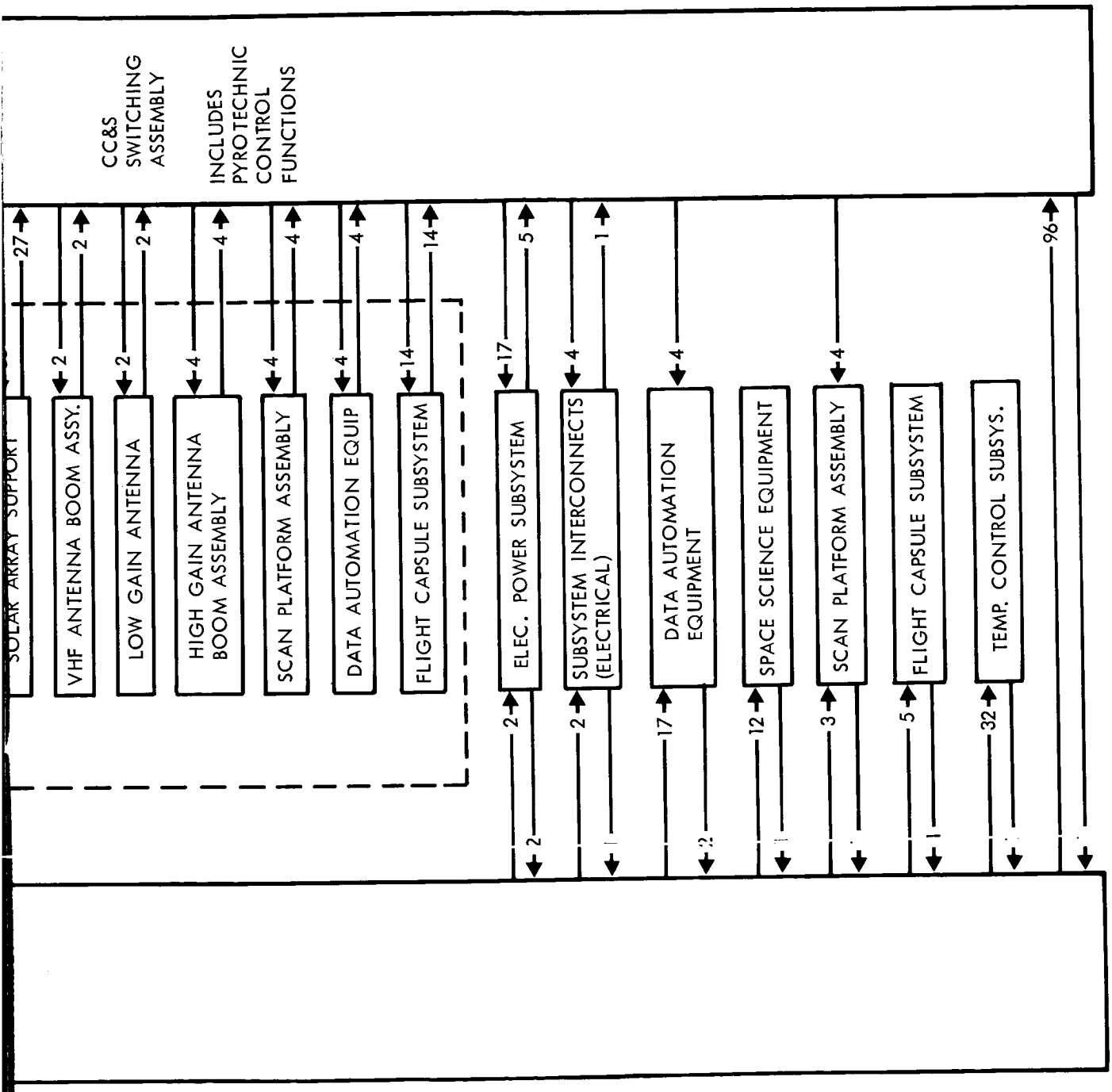

For further information see Figure 4.8-14 and 4.8-15.

Figure 4.8-4: CC & S — Spacecraft Subsystems Interface Block Diagram

4.8.1.2 Major Design Concepts, Requirements, and Constraints

Long-term reliability, minimum ground-to-spacecraft command transmission, repetitive command sequences with few variables, low weight and power consumption, and growth capability are prime factors influencing the design.

The proposed design for the CC&S provides for storage of all preplanned mission events. Normal operation of the spacecraft requires ground-to-spacecraft transmissions only for commanding mission variables. In addition, the CC&S can accept commands from mission operations to reprogram, override, correct errors, and initiate emergency modes. Reliability, the use of space-proven equipment, and performance versatility were factors that lead to the selection of a modified version of the NASA Lunar Orbiter programmer. Reliability is also gained by minimizing the ground-to-spacecraft transmission as the primary control. Ground-to-spacecraft transmission is used as an emergency mode whereby the control and commands can be modified. The entire program of command routines and subroutines is stored in the memories prior to launch. Mission variables (such as roll, pitch, and yaw angular changes; velocity change; and change of times for initiating event execution) are the only commands that must be transmitted, and can be transmitted any time prior to the event. Spacecraft time is generated by the CC&S and event initiation is accomplished by comparison to the onboard time.

Program control will reuse event command sequences, thus minimizing memory storage requirements for repetitive sequences. Program control words

used to execute magnitude commands are address-modified so that the variables are used sequentially each time the command is repeated.

The CC&S is the central element for functional interfaces with the spacecraft subsystems. The preliminary design effort has identified 333 output functions, 68 input functions, and 537 wires as interfaces. This large number of interfaces imposes a design restraint that the CC&S must be able to accommodate changes, both physical and functional, throughout the development and operational phases of the program.

4.8.2 Applicable Documentation

Boeing Documentation

1) D2-82724-3
   "Voyager Program - Reliability Analysis and Prediction Standards"
2) D2-82724-1
   "Voyager Reliability"
3) D2-100234 (Lunar Orbiter)
   "Programmer Functional Analysis"
4) D2-100259 (Lunar Orbiter)
   "Failure Mode and Criticality Analysis"

4.8.3 Functional Description

4.8.3.1 Design

The preferred configuration is presented in the following paragraphs.

Control Assembly--The control assembly consists of two complete data processing units, each containing a 128-word memory. The independent systems are parallel redundant to meet the reliability goal of 0.9940. Both outputs until commanded to switchover. Switching between the two processors outputs until command to switchover. Switching between the two processors will be accomplished by either real time or stored program command. When the switchover command occurs it will cause the issuing-data processor to go to a nonoperational mode and the other data processor to go to the next instruction provided within its own memory. This feature allows continuous transmitted command access to either memory for purposes of program updating, revising, or initiating the program routine in the unused system as the mission progresses. The control assembly is shown in the functional block diagram of Figure 4.8-5.

The control assembly has an input function which controls two running modes of the system. One mode prohibits execution of the stored program, but allows memory loading and verification. Discrete real-time-commands can override this control. The second mode allows normal execution of stored commands, real-time-commands, memory loading, and 11 spacecraft functional interrupts. The second feature is used to control the selection of a redundant system. One output function of each system is an on-off type of command that is directed by ground real-time-command or stored-program-command and provides the input function of mode control to either system.

Description of the control assembly is presented by defining the functions of each unit (individual blocks) shown in Figure 4.8-5.

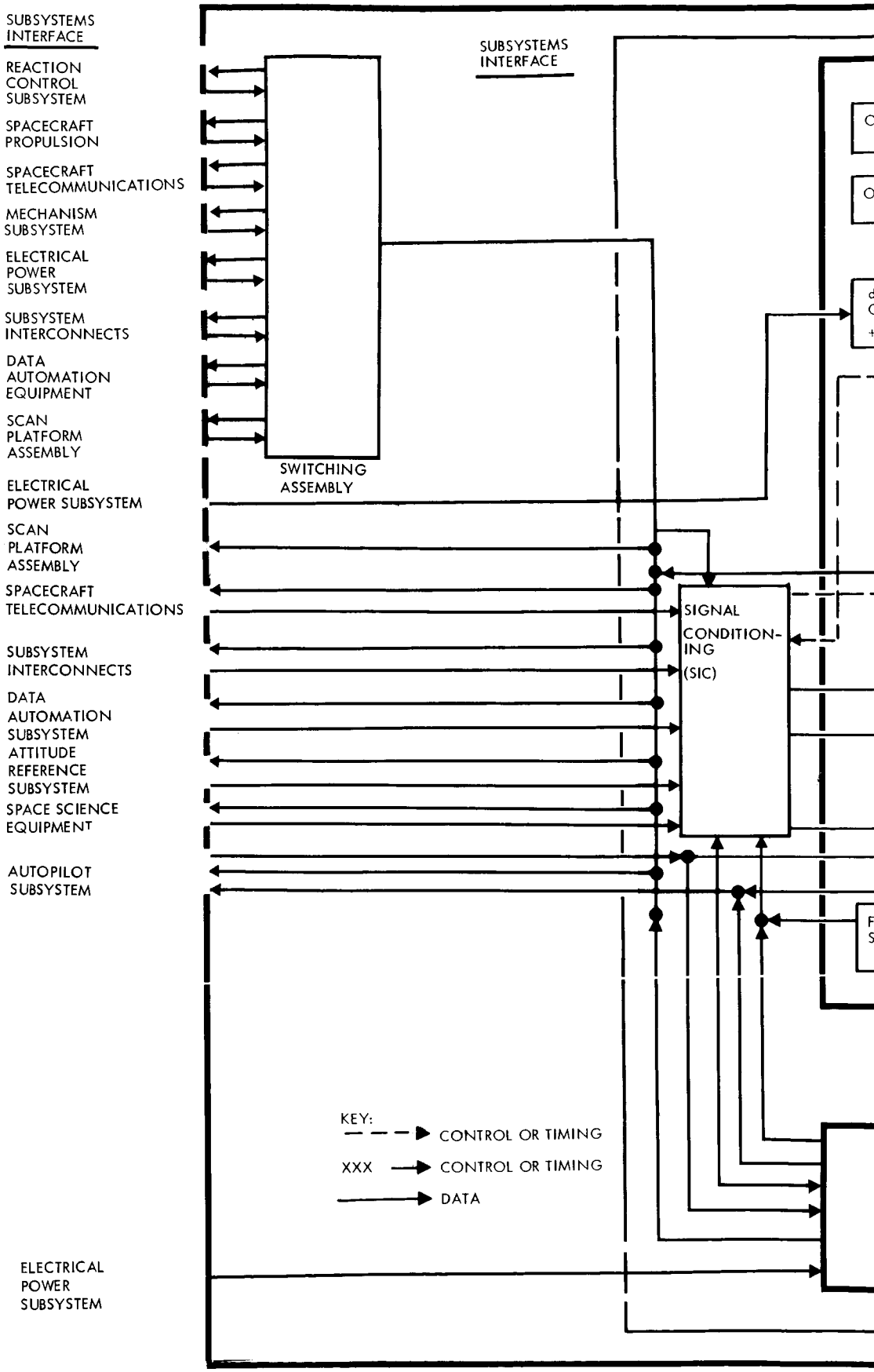
SUBSYSTEMS INTERFACE
REACTION CONTROL SUBSYSTEM
SPACECRAFT PROPULSION
SPACECRAFT TELECOMMUNICATIONS
MECHANISM SUBSYSTEM
ELECTRICAL POWER SUBSYSTEM
SUBSYSTEM INTERCONNECTS
DATA AUTOMATION EQUIPMENT
SCAN PLATFORM ASSEMBLY
SUBSYSTEMS INTERFACE
SWITCHING ASSEMBLY
ELECTRICAL POWER SUBSYSTEM
SCAN PLATFORM ASSEMBLY
SPACECRAFT TELECOMMUNICATIONS
SUBSYSTEM INTERCONNECTS
DATA AUTOMATION SUBSYSTEM
ATTITUDE REFERENCE SUBSYSTEM
SPACE SCIENCE EQUIPMENT
AUTOPILOT SUBSYSTEM
SIGNAL CONDITION-ING (SIC)
KEY:
CONTROL OR TIMING
XXX CONTROL OR TIMING
DATA
ELECTRICAL POWER SUBSYSTEM

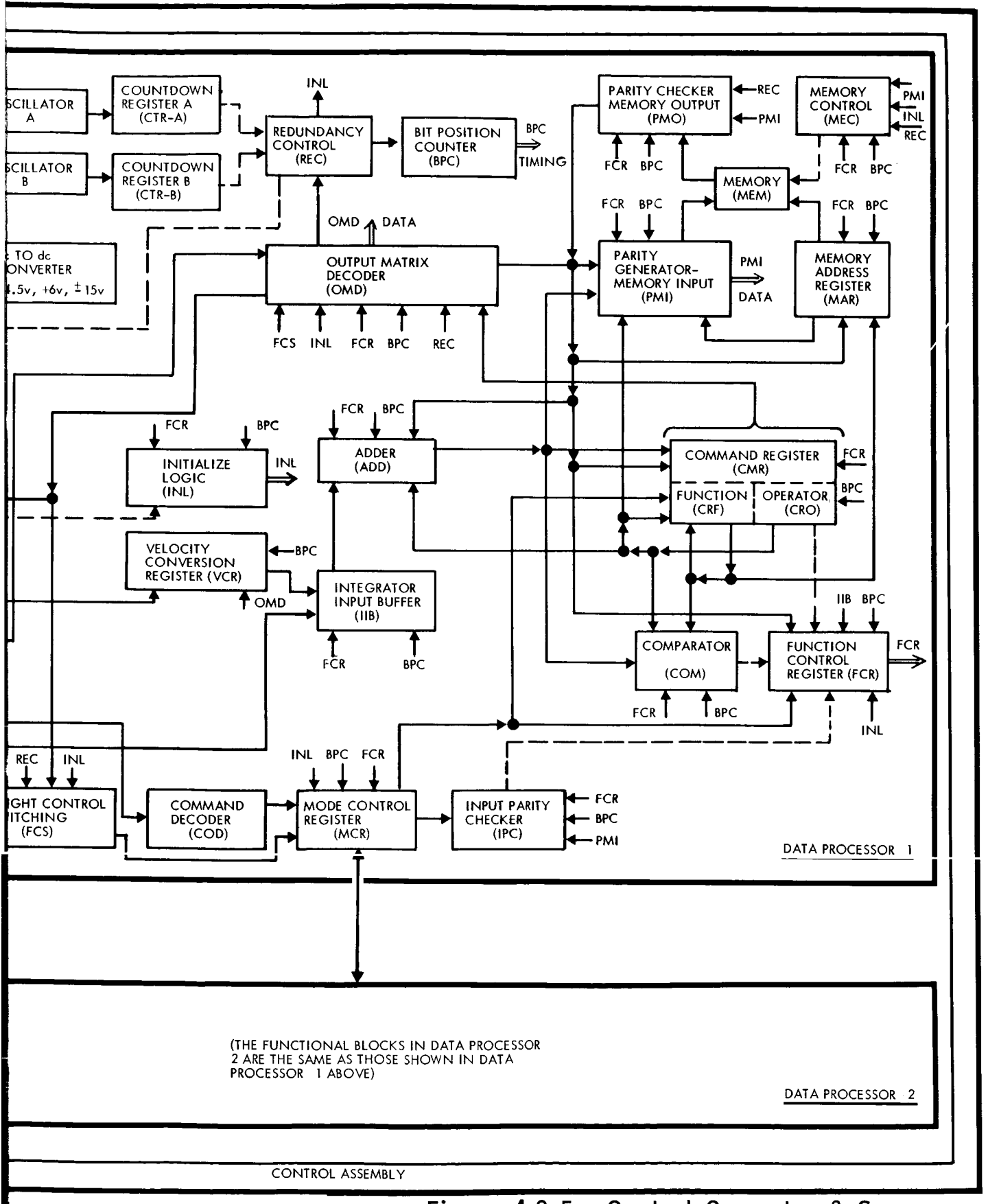

Figure 4.8-5: Central Computer & Sequencer Control Assembly Functional Block Diagram

Signal Conditioner (Inputs)--Each redundant-data processor receives control signals from the common input circuits in the signal conditioner. Twenty-three integrated circuits are employed to convert subsystem voltage levels to the voltage level of the CC&S logic. The circuits also provide noise suppression, load isolation, and minimum susceptibility to short-circuits.

Command Decoder--The command decoder is required for buffering the 1-bit-per-second bit-rate of the command detector output in the telecommunications group to the 2.4 kc bit-rate of the CC&S processing logic. Specifically, the command decoder must (1) receive a command detector in-lock signal indicating data is being received; (2) receive the bit synchronization and 27 data bits; (3) recognize 26 binary zeros prior to the command word bits; (4) recognize a 4-bit pre-set command address; (5) accumulate the entire word before command execution, and (6) hold the entire word for telemetry retransmission. This unit performs a function that is not provided in the NASA Lunar Orbiter program and must be added to accommodate the Voyager design.

Modification alternates to incorporate the command decoder are: (1) provide additional separate sequencing logic and utilize existing storage, and (2) provide additional separate sequencing and storage to accept and accumulate the commands.

The candidate modification (1) would require redesign of the program control logic (function-control register) because the transmitted bit-rate is incompatible with the CC&S data-processing rate. Method 1 decreases

the alternate command paths within the processor. Although this method reduces the parts count (60 vs 80 microcircuits), it does not improve the functional reliability and is therefore an unattractive configuration because of program control logic redesign and loss of alternate command paths.

Method (2) is the selected design and can be implemented without disturbing proven logic design. Method (2) is presented in more detail in the following paragraph.

Bit information and a receiver-in-lock signal is received from the command detector located in the telecommunications group. Twenty-six consecutive zero bits are counted prior to decoding the spacecraft address portion of the message. If consecutive zeros do not occur, or if the receive-in-lock signal is interrupted, the counter is reset and message decoding will not proceed. If the 4-bit decoded spacecraft address agrees with the present address, the remaining command word is routed to the function control register and command register through the mode control register for CC&S processing.

The four spacecraft address flip-flops in the command decoder are initialized during power turn-on. A command word, whose address coincides with the initialized address, is used to reset the address flip-flops to one-of-seven codes particular to each spacecraft. All command words following this address command must have a coinciding address for acceptance. This feature provides versatility and mission independence for the CC&S command decoder design.

Command Register--Command words, from memory or command decoder, are held in this 20-bit register for decoding by the output matrix decoder. The register provides parallel, complemented, and uncomplemented outputs to the output matrix decoder. When time or quantitative commands are being compared, the constant value is circulated in this register and sent to the comparator for comparison with integrated values.

Mode Control Register--The mode control register accepts command information and nine signal interrupts from spacecraft telecommunications, and two occultation signals from the attitude reference subsystem. It sets up the CC&S for:

1) Real-time or stored-program operation;
2) Interrupt commands (stop stored program and execute new command word); and
3) Information requests (telemetry and spacecraft time).

Input Parity Checker--The input parity checker checks the input word from the communications receivers for even parity with two parity bits (bits 26 and 27) as illustrated in Figure 4.8-6.

Function Control Register--The function control register holds the present five-bit operation code and functional mode of the CC&S and combines them with programmer timing to direct the information flow through the programmer. The function control register also controls changes in the programmer operating mode that originate within the programmer.

GROUND TRANSMITTED COMMAND WORD FORMAT

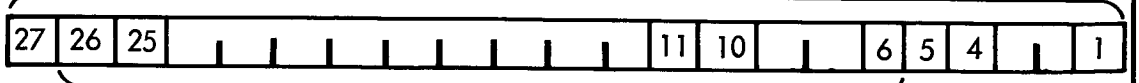

INTERNAL COMMAND WORD FORMAT

BIT NUMBER (1-27)	FUNCTION OR STATE
1 THRU 4	SPACECRAFT ADDRESS
5	TRUE: REAL TIME COMMAND FALSE: STORED PROGRAM COMMAND
6 THRU 10	OPERATION CODE
11 THRU 25	MAGNITUDE OR FUNCTION
26	EVEN PARITY FOR BITS 5-17
27	EVEN PARITY FOR BITS 18-25

GROUND TRANSMITTED TIME WORD FORMAT

INTERNAL TIME WORD FORMAT

BIT NUMBER (1-27)	FUNCTION OR STATE
1 THRU 4	SPACECRAFT ADDRESS
5	FALSE: STORED PROGRAM THIS BIT MUST BE FALSE
6 THRU 25	TIME WORD: 0 to 29.1 HOURS
26	EVEN PARITY FOR BITS 5-17
27	EVEN PARITY FOR BITS 18-25

Figure 4.8-6: Ground Transmitted and Internal Word Formats

Adder--This unit is a half-adder and has logic circuitry which adds 1 bit at a time to a value stored in the memory. The adder is used to add time, position and velocity increments, to increment addresses and to increment the remaining times a jump command can be executed.

Integrator Input Buffer--The integrator buffer receives and holds single increments corresponding to position and velocity until the programmer is ready to receive the information. The buffer also subtracts one from the velocity conversion register when the integrator buffer accepts an increment.

Velocity Conversion Register--The velocity conversion register detects the difference between two different frequencies impressed on it. The input frequencies are in the form of two separate frequencies whose rate sum is constant; the difference rate is variable and proportional to the disturbance measured by the accelerometer. The difference frequency is scaled into 0.1 foot-per-second increments for midcourse velocity changes and orbit trim, and 0.5 foot-per-second increments at orbit insertion.

Memory Address Register--Seven address bits, held in this register, control the addressing of words read in or out of the memory. Addressing of special-purpose memory words, as commanded by the function control register, overrides, but does not destroy, the contents of the memory address register flip-flops. This technique allows all indexing and address-modification-registers to be contained in the memory instead of external flip-flop-registers.

Memory--The memory consists of a magnetic-core plane with associated discrete part-read-and-write circuitry. The memory contains 128-bit word-storage which may be randomly selected. Read in/read out of the 21-bit word is serial, controlled by an internal counter. The basic bit cycle is read/modify/write. The memory accepts data from the command register and adder. Eight specific word locations are employed as spacecraft time-accumulation-register, magnitude-integrating-register, next instruction-address-register, store program word-address-register, occultation time recording registers, interrupted instruction and address-register and telemetry word-transfer. The use of these special word locations reduces the number of active circuit registers. This results in a reduction of power consumption and weight. The selected memory has growth capability.

Additional memory capacity can be incorporated in the CC&S easily by either of two alternate methods.

1) The presently available Lunar Orbiter memory could be modified by doubling the number of cores and increasing the circuitry by approximately 50 percent.
2) Two Lunar Orbiter memories could be incorporated in each processor.

Method 1) imposes a minimum modification on the data proacessor, requiring only the addition of 3 microcircuit flatpacks. This method requires a memory redesign, new specifications, and new testing, which makes this approach undesirable.

Method 2) imposes a modest modification to the data processor requiring 20 microcircuit-flatpacks to interface with the additional memory. This

method has the advantage of using a memory that is off the shelf and providing redundancy in the memory function of the data processor. Method 2) would be a preferred approach if system programming requirements increase to exceed present memory capacity.

Parity Generator - Memory Input--This unit provides buffering between the memory and the programmer logic. The parity generator also provides an even parity bit in bit-position 21 for words transferred into memory.

Memory Control--The memory control gates a 4.8 kc pulse train necessary to read in or read out 21-bit words from memory in phase with the programmer operation. The memory control is controlled by the function-control register and programmer timing.

Parity Checker-Memory Output--This unit provides buffering between the memory sense amplifier and the programmer logic. The parity checker-memory output unit also provides an even parity check on the 21-bit words coming from the memory.

Comparator--The comparator provides serial comparison between a constant value from the command register and an incremented value from memory. Twenty-bit time words, and 15-bit attitude and velocity words are compared. When comparison is reached, the comparator provides a logic signal which causes the CC&S to proceed to the next instruction.

Oscillators and Countdown Register--There are two crystal oscillators in each data processor. Each oscillator drives a countdown register from which all CC&S frequencies and timing are derived. The crystal oscillator

is assembled with discrete parts and provides a basic 614.4 kc output frequency. The oscillator provides an extremely stable, jitter-free clock frequency with an accuracy of 1 part in 10^6. The countdown register generates 0 to plus 4.5 v d.c. square-wave trains of the following frequencies: 614.4 kc; 307.2 kc; 153.6 kc; 76.8 kc; 38.4 kc; 19.2 kc; 4.8 kc; 800 cps; 400 cps; 100 cps; 50 cps; and 10 cps. Two clock-and-countdown registers are used in the system. They are controlled by the redundancy control.

Redundancy Control--The redundancy control provides switching, in event of failure, between the two countdown registers. Control is exercised by a real-time command word through the opposite processor.

Bit-Position Counter--Frequencies (4.8 kc through 10 cps) from the countdown register are combined into distinct intervals of time for purposes of shifting information within the data processor units. Periods of word times, word time portions, and bit times are generated in this unit.

Output Matrix Decoder--Decoding matrices and necessary logic elements provide unique commands and signal formats to all required spacecraft instruments and subsystems. Pulse commands, on-off commands, timing bursts, and gated sequences are formed in this unit. The output gate for each command function also performs the low-level signal-conditioning.

CC&S logic voltage levels are converted to the voltage and current parameters required by each instrument and subsystem. Discrete circuit amplifiers are used. The circuits also provide short circuit protection and meet electro-interference requirements of the spacecraft. The majority of spacecraft functions have redundant output signal conditioner circuits.

High-level signals and their drivers are electrically and physically isolated from low-level signals and devices. High-level signal circuits are enclosed in the switching assembly which is presented in the following section.

Flight Control Switching--Commands from the output matrix decoder, and Sun and Canopus presence signals are combined to provide modes of control for the autopilot subsystem in roll, pitch, and yaw axis, as well as selecting gyro modes of rate or rate integration.

DC to DC Converter--The dc-to-dc converter converts spacecraft voltage into plus 4.5 volts, plus 6 volts, plus 15 volts, and minus 15 volts for the integrated logic circuits, memory and signal conditioning. The converter also provides voltage to the switching assembly.

Initiate Logic--The initiate logic is used to set the internal state of the data processor when power is first turned on to the subsystem. This sets the entire output matrix in the necessary output state. When the subsystem is in the spacecraft and power is applied, the state of the output matrix will determine whether power is turned on or off to those spacecraft elements where power is controlled by the CC&S. Commands must then be issued to the subsystem. To change the power state, the data processor is placed in a nonoperational mode by the initiate logic when power is turned on and must also be commanded from this state if required.

Switching Assembly--The CC&S switching assembly is described in Figure 4.8-7. Low-level signals from the control assembly are converted in the switching assembly to high-current (5-10 amperes) or voltage level (35 volts) signals.

The arming switches are closed by umbilical command and their actuation monitored prior to launch. The inhibit switches provide further protection against inadvertent firing of the squibs. The squib drivers are directly connected to the squib bridgewires. Most of the squib devices require redundant driver circuits and are implemented as shown in Figure 4.8-8. This assembly provides isolation of large signal-transient and electro-magnetic fields from other equipment.

Pyrotechnic switching is further described in Paragraph 4.4.

Command-Word Format--The ground-transmitted command word consists of 27 information-bits, preceded by 26-zero-bits. The order of transmitting the information word begins with the least-significant bit. A receiver in-lock signal is to accompany the data. The ground-transmitted word format, as received by the command decoder, is illustrated in Figure 4.8-6. The four-bit spacecraft address must agree with the address logic to enable word execution. The parity bits are associated with the command-word bits only. The word-error probability for onboard verification is calculated to be 1.27×10^{-8} errors per word. When the word is verified by telemetry return to Earth, the word-error probability becomes 3.18×10^{-13}.

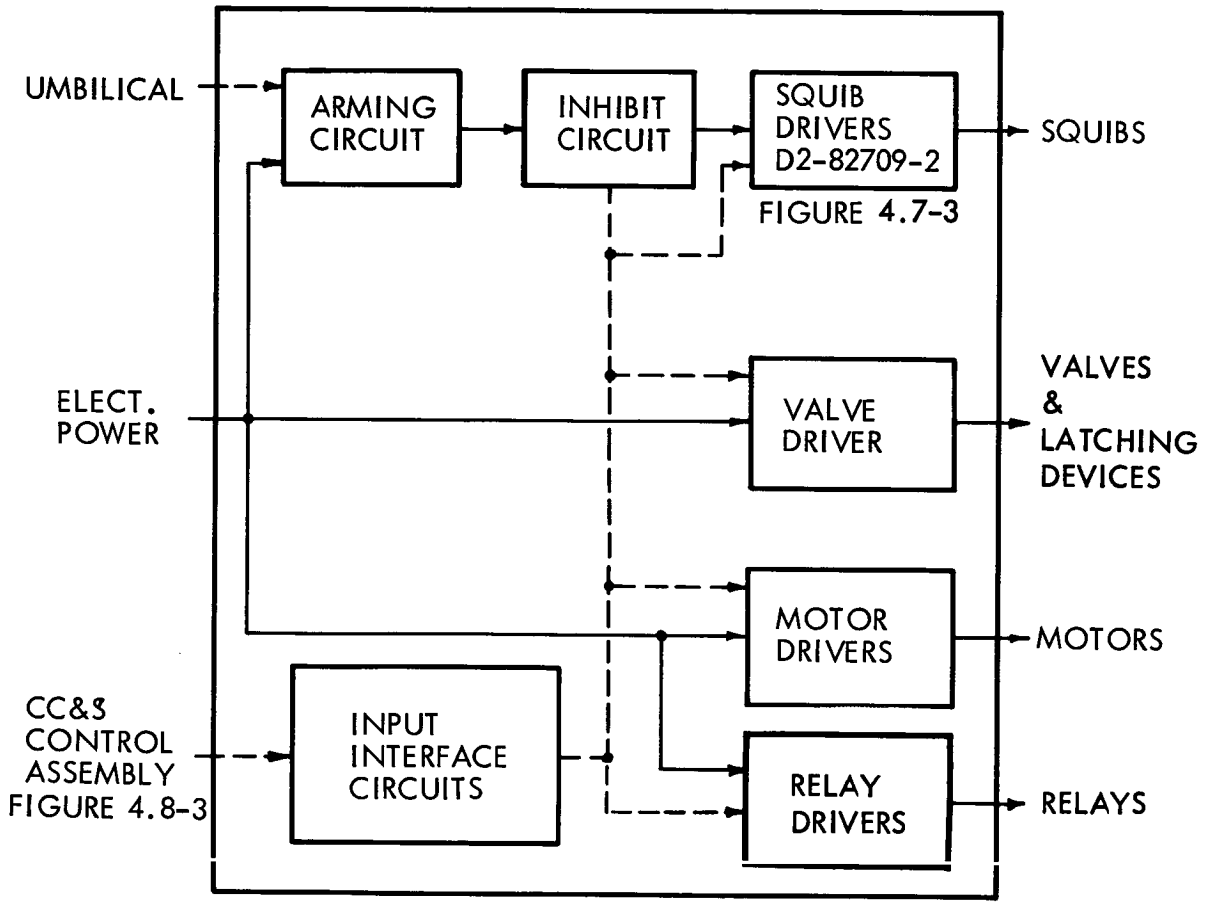

Figure 4.8-7: Switching Assembly

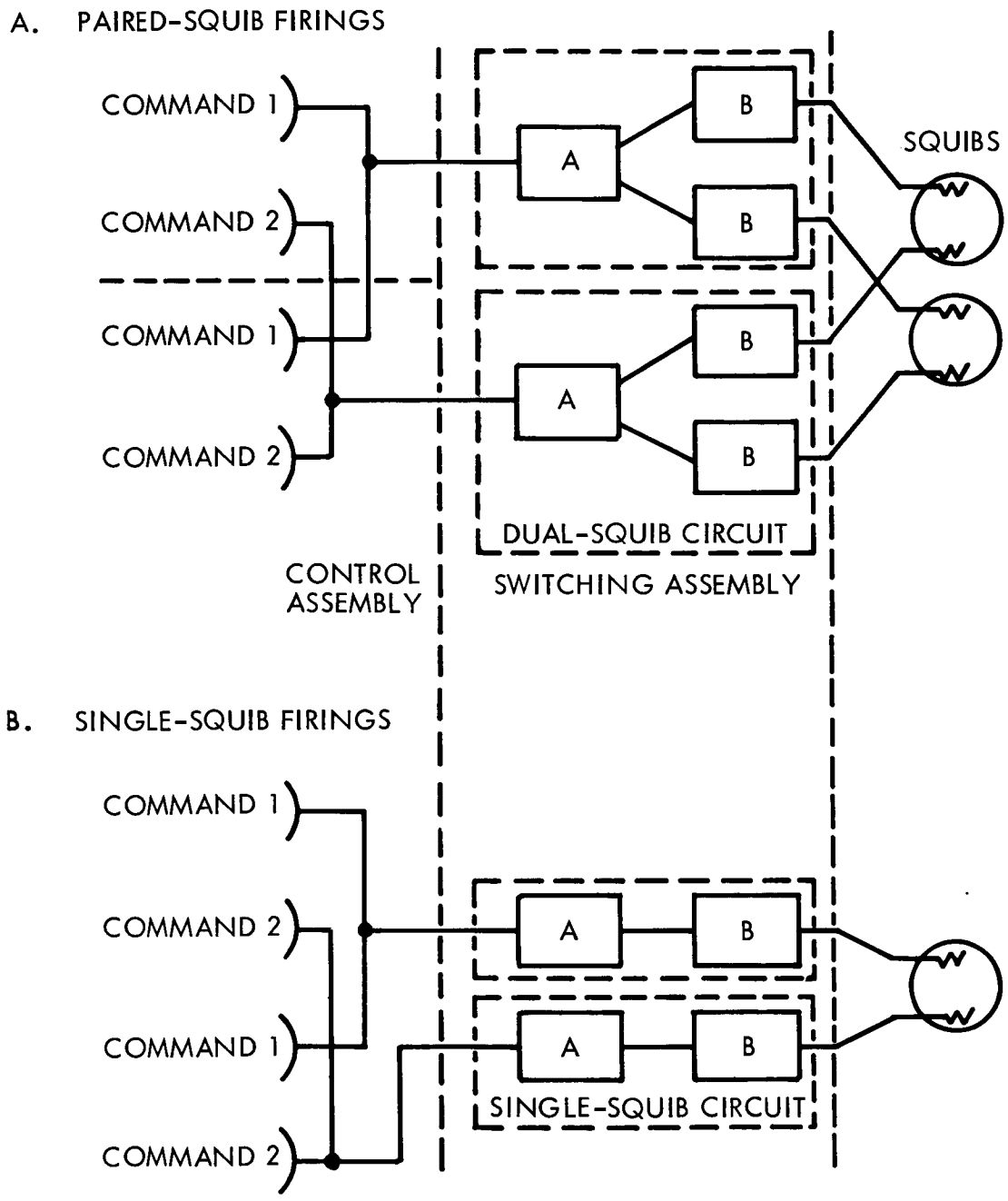

CIRCUIT A FAILURE RATE 0.01228×10^{-6}/hr

CIRCUIT B FAILURE RATE 0.11256×10^{-6}/hr

Figure 4.8-8: Squib Firing Configuration

The first bit of the internal command-word determines a real-time or stored-program mode of operation and is eliminated as the word is transferred from the command decoder.

Instruction Sets--Command word instructions are separated into two sets: those instruction words that control internal functions of the CC&S; and those instruction words that control spacecraft subsystem functions external to the CC&S. Incoming messages are shifted into the command decoder until the entire 27 bits are received. The four-bit spacecraft address code is verified in this unit and is discarded as the message is transferred to the mode-control register. The command word is contained in bits designated 2 through 21. Bit 1 indicates real-time command or stored-program-command and is discarded as the word shifts through the mode control register.

Internal CC&S Commands--The internal operation performed is designated by bits 2 through 6. Commands that are for real-time use, that is, do not require storage, are ignored if they are accidentally stored. Conversely, operations that are intended for stored-program use only are ignored when accompanied with a real-time bit. Description of the internal codes follows:

1) Telemeter Memory (TEM)--Real-time command only. Bits 7 through 13 designate the memory address of the word desired to be telemetered. The address word is transferred to a special memory location which serves as a holding register until it can be transferred to the telecommunication group. This command is used to verify specific stored commands.

2) Wait Time (WAT)--Stored-program command only. Any single bit within bits 7 through 21 represents a binary constant which is added to the present spacecraft time and then compared until equality occurs. Used as a delay between commands.

3) Compare Time (COT)--Stored-program command only. Bits 7 through 13 designate the memory address of a 20-bit word to be compared to spacecraft time. The 20-bit constant is compared until equality is accomplished before executing the next instruction. It is used to initiate an event at a desired spacecraft time. The address is indexed each time the command is executed so that a new value is compared when the command is repeated.

4) Execute Magnitude Minus (EMM)--Stored program command only. Bits 7 through 13 designate the memory address of a spacecraft magnitude command. The address is indexed each time the command is executed so that a new magnitude value is compared when the command is repeated. The minus sign is algebraically added to the spacecraft magnitude command sign to control the maneuver direction.

5) Execute Magnitude Plus (EMP)--Same as EMM except for sign.

6) Store Program Address (SPA)--Real-time command only. Bits 7 through 13 designate the address where the next stored program word transmitted from ground is to be stored. The address is indexed each time a stored program word is received so that the words are sequentially stored until a new SPA command is received.

7) Terminate (TER)--Real-time command only. The function bits (7 through 21) have no significance. The command is used to terminate the present stored program command and advance to the next instruction. Used primarily as a backup command to stop a comparison of time or magnitude.

8) Jump (JMP)--Bits 7 through 13 designate the address of the next instruction to be executed from memory. Bits 14 through 21 is an eight bit binary number, in two's complement form, equivalent to the number of times that the command can be executed. Each time the command is used, the number is incremented. When all zeroes occur because of overflow, the address of the JMP command is ignored and the program advances to the next sequential instruction. When used as real-time command, the present stored program is interrupted and jumps to the address designated by the JMP command. The real-time JMP command is not reused.

9) Jump Modified (JPM)--Same as jump except the address is indexed and there is no limit to the number of repeated executions. Used to select different subroutines.

External CC&S Commands--Eight operation codes provide magnitude commands. Seven operation codes provide discrete functions in independent order and one operation code is provided for sequential discrete functions. All spacecraft commands can be issued as real time or stored-program commands. Description of the external codes follows:

1) Velocity - Low Thrust (VEL)--The fifteen bits of binary magnitude are equivalent to the desired velocity change in 0.1 foot-per-second increments. The command causes low-thrust engine burning and integration of acceleration is compared to the fifteen-bit constant. When equality is achieved, the VEL command is terminated and the program advances. In the real-time mode, the command is valid only when addressed by an internal EMP command.

2) Velocity High Thrust (VEH)--This command initiates firing of the high-thrust, solid-propellant engine. Accelerometer outputs are summed to determine the resultant spacecraft velocity change. The maneuver is timed.

3) Pitch Plus (PIP)--The fifteen-bit binary magnitude is equivalent to 1/200th of a degree of angular movement about the pitch axis. Integration-of-gyro rate is compared to the constant and equality terminates the command. In the real-time mode, the command is used directly and causes a plus-rotation. In the stored-program mode, the command is valid only when addressed by an internal EMP or EMM command. When addressed by an EMP command, the direction of rotation is positive; and an EMM command causes a negative rotation.

4) Pitch Minus (PIM)--Same as PIP except for sign.

5) Roll Plus (ROP)--Same as PIP except movement is about the roll-axis.

6) Roll Minus (ROM)-- Same as ROP except for sign.

7) Yaw Plus (YAP)--Same as PIP except movement is about yaw-axis.

8) Yaw Minus (YAM)--Same as YAP except for sign.

9) Discrete Commands (COM, CON, ACF, ACS, DHS, DAE, CAP)--The seven operation codes are combined with their respective fifteen-bit function codes to produce fifty-two unique function commands per operation code. The function commands are fifty-millisecond pulses to the required spacecraft subsystem or flip-flops are controlled to produce on-off commands.

10) Sequential Discrete Commands (DEP)--Squib firings are numerous and are performed in a defined ordered sequence. The function bits are indexed, each reusing the same command word.

Programming--Maximum efficiency of storage space is obtained by combining individual discrete functions into subroutines that are addressed from a master sequence and reusing as many subroutines as possible. Discrete command words are formatted to provide a maximum number of independent subsystem functions that may occur simultaneously. A typical event sequence for the mission profile is shown in Figure 4.8-9. A corresponding program flow diagram is shown in Figure 4.8-10. Each subroutine returns the program to a compare time which will control the time when the next event is executed. The mission profile command decision block is a series of jump commands directing the program to the various subroutines. A total of 240 command words are estimated for the flight mission. One memory

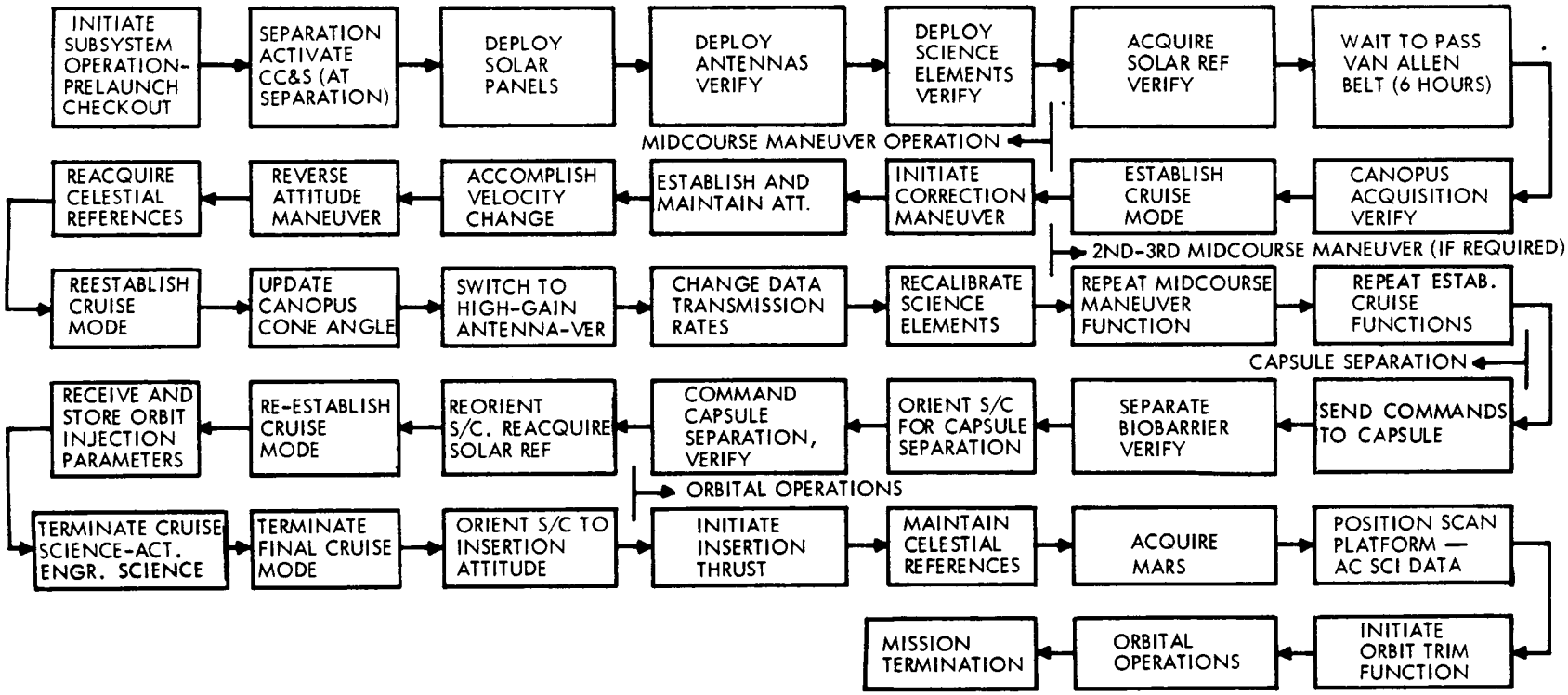

Figure 4.8 -9: Mission Event Sequence — Typical

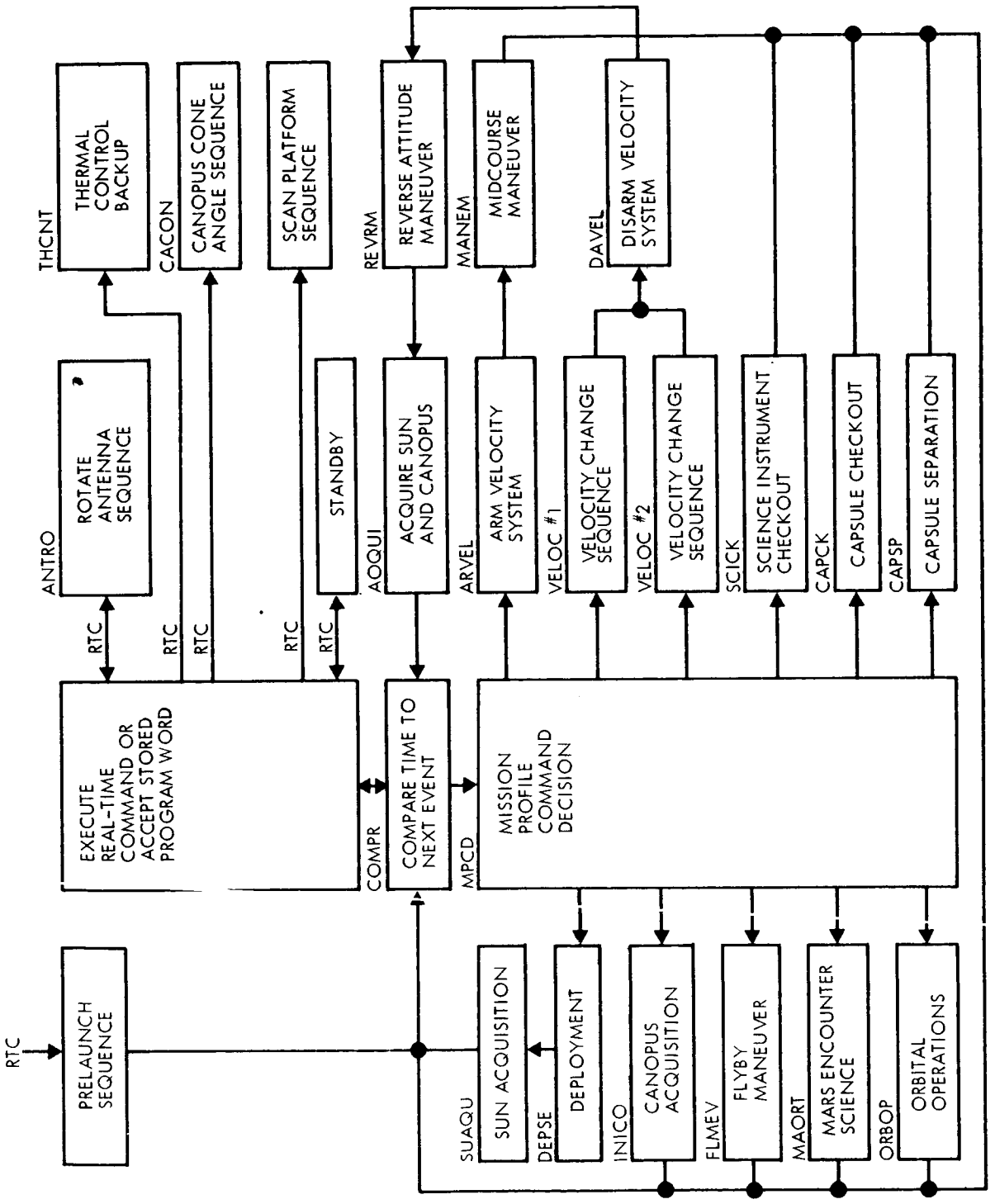

Figure 4.8-10: CC&S Programmer — Flow Diagram

and its processing logic is exercised until the stored program has been executed. The last word of this program causes control to switch to the other memory unit and its processing logic, from which point the flight program continues.

The CC&S clock is implemented with a 20-bit word that is incremented every 0.1 second, and provides a 29.1-hour recycle period. The compare time (COT) command is only capable of equality comparison for a specific time within the recycle period. Because the time between major events is much longer than this period, a special routine shown in Figure 4.8-11 is required for extending the effective time comparison with three-word memory locations. This example is for a 1386-hour, 15-minute, 28-second period.

Stored-word commands will be transferred from the CC&S to the capsule by a minor modification to the control logic of the NASA Lunar Orbiter programmer. In the existing programmer, a real-time telemeter memory command causes a word-transfer from the addressed location specified by the command to a special address for transfer to the telemetry subsystem. A telemetry interrupt causes the transfer of a 20-bit word at a 2.4 kc rate, within a specific 10-millisecond period. The Voyager CC&S would perform this same operation except that the telemeter memory command would be a stored word. When executed it would cause a transfer from the designated address location to another special address for transfer to the capsule. The instruction command will also simulate the interrupt to cause transfer to the capsule. The transfer occurs at the same rate and the entire sequence is performed within the 100 millisecond cycle time of the CC&S. Any (more than 5) number of commands can be transferred.

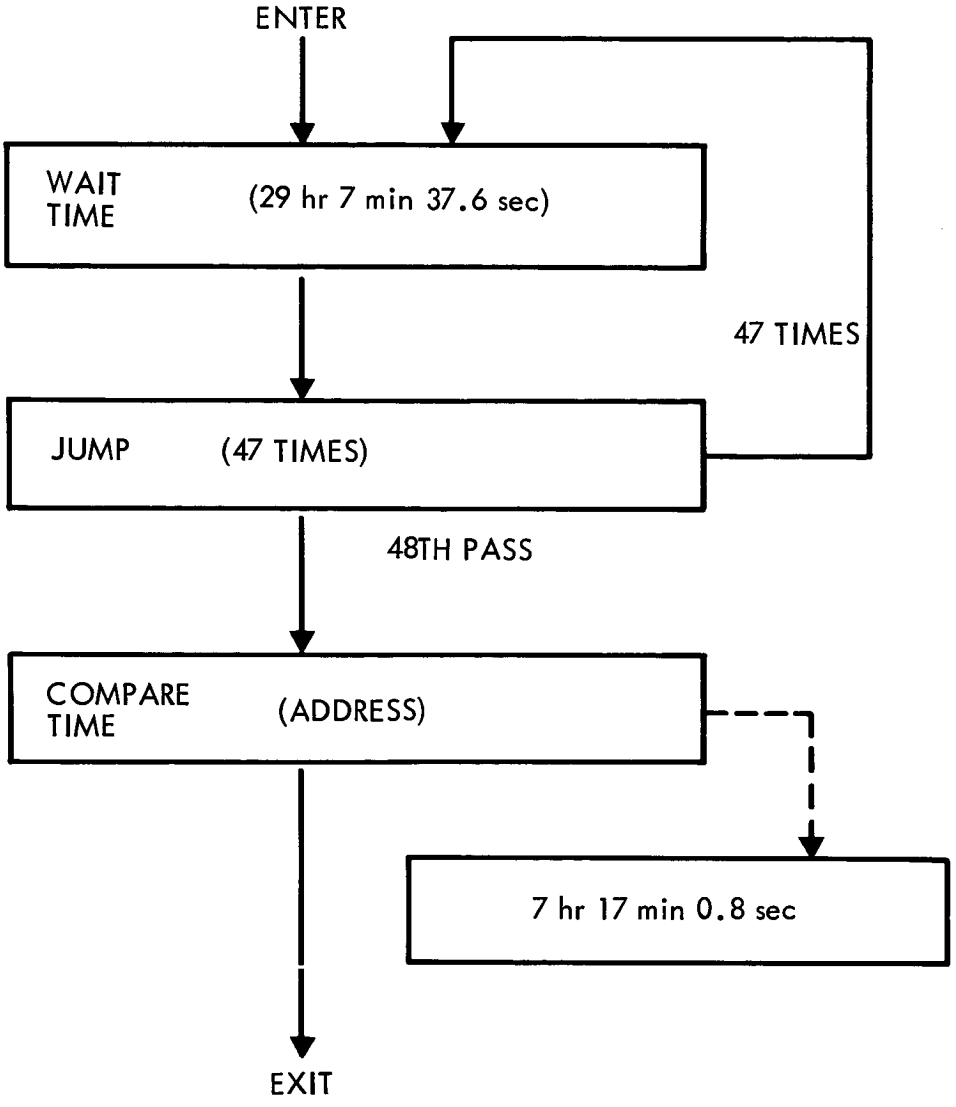

Figure 4.8-11: Extended-Period Time Comparison

Stored commands will be sent to the Data Automation Equipment (DAE) to control the science instruments. The CC&S has the capability to sequence and time the commands that need to be executed in the DAE. A proposed interface shifts (sends) a 20-bit command word into the DAE where it is stored in a 20-bit-register. Decoding will be accomplished within the DAE by switching the appropriate outputs. An alternate approach to the 20-bit register interface is to increase the CC&S output decoding command structure to incorporate within the CC&S the switching functions for controlling the science instruments. This approach provides redundant output-switching through the CC&S output matrix decoder.

Packaging--The CC&S, as the primary onboard means of spacecraft operational control, must maintain reliable operation throughout the mission. This will be accomplished by a variety of means--including circuit design, packaging, and location of the CC&S in relationship to sources of electromagnetic interference.

The role of packaging in this endeavor is to:

1) Provide structural rigidity to prevent physical separation or deformation, loss of electrical contact, and unintended electrical contact;
2) Provide thermal control, to prevent part failure and performance tolerance overrun, by providing sufficient conductance paths and appropriate radiating surfaces;
3) Provide a physical barrier to micrometeorites, radiation, dust particles, abrasion and humidity;
4) Provide shielding to electromagnetic interference;

5) Provide isolation to vibration and shock;

6) Minimize sources and effects of chemical corrosion;

7) Position components and subassemblies in relation to the acceleration and vibration axis, for minimum effect during propulsion phases;

8) Microminiaturize all logic circuitry and thereby offer the reliability advantages of fewer circuit interfaces and all-in-one-house circuit manufacture. The low weight and volume of microelectronics also allows a greater use of redundancy techniques. Use cordwood module techniques for other circuitry;

9) Use the packaging design, and consequently experience, of an existing space program. The CC&S draws upon the experience of the Lunar Orbiter and Minuteman programs.

Integrated circuit parts are used for all logic implementation except the memory and oscillator. The circuits selected will be space-proven, have high reliability with extensive life test data, have high noise immunity, are direct-current-coupled to provide transient noise-rejection, and are low-power devices. The devices will be DTL circuits employing the Nand gate, extender, buffer, and flip-flop as the basic logic elements.

Discrete part circuits are designed using worst-case analysis. Minuteman type high reliability and JPL-approved parts are used.

The memories consist of square-loop ferrite magnetic cores with a high-disturb ratio that is linear over an extended temperature range. Dis-

crete part circuits within the memory use high-reliability parts and are worst-case designed.

The packaging of the CC&S will follow the Lunar Orbiter concept. The microcircuit boards are shown in Figure 4.8-12. The cordwood modules and circuit boards are shown in Figure 4.8-13. Heat transfer is accomplished by conducting the generated heat of electronic parts directly to a package subchassis that functions as a thermal bus. Heat is conducted along this element to a space-facing flange that radiates the heat to space. Steady state thermal control is accomplished by sizing the bus and radiating area to maintain a desired temperature level. Transient thermal control is accomplished through the opening or closure of thermal control louvers.

The packaging concept briefly described above has been qualified for space. Tests include three months of thermal vacuum testing and vibration testing of a programmer production prototype to explore environmental design margins. The test environment exceeded Voyager environmental requirements and was passed successfully by the programmer.

Prior to first usage on Voyager these designs will have been flown a number of times in the Lunar Orbiter spacecraft. For additional discussion on packaging see Section 4.4.2. General reliability design constraints on the CC&S are described in Section 2.2.8.

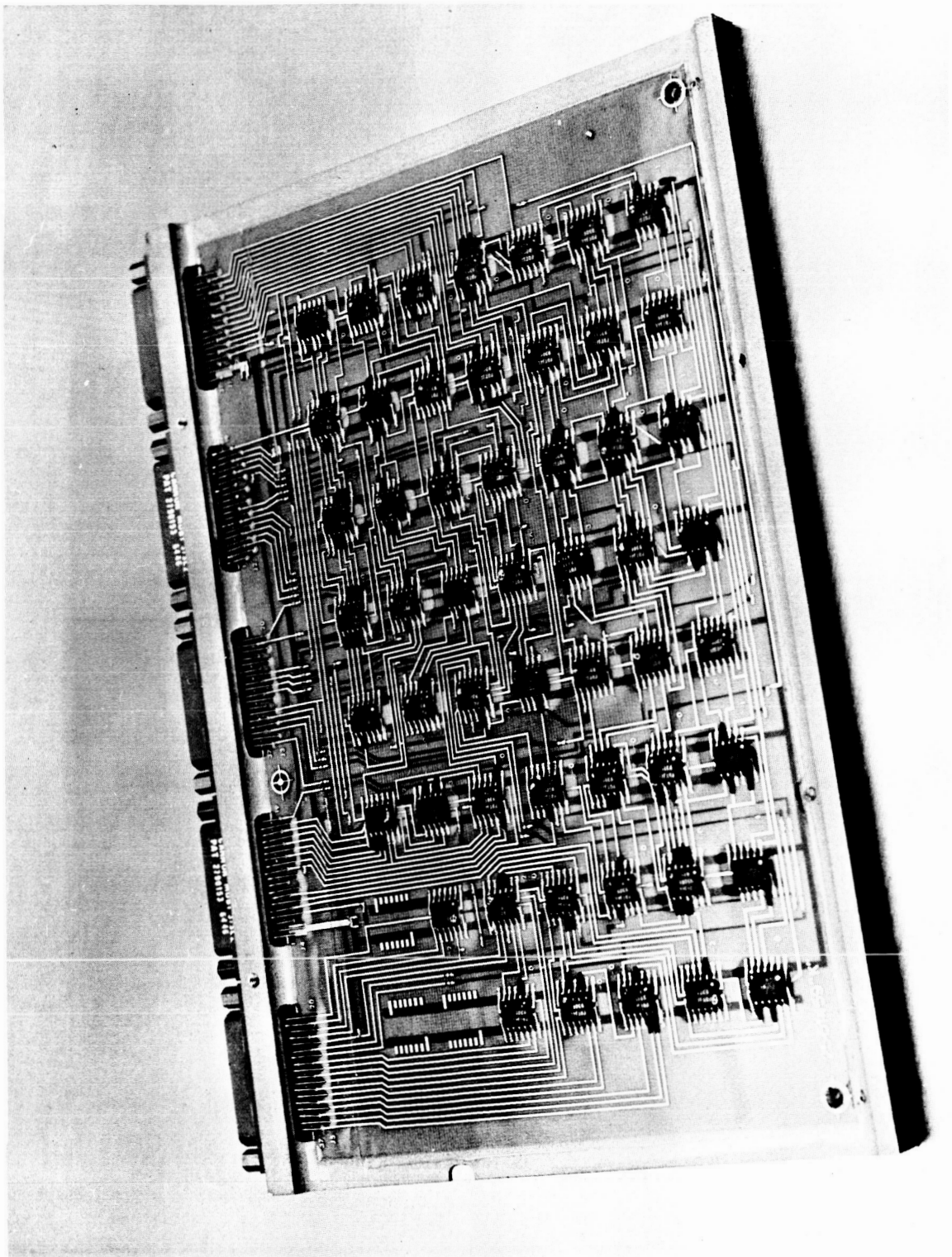

Figure 4.8-12: Lunar Orbiter — Microcircuit Board Assembly Flight Programmer

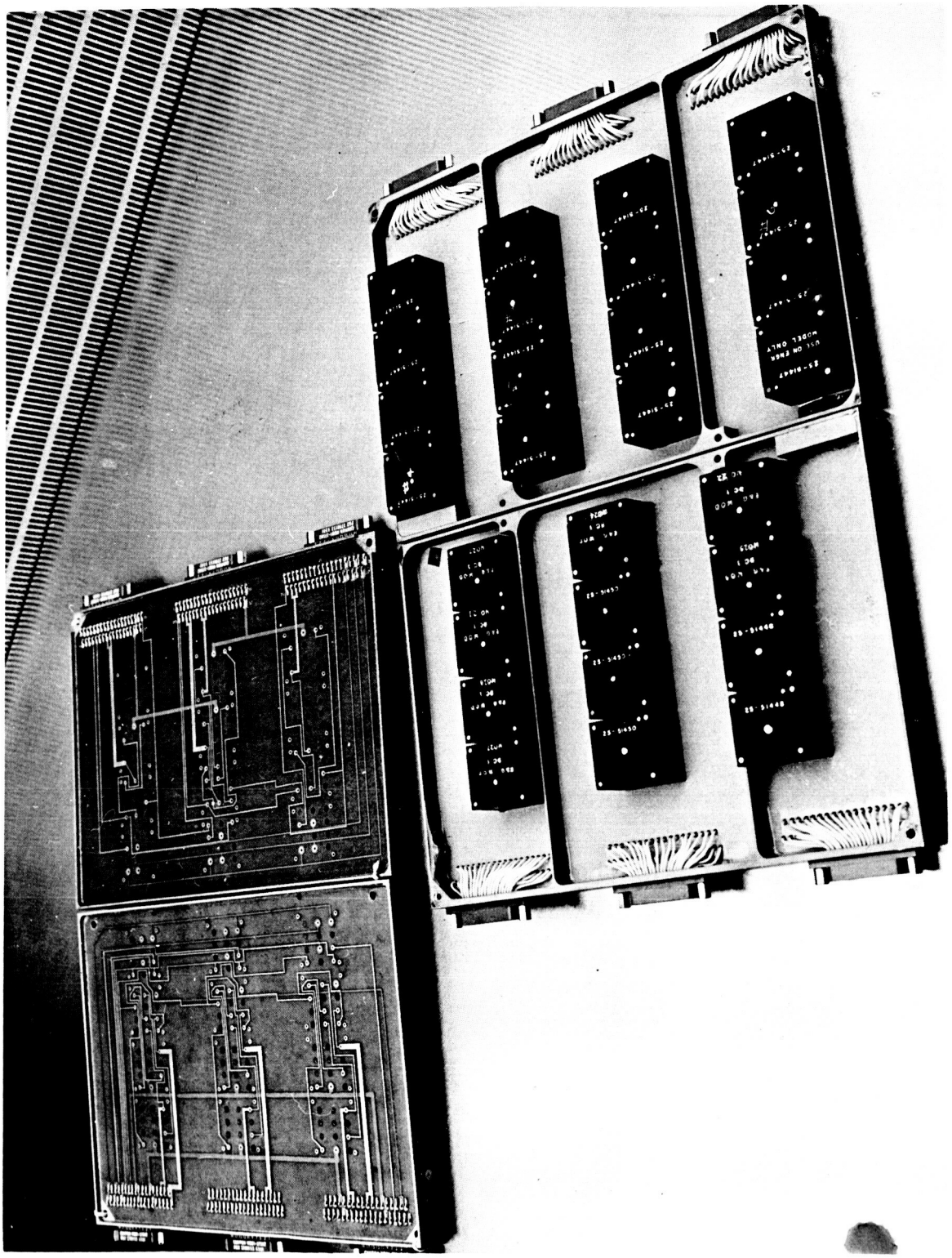

Figure 4.8-13: Lunar Orbiter — Module Board Assembly Flight Programmer

4.8.3.2 Functional Reliability

Long-term reliability is achieved by implementing the CC&S with high-reliability parts, redundancy, serial operation, stored program, real-time backup commands, and work-around modes.

Analysis performed on the preferred configuration results in a reliability assessment of 0.9940. Further detailed assessments are found in Section 3.0 and in Boeing Document D2-82724-1.

Failure Rates and Parts Count--Table 4.8-1 summarizes the parts count and failure rate per unit within the CC&S. The failure rate estimations are derived from Boeing Document D2-82724-3.

Failure Mode and Effects Analysis--The internal processing logic and memory are identical to the Lunar Orbiter programmer. A failure mode and criticality analysis has been performed on the Lunar Orbiter programmer and is documented in Boeing Document D2-100259 ("Failure Mode and Criticality Analysis") Volume 1. The analysis performed on each unit indicated that most single or multiple failures within the unit caused only a minor degradation of the mission objectives. Several work-around modes were available for most single failures.

All stored program commands can be executed on a real-time basis by transmission from ground. Several techniques are available to perform maneuver commands. The stored program can be updated or changed at any time, enabling alternate mission objectives in the event of subsystem

Table 4.8-1: CC&S UNIT FAILURE RATES

Unit	Number of Units	Number of Integrated Circuit Parts Per Unit	Number of Discrete Circuits Per Unit	Unit Failure Rate Per 10^6 Hr.
Input Signal Conditioner	1	23	-	Redundant
Command Logic				
Command Decoder	2	80	-	0.800
Command Register	2	39	-	0.390
Flight Control Switching	2	16.5	-	0.165
Timing Logic				
Oscillator	4	-	7	0.989
Countdown Register	4	45	-	0.450
Bit Position Counter	2	28.5	-	0.285
Redundancy Control	2	30.5	-	0.305
Arithmetic Logic & Memory				
Adder	2	10.5	-	0.105
Comparator	2	6	-	0.006
Integrator Input Buffer	2	4	-	0.040
Velocity Conversion Register	2	27.5	-	0.275
Memory	2	-	8	1.023
Memory Control	2	2.5	-	0.025
Parity Checker-Memory Output	2	7.5	-	0.075
Parity Generator-Memory Input	2	11	-	0.110
Memory Address Register	2	27.5	-	0.275
Control Logic				
Initialize Logic	2	8	-	0.080
Input Parity Checker	2	12	-	0.120
Function Control Register	2	118	-	1.180
Mode Control Register	2	30	-	0.300
Output Matrix Decoder				
Single Functions	2	220	-	2.20
Redundant Functions	2	57	-	Redundant
Power Supply	2	-	1	1.440
Connections (estimated)	9000	-	-	0.900
Switching Assembly				
Relay	2	-	-	0.257
Dual Squib Drivers	53	-	1	0.2374
Single Squib Drivers	2	-	1	0.1248
Solenoid Drivers	8	-	1	0.0645
Relay Drivers	15	-	1	0.0706
Motor Drivers	6	-	1	0.0484
TOTALS				
Integrated Circuits		1675		
Discrete Parts		3725		
Magnetic Cores		5720		

failure. Each processor is complete and redundant to the other. Either one is capable of performing any function, and switching between redundant processors can be performed at any time.

Redundancy Analysis--Major functional blocks used to perform the reliability analysis and the respective reliability assessments are presented in Section 3.0. Critical functions such as squib firings, are actuated by redundant commands through redundant circuitry as illustrated in Figure 4.8-8.

Failure Mode Programming--The programming work-around methods have been established for the Lunar Orbiter programmer. The establishment of these methods was derived from the "Failure Mode and Criticality Analysis," D2-100259. The analysis procedures defined the failed article, the article's function, failure causes, failure modes, the operational effect of the failure, the probability of failure, and the action taken for work-around modes.

Critical Path Analysis--The Lunar Orbiter critical path analysis, in D2-100259, applies for the single-system Voyager CC&S. The redundant system CC&S eliminates the critical paths found in each single system. A cursory treatment of the Voyager CC&S signal paths indicated a critical failure mode in the output circuits. A pair of redundant circuits, connected together at their outputs to provide a single function, could fail such that a true signal occurs when it is not desired. Insurance against such failure modes is provided by circuits with high reliability.

4.8.3.3 Development Status

The Voyager central computer and sequencer subsystem is a modification of the NASA Lunar Orbiter programmer and switching assemblies and as such will draw heavily on the design and test experience of that program. The first Lunar Orbiter is scheduled for a 1966 summer flight with four subsequent flights every 2.5 months. Considerable data will be available from these flights and the preceding qualification test program, which is applicable to Voyager CC&S development.

It is recognized that there are considerable differences in environmental and life requirements between the Lunar Orbiter and Voyager programs. Transit and orbiting times for the Lunar Orbiter are 2-3 days and 20-30 days, respectively. Transit and orbiting times for the Voyager are 7 months and 6 months, respectively. The Voyager will operate further from the Sun, and must withstand micrometeorites for a longer period than the Lunar Orbiter. To satisfy the Voyager CC&S functional requirements, the redundancy features have been added. The vibration and thermal requirements are more severe for the Lunar Orbiter unit than the Voyager. The following modifications to the NASA Lunar Orbiter programmer (control assembly and switching assembly) are planned.

Control Assembly--Instead of discrete part circuits providing input and output interface signal conditioning, integrated circuits will be used.

The data processor (programmer) will be made completely redundant with the exception of noncritical path signal conditioning circuits.

Control circuits will be developed to switch function responsibilities to the second redundant data processor by command or in the event of failure of the first data processor.

The power-converter-regulator design will be modified to meet the revised voltage and power requirements. The transformer windings will be changed because the Voyager spacecraft power subsystem supplies 35 v d.c., ±5 percent, and the converter is designed for 21.4 to 31 v d.c. The regulation will be made more efficient because the input tolerances are reduced.

Wire and connector subassemblies will reflect the redundancy and increase in functions.

Switching Assembly--Additional squib initiation circuits, solenoid drivers, motor drivers, and actuator drivers will be added to accommodate the large increase in the number of functions.

The Lunar Orbiter use of Minuteman high-reliability parts and proven worst-case design for discrete circuits will be retained.

4.8.4 Interface Definition

The defined boundaries of the CC&S control and switching assembly are shown in Figure 4.8-4. The detailed input and output definitions of the CC&S interfaces with other spacecraft subsystems appear in Figure 4.8-14 (control assembly) and Figure 4.8-15 (switching assembly).

AUTOPILOT SUBSYSTEM
MALFUNCTION COMPARATOR SIGNAL
MALFUNCTION COMPARATOR SIGNAL
MALFUNCTION COMPARATOR SIGNAL
MALFUNCTION COMPARATOR SIGNAL
MALFUNCTION COMPARATOR SIGNAL
MALFUNCTION COMPARATOR SIGNAL
MALFUNCTION COMPARATOR SIGNAL
MALFUNCTION COMPARATOR SIGNAL
MALFUNCTION COMPARATOR SIGNAL
MALFUNCTION COMPARATOR SIGNAL
MALFUNCTION COMPARATOR SIGNAL
MALFUNCTION COMPARATOR SIGNAL
DEADBAND CHANGE 0.4°
DEADBAND CHANGE 0.2°
CANOPUS SENSOR
SUN SENSOR INPUT SELECT
SLEW ROLL PLUS
SLEW ROLL MINUS
SLEW PITCH PLUS
SLEW PITCH MINUS
SLEW YAW PLUS
SLEW YAW MINUS
SELECT ROLL GYRO POSITION
SELECT ROLL GYRO RATE
SELECT PITCH GYRO POSITION
SELECT PITCH GYRO RATE
SELECT YAW GYRO POSITION
SELECT YAW GYRO RATE
SELECT REACTION CONTROL 1
SELECT REACTION CONTROL 2
SELECT JET VANE 1
SELECT JET VANE 2
SELECT DERIVATIVE FEED BACK (ON-OFF)
ENABLE INJECTION VALVE DRIVERS
POWER ON
STABILIZATION ROLL AXIS
STABILIZATION PITCH AXIS
STABILIZATION YAW AXIS
RETURN
4 4 4 4 4 4 4 4 4 4 4 4 4 4 4 4 4 4 4 4 4 4 4 4 4 4 4 4 4 4 4 4 4 4 4 4 4 4 4 4 4 4
3 3 2 2 4 4
4 4
4
4
SERIAL DATA
SERIAL DATA
BIT SYNC
BIT SYNC
IN LOCK
IN LOCK
SIGNAL RETURN
RF ON-OFF
RANGING ON-OFF
TRAVELING WAVE TUBE AMP ON-OFF
TRAVELING WAVE TUBE AMP ON-OFF
COMMAND DETECTOR
TRANS-PONDER
NO.1
TRAVEL WAVE TUBE AMPLIF

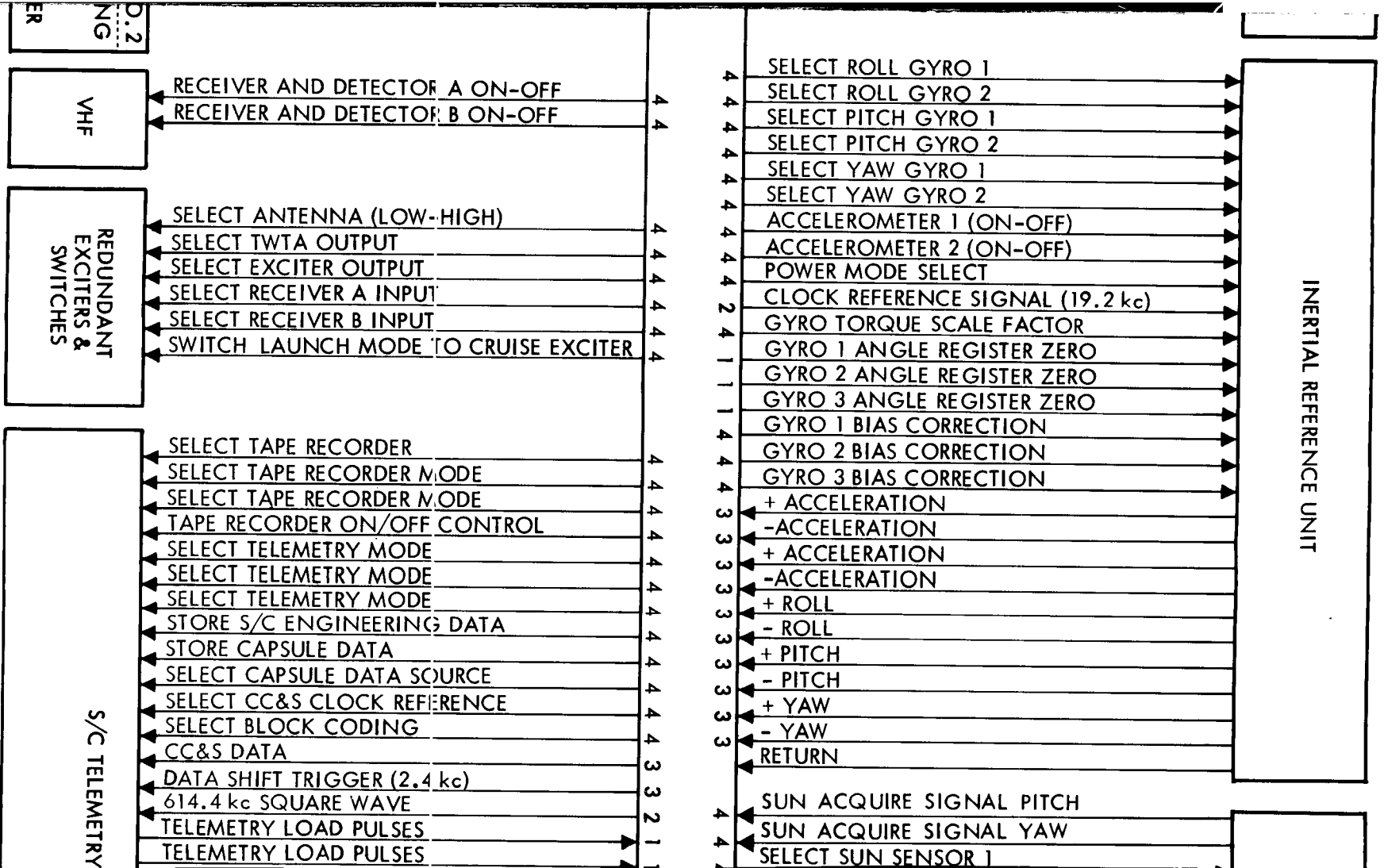
D.2
NG
ER
VHF
RECEIVER AND DETECTOR A ON-OFF
RECEIVER AND DETECTOR B ON-OFF
REDUNDANT EXCITERS & SWITCHES
SELECT ANTENNA (LOW-HIGH)
SELECT TWTA OUTPUT
SELECT EXCITER OUTPUT
SELECT RECEIVER A INPUT
SELECT RECEIVER B INPUT
SWITCH LAUNCH MODE TO CRUISE EXCITER
S/C TELEMETRY
SELECT TAPE RECORDER
SELECT TAPE RECORDER MODE
SELECT TAPE RECORDER MODE
TAPE RECORDER ON/OFF CONTROL
SELECT TELEMETRY MODE
SELECT TELEMETRY MODE
SELECT TELEMETRY MODE
STORE S/C ENGINEERING DATA
STORE CAPSULE DATA
SELECT CAPSULE DATA SOURCE
SELECT CC&S CLOCK REFERENCE
SELECT BLOCK CODING
CC&S DATA
DATA SHIFT TRIGGER (2.4 kc)
614.4 kc SQUARE WAVE
TELEMETRY LOAD PULSES
TELEMETRY LOAD PULSES
SELECT ROLL GYRO 1
SELECT ROLL GYRO 2
SELECT PITCH GYRO 1
SELECT PITCH GYRO 2
SELECT YAW GYRO 1
SELECT YAW GYRO 2
ACCELEROMETER 1 (ON-OFF)
ACCELEROMETER 2 (ON-OFF)
POWER MODE SELECT
CLOCK REFERENCE SIGNAL (19.2 kc)
GYRO TORQUE SCALE FACTOR
GYRO 1 ANGLE REGISTER ZERO
GYRO 2 ANGLE REGISTER ZERO
GYRO 3 ANGLE REGISTER ZERO
GYRO 1 BIAS CORRECTION
GYRO 2 BIAS CORRECTION
GYRO 3 BIAS CORRECTION
+ ACCELERATION
-ACCELERATION
+ ACCELERATION
-ACCELERATION
+ ROLL
- ROLL
+ PITCH
- PITCH
+ YAW
- YAW
RETURN
INERTIAL REFERENCE UNIT
SUN ACQUIRE SIGNAL PITCH
SUN ACQUIRE SIGNAL YAW
SELECT SUN SENSOR 1

SUN SENSORS
STAR TRACKER CANOPUS
NO. 1
NO. 2
SPACECRAFT PROPULSION
SELECT SUN SENSOR 2
COARSE SENSOR OFF
RETURN
CANOPUS (ON-OFF)
CANOPUS SHUTTER (OPEN-CLOSE)
GATE OVERRIDE
CONE ANGLE 1
CONE ANGLE 2
CONE ANGLE 3
CONE ANGLE 4
CONE ANGLE 5
CONE ANGLE 6
CANOPUS PRESENCE
INTENSITY
CHAMBER PRESSURE MONITOR
CC&S CONTROL ASSEMBLY
TELEMETRY LOAD PULSES
PARITY ERROR HALT
CANOPUS ON-OFF 1
CANOPUS ON-OFF 2
POWER MODE SELECT
ACCELEROMETER LOOP
SUN PRESENCE SIGNAL
MAGNITUDE COMMAND IDENTIFICATION 1
MAGNITUDE COMMAND IDENTIFICATION 2
MAGNITUDE COMMAND IDENTIFICATION 3
MAGNITUDE COMMAND IDENTIFICATION 4
MAGNITUDE COMMAND IDENTIFICATION 5
MAGNITUDE COMMAND IDENTIFICATION 6
CHAMBER PRESSURE MONITOR
RETURN
START SPACECRAFT CLOCK
SPACECRAFT CLOCK RETURN
CC&S READY
AND DATA STORAGE SUBSYSTEM
(T&DS)
SUBSYSTEM INTERCONNECT (ELECTRICAL)

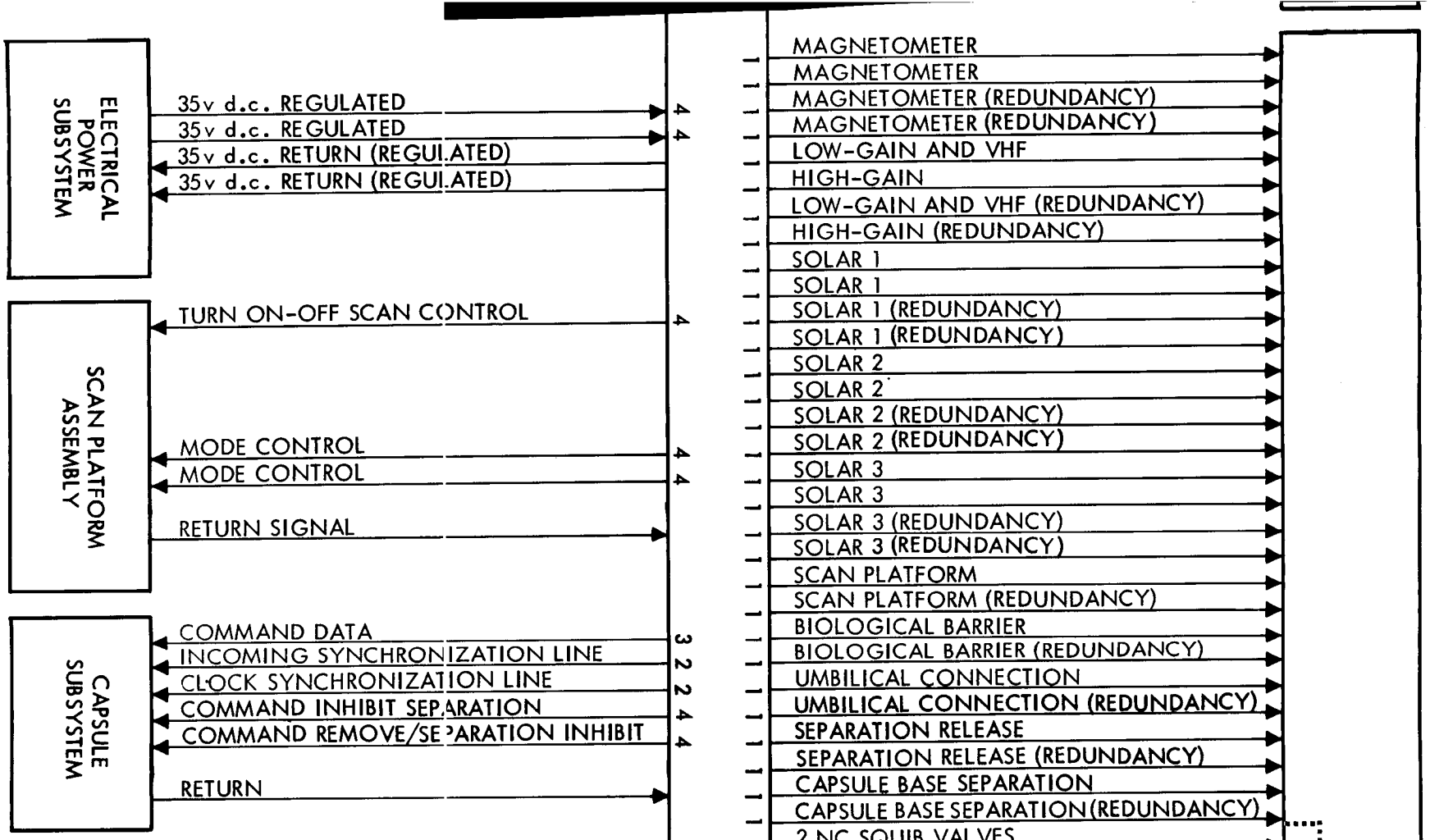
ELECTRICAL POWER SUBSYSTEM
35v d.c. REGULATED
35v d.c. REGULATED
35v d.c. RETURN (REGULATED)
35v d.c. RETURN (REGULATED)
4
4
SCAN PLATFORM ASSEMBLY
TURN ON-OFF SCAN CONTROL
4
MODE CONTROL
MODE CONTROL
4
4
RETURN SIGNAL
CAPSULE SUBSYSTEM
COMMAND DATA
INCOMING SYNCHRONIZATION LINE
CLOCK SYNCHRONIZATION LINE
COMMAND INHIBIT SEPARATION
COMMAND REMOVE/SEPARATION INHIBIT
3
2
2
4
4
RETURN
MAGNETOMETER
MAGNETOMETER
MAGNETOMETER (REDUNDANCY)
MAGNETOMETER (REDUNDANCY)
LOW-GAIN AND VHF
HIGH-GAIN
LOW-GAIN AND VHF (REDUNDANCY)
HIGH-GAIN (REDUNDANCY)
SOLAR 1
SOLAR 1
SOLAR 1 (REDUNDANCY)
SOLAR 1 (REDUNDANCY)
SOLAR 2
SOLAR 2
SOLAR 2 (REDUNDANCY)
SOLAR 2 (REDUNDANCY)
SOLAR 3
SOLAR 3
SOLAR 3 (REDUNDANCY)
SOLAR 3 (REDUNDANCY)
SCAN PLATFORM
SCAN PLATFORM (REDUNDANCY)
BIOLOGICAL BARRIER
BIOLOGICAL BARRIER (REDUNDANCY)
UMBILICAL CONNECTION
UMBILICAL CONNECTION (REDUNDANCY)
SEPARATION RELEASE
SEPARATION RELEASE (REDUNDANCY)
CAPSULE BASE SEPARATION
CAPSULE BASE SEPARATION (REDUNDANCY)
2 NC SOLIB VALVES

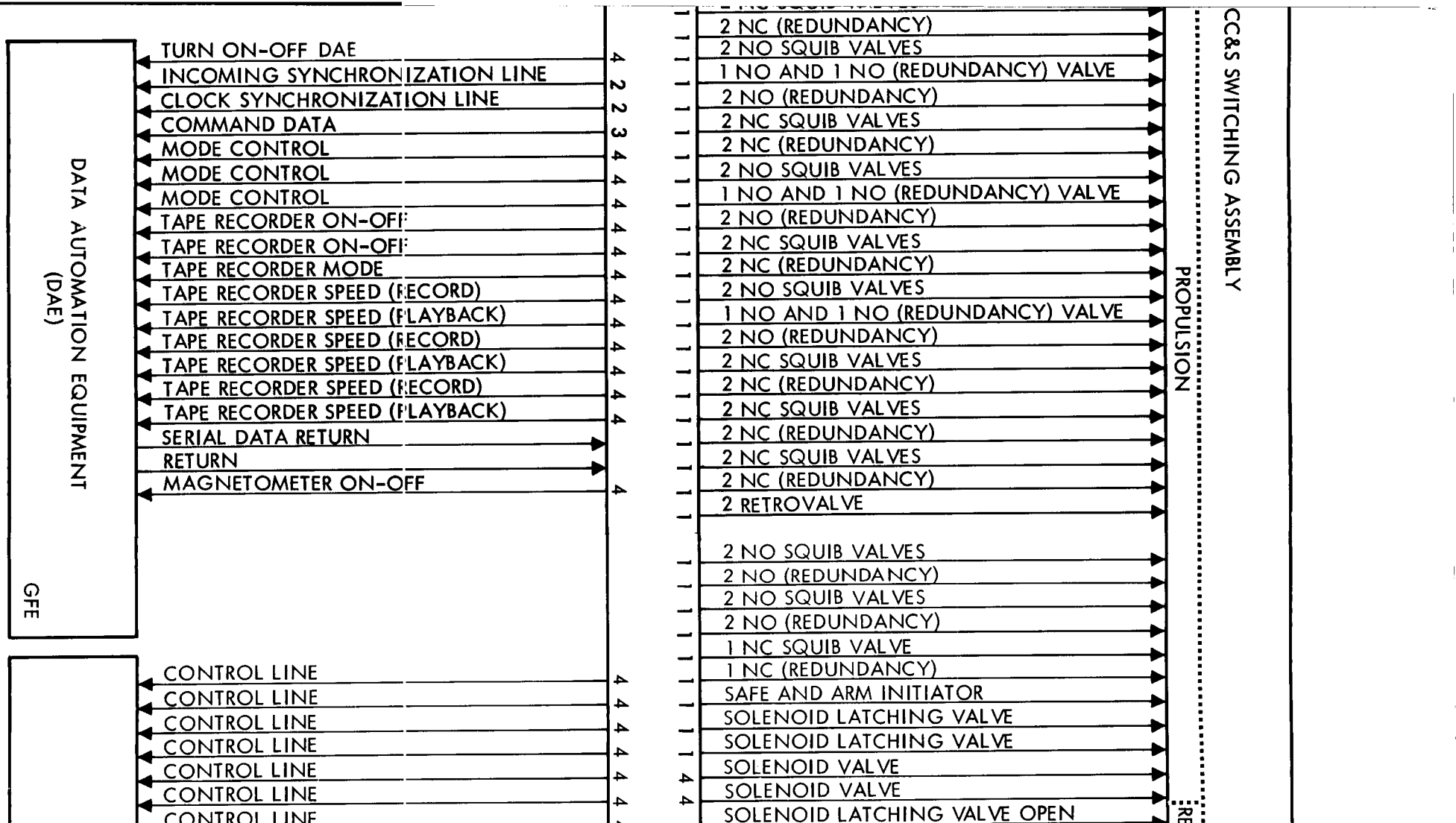
DATA AUTOMATION EQUIPMENT (DAE)
GFE
TURN ON-OFF DAE
INCOMING SYNCHRONIZATION LINE
CLOCK SYNCHRONIZATION LINE
COMMAND DATA
MODE CONTROL
MODE CONTROL
MODE CONTROL
TAPE RECORDER ON-OFF
TAPE RECORDER ON-OFF
TAPE RECORDER MODE
TAPE RECORDER SPEED (RECORD)
TAPE RECORDER SPEED (PLAYBACK)
TAPE RECORDER SPEED (RECORD)
TAPE RECORDER SPEED (PLAYBACK)
TAPE RECORDER SPEED (RECORD)
TAPE RECORDER SPEED (PLAYBACK)
SERIAL DATA RETURN
RETURN
MAGNETOMETER ON-OFF
4 2 2 3 4 4 4 4 4 4 4 4 4 4 4 4 4 4 4
CONTROL LINE
CONTROL LINE
CONTROL LINE
CONTROL LINE
CONTROL LINE
CONTROL LINE
CONTROL LINE
4 4 4 4 4 4 4
CC&S SWITCHING ASSEMBLY
PROPULSION
2 NC (REDUNDANCY)
2 NO SQUIB VALVES
1 NO AND 1 NO (REDUNDANCY) VALVE
2 NO (REDUNDANCY)
2 NC SQUIB VALVES
2 NC (REDUNDANCY)
2 NO SQUIB VALVES
1 NO AND 1 NO (REDUNDANCY) VALVE
2 NO (REDUNDANCY)
2 NC SQUIB VALVES
2 NC (REDUNDANCY)
2 NO SQUIB VALVES
1 NO AND 1 NO (REDUNDANCY) VALVE
2 NO (REDUNDANCY)
2 NC SQUIB VALVES
2 NC (REDUNDANCY)
2 NC SQUIB VALVES
2 NC (REDUNDANCY)
2 NC SQUIB VALVES
2 NC (REDUNDANCY)
2 RETROVALVE
2 NO SQUIB VALVES
2 NO (REDUNDANCY)
2 NO SQUIB VALVES
2 NO (REDUNDANCY)
1 NC SQUIB VALVE
1 NC (REDUNDANCY)
SAFE AND ARM INITIATOR
SOLENOID LATCHING VALVE
SOLENOID LATCHING VALVE
SOLENOID VALVE
SOLENOID VALVE
SOLENOID LATCHING VALVE OPEN
1 1 1

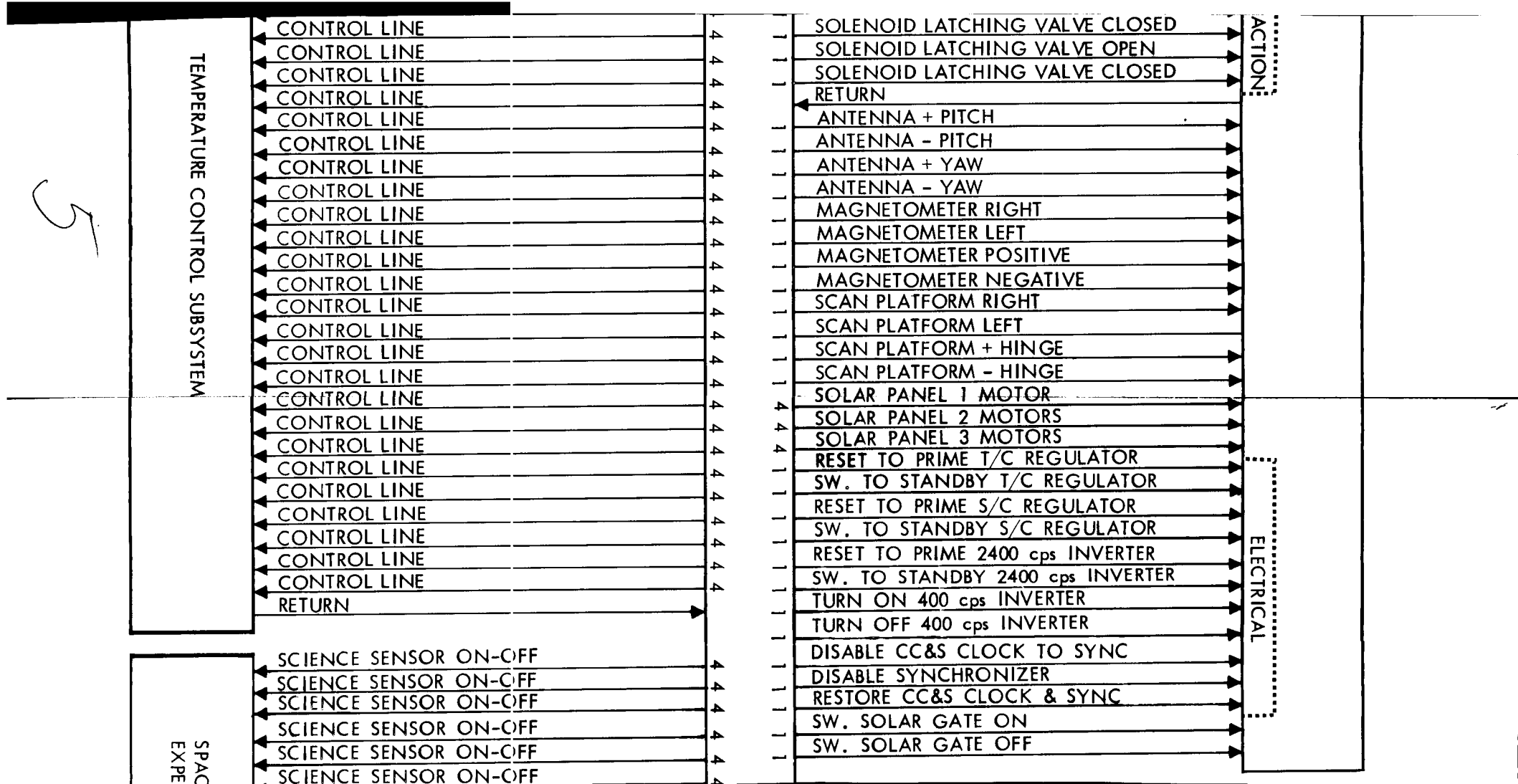
TEMPERATURE CONTROL SUBSYSTEM
CONTROL LINE
CONTROL LINE
CONTROL LINE
CONTROL LINE
CONTROL LINE
CONTROL LINE
CONTROL LINE
CONTROL LINE
CONTROL LINE
CONTROL LINE
CONTROL LINE
CONTROL LINE
CONTROL LINE
CONTROL LINE
CONTROL LINE
CONTROL LINE
CONTROL LINE
CONTROL LINE
CONTROL LINE
CONTROL LINE
CONTROL LINE
RETURN
SCIENCE SENSOR ON-OFF
SCIENCE SENSOR ON-OFF
SCIENCE SENSOR ON-OFF
SCIENCE SENSOR ON-OFF
SCIENCE SENSOR ON-OFF
SOLENOID LATCHING VALVE CLOSED
SOLENOID LATCHING VALVE OPEN
SOLENOID LATCHING VALVE CLOSED
RETURN
ACTION
ANTENNA + PITCH
ANTENNA - PITCH
ANTENNA + YAW
ANTENNA - YAW
MAGNETOMETER RIGHT
MAGNETOMETER LEFT
MAGNETOMETER POSITIVE
MAGNETOMETER NEGATIVE
SCAN PLATFORM RIGHT
SCAN PLATFORM LEFT
SCAN PLATFORM + HINGE
SCAN PLATFORM - HINGE
SOLAR PANEL 1 MOTOR
SOLAR PANEL 2 MOTORS
SOLAR PANEL 3 MOTORS
RESET TO PRIME T/C REGULATOR
SW. TO STANDBY T/C REGULATOR
RESET TO PRIME S/C REGULATOR
SW. TO STANDBY S/C REGULATOR
RESET TO PRIME 2400 cps INVERTER
SW. TO STANDBY 2400 cps INVERTER
TURN ON 400 cps INVERTER
TURN OFF 400 cps INVERTER
DISABLE CC&S CLOCK TO SYNC
DISABLE SYNCHRONIZER
RESTORE CC&S CLOCK & SYNC
SW. SOLAR GATE ON
SW. SOLAR GATE OFF
ELECTRICAL

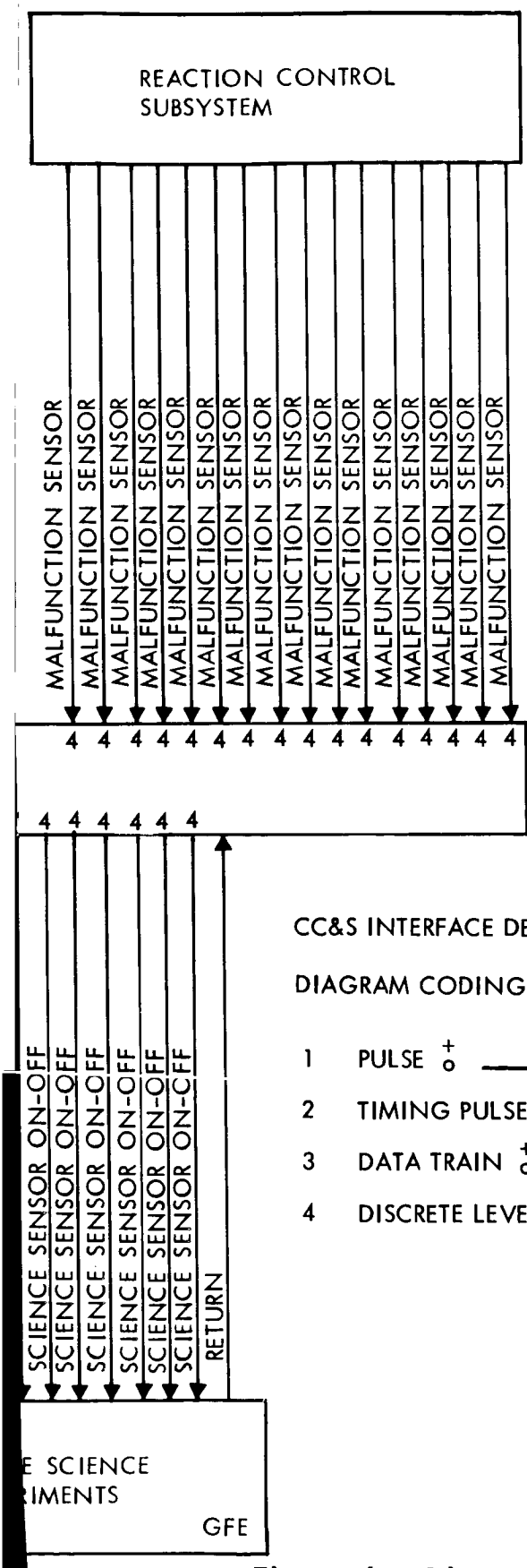

CC&S INTERFACE DEFINITIONS

DIAGRAM CODING

1 PULSE

2 TIMING PULSE TRAIN

3 DATA TRAIN

4 DISCRETE LEVEL VOLTAGE CHANGE

Figure 4.8-14: Control Assembly Interface Diagram

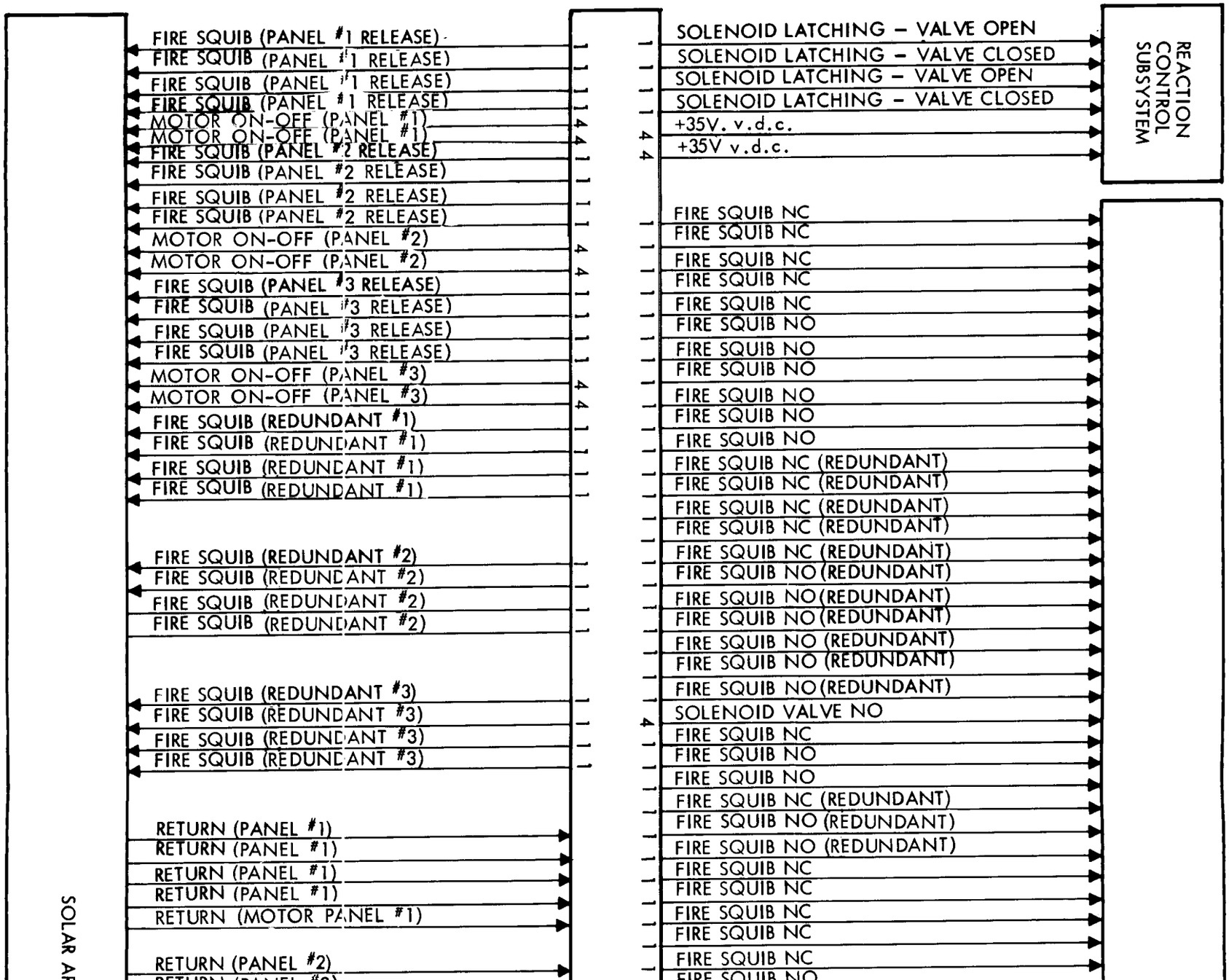
SOLAR ARRAY
FIRE SQUIB (PANEL #1 RELEASE)
FIRE SQUIB (PANEL #1 RELEASE)
FIRE SQUIB (PANEL #1 RELEASE)
FIRE SQUIB (PANEL #1 RELEASE)
MOTOR ON-OFF (PANEL #1)
MOTOR ON-OFF (PANEL #1)
FIRE SQUIB (PANEL #2 RELEASE)
FIRE SQUIB (PANEL #2 RELEASE)
FIRE SQUIB (PANEL #2 RELEASE)
FIRE SQUIB (PANEL #2 RELEASE)
MOTOR ON-OFF (PANEL #2)
MOTOR ON-OFF (PANEL #2)
FIRE SQUIB (PANEL #3 RELEASE)
FIRE SQUIB (PANEL #3 RELEASE)
FIRE SQUIB (PANEL #3 RELEASE)
FIRE SQUIB (PANEL #3 RELEASE)
MOTOR ON-OFF (PANEL #3)
MOTOR ON-OFF (PANEL #3)
FIRE SQUIB (REDUNDANT #1)
FIRE SQUIB (REDUNDANT #1)
FIRE SQUIB (REDUNDANT #1)
FIRE SQUIB (REDUNDANT #1)
FIRE SQUIB (REDUNDANT #2)
FIRE SQUIB (REDUNDANT #2)
FIRE SQUIB (REDUNDANT #2)
FIRE SQUIB (REDUNDANT #2)
FIRE SQUIB (REDUNDANT #3)
FIRE SQUIB (REDUNDANT #3)
FIRE SQUIB (REDUNDANT #3)
FIRE SQUIB (REDUNDANT #3)
RETURN (PANEL #1)
RETURN (PANEL #1)
RETURN (PANEL #1)
RETURN (PANEL #1)
RETURN (MOTOR PANEL #1)
RETURN (PANEL #2)
SOLENOID LATCHING – VALVE OPEN
SOLENOID LATCHING – VALVE CLOSED
SOLENOID LATCHING – VALVE OPEN
SOLENOID LATCHING – VALVE CLOSED
+35V. v.d.c.
+35V v.d.c.
REACTION CONTROL SUBSYSTEM
FIRE SQUIB NC
FIRE SQUIB NC
FIRE SQUIB NC
FIRE SQUIB NC
FIRE SQUIB NC
FIRE SQUIB NO
FIRE SQUIB NO
FIRE SQUIB NO
FIRE SQUIB NO
FIRE SQUIB NO
FIRE SQUIB NC (REDUNDANT)
FIRE SQUIB NC (REDUNDANT)
FIRE SQUIB NC (REDUNDANT)
FIRE SQUIB NC (REDUNDANT)
FIRE SQUIB NC (REDUNDANT)
FIRE SQUIB NO (REDUNDANT)
FIRE SQUIB NO (REDUNDANT)
FIRE SQUIB NO (REDUNDANT)
FIRE SQUIB NO (REDUNDANT)
FIRE SQUIB NO (REDUNDANT)
FIRE SQUIB NO (REDUNDANT)
SOLENOID VALVE NO
FIRE SQUIB NC
FIRE SQUIB NO
FIRE SQUIB NO
FIRE SQUIB NC (REDUNDANT)
FIRE SQUIB NO (REDUNDANT)
FIRE SQUIB NO (REDUNDANT)
FIRE SQUIB NC
FIRE SQUIB NC
FIRE SQUIB NC
FIRE SQUIB NC
FIRE SQUIB NC
FIRE SQUIB NO

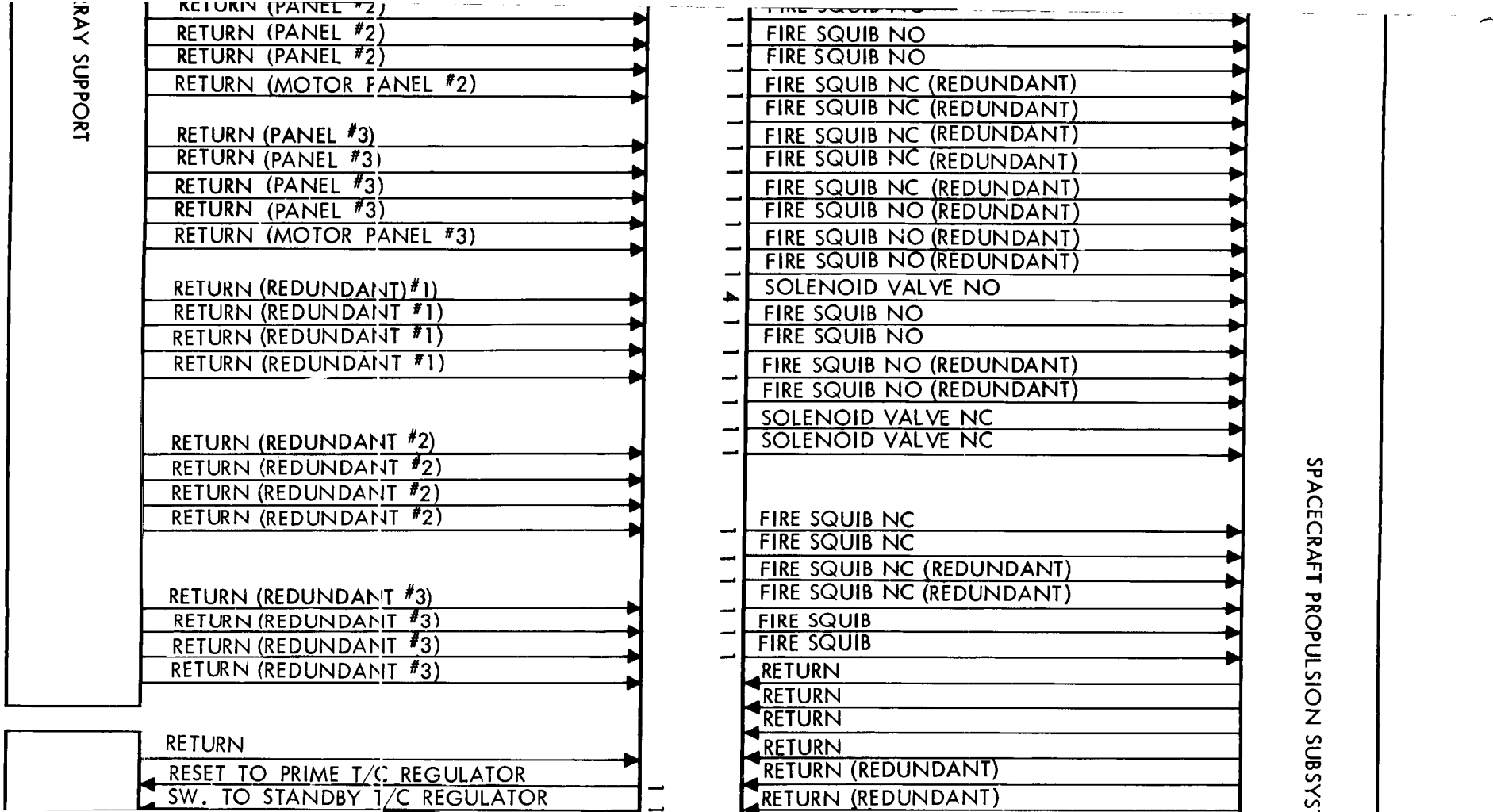
RAY SUPPORT
RETURN (PANEL #2)
RETURN (PANEL #2)
RETURN (PANEL #2)
RETURN (MOTOR PANEL #2)
RETURN (PANEL #3)
RETURN (PANEL #3)
RETURN (PANEL #3)
RETURN (PANEL #3)
RETURN (MOTOR PANEL #3)
RETURN (REDUNDANT) #1)
RETURN (REDUNDANT #1)
RETURN (REDUNDANT #1)
RETURN (REDUNDANT #1)
RETURN (REDUNDANT #2)
RETURN (REDUNDANT #2)
RETURN (REDUNDANT #2)
RETURN (REDUNDANT #2)
RETURN (REDUNDANT #3)
RETURN (REDUNDANT #3)
RETURN (REDUNDANT #3)
RETURN (REDUNDANT #3)
RETURN
RESET TO PRIME T/C REGULATOR
SW. TO STANDBY T/C REGULATOR
FIRE SQUIB NO
FIRE SQUIB NO
FIRE SQUIB NC (REDUNDANT)
FIRE SQUIB NC (REDUNDANT)
FIRE SQUIB NC (REDUNDANT)
FIRE SQUIB NC (REDUNDANT)
FIRE SQUIB NC (REDUNDANT)
FIRE SQUIB NO (REDUNDANT)
FIRE SQUIB NO (REDUNDANT)
FIRE SQUIB NO (REDUNDANT)
SOLENOID VALVE NO
FIRE SQUIB NO
FIRE SQUIB NO
FIRE SQUIB NO (REDUNDANT)
FIRE SQUIB NO (REDUNDANT)
SOLENOID VALVE NC
SOLENOID VALVE NC
FIRE SQUIB NC
FIRE SQUIB NC
FIRE SQUIB NC (REDUNDANT)
FIRE SQUIB NC (REDUNDANT)
FIRE SQUIB
FIRE SQUIB
RETURN
RETURN
RETURN
RETURN
RETURN (REDUNDANT)
RETURN (REDUNDANT)
SPACECRAFT PROPULSION SUBSYS

EM

RETURN
RETURN
RETURN
RETURN
RETURN
RETURN
RETURN
RETURN
RETURN
RETURN
RETURN (REDUNDANT)
RETURN (REDUNDANT)
RETURN (REDUNDANT)
RETURN (REDUNDANT)
RETURN (REDUNDANT)
RETURN (REDUNDANT)
RETURN (REDUNDANT)
RETURN (REDUNDANT)
+35V.v.d.c.
RETURN
RETURN
RETURN
RETURN (REDUNDANT)
RETURN (REDUNDANT)
RETURN (REDUNDANT)
RETURN
RETURN
RETURN
RETURN
RETURN
RETURN
RETURN
RETURN (REDUNDANT)

SWITCHING ASSEMBLY

1 RESET TO PRIME S/C REGULATOR
1 SW. TO STANDBY S/C REGULATOR
1 RESET TO PRIME 2400 cps INVERTER
1 SW. TO STANDBY 2400 cps INVERTER
1 TURN ON 400 cps INVERTER
1 TURN OFF 400 cps INVERTER
1 DISABLE CC&S CLOCK TO SYNC
1 DISABLE SYNCHRONIZER
1 RESTORE CC&S CLOCK & SYNC
1 SW. SOLAR GATE ON
1 SW. SOLAR GATE OFF
4 BATTERY POWER (SQUIBS)
4 BATTERY POWER (SQUIBS)
4 35 v.d.c. REGULATED
4 35 v.d.c. REGULATED
35 v.d.c. RETURN
35 v.d.c. RETURN
BATTERY POWER RETURN
BATTERY POWER RETURN

1 LOW-GAIN RELEASE SQUIB
1 LOW-GAIN RELEASE SQUIB (R)
RETURN
RETURN (REDUNDANT)

1 HIGH-GAIN ANT. RELEASE SQUIB
1 HIGH-GAIN ANT. RELEASE SQUIB
1 HIGH-GAIN ANT. RELEASE SQUIB (R)
1 HIGH-GAIN ANT. RELEASE SQUIB (R)
RETURN
RETURN
RETURN (REDUNDANCY)
RETURN (REDUNDANCY)

ELECTRICAL POWER SUBSYSTEM

LOW-GAIN ANTENNA

HIGH-GAIN ANTENNA BOOM ASSEMBLY

3

CC&S CONTROL ASSEMBLY

SUBSYSTEM INTERCONNECT (ELECTRICAL)

RETURN (REDUNDANT)
RETURN (REDUNDANT)
RETURN (REDUNDANT)
RETURN (REDUNDANT)
RETURN (REDUNDANT)
RETURN (REDUNDANT)
RETURN (REDUNDANT)
+35V.v.d.c.
RETURN
RETURN
RETURN (REDUNDANT)
RETURN (REDUNDANT)
+35V v.d.c.
+35V v.d.c.

"SEE CONTROL ASSEMBLY INTERFACE WITH SWITCHING ASSEMBLY"
96 CONTROL LINES
RETURN

SQUIB ARM
SQUIB DISARM
SQUIB DISARM "A"
SQUIB DISARM "B"
RETURN

4 4 4

1 1 1 1 1

ANTENNA POSITION 0.18° + PITCH
ANTENNA POSITION 0.18° - PITCH
ANTENNA POSITION 0.18° + YAW
ANTENNA POSITION 0.18° - YAW

1 1 1

VHF RELEASE SQUIB
VHF RELEASE SQUIB (R)
RETURN
RETURN (REDUNDANT)

1 1 1 1 1 1 1 1 1 1 1

UNLOCKING SQUIB
UNLOCKING SQUIB
UNLOCKING SQUIB (R)
UNLOCKING SQUIB (R)
RETURN
RETURN
RETURN (REDUNDANT)
RETURN (REDUNDANT)
+ ROLL 1° RIGHT
-ROLL 1° LEFT
+ HINGE 1°
- HINGE 1°

VHF ANTENNA BOOM ASSEMBLY

SCAN PLATFORM ASSEMBLY

4

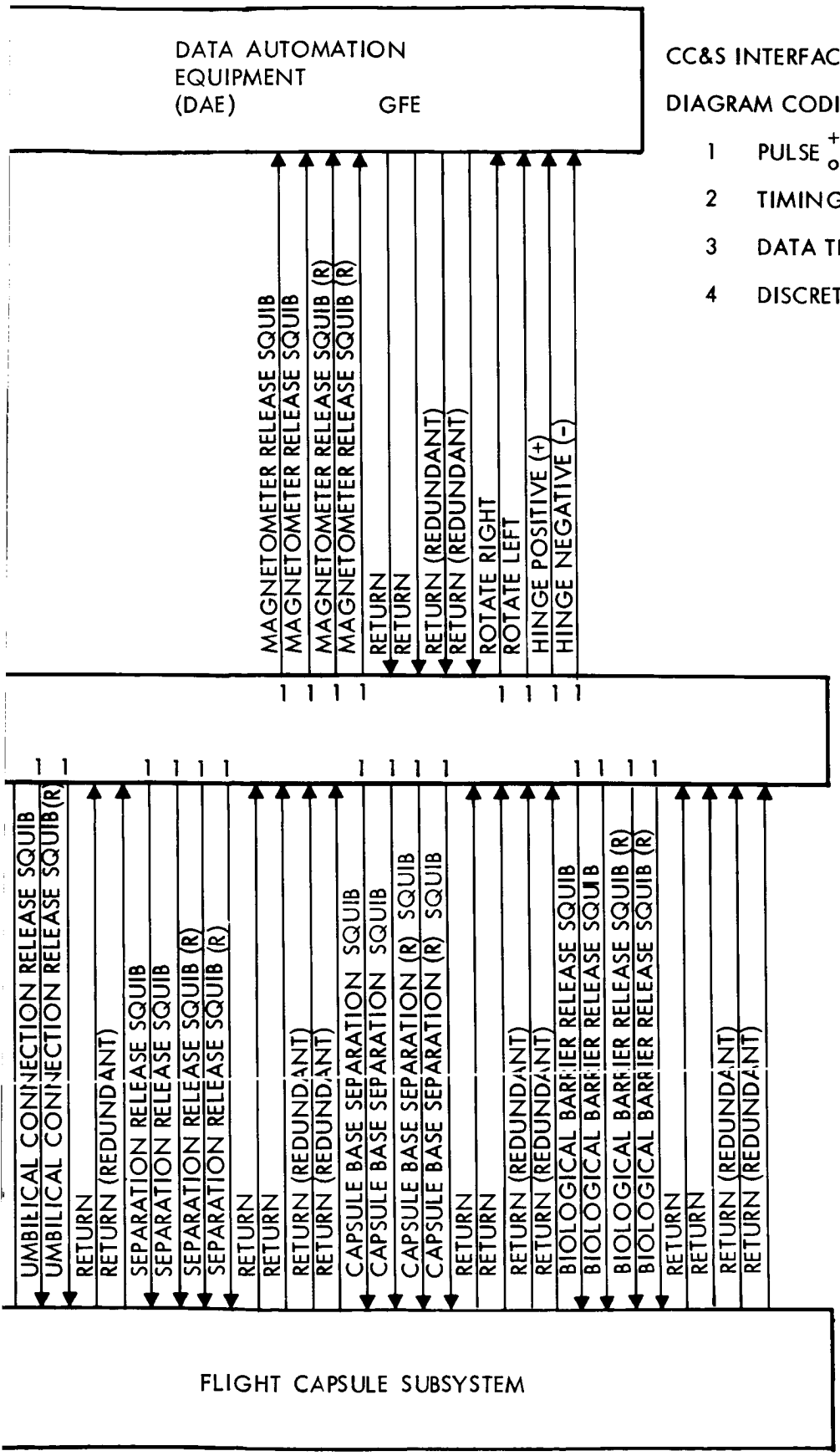

Figure 4.8-15: Switching Assembly Interface Diagram

The electrical inputs and outputs to the CC&S are summarized in Table 4.8-2. The switching assembly will receive signals from the CC&S control assembly and will operate high-voltage and current switching (squib firing and solenoid operations). Output signal rise times and fall times are limited by Miller feedback circuits to suppress RFI generation; the CC&S has no optical interface requirements. It is not an emitter of radioactive or nuclear radiation and the environment which it is subjected to is presented in Paragraph 3.0. Mechanical and thermal interfaces are controlled by packaging design as outlined in Paragraph 4.8.3.1. The CC&S assemblies are:

	Size	Volume	Weight
Control Assembly	8 x 8 x 24 inches	1550 cubic inches	29 pounds
Switching Assembly	8 x 8 x 16 inches	1050 cubic inches	29 pounds

The ambient contribution of the CC&S subsystem to the spacecraft magnetic field is stable, less than 1 gamma in magnitude, and will be measured together with all other contributions during total magnetic mapping. Nonambient contributions of significant proportions may occur during operations of the switching assembly. These also will be determined during total system magnetic mapping. The nonambient contributions are short in duration (seconds or less), infrequent in occurrence, and their time of occurrence is known.

The CC&S will provide four different types of timing signals to the spacecraft subsystems as shown on the control and switching assembly interface diagrams. The four timing pulses are:

Table 4.8-2: CC&S ELECTRICAL INTERFACE SUBSYSTEM SUMMARY

		FUNCTIONS		
	NO. WIRES	INPUTS	OUTPUTS	TOTAL
Autopilot	39	15	23	38
Attitude Reference	56	16	38	54
Reaction Control	22	16	4	20
Propulsion	120	4	58	62
Telecommunications	66	15	49	64
Mechanism	117	0	60	60
Electrical, Power	26	0	19	19
Temperature Control	33	0	32	32
Data Automation Equipment	23	0	21	21
Space Science Experiments	13	0	12	12
Subsystem Interconnects	8	2	5	7
Scan Platform	8	0	7	7
Flight Capsule	6	0	5	5
	537	68	333	401

Kinds of Commands

1) Pulse 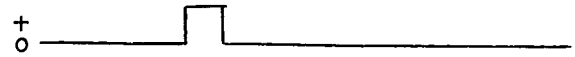

A single 6-volt 50 millisecond pulse used for firing squibs (5 amp minimum), operating latching valves (1.2 amp minimum - 2.2 amps maximum), positioning (10,000 ohms and 1000 μμ farads), single action switching (5 amp minimum)and telemetry load pulses (10,000 ohms and 1000 μμ farads).

2) Timing pulse train 

A 6-volt amplitude clock reference pulse trains (uniform pulses) used for providing clock timing trains of desired frequencies (19.2 kc. to the inertial reference unit and 614.4 kc. to the spacecraft telemetry and data storage subsystem) to the subsystems and for synchronization.

3) Data Train 

A 6-volt amplitude 50-millisecond pulse (10,000 ohms and 1000 μμ farads) of nonuniform spacing used for data transmission between subsystems (20, 21, and 22 bits) and mission operations support (27 bits).

4) Discrete Level Voltage Change 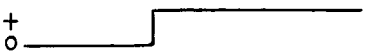

A 6-volt amplitude level voltage will change states of switches (10,000 ohms and 1000 μμ farads), hold relays and solenoids in their closed or open position (1.2 amp minimum to 2.2 amp maximum) and turn switches either ON or OFF (10,000 ohms and 1000 μμ farads).

In Table 4.8-3 the subsystem interfaces are grouped with their corresponding timing signal levels shown with a total of 143 pulses, 9 timing pulse trains, 16 data trains, and 231 discrete level voltage changes for the CC&S subsystems.

4.8.5 Performance Parameters

Table 4.8-4 lists the parameters of the CC&S performance.

4.8.6 Physical Characteristics and Constraints

Physical characteristics are shown in Table 4.8-5. Environmental constraints to which the CC&S are subjected are covered in Section 2.2.

4.8.7 Safety Considerations

No high voltage or explosive devices exist in the CC&S. Inadvertent squib detonation before launch is prevented by ground control inhibiting the squib firing circuits. The squib driver amplifiers in the switching assembly have no power applied to them until commanded by a hard line from the blockhouse to arm the circuits. Circuits used to drive mechanical devices by CC&S commands are also inhibited in the same manner. Design restraints for safety are discussed in detail in Paragraph 2.2.9.

Table 4.8-3: CC&S TIMING SIGNALS AND INTERFACES

	Control Assembly	Switching Assembly	Signals			
			1	2	3	4
Autopilot	X					38
Attitude Reference Subsystem						
Inertial Reference Unit	X		3	1	10	13
Star Tracker	X					22
Sun Sensors	X					5
Reaction Control Subsystem		X	4			
Spacecraft Propulsion	X					4
Spacecraft Propulsion		X	56			2
Spacecraft Telecommunications						
Command Detector	X			2	2	2
Transponder	X					2
Traveling Wave Tube	X					2
VHF	X					2
Redundancy Exciters and RF Switches	X					6
Spacecraft Telemetry and Data Storage Subsystem	X		9	1	2	30
Spacecraft Antenna Subsystem		X	4			
Mechanism Subsystem						
Solar Array Support		X	24			6
VHF Antenna Boom Assembly		X	2			
Low Gain Antenna		X	2			
High Gain Antenna Boom Assy.		X	4			
Reaction Control Subsystem	X					16

Table 4.8-3: (Continued)

	Control Assembly	Switching Assembly	Signals 1	2	3	4
Scan Platform Assembly		X	4			
Data Automation Equipment		X	4			
Flight Capsule Subsystem		X	14			
Electrical Power Subsystem	X					2
Electrical Power Subsystem		X	13			4
Subsystem Interconnects (Electrical)	X			1		1
Subsystem Interconnects (Electrical)		X				3
Data Automation System	X			2	1	14
Data Automation System		X				4
Space Science Experiments	X					12
Scan Platform Assembly	X					3
Scan Platform Assembly		X				4
Flight Capsule Subsystem	X			2	1	2
Temperature Control Subsystem	X					32
TOTALS:			143	9	16	231

Table 4.8-4: CC&S PERFORMANCE CHARACTERISTICS

Reliability	0.9941 for a Total Mission Time of 5880 Hours (245 Days)
Memory - each (2)	
Capacity	128 Words (2688 Bits)
Type	Coincident Current Magnetic Cores
Command Capability	333
Bit Rate	
Operating	2.4 kc
Maximum	5 kc
Word Length	
External	27 Bits
Internal	21 Bits
Word Rate	1 Word/10 milliseconds
Program Modes	Real Time Stored Program Automatic
Program Routines	
Real Time Modes (Highest Priority)	Magnitude Computation, Comparison and Execution Discrete Execution Jump (Instruction Sequence Modification) Terminate Execution Store Program Address Execution Telemeter Memory
Stored Program Mode	Magnitude Computation, Comparison and Execution Discrete Execution Wait Time Computation, Comparison and Execution Jump (Instruction Sequence Modification) Jump Modified (Address Modification) Compare Time Comparison and Execution

Table 4.8-4: CC&S PERFORMANCE CHARACTERISTICS (Continued)

Automatic Modes	Store Sun Occultation Time Store Canopus Occultation Time Spacecraft Time Computation, Comparison and Execution Telemeter Programmer Data Sun Acquisition Control Canopus Acquisition Control Special Reference Control Inertial Reference Control
Storage Modes	
Automatic Sequential Storage	1 Command Word/Stored Word
Random Access Storage	2 Command Words/Stored Word
Computation	
Bit Addition	1 Bit/10 Msec
Serial Comparison	20 Bits/10 Msec
Magnitude Addition	90 Bits/Second
Spacecraft Clock	
Type	Binary
Capacity	29 Hours, 7 Minutes, 39.5 Seconds
Least Significant Bit	0.1 Second
Accuracy	1 Part in 10^6 in 16 Hours
Reset Modes	To Zero - Manual, Total Count, and Command Anytime - Command
Velocity Conversion Register	
Range	$\leq$ 200 pps
Difference	25 Parts in 200
Telemetry	
Memory Storage	9 (20-Bit Words)

Table 4.8-5: CC&S PHYSICAL CHARACTERISTICS AND CONSTRAINTS

WEIGHT	Control Assembly	29 Pounds
	Switching Assembly	29 Pounds
	TOTAL	58 Pounds
POWER	Control Assembly	35 Watts
	Switching Assembly	5.5 Watts
	TOTAL	40.5 Watts
VOLUME	Control Assembly	1550 Cubic Inches
	Switching Assembly	1050 Cubic Inches
DIMENSIONS	Control Assembly	8 x 8 x 24 Inches
	Switching Assembly	8 x 8 x 16 Inches
PARTS COUNT	Discrete	3725
	Integrated Circuits	1675
	Magnetic Cores	5720

PHYSICAL CONSTRAINTS

No special location, position, or configuration required

4.8.8 Control Assembly Optimization

This section discusses three integrated circuit trade studies which are applicable to the design of the Voyager CC&S control assembly logic circuitry. These studies provide a basis for the selection of vendors and the selection of either micro-circuit or discrete part circuit assemblies and investigate integrated circuit seals. The studies were accomplished for the Lunar Orbiter and Minuteman programs and are included here because of the applicability to the Voyager program.

4.8.8.1 Comparison Test of DTL Integrated Circuits

A series of tests on integrated circuits, from three vendors, utilizing physical and material analysis techniques, was conducted to assist in making a source selection decision on the Minuteman program. The major factors considered in these tests were package hermeticity, masking and diffusion, package gas (backfill), surface passivation aluminization (interconnects), and lead bond design and strength. A discussion of the tests, results and conclusions are given in the following paragraphs:

Limited Physical/Mechanical Test--This was a limited test of physical and mechanical properties for the purpose of determining significant differences between parts supplied by three vendors or uncovering serious deficiencies in design and construction. This test represents the first effort in what is expected to be a comprehensive micro-circuit evaluation program. Its limitations of sample sizes and

quantitative results are recognized but justified on the basis of extensive use of test methods similar to those used successfully to evaluate planar transistors.

It is concluded that for the overall physical and mechanical characteristics tested, parts from Vendor A and B are on a par with one another and superior to Vendor C's part. The most significant difference is in the internal lead bond design and workmanship.

Test Procedures--Perform the following test steps on one part from each vendor:

1) Perform a lead bend test per Paragraph 4.5.4.18 of Autonetics specification NA5-15825 (2 oz. - 45^{o} bend) on half of leads. Record number of bends required to break leads.

2) A krypton-85 leak detector test (sensitivity 10^{-11} atm cc/sec minimum) is to be performed before and after the lead bend test of Paragraph 1) above.

3) On the remaining one-half of leads, perform a pull test per method 2036 of MIL-STD-750. Record tension required to break each lead.

4) Perform a thorough internal visual inspection for any evidence of loose conducting material, contamination, scratches or oxide flaws on wafer.

5) Make a judgment as to whether leads could contact one another, the

chip, or the case under environmental stresses or due to manufacturing tolerances.

6) Identify the types of bonds used on the chip and post; note appearance of bonds.

7) Make a qualitative test of the lead bond strength on all internal leads. Note and record any significant observation about the bond area (did pad material come off with bond, etc.).

8) Make a judgment on the uniformity, quality, and adhesive properties of the interconnect and lead contact areas.

9) Make a qualitative test of the die-to-header bond by attempting to pry the chip off the header intact.

10) All test specimens were furnished by the vendor as evaluation test samples. Insofar as is known, the parts were all fabricated in the third or fourth quarter of 1964. These parts were all from the vendor's standard DTL lines.

Test Results--The results of the lead bend and pull tests are as follows:

1) Number of Bends to Break Lead

Lead	1	2	3	4	5
Vendor A	*500	*200	*200	*200	*200
Vendor C	83	105	107	114	122
Vendor B	71	74	77	97	151

* On Lead 1, lead did not break after 500 bends. Remaining leads were cycled 200 times with no breakage occurring.

2) Effects of Lead Bend Tests on Package Hermeticity

	Leak Rate Before Test*	Leak Rate After Test*
Vendor A	10^{-10}	10
Vendor C	10^{-10}	2.5×10^{-4}
Vendor B	10^{-10}	2.5×10^{-8}

*Leak rate given in atm cc/sec.

3) Number of Pounds Tension Required to Break Leads (Average value)

	Pounds	(Lead Dimensions)
Vendor A	4.3	(0.004 x 0.019)
Vendor C	4.0	(0.004 x 0.011)
Vendor B	4.5	(0.004 x 0.016)

There was no evidence of loose conducting material, contamination of obvious oxide scratches or imperfections in any of the specimens examined.

Internal-lead-configuration tests are summarized below.

1) Vendor A--This vendor utilizes an all-aluminum internal lead system. This includes aluminizing the portion of the external lead which extends into the interior of the package (the "post") and to which the internal lead from the chip is attached. This system effectively eliminates the formation of intermetallic compounds such as "purple plague." The lead diameter is approximately 2 mils. The chip bond is relatively long and narrow with considerable area contact giving good mechanical strength. The post bond is identical to the chip bond. The bond appearance is excellent and the lead placement on the pads fairly precise. As with all wedge-type bonds, the leads

come off the bonding pads parallel to the chip and there is some danger of a lead inadvertently touching the edge of the chip due to manufacturing tolerances or environmental stresses. This danger is reduced somewhat by "humping" the lead slightly as it comes off the bonding pad. The leads are drawn fairly taut leaving little if any possibility of a lead drooping down enough to contact the chip. The spacing between leads is uniform and there is essentially no danger of the leads contacting one another.

2) Vendor C--This vendor also utilizes an all-aluminum system, including aluminizing the internal post. The lead is approximately 1 mil in diameter. The chip bond is the familiar small-area thermal-compression wedge bond. The appearance of the chip bonds is relatively poor. All of the bonds examined appeared to have been made with excessive pressure on the bonding tool. This results in nearly cutting through the lead at the heel of the wedge and a consequent reduction in mechanical strength. Also common on these bonds is excessive "toe" at the tip of the bond. This "toe" results from the wedge being made too far from the tip of the lead. "Toes" are known by past experience to be subject to separation by shock and other mechanical forces and thus become loose conducting particles. Excessive pressure was also evident on the post bond but not to the same extent. Many of the post bonds are covered with the glass-like case sealing material as a result of the package sealing operation. Bond placement was also relatively poor. Lead spacing was generally good. Some concern is felt for attaching lead bonds at the center of the chip as was done on one lead in the part examined. When wedge bonds such as these

are used in this manner, the chance of a lead inadvertently contacting a chip interconnect is greatly increased.

3) Vendor B--This vendor utilizes the conventional gold ball thermal compression bond to an aluminum pad. The lead diameter is approximately 1.5 mils. The bond appearance is excellent and the lead placement on the pads very precise as shown in Figure 4.8-16. There was no evidence of purple plague on the bonds examined. Considerable care is evidenced in routing the bend-leads to minimize the probability of the leads contacting the chip.

Internal Lead Bond Strength--These tests are summarized below.

1) Vendor A--In all cases, the lead itself broke when force was applied to approximately the center of the span (No bonds came loose). The bonds themselves were then pried off the chip and indicated excellent mechanical attachment in all cases. In general, pad material under the bond did not come clean off the oxide, indicating good affinity between the aluminum interconnect and the chip surface. The post bond was similarly checked and found to be generally excellent.

2) Vendor C--In all cases the lead separated at the heel of the bond itself. The force required to do this was extremely slight. Generally, the pad material lifted off the chip when the remainder of the bonds were pried off. The bond strength of the post bond was considerably better but here again excessive pressure tended to reduce mechanical bond strength.

3) Vendor B--In all cases the lead itself broke. No bonds came loose. For most bonds, applying force to the bonds themselves caused the

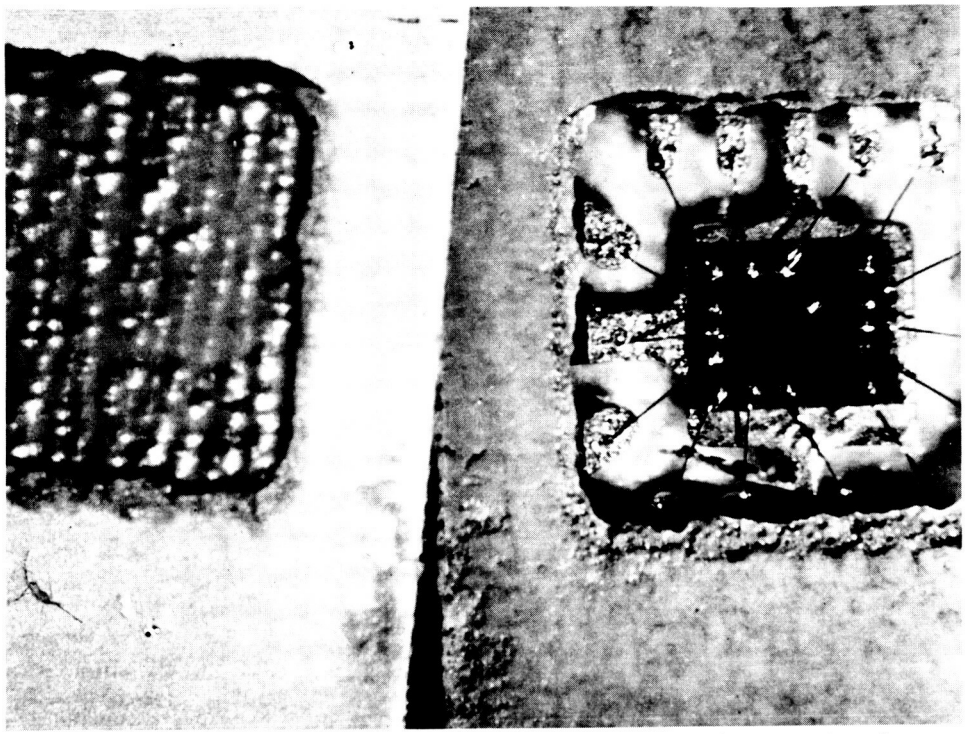

Figure 4.8-16: Vendor B Flat Package with Defective Hermetic Seal

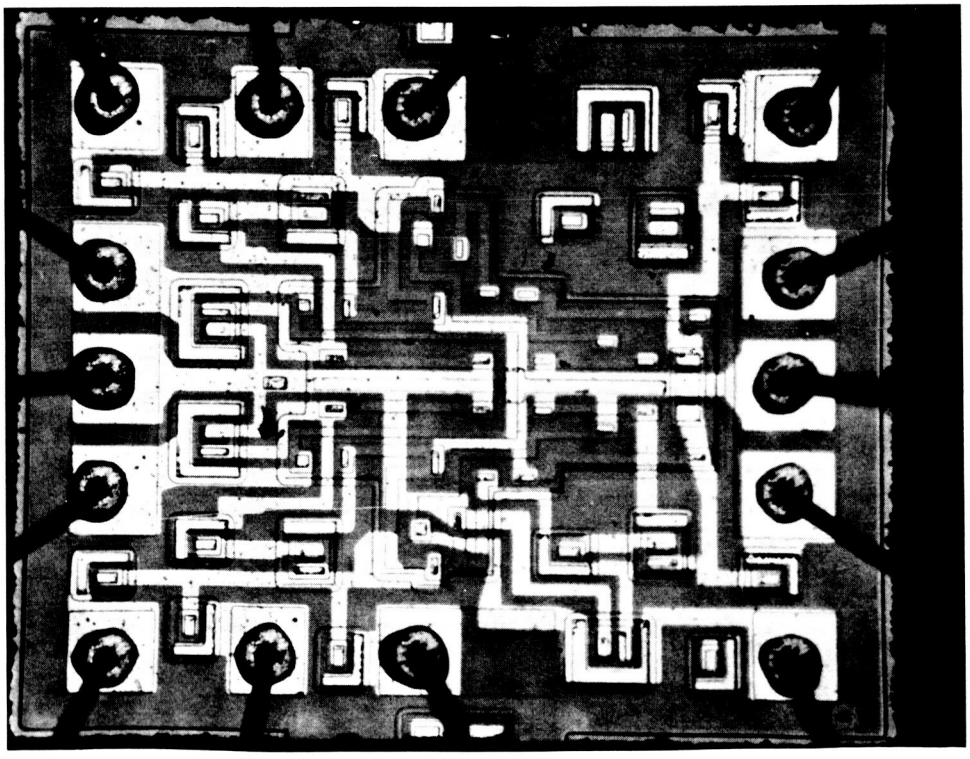

Figure 4.8-17: Vendor B Integrated Circuit — 65X

bond and the pad material to come clear off the oxide. This is considered to indicate an optimum bonding joint for a ball bond. The bond strength was judged to be excellent on all except possibly one of ten bonds. The remaining bond was noticeably weaker but still more than adequate. The post bonds were found to have excellent mechanical strength.

The interconnect and contact pad aluminization was judged to be of good uniformity on all three vendors' parts. The adhesive properties of the Vendor A and B aluminization were judged to be equally good and superior to that of the Vendor C part. The aluminization on the Vendor C part was considerably softer and could be scraped completely off the oxide quite easily. On the Vendor A and B parts hard scraping did not remove the final film of aluminum.

Vendors A and C bond the chip to the glass or ceramic package with a material similar to that used to seal the package. It forms a very hard and tenacious bonding material and exhibited excellent mechanical strength when an attempt was made to pry the chip off the header. Vendor B bonds the chip using a gold eutectic solder. This bond though not quite as strong mechanically as the others was still judged to be excellent.

4.8.8.2 Design Evaluation of DTL Integrated Circuits--Four integrated circuits packaged in ceramic or metal/ceramic flat packs were received for material and design analysis from Vendors A, B and C. In addition, three integrated circuits packaged in low silhouette To-5 cans were received from Vendor C. The information

was requested by the Boeing Aero-Space Division Electronic Parts organization to aid them in selecting a source of integrated circuits for the Minuteman improved data store and processor. Due to short lead time, a complete analysis was not attempted. Those items listed under test procedure were determined to provide the most information in the time allowed.

Rated on the basis of microscopic examination and the observed physical and chemical characteristics of each device, the selection is as follows:

1) Vendor A;
2) Vendor B;
3) Vendor C.

Test Procedure--Vendor samples were dispensed in the following manner:

1) A package gas analysis was performed on one part from each vendor, with the exception of Vendor C which had two To-5 and three flat-packs analyzed.
2) Four flat packs from each vendor and two To-5 packages from Vendor C were tested for hermeticity with Kr^{85}. One flat pack from each vendor was retested in Kr^{85} following a destructive lead bend test.
3) Optical, chemical stain and chemical etch analysis was performed on two flat-packs from each vendor.

Test Results--The tests are summarized below.

1) Hermeticity and Package--Flat packs from each vendor were tested for hermeticity in the Physics of Failure Kr^{85} leak detection apparatus. One of these units from each manufacturer was selected

for a destructive lead bend test and rechecked for hermeticity afterward. The results of these tests are listed in Table 4.8-6.

The To-5 can was gold-plated to facilitate soldering and welding as well as form a good electrical contact for the common connector. The number of leads available on this package are limited to ten by size and geometry. Mechanically they are stronger than the ribbon lead used in conjunction with the flat package. The leads are constructed from gold-plated Kovar (54% Fe, 29% Ni, 17% Co, 0.2% Mn, 0.1% C). 7052 or similar glass is used as a feed through insulator.

Two methods of flat-pack construction were observed. Vendor A and Vendor C use an opaque, all-ceramic construction of 7052 or similar glass that seals well to flat Kovar feed-throughs. The ribbon leads are gold-plated.

Vendor B uses a ceramic package with a transparent back window which evidently serves the purpose of allowing observation of a dyepenetrant used during gross leak testing. The final sealing is accomplished with a prefixed glass-coated Kovar cover.

One such device is shown in Figure 4.8-16. The lid was removed by the simple insertion of a scalpel. Very little force was required for its removal.

An objection is raised to this type of sealing. Ceramic to ceramic makes a better hermetic seal than ceramic to Kovar, simply on the

Table 4.8-6: Kr^{85} HERMETIC SEAL TEST
BEFORE LEAD BEND TEST

Vendor A		Vendor B	
Type 44 #1	10^{-6} atm cc/sec	Type 43	10^{-10} atm cc/sec
Type 44 #2	4×10^{-7} atm cc/sec	Type 44	3×10^{-8} atm cc/sec
Type 42	8×10^{-6} atm cc/sec	Type 43	10^{-10} atm cc/sec
Type 43	10^{-10} atm cc/sec	Type 44	10^{-10} atm cc/sec

Vendor C (Flat Pack)

Type 44	10^{-10} atm cc/sec
Type 43 #1	10^{-10} atm cc/sec
Type 43 #2	10^{-10} atm cc/sec
Type 45	10^{-10} atm cc/sec

Vendor C (To-5)

Type 42	10^{-10} atm cc/sec
Type 44	10^{-10} atm cc/sec

Vendor A		Vendor B		Vendor C	
Type 43	10^{-8} atm cc/sec	Type 43	2.5×10^{-8} atm cc/sec	Type 43 #1	2.5×10^{-4} atm cc/sec

basis that two similar materials wet much better than dissimilar materials.

The vendors are listed as follows in order of their acceptability in the areas of packaging and hermeticity.

a) Vendor C;

b) Vendor A;

c) Vendor B.

2) Package Gas Analysis--A CEC 21-611 mass spectrometer was used for analysis of gas content. The standard system was used for the To-5 can and then modified to increase sensitivity for analysis of the much smaller volumes of the flat-packs.

The results are presented in Table 4.8-7. An estimate of the total gas composition is given in the same column that shows the measured pressure change when the package was opened. The percent of gaseous composition is more accurate for the flat-pack. An error of 50 percent or greater is possible for quantitative estimates of water because of its polar character. Actually, only one package, Vendor C, the To-5 can, had the most desirable atmosphere, relatively inert and dry. There have been a number of studies on the effect of various atmospheres on device characteristics. It appears that an inert atmosphere is still the most desirable. Of more importance, however, is a hermetically tight device which does not allow the atmosphere to change. It is a changing atmosphere of water, oxygen and other

Table 4.8-7: ANALYSIS OF INTEGRATED CIRCUIT PACKAGE GASES
(Figures are given in Mol-Percent with Estimated Error)

Device	Gas	Water	Nitrogen	Oxygen	Argon	Carbon Dioxide	Methalol (?)	P of Package and** Estimate of Content
Vendor C Type 44		-	85 ± 3	13 ± 2	1 ± 0.5	1 ± 0.5	-	1.6 mm est. dry air
Type 44		0.3 + 1	99 ± 1	1 ± 0.5	-	-	-	1.72 mm est. slightly wet nitrogen
Air for the day of analysis		0.03 + 2	83 + 5	14 ± 3	1 ± 0.5	.04 + 0.5	-	50 mm RH 53%
System was then modified to increase sensitivity for flat-packs								
Vendor A Type 42		10 ± 2*	73 ± 5	15 ± 3	1.5 ± 0.5	1 ± 0.5	-	0.225 mm est. wet air
Vendor B Type 44		6 ± 2*	32 ± 5	2.5 ± 0.5	0.25 ± 0.10	10 ± 2	-	0.162 mm est. wet, dirty air
Air for the day		3.5 ± 0.5*	90 ± 5	15 ± 3	1 ± 0.5	0.3 ± 0.10	-	0.225 mm RF 57%
Vendor C Type 44		8 ± 2*	38 ± 7	7 ± 5	0.2 ± 0.1	0.6 ± 0.2	46 ± 15	0.136 mm wet air and methanol
Air for the day		2.5 ± 0.5*	80 ± 5	16 ± 3	0.2 ± 0.1	0.8 ± 0.3	-	0.190 mm RH 62%
Vendor C Type 45		4 ± 1.5*	48 ± 8	10 ± 5	0.2 ± 0.1	0.8 ± 0.3	37 ± 15	0.186 mm wet air and methanol
Type 43		9 ± 2*	39 ± 7	8 ± 5	0.2 ± 0.1	1.0 ± 0.3	43 ± 15	0.190 mm wet air and methanol
Air for the day		10 ± 5*	73 ± 5	16 ± 3	0.5 ± 0.2	0.5 ± 0.2	-	0.190 mm RH 58%

* Probably high by a factor of 2
** Change in chamber pressure after package was opened

rather easily ionizable gases which contribute to oxidation, contamination and other undesirable effects on device performance. Using this criteria the devices were rated as follows:

a) Vendor C To-5;

b) Vendor C Flat-Pack;

c) Vendor A;

d) Vendor B.

The methanol in the Vendor C flat-pack does not appear to be desirable. It was, however, found to be difficult to ionize, as evidenced by the fact that no hydrogen was detected by the mass spectrometer. It would be helpful to know if there is a reason for purposely enclosing methanol or whether it is accomplished unintentionally.

3) Bonding--A different lead-to-chip bonding technique was used by each of the manufacturers. Vendor B uses a conventional gold-to-aluminum nail-head bond. Vendor A uses a long wedge or ultrasonic aluminum-to-aluminum bond, and Vendor C uses a short wedge aluminum-to-aluminum bond. Low magnification observation showed a good degree of accuracy of bond placement by all three manufacturers. The bond quality varied widely.

Vendor B was the only manufacturer represented to use a gold nail-head bond. The bond as observed in Figure 4.8-17 has been accomplished with a good degree of accuracy and uniformity. Purple plague which is inevitable whenever gold and aluminum meet seems to have been controlled to a reasonable degree. One bond was inadvertently lifted during inspection. It was noted that when the bond lifted, it removed

all of the bonding material down to the passivation on the die. This indicates that all of the aluminum in the bond area was consumed in the bonding operation and that the bond did not penetrate the passivation. Both of these features are desirable in a nail-head bond.

Vendor A utilizes an aluminum-to-aluminum bond which is either made ultrasonically or with a wedge made along the axis of the short wedge which is made perpendicular to the axis of the lead. A short wedge bond was noted on what was apparently an earlier Vendor A part. The long wedge bond has a distinct advantage over a short wedge bond, in that there is less deformation of the wire adjacent to the bond and consequently less stress in the wire at that point. Vendor A appears to have achieved a reasonable degree of precision in their bonding operation, although one of the fourteen bonds shown in Figure 4.8-18 was nearly cut in half by the bonding tool.

The poorest bond observed was in two Vendor C To-5 packages. Both devices showed that an excessive amount of pressure was used a number of times during the wedge bonding operation. This can be seen in Figure 4.8-19 where four of the aluminum bonds are grossly smeared. This resulted in an extremely weakened condition and prevented bonds from surviving relatively mild cleaning procedures such as rinsing with distilled water.

Unfortunately, through an error in parts distribution, only one intact Vendor C flat-pack was observed. Three were analyzed for

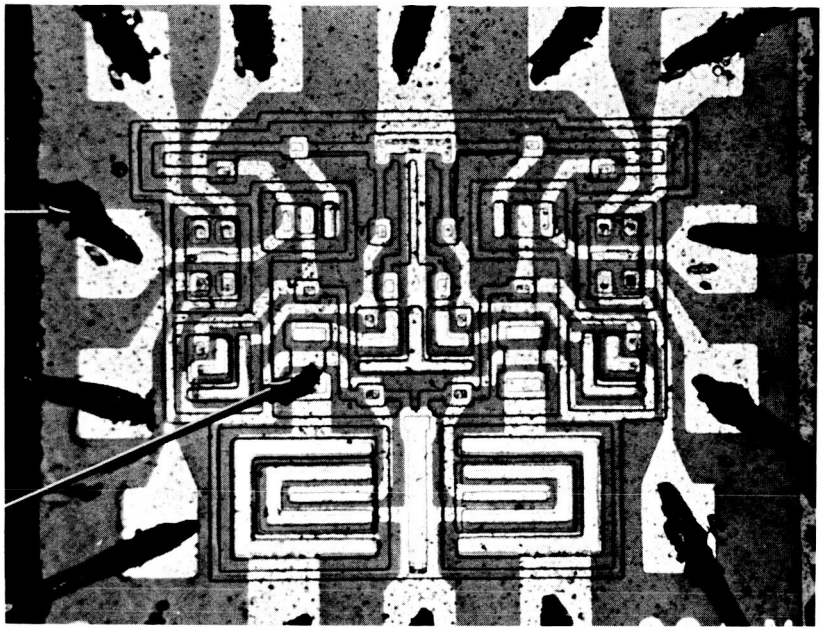

Figure 4.8-18: Vendor A Integrated Circuit Showing Surface Damage

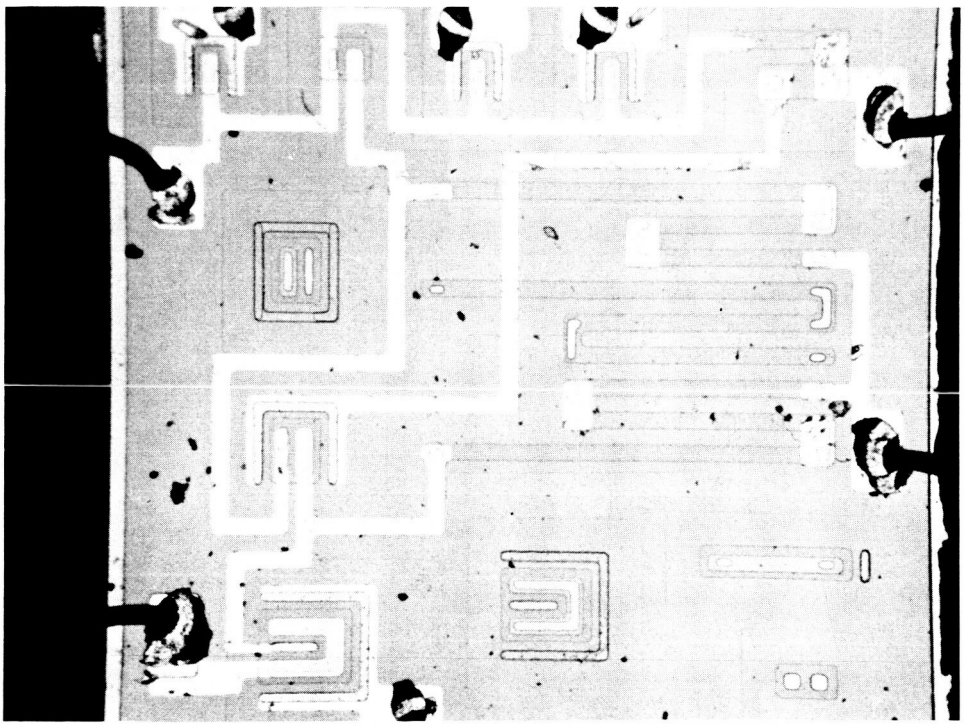

Figure 4.8-19: Vendor C Integrated Circuit

package gas in the mass spectrometer and only partial observation of chip fragments could be accomplished. From what could be observed, the bond quality of the flat-pack was far superior to that found in the To-5 cans. The bonds have an appearance of uniform bonding pressure and accuracy of placement. A check of several bonds was made by measuring the thickness of the aluminum lead at the wedge mark. Of six bonds checked only one showed a greater-than-average thickness.

Because of the fragility experience in observing the bonds found in the Vendor C To-5 package, the flat-pack bonds were further tested by forcing 24-psi pressurized air across the surface of chip both before and after boiling 5 minutes in distilled water. No bond failures were noted. Even two damaged bonds survived quite well. This was a considerable degree better than the To-5 bonds, and the pressurized air test itself was considered more severe than an additional test of centrifuging this same part at 5010 rpm with a force of 3386 g's.

Bonding leads to the external ribbons seemed to be accomplished without difficulty by all three manufacturers.

In the absence of more qualitative data the vendors are listed below in order of ability to make an acceptable bond.

a) Vendor A - Vendor B;

b) Vendor C.

Note that Vendor A and Vendor B are rated the same. Figure 4.8-20 shows a Vendor C chip lead to feed-through lead bonding that is glassed-over. It is not known if this was by accident or design.

4) Mask Alignment--One apparent problem in depositing aluminum interconnects appears to be mask alignment. If a mask is shifted slightly, there is bare silicon exposed from the time the aluminum is deposited until the time the aluminum is sintered. When the aluminum is sintered, there will be a thin layer of oxide grown on the silicon. Any contamination introduced to the silicon while it is not protected could possibly cause excessive leakage current in the device.

The quality of the mask alignment for the aluminum interconnects, in decreasing order, is:

a) Vendor A;

b) Vendor B;

c) Vendor C.

This order is based on the area of silicon left uncovered by the aluminum interconnects. Figure 4.8-21 is one of the least acceptable mask-misalignments observed.

5) Passivation--A uniform passivation of the die is necessary to prevent:

a) premature dielectric breakdown of the silicon oxide between an aluminum interconnect and a component in the die; and

b) "pipe" formation by diffusion of a "n" or "p" dopant into a "p" or "n" region through a hole in the passivation.

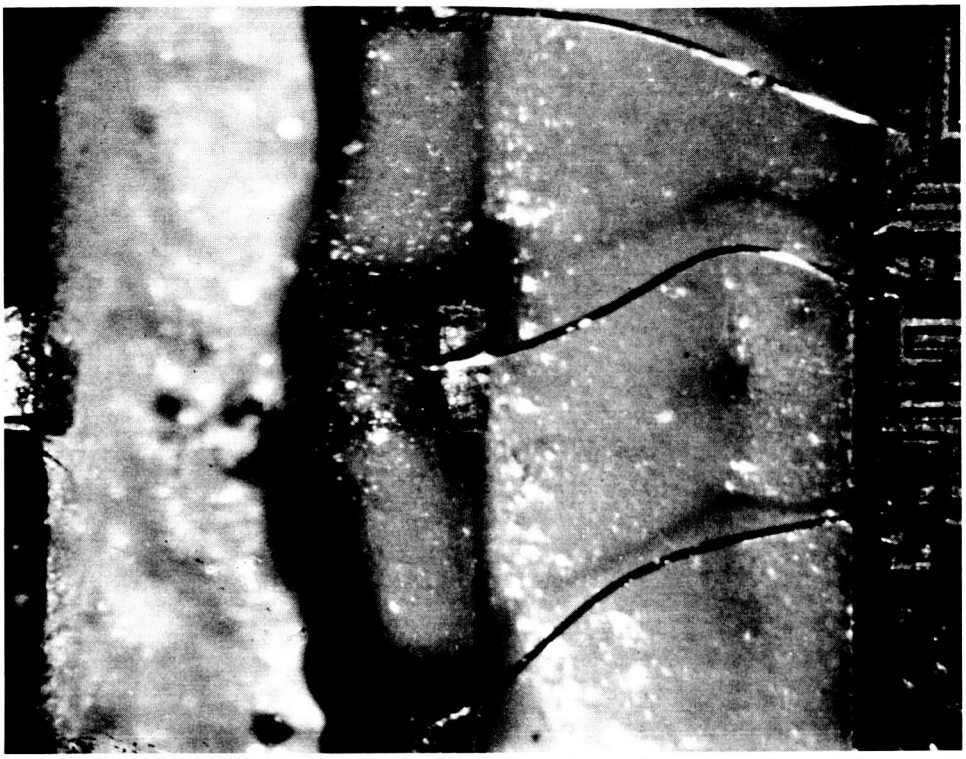

Figure 4.8-20: Vendor C Integrated Circuit Showing Glassed-Over Leads — 37X

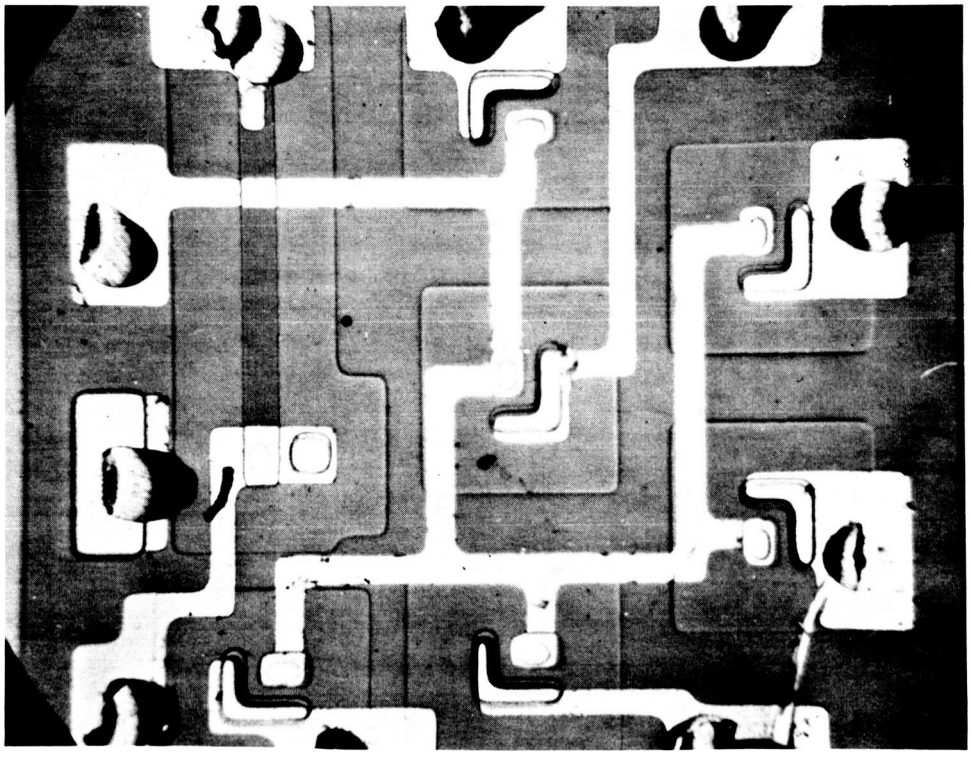

Figure 4.8-21: Vendor C Integrated Circuit — 140X

All three manufacturers were found to have dirt particles on the crystal surface. The degree varied somewhat, but not enough to rate them differently.

Oxide passivation of the crystal surface was found to be defective in all parts observed. Literally hundreds of one and two fringe pinholes were found. Some much larger pinholes having as many as six fringes may be seen in Figures 4.8-22, -23, and -24. Figure 4.8-22 shows a pinhole directly over a resistor diffusion. It was not possible to focus on all five fringes in one photograph, but from the number of fringes (approximately 1200A/fringe) it leaves little doubt that the hole is down to the diffusion itself.

In Figure 4.8-23 the fringe pattern and corresponding hole lies directly over the emitter diffusion and within the aluminum metallization. Five fringes were found. This hole did not become apparent until a chlorine etch was applied.

The hole in Figure 4.8-24 lies in among the metallization geometry. Five to six fringes were found indicating penetration to the silicon crystal.

In some cases (Figure 4.8-25) residual fluoride etchant has removed layers of oxide rather than leaving a small hole. Also seen in this figure next to an isolation diode, is a four or five fringe pinhole (out-of-focus).

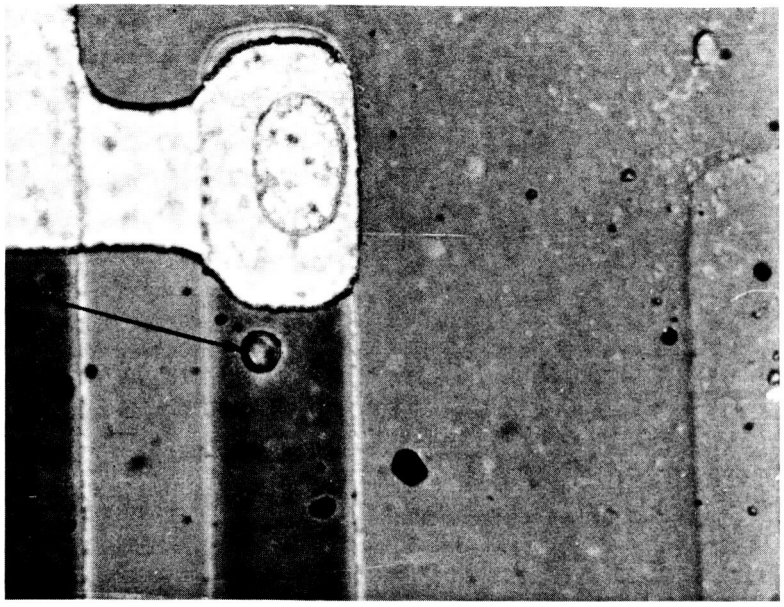

Figure 4.8-22: Vendor C Integrated Circuit Showing Pinhole in Oxide — 765X

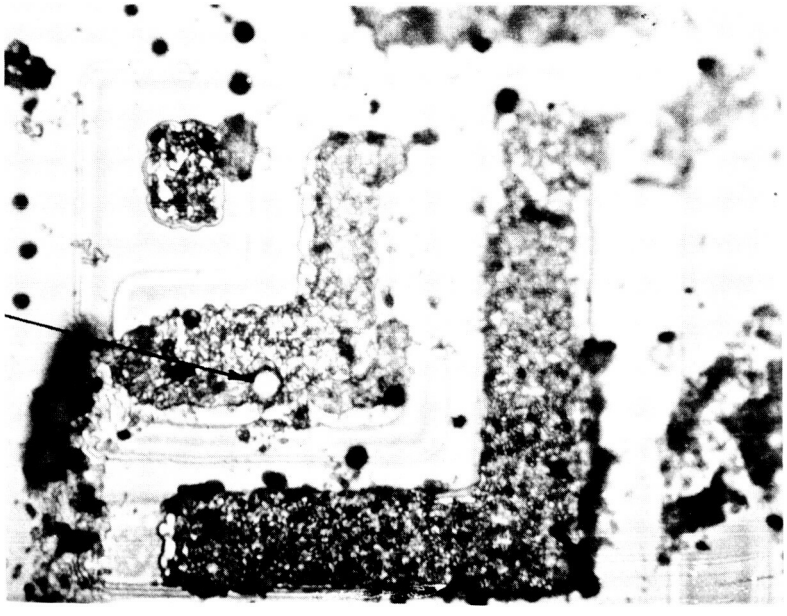

Figure 4.8-23: Vendor A Integrated Circuit Showing Pinhole — 765X

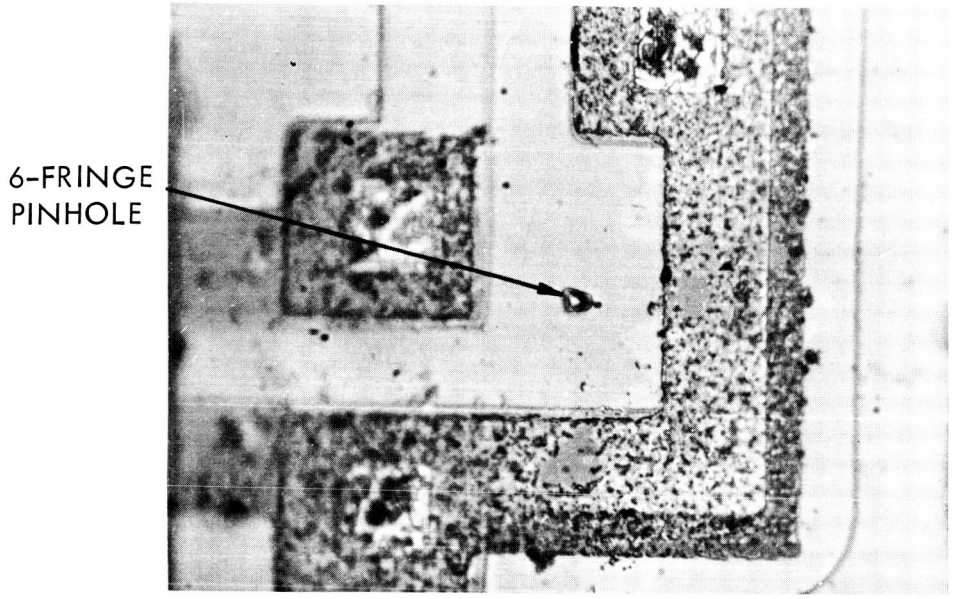

Figure 4.8-24: Vendor B Integrated Circuit Showing Pinhole — 765X

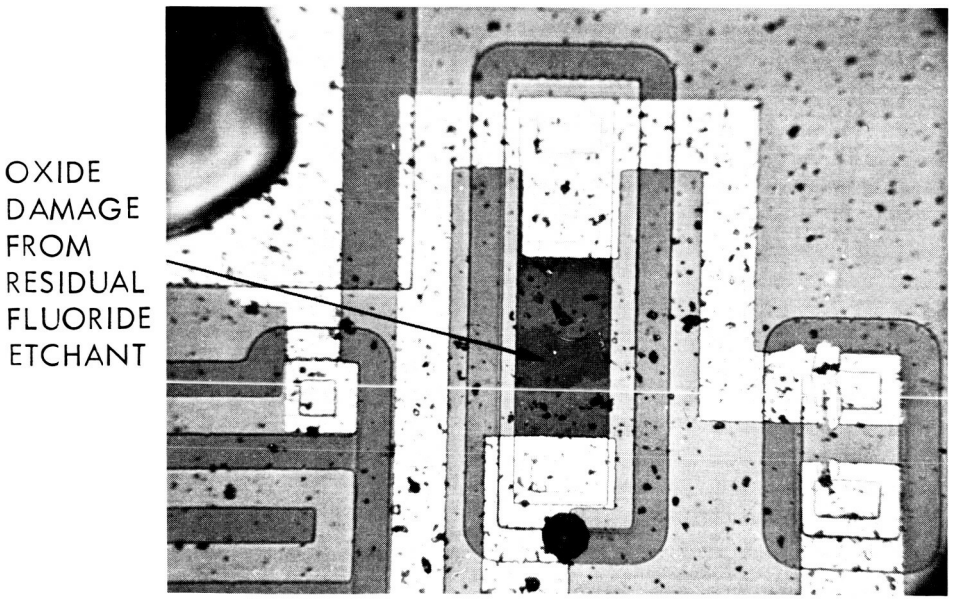

Figure 4.8-25: Vendor B Integrated Circuit with Oxide Damage — 275X

The vendors are listed as follows in order of their acceptability in regard to passivation of the chips.

a) Vendor A - Vendor C;

b) Vendor B.

Note that Vendor A and Vendor C are rated the same.

6) Metallization--All manufacturers were found to have damaged metallization from dragging or misplacing the handling tool on the surface of the chip. In some cases smearing of the aluminum which results from dragging may cause shorts between interconnections. Referring back to Figure 4.8-18, the arrow pointing to the dark spot shows where tool dragging has smeared enough aluminum to give the appearance that aluminum interconnections have shorted. Since no electrical tests were performed, this was not confirmed.

Another objection to this type of damage is the weakened condition of thinned-out aluminum leaves it susceptible to further oxidation to Al_2O_3. With such a device in operation, heat generating currents could accelerate further oxidation, consequently increasing resistance, resulting in a hot-spot and an eventual open condition.

Chromate conversion was applied to study surface charge and diffusion distribution. This technique is best shown in color photography; however, Figure 4.8-26 has enough contrast to show that surface defects or impurities which were included during the metallization process, having a different charge character or distribution, did not stain at all.

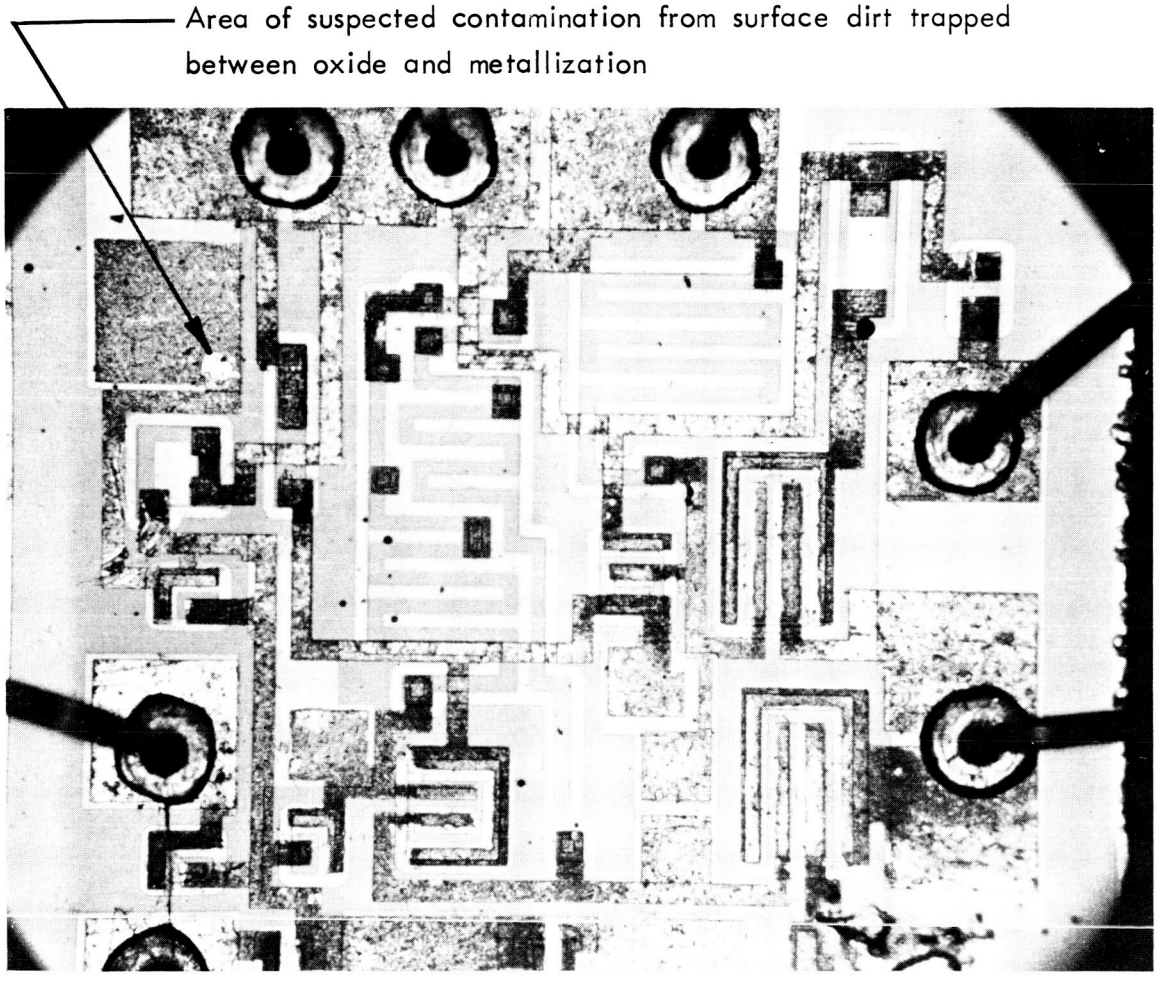

Figure 4.8-26: Vendor B Integrated Circuit at 65X

Quality of aluminizing can have an important bearing on device performance. Too thin metallization can lead to eventual high resistance. Too thick metallization can result in crystallization problems during subsequent sintering operations.

Rated in order of the best quality of aluminizing:

a) Vendor A;

b) Vendor B;

c) Vendor C.

7) Discussion and Conclusion--It is restated that this evaluation is based on microscopic observation, and physical and chemical tests, without knowledge of electrical characteristics of any device included in this analysis. On this basis, six categories of observation and analysis were used to aid in deciding the rating of each manufacturer.

This rating system is presented in Table 4.8-8. Following the title of each category is a number in parenthesis which is a weighting factor that emphasizes the relative importance placed upon each category. As each manufacturer was given three points for first, two for second and one for third, the weighting factor was used as a multiplier to give the total points for that particular category. The points from each category were then totaled to arrive at the final rating based on the cumulative results.

Table 4.8-8: RATING SYSTEM USED FOR EVALUATING INTEGRATED CIRCUITS

		Vendor A	Vendor C	Vendor B
Lead Bonding to Chip	(3)	9	3	9
Interconnecting Metallization	(2)	4	2	4
Hermetic Sealing and Package Quality	(2)	4	6	2
Silicon Oxide Passivation	(2)	4	4	2
Accuracy of Metallization Alignment	(1)	3	1	2
Package Gas Analysis	(1)	2	3	1
Cumulative Total		26	19	20

Employing this criteria, the manufacturers were rated by the Boeing Physics of Failure group as follows:

a) Vendor A;

b) Vendor B;

c) Vendor C.

4.8.8.3 Comparison of Microcircuit and Discrete Part Circuit Assemblies The electronic assemblies which were designed for the "control assembly" in the Lunar Orbiter provide means for comparing some costs, weights and volume of electronic assemblies using integrated circuitry (in this case, flat-packs) with functionally equivalent assemblies using discrete part circuitry.

The computing and logic portion of the "control assembly" was designed around integrated circuits in flat-pack form whereas the remainder of the "control assembly" circuitry was more suitably designed around discrete parts in cordwood module form.

The "flat-pack board assembly," as referred to here, consists of flat packs, connectors and printed circuit boards assembled on a mounting plate. The "module board assembly" consists of encapsulated cordwood modules, connectors, and printed circuit boards assembled on mounting frames.

Assumptions--The data contained herein was obtained from personnel on the Lunar Orbiter program working in circuit design, packaging design,

drafting, parts control, spares and costing. Detailed breakdowns of the production costs are not included in this comparison.

It is estimated the results of this comparison would have been similar whether the discrete parts were assumed to be mounted in cordwood module form or on circuit boards.

The weight comparison made is between the "flat-pack board assemblies" and the "module board assemblies" only and does not include the associated cable and chassis weight.

All of the related costs have not been included in this analysis, but it is assumed that the majority of the significant and direct costs which result in savings, are included. The cost for "spares" is negligible for the cordwood modules because of the small quantity allocated. There was insufficient data to compare costs associated with rejections or repair.

An indirect cost savings not calculated, which will be significant, is that which results from the weight reduction.

Circuit Comparison--The comparison of microcircuit and discrete part circuit assemblies is shown in Tables 4.8-9 through 4.8-13.

4.8.8.4 Integrated Circuit Seal Investigation

The following investigation was conducted by The Boeing Company, Aero-Space Division, Structures and Materials Technology organization (Lunar Orbiter).

Table 4.8-9: SUMMARY OF SAVINGS
USING INTEGRATED CIRCUITS RATHER THAN DISCRETE PARTS

Average Cost Savings per Spacecraft (Based on 12 spacecraft)	$163,708.00
Weight Savings per Spacecraft (See note on weight)	28 lbs.
Volume Savings per Spacecraft	0.51 cu. ft.

Data taken from Tables 4.8-11 and 4.8-12.

Table 4.8-10: LUNAR ORBITER CONTROL ASSEMBLY
COMPUTING AND LOGIC CIRCUIT REQUIREMENTS

	Type of Circuit			
	Dual 4-Input Gate	Clocked Flip-Flop	4-Input Buffer	4-Input Expander
Number of circuits (flat-packs) required per control assembly (Based on Fairchild Microcircuits)	408	122	36	46
Number of parts contained in each circuit (Fairchild Microcircuits)	22	67	30	8
Total number of parts required per control assembly	8976	8174	1080	368

Table 4.8-11: DATA SUMMARY, COMPUTING AND LOGIC CIRCUITRY

USING INTEGRATED CIRCUITS (FLAT-PACKS)

Number of flat-packs required per control assembly (see Table 4.8-10)	Dual 4-input gate	408
	Clocked flip-flop	122
	4-input buffer	36
	4-input expander	46
	Total	612
Number of flat-packs per flat-pack board assembly	Space on boards for a maximum of--	112
	Actual used per assembly (average)--	88
Number of flat-pack board assemblies required per control assembly	7 used (leaves some space for spare circuits)	
Average cost of each flat-pack board assembly (not including cost of packaging and logic design, included below)		
Assembly drawings and artwork	280 manhours at $10/manhour	$2800.00*
Cost of flat-packs	88/assemblies + 2 spares at $15 ea.(Avg.)	1350.00
Cost of testing flat-packs	88/assemblies + 2 spares at $20 ea.(Avg.)	1800.00
Raw materials		56.00
Production labor	98 hrs run time at $21/hr ($21/hr takes care of labor, OH, planning, quality control, etc.)	2058.00
		8064.00

Table 4.8-11 (Continued)

Total cost of flat-pack board assemblies required per control assembly	7 at $8064.00 ea.	$56,448.00
Cost of logic design for all of the computing and logic circuitry in the control assembly	5760 manhours at $10/manhour	$57,600.00 *
Cost of basic package design for the flat-pack board assemblies	1440 manhours at $10/manhour	$14,400.00 *
Total cost of the computing and logic circuitry for the 1st control assembly using flat-pack board assemblies		$128,448.00
Total cost of the computing and logic circuitry for each of the (2nd and on) control assemblies using flat-pack board assemblies	NOTE: Costs marked with an asterisk not incurred on the (2nd and on) vehicle	$36,848.00
Weight of flat-pack board assemblies	7 assemblies at 0.32 lbs/assembly	2.24 lbs.
Volume of flat-pack board assemblies	7 assemblies at 14.69 cu. in./assembly	102.83 cu. in.

Table 4.3-12: DATA SUMMARY, COMPUTING AND LOGIC CIRCUITRY USING DISCRETE PART CIRCUITS (CORDWOOD MODULES)

Number of cordwood modules neeced to incorporate the circuit parts indicated in Table 4.8-10.	at 30 discrete parts per module	Dual 4-input-gate 300 Clocked flip-flop 273 4-input buffer 36 4-input expander 12 Total No. Modules 621
Number of module board assemblies required per control assembly	at 28 modules per module board assembly	Required Assemblies 22
Cost of circuit design for the cordwood modules	4 module circuit designs required at 160 manhours/circuit and $10/manhour	* $6,400.00
Cost of assembly drawings and artwork for cordwood modules	4 different modules at 56 manhours/ module and $10/manhour	* $2,240.00
Cost of assembly drawings and artwork for module board assembly drawings	160 manhours/assembly at $10/ manhour	Total cost (12 assys) *$35,200.00
Cost of parts and materials for the module board assemblies	at $3566.00/assembly	Total cost (22 assys) $78,452.00
Cost of testing discrete parts	at $1.00/discrete part and 30 parts/module and 621 modules	$18,630.00

Table 4.8-12 (Continued)

Total cost of production labor for the module board assemblies	217 hours run time/assy at $21.00/hr ($21.00/hr takes care of labor, OH, planning, quality control, etc.)	Total cost - $100,254.00
Cost of logic design for all of the computing and logic circuitry in the control assy	5760 manhours at $10.00/manhour	*$ 57,600.00
Cost of basic package design for the cordwood modules and the module board assemblies	2880 manhours at $10.00/manhour	$ 28,800.00
Total cost of computing and logic circuitry for the 1st control assembly using module board assemblies		$327,576.00
Total cost of computing and logic circuitry for the 2nd and on control assembly using module board assemblies	NOTE: Costs marked with an asterisk not incurred on the (2nd and on) vehicle	$197,336.00
Weight of module board assemblies	22 assys at 1.357 lbs/assy	30 lbs.
Volume of module board assemblies	22 assys at 45 cu. in./assy	990 cu. in.

Table 4.8-13: TOTAL PROGRAMMER OR CONTROL ASSEMBLY

		Microelectronic Version	Equivalent Discrete
Reliability F/hr.		70×10^{-6}	-
Size		990 cu. in.	1700 cu. in.
Weight	Logic	2.24 lbs.	30 lbs.
	Total	SW Assembly 6.3 lbs. Control Assembly 18.74 lbs.	46.5 lbs.
Production Cost/ea.		$145 K	$305 K
Design Cost	Logic	$ 72 K	$130 K
	Balance	Same	Same
Power Consumption		40W	50W

The subject investigation was conducted using Fairchild integrated circuit flat-packs with unformed straight leads (electrical rejects) and with formed leads (production parts received for use in production hardware).

Figures 4.8-27 and -28 are external views of typical integrated circuits in a flat-pack configuration taken at a magnification of 15X. These photos were taken of the flat-packs as received in an endeavor to ascertain a possible correlation between external physical appearance and internal defects which might cause leakage. These pictures showed a surface crazing of the glass seal and the glass miniscus on the leads.

Three production flat-packs were leak checked after removing the epoxy paint from the body by solvent softening and scrubbing. This was necessary because the paint absorbs the tracer gas. The results of the leak tests showed an average leak rate of 10^{-11} cc/second, which is considerably less than the minimum requirements. Had any of these tests showed an unacceptable leak rate, the flat-packs would have been sectioned to find the cause of the leak.

Two production flat-packs and two reject flat-packs were sectioned and photographed at a magnification of 100X at several levels through the seal area. No defects which would affect the integrity of the seal were noted. Some porosity existed in all the seals but consisted of very small bubbles entirely surrounded by the glass seal. A dark line which at first looked like a crack was found, but upon further polishing and study it was determined to be a stringing condition in the glass.

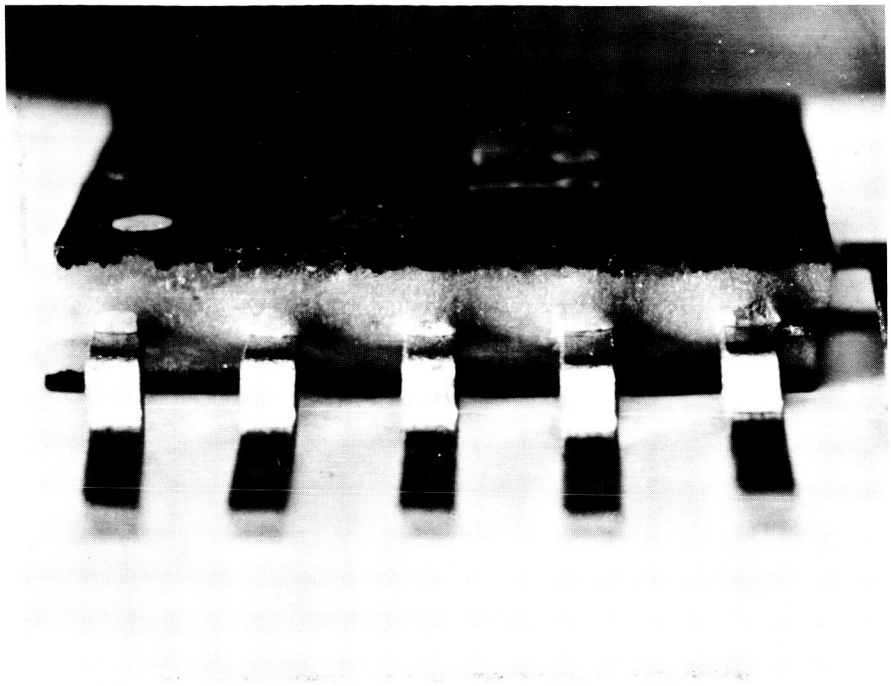

Figure 4.8-27: Integrated Circuit—Side View 15X

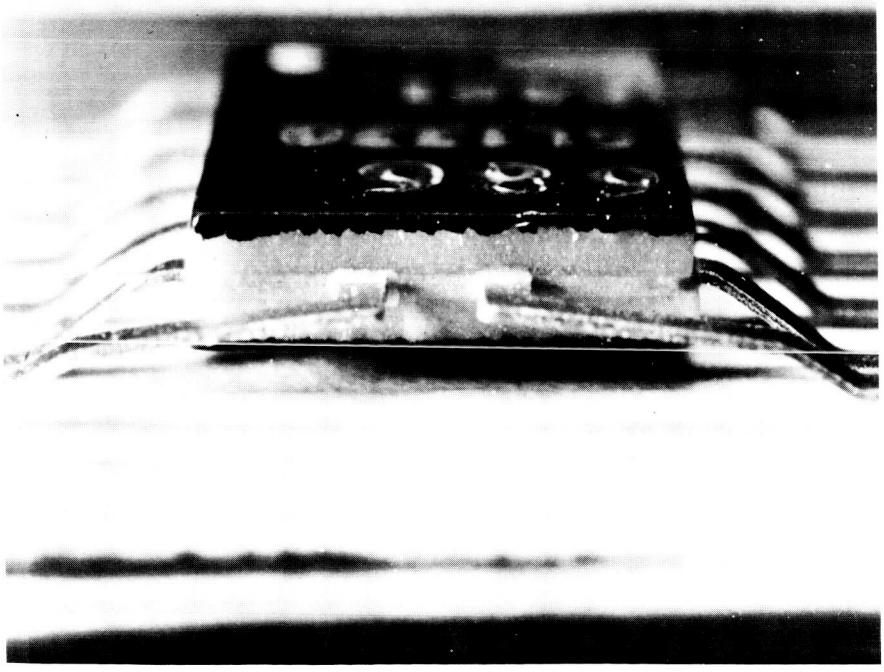

Figure 4.8-28: Integrated Circuit—End View 15X

The random location and discontinuous nature of the lines precluded the possibility of a crack in the seal. Figures 4.8-29 through 4.8-32 are sections through the seal areas at a magnification of 100X. Figure 4.8-29 is taken just inside the glass seal of the package. It will be noted that there are dark lines which might be cracks. Figure 4.8-30 is a view of the same seal a few thousandths further into the seal area. Note that the apparent cracks have moved substantially from the location in Figure 4.8-29 Figures 4.8-31 and 4.8-32 were taken still deeper in the seal area and it can be seen that the cracks have now disappeared entirely. From this investigation it was concluded that the seals are satisfactory and leak check tests verified this. The small dark spots in the seal area are caused by a material in the glass seal which is included to prevent propagation of cracks. Upon polishing, this material comes out and leaves a small void, which is a dark spot in the picture.

4.8.9 Switching Assembly Trade Study

4.8.9.1 Comparison of Mariner C and Lunar Orbiter Squib Circuits

This section documents the Boeing response to a NASA request to compare the JPL Mariner C and Boeing Lunar Orbiter squib circuits. The basis for comparison includes the following items.

1) The circuit will be required to deliver a minimum of 5.0 amperes for a minimum of 5 milliseconds to a 0.9- to 1.20-ohms bridgewire.
2) The Boeing Minuteman derating techniques are applicable to both circuits; thus, established reliability data and comparable conservative design levels can be used for the study.
3) JPL space-proven parts are to be considered for the SCR circuit, if the benefit of qualified parts and circuitry is to be retained.

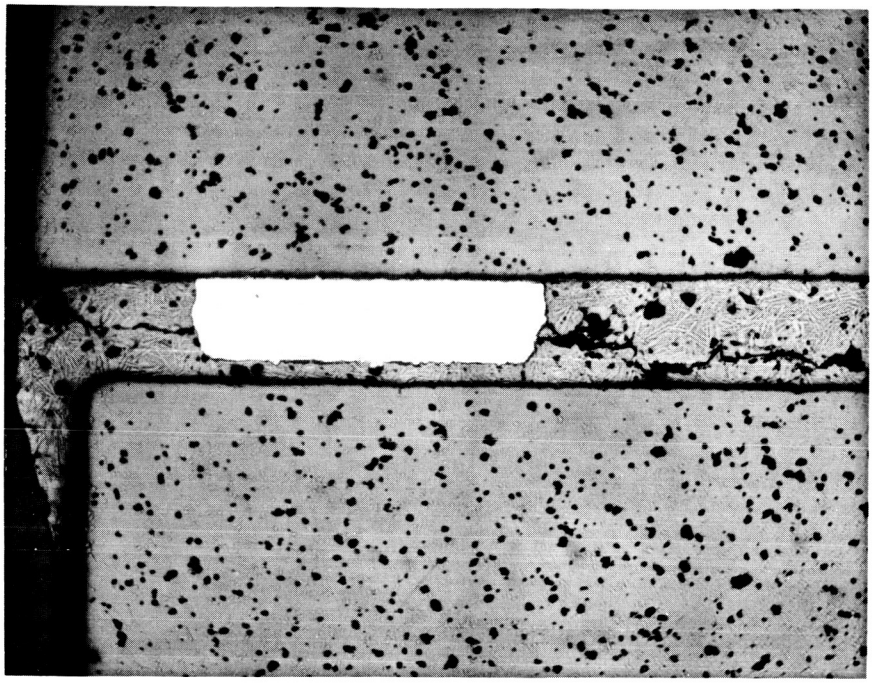

Figure 4.8-29: Cross Section of Beginning of Seal Area — 100X

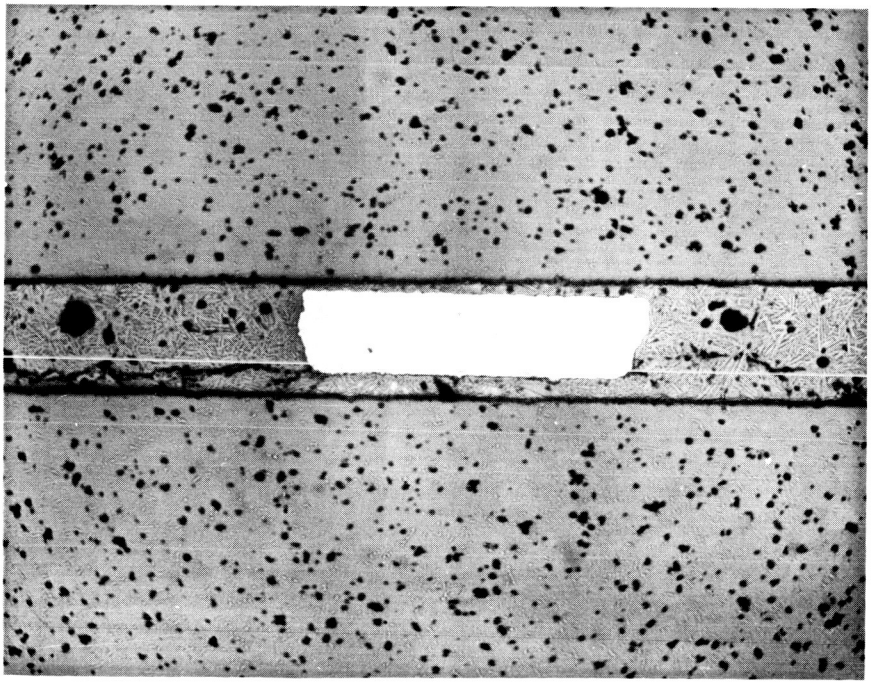

Figure 4.8-30: Cross Section of Seal Area Past Figure 4.8-29 — 100X

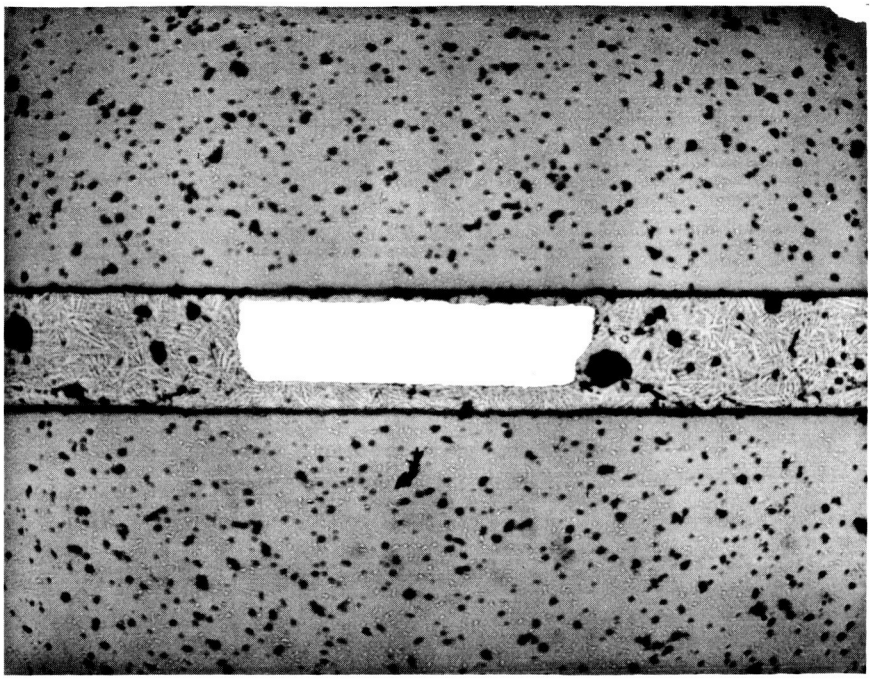

Figure 4.8-31: Cross Section of Seal Area Past Figure 4.8-30 — 100X

Figure 4.8-32: Cross Section of Seal Area Past Figure 4.8-31 — 100X

4) The circuits will be evaluated on the basis of survival from a shorted squib condition.

5) Eighteen bridgewires are to be fired by a redundant system so that no single component failure prevents function actuation by one of two bridgewires per function.

6) Changes to associated subsystems (e.g., power subsystem and wiring) will not be considered.

Of the five NASA comparison factors, weight, reliability, and failure modes favor the Boeing circuit, and complexity favors the JPL circuit. Power differences are negligible.

Different design conditions apply for the Lunar Orbiter and the Mariner C, especially in power and signal source conditions. It is concluded that the trades favoring the Boeing circuit outweigh those favoring the JPL circuit for the Lunar Orbiter.

Some of the facts about the Mariner C squib circuitry were the result of a telephone conversation between Walter S. Wuest, JPL, and Robert Charters and Donn Larsen, Boeing, on January 7, 1965. These facts are as follows:

1) A 1-amp, 1-watt, no-fire squib similar to the Lunar Orbiter squib is used (1.1 $\pm$0.1 ohm).

2) The firing supply source is a transformer-rectifier unit fed from a well-regulated 2.4-kc supply. The transformer-rectifier output is held to within a few percent of 27 v.d.c.

3) A capacitor charge-limiting resistor of 3000 ohms was used to ensure SCR turnoff.

4) The capacitor was rated for 30 v.d.c.; 10-percent derating to 27 v.d.c. was used.

5) The capacitor size was 1800 mfd for each squib fired in parallel.

6) The 3.5 amp must fire 5 amp recommended firing levels were not used. They arrived at a 2-1 energy margin by firing a set of squibs; the capacitor size was based on this energy level.

7) A 1-ohm, 2.5=watt resistor was used in series with the squib between cathode and ground.

8) The squib circuit wire resistance is 0.4 maximum.

9) The General Electric Hi-rel SCR is screened for a maximum gating current of 50 ma and a minimum turnoff current of 10 ma.

10) The capacitor is screened for leakage, voltage, and loss of electrolyte under vacuum, thermal test conditions.

11) The capacitor is of the General Electric 15K series and weighs 125 grams.

Physical Comparison--The Mariner C and Lunar Orbiter squib circuits are compared in complexity, weight, volume, and power consumption in Tables 4.8-14, -15, and -16.

Circuit Analysis--The following pages provide an analysis of the Mariner C squib circuitry compared to the Lunar Orbiter circuitry. Figure 4.8-33 describes the circuits for such an application, and Figure 4.8-34 compares the Mariner C and Lunar Orbiter circuits for sensitivity.

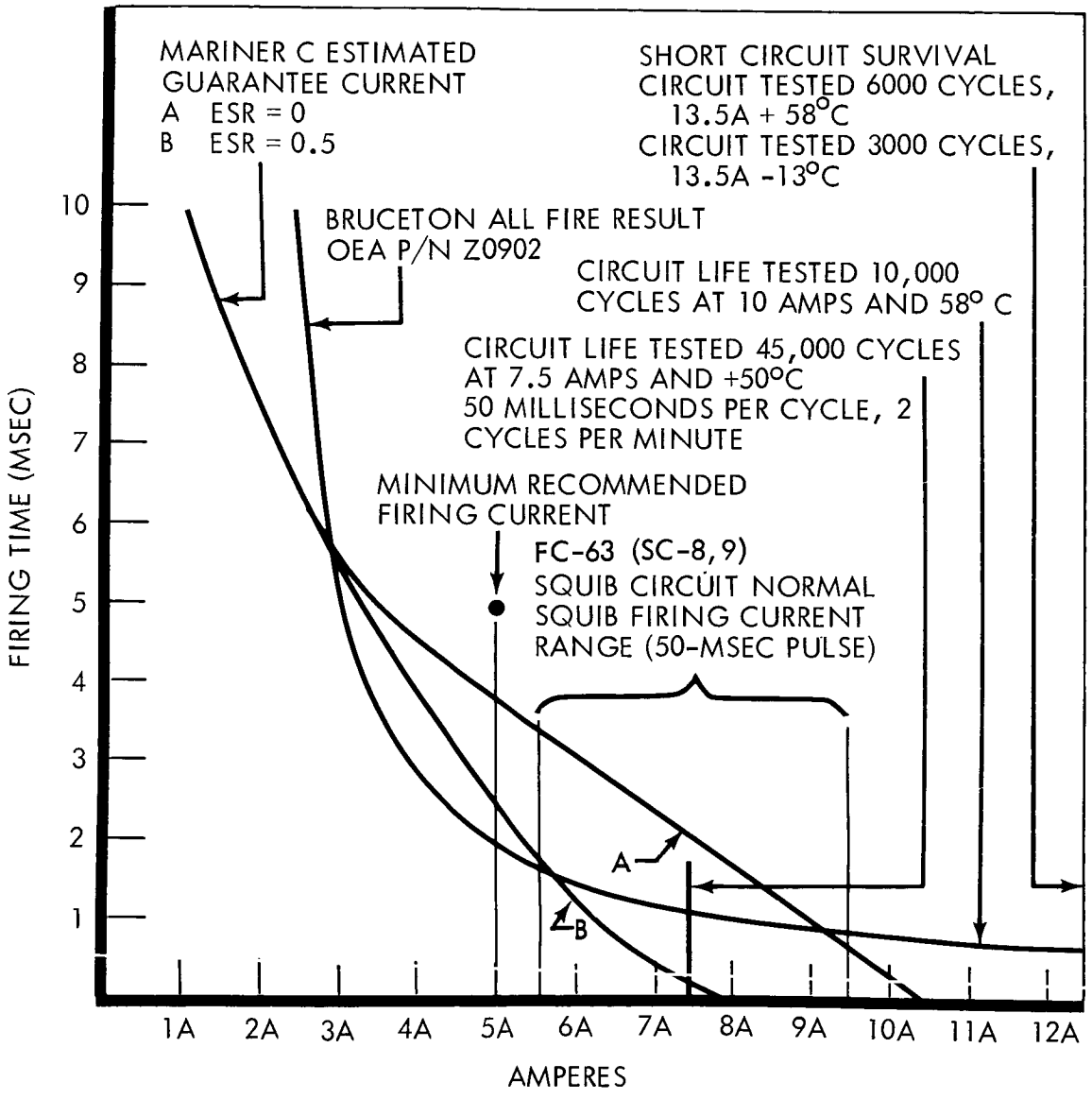

TYPICAL 1 WATT— 1 AMP NO FIRE BRIDGEWIRE BRUCETON PLOT COMPARED WITH THE JPL CIRCUIT "AS IS" AND LO CIRCUIT CAPABILITIES

Figure 4.8-34: Bridgewire Sensitivity vs JPL SCR Circuit and L. O. Circuit Capability

Table 4.8-14: MARINER C AND LUNAR ORBITER SQUIB-FIRING-CIRCUIT COMPARISON SUMMARY

	MARINER C CIRCUIT	LUNAR ORBITER CIRCUIT
NASA-Requested Comparison Factors		
Weight (Module Basis)	3858 grams	502 grams
Power		
Off-State**	0.990 watt	0.900 watt
On-State**	0.106 watt	0.145 watt
Complexity (Total Electronic Parts in Switching Assembly)	304	348
Reliability and Failure Modes		
Total Failure Rate ($\lambda \times 10^{-6}$ Failures/hr)	6.8	1.9
Failure Rate, Single-Thread	0.64	0.26
Reliability, Inadvertent Firing (All Circuits)	0.9994	0.9997
Reliability, Failure to Fire (Single-Thread)	0.9997	0.9999
Other Important Comparison Factors		
Volume (Module Basis)	71 cu. in.	23 cu. in.
Shorted Squib, Current Limiting	None	1.9
Short-Pulse EI Susceptibility	More	Less
Generated, Radiated Interference	More	Less
Generated, Conducted Interference	Less	More
Peak Battery Drain	Very Small	Very Large
Presently Identifiable, Qualified* Parts Available	No	Yes
Part Screening to New (Unwritten) Specifications	2	None

* Or qualification in process.
** Does not include current limiting or switch drop.

Table 4.8-15; MARINER C AND LUNAR ORBITER SQUIB-CIRCUIT COMPLEXITY, WEIGHT, VOLUME SUMMARY

PART DESCRIPTION	QTY PER S/A	TOTAL PARTS	WEIGHT PER UNIT	TOTAL WEIGHT	VOLUME PER UNIT	TOTAL VOLUME
Mariner C						
SC-8 Equivalent Module: R1-R14, Q1-Q4, C1-C5, CR-1, CR-2	10	240	22	220	1.10	11.0
SC-9a, 9b (SCR-1,-2)	9	18	11	198	0.55	9.9
SC-10 Equivalent Module: CR-1, CR-7, K-1, R02, R-4	1	10	65	65	1.8	1.8
Module A, Module B: R1, C1-C3	9	36	375	3375	5.4	48.6
		304		3858		71.3
Lunar Orbiter Circuit						
SC-8 Module A: R1-R20, Q1-Q6, CR-1, CR-2, C1-C4	8	256	22	176	1.10	8.8
SC-8 Module B: R1-R11, R13, R14, Q1-Q4 CR-1, CR-2, C1-C3	2	44	22	44	1.10	2.2
SC-10 Module: CR-1, CR-7, R-1, R-4 K-1	1	12	86	86	2.3	2.3
SC-9(a), SC-9(b)	18	36	11	196	0.55	9.9
		348		502		23.1

Table 4.8-16: SQUIB-CIRCUIT POWER-CONSUMPTION BREAKDOWN

	MARINER C	LUNAR ORBITER
	Watts	
Off-State		
Noise Immunity	0.270	0.270
Leakage (Estimated)	0.360	0.270
Bias	0.360	0.360
Total (18 Circuits)	0.990	0.900
Per Circuit	0.055	0.050
On-State		
Peak Power per Squib (Average Circuit 27 v.d.c. 1 Squib, 0.5 Wire)	486.0	210.0
Switch Power Consumption per Two Squibs, Not Including Limiting or Output Device	0.106	0.145
Battery Drain per Squib due to Squib Current	2.05[1] watt-sec	0.8[2] watt-sec

[1] Based on charging cycle.
[2] Based on firing cycle.

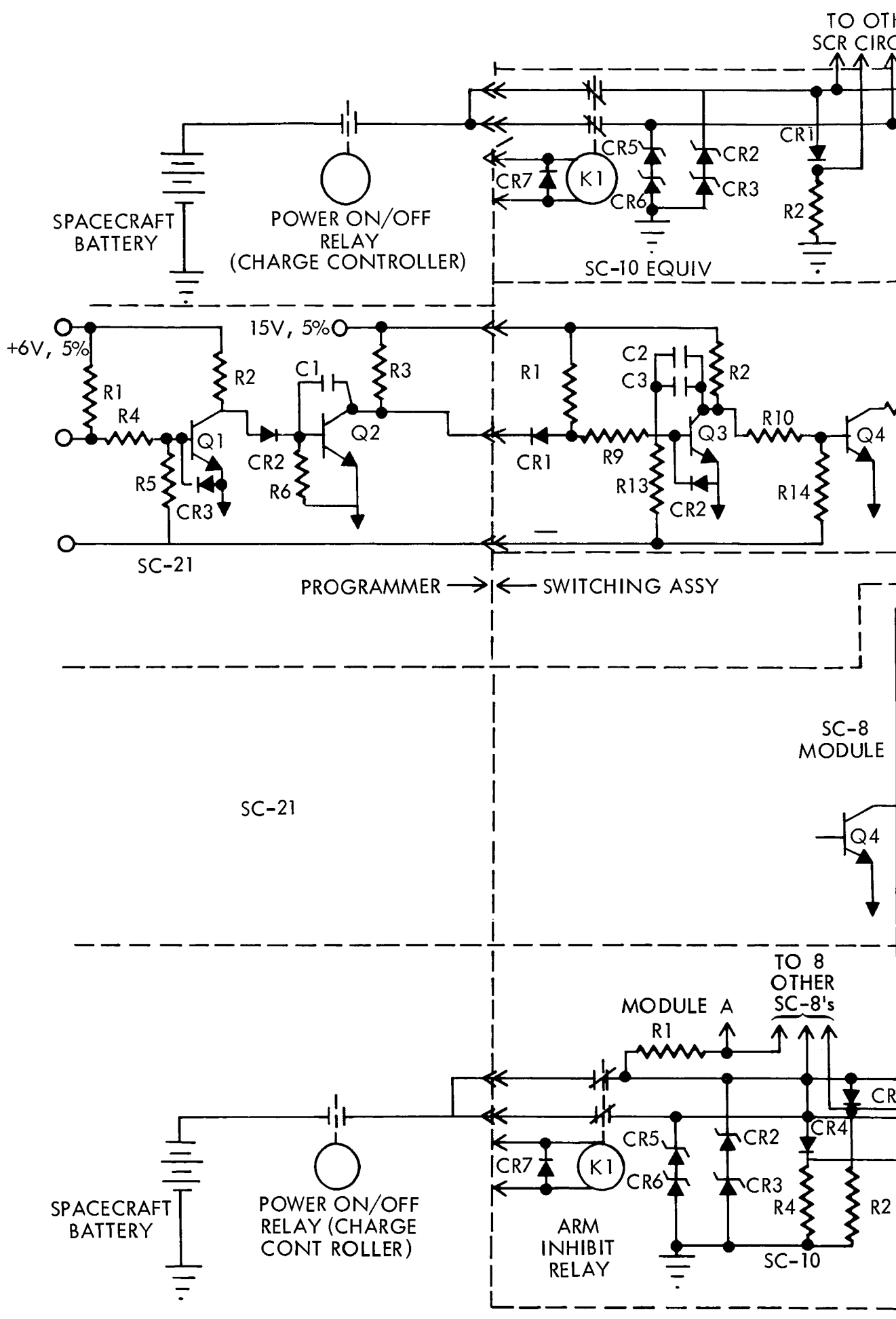
TO OTH
SCR CIRC
CR1
CR5
CR2
CR7
K1
CR3
CR6
R2
SPACECRAFT BATTERY
POWER ON/OFF RELAY (CHARGE CONTROLLER)
SC-10 EQUIV
+6V, 5%
15V, 5%
R1
R2
C1
R3
R4
Q1
Q2
CR2
R6
R5
CR3
SC-21
C2
C3
R1
R2
R10
Q3
Q4
CR1
R9
R13
CR2
R14
PROGRAMMER
SWITCHING ASSY
SC-8 MODULE
SC-21
Q4
TO 8 OTHER SC-8's
MODULE A
R1
CR
CR4
CR5
CR2
CR7
K1
CR6
CR3
R4
R2
SPACECRAFT BATTERY
POWER ON/OFF RELAY (CHARGE CONT ROLLER)
ARM INHIBIT RELAY
SC-10

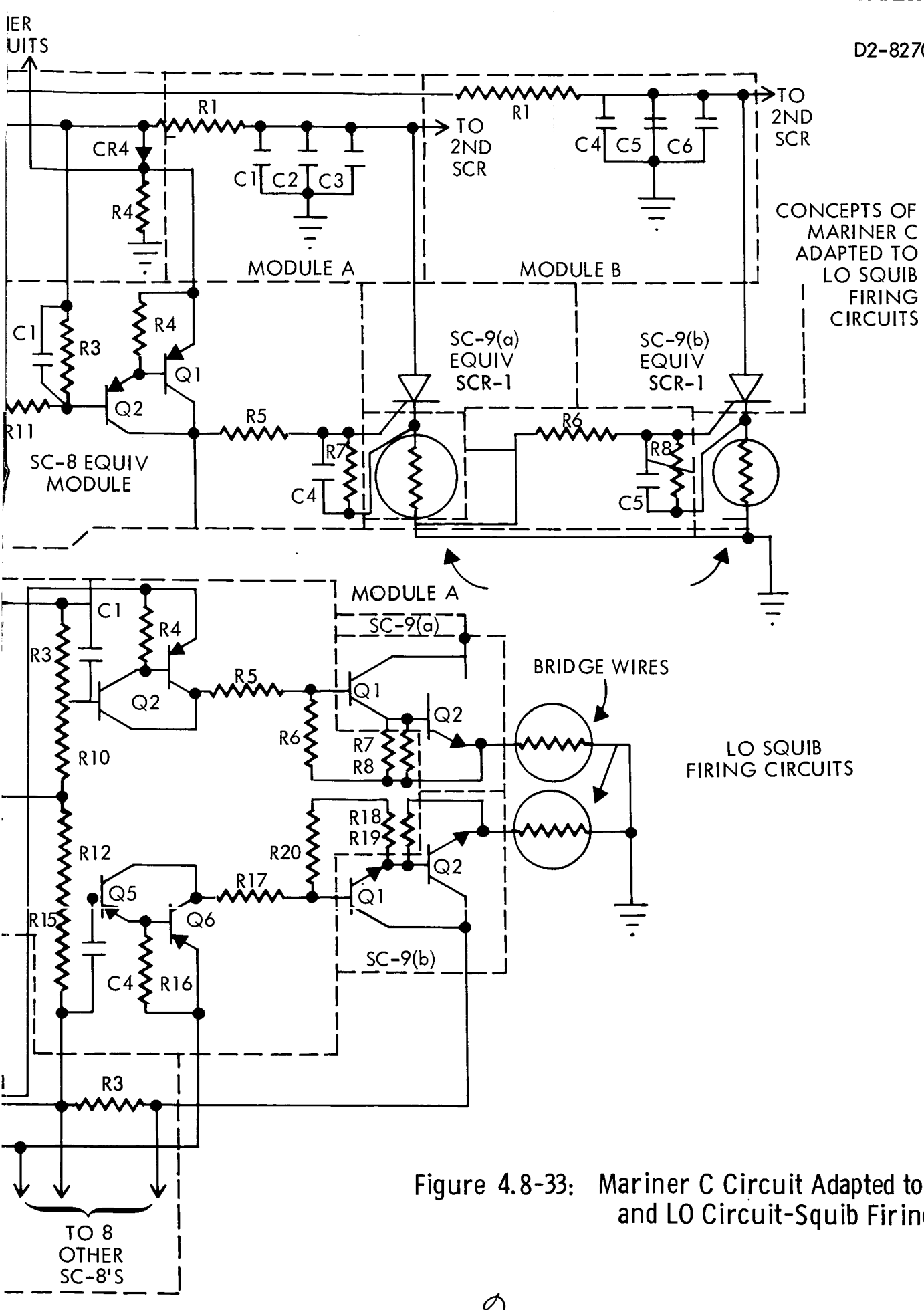

Figure 4.8-33: Mariner C Circuit Adapted to LO and LO Circuit-Squib Firing

SCR Turnoff Circuit Analysis

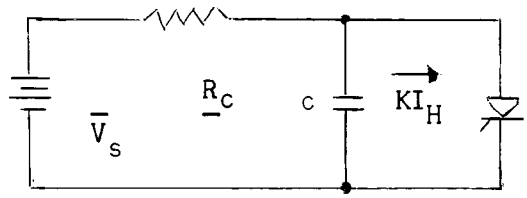

Requirements: SCR Circuit must turn off after squib firing via reducing available anode current below minimum holding level.

$$\therefore \quad \underline{R}_C = \frac{\bar{V}_s}{KI_H}$$

where K is a weighting factor for holding current degradation with time.

From Mariner C:

$$K = \frac{V_s'}{R'_c \; I_H} = \frac{27 \text{ v}}{3K \times 10ma} = 0.9$$

Assumptions: SCR's screened as in Mariner C program for I_H minimum of 10 m.a.

Conditions: Firing circuit resistances are negligible.

Solution:

$$\underline{R}_C = \frac{31.6 \text{ v}}{0.9 \times 10ma} = 3.51 \text{ K}$$

Select: $R_C = 3.6K \pm 1$ percent initial, ± 2.5 percent final

Discharge circuit conditions: Current limiting

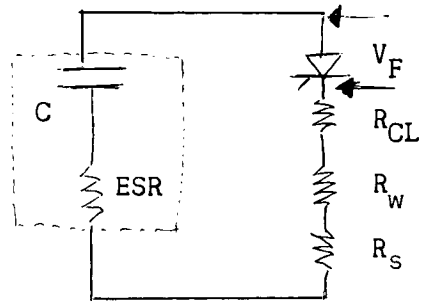

Requirement: Circuit must survive and not cause further system degradation for shorted squib condition:

$$\underline{R}_{CL} = \frac{\bar{V}_s}{\bar{I}_F} - (\underline{R}_W + \underline{R}_S + \underline{ESR})$$

Reliability Comparison--Tables 4.8-17 and -18 and the "Failure Mode, Effect, and Criticality Analysis" sheets (Table 4.8-19) provide a reliability comparison between the Mariner C and Lunar Orbiter squib circuits. In addition to "Actions" listed in the attached "Failure Mode, Effect, and Criticality Analysis," the following coded sections appear at applicable places in that column:

1) Adequate component power derating;
2) Adequate component tolerance derating;
3) Screened components;
4) Welded module connections;
5) Prepotting and postpotting tests;
6) Lowest power or other stress in quiescent state;
7) Adequate I_{CBO} derating;
8) Adequate voltage derating.

Mariner C Single-Thread Circuit Reliability

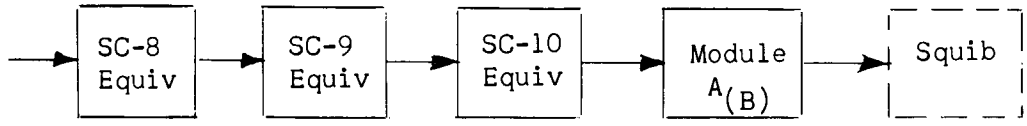

$\lambda = 0.104 \times 10^{-6}$ F/hr $\quad \lambda = 0.25 \times 10^{-6}$ F/hr $\quad \lambda = 0.128 \times 10^{-6}$ F/hr $\quad \lambda = 0.160 \times 10^{-6}$ F/hr

$$\lambda T = 0.642 \times 10^{-6} \text{ F/hr}$$

Mission $\lambda M = \lambda_T t = 0.642 \times 10^{-6} \times 720 = 462 \times 10^{-6}$ F/Mission

Mission Reliability = $1 - \lambda M = 0.9995$

Table 4.8-17: FAILURE MODES COMPARISON (SINGLE-THREAD BASIS)

x 10^{-6} FAILURES PER HOUR

LUNAR ORBITER CIRCUIT	SC-21	SC-8	SC-9	SC-10	Total
1) Inadvertent Squib Firing	0.0056	0.0074	0.0002	0.001	0.0142
2) Failure to Fire Bridgewire(s)	0.0099	0.0836	0.0224	0.0001	0.1160
3) Failure to Turn Off After Firing (Presumes Partial Squib Short)	--	0.0131	0.0055	--	0.0186
4) Other	0.0027	0.0064	--	0.1100	0.1191
5) None	0.0076	0.0083	--	0.0470	0.0629

Reliability--Inadvertent Firing (18 circuits) = 0.9997
Reliability--Failure to Fire (Single-Thread) = 0.9999

MARINER C TYPE CIRCUIT	SC-21	SC-8 (Equiv.)	SC-9 (Equiv.)	SC-10	Module A	Total
1) Inadvertent Squib Firing	0.0056	0.0366	0.0501	0.0010	--	0.0933
2) Failure to Fire Bridgewire(s)	0.0099	0.0822	0.10	0.0001	0.1415	0.3337
3) Failure to Turn Off After Firing	--	0.0079	0.10	--	0.0003	0.1082
4) Other	0.0027	0.0006	--	0.1100	0.0100	0.1233
5) None	0.0076	0.0139	--	0.0470	--	0.0685

Reliability--Inadvertent Firing (18 circiits) = 0.9994
Reliability--Failure to Fire (Single-Thread) = 0.9997

Table 4.8-18: MARINER C AND LUNAR ORBITER SQUIB-CIRCUIT FAILURE-RATE BREAKDOWN

COMPONENT	$\lambda \times 10^{-5}$ FAILURES/HR PER UNIT	TOTAL PER SINGLE CIRCUIT	UNITS PER S/A	TOTAL PER S/A
JPL Mariner C Circuits				
SC-8 Equivalent Module		0.104		
R1-R4, R7-R11, R13, R14	0.0018	0.0216	128	0.23
Q3, Q4	0.003	0.006	20	0.06
Q2	0.007	0.007	10	0.07
Q1	0.03	0.03	10	0.30
C1, C2, C3	0.001	0.003	10	0.03
C4	0.035	0.035	18	0.63
R5, R6	0.01	0.01	18	0.18
CR-1, CR-2	0.002	0.004	20	0.08
SC-9 Equivalent Module		0.25		
SCR-1	0.25	0.25	18	4.50
SC-10 Equivalent Module		0.128		
K1	0.1	0.05	1	0.10
CR-1, CR-4, CR-7	0.02	0.04	3	0.06
CR-2, -3, -5, -6	0.01	0.02	4	0.04
R2, R4	0.018	0.018	2	0.036
Modules A, B		0.16		
C1, C2, C3	0.05	0.15	27	0.405
R1	0.01	0.01	9	0.09
				6.811
Lunar Orbiter				
SC-8 Module		0.102		
R1-R4, R6-R16, R18-R20	0.0018	0.0216	168	0.305
R5, R17	0.01	0.01	18	0.18
Q3, Q4	0.003	0.006	20	0.06
Q2	0.007	0.007	18	0.126
Q1	0.03	0.03	18	0.54
C1, 2, 3, 4	0.001	0.004	40	0.04
CR-1, CR-2	0.002	0.004	20	0.08
SC-9		0.02		
Q1, Q2	0.01	0.02	36	0.36
SC-10		0.138		
K-1	0.10	0.05	1	0.10
CR-1, -4, -7	0.02	0.04	3	0.06
CR-2, -3, -5, -6	0.01	0.02	4	0.04
R4, R2	0.018	0.018	2	0.036
R1, R3	0.01	0.01	2	0.02
				1.947

Lunar Orbiter Single-Thread Circuit Reliability

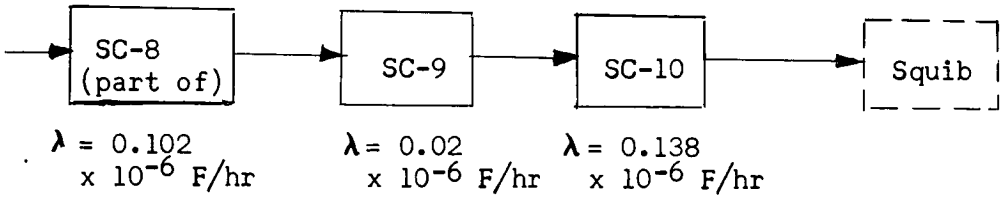

$\lambda = 0.102 \times 10^{-6}$ F/hr $\quad \lambda = 0.02 \times 10^{-6}$ F/hr $\quad \lambda = 0.138 \times 10^{-6}$ F/hr

$$\lambda T = 0.260 \times 10^{-6} \text{ F/hr}$$

Mission $\lambda M = \lambda_T t = 0.260 \times 10^{-6} \times 720 = 187 \times 10^{-6}$ F/M

Mission Reliability = $1 - \lambda M = 0.9998$

(1) COMPONENT SUBSYSTEM OR SYSTEM	C
(4) USED ON COMPONENT SUBSYSTEM OR SYSTEM	A
(7) SUPPLIER OR RESP ORGN	F

ARTICLE & IDENTIFICATION (10)	(11) ARTICLE FUNCTION
SC-21* Level Amplifier, Waveform Control	
1) R-1 Resistor	Bias, pull up, turn on, noise margin
2) R4 Resistor	Base drive, noise margin
3) R5 Resistor	Bias, turn off, noise margin
4) Q1 Transistor	Threshold gate — level amplifier
5) CR-3 Diode	Q1 vebo protection

* Same as FC-44-4

** Worst-case minimum noise margin

FAILURE MODE, EFFECT, & CRITICALITY ANALYSI

B INTERFACE OUTPUT CIRCUIT, SOURCE, PROGRAMMER OMD, LOAD, SQU

CONTROL ASSEMBLY FLIGHT ELECTRONICS	(2) DRAWING NUMBER
ATTITUDE CONTROL SYSTEM INSTALLATION	(5) USED ON DRAWING NUM
LIGHT PROGRAMMER DESIGN (BOEING)	(8) PREPARED BY D

(12) MODES & CAUSES OF FAILURE	(13) OPERATIONAL EFFECT	
	PRIMARY	SECONDARY
a) Resistance increase	a) Reduced noise margin	a) None
b) Resistor opens	b) Q1 held off	b) Inadvertent squib fire command
c) Resistance decreases	c) Q1 hard to turn off	c) Failure to fire bridge wire
a) Resistance increases	a) Reduced noise margin	a) None
b) Resistor opens	b) Q1 held off	b) Inadvertent squib fire command
c) Resistance decreases	c) Q1 held on	c) Failure to fire bridge wire
a) Resistance increase	a) Q1 hard to turn off	a) Failure to fire bridge wire
b) Resistor opens	b) Q1 held on	b) Failure to fire bridge wire
c) Resistance decreases	c) Reduced noise margin	c) None
a) Any open connection loss h_{FE}	a) Q2 held on	a) Inadvertent squib fire command
b) I_{CBO} increase C-B or CE short	b) Q2 held off	b) Failure to fire bridge wire
a) Diode open	a) Vebo exceeded although I_{EBO} limited during squib fire command	a) None
b) Diode leakage (I_R) excessive	b) Reduced noise margin	b) None

Table 4.8-19:

	(3) BOEING SPEC
IBER 25-51412-1	(6) DATE 1/10/65
onn E. Larsen	(9) APPROVED BY

PROB OF OCCURRENCE (14) $\times 10^{-6}$	SEVERITY RATING (15)	(16) ACTION TO MINIMIZE FAILURE MODE SUSCEPTIBILITY
0.0006	C	a) R = 100% required to reduce noise margin** to zero (1) (2) (3) (4) (5) (6)
0.0008	A-C	b) (1) (3) (4) (5) (6) — Arm inhibit relay — short mission time during which failure is critical
0.0006	C	c) Redundant squib circuit (1) (2) (3) (5)
0.0006	C	a) R = +30% required to reduce noise margin** to zero
0.0008	A-C	b) Same as 1 b) above
0.0006	C	c) Same as 1 c) above
0.0006	C	a) Same as 1 c) above
0.0008	C	b) Same as 1 c) above
0.0006	C	c) R = 30% required to reduce noise margin** to zero
0.0027	A-C	a) (1) (3) (4) (5) — Arm inhibit relay — short mission time during which failure is critical
0.0003	C	b) (1) (3) (5) (7) (8) — Redundant squib circuit
0.0025	C	a) (1) (3) (4) (5) (6) (8)
0.0005	C	b) Leakage must increase by over 30 times worst-case limit to reduce noise margin to zero (1) (3) (5) (6) (8)

(1) COMPONENT SUBSYSTEM OR SYST	
(10) ARTICLE & IDENTIFICATION	(11) ARTICLE FUNCTION
SC-21 Continued	
6) R2 Resistor	Bias, turn on waveform control
7) CR-2 Diode	Bias, turn off
8) C-1 Capacitor	Waveform control
9) R-6 Resistor	Turn off bias waveform control
10) Q_2 Transistor	Waveform control integrator level amplifier
11) R3 Resistor	Collector supply transistor

* No single circuit where generated E-I e

FAILURE MODE, EFFECT, & CRITICALITY ANALYSIS — CONTI

EM	Squib Interface Output Circuit (continued)	(2) DRAWING NU
(12) MODES & CAUSES OF FAILURE	(13) OPERATIONAL EFFECT	
	PRIMARY	SECONDARY
a) Resistance increase	a) Increased waveform delay time	a) None
b) Resistance decrease	b) Decreased noise margin waveform	b) SC-21 output waveform exceeds E-1 spec.
c) Resistor opens	c) Q_2 held off	c) Failure to fire bridge wire
a) Diode opens	a) Q_2 held off	a) Failure to fire bridge wire
b) Diode leakage (I_R) excessive	b) Reduced rise time	b) SC-21 output waveform exceeds E-1 spec.
a) Increased capacity	a) SC-21 rise time increases	a) None
b) Decreased capacity	b) SC-21 delay time decreases	b) SC-21 output waveform exceeds E-1 spec.
a) Increased resistance	a) SC-21 delay time decreases rise time increases	a) Same as 8 b) above.
b) Decreased resistance	b) SC-21 delay time increases; rise time increases; reduced Q_2 drive	b) Possible failure to fire squib.
c) Resistor open	c) Q_2 may turn on due to I_{CBO} of Q_2	c) Inadvertent squ fire command
a) Any contact open h_{FE} decrease	a) Q_2 held off	a) Failure to fire bridge wire
b) C-E or C-B short I_{CBO} increases	b) Q_2 held on	b) Inadvertent squ fire command
a) Resistance increase	a) Decreased noise margin	a) None
b) Resistance decrease	b) Increased noise margin	b) Possible failure to fire bridge wire

xceeds spec and creates a problem since control is based on cumulative effect.

NUATION SHEET

Table 4.8-19 : —Continuation Sheet

MBER		(3) BOEING SPEC
(14) PROB OF OCCUR	(15) SEVERITY RATING	(16) ACTION TO MINIMIZE FAILURE MODE SUSCEPTIBILITY
0.0006	C or lower	a) (1) (2) (3) (5) —Results in reduced E-I generation.
0.0006	C or lower	b) R_2 must decrease by more than 50% to pull Q_1 out of saturation. (1) (2) (3) (5).
0.0008	C	c) Redundant squib circuit (1) (3) (4) (5).
0.0025	C	a) Redundant squib circuit (1) (3) (4) (5) (6) (8).
0.0005	C or lower	b) (1) (3) (5) (6) (8).
0.001	C or lower	a) Results in reduced E-I generation (2) (3) (8).
0.001	C or lower	b) (2) (3) (8).
0.0006	C or lower	a) (1) (2) (3) (5) (6) (7).
0.0006	C	b) Redundant squib circuit (1) (2) (3) (5) (6).
0.0008	A	c) (1) (2) (3) (4) (5) (6) I_{CBO} = 0.35 a) required to reduce output to 4.5 volts min.
0.0025	C	a) Redundant squib firing circuit.
0.0005	A-C	b) (1) (2) (3) (5) (6) (7) (8).
0.0006	C	a) Resistance must increase by 250% to reduce noise margin to zero (1) (2) (3) (4) (5) (6).
0.0006	C	b) Redundant squib firing circuit (1) (2) (3) (4) (5) (6).

(1) COMPONENT SUBSYSTEM OR SYSTEM	SWITCHING ASSEMBLY
(4) USED ON COMPONENT SUBSYSTEM OR SYSTEM	ATTITUDE CONTROL SYSTEM INSTALLATION LUNAR ORBITER
(7) SUPPLIER OR RESP ORGN	PROGRAMMER DESIGN GROUP, BOEING

ARTICLE & IDENTIFICATION (10)	ARTICLE FUNCTION (11)	MODES & CAUSES OF FAILURE (12)	(13) OPERATIO PRIMARY
SC-8 Module	Noise immunity and d.c. level amplifier — squib firing circuits		
1) CR-1 Diode	Noise margin	a) Diode opens	a) Q3 held on
		b) Diode leakage increases	b) Increased susceptibility to 100 volt sec E-1
2) R-1 Resistor	Bias — Q3 turn on — noise immunity	a) Resistance increase (2.5%)	a) Reduced d.c. noise margin
		b) Resistance decrease (2.5%)	b) Q3 may be held on
		c) Resistor opens	c) Q3 held on
3) R-9 Resistor	Base drive — Q3 noise margin	a) Resistance increase (2.5%)	a) Reduced d.c. noise margin
		b) Resistance decrease (2.5%)	b) Q3 may be held on
		c) Resistor opens	c) Q3 held off
4) R-13 Resistor	Bias — Q3 turn off noise margin	a) Resistance increase (2.5%)	a) Reduced d.c. noise margin Q3 off
		b) Resistance decrease	b) Reduced d.c. noise margin Q3 on
		c) Resistor opens	c) Q3 held on
5) CR-2 Diode	Base clamp reduce vebo	a) Diode opens	a) Q3 collector rise to 17-20 volts during turn on
		b) Diode leakage increases	b) Q3 failure to turn on after squib firing

Table 4.8-19: — Continuation Sheet

DRAWING (2) NUMBER 25-51661	BOEING (3) SPEC D2-100254
USED ON (5) DRAWING NUMBER 25-51412-1	(6) DATE 2/6/65
(8) PREPARED BY Donn E. Larsen	(9) APPROVED BY

)NAL EFFECT SECONDARY	PROB OF OCCURRENCE (14)	SEVERITY RATING (15)	ACTION TO MINIMIZE FAILURE MODE SUSCEPTIBILITY (16)
a) Failure to fire bridge wire	0.0018	C	a) Redundant squib firing circuit (1) (3) (4) (5) (6) (8)
b) None	0.0002	C	b) Back up noise rejection in R3 R11 C1 filter (R12 R_{15} C4 also) (1) (3) (4) (5) (6) (8)
a) None	0.0006	C	a) R1 must increase 30% to reduce noise margin to zero (1) (2) (3) (4) (5) (6)
b) Possible failure to fire bridge wire	0.0006	C	b) Redundant squib circuit source can handle R1 = 3K (1) (2) (3) (4) (5) (6)
c) Inadvertent squib fire command	0.0006	A-C	c) (1) (3) (4) (5) (6)
a) None	0.0006	C	a) R9 must increase 50% to reduce noise margin to zero (1) (2) (3) (4) (5)
b) Possible failure to fire bridge wire	0.0006	C	b) Redundant squib firing circuit (1) (2) (3) (4) (5)
c) Inadvertent squib fire command	0.0006	A-C	c) (1) (3) (4) (5)
a) None	0.0006	C	a) R2 must increase by 140% to reduce noise margin to zero (1) (2) (3) (4) (5)
b) None	0.0006	C	b) R2 must decrease by 20% to reduce noise margin to zero (1) (2) (3) (4) (5)
c) Failure to fire bridge wire	0.0006	C	c) Redundant squib firing circuit (1) (3) (4) (5)
a) None	0.0018	C or lower	a) (1) (3) (4) (5)
b) Continuous squib fire command	0.0002	C	b) (1) ( ) (5) (6)

(1) COMPONENT SUBSYSTEM OR SYSTEM		SWITCHING ASSEMBLY	
(10) ARTICLE & IDENTIFICATION	(11) ARTICLE FUNCTION	(12) MODES & CAUSES OF FAILURE	(13) OPERATION PRIMARY
SC-8 Module (continued)			
6) C-2 or C-3 Capacitor	Short pulse noise rejection	a) Increase capacity ±8%	a) Increase noise rejection
		b) Decrease capacity ±8%	b) Decreased pulse rejection*
		c) Capacitor opens	c) Decreased pulse rejection*
		d) Capacitor shorted or leakage	d) Q3 held on
7) Q_3 Transistor	Threshold gate — d.c. amplifier — noise pulse integrator	a) Any terminal fails open loss h_{FE}	a) Q4 held on
		b) Fails shorted I_{CBO} increase	b) Q4 held off
8) R2 Resistor	Bias — Q4 turn on noise immunity	a) Resistance increase 2.5%	a) Q4 may be held off at 54K
		b) Resistance decreases 2.5%	b) Decreased short pulse noise rejection
		c) Resistor opens	c) Q4 held off
9) R10 Resistor	Base drive — Q4	a) Resistance increase	a) Reduced Q4 drive
		b) Resistance decrease	b) Increased Q4 drive
		c) Resistor opens	c) Q4 held off
10) R14 Resistor	Bias — Q4 turn off	a) Resistance increases 2.5%	a) Decreased turn-off bias
		b) Resistance decrease 2.5%	b) Increased turn-off bias
		c) Resistor opens	c) Q4 may turn on at 60°C

ANALYSIS — CONTINUATION SHEET

R — SC-8 MODULE

Table 4.8-19: — Continuation Sheet

(2) DRAWING NUMBER 25-51661			(3) BOEING SPEC D2-100254
AL EFFECT SECONDARY	(14) PROB OF OCCUR	(15) SEVERITY RATING	(16) ACTION TO MINIMIZE FAILURE MODE SUSCEPTIBILITY
a) None	0.0003	C	a) (3)
b) None	0.0003	C	b) (2) (3) (5) (6) — Back up noise rejection R11, R3, C1
c) Short pulse energy to squib 10 wt peak at 120 cps, 10μ.s. 10 Mw average if both capacitors open	0.0003	C	c) (2) (3) (5) (6) — Back up d.c. and noise rejection and filter R11, R3, C1 (R12, R15, C4)
d) Failure to fire bridge wire	0.0001	C	d) (3) (5) (6) — Glass dielectric capacitor selected — highest quality
a) Inadvertent squib fire command	0.0027	A-C	a) (1) (2) (3) (4) (5)
b) Failure to fire bridge wire	0.0003	C	b) (1) (2) (3) (5) (7) (8)
a) Possible failure to fire bridge wire	0.0006	C	a) (1) (2) (3) ( ) (5) redundant squib firing circuit
b) None	0.0006	C	b) R's = 10% affects pulse width rejection 10% (insensitive)
c) Failure to fire bridge wire	0.0006	C	c) Redundant firing circuit
a) None	0.0006	C or lower	a) R10 must increase by 60% to hold Q_4 off (1) (2) (3) (4) (5) (6)
b) None	0.0006	C or lower	b) R10 4K required to turn on Q_4 (1) (2) (3) (5) (6).
c) Failure to fire squib	0.0006	C	c) Redundant squib firing circuit (1) (2) (3) (4) (5) (6)
a) None	0.0006	C or lower	a) R14 100K required to turn on Q_4 (1) (2) (3) (4) (5)
b) None	0.0006	C or lower	b) R14 235K required to hold Q_4 off (1) (2) (3) (5)
c) Possible squib fire command	0.0006	A-C	c) $V_{CE(SAT)}$ + (I_{CBO} and I_{EBO}) R10 = 0.20 + (3.2 + 0) 11K 0.25 = V_{BE}. (1) (3) (4) (5)

(1) COMPONENT SUBSYSTEM OR SYSTEM SWITCHING ASSEMBLY

(10) ARTICLE & IDENTIFICATION	(11) ARTICLE FUNCTION	(12) MODES & CAUSES OF FAILURE	(13) OPERATIO PRIMARY
SC-8 Module (continued)			
11) Q_4 Transistor	Amplifier — switch	a) C or E terminal opens loss h_{FE}	a) Q2 Q5 held off
		b) Fails shorted — high I_{CBO}	b) Q2 Q5 turned on
12) R-10 Resistor (R-12)	Base drive — ground noise filter	a) Resistance increase	a) Decreased Q2 Q5 turn in bias
		b) Resistance decrease	b) Q4 may fail to saturate
		c) Resistor opens	c) Q2 (Q5) held off
13) R-3 Resistor (R-15)	Bias — Q2 (Q5) turn off	a) Resistance increase	a) Reduced turn off I_{CBO} margin
		b) Resistance decrease	b) Reduced Q2 (Q5) base drive
		c) Resistor opens	c) Possible Q2 (Q5) turn on
14) C-1 or C-4 Capacitor	Ground noise filter — power supply conducted interference filter	a) Capacitance increase	a) Improved noise rejection
		b) Capacitance decrease	b) Reduced noise rejection
		c) Capacitor open	c) Squib command outpu for duration of P-5 noise
		d) Capacitor leakage or short	d) Q2 (Q5) may be held off
15) Q2 (Q5) Transistor	Switch — amplifier part of Darlington pair	a) C-E open	a) Q1 (Q6) held off
		b) High I_{CBO} C-B, C-E short I) Before normal command II) During or after	b) Q1 (Q6) held on
		c) Loss h_{FE}	c) Reduced gain

Table 4.8-19: —Continuation Sheet

Y ANALYSIS — CONTINUATION SHEET
NAR ORBITER — SC-8 MODULE

Table 4.8-19: —Continuation Sheet

(2) DRAWING NUMBER 25-51661			(3) BOEING SPEC D2-100254
ONAL EFFECT SECONDARY	(14) PROB OF OCCURRENCE	SEVERITY (15) RATING	(16) ACTION TO MINIMIZE FAILURE MODE SUSCEPTIBILITY
a) Failure to fire bridge wire	0.0027	C	a) Redundant squib circuit (1) (3) (4) (5) (6)
b) Inadvertent squib fire command	0.0003	A-C	b) (1) (2) (3) (4) (5) (6) (7) (8)
a) Possible failure to fire bridge wire	0.0006	C	a) Sufficient gain in balance of switch amplifier to compensate for loss of Q2 (Q5) base drive (1) (2) (3) (5) (6) redundant squib circuit
b) Possible failure to fire bridge wire	0.0006	C	b) Same as above
c) Failure to fire bridge wire	0.0006	C	c) Redundant squib circuit (3) (4)
a) Continuous squib fire command possible after normal command	0.0006	C	a) (1) (2) (3) (5) (6) (7)
b) Possible failure to fire bridge wire	0.0006	C	b) Sufficient gain in balance of switch to offset loss of Q2 (Q5) base drive (1) (2) (3) (5) (6).
c) Possible inadvertent squib fire command	0.0006	A-C	c) Back up turn off via I_{CEO_2} R4 (I_{CEO_5} R16) V_{BE_2} (V_{BE_5}) off and R6 (R18)
a) None	0.0003	C or lower	a) (3)
b) Increased possibility of noise to squib	0.0003	C	b) Capacitance forms only portion of filter (C_{OB} Q4 R11 R3 C1 (R12 R15 C4) (3)
t c) Possible squib firing in high interference environment	0.0003	A-C	c) Bridge wire requires more energy than expected E-I (see 6 c)
d) Failure to fire bridge wire	0.0001	C	d) Capacitor type selection redundant squib circuit (1) (2) (3) (5) (6) (8)
a) Failure to fire bridge wire	0.0060	C	a) Redundant bridge wire
b) I) Inadvertent squib fire command	0.0001	A	b) (1) (2) ( ) (4) (5) (6) (7) (8) component screened for BV_{CEO}
II) Continuous squib fire command	0.0005	C	
c) Possible failure to fire bridge wire	0.0004	C	c) (2) Balance of amplifier offsets loss h_{FE}

COMPONENT (1) SUBSYSTEM OR SYSTEM		SWITCHING ASSEMBLY		
ARTICLE & IDENTIFICATION (10)		ARTICLE (11) FUNCTION	MODES & (12) CAUSES OF FAILURE	(13) OPERATION PRIMARY
SC-8 Module (continued)			a) Resistance increase	a) Lower I_{CBO} margin
16)	R4 (R16) Resistor	Bias — turn off Q1 (Q6)	b) Resistance decrease	b) Reduced Q1 (Q6) base drive
			c) Resistor opens	c) Q1, Q6 may be turned on at temperature extremes
17)	Q1 (Q6) Transistor	Switch — amplifier part of Darlington pair	a) C or E open	a) No SC-8 output (1 side)
			b) C-B, C-E short I. Before fire command II. After fire command	b) SC-8 squib fire command output
			c) Loss h_{FE}	c) Reduced output SC-8
			d) High I_{CBO}	d) SC-8 output continuous after normal firing
18)	R5 (R17) Resistor	Input drive limiting SC-9	a) Resistance increase	a) Reduced SC-9 drive
			b) Resistance decrease shorted turns	b) Q1 (Q6) may pull out sat. during normal firing and short
			c) Resistor opens	c) No output to one SC-9
19)	R6 (R20) Resistor	Bias, SC-9 Q1 turn off	a) Resistance increase	a) SC-9 Q1 may fail to turn off following normal squib firing
			b) Resistance decrease	b) Reduced drive to SC-9
			c) Resistor open	c) Increased leakage output of SC-9

Table 4.8-19: —Continuation Sheet

IS — CONTINUATION SHEET
:R — SC-8 MODULE

Table 4.8-19: —Continuation Sheet

DRAWING (2) NUMBER 25-51661			BOEING (3) SPEC D2-100254
AL EFFECT SECONDARY	PROB OF OCCURRENCE (14)	SEVERITY RATING (15)	ACTION TO MINIMIZE (16) FAILURE MODE SUSCEPTIBILITY
a) Possible continuous squib fire command	0.0006	C	a) (1) (2) (3) (5) (6) (7)
b) Possible failure to fire squib	0.0006	C	b) (1) (2) (3) (5) (6) Reserve gain in balance of amplifier
c) Possible inadvertent squib fire command	0.0006	A-C	c) (I_{CEO} + I_{CBO_2} + I_{CBO_1} (SC-9)) R_7 V_{BE} (off) is backup turn off (1) (3) (4) (5) (6) (7)
a) Failure to fire bridge wire	0.060	C	a) Redundant squib circuit (1) (3) (4) (5) (6) (8)
b) I) Inadvertent squib fire command	0.001	A-C	b) (1) (2) (3) (5) (6) (8) Q_1, Q_6 screened for BV_{CEO}
II) Continuous squib fire command	0.003		
c) Possible failure to fire bridge wire	0.003	C	c) (2) (3) (5) Redundant squib circuit reserve overall gain
d) Continuous squib firing command after normal command	0.003	C	d) (1) (2) (3) (6) (7) (8)
a) SC-9 may not saturate for shorted squib	0.004	C	a) SC-9 input limits — gain derated provides reserve capability to saturate (1) (2) (3) (4) (5) (6)
b) Continuous squib firing command after normal command	0.004	C	b) Reserve gain in Q_1 Q_2 (Q_5 Q_6), (1) — Hi-Rel wire-wound resistor, component rated for 10X steady-state power for 10 sec — used at 1.5X rated power for 50 msec (2) (3) (4) (5) (6).
c) Failure to fire bridge wire	0.002	C	c) Redundant squib circuit wire wound resistor (3) (4) (5)
a) Continuous squib fire command following normal command	0.0006	C	a) (1) (2) (3) (4) (5) (6) (7)
b) Reduced SC-9 output	0.0006	C	b) Adequate reserve gain SC-8 and SC-9 (1)
c) Increased leakage to bridge wire	0.0006	C	c) R7, R8 (R18, R19) backup R6, (R20) to swamp I_{CEO} or Q1 of SC-9, and I_{CBO} Q_1 (Q_6) of SC-8

(1) COMPONENT SUBSYSTEM OR SYSTEM		SWITCHING ASSEMBLY	
ARTICLE & IDENTIFICATION (10)	ARTICLE FUNCTION (11)	MODES & CAUSES OF FAILURE (12)	(13) OPERATIO PRIMARY
SC-8 Module (continued)			
20) R7 or R8 (R18 or R19)	Bias — turn off Q2 of SC-9	a) Resistance increase	a) Increase SC-9 leakage output
		b) Resistance decrease	b) Reduced SC-9 Q2 drive
		c) Resistor opens	c) SC-9 Q2 may fail to turn off after normal squib firing

Table 4.8-19: —Continuation Sheet

Y ANALYSIS — CONTINUATION SHEET
IAR ORBITER — SC-8 MODULE

DRAWING (2) NUMBER 25-51661			BOEING (3) SPEC D2-100254
NAL EFFECT SECONDARY	PROB OF OCCURRENCE (14)	SEVERITY RATING (15)	(16) ACTION TO MINIMIZE FAILURE MODE SUSCEPTIBILITY
a) Increased leakage to squib	0.0006	C	a) Circuit designed for R7 R8 = 21 ohms max. (or R7 or R8 increase to more than 50 's) (1) (2) (3) (4) (5) (6) (7).
b) Possible failure to fire bridge wire	0.0006	C	b) Reserve gain SC-9 (1) (2) (3) (5) (6).
c) Continuous squib fire command following normal command	0.0006	C	c) R8 provides turn off as T5 cools down if squib is not low-resistance shorted.

FAILURE MODE, EFFECT, AND CRITICA
SQUIB FIRING — LUNAR C

(1) COMPONENT SUBSYSTEM OR SYSTEM		SWITCHING ASSEMBLY	
ARTICLE IDENTIFICATION (10)	ARTICLE FUNCTION (11)	MODES & CAUSES OF FAILURES (12)	(13) PRIMA
SC-9 Module	Switch - Amplifier Power		
1. Q1 Transistor	Switch - amplifier part of Darlington pair	a) C or E open	a) No SC-9
		b) Excess I_{CBO} C-B, C-E short I) Before normal squib command II) During or after normal command	b) Q_2 held
		c) Loss of h_{FE}	c) Reduced output
2. Q2 Transistor	Switch - amplifier part of Darlington pair	a) C or E open	a) No SC-9
		b) Excess I_{CBO} C-B, C-E short I) Before normal squib command II) During or after normal command	b) Q_2 held
		c) Loss of h_{FE}	c) Reduced output

Table 4.8-19: —Continuation Sheet

LITY ANALYSIS — CONTINUATION SHEET
ORBITER — SC-10

	(2) DRAWING NUMBER 25-51661			(3) BOEING SPEC D2-100234
OPERATIONAL EFFECT		PROB OF OCCUR (14)	SEVERITY RATING (15)	ACTION TO MINIMIZE FAILURE MODE SUSCEPTIBILITY (16)
RY	SECONDARY			
? output	a) Failure to fire bridgewire	0.009	C	a) Redundant squib circuit (1) (3) (4) (5) (6)
on	b) I) Inadvertent squib fire command II) Failure to turn off squib command output	0.0001 0.005	A	b) (1) (2) (3) (5) (6) (7) (8) R7, R8, R18, R19, reduce I_{CEO} increase effect due to excess I_{CBO}
SC-9	c) Possible failure to fire bridgewire	0.004	C	c) Redundant squib circuit (2) (3) (5)
? output	a) Failure to fire bridgewire	0.009	C	a) Redundant squib circuit (3) (4) (5)
on	b) I) Inadvertent squib fire command II) Failure to turn off squib command output	0.0001 0.0005	A C	
SC-9	c) Possible failure to fire bridgewire	0.0004	C	c) Redundant squib circuit (2) (3) (5)

(1) COMPONENT SUBSYSTEM OR SYSTEM		SWITCHING ASSEMBLY	
ARTICLE IDENTIFICATION (10)	ARTICLE FUNCTION (11)	MODES & CAUSES OF FAILURE (12)	(13) PRIM
SC-10 1) K1 Relay	Arm inhibit, bias, and noise clamp Prevent squib firing during exercise of programmer after squib installation	a) Failure to energize	a) Provide between troller po contacts circuits
		b) Failure to de-energize	b) Failure t circuits
		c) Normally closed contacts fail to open	c) No disar on launc
		d) Normally closed contacts fail to close	d) No arm on launc
2) CR-7 Diode	Relay E-I suppression	a) Diode opens	a) Noise pu rated du energizc relay
		b) Diode shorts	b) Failure relay (a
3) CR-5, CR-6, CR-2, or CR-3 zener diodes	Noise clamp	a) Zener voltage decrease (to 20% out of tolerance)	a) Improve ing
		b) Zener voltage increase (to 15% out of tolerance)	b) Degrade clampin
		c) Zener opens	c) Predicte trig circuits second Q1, Q2
		d) Zener short	d) Probabl of conn relay c

Y ANALYSIS — CONTINUATION SHEET

– LUNAR ORBITER — SC-10

Table 4.8-19: — Continuation Sheet

	(2) DRAWING NUMBER 25-51661			(3) BOEING SPEC D2-100254
OPERATIONAL EFFECT		PROB OF OCCURRENCE (14)	SEVERITY RATING (15)	ACTION TO MINIMIZE FAILURE MODE SUSCEPTIBILITY (16)
ARY	SECONDARY			
ontinuity harge con- wer on-off and squib	a) Cessation of S/C test operations	0.001	C	a) Component qualification to controlled spec test cycled to increase confidence
arm squib	b) Stop launch countdown	0.000 +	C	b) Same as a) above
m indication h console	c) Stop launch countdown	0.045	C	c) Same as a) above
ndication h console	d) Stop launch countdown	0.045	C	d) Same as a) above
lse gene- ring de- ition of K-1	a) Possible noise triggering of S/A circuits	0.018	C	a) Screened parts module tests
o energize m inhibit)	b) Stop launch countdown	0.002	C	b) Same as 1) a) above
d noise clamp-	a) None	0.009	C or lower	a) Component selection screening, confidence test, derating
d noise g	b) None	0.010	C or lower	b) Q2, Q5, Q6 BV_{CEO} screened to 47 volts minimum
d 20 μsec gering squib possible breakdown , Q5, Q6	c) Possible in- advertent squib firing	0.001	A-C	c) Component selection screening
e burn open ector pins or ntacts	d) Failure to squib redundancy	0.0001	A-C	d) Same as c) above

(1) COMPONENT SUBSYSTEM OR SYSTEM		SWITCHING ASSEMBLY	
ARTICLE IDENTIFICATION (10)	ARTICLE FUNCTION (11)	MODES & CAUSES OF FAILURE (12)	(13) OPERATIO
			PRIMARY
SC-10 (continued)			
4) CR-1 or CR-4 Diode	SC-8 Q1, Q2 (Q5, Q6) part of ground noise filter threshold	a) Diode fails open	a) V_{EBO} Q1 Q2 exceeded (Q5 Q6) — loss of redundancy 9 squib circuits
		b) Diode fails shorted	b) Reduced ground noise immunity
5) R2 (R4) Resistor	Diode — voltage control	a) Resistance increase 2.5, -10%	a) Reduced ground noise immunity
		b) Resistance decrease 2.5, -10%	b) Improved ground noise immunity
		c) Resistor opens	c) Reduced ground noise immunity
6) R1 (R3)	Resistor — current limiting	a) Resistance decrease	a) Increased SC-9 output current
		b) Resistance increase	b) Decreased SC-9 output
		c) Resistor opens	c) No output 1-9 SC-9 squib firing circuits

Table 4.8-19: — Continuation Sheet

Y ANALYSIS — CONTINUATION SHEET
- LUNAR ORBITER — SC-10

(2) DRAWING NUMBER 25-51661			(3) BOEING SPEC D2-100254
NAL EFFECT SECONDARY	PROB'OF OCCURRENCE (14)	SEVERITY RATING (15)	ACTION TO MINIMIZE FAILURE MODE SUSCEPTIBILITY (16)
	0.018	B-C	a) Power limited to 3 milliwatts, current limited to 3 ma Acts as zener Redundant circuits
a) Failure to fire all bridgewires			
	0.002	C	b) Predicted noise provides inadequate energy to squib circuit V_{BE_1}, V_{BE_2} provide backup noise threshold
b) Possible ground noise triggering of squib circuit	0.006	C	a) Circuit insensitive to 10% changes in R_2 (R_4)
a) None	0.006	C or lower	b)
b) None	0.006		c) V_{BE} of Q1, Q2 + V_F of diode provide backup noise threshold.
c) None	0.003	C	a) Circuit designed for -8% (1% initial resistor) commercial vendor (Minuteman) recommendation Component qualification to specific application
a) None			
b) None	0.003	C	b) 50% increase in resistance would allow current above Bruceton all fire curve Also see a) above Circuit designed for +5% increase to provide 5 amps min
c) None			
	0.004	B-C	c) Redundant squib firing circuits depending on independent resistor

(1) COMPONENT SUBSYSTEM OR SYSTEM	CONTROL AND SWITCHING ASSEMBLY		
ARTICLE IDENTIFICATION (10)	ARTICLE FUNCTION (11)	MODES & CAUSES OF FAILURE (12)	(13) OPERATIO
			PRIMARY
Interconnecting wiring			
1) SC-21, SC-8, SC-9, SC-10	Provide 5 Amp, to squibs	a) Turn on during power energize cycle	a) SC-9 output to squib
2) +15 volt wire	Bias gate	a) Open connection to one SC-21 only	a) SC-9 output held off
		b) Open connection to SC-21 mother board	b) Loss of redundancy
4) -15 volt	Bias gate	a) Open connection to one SC-21	a) Q1 or Q4 fail to turn off during squib fire command
		b) Open connection to SC-21 mother board	b) Loss redundancy
5) +6 volt	Bias gate	a) Open connection to one SC-21	a) SC-21 output stays at level one
		b) Open connection to SC-21 mother board	b) Loss of redundancy
7) Digital return	Regulated power return	a) Open connection to one SC-21	a) SC-21 output stays at level one
		b) Open connection to mother board	b) Loss of redundancy

Note 1 - Add confidence testing of wiring to each item

— CONTINUATION SHEET

CONNECTING WIRING

Table 4.8-19: — Continuation Sheet

(2) DRAWING NUMBER 25-51661			(3) BOEING SPEC D2-100254
NAL EFFECT SECONDARY	PROB OF OCCURRENCE (14)	SEVERITY RATING (15)	ACTION TO MINIMIZE FAILURE MODE SUSCEPTILITY (16)
a) Inadvertent squib firing all squibs	100%	A Procedure control	a) Energize arm inhibit relay prior to application or S/C power from ground or batteries
a) Failure to fire 2 bridgewires	0.00012	C	a) Redundant squib firing circuits
b) None	0.00012	C	b) Redundant wires to mother board
a) Possible failure to fire squib	0.00012	C	a) Redundant squib circuit
b) None	0.00012	C	b) Redundant wires to mother board
a) Failure to fire 2 bridgewires	0.00012	C	a) Redundant squib circuits
b) None	0.00012	C	b) Redundant wires to mother board
a) Failure to fire 2 bridgewires	0.00012	C	a) Redundant wires to mother board
b) None	0.00012	C	b) Redundant wires to mother board

(1) COMPONENT SUBSYSTEM OR SYSTEM	
(10) ARTICLE IDENTIFICATION	(11) ARTICLE FUNCTION
1) Signal input wire	Interconnect O M D to S I C (SC-21)
2) Signal output wire	Interconnect SC-21 in control assembly with SC-8 in switching assembly
3) SC-8 to SC-9 etched circuit	SC-8 output to SC-9 input
4) SC-8 + 15v input	Bias-switching amplifier
5) SC-8 - 15v input	Bias-switching amplifier
6) SC-8 digital return input	Regulated power return to control assembly power supply

FAILURE MODE, EFFECT, & CRITICALITY ANALYSIS — (
SQUIB FIRING CIRCUITS — LUNAR ORBITER — INTERC

CONTROL AND SWITCHING ASSEMBLY

(12) MODES & CAUSES OF FAILURE	(13) OPERATIO PRIMARY
a) Open wire	a) SC-21 output held at "logic L"
a) Open wire	a) SC-8 output held at "off"
a) Open wire	a) SC-9 output held off
a) Open circuit to one SC-8 module on mother board	a) SC-9 output held off
b) Open wire to SC-8 mother board from control assembly power supply bus	b) Loss of redundancy
a) Open circuit to SC-8 module on mother board	a) Loss of reserve Q_4 turn off current
b) Open wire to SC-8 mother board from control assembly power supply bus	b) Loss of redundancy
a) Open wire to SC-8 module	a) No SC-8 output
b) Open wire to SC-8 mother board	b) Loss of redundancy

2

Table 4.8-19: — Continuation Sheet

CONTINUATION SHEET
ONNECTING WIRING

(2) DRAWING NUMBER 25-51661			(3) BOEING SPEC D2-100254
NAL EFFECT SECONDARY	(14) PROB OF OCCUR	(15) SEVERITY RATING	ACTION TO MINIMIZE FAILURE MODE SUSCEPTIBILITY
a) Failure to fire 2 bridgewires	0.00012	C	a) Redundant squib circuits
a) Failure to fire bridgewire	0.00012	C	a) See above
a) Failure to fire bridgewire	0.00012 X2	C	a) See above
a) Failure to fire 2 bridgewires	0.00012	C	a) See above
b) None	0.00012	C or lower	b) Redundant wires to mother board from control assembly.
a) None	0.00012	C or lower	a) Q_3 saturates harder and together with I_{CBO} R10 remains below V_{BE} (off) max of Q4, holding Q4 off
b) None	0.00012	C or lower	b) Redundant wires from control assembly power supply terminal bus
a) Failure to fire 2 bridgewires	0.00012	C	a) Redundant squib circuits
b) None	0.00012	C or lower	b) Redundant wires to mother board from control assembly power supply terminals

3

FAILURE MODE, EFFECT, & CRITICALITY A

SQUIB FIRING CIRCUIT—LUNAR ORBITE

(1) COMPONENT SUBSYSTEM OR SYSTEM		SWITCHING ASSEMBLY	
ARTICLE IDENTIFICATION (10)	ARTICLE FUNCTION (11)	MODES & CAUSES OF FAILURE (12)	(13) OPE PRIMARY
Interconnecting wire	Power and power returns		
1) +28 v.d.c. squib power	Power to switching assembly for squib firing	a) Open +28 v.d.c. wire to SC-10 module or open 28 v.d.c. return	a) Loss of red

Table 4.8-19: — Continuation Sheet

NALYSIS — CONTINUATION SHEET

R — INTERCONNECTING WIRING

	(2) DRAWING NUMBER 25-51661			(3) BOEING SPEC D2-100254
RATIONAL EFFECT		PROB OF OCCURRENCE (14)	SEVERITY RATING (15)	ACTION TO MINIMIZE FAILURE MODE SUSCEPTIBILITY (16)
Y	SECONDARY			
undancy	a) None	0.00012 X2	C	a) Redundant wiring from power subsystem terminals into SC-9 module and out to external connector pins.

(1) COMPONENT SUBSYSTEM OR SYSTEM		NASA COMPARISON REQUEST	
ARTICLE IDENTIFICATION (10)	ARTICLE FUNCTION (11)	MODES & CAUSES OF FAILURE (12)	(13 PRIMAR
SC-8 equiv module	SCR trigger amplifier	Same as SC-8 for L O except delete R5, R6, R7, R8, R12, R15, C4, Q5, Q6, R16, R17, R18, R19, R20, and replace with:	
1) R5 Resistor (R_6)	Gate current limiter filter component	a) Resistance increase	a) Reduced SC-
		b) Resistance decrease	b) Decreased no tion
		c) Resistor opens	c) No SC-8 out
2) R7 Resistor (R_8)	Bias turn off	a) Resistance increase	a) SCR may turn to Q1 I_{CBO}
		b) Resistance decrease	b) Reduced SC-
		c) Resistor opens	c) Increased SC and I_{CBO} ou
3) C4, C5, capacitor	Filter, SCR noise input	a) Capacity increase	a) Increased noi rejection
		b) Capacity decrease high power factor	b) Decreased no rejection
		c) Capacitor opens	c) No noise reje in SCR input
		d) Capacitor shorts	d) No SC-8 outp

Table 4.8-19: —Continuation Sheet

TY ANALYSIS — CONTINUATION SHEET
NER C TYPE — SC-8 DEVIATIONS

	(2) DRAWING NUMBER			(3) BOEING SPEC
) OPERATIONAL EFFECT		PROB OF OCCURRENCE (14)	SEVERITY RATING (15)	ACTION TO MINIMIZE FAILURE MODE SUSCEPTIBILITY (16)
Y	SECONDARY			
3 output	a) Possible failure to fire bridgewire	0.003	C	a) Redundant firing circuit
ise rejec-	b) Possible inadvertent squib fire command	0.003	A-C	b) Design R5, R7, C4, filter for insensitivity to R_5
ut (1 side)	c) Failure to fire bridgewire	0.004	C	c) Redundant firing circuit
on due	a) Possible inadvertent squib fire command	0.0006	A-C	a) Proper deratings
3 output	b) None	0.0006	C	b) Reserve gain adequate to fire SCR
8 noise put	c) Possible inadvertent squib fire command	0.0006	C	c) Welded connections proper deratings event likely to occur only during firings
e	a) None	0.005	C or lower	a) Screened components
se	b) Possible inadvertent squib firing	0.010	A-C	b) Screened components proper deratings
ction	c) Inadvertent squib fire command — probable	0.015	A-C	c) Reduce SCR gate lead length - proper lead dress, (multiple - capacitors possible)
ut	d) Failure to fire bridgewire	0.005	C	d) Redundant circuit component derating

FAILURE MODE, EFFECT, & CRITI

SQUIB FIRING CIRCUIT — N

(1) COMPONENT SUBSYSTEM SYSTEM		NASA COMPARISON REQUEST	
ARTICLE IDENTIFICATION (10)	ARTICLE FUNCTION (11)	MODES & CAUSES OF FAILURE (12)	(13) PRIMA
SC-9 equiv module	Provide squib firing power		
1) SCR-1 silicon controlled rectifier	Gate, power	a) Any terminal open	a) No SC-9
		b) Excess leakage I I A-G II I A-K	b) I SCR tu II Reduc capacitor
		c) Decreased I_H	c) SCR rema after norm
		d) V_{BO} breakdown	d) SCR forwa over

Table 4.8-19: —Continuation Sheet

CALITY ANALYSIS — CONTINUATION SHEET

MARINER C TYPE — SC-9 EQUIVALENT

	(2) DRAWING NUMBER			(3) BOEING SPEC
OPERATIONAL EFFECT		PROB OF OCCURRENCE (14)	SEVERITY RATING (15)	ACTION TO MINIMIZE FAILURE MODE SUSCEPTIBILITY (16)
RY	SECONDARY			
output	a) No squib fire command	0.05	C	a) Screened components
rns on ed output source	b) I Inadvertent squib fire command	0.05	A-C	b) Screened components adequate deratings contamination control
	II Possible failure to fire squib	0.05	C	
ns on al firing	c) 2nd SCR sharing module A or B fails to fire	0.10	C	c) Redundant circuits screened components
rd break-	d) Inadvertent squib fire command	0.0001	A	d) Adequate V_{BO} derating

FAILURE MODE, EFFECT, & CRITICALITY

SQUIB FIRING CIRCUIT — MARI

(1) COMPONENT SUBSYSTEM OR SYSTEM	NASA COMPARISON REQUEST		
(10) ARTICLE IDENTIFICATION	(11) ARTICLE FUNCTION	(12) MODES & CAUSES OF FAILURE	(13) OPERA PRIMARY
Module A	Modified power source for squib firing		
1) C1, C2, or C3	Energy storage squib firing	a) Capacity decrease high power factor	a) Reduced energy output
		b) Capacity increase	b) Increased energy output
		c) Capacitor short	c) No energy output
		d) Capacitor open	d) No energy output
2) R1 Resistor	Capacitor charging SCR turn off control	a) Resistance increase	a) Increased charging time
		b) Resistance decrease	b) SCR's fail to turn off
		c) Resistor opens	c) No energy output

ANALYSIS — CONTINUATION SHEET

NER C TYPE — MODULE A

Table 4.8-19: — Continuation Sheet

(2) DRAWING NUMBER			(3) BOEING SPEC
TIONAL EFFECT SECONDARY	(14) PROB OF OCCURRENCE	(15) SEVERITY RATING	(16) ACTION TO MINIMIZE FAILURE MODE SUSCEPTIBILITY
a) Possible failure to fire bridgewire	0.05	C	a) Redundant circuits
b) Increased recharging time	0.01	Lower than C	b) Screened components
c) Failure to fire 2 bridgewires	0.04	C	c) Redundant circuits
d) Failure to fire 2 bridgewires	0.005	C	d) Redundant circuits screening
a) Possible failure to fire bridgewire	0.0006	C	a) Redundant circuits screening
b) Continuous squib fire command if bridgewire opens 2.8K failure to fire 2nd bridge-wire	0.0006	C	b) Redundant circuits screening
c) Failure to fire 2 bridgewires	0.0006	C	c) Redundant circuits screening

ERRATA (Continued)

Volume A

Page No.	Paragraph, Table, or Figure No.	
4.1-97	Para. 4.1.3.3	Line 13: Delete reference (D2-82709-2, Section 4.1.8). Add: ("Philco Document WDL-TDR-2531, Section 4.0.)
4.1-103	Table 4.1-11	Change: "Image Rejection" line from "8 db MIN to INPUT f's OF 8 & 46 Mc" to "80 db MIN to INPUT f's OF 10 & 46 Mc"
4.1-112	Table 4.1-14	Column "Pointing Loss (db)" Change "3d db" to "3-4 db"
4.1-130	Table 4.1-16	Change line "Low Gain Antenna" Column "Gain" (See Figure 4.1.3.4-7) to "(See Fig. 4.1-23, Vol. II)" Change reference "Figure 4.1.3.4-8" to "Figure 4.1-29"
4.1-134	Table 4.1-18	Line 2 of "Mechanical Interface" Change: "on an interval" to "integral"
4.1-146	Para. 4.1.4	Line 15: Change: "Figure 4.1-33" to "Figure 4.1-30"
4.1-170	Table 4.1.4-7	Move numerical designations from "Source of Loss" line to "Telemetry Mode" line Move vertical divider between "5" and "6" one numerical column to right.
4.1-178		Change summation signs to pi signs in second formula on page.
4.1-263	Figure 4.1.4-35	Change 0 = 0.0152" to "0.0512"
4.1-301	Para. 4.1.5	Line 3: Change: D2-23834-1, Revision A to "D2-82724-3, Revision B."

ERRATA (Continued)

Volume A

Page No.	Paragraph, Table, or Figure No.	
4.3-1	Para. 4.3	Line 11. Change from "395 pounds" to "410 pounds."
4.3-3	Table 4.3-1	Change: "Minimum V (Orbit Time)" to: "Minimum V (Orbit Trim)"
4.3-9	Para. 4.3.3.1	Change last sentence from: "These tanks contain 395" to: "These tanks contain 395 usable plus 15 residual."
4.3-13	Para. 4.3.3.1	Change page no. from: 4.3-13 to 4.3-17
4.3-17	Para. 4.3.3.1	Change page no. from: 4.3-17 to 4.3-13
4.3-21	Table 4.3-4	On burn time line Change: "982" to "982 seconds" On "size length" line Change: "5.72" in. to "8.52 in.
4.3-22	Figure 4.3-7	Change: 1.30" to 2.0" Change: 0.80" to 1.0" Change: 3.62" to 5.02" Delete: 5.72"
4.3-24	Figure 4.3-9	Change: 1.30 to 2.0 Change 2.10 to 3.0 Change: 5.72 to 8.2
4.3-28	Para. 4.3.3.1	Line 12: Change: "The signals from the pressure transducers are fed into a MDS signal conditioner which compares pressure transducer will not result in an engine-out signal." to: The signals from the pressure transducers are fed into a MDS signal conditioner which compares pressure transducer outputs. Threshold level is set such that a malfunctioning pressure transducer will not result in an engine-out signal."

ERRATA (Continued)

Volume A

Page No.	Paragraph, Table, or Figure No.	
4.3-34	Table 4.3-7	Change: "Ignition Delay Time" from 70M/sec to 70 milli-sec." Change reference: Change "*Add 33 lb to "* Add 38 lb."
4.3-36	Para. 4.3.3.2	Line 2: Change "30-pound" to "38-pound."
4.3-51	Table 4.3-10	Change valve position indicators "(2)" to "(4)"
4.3-53	Figure 4.3-19	Draw horizontal lines from both filters to both regulators (in center of page)
4.3-60	Para. 4.3.5.1	Change Line 1 callout from: 0.9973 to "0.9968."
4.3-62	Table 4.3-13	N_2H_4 Propellant Weight: Change from 395 to "410"
4.3-65	Table 4.3-15	In-Orbit: Change: "Inerts from 70 to "62" "Solid Motor from (30) to (38)"
4.3-71	Table 4.3-16	Change Structural Support -- Solid Rocket Motor from 30 to "38"
4.4-31	Figure 4.4-10	Change T = 40°F to "T = -60°F"
4.4-33	Figure 4.4-12	Add: Abscissa title: "TIME FROM PERIAPSIS (HRS)"
4.6-10	Table 4.6-2	Inertial Hold: Change from 0.2° to "0.6°."

ERRATA (Continued)

Volume A

Page No.	Paragraph, Table, or Figure No.	
4.6-45	Table 4.6-7A	Change all reference from (fps) to (mps) Delete: Magnitude $7x10^{-5}$ $5.4x10^{-3}$ Add: "Stability (90 days) $1x5\ 10^{-4}$ 11.55×10^{-3}" Change: Temperature Coefficient Velocity Error from 1.65 to "6.93." Change: Noise Velocity Error from .55 to "2.31" Change: Vibration Velocity Error from .01 to ".03" Change: "Trimmed to within" Velocity Error from 5.9 to "13.2" Delete: "Trimmed to Within" Allowable Velocity Error 0.03. Change: Total RSS Error Velocity Error from 0.011 to "0.017." Change: "Time of thrust" - 2.4 seconds to "= 7.85 seconds."
4.6-60	Figure 4.6-19	Delete: "From CC&S, Divider Register block.
4.7-3		Add: Figure number and title: "Figure 4.7-2, REACTION CONTROL SUBSYSTEM."
4.7-7	Para. 4.7.1	Line 12: Change reference from Section 4.7 to "Section 4.6."
4.7-12	Para. 4.7.3.3	Change: Reference from Section 3.4.5.4 to "Section 3.3."
4.7-18	Para. 4.7.6.3	Line 4. Change "0.4" to "0.02."
4.7-19	Figure 4.7-5	Divide: All ordinate scale numbers by 5.
4.7-20	Figure 4.7-6	Add: Footnote: "Approximate solar pressure is shown too high by a factor of 2."
4.7-22	Table 4.7-4	Change: All reference to "Pitch" to "Yaw."

ERRATA (Continued)

Volume A

Page No.	Paragraph, Table, or Figure No.		
4.8.5	Figure 4.8-3	Change:	Figure number and title from "4.8-3 Central Computer and Sequencer Functional Block Diagram" to: "Figure 4.8-5, Central Computer and Sequencer Control Assembly Functional Block Diagram."
4.8-17	Figure 4.8-5	Change:	Figure and title from "4.8-5 Central Computer and Sequencer Control Assembly Functional Block Diagram," to "Figure 4,8-3 Central Computer and Sequencer Functional Block Diagram."

ERRATE

Page No.	Paragraph, Table, or Figure No.	
3- 109	Table 3-9	Delete table
3-92	Fig. 3-31	Change: "Launch Vehicle 6026 Spacecraft Bus and Propulsion" To: Launch Vehicle 6016 or 6026 Spacecraft Bus and Propulsion" Change: "Launch Vehicle 6026 Spacecraft Bus, Propulsion, and Planetary Science Payload" To: "Launch Vehicle, 6016 or 6026 Spacecraft Bus, Propulsion, and Planetary Science Payload" Change: "6015 Spacecraft Bus Propulsion and Plantary Science Payload" To: Launch Vehicle, 6015 Spacecraft Bus Propulsion and Planetary Science Payload." Delete: "6016 Spacecraft Bus, Propulsion, and Planetary Science Payload" (and associated graph)
4.1-18	Para. 4.1.2.2	Delete: Last line on page: "A single subcarrier modulator in the spacecraft"
4.1-23	Table 4.1-2	Delete: Note 4) "Section 4.1.7" Add: Note 4) "Section 4.1.6"
4.1-33	Para. 4.1.2.3	Delete: General Electric II Add: General Electric II
4.1-38	Para. 4.1.2.4	Line II: Delete last figure in equation "III" Add: "191" Line 13: Delete "that B_L53.5 cps." Add: "that B_L33.5 CPS."
4.1-47	Para. 4.1.3.3	Change last two sentences on page to read: "This crossmultiplication of noisy signal produces an SNR degradation that has been calculated by Springett. 22 The band limiting effect of the filter at points 1 and 2 improves the SNR of the signal to the crossmultiplier."
4.1-61	Para. 4.1.4.1	Delete: "f) Phase Instability (nominal); Less than 2 degrees peak in $2B_{LO}$=cps" Add: "f) Phase Instability (nominal): less than 2 degrees peak in $2B_{LO}$= 20 cps
4.1-66	Para. 4.1.4.1	Line 15: Delete: "TDA'S have been space qualified Add: "TDA's have been evaluated for"